Ion Exchange and Solvent Extraction

A Series of Advances

Volume 19

Edited by
BRUCE A. MOYER

Ion Exchange and Solvent Extraction

A Series of Advances

Volume 19

ION EXCHANGE AND SOLVENT EXTRACTION SERIES

Series editors

Arup K. Sengupta
Bruce A. Moyer

Founding Editors

Jacob A Marinsky
Yizhak Marcus

Contents of Other Volumes

Ion Exchange and Solvent Extraction

A Series of Advances

Volume 19

Edited by

BRUCE A. MOYER

CRC Press
Taylor & Francis Group
Boca Raton   London   New York

CRC Press is an imprint of the
Taylor & Francis Group, an **informa** business

Contents

Preface

Volume 19 of the series *Ion Exchange and Solvent Extraction* devotes itself to a comprehensive look at the progress of science underlying solvent extraction in its role as the central technique for the reprocessing of commercial spent nuclear fuel. Perhaps one of the most difficult separation challenges imaginable is the partitioning of the components of nuclear fuel that has been "burned up" in a nuclear reactor. Not only does this challenge lie in the selective removal of certain actinides and fission products in a mixture of over a third of the periodic table, but also the separations must be carried out in a field of intense radioactivity. Moreover, the sought decontamination factors are ambitious, and the range of concentrations of metals to be removed varies from on the order of milligrams per liter to over hundreds of grams per liter. As if this is not enough, we demand group separations and even simultaneous extractions of metal species that are quite disparate, even simultaneous extraction of cations and anions. Early practitioners soon recognized the power of solvent extraction as a technique that possessed high selectivity and also offered the robustness and simplicity needed for operation behind thick concrete shielding. The flexibility of stagewise flowsheet design was especially appealing. Indeed, solvent-extraction chemistry developed over a half-century ago is still widely practiced in the world, and it may even be said that solvent extraction itself as a technique for the industrial separation of metals owes its birth to the problem of nuclear separations.

Now, more than six decades after the dawn of the nuclear era, a period of transformation—some say a renaissance—has begun in nuclear technologies in all parts of the fuel cycle, and this naturally includes a transformation in the practice of solvent extraction. In view of the peaking of world oil supplies, growing concerns about global warming and its potential connection with the burning of fossil fuels, and domestic needs for energy independence, more countries are turning to greater use of nuclear energy as part of their energy policy. At the same time, it is recognized that long-term use of nuclear energy will necessitate the development of better technology to separate and recycle those components that either add energy value or that, because of their long-term hazard, need to be destroyed by transmutation. Thus, the long-term vision of many workers in the field entails a proliferation-free nuclear-energy economy in which little waste is stored or released to the environment. Motivated by such goals, research has not stood still over the past few decades, and now there exist new understanding, new molecules, new processes, and new contacting methods that can be used in future plants for commercial reprocessing. What is more, the momentum of current research coupled with powerful new tools available for conducting research promises major advances in the field.

In view of the heightened challenges and accompanying transformations in the field of spent nuclear fuel reprocessing, this volume aims to capture recent progress as it can be described today and looks ahead to potential developments. An overview chapter on the basic strategies in reprocessing introduces the book, defining the goals being pursued in different countries and the accompanying technical

challenges being addressed. The next three chapters present a range of new molecules that have been synthesized and tested toward gaining increased selectivity and performance for specific purposes, such as the group separation of actinides from lanthanides. New classes of molecules such as calixarenes, bis(triazinyl)pyridines, and diamides show an increasing sophistication over previous generations of simpler extractants, taking advantage of the unique economics of nuclear separations. Compared with the hydrometallurgical recovery of metals from ores, separations in the nuclear industry, where the capital and operating costs are dominated by factors other than the price of the extractants, benefit from the considerable variety of applicable molecular frameworks that can be used. If molecules of greater complexity can be afforded and are needed for certain tasks, then molecular design must be pursued, for the high cost of synthesis and testing of new compounds for radiochemical separations necessitates testing fewer compounds. Design techniques must pinpoint effective structures prior to synthesis, and one chapter addresses a new approach to the discovery of even more powerful extractants. It is also known that some objectives can be accomplished by mixing extractants, as the next chapter discusses, but can one generalize some measure of rules that provide some predictability? Despite all the attempts to design superior extractants, the phenomenon of phase splitting or third-phase formation has remained one of the factors impeding progress since the earliest use of solvent extraction. It can be said that the "ungainly" molecular structures of the most successful extractants owe their origin in part to avoidance of third phases. Unfortunately, the understanding needed to overcome this problem by rational vs. empirical means has been limited until recently, as described in another chapter. The theme of understanding-leading-to-predictability is continued in addressing the inevitable problem of the effects of intense radiation on the solvent and its performance. If a new extractant cannot survive radiolysis conditions, then its usefulness in reprocessing is severely limited. But, can we predict in advance such instability? Nuclear separations often raise the question of accountability, requiring accurate real-time analytical capabilities, which are needed for good process control in any case. Accordingly, advances in analytical techniques, many based not surprisingly on reagents familiar in process separations, are covered. The development of new types of centrifugal contactors for more efficient processing is also described, for increasing throughput reduces footprints and corresponding costs. Higher throughput also reduces solvent inventory, further enabling the use of expensive designer extractants, and reduced phase-contact times minimize solvent degradation. Finally, a forward-looking chapter caps off the volume by considering new chemistry that may offer the potential for further advances in the future, using novel media such as ionic liquids and supercritical solvents.

In view of its comprehensive coverage, this volume is intended as a necessary reference for anyone interested in the basic chemistry of nuclear fuel reprocessing, including students, academicians, government researchers, industrial practitioners, and even policymakers. It should present a foundation for new research, as it not only describes the state of our knowledge, but also covers research tools, such as new methods for molecular design, spectroscopic techniques, and analytical methods. It should help applied chemists usher in the next era of nuclear technologies, as they will have a much better understanding of the systems they are working with. It should help

in the process of setting nuclear policy, as it defines what our capabilities are, at least in principle, upon further development. Although directed at nuclear separations, this volume should also prove useful to solvent-extraction chemists in hydrometallurgy, practicing the recovery of metals from ore, scrap, etc., in that the same new research tools are available for the study of any liquid-liquid system. Moreover, certain aspects of solvent extraction, such as third-phase formation, extractant design, and process-stream analysis, challenge all researchers and practitioners in the field. Therefore, Volume 19 of the series *Ion Exchange and Solvent Extraction* seems a timely one for many reasons and a fitting presentation of the state of the art in solvent extraction.

Editor

Bruce A. Moyer has 30 years of experience in R&D on solvent extraction and ion exchange, focusing on radionuclide separations for environmental and waste cleanup, nuclear fuel cycles, and national security applications in the USDOE complex. Dr. Moyer leads the Chemical Separations Group of ORNL's Chemical Sciences Division. He is editor of the journal *Solvent Extraction and Ion Exchange* and recently served as technical program chair and editor in chief of the proceedings of the International Solvent Extraction Conference ISEC 2008. He has nine patents and over one hundred and fifty career publications. He is a co-inventor of the Caustic-Side Solvent Extraction (CSSX) process deployed at the USDOE Savannah River Site for cesium removal from high-level waste. Dr. Moyer was also a co-inventor of BiQuat anion-exchange resin (IR-100 Award, 2004), successfully demonstrated for both pertechnetate and perchlorate removal from groundwater at DOE and DOD sites. Dr. Moyer graduated summa cum laude from Duke University in 1974 (Phi Beta Kappa) with a BS in chemistry and from the University of North Carolina at Chapel Hill in 1979 with a PhD in inorganic chemistry.

Contributors

Vasily A. Babain
VG Khlopin Radium Institute
St. Petersburg, Russia

P. Bauduin
(Until 2007)
Commissariat à l'Énergie Atomique
CEA Saclay
DSM/IRAMIS/SCM/LIONS
Gif-sur-Yvette, France

and

(From 2007)
Institut de Chimie Séparative de
    Marcoule
UMR5257
Bagnols-sur-Cèze, France

Laurence Berthon
Commissariat á l'Energie Atomique,
CEA Marcoule
Bagnols-sur-Cèze, France

Marie-Christine Charbonnel
Commissariat à l'Énergie Atomique
CEA Marcoule
Bagnols-sur-Cèze, France

Mark L. Dietz
Department of Chemistry and
    Biochemistry
University of Wisconsin-Milwaukee
Milwaukee, Wisconsin

Jean François Dozol
CEA, DEN, Cadarache
Saint Paul Lez Durance, France

Oleg B. Egorov
IsoRay Medical Inc.
Richland, Washington

Jay W. Grate
Pacific Northwest National Laboratory
Richland, Washington

Clément Hill
Commissariat à l'Énergie Atomique
CEA Marcoule
Bagnols-sur-Cèze, France

Ralph A. Leonard
Chemical Sciences and Engineering
    Division
Argonne National Laboratory
Argonne, Illinois

Rainer Ludwig
International Atomic Energy Agency
    A-1400
Vienna, Austria

Vijay K. Manchanda
Radiochemistry Division
Bhabha Atomic Research Centre
Mumbai, India

P.K. Mohapatra
Radiochemistry Division
Bhabha Atomic Research Centre
Mumbai, India

Yasuji Morita
Japan Atomic Energy Agency
Tokai-Mura, Ibaraki-ken, Japan

Matthew J. O'Hara
Pacific Northwest National Laboratory
Richland, Washington

P.N. Pathak
Radiochemistry Division
Bhabha Atomic Research Centre
Mumbai, India

Vitaly Solov'ev
Institute of Physical Chemistry and
    Electrochemistry of Russian
    Academy of Sciences
Moscow, Russia

Shoichi Tachimori
Sec. Nuclear Safety Commission, CAO
Tokyo, Japan

Fabienne Testard
Commissariat à l'Énergie Atomique
CEA Saclay
DSM/IRAMIS/SCM/LIONS
Gif-sur-Yvette, France

Alexandre Varnek
Laboratoire d'Infochimie
UMR 7177 CNRS
Université Louis Pasteur
Strasbourg, France

Th. Zemb
Institut de Chimie Séparative de
    Marcoule
UMR5257
Bagnols-sur-Cèze, France

1 Overview of Solvent Extraction Chemistry for Reprocessing

Shoichi Tachimori
Sec. Nuclear Safety Commission (Retired)

Yasuji Morita
Japan Atomic Energy Agency

CONTENTS

1.1 INTRODUCTION

1.1.1 CURRENT STATUS

Reprocessing of spent nuclear fuel (SNF) has been, for a half-century, playing a central role in an enhanced utilization of nuclear energy. In the first generation of reprocessing, about 7.5–8.0×10^5 t of low burn-up uranium was processed during the Cold War era to recover ca. 300 t weapon-grade plutonium. In the second generation, on the contrary, reprocessing has been used to improve the peaceful utilization of nuclear energy, and ca. 1.0×10^5 t of civil high burn-up fuel, which is almost one-third of the total civil SNF evolved worldwide, has been reprocessed mostly in Europe by now (*1–3*).

The sum total of electricity generated by means of nuclear power worldwide till the end of 2007 is almost 5.8×10^{13} kWh, which is 14 times that generated in the United States in 2006.

Changing the point of view to material transformation, a nuclear reactor yields both fission products (FPs) and transuranic elements (TRUs). One-day operation of a 1GWe- nuclear power plant consumes ca. 3.2 kg actinides by fission reactions producing almost the same amounts of FPs, and simultaneously yields ca. 1.0 kg TRUs (mostly Pu), which is a remainder of TRUs produced by (n,γ) and (n,2n) reactions of U and burnt, on an assumption of an average burn-up of 30 GWD/t. Hence, humanity will realize, taking until 2010, the transmutation of ca. 10^4 t of U (^{235}U and ^{238}U) into FPs (ca. 7700 t), Pu (ca. 2300 t, assuming an average burn-up of 30 GWD/t), and minor actinides (MAs; Np, Am, Cm) by modern nuclear technology. Specifically, the main useful products include: Ru, 490 t; Rh, 110 t; Pd, 250 t; ^{99}Tc, 170 t; ^{241}Am (^{241}Pu), 300 t; ^{243}Am, 10 t; ^{244}Cm, 1.6 t, etc.

Although the main incentive of reprocessing is to use uranium resources effectively by recovering and recycling the Pu and U remaining in the SNF, the real feature of the Pu flow in the current world can be described as follows:

1. Pu production in contemporary power reactors is ca. 90–100 t/year.
2. Pu separation by reprocessing is ca. 20–30 t/year.
3. About two-thirds of the separated Pu are used in mixed oxide (MOX) fuel fabrication.
4. The residual "excess" civilian Pu has been accumulating in several countries, and the gross amounts of Pu stored were estimated to be ca. 250 t at the end of 2006.

After a peak at 2010, the amount of Pu stored is supposed to start decreasing due to the expected increase in MOX fuel fabrication and its usage in Light Water Reactors (LWRs). Obviously, the utilization of MOX fuel by LWRs would gradually reach a balance in which the fissile Pu in the LWR fuel is ca. 5% of the total fuels. Consequently, the utilization of U resources would not be drastically improved. The ultimate utilization will be attained in the Fast Breeder Reactor (FBR) fuel cycle, in which a conversion of fertile ^{238}U to ^{239}Pu overwhelms the consumption of the ^{239}Pu.

In the second-generation reprocessing, the applied separation technology has been the PUREX process, an acronym of Plutonium Uranium Reduction Extraction (*4*) based on a liquid-liquid extraction with tri-*n*-butyl phosphate (TBP) in *n*-paraffin diluent, which selectively recovers Pu and U on an industrial scale.

Growing concerns about global environmental issues and the risk of nuclear proliferation led to the evolution of additional requirements for the future sustainable utilization of nuclear energy. The requirements are:

1. Drastically reduce the potential impact of radioactive wastes on the environment, that is, the long-term radiotoxicity or exposure risk, particularly attributable to the high-level waste (HLW) to be disposed of.
2. Further improve proliferation resistance (PR) and safety. The essential elements to enhance nonproliferation of nuclear weapons or to suppress harmful usage of nuclear power are to (i) decrease the global inventory of separated fissile nuclides, including the existing warheads; (ii) make the

handling of special nuclear materials not authorized by IAEA extremely difficult; and (iii) disseminate worldwide renunciation of nonpeaceful utilization of nuclear materials.

3. Minimize the cost of the disposal of HLW in a deep geological repository by reducing not only the volume of the wastes, but also the heat load of the wastes.

In response to these requirements, various projects have been conducted so far. An elaborate idea of Partitioning and Transmutation (P&T) was revised and has been investigated among the OECD and non-OECD countries. The P&T strategy consists of a "partitioning process" and a "transmutation cycle." In the former, most of the TRUs (Np, Pu, Am, and Cm), long-lived FPs (LLFP) (^{129}I and ^{99}Tc), and heat-generating nuclides (^{90}Sr and ^{137}Cs) are partitioned in addition to U by chemical separation to realize (1) and (3) above. During the first 300 years after discharge of the SNF from a reactor, the thermal burden of the HLW on the repository, prevailing with ^{90}Sr and ^{137}Cs, restricts the design conditions of the repository, and, consequently, removal of these heat-generating nuclides from the HLW relaxes the specifications of a repository (*5*). After about 300 to 500 years, the radiotoxicity of the HLW is dominated by the MAs. After more than 200,000 years, the radiotoxicity of the HLW reaches the uranium-ore radiotoxicity threshold, which is regarded as nonhazardous to the environment. Thereby, the removal of all the MAs from the HLW markedly reduces the long-term radiotoxicity of the consequent waste and makes it below that of the original uranium ore after 3000 years. In the transmutation cycle, contributing to (1) and (2)-(i) above, the MAs and some LLFPs recovered are transmuted in a fast neutron reactor (FR) and accelerator driven system (ADS).

During the last few decades, considerable scientific and technical efforts have been devoted to develop partitioning/reprocessing processes in the frame of domestic and international projects: SPIN (France), OMEGA (Japan), bilateral cooperation and EURATOM Framework Programs 5 and 6 (NEWPART, PARTNEW, EUROPART, CALIXPART, PYROREP) (*6, 7*). Significant scientific and technical progress has been made. In Europe, the newest R&D program relating to P&T studies started in 2007 under the 7th EU Framework Program FP7 (*8*).

Parallel with these programs, an ambitious project, the Global Nuclear Energy Partnership (GNEP), has been launched following the Advanced Fuel Cycle Initiative (AFCI) in the United States (*9–11*). This is a historical "turning-point" of the fuel cycle strategy of the United States from the once-through to the closed fuel cycle. Consequently, fruitful results of separation science and technology, including R&D for UREX+ (URanium Extraction plus) systems, have been emerging.

From the viewpoint of reducing the potential impact of radioactive wastes on the environment, a large-scale scientific and technical challenge has been devoted to addressing the issues of "legacy of defense waste" in the United States. Various separation technologies to remove actinides (Ans), ^{137}Cs, ^{90}Sr, and ^{99}Tc from the complicated wastes stored in tanks at Hanford, Savannah River, and Idaho sites have been assessed, developed, and tested with real wastes under the collaboration of National Laboratories, private companies, and universities in the United States (*12–15*).

1.1.2 Peculiarities of Recent Progress

During the last few decades, the evolution of separation science and technology for reprocessing has obviously been affected by the progress of modern science and technologies, including actinide chemistry, computer science, information technology, an expanding knowledge base composed of a lot of fundamental and theoretical insights and experimental data, and highly sophisticated technologies. Some prominent achievements showing this feature symbolically are: (1) research teams in Marcoule and in Sellafield have successfully demonstrated control of the behavior of Np in the PUREX process; (2) research groups in the United States and in France have clarified the mesoscopic structure and the mechanism of third-phase formation (TPF) in extraction systems of TBP, diamides, and others; and (3) the debut of many novel extractants intentionally designed for specific separation purposes.

The first work depends essentially on an accurate and reliable analysis by using sophisticated simulation codes, such as, PAREX of CEA and SpeedUp (Aspen Plus) of British Nuclear Fuels Ltd. (BNFL), which were independently developed and verified by a large number of distribution and kinetics data of Np for redox reactions. The flowsheet conditions of the first cycle of the PUREX process were determined by CEA (*16–18*) with respect to coextraction of Np with U and Pu, and flowsheets of splitting Np from a U-stream were determined by BNFL (*19, 20*). The former flowsheets were validated by experiments using a genuine SNF and dedicated pulsed columns equipped with sensitive probes in the heavily shielded cell Chaîne Blindée Procédé (CBP) at the ATALANTE facility (CEA/Marcoule). The latter were validated by tests on a hot bench at Sellafield. Satisfactory results of Np extraction and stripping were obtained with a yield greater than 99%. Those rigs are well accommodated with high-level analytical lines.

TPF, splitting of an organic phase into two phases, has been an unwanted phenomenon not only in the PUREX process, but also in many, if not most, liquid-liquid extraction systems, for example DIAMEX (DIAMide EXtraction). Despite its significance, TPF remains insufficiently understood. Chiarizia et al. applied the small-angle neutron scattering (SANS) technique to investigate TPF in the TBP solvent system (*21, 22*). The SANS data were obtained by using the very intense neutron beam from the Intense pulsed neutron source (IPNS) at Argonne National Laboratory (ANL) and analyzed by virtue of Baxter's "sticky spheres" model. In addition, the inner-sphere structure of the TBP-U(VI)-NO$_3^-$ complex in the third phase was studied by measuring the X-ray absorption fine structure (XAFS) at a beam-line of the Advanced photon source (APS) at ANL. Consequently, the mechanism of aggregation involving the self-assembly of small reverse micelles of TBP-metal complex and HNO$_3$ was proposed. The findings elucidate the structure of the third phase and feature the physical chemistry of the system. The aggregation phenomenon is governed by two contrasting physical forces in an organic solvent: attractive and dispersive. Similar results were reported for diamide extraction systems by Madic et al., who used the small-angle X-ray scattering (SAXS) technique for analysis (*23*). They also used Baxter's "sticky spheres" model.

The motivation of the third achievement is ascribed to the fact that the influence of the invention of an ideal extractant possessing a high affinity and selectivity

toward a specified nuclide is so great as to expand the possibility of separations and to reduce the cost of a whole process significantly, and that the methodologies are well matured due to the progress of computer technology and software, complex chemistry, and synthetic organic chemistry.

These successful achievements were heavily owing to fundamental research, which induces synergism between fundamental and applied research. In addition, various collaborations among domestic and international researchers were also synergistic, and the development was thereby accelerated. The reprocessing technology, in this way, continues to evolve with the rapid progress of surrounding science and technology.

1.2 EVOLUTION OF SOLVENT-EXTRACTION SYSTEMS FOR REPROCESSING

Many review papers covering a broad spectrum of R&D issues of reprocessing were published during the period from the end of the twentieth century to the dawn of the new century (*24–31*). For the modernization of PUREX technology, which has already been practiced on an industrial scale for a half-century, the main R&D issues challenged were to

1. Optimize each application of PUREX and the overall process to attain sufficiently improved performance by refinement of flowsheet conditions using reliable and accurate software (i.e., database and simulation code) and by sophistication of process-control methods.
2. Introduce novel processes for improved PUREX concepts (i.e., control of Tc, Np, and iodine) and advanced methods, such as reagent's regeneration process.
3. Develop the hardware (e.g., centrifugal contactors, sensors, and other devices) and accompanying equipment, such as waste-treatment systems.
4. Address issues remaining unsolved in the PUREX process, namely, TPF, and topics in understanding the process fundamentally and thoroughly.

The ultimate goal for PUREX will be establishing an advanced single-cycle process (*32, 33*).

On the other hand, for the establishment of novel liquid-liquid extraction processes, many subjects, from fundamentals to plant-scale application steps, are to be solved generally as follows:

1. Design and develop a novel molecule that provides satisfactory separation of a target nuclide. It should be easily synthesized.
2. Build a core extraction system: choose components such as extractant, diluent, modifier, scrubbing/stripping agents, aqueous-phase conditions, etc.
3. Collect intrinsic data pertaining to the emerging process: liquid-liquid distribution, kinetics, hydrolytic and radiolytic stability, and the maximum metal loading in an organic phase without TPF, referred to as the limiting organic concentration (LOC). Consequently, build a database.

4. Develop a process simulation code to contrive objective flowsheets and to predict and optimize performance.
5. Establish the flowsheets by using the simulation code and the database, and perform small-scale countercurrent experiments to verify the flowsheets.
6. Assess quality and quantity of products and wastes arising through the treatment of product and raffinate streams, which contain not only nitric acid, but also organic compounds (i.e., complexants, reductants, etc.). The treatment methods significantly affect the cost and safety issues of the reprocessing.

The following sections review recent findings and progress achieved on liquid-liquid extraction systems dedicated to reprocessing of the SNFs.

1.2.1 IMPROVED PUREX PROCESS

Although the PUREX process is regarded as a well-matured chemical technology in the nuclear industry, owing to its complex chemistry, high radiation field, evolution of the fuels to be processed (i.e., extended high burn-up and MOX fuel), safety and economical issues, and its principal position in establishing the nuclear fuel cycle, both fundamental and application studies have been continued.

Precise process simulation codes are vital tools to design and optimize a process flowsheet of countercurrent liquid-liquid extraction. The central core of such codes generally consists of programs quantifying the liquid-liquid equilibrium of solutes and the kinetics of chemical reactions involved in the system. Baes et al. of Oak Ridge National Laboratory (ORNL) have established models for the thermodynamics of two-phase equilibrium systems, and the latest version, SXFIT, is a general model, theoretically treating a limitless number of components for extraction systems (*34, 35*). Kumar and Koganti of Indira Gandhi Centre for Atomic Research (IGCAR, India) have presented many empirical models to calculate equilibrium states of the solutes, including boundaries of TPF in the TBP/*n*-dodecane system (*36–40*). Such modeling efforts have also been performed worldwide (*41–44*).

As a consequence, corporations operating PUREX plants have been using sophisticated process simulation codes, including the PAREX code in France (*45–47*), SpeedUp (Aspen Plus) in the UK (*48*), and SIMPSEX code in India (*49–51*). Argonne Model for Universal Solvent Extraction (AMUSE) code in the United States was contrived not only for PUREX, but for UREX+ processes (*52*), which will be mentioned later. In Japan, similar efforts have also been made (*53–55*).

As the PUREX process is operated under an extremely strong radiation field with nitric acid, the radiolytic and hydrolytic degradation of TBP/*n*-paraffin solvent and its influence on the process performance have long been investigated, and the studies are continuing (*56–65*). The degraded solvent should be regenerated for recycling, and one of the main reasons for the successful operation of the La Hague reprocessing plants is an advanced solvent cleanup by vacuum distillation (*66*).

The behavior of Tc in the PUREX process was first reported by Siddall in 1959 (*67*), and since then, not only its distribution (*68*), but also its detrimental effects (*69*) have been clarified. Thus, control of Tc in the PUREX process was envisaged in that most of the dissolved Tc is finally directed to the raffinate stream at the first cycle

(*70*). French researchers have verified that more than 99% of dissolved Tc could be stripped and put into the raffinate successfully (*16–18*).

As the requirements of U-product specification are very severe with respect to Np content (125 Bq/g U, according to ASTM C788-03), and due to its behavior in geological systems, Np should be removed quantitatively from a waste disposed in a repository. Therefore, sophisticated control of Np in the PUREX process has been strongly urged. As the distribution of Np valence state as IV, V, or VI varies depending on the system, many investigations have been devoted to the kinetics of redox reactions of Np in systems relating to PUREX. Studies are classified into two categories: those in HNO_3–HNO_2 systems (*71–76*) and those with reductants (*77–85*). Based on the valuable knowledge obtained and by virtue of excellent computer codes, very promising results of "Np management" in the PUREX process have been obtained at the hot cell in France and UK, as explained in Section 1.1.2 (*16–20*).

The phenomenon of TPF is a disturbing one to be avoided for an application of liquid-liquid extraction. For the PUREX process, the conditions of TPF as functions of concentrations of HNO_3, U(VI), U(IV), and Pu(IV); diluent; and temperature were investigated thoroughly (*86–88*). The conditions are commonly expressed in terms of LOC. The scientific elucidation, however, of the TPF, dealing with compositions/speciation and structure of the phases, causes of the phase splitting and its mechanism, thermodynamic features of TPF, reasons for difference of the LOCs with respect to metals and acids, had been deficient.

As explained in Section 1.1.2, with the advent of advanced machines such as strong neutron sources or X-ray sources, structural analysis of liquid samples by SANS, SAXS, and XAFS has enabled the rigorous study of not only metal-ligand complexes, but also TPF. Using these techniques, Chiarizia et al., Madic et al., and others have addressed the TPF issues vigorously (*21–23, 89–97*). Using Baxter's "sticky spheres" model, they showed that the extracted metal-ligand species exist as reverse micelles. Consequently, the TPF was explained (*21*) in accordance with the idea that the small reverse micelles formed by the TBP in an organic phase are subject to two opposing physical forces: (1) thermal energy tends to keep the micelles, dispersed in the solvent; and (2) intermicellar attraction causes micellar adhesion. The latter is the van der Waals force between the polar cores of the reverse micelles and the attraction becomes stronger as increasing amounts of polar solutes are transferred into the TBP phase. When the energy of attraction between the micelles in solution becomes about twice the average thermal energy ($\sim 2k_BT$, where k_B is the Boltzman constant), the reverse micelles start to self-assemble. Regarding how rapidly the energy of (2) reaches the critical value, $2k_BT$ strongly depends on the charge and radius of the extracted cation, its ionization potential, and hydration enthalpy for the extracted nitrates. In a recent report, Berthon et al. (*98*) investigated the effect of alkyl chain length of both diamide and diluent on the phase splitting of an organic phase. They explained that the attractive force between polar cores of reverse micelles increases with a decrease of chain length of the diamide and with an increase of that of diluent. Diluent molecules, having shorter (or branched) chains, penetrate the apolar layer of reverse micelles, which results in swelling of the layer, and thus the attractive force between the micelles' cores decreases. These findings provide an insight into TPF, and further studies would be expected to identify, a route to prevent the TPF.

It is well recognized that centrifugal contactors in a reprocessing plant reduce the total cost and are, thus, superior to a plant installed with very big or tall pulsed columns. In addition, as recent LWRs discharge UO_2 fuels of very high burn-up (~55 GWD/MT) and MOX fuels, which increase the radiation intensity of the SNF drastically, a very short contact time of an organic solvent with an aqueous solution is preferable. Thus, development of annular centrifugal contactors has steadily progressed (*99–103*).

Recently, the CO-EXtraction (COEX) process was proposed by AREVA-France (*104*). The COEX process initially coextracts all of the U and Pu, and subsequently splits them into a U stream and a Pu stream containing an equal amount of U. In addition, a hydrometallurgical co-conversion process is coinstalled in an "integrated recycling plant," which produces homogenous mixed actinide oxides (*105, 106*). Thus, the PR is enhanced.

A key technology that is imperative to society should have, and be prepared with, alternatives at all times. Thus, different kinds of monodentate extractants have been investigated worldwide. They are monoamides (*107–115*), dialkylsulfoxides (*116–121*), and trialkyl (*122, 123*) and tricyclohexyl phosphates (*124*).

1.2.2   Advanced Processes

As discussed in Section 1.1.1, the requirements for the reprocessing of SNF have shifted due to the evolution of global politics and concerns about environmental issues. Consequently, to satisfy the new requirements, the kinds of radionuclides to be separated from SNF before disposition to a repository as waste are expected to increase compared to the development of new processes with the PUREX process. Now, separation chemists should recognize, before they start, how much (yield) and what quality (specifications) are required for products of the respective nuclides separated. This goal is, of course, deduced from the defined purpose of a respective project. Table 1.1 shows examples of the goals for separation in the OMEGA project (*125*) and GNEP (AFCI) project (*126*). The goals of the OMEGA project were defined by expecting advanced future technologies. The target nuclides elaborated were not only U and Pu, but also MAs and some FPs.

Similar goals or criteria of the French SPIN program cannot be found, but the recovery targets of the CEA were described (*18*) explicitly as,

1. 99.9% of the americium and curium present in the PUREX raffinate
2. More than 99% of the neptunium and iodine present in the original spent fuel
3. More than 99% of the technetium present in the PUREX raffinate
4. 99.9% of the cesium present in the PUREX raffinate

Complete achievement of the above goals seems very difficult when we assume nothing but the existing extractants. Therefore, the principal tasks are to develop novel extractants that are satisfactorily applicable to actual processes for target nuclides. Thus, many researchers, aiming at a specific nuclide, have pursued elaborate investigations, such as "molecular design" or "molecular modeling," through analytical and experimental approaches.

TABLE 1.1

Examples of the Partitioning Goals (Recovery Yield, Product Purity) for Long-lived Nuclides

Objectives	OMEGA Project[a] Expecting Progress of Science and Technology in Future		AFCI Project (UREX+1a Process)[b] Changeable with Variation of UREX+Processes			
Radiotoxicity						
Relative values to the values of once-through spent fuel (LWR)	Decrease to 1/1000 after 100 Years of Disposal		The Requirements are not in View of Radiotoxicity but of Better Utilization of Resources			
	U	>99.9%	S or T	Np	>99%	Recycling	Recycle to LWR/ALWR requires MOX fuel spec.
	Np	>99.9%	T (fast)	Pu	>99%	Recycling	ASTM C833-01 <3 mg Lns/g (U + TRU) DF (Pu) > 10⁵
	Pu	>99.99%	T (therm., fast)				
	Am	>99.99%	T (fast)				
	Cm	>99.9%	S or T (fast)				
	Sr	>99%	S				
	Cs	>99%	S				
	Tc-99	>99.9%	S or T (therm)?				
Repository capacity	Increase five-fold			Decrease mass and heat-load of waste for disposal			
	Sr	>99%	S	Sr	>99%	Heat-load =	S: as Class C LLW 10CFR61.55
	Cs	>99%	S	Cs	>99%	Σother FP's	TRU < 3700 Bq/g product

(Continued)

TABLE 1.1 (Continued)

Objectives	OMEGA Project[a] Expecting Progress of Science and Technology in Future	AFCI Project (UREX+1a Process)[b] Changeable with Variation of UREX+Processes
Radiotoxicity	Decrease to 1/1000 after 100 Years of Disposal	The Requirements are not in View of Radiotoxicity but of Better Utilization of Resources
	Others: Mo, Ba, Te, Rb, Y, lanthanides, platinum groups	U — >95% — Mass — S: as Class C LLW / Recycle: ASTM C788-3
		Am and Cm — >99.9% — Heat-load < 1/100 — T (fast): if MOX is assumed: ASTM C833-01 / <20 mg Lns/g (U + TRU)
Dose risk	Decrease to 1/100	Decrease off-site dose to <1/20
	I-129 — >99.9% — S or T (therm)?	I-129 — >95% — S or T (therm) — T: 4 µg F. Ans/g I
	C-14 — >90% — S	Tc-99 — >95% — S or T (therm) — T: 16 µg F. Ans/g Tc
	Cl-36 — >90% — S	

Sources:

a Takano, H., Ikegami, T. 2002. Activities on R&D of partitioning and transmutation in Japan. 7th Information Exchange Meeting on Actinide and Fission Product Partitioning and Transmutation. 23–35. Jeju, Korea Oct. 14–16;

b Pereira, C., Vandegrift, G.F., Regalbuto, M.C., Bakel, Al., Bowers, D., Gelis, A.V., Hebden, A.S., Maggos, L.E., Stepinski, D., Tsai, Y., Laidler, J.J. 2007. Lab-scale demonstration of the UREX+1a process using spent fuel. Proceedings of WM'07, Tucson, AZ, February 25 to March 1.

Note: S: storage. T: transmute by thermal (therm) or fast (fast) neutrons. F. Ans: fissile actinides.

ASTM C788-98: Standard specification for nuclear-grade uranyl nitrate solution or crystals.

ASTM C833-01: Standard specification for sintered (uranium–plutonium) dioxide pellets.

1.2.2.1 Molecular Modeling Approach

Molecular design has enjoyed a long history, from the preliminary "trial-and-error" stage to the contemporary computer-aided "molecular modeling" stage. In this chapter, the latter, *in silico design*, for nuclear applications is focused on and reviewed.

Design of a novel ligand that shows affinity to specified metals entails a toolbox containing knowledge bases, computer codes, and synthetic methods for organics. The knowledge bases are, for example, OECD/NEA's Thermochemical Database (*127, 128*), solvent-extraction database and programs for analysis (*129–132*). Although methodologies of modeling, how to use the tools, depend heavily on the researcher's expertise, requisite criteria for design is the knowledge about the relationship between ligand structure and the nature of metal-donor group interactions; quantitative structure-activity relationship (QSAR). Many investigations to establish methodologies for designing ligands possessing high affinity and selectivity to specified metal ions have appeared during the past decade (*133–150*). Computational chemistry plays an essential role in these investigations, namely, molecular mechanics (MM) and molecular orbital (MO) calculations. It has been efficiently used to obtain an optimized structure of a molecule and to determine appropriate descriptors, resulting in a good QSAR with experimental properties. Hay of Pacific Northwest National Laboratory (PNNL) and others have progressed a research project for computational design of metal ion sequestering ligands (*151–156*). Initially, they developed a molecule-building software, HostDesigner. It generates a large number of candidate molecular architectures, incorporating sets of donor groups and molecular fragments given by users. HostDesigner screens many candidate architectures with respect to complementarity for a targeted metal ion and finally outputs a list of lead candidates for further evaluation. In the next step, the candidates are evaluated and prioritized more accurately with respect to their binding affinity for a specified metal ion guest by using MM models, for example, MMX, MM3, and AMBER. MM models partition the steric energy into stretching, bending, torsion, and nonbonded (Van der Waals, electrostatics, hydrogen bonding) interactions. The process of parameterizing these models requires knowledge of the geometries and potential energy surfaces for each individual interaction, which are precisely the criteria needed to evaluate metal ion complementarity. A successful achievement of the strategy was demonstrated by the design of a bicyclic diamide (*157–159*).

Varnek of Université Louis Pasteur gives a comprehensive explanation of QSAR methodology (see Chapter 5 of this volume).

Molecular design ultimately requires a solid comprehension of a liquid-liquid extraction system not only in an equilibrium state of a system, but also in the form of intermediate complexes and dynamic processes taking place mainly at the liquid-liquid interface. Molecular dynamic (MD) simulation reproduces the orientation of the reacting agents and the intermediate complexes at the interface rather precisely (*160– 162*), and consequently reflects the stability of metal-ligand complexes and selectivity of the reactions. Striking investigations with MD simulation have been accomplished by Wipff et al. (*163–171*), where a topical one is a phenomenon with TBP and UO_2^{2+} (*167–169*). MD computations have been advancing in various systems (*172–174*), and because they treat systems as inherently consisting of large numbers of atoms and molecules, the capability of MD simulation depends entirely on the progress

of computer performance and computational techniques. In the future, molecular modeling could be easily accomplished at a level of practical applications.

1.2.2.2   Novel Extractants and Processes

Usually, a novel extractant is developed aiming for an application for a specific separation purpose. Therefore, in the present chapter, novel extractants were categorized and reviewed according to a specific purpose for reprocessing.

1.2.2.2.1   Uranium-Selective Extraction

As U is the major component of a SNF see Table 1.2, its initial separation in reprocessing alleviates the mass burden of following steps and is considered preferable. The UREX process developed in the AFCI program of the United States is based on the PUREX process (30 vol % TBP in *n*-dodecane) and suppression of extractions of Pu and Np by reduction/complexation (*175–182*). Plutonium and Np are reduced by acetohydroxamic acid (AHA, $CH_3CONHOH$) to Pu(III), Np(V), and Np(IV). U is kept in an extractable U(VI) state. Although Np(IV) is also extractable, AHA forms a complex with Np(IV) that is soluble in the aqueous phase. In the case where reoxidation of Pu(III) occurs, the Pu(IV) also transfers to the aqueous phase by forming a Pu(IV)-AHA complex. Thus, U is exclusively extracted. AHA decomposes to hydroxylamine and acetic acid (*176*).

The reaction rate of AHA is large enough to use centrifugal contactors. Process experiments with real SNF in a series of centrifugal contactors have demonstrated a separation of highly pure U with a yield of >99.99% (*126, 183–188*). The UREX+ process also enables the effective separation of Tc (*189*).

For the design of UREX flowsheets, the AMUSE code has been used effectively. AMUSE is an updated version of the Generic TRUEX Model (GTM), which was developed during the 1980s and 1990s to design multistage countercurrent flowsheets for the TRans-Uranium EXtraction (TRUEX) process (*190*). GTM was renewed by adopting the SASSE model (Spreadsheet Algorithm for Stagewise Solvent Extraction) (*191–194*), a modified version of the SEPHIS code (*195*) and Spreadsheet Algorithm for Speciation and Partitioning Equilibria (SASPE). The prominent feature of AMUSE (*196–198*) involves (1) calculating very accurate distribution values using thermodynamic activities for H^+, NO_3^-, and water to fit experimental data to equilibrium equations (*199*); and (2) building the model in a modular format with the easily programmed and user-friendly Microsoft Excel. Thus, the AMUSE code is applicable to design and optimization of solvent-extraction flowsheets of not only UREX, PUREX, and TRUEX, but also SREX, CSSX, and NPEX processes. Application to other processes, for example, CCD-PEG and TALSPEAK, is promising.

N,N-dialkylamides are monodentate ligands that show extraction properties for Ans similar to TBP. When a highly branched structure is incorporated into the alkyl groups of the amide molecule, the resulting amide exhibits steric hindrance in the extraction of Ans (*200–202*). This effect is larger for Pu(IV) than U(VI) and causes an increase in separation factor; $SF[U(VI)/Pu(IV)] = D(U_{VI})/D(Pu_{IV})$, where $D(M)$ is the distribution ratio of M. A research group from the Japan Atomic Energy Agency (JAEA, formerly JAERI) has adopted *N,N*-di-octyl-2-ethylbutanamide (DO2EBA) as the extractant of the Branched-AlkylMonoAmide (BAMA) process

TABLE 1.2

Elemental Compositions of various Spent Fuels and Liquid Concentrations in a Dissolved Solution

Element	Amounts (kg) and Concentration (g/L or mM) for 1 t of Spent Fuel[a]					
	PWR (UO$_2$), 60 GWD/t[b]		PWR (MOX), 60 GWD/t[c]		FBR (MOX), 90 GWD/t[d]	
U	924 kg	264 g/L	881 kg	252 g/L	776 kg	222 g/L
Pu	12.8	3.66 (15.3 mM)	51.7	14.8 (62 mM)	128	36.6 (153 mM)
Np	0.93	0.265 (1.12 mM)	0.21	0.061 (0.26 mM)	0.466	0.133 (0.56 mM)
Am	0.78	0.223 (0.92 mM)	4.80	1.37 (5.67 mM)	4.60	1.31 (5.43 mM)
Cm	0.13	0.037 (0.15 mM)	1.17	0.334 (1.37 mM)	1.36	0.389 (1.60 mM)
Total An	939 kg	268 g/L	939 kg	268 g/L	911 kg	260 g/L
Sr	1.45	0.41 (4.65 mM)	0.72	0.205 (2.30 mM)	1.06	0.303 (3.36 mM)
Zr	6.44	1.84 (19.6 mM)	4.52	1.29 (13.7 mM)	6.21	1.77 (18.6 mM)
Mo	6.02	1.72 (17.6 mM)	5.54	1.58 (16.2 mM)	7.57	2.16 (22.0 mM)
Tc	1.36	0.39 (3.92 mM)	1.34	0.383 (3.87 mM)	1.86	0.531 (5.36 mM)
Cs	4.71	1.35 (9.97 mM)	5.44	1.55 (11.5 mM)	8.73	2.49 (18.3 mM)
Ln (La–Gd)	17.8	5.08 (35.5 mM)	16.4	4.69 (32.7 mM)	29.0	8.29 (58 mM)
Total FP[e]	51.2 kg	14.6 g/L	50.7 kg	14.5 g/L	78.0 kg	22.3 g/L

a Liquid concentration calculated by supposing 1000 kg of spent fuel is dissolved in 3.5 m^3 of nitric acid solution.

b PWR (UO$_2$) fuel: initial enrichment 5.0 wt %; 5 years cooling.

c PWR (MOX) fuel: initial Pu content, 7.9 wt %; fissile Pu content, 69% of total Pu; ^{235}U content, 0.23 wt %; 5 years cooling.

d FBR (MOX) fuel: initial Pu content, ca. 20 wt %; 4 years cooling.

e Total FP does not include rare gases (Kr, Xe) and iodine.

and successfully demonstrated the selective recovery of U(VI). Neptunium(VI) extracted simultaneously with U(VI) was scrubbed and removed by AHA (*203, 204*). The CEA group proposed *N,N*-di-(2-ethylhexyl)-*iso*-butanamide (D2EH*i*BA) for the selective extraction of U in the concept of GANEX (Grouped ActiNide EXtraction) (*205*) (Figure 1.1).

1.2.2.2.2   Extraction of Transuranium Elements

Processes for separating Pu in pure form are not included in the present review because of the restriction consistent with the nonproliferation rule. Thus, processes and extractants capable of extracting TRUs were reviewed. Methods for the separation of TRUs contrived so far can be categorized in four ways:

A. Extract all Ans, including Am and Cm, simultaneously from a feed solution of relatively high nitric acid concentrations, leaving all other elements including lanthanides (Lns). Probably U (and Np) is removed in advance.

B. Extract Ans with Lns in an extraction stage of high acidity and strip only Ans in a stripping stage. Lns must be kept in an organic phase under the Ans-strip conditions. Finally, Lns are stripped. This is a one-cycle process.

C. Extract Ans with Lns from highly acidic aqueous solution at the first cycle and then separate Ans from Lns in the second (low acid) cycle. The extractants used in the respective cycles would be nonidentical.

D. Use a mixture of two extractants; one enables extraction of both Ans and Lns from high acid solutions and the other enables extraction of Ans and Lns at low acidities. By using the mixed extractants, method (B) of one cycle is satisfied.

Actually, ligands capable of utilizing method (A) have not yet been developed. Ligands having N-donors and exhibiting a high SF[Ans/Lns] value in an acidic region are under investigation (see Section 1.2.2.2.2). Ligands such as carbamoylmethylphosphine oxides (CMPO) and diamides are candidates for method (B). However, most selective stripping of Ans is undertaken by using complexants under conditions of low acidity or pH region where the bidentate extractants lose their affinity toward Lns. Therefore, other methods were contrived as alternatives.

Based on the above considerations, Ans extraction systems following the methods (C) and (D) are reviewed below.

D2EH*i*BA   DO2EBA
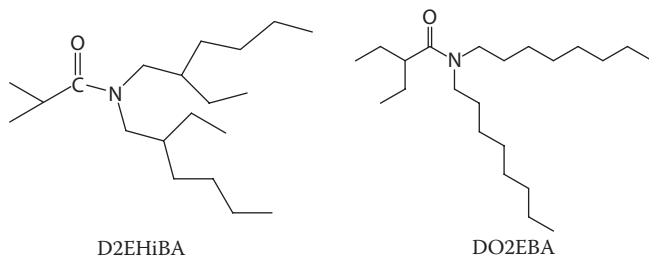
FIGURE 1.1   Structure of branched monoamides.

1.2.2.2.2.1   Simultaneous Extraction of Ans and Lns

CMPO. Among the bidentate extractants reported, octyl(phenyl)-*N,N*'-di-*iso*-butyl carbamoyl-methylphosphine oxide (OΦD(*i*B)CMPO) is the most popular and thoroughly utilized extractant, which was developed by Horwitz et al. of ANL (*212*). It has been used in the TRUEX process and applied preponderantly to various objectives in the United States during the 1980s (*206*). A wide range of nitric acid concentrations of feed solution, for example, 1 to 6 M HNO_3, is applicable to the TRUEX process. OΦD(*i*B)CMPO is used as dissolved in 1.2 to 1.4 M TBP-paraffin solvent. The quantity of TBP used for OΦD(*i*B)CMPO is a function of the chain length and branching of the paraffinic hydrocarbon. A similar CMPO, diphenyl-*N,N*'-di-*n*-butylcarbamoyl-methylphosphine oxide (DΦDBCMPO), whose characteristics have been compared with those of OΦD(*i*B)CMPO (*206*), was developed by Russian researchers (*207*). The Russian CMPO is not sufficiently soluble in the above solvent, but it dissolves in a polar organofluorine compound (Fluoropol-732, 1-nitro-3-(trifluoromethyl)benzene), and thus eliminates TBP, whose degradation products must be washed out sufficiently during operation. Studies on hydrolysis and radiolysis of OΦD(*i*B)CMPO have been carried out intensively, and the degradation products and their effects on the extraction systems of CMPO have been identified (*208, 209*). A trace amount of impurities or degradation products of CMPO-TBP, especially acidic compounds, significantly affects the extraction behavior toward Ans and Lns in the low acid region used in stripping. Consequently, high performance of cleanup methods for the recycled solvent is definitely needed for the TRUEX process and has been envisaged (*210, 211*). Usually, extraction of multivalent elements (i.e., Fe, Zr, Mo, and Pd) is suppressed by the addition of oxalic acid to the feed solution or to scrubbing stages.

To design and optimize flowsheets most appropriate for the objective application, the GTM program has been used (*212, 213*). After the 1990s, the application of the TRUEX process for practical purposes has been implemented successfully (*214–219*), parallel to fundamental investigations (*220–225*).

Malonamide. Malonamides (MAMs) are the most extensively investigated extractant in Europe (*226–245*), under the terms of French law of 30 December 1991. MAMs have two carbonyl oxygens, which are electron donors and bind to actinides (*246*). Based on the wealth of data and molecular modeling expertise, the molecular formula was optimized in view of good extraction and stripping, solubility and loading capacity of the metal-complex in diluent, conditions of TPF, and hydrolytic and radiolytic stability (*247, 248*). Consequently, *N,N*'-dimethyl-*N,N*'-dioctylhexylethoxy-malonamide (DMDOHEMA) was assigned as an extractant of the DIAMEX process. The diluent used is the same as the one used in the La Hague plants, TPH, which is an industrial blend of branched alkanes obtained by polymerization of propylene and hydrogenation of the formed tetramers. The DIAMEX flowsheets have been contrived and optimized by using the PAREX code. The concentration of nitric acid in feed solutions is allowed to be 3–5 M. Verification experiments have been carried out with a genuine HA raffinate at the ATALANTE facility (*16–18*). The main results obtained by using 0.65 M DMDOHEMA/TPH solvent up to 2004 are that (a) recovery yields of An(III) and Ln(III) were >99.9%; (b) decontamination of the main disturbing elements, Zr and Mo (by oxalic acid) and Pd (by *N*-(2-hydroxylethyl)ethylenediamine-*N,N*',*N*'-triacetic acid; HEDTA) was satisfactory; and (c) effects of degradation products of

DMDOHEMA were limited and did not exert disturbing effects on the implementation of the DIAMEX process.

In the United States, Lumetta et al. designed a MAM molecule by a method of MM calculation, which gives a molecular formula with the most favorable total strain energy (*157–159*). The MAM ligand (L_{MAM}) thus designed was chemically synthesized, and the X-ray crystal structure of the complex $Eu(L_{DMA})_2(NO_3)_3$ exhibited the same chelate conformation as predicted by the MM model, and moreover, its lipophilic derivative was synthesized and used for the verification experiments of solvent extraction. Very interestingly, it revealed a dramatic increase in the distribution ratio of Eu(III), namely 7 orders of magnitude larger than a typical L_{DMA} (*157*). The extracted complexes of An(III) or Ln(III) in MAM-TPH extraction system are represented as $M(NO_3)_3(L_{MAM})_2$, where M = An(III) and Ln(III).

Actually, TPF is also a problem of MAM extraction systems (*23, 249, 250*), and thus various investigations on TPF and the structural studies on the extracted metal-MAM complexes have been carried out. Formation of reverse micelles and their aggregation were discussed (*251–254*).

Diglycolamide. Owing to the relatively weak affinity and poor preorganization (*157*) of the two carbonyl groups of MAM for the Ans and Lns ions, the DIAMEX process requires a higher concentration of DMDOHEMA, 0.5 M, and more extraction stages than the TRUEX process. JAEA researchers investigated the affinity-strengthening effect of ether oxygens introduced between the two amide groups of MAM, supposing a family of podands, and found only one ether oxygen is the strongest (*255–258*). Consequently, diglycolic amides (DGA) were deemed to bind to Ans(III) and Lns(III) ions in a definitive tridentate fashion. This feature was confirmed by an XAFS study (*257*).

The molecular formula of DGA was optimized, and *N,N,N',N'*-tetraoctyl diglycolamide (TODGA) was chosen for process applications (*259, 260*). The monoamide DHOA was used as a phase modifier of the TODGA/*n*-dodecane solvent to improve the solubility of the metal-TODGA complex (*261*). The basic extraction reaction of TODGA with An and Ln ions and the stoichiometry of their metal-TODGA complexes formed in the organic phase are similar to those of MAMs, including reverse-micelle formation and their aggregation (*262–264*). But, interestingly, the extractability of TODGA for actinide ions follows the order Th(IV) $\simeq$ Am(III) > Pu(IV) > U(VI) $\gg$ Np(V), and *D*(M) versus atomic number of Lns apparently follows a very different pattern as compared with MAMs (*256*). Hydrolytic and radiolytic stabilities were studied (*265–267*), and the results showed that *n*-dodecane has a sensitization effect on the radiolysis of amides, owing mainly to a charge transfer from radical cations of *n*-dodecane to the amide molecules in the primary process (*266*). This result was supported by the difference in the ionization potentials between *n*-dodecane and amides. The radiolytic effects on the practical extraction systems of Ans by TODGA-DHOA/*n*-dodecane solvent were, however, found to be insignificant (*275*). Modolo et al. have demonstrated high performance of the TODGA-process for Ans-Lns coextraction with TODGA-TPH (*268, 269*) or TODGA-TBP-TPH (*270–273*) solvents using genuine HLW.

The extracted complexes of An(III) or Ln(III) in the TODGA-*n*-paraffin extraction system are represented as $ML_2(NO_3)_3$ or $ML_4(NO_3)_3$ (reverse micelle including H_2O and HNO_3 molecules), where M = An(III) or Ln(III) and L = TODGA. Due to the

promising extraction propensity of TODGA, not only basic studies but also various R&D works for applications have been envisaged and demonstrated (*274–277*). Tian et al. investigated the distribution equilibria and thermodynamics of U(VI), Np(V), Pu(IV), Am(III), and TcO$_4^-$ with another DGA, *N,N,N',N'*-tetra*iso*-butyl-3-oxa-glutaramide (T*i*BOGA) (*278*). The extractability of T*i*BOGA in 40/60% (V/V) 1-octanol/kerosene for the ions follows the order Am(III) ≫ Pu(IV) > U(VI) ≃ Tc(VII) > Np(V). Mowafy et al. compared the extractability of several diglycolamides having different alkyl groups with amidic nitrogen, using benzene as diluent (*279*).

TRPO. The trialkyl phosphine oxide (TRPO) process was developed at Tsinghua University in China during the 1990s (*280–282*). TRPO is the trademark of a commercial product in China, consisting of a mixture of phosphine oxides with alkyl groups of different C number. For the extraction of Ans (and Lns), 30 vol % TRPO in kerosene was used from an aqueous solution of nitric acid concentration of 0.5–1 M. Ans (and Lns) were stripped with a 5–6 M HNO$_3$ solution. Technetium(VII) is also efficiently extracted by the solvent and stripped by water (*283*). When TRPO degrades radiolytically, polymeric products prevent effective stripping of Pu (*284–286*). The TRPO process has been tested in China (*287*) and at the ITU in Karlsruhe (*288, 289*) with genuine HLW; its performance was appraised as being satisfactory. Recently, from the viewpoint of integration of PUREX and TRPO processes, a simplified TRPO flowsheets has been proposed (*290*).

DIDPA. Application of di-isodecyl phosphoric acid (DIDPA) to the extraction of Ans(III) and Lns(III) was initiated at JAEA in the 1970s (*291, 292*). Then it was fully investigated in the frame of the Partitioning and Transmutation program. For the extraction of Ans (and Lns), 0.5 M DIDPA-0.1 M TBP in *n*-dodecane was contacted with an aqueous solution of nitric acid concentration of ~0.5 M. In the second cycle, from the re-extracted Ans and Lns, Ans were stripped by 0.05 M diethylene-triamine-*N,N,N',N'',N''*-pentaacetic acid (DTPA) solution, leaving Lns in the organic phase in the manner of the Reversed TALSPEAK process (*358*). Lns were stripped by 4 M HNO$_3$. The process was tested in a hot-cell with a genuine HLW solution at the NUCEF facility of JAEA (*293*) and at the Institute for Transuranium Elements (ITU) in Karlsruhe (*294*). A recovery yield of 99.99% of Am and Cm was achieved. The process requires denitration of HLW in adjusting the feed, which produces precipitates of Mo, Zr, etc. Thus, it could, by filtration, remove most of the Mo and Zr, which are troublesome in the latter processes (Figure 1.2).

Scrubbing and stripping. Conditions of scrubbing and stripping are very important from the viewpoint of process performance, as they determine the purity and recovery yield of a product. The former selectively removes contaminating solutes from the main extractable solute in an organic phase. The latter strips the objective solutes selectively and successively from the organic phase. Scrubbing and stripping produce aqueous streams to be treated next, as a product or waste. Therefore, their chemical compositions are carefully determined to minimize the cost and the wastes. Some examples are shown in Table 1.3. The ligands that extract Ans usually exhibit affinity for multivalent metal ions, such as Fe(III), Mo(VI), Zr(IV), Pd(II), and Ru, and they are coextracted with Ans. Thus, most processes shown in Table 1.3 utilize complexing reagents that hold back the impurity elements by selective complexation in the aqueous phase. Oxalic acid is commonly used as a
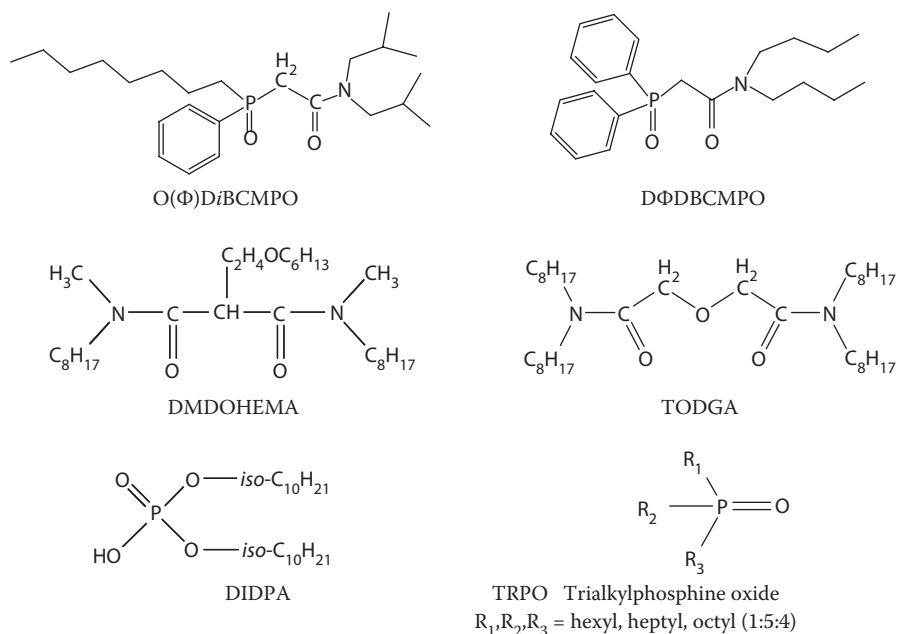
FIGURE 1.2 Structure of extractants used for extraction of actinides and lanthanides.

typical complexant. Some reductants, for example, HAN, AHA, and H_2O_2, are also used for effective scrubbing and stripping. Most reagents used are salt-free, except for Na_2CO_3, and easily decomposable.

1.2.2.2.2.2 Separation between Ans and Lns Both Ans(III) and Lns(III) are classified as hard ions and react with hard donors, such as oxygen, very similarly because of the coincidence of ionic size and charge density. On the other hand, the nature of 5f electrons, that is, large relativistic effect, itinerant nature, and a degree of covalency (though small), makes the behavior of An(III) ions slightly softer than Ln(III) ions. Consequently, most group separations of Ans(III) and Lns(III) were attributed to the ligands possessing soft donors with sulfur or nitrogen atoms. Nash has presented a detailed discussion concerning the actinide separations (*295*).

On the premise of the transmutation of Ans (particularly Am and Cm) by fast neutrons, the Ans recovered must be adequately decontaminated from Lns. The required decontamination factor (DF) should be considered from the viewpoints of neutron absorption cross sections of Lns and interactions of Lns (in target) with the cladding material; see Table 1.1 (condition described in ASTM C833-01: <20 mg Lns/g TRU). Taking the compositions of spent fuel to be reprocessed into account (see Table 1.2), the DF required is ca. 1000 for PWR-UO$_2$ (60 GWD/t) and 140 for PWR-MOX (60 GWD/t). Thus, a DF of about 2000 will be a tentative goal.

Sulfur* donors *of the dithiophosphinic acid type. In 1994, Jarvinen et al of Los Alamos National Laboratory (LANL) et al. reported significantly large separation

TABLE 1.3
Examples of the Compositions of Scrubbing and Stripping in Processes for Actinides Separation

Process	Scrubbing		Stripping		
	Reagent	Remarks	1: Am, Cm	2: Pu, Np, etc.	3: U, etc.
TRUEX (USA)	(1): 8 M HNO_3-0.003 M Oxalic acid (2): 0.05 M HNO_3-HAN	JAEA-SETFICS (2): To strip HNO_3	0.01 M HNO_3-DTPA	0.01 M HNO_3-0.01 M HAN	(1): 0.2 M Hydrazine Oxalate (2): 0.02 M Hydrazine Carbonate
TRUEX (Russia)	2 M HNO_3		0.5 M HNO_3-7.0 g/L AHA	10 g/L citric acid-5 g/L DTPA	
DIAMEX	2.8 M HNO_3 - 0.2 M Oxalic acid-0.015 M HEDTA		0.05 M HNO_3		0.3 M Na_2CO_3-0.01 M HEDTA
DIDPA	0.5 M HNO_3 - 1.0 M H_2O_2	To reduce Np(V) to Np(IV)	4.0 M HNO_3	0.8 M Oxalic acid	1.5 M Na_2CO_3
TRPO	1.0 M HNO_3		5-4 M HNO_3	0.5 M Oxalic acid-0.05 M HNO_3	5% Na_2CO_3
TODGA	1 M HNO_3-0.4 M Oxalic acid-0.2 M HEDTA	Tested by Modolo	0.01 M HNO_3		
UREX-NPEX	Dil HNO_3-complexant	Keep Np and Pu as Np(IV), Pu(IV)		Dil HNO_3-complexant	

Note: HEDTA: N-hydroxyethylethylenediamine-N,N',N'-triacetic acid; AHA: aceto-hydroxamic acid; DTPA: diethylenetriamine-N,N,N',N',N''-pentaacetic acid.

factors (SF[Am/Eu]) in extraction systems of dicyclohexyldithiophosphinic acid-TBP and Cyanex 301-TBP. The addition of TBP increased both distribution ratios and SFs (*296*). In 1995, Zhu et al. (Tsinghua University) reported extraordinary large values of SF[Ans(III)/Lns(III)]; they obtained SF[Am(III)/Eu(III)] = 4900 by using purified bis(2,4,4-trimethylpentyl) dithiophosphinic acid, a major component (~80%) of Cyanex 301 (*297, 298*). Process flowsheets were developed and tested in China with genuine HLW (*299–301*). By applying a synergistic combination with TBP, larger SF values could be obtained. To elucidate the large SF values, investigations have been pursued to compare the extraction characteristics of three kinds of dialkyl-dithiophosphinic acids with *n*-octyl-, 1-methylheptyl, and 2-ethylhexyl groups (*302*), and to study the structure of extraction complexes of Ans(III) and Lns(III) by XAFS (*303*), influence of aggregation to extraction (*304*), and speciation of the aggregate with Nd^{3+} (*305*). It has been well appreciated that the instability of the extractant is the main drawback of the Cyanex 301-based process. Thus, the radiolytic behavior of Cyanex 301 has been investigated (*306, 307*). Another drawback is the rather high pH (3.5–4) required for the aqueous solution. The control of pH is fairly difficult in a large-scale countercurrent process.

In the framework of the AFCI program, Peterman et al. of Idaho National Laboratory (INL) have examined the feasibility of using the Cyanex 301 system for treating an ammonium acetate/acetic acid buffered solution (*308*), which was used in the TRUEX process as a strip solution of Ans and Lns. A solvent comprised of 0.25 M Cyanex 301 and 0.37 M TBP in *n*-dodecane was studied. At a region of specific pH value, the intergroup separation of Am + Cm and Lns was concluded to be possible, and it was claimed that a method for removal of degradation products is needed in order to develop a viable large-scale Cyanex 301 process. In recent communications, incredibly large SF[Am/Eu] values, 4 orders of magnitude, were reported by Bhattacharyya et al. of Bhabha Atomic Research Centre (BARC, India) with a binary mixture of purified Cyanex 301 and N-donor ligands (*309*). The solvent

CYANEX 301
bis(2,4,4-trimethylpentyl)
di-thiophosphinic acid

$(ClPh)_2PS_2H$
di(chlorophenyl)
di-thiophosphinic acid
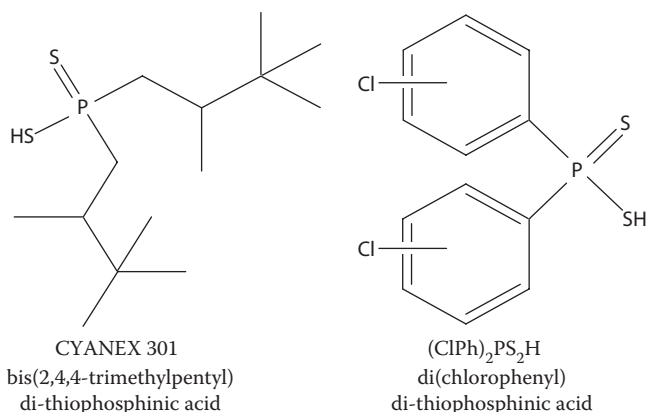
FIGURE 1.3 Structure of sulfur donors used for intergroup separation of Ans(III) and Lns(III).

used was 0.1 M Cyanex 301−0.01 M 1,10-phenanthroline (phen) or −0.025 M 2,2'-bipyridine (bipy) in toluene.

Modolo et al. of Forschungszentrum Jülich (FZJ) have synthesized a new soft ligand, an aromatic dithiophosphinic acid, by substituting phenyl groups in place of alkyl groups and incorporating chlorine into the phenyl rings. The resulting bis(chlorophenyl) dithiophosphinic acid, $(ClPh)_2PS_2H$, exhibited more powerful extractability and radiation stability than Cyanex 301. TOPO was selected as a synergist, and a solvent comprised of 0.5 M $(ClPh)_2PS_2H$ and 0.15 M TOPO in *tert*-butylbenzene/20% isooctane/2% TBP was proposed (*310, 311*). When the solvent was contacted with 0.5 M HNO_3 solution, a SF[Am(III)/Eu(III)] value of ca. 30 was obtained. Thus, the ALINA (Actinide(III)-Lanthanide INtergroup separation from Acidic medium) process was contrived (*312–314*) and tested with a setup of centrifugal contactors with a feed solution simulating raffinate from the DIAMEX process (*315, 316*). The results were satisfactory, and the An product contained 1–3% of Lns, and the recovery yield of Am was >99.9% (Figure 1.3).

In order to elucidate the high selectivity of $(ClPh)_2PS_2H$, structural investigations on the complexes of Cm(III) with $(ClPh)_2PS_2H$ and three different neutral complexing agents as synergists in *tert*-butylbenzene have been performed by EXAFS and TRLFS (*317*). The results were compared with those from the corresponding Eu(III) complexes. It was found that (a) the bidentate $(ClPh)_2PS_2H$ and oxygen donor of the neutral synergists are directly coordinated to the metal cation; (b) no water is coordinated to either extracted Cm(III) or Eu(III) complexes; (c) the sulfur donors of $(ClPh)_2PS_2H$ preferentially bind to Cm(III), whereas oxygen donor preferentially binds to Eu(III). It was concluded that a good selectivity in the system is correlated with a high ratio of the sulfur coordination number to oxygen coordination number. This feature is very different from EXAFS results by Jensen and Bond (*318*), where no structural differences were found between Cm(III) and Eu(III) complexed with bis(2,4,4-trimethylpentyl)dithiophosphinic acid without synergist.

From the viewpoint of wastes coming from the solvent and extractant, the process with S-donors has issues inherent to sulfur. Namely, sulfur is poorly soluble in borosilicate waste forms and causes problems in vitrification. Further, it does not conform to the CHON principle (*319*), meaning that it is not completely incinerable (see below).

Nitrogen donors. French scientists advocated the principle of "CHON," which means usage of chemical reagents composed of elements C, H, O, and N atoms exclusively, and therefore such reagents may be completely incinerable (*319*). Monoamides, diamides, and N-donors were developed in accord with the CHON principle. There are pros and cons to pursuing this principle in developing novel extractants. It is interesting that the term "incinerable" reminds us of nuclear "incineration," which is another expression of transmutation. Supposing a radioactive waste including long-lived radionuclides, in the case that the nuclides are incinerable (transmutable), they will be transmuted, but in the case that they are not incinerable, the radioactive waste would be sent to our descendants. By the same token, CHON reagents would be beneficial in waste management for a long time span.

In the frameworks of international cooperation in Europe, FP5 and FP6, many kinds of N-donors have been synthesized and investigated for their capability of separating Am(III) and Cm(III) from Lns(III). Madic (CEA) took the leadership for the

*i*Pr-BTP
2,6-bis(5,6-isopropyl-1,2,4-triazin-3yl)-pyridine

TPTZ
2,4,6-tri(2-pyridyl)-1,3,5-triazine

C5-BTBP
6,6′-bis (5,6-dipentyl[1,2,4]triazin-3-yl)
[2,2′]bipyridine

TMAHDPTZ
2-(3,5,5-trimethylhexanoyl-amino)-
4,6-di (pyridin-2-yl)-1,3,5-triazine
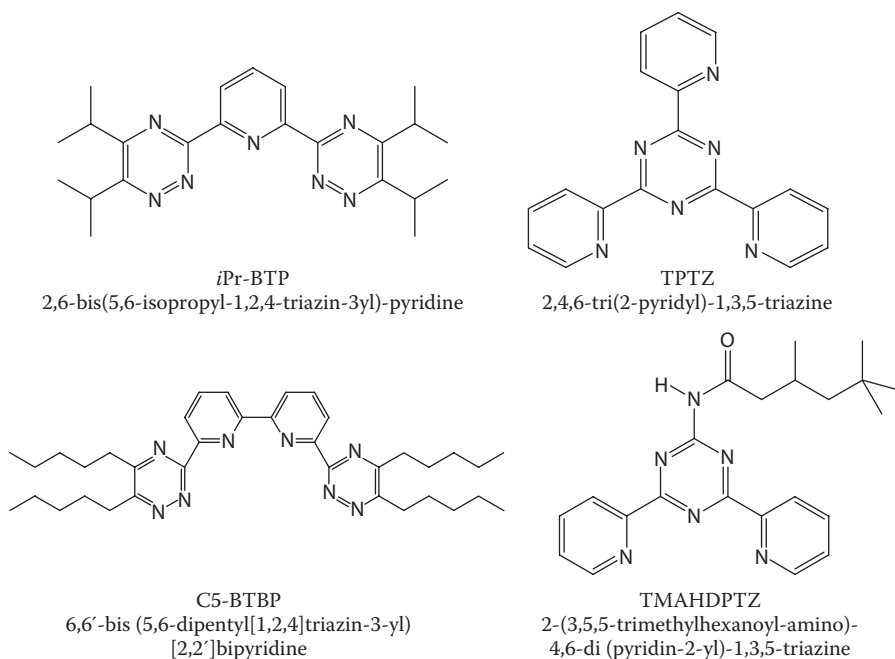
FIGURE 1.4   Structure of nitrogen donors used for intergroup separation of Ans(III) and Lns(III).

R&D works. The main N-donors investigated are picolinamides (2-pyridine carboxy-amide) (*320–322*), 2,4,6-tri(2-pyridyl)-1,3,5-triazines (TPTZ) (*323, 324*), 2-(3,5,5-trimethylhexanoylamino)-4,6-di(pyridine-2-yl)-1,3,5-triazine (TMAHDPTZ) (*325*), bis-triazinyl-1,2,4-pyridines (BTP) (*241, 242, 326–337*), and 6,6'-bis(5,6-dialkyl-1, 2,4-triazin-3-yl)-2,2'-bipyridines (BTBP) (*338–346*). These nitrogen-bearing ligands (Figure 1.4), generally used with a synergist, were tested and assessed with regard to solubility, extractability, selectivity (SF), stability (hydrolysis and radiolysis), aqueous conditions (pH, acidity) where the ligand works, and availability and cost of synthesis. TMAHDPTZ, a substituted TPTZ, developed at the CEA, needs a synergist such as a carboxylic acid. Octanoic acid or $C_9H_{18}BrCOOH$ was chosen, and a flowsheet for the SANEX process (Separation of ActiNide(III) elements by EXtraction) was defined; the solvent contained 0.04 M TMHADPTZ and 2 M octanoic acid in TPH, and the flowsheets were tested with genuine HLW (*329*). The TMAHDPTZ-octanoic acid (RH) mixture needs a feed solution in an elevated pH range, whereas the acidity of the product stream of the DIAMEX process is 0.5 M HNO_3. Thus, for pH control, a gly-colic acid/Na glycolate buffer was adopted. The formula of the extracted An-complex is represented as An(III)(TPTZ)(R.RH)$_3$.

After the success of Kolarik (FZK) (*326, 327*), many BTPs were synthesized and tested as a candidate ligand for SANEX process in the frame of the NEWPART project (*487*). Among them 2,6-bis-(5,6-di-*n*-propyl-1,2,4-triazin-3-yl)pyridine (*n*Pr-BTP), without synergist, exhibited the best performance, for which SF[Am(III)/Eu(III)] is >100; the feed acidity can be as high as 1 M HNO_3, and with use of 0.04 M

*n*Pr-BTP in TPH/*n*-octanol (70/30 vol %) a hot test with a genuine solution was performed at ATALANTE and ITU (*328*). The results revealed some problems, including fairly rapid degradation of *n*Pr-BTP by hydrolysis and radiolysis (*329, 336*). The sensitive position to the hydrolysis and radiolysis was identified to be the α carbon atoms of alkyl groups attached to triazinyls. Then, the 2,6-bis-(5,6-di-isopropyl-1, 2,4-triazin-3-yl)pyridine (*i*Pr-BTP) solvent comprised of 0.01 M *i*Pr-BTP and 0.5 M DMDOHEMA in *n*-octanol as an alternative was employed. To improve the kinetics of extraction and back-extraction, DMDOHEMA was used as a mass-transfer catalyst (*337*). From the hot test, (1) the scientific feasibility of the BTP process was confirmed, and (2) *i*Pr-BTP was also shown not to be sufficiently resistant to radiolysis. Consequently, other types of BTPs, namely, bis(cyclohexyl-tetramethyl) BTP and bis(benzo-cyclohexyl-tetramethyl) BTP were investigated. The extracted An-complex with BTP in octanol is represented as $[An(III)(BTP)_3(NO_3)_3]$.

Workers at Reading University in the UK, having synthesized many N-donors including BTPs, have developed ligands of the BTBP family, which can act as tetradentate ligands to metal ions (*338–346*). For applications, BTBP was modified by attaching several side chains or groups to the core structure, and the molecules prepared were investigated for their physicochemical nature, extraction properties particularly of SF[Am(III)/Ln(III)], and their stability against hydrolysis and radiolysis. Some BTBPs exhibited very promising features. Development of a BTBP process is under way.

Soft-hard hybrid donors. As picolinamides (2-pyridine carboxyamides) extract An(III) from a weakly acidic solution, <0.2 M HNO_3, and its separation ability is rather low, SF[Am(III)/Eu(III)] <10 (*321*), some pyridine-2,6-dicarboxyamides (PDA) were investigated (*347–354*). Although PDAs showed higher extraction of An(III) owing to two carbonyl groups in acidic solution, the SF values were not improved. This limit is ascribed to the ability of N-donors of the pyridine group in discriminating between 4f- and 5f-elements. Thus, Yaita et al. have pursued a new soft (N)-hard (O) hybrid donor, phenanthroline-amide; N-*n*-octyl-N-tolyl-1,10-phenanthroline-2-carboxyamide: OcTolPTA (Figure 1.5), which exhibited a SF(Am/Eu) value of ca. 20 at an aqueous concentration of 1 M HNO_3 (*355*).

Actinide chemistry involving soft donors and separation of Ans and Lns by tailormade soft donors has been prevailing worldwide because its fruits are highly valuable in separation science and technology especially for the advanced reprocessing and partitioning.

Usage of hydrophilic complexants. Since the early report by Weaver and Kappelman (*356*), the Trivalent Actinide-Lanthanide Separations by Phosphorus-reagent Extraction from Aqueous Komplexes (TALSPEAK) is still considered highly applicable for Am(III)/Ln(III) separations (*357–361*). In the newest program of the AFCI, it has been revived in the UREX+ process (*362*). The Reverse TALSPEAK process, a single-cycle process, is preferable to TALSPEAK, a two-cycle process. Both processes have several drawbacks, namely, inability to extract Ans (-Lns) from acidic aqueous solutions and necessity to maintain the pH and reagent concentrations within a narrow range, significant solubility of organic-phase components in the aqueous phase at high carboxylic acid concentrations, deleterious effects of some impurity ions such as Zr(IV), and production of salt wastes. Consequently, modifications are needed for application of TALSPEAK in

N,N'-dimethyl-*N,N'*-diphenylpyridine-
2, 6-dicarboxyamide

Picolinamide
(2-pyridine carboxyamide)

OcTolPTA
N-octyl-N-tolyl-1,10-phenanthroline-
2-carboxyamide
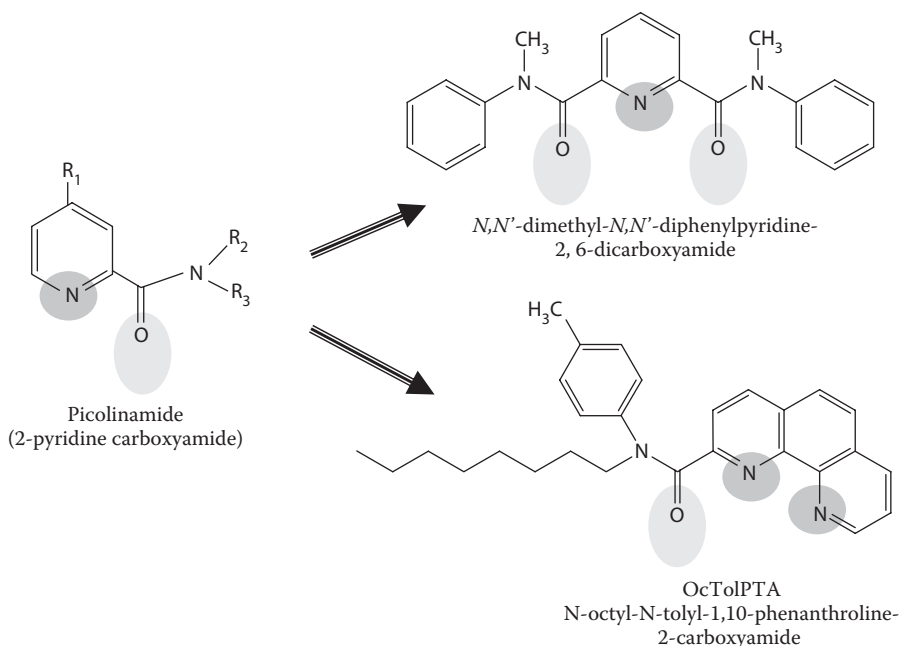
FIGURE 1.5   Structure of soft-hard hybrid donors used for intergroup separation of Ans(III) and Lns(III).

advanced reprocessing. It was shown that replacing the glycolic or lactic acid with citric acid eliminates or greatly reduces the deleterious effects caused by impurities on Ans-Lns separation and TPF. Citrate-based TALSPEAK can tolerate appreciable changes in pH and reagent concentrations, and no significant loss of organic phase was observed (*360–362*).

   The Reverse TALSPEAK process, a single-cycle process, was modified by the addition of diamide or CMPO, which extract Ans(III) and Lns(III) from a high nitric acid solution, where di(2-ethylhexyl)phosphoric acid (HDEHP) has the least ability of extraction. Thus, the French PALADIN (Partition of Actinides and Lanthanides with Acidic extractant, Diamide and INcinerable complexants) process utilizes a combination of malonamide and organophosphoric acid (*363–370*). A hot test was conducted at ATALANTE by using a mixed solvent, 0.5 M DMDOHEMA and 0.3 M HDEHP in TPH, and a strip solution containing 0.25–0.5 M HEDTA and 0.5 M citric acid pH 3. The results showed that the mixed extractant extracts Ans and Lns simultaneously and strips only Ans by means of HEDTA in a single cycle: yield of Am > 99.9% and Cm > 99.7%; DF for Lns is ca. 800. Thus, it is envisaged to integrate DIAMEX and SANEX processes into a single process (*364*). However, some drawbacks were found (*365*): (1) HDEHP extracts Zr and Mo strongly in the extraction stage; processes for removal of Mo and Zr from a solvent are needed for the recycle of the solvent; and (2) HDEHP exerted an antagonistic effect on the extraction of Ans and Lns with DMDOHEMA. These problems could be avoided by adding a partitioning stage to split out two solvents, DMDOHEMA-TPH and HDEHP, by exploiting a higher

alkaline-side aqueous solubility of HDEHP-salt than DMDOHEMA. Consequently, the solvent used for the extraction step was 0.65 M DMDOHEMA-TPH. Finally, an overall assessment was made for three candidate organophosphoric acids: HDEHP, bis(1,3-dimethylbutyl) phosphoric acid, and di(1-hexyl) phosphoric acid (*365*).

Dhami et al. of BARC studied another mixed solvent system, 0.2 M CMPO −0.3 M HDEHP in *n*-paraffin, and a strip solution of 0.4 M hydrazine hydrate-0.4 M formic acid-0.05 M DTPA (*371*). The extraction performance of the process was also satisfactory.

For the separation of Ans from Lns, many other methods or strategies, including novel extractants, have been reported (*372–380*). These studies have produced varying degrees of promise, though progress is still at an early stage. They serve to show the intensity of interest in the area of An(III)/Ln(III) separations.

1.2.2.2.3 Extraction of Cesium and Strontium

A comprehensive review of the extraction of strontium and cesium was made by Dozol et al. (*381*). In the United States, there are many HLW tanks storing alkaline waste solution and sludge, and thereby energetic and continuing R&D with liquid-liquid extraction has been devoted to the removal of ^{137}Cs and ^{90}Sr, which are the main sources of soluble radioactivity. In the present article, solvent-extraction methods mostly used for nitric acid systems are reviewed and summarized (Table 1.4). Some of the reagents tested are shown in Figure 1.6.

1.2.2.2.3.1 Single-element Separation Extraction of Cs^{+} ion is fairly difficult due to the small charge density of the atomic surface. Thus, calix-crowns were preferentially used for the extraction, because they trap Cs^{+} ion not only by coordinating with the crown ring, but also by interaction with the π-electrons of the phenyl rings of the calixarene (*382, 383*). On the other hand, many reports appeared concerning extraction of Sr^{2+} from acidic solutions by crown ethers (*384*).

Crown ethers. Horwitz et al. evaluated 4,4(5)-di-(*t*-butylcyclohexano)-18-crown-6 (D*t*BuCH18C6) in various organic diluents for the removal of Sr from acid solutions (*385, 386*). The authors have demonstrated a relationship between the value of the extraction constant of Sr and the solubility of water in the organic diluent. The presence of water in the diluent obviates the need for complete dehydration of the nitrate ion associated with Sr^{2+} for its transfer into the organic phase. As the diluent of choice, *n*-octanol was selected for further development. D*t*BuCH18C6 has a low solubility in the aqueous phase and exhibits linearity of its D(Sr) versus its concentration. In 1995, the ANL research group reported the replacement of the 1-octanol in the SREX process with a hydrocarbon diluent, Isopar L, because low concentrations of 1-octanol, which are carried via the aqueous phase to downstream processes, reduce the performance of the processes (*387, 388*). This incompatibility is significant when the SREX process is followed by the TRUEX or PUREX processes. TBP was chosen as a modifier of the Isopar L diluent, because it showed higher D(Sr) values. The SREX process was efficiently applied to the HLW at INL till 1998 (*389–394*). The extracted complexes are represented as [SrL^{2+}(NO$_3$)$_2$], where L = crown ether.

Calix-crowns. In France, exploratory studies of calix-crown molecules have been conducted by Dozol et al. (CEA) with the cooperation of ligand synthesis by Ungaro

TABLE 1.4
Liquid-liquid Extraction Systems for Separation of Strontium and Cesium from Acid Solutions

Category	Targets	Process	Extractants	Modifier	Diluent	Remarks
Crown Ether, Calix-Crown						
Single-element extraction systems	Sr	SREX	0.15 M DtBuCH18C6	1.2–1.5 M TBP	Isopar L	Applied to real waste at INL
	Cs	CCCEX	0.062 M DOC[4]C6	1.5 M TBP	TPH	Tested with genuine raffinate
	Cs	CCCEX	0.1 M Calix R14	1 M MA2	TPH	Tested with genuine raffinate
	Cs	CSSX	0.01 M BOBCalixC6	0.5 M Cs-7SB	Isopar L	Caustic-side, effective to acidic waste
Others						
	Cs	Tsinghua U.	0.025 M iPr-C[4]C6	—	n-Octanol	Laboratory test
	Cs	BARC	4.8×10^{-3} M CC-C	—	Nitrobenzene	Laboratory test
	Cs	ARTIST (Cs)	0.01 M DOC[4]C6	10 vol % DHOA	n-Octanol	Laboratory test
	Sr	ARTIST (Sr)	0.2 M TODGA	—	n-Dodecane	Laboratory test
Crown Ether, Calix-Crown						
Multi-element extraction systems	Sr, Cs	FPEX	0.075 M DtBuCH18C6- 0.007 M BOBCalixC6	0.75 M Cs-7SB	Isopar L	0.003 M trioctylamine (TOA)

Sr, Cs	Russian	0.05 M DCH18C6-0.1 M DB21C7	$C_nH_{2n+1}O(C_2H_4-O)_2H$: $n = 12-14$	$H(CF_2CF_2)_3-CH_2OH$	Feed > 2 M HNO$_3$ Recovery yield > 99.5% Cs, Sr
		Chlorinated Cobalt dicarbollide/PEG (–CMPO)			
Sr, Cs	CCD/PEG	0.06–0.13 M CCD-1 vol % Triton X100		FS-13	Industrial operation
Sr, Cs, Ans	UNEX	0.08 M H$^+$CCD-0.5 vol % PEG 400–0.02 M DPhDBCMPO		FS-13	Tested with genuine raffinate

Note: DOC[4]C6: Calix[4]arene-1,3-(di-octyloxy)-2,4-crown-6. Calix R14 Calix[4]arene-1,3-[di(2-4diethyl-heptylethoxy)oxy]-2,4-crown-6. BOBCalixC6: Calix[4]arene-1,3[bis-(*tert*-octylbenzo)-2,4-crown-6. *i*Pr-C[4]C6: Calix[4]arene-1,3[bis-(2-propyloxy)]-2,4-crown-6. CC-C: Calix[4]arene-di(naphtho-crown-6). Triton X100: A commercial product of Union Carbide Chemicals and Plastics Co. Inc. *t*-Oct-C$_6$H$_4$-(–OC$_2$H$_4$)$_n$OH [$n = 9–10$].

PEG 400: polyethylene glycol, H–(OCH$_2$CH$_2$)nOH [$n = 8–9$]. MA2: methyloctyl-2-dimethyl-butanamide. FS-13: phenyl trifluoromethyl sulfone.

Cs-7SB: 1-(2,2,3,3-tetrafluoropropoxy)-3-(4-*sec*-butylphenoxy)-2-propanol.

iPr-C[4]C6

Calix R14

BEHBCalixC6-NH2

DOC[4]C6

BNCalixC6

DtBuCH18C6

BOBCalixC6

BEHBCalixC6
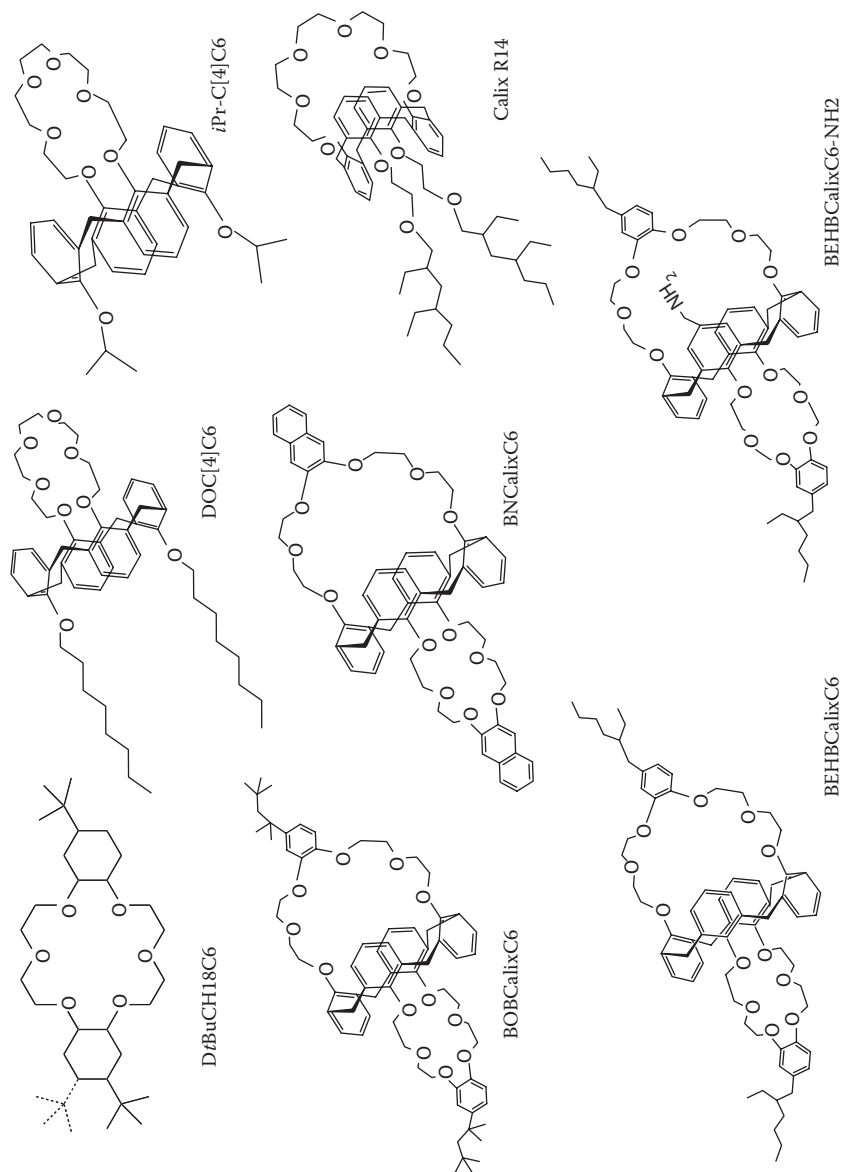
FIGURE 1.6   Structure of extractants used for extraction of Cs and Sr.

of Parma (monocrown-calixarenes) and Vicens of l'ECPM of Strasbourg (biscrown-calixarenes) (*395–404*). Hot tests with raffinate from reprocessing of MOX fuel were started at the CARMEN cell at Fontenay-aux-Roses in 1995. Several monocrown-calixarenes were chosen, and the combinations of extractant/modifier/diluent were optimized. Important factors taken into account were good kinetics, sufficient extraction of Cs from acidities of the feed solution >2 M, effective stripping by dilute HNO_3, TPF, stability and effect of degradation products, high selectivity, and diluent compatibility with DIAMEX and PUREX processes. Consequently, the following two systems were selected as candidates. (1) 0.062 M DOC[4]C6/1.5 M TBP/TPH, and (2) 0.1 M Calix R14/1 M N-methyloctyl-2-dimethyl-butanamide/TPH (*402, 403*). The flowsheets for the respective systems were established by using calculation code (*365*). Verification tests have been conducted at the ATALANTE facility by using genuine raffinate solution, 4 M HNO_3-0.2 M oxalic acid, demonstrating recovery yields of 99.8–99.9% [137]Cs. Only 0.01% of the ^{137}Cs was found in the final organic solvent. These excellent results prove their systems as being promising. Rais et al. proposed the solvent DOC[4]C6 dissolved in 90 vol % 1-*n*-octanol-10 vol % dihexyloctanamide (DHOA) following the CHON principle (*405*). Researchers at Tsinghua University and BARC used extractants, *i*Pr-C[4]C6 (*406*) and calix[4]arene-bis(naphthocrown-6) (*407*), respectively.

A research group at ORNL developed the CSSX (Caustic-Side Solvent eXtraction) process for removal of cesium from alkaline waste solutions utilizing a novel ligand, calix[4]arene-1,3-bis(*tert*-octylbenzo)-2,4-crown-6 (BOBCalixC6) (*408–415*). The extracting solvent is 0.01 M BOBCalixC6/0.50 M Cs-7SB/0.001 M trioctylamine (TOA)/Isopal L, where Cs-7SB is a modifier, and TOA is a suppressor added as a counterion of organophilic anion surfactant-impurities which impair stripping of Cs (*416*). Although the CSSX process was aiming at the alkaline-waste decontamination, namely SRS tank waste, the solvent could be regarded as applicable to acidic waste also (see FPEX process below). However, BOBCalixC6 is susceptible to nitration and is best replaced by alternative calix-crowns for acid-side use (*410*).

Moyer et al. of ORNL have been exploiting new kinds of calix-crown molecules for Cs extraction: a calix-crown bearing branched aliphatic groups for greater solubility, calix[4]arene-bis[4-(2-ethylhexyl)benzo-crown-6] (BEHBCalixC6) (*417, 418*), and pH-switchable calix-crowns bearing amino functionalities, such as BEHBCalixC6-NH_2 (*419–421*). These efforts open up possibilities for a next generation of extractants, though mostly intended for treatment of alkaline solutions.

Diglycol amides. TODGA and other diglycol amides displayed an affinity toward Ca(II) and Sr(II) from 2–3 M HNO_3 solutions (*422*). Thereby, recovery of not only Ans-Lns but also Sr(II) from spent fuels is contemplated (*279, 422, 423*). The extracted complexes are represented as $[Sr(NO_3)_2L_2(HNO_3)]$, where L = TODGA.

1.2.2.2.3.2 Multielement Separation FPEX process. During the course of development of the UREX+ processes, the Fission Product EXtraction (FPEX) process, based on a combined solvent containing two extractants, DtBu18C6 (SREX for Sr) and BOBCalixC6 (CSSX for Cs), has been envisaged (*424–430*). An interesting point is that a modifier Cs-7SB, used in the CSSX process, exhibited a synergistic effect in Sr extraction, and thereby TBP, used as a modifier in the SREX process, was eliminated in the FPEX process. Also, it had been found in the development of

CSSX that hydrogen-bond donor modifiers were most effective for Cs extraction, TBP being a poor modifier by comparison (*413*). The results of preliminary tests showed that the process is effective at selectively extracting Cs and Sr from solutions of nitric acid concentration between 0.5 and 2.5 M. Cesium and Sr can be stripped from the solvent with 0.01 M HNO_3 solution.

CCD/PEG process. Dicarbollide anion {[π-(3)-1,2-$C_2B_9H_{11}$]$_2$Co}, a bulky lipophilic anion that dissociates from its associated cation almost completely in a polar solvent, was first reported by Rais and Selucký of the Nuclear Research Institute Řež plc (NRI, Czech Republic) as an extractant for alkali metals (*431*). Generally, a hexachloro derivative, chlorinated cobalt dicarbollide, [(8,9,12-Cl_3-$C_2B_9H_8$)$_2$-3-Co]$^-$ (CCD), is used because of an increase in chemical and radiation stability (*432–434*). The addition of polyethylene glycols (PEG) to the CCD solvent imparts effective extraction of alkaline-earth metals (*435*). Applications of CCD/PEG have been contrived, as described in a detailed review article written by Rais et al. (*436*). The extraction system with CCD has some important drawbacks: (1) it needs polar aromatic or aliphatic nitro-compound diluents, which are environmentally toxic; and (2) it would release chloride ions during reprocessing and cause corrosion of the facility materials. Efforts toward increasing the solubility of CCD in nonpolar solvents have been focused on alkylation of CCD (*437, 438*). The CCD/PEG process is most effective when the nitric acid concentration in the feed is lower than 1 M. The extracted species of Cs^+ and Sr^{2+} are represented as $[Cs^+ CCD^-]_{org}$ and $[S_r^{2+}(CCD^-)_2]_{org}$, respectively, where cationic and anionic species are free ions in the organic phase.

In the 1980s, Russian scientists, in close cooperation with Czech scientists, initiated R&D for a Cs-Sr combined extraction process for large-scale applications (*439–441*). After successful R&D, the first commercial separation plant, the UE-35 facility, was constructed at the Mayak reprocessing plant RT-1 (*442*). UE-35 was put into operation in August 1996 and, prior to 2001, had processed 1180 m^3 of HLW by the CCD/PEG process, recovering a total of ca. 2×10^{18} Bq (50 MCi) of ^{90}Sr and ^{137}Cs (*443–445*). Based on these experiences with CCD/PEG, Esimantovskii et al. reported that the process for treatment of the aqueous products of the HAW-partitioning flowsheet with CCD is fire-, explosion-, and corrosion-proof (*446*). The CCD-PEG process is a candidate for application in the UREX+ process.

UNEX process. An exhaustive extraction of Sr/Cs and all Ans (-Lns) by one cycle seems efficient and economical for the exclusive purpose of waste treatment either on the acid- or alkaline-side. This idea was developed in the collaboration framework of America (INL) and Russia (Khlopin Radium Institute) (*443, 444*). Among many candidate mixtures of extractants, including CCD/PEG, CMPO, and TRPO, a mixture of Russian CMPO, CCD, and PEG in FS-13 diluent was chosen. The flow-sheets, named the UNiversal EXtraction (UNEX) process, were tested at Idaho and at the Mining and Chemical Combine (MCC) in Russia (*30, 447–454*) with genuine HLW. Recently, a change of stripping reagents from guanidine carbonate to methylamine carbonate (MAC), which can be recycled by distillation, has been reported. The resulting solidification process of the strip product is less complex, cheaper, faster, and safer due to the reduction of the consumption of organic chemicals (*454, 455*). Romanovskiy et al. proposed a drastic variation of extractant, namely, from CMPO to diamide (*456*). Diamides as alternatives are 2,6-pyridine dicarboxyamide

derivatives, whose advantages include much simpler synthesis, larger solubility of their metal solvates in the diluent, and stronger affinity for An(III) versus Ln(III).

For the extraction of Cs or/and Sr, many other extraction systems have been reported (*457–462*).

A variety of novel extracting systems have been developed and reported with an increasing number of new extractants and accumulating knowledge. Although they are not treated comprehensively here, their contribution to the progress of separation science and technology is significant as a whole (*463–467*).

1.2.3   CONSOLIDATED FLOW CONCEPTS OF ADVANCED REPROCESSING

Several consolidated flow concepts (CFCs) of advanced reprocessing have been proposed. The overall goal of a CFC could be attained by a combination of the performance of constituent elemental processes of the CFC. Technologically, it seems inappropriate to discuss the proposed CFCs in detail, because the elemental separation technologies are still evolving and immature, and some may be replaced by others in some cases. Three CFCs are, therefore, briefly explained here for comparison.

In the United States, variants of UREX+ flowsheets were proposed by the DOE in the frame of the GNEP as a principal process for the next generation. The transition from a once-through fuel cycle to a closed fuel cycle requires a staged approach. In stage 1, reprocessing of spent fuel is restored by modifying existing aqueous-based schemes. In stage 2, the recycling of Pu and certain MAs and the environmentally safe disposal of other FPs are the main objectives. In stage 3, the focus is on achieving a closed fuel cycle with actinide transmutation in which all fissile and fertile materials are recycled. Thus, in view of the accumulation of spent fuels, evolution of Gen III (plus) reactors, limited capacity of the Yucca Mountain repository, homogeneous and heterogeneous recycling of all transuranics to the Gen IV (fast) reactors, PR capability, and constraints on the progress of separation technologies, CFCs of the UREX+ family, including UREX+1, UREX+1a, UREX+2, UREX+3, and UREX+4, were proposed (*10*). As an example, the CFC of UREX+3 (Figure 1.7), which is supposed to treat LWR spent fuels based fully on hydrometallurgical processes, separately recovers "Pu-Np" and "Am-Cm" for heterogeneous recycling in the Gen IV (fast) reactors. The CFC of UREX+3 is comprised of several processes: 30 vol % TBP-NPH is used as an extracting solvent for U. Tc is coextracted with U and is removed by a high-acid strip in the presence of AHA prior to recovering U. The Pu-Np recovery is accomplished by the NPEX process after adjusting the valence state of Pu-Np to Pu(IV)-Np(IV). The TRUEX process is applied to the extraction of Am-Cm-Lns, and for the separation of Am-Cm from Lns, a TALSPEAK process is envisaged (*468*). Simultaneous isolation of Cs and Sr is performed by the CCD/PEG process.

The French CEA has been developing the GANEX concept, which is an advanced process to be applied to the homogeneous recycling of all actinides to Gen IV (fast) reactors (*205, 469–471*). Figure 1.8 shows the CFC of GANEX, which adopts the one-cycle "DIAMEX + SANEX." Because the GANEX process separates Am-Cm(-Lns) as an admixture of Pu-Np, the extraction characteristics of the mixed solvent 0.6 M DMDOHEMA and 0.3 M HDEHP in TPH for Pu(IV) and Np(IV,V,VI) were examined. D(M) values and group separation of Ans from Lns were satisfactory. LOC value
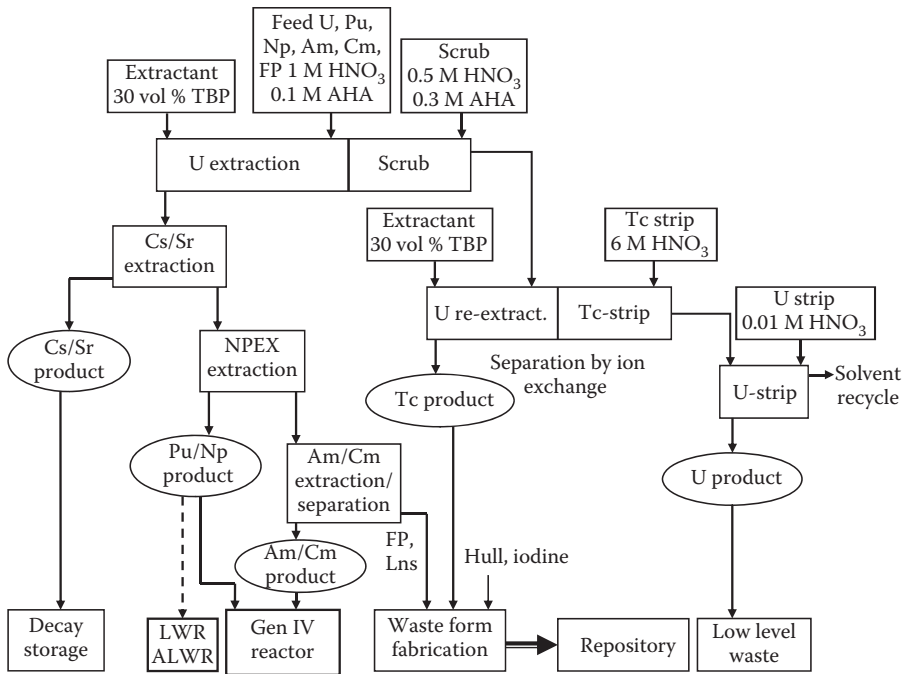
FIGURE 1.7 Conceptual flowsheet of UREX+3 for processing of LWR spent fuel.

with Ce(III) was higher than 0.3 M at an aqueous acidity of 3 M HNO_3 and 0.08 M at pH 3 (*471*). The isolation of FPs, namely ^{135}Cs, is not shown in the GANEX process.

Taking the CHON principle into consideration, a research group at JAEA proposed the Amide-based Radio-resources Treatment with Interim Storage of Transuranics (ARTIST) concept (*203, 472–474*) for the Gen III+, IV reactor fuels (Figure 1.9). It is comprised of the BAMA process for selective U(VI) extraction, TODGA-I and -II processes for separation of all transuranics and separation of Sr, respectively, and the DOC[4]C6 process for Cs recovery. Interim storage of all transuranics recovered by the TODGA-I process was proposed. The admixture of TRUs and Lns satisfies the IAEA's threshold for self-protection, 1 Sv/hr at 1 m, and thereby is actually a PR product. From this admixture, Pu is to be separated, mixed with U, and fabricated to MOX fuel for recycling to the Gen III+ reactors by PR modes in a combination of the separation process and the fuel fabrication process. TRUs are to be separated from Lns by an N-O hybrid donor, *N*-octyl-*N*-tolyl-1,10-phenanthroline-2-carboxyamide, fabricated to MAs oxide fuel, and burned in the FBR.

The CFCs shown in Figures 1.7–1.9 are futuristic and therefore, will evolve steadily in accord with circumstances. There are other well-known CFCs: NEXT (*475*) in Japan and Total Partitioning Process in China (*476, 477*).

As described above, various separation processes and CFCs have been developed and proposed, aiming at the modification of the current PUREX process and reformation of the Improved PUREX and also aiming at the establishment of advanced reprocessing processes. Figure 1.10 shows a classification scheme for these processes and CFCs.
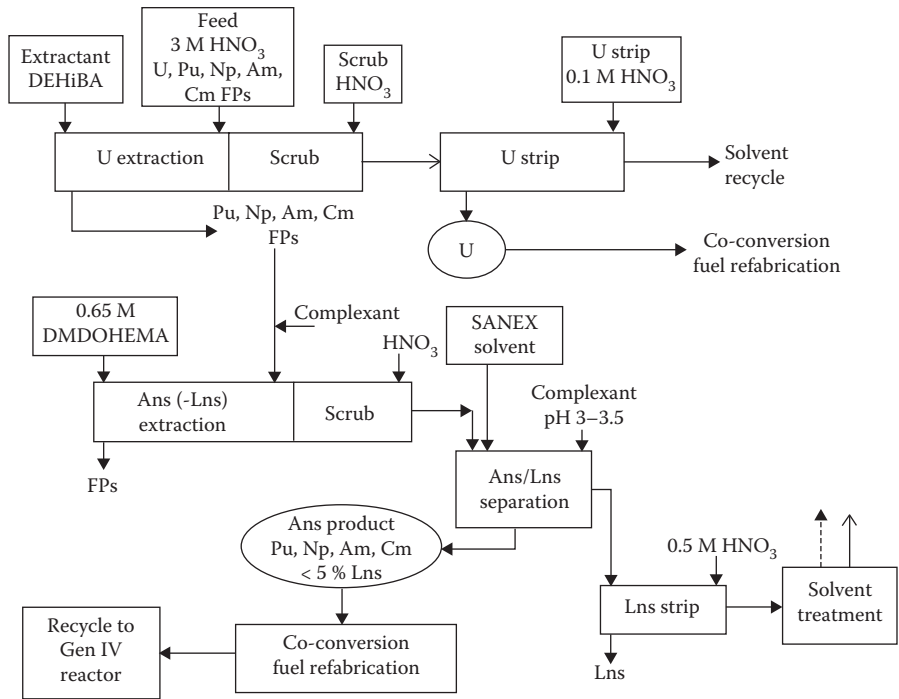
FIGURE 1.8 Conceptual flowsheet of GANEX with a single cycle DIAMEX-SANEX process.
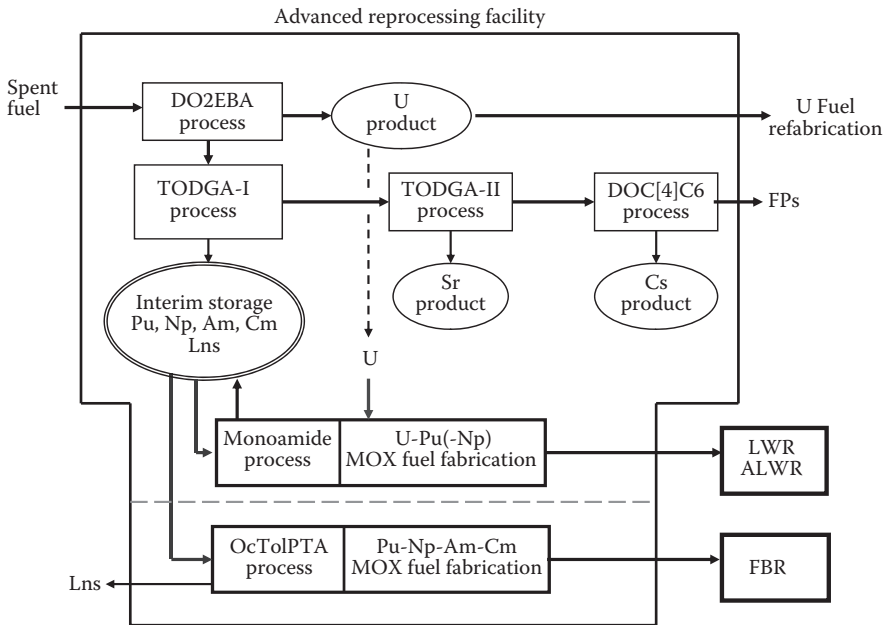
FIGURE 1.9 Conceptual flowsheet of ARTIST for advanced fuel cycle.
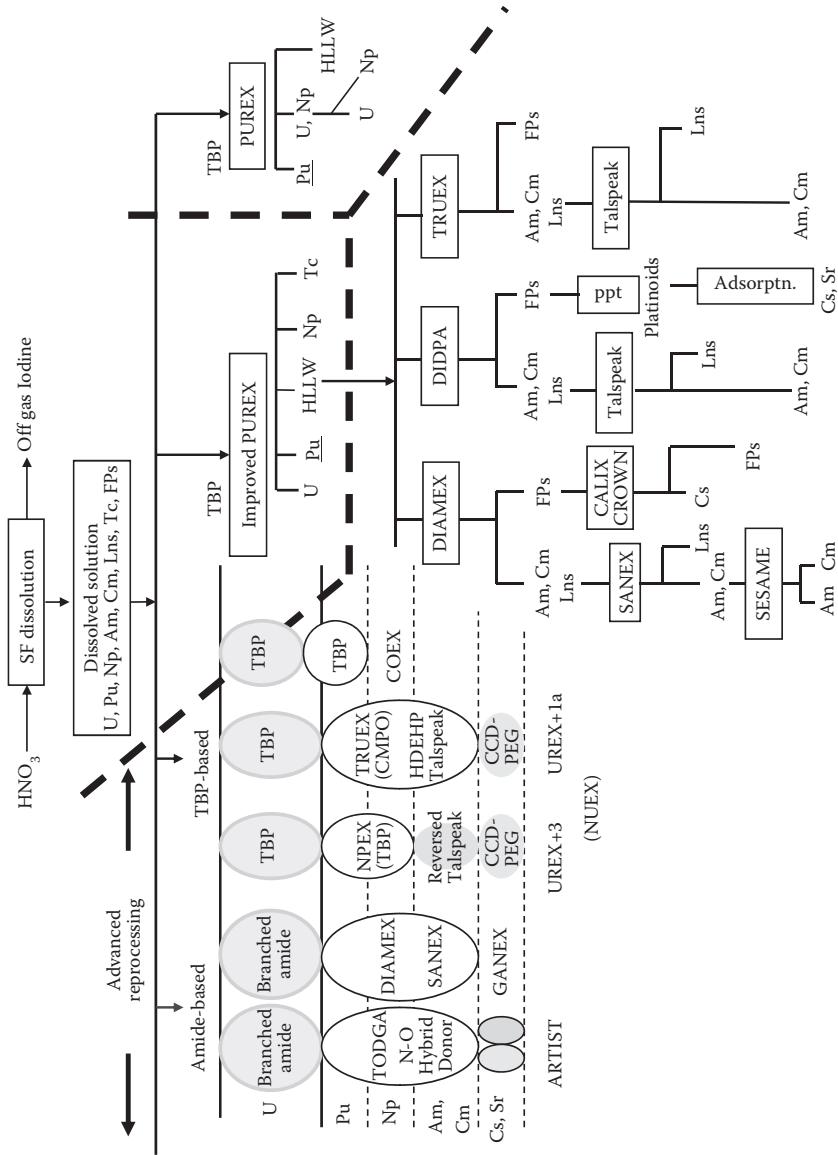
FIGURE 1.10 Classification scheme of separation processes developed and proposed for the reprocessing or partitioning.

The technologies applied to the LWR fuel-reprocessing facilities of the next generation are especially required to be highly proven and PR. In the latter regards, processes producing mixed Pu products, Pu with U (50/50) (COEX), Pu with Np (UREX+2, +3, and NUEX), or Pu with MAs (-Lns) (GANEX, ARTIST, and UREX+1a) are likely candidates with additional elemental processes. The Pu-MAs mixed products are used as fuels for the Gen IV reactors. As the proliferation-resistant capability is different among these products (*478*), there are critical arguments on this issue in the United States (*479*). As far as the fuel cycle of Gen IV reactors is concerned, separation processes with pyrometallurgical technologies are recommended if they are well matured.

1.3   FUTURE PROSPECTS

For various human activities in the twenty-first century, a new concept, sustainability, is a crucial idea. Sustainable development implies that the development of our generation should not constrain the development of the future generation. Accordingly, we should seriously take into account such key factors as economic, environmental, and social impacts, on the global scale and long time span. Among the methodologies to realize sustainable development, recycling is universal, implying maximization of efficient utilization of energy and material resources, minimization of wastes, and consequent reduction in cost. It has matured in the material civilization of the twentieth century. Due to the intrinsic nuclear characteristics of actinides and FPs, recycled usage of the fissile actinides is inevitably needed to maximize the efficiency of actinide utilization. By virtue of separation chemistry and technology, this fundamental concept has been successfully pursued in the reprocessing of nuclear fuel for a half-century. Thus, the main feature of advanced reprocessing should be in accord with "sustainability," keeping strong relations with (1) the evolution of nuclear physics and technology, that is, Gen IV reactors and ADSs, and (2) the progressive pursuit of PR. Although burning of Pu by recycling increases an intrinsic PR effectively, the PR during the reprocessing stage is also to be improved. Then, how could separation chemists and engineers take up this challenge and develop the separation technologies for advanced reprocessing, a pivotal function of a nuclear fuel cycle of the next generation?

A general answer will be to realize the best performance of separation processes and to contrive an ideal actinide-recycling flowscheme for SNF. In the process of liquid-liquid extraction, specifically, the goals to be realized are high extractability and selectivity, rapid kinetics, no TPF, high throughput, minimal secondary wastes, salt-free and CHON principle reagents, and stable and safe operation. These goals will be achieved through the following accomplishments:

1. Design and synthesis of novel ligand molecules that satisfy the above conditions for target metals. Good compatibility of the ligand or metal-ligand complexes with a paraffinic diluent is a central issue to be solved.
2. Choice of ideal scrub and strip reagents and complexants, resulting in a product of the highest purity and yield, an easy post-treatment of the stripped product, and the least amount of secondary wastes.

3. Elucidation of the phenomenon of TPF by studies of extraction mechanism and structure of metal complexes in the liquid phase and the mesoscopic features of the third-phases formed. Finally, the method of eliminating TPF is to be pursued.
4. Investigation of the liquid-liquid interface, where the main reactions and mass-transfer occur, and understanding its microscopic features and its role in the kinetics thoroughly, for example by MD simulation and physical observations. The interface has hidden potential for future applications.

There is certainly a prospect of sure and steady progress due to favorable circumstances: (i) a menu of tools for molecular design, that is, databases, computer codes, and computers, has steadily become richer; (ii) much expertise and new methodologies are accumulating; and (iii) high-quality analytical instruments and high-tech machines, that is, synchrotron radiation facilities and strong neutron sources, are increasing worldwide and opened to users. As for facilities capable of treating high-level radioactive materials, although they are very expensive and located in limited places, various forms of cooperative utilization will be intentionally pursued. A small experimental apparatus such as a microplant developed at the Chalmers University of Technology (*480*) will be beneficial, though somewhat limited.

Due to limited space, reports pertaining to rather futuristic technologies, such as, supercritical fluid extraction (*481–484*) and biphasic aqueous extraction (*485, 486*), were not referred to here (see Chapter 11). Nevertheless, these lead to new and very different avenues for future progress in developing advanced reprocessing technologies.

In conclusion, several issues relating to human science are to be mentioned,

1. Human resources: researchers having good qualifications and expertise should be recruited.
2. Cooperation: international, domestic, and cross-disciplinary collaborations are a requisite. GNEP and Framework Programs of the EU are good examples. In particular, support by synthetic chemists is critical.
3. Education: to stimulate young researchers, good materials (textbooks, books), good practices (exciting experiences), opportunities of in situ exercises and schools should be offered to them. The Institute of Separation Chemistry of Marcoule (ICSM) is a good example.

REFERENCES

1. Multilateral Approaches to the Nuclear Fuel Cycle: Expert Group Report submitted to the Director General of the International Atomic Energy Agency. 2005. INFCIRC/640.
2. Status and Trends in Spent Fuel Reprocessing, IAEA, September 2005. IAEA-TECDOC-1467.
3. Nuclear Energy Data. 2008. 2008. NEA No. 6347, Nuclear Energy Agency, OECD, Paris.
4. Coleman, C.F., Leuze, R.E. 1978. Some milestone solvent extraction processes at the Oak Ridge National Laboratory. *J. Tennessee Acad. Sci*. 53 (3): 102–107.
5. Forsberg, C.W. 2000. Rethinking high-level waste disposal: Separate disposal of high-heat radionuclides (^{90}Sr and ^{137}Cs). *Nucl. Technol.* 131: 252–268.

6. Madic, C., Lecomte, M., Dozol, J.F., Boussier, H. 2004. Advanced chemical separations of minor actinides from high active nuclear wastes. EURADWASTE'04, Luxembourg, Belgium, March 24 to April 1.

7. Madic, C., Hudson, M.J., Baron, P. et al. 2006. EUROPART: European research programme for partitioning of minor actinides within high active wastes issuing from the reprocessing of spent nuclear fuels. 9th OECD/NEA Information Exchange Meeting (IEM) on actinide (An) and fission product (FP) partitioning and transmutation (P&T), Nîmes, France, September 25–29.

8. Bhatnagar, V. 2006. Overview of EU activities in P&T research in the EURATOM 6th and 7th Framework Programmes. 9th OECD/NEA IEM on An and FP P&T, Nîmes, France, September 25–29.

9. GNEP Technical Integration Office, INL. US Department of Energy. 2007. Global nuclear energy partnership technology development plan. GNEP-TECH-TR-PP-2007-00020, Rev 0.

10. US Department of Energy. 2005. Advanced fuel cycle initiative (AFCI) Program plan.

11. US Department of Energy. 2005. Report to Congress, advanced fuel cycle initiative: Objectives, approach, and technology summary.

12. Office of Environmental Management, Office of Technology Development. 1994. Efficient separations and processing integrated program (ESP-IP). Technology summary. DOE/EM-0126P.

13. Office of Environmental Management, Office of Technology Development. 1995. Efficient separations and processing crosscutting program. Technology summary. DOE/EM-0249.

14. US Department of Energy. 1996. Radioactive tank waste remediation focus area. DOE/EM-0295. August.

15. Committee on the Management of Certain Radioactive Waste Streams Stored in Tanks at Three Department of Energy Sites: National Research Council. 2006. Tank waste retrieval, processing, and on-site disposal at three Department of Energy sites: Final Report. National Academy of Sciences.

16. Law of 30 December 1991 – High level and long lived radioactive waste/research and results: Separation and transmutation of long-lived radionuclides. Report Direction 1. Final report. December 2005. CEA/DEN/DDIN/2005-568.

17. Baron, P., Lorrain, B., Boullis, B. 2006. Progress in partitioning: Activities in ATALANTE. 9th OECD/NEA IEM on An and FP of P&T, Nîmes, France, September 25–29.

18. Nuclear Energy Agency, OECD. 2006. French R&D on the partitioning and transmutation of long-lived radionuclides. An international peer review of the 2005 CEA Report. NEA No. 6210.

19. Fox, O.D., Jones, C.J., Birkett, J.E. et al. 2006. Advanced PUREX flowsheets for future Np and Pu fuel cycle demands. In *Separations for the Nuclear Fuel Cycle in the 21st Century*. Lumetta, G.J. et al. Eds. ACS Symposium Series Vol. 933, American Chemical Society, Washington, DC, pp. 89–102.

20. Taylor, R.J., Denniss, I.S., Wallwork, A.L. 1997. Neptunium control in an advanced Purex process. *Nuclear Energy* 36 (1): 39–46.

21. Chiarizia, R. 2006. Mechanism and energetics of third phase formation in TBP solvent extraction of metal salts. IPNS Progress Report 2001–2006. In *Celebration of the 25th Anniversary of IPNS*. ANL-06/54. Argonne National Laboratory.

22. Chiarizia, R., Nash, K.L., Jensen, M.P., Thiyagarajan, P., Littrell, K.C. 2003. Application of the Baxter model for hard-spheres with surface adhesion to SANS data for the U(VI)-HNO_3, TBP-n-dodecane system. *Langmuir* 19 (23): 9592–9599.

23. Abecassis, B., Testard, F., Zemb, Th., Berthon, L., Madic, C. 2003. Effect of n-octanol on the structure at the supramolecular scale of concentrated dimethyldioctylhexyl-ethoxy malonamide extractant solutions. *Langmuir* 19 (17): 6638–6644.

24. Nash, K.L. 2006. Twenty-first century approaches to actinide partitioning. In *Separations for the Nuclear Fuel Cycle in the 21st Century*. Lumetta, G.J. et al. Eds. ACS Symposium Series Vol. 933, American Chemical Society, Washington, DC, pp. 21–40.

25. Todd, T.A., Wigeland, R.A. 2006. Advanced separation technologies for processing spent nuclear fuel and the potential benefits to a geologic repository. In *Separations for the Nuclear Fuel Cycle in the 21st Century*. Lumetta, G.J. et al. Eds. ACS Symposium Series Vol. 933, American Chemical Society, Washington, DC, pp. 41–55.

26. Mathur, J.N., Murali, M.S., Nash, K.L. 2001. Actinide partitioning – A review. *Solvent Extr. Ion Exch.* 19 (3): 357–390.

27. Horwitz, E.P., Schultz, W.W. 1999. Solvent extraction in the treatment of acidic high-level liquid waste; Where do we stand? In *Metal Ion Separation and Preconcentration: Progress and Opportunities*. Bond, A.H., Dietz, M.L., Rogers, R.D. Eds. ACS Symposium Series 716, American Chemical Society, Washington, DC, pp. 20–50.

28. Choppin, G.R. 1999. Overview of chemical separation methods and technologies. In *Chemical Separation Technologies and Related Methods of Nuclear Waste Management: Application, Problems and Research Needs*. Choppin, G.R., Khankhasayev, M.Kh. Eds. Kluwer Academic, Netherlands, pp. 1–15.

29. Wymer, R.G. 1999. Reprocessing of nuclear fuel. In *Chemical Separation Technologies and Related Methods of Nuclear Waste Management: Application, Problems and Research Needs*. Choppin, G.R., Khankhasayev, M.Kh. Eds. Kluwer Academic, Netherlands, pp. 29–52.

30. Babain, V.V., Shadrin, A.Yu. 1999. New extraction technologies for management of radioactive wastes. In *Chemical Separation Technologies and Related Methods of Nuclear Waste Management: Application, Problems and Research Needs*. Choppin, G.R., Khankhasayev, M.Kh. Eds. Kluwer Academic, Netherlands, pp. 135–154.

31. Musikas, C. 1997. Completely incinerable extractants for the nuclear industry. A review. *Min. Pro. Ext. Met. Rev.* 17: 109–142.

32. Bretault, P., Houdin, P., Emin, J.L., Baron, P. 2005. The reprocessing plant of the future: A single extraction cycle. Proc. WM'05 Conference, February 27 to March 3, 2005, Tucson, AZ.

33. Birkett, J.E., Carrott, M.J., Fox, O.D. et al. 2007. Controlling neptunium and plutonium within single cycle solvent extraction flowsheets for advanced fuel cycles. *J. Nucl. Sci. Technol.* 44 (3): 337–343.

34. Baes, C.F. Jr. 1998. SXLSQI A program for modeling solvent extraction systems. Oak Ridge National Laboratory Report. ORNL/TM-13604.

35. Baes, C.F. Jr. 2001. Modeling solvent extraction systems with SXFIT. *Solvent Extr. Ion Exch.* 19 (2): 193–213.

36. Kumar, Sh., Koganti, S.B. 1996. Empirical modeling of Pu(IV) third phase formation in 30% TBP/*n*-dodecane system. *J. Nucl. Sci. Technol.* 33 (12): 1003–1005.

37. Kumar, Sh., Koganti, S.B. 1997. A numerical model for boundary acid concentration for prevention of polymerization at macro Pu concentrations. *J. Nucl. Sci. Technol.* 34 (10): 1027–1028.

38. Kumar, Sh., Koganti, S.B. 2001. Modelling of tritium distribution coefficients in 30 vol% TBP/*n*-dodecane/$UO_2(NO_3)_2$/nitric acid system. *Indian J. Chem. Technol.* 8 (1): 51–53.

39. Kumar, Sh., Koganti, S.B. 2001. Modelling of Np(VI) and Np(IV) distribution coefficients in 30% TBP/*n*-dodecane/nitric acid/water system. *Indian J. Chem. Technol.* 8 (1): 41–43.

40. Kumar, Sh., Koganti, S.B. 2003. An empirical correlation for Pu(III) distribution coefficients in 30% TBP/*n*-dodecane PUREX system in the presence of U(VI), U(IV), Pu(IV), Pu(III), and hydrazine nitrate. *Solvent Extr. Ion Exch.* 21 (3): 369–380.

41. Tachimori, S. 1991. Numerical simulation for chemical reactions of actinide elements in aqueous nitric acid solution. *J. Nucl. Sci. Technol.* 28 (3): 218–227.
42. Mokili, B., Poitrenaud, C. 1995. Modeling of nitric acid and water from aqueous solutions containing a salting-out agent by tri-butylphosphate. *Solvent Extr. Ion Exch.* 13 (4): 731–754.
43. Comor, J.J., Tolic, A.S., Kopecni, M.M., Petkovic, D.J. 1999. Modeling of the simultaneous extraction of nitric acid and uranyl nitrate with tri-*n*-butyl phosphate. Application to extraction operation. *Sep. Sci. Technol.* 34 (1): 115–122.
44. Sagar, V., Chetty, K.V., Sood, D.D. 2000. Extraction of Pu(III) by TBP in presence of uranium. *Solvent Extr. Ion Exch.* 18 (2): 307–317.
45. Baron, P., Boullis, B. 1987. Modeling of uranium/plutonium splitting in PUREX process. *I. Chem. E. Symposium, Series No. 103*, Extraction'87, June 23–26, Dounreay, UK, p. 323.
46. Baron, P., Duhamet, J. 1988. Simulation of uranium/plutonium splitting in a pulsed column in the PUREX process. *Proc. ISEC 88, Vol. IV*, Moscow, p. 204.
47. Dinh, B., Mauborgne, B., Baron, P. 1992. Dynamic simulation of extraction operations: Application in nuclear fuel reprocessing. In *European Symposium on Computer Aided Process Engineering-2*, ESCAPE 2, October 5–7, Toulouse, France.
48. Wallwork, A.L., Denniss, I.S., Taylor, R.J. et al. 1999. Modelling of advanced flowsheets using data from miniature contactor trials. *Nucl. Energy* 38 (1): 31–35.
49. Kumar, Sh., Koganti, S.B. 2002. Development and application of computer code SIMPSEX for simulation of FBR fuel reprocessing flowsheet. IGC Report. IGC-234.
50. Kumar, Sh., Koganti, S.B. 2004. Development and application of computer code SIMPSEX for simulation of FBR fuel reprocessing flowsheet III: Additional benchmarking results for HAN and U(IV) based U-Pu partitioning and a HAN based alternative partitioning step for FBTR fuel reprocessing. IGC Report. BIGC-257.
51. Kumar, Sh., Koganti, S.B. 2005. FBR MOX fuel reprocessing II: Computer simulation of mixer settler experiments (reprocessing of 70%UO_2 + 30%PuO_2 Dounreay and KNK fuels) by indigenous computer code SIMPSEX. Proc. ISEC 2005, Beijing, China, September 19–23.
52. Coy, F.B. 2002. Developing computer models for the UREX solvent extraction process and performing a sensitivity analysis of variables used for optimizing flowsheets for actinide transmutation. Thesis. The University of Texas at Austin.
53. Tachimori, S. 1994. EXTRA-M: A computing code system for analysis of the Purex process with mixer settlers for reprocessing. JAERI Report. JAERI 1331.
54. Asakura, T., Sato, M., Matsumura, M., Morita, Y. 1999. Simulation code of chemical separation process of spent fuel reprocessing: Tool for process development and safety research. Proc. 2nd NUCEF Intern. Symp. NUCEF'98. JAERI Report. JAERI-Conf 99-004 Part I.
55. Ueda, Y., Matsumoto, S. 2003. Algebraic equation for solvent extraction flow sheet under existence of abnormal flows. *Nucl. Technol.* 144: 400–406.
56. Neace, J.C. 1983. Diluent degradation products in the Purex solvent. *Sep. Sci. Technol.* 18 (14–15): 1581–1594.
57. Tahraqui, A., Morris, J.H. 1995. Decomposition of solvent extraction media during nuclear reprocessing: Literature review. *Sep. Sci. Technol.* 30 (13): 2603–2630.
58. Tripathi, S.C., Sumathi, S., Ramanujam, A. 1999. Effects of solvent recycling on radiolytic degradation of 30% tributyl phosphate-*n*-dodecane-HNO_3 system. *Sep. Sci. Technol.* 34 (14): 2887–2903.
59. May, I., Taylor, R.J., Wallovork, A.J. et al. 2000. The influence of DBP on actinide extraction by 30% TBP. *Radiochim. Acta* 88: 283–293.
60. Powell, B.A. 2001. Uranium di-*n*-butylphosphate chemistry. MS Thesis. Clemson University.

61. Tripathi, S.C., Bindu, P., Ramanujam, A. 2001. Studies on the identification of harmful radiolytic products of 30% TBP-*n*-dodecane-HNO$_3$ by gas-liquid chromatography. I. Formation of diluent degradation products and their role in Pu retention behavior. *Sep. Sci. Technol.* 36 (7): 1463–1478.

62. Tripathi, S.C., Ramanujam, A., Gupta, K.K., Bindu, P. 2001. Studies on the identification of harmful radiolytic products of 30% TBP-*n*-dodecane-HNO$_3$ by gas-liquid chromatography. II. Formation and characterization of high molecular weight organophosphates. *Sep. Sci. Technol.* 36 (13): 2863–2883.

63. Ikeda, H., Suzuki, A. 2001. Empirical correlations for radiolytic degradation of *n*-dodecane density viscosity and phase separation time. *J. Nucl. Sci. Technol.* 38 (12): 1138–1140.

64. Tripathi, S.C., Ramanujam, A. 2003. Effect of radiation-induced physicochemical transformations on density and viscosity of 30% TBP-*n*-dodecane-HNO$_3$. *Sep. Sci. Technol.* 38 (10): 2307–2326.

65. Venkatesan, K.A., Robertselvan, B., Antony, M.P., Srinivasan, T.G., Rao, P.R.V. 2006. Physicochemical and plutonium retention properties of hydrolytic and radiolytically degraded tri-*n*-amylphosphate. *Solvent Extr. Ion Exch.* 24 (5): 747–763.

66. Drain, F., Moulin, J.P., Gillet, B. 2000. Advanced solvent management in the La Hague reprocessing plants. AIChE Spring Meeting, March 5–9, Atlanta, GA.

67. Siddall, T.H. 1959. Behavior of technetium in the Purex process. DP-364.

68. Kanellakopulos, B., Konig, C.P. 1983. On the extraction behavior of technetium with respect to the Purex process. *Radiochim. Acta* 33: 169–175.

69. Garraway, J., Wilson, P.D. 1984. Technetium-catalysed oxidation of hydrazine by nitric acid. *J. Less-Common Metals* 97: 191–204.

70. Tachimori, S. 1994. Simulation study on behavior of technetium and its controlled strip during codecontamination process of fuel reprocessing. *J. Nucl. Sci. Technol.* 31 (5): 456–462.

71. Koltunov, V.S., Frolov, K.M., Sinev, M.Y., Isaev, Y.V. 1992. Kinetics of redox reactions of U, Np and Pu in TBP solutions: III. Oxidation of Np(V) by nitrous acid in nitric acid solution. *Radiokhimiya* 34: 118–123.

72. Koltunov, V.S., Frolov, K.M., Sinev, M.Y., Isaev, Y.V. 1993. Kinetics of redox reactions of U, Np and Pu redox reactions in TBP solutions: IV. Np(VI) reduction by HNO$_2$. *Soviet Radiochem.* 34: 450–453.

73. Tochiyama, O., Nakamura, Y., Hirota, M., Inoue, Y. 1995. Kinetics of nitrous acid-catalyzed oxidation of neptunium in nitric acid – TBP extraction system. *J. Nucl. Sci. Technol.* 32: 118–124.

74. Gaquer, I., Moisy, P., Madic, C. 1996. Redox chemistry of Np(VI)/Np(V) couple in nitric/nitrous acid aqueous media. 4th Int. Conf. on Nuclear and Radiochemistry, NRC4, St-Malo, France, September 8–13.

75. Homma, S., Takanashi, M., Koga, J., Matsumoto, S., Ozawa, M. 1996. An approach for evaluating equilibrium and rate constants for the reaction of Np(V) with nitric acid in the PUREX process using process data. *Nucl. Technol.* 116: 108–114.

76. Taylor, R.J., Koltunov, V.S., Savilova, O.A. et al. 1998. The oxidation of Np(IV) by nitric acid in 100% TBP and diluted TBP/nododecane solutions. *J. Alloys Compds.* 271–273: 817–820.

77. Taylor, R.J., May, I., Wallwork, A.L. et al. 1998. The application of formo- and aceto-hydroxamic acids in nuclear fuel reprocessing. *J. Alloys Compds.* 271–273: 534–537.

78. Taylor, R.J., May, I., Koltunov, V.S. et al. 1998. Kinetic and solvent extraction studies of the selective reduction of Np(VI) by new salt free reducing agents. *Radiochim. Acta* 81: 149–156.

79. Uchiyama, G., Asakura, T., Hotoku, S., Fujine, S. 1998. The separation of neptunium and technetium in an advanced PUREX process. *Solvent Extr. Ion Exch.* 16 (5): 1191–1213.

80. Taylor, R.J., May, I. 1999. The reduction of actinide ions by hydroxamic acids. *Czech. J. Phys.* 49: 617–621.
81. Koltunov, V.S., Taylor, R.J., Baranov, S.M., Mezhov, E.A., May, I. 1999. The reduction of plutonium(IV) and neptunium(VI) ions by N,N-ethyl(hydroxyethyl) hydroxylamine in nitric acid. *Radiochim. Acta* 86: 115–121.
82. Karraker, D.G., Rudisill, T.S., Thompson, M.C. 2001. Studies of the effect of acetohydroxamic acid on distribution of plutonium and neptunium by 30vol% tributyl phosphate. WSRC-TR-2001-00509.
83. Anyun, Z., Jingxin, H., Xianye, Z., Fangding, W. 2001. Hydroxylamine derivatives in PUREX process, VI. Study on the partitioning of uranium/neptunium and uranium/ plutonium with N,N-diethylhydroxylamine in the purification cycle of uranium contactor. *Solvent Extr. Ion Exch.* 19 (6): 965–979.
84. Zhu, Z., He, J., Zhang, Z. et al. 2004. Uranium/plutonium and uranium/neptunium separation by the Purex process using hydroxyurea. *J. Radioanal. Nucl. Chem.* 262 (3): 707–711.
85. Koltunov, V.S., Taylor, R.J., Baranov, S.M. et al. 2000. Acetaldoxime – A promising reducing agent for Pu and Np ions in the Purex process. In Scientific research on the back-end of the fuel cycle for the 21st century, ATALANTE 2000, October 24–26, Avignon, France, 01–06.
86. Rao, P.R.V., Kolarik, Z. 1996. A review of third phase formation in extraction of actinides by neutral organophosphorus extractants. *Solvent Extr. Ion Exch.* 14 (6): 955–993.
87. Osseo-Asare, K. 1991. Aggregation, reversed micelles and microemulsions in liquid-liquid extraction: The tri-*n*-butyl phosphate-diluent-water-electrolyte system. *Adv. Colloid Interface Sci.* 37: 123–173.
88. Osseo-Asare, K. 2002. Microemulsions and third phase formation. In *Proc. Int. Solv. Extr. Conf. ISEC 2002*. Sole, K.C., Cole, P.M., Preston, J.S., Robinson, D.J. Eds. South African Institute of Mining and Metallurgy, Cape Town, South Africa, March 18–21, Chris Van Rensburg Pub. Ltd., Melville, Johannesburg, pp. 118–124.
89. Jensen, M.P., Chiarizia, R., Ferrato, J.R. et al. 2002. New insights in third phase formation in the U(VI)-HNO₃, TBP-alkane system. In *Proc. ISEC'2002*. Sole, K.C., Cole, P.M., Preston, J.S., Robinson, D.J. Eds. South African Institute of Mining and Metallurgy, Cape Town, South Africa, March 18–21, Chris van Rensburg, Melville, pp. 1137–1142.
90. Chiarizia, R., Jensen, M.P., Borkowski, M. et al. 2003. Third phase formation revisited: The U(VI), HNO₃-TBP, *n*-dodecane system. *Solvent Extr. Ion Exch.* 21 (1): 1–27.
91. Chiarizia, R., Jensen, M.P., Borkowski, M. et al. 2003. SANS study of third phase formation in the U(VI), HNO₃/TBP, *n*-dodecane system. *Sep. Sci. Technol.* 38 (12&13): 3313–3331.
92. Chiarizia, R., Thiyagarajan, P., Jensen, M.P. et al. 2003. Third phase formation in TBP solvent extraction systems as a result of interaction between reverse micelles. In *Leaching and Solution Purification*, Vol. 1. Proc. Hydrometallurgy 2003; 5th Int. Conf. in Honor of Prof. I. Ritchie. Young, C.A. et al. Eds. The Minerals, Metals and Materials Society, Warrendale, PA, pp. 917–928.
93. Nave, A., Mandin, C., Martinet, L. et al. 2004. Supramolecular organization of tri-*n*-butylphosphate in organic diluent on approaching third phase transition. *Phys. Chem. Chem. Phys.* 6: 799–808.
94. Chiarizia, R., Jensen, M.P., Borkowski, M., Thiyagarajan, P., Littrell, K.C. 2004. Interpretation of third phase formation in the Th(IV)-HNO₃, TBP-*n*-octane system with Baxter's "sticky spheres" model. *Solvent Extr. Ion Exch.* 22 (3): 325–351.
95. Chiarizia, R., Jensen, M.P., Rickert, P.G. et al. 2004. Extraction of zirconium nitrate by TBP in *n*-octane: Influence of cation type on third phase formation according to the "sticky spheres" model. *Langmuir* 20 (25): 10798–10808.

96. Plaue, J., Gelis, A., Czerwinski, K., Thiyagarajan, P., Chiarizia, R. 2006. Small-angle neutron scattering study of plutonium third phase formation in 30% TBP/HNO$_3$/alkane diluent systems. *Solvent Extr. Ion Exch.* 24 (3): 283–298.

97. Chiarizia, R., Briand, A. 2007. Third phase formation in the extraction of inorganic acids by TBP in *n*-octane. *Solvent Extr. Ion Exch.* 25 (3): 351–371.

98. Berthon, L., Martinet, L., Testard, F., Madic, C., Zemb, T. 2007. Solvent penetration and sterical stabilization of reverse aggregates based on the DIAMEX process extracting molecules: Consequences for the third phase formation. *Solvent Extr. Ion Exch.* 25 (5): 545–576.

99. Jenkins, J.A., Mills, A.L., Thompson, P.J., Jubin, R.T. 1993. Performance of centrifugal contactors on uranium and plutonium active PUREX flowsheets. In *Solvent Extraction in the Process Industries: ISEC 93*, York, UK, September 16–21. Logsdail, D.H., Slater, M.J. Eds. Elsevier Applied Science, London and New York.

100. Meikrantz, D.H., Law, J., Todd, T. 2007. Design attributes and scale up testing of annular centrifugal contactors. Chemical Engineering Division of the AIChE Spring National Meeting, April 10–14, 2005, Atlanta, GA. INL/CON-05-00088.

101. Mann, N.R., Garn, T.G., Meikrantz, D., Law, J., Todd, T. 2007. Clean-in-place and reliability testing of a commercial 12.5 cm annular centrifugal contactor at the INL. GLOBAL 2007, Boise, ID, September 9–13. INL/CONF-07-12171.

102. Meikrantz, D.H., Garn, T., Mann, N., Law, J., Todd, T. 2007. Hydraulic performance and mass transfer efficiency of engineering scale centrifugal contactors. In *Advanced Nuclear Fuel Cycles and Systems*. Global 2007, Boise, ID, September 9–13. INL/CONF-07-12167.

103. Okamura, N., Takeuchi, M., Ogino, H., Kase, T., Koizumi, T. 2007. Development of centrifugal contactor with high reliability. GLOBAL 2007, Boise, ID, September 9–13.

104. The Boston Consulting Group. 2006. Economic assessment of used nuclear fuel management in the United States. July 2006. This report was prepared for AREVA. http://www.bcg.com/publications/files/2116202EconomicAssessmentReport24Jul0SR.pdf.

105. Arab-Chapelet, B., Nowogrocki, G., Abraham, F., Grandjean, S. 2005. U(IV)/Ln(III) unexpected mixed site in polymetallic oxalate complexes. Part II. Substitution of U(IV) for Ln(III) in the new oxalates (N$_2$H$_5$)Ln(C$_2$O$_4$)$_2$ nH$_2$O (Ln = Nd, Gd). *J. Solid State Chem.* 178: 3055–3065.

106. Grandjean, S., Arab-Chapelet, B., Robinsson, A-C. et al. 2007. Synthesis of mixed actinide compounds by hydrometallurgical co-conversion methods. In *Advanced Nuclear Fuel Cycles and Systems*. Global 2007, Boise, ID, September 9–13, pp. 98–105.

107. Pathak, P.N., Veeraraghavan, R., Prabhu, D.R., Mahajan, G.R., Manchanda, V.K. 1999. Separation studies of uranium and thorium using di-2-ethylhexylisobutyramide (D2EHIBA). *Sep. Sci. Technol.* 34 (13): 2601–2614.

108. Suzuki, S., Tamura, K., Tachimori, S., Usui, Y. 1999. Extraction of uranium(VI) and plutonium(IV) from nitric acid solution by substituted cyclic amides. *Solvent Extr. Res. Dev. Jpn.* 6: 72–79.

109. Suzuki, S., Tamura, K., Tachimori, S., Usui, Y. 1999. Solvent extraction of technetium (VII) by cyclic amides. *J. Radioanal. Nucl. Chem.* 239 (2): 377–380.

110. Gupta, K.K., Manchanda, V.K., Subramanian, M.S., Singh, R.K. 2000. N,N-dihexylhexanamide: A promising extractant for nuclear fuel reprocessing. *Sep. Sci. Technol.* 35 (10): 1603–1617.

111. Gupta, K.K., Manchanda, V.K., Sriram, S. et al. 2000. Third phase formation in the extraction of uranyl nitrate by N,N-dialkyl aliphatic amides. *Solvent Extr. Ion Exch.* 18 (3): 421–439.

112. Pathak, P.N., Kumbhare, L.B., Manchanda, V.K. 2001. Effect of structure of N,N-dialkyl amides on the extraction of U(VI) and Th(IV): A thermodynamic study. *Radiochim. Acta* 89: 447–452.

113. Manchanda, V.K., Ruikar, P.B., Sriram, S. et al. 2001. Distribution behaviour of U(VI), Pu(IV), Am(III) and Zr(IV) with N,N-dihexyl octanamide under uranium-loading conditions. *Nucl. Technol.* 134: 231–240.

114. Vidyalakshmi, V., Subramanian, M.S., Srinivasan, T.G., Rao, P.R.V. 2001. Effect of extractant structure on third phase formation in the extraction of uranium and nitric acid by N,N-dialkyl amides. *Solvent Extr. Ion Exch.* 19 (1): 37–49.

115. Vidyalakshmi, V., Subramanian, M.S., Rajeswari, S., Srinivasan, T.G., Rao, P.R.V. 2003. Interfacial tension studies of N,N-dialkyl amides. *Solvent Extr. Ion Exch.* 21 (3): 399–412.

116. Moyer, B.A., Caley, C.E. 1988. Hydration and aggregation of monofunctional sulfoxide and other neutral oxygen-donor extractants: The di(2-ethylhexyl)sulfoxide, dodecane, water system. *Solvent Extr. Ion Exch.* 6 (5): 785–817.

117. Prabhu, D.R., Mahajan, G.R., Murali, M. et al. 1992. Di(2-ethylhexyl)sulfoxide as an extractant for plutonium(IV) from nitric acid medium. *J. Radioanal. Nucl. Chem.* 162 (1): 91–97.

118. Kumar, Sh., Koganti, S.B. 1998. A Setchenow type model for Pu(IV) third phase formation in nitric acid-bis(2-ethylhexyl)sulphoxide/dodecane biphasic system at 298.15K. *Solvent Extr. Ion Exch.* 16 (3): 829–841.

119. Preston, J.S., du Preez, A.C. 1999. The influence of extractant structure on the solvent extraction of uranium(VI) and thorium(IV) from nitrate media by dialkyl sulphoxides. *J. Chem. Technol. Biotechnol.* 69 (1): 86–92.

120. Moyer, B.A., Baes Jr. C.F., Case, F.I., Driver, J.L. 2001. Liquid-liquid equilibrium analysis in perspective II. Complete model of water, nitric acid, and uranyl nitrate extraction by di-2-ethylhexyl sulfoxide in dodecane. *Solvent Extr. Ion Exch.* 19 (5): 757–790.

121. Kolarik, Z. 2004. Sulfoxide extractants and synergists. In *Ion Exchange and Solvent Extraction*, *A Series of Advances*, Vol. 17. Marcus, Y., SenGupta, A.K., Marinsky, J.A. Eds. Marcel Dekker, New York, pp. 165–242.

122. Suresh, A., Srinivasan, T.G., Vasudeva Rao, P.R. 1994. Extraction of U(VI), Pu(IV) and Th(IV) by some trialkyl phosphates. *Solvent Extr. Ion Exch.* 12 (4): 727–744.

123. Prasanna, R., Suresh, A., Srinivasan, T.G., Vasudeva Rao, P.R. 1997. Extraction of nitric acid by some trialkyl phosphates. *J. Radioanal. Nucl. Chem.* 222 (1–2): 231–234.

124. Brahmmananda Rao, C.V.S., Suresh, A., Srinivasan, T.G., Vasudeva Rao, P.R. 2003. Tricyclohexyl phosphate – A unique member in the neutral organophosphate family. *Solvent Extr. Ion Exch.* 21 (2): 221–238.

125. Takano, H., Ikegami, T. 2002. Activities on R&D of partitioning and transmutation in Japan. 7th OECD/NEA IEM on An and FPs P&T. 23–35, Jeju, Korea, October 14–16, pp. 29–41.

126. Pereira, C., Vandegrift, G.F., Regalbuto, M.C. et al. 2007. Lab-scale demonstration of the UREX + 1a process using spent fuel. Proc. of WM'07, Tucson, AZ, February 25 to March 1.

127. Guillaumont, R., Fanghanel, T., Fuger, J., Grenthe, I., Neck, V. 2003. *Update on the Chemical Thermodynamics of Uranium, Neptunium, Plutonium, Americium and Technetium*. Elsevier Science, North Holland, Amsterdam, p. 919.

128. Hummel, W., Anderegg, G., Puigdomenech, I., Rao, L., Tochiyama, O. 2005. *Chemical Thermodynamics of Compounds and Complexes of U, Np, Pu, Am, Tc, Se, Ni, and Zr with Selected Organic Ligands*. Elsevier Science, North Holland, Amsterdam, p. 1088.

129. Varnek, A., Wipff, G., Solov'ev, V.P. 2001. Towards an information system on solvent extraction. *Solvent Extr. Ion Exch.* 19 (5): 791–837.

130. Solvent eXtraction Database SXD. 2006. http://infochim.u-strasbg.fr/sxd.

131. Katritzky, A.R., Karelson, M., Petrukhin, R. 1994. The CODESSA PRO project: Comprehensive descriptors for structural and statistical analysis. http://www.codessa-pro.com/manual/manual.htm.

132. ISIDA In Silico Design and Data Analysis Project. http://infochim.u-strasbg.fr/recherche/isida/index.php.
133. Katritzky, A.R., Karelson, M., Lobanov, V.S. 1996. Quantum-chemical descriptors in QSAR/QSPR studies. *Chem. Rev.* 96 (3): 1027–1043.
134. Comba, P., Gloe, K., Inoue, K., Krueger, T., Stephan, H., Yoshizuka, K. 1998. Molecular mechanics calculations and the metal ion selective extraction of lanthanoids. *Inorg. Chem.* 37 (13): 3310–3315.
135. Rabbe, C., Madic, C., Godard, A. 1998. Molecular modeling study of uranyl nitrate extraction with monoamides I. Quantum chemistry approach. *Solvent Extr. Ion Exch.* 16 (1): 91–103.
136. Rabbe, C., Sella, C., Madic, C., Godard, A. 1999. Molecular modeling study of uranyl nitrate extraction with monoamides. II. Molecular mechanics and lipophilicity calculations. Structure-activity relationships. *Solvent Extr. Ion Exch.* 17 (1): 87–112.
137. Goto, M., Matsumoto, S., Uezu, K. et al. 1999. Development and computational modeling of novel bifunctional organophosphorus extractants for lanthanoid separation. *Sep. Sci. Technol.* 34 (11): 2125–2139.
138. Varnek, A., Wipff, G., Solov'ev, V.P. 2002. Assessment of the macrocyclic effect for the complexation of crown-ethers with alkali cations using substructural molecular fragments. *J. Chem. Inf. Comput. Sci.* 42: 812–829.
139. Boehme, C., Coupez, B., Wipff, G. 2002. Interaction of M^{3+} lanthanide cations with malonamide ligands and their thia analogues: A quantum mechanics study of monodentate vs bidentate binding, counterion effects and ligand protonation. *J. Phys. Chem. A* 106: 6487–6498.
140. Coupez, B., Boehme, C., Wipff, G. 2002. Interaction of bifunctional carbonyl and phosphoryl ligands with M^{3+} lanthanide cations: How strong is the bidentate effect? The role of ligand size and counterions investigated by quantum mechanics. *Phys. Chem.* 4: 5716–5729.
141. Sachleben, R.A., Bryan, J.C., Engle, N.L. et al. 2003. Rational design of cesium-selective ionophores: Dihydrocalix[4]arene crown-6 ethers. *Eur. J. Org. Chem.* 2003 (24): 4862–4869.
142. Hay, B.P., Werner, E.J., Raymond, K.N. 2004. Estimating the number of bound waters in Gd(III) complexes revisited. Improved methods for the prediction of q-values. *Bioconjugate Chem*. 15 (6): 1496–1502.
143. Drew, M.G.B., Hudson, M.J., Youngs, T.G.A. 2004. QSAR studies of multidentate nitrogen ligands used in lanthanide and actinide extraction processes. *J. Alloys Compds.* 374: 408–415.
144. Varnek, A., Fourches, D., Solov'ev, V.P. et al. 2004. In Silico design of new uranyl extractants based on phosphoryl-containing podands: QSPR studies, generation and screening of virtual combinatorial library and experimental tests. *J. Chem. Inf. Comput. Sci.* 44 (4): 1365–1382.
145. Yoshizuka, K. 2004. Advance of computational technology for simulating solvent extraction. *Anal. Sci.* 20 (5): 761–765.
146. Yoshizuka, K., Shinohara, T., Shigematsu, H., Kuroki, S., Inoue, K. 2006. Solvent extraction and molecular modeling of uranyl and thorium ions with organophosphorus extractants. *Solvent Extr. Res. Dev. Jpn.* 13: 115–122.
147. Svetlitski, R., Lomaka, A., Karelson, M. 2006. QSPR modeling of lanthanide-organic complex stability constants. *Sep. Sci. Technol.* 41 (1): 197–216.
148. Solov'ev, V.P., Kireeva, N.V., Tsivadze, A.Yu., Varnek, A. 2006. Structure-property modeling of complexation of strontium cation by organic ligands. *J. Struct. Chem.* 47: 311–325.
149. Varnek, A., Fourches, D., Solov'ev, V.P. et al. 2007. Successful "In Silico" design of new efficient uranyl binders. *Solvent Extr. Ion Exch.* 25 (4): 433–462.
150. Varnek, A., Fourches, D., Sieffert, N. et al. 2007. QSPR modeling of the Am^{III}/Eu^{III} separation factor: How far can we predict ? *Solvent Extr. Ion Exch.* 25 (1): 1–26.

151. Hay, B.P. 1999. A molecular mechanics method for predicting the influence of ligand structure on metal ion binding affinity. In *Metal Ion Separation and Preconcentration Progress and Opportunities.* Bond, A.H., Dietz, M.L., Rogers, R.D. Eds. ACS Symposium Series 716, American Chemical Society, Washington, DC, pp. 102–113.

152. Nicholas, J.B., Dixon, D.A., Hay, B.P. 1999. Ab initio molecular orbital study of cation-binding between the alkali metal cations and benzene. *J. Phys. Chem.* 103: 1394–1400.

153. Hay, B.P., Nicholas, J.B. 2000. Novel binding modes in tetramethoxycalix[4]arene: Implications for ligand design. *J. Am. Chem. Soc.* 122: 10083–10089.

154. Hay, B.P., Hancock, R.D. 2001. The role of donor group orientation as a factor in metal ion recognition by ligands. *Coord. Chem. Rev.* 212: 61–78.

155. Hay, B.P., Firman, T.K. 2002. HostDesigner: A Program for the de novo structure-based design of molecular receptors with binding sites that complement metal ion guests. *Inorg. Chem.* 41 (21): 5502–5512.

156. Hay, B.P., Firman, T.K., Lumetta, G.J. et al. 2004. Toward the computer–aided design of metal ion sequestering agents. *J. Alloys Compds.* 374: 416–419.

157. Lumetta, G.J., Rapko, B.M., Garza, P.A. et al. 2002. Deliberate design of ligand architecture yields dramatic enhancement of metal ion affinity. *J. Am. Chem. Soc.* 124: 5644–5645.

158. Lumetta, G.J., Rapko, B.M., Hay, B.P. et al. 2002. A novel bicyclic diamide with high binding affinity for trivalent f-block elements. *Solvent Extr. Ion Exch.* 21 (1): 29–39.

159. Sinkov, S.I., Rapko, B.M., Lumetta, G.J. et al. 2004. Bicyclic and acyclic diamides: Comparison of their aqueous phase binding constants with Nd(III), Am(III), Pu(IV), Np(V), Pu(VI) and U(VI). *Inorg. Chem.* 43 (26): 8404–8413.

160. Benjamin, I. 1996. Chemical reactions and salvation at liquid interfaces: A microscopic perspective. *Chem. Rev.* 96 (4): 1449–1475.

161. Benjamin, I. 1997. Molecular structure and dynamics at liquid-liquid interfaces. *Ann. Rev. Phys. Chem.* 48: 407–451.

162. Guilbaud, P., Wipff, G. 1996. MD simulations on UO_2^{2+} and Sr^{2+} complexes with CMPO derivatives in aqueous solution and at a water/chloroform interface. *New J. Chem.* 20: 631–642.

163. Thuéry, P., Nierlich, M., Bryan, J.C. et al. 1997. Crown ether conformations in 1,3-calix[4]arene bis(crown ether): Crystal structures of a cesium complex and solvent adducts and molecular dynamics simulations. *J. Chem. Soc. Dalton Trans.* 1997 (22): 4191–4202.

164. Toxler, L., Wipff, G. 1998. Interfacial behaviour of ionophoric systems: Molecular dynamics studies on 18-crown-6 and its complexes at the water-chloroform interface. *Anal. Sci.* 14: 43–56.

165. Baaden, M., Berny, F., Muzet, N., Troxler, L., Wipff, G. 2000. Interfacial features of assisted liquid-liquid extraction of uranyl and cesium salts: A molecular dynamics investigation. In *Calixarenes for Separation.* Lumetta, G., Rogers, R., Gopalan, A. Eds. ACS Symposium Series 757, American Chemical Society, Washington, DC, pp. 71–85.

166. Boehme, C., Wipff, G. 2001. The energetic and structural effects of steric crowding in phosphate and dithiophosphinate complexes of M^{3+} lanthanide cations. A computational study. *Chem. Eur. J.* 7: 1398–1407.

167. Baaden, M., Berny, F., Wipff, G. 2001. The chloroform/TBP/aqueous nitric acid interfacial system: A molecular dynamics investigation. *J. Mol. Liquids* 90: 3–12.

168. Baaden, M., Burgard, M., Wipff, G. 2001. TBP at the water-oil interface: The effect of TBP concentration and water acidity investigated by molecular dynamics simulations. *Phys. Chem. B* 105: 11131–11141.

169. Baaden, M., Schurhammer, R., Wipff, G. 2002. Molecular dynamics study of the uranyl extraction by TBP: Demixing of water/oil/TBP solutions with a comparison of super-critical CO_2 and chloroform. *J. Phys. Chem. B* 106: 434–441.

170. Baaden, M., Berny, F., Madic, C., Schurhammer, R., Wipff, G. 2003. Theoretical studies on lanthanide cation extraction by picolinamides: Ligand-cation interactions and interfacial behavior. *Solvent Extr. Ion Exch.* 21 (2): 199–220.

171. Jost, P., Galand, P.J.N., Schurhammer, R., Wipff, G. 2007. Supramolecular interactions of cryptates in concentrated solutions: The effect of solvent and counterions investigated by MD simulations. *Solvent Extr. Ion Exch.* 25 (2): 257–271.

172. Hirata, M., Guilbaud, P., Dobler, M., Tachimori, S. 2003. Molecular dynamics simulations for the complexexation of Ln^{3+} and UO_2^{2+} ions with tridentate ligands diglycolamide (DGA). *Phys. Chem. Chem. Phys.* 5: 691–695.

173. Raman, S., Ashcraft, R.W., Vial, M., Klasky, M.L. 2005. Oxidation of hydroxylamine by nitrous and nitric acids. Model development from first principle SCRF calculations. *J. Phys. Chem. A, Mol. Spectrosc. Kinet. Environ. Gen. Theory* 109 (38): 8526–8536.

174. Riedleder, A.J., Kentish, S.E., Perera, J.M., Stevens, G.W. 2007. Structural investigation of a water/n-heptane interface: A molecular dynamics study. *Solvent Extr. Ion Exch.* 25 (1): 41–52.

175. Butler, R.J., Sinkov, S., Renshaw, J.C. et al. 2000. Reactions of plutonium with acetohydroxamic acid in aqueous solution: First results. ATALANTE 2000, Avignon, France, October 24–26, P2-09.

176. Nuñez, L., Vandegrift, G.F. 2000. Evaluation of hydroxamic acid in uranium extraction process: Literature review. ANL-00/35.

177. Karraker, D.G., Rudisill, T.S., Thompson, M.C. 2001. Studies of the effect of acetohydroxamic acid on distribution of plutonium and neptunium by 30 vol % tributyl phosphate. WSRC-TR-2001-00509.

178. Karraker, D.G. 2002. Radiation chemistry of acetohydroxamic acid in the UREX process. WSRC-TR-2002-00283.

179. Bruso, J., Tkac, P., Matteson, B., Paulenova, A. 2006. Reduction and complexation kinetics of M(IV) in the presence of acetohydroxamic acid. ACS Annual Meeting, Atlanta, GA, March.

180. Alyapyshev, M., Paulenova, A., Cleveland, M.A., Bruso, J.E., Tkac, P. 2007. Hydrolysis of acetohydroxamic acid under UREX + conditions. GLOBAL 2007, Boise, ID, September 9–13.

181. Carrott, M.J., Fox, O.D., Maher, C.J. et al. 2007. Solvent extraction behavior of plutonium (IV) ions in the presence of simple hydroxamic acids. *Solvent Extr. Ion Exch.* 25 (6): 723–745.

182. Taylor, R.J., Sinkov, S.I., Choppin, G.R., May, I. 2008. Solvent extraction behavior of neptunium(IV) ions between nitric acid and diluted 30 % tri-butyl phosphate in the presence of simple hydroxamic acids. *Solvent Extr. Ion Exch.* 26 (1): 41–61.

183. AAA Quarterly Report, Apr–Jun, 2001; LA-UR-01-4283, Jul–Sept, 2001; LA-UR-01-6111, Oct-Dec, 2001; LA-UR-02-0724, Jan–Mar, 2002; LA-UR-02-2630, Apr–Jun, 2002; LA-UR-02-5515, Jul–Sept 2002; LA-UR-02-7220.

184. Thompson, M.C., Norato, M.A., Kessinger, G.F. et al. 2002. Demonstration of the UREX solvent extraction process with Dresden reactor fuel solution. WSRC-TR-2002-00444.

185. Vandegrift, G.F., Regalbuto, M.C., Aase, S.B. et al. 2004. Designing and demonstration of the UREX + process using spent nuclear fuel. ATALANTE 2004, Nîmes, France, June 21–24, O12-01.

186. Vandegrift, G.F., Regalbuto, M.C., Aase, S.B. et al. 2004. Lab-scale demonstration of the UREX + process. WM'04 Conf. February 29 to March 4, Tucson, AZ. WM-4323.

187. Pereira, C., Vandegrift, G.F., Regalbuto, M.C., Aase, S.B. 2005. Lab-scale demonstration of the UREX + 2 process using spent fuel. WM'05 Conf. February 27 to March 3, Tucson, AZ.

188. Matteson, B., Bruso, J., Tkac, P., Paulenova, A. 2006. Extraction systems effects of nitrate on extraction of tetravalent metals in UREX + . ACS Annual Meeting, Atlanta, GA, March.

189. Norman, C.S., Moses, A. Jr., Thomas, M. 2001. Technetium and iodine separations in the UREX process. LA-UR-01-6607.

190. Vandegrift, G.F., Copple, J.M., Chamberlain, D.B. et al. 1992. The generic TRUEX model: Operating manual for the IBM-PC compatible and Macintosh computers, Chemical Technology Division, Argonne National Laboratory. ANL-92/41.

191. Leonard, R.A., Regalbuto, M.C. 1994. A spreadsheet algorithm for stagewise solvent extraction. *Solvent Extr. Ion Exch.* 12 (5): 909–930.

192. Laurinat, J.E. 2006. SASSE modeling of first cycle neptunium(VI) recovery flowsheet. WSRC-TR-2006-00104, Rev.0.

193. Laurinat, J.E. 2006. SASSE modeling of first cycle neptunium(IV) recovery flowsheet. WSRC-TR-2006-00187, Rev.0.

194. Laurinat, J.E. 2007. SASSE modeling of a uranium/molybdenum separation flowsheet. WSRC-STI-2007-00111.

195. Mitchell, A.D. 1979. SEPHIS-MOD4: A user's manual to revised model of the Purex solvent extraction system. ORNL-5471.

196. Regalbuto, M.C., Vandegrift, G.F., Bakel, A.J., Copple, J.M., Pereira, C. 2003. Development of the AMUSE code. *AFCI Quarterly Review*, January, Albuquerque, NM.

197. Regalbuto, M.C., Copple, J.M., Leonard, R., Pereira, C., Vandegrift, G.F. 2004. Solvent extraction process development for partitioning and transmutation of spent fuel. 8th OECD/NEA IEM on An and FP P&T, Las Vegas, NV, November 9–11, 2004.

198. Regalbuto, M.C. 2006. Chemical reprocessing plant simulation. Advanced simulations: A critical tool for future nuclear fuel cycles, Lawrence Livermore National Laboratory, December 14–16.

199. Bromley, L.A. 1973. Thermodynamic properties of strong electrolytes in aqueous solutions. *AIChE J.* 19 (2): 313–320.

200. Pathak, P.N., Kumbhare, L.B., Manchanda, V.K. 2001. Structural effects in N,N-dialkyl amides on their extraction behavior toward uranium and thorium. *Solvent Extr. Ion Exch.* 19 (1): 105–126.

201. Pathak, P.N., Prabhu, D.R., Ruikar, P.B., Manchanda, V.K. 2002. Evaluation of di(2-ethylhexyl) isobutyramide (D2EHIBA) as a process extractant for the recovery of ^{233}U from irradiated Th. *Solvent Extr. Ion Exch.* 20 (3): 293–311.

202. Manchanda, V.K., Pathak, P.N., Rao, A.K. 2004. Di(2-ethylhexyl) pivalamide (D2EHPVA): A promising extractant for selective removal of uranium from high level nuclear waste solutions. *Solvent Extr. Ion Exch.* 22 (3): 353–375.

203. Suzuki, S., Sasaki, Y., Yaita, T., Kimura, T. 2004. Study on selective separation of uranium by N,N-dialkylamide in ARTIST process. Proc. ATALANTE 2004, Nîmes, France, June 21–25.

204. Suzuki, S., Yaita, T., Sugo, Y., Kimura, T. 2007. Study on selective separation of uranium(VI) by new N,N-dialkyl carboxy amides. GLOBAL 2007, Boise, ID, September 9–13.

205. Baron, P., Masson, M., Rostaing, C., Boullis, B. 2007. Advanced separation processes for sustainable nuclear systems. GLOBAL 2007, Boise, ID, September 9–13.

206. Horwitz, E.P., Schultz, W.W. 1999. Solvent extraction in the treatment of acidic high-level liquid waste; Where do we stand? In *Metal Ion Separation and Preconcentration: Progress and Opportunities.* Bond, A.H., Dietz, M.L., Rogers, R.D. Eds. ACS Symposium Series 716, American Chemical Society, Washington, DC, pp. 20–50.

207. Litvina, M.N., Chmutova, M.K., Myasoedov, B.F., Kabachnik, M.I. 1996. Extraction and separation factors of lanthanides and americium in aqueous nitric acid- diaryl(dialkyl)-(dialkylcarbamoyl-methyl)phosphine oxide systems. *Radiochemistry* 38 (6): 494–499.

208. Buchholz, B.A., Nunez, L., Vandegriff, G.F. 1996. Effect of α-radiolysis on TRUEX-NPH solvent. *Sep. Sci. Technol.* 31 (16): 2231–2243.

209. Mathur, J.N., Murali, M.S., Ruikar, P.B. et al. 1998. Degradation, clean-up and reusability of octylphenyl-N,N-diisobutyl-carbamoylmethylphosphine oxide (CMPO) during partitioning of minor actinides from high level waste (HLW) solution. *Sep. Sci. Technol.* 33 (14): 2179–2196.

210. Chiarizia, R., Horwitz, E.P. 1990. Secondary clean up of TRUEX process solvent. *Solvent Extr. Ion Exch.* 8 (6): 907–941.

211. Horwitz, E.P., Diamond, H., Gatrone, R.C., Nash, K.L. 1990. TUCS: A new class of aqueous complexing agents for use in solvent extraction processes. ISEC'90, Kyoto, Japan, July 16–21. ANL/CP-71262.

212. Vandegrift, G.F., Chaiko, D.J., Chamberlain, D.B. et al. 1990. *The Generic TRUEX Model*, Volume Two: Description of the Chemistry and Engineering Principles Used in the Model. ANL89/18, Volume Three: Experimental Database Generated in Support of the Model. ANL-89/19.

213. Vandegrift, G.F., Regalbuto, M.C. 1995. Validation of the generic TRUEX model using data from TRUEX demonstrations with actual high-level waste. *5th Int. Conf. on Radioactive Waste Management and Environmental Remediation*. ICEM'95, Berlin, Germany, 3–9 September, Vol. 1, p. 457.

214. Chiarizia, R., Gasparini, G.M., Casarci, M., Rossi, M., Grossi, G. 1993. Italian experience with the TRUEX process. GLOBAL'93: *Future Nuclear Systems: Emerging Fuel Cycles and Waste Disposal Options*. Seattle, WA, September 12–17.

215. Ozawa, M., Hirano, H., Koma, Y., Kawata, T. 1995. Enhancing actinides separation by consolidated PUREX and TRUEX processes intensified by salt-free requisite. *Int. Conf. Evaluation of Emerging Nuclear Fuel Cycle Systems*. GLOBAL '95, Vol. 1, Versailles, France, September 11–14, pp. 585–594.

216. Brewer, K.N., Herbst, R.S., Gam, T. et al. 1996. A comparison of TRUEX and CMP solvent extraction processes for actinide removal from ICPP wastes. INEL-96/0094. Idaho National Engineering and Environmental Laboratory.

217. Chamberlain, D.B., Conner, C., Hutter, J.C. et al. 1997. TRUEX processing of plutonium analytical solutions at Argonne National Laboratory. *Sep. Sci. Technol.* 32 (1–4): 303–326.

218. Chitnis, R.R., Wattal, P.K., Ramanujam, A. et al. 1999. Recovery of actinides extracted by TRUEX solvent from high-level waste using complexing agents II. Counter-current studies. *J. Radioanal. Nucl. Chem.* 240 (3): 727–730.

219. Law, J.D., Herbst, R.S., Todd, T.A. 2002. Integrated AMP-PAN, TRUEX, and SREX testing. II. Flowsheet testing for separation of radionuclides from actual acidic radioactive waste. *Sep. Sci. Technol.* 37 (6): 1353–1373.

220. Diamond, H., Thiyagarajan, P., Herlinger, A.W., Horwitz, E.P. 1990. Small-angle neutron scattering studies of praseodymium-CMPO polymerization. *Solvent Extr. Ion Exch.* 8 (3): 503–513.

221. Nagasaki, S., Wisnubroto, D.S., Enokida, Y., Suzuki, A. 1994. Neptunium separation from nitric acid solutions with CMPO. 4th Int. Conf. Nuclear Fuel Reprocessing and Waste Management, RECOD '94: Proceedings Vol. 3, London, UK, April 24–28.

222. Takeuchi, M., Tanaka, S., Yamawaki, M., Tachimori, S. 1995. Numerical modeling for coextraction of Tc(VII) with U(VI) by n-octyl(phenyl)-N,N-diisobutylcarbamoyl methylphosphine oxide from nitric acid solution. *J. Nucl. Sci. Technol.* 32 (5): 450–455.

223. Brewer, K.N., Herbst, R.S., Todd, T.A., Christian, J.D. 1998. Zirconium extraction into octyl-(phenyl)-N,N-diisobutylcarbamoylmethylphosphine oxide and tributyl phosphate. *Solvent Extr. Ion Exch.* 16 (4): 1047–1066.

224. Fujii, T., Yamana, H., Watanabe, M., Moriyama, H. 2001. Extraction of molybdenum from nitric acid by octyl(phenyl)-N,N-diisobutylcarbamoylmethyl phosphine oxide. *Solvent Extr. Ion Exch.* 19 (1): 127–141.

225. Belair, S., Labet, A., Mariet, C., Dannus, P. 2005. Modeling of the extraction of nitric acid and neodymium nitrate from aqueous solutions over a wide range of activities by CMPO. *Solvent Extr. Ion Exch.* 23 (4): 481–499.

226. Musikas, C. 1987. Potentiality of non-organophosphours extractants in chemical separations of actinides. 5th Symposium on Separation Science and Technology for Energy Applications, Knoxville, TN, October 26–29.

227. Musikas, C., Condamines, N., Charbonnel, M.C., Hubert, H. 1989. Actinide complexes in solvent extraction. The Amide Type of Extractants, Actinides '89 Conference, Tashkent, USSR, September 24–29. CEA-CONF-10061.

228. Cuillerdier, C., Musikas, C., Hoel, P., Nigond, L., Vitart, X. 1991. Malonamides as new extractants for nuclear waste solutions. *Sep. Sci. Technol.* 26 (9): 1229–1244.

229. Nigond, N., Condamine, P.Y., Cordier, J. et al. 1995. Recent advances in the treatment of nuclear waste by the use of the diamide and picolinamide extractant. *Sep. Sci. Technol.* 30 (7–9): 2075–2099.

230. Charbonnel, M.C., Berthon, L. 1997. Optimization of the extractant molecule for the DIAMEX process. In *Rapport Scientifique de la Direction du Cycle de Combustible (DCC)*. Report CEA-R-5801, pp. 114–119.

231. Spjuth, L., Liljenzin, J.-O., Skalberg, M. et al. 1997. Extraction of actinides and lanthanides from nitric acid solution by malonamides. *Radiochim. Acta* 78: 39–46.

232. Chan, G.Y.S., Drew, M.G.B., Hudson, M.J. et al. 1997. Solvent extraction of metal ions from nitric acid solutions using N,N'-substituted malonamides. Experimental and crystallographic evidence for two mechanisms of extraction, metal complexation and ion-pair formation. *J. Chem. Soc. Dalton Trans.* 1997 (4): 649–660.

233. Smith, B.F., Wilson, K.V., Gibson, R.R., Jones, M.M., Jarvinen, G.D. 1997. Amides as phase modifiers for N,N'-tetraalkylmalonamide extraction of actinides and lanthanides from nitric acid solutions. *Sep. Sci. Technol.* 32 (1–4): 149–173.

234. Madic, C., Hudson, C. 1998. High level liquid waste partitioning by means of completely incinerable extractants. EUR 18038 EN. European Commission on Nuclear Science and Technology, Luxembourg.

235. Byers, P. 1998. Novel extraction reagents for the solvent extraction of lanthanides and trivalent actinides. Ph.D. Thesis. University of Reading.

236. Spjuth, L. 1999. Solvent extraction studies with substituted malonamides and oligopyridines. Ph.D. Thesis. Chalmers University of Technology, Gothenburg.

237. Spjuth, L., Liljenzin, J-O., Hudson, M.J. et al. 2000. Comparison of extraction behaviour and basicity of some substituted malonamides. *Solvent Extr. Ion Exch.* 18 (1): 1–23.

238. Madic, C., Hudson, M.J., Liljenzin, J-O. et al. 2000. New partitioning techniques for minor actinides. EUR 19149. European Commission, Luxembourg.

239. Facchini, A., Amato, L., Modolo, G. et al. 2000. Transient- and steady-state concentration profiles in a DIAMEX-like countercurrent process for An(III) Ln(III) separation. *Sep. Sci. Technol.* 35 (7): 1055–1068.

240. Malmbeck, R., Courson, O., Pagliosa, G. et al. 2000. Partitioning of minor actinides from HLLW using the DIAMEX process. Part 2 – "Hot" continuous counter-current experiment. *Radiochim. Acta* 88: 865–871.

241. Charbonnel, M.C., Flandin, J.L., Giroux, S. et al. 2002. Extraction of Ln(III) and Am(III) from nitrate media by malonamides and polydentate N-bearing ligands. In *Proc. ISEC'2002*. Sole, K.C., Cole, P.M., Preston, J.S., Robinson, D.J. Eds. South African Institute of Mining and Metallurgy, Cape Town, South Africa, March 18–21, Chris van Rensburg, Melville, Vol. 2, pp. 1154–1160.

242. Madic, C., Testard, F., Hudson, M.J. et al. 2004. PARTNEW – New solvent extraction processes for minor actinides-final report. CEA-R-6066.

243. Serrano-Purroy, D., Baron, P., Christiansen, B. et al. 2005. Recovery of minor actinides from HLLW using the DIAMEX process. *Radiochim. Acta* 93 (3): 351–355.

244. Serrano-Purroy, D., Christiansen, B., Glatz, J-P., Malmbeck, R., Modolo, G. 2005. Towards a DIAMEX process using high active concentrate. *Radiochim. Acta* 93 (3): 357–361.

245. Modolo, G., Vijgen, H., Serrano-Purroy, D. et al. 2007. DIAMEX counter-current extraction process for recovery of trivalent actinides from simulated high active concentrate. *Sep. Sci. Technol.* 42 (3): 439–452.

246. Nakamura, T., Miyake, C. 1995. Extraction of lanthanide(III) and uranyl(VI) from nitric acid solution by N,N'-dimethyl-N,N'-dibutylmalonamide. *Solvent Extr. Ion Exch.* 13 (2): 253–273.

247. Nicol, C., Cames, B., Margot, L., Ramain, L. 2000. DIAMEX solvent regeneration studies. ATALANTE 2000, Avignon, France, October 24–26, pp. 3–22.

248. Berthon, L., Morel, J.M., Zorz, N. et al. 2001. DIAMEX process for minor actinide partitioning: Hydrolytic and radiolytic degradations of malonamide extractants. *Sep. Sci. Technol.* 36 (5&6): 709–728.

249. Erlinger, C.V. 1998. Towards a physical interpretation of third phase formation in liquid-liquid extraction. Application to the DIAMEX process for the treatment of high radioactive nuclear wastes. Thesis. University Paris XI, Paris.

250. Erlinger, C., Gazeau, D., Zemb, Th. et al. 1998. Effect of nitric acid extraction on phase behavior, microstructure and interactions between primary aggregates in the system dimethyldibutyl-tetradecylmalonamide (DMDBTDMA)/*n*-dodecane/water: A phase analysis and small-angle X-ray scattering (SAXS) characterization study. *Solvent Extr. Ion Exch.* 16: 707–738.

251. Erlinger, C., Belloni, L., Zemb, Th., Madic, C. 1999. Attractive interactions between reverse aggregates and phase separation in concentrated malonamide extractant solutions. *Langmuir* 15 (7): 2290–2300.

252. Lefrancois, L., Belnet, F., Noel, D., Tondre, C. 1999. An attempt to theoretically predict third-phase formation in the dimethyldibutyltetradecylmalonamide (DMDBTDMA)/dodecane/water/nitric acid extraction system. *Sep. Sci. Technol.* 34 (5): 755–770.

253. Berthon, C., Guilbaud, P., Bousquet, M., Gimenez, C. 2002. Structural studies by NMR and molecular dynamic calculations of lanthanide complexes with ethoxy malonamides in solution. In *ISEC'02, Proc Int Solvent Extr Conf*. Sole, K.C., Cole, P.M., Preston, J.S., Robinson, D.J. Eds. Cape Town, South Africa, March 18–21, Chris van Rensburg, Melville, pp. 1148–1153.

254. Martinet, L., Berthon, L., Peineau, N., Madic, C., Zemb, T. 2002. Aggregation of the solvates formed in liquid-liquid extraction of metallic cations by malonamides: Study of the Nd(NO₃)₃/H₂O/LiNO₃/DMDBTDMA/dodecane system. In *Proc ISEC'02*. Sole, K.C., Cole, P.M., Preston, J.S., Robinson, D.J. Eds. Cape Town, South Africa, March 18–21, Chris van Rensburg, Melville, pp. 1161–1167.

255. Narita, H., Yaita, T., Tamura, K., Tachimori, S. 1998. Solvent extraction of trivalent lanthanide ions with N,N'-dimethyl-N,N'-diphenyl-3-oxapentanediamide. *Radiochim. Acta* 81 (4): 223–226.

256. Narita, H., Yaita, T., Tamura, K., Tachimori, S. 1999. Study on the extraction of trivalent lanthanide ions with N,N'-dimethyl-N,N'-diphenyl-malonamide and -diglycol-amide. *J. Radioanal. Nucl. Chem.* 239 (2): 381–384.

257. Narita, H., Yaita, T., Tachimori, S. 1999. Extraction behavior for trivalent lanthanides with amides and EXAFS study of their complexes. In *Solvent Extraction for the 21st Century. Proc ISEC'99*, Barcelona, Spain, July 11–16, Cox, M., Hidalgo, M. Valiente, M. Eds. Society of Chemical Industry, London, 2001; Vol. 1: 693–696.

258. Narita, H., Yaita, T., Tachimori, S. 2004. Extraction of lanthanides with N,N'-dimethyl-N,N'-diphenyl-malonamide and -3,6-dioxaoctanediamide. *Solvent Extr. Ion Exch.* 22 (2): 135–145.

259. Sasaki, Y., Sugo, Y., Suzuki, S., Tachimori, S. 2001. The novel extractants, diglycolamides, for the extraction of lanthanides and actinides in HNO$_3$-n-dodecane system. *Solvent Extr. Ion Exch.* 19 (1): 91–103.

260. Sasaki, Y., Tachimori, S. 2002. Extraction of actinides(III), (IV), (V), (VI) and lanthanides(III) by structurally tailored diamides. *Solvent Extr. Ion Exch.* 20 (1): 21–34.

261. Tachimori, S., Sasaki, Y., Suzuki, S. 2002. Modification of TODGA-n-dodecane solvent with a monoamide for high loading of lanthanides(III) and actinides(III). *Solvent Extr. Ion Exch.* 20 (6): 687–699.

262. Nave, S., Modolo, G., Madic, C., Testard, F. 2004. Aggregation properties of N,N,N',N'-tetraoctyl-3-oxapentanediamide (TODGA) in n-dodecane. *Solvent Extr. Ion Exch.* 22 (4): 527–551.

263. Yaita, T., Herlinger, A.W., Thiyagarajan, P., Jensen, M.P. 2004. Influence of extractant aggregation on the extraction of trivalent f-element cations by a tetraalkyldiglycolamide. *Solvent Extr. Ion Exch.* 22 (4): 553–571.

264. Jensen, M.P., Yaita, T., Chiarizia, R. 2007. Reverse micelle formation in the partitioning of trivalent f-element cations by biphasic systems containing a tetraalkyldiglycolamide. *Langmuir* 23 (9): 4765–4774.

265. Sugo, Y., Sasaki, Y., Tachimori, S. 2002. Studies on hydrolysis and radiolysis of N,N,N',N'-tetraoctyl-3-oxapentane-1,5-diamide. *Radiochim. Acta* 90 (3): 161–165.

266. Sugo, Y., Izumi, Y., Yoshida, Y. et al. 2007. Influence of diluent on radiolysis of amides in organic solution. *Rad. Phys. Chem.* 76 (5): 794–800.

267. Sugo, Y., Sasaki, Y., Kimura, T., Sekine, T. 2007. Attempts to improve a radiolytic stability of amidic extractants. *GLOBAL 2007*, Boise, ID, September 9–13, pp. 1870–1873.

268. Modolo, G., Vijgen, H., Schreinemachers, C., Baron, P., Dinh, B. 2003. TODGA process development for partitioning of actinides(III) from PUREX raffinate. *GLOBAL 2003*, New Orleans, LA, November 16–20, pp. 1926–1930.

269. Modolo, G., Asp, H., Schreinemachers, C., Vijgen, H. 2006. Development of a TODGA-process for co-separation of trivalent actinides and lanthanides from a high active raffinate. 9th OECD/NEA IEM on An and FP P&T, Nîmes, France, September 25–29.

270. Magnusson, D., Christiansen, B., Glatz, J.P. et al. 2007. Partitioning of minor actinides from PUREX raffinate by the TODGA process. *GLOBAL 2007*, Boise, ID, September 9–13, pp. 713–718.

271. Modolo, G., Asp, H., Vijgen, H. et al. 2007. Demonstration of a TODGA/TBP process for recovery of trivalent actinides and lanthanides from a PUREX raffinate. *GLOBAL 2007*, Boise, ID, September 9–13, pp. 1111–1116.

272. Modolo, G., Asp, H., Schreinemachers, C., Vijgen, H. 2007. Development of a TODGA based process for partitioning of actinides from a PUREX raffinate Part I: Batch extraction optimization studies and stability tests. *Solvent Extr. Ion Exch*. 25 (6): 703–721.

273. Modolo, G., Asp, H., Vijgen, H. et al. 2008. Demonstration of a TODGA-based continuous counter-current extraction process for the partitioning of actinides from a simulated PUREX raffinate, Part II: Centrifugal contactor runs. *Solvent Extr. Ion Exch*. 26 (1): 62–76.

274. Suzuki, H., Sasaki, Y., Sugo, Y., Apichaibukol, A., Kimura, T. 2004. Extraction and separation of Am(III) and Sr(II) by N,N,N',N'-tetraoctyl-3-oxapentanediamide (TODGA). *Radiochim. Acta* 92 (8): 463–466.

275. Apichaibukol, A., Sasaki, Y., Morita, Y. 2004. Effect of DTPA on the extraction of actinides(III) and lanthanides(III) from nitrate solution into TODGA/*n*-dodecane. *Solvent Extr. Ion Exch.* 22 (6): 997–1011.

276. Ansari, S.A., Pathak, P.N., Manchanda, V.K., Husain, M., Prasad, A.K., Parmar, V.S. 2005. N,N,N',N'-Tetraoctyl diglycolamide (TODGA): A promising extractant for actinide-partitioning from high-level waste (HLW). *Solvent Extr. Ion Exch.* 23 (4): 463–479.

277. Ansari, S.A., Pathak, P.N., Husain, M. et al. 2006. Extraction of actinides using N,N,N',N'-tetraalkyl-diglycolamide (TODGA): A thermodynamic study. *Radiochim. Acta* 94 (6–7): 307–312.

278. Tian, G., Zhang, P., Wang, J., Rao, L. 2005. Extraction of actinide(III, IV, V, VI) ions and TcO$_4^-$ by N,N,N',N'-tetraisobutyl-3-oxa-glutaramide. *Solvent Extr. Ion Exch.* 23 (5): 631–643.

279. Mowafy, E.A., Aly, H.F. 2007. Synthesis of some N,N,N',N'-tetraalkyl-3-oxa- pentane-1.5,-diamides and their application in solvent extraction. *Solvent Extr. Ion Exch.* 25 (2): 205–224.

280. Apostilidos, C., Meester, R., de Koch, L. et al. 1990. The extraction of actinides and other constituents from highly-active waste (HAW) by trialkyl phosphine oxide (TRPO). Technical seminar on new separation chemistry techniques for radioactive waste and other specific applications, Rome (Italy), May 16–18. EUR-13390-EN.

281. Zhu, Y., Song, C. 1992. Recovery of neptunium, plutonium and americium from highly active waste. Tri-alkyl phosphine oxide extraction. In *Transuranium Elements: A Half Century*. Morss, L.R. Fuger, J., Eds. ACS, Washington, DC, pp. 318–330.

282. Zhu, Y., Jiao, R. 1994. Chinese experience in the removal of actinides from highly active waste by trialkyl phosphine oxide extraction. *Nucl. Technol.* 108: 361–369.

283. Feng, X., Song, C. 2001. The extraction and stripping behavior of heptavalent technetium with trialkyl phosphine oxide. *Solvent Extr. Ion Exch.* 19 (1): 51–60.

284. Dziwinski, E., Szymanowski, J. 1998. Composition of Cyanex 923, Cyanex 921 and TOPO. *Solvent Extr. Ion Exch.* 16 (6): 1515–1525.

285. Zhang, P., Song, C.L., Liang, J.F., Xin, R.X. 2001. Extraction and retention of plutonium with γ-irradiated 30% trialkylphosphine oxide-kerosene solution. *Solvent Extr. Ion Exch.* 19 (1): 79–89.

286. Zhang, P., Song, C.L., Liang, J.F., Xin, R.X. 2003. Identification of radiolytic degradation products of γ-irradiated 30% trialkylphosphine oxide-kerosene solution. *Solvent Extr. Ion Exch.* 21 (1): 91–108.

287. Wang, J., Song, C. 2001. Hot test of trialkyl phosphine oxide (TRPO) for removing actinides from highly saline high-level liquid waste (HLLW). *Solvent Extr. Ion Exch.* 19 (1): 231–242.

288. Glatz, J.P., Song, C., Koch, L., Bokelund, H.M., He, X. 1995. Hot tests of the TRPO process for the removal of TRU elements from HLLW. Int. Conf. Evaluation of Emerging Nuclear Fuel Cycle Systems. GLOBAL'95, Versaille, France, September 11–14.

289. Song, C., Glatz, J.P. 1996. Mathematical model for the extraction of americium from HLLW by 30 % TRPO and its experimental verification. In *A Value Adding Through Solvent Extraction*. Proc ISEC'96, Vol. 2, The University of Melbourne, Australia, March 19–23.

290. Liu, X., Liang, J., Xu, J. 2004. Simplified Chinese TRPO process to extract and recover transuranium elements from high-level waste. *Solvent Extr. Ion Exch.* 22 (2): 163–173.

291. Tachimori, S., Sato, A., Nakamura, H. 1978. Extraction of lanthanides(III) with di-*iso*-decyl phosphoric acid from nitric acid solution. *J. Nucl. Sci. Technol.* 15: 421–425.

292. Tachimori, S., Sato, A., Nakamura, H. 1979. Separation of transplutonium and rare-earth elements by extraction with di-*iso*-decyl phosphoric acid from DTPA solution. *J. Nucl. Sci. Technol.* 16: 434–440.

293. Morita, Y., Yamaguchi, I., Kondo, Y. et al. 1995. Safety and environmental aspects of partitioning and transmutation of actinides and fission products. IAEA-TECDOC-783. IAEA, Vienna, p. 93.

294. Morita, Y., Kubota, M., Glatz, J.P. et al. 1996. Actinide partitioning from HLW in a continuous DIDPA extraction process by means of centrifugal extractors. *Solvent Extr. Ion Exch.* 14 (3): 385–400.

295. Nash, K.L. 1993. A review of the basic chemistry and recent developments in trivalent f-elements separations. *Solvent Extr. Ion Exch.* 11 (4): 729–768.

296. Jarvinen, G., Barrans, R., Schroeder, N. et al. 1994. Selective extraction of trivalent actinides from lanthanides with dithiophosphinic acids and tributylphosphate. American Chemical Society, San Diego, CA, March. LA-UR-94-4350.

297. Zhu, Y. 1995. The separation of americium from light lanthanides by Cyanex 301 extraction. *Radiochim. Acta* 68 (1): 95–98.

298. Zhu, Y., Chen, J., Jiao, R. 1996. Extraction of Am(III) and Eu(III) from nitrate solution with purified cyanex 301. *Solvent Extr. Ion Exch.* 14 (1): 61–68.

299. Chen, J., Jiao, R., Zhu, Y. 1997. A cross-flow hot test for separating Am from fission product lanthanide by bis(2,4,4-trimethylpentyl)dithiophosphinic acid. *Radiochim. Acta* 76 (3/4): 129–130.

300. Chen, J., Zhu, Y., Jiao, R. 1998. Separation of Am(III) from fission product lanthanides by bis(2,4,4-trimethylpentyl)dithiophosphinic acid (HBTMPDTP) extraction – Process parameters calculation. *Nucl. Technol.* 122 (1): 64–71.

301. Chen, J., Tian, G., Jiao, R., Zhu, Y. 2001. A hot test for separating americium from fission product lanthanides by purified Cyanex 301 extraction in centrifugal contactors. Actinides 2001, Hayama, Japan, November 4–9.

302. Tian, G., Zhu, Y., Xu, J. 2001. Extraction of Am(III) and Ln(III) by dialkyldithio phosphinic acid with different alkyl groups. *Solvent Extr. Ion Exch.* 19 (6): 993–1005.

303. Tian, G., Zhu, Y., Xu, J. 2001. Characterization of extraction complexes of Am(III) and Nd(III) with dialkyldithiophosphinic acid by extended X-ray absorption fine structure spectroscopy. Actinides 2001, Hayama, Japan November 4–9.

304. Jensen, M.P., Bond, A.H. 2002. Influence of aggregation on the extraction of trivalent lanthanide and actinide cations by purified Cyanex 272, Cyanex 301, and Cyanex 302. *Radiochim. Acta* 90 (4): 205–209.

305. Jensen, M.P., Chiarizia, R., Urban, V., Nash, K.L. 2001. Aggregation of the neodymium complexes of HDEHP, CYANEX 272, CYANEX 302, and CYANEX 301 in toluene. NUCEF 2001, Tokai-mura, Japan, October 31 to November 2.

306. Chen, J., Jiao, R., Zhu, Y. 1996. A study on the radiolytic stability of commercial and purified CYANEX 301. *Solvent Extr. Ion Exch.* 14 (2): 555–565.

307. Modolo, G., Odoj, R. 1998. Influence of the purity and irradiation stability of Cyanex 301 on the separation of trivalent actinides from lanthanides by solvent extraction. *J. Radioanal. Nucl. Chem.* 228 (1–2): 83–89.

308. Peterman, D.R., Law, J.D., Todd, T.A., Tillotson, R.D. 2006. Use of Cyanex-301 for separation of Am/Cm from lanthanides in an advanced nuclear fuel cycle. In *Separations for the Nuclear Fuel Cycle in the 21st Century*. Lumetta, G.J. et al. Eds. ACS Symposium Series Vol. 933, American Chemical Society, Washington, DC, pp. 251–259.

309. Bhattacharyya, A., Mohapatra, P.K., Manchanda, V.K. 2006. Separation of americium(III) and europium(III) from nitrate medium using a binary mixture of Cyanex-301 with N-donor ligands. *Solvent Extr. Ion Exch.* 24 (1): 1–17.

310. Modolo, G., Odoj, R. 1999. Actinides(III)-lanthanides group separation from nitric acid using new aromatic diorganyldithiophosphinic acids. 5th OECD/NEA IEM on An and FP P&T. SCK-CEN, Mol, Belgium, November 25–27, 1998.

311. Modolo, G., Odoj, R. 1999. Synergistic selective extraction of actinides(III) over lanthanides from nitric acid using new aromatic diorganyldithiophosphinic acids and neutral organophosphorus compounds. *Solvent Extr. Ion Exch.* 17 (1): 33–53.

312. Modolo, G., Seekamp, S., Vijgen, H., Scharf, K., Baron, P. 2001. Recent developments in the ALINA process for An(III)/Ln(III) group separation during the partitioning of minor actinides. Proc 8th Int Conf Radioactive Waste Management and Environmental Remediation, ICEM 01, Bruges, Belgium, September 30 to October 4. ASME.

313. Modolo, G., Seekamp, S., Nabet, S. 2002. Development of an extraction process for separation of actinoids(III)/lanthanoids(III) with the aid of dithiophosphinic acids. *Chem. Ing. Tech.* 74 (3): 261–265.

314. Geist, A., Modolo, G., Weigl, M. 2003. SANEX-IV process development studies: Di(chlorophenyl)dithiophosphinic acid as selective extractant for actinides(III). Proc Int Workshop on P&T and ADS Development. SCK-CEN, Mol, Belgium, October 6–8.

315. Christiansen, B., Apostolidis, C., Carlos, R. et al. 2004. Advanced aqueous reprocessing in P&T strategies: Process demonstrations on genuine fuels and targets. *Radiochim. Acta* 92 (8): 475–480.

316. Gompper, K., Geist, A., Modolo, G. et al. 2005. R&D on partitioning at the German Research Centers Karlsruhe and Jülich. Proc. GLOBAL 2005, Tsukuba, Japan, October 9–13. Paper No. 059.

317. Weigl, M., Denecke, M.A., Panak, P.J., Geist, A., Gompper, K. 2005. EXAFS and time-resolved laser fluorescence spectroscopy (TRLFS) investigations of the structure of Cm(III)/Eu(III) complexed with di(chlorophenyl)dithiophosphinic acid and different synergistic agents. *Dalton Trans.* 2005 (7): 1281–1286.

318. Jensen, M.P., Bond, A.H. 2002. Comparison of covalency in the complexes of trivalent actinide and lanthanide cations. *J. Am. Chem. Soc.* 124 (33): 9870–9877.

319. Baudin, G. 1992. The French situation on long lived radioisotope separation studies (Puretex and Actinex programs). 2nd OECD/NEA IEM on An and FP P&T, ANL, November 11–13.

320. Cordier, P.Y., Condamines, N. 1993. De nouvelles Molécules pour la Séparation des Actinides: Les Picolinamides. GECOM-CONCOORD'93, La-Lomde-Les-Maures, France, May.

321. Cordier, P.-Y. 1996. Separation of actinides(III) and lanthanides(III) by liquid-liquid extraction with the novel molecules: The picolinamides. Thesis. Blaise Pascal Clermont-Ferrand University.

322. Nigond, L., Condamines, N., Cordier, P.Y. et al. 1995. Recent advances in the treatment of nuclear wastes by the use of diamide and picolinamide extractants. *Sep. Sci. Technol.* 30 (7–9): 2075–2099.

323. Chan, G.Y.S., Drew, M.G.B., Hudson, M.J. et al. 1996. Complexation of 2,4,6-tri-tert-butylpyridine-1,3,5-triazine Ligand (L) with the cerium (IV) nitrate anion. *Polyhedron* 15 (19): 3385–3398.

324. Miguirditchian, M., Guillaneux, D., Guillaumont, D. et al. 2005. Thermodynamic study of the complexation of trivalent actinide and lanthanide cations by ADPTZ, a tridentate N-donor ligand. *Inorg. Chem.* 44 (5): 1404–1412.

325. Hudson, M., Drew, M.G.B., Iveson, P.B., Madic, C., Russell, M.L. 2000. Partitioning-separation of metal ions using heterocyclic ligands. 6th OECD/NEA IEM on An and FP P&T. Madrid, Spain, December 11–13.

326. Kolarik, Z., Müllich, U., Gassner, F. 1999. Selective extraction of Am(III) over Eu(III) by 2,6-ditriazolyl- and 2,6-ditriazinylpyridines. *Solvent Extr. Ion Exch.* 17 (1): 23–32.

327. Kolarik, Z., Müllich, U., Gassner, F. 1999. Extraction of Am(III) and Eu(III) nitrates by 2,6-di-(5,6-dipropyl-1,2,4-triazin-3-yl)pyridines. *Solvent Extr. Ion Exch.* 17 (5): 1155–1170.

328. Sätmark, B., Courson, O., Malmbeck, R. et al. 2000. Separation of minor actinides from a genuine Ma/Ln fraction. 6th OECD/NEA IEM on An and FP P&T, Madrid, Spain, December 11–13.

329. Madic, C., Lecomte, M., Baron, P., Boullis, P. 2002. Separation of long-lived radionuclides from high-active nuclear wastes. *Comptes Rendus Physique* 3 (7): 797–811.

330. Hill, C., Guillaneux, D., Berthon, L., Madic, C. 2002. SANEX-BTP process development studies. *J. Nucl. Sci. Technol.* (Suppl 3): 309–312.

331. Boubals, N., Drew, M.G.B., Hill, C. et al. 2002. Americium (III) and eruopium (III) solvent extraction studies of amide-substituted triazine ligands and complexes formed with ytterbium (III). *J. Chem. Soc. Dalton Trans.* 2002 (1): 55–62.

332. Karmazin, L., Mazzanti, M., Gateau, C., Hill, C., Pecaut, J. 2002. The important effect of ligand architecture on the selectivity of metal ion recognition in An(III)/Ln(III) separation with N-donor extractants. *Chem. Commun.* 2892–2893.

333. Kolarik, Z. 2003. Extraction of selected mono- to tetravalent metal ions by 2,6-di(5,6-dialkyl-1,2,4-triazin-3-yl)pyridines. *Solvent Extr. Ion Exch.* 21 (3): 381–397.

334. Hudson, M.J., Drew, M.G.B., Foreman, M.R.St.J. et al. 2003. The coordination chemistry of 1,2,4-triazinyl bipyridines with lanthanide(III) elements-implications for the partitioning of americium(III). *J. Chem. Soc. Dalton Trans.* 2003 (9): 1675–1685.

335. Bilancia, G., Facchini, A., Ferrando, M. et al. 2005. Selective actinide extraction with a tri-synergistic mixture using a centrifugal contactor battery. *Solvent Extr. Ion Exch.* 23 (6): 773–780.

336. Hill, C., Berthon, L., Madic, C. 2005. Study of the stability of BTP extractants under radiolysis. Proc Int Conf Nuclear Energy Systems for Future Generation and Global Sustainability. GLOBAL 2005, Tsukuba, Japan, October 9–13.

337. Weigl, M., Geist, A., Mullich, U., Gompper, K. 2006. Kinetics of americium(III) extraction and back extraction with BTP. *Solvent Extr. Ion Exch.* 24 (6): 845–860.

338. Drew, M.G.B., Foreman, M.R.S., Hill, C., Hudson, M.J., Madic, C. 2005. 6,6'-Bis-(5,6-diethyl-[1,2,4]triazin-3-yl)-[2,2']bipyridinyl the first example of a new class of quadridentate heterocyclic extraction reagents for the separation of americium(III) and europium(III). *Inorg. Chem. Commun.* 8 (3): 239–241.

339. Denecke, M.A., Rossberg, A., Panak, P.J. 2005. Characterization and comparison of Cm(III) and Eu(III) complexed with 2,6-di(5,6-dipropyl-1,2,4-triazin-3-yl)pyridine using EXAFS, TRFLS, and quantum-chemical methods. *Inorg. Chem.* 44 (23): 8418–8425.

340. Foreman, M.R.St.J., Hudson, M.J., Geist, A., Madic, C., Weigl, M. 2005. An investigation into the extraction of americium(III), lanthanides and D-block metals by 6,6'-bis-(5,6-dipentyl-[1,2,4]triazin-3-yl)-[2,2']bipyridinyl (C$_5$-BTBP). *Solvent Extr. Ion Exch.* 23 (5): 645–662.

341. Foreman, M.R.S., Hudson, M.J., Drew, G.B.D., Hill, C., Madic, C. 2006. Complexes formed between the quadridentate, heterocyclic molecules 6,6'-bis-(5,6-dialkyl-1,2,4-triazin-3-yl)-2,2'-bipyridine (BTBP) and lanthanides(III): Implications for the partitioning of actinides(III) and lanthanides(III). *Dalton Trans.* 13: 1645–1653.

342. Nilsson, M., Andersson, S., Drouet, F. et al. 2006. Extraction properties of 6,6′-bis-(5,6-dipentyl-[1,2,4]triazin-3-yl)-[2,2']bipyridinyl. *Solvent Extr. Ion Exch.* 24 (3): 299–318.

343. Geist, A., Hill, C., Modolo, G. et al. 2006. 6,6'-Bis(5,5,8,8-tetramethyl-5,6,7,8-tetrahydro-benzo[1,2,4]triazin-3-yl)[2,2']bipyridine, an effective extracting agent for the separation of americium(III) and curium(III) from the lanthanides. *Solvent Extr. Ion Exch.* 24 (4): 463–483.

344. Nilsson, M., Ekberg, C., Foreman, M. et al. 2006. Separation of actinides(III) from lanthanides(III) in simulated nuclear waste streams using 6,6'-bis-(5,6-dipentyl-[1,2,4]triazin-3-yl)-[2,2']bipyridinyl (C5-BTBP) in cyclohexanone. *Solvent Extr. Ion Exch.* 24 (6): 823–843.

345. Retegan, T., Ekberg, C., Dubois, I. et al. 2007. Extraction of actinides with different 6,6-bis(5,6-dialkyl-[1,2,4]-triazin-3-yl)-[2,2']-pyridines (BTBPs). *Solvent Extr. Ion Exch.* 25 (4): 417–431.

346. Dubois, I., Ekberg, C., Englund, S. et al. 2007. Partitioning and transmutation: Annual report 2006. Nuclear Chemistry, Department of Chemical and Biological Engineering, Chalmers University of Technology.

347. Mowafy, E.A., Shalash, A.M., El-Naggar, I.M. 2003. Extraction of certain radionuclides by bipicolinamides as new extractants from nitric acid medium. *Indian J. Chem.* 42A (12): 3012–3016.

348. Shimada, A., Yaita, T., Narita, H., Tachimori, S., Okuno, K. 2004. Extraction studies of lanthanide(III) ions with N,N'-dimethyl-N,N'-diphenylpyridine-2,6-dicarboxyamide (DMDPhPDA) from nitric acid solutions. *Solvent Extr. Ion Exch.* 22 (2): 147–161.

349. Alyapyshev, M.Yu., Babain, V.A., Smirnov, I.V. 2004. Extractive properties of synergistic mixtures of dipicolinic acid diamides and chlorinated cobalt dicarbollide. *Radiochemistry* 46 (3): 270–271.

350. Yaita, T., Shiwaku, H., Suzuki, S. et al. 2005. XAFS and spectroscopic characterization for the structure and electronic structure of Ce-DMDPhPDA complexes in methanol. *Physica. Scripta* **T115**: 302–305.

351. Alyapyshev, M.Yu., Babain, V.A., Smirnov, I.V., Shadrin, A.Yu. 2006. Separation of americium and europium from solutions of nitric and perchloric acid using dipicolinic acid diamides. *Czech. J. Phys.* 56, Suppl. D: D469–D475.

352. Babain, V.A., Alyapyshev, M.Yu., Smirnov, I.V., Shadrin, A.Yu. 2006. Extraction of Am and Eu with N,N'-substituted pyridine-2,6-dicarboxamides in fluorinated diluents. *Radiochemistry* 48 (4): 369–373.

353. Alyapyshev, M.Yu., Babain, V.A., Antonov, N.G., Smirnov, I.V. 2006. Extraction of americium and europium from perchloric acid solutions with N,N,N',N'- tetraalkylpyridine-2,6-dicarboxamides. *Russ. J. Appl. Chem.* 79 (11): 1808–1815.

354. Babain, V.A., Alyapyshev, M.Yu., Kiseleva, R.N. 2007. Metal extraction by N,N′-dialkyl-N,N′-diaryl-dipicolinamides from nitric acid solutions. *Radiochim. Acta* 95 (4): 217–223.

355. Yaita, T., Kobayashi, T., Suzuki, S. et al. 2006. Molecular design and development for hybrid donor type ligands with oxygen and nitrogen for simultaneous separation of actinides(III, IV, VI) from lanthanides. 15th Symposium on Separation Science and Technology for Energy Applications, Gatlinburg, TN, October 21–25.

356. Weaver, B.S., Kappelmann, F.A. 1964. Talspeak: A new method of separating americium and curium from lanthanides by extraction from an aqueous solution of aminopolyacetic acid complex with a monoacidic phosphate or phosphonate. ORNL-3559.

357. Persson, G., Svantesson, I., Wingefors, S., Liljenzin, J-O. 1984. Hot test of a TALSPEAK procedure for separation of actinides and lanthanides using Recirculating DTPA-Lactic acid solution. *Solvent Extr. Ion Exch.* 2 (1): 89–113.

358. Svantesson, I. 1984. A reversed TALSPEAK process for the separation of actinides from lanthanides. Thesis. Chalmers University of Technology, Göteborg.

359. Persson, G., Wingefors, S., Liljenzin, J-O., Svantesson, I. 1984. The CTH-process for HLLW treatment: Part II – Hot test. *Radiochim. Acta* 35: 163–172.

360. Del-Cul, G.D., Bond, W.D., Toth, L.M. et al. 1994. Citrate based "TALSPEAK" lanthanide-actinide separation process. ORNL/TM-12785.

361. Nilsson, M., Nash, K.L. 2007. Review article: A review of the development and operational characteristics of the TALSPEAK process. *Solvent Extr. Ion Exch.* 25 (6): 665–701.

362. Collins, E.D., Benker, D.E., Bailey, P.D. et al. 2005. Hot test evaluation of the TALSPEAK process. Proc. GLOBAL 2005, Tsukuba, Japan, October 9–13. Paper No. 186.

363. Hérés, X., Nicol, C., Bisel, L., Baron, P., Ramain, L. 1999. PALADIN: A one step process for actinide(III)/fission product separation. *Proc. GLOBAL'99, Nuclear Technology – Bridging the Millennia*, Jackson Hole, WY, August 29 to September 3, pp. 585–591.

364. Direction de l'Energie Nucléaire, CEA. Rapport sur la faisabilité scientifique de la séparation poussée. Rapport Technique DEN/DDIN/DPRGD/2001/2.

365. Direction de l'Energie Nucléaire, CEA. Faisabilité technique de la séparation poussée. Rapport Technique DEN/VRH/DRCP/2004/1, pp. 23–42.

366. Mauborgne, B., Hérés, X., Lecomte, M., Baron, P. 2007. Cyclic method for separating chemical elements present in an aqueous solution. US Patent 7157003.

367. Gannaz, B. 2006. Spéciation Moléculaire et Supramoléculaire de Systémes d'Extraction Liquid-Liquid ā Base de Malonamide et/ou d'Acides Dialkyl phosphoriques pour la Séparation An(III)/ Ln(III). PhD Thesis. University of Paris XI.

368. Gannaz, B., Chiarizia R., Antonio, M.R., Hill, C., Cote, G. 2007. Extraction of lanthanides(III) and Am(III) by mixtures of malonamide and dialkylphosphoric acid. *Solvent Extr. Ion Exch.* 25 (3): 313–337.

369. Hérés, X., Ameil, E., Martiniz, I., Baron, P., Hill, C. 2007. Extractant separation in DIAMEX-SANEX process. GLOBAL 2007, Boise, ID, September 9–13.

370. Bisel, I., Cames, B., Faucon, M., Rudloff, D., Saucerotte, B. 2007. DIAMEX-SANEX solvent behavior under continuous degradation and regeneration operation. GLOBAL 2007, Boise, ID, September 9–13.

371. Dhami, P.S., Chitnis, R.R., Gopalakrishnan, V. et al. 2001. Studies on the partitioning of actinides from high level waste using a mixture of HDEHP and CMPO as extractant. *Sep. Sci. Technol.* 36 (2): 325–335.

372. Rais, J., Tachimori, S. 1994. Extraction separation of tervalent americium and lanthanides in the presence of some soft and hard donors and dicarbollide. *Sep. Sci. Technol.* 29 (10): 1347–1365.

373. Yordanov, A.T., Whittlesey, B.R., Roundhill, D.M. 1998. Calixarenes derivatized with sulfur-containing functionalities as selective extractants for heavy and precious metal ions. *Inorg. Chem.* 37 (14): 3526–3531.

374. Jensen, M.P., Bond, A.H. 2002. Comparison of covalency in the complexes of trivalent actinide and lanthanide cations. *J. Am. Chem. Soc.* 124 (33): 9870–9877.

375. Peters, M.W., Werner, E.J., Scott, M.J. 2002. Enhanced selectivity for actinides over lanthanides with CMPO ligands secured to a C-3 symmetric triphenoxymethane platform. *Inorg. Chem.* 41 (7): 1707–1716.

376. Nash, K.L., Lavallette, C., Borkowski, M., Paine, R.T., Gan, X. 2002. Features of the thermodynamics of two-phase distribution reactions of americium(III) and europium (III) nitrates into solutions of 2,6-bis[(di-2-ethylhexylphosphino)methyl]pyridine-N,P,P-trioxide. *Inorg. Chem.* 41 (22): 5849–5858.

377. Hudson, M.J. 2003. Some new strategies for the chemical separation of actinides and lanthanides. *Czech. J. Phys.* 53 (Suppl. 1): A305–A311.

378. Schmidt, C., Saadioui, M., Böhmer, V. et al. 2003. Modification of calix[4]arenes with CMPO-functions at the wide rim. Synthesis, solution behavior, and separation of actinides from lanthanides. *Org. Biomol. Chem.* 1: 4089–4096.

379. Watanabe, M., Mirvaliev, R., Tachimori, S. et al. 2004. Selective extraction of americium(III) over macroscopic concentration of lanthanides(III) by synergistic system of TPEN and D2EHPA in 1-octanol. *Solvent Extr. Ion Exch.* 22 (3): 377–390.

380. Nuclear Energy Research Initiative (NERI) Final Report. 2005. Advanced extraction methods for actinide/lanthanide separations. Submitted by: University of Florida, PI: Scott, M.J., collaborating organization: Argonne National Laboratory. PNNL-13221.

381. Dozol, J.F., Dozol, M., Macias, R.M. 2000. Extraction of strontium and cesium by dicarbollides, crown ethers and functionalized calixarenes. *J. Incl. Phenom. Macrocycl. Chem.* 38 (1–4): 1–22.

382. Ikeda, A., Shinkai, S. 1992. Unusually high ionophoricity of 1,3-alternate- calix[4] arenes-*pi*-donor participation in the complexation of cations. *Tetrahedron Lett.* 33: 7385–7388.

383. Ikeda, A., Tsuzuki, H., Shinkai, S. 1994. X-ray crystallographic studies of a 1,3-alternate-calix[4]arene Na$^+$ complex – Is the cation-pi interaction operative between the benzene rings and Na$^+$? *Tetrahedron Lett.* 35: 8417–8420.
384. Orth, R.J., Kurath, D.E. 1994. Review and assessment of technologies for the separation of strontium from alkaline and acidic media. PNL-9053.
385. Horwitz, E.P., Dietz, M.L., Fisher, D.E. 1990. Extraction of strontium from nitric acid solutions using dicyclohexano-18-crown-6 and its derivatives. *Solvent Extr. Ion Exch.* 8 (4&5): 557–572.
386. Horwitz, E.P., Dietz, M.L., Fisher, D.E. 1991. SREX: A new process for the extraction and recovery of strontium from acidic nuclear waste streams. *Solvent Extr. Ion Exch.* 9 (1): 1–25.
387. Dietz, M.L., Horwitz, E.P., Rogers, R.D. 1995. Extraction of strontium from acidic nitrate media using a modified PUREX solvent. *Solvent Extr. Ion Exch.* 13 (1): 1–17.
388. Wood, D.J., Tranter, T.J., Todd, T.A. 1995. Effect of the interference of alkali and alkaline earth metal ions on the extraction of ^{90}Sr from acidic nuclear waste solutions by 18-crown-6 derivatives in 1-octanol. *Solvent Extr. Ion Exch.* 13 (5): 829–844.
389. Law, J.D., Wood, D.J., Herbst, R.S. 1997. Development and testing of SREX flowsheets for treatment of Idaho Chemical Processing Plant sodium-bearing waste using centrifugal contactors. *Sep. Sci. Technol.* 32 (1–4): 223–240.
390. Wood, D.J., Law, J.D. 1997. Evaluation of the SREX solvent extraction process for the removal of ^{90}Sr and hazardous metals from acidic nuclear waste solution containing high concentrations of interfering alkali metal ions. *Sep. Sci. Technol.* 32 (1–4): 241–253.
391. Law, J.D., Wood, D.J., Herbst, R.S. 1997. Development and testing of SREX flowsheets for treatment of Idaho Chemical Processing Plant sodium-bearing waste using centrifugal contactors. *Sep. Sci. Technol.* 32 (1–4): 223–240.
392. Innovative Technology Summary Report. 1998. TRUEX/SREX Demonstration, Tanks Focus Area. DOE/EM-0419. Office of Science and Technology of USDOE.
393. Wood, D.J., Law, J.D., Todd, T.A. 1998. Demonstration of a SREX process for the treatment of actual high activity waste at the INEEL using centrifugal contactors. Science and Technology for Disposal of Radioactive Tank Waste, Schulx, W.W., Lombardo, N.J. Eds. Plenum, New York, pp. 255–268.
394. Law, J.D., Wood, D.J., Todd, T.A. 1999. Development of a SREX flowsheet for the separation of strontium from dissolved INEEL zirconium calcine. INEEL/EXT-99-00001.
395. Casnati, A., Pochini, A., Ungaro, R. et al. 1995. Synthesis, complexation and membrane transport studies of 1,3-alternate calyx[4]arene crown-6 conformers: A new class of cesium selective ionophores. *J. Am. Chem. Soc.* 117: 2767–2777.
396. Dozol, J.F., Bohmer, V., McKervey, A. et al. 1997. New macrocyclic extractants for radioactive waste treatment: Ionizable crown ethers and functionalized calixarenes. Report EUR-17615.
397. Dozol, J.F., Simon, N., Lamare, V. et al. 1999. A solution for cesium removal from high-salinity acidic or alkaline liquid waste: The crown calyx[4]arene. *Sep. Sci. Technol.* 34 (6–7): 877–909.
398. Dozol, J.E., Schwing-Weill, M.J., Arnaud-Neu, F. et al. 2000. Extraction and selective separation of long-lived nuclides by functionalized macrocycles; European Commission, Nuclear Science and Technology Report. EUR 19605.
399. Dozol, J.-F., Lamare, V., Simon, N., Ungaro, R., Casnati, A. 2000. Extraction of cesium by calix[4]arene-crown-6: From synthesis to process. In *Calixarene for Separations.* Lumetta, G.J., Rogers, R.D., Gopalan, A.S. Eds. ACS Symposium Series No. 757, American Chemical Society, Washington, DC, pp. 12–25.
400. Casnati, A., Sansone, F., Dozol, J.F. 2001. New calyx[4]arene-monobenzo- and dibenzo-crown-6 as cesium selective ionophores in the radioactive waste treatment: Synthesis, complexation and extraction properties. *J. Incl. Phenom. Macro. Chem.* 41 (1–4): 193–200.

401. Jankowski, C.K., Dozol, J.F., Allain, F. et al. 2002. Nitration of calixcrown 6 influence on extracting abilities. Use of cesium salts for detection of crown ether macrocycles with the electrospray ionization mass spectrometry technique. *Polish J. Chem.* 76: 701–709.

402. Direction de l'Energie Nucléaire, CEA. *Rapport sur la faisabilité scientifique de la séparation poussée. Technical Report, 2001.* DEN/DDIN/RT-DPRGD/2001/2, pp. 102–112.

403. Direction de l'Energie Nucléaire, CEA. *Faisabilité technique de la séparation poussée. Technical Report, 2004.* DEN/VRH/DRCP/2004/1, pp. 171–180.

404. Simon, N., Tournois, B., Eymard, S. et al. 2004. Cs selective extraction from high level liquid wastes with crown calixarenes: Where are we today? Atalante, Nîmes, France, June 21–25, pp. 1–57.

405. Alexova, J., Širova, M., Rais, J. et al. 2008. Development of a process for the extraction of ^{137}Cs from acidic HLLW based on crowncalix extractant – Use of dialkylamide modifier. In *Solvent Extraction: Fundamentals to Industrial Applications. ISEC 2008.*, Moyer B.A. Ed., September 15–19, Tucson, Arizona, Canadian Institute of Mining, Metallurgy and Petroleum, pp. 653–658.

406. Wang, J.W., Zhu, X., Song, C. 2005. Extraction performance of Cs by 25,27-bis(2-propyloxy)calix[4]-26,28-crown-6 (iPr-C[4]C-6) in *n*-octanol. *Sep. Sci. Technol.* 40 (16): 3381–3392.

407. Mohapatra, P.K., Ansari, S.A., Sarkar, A., Bhattacharyya, A., Manchanda, V.K. 2006. Evaluation of calix-crown ionophores for selective separation of radio-esium from acidic nuclear waste solution. *Anal. Chim. Acta* 571 (2): 308–314.

408. Bonnesen, P.V., Delmau, L.H., Haverlock, T.J., Moyer, B.A. 1998. Alkaline-side extraction of cesium from Savannah River tank waste using a calixarene-crown ether extractant. ORNL/TM-13704.

409. Sachleben, R.A., Bonnesen, P.V., Desazeaud, T. et al. 1999. Surveying the extraction of cesium nitrate by 1,3-alternate calix[4]arene crown-6 ethers in 1,2-dichloroethane. *Solvent Extr. Ion Exch.* 17 (6): 1445–1459.

410. Bonnesen, P.V., Haverlock, T.J., Engle, N.L., Sachleben, R.A., Moyer, B.A. 2000. Development of process chemistry for the removal of cesium from acidic nuclear waste by calix[4]arene-crown-6 ethers. In *Calixarene Molecules for Separations.* Lumetta, G.J., Rogers, R.D., Gopalan, A.S. Eds. ACS Symposium Series Vol. 757, American Chemical Society, Washington, DC, pp. 26–44.

411. Delmau, L.H., Bostick, D.A., Haverlock, T.J., Moyer, B.A. 2002. Caustic-side solvent extraction: Extended equilibrium modeling of cesium and potassium distribution behavior. Oak Ridge National Laboratory Report. ORNL/TM-2002/116.

412. Delmau, L.H., Birdwell, J.F. Jr., Bonnesen, P.V. et al. 2002. Caustic-side solvent extraction: Chemical and physical properties of the optimized solvent. Oak Ridge National Laboratory. ORNL/TM-2002/190.

413. Bonnesen, P.V., Delmau, L.H., Moyer, B.A., Lumetta, G.J. 2003. Development of effective solvent modifiers for the solvent extraction of cesium from alkaline high-level tank waste. *Solvent Extr. Ion Exch.* 21 (2): 141–170.

414. Leonard, R.A., Aase, S.B., Arafat, H.A. et al. 2003. Experimental verification of caustic-side solvent extraction for removal of cesium from tank waste. *Solvent Extr. Ion Exch.* 21 (4): 505–526.

415. Moyer, B.A., Birdwell, J.F. Jr., Bonnesen, P.V., Delmau, L.H. 2005. Use of macrocycles in nuclear-waste cleanup: A real-world application of a calixcrown in technology for the separation of cesium. In *Macrocyclic Chemistry – Current Trends and Future Prospectives.* Gloe K. Ed., Springer, Dordrecht, pp. 383–405.

416. Delmau, L.H., Bonnesen, P.V., Moyer, B.A. 2004. A solution to stripping problems caused by organophilic anion impurities in crown-ether based solvent extraction systems: A case study of cesium removal from radioactive wastes. *Hydrometallurgy* 72 (1–2): 9–19.

417. Engle, N.L., Bonnesen, P.V., Tomkins, B.A., Haverlock, T.J., Moyer, B.A. 2004. Synthesis and properties of calix[4]arene-bis[4-(2-ethylhexyl)benzo-crown-6], a cesium extractant with improved solubility. *Solvent Extr. Ion Exch.* 22 (4): 611–636.

418. Moyer, B.A., Bazelaire, E., Bonnesen, P.V. et al. 2005. Next generation extractants for cesium separation from high-level waste: From fundamental concepts to site implementation. FY 2005 Annual Report, Environmental Management Science Program, Project #73803.

419. Bazelaire, E., Bonnesen, P.B., Delmau, L.H. et al. 2003. New amino-functionalized 1,3-alternate calyx[4]arene bis- and mono-(benzo-crown-6 ethers) for pH-switched cesium nitrate extraction. *Tetrahedron Lett.* 44 (29): 5397–5401.

420. Bazelaire, E., Gorbunova, M.G., Bonnesen, P.V., Moyer, B.A., Delmau, L.H. 2004. pH-switchable cesium nitrate extraction with calyx[4]arene mono and bis(benzo-crown-6) ethers bearing amino functionalities. *Solvent Extr. Ion Exch.* 22 (4): 637–661.

421. Harmon, B.W., Ensor, D.D., Delmau, L.H., Moyer B.A. 2007. Extraction of cesium by a calix[4]arene-crown-6 ether bearing a pendant amine group. *Solvent Extr. Ion Exch.* 25 (3): 373–388.

422. Tachimori, S., Suzuki, Y., Sasaki, Y., Apichaibukol, A. 2003. Solvent extraction of alkaline earth metal ions by diglycolic amides from nitric acid solutions. *Solvent Extr. Ion Exch.* 21 (5): 707–715.

423. Tian, G., Wang, J., Shen, Y., Rao, L. 2005. Extraction of strontium from HLLW using N,N,N',N'-tetraisobutyl-3-oxa-glutaramide. *Solvent Extr. Ion Exch.* 23 (4): 519–528.

424. Sachleben, R.A., Bonnesen, P.V., Descazeaud, T. et al. 1999. Surveying the extraction of cesium nitrate by 1,3-alternate calix[4]arene crown-6 ethers in 1,2-dichloroethane. *Solvent Extr. Ion Exch.* 17 (6): 1445–1459.

425. Riddle, C.L., Baker, J.D., Law, J.D. et al. 2004. Development of a novel solvent for the simultaneous separation of strontium and cesium from dissolved spent nuclear fuel solutions. Americas Nuclear Energy Symposium (ANES 2004), Deauville Beach Resort, Miami Beach, FL, October 3–6.

426. Riddle, C.L., Baker, J.D., Law, J.D. et al. 2005. Fission product extraction (FPEX): Development of a novel solvent for the simultaneous separation of strontium and cesium from acidic solutions. *Solvent Extr. Ion Exch.* 23 (3): 449–461.

427. Todd, T.A., Law, J.D., Herbst, R.S. et al. 2005. Advanced technologies for the simultaneous separation of cesium and strontium from spent nuclear fuel. WM'05 Conf, February 27 to March 3, Tucson, AZ.

428. Law, J.D., Garn, T.G., Herbst, R.S. et al. 2006. Development of cesium and strontium separation and immobilization technologies in support of an advanced nuclear fuel cycle. WM'06 Conf, February 26 to March 2, Tucson, AZ. INL/CON-05-00970.

429. Mincher, B.J., Peterman, D.R., Riddle, C.L. et al. 2006. Gamma ray radiolysis of the FPEX solvent. 9th OECD/NEA IEM on An and FP P&T, Nîmes, France, September 25–29. INL/CON-06-11724.

430. Delmau, L.H., Bonnesen, P.V., Engle, N.L. et al. 2006. Combined extraction of cesium and strontium from alkaline nitrate solutions. *Solvent Extr. Ion Exch.* 24 (2): 197–217.

431. Rais, J., Seluck, P., Kyrš, M. 1976. Extraction of alkali-metals into nitrobenzene in presence of univalent polyhedral borate anion. *J. Inorg. Nucl. Chem.* 38: 1376–1378.

432. Rais, J., Plesek, J., Seluck, P., Kyrš, M., Kadlecova, L. 1991. Extraction of cesium with derivatives of carborane into nitrobenzene. *J. Radioanal. Nucl. Chem.* 148 (2): 349–357.

433. Matel, L., Cech, R., Macasek, F., Hermanek, S., Plesek, J. 1977. Radiolysis of the bis(1,2-dicarbollyl)cobalt(III) ion in nitrobenzene-bromoform mixture. I. A final product of radiolysis. *Radiochem. Radioanal. Lett.* 29: 317–324.

434. Mincher, B.J., Herbst, R.S., Tillotson, R.D. 2007. Radiation effects on the performance of HCCD-PEG for Cs and Sr extraction. *Solvent Extr. Ion Exch.* 25 (6): 747–755.

435. Kyrš, M., Seluck, P. 1993. A rapid separation of Sr from Ca by solvent extraction with dicarbollides in the presence of EDTA and polyethylene glycols. *J. Radioanal. Nucl. Chem. Art.* 174 (1): 153–165.

436. Rais, J., Grüner, B. 2004. Extraction with metal bis(dicarbollide) anions: Metal bis(dicarbollide) extractants and their applications in separation chemistry. In *Ion Exchange and Solvent Extraction*, *A Series of Advances* Vol. 17. Marcus, Y., SenGupta, A.K., Marinsky, J.A. Eds. Marcel Dekker, New York, pp. 243–334.

437. Miller, R.L., Pinkerton, A.B., Hurlburt, P.K., Abney, K.D. 1995. Extraction of cesium and strontium into hydrocarbon solvents using tetra-C-alkyl cobalt dicarbollide. *Solvent Extr. Ion Exch.* 13 (5): 831–827.

438. Chamberlin, R.M., Abney, K.D. 1999. Strontium and cesium extraction into hydro-carbons using alkyl cobalt dicarbollide and polyethylene glycols. *J. Radioanal. Nucl. Chem.* 240 (2): 547–553.

439. Galkin, B.Y., Esimantovskiy, V.M., Lazarev, L.N. et al. 1988. *Proc. ISEC-88*, Vol. 4, Nauka, Moscow, p. 215.

440. Galkin, B.Ya., Shishkin, D.N. 2001. Extraction withdrawal of cesium and strontium radionuclides from the solution of spent nuclear fuel. In *Back-End of the Fuel Cycle: From Research to Solutions.* GLOBAL 2001, September 9–13, Paris, France.

441. Law, J.D., Garn, T.G., Herbst, R.S. et al. 2005. Development of cesium and strontium separation and immobilization technologies in support of an advanced nuclear fuel cycle. WM'05, Tucson, AZ, February 27 to March 3. INL/CON-05-00970.

442. Dzekun, E.G., Glagolenko, Y.V., Drojko, E.G. et al. 1996. Industrial-scale plant for HLW partitioning in Russia. *Proceedings Int Topical Meeting Nuclear Hazardous Waste Management*, *SPECTRUM'96*, American Nuclear Society, La Grange Park, IL, Seattle, WA, August 18–23, pp. 2138–2139.

443. Romanovsky, V.N**.** 1998. R&D activities on partitioning in Russia. Fifth OECD/NEA IEM on An and FP P&T, Mol, Belgium, November 25–27.

444. Romanovsky, V.N. 2002. U.S.-Russian Cooperative Program in Research and Development of Chemical Separation Technologies. In *Chemical Separations in Nuclear Waste Management.* Choppin, G.R., Khankhasayev, M.K., Plend, H.S. Eds. Battelle Press, Columbus, OH. DOE/EM-0591.

445. Myasoedov, B.F. 2007. Chemical treatment of high-level waste for utilization. An international spent nuclear fuel storage facility – Exploring a Russian site as a prototype. *Proc of Int Workshop*. Schweitzer, G.E., Sharber, A.C. Eds. National Academy of Sciences, Washington, DC, pp. 199–207.

446. Esimantovskii, V.M., Galkin, B.Ya., Dzekun, E.G. et al. 1992. Technological tests of HAW partitioning with the use of chlorinated cobalt dicarbollide. WM'92, Tucson, AZ, March 1.

447. Todd, T.A., Romanovskiy, V.N., Brewer, K.N. et al. 1999. Development of a universal cobalt dicarbollide solvent for the removal of actinides, cesium and strontium from acidic wastes. *Proc ISEC'99*, Barcelona, Spain, July 11–16, pp. 1345–1349.

448. Romanovskiy, V.N., Smirnov, I.V., Babain, V.A. et al. 2001. The universal solvent extraction (UNEX) process. I. Development of the UNEX process solvent for the separation of cesium, strontium, and the actinides from acidic radioactive waste. *Solvent Extr. Ion Exch.* 19 (1): 1–21.

449. Law, J.D., Herbst, R.S., Todd, T.A. et al. 2001. The universal solvent extraction (UNEX) process. II. Flowsheet development and demonstration of the UREX process for the separation of cesium, strontium, and actinides from actual acidic radioactive waste. *Solvent Extr. Ion Exch.* 19 (1): 23–36.

450. Herbst, R.S., Law, J.D., Todd, T.A. et al. 2002. Universal solvent extraction (UNEX) flowsheet testing for the removal of cesium, strontium, and actinides elements from radioactive, acidic dissolved waste. *Solvent Extr. Ion Exch.* 20 (4–5): 429–445.

451. Herbst, R.S., Law, J.D., Todd, T.A. et al. 2003. Development of the universal extraction (UNEX) process for the simultaneous recovery of Cs, Sr, and actinides from acidic radioactive wastes. *Sep. Sci. Technol.* 38 (12&13): 2685–2708.

452. Todd, T.A., Batcheller, T.A., Law, J.D., Herbst, R.S. 2004. Cesium and strontium separation technologies literature review. INEEL/EXT-04-01895.

453. Smirnov, I.V., Babain, V.A., Shadrin, A.Yu. et al. 2005. Extraction of americium and europium by diphosphine dioxides and their mixtures with chlorinated cobalt dicarbollide. *Solvent Extr. Ion Exch.* 23 (1): 1–21.

454. Law, J.D., Herbst, R.S., Peterman, D.R. et al. 2005. Development of a regenerable strip reagent for treatment of acidic, radioactive waste with cobalt dicarbollide based solvent extraction processes. *Solvent Extr. Ion Exch.* 23 (1): 59–84.

455. Romanovskiy, V.N., Smirnov, I.V., Babain, V.A. et al. 2005. UNEX-process. State of the art and outlook. Proc GLOBAL 2005, Tsukuba, Japan, October 9–13. Paper No. 353.

456. Romanovskiy, V.N., Babain, V.A., Alyapyshev, M.Yu. et al. 2006. Radionuclide extraction by 2,6-pyridinedicarboxylamide derivatives and chlorinated cobalt dicarbollide. *Sep. Sci. Technol.* 41 (10): 2111–2127.

457. Bond, A.H., Chiarizia, R., Huber, V.J. et al. 1999. Synergistic solvent extraction of alkaline earth cations by mixtures of di-*n*-octylphosphoric acid and stereoisomers of dicyclohexano-18-crown-6. *Anal. Chem.* 71 (14): 2757–2765.

458. McAlister, D.R., Chiarizia, R., Dietz, M.L., Herlinger, A.W., Zalupski, P.R. 2002. Extraction of alkaline earth and actinide cations by mixture of di(2-ethylhexyl)alkylene- diphosphonic acids and neutral synergists. *Solvent Extr. Ion Exch.* 20 (4–5): 447–469.

459. Grüner, B., Plesek, J., Baca, J. et al. 2002. Crown ether substituted cobalt bis(dicarbollide) ions as selective extraction agents for removal of Cs^+ and Sr^{2+} from nuclear waste. *New J. Chem.* 26 (7): 867–875.

460. White, T.L., Peterson, R.A., Wilmarth, W.R. et al. 2003. Stability study of Cs extraction solvent. *Sep. Sci. Technol.* 38 (12&13): 2667–2683.

461. Mohapatra, P.K., Ansari, S.A., Sarkar, A., Bhattacharyya, A., Manchanda, V.K. 2006. Evaluation of calix-crown ionophores for selective separation of radio-cesium from acidic nuclear waste solution. *Anal. Chim. Acta* 571 (2): 308–314.

462. Yakshin, V.V., Vilkova, O.N., Tsarenko, N.A. et al. 2006. Molecular design of macrocyclic extractants for extraction and separation of alkali and alkaline-earth metals. *Russ. J. Coord. Chem.* 32 (2): 77–81.

463. Arnaud-Neu, F., Böhmer, V., Dozol, J.F. et al. 1996. Calixarenes with diphenylphosphoryl acetamide functions at the upper rim. A new class of highly efficient extractants for lanthanides and actinides. *J. Chem. Soc. Perkin Trans.* 2 (1): 1175–1182.

464. Wen, Y., Qin, Z., Liu, W. 2001. Extraction of americium(III) and europium(III) with two open chain crown ethers of amide type. *J. Radioanal. Nucl. Chem.* 250 (2): 285–289.

465. Brahmmananda Rao, C.V.S., Suresh, A., Srinivasan, T.G., Vasudeva Rao, P.R. 2003. Tricyclohexyl phosphate – A unique member in the neutral organophosphate family. *Solvent Extr. Ion Exch.* 21 (2): 221–238.

466. Matloka, K., Gelis, A., Regalbuto, M., Vandegrift, G., Scott, M.J. 2005. Highly efficient binding of trivalent f-elements from acidic media with a C_3-symmetric tripodal ligand containing diglycolamide arms. *J. Chem. Soc. Dalton Trans.* 2005 (23): 3719–3721.

467. Matloka, K., Gelis, A., Regalbuto, M., Vandegriff, G., Scott, M. 2006. C3-symmetric tripodal thio/diglycolamide-based ligands for trivalent f-element separations. *Sep. Sci. Technol.* 41 (10): 2129–2146.

468. Collins, E.D., Benker, D.E., Felker, L.K. et al. 2005. Development of the UREX + 3 flowsheet – An advanced separations process for spent fuel processing. ANS 2005 Winter Meeting, Washington, DC, November 17.

469. Adnet, J.M., Miguirditchian, M., Hill, C. et al. 2005. Development of new hydrometallurgical processes for actinide recovery: GANEX concept. Proc GLOBAL 2005, Tsukuba, Japan, October 9–13. Paper No. 119.

470. Baron, P., Lorrain, B., Boullis, B. 2006. Progress in partitioning: Activities in ATALANTE. Ninth OECD/NEA IEM on An and FP P&T, Nîmes, France, September 25–29.

471. Miguirditchian, M., Chareyre, L., Heres, X. et al. 2007. GANEX: Adaptation of the DIAMEX-SANEX process for the group actinide separation. GLOBAL 2007, Boise, ID, September 9–13.

472. Tachimori, S., Yaita, T., Suzuki, S., Rais, J. 2008. Development of CHON- extractants and proliferation resistant advanced reprocessing: ARTIST, in Japan. Proc DAE-BRNS Biennial Symp on *Emerging Trends in Separation Science and Technology*, SESTEC-2008, University of Delhi, March 12–14, pp. 18–24.

473. Morita, Y., Sasaki, Y., Tachimori, S. 2001. Development of TODGA extraction process for high-level liquid waste: Preliminary evaluation of actinide separation by calculation. Proc GLOBAL 2001, Paris, France, September 9–13.

474. Sasaki, Y., Suzuki, S., Tachimori, S., Kimura, T. 2003. An innovative chemical separation process (ARTIST) for treatment of spent nuclear fuel. GLOBAL 2003, New Orleans, LA, November 16–20.

475. Takata, T., Koma, Y., Sato, K. et al. 2004. Conceptual design study on advanced aqueous reprocessing system for fast reactor fuel cycle. *J. Nucl. Sci. Technol.* 41 (3): 307–314.

476. Song, C., Wang, J., Jiao, R. 1999. Hot test of Total Partitioning process for the treatment of high saline HLLW. In GLOBAL'99, Jackson Hole, WY, August 29 to September 3.

477. Song, C. 2000. Study on partitioning of long lived nuclides from HLLW in Tsinghua University. Proc 5th Int Symp on *Energy Future in the Asia/Pacific Region*, Beijing, China, March 27–29, pp. 89–99.

478. Kang, J., von Hippel, F. 2005. Limited proliferation-resistance benefits from recycling unseparated transuranics and lanthanides from light-water reactor spent fuel. *Science and Global Security* 13: 169–181.

479. Hippel, F. 2007. Managing spent fuel in the United States: The illogic of reprocessing. Research Report No. 3, International Panel on Fissile Materials.

480. Skarnemark, G., Andersson, S., Eberhardt, K. et al. 2005. A micro reactor for continuous multistage solvent extraction. ISEC 2005, Beijing, China, September 19–23.

481. Shimada, T., Ogumo, S., Sawada, K., Enokida, Y., Yamamoto, I. 2006. Selective extraction of uranium from a mixture of metal or metal oxides by a tri-n-butyl- phosphate complex with HNO_3 and H_2O in supercritical CO_2. *Anal. Sci.* 22 (11): 1387–1391.

482. Shimada, T., Ogumo, S., Ishihara, N., Kosaka, Y., Mori, Y. 2002. A study on the technique of spent fuel reprocessing with supercritical fluid direct extraction method (Super-DIRECT method). *J. Nucl. Sci. Technol.* Suppl. 3: 757–760.

483. Enokida, Y., El-Fatah, S.A., Wai, C.M. 2002. Ultrasound-enhanced dissolution of UO_2 in supercritical CO_2 containing a CO_2-philic complexant of tri-n-butylphosphate and nitric acid. *Ind. Eng. Chem. Res.* 41 (9): 2282–2286.

484. Lin, Y., Liu, C., Wu, H., Yak, H.K., Wai, C.M. 2003. Supercritical fluid extraction of toxic heavy metals and uranium from acidic solutions with sulfur-containing organophosphorus reagents. *Ind. Eng. Chem. Res.* 42 (7): 1400–1405.

485. Dietz, M.L. 2006. Ionic liquids as extraction solvent: Where do we stand? *Sep. Sci. Technol.* 41 (10): 2047–2063.

486. Luo, H., Dai, S., Bonnesen, P.V. et al. 2006. A striking effect of ionic-liquid anions in the extraction of Sr^{2+} and Cs^+ by dicyclohexano-18-crown-6. *Solvent Extr. Ion Exch.* 24 (1): 19–31.

487. Kolarik, Z. 2008. Complexation and Separation of lanthanides (III) and actinides (III) by heterocyclic–donors in solutions. *Chem. Rev.* 108: 4208–4252.

2 New Developments in Thorium, Uranium, and Plutonium Extraction

Vijay K. Manchanda, P.N. Pathak,
and P.K. Mohapatra
Bhabha Atomic Research Center

CONTENTS

2.1   INTRODUCTION

Two of the major consequences of neutron-induced nuclear reactions with natural uranium targets, nuclear fission and production of trans-uranium elements, have contributed significantly to the separation chemistry of actinides. Since the early days of the Manhattan Project, much of the interest centered on the separation of trace amounts of plutonium from a large excess of uranium and a moderate concentration of fission and decay products. Solvent extraction and ion exchange have played a key role in isolation, separation, and purification of uranium and plutonium, both at analytical and industrial scale. Sustained interest in improved nuclear fuel-reprocessing methods and growing concern for the fate of actinides at potential waste-disposal sites provide continuous motivation for investigating the complexation and separation behavior of actinides. Separation chemistry of actinides plays a pivotal role at different stages of the nuclear fuel cycle: (a) recovery and purification from ores, (b) chemical quality control of nuclear fuels, (c) fuel reprocessing, and (d) waste management. Apart from these applications, the actinides display a fascinating chemistry in solution (e.g., disproportionation, variable oxidation state, colloid formation, and polymerization), which provides sufficient justification for solution chemists to investigate their basic complexation and separation behavior (*1*).

Over the last six decades, a significant amount of work has been done in this area of nuclear science and technology. In the present review, an attempt has been made to highlight the recent developments in this branch of science concerning the actinide elements with special reference to thorium, uranium, and plutonium, specific isotopes of which are being used as fissile/fertile materials.

2.2   BASIC CHEMICAL PROPERTIES

Actinides, particularly the lighter ones, display multiple oxidation states and complex chemical behavior, which makes their chemistry quite fascinating. Some isotopes of these elements, such as ^{232}Th, ^{233,235,238}U, and ^{239}Pu, are important for the nuclear industry due to their utility as fissile/fertile materials. Therefore, the separation chemistry of different oxidation states of Th, U, and Pu need to be reviewed with respect to both basic as well as applied aspects. Some fundamental chemical properties of the lighter actinides, including oxidation states, hydrolysis, and complexation characteristics form the basis of their separation.

2.2.1   Oxidation States

In spite of considerable similarities between the chemical properties of lanthanides and actinides, the trivalent oxidation state is not stable for the early members of the actinide series. Due to larger ionic radii and the presence of shielding electrons, the 5f electrons of actinides are subjected to a weaker attraction from the nuclear charge than the corresponding 4f electrons of lanthanides. The greater stability of tetrapositive ions of actinides such as Th and Pu is attributed to the smaller values of fourth ionization potential for 5f electrons compared to 4f electrons of lanthanides, an effect that has been observed in aqueous solution of Th and Ce (*2*). Thus, thorium

exists in the aqueous phase only as Th(IV), whereas the oxidation state 3+ becomes dominant only for elements after plutonium. All the oxidation states are well known except the rare 7+ states for Np and Pu (*3*). The actinide ions in the 7+ oxidation state behave as very strong acids and are immediately hydrolyzed to oxoanions, such as MO_5^{3-}. The chemistry of Pu is particularly interesting in view of its ability to coexist in four different oxidation states: 3+, 4+, 5+, and 6+. Penta- and hexavalent actinide ions exist in acid solution as the oxygenated cations, MO_2^+ and MO_2^{2+}, which are remarkably stable. The subsequent discussion is broadly restricted to the extraction behavior of only tetravalent actinides such as Th(IV), Pu(IV), and hexavalent actinides such as U(VI).

2.2.2 Hydrolysis

The actinide ions in 5+ and 6+ oxidation states are prone to severe hydrolysis as compared to lower oxidation states in view of their high ionic potentials. Consequently, these oxidation states exist as the actinyl ions MO_2^+ and MO_2^{2+} even under acidic conditions, which can further hydrolyze under high pH conditions. The oxygen atoms of these ions do not possess any basic property and thus do not interact with protons. The tetravalent ions do not exist as the oxy-cations and can be readily hydrolyzed at low to moderate pH solutions. The degree of hydrolysis for actinide ions decreases in the order: $M^{4+} > MO_2^{2+} > M^{3+} > MO_2^+$, which is similar to their complex formation properties (*4*). In general, the hydrolysis of the actinides ions can be represented as follows:

$$M(H_2O)_x^{n+} \rightleftharpoons M(OH)_x^{(n-x)+} + xH^+ \tag{2.1}$$
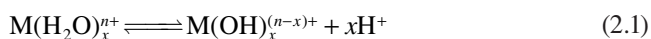
The Th^{4+} ion, due to its larger size and lower ionic potential, is quite different from other tetravalent actinide ions, as it does not undergo hydrolysis as readily as U^{4+} or Pu^{4+} ions (*5*). Tetravalent U and Pu ions hydrolyze first in a simple reaction, as given by Equation 2.1, which is followed by a slow irreversible polymerization of hydrolyzed products.

2.2.3 Complexation of Actinides

The high-oxidation state actinide ions are referred to as hard acids and exhibit strong tendency to form complexes with hard-base ligands, especially those with oxygen donor atoms. Based on the complexation behavior of actinide ions with various complexing agents and extractants, suitable separation and purification methods have been devised. An important factor that determines the strength of the complex formed is the ionic potential (or charge density) of the metal ion, which is the ratio of ionic charge to ionic radius. Higher ionic potential corresponds to greater electrostatic attraction between cations and anions, and hence stronger complexes are formed. This generalization is, however, valid only when primarily ionic bonds are formed. The complexing strength of actinide ions in different oxidation states follows the order $M^{4+} > MO_2^{2+} > M^{3+} > MO_2^+$. Similarly, for the given metal ions in the

same oxidation state, the complexing ability increases with the atomic number due to the increased ionic potential as a result of the "actinide contraction" (*6*). For anions, the tendency to form complexes with a given actinide ion generally varies in the same manner as their abilities to bind with hydrogen ion (*7*). For monovalent ligands, the complexing tendency generally decreases in the order $F^- > NO_3^- > Cl^- > Br^- > I^- > ClO_4^-$ (*8*). The divalent anions usually form stronger complexes than the monovalent anions and their complexing ability decreases in the order $CO_3^{2-} > SO_3^{2-} > C_2O_4^{2-} > SO_4^{2-}$. The complexing ability of some of the organic ligands with a given actinide ion follows the trend EDTA > citrate > oxalate > HIBA > lactate > acetate. However, factors like hybridization involving 5f orbitals, steric effects, and hydration of metal ions influence the tendency of complexation significantly for early actinides.

2.3   SOLVENT-EXTRACTION STUDIES

Organic extractants facilitate the transfer of the metal ions from the aqueous phase to the organic phase in solvent extraction. Based on the nature of the organic extractant, the metal ion, and the diluent, effective separation methods can be devised. Uranium extraction into diethyl ether from nitrate medium by salting out is perhaps one of the first uses of solvent extraction for large-scale actinide processing (*9*). In this case, ether not only acts as the diluent, it also acts as the extractant, which works according to the solvation mechanism (discussed below).

The organic extractants used for the separation of metal ions broadly fall into three classes, chelating extractants, solvating extractants, and ion-pair extractants. For the first two classes, usually nonpolar organic diluent is preferred. On the other hand, polar diluents are preferred in the case of ion-pair extraction.

 i. Chelating extractants. These extractants form chelate complexes, and many of them are weak acids. Usually, they dissociate at low pH to form anionic ligands that form strong complexes with the metal ions. Examples of this type of extraction are the extraction of Pu(IV) and Th(IV) by 2-thenoyltrifluoroacetone (HTTA) (*10*) and extraction of U(VI) by organophosphoric acid extractants such as di(2-ethylhexyl) phosphoric acid (DEHPA) (*11*), respectively. Commonly used chelating extractants such as beta-diketones, tropolones, and oximes have limited solubility in the organic diluents and hence have limited process applications. However, they are excellent analytical reagents.

 ii. Solvating extractants. Solvating extractants are widely used in the nuclear fuel cycle. Usually, the extraction of metal ions proceeds via replacement of water molecules by basic donor atoms (such as O, S, or N) of the neutral ligands. Well-known examples are the extraction of Pu(IV) and U(VI) by tri-*n*-butyl phosphate (TBP) and octylphenyl-*N,N*-di-*iso*-butylcarbamoylmethyl phosphine oxide (CMPO) from nitric acid medium (*12*).

 iii. Ion-pair extractants. This type of extraction proceeds with the formation of ion-pair species between the metal-bearing ions and counterions provided by ligands. Acidic ligands provide anions by liberating protons, which then complex with the metal cations to form an ion pair. On the other hand, basic

ligands provide cations that complex with aqueous anionic metal complexes to form ion pairs. Examples of acidic extractants are sulfonic acids (*13*), carboxylic acids (*14*), and those of basic extractants are amines and quaternary ammonium salts (*15*).

2.3.1 CHELATING EXTRACTANTS

Chelating extractants such as beta-diketones, tropolones, hydroxyoximes, and 8-hydroxyquinolines (Figure 2.1), have been used extensively for the extraction of actinide ions from moderate to weakly acidic solutions (*15–17*). Beta-diketones such as acetylacetone (acac), HTTA, benzoyl trifluoroacetone (BTFA), and dibenzoylmethane (HDBM) have been commonly used for the separation of actinide ions. The extraction mechanism involved formation of the enol form of the beta-diketone prior to complexation and extraction of the metal ion (Figure 2.2).

It is also reported that beta-diketones, such as HTTA, hydrolyze at higher pH values, leading to the formation of acetylthiophene and trifluoroacetic acid (*19, 20*). Even for the hydrolysis reaction, the formation of enolate ion was found to be an active intermediate (*19*). Limitations such as aqueous solubility, photolytic and chemical degradation, and limited solubility in the organic diluents have restricted their applications to analytical work. Favorable extraction along with strong absorption of its complex (λ_{max} = 417 nm; ε = 14,000 M^{-1} cm^{-1}) makes HDBM a useful spectrophotometric reagent for uranium analysis. HTTA is commonly employed for the analytical separations of metal ions (*21*). One of the early reports on U(VI) extraction by beta-diketones is the extraction of uranyl ion by benzoylacetone (*22*). Apart from the acid dissociation constant (pK_a) and partition coefficient of the ligand (P_L), the effectiveness of the separation is governed by the complex formation constant, partition coefficient of the metal-beta-diketonate, and kinetics of its extraction.
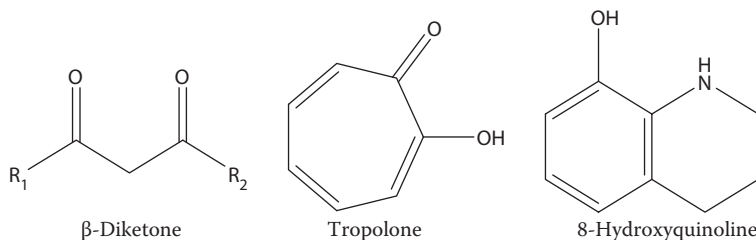
FIGURE 2.1 Structural representation of some chelating extractants.

β-Diketone   Tropolone   8-Hydroxyquinoline
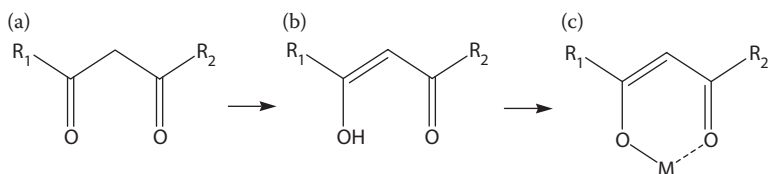
FIGURE 2.2 Structural representation of the (a) keto-form, (b) enol-form, and (c) metal complex.

As the complex formation is preceded by the acid dissociation of the beta-diketone, its pK_a value has an inverse dependence on the metal extraction efficiency (*23*), the lower the pK_a value of the beta-diketone becomes, the higher its efficiency as an extractantis. This inverse linear correlation of the pK_a of the beta-diketone with its extraction constant was reported by Batzar et al. using acyclic ligands, HTTA (Figure 2.3a), HDBM, acac, etc., for U(VI) extraction (*23*). However, these beta-diketones are capable of extracting tetravalent actinides from moderate acidic solutions and hexavalent actinides from weakly acidic solutions. They extract trivalent actinides poorly. Beta-diketones containing a heterocyclic moiety such as HPAI (3-phenyl-4-acetyl-5-isoxazolone, pK_a: 1.31; Figure 2.3b), HPBI (3-phenyl-4-benzoyl-5-isoxazolone, pK_a: 1.12; Figure 2.3b), and HPMBP (1-phenyl-3-methyl-4-benzoyl-5-pyrazolone, pK_a: 4.10; Figure 2.3c) have been employed for the extraction of actinides from acidic/complexing media. The tetravalent actinide ions are usually extracted more efficiently than hexavalent uranium (Table 2.1). The inverse linear correlation of extraction constant (log K_{ex}) with respect to the pK_a of the extractant (observed distinctly in the case of U(VI)-acyclic beta-diketones) was not observed for Pu(IV) with beta-diketones like HPMBP and HPBI, in which the heterocyclic ring contained one of the ketonic groups. It was ascribed to the increased stereochemical constraints (*24*). However, very large extraction constants of Pu(IV) with HPMBP led to the development of

R = Thenoyl; HTTA
R = Ph; BTFA

R = Ph; HPBI
R = Me; HPAI
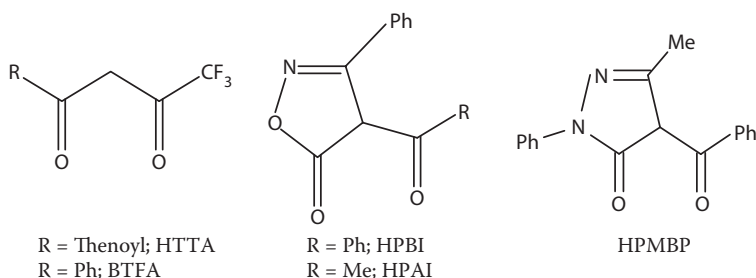
HPMBP

FIGURE 2.3　Structures of some beta-diketones used for the extraction of actinides.

TABLE 2.1

Two-phase Extraction Constants for Actinides with Several Beta-Diketones

Metal Ion	Log K_{ex}		
	HTTA	**HPMBP**	**HPBI**
pK_a	6.24	4.10	1.12
U(VI)	−2.44 (*28*)	0.63 (*27*)	1.40 (*28*)
Th(IV)	2.25 (*29*)	6.96 (*29*)	8.26 (*30*)
U(IV)	5.42 (*32*)	–	–
Np(IV)	5.68 (*32*)	–	10.11 (*34*)
Pu(IV)	7.31 (*32*)	13.75 (*33*)	10.76 (*24*)

analytical procedures for the determination of Pu(IV) in the dissolver solution of the PUREX process as well as for the separation of Pu(IV) and U(VI) in the supernatant of the oxalate conversion process (*25, 26*). Unlike the beta-diketones, which form six-membered chelate rings with the metal ions, tropolones (with two O atoms coordinating) and oximes (with one O and one N as donor atoms) form 5-membered chelate rings.

Organophosphorous acidic extractants such as DEHPA, dibutylphosphoric acid (DBP), 2-ethylhexyl phosphonic acid (PC-88A), and bis(trimethylpentyl) phosphinic acid (Cyanex-272) are employed for process applications (*36*). Their high organic-phase solubility is based on the fact that they exist predominantly in dimeric form in the organic phase. Peppard et al. have investigated the extraction behavior of tetravalent and hexavalent actinide ions using DEHPA, which exists as dimers in non-polar diluents (*11*). The extracted species for tetravalent and hexavalent actinide ions are $MY_2(HY_2)_2$ and $M(HY_2)_2$ (where Y represents the anion of monomer HY, and HY_2 the anion of dimer H_2Y_2), respectively, as depicted in the following extraction equilibria:

$$M^{4+} + 3(HY)_2 \rightleftharpoons M(HY_2)_2Y_2 + 4H^+ \tag{2.2}$$

$$MO_2^{2+} + 2(HY)_2 \rightleftharpoons MO_2(HY_2)_2 + 2H^+ \tag{2.3}$$
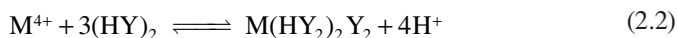
The nature of extracted species depends on the nature of the aqueous-phase acid and its concentration. Whereas $Pu(HY_2)_2Y_2$ was reported to get extracted from sulfuric acid medium, three species, $PuY_2(HY_2)_2$, $Pu(NO_3)Y(HY_2)_2$, and $Pu(NO_3)_2(HY_2)_2$, were coextracted from nitrate medium with increasing concentration of nitrate ion (*36*). The strong ability of DEHPA to extract UO_2^{2+} is utilized in the DAPEX process for the recovery of uranium from sulfuric acid leach liquors (*37*). In this process, 0.1 M DEHPA is modified with 0.1 M TBP or *iso*-decanol (to prevent third-phase formation) in kerosene. DEHPA is also used along with trinoctyl phosphine oxide (TOPO) for the recovery of U from phosphoric acid medium. Another commercially available organophosphoric acid, octylphenyl phosphoric acid (OPPA), has also been found promising for uranium recovery from phosphoric acid medium (*38*). OPPA is a mixture of dioctylphenyl phosphoric acid (DOPPA) and monooctylphenyl phosphoric acid (MOPPA). It extracts U(IV) preferentially over U(VI). Mithapara et al. studied the extraction behavior of Pu(IV) using this reagent (*39*). Several analytical applications for the recovery of U(VI) and Pu(IV) from various mineral acid solutions using DBP and PC-88A have been reported in the literature (*40–42*).

2.3.2 SOLVATING EXTRACTANTS

While pH plays an important role in the extraction of metal ions by the acidic chelating extractants, counteranions such as NO_3^-, Cl^-, etc., significantly influence the extraction of metal ions by solvating extractants (L) like TBP, TOPO, etc. The extracted species thus forms solvating species such as $MX_4 \cdot nL$ or $MO_2X_2 \cdot nL$ for tetravalent and hexavalent actinide ions, respectively, where X is a representative counteranion and *n* is the number of ligand molecules in the extracted species. In

general, n is 2 for both tetra- and hexavalent actinide ions, whereas it is 3 for trivalent actinide ions. Exceptions are seen for Th(IV) extraction at high ligand-to-metal ion concentration ratio, where species of the type $Th(NO_3)_4 \cdot 3L$ are reported. Such solvating type mechanism also operates for the extraction of tetra- and hexavalent actinides from nitrate medium using diethyl ether as well as hexone (MIBK) as the solvent. These solvents are used in the well-known BUTEX and REDOX processes originally proposed for fuel reprocessing in the early 1950s (43, 44). However, the low flash point of these solvents and the requirement of large concentrations of "salting-out" agents were found to be the drawbacks of these processes. TBP (Figure 2.4), a neutral donor ligand working according to the solvation mechanism, has been extensively used for the reprocessing of irradiated fuels in the well-known "PUREX" (Plutonium Uranium Reduction EXtraction) process. The extraction mechanism involves the following extraction equilibria:

$$Pu^{4+} + 4NO_3^- + 2TBP_{(o)} \rightleftharpoons Pu(NO_3)_4 \cdot 2TBP \tag{2.4}$$

$$UO_2^{2+} + 2NO_3^- + 2TBP_{(o)} \rightleftharpoons UO_2(NO_3)_2 \cdot 2TBP \tag{2.5}$$
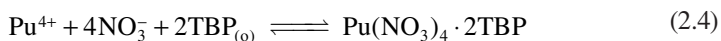
The metal ion extraction should increase with the increase in extractant concentration as well as with nitrate ion concentration. With the increasing concentration of nitric acid, beyond a point however, a decrease in metal ion extraction is observed, which is ascribed primarily to the (i) formation of anionic actinide complexes, and (ii) decrease of extractant concentration caused by nitric acid extractant complex formation. The latter is represented as:

$$TBP_{(o)} + NO_3^- + H^+ \xrightleftharpoons{K_H} TBP \cdot HNO_{3(o)} \tag{2.6}$$

where K_H is the acid uptake constant of TBP. The log K_H values for TBP and TOPO are 0.17 and 8.9, respectively (28).

The radiolytic and chemical degradation of TBP gives rise to monobutylphosphoric acid (MBP) and DBP, which are powerful extractants under low acidic conditions. As stripping in the PUREX process is carried out under such
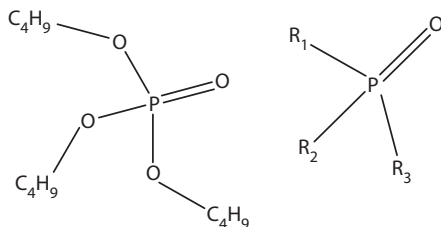
FIGURE 2.4　Structures of TBP and trialkyl phosphine oxide $R_1 = R_2 = R_3 = n$-octyl: TOPO.

conditions, the presence of MBP and DBP along with TBP adversely influences the process. Formation of synergistic species of both U(VI) and Pu(IV) involving TBP and the degradation products (such as MBP and DBP) makes the stripping of these ions more cumbersome. These degradation products also extract some fission products under PUREX feed conditions and influence the decontamination factors (DFs). TBP extracts U(VI) better at ambient temperature as compared to Pu(IV). On the other hand, it extracts Pu(IV) better at higher temperatures as compared to U(VI). This principle has been used in the improved PUREX (IMPUREX) process recommended for Pu recovery from fast reactor spent fuel (*45*). The contrasting effects of temperature on the extraction behavior are due to stronger hydration as well as more stringent stereochemical requirements of Pu(IV) as compared to U(VI).

Higher homologues of TBP were evaluated for the extraction of U(VI) and Pu(IV), and stereochemical isomers of TBP were evaluated for the separation of U(VI) from Th(IV). Triamyl phosphate (TAP) and its branched isomer triisoamyl phosphate (TiAP) have been identified as alternative extractants having very low aqueous solubility and no third-phase formation problem with plutonium (*46–48*). The effect of temperature on the extraction of U(VI) from nitric acid medium by TAP/*n*-dodecane was studied at varying extractant concentration and aqueous-phase acidity (*49*). Trialkylphosphates were also evaluated for the extraction of U(VI) and Th(IV) ions (*47*). It was observed that the distribution ratio for the extraction of Th(IV) is drastically suppressed by the introduction of branching at the first carbon atom of the alkyl group. In this context, Suresh et al. investigated the extraction of uranium and thorium by tri-*sec*-butyl phosphate (TsBP) and tri-*iso*-butyl phosphate (TiBP) (*50, 51*). Higher homologues of TBP, like tri-*n*-hexyl phosphate (THP) and tris(2-ethylhexyl) phosphate (TEHP), were reported to have higher extraction ability with reduced tendency toward third-phase formation (*52, 53*). The esters with bulkier substituents in place of the butyl group were proposed to be of practical value for the process applications in uranium and thorium separation (*54*). The limiting organic-phase concentration (LOC) of thorium in equilibrium with aqueous nitric acid-thorium nitrate was reported to decrease in the order THP > TAP > TBP. It was expected that with higher homologues like TEHP, an even better loading of thorium could be achieved without the risk of third-phase formation. Pathak et al. showed that TEHP can be a better choice for U/Th separation as compared to TBP and TsBP (*55*).

There are many other neutral organophosphorus compounds that have similar extraction mechanism, but they offer a wide range of extraction ability for the metal ions. As a matter of rule, for the neutral compounds, the extraction power increases markedly as the number of direct C–P bond increases in the series, which can be given as phosphate < phosphonate < phosphinate < phosphine oxide. TOPO (Figure 2.4) is a powerful neutral extractant for many tetra- and hexavalent actinide ions. Its use along with DEHPA for U recovery in the Wet Process Phosphoric Acid (WPPA) process is well known (*56*). Studies with mixed trialkyl phosphine oxides (TRPO) have also shown high extraction of tri-, tetra-, and hexavalent actinides from high-level waste (HLW) (*57*). The effect of nature of the mineral acid on uranium extraction has been investigated by Petkovic et al., who

reported extraction of disolvate species, with the log K_{ex} values as 8.11, 5.27, and 4.12 for HNO_3, HCl, and H_2SO_4, respectively (*58*).

Recently, another class of neutral organophosphorus compounds, namely, *N,N*-dialkyl carbamoyl methyl phosphonate (CMP) (*59*) and its phosphine oxide analog (CMPO) have received attention due to their ability to extract even trivalent actinides from acidic solutions along with the hexa- and tetravalent actinide ions. These bidentate phosphorus-based neutral extractants are reported to be stronger extractants as compared to TOPO (*59–62*). Pu(IV) and U(VI) are extracted as per the following extraction equilibria:

$$Pu^{4+} + 4NO_3^- + 2CMPO_{(o)} \rightleftharpoons Pu(NO_3)_4 \cdot 2CMPO \qquad (2.7)$$

$$UO_2^{2+} + 2NO_3^- + 2CMPO_{(o)} \rightleftharpoons UO_2(NO_3)_2 \cdot 2CMPO \qquad (2.8)$$
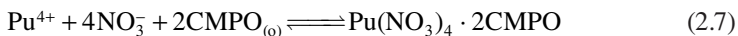
Due to the ease of formation of third phase with CMPO, many literature reports are based on the use of the mixture of 0.2 M CMPO + 1.2 M TBP as the solvent (*63*). This mixture has also been used in the TRUEX process recommended for the partitioning of minor actinides from HLW. Some applications of CMPO for the separation of Pu include its recovery from assorted laboratory wastes and oxalate supernatant (*64, 65*).

Due to several distinct advantages over TBP (see Section 2.8.2), dialkylamides are being considered as alternatives to TBP for process applications. Basic studies on the effect of the structure of *N,N*-dialkylamides with varying alkyl substituents on the carbon atom adjacent to carbonyl group, namely, di-(2-ethylhexyl)acetamide (D2EHAA), di-(2-ethylhexyl)propionamide (D2EHPRA), di-(2-ethylhexyl)isobutyramide (D2EHIBA), and di-(2-ethylhexyl)pivalamide (D2EHPVA), on the extraction of U(VI) and Th(IV) have been carried out (*66, 67*). The conditional extraction constants (K_{ex}) for uranium are found to vary in the order: D2EHAA (34.0 ± 2.0) > D2EHPRA (5.6 ± 0.4) > D2EHIBA (1.2 ± 0.1) > D2EHPVA (0.51 ± 0.03). A third phase has been observed in the case of 1 M D2EHAA (≥1 M HNO_3) and 1 M D2EHPRA (≥3 M HNO_3) in the presence of macro concentrations of thorium. The separation factor (SF = D_U / D_{Th}) for D2EHPVA is distinctly larger as compared to other amides as well as to TBP. Studies have revealed that successive alkylation of the C_c atom adjacent to the carbonyl group greatly suppresses the extraction of tetravalent actinides and fission products as compared to the hexavalent metal ions and, therefore, holds promise for the separation of U(VI) from Th(IV). Large numbers of amides were evaluated for their extraction behavior with respect to U/Th separation (Table 2.2) (*66–72*).

Vidyalakshmi et al. studied the influence of the molecular structure of amides on the extraction of uranium and nitric acid (*73*). Gupta et al. showed that from moderately acidic medium (3.5 M HNO_3), U(VI) and Pu(IV) are extracted by amides (viz. dihexylhexanamide, DHHA; dihexyloctanamide, DHOA; and dihexyldecanamide, DHDA) via the solvation mechanism similar to TBP. The log K_{ex} values for the solvated species involving amides were lower than TBP for U(VI), but higher than TBP for Pu(IV) (*74–76*). At higher nitric acid concentration, the amides undergo protonation (HAmide$^+$) and extract U(VI) and Pu(IV) as ion pairs of the type $[UO_2(NO_3)_3^-]$ [HAmide$^+$] and $[Pu(NO_3)_6^{2-}]$ [HAmide$^+$]$_2$. Thus, the amides differ from TBP (solvated species) with respect to the nature of extracted species at high acidity.

TABLE 2.2

Evaluation of Branched-Chain Amides for the Separation of ^{233}U from Irradiated ^{232}Th (*69*)
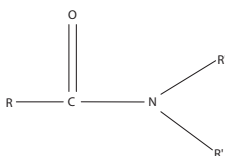
Amide	R	R'	D_U	D_{Th}	SF
D2EHIBA	$(CH_3)_2CH$	$C_4H_9CH(C_2H_5)CH_2$	3.70	1.0×10^{-2}	370
DIB2EHA	$CH_3(CH_2)_3CH(C_2H_5)$	$(CH_3)_2CHCH_2$	4.70	1.34×10^{-2}	351
DOIBA	$(CH_3)_2CH$	C_8H_{17}	5.84	1.42×10^{-2}	411
DO2EHA	$CH_3(CH_2)_3CH(C_2H_5)$	C_8H_{17}	6.58	1.85×10^{-2}	356
D2EHBA	C_3H_7	$C_4H_9CH(C_2H_5)CH_2$	8.36	6.01×10^{-2}	139
D2EHPRA	CH_3CH_2	$C_4H_9CH(C_2H_5)CH_2$	9.7	0.1	97
D2EHAA	CH_3	$C_4H_9CH(C_2H_5)CH_2$	19.10	1.12	17
DHOA	C_7H_{15}	C_6H_{13}	12.40	0.59	21
DHDA	C_9H_{19}	C_6H_{13}	11.62	0.45	26
DBDA	C_9H_{19}	C_4H_9	11.48	0.96	12
DHHA	C_5H_{11}	C_6H_{13}	12.80	0.80	16
TBP	–	–	40	4	10

Source: Pathak, P.N.; Veeraraghavan, R.; Ruikar, P.B.; Manchanda, V.K., *Radiochim: Acta*, 86, 129–134, 1999. With permission.

Note: Concentration of the extractant: 1 M; Diluent: *n*-dodecane; Aqueous phase: 4 M HNO$_3$; Temperature: 25°C; SF: D_U/D_{Th} (using ^{233}U / ^{234}Th tracer only).

Ruikar et al. investigated the extraction behavior of U(VI) and Pu(IV) from 3.5 M HNO$_3$ medium with gamma-irradiated amides (*77, 78*). The distribution ratio of U(VI) decreased gradually with increased dose (up to 5×10^5 Gray) and became almost constant thereafter. By contrast, the distribution ratio of Pu(IV) decreased gradually up to 4×10^5 Gray dose and increased thereafter, indicating the synergistic effect of radiolytic products at higher dose.

Extraction of actinides has also been reported with substituted malonamides like *N,N'*-di-methyl-*N,N'*-di-*n*-butyl-tetradecylmalonamide (DMDBTDMA) (*79*), for which the extracted species for Pu(IV) and U(VI) are observed to be Pu(NO$_3$)$_4 \cdot$ 3DMDBTDMA and UO$_2$(NO$_3$)$_2 \cdot$ 2DMDBTDMA, respectively. The extraction by malonamides also suffers from a drawback of third-phase formation, necessitating the use of a modifier at higher acidity and high metal loadings. Several variants of substituted malonamides have also been used, the most promising for actinide partitioning being *N,N'*-dimethyl-*N,N'*-di-*n*-octyl-hexylethoxymalonamide (DMDOHEMA) (*80*). Another promising diamide extractant is *N,N,N'N'*-tetraoctyl-3-oxapentane-1,5-diamide (TODGA), which has been proved to be the most efficient extractant for the trivalent actinide ions from acidic media (*81–83*).

Preston et al. studied the solvent extraction and separation behavior of U(VI) and Th(IV) from sodium nitrate solutions (0.2–6.0 M), emloying a series of dialkyl sulfoxides with different structures (*84*). For the isomeric compounds of R_2SO with C_8 alkyl groups, the SFs increase in the order: R = *n*-octyl > 2-ethylhexyl, which is also the order of increasing steric hindrance of the alkyl group. For these compounds, the extracted metal complexes reported were $UO_2(NO_3)_2 \cdot 2R_2SO$ and $Th(NO_3)_4 \cdot 3R_2SO$. The extraction of Np(IV), Np(VI), Pu(IV), and U(VI) from nitric acid medium has been carried out with dibutyldecanamide (DBDA), DHDA, bis-2-ethylhexylsulfoxide (BEHSO), and CMPO using *n*-dodecane as the diluent (*85*). The order of extraction for the metal ions was CMPO > BEHSO > DHDA > DBDA. The species extracted into the organic phase were found to be the disolvate with all the extractants for hexavalent metal ions such as Np(VI) and U(VI) and also with tetravalent ions like Np(IV) and Pu(IV) in the case of BEHSO and CMPO. However, in the case of DBDA and DHDA, Np(IV) and Pu(IV) were extracted as the trisolvate species. In general, log K_{ex} (two-phase extraction constant) increased with increasing basicity of the extractants. Sato et al. had investigated the uptake of U from HCl medium using dihexyl sulfoxide (*86*). The liquid-liquid extraction behavior of plutonium(IV) from aqueous nitric acid media into *n*-dodecane by BEHSO indicated increased extraction with increasing nitric acid concentration up to 6 M HNO_3, beyond which a decrease was observed (*87*). Higher extractability of U(VI) led to the decrease in Pu(IV) extraction under loading conditions. Similar to CMPO, bifunctional carbamoyl methyl sulfoxides were also used for the extraction of actinides from acidic medium. Uranium extraction using phenyl-*N,N*-dibutylcarbamoylmethyl sulfoxide (PCMSO) from acidic nitrate media suggested no internal buffering action, as the distribution ratio values were much lower as compared to CMPO (*88*). Another report indicated no extraction of trivalent actinides, though moderate extraction of Pu(IV) and U(VI) was observed. X-ray crystal structure data has confirmed the bidentate nature of the ligand (*89*). Shukla et al. studied the

---

TABLE 2.3

Extraction Constants of some Actinide Ions from Nitric Acid Medium Using Solvating Extractants along with the Acid Uptake Constant (K_H)

		Log K_{ex}		
Extractant	**K_H**	**−Th(IV)**	**−Pu(IV)**	**−U(VI)**
TBP	0.16	−0.07	2.04	1.35
TOPO (*24*)	8.9	–	6.84	5.58 (*91*)[a]
DHOA (*76*)	0.19	1.48	3.55	1.49
D2EHIBA (*66*)	0.12	−1.62	−1.44	−0.06
DMDBTDMA (*79*)	0.32	–	5.4	2.2
CMPO (*62*)	2.0	6.61 (*92*)[a]	4.7	2.8
TODGA (*83*)	4.0	–	8.6	4.9

[a] *N,N*-diphenyldimethylCMPO in dichloromethane.

extraction behavior of Pu(IV) and U(VI) from aqueous nitric acid media using di-n-octylsulfoxide (DOSO) as the extractant (*90*). Extraction constants for some actinide ions with neutral extractants are listed in Table 2.3. It is clearly seen that TOPO has the largest extracting power among the monodentate ligands, while TODGA is the strongest extractant among the polydentate ligands.

2.3.3 EXTRACTION BY ION PAIRS

Tertiary amines and quaternary ammonium compounds have been used for the extraction of actinide ions from relatively high concentrations of acids and salts. In these cases, the ammonium compounds form reverse micelles in the organic phase (*93*). The amine solutions are necessarily pre-equilibrated with acid solutions to form anionic-exchange sites, which subsequently exchange with the anionic complexes of metal ions. These extractants are termed liquid anion exchangers. Extraction of actinides increases with the chain length of amine extractants due to increasing organophilicity, which increases the partition coefficient of the extractant and hence, the distribution ratios. Tri-n-octyl amine (TOA), trilauryl amine (TLA), and Alamine 336 have been extensively used for actinide extraction. However, tetravalent actinides form their anionic complexes readily and are better extracted as compared to hexavalent actinides. Alamine 336 is used for the recovery of U(VI) from the sulfate leach liquor as per the following extraction equilibrium:

$$2R_3N + H_2SO_4 \rightleftharpoons (R_3NH^+)_2SO_4^{2-} \tag{2.9}$$

$$2(R_3NH^+)_2SO_4^{2-} + UO_2(SO_4)_3^{4-} \rightleftharpoons (R_3NH^+)_4[UO_2(SO_4)_3^{4-}] + 2SO_4^{2-} \tag{2.10}$$
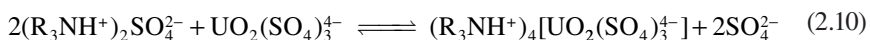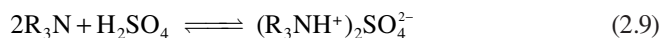
This process is termed the AMEX or PURLEX process and has better decontamination from the associated impurities as compared to the DAPEX process described above (*94, 95*). In view of its high specificity for Pu(IV) over U(VI), the TLA process has been suggested for the recovery of Pu from the spent fuel. It shows >99.9% recovery of Pu and DF > 10^3 for fission products such as Zr and Nb. Alamine 336 is recommended for the separation of trivalent actinides from trivalent lanthanides in the TRAMEX process. The extraction of hexavalent actinides using tertiary amines varies with the nature of aqueous phase acid and its concentration (*96*). The extraction of U(VI) from sulfuric acid medium is larger at low acid concentration as compared with those from HCl or HNO$_3$ medium. The relative extractability follows the trend: H$_2$SO$_4$ > HCl > HNO$_3$ at low acidity (<2 M), which changes to HCl > HNO$_3$> H$_2$SO$_4$ (>2 M). Aliquat 336 is used for separating ^{234}Th from natural U where feed contains the mixture in 6 M HCl (*30*). A report on the extraction of uranium and plutonium from hydrochloric acid solution using tri(isooctyl)amine dissolved in xylene or methylisobutyl ketone (MIBK) indicates that U and Pu are separated from thorium, alkali metals, alkaline earths, rare earths, zirconium, niobium, and ruthenium, as the latter elements do not form extractable anionic species (*97*). The extraction of Np(IV), Pu(IV), and U(VI) from aqueous hydrochloric acid into tertiary and quaternary amines such as Aliquat-336, tetraheptylammonium chloride, and Hyamine-1622 were reported to involve species such as NpCl$_6^{2-}$, PuCl$_6^{2-}$, and UO$_2$Cl$_4^{2-}$,

which was supported by absorption spectrophotometry (*98*). In another report, the extraction behavior of technetium and actinides such as thorium, uranium, neptunium, plutonium, americium, and curium from nitric acid medium was investigated using Aliquat-336 in 1,3-diisopropyl benzene as the extractant (*99*). Distribution data obtained are modeled by anion exchange (technetium) and ion-pair formation mechanisms (actinides) with the extraction of nitric acid included to account for the lowering of the free extractant concentration. Takahashi et al. developed a selective and very effective concentration method for uranium(VI) by the homogeneous liquid-liquid extraction method based on the ion-pair separation of perfluorooctanoate ion (PFOA⁻) with tetrabutylammonium ion (TBA⁺) and acetate as the complexing agent, which formed anionic U-bearing species such as $UO_2(CH_3COO)_3^-$ (*100*). There are several other reports on the ion-pair extraction of actinide ions that involved neutral donor ligands. In those studies, diluents played an important role in deciding the nature of extracted species. Mohapatra et al. studied the ion-pair extraction behavior of uranyl ion from aqueous picrate solutions (pH 3.0) employing several crown ethers such as benzo-15-crown-5 (B15C5), 18-crown-6 (18C6), dibenzo-18-crown-6 (DB18C6), and dibenzo-24-crown-8 (DB24C8) in chloroform (*101*). The stoichiometry of the extracted species corresponded to $[UO_2(\text{crown ether})_n]^{2+} \cdot [\text{pic}^-]_2$, where $n = 1.5$ for B15C5 and 1 for 18C6 as well as DB18C6. Adducts of DB24C8 could not be observed, as practically no extraction was possible using this reagent. Interestingly, in this report, trivalent lanthanides were extracted to a much larger extent than the uranyl ion. In another study, Am^{3+} was extracted to a much higher extent than UO_2^{2+} ion, when 18C6 in $CHCl_3$ was used as the extractant and picrate ion was used as the counteranion (*102*). The same authors have observed similar unusual extraction behavior of Am^{3+} and UO_2^{2+} using TBP and DOSO as extractant and picrate as the counteranion. The inner-sphere water molecules and their substitution by the oxo donor molecules appeared to influence the extraction constants of these metal ions, which was corroborated with the help of thermodynamic parameters (*103*).

2.3.4 Synergistic Extraction

"Synergism" refers to the phenomenon where the extraction of metal ions in the presence of two or more extractants is more than that expected from the sum total of the individual extractants. Though solvent extraction of actinides using a single extractant is discussed above, there are numerous applications of synergistic extraction using a combination of suitable extractants. Major advantages of the synergistic extraction include low ligand inventory and the possibility of extraction from a high concentration of acids or complexing agents. Well-known examples of synergistic extraction are the extraction of U(VI) and Pu(IV) from nitric acid medium by a mixture of a beta-diketone (such as HTTA) and neutral oxo donors such as TBP and TOPO (Figure 2.4) (*23*). A linear correlation between the adduct formation constant and ligand basicity was observed (*24*). No role of stereochemistry of auxiliary ligand (substituted amides) was observed for U(VI) extraction with primary ligands such as HTTA, HPMBP, or HPBI (*104–106*). The synergistic extraction systems are influenced by side reactions in the aqueous phase, side reactions in the organic phase, and interactions between the primary and auxiliary ligands wherein diluent plays

an important role (*107*). Dialkyl amides when used as the auxiliary ligand yielded enhancement in the extraction as predicted by their K_H values (*66*). Manchanda et al. have investigated the adduct formation of U(VI)-TTA complexes with several amine oxides and observed a combined role of ligand basicity and stereochemistry, but no significant role of back bonding from U to the π^* orbitals of the amine oxides (*108*). Subramanian et al. indicated that the adduct formation with sulfoxides is less pronounced as compared to that with phosphine oxides (*109*).

Though TBP and DOSO adducts of Pu(IV) were observed when HTTA was used as the primary extractant, no such adducts were reported with the Pu(IV)-HPMBP system (*110, 111*). On the other hand, synergism was observed for Pu(IV) extraction with HTTA, HPMBP, and HPBI (with stringent stereochemical requirements) when TOPO was used as the auxiliary ligand (*27, 33*). Other tetravalent actinide ions such as Th(IV) and Np(IV) have shown similar extraction behavior (*29, 30, 34*). Some adduct formation constants (K_s) for U(VI) and tetravalent actinide ions are listed in Table 2.4. It is necessary to consider both electronic and steric factors of the ligands to explain the observed trends.

Studies on the synergistic extraction of hexavalent uranium and hexavalent plutonium in HNO_3 medium with HTTA and HPMBP in combination with neutral donor(s), namely, diphenyl sulfoxide (DPSO), TBP, and TOPO (monofunctional) and dibutyldiethyl Carbomoyl methyl phosphonate (DBDECMP), dihexylethyl carbomyl methyl phosphonate (DHDECMP), CMPO (bifunctional), suggested a linear correlation of the equilibrium constant for the organic-phase synergistic reaction (log K_s) of both U(VI) and Pu(VI) with the basicity (log K_H) of the donor (both mono- and bifunctional) indicating bifunctional donors also behave as monofunctional. This was supported by the thermodynamic data obtained by carrying out distribution studies at variable temperatures (*112*). On the other hand, synergistic extraction of U(VI) using acylpyrazolones and crown ethers showed lower enhancements as compared to TBP as the auxiliary ligands, which was ascribed to the stereochemical effects and unusual conformations of the crown ethers (*113*).

Synergistic extraction, in the system DEHPA and TOPO, is quite interesting for its ability to extract uranium from high concentrations of phosphoric acid (*38*). This finds application in the recovery of uranium from dilute phosphoric acid medium in

TABLE 2.4

Ternary Adduct Formation Constants of Early Actinide Ions with some Beta-Diketones

	Log K_s					
	HTTA		HPMBP		HPBI	
	TBP	TOPO	TBP	TOPO	TBP	TOPO
U(VI)	5.10	7.05	4.28	6.45	5.12 (*28*)	8.70 (*28*)
Th(IV)	4.63 (*111*)	7.50 (*111*)	–	6.28 (*29*)	6.70 (*30*)	8.56 (*30*)
Np(IV)	–	5.66 (*111*)	–	–	–	7.14 (*24*)
Pu(IV)	–	4.95 (*111*)	–	3.91 (*33*)	–	4.85 (*34*)

the WPPA process, which contains about 50–200 ppm U. Usually, 0.5 M DEHPA + 0.125 M TOPO in kerosene is used for the extraction of U(VI), where the U oxidation state is adjusted by the $NaClO_3/H_2O_2$ oxidizing mixture. The stripping of U(VI) to U(IV) by Fe^{2+} is the key in this process. Stronger complexing ability of U(IV) with phosphate ion helps in transferring the extracted metal ion back to the aqueous phase in the stripping cycle. The extraction of uranium(VI) from hydrochloric acid medium with PC-88A and neutral organophosphorous donors like TBP, TOPO, and Cyanex 923 (S) in *n*-dodecane gave synergistic enhancement in the order Cyanex 923 > TOPO > TBP (*114*). The species extracted with PC-88A alone is $UO_2(HA_2)_2$, whereas with S alone, it is $UO_2Cl_2\cdot2S$, and with the synergistic mixtures it is $UO_2(HA_2)_2\cdot S$.

Otu has reported the extraction of thorium(IV) and uranium(VI) from nitric acid solutions into a synergistic extraction system containing 2-ethylhexyl phenylphosphonic acid (HEHP) and micellar dinonylnaphthalene sulfonic acid (HDNNS) (*13*). Synergistic enhancement factor of 67 and 11 were observed for Th(IV) and U(VI), respectively, from 1 M HNO_3. Although HDNNS shows better separation of thorium and uranium, the mixed ligand system exhibits superior extractability for both metals ions. Extraction studies of uranium(VI) with LIX-860 (HX represented by the chemical formula $C_{12}H_{25}(C_6H_{13})OHCHNOH$) and its mixture with Versatic-10 (HR, mixture of tertiary monocarboxylic acids containing a total of 10 carbon atoms) have indicated extraction of mixed species such as $UO_2X_2(HR)_n$, $UO_2R_2(HX)_n$, and $UO_2RX\,(HX)_n(HR)_n$ in the synergistic extraction system. The extraction efficiency changed with the nature of the diluent (*14*).

Few studies are available on synergistic extraction using amines as the primary extractant. Sriram et al. studied the distribution behavior of U(VI) from H_2SO_4 (0.1 M) using mixtures of Alamine 336 with three different neutral oxo donors, namely, DHOA, TBP, and TOPO, in several diluents (*115*). The stoichiometry of species extracted in dodecane medium was found to vary with the nature of the oxo donor. In the case of Alamine 336-DHOA mixture $\{R_3NH\}_4UO_2(SO_4)_3$, DHOA appears to dominate. Synergistic enhancement in D_U values varied in the order DHOA < TBP < TOPO, which follows the trend of their basicities. In nitrobenzene medium, antagonism was observed.

2.4   SPECTROSCOPIC STUDIES ON EXTRACTED SPECIES

Several spectroscopic techniques, namely, Ultraviolet-Visible Spectroscopy (UV–Vis), Infrared (IR), Nuclear Magnetic Resonance (NMR), etc., have been used for understanding the mechanism of solvent-extraction processes and identification of extracted species. Berthon et al. reviewed the use of NMR techniques in solvent-extraction studies for monoamides, malonamides, picolinamides, and TBP (*116, 117*). NMR spectroscopy was used as a tool to identify the structural parameters that control selectivity and efficiency of extraction of metal ions. ^{13}C NMR relaxation-time data were used to determine the distances between the carbon atoms of the monoamide ligands and the actinides centers. The ^{1}H, ^{2}H, and ^{13}C NMR spectra analysis of the solvent organic phases indicated malonamide dimer formation at low concentrations. However, at higher ligand concentrations, micelle formation was observed. NMR studies were also used to understand nitric acid extraction mechanisms. Before obtaining conformational information from ^{13}C relaxation times, the stoichiometries of the

extracted species were established. This helped in assigning the NMR spectra to the monoamides and to understand the fast-exchange process. Similarly, the exchange reactions of TBP and CMP in U(VI)-nitrato complexes with TBP or CMP were studied by ^{31}P NMR spectroscopy in solvents like CD_3COCD_3 and CD_2Cl_2 solvents (*118*). The number of TBP molecules coordinated to uranyl nitrate was determined to be 1 in CD_3COCD_3 and 2 in CD_2Cl_2 by ^{31}P NMR signals of free and coordinated TBP. Similarly, the number of coordinated CMP was evaluated as 1 in CD_3COCD_3. The exchange rate of TBP in U(VI)-TBP was independent of the free TBP concentration, whereas that in U(VI)-CMP was dependent on free CMP concentration.

May et al. investigated the extraction behavior of U(VI), U(IV), Np(IV), and Pu(IV) complexation with dibutyl phosphoric acid (HDBP) in 30% TBP/organic diluent solutions (*119*). Spectroscopic analysis of organic phases by ^{31}P NMR, absorption spectroscopy, and Extended X-ray Absorption Fine Structure Spectroscopy (EXAFS) indicated that U(VI) formed a range of complexes with HDBP. At comparatively high HNO_3 loading in the organic phase, HDBP can displace TBP groups to form either $UO_2(NO_3)_2(HDBP)(TBP)$ or $UO_2(NO_3)_2(HDBP)_2$. At lower HNO_3 loadings, HDBP can also deprotonate and act as a chelate ligand, displacing nitrates to form either $UO_2(DBP)_2(HDBP)_x$ or $UO_2(NO_3)(DBP)(HDBP)_x$ (where $x = 1$ or 2). Distribution data and absorption spectroscopy also indicated that Np(IV) formed at least two complexes in which nitrate groups are displaced by the DBP$^-$ anion. In contrast, for U(IV), it is almost certain that TBP groups are displaced by HDBP at increased HDBP loading, forming $U(NO_3)_4(HDBP)(TBP)$. However, there was no evidence for the displacement of nitrates. Pu(IV) distribution data suggested that complex reactions were taking place in both the phases. Nevertheless, HDBP does readily complex with Pu(IV), displacing nitrates from the Pu(IV) species formed in the organic phase. IR and visible spectra of $UO_2(NO_3)_2 \cdot 2DHOA$ isolated from the organic phase confirmed the formation of a single inner-sphere complex where the metal amide coordination was through the carbonyl oxygen of DHOA. The Proton Magnetic Resonance (PMR) spectra indicated the existence of restricted rotation around the C-N bond (*120*). Subramanian et al. suggested similar restricted rotation around the C-S bond in synergistic complexes of the type $UO_2(beta\text{-}diketone)_2 \cdot DOSO$. The bidentate nature of both beta-diketones in these complexes was confirmed by PMR and IR spectral studies (*121*).

Shifts in the asymmetric stretching frequencies of N-O group (amine in oxides), S-O group (in sulfoxides), and P-O (in phosphine oxides) were correlated with the adduct formation constants in the organic phase (*121–124*). IR spectroscopy was used to identify the coordination of nitrate groups to metal cations and of the extractant molecules. Ruikar et al. described a method for the quantitative estimation of some organic extractants such as TBP, DOSO, and dibutyldecanamide (DBDA) (*125*). These studies indicated that Beer's law was obeyed in the concentration range of 0.01–0.2 M. The method was applied for the determination of amide contents of irradiated di-*n*-alkylamides.

2.5 THIRD-PHASE FORMATION STUDIES

The term "Third-Phase Formation" in solvent extraction refers to a phenomenon in which the organic phase splits into two phases (*126*). One of the two phases is diluent rich, whereas the other is rich in extractant and also contains the metal solvate. Third-

phase formation behavior of any extractant for a particular metal ion under a specified condition is expressed in terms of LOC. This refers to the concentration of the metal ion in the organic phase beyond which the organic phase splits into two phases.

TBP forms a third phase during the extraction of tetravalent metal ions such as Pu(IV), U(IV), and Th(IV). The formation of a third phase during countercurrent extraction may lead to "flooding," severely affecting the hydrodynamics of the processes. Also, accumulation of a Pu-rich third phase may lead to a criticality problem. The conditions leading to the formation of third-phase must be avoided in solvent-extraction processes. Major factors that affect third-phase formation are (i) organic-phase composition (nature and concentration of diluent and extractant concentration), (ii) aqueous-phase composition, and (iii) temperature. Extensive studies have been carried out to understand the third-phase formation phenomenon for different organophosphorous extractants like TBP, TAP, TsBP, tricyclohexyl phosphate (TcyHP), diamylamyl phosphonate (DAAP), CMPO, amines, etc., under different experimental conditions (*127–133*). Rao et al. reported that during Th(IV) extraction with trialkyl phosphates like TBP and TAP, the LOC values (a) increased with extractant concentration and the carbon chain length of the alkyl group, and (b) decreased with increased aqueous-phase acidity. Comparison of the third-phase formation behavior of Th(IV) with Pu(IV) showed that the problem of third-phase formation is more severe with the former than with the latter. Recently, it was observed that TcyHP formed a third phase during the extraction of U(VI), which is not reported during the extraction with TBP (*132*). No third phase is observed during the extraction of uranium during reprocessing of the spent nuclear fuel from thermal reactors due to the presence of low concentrations of Pu in the feed solutions. However, during the fast-reactor fuel reprocessing, one has to optimize the conditions to avoid third-phase formation in view of the relatively larger concentration of Pu in the feed solutions.

It was observed that third-phase formation is almost instantaneous in trialkyl phosphates and in amine systems. By contrast, Gasparini reported that third phase formation in the case of dialkyl amides is kinetically slow (*134, 135*). Among the amides studied, *N,N* dihexyl derivatives of *n*-hexanamide (DHHA), *n*-octanamide (DHOA), and *n*-decanamide (DHDA) were identified as suitable candidates for actinide extraction (*74–76*). The LOC value of Pu(IV) in DHOA-*n*-dodecane system increased from 0.12 mol/L (at 1 M HNO_3) to 0.2 mol/L (at 3.3 M HNO_3); thereafter the value decreased gradually to 0.055 mol/L at 7 M HNO_3 (136). This variation in the trend can be due to the change in the proportions of the extractable species like $Pu(NO_3)_4 \cdot 2DHOA$, $HNO_3 \cdot DHOA$, and $[Pu(NO_3)_6]^{2-}[HDHOA]_2^+$ with varying aqueous-phase nitric acid concentration. At lower nitric acid concentrations (0.5–1 M), the third phase appeared in the form of crud, which can be attributed to the extensive aggregation of the extractable species in the organic phase (137–141).

Unlike the TBP system, third phases appear in the amide extraction system under high uranium loading conditions (*75*). The LOCs for U(VI), using 1 M DHHA and 1 M DHOA in *n*-dodecane obtained as a function of equilibrium nitric acid concentration of the aqueous phase (1–8 M) at 25°C, were measured. The LOC values for both amides decreased regularly with nitric acid molarity in the aqueous phase. The LOC value ranged from 0.37 mol/L (at 1 M HNO_3) to 0.088 mol/L (at 6.6 M HNO_3) for

DHHA and 0.43 mol/L (at 1 M HNO$_3$) to 0.17 mol/L (at 7.7 M HNO$_3$) for DHOA. The effect of nitric acid on the LOC of uranium was explained as due to the competition of amide for HNO$_3$ and UO$_2$(NO$_3$)$_2$ molecules. Uranium loading capacities of 1 M solutions of the amides in *n*-dodecane at 3.0 M HNO$_3$ are evaluated to be 0.29 mol/L for DHHA and 0.40 mol/L for DHOA. Apart from the influence of nitric acid, the influence of NaNO$_3$, temperature, and ionic strength was also studied on the LOC of uranium.

Recently, Jha et al. reported that straight-chain amides showed an increase in Th-LOC values with the total number of carbon atoms and the carbon chain length on the carbonyl group (*142*).

The LOC values for Th(IV) for DHOA, DHDA, and TBP as the extractants were marginally higher in *n*-dodecane as compared to normal paraffinic hydrocarbon (NPH). The LOC data in the U(VI)-DHDA/*n*-dodecane system indicated no definite trend from 0.5 to 5 M HNO$_3$. However, no crud formation was observed at higher nitric acid concentration (from 5.5 to 8 M), and the LOC values decreased from 0.29 mol/L (at 5.6 M HNO$_3$) to 0.16 mol/L (at 8 M HNO$_3$).

Spectroscopic techniques such as visible and IR spectroscopy, EXAFS, and Small Angle Neutron Scattering (SANS) have been used for characterizing the third-phase formed during the extraction of Th(IV) and Zr(IV), and nitric acid by TBP (*137–141*). Chiarizia et al. investigated the U(VI)-HNO$_3$-TBP, *n*-dodecane system to gain insight on the coordination chemistry and structure evolution of the species formed in the organic phase before and after third-phase formation (*137, 138*). Chemical analyses, spectroscopic and EXAFS data indicate that U(VI) is extracted as the UO$_2$(NO$_3$)$_2$·2TBP adduct, whereas the third-phase species have the average composition UO$_2$(NO$_3$)$_2$·2TBP·HNO$_3$. SANS measurements on TBP solutions loaded with only HNO$_3$ or with increasing amounts of U(VI) have revealed the presence, before phase splitting, of ellipsoidal aggregates with the major and minor axes up to about 64 and 15 Å, respectively. The formation of these aggregates, very likely of the reverse micelle-type, is observed in all cases, that is, only HNO$_3$, only UO$_2$(NO$_3$)$_2$, or both HNO$_3$ and UO$_2$(NO$_3$)$_2$ (when extracted by the TBP solution). Upon third-phase formation, the SANS data revealed the presence of smaller aggregates in the light organic phase, whereas the heavy organic phase contained pockets of diluent, each with an average of about two molecules of *n*-dodecane.

Borkowski et al. studied the third-phase formation in Th(NO$_3$)$_4$ extraction from 1 M HNO$_3$ by 20% TBP in *n*-octane (*139, 140*). Chemical analyses showed that Th(IV) existed in the organic phase mainly as the trisolvate Th(NO$_3$)$_4$·3(TBP). The third phase also contains a small amount of HNO$_3$, presumably hydrogen-bonded to the trisolvate complex. SANS measurements on TBP solutions loaded with only HNO$_3$ or with increasing amounts of Th(IV) revealed the presence, before phase splitting, of large ellipsoidal aggregates with the parallel and perpendicular axes having lengths up to about 230 and 24 Å, respectively. Although the formation of these aggregates was observed in all cases, that is, when only HNO$_3$, only Th(NO$_3$)$_4$, or both HNO$_3$ and Th(NO$_3$)$_4$ are extracted by the TBP solution, the size of the aggregates is largest in the latter case. Similar observations were made during the extraction of Zr(IV) from nitric acid medium by TBP/*n*-octane (*141*). SANS study showed an increased scattering intensity with increased extraction

of $Zr(NO_3)_4$ into the organic phase, which was attributed to interactions between small reverse micelle-like particles containing two to three TBP molecules. The particles interact through attractive forces between their polar cores with a potential energy exceeding $2k_BT$. The interparticle attractions lead to the third-phase formation.

2.6 MODELING

Auwer et al. used X-ray Absorption Spectroscopy (XAS) to study various U, Np, and Pu nitrato coordination complexes of the type $AnO_2(NO_3)_2 \cdot TBP$ (*143*). No significant variation in the actinide environment was noticed across the series UO_2^{2+}, NpO_2^{2+}, and PuO_2^{2+}. Relativistic molecular orbital calculations for $(UO_2(NO_3)_2(TBPO)_2)$, $(UO_2(NO_3)_2(TBP)_2)$, $(UO_2(NO_3)_2(TMP)_2)$ (TMP is trimethylphosphate), and $(UO_2(NO_3)_2(H_2O)_2)$ using the discrete-variational Dirac-Slater molecular orbital method showed that the bonds between uranium and the ligands of these complexes have a degree of covalent character (*144*). There is a close relationship between the ligand-displacement ability in complexes of the type $(UO_2X_2L_2)$ (X = Cl, NO_3) and effective charges of atoms to be coordinated in each ligand. The strength of bond between ligands and the central uranium atom is calculated by Mulliken population analysis. From these calculated results, it was shown that the overlap population on TBP with a central uranium atom is larger than that on TMP.

Rabbe et al. applied the molecular orbital approach to establish structure-activity relationships on a database of 22 monoamides used as U(VI) nitrate extractants (*145*). Semiempirical calculations on the monoamides were carried out using the AM1 self-consistent field method. A quantitative relationship was established between the U(VI) nitrate distribution ratio and a charge parameter of the monoamide extractant. Further, it was found that predominant factors determining the extracting ability of a monoamide were of three kinds: (1) electron density of the coordinating atoms or groups, which should be as high as possible; (2) steric effects, which should be as low as possible; and (3) lipophilicity of the ligands, which should be above a minimum threshold value (*146*). Molecular mechanics calculations were done on $UO_2(NO_3)_2A_2$ complexes in order to determine the influence of steric effects on the formation of these compounds. Calculations of monoamide lipophilicity using Rekker's method showed that all the molecules of the database were lipophilic enough and, consequently, this parameter was not significantly important for the extraction of uranyl nitrate by these monoamides. In this context, assuming that the alkyl group (attached to N atom) does not influence the charge parameter, Pathak et al. used the reported values of *N,N*-dibutylacetamide, *N,N*-dibutylpropionamide, *N,N*-dibutylisobutyramide, and *N,N*-dibutylpivalamide for di(2-ethylhexyl) derivatives of acetamide (D2EHAA), propionamide (D2EHPRA), isobutyramide (D2EHIBA), and pivalamide (D2EHPVA), respectively (*66, 67*). It was observed that $\log D_U$, $\log D_{Th}$, as well as K_H varied linearly with the total electron density of the selected amides, irrespective of acidity. It appeared that the charge density accounts both for electronic as well as steric factors relevant to the branching of the alkyl substituents on the C_α atom. Dramatic changes in the actinide coordination sphere appeared when the An(VI) metal was reduced to An(IV).

Solovkin et al. constructed a model describing the kinetics and equilibrium in systems involving complexation and solvent extraction of tetravalent uranium, plutonium, and neptunium in aqueous solutions of nitric acid/sulfuric acid with a TBP-*n*-alkane mixture (*147*). Koganti and coworkers have worked extensively on the development of SIMPSEX code relevant for fuel reprocessing (*148–151*). The model is specific to mixer-settler contactors and is restricted to mass-transfer equilibrium. The code has been validated with the experimental data available in the literature. Empirical models for third-phase formation, limiting acid concentration for the prevention of Pu(IV) polymerization were developed and incorporated into the SIMPSEX code. Salting-effect models were proposed for third-phase formation behavior of U(VI), U(IV), Pu(IV), and Th(IV) in solvent-extraction systems using TBP as the extractant (*152*). Conventionally, the composition of the actinide-TBP solvate is assumed to be the same in the unpartitioned organic phase and the third-phase.

2.7   SPENT-FUEL REPROCESSING

Nuclear power constitutes about 15% of the total electricity produced worldwide (350 GWe) (*153*). In all, 30 countries are engaged in this activity with about 450 nuclear power reactors currently in operation. The extent of occurrence of uranium in nature would have set the limit for growth of the nuclear energy, as is the case with other fossil fuels like coal and oil. However, the possibility to synthesize ^{239}Pu and ^{233}U overcame this limitation. These fissile materials are produced in nuclear reactors by the irradiation of naturally occurring uranium and thorium. These fissile isotopes can be recovered from the spent nuclear fuel or especially irradiated targets. Nuclear-fuel reprocessing is the operation of recovering the nuclear-grade uranium and plutonium from the spent fuel, which is a complex chemical/radiological mixture containing isotopes of more than 30 elements at varying concentrations. Reprocessing is an important element for the long-term global nuclear power scenario, which is the major motivation to develop novel schemes for the separation of thorium, uranium, and plutonium from other elements with high DFs. Spent fuel produced worldwide up to 1997 was around 200,000 t, and it is expected to reach 340,000 t by the year 2010 (*153*). However, out of this, only about 80,000 t has been reprocessed so far. France and the UK are the leading nations engaged in fuel reprocessing and recycling of uranium and plutonium.

Salient features of any fuel-reprocessing scheme are:

a. Sufficient cooling of spent fuel to allow decay of short-lived fission products
b. Quantitative recovery of U and Pu
c. High DFs (with respect to the fission products and structural materials) to ensure nuclear purity of U and Pu
d. Remote control operations to avoid personnel exposure

It is desirable to install specially designed reprocessing equipment behind massive concrete shielding (sometimes as much as 1.5 m thick) to protect personnel from

high radiation fields. Another important difference between traditional and nuclear chemical engineering is the need to provide a design that precludes criticality accidents caused by the presence of sufficient fissile material above certain concentration and in certain physical states/shapes.

2.7.1 PUREX PROCESS AND RECENT DEVELOPMENTS

The PUREX process is based on the extraction of Pu(IV) and U(VI) as $Pu(NO_3)_4 \cdot 2TBP$ and $UO_2(NO_3)_2 \cdot 2TBP$ complexes from moderate nitric acid (~3 M) (*154–162*). Most of the other elements in monovalent, divalent, trivalent, and pentavalent states do not form sufficiently strong neutral nitrate complexes that can be made organophilic by TBP. Mutual separation of U and Pu is achieved by reducing Pu to Pu(III) without affecting the oxidation state of U. Back-extraction of U is carried out by contacting the organic phase with the aqueous phase of low nitrate concentration. Solvent needs to be freed from the degradation products, and Na_2CO_3 has always been used for this. The salient features of the PUREX process are:

1. Decladding/dissolution of spent fuel in concentrated nitric acid
2. Feed adjustment [oxidation state of Pu to Pu(IV)]
3. Co-extraction of U(VI)/Pu(IV) with 30% TBP/*n*-dodecane as solvent
4. Scrubbing of fission products
5. Partitioning of Pu by reduction to Pu(III)
6. Back-extraction of uranium
7. Purification cycle for Pu
8. Purification cycle for U
9. Regeneration/recycle of the solvent
10. Pu and U reconversion to their oxides
11. HLW (raffinate of the coextraction cycle) disposal

The aim of the extraction step is to separate U and Pu together from fission products. After adjustment of the composition of the dissolver solution, it is fed to the center of a pulse column, which may have an extraction as well as scrub section. The nuclear industry has made significant contributions in the development of liquid-liquid contactors for the separation of one or more solutes from feed solutions, wherein they provide a more economical alternative compared to other unit operations. The various equipment that is used can be broadly classified into three categories: (1) mixer-settlers; (2) liquid pulsed sieve-plate columns; and (3) centrifugal contactors. Each one has its own merits. Mixer-settlers score over the other contactors in their simple design and reliable operation over a wide range of process conditions. Recently, air-pulsed mixer-settlers of different designs are also in use in the fuel-reprocessing industry (*163*). A solvent stream, 30% TBP-*n*-dodecane is fed at the bottom of the contactor, and a stream of 2–3 M scrub solution of HNO_3 enters the contactor from the top. U and Pu are extracted together by the solvent stream; the scrub stream eliminates most of the fission products co-extracted with U and Pu. A high loading of U in the solvent phase helps to reduce the extraction of fission products (as the available free TBP concentration decreases). On the other hand, a very high U

loading decreases the extraction of valuable Pu. Therefore, an optimum saturation of 60–80% is generally preferred.

The loaded and scrubbed solvent, containing U and Pu from the extraction/scrub column, is taken to the partitioning contactor, where U and Pu are separated from each other. Back-extracting Pu from the TBP phase achieves this by reducing it to a trivalent state with U(IV)-hydrazine. The aqueous Pu(III) stream is scrubbed by TBP to remove the excess U(IV), which has sufficient extractability in the TBP phase. An aqueous scrub with U(IV) and hydrazine in dilute nitric acid is introduced from the top of the column to remove the residual Pu from the U-bearing organic phase that leaves the column from the top. The U-bearing organic stream is stripped of U in the strip contactor using dilute nitric acid (0.01 M). Low acidity helps the stripping of U. The organic feed contains some HNO_3, which increases the acidity of the aqueous stream. After this cycle, the solvent is generally sent for Na_2CO_3 washing to remove the degradation products of TBP.

The aqueous U product with trace-level impurities is taken to evaporators for concentration, and after conditioning at 1 M HNO_3, U(IV)-hydrazine is added to reduce Pu(IV) to Pu(III), and then it is fed to the compound contactor where U is again extracted by TBP to a higher saturation level. Pu(III) and fission products remain in the aqueous phase. The loaded solvent is stripped in another column with 0.01 M HNO_3. The final U product is concentrated and precipitated as ammonium diuranate, filtered, and calcined to get UO_2. After the separation from the bulk of the U in the first cycle, the Pu stream is once again passed through a solvent-extraction cycle to remove the traces of U and fission products present, as well as to obtain the desired product concentration required for precipitation. Here, 20% TBP is preferred as extractant, as the feed is devoid of bulk U. As an alternative, final purification is sometimes carried out by an anion-exchange process (*164*). The final Pu product is precipitated as plutonium(IV) oxalate, filtered, and calcined to get PuO_2.

Table 2.5 summarizes the developments at the four major stages of the PUREX process. The success of the process is measured by the quantitative recovery (>99.9%) of U and Pu with high DFs (DF > 10^6) from the fission products and structural materials. There is also growing concern about the volumes of radioactive waste generated during fuel reprocessing. There have been continuous R&D efforts in radiochemical laboratories toward these ends.

As a consequence, whereas $NaNO_2$ was employed for feed adjustment of the reprocessing solution in the earlier plants, N_2O_4 is being used increasingly for this purpose today. Similarly, in the partitioning cycle, U(IV) has replaced ferrous sulfamate. The

TABLE 2.5

Developments in the PUREX Process

Stage	Original	Development	References
Feed adjustment	$NaNO_2$	N_2O_4, electrolytic	(*160*)
Co-decontamination	3 M HNO_3	5 M HNO_3, 50°C (IMPUREX)	(*45*)
Partitioning	$Fe(NH_2SO_3)_2$	U(IV)-hydrazine, electrolytic	(*164*)
Solvent treatment	Na_2CO_3	Hydrazine carbonate	(*164*)

addition of U in the process is an acceptable proposal, as it can be conveniently diverted to the uranium PUREX stream. Regeneration of solvent demands the elimination of acidic degradation products like monobutyl phosphoric acid (H_2MBP) and HDBP with an alkaline wash. In this context, commonly used Na_2CO_3 contributes significantly toward the generation of large salt volumes. Whereas electrolytic methods are becoming increasingly popular to restrict the waste volumes for the first two steps, hydrazine carbonate is a potential candidate to replace Na_2CO_3 for solvent treatment. There is also an effort to improve the PUREX process (IMPUREX) by adjusting the feed acidity to 5 M instead of 3 M and the temperature to 50°C (instead of ambient temperature) (*45*). These modifications are expected to yield Pu product with improved DF from fission products like Zr and Ru.

Ban et al. reviewed the reduction properties of several salt-free reagents for Np(VI) and Pu(IV) to choose selective reductants that reduce only Np(VI) to Np(V) for separating Np from U and Pu in TBP by reductive back-extraction (*165*). Allylhydrazine was proposed as a candidate for selective Np(VI) reduction, and it was confirmed by a batch experiment that allylhydrazine reduced almost all Np(VI) to Np(V) and back-extracted Np from the organic phase (30% TBP/*n*-dodecane) to the aqueous phase (3 M HNO_3) within 10 minutes. A continuous countercurrent experiment using a miniature mixer-settler was carried out with allylhydrazine at room temperature. At least 91% of Np(VI) fed to the mixer-settler was selectively reduced to Np(V) and separated from U and Pu.

Hydroxyurea dissolved in nitric acid can efficiently strip plutonium and neptunium from tributylphosphate (TBP) and has little influence on the uranium distribution between the two phases (*166*). The SFs of uranium/plutonium and uranium/neptunium can reach values as high as 4.7×10^4 and 260, respectively. This indicates that hydroxyurea is a promising salt-free agent for the separation of uranium from plutonium and neptunium. The hydrolysis and polymerization of Pu(IV) can cause serious problems during the aqueous processing of spent fuel and nuclear wastes, whenever acidity in the pH range is encountered. Several studies describing the liquid/liquid extraction behavior of polymeric Pu(IV) showed that poor plutonium extraction was accompanied by the appearance of an interfacial crud or third phase. Crud is an emulsion stabilized by finely dispersed solids. Insoluble residues can also be formed by the complexation of degradation products of TBP with Zr(IV) and Pu(IV) (*167*).

As a part of the Advanced Fuel Cycle Initiative (AFCI), Argonne National Laboratory has developed the Uranium Extraction Process (UREX+ process), which consists of five solvent-extraction processes that separate dissolved spent fuel into seven fractions (*168*). The five solvent-extraction processes were: (i) UREX, quantitative extraction of uranium and technetium; (ii) Chlorinated Cobalt Dicarbollide-Polyethylene Glycol (CCD-PEG), recovery of Cs and Sr; (iii) Neptunium Plutonium Extraction (NPEX), recovery of plutonium and neptunium; (iv) TRUEX: recovery of Am, Cm, and Rare Earth Element (REE) fission products; and (v) Cyanex 301: separation of Am and Cm from REEs. Under the Global Nuclear Energy Partnership (GNEP) program led by the United States, efforts are being made by countries with a developed nuclear technological base to provide safe nuclear power to other countries and to minimize proliferation concerns worldwide (*169–173*). There is a renewed international interest in the development of new separation schemes for coprocessing of U/Pu present in dissolver solution. This has an additional advantage with

respect to criticality problems. The coprocessing option appears particularly promising for the reprocessing of Pu-based fast reactor spent fuels. In this approach, the recycling of spent nuclear fuel will be done without separating out pure plutonium. This will help in nuclear nonproliferation, recovery, and reuse of fuel resources. The long-lived fission products such as ^{99}Tc and [129]I will be separated and immobilized before disposal in repositories. Short-lived fission products such as ^{137}Cs and ^{90}Sr will be allowed to decay until they meet the requirements for disposal as low-level waste. Transuranics such as Pu, Np, Am, and Cm will be separated from the fission products so that they could be fabricated into fuel for an Advanced Burner Reactor (ABR). Birket et al. reviewed the recent developments in the PUREX process for nuclear-fuel reprocessing and have recommended U/Pu coprocessing and Pu/Np costripping. Aqueous soluble simple hydroxamic acids, for example, formo- and aceto-hydroxamic acids, are very effective for the separation of uranium from neptunium and plutonium (*174–178*). The strength of interaction of the hydroxamic acids has been quantified by determination of stability constants.

Recently, straight chain *N,N*-dihexyloctanamide (DHOA) was evaluated for the coprocessing of spent nuclear fuel (*179*). Batch extraction studies suggested that DHOA is a better choice for coprocessing of spent nuclear fuel than TBP. It offers better extraction of Pu under feed conditions (4 M HNO_3) and easy stripping at 0.5 M HNO_3 without using any reducing agent. This observation was attributed to the formation of disolvated species at 0.5 M HNO_3; whereas more than two DHOA molecules were involved in the extracted species at 4 M HNO_3.

2.7.2 THORIUM FUEL REPROCESSING

In order to make use of thorium as a nuclear resource for power generation, development of efficient separation processes are necessary to recover [233]U from irradiated thorium and fission products. The THORium uranium EXtraction (THOREX) process has not been commercially used as much as the PUREX process due to lack of exploitation of thorium as an energy resource (*157, 180*). Extensive work carried out at ORNL during the fifties and sixties led to the development of various versions of the THOREX process given in Table 2.6. The stable nature of thorium dioxide poses difficulties in its dissolution in nitric acid. A small amount of fluoride addition to nitric acid is required for the dissolution of more inert thorium (*181*).

Salient features of the THOREX process are:

1. Difficulty in dissolution of irradiated thoria.
2. [233]Pa, formed by neutron capture of [232]Th, decays to [233]U with a half-life of 27.4 days. This necessitates a longer cooling period for the complete recovery of [233]U in one step.
3. The contamination due to [232]U in the recovered [233]U product leads to intense gamma radiation, which requires specially designed shielded facilities during fuel reprocessing and fuel fabrication.

The use of fluoride ion, however, enhances the corrosion of stainless steel equipment. This problem is mitigated by the addition of appropriate amounts of aluminium

TABLE 2.6

Various Schemes for the Separation of Uranium and Thorium

Process	Details	Medium	Extractant	References
Hexone – ^{233}U	Extraction of ^{233}U	Acid deficient	Hexone[a]	(182)
Interim – 23	Extraction of ^{233}U	Acidic	1.5% TBP	(183)
THOREX No. 1	Selective extraction	Acidic		(184)
	Pa		DIBC[b]	
	U		5% TBP	
	Th		45% TBP	
THOREX No. 2	Co-extraction of U and Th	Acid deficient	42.5% TBP	(185)
Acid THOREX	Co-extraction of U and Th	Acidic	30% TBP	(186)
THOREX	Extraction of ^{233}U	Acidic	5% TBP	(187)

[a]　4-Methyl-2-pentanone.

[b]　2,6-Dimethyl 4-heptanol.

(in the form of $Al(NO_3)_3$) to complex the excess fluoride, thus, limiting the concentration of free fluoride ion (188). Thorium metal dissolves without much difficulty in 10–15 M HNO_3 containing HF (~0.03 M). During the dissolution of zircaloy-clad thorium fuel, dissolution of the zirconium clad takes place to a small extent along with the thorium fuel, and this has to be taken into account during subsequent solvent-extraction steps (189). TBP has been used principally as the extractant for the selective extraction of ^{233}U over ^{232}Th. Depending on the requirement whether both thorium and ^{233}U are to be recovered or only ^{233}U is to be extracted, the concentration of TBP is judiciously chosen. TBP (5%) has been used as the extractant for the selective extraction of ^{233}U (187). Thorium and ^{233}U have been co-extracted employing 30% TBP. The coextraction of thorium and ^{233}U leads to third-phase formation (186). To avoid third-phase formation, the solvent loading of TBP phase with thorium is restricted to values much lower than that normally employed in the case of uranium. After one cycle of extraction, scrubbing, and stripping, the aqueous ^{233}U stream contains significant amounts of thorium, minor quantities of other actinides, and fission products. Three alternative methods are used for the purification of product ^{233}U.

1. Anion exchange in hydrochloric acid/acetic acid medium for selective sorption of uranium as its anionic chloride/acetate complex (190, 191).
2. Cation exchange in nitric acid for preferential sorption and removal of tetravalent thorium (192).
3. Precipitation and separation of thorium from ^{233}U as oxalate (193, 194).

Even though in the THOREX process ^{233}U can be preferentially recovered from irradiated thorium fuel by using an extraction flowsheet based on 5% TBP/*n*-dodecane as the extractant, further lowering of the concentration of TBP in the solvent has certain advantages in terms of reduced co-extraction of thorium and fission products (195, 196). Ramanujam et al. reported a sequential precipitation technique

for the separation of uranium and thorium present in the uranium product stream of a single-cycle 5% TBP THOREX process (*193*). It involved the precipitation of thorium as oxalate in 1 M HNO_3 medium at 60°C–70°C and, after filtration, precipitation of uranium as ammonium diuranate at 80°C–90°C from the oxalate supernatant. This technique offered several advantages over the ion-exchange process normally used for treating these products.

2.7.3 COMPARISON OF PUREX AND THOREX PROCESSES

Table 2.7 compares the salient features of PUREX and THOREX processes. Whereas uranium is the major component in the PUREX feed, thorium is in macro concentration in the THOREX feed solutions. U and Pu are co-extracted in the PUREX process, employing 30% TBP as extractant. Separation of U and Pu in the PUREX process is based on the conversion of Pu(IV) to Pu(III), which is poorly extracted by 30% TBP. However, Th(IV) cannot be reduced. In the THOREX process, therefore, selective extraction of U over Th is carried out using 5% TBP solution in *n*-dodecane. LOC values (g/L) of the bulk elements (i.e., U and Th) in the PUREX and THOREX processes are ~120 and 25, respectively. A scrub cycle is essential in both the processes to improve decontamination from fission products. Decay products of ^{232}U-^{228}Th (especially ^{212}Bi and ^{208}Tl) are hard gamma emitters, which necessitates additional shielding arrangements during reprocessing as compared to that needed in the PUREX process in view of the softer gammas (60 keV) emitted by ^{241}Am.

2.8 ALTERNATIVE EXTRACTANTS

2.8.1 ORGANOPHOSPHOROUS EXTRACTANTS

Though TBP is the work horse for spent fuel reprocessing, its use has shown some limitations, such as high aqueous solubility (~0.4 g/L), deleterious nature of degradation products, and the problems of third-phase formation with tetravalent Pu and Th. In the context of short-cooled fast-reactor fuel reprocessing, these drawbacks of TBP are of serious concern. There is an interest, therefore, to develop alternative extractants. Process flowsheets have been suggested with high temperature (IMPUREX Process) during extraction to avoid plutonium reflux and third-phase formation (*45*). TAP and its branched isomer TiAP have been identified as alternative extractants, having very low aqueous solubility and no third-phase formation problem with plutonium (*46–48*). The effect of temperature on the extraction of U(VI) from nitric acid medium by TAP/*n*-dodecane was studied at varying extractant concentration and aqueous-phase acidity (*49*). Extraction of uranium by TAP is an enthalpy-controlled process.

Hydrolytic and radiolytic degradation of TAP solution in normal paraffinic hydrocarbon (NPH) in the presence of nitric acid was investigated. Physicochemical properties such as density, viscosity, and phase-disengagement time (PDT) were measured for undegraded and degraded solutions (*197*). The variations in these parameters were not very different from those obtained with degraded TBP. Thus, the hydrodynamic problems expected during the solvent-extraction process with TAP would be similar to those encountered with TBP/NPH system. The influence of chemical

TABLE 2.7

Comparison of PUREX and THOREX Process

Feature	PUREX Process (PHWR fuel)	THOREX Process (J-rods in Research Reactor)
Feed composition	~300 g/L U+~1 g/L Pu+MA^a+FPs^b in 3 M HNO$_3$	~200 g/L Th+~200 mg/L U+FPs in 4 M HNO$_3$
Extractant	30% TBP in *n*-dodecane	5% TBP in *n*-dodecane
Principal radionuclide	Pu (^{239}Pu)	U (^{233}U)
Precursor of principal radionuclides	^{239}Np ($t_{1/2}$=2.3 d)	^{233}Pa ($t_{1/2}$=27 d)
Separation schemes	Co-extraction of Pu(IV) and U(VI) preferentially over MAs and FPs; scrub cycle to improve DF from FPs; partition of Pu(III) from U(VI)/U(IV)	Preferential extraction of U(VI) over Th(IV) and FPs; scrub cycle to improve DF from Th as well as FPs
LOC and stoichiometry of extracted species of the bulk elements	>120 g/L U; UO$_2$(NO$_3$)$_2$·2TBP	25 g/L Th^c; Th(NO$_3$)$_4$·3TBP
Production of long-lived minor actinides	Significant	Negligible
Radiologically important radionuclide	^{241}Pu(14.9 y)–^{241}Am (433 y)	^{233}U(72 y)–^{228}Th (2 y) decay to ^{212}Bi/^{208}Tl

^{a} Minor actinides.
^{b} Fission products.
^{c} In 1M TBP.

and radiation-induced reactions in TAP-NPH-HNO$_3$ on plutonium retention in the organic phase has also been assessed.

Even though a TBP-based THOREX process has been employed for the reprocessing of spent thorium fuels, there are certain inherent problems like third-phase formation and low SF for U/Th separation, which necessitate the development of alternative extractants. Siddall, Mason, and Griffin suggested that, in the absence of steric effects in organophosphorus ligands, the extraction of both U(VI) and Th(IV) increases as the basicity of the coordinating P = O of the neutral extractant increases (*198, 199*). However, among the homologous series of neutral phosphate, phosphonate, phosphinate, and phosphine oxide, phosphate has the least basic phosphoryl oxygen of the series and gives the largest SF for U/Th separation. In this connection, several trialkylphosphates were developed and tested for the extraction of U(VI) and Th(IV) ions (*47*). It was observed that the distribution ratio for the extraction of Th(IV) is drastically suppressed by the introduction of branching at the first carbon atom of the alkyl group.

Suresh et al. investigated the extraction of uranium and thorium by TsBP and TiBP (isomers of TBP with branched carbon chain) as an alternative choice for TBP (*47*). Higher homologues of TBP, for example, THP and TEHP, were reported to have higher extraction ability with reduced tendency toward third-phase formation (*50, 51*). The esters with bulkier substituents in place of the butyl group were proposed to be of practical value for the process applications in uranium and thorium separation (*54*). The LOC of thorium in equilibrium with aqueous nitric acid-thorium nitrate was reported to decrease in the order THP > TAP > TBP. Pathak et al. showed that TEHP can be a better choice for U/Th separation compared to TBP and TsBP (*55*).

Brahmmananda Rao et al. synthesized TcyHP, having three closed bulky aliphatic rings and compared the extraction of U(VI) and Th(IV) with those of TBP, TsBP, and THP (*132*). The distribution ratios for extraction of U(VI) and Th(IV) by TcyHP at all acidities were almost double the value for THP. One of the major drawbacks of the extraction of U(VI) and Th(IV) by TcyHP was the formation of a third-phase during extraction. Typically, the Th(IV)-LOC value at neutral acidity for 1.1 M TcyHP/*n*-dodecane was ~25 g/L, whereas that of 1.1 M TBP/*n*-dodecane was 52 g/L. The most striking observation was that the extraction of uranium by TcyHP/*n*-dodecane from neutral medium led to third-phase formation even with a loading of 3.1 g/L, whereas other trialkyl phosphates did not form a third phase at all during extraction of U(VI) under comparable conditions. However, in the process for recovery of [233]U from irradiated thorium, when the uranium concentration was in the millimolar range, the higher U/Th SFs achieved with TcyHP could prove to be an advantage.

2.8.2 N,N-Dialkyl Amides as Extractants

Since the pioneering work of Siddall, *N,N*-dialkyl amides have been evaluated extensively as alternative extractants to TBP (*200, 201*). The salient features of amides as extractants are (i) low volume of secondary waste generated (completely incinerable), (ii) innocuous nature of chemical and radiolytic degradation products (better decontamination from fission products and regeneration/clean up easier), (iii) low aqueous-phase solubility, (iv) final U and Pu products streams are free of P contamination, and (v) ease of synthesis. However, LOC values of U and Pu as well as viscosity are

unfavorable with respect to TBP. In view of the fact that physicochemical properties of amides can be tuned by the judicious choice of the alkyl groups, this group of extractants has received attention as an alternative to TBP. An increase in the chain length, particularly adjacent to the carbonyl group, improves the extraction ability and LOC of metal ions. However, it adversely influences the phase disengagement time, hydraulic behavior, and the aqueous solubility of degradation products.

Musikas and co-workers studied extensively the extraction behavior of inorganic acids and U/Pu extraction chemistry with *N,N*-dialkyl amides (*202–205*). Based on the extraction data, they proposed certain dialkyl amides suitable for the reprocessing of irradiated nuclear fuels in nitric acid media. Most of the work reported earlier on amides referred to either aromatic or substituted aliphatic hydrocarbons employed as diluents. However, these diluents are not suitable for commercial-scale reprocessing due to their poor radiation and chemical stability in the presence of nitric acid, as well as their tendency to form a three-phase system.

Recently, a systematic attempt has been made in the authors' laboratory to investigate (a) linear dialkyl amides as an alternative to TBP (as in the PUREX process) for their recovery and purification of Pu, and (b) branched dialkyl amides as alternatives to TBP (as in the THOREX process) for the recovery and purification of uranium (*66–72, 74–78*). Several dialkyl amides were synthesized and evaluated for their extraction behavior toward U(VI), Pu(IV), Am(III), and fission products from nitric acid medium employing *n*-dodecane as the diluent. *N,N*-dihexyl derivatives of hexanamide (DHHA), octanamide (DHOA), and decanamide (DHDA) were found to be promising among a large number of extractants studied. These ligands readily dissolved in *n*-dodecane and did not form third phases with nitric acid (up to 7 M). The nature of extracted species formed in the organic phase, the corresponding two-phase extraction constants, the influence of U loading on third-phase formation and on distribution data, and the effect of gamma irradiation as well as of temperature have been investigated (*74–78, 205*). Laboratory batch studies as well as mixer-settler studies were performed with DHOA and compared with those of TBP. Figure 2.5a shows the differences in the behavior of
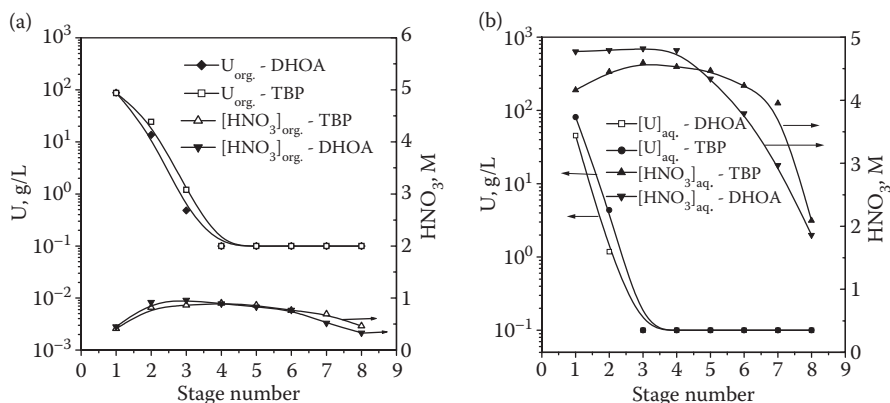
FIGURE 2.5   (a) Stage-analysis data of DHOA and TBP in uranium extraction cycle. (b) Stage-analysis data of DHOA and TBP in uranium stripping cycle. (From Manchanda, V.K.; Pathak, P.N., *Sep. Pur. Technol.*, 35, 85–103, 2004. With permission.)

the two extractants. The aqueous uranium concentration for DHOA system is lower, but the acidity is higher as compared to the TBP system at stage 1 as well as at stage 2. Whereas approximately 215 g/L U was extracted in the 1st stage for DHOA, only 180 g/L was extracted in the case of 1.1 M TBP. Figure 2.5b shows the superior stripping behavior of 1.1 M DHOA as compared to that of 1.1 M TBP.

From extensive studies with linear and branched-chain dialkyl amides, it was concluded that branched-chain D2EHIBA was a promising candidate for the separation of ^{233}U from irradiated thorium. Further distribution behavior of U(VI) and Th(IV) was studied employing 0.5 M D2EHIBA/n-dodecane as a function of nitric acid concentration in the presence of 0.05 M HF + 0.1 M Al(NO$_3$)$_3$ and 200 g/LTh. Fission-product distribution behavior has been investigated under THOREX feed conditions. Mixer-settler studies were carried out on THOREX feed solution consisting of [Th] = 200 g/L, [U] = ~210 mg/L, [HNO$_3$] = 4.0 M, [HF] = ~0.05 M, and [Al(NO$_3$)$_3$] = ~0.1 M, using 0.5 M D2EHIBA as well as 5% TBP solutions in n-dodecane as extractants (68–72).

Table 2.8 summarizes the results obtained during 12-stage mixer-settler runs carried out using 0.5 M D2EHIBA and 5% TBP on THOREX feed solution ([Th] = 207 g/L, [U] = 202 mg/L, [HNO$_3$] = ~4 M, [HF] = ~0.01 M, and [Al(NO$_3$)$_3$] = ~0.1 M). Loss of uranium to the raffinate is significantly lower in the case of 0.5 M D2EHIBA (1%) than in the case of 5% TBP (5%).

It is clear that significant decontamination of U over Th is achieved in the case of 0.5 M D2EHIBA as compared to that of 5% TBP [DF ~1.2 × 10^3 (0.5 M D2EHIBA) and ~40 (5% TBP)]. In view of higher extractant concentration in the case of D2EHIBA (0.5 M), acid uptake is significantly larger than that of 5% TBP (0.18 M).

TABLE 2.8

Comparison of Performance of 0.5 M D2EHIBA with 5% TBP During Mixer-Settler Runs

Parameter	0.5 M D2EHIBA	5% TBP (0.18 M)
Uranium loss (%)	1%	5%
Thorium uptake (g/L)	0.18	5.9
Acid uptake (M)	0.4	0.17
	After Stripping	
[U]$_{org.}$ (mg/L)	Not detected (<1)	5
[Th]$_{org.}$ (mg/L)	Not detected (<1)	16
[HNO$_3$] (M)	0.03	0.005
DF[a]	~1.2×10^3 (~10^6)	~40

Source: Pathak, P.N.; Prabhu, D.R.; Kanekar, A.S.; Ruikar, P.B.; Bhattacharyya, A.; Mohapatra, P.K.; Manchanda, V.K., *Ind. Eng. Chem., Res.* 43, 4369–4375, 2004. With permission.

Note: Number in bracket refers to overall DF of U over Th; Strippant: distilled water.

[a] After extraction cycle.

2.9   NOVEL TECHNIQUES

Solvent-extraction processes are extensively employed in hydrometallurgy opera-tions for the recovery of metal ions at industrial scale (in quantities larger than kilo-grams). However, a major problem associated with this technique is the generation of large volumes of secondary waste and handling of large volumes of inflammable diluents. At times, the extractant cost may be too high to permit its use in large-scale solvent-extraction processes. It is, therefore, imperative to look for alternative tech-niques where the ligand inventory is lower, particularly when the metal quantities involved are in the grams/milligrams range. In this connection, several techniques like Hollow fiber supported liquid membrane (HFSLM), Magnetically Assisted Chemical Separation (MACS), and Extraction Chromatography (EC) are being evaluated for the recovery of metal ions from relatively lean solutions (*206–214*). All these techniques are based on metal ion solvent-extraction data.

2.9.1   EXTRACTION CHROMATOGRAPHY

The EC technique combines the versatility of solvent-extraction and chromato-graphic techniques. However, one important difference between solvent-extraction and chromatography processes is the change in the activities of the extractant and the extracted complex due to the influence of the EC support. Another difference is the non-attainment of the thermodynamic equilibrium when EC is performed in a column. These differences do not influence the chemical steps of transfer of the sol-ute from one phase to another (*214*). Traditionally, the final purification of ^{233}U and Pu products in the reprocessing of Th/U-based spent fuel has been achieved by ion-exchange chromatography. The recent developments in EC technique include evalu-ation of new extractants for the uptake of actinides from different aqueous media. This technique can be particularly useful for the treatment of low actinide activity levels in effluent streams. Currently, the emphasis is on the chemical grafting of the extractant molecules on solid supports to enhance the stability of the extraction-chromatographic resin material.

Madic and coworkers have carried out a pilot-scale investigation to evaluate the possible application of the extraction-chromatographic method for the partitioning of alpha emitters from liquid wastes emanating from a fuel-reprocessing facility, with an aim to obtain pure AmO_2, which can be used for alpha, gamma, and neutron sources (*215*). The process developed for alpha partitioning had two steps: (i) the extraction of macro amounts of uranium with 30% TBP in dodecane in mixer-set-tlers, and then (ii) coextraction of ^{237}Np, ^{239}Pu, and ^{241}Am by EC on a macro column filled with di-*n*-hexyloctoxymethylphosphine oxide sorbed on an inert support. In each run, about 200 L of initial waste were decontaminated from alpha emitters. The loading step was followed by selective elution of americium, neptunium, and plu-tonium. Silica gel was used as an inert support for the extraction-chromatographic separation of actinides and lanthanides from HNO_3 and synthetic HLW solutions (*216*). Using CMPO impregnated silica gel, high sorption of Pu, Am, and U was obtained from the U-depleted HLW solution. These metal ions were subsequently eluted using different eluents. Similarly, Cyanex 923 sorbed on Chromosorb-W was

used as the stationary phase in the extraction-chromatographic separation of actinide ions from simulated HLW (devoid of uranium) (*212*). The uptake behavior of U(VI), Pu(IV), Am(III), and Fe(III) was studied batch. Schulte et al. evaluated the application of the EC technique to actinide decontamination from hydrochloric acid effluent streams to reduce the loss of radioactivity to the environment and the hazard of the associated solid waste (*217*).

The chemical anchoring of the extractant molecule with the polymeric matrix of the resin beads can overcome the problem of loss of impregnated extractant from the pores of the solid support. Recently, Ansari et al. reported a novel malonamide grafted polystyrene-divinyl benzene resin for extraction, preconcentration, and separation of actinides (*218, 219*). The grafted resin exhibited stronger binding for hexavalent and tetravalent actinides such as U(VI), Th(IV), and Pu(IV) over trivalent actinides, namely, Am(III) and Pu(III). Batch studies on solid-phase extraction performed over a wide range of acid solution (0.01–6 M HNO_3) revealed that the components of a ternary mixture of uranium, americium, and plutonium or thorium, americium, and plutonium could be separated from each other at 1 M HNO_3. Desorption of U(VI), Pu(IV), and Am(III) from the loaded resin was efficiently carried out using 0.1 M α-HIBA, 0.25 M oxalic acid, and 0.01 M EDTA, respectively. Quantitative preconcentration of actinide ions such as Th(IV) and U(VI) was possible from 3 M HNO_3 solution. The practical utility of the grafted resin was evaluated by uranium sorption measurements in several successive cycles. The sorption efficiency of the resin with respect to uranyl ion remained unchanged even after 30 days of continuous use. The surface morphology of the resin was monitored with the help of scanning electron microscopy (SEM).

Subramanian and coworkers developed polymeric sorbents using different support materials (such as Merrifield chloromethylated resin, Amberlite XAD 16) and complexing ligands (amides, phosphonic acids, TTA), and evaluated their binding affinity for U(VI) over other diverse ions, even under high acidities. The practical utility of these sorbents was demonstrated using simulated waste solutions (*220–222*). Shamsipur et al. reported the solid-phase extraction of ultra trace U(VI) in natural waters using octadecyl silica membrane disks modified by TOPO (*223*). The method was found satisfactory for the extraction and determination of uranium from different water samples.

2.9.2 Supercritical Fluid Extraction (SFE)

The last two decades have seen an increased interest in the use of supercritical fluids in separation science. Supercritical CO_2 has often been employed as a naturally occurring medium for the separation, purification, and determination of organic substances in environmental samples. However, there are only limited reports on the use of supercritical fluid as solvent in the separation of metal ions from solutions as well as various solid matrices. The supercritical fluid extraction (SFE) technology offers several advantages over conventional solvent-based methods, including the ability to extract radionuclides directly from solids, easy separation of solutes from CO_2, and minimization of waste generation. It can easily be removed from the extracted substances by degasification under atmospheric pressure and temperature.

As supercritical fluid is able to dissolve analytes directly from solid materials, sample dissolution is not a necessary condition for SFE.

In the nineties, Wai et al. initiated the work on the separation of lanthanides and actinides through a supercritical fluid route (*224–228*). Supercritical fluid carbon dioxide (SF-CO_2) is capable of extracting radionuclides including cesium, strontium, uranium, plutonium, and lanthanides directly from liquid and solid samples with proper complexing agents (*229–233*). Of particular interest is the ability of SF-CO_2 to dissolve uranium dioxide directly using a CO_2-soluble TBP-HNO_3 extractant to form a soluble $UO_2(NO_3)_2(TBP)_2$ complex that can be separated from Cs, Sr, and other transition metals (*234–236*). This method has also shown promise to dissolve plutonium dioxide in SF-CO_2. Direct extraction of metal ions by supercritical fluid is highly inefficient primarily because of the charge-neutralization requirement and weak solute-solvent interactions. However, when metal ions are bound to organic ligands, they may become quite soluble in supercritical CO_2. Similar to the conventional solvent extraction, solvating/chelating extractants are employed to facilitate the dissolution of metal ion in supercritical fluid. The basic requirements for SFE are (i) supercritical fluid must be able to dissolve both ligand and metal complex in sufficient quantities, (ii) ligand must be able to access the metal ion present in the sample, and (iii) metal complex must be transported in supercritical fluid without significant decomposition. Efficient extraction also requires good control over temperature and pressure of supercritical fluid. Table 2.9 lists some of the recent studies on U(VI) and Th(IV) using different extractants as modifiers. Trofimov et al. investigated the effects of calcination temperatures on the dissolution of individual actinide oxides from mixtures, as well as of solid solutions U-Pu, U-Np, U-Am, and U-Pu-Eu oxides in SF-CO_2 containing the TBP-HNO_3 complex (*248*). The effect of the calcination temperature of solid solutions of dioxides on the separation of actinides during SFE was also studied. It was shown for the first time that milligram amounts of uranium oxide could be quantitatively dissolved in SF-CO_2 containing TBP-HNO_3 and efficiently separated from Pu, Np, and Th during SFE of mechanical mixture of these oxides (*249*). However, both U and Pu are quantitatively dissolved in SF-CO_2 containing TBP·HNO_3 during SFE from solid solutions of U-Pu dioxide. An increase of the calcination temperature of the mixed U(IV)-Pu(IV) oxide from 850°C to 1200°C showed no influence on the relative extraction yield of these actinides during SFE. It is found that uranium and plutonium are directly extracted from unirradiated mixed oxide (MOX) fuel by SF-CO_2 containing TBP-HNO_3 (*250*). It is likely that it is easier to directly extract uranium and plutonium from irradiated than unirradiated fuel. Studies are underway on the Super-DIREX process for reprocessing of spent fuel, which has shown high efficiency (*251*). Dependence of the extraction efficiency on dissolution temperature, Pu content, oxide/TBP-HNO_3 complex ratio, and effect of oxidation have been investigated. Clifford et al. presented a model for the analysis of the results of extraction of uranium in a flow system by supercritical fluid modified with TBP from a nitric acid matrix in which the extraction is not limited by the solubility of the uranium species (*252*). The model used is that of diffusion out of a sphere into a medium in which the extracted uranium is infinitely dilute. Although not a completely accurate representation of the liquid-supercritical fluid system, the model is shown to be a reasonable representation. A UV irradiation experiment

TABLE 2.9
Highlights of Recent SFE Studies on Actinides Ions

Metal Ion	Medium/sample	Extractant	Remarks	Reference
U(VI)	Nitric acid	TBP	Extraction mechanism identical to solvent extraction; ultrasonic can enhance dissolution of UO_2	(234–238)
Th(IV); U(VI)	Nitric acid	TBP, TBPO, TOPO, TPPO	Extraction efficiency follows the order of the basicity of extractants	(239, 240)
Th(IV); U(VI)	Solid (filter papers/sand)	TTA/TBP	Quantitative extraction with TTA/TBP mixture	(241, 242)
U(VI); Th(IV)	Solid (tissue paper/oxide)	TOPO, TBP, acac, HDEHP, CMPO, etc.	Nature of extractant and preheating of tissue paper affected the extraction behavior of uranium	(243–245)
Pu(IV), Am(III)	Teflon, stainless steel and glass waste matrices	CMPO	Recovery of Pu and Am demonstrated	(246)
U(VI); Pu(IV)	Simulated spent fuel	TBP, MIBK, DMDOHEMA, etc.	Recovery of U(VI), Pu(IV) demonstrated Countercurrent chromatography used	(247)

Note: TBPO, tributylphosphine oxide. TOPO, trioctylphosphine oxide. TPPO, triphenylphosphine oxide. acac, acetyl acetone. HDEHP, di(2-ethylhexyl)phosphoric acid. MIBK, methylisobutyl ketone. DMDOHEMA, *N,N*-dimethyl-*N,N*-dioctylhexylethoxymalonamide.

showed photochemical reduction of UO_2^{2+}-TBP complex by ethanol in supercritical carbon dioxide (*253*).

2.9.3   MEMBRANE-BASED SEPARATION STUDIES

This branch of separation science has gained attention in the past few decades essentially due to its cost effectiveness in the treatment of industrial effluents, water purification, gas separation, etc. (*254–260*). Carrier-mediated transport of metal ions across liquid membranes is one of the options for the recovery of valuable metals from various waste streams. This is of great relevance in the nuclear industry in view of the stringent nuclear-waste management regulations. In this context, few attempts have been made for the recovery of radiologically toxic, long-lived, actinides and fission products employing extractants like CMPO, DMDBTDMA, and Aliquat 336, etc. (*261–271*). Amongst several membrane-based techniques, supported liquid membranes (SLMs) are particularly fascinating essentially due to their selectivity and simplicity. However, SLM-based separations have a major disadvantage of physical stability. Due to the advent of polymer inclusion membranes (PIM) and HFSLMs, several groups have shown keen interest in these techniques. Whereas hollow-fiber based separations offer the distinct advantage of efficient mass transfer due to large surface-to-volume ratio, PIMs offer the advantage of carrier immobility (*272–274*).

Amines were used as carriers for uranium recovery from acidic solutions. Babcock et al. showed that coupled transport of uranium from a sulfate medium using tertiary amine as the carrier is quite efficient (*265, 275, 276*). Mohapatra et al. reported the selective transport of U(VI) over Th(IV) from HCl medium using Aliquat 336/chloroform as the carrier (*265*). This study suggested that a significant amount of acid transport affected the uranium transport across the membrane. Shailesh et al. reported the U/Th separation studies using D2EHIBA as a carrier for SLM (*277*). Microporous polytetrafluoroethylene (PTFE) membrane was used as the polymeric support for the transport studies of uranium from a feed in nitric acid medium. The effect of experimental parameters, namely, role of diluent, carrier concentration, feed acidity, and metal ion concentrations on U/Th transport, was investigated (Figure 2.6). A model describing the transport mechanism was proposed.

Hollow-fiber nondispersive extraction (HFNDX) showed very fast transport (within 20 minutes) of uranium from a feed containing 10 g/L U in 4 M HNO_3, using DHOA as the carrier (*278*). Similar studies are being done at Bhabha Atomic Research Centre, Mumbai, India, on the evaluation of TODGA for the partitioning of actinides from HLW solutions. The HFSLM technique was used for the decontamination of the severely contaminated Hanford site groundwater, using dialkylphosphinc acid (Cyanex-272) as the carrier (*272*). Selective transport of Pu^4 over other long-lived fission-product contaminants from aqueous acidic solutions through an organic bulk-liquid membrane (BLM) and flat-sheet SLM containing TBP as the mobile carrier and dodecane as the membrane solvent has been reported. Extremely dilute to moderately concentrated plutonium nitrate solutions (10^{-5} M) in ~2–3 M HNO_3 were used as the source phase. With an increase in carrier concentration in the organic membrane, both the amount of plutonium that can
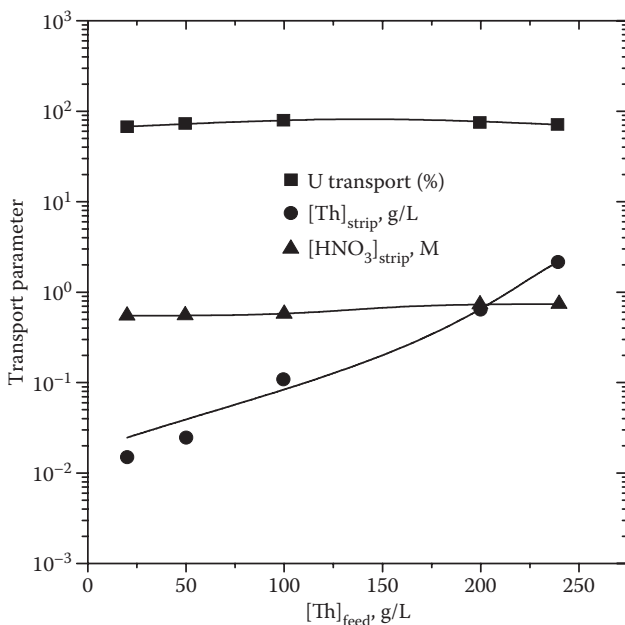
FIGURE 2.6 Variation of U, Th, and nitric acid transport with feed Th concentration. Carrier: 1 M D2EHIBA/*n*-dodecane. Strip: pH 2 solution. Feed acidity: 4 M HNO3. $[U]_{feed}$ = ~200 mg/L. Duration: 8 h. (From Shailesh, S.; Pathak, P.N.; Mohapatra, P.K.; Manchanda, V.K., *J. Membr. Sci.* 272, 143–151, 2006. With permission.)

be extracted into the membrane and the viscosity of the organic solution increases. These opposing effects result in maximum plutonium permeation with about 30% TBP in dodecane, while enhanced acidity of the strip side adversely affects the partitioning of the cation into the product side. Among several aqueous reagents tested, 0.5 M ascorbic acid was found to be the most efficient strippant. Rathore et al. used TBP as the carrier for the transport of Pu(IV) from nitric acid medium by the HFSLM method. Transport of Pu(IV) from nitric acid medium across a HFSLM was also studied using Aliquat 336 as the carrier. This technique was further used for the recovery of Pu from oxalate-bearing wastes generated during the reconversion process (*273, 274*).

2.9.4 MAGNETICALLY ASSISTED CHEMICAL SEPARATION

Conventionally, ion-exchange and solvent-extraction technologies have been used for the separation and recovery of transuranics and other hazardous metal ions from waste solutions of different origins. However, due to the requirements of bulky equipment, large chemical inventories, and large volumes of secondary wastes, there is a need to develop new technologies that can overcome the drawbacks of the solvent-extraction technique. In this connection, MACS provides a promising alternative to solvent extraction (*279–285*). In this process, tiny ferromagnetic particles coated

with extractant are used for selective removal of radionuclides and hazardous metal ions. The contaminant-loaded particles are then recovered from the waste solutions using a magnetic field. The contaminants attached to the magnetic particles are subsequently removed using a small volume of strippant, and then the particles are recycled. This mode of separation is novel, simple, compact, and low in cost. Work done at ANL, USA, has demonstrated the effectiveness of this technique.

At BARC, DMDBTDMA as well as TODGA-coated magnetic particles (cross-linked polyacrylamide and acrylic acid entrapping charcoal and iron oxide) were evaluated for possible application in the partitioning of actinides, lanthanides, and fission products from pure nitric acid solutions as well as from simulated pressurized heavy-water reactor-high-level waste (PHWR-SHLW) (*286–288*). Uptake profiles of various metal ions, including Pu(IV) and U(VI), were obtained as a function of time and nitric acid concentration by batch studies using DMDBTDMA/TODGA-coated magnetic particles. The order of uptake followed the order Pu(IV) > U(VI) > Am(III) > Eu(III) > Sr(II) > Cs(I) in both nitric acid and SHLW. The stability and recycling capacity of the DMDBTDMA/TODGA-coated magnetic particles was also assessed. Similarly, Cyanex 923-coated magnetic particles were also evaluated for uptake of metal ions from waste streams.

2.10　FUTURE PERSPECTIVES

Solvent extraction has played a key role in the separation of actinides both at industrial scale as well as for analytical applications. New challenges in the nuclear industry relate to the (a) recovery of uranium from lean natural resources (including phosphate rocks and oceans), (b) development of proliferation-resistant flowsheets for the reprocessing of spent fuels of thermal reactors, (c) development of novel extractants which are amenable for high radiation dose as well as for high Pu loading for fast-reactor fuel reprocessing, and (d) development of efficient schemes to recover alpha emitters quantitatively from the radioactive waste effluents. Basic extraction/stripping data with unirradiated and irradiated solvents of different oxidation states of actinides under widely varying aqueous media composition is critical for the development of any new separation scheme. In view of the presence of hard gamma emitters emanating from ^{232}U, there has been very little attention paid so far to the development of flowsheets for the efficient recovery of ^{233}U from the irradiated Th used for flux flattening in thermal reactors or as blanket in fast reactors. In this context, there is a need to (i) develop efficient dissolution schemes for irradiated ThO$_2$, (ii) develop innovative schemes to integrate reprocessing and fabrication stages of (Th, ^{233}U)O$_2$ fuel to reduce the problem of ^{232}U decay products, and (iii) improve our understanding of separation chemistry of Pa.

In recent years, there has been increasing interest in developing green solvents to minimize the adverse impact on the environment. In the nuclear industry, particular emphasis is on reducing the secondary waste volume as well as on reducing the ligand inventory. There is a paradigm shift in the choice of new extractants based on C, H, O, N elements (to ensure their complete incinerability). Alternative techniques, such as, EC, SFE, hollow-fiber based SLMs, and magnetically assisted chemical separations, need to be developed, which are essentially based on the principle of

solvent extraction but allow large reduction in the ligand inventory, thereby facilitating the use of exotic ligands in process solvents.

REFERENCES

1. Katz, J.J.; Seaborg, G.T.; Morss, L.R. (Eds.) *The Chemistry of Actinide Elements*, Vol. 1 & 2, Chapman and Hall, New York (1986).

2. Cunningham, B.B. *Proc. of XVII International Congress of Pure and Applied Chemistry*, Butterworths, London (1960), Vol. 1, p. 64.

3. Spitsyn, V.I; Gelman, A.D.; Krot, N.N.; Mefodiyeva, M.P.; Zacharova, F.A.; Komokov, Y.A.; Shilov, V.P.; Smirnovam, I.V. Heptavalent state of neptunium and plutonium, *J. Inorg. Nucl. Chem.* 31 (1969) 2733–2745.

4. Kraus, K.A. *Proc. Ist U.N. Conf. Peaceful Uses of Atomic Energy*, Geneva (1956), Vol. 7, p. 245.

5. Haissinsky, M. *Nuclear Chemistry and its Applications* (English ed.), Addison-Wesley, Reading, MA (1964), p. 233.

6. Ahrland, S.; Liljenzin, J.O.; Rydberg, J. Solution chemistry, In *Comprehensive Inorganic Chemistry*, J.C. Bailar Jr., H.J. Emeleus, R. Nyhlom, and A.F.T. Dickenson (Eds.), Pergamon Press, Oxford (1973), Vol. 5, p. 514.

7. Jones, A.D.; Choppin, G.R. Complexes of actinide ions in aqueous solution, *Actinides Rev.* 1 (1969) 311–336.

8. Martell, A.E.; Smith, R.M.; Motekaitis, R.J. *NIST Critically Selected Stability Constants of Metal Complexes Data Base, Version 5.0*, Texas A&M University, College Station, TX, (1998).

9. Howells, G.R.; Hughes, T.G.; Mackey, D.R.; Saddington, K. *Proc. 2nd UN Int. Conf. on Peaceful Uses of Atomic Energy*, Geneva (1958) pp. 3–24.

10. Ramanujam, A.; Nadkarni, M.N.; Ramakrishna, V.V.; Patil, S.K. Studies on the HTTA extraction of tetravalent actinides, *J. Radioanal. Chem.* 42 (1978) 349–357.

11. Peppard, D.F.; Mason, G.W.; McCarty, S. Extraction of thorium(IV) by di esters of orthophosphoric acid, $(GO)_2PO(OH)$, *J. Inorg. Nucl. Chem.* 13 (1960) 138–150.

12. Bagawde, S.V.; Vasudeva Rao, P.R.; Ramakrishna, V.V.; Patil, S.K. The effect of temperature on the extraction of uranium(VI) from nitric acid by tri-n-butyl-phosphate, *J. Inorg. Nucl. Chem.* 40 (1978) 1913–1918.

13. Otu, E.O. The synergistic extraction of thorium(IV) and uranium(VI) by 2-ethylhexyl phenylphosphonic acid and micelles of dinonylnaphthalene sulphonic acid, *Solvent Extr. Ion Exch.* 15 (1997) 1–13.

14. Mohanty, S.P.; Mohanty, I.; Mishra, S.; Chakravortty, V. Extraction of uranium(VI) with a binary mixture of LIX-860 and Versatic-10, *J. Radioanal. Nucl. Chem.* 227 (1998) 99–103.

15. Eyal, A.M.; Canari, R. pH dependence of carboxylic and mineral acid extraction by amine-based extractants: Effects of pKa, amine basicity, and diluent properties, *Ind. Eng. Chem. Res.* 34 (1995) 1789–1798.

16. Stary, J. *The Extraction of Metal Chelates*, Pergamon, Oxford (1964).

17. Stary, J.; Freiser, H. *Equilibrium Constants of Liquid-Liquid Distribution Reactions, Part 4. Chelating Extractants*, Pergamon, Oxford (IUPAC Chem. Data Series No. 18) (1978).

18. Sekine, T.; Dyrssen, D. Solvent extraction of metal ions with mixed ligands – IV. Extraction of Eu(III) with chelating acids and neutral adduct-forming ligands, *J. Inorg. Nucl. Chem.* 29 (1967) 1475–1480.

19. Cook, E.H.; Taft, R.W. Concerning the behavior of aqueous thenoyltrifluoroacetone. *J. Am. Chem. Soc.* 74 (1952) 6103–6104.

20. Manchanda, V.K.; Chang, C.A. Solvent extraction studies of lanthanum(III) and neodymium(III) with ionizable macrocyclic ligands and thenoyltrifluoroacetone, *Anal. Chem.* 58 (1988) 2269–2275.

21. De, A.K.; Khopkar, S.M.; Chalmers, R.A. *Solvent Extraction of Metals*, Van Nostrand Reinhold, London (1970).

22. Starý, J.; Prášilová, J. Extraction and ion exchange investigation of uranium(VI) chelates, *J. Inorg. Nucl. Chem.* 17 (1961) 361–365.

23. Batzar, K.; Goldberg, D.E.; Newman, L.J. Effect of β-diketone structure on the synergistic extraction of uranyl ion by tributylphosphate, *J. Inorg. Nucl. Chem.* 29 (1967) 1511–1518.

24. Mohapatra, P.K.; Manchanda, V.K. Role of ligand basicity and stereochemistry in the extraction of plutonium(IV) isoxazolonates, *Radiochim. Acta* 91 (2003) 705–712.

25. Mohapatra, P.K.; Ruikar, P.B.; Manchanda, V.K. Recovery of plutonium from oxalate supernatant using 1-phenyl-3-methyl-4-benzoyl-5-pyrazolone, *J. Radioanal. Nucl. Chem.* 270 (2006) 345–348.

26. Manchanda, V.K.; Gupta, K.K.; Vardarajan, N.; Singh, R.K. *Proceeding of Nuclear and Radiochemistry Symposium*, NUCAR-97, Saha Institute of Nuclear Physics (SINP), Calcutta (1997), p. 184.

27. Bacher, W.; Keller, C. 4-Acyl-substituierte 1-phenyl-3-methyl-pyrazolone-5 als chelatbildner für actinidenionen, *J. Inorg. Nucl. Chem.* 35 (1973) 2945–2956.

28. Mansingh, P.S.; Veeraraghavan, R.; Mohapatra, P.K.; Manchanda, V.K.; Dash, K.C. Adduct formation of a uranyl isoxazolonate with organophilic neutral oxodonors, *Radiochim. Acta* 72 (1996) 127–132.

29. Mohapatra, P.K.; Veeraraghavan, R.; Manchanda, V.K. Extraction of thorium(IV) by a mixture of 1-phenyl-3-methyl-4-benzoyl-5-pyrazolone and tri-n-octyl phosphine oxide, *J. Radioanal. Nucl. Chem.* 240 (1999) 31–38.

30. Thakur, P.; Veeraraghavan, R.; Mohapatra, P.K.; Manchanda, V.K.; Dash, K.C. Extraction of ternary complexes of thorium(IV) with 3-phenyl-4-benzoyl-5-isoxazolone and neutral donors from nitric acid medium, *Talanta* 43 (1996) 1305–1312.

31. Ramanujam, A.; Gudi, N.M.; Nadkarni, M.N.; Patil, S.K.; Ramakrishna, V.V. DAE Nuclear Chemical and Radiochemical Symposium, Waltair, India, Paper No. AC-18 (1980).

32. Sajun, M.S.; Ramakrishna, V.V.; Patil, S.K. Synergistic extraction of tetravalent actinides by mixtures of a β-diketone and a sulfoxide, *J. Radioanal. Chem.* 63 (1981) 57–63.

33. Manchanda, V.K.; Mohapatra, P.K. Extraction of plutonium(IV) with 1-phenyl-3-methyl-4-benzoyl-pyrazolone-5-one and tri-*n*-octylphosphine oxide, *Radiochim. Acta* 60 (1993) 185–188.

34. Banerjee, S.; Mohapatra, P.K.; Bhattacharyya, A.; Basu, S.; Manchanda, V.K. Extraction of tetravalent neptunium isoxazolonates as their TOPO adducts, *Radiochim. Acta* 92 (2004) 95–99.

35. Deshpande, S.M.; Mishra, S.L.; Gajankush, R.B.; Thakur, N.V.; Koppikar, K.S. Recovery of high purity Y_2O_3 by solvent extraction route using organophosphorus extractants, *Min. Process. Extr. Metall. Rev.* 10 (1992) 267–273.

36. Phal, D.G.; Kannan, S.; Ramakrishna, V.V.; Patil, S.K. Studies on the solvent extraction behaviour of Pu(IV) from sulfuric acid medium into di-2-ethylhexylphosphoric acid (HDEHP), *J. Radioanal. Nucl. Chem.* 152 (1991) 137–150.

37. Blake, C.A. Jr.; Baes, C.F. Jr.; Brown, K.B.; Coleman, C.F.; White, J.C. Solvent extraction of uranium and other metals by acidic and neutral organophosphorus compounds, In *Peaceful Uses of Atomic Energy. Vol. 28, Basic Chemistry in Nuclear Energy,* United Nations, Geneva (1958), pp. 289–298.

38. Hurst, F.J.; Crouse, D.J. Recovery of uranium from wet-process phosphoric acid by extraction with octylphenylphosphoric acid, *Ind. Eng. Chem. Proc.* 13 (1974) 286–291.

39. Mithapara, P.D.; Manchanda, V.K.; Natarajan, P.R. Extraction studies of Pu(IV) with octylphenyl acid phosphate, *J. Radioanal. Nucl. Chem.* 83 (1984) 301–307.

40. Gopalkrishnan, M.; Radhakrishnan, K.; Dhami, P.S.; Kulkarni, V.T.; Joshi, M.V.; Patwardhan, A.B.; Mathur, J.N. Determination of trace impurities in uranium, thorium and plutonium matrices by solvent extraction and inductively coupled plasma atomic emission spectrometry, *Talanta* 44 (1997) 169–176.

41. Mapara, P.M.; Godbole, A.G.; Swarup, R.; Nagar, M.S. Extraction of uranium and plutonium from oxalate bearing solutions using phosphonic acid: Solvent extraction, extraction chromatography and infrared studies, *J. Radioanal. Nucl. Chem.* 240 (1999) 631–635.

42. Chetty, K.V.; Gamare, J.S.; Godbole, A.G.; Vaidya, V.N. Recovery of plutonium from uranium analytical waste solution containing phosphate using 2-ethylhexyl 2-ethylhexyl phosphonic acid (PC88A), *J. Radioanal. Nucl. Chem.* 269 (2006) 15–20.

43. Howells, G.R.; Hughes, T.G.; Mackey, D.R.; Saddington, K. *Proceedings of 2nd Peaceful Uses of Atomic Energy*, United Nations, Geneva (1958), Vol. 17, p. 3.

44. Lawroski, S.; Levenson, M. USAEC Report, TID 7534 (1957).

45. Schmieder, H.; Petrich, G. A concept for an improved Purex process, *Radiochim. Acta* 48 (1989) 181–192.

46. Burger, L.L. The neutral organophosphorus compounds as extractants, *Nucl. Sci. Eng.* 16 (1963) 428–439.

47. Suresh, A.; Srinivasan, T.G.; Vasudeva Rao, P.R. Extraction of U(VI), Pu(IV) and Th(IV) by some trialkyl phosphates, *Solvent Extr. Ion Exch.* 12 (1994) 727–744.

48. Srinivasan, T.G.; Suresh, A.; Prasanna, R.; Jayanthi, N.; Vasudeva Rao, P.R. Metal-solvate stoichiometry evaluation in extractions by solvating type neutral extractants – A novel approach, *Solvent Extr. Ion Exch.* 14 (1996) 443–458.

49. Srinivasan, T.G.; Vasudeva Rao, P.R.; Sood, D.D. The effect of temperature on the extraction of uranium(VI) from nitric acid by tri-n-amyl phosphate, *Solvent Extr. Ion Exch.* 15 (1997) 15–31.

50. Suresh, A.; Subramaniam, S.; Srinivasan, T.G.; Vasudeva Rao, P.R. Studies on U-Th separation using tri-sec-butyl phosphate, *Solvent Extr. Ion Exch.* 13 (1995) 415–430.

51. Suresh, A.; Srinivasan, T.G.; Vasudeva Rao, P.R.; Rajagopalan, C.V.; Koganti, S.B. U/Th separation by counter-current liquid-liquid extraction with tri-sec butyl phosphate by using an ejector mixer-settler, *Sep. Sci. Technol.* 39 (2005) 2477–2496.

52. Crouse, D.J.; Arnold, W.D.; Hurst, F.J. *Proc. Int. Solv. Extr. Conference*, ISEC-83, Denver, CO (1983), p. 90.

53. Nikiforov, A.S.; Zakharkin, B.S.; Renard, Eh.V.; Rozen, A.M.; Smetanin, E.Y. *Proc. Int. Conf., Actinides-89*, Tashkent (1989), p. 20.

54. Siddall III, T.H. The effects of altering alkyl substituents in trialkyl phosphates on the extraction of actinides, *J. Inorg. Nucl. Chem.* 13 (1960) 151–155.

55. Pathak, P.N.; Veeraraghavan, R.; Manchanda, V.K. Separation of uranium and thorium using tris(2-ethylhexyl) phosphate as extractant, *J. Radioanal. Nucl. Chem.* 240 (1999) 15–18.

56. Hurst; F.J. Recovery of uranium from wet-process phosphoric acid by solvent extraction, *Trans. Soc. Min. Eng. AIME* 262 (1977) 240–248.

57. Apostolidis, C.; Meester, R. De.; Koch, L.; Molinet, R.; Liang, J.; Zhu, Y. The Extraction of Actinides and Other Constituents from Highly Active Waste (HAW) by Triallkyl Phosphine Oxide. In *New Separation Techniques for Radioactive Waste and Other Specific Applications*, L. Cecille, M. Casa, and L. Pietrelli (Eds.), Elsevier Applied Science, Rome; Italy (1990), p. 80.

58. Petkovic, D.M.; Kopecni, M.M.; Mltrovic, A.A. Solvent extraction of nitric, hydrochloric and sulfuric acid and their uranyl salts with tri-n-octylphosphine oxide, *Solvent Extr. Ion Exch.* 10 (1992) 685–696.

59. Horwitz, E.P.; Kalina, D.G.; Kaplan, L.; Mason, W.G.; Diamond, H. Selected alkyl(phenyl)-*N,N*-dialkylcarbamoylmethylphosphine oxides as extractants for Am(III) from nitric acid media, *Sep. Sci. Technol.* 17 (1982) 1261–1279.
60. Siddall, Jr. T.H. Bidentate organophosphorus compounds as extractants-II. Extraction mechanisms for cerium(III) nitrate, *J. Inorg. Nucl. Chem.* 26 (1964) 1991–2003.
61. Horwitz, E.P.; Muscatello, A.C.; Kalina, D.G.; Kaplan, L. The extraction of Selected transplutonium(III) and lanthanide(III) ions by dihexyl-*N,N*-diethylcarbamoylmethylphosphonate from aqueous nitrate media, *Sep. Sci. Technol.* 16 (1981) 417–437.
62. Mathur, J.N.; Nash, K.L. Thermodynamics of extraction of Am(III) and Eu(III) from nitrate and thiocyanate media with octyl(phenyl)-N,N-diisobutylcarbamoylmethylphosphine oxide, *Solvent Extr. Ion Exch.* 16 (1998) 1341–1356.
63. Schulz, W.W.; Horwitz, E.P. TRUEX process and the management of liquid TRU Waste, *Sep. Sci. Technol.* 23 (1998) 1191–1210.
64. Nagar, M.S.; Ruikar, P.B.; Mathur, J.N. Recovery of plutonium from assorted laboratory wastes, *J. Radioanal. Nucl. Chem.* 222 (1997) 243–245.
65. Michael, K.M.; Rizvi, G.H.; Mathur, J.N.; Ramanujam, A. Separation and recovery of uranium and plutonium from oxalate supernatant, *J. Radioanal. Nucl. Chem.* 246 (2000) 355–359.
66. Pathak, P.N.; Kumbhare, L.B.; Manchanda, V.K. Structural effects in n n-dialkyl amides on their extraction behavior toward uranium and thorium, *Solvent Extr. Ion Exch.* 19 (2001) 105–126.
67. Pathak, P.N.; Kumbhare, L.B.; Manchanda, V.K. Effect of structure of N,N dialkyl amides on the extraction of U(VI) and Th(IV): A thermodynamic study, *Radiochim. Acta* 89 (2001) 447–452.
68. Pathak, P.N.; Veeraraghavan, R.; Prabhu, D.R.; Mahajan, G.R.; Manchanda, V.K. Separation studies of uranium and thorium using di-2-ethylhexyl isobutyramide (D2EHIBA), *Sep. Sci. Technol.* 34 (1999) 2601–2614.
69. Pathak, P.N.; Veeraraghavan, R.; Ruikar, P.B.; Manchanda, V.K. Solvent extraction studies on Th(IV), Pa(V) and U(VI) from nitric acid medium using di-2-ethylhexyl isobutyramide (D2EHIBA), *Radiochim. Acta* 86 (1999) 129–134.
70. Pathak, P.N.; Prabhu, D.R.; Manchanda, V.K. Distribution behaviour of U(VI), Th(IV) and Pa(V) from nitric acid medium using linear and branched chain extractants, *Solvent Extr. Ion Exch.* 18 (2000) 821–840.
71. Pathak, P.N.; Prabhu, D.R.; Ruikar, P.B.; Manchanda, V.K. Evaluation of di(2-ethylhexyl)isobutyramide (D2EHIBA) as a process extractant for the recovery of [233]U from irradiated Th, *Solvent Extr. Ion Exch.* 20 (2002) 293–311.
72. Pathak, P.N.; Prabhu, D.R.; Kanekar, A.S.; Ruikar, P.B.; Bhattacharyya, A.; Mohapatra, P.K.; Manchanda, V.K. Distribution behavior of U(VI), Th(IV), and fission products with di(2-ethylhexyl) isobutyramide under process conditions, *Ind. Eng. Chem. Res.* 43 (2004) 4369–4375.
73. Vidyalakshmi, V.; Subramanian, M.S.; Srinivasan, T.G.; Vasudeva Rao, P.R. Effect of extractant structure on third phase formation in the extraction of uranium and nitric acid by n-dialkyl amides, *Solvent Extr. Ion Exch.* 19 (2001) 37–49.
74. Gupta, K.K.; Manchanda, V.K.; Subramanian, M.S.; Singh, R.K. N,N-Dihexyl hexanamide: A promising extractant for nuclear fuel reprocessing, *Sep. Sci. Technol.* 35 (2000) 1603–1617.
75. Gupta, K.K.; Manchanda, V.K.; Sriram, S.; Thomas, G.; Kulkarni, P.G.; Singh, R.K. Third phase formation in the extraction of uranyl nitrate by N,N-dialkyl aliphatic amides, *Solvent Extr. Ion Exch.* 18 (2000) 421–439.
76. Gupta, K.K.; Manchanda, V.K.; Subramanian, M.S.; Singh, R.K. Solvent extraction studies on U(VI), Pu(IV), and fission products using N,N-dihexyloctanamide, *Solvent Extr. Ion Exch.* 18 (2000) 273–292.

77. Ruikar, P.B.; Nagar, M.S.; Subramanian, M.S.; Gupta, K.K.; Varadarajan, N.; Singh, R.K. Extraction behavior of uranium(VI), plutonium(IV) and some fission products with gamma pre-irradiated n-dodecane solutions of N,N'-dihexyl substituted amides, *J. Radioanal. Nucl. Chem.* 196 (1995) 171–178.

78. Ruikar, P.B.; Nagar, M.S.; Subramanian, M.S. Extraction of uranium, plutonium and some fission products with γ-irradiated unsymmetrical and branched chain dialkylamides, *J. Radioanal. Nucl. Chem.* 176 (1993) 103–111.

79. Mahajan, G.R.; Prabhu, D.R.; Manchanda, V.K.; Badheka, L.P. Substituted malonamides as extractants for partitioning of actinides from nuclear waste solutions, *Waste Management* 18 (1998) 125–133.

80. Berthon, L.; Morel, J.M.; Zorz, N.; Nicol, C.; Virelizier, H.; Madic, C. Diamex process for minor actinide partitioning: Hydrolytic and radiolytic degradations of malonamide extractants, *Sep. Sci. Technol.* 36 (2001) 709–728.

81. Sasaki, Y.; Sugo, Y.; Suzuki, S.; Tachimori, S. The novel extractants diglycolamides for the extraction of lanthanides and actinides in HNO3-*n*-dodecane system, *Solvent Extr. Ion Exch.* 19 (2001) 91–103.

82. Ansari, S.A.; Pathak, P.N.; Manchanda, V.K.; Husain, M.; Prasad, A.K.; Parmar, V.S. N,N,N',N'-Tetraoctyl diglycolamide (TODGA): A promising extractant for actinide-partitioning from high-level waste (HLW), *Solvent Extr. Ion Exch.* 23 (2005) 463–479.

83. Ansari, S.A.; Pathak, P.N.; Hussain, M.F.; Prasad, A.; Parmar, V.S.; Manchanda, V.K. Extraction of actinides using N, N, N', N'-tetraoctyl diglycolamide (TODGA): A thermodynamic study, *Radiochim. Acta* 94 (2006) 307–312.

84. Preston, J.S.; du Preez, A.C. The influence of extractant structure on the solvent extraction of uranium(VI) and thorium(IV) from nitrate media by dialkyl sulphoxides, *J. Chem. Technol. Biotechnol.* 69 (1997) 86–92.

85. Mathur, J.N.; Ruikar, P.B.; Balarama Krishna, M.V.; Murali, M.S.; Nagar, M.S.; Iyer, R.H. Extraction of Np(IV), Np(VI), Pu(IV) and U(VI) with Amides, BEHSO and CMPO from nitric acid medium, *Radiochim. Acta* 73 (1996) 199–206.

86. Sato, T.; Adachi, K.; Sato, K. Liquid-liquid extraction of uranium(VI) from hydrochloric acid solutions by dihexyl sulphoxide, *Solvent Extr. Res. Dev. Jpn.* 13 (2006) 73–81.

87. Prabhu, D.R.; Mahajan, G.R.; Murali, M.S.; Shukla, J.P.; Nair, G.M.; Natarajan, P.R. Di(2-ethylhexyl)sulfoxide as an extractant for plutonium(IV) from nitric acid medium, *J. Radioanal. Nucl. Chem.* 162 (1992) 91–97.

88. Jing-Tian, H.; Guo-Xin, S.; Hua, S.; Shu-Feng, C.; Bo-Rong, B. Phenyl-N,N-dibutylcarbamoylmethyl sulfoxide as a new bifunctional extractant for extraction of uranium(VI) in toluene, *J. Radioanal. Nucl. Chem.* 242 (1999) 821–824.

89. Kannan, S.; Chetty, K.V.; Venugopal, V.; Drew, M.G.B. Extraction and coordination studies of the unexplored bifunctional ligand carbamoyl methyl sulfoxide (CMSO) with uranium(VI) and cerium(III) nitrates. Synthesis and structures of $[UO_2(NO_3)_2(PhSOCH_2CONiBu_2)]$ and $[Ce(NO_3)_3(PhSOCH_2CONBu_2)_2]$, *Dalton Trans.* (2004) 3604–3610.

90. Shukla, J.P.; Pai, S.A.; Subramanian, M.S. Solvent extraction of plutonium(IV), uranium(VI), and some fission products with di-*n*-octylsulfoxide, *Sep. Sci. Technol.* 14 (1979) 883–894.

91. Yong-Jun, Z. Extraction of trivalent actinides with phosphine oxides, In *Handbook on the Physics and Chemistry of Actinides*, A.J. Freeman and C. Keller (Eds.), Elsevier Science, Amsterdam, North Holland (1985), p. 482.

92. Yaftian, M.R.; Hassanzadeh, L.; Eshraghi, M.E.; Matt; D. Solvent extraction of thorium (IV) and europium (III) ions by diphenyl-N,N-dimethylcarbamoylmethylphosphine oxide from aqueous nitrate media, *Sep. Purif. Tech.* 31 (2003) 261–268.

93. Yatsenko, N.A.; Palant, A.A. Micelle formation in liquid-liquid extraction of tungsten(VI), molybdenum(VI), and rhenium(VII) by diisododecylamine, dioctylamine, and trioctylamine from sulfuric acid solutions, *Russ. J. Inorg. Chem.* 45 (2000) 1460–1464.

94. Gupta, C.K.; Mukherjee, T.K. *Hydrometallurgy in Extraction Processes*, CRC Press, Boca Raton, FL (1990).

95. Uranium Extraction Technology. Technical Reports Series No. 359, International Atomic Energy Agency (IAEA), Vienna (1993).

96. Choppin, G.R.; Khankhasayev, M.K. *Chemical Separation Technologies and Related Methods of Nuclear Waste Management: Applications, Problems, and Research Needs*, Springer, Dubaa; Russia (1999).

97. Moore, F.L. Liquid-liquid extraction of uranium and plutonium from hydrochloric acid solution with tri(iso-octyl)amine: Separation from thorium and fission products, *Anal. Chem.* 30 (1958) 908–911.

98. Bhandiwad, V.R.; Swarup, R.; Patil, S.K. Extraction of actinides by quaternary amines from hydrochloric acid medium, *J. Radioanal. Chem.* 52 (1979) 5–14.

99. Landgren, A.; Liljenzin, J.O. Extraction behaviour of technetium and actinides in the aliquat-336/nitric acid system, *Solvent Extr. Ion Exch.* 17 (1999) 1387–1401.

100. Takahashi, A.; Ueki, Y.; Igarashi, S. Homogeneous liquid-liquid extraction of uranium(VI) from acetate aqueous solution, *Anal. Chim. Acta* 387 (1999) 71–75.

101. Mohapatra, P.K.; Manchanda, V.K. Ion-pair extraction of uranyl ion from aqueous medium using crown ethers, *Talanta* 47 (1998) 1271–1278.

102. Mohapatra, P.K.; Manchanda, V.K. An unusual extraction behavior of americium(III) and dioxouranium(VI) from picric acid medium using 18-crown-6 as neutral oxodonor, *J. Radioanal Nucl. Chem.* 241 (1999) 101–105.

103. Mohapatra, P.K.; Manchanda, V.K. The unusual extraction behavior of americium(III) and dioxouranium(VI) from picric acid medium using neutral oxodonors: II. A thermo-dynamic study, *J. Radioanal. Nucl. Chem.* 240 (1999) 159–164.

104. Banerjee, S.; Bhattacharya, A.; Mohapatra, P.K.; Basu, S.; Manchanda, V.K. Extraction of the uranyl ion with 3-phenyl-4-benzoyl-5-isoxazolone (HPBI) and neutral donors from dilute nitric acid medium, *Radiochim. Acta* 91 (2003) 729–736.

105. Bhattacharyya, A.; Banerjee, S.; Mohapatra, P.K.; Basu, S.; Manchanda, V.K. Extraction of ternary beta-diketonates of uranyl ion using some substituted monoamides, *Solvent Extr. Ion Exch*. 21 (2003) 687–705.

106. Bhattacharyya, A.; Banerjee, S.; Mohapatra, P.K.; Basu, S.; Manchanda, V.K. Role of ligand structure and basicity on the extraction of uranyl isoxazolonate adducts, *Solvent Extr. Ion Exch*. 22 (2004) 13–29.

107. Duyckaerts, G.; Desreux, J.F. *International Solvent Extraction Conference*, ISEC 77, Belgium (1977), pp. 73–86.

108. Manchanda, V.K.; Shukla, J.P.; Subramanian, M.S. Coordination of uranyl bis(thenoyltrifluoroacetonate) with some heterocyclic n-oxides, *J. Inorg. Nucl. Chem.* 36 (1974) 2595–2598.

109. Subramanian, M.S.; Viswanatha, A. Complexes of uranyl diketones with aromatic sul-phoxides, *J. Inorg. Nucl. Chem.* 31 (1969) 2575–2585.

110. Patil, S.K.; Ramakrishna, V.V.; Hara Prakash, B. Synergistic extraction of Pu(IV) by mixtures of HTTA with TBP and DBBP, *Sep. Sci. Technol.* 15 (1980) 131–144.

111. Patil, S.K.; Ramakrishna, V.V.; Kartha, P.K.S.; Gudi, N.M. Synergistic extraction of plutonium(IV) from nitric acid medium by mixtures of TOPO and HTTA, *Sep. Sci. Technol.* 15 (1980) 1459–1469.

112. Pai, S.A.; Lohitakshan, K.V.; Mithapara, P.D.; Aggarwal, S.K. Solvent extraction of uranium(VI), plutonium(VI) and americium(III) with HTTA/HPMBP using mono- and bi-functional neutral donors: synergism and thermodynamics, *J. Radioanal. Nucl. Chem.* 245 (2000) 623–628.

113. Mundra, S.K.; Pai, S.A.; Subramanian, M.S. Synergistic extraction of uranyl ion with acylpyrazolones and dicyclohexano-18-crown-6, *J. Radioanal. Chem. Articles* 116 (1987) 203–211.

114. Singh, D.K.; Singh, H.; Mathur, J.N. Synergistic extraction of U(VI) with mixtures of 2-ethylhexyl phosphonic acid-mono-2-ethylhexyl ester (PC-88A) and TBP, TOPO or Cyanex 923, *Radiochim. Acta* 89 (2001) 573–578.

115. Sriram, S.; Veeraraghavan, R.; Manchanda, V.K. Synergistic extraction of uranium(VI) by alamine 336 in the presence of neutral oxodonors, *Radiochim. Acta* 84 (1999) 153–157.

116. Berthon, C.; Vaufrey, F.; Livet, J.; Madic, C.; Hudson, M.J. ISEC'96. Value adding through solvent extraction, Shallcross, D.C.; Paimin, R.; Prvcic, L.M. (Eds.) *Proceedings of the International Solvent Extraction Conference 1996*, The University of Melbourne, Melbourne, VIC (Australia) (1996), Vol. 2, 883, pp. 1349–1354.

117. Berthon, C.; Chachaty, C. NMR and IR spectrometric studies of monoamide complexes with plutonium(IV) and lanthanide(III) nitrates, *Solvent Extr. Ion Exch.* 13 (1995) 781–812.

118. Hatakeyama, K.; Park, Y.-Y.; Tomiyasu, H.; Wada, Y.; Ikeda, Y. A nuclear magnetic resonance study on ligand exchange reactions in U(VI) nitrato complexes with ligands containing phosphoryl group in non-aqueous solvents, *J. Nucl. Sci. Technol. Tokyo* 34 (1997) 298–303.

119. May, I.; Livens, F.R.; Taylor, R.J.; Wallwork, A.L.; Hastings, J.J.; Fedorov, Y.S.; Zilberman, B.Y.; Mishin, E.N.; Arkhipov, S.A.; Blazheva, I.V.; Poverkova, L.Y.; Charnock, J.M. The influence of dibutylphosphate on actinide extraction by 30% tributylphosphate, *Radiochim. Acta* 88 (2000) 283–290.

120. Sriram, S.; Ruikar, P.B.; Nagar, M.S.; Kalsi, P.C.; Manchanda, V.K. Physicochemical studies on uranium(VI) complexes of N,N-dialkylamides, *J. Ind. Chem. Soc.* 79 (2002) 498–501.

121. Subramanian, M.S.; Pai, S.A.; Manchanda, V.K. Acid dissociation of some beta diketones in mixtures of water and dioxane – A thermodynamic study, *Aust. J. Chem.* 26 (1973) 85–89.

122. Manchanda, V.K.; Subramanian, M.S. Infrared and P.M.R. investigations of some complexes of uranyl beta diketonates with methyl substituted pyridine N-oxides, *Aust. J. Chem.* 27 (1974) 1573–1577.

123. Manchanda, V.K.; Subramanian, M.S. IR and PMR studies of some uranyl beta-diketones oxodonor adducts, *Acta Chim. Acad. Sci. Hung.* 111 (1982) 63–67.

124. Manchanda, V.K.; Shukla, J.P.; Subramanian, M.S. Coordination of uranyl bis(thenoyltrifluoroacetonate) with some heterocyclic *N*-oxides, *J. Inorg. Nucl. Chem.* 36 (1974) 2595–2598.

125. Ruikar, P.B.; Nagar, M.S.; Subramanian, M.S. Quantitative analysis of some extractants by infrared spectrometry, *J. Radioanal. Nucl. Chem. Lett.* 155 (1991) 371–376.

126. Kertes, A.S. *Proceedings of International Solvent Extraction Conference*, ISEC-65 (1965), p. 377.

127. Vasudeva Rao, P.R.; Kolarik, Z. A review of third phase formation in extraction of actinides by neutral organophosphorus extractant**s**, *Solvent Extr. Ion Exch.* 14 (1996) 955–993.

128. Srinivasan, T.G.; Ahmed, M.K.; Shakila, A.M.; Dhamodaran, R.; Vasudeva Rao, P.R.; Mathews, C.K. Third phase formation in the extraction of plutonium by tri-normal-butyl phosphate, *Radiochim. Acta* 40 (1986) 151–154.

129. Vasudeva Rao, P.R. Extraction of actinides by trialkyl phosphates, *Min. Process. Extr. Metall. Rev.* 18 (1998) 309–331.

130. Vasudeva Rao, P.R.; Srinivasan, T.G. *Proceedings of Nuclear and Radiochemistry Symposium*, *NUCAR 2001*, University of Pune, Pune, February 7–10 (2001), p. 59.

131. Suresh, A.; Deivanayaki, R.; Srinivasan, T.G.; Vasudeva Rao, P.R. *Nuclear and Radiochemistry Symposium*, NUCAR-2005, Amritsar (India), March 15–18 (2005), pp. 135–136.

132. Brahammanada Rao, C.V.S.; Suresh, A.; Srinivasan, T.G.; Vasudeva Rao, P.R., Tricyclohexylphosphate – A unique member in the neutral organophosphate family, *Solvent Extr. Ion Exch.* 21 (2003) 221–238.

133. Brahammanada Rao, C.V.S.; Srinivasan, T.G.; Vasudeva Rao, P.R. Studies on the extraction of actinides by diamyl amyl phosphonate, *Solvent Extr. Ion Exch.* 25 (2007) 771–789.

134. Gasparini, G.M.; Grossi, G. Application of *N,N*-dialkyl aliphatic amides in the separation of some actinides, *Sep. Sci. Technol.* 15 (1979) 825–844.

135. Gasparini, G.M.; Grossi, G. Long chain disubstituted aliphatic amides as extracting agents in industrial applications of solvent extraction, *Solvent Extr. Ion Exch.* 14 (1986) 1233–1271.

136. Jha, R.K.; Gupta, K.K.; Kulkarni, P.G.; Gurba, P.B.; Janardan, P.; Changrani, R.D.; Dey, P.K.; Pathak, P.N.; Manchanda, V.K. *Proceedings of DAE-BRNS Symposium on Emerging Trends in Separation Science and Technology*, *SESTEC-2006*, Mumbai, India, September 29 to October 1 (2006), C-11, pp. 154.

137. Chiarizia, R.; Jensen, M.P.; Borkowski, M.; Ferraro, J.R.; Thiyagarajan, P.; Littrell, K.C. Third phase formation revisited: The U(VI), HNO_3-TBP, *n*-dodecane system, *Solvent Extr. Ion Exch.* 21 (2003) 1–27.

138. Chiarizia, R.; Jensen, M.P.; Borkowski, M.; Ferraro, J.R.; Thiyagarajan, P.; Littrell, K.C. SANS study of third phase formation in the U(VI)-HNO_3/TBP-*n*-dodecane system, *Sep. Sci. Technol.* 38 (2003) 3313–3331.

139. Borkowski, M.; Chiariza, R.; Jensen, M.P.; Ferraro, J.R.; Thiyagarajan, P.; Littrel, K.C. SANS study of third phase formation in the Th(IV)-HNO_3/TBP-*n*-octane system, *Sep. Sci. Technol.* 38 (2003) 3333–3351.

140. Chiariza, R.; Jensen, M.P.; Borkowski, M.; Thiyagarajan, P.; Littrel, K.C. Interpretation of third phase formation in the Th(IV)-HNO_3, TBP-n-octane system with Baxter's "sticky spheres" model, *Solvent Extr. Ion Exch.* 22 (2004) 325–351.

141. Chiariza, R.; Jensen, M.P.; Rickert, P.G.; Kolarik, Z.; Borkowski, M.; Thiyagarajan, P. Extraction of zirconium nitrate by TBP in n-octane: Influence of cation type on third phase formation according to the "sticky spheres" model, *Langmuir* 20 (2004) 10798–10808.

142. Jha, R.K.; Gupta, K.K.; Kulkarni, P.G.; Gurba, P.B.; Janardan, P.; Changrani, R.D.; Dey, P.K.; Pathak, P.N.; Manchanda, V.K. Third phase formation studies in the extraction of Th(IV) and U(VI) by N,N-dialkyl aliphatic amides, *Desalination* 232 (2008) 225–233.

143. Den Auwer, C.C.; Revel, R.; Charbonnel, M.C.; Presson, M.T.; Conradson, S.D.; Simoni, E.; Le Du, J.F.; Madic, C. Actinide coordination sphere in various U, Np and Pu nitrato coordination complexes, *J. Synch. Rad.* 6 (1999) 101–104.

144. Oda, Y.; Funasaka, H.; Nakamura, Y.; Adachi, H. Discreter variational Dirac-slater calculation of Urangl (VI) nitrate complexes, *J. Alloys Comp.* 255 (1997) 24–30.

145. Rabbe, C.; Madic, C.; Godard, A. Molecular modeling study of uranyl nitrate extraction with monoamides I. Quantum chemistry approach, *Solvent Extr. Ion Exch.* 16 (1998) 1091–1109.

146. Rabbe, C.; Madic, C.; Sella, C.; Godard, A. Molecular modeling study of uranyl nitrate extraction with monoamides II. Molecular mechanics and lipophilicity calculations. Structure-activity relationships, *Solvent Extr. Ion Exch.* 17 (1999) 87–112.

147. Solovkin, A.S.; Rubisov, V.N.; Smelov, V.S.; Druzherukov, V.I.; Starikov, V.M.; Muratova, G.G. Simulating equilibria in two-phase systems: H_2O-HNO_3-H_2SO_4-An(IV)-tri-*n*-butyl-phosphate-*n*-alkanes, *Sov. Atomic Energy* (English Trans.) 62 (1987) 385–390.

148. Pandey, N.K.; Koganti, S.B. Simulation of electro-mixer-settler for the partitioning of uranium and plutonium in PUREX process, *Ind. J. Chem. Technol.* 11 (2004) 535–547.

149. Kumar, S.; Kumar, R.; Koganti, S.B. Indira Gandhi Centre for Atomic Research, Kalpakkam (India), Report, IGC-273 (2005).

150. Kumar, S.; Koganti, S.B. Development and application of a computer code SIMPSEX for simulation of FBR reprocessing flowsheets, Report IGC–234 (2002).
151. Kumar, S.; Koganti, S.B. Indira Gandhi Centre for Atomic Research, Kalpakkam (India), Report; IGC-230 (2002).
152. Kumar, S.; Koganti, S.B. Indira Gandhi Centre for Atomic Research, Kalpakkam (India), Report; IGC-229 (2002).
153. Status and Trends of Spent Fuel Reprocessing, IAEA TECDOC-1103 (1999).
154. McKay, H.A.C.; Miles, J.H.; Swanson, J.L. In *Science and Technology of Tributyl Phosphate*, W.W. Schulz, L.L. Burger, J.D. Navratil, and K.P. Bender (Eds.), CRC Press, Boca Raton, FL (1990), Vol. 3, Chapter 1.
155. Wick, O.J. *Plutonium Handbook: A Guide to the Technology*, Gordon and Breach, New York (1967) Vol. II.
156. Stevenson, R.L.; Smith, P.E. In *Reactor HandBook (Fuel Reprocessing)*, S.M. Stoller and R.B. Richards (Eds.), Interscience, New York (1961), Vol. 2.
157. Ebert, K., Reprocessing of spent nuclear fuel: Status and prospects, *Nucl. Energy* 27 (1988) 361–365.
158. Sekine, T. In *Solvent Extraction 1990*, T. Sekine (Ed.) Pt A, Elsevier Science, Amsterdam (1992), p. 747.
159. Anderson, B.; Frew, J.D.; Pugh, O.; Thomson, P.J. Reprocessing the fuel from the prototype fast reactor (PFR), *Nucl. Eng.* 35 (1994) 129–133.
160. Benedict, M.; Pigford, T.H.; Levi, H.W. *Nuclear Chemical Engineering*, McGraw-Hill, New York (1981).
161. Bodansky, D. Reprocessing spent nuclear fuel, *Phys. Today* (2006) 80–81.
162. Rajagopalan, C.V.; Periasamy, K.; Koganti, S.B. ACE-94: Advances in Chemical Engineering in Nuclear and Process Industries, Mumbai (India), 9–11 June 1994, pp. 517–523.
163. Ramanujam, A.; Venkataraman, N. Spent fuel reprocessing, In *Facets of Nuclear Science and Technology*, S.K. Aggarwal and D.D. Sood (Eds.), Department of Atomic Energy, Mumbai, India (1996), pp. 137–147.
164. Sood, D.D.; Patil, S.K. Chemistry of nuclear fuel reprocessing: Current status, *J. Radioanal. Nucl. Chem.* 203 (1999) 547–573.
165. Ban, Y.; Asakura, T.; Morita, Y. GLOBAL 2005: International Conference on Nuclear Energy Systems for Future Generation and Global Sustainability, Tsukuba, Ibaraki (Japan) 9–13 October, 2005.
166. Zhaowu, Z.; Jianyu, H.; Zefu, Z.; Yu, Z.; Jianmin, Z.; Weifang, Z. Uranium/plutonium and uranium/neptunium separation by the Purex process using hydroxyurea, *J. Radioanal. Nucl. Chem.* 262 (2004) 707–711.
167. Hiroshi, S.; Atsushi, I.; Chuzaburo, T.; Shigehiko, M.; Syouzo, Y.; Takao, A. *International Conference on Nuclear Fuel Reprocessing and Waste Management*, RECOD'91, Sendai (Japan), 14–18 April 1991, pp. 786–789.
168. Vandegrift, G.F.; Regalbuto, M.C.; Aase, S.; Bakel, A.; Battisti, T.J.; Bowers, D.; Byrnes, J.P.; Clark, M.A.; Emery, J.W.; Falkenberg, J.R.; Gelis, A.V.; Pereira, C.; Hafenrichter, L.; Tsai, Y.; Quigley, K.J.; Vander Pol, M.H. Designing and demonstration of the UREX + process using spent nuclear fuel, ATLANTE 2004, June 21–25, 2004.
169. GNEP Strategic Plan, GNEP-167312, Rev 0, January 2007.
170. Knighton, J.B.; Baldwin, C.E. Pyrochemical Coprocessing of Uranium Dioxide-Plutonium Dioxide LMFBR Fuel by the Salt Transport Method, Rocky Flats Report RFP-2887, CONF-790415-29 (1979).
171. Zabunoğlu, O.H.; Özdemir, L. Purex co-processing of spent LWR fuels: Comparative fuel cycle cost analyses, *Ann. Nucl. Energy* 32 (2005) 137–149.
172. Zabunoğlu, O.H.; Özdemir, L. Purex co-processing of spent LWR fuels: Flow sheet, *Ann. Nucl. Energy* 32 (2005) 151–162.

173. Sunanta, P.; Reiner, P. Recycling of actinides in light water reactors, *Nucl. Technol.* 51 (1980) 7–12.

174. Birkett, J.E.; Carrott, M.J.; Fox, O.D.; Jones, C.J.; Maher, C.J.; Roube, C.V.; Raylor, R.J.; Woodhead, D.A. Recent developments in the Purex process for nuclear fuel reprocessing: Complexant based stripping for uranium/plutonium separation, *Chimia* 59 (2005) 898–904.

175. Carrott, M.J.; Fox, O.D.; LeGurun, G.; Jones, C.J.; Mason, C.; Taylor, R.J.; Andirieux, F.P.L.; Boxall, C. Oxidation-reduction reactions of simple hydroxamic acids and plutonium(IV) ions in nitric acid, *Radiochim. Acta* 96 (2008) 333–343.

176. Carrott, M.J.; Fox, O.D.; Maher, C.J.; Mason, C.; Taylor, R.J.; Sinkov, S.I.; Choppin, G.R. Solvent extraction behavior of plutonium (IV) ions in the presence of simple hydroxamic acids, *Solvent Extr. Ion Exch.* 25 (2007) 723–745.

177. Taylor, R.J.; Sinkov, S.I.; Choppin, G.R.; May, I. Solvent extraction behavior of neptunium (IV) ions between nitric acid and diluted 30% tri-butyl phosphate in the presence of simple hydroxamic acids. *Solvent Extr. Ion Exch.* 26 (2008) 41–61.

178. Sinkov, S.I.; Choppin, G.R.; Taylor, R.J. Spectrophotometry and luminescence spectroscopy of acetohydroxamate complexes of trivalent lanthanide and actinide ions, *J. Solut. Chem.*, 36 (2007) 815–830.

179. Pathak, P.N.; Prabhu, D.R.; Kanekar, A.S.; Manchanda, V.K. Recent R&D Studies Related to Spent Nuclear Fuel Reprocessing. Presented in Plutonium Futures "The Science" 2008 Conference held at Dijon, France, July 7–11, 2008.

180. Bond, W.D. Thorex process, In *Science and Technology of Tributyl Phosphate*, W.W. Schulz, K.P. Bender, L.L. Burger, and J.D. Navratil (Eds.), Vol. 3, *Applications of Tributyl Phosphate in Nuclear Fuel Processing*, CRC Press, Boca Raton, FL (1990), pp. 225–247.

181. Rathvon, H.C.; Blasewitz, A.G.; Maher, R.; Eargle, Jr., J.C.; Wible, A.E. *Proceedings of International Thorium Fuel Cycle Symposium* (1966), p. 765.

182. Fergusan, D.E.; Nicholsan, E.L. USAEC Report, ORNL – 715, Oak Ridge National Laboratory, July 27, 1950.

183. Hylton, C.D. USAEC Report, ORNL – 1425, Oak Ridge National Laboratory, December 30, 1952.

184. Gresky, A.T.; Bennet, M.R.; Brandt, S.S.; McDuffee, W.T.; Savolainen, J.E. USAEC Report, ORNL – 1367, Oak Ridge National Laboratory, January 2, 1953.

185. Bruce, F.R.; Shank, E.M.; Brooksbank, R.E.; Parroff, J.R.; Sadowski, G.S. *Proceedings Second United Nations International Conference on Peaceful Uses of Atomic Energy* (1958), Vol. 17, p. 49.

186. Rainey, R.H.; Moore, J.H. USAEC Report, ORNL – 3155, Oak Ridge National Laboratory, May, 1952.

187. Balasubramaniam, G.R.; Chitnis, R.T.; Ramanujam, A.; Venkatesan, M. Report, BARC – 940, Bhabha Atomic Research Centre, Mumbai, India (1977).

188. Vijayan, K.; Shinde, S.S.; Jambunathan, U.; Ramanujam, A. *Proceedings of Annual Conference of Indian Nuclear Society*, INSAC-2000/50, Mumbai, June 1–2, 2000, p. 148.

189. Sinalkar, N.M.; Janardanan, C.; Vijayan, K.; Shinde, S.S.; Jambunathan, U.; Ramanujam, A. *Nuclear and Radiochemistry Symposium*, NUCAR-2001, CARM-37, University of Pune, Pune, February 7–10, 2001, p. 210.

190. Srinivasan, N.; Nadkarni, M.N.; Balasubramanian, G.R.; Chitnis, R.T.; Siddiqui, H.R. Report, BARC – 643, Bhabha Atomic Research Centre, Mumbai, India (1972).

191. Mukherjee, A.; Kulkarni, R.T.; Rege, S.G.; Achuthan, P.V. Proceedings of DAE Symposium on Radiochemistry and Radiation Chemistry, SC-12, University of Pune, Pune (1982).

192. Chitnis, R.T.; Rajappan, K.G.; Kumar, S.V.; Nadkarni, M.N. Report, BARC – 1003, Bhabha Atomic Research Centre, Mumbai, India (1979).

193. Ramanujam, A.; Dhami, P.S.; Gopalkrishnan, V.; Mukherjee, A.; Dhumwad, R.K. Report, BARC – 1486, Bhabha Atomic Research Centre, Mumbai, India (1989).
194. Govindan, P.; Palamalai, A.; Vijayan, K.S.; Raja, M.; Parthasarathy, S.; Mohan, S.V.; Subba Rao, R.V. Purification of 233U from thorium and iron in the reprocessing of irradiated thorium oxide rods, *J. Radioanal. Nucl. Chem.* 246 (2000) 441–444.
195. Chitnis, R.R.; Dhami, P.S.; Ramanujam, A.; Kansara, V.P. Bhabha Atomic Research Centre, Mumbai (India), BARC Report, BARC-2001/E/030.
196. Kedari, C.S.; Sinalkar, N.; Dhami, P.S.; Achuthan, P.V.; Vijayan, K.; Moorthy, A.D.; Jambunathan, U.; Munshi, S.K.; Dey, P.K. Report, BARC-2005/E/024.
197. Venkatesan, K.A.; Robertselvan, B.; Antony, M.P.; Srinivasan, T.G.; Vasudeva Rao, P.R. Physiochemical and plutonium retention properties of hydrolytic and radiolytically degraded tri-*n*-amylphosphate, *Solvent Extr. Ion Exch.* 24 (2006) 747–763.
198. Siddall III, T.H. Trialkyl phosphates and dialkyl alkylphosphonates in uranium and thorium extraction, *Ind. Eng. Chem.* 51 (1959) 41–44.
199. Mason, G.W.; Griffin, H.E. Demonstration of the potential for designing extractants with preselected extraction properties: possible application to reactor fuel reprocessing, In *Actinide Separations*, J.D. Navratil and W.W. Schulz (Eds.), American Chemical Society, Washington, DC (1980), pp. 89–99.
200. Siddall III, T.H. Effects of structure of *N,N*-disubstituted amides on their extraction of actinide and zirconium nitrates and of nitric acid, *J. Phys. Chem.* 64 (1960) 1863–1866.
201. Siddall III, T.H. USAEC Report DP – 541, E. I. Du Pont de Nemours and Co. Alken, SC (1961).
202. Musikas, C.; Condamines, C.; Cuillerdier, C.; Nigond, L. International Symposium on Radiochemistry and Radiation Chemistry – Plutonium 50, Bombay (India), 4–7 February, 1991.
203. Musikas, C.; Condamines, N.; Cuillerdier, C. ISEC'90: International Solvent Extraction Conference, Kyoto (Japan), 16–21 July, 1990.
204. Musikas, C. Potentiality of nonorganophosphorus extractants in chemical separations of actinides, *Sep. Sci. Technol.* 23 (1988) 1211–1226.
205. Manchanda, V.K.; Pathak, P.N. Amides and diamides as promising extractants in the back end of the nuclear fuel cycle: An overview, *Sep. Pur. Technol.* 35 (2004) 85–103.
206. Danesi, P.R.; Horwitz, E.P.; Rickert, P.G. Rate and mechanism of facilitated americium(III) transport through a supported liquid membrane containing a bifunctional organophosphorous mobile carrier, *J. Phys. Chem.* 87 (1983) 4708–4715.
207. Sriram, S.; Manchanda, V.K. Transport of metal ions across a supported liquid membrane (SLM) using dimethyldibutyl-tetradecyl-1,3-malonamide (DMDBTDMA) as the carrier, *Solvent Extr. Ion Exch.* 20 (2002) 97–114.
208. Kaminski, M.D.; Nunez, L. Extractant-coated magnetic particles for cobalt and nickel recovery from acidic solution, *J. Magn. Magn. Mater.* 194 (1999) 31–36.
209. Nunez, L.; Buchholz, B.A.; Vandergrift, G.F. Waste remediation using in situ magnetically assisted chemical separation, *Sep. Sci. Technol.* 30 (1995) 1455–1471.
210. Mathur, J.N.; Murali, M.S.; Iyer, R.H.; Ramanujam, A.; Dhami, P.S.; Gopalkrishnan, V.; Rao, M.K.; Badheka, L.P.; Banerji, A. Extraction chromatographic separation of minor actinides from purex high-level wastes using CMPO, *Nucl. Technol.* 109 (1995) 216–225.
211. Yamaura, M.; Matsuda, H.T. Actinides and fission products extraction behavior in TBP/XAD7 chromatographic column, *J. Radioanal Nucl. Chem.* 224 (1997) 83–87.
212. Ansari, S.A.; Murali, M.S.; Pathak, P.N.; Manchanda, V.K. Extraction chromatography of actinides using cyanex-923 as stationary phase, *Solvent Extr. Ion Exch.* 22 (2004) 1013–1036.

213. Mohapatra, P.K.; Sriram, S.; Manchanda, V.K.; Badheka, L.P. Uptake of metal ions by extraction chromatography using dimethyl dibutyl tetradecyl-1,3-malonamide (DMDBTDMA) as the stationary phase, *Sep. Sci. Technol*. 35 (1999) 39–55.

214. Braun, T.; Ghersini, G. *Extraction Chromatography*, Vol. 2, Elsevier Scientific, New York, 1975.

215. Madic, C.; Kertesz, C.; Sontag, R.; Koehly, G. Application of extraction chromatography to the recovery of neptunium, plutonium and americium from an industrial waste, *Sep. Sci. Technol.* 15 (1980) 745–762.

216. Naik, P.W.; Dhami, P.S.; Misra, S.K.; Jambunathan, U.; Mathur, J.N. Use of organophosphorus extractants impregnated on silica gel for the extraction chromatographic separation of minor actinides from high level waste solutions, *J. Radioanal. Nucl. Chem.* 257 (2003) 327–332.

217. Schulte, L.D.; McKee, S.D.; Salazar, R.R. Annual Meeting of the American Nuclear Society (ANS), Reno, NV, 16–20 June, 1996.

218. Ansari, S.A.; Mohapatra, P.K.; Manchanda, V.K. Synthesis of N,N'-dimethyl-N,N'-dibutyl malonamide functionalized polymer and its sorption affinities towards U(VI) and Th(IV) ions, *Talanta* 73 (2007) 878–885.

219. Ansari, S.A.; Mohapatra, P.K.; Manchanda, V.K. A novel malonamide grafted polystyrene-divinyl benzene resin for extraction, pre-concentration and separation of actinides, *J. Hazard. Mater.* 161 (2009) 1323–1329.

220. Prabhakaran, D.; Subramanian, M.S. Selective extraction of U(VI) over Th(IV) from acidic streams using di-bis(2-ethylhexyl) malonamide anchored chloromethylated polymeric matrix, *Talanta* 65 (2005) 179–184.

221. Shiva Kesava Raju, Ch.; Subramanian, M.S. Sequential separation of lanthanides, thorium and uranium using novel solid phase extraction method from high acidic nuclear wastes, *J. Hazard. Mater*. 145 (2007) 315–322.

222. Maheshwari, M.A.; Subramanian, M.S. AXAD-16-3,4-dihydroxy benzoyl methyl phosphonic acid: A selective preconcentrator for U and Th from acidic waste streams and environmental samples, *React. Funct. Polymer* 62 (2005) 105–114.

223. Shamsipur, M.; Ghiasvand, A.R.; Yamini, Y. Solid-phase extraction of ultratrace uranium(VI) in natural waters using octadecyl silica membrane disks modified by tri-N-octylphosphine oxide and its spectrophotometric determination with dibenzoylmethane, *Anal. Chem.* 65 (1999) 4892–4895.

224. Wai, C.M.; Lin, Y.; Ji, M.; Toews, K.L.; Smart, N.G. Extraction and separation of uranium and lanthanides with supercritical fluids, *ACS Symposium Series* 716 (1999) 390–400.

225. Burford, M.D.; Ozel, M.Z.; Clifford, A.A.; Bartle, K.D.; Lin, Y.; Wai, C.M.; Smart, N.G. Extraction and recovery of metals using a supercritical fluid with chelating agents, *Analyst* 124 (1999) 609–614.

226. Lin, Y.; Smart, N.G.; Wai, C.M. Supercritical fluid extraction and chromatography of metal chelates and organometallic compounds, *Trends Anal. Chem.* 14 (1995) 123–133.

227. Wai, C.M.; Wang, S. Supercritical fluid extraction: Metals as complexes, *J. Chrom. A* 785 (1997) 369–383.

228. Lin, Y.; Wu, H.; Smart, N.; Wai, C.M. Investigation of adducts of lanthanide and uranium β-diketonates with organophosphorus Lewis bases by supercritical fluid chromatography, *J. Chrom. A* 793 (1998) 107–113.

229. Wai, C.M.; Kulyako, Y.; Yak, H.K.; Chen, X.; Lee, S.J. Selective extraction of strontium with supercritical fluid carbon dioxide, *Chem. Comm.* 24 (1999) 2533–2534.

230. Wai, C.M. Supercritical fluid extraction of radionuclides: A green technology for nuclear waste management, *ACS Symposium Series* 943 (2006) 161–170.

231. Wai, C.M. Reprocessing spent nuclear fuel with supercritical carbon dioxide, *ACS Symposium Series* 933 (2006) 57–67.

232. Chiu, K.H.; Yak, H.K.; Wang, J.S.; Wai, C.M. Supercritical fluid extraction of mixed wastes, *Green Chem.* 6 (2004) 502–506.
233. Clifford, A.A.; Zhu, S.; Smart, N.G.; Lin, Y.; Wai, C.M.; Yoshida, Z.; Meguro, Y.; Iso, S. Modelling of the extraction of uranium with supercritical carbon dioxide, *J. Nucl. Sci. Tech.* 38 (2001) 433–438.
234. Samsonov, M.D.; Wai, C.M.; Lee, S.-C.; Kulyako, Y.; Smart, N.G. Dissolution of uranium dioxide in supercritical fluid carbon dioxide, *Chem. Comm.* (2001) 1868–1869.
235. Meguro, Y.; Iso, S.; Yoshida, Z.; Tomioka, O.; Enokida, Y.; Yamamoto, I. Decontamination of uranium oxides from solid wastes by supercritical CO_2 fluid leaching method using HNO3-TBP complex as a reactant, *J. Supercrit. Fluids* 31 (2004) 141–147.
236. Trofimov, T.I.; Samsonov, M.D.; Kulyako, Y.M.; Myasoedov, B.F. Dissolution and extraction of actinide oxides in supercritical carbon dioxide containing the complex of tri-n-butylphosphate with nitric acid, *C.R. Chimie* 7 (2004) 1209–1213.
237. Samsonov, M.D.; Trofimov, T.I.; Kulyako, Y.M.; Myasoedov, B.F. Recovery of actinides from their dioxides using supercritical CO_2 containing the adduct of tributyl phosphate with nitric acid, *Radiochemistry* 49 (2007) 246–250.
238. Enokida, Y.; Al-Fatah, S.A.; Wai, C.M. Ultrasound-enhanced dissolution of UO2 in supercritical CO_2 containing a CO_2-philic complexant of tri-n-butylphosphate and nitric acid, *Ind. Eng. Chem. Res.* 41 (2002) 2282–2286.
239. Toews, K.L.; Smart, N.G.; Wai, C.M. Complexation and transport of uranyl nitrate in supercritical carbon dioxide with organophosphorus reagents, *Radiochim. Acta* 75 (1996) 179–184.
240. Meguro, Y.; Iso, S.; Takeishi, H.; Yoshida, Z. Extraction of uranium(VI) in nitric acid solution with supercritical carbon dioxide fluid containing tributylphosphate, *Radiochim. Acta* 75 (1996) 185–191.
241. Lin, Y.; Smart, N.G.; Wai, C.M. Supercritical fluid extraction of uranium and thorium from nitric acid solutions with organophosphorus reagents, *Environ. Sci. Tech.* 29 (1995) 2706–2708.
242. Lin, Y.; Wai, C.M.; Jean, F.M.; Brauer, R.D. Supercritical fluid extraction of thorium and uranium ions from solid and liquid materials with fluorinated β-Diketones and tributyl phosphate, *Environ. Sci. Tech.* 28 (1994) 1190–1193.
243. Kumar, R.; Sivaraman, N.; Srinivasan, T.G.; Vasudeva Rao, P.R. Studies on the supercritical fluid extraction of uranium from tissue matrix, *Radiochim. Acta* 90 (2002) 141–145.
244. Kumar, R.; Sivaraman, N.; Vadivu, E.S.; Srinivasan, T.G.; Vasudeva Rao, P.R. Complete removal of uranyl nitrate from tissue matrix using supercritical fluid extraction, *Radiochim. Acta* 91 (2003) 197–201.
245. Kumar, P.; Pal, A.; Saxena, M.K.; Ramakumar, K.L. Supercritical fluid extraction of thorium from tissue paper matrix employing organophosphorous reagents, *Radiochim. Acta* 95 (2007) 701–708.
246. Kumar, R.; Sivaraman, N.; Sujatha, K.; Srinivasan, T.G.; Vasudeva Rao, P.R. Removal of plutonium and americium from waste matrices by supercritical carbon dioxide extraction, *Radiochim. Acta* 95 (2007) 577–584.
247. Myasoedov, B.F.; Kulyako, Y.M.; Trofimov, T.I.; Samsonov, M.D.; Malikov D.A. Recovery of U and Pu from simulated spent nuclear fuel by adducts of organic reagents with HNO_3 followed by their separation from fission products by countercurrent chromatography, Plutonium Futures – *The Science* 2008, Dijon, France, July 7–11.
248. Trofimov, T.I.; Samsonov, M.D.; Kulyako, Y.M.; Myasoedov, B.F. Dissolution and extraction of actinide oxides in supercritical carbon dioxide containing the complex of tri-n-butylphosphate with nitric acid, *C.R. Chimie* (2004) 1209–1213.
249. Samsonov, M.D.; Trofimov, T.I.; Vinokurov, S.E.; Myasoedov, B.F.; Lee, S.C.; Wai, C.M. Actinide 2001, *International Conference Hayama*, Kanagawa (Japan) 4–9 November, pp. 263–266.

250. Miura, S.; Kamiya, M.; Miyachi, S.; Koyama, T.; Ogumo, S.; Shimada, T.; Mori, Y.; Enokida, Y. GLOBAL 2005: International Conference on Nuclear Energy Systems for Future Generation and Global Sustainability, Tsukuba, Ibaraki (Japan) 9–13 October, 2005.

251. Miura, S.; Kamiya, M.; Nomura, K.; Koyama, T.; Ogum, S.; Shimada, T.; Mori, Y.; Enokida, Y. Atalante 2004 Conference: Advances for Future Nuclear Fuel Cycles, Nimes (France) 21–24 June, 2004.

252. Clifford, A.A.; Zhu, S.; Smart, N.G.; Lin, Y.; Wai, C.M.; Yoshida, Z.; Meguro, Y.; Iso, S. Modelling of the extraction of uranium with supercritical carbon dioxide, *J. Nucl. Sci. Technol. Tokyo* 38 (6) (2001) 433–438.

253. Park, Y.Y.; Fazekas, Z.; Harada, M.; Ikeda, Y.; Yamamura, T.; Tomiyasu, H. Japan-Korea Seminar on Advanced Reactors Tokyo (Japan) 19–20 October 2000; *Bull. Res. Lab. Nucl.* Reactors-Tokyo-Institute-of-Technology (2000), Vol. 3 (special issue) pp. 160–162.

254. Ho, W.S.W.; Sirkar, K.K. *Membrane Handbook*, Van Nostrand Reinhold, New York, 1992.

255. Boyadzhiev, L.; Lazarova, Z. Liquid membranes (liquid pertraction) In *Membrane Separations Technology, Principles, and Applications*, R.D. Noble and S.A. Stern (Eds.), Elsevier Science B.V., Amsterdam (1995).

256. Zhang, R. *Separation Techniques by Liquid Membranes*, Jiangxi Renmin, Nanchang (1984).

257. Mohapatra, P.K.; Manchanda, V.K. Liquid membrane based separations of actinides and fission products, *Ind. J. Chem.* 42A (2003) 2925–2938.

258. IUPAC Technical Report Series No. 431, Application of Membrane Technologies for Liquid Waste Processing, IAEA, Vienna (2004).

259. Choppin, G.R.; Morgenstern, A. Radionuclide separations in radioactive waste disposal, *J. Radioanal. Nucl. Chem.* 243 (2000) 45–51.

260. Advanced technologies for the treatment of low and intermediate level radioactive wastes, IAEA Technical Report, Series No. 370, International Atomic Energy Agency, Vienna, Austria, 1994.

261. Sriram, S.; Mohapatra, P.K.; Pandey, A.K.; Manchanda, V.K.; Badheka, L.P. Facilitated transport of americium(III) from nitric acid media using dimethyldibutyltetradecyl-1,3-malonamide, *J. Memb. Sci.* 177 (2000) 163–175.

262. Danesi, P.R. Separation of metal species by supported liquid membranes, *Sep. Sci. Technol.* 19 (1985) 857–894.

263. Danesi, P.R.; Chiarizia, R.; Rickert, P.; Horwitz, E.P. Separation of actinides and lanthanides from acidic nuclear wastes by supported liquid membranes, *Solvent Extr. Ion Exch.* 3 (1985) 111–147.

264. Muscatello, A.C.; Navratil, J.D. Americium removal from nitric acid waste stream, *J. Radioanal. Nucl. Chem.* 128 (2005) 449–462.

265. Mohapatra, P.K.; Lakshmi, D.S.; Mohan, D.; Manchanda, V.K. Uranium pertraction across a PTFE flat sheet membrane containing Aliquat 336 as the carrier, *Sep. Pur. Technol.* 51 (2006) 24–30.

266. Mohapatra, P.K.; Lakshmi, D.S.; Mohan, D.; Manchanda, V.K. Selective transport of cesium using a supported liquid membrane containing di-t-butyl benzo 18 crown 6 as the carrier, *J. Membr. Sci.* 232 (2004) 133–139.

267. Mohapatra, P.K.; Pathak, P.N.; Kelkar, A.; Manchanda, V.K. Novel polymer inclusion membrane containing a macrocyclic ionophore for selective removal of strontium from nuclear waste solution, *New J. Chem.* 28 (2004) 1004–1009.

268. Joshi, J.M.; Manchanda Pathak, P.N.; Pandey, A.K.; Manchanda, V.K. Optode for uranium(VI) determination in aqueous medium, *Talanta* 76 (2008) 60–65.

269. Mohapatra, P.K.; Pathak, P.N.; Kelkar, A.; Manchanda, V.K. Novel polymer inclusion membrane containing a macrocyclic ionophore for selective removal of strontium from nuclear waste solution, *New J. Chem.* 28 (2004) 1004–1009.

270. Noble, R.D.; Koval, C.A.; Pellegrino, J.J. Facilitated transport membrane systems, *Chem. Eng. Prog.* 85 (1989) 58–70.

271. Izatt, R.M.; Lamb, J.D.; Bruening, R.L. Comparison of bulk, emulsion, thin sheet supported, and hollow fiber supported liquid membranes in macrocycle-mediated cation separations, *Sep. Sci. Technol.* 23 (1988) 1645–1658.

272. Chiarizia, R.; Horwitz, E.P.; Rickert, P.G.; Hodgson, K.M. Application of supported liquid membranes for removal of uranium from groundwater, *Sep. Sci. Technol.* 25 (1990) 1571–1586.

273. Rathore, N.S.; Sonawane, J.V.; Kumar, A.; Venugopalan, A.K.; Singh, R.K.; Bajpai, D.D.; Shukla, J.P. Hollow fiber supported liquid membrane: A novel technique for separation and recovery of plutonium from aqueous acidic wastes, *J. Membr. Sci.* 189 (2001) 119–128.

274. Rathore, N.S.; Sonawane, J.V.; Kumar, A.; Venugopalan, A.K.; Singh, R.K.; Bajpai, D.D.; Shukla, J.P. *NUCAR 99: Nuclear and Radiochemistry Symposium*, Mumbai (India) 19–22 January 1999, pp. 153–154.

275. Babcock, W.C.; Baker, R.W.; Kelly, D.J.; LaChapelle, E.D. International Solvent Extraction Conference, ISEC-80, Liege, Belgium.

276. Subba Rao, R.V.; Sivakumar, P.; Natarajan, R.; Vasudeva Rao, P.R. Effect of Aliquat 336 concentration on transportation of hydrochloric acid across supported liquid membrane, *J. Radioanal. Nucl. Chem.* 252 (1) (2002) 95–98.

277. Shailesh, S.; Pathak, P.N.; Mohapatra, P.K.; Manchanda, V.K. Transport studies of uranium across a supported liquid membrane containing N,N-di(2-ethylhexyl) isobutyramide (D2EHIBA) as the carrier, *J. Membr. Sci.* 272 (2006) 143–151.

278. Patil, C.B.; Mohapatra, P.K.; Singh, R.R.; Gurba, P.B.; Janardan, P.; Changrani, R.D.; Manchanda, V.K. Transport of uranium from nitric acid solution by non-dispersive solvent extraction using a hollow fibre contactor, *Radiochim. Acta* 94 (2006) 331–334.

279. Kaminski, M.D.; Nunez, L. Cesium extraction from a novel chemical decontamination process solvent using magnetic microparticles, *Sep. Sci. Technol.* 37 (2002) 3703–3714.

280. Nunez, L.; Kaminski, M.D. Transuranic separation using organophosphorus extractants adsorbed onto super paramagnetic carriers, *J. Magn. Magn. Mater.* 194 (1999) 102–107.

281. Kaminski, M.D.; Landsberger, S.; Nunez, L.; Vandegrift, G.F. Sorption capacity of ferromagnetic microparticles coated with CMPO, *Sep. Sci. Technol.* 32 (1997) 115–126.

282. Buchholz, B.A.; Tuaazon, H.E.; Kaminski, M.D.; Aase, S.B.; Nunez, L.; Vandegrift, G.F. Optimizing the coating process of organic actinide extractants on magnetically assisted chemical separation particles, *Sep. Pur. Technol.* 11 (1997) 211–219.

283. Nunez, L.; Buchholz, B.A.; Vandegrift, G.F. Radiolysis and hydrolysis of magnetically assisted chemical separation particles, *Sep. Sci. Technol.* 31 (1996) 1933–1952.

284. Mathews, S.E.; Parzuchoski, P.; Garcia-Carrera, A.; Grüttner, C.; Dozol, J.F.; Bohmer, V. Extraction of lanthanides and actinides by a magnetically assisted chemical separation technique based on CMPO-calix[4]arenas, *Chem. Commun.* 5 (2001) 417–418.

285. Kaminski, M.D.; Nunez, L.; Visser, A.V. Evaluation of extractant-coated ferromagnetic microparticles for the recovery of hazardous metals from waste solution, *Sep. Sci. Technol.* 34 (1999) 1103–1120.

286. Shaibu, B.S.; Reddy, M.L.P.; Prabhu, D.R.; Kanekar, A.S.; Manchanda, V.K. N,N'-dimethyl-N, N'-dibutyl tetradecyl malonamide impregnated magnetic particles for the extraction and separation of radionuclides from nuclear waste streams, *Radiochim. Acta* 94 (2006) 267–273.

287. Shaibu, B.S.; Reddy, M.L.P.; Bhattacharyya, A.; Manchanda, V.K. Evaluation of Cyanex 923-coated magnetic particles for the extraction and separation of lanthanides and actinides from nuclear waste streams, *J. Magn. Magn. Mater*. 301 (2006) 312–318.

288. Shaibu, B.S.; Reddy, M.L.P.; Prabhu, D.R.; Kanekar, A.S.; Manchanda, V.K. N,N,N',N'-tetraoctyl-3-oxapentane-1,5-diamide impregnated magnetic particles for the uptake of lanthanides and actinides from nuclear waste streams, *Radiochim. Acta* 95 (2007) 159–164.

3 Overview of Recent Advances in An(III)/Ln(III) Separation by Solvent Extraction

Clément Hill
Commissariat à l'Énergie Atomique

CONTENTS

3.1 INTRODUCTION

3.1.1 Why Should Trivalent Actinides Be Separated?

Spent nuclear fuel from any current power reactor contains uranium and plutonium, in proportions such that their recovery becomes an economically justifiable operation that also saves natural uranium resources. Industrial reprocessing of spent nuclear fuel through the PUREX process (*1–4*) aims at partitioning uranium (U) and plutonium (Pu) from the fission products and the minor actinides (neptunium (Np), americium (Am), curium (Cm), californium (Cf), etc.), so designated because of their small quantities per ton of metallic fuel compared with U and Pu. Reprocessed plutonium can be used to fabricate mixed oxide (MOX) fuel, whereas reprocessed uranium can be stored as a valuable material. Furthermore, by conditioning the highly active PUREX raffinates in glass and the fuel claddings and hulls in concrete matrices, reprocessing of spent nuclear fuel considerably reduces the final waste volume requiring disposal in deep geological repositories.

Regarding the evolution of the radiotoxic inventory of nuclear waste on a geological time scale, it has been calculated that the potential hazard of vitrified waste still exceeds 10,000 years if only U and Pu are separated from the spent fuel. However, the removal of minor actinides followed by transmutation into shorter-lived radionuclides would reduce this period to 300–500 years, in contrast with the 200,000-year period estimated in the case of the direct disposal of spent nuclear fuel. That is the reason why the P&T strategy, namely the partitioning of minor actinides from highly active PUREX raffinates (or, if possible, directly from the spent nuclear fuel dissolution solutions) followed by their transmutation in dedicated nuclear reactors, has consensually been adopted among the Organization for Economic Cooperation and Development/Nuclear Energy Agency (OECD/NEA) countries as the best strategy to reduce long-term nuclear-waste radiotoxicity (*5*). In Japan, the OMEGA program (Option for Making Extra Gains of Actinides and Fission Products Generated in Nuclear Fuel Cycle) was initiated in 1988 (*6, 7*). In France, two Waste Management Acts were enacted in 1991 and 2006 to organize French research programs on the partitioning and transmutation of long-lived radionuclides and help prepare the construction of both an industrial minor-actinide partitioning facility and an actinide-burner reactor by 2020 (*8–15*). EURATOM has funded many collaborative projects among European research institutes in the field of P&T since the 1990s (*16–23*). In 2003, the U.S. Department of Energy instituted a new program: the Advanced Fuel Cycle Initiative (an outgrowth of former programs, Advanced Accelerator Applications and Accelerator Transmutation of Waste), which intends to provide the technologies necessary for cost-effective and environmentally sound processing of spent nuclear fuel by 2025 (*24–27*).

As no technology can selectively transmute minor actinides to a degree meaningful for waste management while they are contained in the spent nuclear fuel, these elements must be separated from the neutron-absorbing elements before being properly transmuted. In the case of trivalent minor actinides, this preliminary step is further necessary because of the following reasons:

- Trivalent actinides (An(III), from Am(III) to Cf(III)) are poorly extracted by tributyl phosphate (TBP); only Np can be separated by modifying the

PUREX experimental conditions; hence, a demand exists for the design of new extracting agents for the recovery of An(III).

- Lanthanides, which account for about one-third of the fission products, are strong neutron-absorbing elements and predominantly exist as trivalent cations in acidic aqueous solutions; the solution chemistry of transplutonium elements (TPEs) thus, resembles that of lanthanides (*28–31*).

The separation of the trivalent 4*f* and 5*f* elements has therefore become a challenging key issue in the technical feasibility demonstration and success of the P&T strategy.

Difficulties that must be overcome when developing a new separation process include the need to:

- Ensure high An(III) recovery yields
- Ensure high An(III) decontamination factors (DFs) toward other elements initially present in the feed stream
- Minimize changes in the highly active feed composition to avoid forming precipitates, the occurrence of which could trap minor actinides and thus decrease their recovery yields
- Minimize secondary waste generation
- Ensure fast mass transfer to shorten the process time and allow the use of small-volume contactors (*32, 33*)

3.1.2 How to Separate Trivalent Actinides?

Although numerous separation processes exist, they all belong to only two main categories: aqueous and dry. Aqueous processes are mainly employed for radionuclides in the form of oxides; dry processes can be used for both metallic and oxide forms. Hydrometallurgical processes (the focus of this review) involve liquid-liquid extraction (solvent extraction) and can easily be implemented at industrial scale through remotely handled continuous operations. They rely on the dissolution of the elements constituting the spent nuclear fuel in an acidic solution, usually a heated solution of concentrated nitric acid, which stabilizes a fairly wide range of oxidation states of the dissolved elements. Furthermore, the prepared nitric feed is not too corrosive toward stainless-steel devices compared with other mineral acids. The chemical behavior of the dissolved elements can thus be controlled by their oxidation states. The target elements, for example the An(III), will undergo complexation reactions:

- Either in the bulk aqueous phase, through specific interactions with hydrophilic chemicals introduced at the different steps of the partitioning process (e.g., extraction or stripping steps), or
- After diffusion to the interface, through specific interactions with lipophilic chemicals incorporated in the organic solvent.

The separation of An(III) will thus be achieved either by selective extraction or by selective complexation in the aqueous phase. These two different modes will be illustrated by many examples in this review. Although favorable to an industrial

implementation, as the amount of An(III) is much smaller than that of the fission products contained in the spent fuel, the selective extraction of An(III) is rather difficult to achieve, especially when the feed contains many other cationic species, as it requires the design of very selective extracting agents. There is currently no identified partitioning process that can selectively extract the An(III) directly from a spent nuclear fuel dissolution solution nor from a nonpretreated PUREX raffinate. As it will be discussed hereafter, most of the processes described in the literature extract the An(III) selectively from an An(III) + Ln(III) solution issued from a first-step process, which has separated the An(III) + Ln(III) fraction from a PUREX highly active raffinate. Examples of such first steps are TRUEX, TRPO, DIAMEX, and DIDPA (first step) processes. Examples of An(III)/Ln(III) second-step separation processes are CYANEX 301, ALINA, and all the systems involving nitrogen polydentate ligands, such as polypyridines or polytriazines (TPTZ, BTP, or BTBP). There are, however, a few processes that allow the An(III)/Ln(III) partitioning by the selective complexation of the An(III) in the aqueous phase, either at the extraction or at the stripping steps. A preliminary pH adjustment by denitration (or acidity reduction/neutralization) of the feed is nevertheless necessary to enable the selective complexation of the An(III) by hydrophilic agents when they are directly introduced in the feed, such as in the TALSPEAK process. In case the selective hydrophilic agent is introduced in the stripping solution, such as in the "reverse" TALSPEAK, DIDPA (second step), SETFICS, and DIAMEX-SANEX/ HDEHP processes, the loading capacity of the organic solvent must be very high to avoid third-phase formation, as some fission products, such as Mo, Zr, Ru, and Pd might also be coextracted with the trivalent lanthanides and actinides.

3.1.3 MOLECULAR ENGINEERING: TOWARD A RATIONAL CONCEPTION OF THE EXTRACTANTS

Among the various parameters to take into account when developing a new separation system for An(III)/Ln(III) separation, the most important ones are the following (*28, 29, 32–39*):

- Affinity toward the target An(III), which should be high under the extraction conditions (high loading capacity without third-phase formation or precipitation) and low under the stripping (back-extraction) conditions (the reversible reaction should be controlled by simple parameters, such as nitrate or proton concentrations).
- Selectivity toward the An(III) versus the mineral acid (usually nitric acid) and the other metallic cations present in the feed. The higher the selectivity attained, the fewer the process stages required, and thus the more compact the industrial footprint.
- Kinetics of phase transfer should be sufficiently fast, both at the extraction and stripping steps, to allow short-residence time contactors to be employed. In pulsed columns, the contacting time averages a few minutes, while in centrifugal contactors, this contacting time might shorten to only a few seconds.

- Coalescence of both the organic and the aqueous phases at each step of the process, which ensures good hydraulic properties (no phase entrainment, no stable emulsion).
- Stability of both the organic diluent and the extractant, which should be the highest possible. However, as the latter will inevitably age and degrade through hydrolysis and radiolysis, its degradation compounds should not disturb the implementation of the separation process and should be easily eliminated by specific washing.
- Secondary waste produced by the implementation of the separation process should be as low as possible. Some current strategies rely on the development of extraction systems based on only four atoms, C, H, O, and N, to convert the spent solvent into environmentally friendly gases.

Therefore, in their quest to design new An(III) selective ligands or extractants, chemists have to consider many criteria, such as:

- The ligand structure (nature of constituting atoms), which will directly condition its hydrolytic/radiolytic stability and impose the nature of its degradation compounds (as secondary waste).
- The nature of the electron-donor atom(s) introduced in the skeleton of the ligand and their electronic densities, which will define the ligand affinity and selectivity toward the An(III).
- The ligand denticity (number and location of the electron donor atoms), which will tune its selectivity toward the target An(III).
- The choice of the substituting groups grafted on the structure of the ligand, which will affect (i) its affinity and selectivity toward the target An(III) (a steric hindrance of its coordination sites will, for instance, decrease its extraction properties); (ii) its hydrophilicity or lipophilicity, which plays in important role in the kinetics of phase transfer and hydraulic properties (e.g., coalescence of the organic phase and aggregation of extractant molecules in the solvent); and (iii) its hydrolytic/radiolytic stability.

To design ever more efficient new ligands, chemists today may benefit from the thriving analytical techniques developed to thoroughly investigate complex formation, metal extraction, and chemical degradation mechanisms (e.g., X-ray crystallography, X-ray absorption, infrared and Raman spectroscopies, time-resolved laser-induced fluorimetry, small-angle neutron/X-ray scattering, nuclear magnetic resonance, or electrospray-ionization mass-spectrometry (*40–53*)), as well as from the accurate theoretical modeling approaches (quantum chemistry and molecular dynamics calculations (*54–57*)).

Since the 1960s, considerable efforts have been devoted worldwide to develop viable An(III)/Ln(III) separation systems, either by liquid-liquid extraction, precipitation, or ion-exchange chromatography. These systems have been regularly reported in comprehensive reviews covering various issues of actinide and lanthanide separations, such as the basics of actinide solution chemistry in aqueous/

organic media, historical background, and emerging techniques that may figure prominently in future developments of actinide separation options (*28, 29, 34–39, 58*). The latest review was published in 2006, highlighting the significant role of soft-donor ligands in the observed An(III)/Ln(III) selectivity and emphasizing the generic flowsheets of the most mature processes developed throughout the world to separate the actinides from the spent-fuel dissolution liquors, such as PUREX, TRUEX, TRPO, DIDPA, UNEX, SETFICS, DIAMEX, and SANEX (*39*). However, although important results have been achieved (concept feasibility assessment at laboratory scale on highly active feeds), to date, none of these separation processes have been developed industrially to ensure the closure of the fuel cycle by selective recovery of the trivalent minor actinides for subsequent transmutation in dedicated reactors.

This review will not consider all aspects of An(III)/Ln(III) separation, but will focus on the latest achievements of solvent-extraction processes developed around the world to separate An(III) from Ln(III) in acidic media. Only systems whose concept feasibility has been assessed through the implementation of countercurrent tests either at laboratory or pilot scales will be described. The reader will find more information in the above-mentioned reviews about some new organic solvents studied for An(III)/Ln(III) separation, but which have not yet been developed up to the process-design stage. The following review will focus only on the studies that have been published in the open literature since the 1990s, and that have not been screened out in previous reviews. It will also include papers published or reported during international conferences during the last couple of years.

3.2   FUNDAMENTAL FEATURES OF HYDROMETALLURGY

3.2.1   Applicable Principles of Solvent Extraction

Hydrometallurgy aims to produce pure metallic species from rather complex solutions. This is typically the case for spent nuclear fuel dissolution liquors, which contain about one-third of the Mendeleyev periodic table. The first step of a hydrometallurgical process usually involves preparing the aqueous feed by dissolving the crude solid material containing the metallic species to be recovered and all sorts of impurities in a suitable aqueous matrix (*59*). In the case of spent nuclear fuel, the dissolution matrix is nitric acid, and the highest dissolution yields are required to minimize actinide losses in the waste (*60*). The target elements are then extracted from this acidic dissolution liquor by contacting it with an immiscible organic solvent containing one (or more) efficient and selective extracting agent(s), which can simultaneously undergo multiple reaction equilibria, often with the help of aqueous complexants and redox agents. The role of the organic diluent is to confer the separation system with the physical properties required for process development: density, surface and vapor tensions, flash point, etc. Preferred diluents for nuclear applications are aliphatic hydrocarbons (e.g., *n*-dodecane, odorless kerosene, isoparaffinic hydrocarbons, etc.) because of their good hydraulics, low aqueous solubility, and resistance to radiation degradation (*32, 33*). The dispersion that takes place during the mixing of the aqueous and the organic phases increases the exchange surface

area (all the more so as the droplets are small), thus increasing the diffusion of the concerned species from the bulk to the interface, the probability for their meeting at the interface, and thus the kinetics of complexation reactions. Preferred devices for achieving this mixing in reprocessing are either discontinuous, such as mixer-settlers and annular centrifugal contactors, or continuous, such as pulsed columns (*61*).

When chemical equilibrium is approached (the chemical potentials of the respective species are equal in both phases), the physical separation of the two phases is achieved either through natural gravity or centrifugation forces. This results in an enriched organic phase that can consequently be contacted with a suitable stripping solution to concentrate the target element(s) into a suitable form for the next step of the reprocessing scheme (e.g., new feed solution, precursor materials for waste conditioning or fuel fabrication) and a depleted aqueous phase (raffinate). This procedure can be repeated countercurrently until the desired recovery and decontamination yields are obtained. Such flexibility in flowsheet design and all-liquid reprocessing takes advantage of a broad range of solvent-extraction chemistry (*62*).

The extraction of a given metallic cation M^{n+} into an organic solvent proceeds either through its coextraction with some of the anions initially present in the aqueous feed (two different mechanisms (1) and (2) are distinguished) or through its exchange with proton(s) from the organic solvent to conserve phase neutrality (mechanism (3)):

1. "Solvate extraction" occurs when a neutral extracting agent (usually a ligand bearing electron donor atoms, such as oxygen in octyl(phenyl)-*N,N*-dii*so*butylcarbamoylmethyl-phosphine oxide (CMPO), used in the TRUEX process) coextracts both the cation and the anion(s) to form intimate, partially, or fully dissociated neutral complexes in the organic phase, depending on the dissociation constant of the organic diluent.
2. "Anion exchange" occurs when an ion pair is formed in the organic phase between the positively charged extracting agent (usually a quaternary or protonated tertiary amine, such as Aliquat 336 used in the TRAMEX process) and the negatively charged complex containing the metallic cation (usually formed in the aqueous feed because of an excess of concentration of anions that complex the targeted metallic cation).
3. "Proton exchange" or "cation exchange" occurs when the metallic cation is extracted through the exchange of proton(s) from the organic acidic extracting agent (such as HDEHP in the TALSPEAK process), which sometimes belongs to a synergistic mixture.

The reasons why solvent extraction has become the reference technique for the reprocessing of spent nuclear fuels at industrial scale (and will probably also be chosen in the future for the recovery of long-lived radionuclides) are the following (*32, 33*):

- The choice is wide for the formulation of the chemical system developed to separate the target species (e.g., number and nature of the extracting agent(s), including the use of binary synergistic systems or phase modifiers, concentration of species, nature of the organic diluent).

- The desired separation and purification specifications are easily obtained by successive extraction-scrubbing-stripping steps. Flowsheet design is very flexible.
- The separation processes involving all-liquid operations can be implemented continuously, which, is very advantageous industrially, as it ensures high throughputs.
- The criticality risks can be almost completely cancelled by designing devices that fulfill specific safety geometric requirements.
- The energy input for running hydrometallurgical processes is usually small (room temperature, normal pressure).

However, it is also fair to say that concerns about proliferation have been a problem, in that solvent-extraction methods have created the possibility to separate plutonium. Furthermore, nuclear researchers have to address several problems when developing partitioning processes, such as the use of flammable liquids, the disposal of spent solvents, as well as the fate of the chemicals introduced in the various parts of the processes to improve their performances (e.g., complexants and buffers added to the feeds or stripping solutions).

3.2.2 Thermodynamics of Solvent Extraction Pertaining to *f*-Elements

3.2.2.1 Properties of Trivalent Actinides and Lanthanides

Today, it is accepted that lanthanides (4*f* elements) and transplutonium actinides (5*f* elements) possess relatively similar physical and chemical properties (*28–31, 63*) including:

- A stable trivalent oxidation state in acidic aqueous solutions
- Decreasing cation radii along the series resulting from the inability of the relatively small spatial extension of the 4*f* and 5*f* electrons to compensate for the steadily increasing nuclear charge
- Similar cation radii for certain An(III) and Ln(III)
- First-coordination-sphere hydration numbers ranging from 9 (at the beginning of the series) to 8 (at the end of the series)
- Hard electron-acceptor properties according to Pearson's theory of hard and soft acids and bases (*64*), which favor electrostatic interactions with oxygen-bearing ligands (hard donors), such as ligands bearing -C=O or -P=O groups

From the early 1980s, it has also been assumed that the slightly greater spatial extension of the 5*f* orbitals was responsible for the existence of some degree of covalence (or polarizability) in the bonding interactions between An(III) and soft bases, such as sulfur- or nitrogen-bearing ligands (*65–69*). Recent thermodynamic studies exploiting accurate analytical techniques, such as microcalorimetry, nuclear magnetic resonance, extended X-ray absorption fine structure, X-ray crystallography or mass spectrometry, providing a better comprehension of the complexation/extraction

mechanisms, have highlighted differences in the behaviors of trivalent actinides and lanthanides (*54–56, 70*). The higher enthalpy terms for An(III) are often assumed to be in line with a higher degree of covalence within the metal-ligand bonds. Furthermore, density functional theory (DFT) calculations have recently managed to account for the experimental relative stabilities of methyl-2,6-bis(1,2,4-triazin-3-yl) pyridine (Me-BTP) complexes with Ce(III) and U(III). In particular, the significant shortening of the U-N distances with respect to those of Ce-N ($\Delta d = 0.09$ Å) in the Me-BTP complexes has been rationalized in terms of π back-bonding interactions between uranium $5f$ orbitals and the ligand π^* levels (*54, 55*). Computational modeling through DFT calculations has also confirmed the experimentally determined metrical parameters of $M[N(EPR_2)_2]_3$ neutral complexes (M = An, Ln; E = S, Se, Te; R = Ph, iPr), in which the An-E bond lengths (An = U, Pu) appear shorter than the Ln-E bond lengths (Ln = La, Ce) for metal ions of similar ionic radii. These results seem consistent with an increase in covalent interactions in the actinide bonding relative to the lanthanide bonding due to an increase in f-orbital participation in the An-E bonds (*56*).

3.2.2.2 Solvate Extraction of Trivalent 4*f* and 5*f* Elements

The solvate extraction mechanism of trivalent $4f$ and $5f$ elements can be described by the following equilibrium, where A^- symbolizes the anion of the aqueous phase and E is the neutral solvation agent of the organic phase (overbars account for species in the organic phase, where residual aqueous molecules might also hydrate the extracted complex):

$$M^{3+} + 3A^- + e\overline{E} \underset{}{\overset{K_{ex}}{\rightleftharpoons}} \overline{MA_3E_e} \tag{3.1}$$

As a rough approximation (neglecting the activity coefficients), the distribution ratio of a given trivalent metallic cation (D_M) can be derived from the logarithm expression of the concentration equilibrium constant K_{ex}:

$$\log D_M = 3\log[A^-] + e\log[\overline{E}] + \log K_{ex}$$

Accordingly, D_M increases with both the concentration of the neutral solvation agent, E, initially present in the organic phase, and that of the mineral anion, A^-, initially present in the aqueous phase. Inversely, the back-extraction of the trivalent element is favored by a decrease of the concentration of A^- in the aqueous solution.

For a given ionic strength, D_M depends on the nature of the coextracted anion A^-. To allow the formation and extraction of the neutral complex, the coextracted mineral anion A^- has to lose part (or all) of its hydration shell. The smaller the hydration energy of the mineral anion is, the easier is its transfer to the organic phase, and thus the higher is the affinity of the solvation extractant toward trivalent $4f$ and $5f$ elements (*29, 76*), as observed in the series chloride < nitrate < perchlorate < pertechnetate, which inversely follows the anion hydration energy order $\Delta G_h(Cl^-) > \Delta G_h(NO_3^-) > \Delta G_h(ClO_4^-) > \Delta G_h(TcO_4^-)$.

If the source of anions A^- is a mineral acid, a competitive proton-extraction reaction might occur, which will decrease the affinity of the neutral solvation agent for the target trivalent elements:

$$n\{H^+, A^-\} + \overline{E} \rightleftharpoons \overline{(HA)_n E} \tag{3.2}$$

On the other hand, if the source of anions A^- is an organophilic acid, already present in the organic phase, a synergistic effect might be observed between the two extractants, but the extraction mechanism will resemble that of a cation exchange (see Section 3):

$$M^{3+} + e\overline{E} + n\overline{(HA)_2} \xrightleftharpoons{K_{ex}} \overline{ME_e A_3 (HA)_{2n-3}} + 3H^+ \tag{3.3}$$

Neutral extracting agents possessing oxygen-donor atoms (hard bases) in their structure easily coordinate trivalent lanthanide and actinide cations, but do not discriminate between the two families of elements, because the ion-dipole (or ion-induced dipole type) interactions mostly rely on the charge densities of the electron donor and acceptor atoms. As a result, the similar cation radii of some An(III) and Ln(III) and the constriction of the cation radius along the two series of f elements make An(III)/Ln(III) separation essentially impossible from nitric acid media. They can be separated, however, if soft-donor anions, such as thiocyanates, SCN^-, are introduced in the feed (*34, 35, 39, 77*).

Neutral oxygen-donor extracting agents coordinate either through monodentate, bidentate, or polydentate modes. However, the higher the degree of coordination of the neutral oxygen-donor extractant to the trivalent cation is, the stronger are the metal-ligand bonding interactions because of the increased entropy-variation term ($\Delta S > 0$), due to the increased system disorder caused by dehydration of the metallic cations (*78*).

Among the monodentate oxygen phosphorus donor extractants widely used for trivalent $4f$ and $5f$ element extraction, one can cite the Neutral organo phosphorous compounds (NOPCs), such as phosphine oxides $R_3P = O$ used in the Chinese TRPO process (*79*). The higher the negative charge density on the oxygen atom of the P=O moiety is, the higher is the affinity of the ligand for a given trivalent $4f$ or $5f$ element salt. Therefore, the order observed for the extraction of trivalent $4f$ and $5f$ elements by monodentate NOPCs follows the inductive effects of the R and RO substituents: $R_3P=O > RO(R')_2P=O > (RO)_2R'P=O > (RO)_3P=O$ (*80, 81*). Because R substituents induce a higher basicity than RO substituents, phosphates are very poor solvation agents of trivalent elements and require a very high salting-out effect.

Bidentate oxygen-donor extractants include the neutral diamide compounds, such as the malonamides used in the French DIAMEX and DIAMEX-SANEX processes, $RR'N(C=O)-CHR''-(C=O)NRR'$; the bisphosphine oxides, $RR'(P=O)- CHR''-(P=O)RR'$; the carbamoyl-(methyl)-phosphinates, $ROR'O(P=O)-(CH_2)_{n=0 \text{ or } 1}-(C=O)NRR'$; or the more efficient carbamoyl-methyl-phosphine oxides, $RR'(P=O)-CHR''-(C=O)$

NRR′, such as CMPO used in several processes (e.g., American or Russian TRUEX, Japanese SETFICS processes). The bifunctional nature of these extractants reduces the impact of competition between HNO_3 and the target metal cations.

Among the terdentate oxygen-donor extractants are the neutral diglycolamide compounds, $RR′N(C=O)-CH_2-O-CH_2-(C=O)NRR′$, used in the Japanese TODGA process.

In all the preceding chemical schemes, R, R′, and R″ represent linear or branched alkyl or phenyl substituents.

Conversely, neutral extracting agents possessing nitrogen electron-donor atoms in their structure (soft bases) will easily discriminate between An(III) and Ln(III) even from nitric acid feeds, thanks to covalently hinted An(III)-N interactions, the best example being the terdentate bis-triazinyl-pyridines (BTPs) or the tetradentate bis-triazinyl-bis-pyridines (BTBP).

3.2.2.3   Cation-Exchange Extraction of Trivalent 4*f* and 5*f* Elements

In simple cases, which tend to be rare, the cation exchanger exists in a monomeric form in the organic phase, mostly found in the case of the chelating β-diketone extractants, $RR′(C=O)-CHR″-(C=O)RR′$. In other cases, such as for the carboxylic acids or the dialkyl-phosphorus acids, dimers predominantly exist in less polar organic phases (*82, 83*). The extraction mechanism of trivalent 4*f* and 5*f* elements can often be described by the following equilibrium, where HA symbolizes the proton exchanger initially present in the organic phase (superscripts account for species in the organic phase):
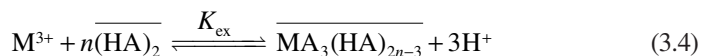
$$M^{3+} + n\overline{(HA)_2} \underset{}{\overset{K_{ex}}{\rightleftharpoons}} \overline{MA_3(HA)_{2n-3}} + 3H^+ \tag{3.4}$$

As a rough approximation (neglecting the activity coefficients), the distribution ratio of the metallic cation (D_M) can be derived from the logarithm expression of the equilibrium constant (K_{ex}):

$$\log D_M = n\log[\overline{(HA)_2}] + 3pH + \log K_{ex}$$

This relation clearly underscores the critical role of the aqueous phase acidity (or pH).

There are various types of organic proton exchangers (*34, 35, 38*). Diesters of phosphoric acid, $(RO)_2P=O(OH)$, phosphonic acids, $R(RO)P=O(OH)$, and phosphinic acids, $R_2P=O(OH)$, where R represents linear or branched alkyl or phenyl substituents, are the most common cation exchangers developed in liquid-liquid extraction for the extraction of trivalent 4*f* and 5*f* elements. They were initially developed for the American TALSPEAK and the Japanese DIDPA processes and have recently been introduced in the French DIAMEX-SANEX process. As for previously described NOPCs, these organophosphorus acids present oxygen-donor atoms (hard bases) in their structures and therefore will easily coordinate trivalent lanthanide and actinide cations, but they will not allow complete discrimination of the two families of elements. However, contrary to previously described neutral organophosphorus

solvation extractants, the order observed for the extraction of trivalent 4*f* and 5*f* elements by organophosphorus acids follows the reverse inductive effects of R and RO substituents: $(RO)_2P=O(OH) > R(RO)P=O(OH) > R_2P=O(OH)$ (*84*).

Alkyl substituents, which increase the basicity compared with RO substituents, make the proton less labile.

Mono- and disulfur substitutes of diesters of phosphoric acids, phosphonic acids, and phosphinic acids, possessing soft-donor atoms in their structures, present large An(III)/Ln(III) selectivities, especially the dialkyl-dithiophosphinic acid used in the Chinese CYANEX 301 process or its chlorophenyl derivative used in the German ALINA process.

Some carboxylic acids, such as bromodecanoic acid, are soluble in hydrocarbon diluents and may be used as cation exchangers. However, due to their usually high pK_a values compared with those of organophosphorus acids or sulfonic acids, the use of these carboxylic acids is restricted to buffered feeds.

3.3 RECENT ADVANCES IN An(III)/Ln(III) SEPARATION BY SOLVENT-EXTRACTION PROCESSES

Until now, the research carried out worldwide for An(III)/Ln(III) separation by solvent extraction has been motivated by two different objectives:

1. Solve the critical problem arising from the legacy of decades of military research programs: how to decontaminate the highly active liquid waste and sludge containing large quantities of alpha emitters?
2. Address the challenges of long-term nuclear-waste storage: how to reduce the radiotoxicity of the final waste to be disposed of in underground repositories?

Today, the Generation IV roadmap requirements and the Global Nuclear Energy Partnership (GNEP) initiated by the United States (*85*) encourage radiochemists to develop hydrometallurgical separation processes that tackle a single challenge: how to recover the minor actinides from the spent-fuel dissolution liquors, selectively or together with other actinides, in order to fabricate new fuels or targets for transmutation in dedicated reactors? This would make possible the closure of the nuclear fuel cycle and demonstrate the sustainability of nuclear energy for the next centuries (*86, 87*).

However, due to the chemical similarities of the trivalent actinide and lanthanide elements, historically, it has been easier to develop step-by-step processes: first, An(III) + Ln(III) coextraction processes, which also address the problem of waste alpha decontamination, and second, An(III)/Ln(III) separation processes, which can only be implemented on the solutions produced by the first-step processes. Today, however, a few processes are available that allow recovery of the trivalent actinides in a single step from highly active liquid waste.

This review will exclusively deal with studies related to solvent-extraction processes (neither solid-phase precipitation nor ion-exchange chromatography) aiming at separating trivalent actinides from PUREX raffinates or spent-fuel dissolution

liquors. Only the systems that have been developed up to the implementation of cold, spiked, or highly active countercurrent tests at laboratory scale or in industrial pilot plants will be described: first, the two-cycle processes, and second, the single-cycle processes.

3.3.1 Two-cycle Processes

3.3.1.1 First Step: An(III) + Ln(III) Separation from the Rest of the Fission Products

In each country concerned with the reprocessing of spent nuclear fuel arising from civil or military applications, the highly active waste (HAW) that has been generated for decades by the PUREX or similar processes is still currently stored on the reprocessing plant sites, either as a liquid sludge contained in tanks or as a solid in vitrified or cemented matrices. HAW usually contains large quantities of alpha emitters (minor actinides, such as Np and TPEs) that increase its long-term radiotoxicity. Therefore, the solvent-extraction processes developed in the early 1980s aimed at achieving high minor-actinide DFs (e.g., American TRUEX and Russian-American UNEX), but not at separating trivalent actinides from lanthanides: they involved highly efficient bidentate and chelating extracting agents bearing oxygen-donor atoms. On the contrary, other solvent-extraction processes based also on oxygen-donor extracting agents, such as Chinese TRPO, Japanese DIDPA (first cycle), and French DIAMEX processes, were developed as head-end steps of An(III)/Ln(III) partitioning schemes. The concept feasibility of all these processes has already been validated on genuine highly active feeds, and their recent developments mainly deal with the following issues:

- Process comprehension, such as the study of aggregation phenomena to predict third-phase formation.
- Minor experimental modifications, such as the use of hydrophilic complexants to ease the scrubbing and stripping of the loaded solvents and simplify the flowsheets.
- Optimization of the extractant skeleton or the diluent nature to improve extraction or separation yields.

These developments will hereafter be described for each family of extractants from NOPCs to amino compounds, and for each topic, results will be sorted chronologically by country.

3.3.1.1.1 Phosphate and Phosphonate Derivatives

The enthalpies of extraction of U(VI) and Am(III) nitrates by neutral organophosphate extractants, such as tri-*n*-butyl phosphate (TBP), tri-*n*-amyl phosphate (TAP), tri-*sec*-butyl phosphate (TsBP), tri-*iso*-amyl phosphate (TiAP), and tri-*n*-hexyl phosphate (THP) have been determined in *n*-dodecane over the temperature range 283–333 K (*88*). Am extraction becomes more exothermic in the following order: THP~TiAP < TAP < TsBP < TBP, highlighting the steric hindrance caused by branched substituents compared with linear homologues and long-chain substituents

(hexyl) compared with shorter ones (butyl) in the Am(III)-trisolvates extracted by trialkyl phosphates.

Diamylamyl phosphonate (DAAP) has been evaluated as a substitute for TBP to extract U(VI), Th(IV), Pu(IV), and Am(III) in *n*-dodecane (*89*). Some important physical properties of this extractant (density, viscosity, surface tension, and phase disengagement time) that should fulfill specific requirements for industrial applications were measured and compared to those of TBP. However, although higher than in the case of TBP, D_{Am} only reaches 0.16 at 303 K for [HNO_3] = 1.5 M and [DAAP] = 1.1 M in *n*-dodecane. It remains poor compared with other tetravalent and hexavalent actinides. The trend shows a steep rise of D_{Am} values with [HNO_3] from 0.5 to 1.5 M, followed by a gradual fall. It is, however, assumed from this study that higher concentrations of DAAP, or even neat DAAP, could lead to appreciable D_{Am} values, enabling DAAP application in trivalent actinide extraction.

3.3.1.1.2 Trialkyl-phosphine Oxides: The TRPO Process

The TRPO process was developed at the Institute of Nuclear Energy Technology (INET, Tsinghua University, Beijing, China) in the 1980s to recover the transuranium elements (TRU) from highly active defense waste (*90*). It uses a mixture of trialkyl phosphine oxides (TRPO, with $C_6 < R < C_8$ or CYANEX 923 dissolved at 30% in kerosene), which can extract An(III) and Ln(III) if the feed acidity is decreased to less than 1 M HNO_3. An(III) and Ln(III) are then selectively stripped from the loaded solvent (containing other extracted actinides) in 5.5 M HNO_3. Np and Pu are recovered in 0.6 M oxalic acid and U in a 5% sodium carbonate solution. However, the presence of Fe(III) causes third-phase formation, which can be avoided either by adding TBP or *n*-octanol to the TRPO solvent, or by diluting the feed (*91*).

A 72-hour inactive test was performed to validate the whole process scheme in five pulse columns and 24 stages of centrifugal contactors at the INET (*92*). Nd and Zr simulated Am and Pu, respectively. DFs (expressed as the ratios: [M]$_{feed}\phi_{feed}$/[M]$_{raff}\phi_{raff}$, where ϕ represents the flow-rate of solute M) greater than 3000, 500, and 1000 were obtained for U, Nd, and Zr, respectively, thus demonstrating the feasibility and reliability of the TRPO process scheme.

Previous active countercurrent tests performed in compact contactors (10 mm in diameter, 4−5 mL holdup per stage) on highly saline waste (~380 g/L of Na, Al, Fe, Cr, and Ni) had demonstrated that 99.9% of the actinides could be recovered with the rare earth elements (REEs) in six stages (*93*).

A new concept integrating both the PUREX and the TRPO processes is proposed by the INET researchers. This simplified PUREX-TRPO process uses a binary mixture of TBP (20%) and TRPO (20%) in kerosene to extract all actinides including TPEs, which can be back-extracted together with the trivalent lanthanides in a 5.5 M HNO_3 solution as in the TRPO process (*94*).

As part of a process comparison campaign carried out by the Institute for TPEs (ITU, Karlsruhe, Germany), a TRPO flowsheet was implemented countercurrently in 22 miniature centrifugal contactors. The process used six stages for extraction, two stages for the first scrub with 1 M HNO_3, four stages for stripping the

An(III) + Ln(III) fraction with 5.5 M HNO_3, two stages for the second scrub with 0.6 M oxalic acid, four stages for stripping the Np + Pu fraction with 0.6 M oxalic acid, and finally four stages for stripping U with 5% Na_2CO_3. It involved a mixture of trialkyl(C_6-C_8) phosphine oxides (TRPO) dissolved at 30% in *n*-dodecane as the organic solvent and a genuine PUREX raffinate (obtained from reprocessing commercial spent (light water reactor) LWR fuel) denitrated to 0.7 M HNO_3 as the aqueous feed. Despite the fact that this preceding denitration of the high-level liquid waste (HLLW) with formic acid might have implied a risk of precipitation and hence losses of minor actinides, the DFs obtained for the raffinate (in the extraction section) and for the organic solvent (in the stripping section) were, respectively, higher than 800 and equal to 730 for Am(III), and higher than 200 and equal to 780 for Cm(III). The overall recovery yields for Am(III) and Cm(III) were 99.7 and 99%, respectively. Losses of the trivalent minor actinides in the Np + Pu fraction (~0.13%) and in the U output (0.14% for Am(III) and 0.35% for Cm(III)) were higher than in the spent solvent (0.03% for Am(III) and 0.09% for Cm(III)) (*95, 96*).

3.3.1.1.3   Bidentate Neutral Organophosphorus Compounds

3.3.1.1.3.1   CMPO: The TRUEX Process   The TRUEX (TRansUranium EXtraction) process (*97, 98*), developed at the Argonne National Laboratory (ANL) in the 1980s to decontaminate Cold War legacy transuranic waste (arising from plutonium production for nuclear weapon manufacturing), uses a mixture of TBP and CMPO (Figure 3.1) that allows all minor actinides (and the lanthanides) to be extracted from acidic media (up to 5 M nitric acid). However, it requires a PUREX (or similar) process as its front-end.

The TRUEX solvent ([CMPO] = 0.2 M + [TBP] = 1.4 M in *n*-dodecane) was employed to decontaminate samples of sludge arising from the concentration (by evaporation of water) and neutralization (with caustic) of the acidic waste of Melton Valley Storage Tank W-25 at the Oak Ridge National Laboratory. The sludge was quantitatively (~80%) dissolved in concentrated nitric acid after caustic leaching treatment (*99*). Two campaigns of batch liquid-liquid extraction tests (at 2.9 and 1.6 M HNO_3, respectively) were successfully carried out, although gel formation disturbed the experiments. More than 95% of Eu, Pu, Cm, Th, and U were removed in only one step from the aqueous feeds. Mercury and vanadium also appeared to be extracted. The analytical results were in good agreement with
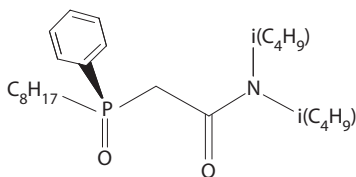
FIGURE 3.1   *n*-Octyl-phenyl-*N,N′*-di(*iso*)butyl-carbamoyl-methyl phosphine oxide (CMPO) used in the TRUEX process.

the values predicted by the Generic TRUEX Model (GMT), a thermodynamic model developed during the 1980s to design TRUEX flowsheets, and grounded on mass-action laws describing the extraction of ionic species by neutral organic ligands (*100*).

Since the launching of the Advanced Fuel Cycle Initiative (AFCI) program in the United States, the TRUEX solvent has been integrated in the five-step UREX+ process, initially consisting of five solvent-extraction steps to separate the constituents of dissolved spent nuclear fuels into seven fractions (*101*):

1. Following dissolution, uranium and technetium are recovered from the feed in separate product streams.
2. In the next step, which was designed by researchers of the Idaho National Laboratory (INL, Idaho), cesium and strontium are removed from the UREX raffinates.
3. After feed acidity adjustment, plutonium and neptunium are recovered in the NPEX process, with high yields and sufficiently low impurity levels to make them suitable for MOX fuel fabrication.
4. The raffinate of the NPEX process is fed, without acidity adjustment, to a TRUEX step, where the minor actinides and the REEs are recovered.
5. Eventually, the TRUEX product is fed directly to a CYANEX 301 step, where the minor actinides are purified from the REEs.

At the end of 2003, the complete UREX+ solvent-extraction process was assessed and validated using multistage countercurrent centrifugal contactors at ANL. It was run twice in three multistage 2-cm centrifugal contactors, initially with a simulated dissolved spent fuel, and subsequently with a feed obtained by dissolving in nitric acid an irradiated uranium-oxide pin of spent Big Rock Point fuel (initially enriched at 4.6% with ^{235}U, containing 1% of gadolinium burnable poison, burned up to 29,600 MWd/MT, and cooled for 21 years). The volume and concentration of the initial nitric acid solution was adjusted to provide a uranium solution appropriate to the low-acid requirements of the UREX process. The process flowsheets were designed with the help of the Argonne Model for Universal Solvent Extraction (AMUSE) code, an updated version of the former GMT code. Because of the number of stages available and the low stage efficiency of the 2-cm centrifugal contactors, the flowsheets expected for plant use would be significantly different.

Americium, curium, REEs, and residual plutonium and neptunium were all extracted by the TRUEX solvent ([CMPO] = 0.2 M + [TBP] = 1.4 M in *n*-dodecane). Some fission products were also extracted and had to be scrubbed from the solvent. Although the lighter rare earths were considerably more extractable than the heavier rare earths, flowsheets could easily be designed to give complete separation of Am and Cm from all rare earths. The TRUEX flowsheet tested Figure 3.2) was unique to the UREX+ process by having three scrub sections. In the first scrub section, the impurities were removed from the solvent using oxalic acid. The second scrub used moderately concentrated nitric acid to scrub oxalic acid from the solvent. The third scrub section used relatively dilute nitric acid to lower the concentration of nitric acid in the loaded solvent and ease the stripping of the actinide and REEs. The stripping
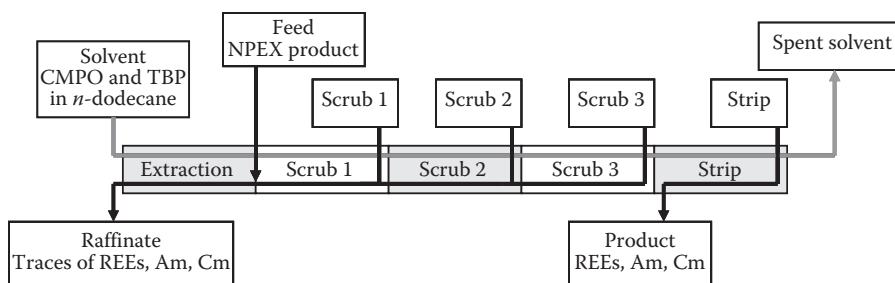
FIGURE 3.2 TRUEX process flowsheet used in the UREX+ demonstration run by ANL. (From Vandegrift, G.F., Regalbuto, M.C., Aase, S., Bakel, A., Battisti, A.T., Bowers, D., Byrnes, J.P., Clark, M.A., Cummings, D.G., Emery, J.W., Falkenberg, J.R., Gelis, A.V., Pereira, C., Hafenrichter, L., Tsai, Y., Quigley, K.J., Vander Pol, M.H. 2004. *ATALANTE 2004: Advances for Future Nuclear Cycles,* June 2004, Nîmes, France.)

section used a weakly complexing salt to back-extract the trivalent elements and maintain a pH between 3 and 4, allowing the subsequent direct implementation of the CYANEX 301 solvent.

Recently, a suite of processes collectively known as UREX+ (i.e., UREX + 1, UREX + 1a, UREX + 2, UREX + 3, UREX + 4) has been designed to meet a number of the GNEP targets (*102*).

The current American reference process is the UREX + 3, consisting of several solvent-extraction steps that separate the constituents of the dissolved spent nuclear fuels into three main products (*27*):

1. Uranium
2. A mixture of uranium, neptunium, and plutonium to fabricate new mixed actinide-fuels (either metallic or oxides)
3. A mixture of americium and curium

Following spent nuclear-fuel dissolution, the UREX+ Codecon Process flowsheet allows (i) partial recovery of uranium on one side of the multistage contactor-bank (uranium being coextracted with technetium in a PUREX-like solvent), and (ii) complete recovery of neptunium and plutonium (stripped with a reducing hydroxylamine nitrate (HAN) solution) together with the remaining uranium, on the other side of the contactor-bank. The UREX+ raffinate is fed (without acidity adjustment) to a TRUEX step, where the trivalent minor actinides and the REEs are co-recovered in a TRUEX output stream, which is then fed (after acidity adjustment) to a TALSPEAK step to separate Am(III) and Cm(III) from the Ln(III). Cesium and strontium are removed from the TRUEX raffinate by implementing the FPEX process. They are subsequently combined with the lanthanides (recovered in the TALSPEAK raffinate) in high-level waste forms, whereas the other metallic fission products are turned into metal waste forms.

Under the 3rd EURATOM Framework Program on the management and disposal of radioactive wastes, Italian researchers of the National Commission for Research and Development of Nuclear and Alternative Energy Sources (ENEA) tested a TRUEX flowsheet, aiming at achieving an alpha decontamination factor (DF) greater

than 1000 together with a reduction of the lanthanides/americium weight ratio by a factor of about 200 (*103*). The solvent consisted of TBP (1.4 M) and two derivatives of CMPO, namely octyl phenyl di*iso*butyl CMPO (OϕCMPO, 0.2 M in *n*-dodecane) and diphenyl di*iso*butyl CMPO (Ph$_2$Bu$_2$CMPO, 0.2 M in *o*-xylene).

As part of a process comparison campaign carried out by ITU, a TRUEX flow-sheet was implemented countercurrently in 24 miniature centrifugal contactors (*95, 96*). In this flowsheet, six stages were used for extraction, six stages for the scrub with 0.2 M HNO$_3$ and 0.01 M oxalic acid, four stages for stripping the An(III) + Ln(III) fraction with 0.05 M HNO$_3$, four stages for stripping the Np + Pu fraction with 0.05 M HNO$_3$ and 0.05 M HF, and finally four stages for stripping U with 5% Na$_2$CO$_3$. It involved a mixture of CMPO and TBP, dissolved at 0.2 and 1.4 M in *n*-dode-cane as the organic solvent, respectively, and a genuine PUREX raffinate (obtained from reprocessing commercial spent LWR fuel) as the aqueous feed (2 M HNO$_3$). At equilibrium, feed DFs greater than 1200 for Cm(III) and 7700 for Am(III) were obtained. However, due to an accumulation of Am(III) and Cm(III) in the organic phase all along the back-extraction section, only small amounts of the latter elements were found in the An(III) + Ln(III) fraction (7% and 13% of Am(III) and Cm(III), respectively), while part of these two elements appeared down-stream in the Np + Pu product (7% and 10% of Am(III) and Cm(III), respectively) and in the U product (5% and 7% of Am(III) and Cm(III), respectively). Only a small amount remained in the spent solvent, 0.4 and 0.3% of Am(III) and Cm(III), respectively. This was believed to be caused by the too high nitric acid concentration in the loaded organic solvent in the An(III) back-extraction section. Hence, the trivalent minor actinide recovery yield is expected to be improved by reducing this acidity.

At the Indian Bhabha Atomic Research Center, inactive engineering-scale coun-tercurrent tests have been conducted with a TRUEX solvent to validate the extrac-tion of La(III) and Ce(III) (used to mimic An(III) and Ln(III) bulk separation) from a surrogate feed ([HNO$_3$] = 4 M) simulating a PUREX raffinate issued from the reprocessing of a long-cooled pressurized heavy-water reactor spent fuel (*104*). Over a period of approximately 10 hours, 300 L of the surrogate feed was treated in com-bined airlift mixer-settler units (10 stages, 20−30 L/h throughput) by a solvent com-posed of CMPO (0.25 M) and TBP (1.2 M) dissolved in *n*-dodecane. La(III) and Ce(III) were quantitatively stripped in a ternary mixture of NaOH (1.5 M), formic acid (1.5 M), and DTPA (0.05 M). Third-phase formation was not encountered in the five-extraction stages or in the five stripping stages. The final streams showed negli-gible amounts of entrained phases. The overall mass balances were satisfactory.

In Japan, a 16-stage TRUEX flowsheet involving a solvent composed of CMPO (0.2 M) and TBP (1 M), dissolved in *n*-dodecane, was implemented in batch experi-ments. The extraction of short-lived fission products ([93]Y, [99]Mo, [97]Zr, [122]Sb, [132]Te, [133]I, and [143]Ce, produced by neutron irradiation) and neptunium was investigated. The distribution ratios of all these elements were experimentally determined as a function of various parameters, such as the concentrations of nitric acid, uranium, and oxalic acid. The acid dependence of Np and Zr was clearly observed, and oxalic acid was effective in limiting Zr extraction. High distribution ratios were observed for Y(III) and Ce(III), simulating Am(III). The lack of reproducibility of the distribution ratios of Mo was attributed to differences in preparation protocols. The extraction of Te was

explained by considering the presence of neutral and anionic species (*105–107*). The modified SEPHIS code was employed to evaluate the distribution of HNO_3 in each of the 16 stages of the extraction-scrubbing bank. The SEPHIS code is a Fortran computer code, developed at Oak Ridge National Laboratory in 1975 to solve the material balances of countercurrent solvent-extraction processes, which includes algorithms to predict the distribution ratios for Pu and U based on TBP concentration, extractable and nonextractable nitrate concentrations, and Pu and U metal ion concentrations. From the obtained $[HNO_3]_{aq}$ values, the distribution ratios of Ce, Mo, Pd, and Sb were estimated in each stage using experimental D_M curves or literature data for the actinides. The concentration profiles of all elements were then calculated thanks to the multistage extraction simulation code. The recovery of the TRU by the TRUEX solvent was expected to be effective from 1 to 3 M HNO_3 in the presence of oxalic acid and oxidizing agent. However, this TRUEX flowsheet still requires further improvement to obtain higher performances for Mo and Pd decontamination.

The extraction behavior of nitric acid into a TRUEX solvent (0.2 M CMPO and 1 M TBP in *n*-dodecane) was studied for 0.1–7 M HNO_3 (*108*). The effective CMPO concentration was estimated from the extraction results of lanthanum nitrate, and the following relationship was proposed: $[CMPO]/[CMPO]_{ini}$ (%) = $\exp(4.706-1.099$ $[HNO_3] + 0.1005[HNO_3]^2-0.0089[HNO_3]^3)$, based on the formation of (HNO_3) (CMPO) and $(HNO_3)_2$(CMPO) complexes and the activity coefficients calculated by the Zdanovskii–Mikulin rule. The applicability of the effective CMPO concentration to model the extraction of other elements was demonstrated for cerium and ytterbium nitrates:

$$M^{3+} + 3NO_3^- + 3\overline{CMPO} \xrightleftharpoons{K_{ex}} \overline{M(NO_3)_3CMPO_3} \qquad (3.5)$$
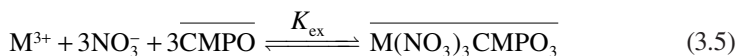
However, this speciation is a bit different from the one previously determined using the Mikulin–Sergievskii–Dannus' model for the extraction of neodymium nitrate by CMPO (alone) in nitrophenylhexyl ether (NPHE), also called 1-(hexyloxy)-2-nitrobenzene (*109*). A satisfactory description of the distribution of neodymium nitrate has been obtained over a wide range of neodymium and nitric acid concentrations in the aqueous phase by taking into account the formation of the following complexes involving CMPO: $Nd(NO_3)_3(CMPO)_{n=1-3}$ and $Nd(NO_3)_3(HNO_3)$ $(CMPO)_{n=1-3}$. The stoichiometric mean activity coefficients of the components in binary aqueous phases had been determined by interpolating experimental data published in the literature. For mixtures, they have been calculated from experimental data using the Mikulin's equation, whereas the activity coefficients of the species in the organic phase have been calculated from the Sergievskii–Dannus' equation.

3.3.1.1.3.2 Carbamoylmethyl Phosphine Oxide Derivatives The physicochemical properties of various aryl derivatives of CMPO have been investigated at the Vernadsky Institute of Geochemistry and Analytical Chemistry. Extraction of americium and lanthanides from nitric acid with solutions of diphenyl- and dibutyl-(diethylcarbamoylmethyl) phosphine oxides (Ph_2Et_2-CMPO and Bu_2Et_2-CMPO) in dichloroethane have been investigated as a function of the concentrations of the extractants and nitric acid (*110, 111*). The observed dependences are characterized

by a pronounced tetrad effect for Bu_2Et_2-CMPO, and a steeper slope but no tetrad effect for Ph_2Et_2-CMPO. Both extractants show low selectivity toward Am(III), but the Am(III)/Ln(III) separation factor increases with the Ln(III) atomic number.

Diphenyl-(dibutylcarbamoylmethyl) phosphine oxide (Ph_2Bu_2-CMPO) was shown able to effectively extract actinide and REEs from acidic solutions, without its preliminary dissolution in an organic solvent (*112–114*). Initially solid, Ph_2Bu_2-CMPO powder changes its state of aggregation when contacted with 4 M HNO_3 and turns into a colorless viscous liquid complex (a liquid reagent that does not mix with aqueous phase). The extraction behaviors of praseodymium(III), americium, neptunium, and plutonium in various oxidation states were assessed using the liquid reagent Ph_2Bu_2-CMPO·HNO_3·nH_2O (where $n = 2$–3). The extraction yields appeared to be greater than with conventional solvent extraction, although redox reactions occurred during the extraction process (e.g., Pu(III), Np(V), and Am(VI) are not stable on contact with the liquid reagent phase). The redox potential of the liquid reagent was estimated around +1.5 V, based on the formal redox potentials of Pu(IV)/(Pu(III), Np(IV)/Np(V), and Am(VI)/Am(V).

The extraction of Am(III) was investigated in greater detail for different nitric acid concentrations and salt contents: Al (5–15 g/L), Na (5–20 g/L), Ca (0.5–2.0 g/L), Cr (0.5–2.5 g/L), and Fe (0.5–5.0 g/L). The completeness of extraction of Am was determined by the amount of Ph_2Bu_2-CMPO·HNO_3 compound involved and depended on the concentration of nitric acid and the duration of the contact time of the phases (*115*). In solvent-extraction systems involving organic diluents, the extraction of the target elements and that of nitric acid are usually in competition. Conversely, in the particular case of metal extraction into an acidified Ph_2Bu_2-CMPO phase (without any organic diluent), both processes favor the extraction of Am, as if the salting out of the acid results in a more complete formation of the liquid reagent. The extraction of Am(III) from solutions of Al salts showed that when the acid and salt concentrations increase, the extraction yield of Am(III) also increases, and the time of establishment of extraction equilibrium shortens. This peculiarity could become an advantage for processing acidic HAW, because the use of toxic and environmentally hazardous organic solvents would be avoided.

3.3.1.1.3.3   The UNEX Process: A Universal Solvent   Intensive collaboration between the INL and the Khlopin Radium Institute of Saint Petersburg (KRI, Russia) since 1994 has resulted in the development of the UNEX process for the treatment of radioactive waste stored at the INL (116–125). The UNEX process is based on the following tertiary solvent:

- A chlorinated cobalt dicarbollide (CCD, Figure 3.3) originally developed in the mid-1970s by Czechoslovakian researchers and later implemented in Russia to remove cesium from acidic solutions
- Polyethylene glycol (PEG-400), which helps strontium removal
- Diphenyl-*N,N*-di*iso*butylcarbamoylmethylphosphine oxide (Ph$_2$-CMPO, Figure 3.3), a bidentate neutral organophosphorus compound (BNOPC) derived from the TRUEX process, which proved to be efficient for the removal of actinides and REEs.
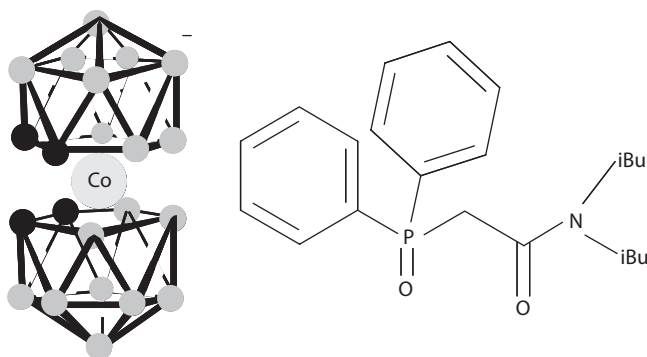
FIGURE 3.3   Cobalt dicarbollide and Ph$_2$-CMPO used in the UNEX process.

Testing and demonstration of concept feasibility of the UNEX process has been completed on batch contact studies using simulated and genuine sodium-bearing acidic waste stored in underground stainless steel tanks at the INL. DFs of 99.7% for Sr, >95% for Cs, and 99.99% for actinides were achieved with a solvent composed of CCD, PEG, and Ph$_2$-CMPO, dissolved in either a light or a heavy non-nitroaromatic diluent (respectively less or more dense than the aqueous feed).

Several countercurrent pilot plant tests have been run in centrifugal contactors:

- Two countercurrent tests were carried out with simulated waste at the INL (*116, 117*). The first flowsheet implemented (11 extraction stages, 1 scrub stage, 6 Cs/Sr strip stages, 3 actinide strip stages, and 5 solvent wash stages) failed because of flooding in the aqueous solution exiting the Cs strip section, and large quantities of Zr precipitate were observed in each of the Cs strip stages. The removal efficiencies from the feed were 99.7%, >99.98%, and >99.92% for Cs, Sr, and Eu (used as Am surrogate), respectively. The second flowsheet was modified to prevent the problems encountered during the first run (citric acid was added in the aqueous feed to avoid Zr extraction, as well as in the scrub and Cs/Sr strip solutions, to scrub potentially extractable Zr). It was implemented without flooding or precipitate formation in the contactors. However, the organic solvent precipitated after many recycles and washings, either because of a lack of solubility of Ph$_2$-CMPO in the light non-nitroaromatic diluent or because of a change of its formulation through recycling. The removal efficiencies from the feed were high, 99.7 and 99.97%, for Cs and Sr, respectively, but lower than 5% for Eu, probably due to Ph$_2$-CMPO precipitation.
- A countercurrent test on a simulated waste was successfully completed at KRI without flooding, third-phase formation, or precipitation of Ph2-CMPO, thanks to the use of *meta*-nitrobenzotrifluoride (Fluoropole-732) as the organic diluent. In this test, 2 cascades of 12 centrifugal contactors were arranged in a circle: eight extraction stages, five stages of Sr and rare-earth

strip, six stages of Cs strip, and five stages of solvent wash. The removal efficiencies obtained for the radionuclides were all better than 99.8%, except for Am which was 99.2%.

- One countercurrent test treated 1.7 L of genuine radioactive tank waste at INL. The flowsheet (Figure 3.4) was successfully implemented without flooding, third-phase formation or precipitation, in a 24-stage pilot plant (2-cm centrifugal contactors) designed and built at ANL. The removal efficiencies from the feed were 99.95%, 99.985%, and 95.2% for ^{137}Cs, ^{90}Sr, and the total alpha emitters, respectively. The lower-than-expected alpha removal efficiency was assumed to be due to loading of the Ph_2-CMPO by fission products, such as Fe and Mo (*118, 121*).

- Long-term countercurrent tests (one lasting 128 hours) were performed in the hot cells of the Mining and Chemical Combine (MCC, Zheleznogorsk, Russia) in the framework of a DOE Project with Sandia National Laboratories. The tests were carried out under dynamic conditions in EZ-33 centrifugal contactors made by NIKIMT (*122*) and involved a solvent composed of CCD, CMPO, and PEG-400, respectively, dissolved at 0.08 M, 0.015 M, and 0.4 vol% in phenyltrifluoromethylsulfone (FS-13). The recycled extractant completed a total of 70 cycles, and its characteristics did not vary significantly during the test. The following recovery degrees of target radionuclides were calculated from their content in the genuine raffinate: >99.95% Cs, >99.99% Sr, and >99.7% gross alpha-activity.

The feasibility of recovering hazardous radionuclides from acidic waste solutions by the UNEX process is demonstrated. However, the tests also confirm that the solvent composition should be adjusted to attain optimum results depending on the waste composition (*123*). Besides, traditional UNEX process has some drawbacks:

- Stripping solutions contain large amounts of guanidine carbonate (0.5–1 M) and diethylene-triamine-pentaacetic acid (DTPA) (*124*). Though,
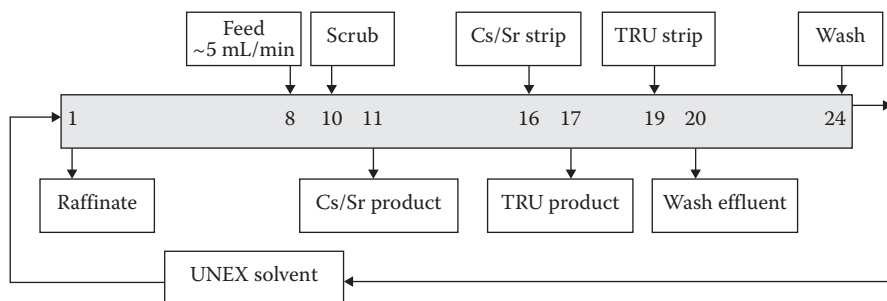
FIGURE 3.4 Universal extraction process flowsheet (UNEX). (From Law, J.D., Herbst, R.S., Todd, T.A., Wood, D.J., Romanovskiy, V.N., Esimantovskiy, V.N., Smirnov, I.V., Babain, V.A., Zaïtsev, B.N. 1999. *Global 1999: Nuclear Technology – Bridging the Millennia*, August–September 1999, Jackson Hole, WY.)

studies have shown that solutions of methylamine carbonate and DTPA or methylamine carbonate and nitrilotriacetic acid (NTA) were as efficient as the guanidine carbonate and DTPA solution to strip the target extracted elements. Furthermore, methylamine carbonate is easily regenerated by distillation.

- The UNEX solvent seems to be of limited utility for reprocessing acidic solutions containing large quantities of lanthanides and/or actinides such as dissolved spent nuclear fuel solutions. These constraints are primarily attributed to the limited solubility of Ph_2-CMPO and of its metallic complexes in the UNEX solvent. That is why diamide derivatives of dipicolinic acid Figure 3.5) have recently been suggested as alternative An + Ln(III) extractants. The tetrabutyl derivative shows the most promising results for the extraction of trivalent elements, but it requires the presence of CCD and PEG-400 as synergistic agents in the FS-13 diluent (*123, 125*).

A procedure based on condensation with phenol and paraform (used as formaldehyde source) was developed to convert spent UNEX solvent (CCD, PEG-400, Ph_2-CMPO, and FS-13) into a solid infusible resin for disposal. The resulting material is insoluble in aqueous alkali and acidic solutions and organic solvents. Incorporation of FS-13 in the cross-linked polymer was confirmed by physicochemical methods. Resistance of the cured resin to high temperatures was proven by thermogravimetry (*126*). This procedure is assumed to be applicable to other organic wastes containing weakly reactive aromatic compounds, such as Fluoropole-732, 1,2-dichlorobenzene, and nitrobenzene.

3.3.1.1.3.4 Diphosphine Dioxides   BNOPCs, such as diphosphine dioxides, have been considered for the recovery of transplutonium elements and REEs from HAWs (*127*). These chelating compounds exhibit enhanced extractive power compared with CMPO or malonamide compounds (*128*) due to their bidentate coordination potential. "Anomalous aryl strengthening effects" (due to an increase in substituent electronegativity, but a decrease in diphosphine dioxide basicity) are often observed when NOPCs coordinate metal cations in a bidentate mode. The resulting six-membered ring (Figure 3.6, $n = 1$) has actually a greater acceptor power, and the phenyl substituents at the phosphorus atoms turn from electron acceptors into electron donor moieties (*129*). Therefore, the extraction constants of bidentate NOPCs are higher by a factor of 10^5 than those of monodentate NOPCs, such as trioctyl phosphine oxide (TOPO).
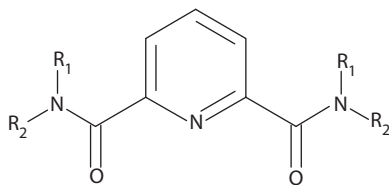
FIGURE 3.5   2,6-Pyridinedicarboxamide derivates investigated for the UNEX process.
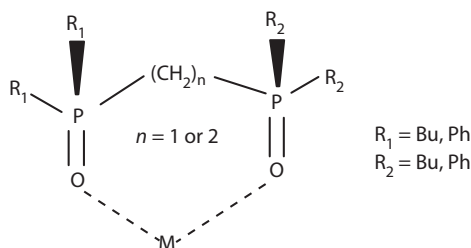
FIGURE 3.6 Bidentate neutral organophosphorus compounds (BNOPCs): diphosphine dioxides.

Another explanation for the incredibly strong extractive power of BNOPCs could be the change at high acidity of the mechanism of metal ion extraction from solvate to cation exchange. It was observed and confirmed by IR spectroscopy and ESI-MS studies that cationic complexes of BNOPCs with proton hydrates or lithium cation easily form in polar organic solvents, such as dichloroethane, *meta*-nitrobenzotrifluoride, and trifluoromethyl phenyl sulfone, which promote acid dissociation in the organic phase. The pre-existing proton hydrates also orientate the donor centers of the BNOPC molecules in an optimized configuration for metal-cation interaction. Europium extraction, for instance, proceeds substantially better in the presence of BNOPC complexes with hydrated protons (when the cation-exchange mechanism is possible) than in the case of the solvate mechanism. It was assumed that the latter reaction pathway, where the extractant molecules have to displace the water molecules from the metal cation hydration shell, was less energetically favorable than the cation-exchange reaction pathway in which the exchanged protons are released and hydrated by the water molecules stemming from the simultaneously occurring dehydration of the metal cation.

The major drawback of phenyl derivatives of BNOPCs is that they are only scarcely soluble in classical hydrocarbon diluents without the addition of massive amounts of phase modifiers, such as TBP or TOPO. They are, however, soluble in halogenated and nitro-halogenated organic diluents (*130*). Furthermore, the anomalous aryl strengthening effect also increases the extraction of other fission products, such as Zr, Mo, Tc, and Fe, which can only be avoided by introducing specific hydrophilic complexants (e.g., acetohydroxamic acid).

Alkylene-bis(diphenylphosphine) dioxides seem to be more soluble in halogenated organic diluents than methylene-bis(diphenylphosphine) dioxides and present different extraction features toward An(III) (*131*).

3.3.1.1.4 Di-iso-decylphosphoric Acid: The DIDPA Process

A four-group partitioning scheme was initially proposed by research teams from the former Japan Atomic Energy Research Institute (JAERI, today JAEA, Japan Atomic Energy Agency) to treat highly active PUREX raffinates (*132*). It consists the separations of

1. TRU for further transmutation
2. Tc and platinum-group metals (PGM)

3. Thermal fission products, Cs and Sr to reduce the costs of the underground repository
4. Other fission products to be disposed of in a geological repository

As described in Figure 3.7, TRU separation is performed by implementing the DIDPA process on pretreated PUREX raffinates. A front-end denitration step by formic acid is thus required to reduce the nitric acid concentration of the feed down to 0.5 M to allow the TRU elements to be extracted by the cation exchanger di-*iso*-decyl-phosphoric acid (DIDPA). This preliminary step, however, induces the precipitation of Mo and Zr (and thus the potential carrying of Pu), which requires filtration steps. The TRU and Ln(III) elements are coextracted by a solvent composed of the dimerized DIDPA and TBP, dissolved at 0.5 and 0.1 M, respectively, in *n*-dodecane. The An(III) + Ln(III) fraction is back-extracted into a concentrated 4 M nitric acid solution, whereas Np and Pu are selectively stripped by oxalic acid.

Several validation tests of the four-group partitioning scheme (including the first cycle TRU + Ln(III) coextraction by the DIDPA process) were carried out at JAERI, from the early 1980s to 1998, on genuine highly active PUREX raffinates (134–136), but the research program seems to be over now:
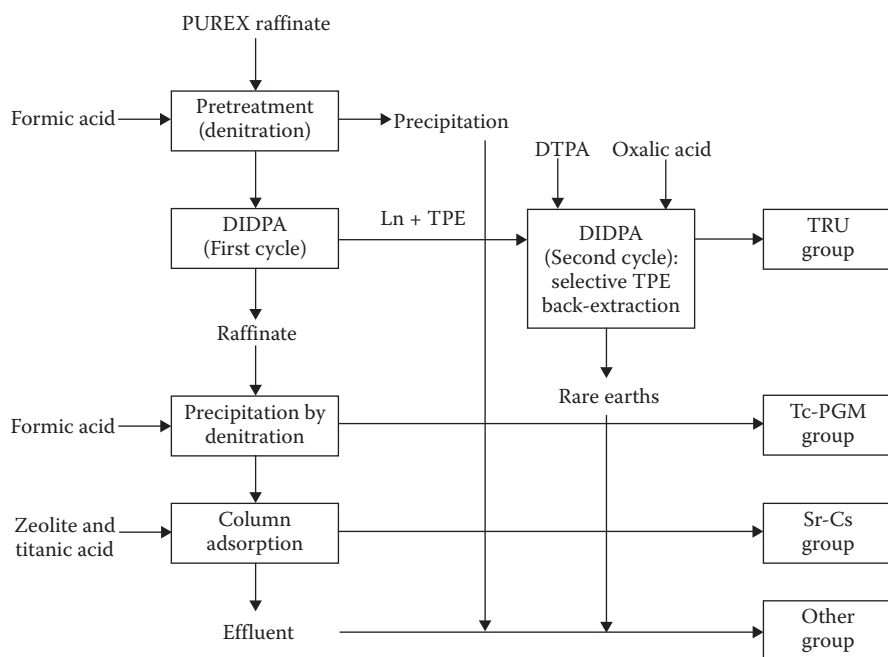
FIGURE 3.7 Four-group partitioning process scheme involving the DIDPA process. (Courtesy of Kubota, M., Morita, Y., Yamaguchi, I., Yamagishi, I., Fujiwara, T., Watanabe, M., Mizoguchi, K., Tatsugae, R., *NUCEF'98 Symposium Working Group*, November 1998, Hitachinaka, Ibaraki, Japan.)

- In 1983, the DIDPA process was tested on 1.2 L of genuine HAW (200 Ci) using mixer-settlers. This test gave satisfactory results for the recovery of Am and Cm from the feed.
- A countercurrent semihot test was later implemented in 24 miniature centrifugal contactors: eight stages for the extraction, four stages for the scrubbing, four stages for the An(III) + Ln(III) stripping with 4 M HNO_3, and eight stages for the Np + Pu stripping with 0.8 M oxalic acid. As only 12 stages could be set up in the hot cell, the flowsheet was run in two successive sequences. The feed originated from a stored concentrate of various reprocessed LWR fuels, centrifuged to remove the precipitate, and further diluted 11 times with HNO_3 (instead of normal denitration method) to adjust its acidity down to 0.5 M. The solvent was a mixture of DIDPA (0.5 M) and TBP (0.1 M) dissolved in *n*-dodecane (*133*). Due to the limited number of stages, the process conditions selected were not fully successful in achieving high recovery yields for the actinides: 98.4% of Cm(III), 97.9% of Am(III), 91.9% of Pu, but only 72.6% of Np were stripped. It was, however, assumed that the actinide extraction and back-extraction efficiencies could be raised by increasing the number of stages, the concentration of oxalic acid, and the temperature.
- In 1998, the four-group partitioning process was tested on 2 L of a genuine HAW (issued from the reprocessing of a 8-GWd/MT spent fuel), denitrated down to 0.5 HNO_3 with formic acid and filtered to remove the colloids (stabilized by the addition of $Mo(H_3PO_4)$) and precipitates. Two batteries of 16 mixer-settlers Figure 3.8) were installed in the Nuclear Fuel Cycle Safety Engineering Research Facility (NUCEF). In seven stages of extraction and four stages of scrubbing, more than 99.99% of Am(III) and Cm(III) were extracted, and more than 99.98% of the latter two elements were back-extracted in five stages with 4 M nitric acid. Np and Pu were extracted simultaneously, and more than 99.6% and 99.9% of Np and Pu, respectively, were back-extracted in 16 stages with 0.8 M oxalic acid.

As part of a process comparison campaign carried out at the ITU, a DIDPA flowsheet was implemented countercurrently in 24 miniature centrifugal contactors:
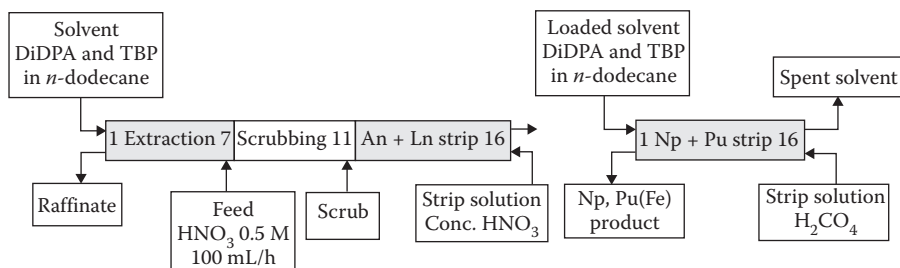
FIGURE 3.8   The DIDPA process (first cycle) tested in NUCEF in 1998. (Courtesy of Morita, Y., Yamaguchi, I., Fujiwara, T., Koizumi, H., Kubota, M., *NUCEF'98 Symposium Working Group*, November 1998, Hitachinaka, Ibaraki, Japan.)

eight stages were used for extraction, four stages for the scrub with 0.5 M HNO_3 and 1 M oxalic acid, four stages for stripping the An(III) + Ln(III) fraction with 4 M HNO_3, and eight stages for stripping the Np + Pu fraction with 0.8 M oxalic acid. It involved a mixture of DIDPA and TBP, respectively dissolved at 0.5 and 0.1 M in *n*-dodecane, as the organic solvent, and a genuine PUREX raffinate (obtained by reprocessing commercial LWR spent fuels) denitrated with formic acid, as the aqueous feed (0.5 M HNO_3). Feed DFs greater than 770 were obtained for the minor actinides. The overall recovery yields for Am(III) and Cm(III) were 97.9 and 98.4%, respectively (*95, 96*).

3.3.1.1.5 Malonamides

In the 1980s, French researchers from the Commissariat à l'Énergie Atomique (CEA) proposed the use of diamide extractants to separate minor actinides from PUREX raffinates and among the diamides those belonging to the malonamide sub-group, with the general formula RR′N(C=O)-CHR″-(C=O)NRR′, where R, R′, and R″ represent hydrogen or hydrocarbon substituents (*137*). These bidentate extractants are soluble in hydrogenated tetrapropene (HTP), the organic hydrocarbon diluent used in the PUREX process at the AREVA La Hague reprocessing plant. Furthermore, carboxylic degradation products of malonamides are less detrimental to the back-extraction of minor actinides in diluted nitric acid than the organophosphoric derivates of degraded BNOPCs.

3.3.1.1.5.1 DMDBTDMA: Former DIAMEX Reference Molecule

Until 1999, *N,N′*-dimethyl-*N,N′*-dibutyltetradecylmalonamide (DMDBTDMA, Figure 3.9) was considered the best malonamide to develop the DIAMEX (DIAMide EXtraction) process, with regard to thermodynamics (i.e., ligand lipopholicity, affinity toward trivalent minor actinide nitrates, and third-phase occurrence) as well as kinetic issues (the kinetic extraction rates of Am(III) and Cm(III) were found to be close to that of Eu(III)). DMDBTDMA extracts trivalent metal nitrates from acidic solutions mainly through a solvation mechanism, thus allowing their stripping in diluted nitric acid. The stoichiometry of the extracted complexes at saturation was shown to be M(III)(DMDBTDMA)$_2$(NO$_3$)$_3$, but higher stoichiometries can be observed owing to the aggregation of the malonamide (*138–141*). Among the 4*f* series, the affinity of the malonamide decreases as the atomic number of the trivalent lanthanide increases (*142*).
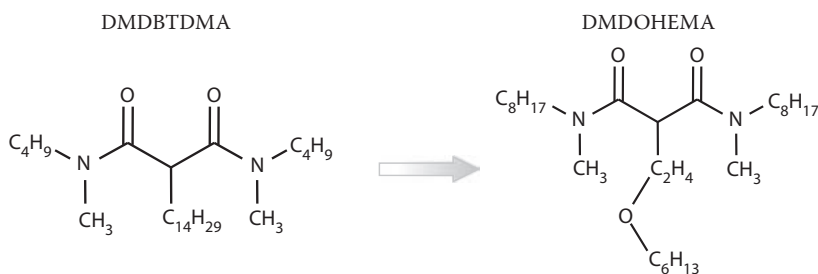
FIGURE 3.9 Evolution of the diamide structure of the DIAMEX process.

Three countercurrent hot tests were performed in mixer-settlers at the CEA Fontenay-aux-Roses in 1993, with six, two, and eight stages, respectively for the extraction, scrub, and strip sections. A high O/A flow rate was set to avoid third-phase formation. Ketomalonic acid and hydrogen peroxide were introduced in the feed to prevent Zr and Mo, respectively, from being coextracted (*143, 144*). Although globally satisfactory (good alpha decontamination of the feed, good stripping from the loaded solvent, and prevention of Zr extraction), these preliminary hot tests nevertheless identified the difficulties of separating Ru (which remained in the solvent) and Mo.

After the flowsheet was assessed on a surrogate feed (*145*), a countercurrent hot test was implemented in 16 miniature centrifugal extractors by teams from the ITU during the NEWPART collaborative project (*17, 95, 96, 145, 146*) under the Fourth EURATOM Framework Program. It involved DMDBTDMA (purified on Alumina-B before use) dissolved at 0.5 M in HTP and a genuine PUREX raffinate obtained by reprocessing a commercial LWR spent fuel (45.2 GWd/tM), further adjusted at 3.5 M nitric acid. Feed DFs greater than 400 for Ln(III), 275 for Am(III), and 70 for Cm(III) were achieved with only six extraction stages (although the rather low DF values of the latter two elements might be due to the contamination background in the hot cell facility). Coextraction of Mo and Zr was efficiently prevented by adding 0.1 M oxalic acid into the feed and using four scrubbing stages with a solution consisting of 3.5 M HNO_3 and 0.3 M oxalic acid. The back-extraction of the trivalent elements also proved to be very efficient in 0.1 M HNO_3, as solvent DFs greater than 2000 for Am(III) and equal to 425 for Cm(III) were obtained in only four stages (two complementary acid scrubbing stages were set up before the stripping section). The overall recovery yields for Am(III) and Cm(III) were 99.6% and 99.2%, respectively. However, palladium and ruthenium were also coextracted (>99.9% for Pd and 5.7% for Ru) and stripped (98.5% for Pd and 5% for Ru) with the An(III) + Ln(III) fraction, thus requiring further investigations, especially to avoid Pd extraction.

3.3.1.1.5.2   DMDOHEMA: The New DIAMEX Reference Molecule   Laboratory studies have been undertaken at the CEA Marcoule to optimize the structure of the malonamide from the standpoint of its affinity for trivalent elements, its loading capacity, and the ease of managing its degradation compounds. The new reference molecule, *N,N′*-dimethyl-*N,N′*-dioctylhexylethoxymalonamide (DMDOHEMA, Figure 3.9), exhibits an oxygen atom in its central chain, which enhances its extractive properties toward trivalent elements and shortens its degradation compounds formed by acidic hydrolysis and radiolysis (*147*). Hydrolytic and radiolytic degradation of DMDOHEMA has been qualitatively and quantitatively characterized (*148, 149*). The degradation compounds with the most detrimental effect on the extraction efficiency of DMDOHEMA are first methyloctylamine, followed by the carboxylic acids and a monoamide. Regeneration of the spent DMDOHEMA solvent has been optimized using specific alkali washings (*145, 150, 151*).

The DMDOHEMA flowsheet was first adapted from that of DMDBTDMA thanks to the PAREX process simulator code, and inactive countercurrent tests have been performed in mixer-settlers. Nitric acidity was decreased from 3.5 to 3 M in the

extraction-scrubbing section to prevent Fe extraction, the O/A flow-rate was reduced to save solvent consumption, and the aqueous stripping flow rate was reduced to concentrate the back-extracted trivalent f elements. The inactive runs confirmed the choice of DMDOHEMA as the new reference DIAMEX extractant in that the hydrolytic behavior was correct, and the Ln(III) extraction performance was as good as observed with DMDBTDMA. The elimination of Zr was quantitative, and the elimination of Mo, Ru, and Fe was much better than with DMDBTDMA: 99.7% for Mo, 79% for Ru, and 98.1% for Fe, in the case of DMDOHEMA, compared with 95%, 50%, and 27%, respectively in the case of DMDBTDMA (*152*).

These promising results were confirmed by a countercurrent hot test carried out in 16 miniature centrifugal extractors at the ITU, during the NEWPART collaborative project under the Fourth EURATOM Framework Program (*96, 145*). DMDOHEMA was dissolved at 0.65 M in HTP, and the feed was a genuine PUREX raffinate (obtained by reprocessing a commercial LWR spent fuel) adjusted at 3.7 M nitric acid. Oxalic acid (0.1 M) and N-(2-hydroxyethyl)ethylenediamine-*N,N′,N′*-triacetic acid (HEDTA, 0.01 M) were added to the feed to limit the extraction of Mo and Zr on the one hand, and Pd on the other hand. The flowsheet consisted of five extraction stages, five scrubbing stages (Mo-Zr and Pd were efficiently scrubbed by a solution of 0.2 M oxalic acid + 0.015 M HEDTA), two acid scrub stages (with 1 M HNO_3), and four strip stages (with 0.1 M HNO_3). The overall recovery yields for Am(III) and Cm(III) were better than in the case of the DMDBTDMA hot test, almost 100% and 99.7%, respectively.

From 1999 to 2005, several countercurrent tests were carried out in laboratory scale mixer-settlers, centrifugal contactors, or rotating ("Couette-Taylor" effect) columns, in the G1 and ATALANTE facilities at the CEA Marcoule, using surrogate (*153*), spiked, or highly active (*3, 15, 147, 154*) PUREX raffinates as the aqueous feeds, and the new reference molecule DMDOHEMA dissolved in HTP as the organic solvent. These tests, as well as long-term hydrolysis/radiolysis endurance tests performed in the MARCEL facility, all aimed at assessing and validating the industrial feasibility of the DIAMEX process implementation. An example of a DIAMEX flowsheet tested in 2000 in miniature centrifugal extractors (ECLHA, developed at the CEA Marcoule) on a genuine highly active PUREX raffinate is shown in Figure 3.10. The hydrodynamic behavior of the solvent recycled six times was excellent during the 37-hour hot test, although it stemmed from a previous hot test carried out in 1999 and had been reused without any particular pretreatment. As shown in Figure 3.10, high An(III) and Ln(III) recovery yields and high DFs versus Mo, Zr, and Pd were obtained thanks to the use of oxalic acid (for Mo and Zr) and HEDTA for Pd in the feed and scrubbing solutions. In the 1999 hot test, for instance, approximately 60% of the Pd initially present in the feed had followed the An(III) + Ln(III) product.

Two DIAMEX/DMDOHEMA hot tests have also been successfully carried out at the ITU, during the PARTNEW collaborative project under the Fifth EURATOM Framework Program (*18*). They involved either a genuine PUREX High Active Raffinate (HAR) or a High Active Concentrate (HAC), obtained after the concentration (by a factor of ~10) through denitration using formic acid, of a PUREX HAR produced by reprocessing a commercial MOX fuel (~30 GWd/tM).

Solvent
DMDOHEMA in HTP

Spent solvent

| 1 Extraction 13 | 1st Scrub 18 | 2nd Scrub 20 | | 1 An + Ln strip 8 |

Raffinate
Am(III)<0.1%
Cm(III)<0.1%
Pd>99.8%
Y~40%

Feed
MOX
HNO$_3$, 3 M
Oxalic acid
HEDTA
122 mL/h

Scrub
HNO$_3$
Oxalic acid
HEDTA

Acid scrub
HNO$_3$

An + Ln product
An(III)>99%
Pd<0.2%
Y~60%
Zr<0.2% (D.L.)
Mo<0.3% (D.L.)

Strip solution
Diluted HNO$_3$
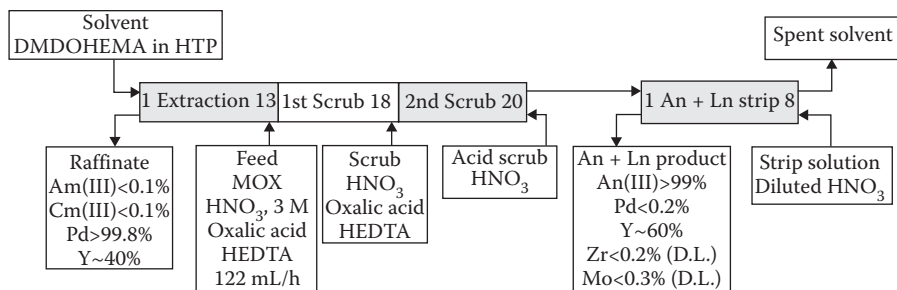
FIGURE 3.10 DIAMEX process flowsheet tested at the CEA Marcoule in 2000 with DMDOHEMA. (Courtesy of Madic, C., Lecomte, M., Baron, P., Boullis, B., *Compte-Rendu de Physique*, 3, 797–811, 2002.)

Solvent
DMDOHEMA in HTP

Spent solvent

| 1 | 4 | 5 | 8 | 9 | 12 | | 13 | 16 |

Raffinate

Feed
HNO$_3$~4 M
Oxalic acid
HEDTA
51 mL/h

Scrub
HNO$_3$
Oxalic acid
HEDTA

Acid scrub
HNO$_3$

An + Ln
product

Strip solution
Diluted HNO$_3$
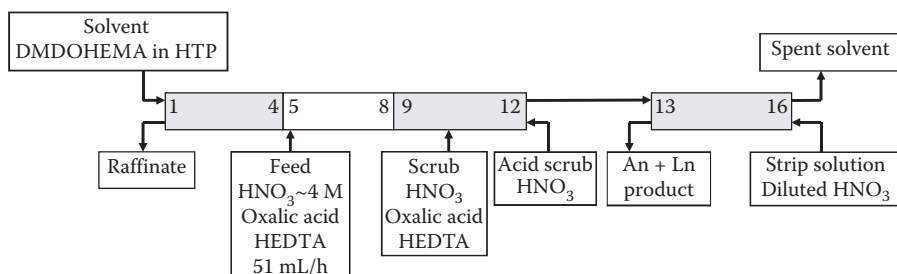
FIGURE 3.11 DIAMEX HAR process flowsheet tested at the ITU with DMDOHEMA. (Courtesy of Serrano-Purroy, D., Baron, P., Christiansen, B., Malmbeck, R., Sorel, C., Glatz, J.P. 2005. *Radiochimica Acta*, 93, 351–355, 2005.)

The DIAMEX HAR hot test was implemented in a 16-stage centrifugal-contactor setup without solvent recirculation: five stages for extraction, five stages for scrubbing, two stages for acid scrubbing of the organic phase, and four stages for back-extraction (Figure 3.11).

The extraction profiles were modeled with the PAREX code (developed at the CEA) and the results compared with earlier data obtained with DMDBTDMA. The five extraction stages were sufficient to achieve feed decontamination factors above 2200 and 320 for Am(III) and Cm(III), respectively. The extraction of Mo, Zr, and Pd was efficiently prevented using oxalic acid and HEDTA scrubbing, but not that of Tc, Y, and to some extent Ru. The back-extraction proved to be very efficient, yielding more than 99.9% recovery of Am(III) and Cm(III) in only four stages. The An(III) + Ln(III) fraction was collected in 0.5 M HNO$_3$, ready for the next separation process (*155*). The DIAMEX HAC hot test was also implemented in a 16-stage centrifugal contactor setup at the ITU, after validation of the process flowsheet on a spiked countercurrent test carried out on a surrogate concentrated feed at the ForschungsZentrum Jülich (FZJ, Germany) (*156, 157*). The flowsheet applied was very close to the one described in Figure 3.11, except that the nitric acidity of the feed was 4.1 M, the HEDTA concentration was decreased to 0.05 and 0.01 M, respectively in the feed and scrub solutions, and the nitric acidity of the stripping

solution was increased to 0.3 M. As for the DIAMEX HAR hot test, the back-extraction of Am(III) and Cm(III) also proved to be very efficient, with more than 99.7 and 99.9%, respectively, recovered in only four stages. DFs were higher than 5000 for the most abundant Ln(III), higher than 20,000 for Am(III), and higher than 10,000 for Cm(III), thus confirming the efficiency of DMDOHEMA for extracting trivalent lanthanides and minor actinides. The addition of oxalic acid and HEDTA effectively prevented coextraction of Mo, Zr, and Pd. Most fission products were not extracted, the exception being Tc (DF = 217), Y (DF = 85), and Ru (DF = 1.1) (*158, 159*).

Also during the PARTNEW collaborative project, miniature Hollow Fiber Modules (HFM) from Celgard Liqui-Cel 2.5×8 Extra-Flow type, consisting of bunches of 100 to 1000 Celgard X30-240 hollow fibers (0.24 mm inside diameter, 0.30 mm outside diameter, 0.02 μm average pore size, 40% porosity) potted in 15–30 cm long glass tubes, were used as phase contactors at the Institut für Nukleare Entsorgung (INE, Karlsruhe, Germany) to carry out several counter-current DIAMEX/DMDOHEMA tests on inactive and spiked surrogate PUREX raffinates.

As organic and aqueous phases are macroscopically separated by the membrane, HFM offer several hydrodynamic advantages over other contactors, such as the absence of flooding and entrainment, or the reduction of feed consumption (*160, 161*). The flowsheets tested in HFM were similar to those developed for centrifugal contactor tests. Computer codes based on equilibrium (*162*) and kinetics data, diffusion coefficients (in both phases and in the membrane pores), and a hydrodynamic description of the module, were established to calculate transient and steady-state effluent concentrations. It was demonstrated that, by selecting appropriate flow rates (as mass transfer is mainly controlled by diffusion), very high DFs ($DF_{Am} = 20,000$ and $DF_{Cm} = 830$) could be achieved. Am(III) and Cm(III) back-extraction efficiency was up to 99.87%.

3.3.1.1.6   Diglycolamides

3.3.1.1.6.1   TODGA Process   Because of the difficulties encountered when implementing the DIDPA process (especially during the feed denitration/filtration steps), researchers from the former Japan Atomic Energy Research Institute (JAERI, today JAEA) have revised their approach to minor-actinide partitioning from the standpoint of ecology, proliferation-resistance, waste minimization, safety, and economy. A new partitioning concept named Amide-based Radio-resources Treatment with Interim Storage of Transuranics (ARTIST) was thus proposed in the early 2000s for the treatment of spent fuels (*163*). ARTIST comprises two main steps:

1. The exclusive isolation of uranium at the front-end by an amide extractant (BAMA process using a Branched Alkyl MonoAmide)
2. The overall recovery of TRU and lanthanides

However, several optional processes are also envisaged to address GEN IV concerns: (i) selective recovery of Pu to produce MOX fuels, (ii) separation of TRU from lanthanides to prepare targets for the transmutation of TRU in Accelerator-driven

systems (ADS), and (iii) isolation of Cs and Sr to reduce the underground disposal cost.

As substitutes for DIDPA extractant, many amides and diamides have been synthesized and tested for TRU partitioning. It was found that the modification of bidentate malonamides into tridentate diglycolic amides (DGA) resulted in more efficient extractants than DMDOHEMA toward all actinides (An(III–VI)), and sometimes even better than CMPO. The nature of the N-substituents (alkyl chain length or branching) of the DGA compounds is of importance for metal ion extraction. For instance, the $D_{U(VI)}$ value decreases as the alkyl chain length increases through the series $C_3H_7 > C_4H_9 > C_6H_{13} > C_8H_{17}$ (*164, 165*). Among the different DGA compounds investigated, bearing various alkyl chain lengths on their amide moieties, *N,N,N′,N′*-tetraoctyl-3-oxapentanediamide (TODGA, Figure 3.12) appeared to be the best extractant of actinides and lanthanides (*166–171*). Actinide extractability decreases in the following order An(IV) ≥ An(III) > An(VI) > An(V), whereas that of the fission products is relatively small, except for Zr(IV), Sr(II), and of course Ln(III). Contrary to the behavior observed with the malonamides, the extraction of Ln(III) increases with the atomic number in the case of TODGA.

The polarity of the organic diluent plays an important role in extraction. The $D_{M(III)}$ values decrease in the order *n*-octanol~*n*-dodecane > dichloroethane > toluene > chloroform, probably because the oxygen-donor atoms of the DGA compound interact with the aromatic and halogenated organic diluents (*169, 172*). In polar diluents such as *n*-octanol, $M(TODGA)_2(NO_3)_3$ complexes are extracted, whereas metal complexes require three or more TODGA molecules to remain stable in nonpolar organic diluents such as toluene or *n*-dodecane, where HNO_3 molecules are assumed to take part in the complex extraction reaction. When a nonpolar diluent such as *n*-dodecane is used, TODGA solvent is prone to form a third phase with relatively low organic concentrations of metal nitrates. For instance, the Nd(III) loading capacity of a solution of 0.1 M TODGA in *n*-dodecane is 0.008 M at [HNO_3] = 3 M. This disadvantage in the case of industrial application can be overcome by adding a phase modifier to the organic solvent. For instance, if the concentration of *N,N*-dihexyl-octanamide (added to TODGA) exceeds 0.5 M in *n*-dodecane, no third phase is observed, but the D_{Nd} value is decreased, while that of D_{HNO_3} is increased compared with neat TODGA/*n*-dodecane (*173, 174*). TBP (0.5 M) also significantly increases the Nd(III) loading capacity of TODGA (from 11 to 20 mM, for [HNO_3] = 3 M and [TODGA] = 0.1 M in HTP). However, the presence of TBP enhances the extraction of both oxalic acid (introduced in the feed to prevent Zr extraction) and nitric acid, which can generate precipitation problems while stripping the Ln(III) from the loaded solvent.
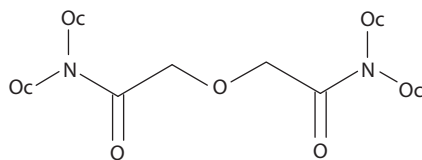
FIGURE 3.12   Tridentate *N,N,N′,N′*-tetraoctyl-3-oxapentanediamide: TODGA.

The studies of metal ion/TODGA complexes in organic diluents present unusual features, which are difficult to interpret by traditional coordination chemistry: (i) the form of the extracted An:TODGA complexes appears to change as nitric acid concentration increases in the aqueous phase; (ii) significant amounts of nitric acid are coextracted into the organic phase; and (iii) measurements based on simple equilibrium thermodynamics suggest the participation of four TODGA molecules in the extracted An(III) nitrates, which is more than can reasonably be accommodated in the inner coordination sphere of these cations (*175*). An explanation of these peculiarities was given by small-angle neutron scattering (SANS) investigations combined with vapor-pressure osmometry and tensiometry measurements of solutions of 0.1 M TODGA in alkane diluents, equilibrated with aqueous solutions of nitric or hydrochloric acids in the presence and absence of Nd(III). In metal-free nitric acid media, partial formation of TODGA dimers was observed at low acidities, whereas for nitric acid concentrations exceeding 0.7 M, polydisperse mixtures of TODGA monomers, dimers, and small reverse micelles (tetramers) were revealed by SANS experiments. No micellization was observed in metal-free hydrochloric acid, but the tetrameric reverse micelles of TODGA appeared as soon as $Nd(NO_3)_3$ or $NdCl_3$ were extracted into *n*-octane. The size and morphology of the micelles changed little in the presence of Nd(III), but the Baxter model applied to the SANS spectra revealed significant interparticle attractions between the polar cores of the micelles that increased by raising the concentrations of nitric acid and Nd(III) in the organic phase. This could explain the unusual extractive behavior of TODGA toward An(III) and Ln(III) in alkanes (*176*).

Work has been pursued in Europe in recent years, especially during the collaborative projects PARTNEW (*18*) and EUROPART (*23*) under the Fifth and Sixth EURATOM Framework Programs, to develop a viable TODGA process for An(III) + Ln(III) recovery from PUREX raffinates. During the PARTNEW project, two consecutive tracer tests have been carried out in miniature centrifugal contactors at the FZJ. In both tests, the feed was a surrogate PUREX raffinate spiked with [152]Eu(III), [241]Am(III), and [244]Cm(III), and the solvent consisted of TODGA dissolved at 0.2 M in HTP:

- The first countercurrent test was implemented in 12 stages: four extraction stages, four scrubbing stages (with 1 M HNO_3, 0.1 M oxalic acid, and 0.05 M HEDTA), and four stripping stages in 0.01 M HNO_3. 99.95% Am(III) and >99.8% La-Gd(III) were recovered from the surrogate feed. However, the An(III) + Ln(III) product solution also contained some contaminants: 9% Sr and 4% Mo.
- The second flowsheet was therefore implemented in 24 stages (Figure 3.13) (*177*). This time, the An(III) + Ln(III) product solution contained only 0.66% Sr and 1.31% Mo. However, the large amounts of oxalic acid (up to 0.4 M) introduced in the feed and scrubbing solutions to avoid Zr extraction led to partial precipitation of An(III) and Ln(III) oxalates in the low acidity conditions of the stripping section.

Therefore, extensive batch extraction studies have been carried out during the EUROPART project to optimize the system formulation. A mixture composed of

```
                                                              ┌──────────────┐
                                                              │ Spent solvent│
                                                              │ An(III)<0.04%│
                                                              │ Ln(III)<0.03%│
                                                              │   Mo~3.3%    │
                                                              │   Ru~15%     │
                                                              │    Y~6%      │
                                                              └──────────────┘
                                                                     ▲
┌──────────────┐                                                     │
│   Solvent    │                                                     │
│ TODGA in HTP │                                                     │
└──────────────┘                                                     │
       │                                                             │
       ▼                                                             │
┌──────────────┬──────────────┬──────────────┬──────────────────────────────┐
│1 Extraction 7│ Scrubbing 13 │ Scrubbing  16│ 17  Stripping  24            │
└──────────────┴──────────────┴──────────────┴──────────────────────────────┘
   │                │              │              │              │
   ▼                ▼              ▼              ▼              ▼
┌─────────┐  ┌──────────┐  ┌──────────┐ ┌──────────┐ ┌──────────────┐ ┌──────────────┐
│Raffinate│  │  Feed    │  │  Scrub   │ │Acid scrub│ │ An + Ln      │ │Strip solution│
│An(III)  │  │  PUREX   │  │  HNO₃    │ │  HNO₃    │ │ product      │ │Diluted HNO₃  │
│<D.L.    │  │raffinate │  │Oxalic    │ └──────────┘ │An(III)>99.9% │ └──────────────┘
│Ln(III)  │  │HNO₃ 3 M  │  │ acid     │             │Ln(III)>99.9% │
│<D.L.    │  │Oxalic    │  │HEDTA     │             │  Pd~1%       │
│Zr>99.9% │  │ acid     │  └──────────┘             │  Mo~1.3%     │
│Mo~95%   │  │HEDTA     │                           │  Sr~0.6%     │
│Ru~84%   │  └──────────┘                           └──────────────┘
│Rest of  │
│FP>99.5% │
└─────────┘
```
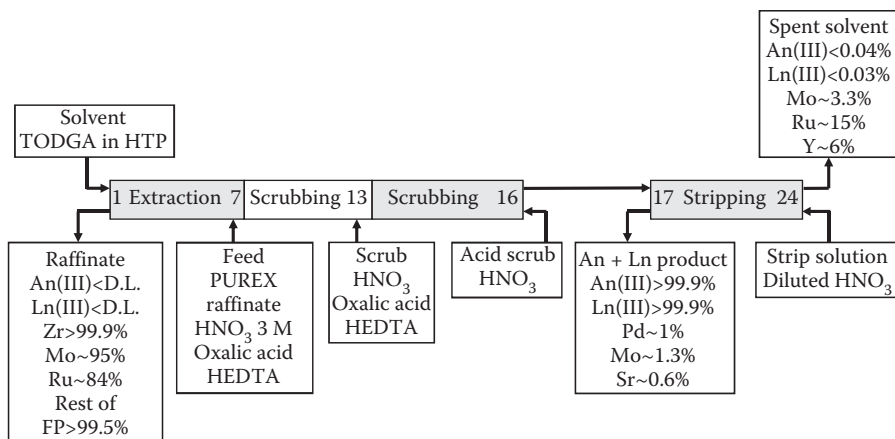
FIGURE 3.13 TODGA process flowsheet tested at the FZJ on a surrogate PUREX raffinate. (Modolo, G., Vijgen, H., Schreinemachers, C., Baron, P., Dinh, B., *Global 2003, Atoms for Prosperity: Updating Eisenhower's Global Vision for Nuclear Energy*, November 2003, New Orleans, LA.)

TODGA (0.2 M) and TBP (0.5 M), added as a phase modifier to increase the loading capacity of TODGA in HTP, was finally proposed to design flowsheets for the coextraction of An(III) and Ln(III) from PUREX raffinates. As for the French DIAMEX process, the extraction of Mo, Zr, and Pd was avoided by the addition of oxalic acid and HEDTA in the feed and scrub solutions, but the oxalic acid concentration was reduced to less than 0.3 M to prevent oxalates of An(III) and Ln(III) from precipitating in the stripping step (because of the transfer of oxalic acid by TBP from the extraction bank to the stripping bank) (*178*). Countercurrent spiked and hot tests were carried out in 2006 in centrifugal contactors at the FZJ and the ITU, respectively, and confirmed the potentiality of the TODGA/TBP/HTP solvent to coextract An(III) and Ln(III) from PUREX raffinates:

- In the spiked tests performed at the FZJ (*179, 180*), the feed solution simulated a PUREX raffinate spiked with [241]Am(III), [244]Cm(III), [252]Cf(III), [152]Eu(III), and [137]Cs(I). More than 99.9% of the trivalent lanthanides and actinides were extracted and back-extracted. Very high DFs versus most of the fission products (except ruthenium, 10% of which was coextracted and only 3% back-extracted) were obtained by implementing the flowsheet described in Figure 3.14 in two successive steps (first-day extraction and scrubbing steps over 6 hours, and second-day stripping step over 2.5 hours) using 16 centrifugal contactors designed at Tsinghua University (Beijing, China) and installed in radiochemical hoods at the FZJ.
- Thanks to these promising results, two hot tests were further carried out in the hot cells of the ITU (*181, 182*) on a genuine highly active PUREX raffinate obtained by reprocessing ~500 g of a UO_2 commercial reactor spent fuel (60 GWd/t). Oxalic acid and HEDTA were added to the PUREX high-activity raffinates, and its acidity was adjusted to ~4.4 M. The flowsheet tested was
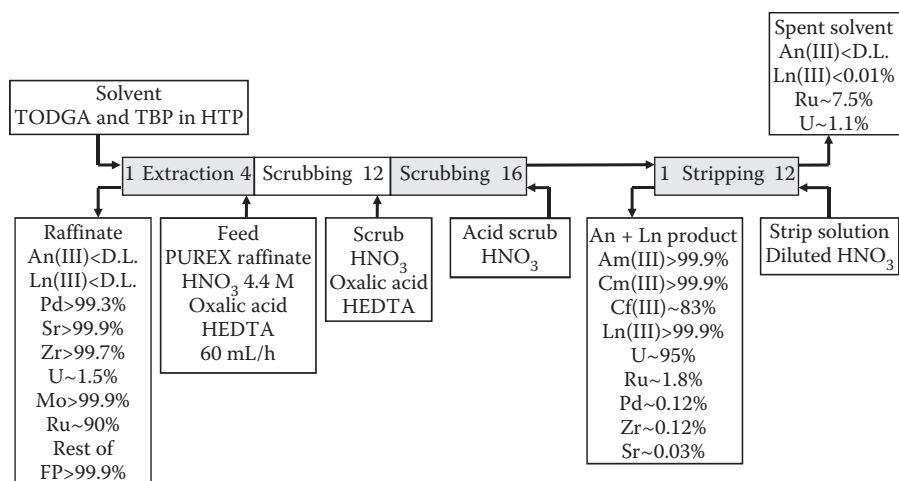
FIGURE 3.14 TODGA/TBP process flowsheet tested at the FZJ on a surrogate PUREX raffinate. (Courtesy of Modolo, G., Asp, H., Vijgen, H., Malmbeck, R., Magnusson, D., Sorel, C., *Global 2007: Advanced Nuclear Fuel Cycles and Systems*, September 2007, Boise, ID.)

similar to that described in Figure 3.14, except that the stripping bank consisted of 16 stages. The flowsheet was therefore implemented in two successive steps, because only 16 miniature laboratory centrifuges (of the BXP012 type manufactured by Rousselet-Robatel Inc., France) were available in the hot cells. The extraction and scrubbing were run during one day and the organic phase (TODGA and TBP, respectively dissolved at 0.2 and 0.5 M in HTP), which was collected after equilibrium was reached, was stripped the day after. Both actinides ([Np + Am + Cm]~190 mg/L) and lanthanides (~1.7 g/L) were extremely efficiently extracted and back-extracted (> 99.9%), with DFs exceeding 1000 for the Ln(III) (being maximum for Pr and Nd and comparable with earlier DIAMEX experiments) and reaching 40,000 for Am(III) and Cm(III). Y was also strongly extracted: it followed the lanthanides and the actinides, ending up in the product fraction. Sr, Zr, and Mo were coextracted to some extent, but efficiently scrubbed. Pd was efficiently held in the aqueous stream thanks to HEDTA complexation in the scrub sections. Of the extracted Ru, around 1% ended up in the An(III) + Ln(III) product fraction, while 17% remained in the spent solvent and should be further removed by a specific solvent treatment before recycling.

The hydrolytic and radiolytic stabilities of TODGA/HTP and TODGA/TBP/HTP solvents have been studied both by the FZJ and JAEA research teams:

- At the FZJ, it was shown that the TODGA solvent was very stable over a period of 60 days of contact with 3 M nitric acid. It also easily sustained an absorbed dose of 600 kGy (dose rate of 1.9 kGy/h). However, for higher doses (up to 1 MGy), a slight decrease of $D_{M(III)}$ values was observed for

Am(III) but not for Eu(III). Obviously, TODGA degradation was higher in the presence of 3 M nitric acid (*183*).

- At JAEA, it was demonstrated that the concentration of TODGA (pre-equilibrated with 3.0 M HNO$_3$) in *n*-dodecane decreased exponentially with the integrated dose (for a dose rate of 4.8 kGy/h), although the extractabilities of the actinide ions were maintained at high acidity even after 422 kGy. On the other hand, at low acidity, the values of $D_{M(III)}$ were increased by irradiation. These results are assumed to be due to the radiolytic degradation product, *N,N*-dioctyl-3-oxapentan-1,5-amic acid, which plays an appreciable extracting role as a proton exchanger at low acidity and as a synergist on the extraction at high acidity (*184*). Nevertheless, the radiolytic stability of TODGA could be largely improved by the addition of suitable compounds, such as *N,N*-dioctylhexanamide (DOHA), in the TODGA/*n*-dodecane solution (*185*). Moreover, the use of an organic diluent with an ionization potential lower than that of TODGA (e.g., *n*-octanol, benzene, di-*iso*-propylbenzene, nitrobenzene, benzylalcohol) also protects TODGA extractant. Furthermore, it was confirmed that aromatic substitution of DGA compounds promoted their radiolytic resistance compared with alkyl substitution.

3.3.1.1.6.2 TODGA Derivatives   Three tetraalkyl-3-oxa-pentanediamides studied in China, namely *N,N,N′,N′*-tetrabutyl-3-oxa-pentanediamide (TBOPDA), *N,N,N′,N′*-tetrahexyl-3-oxa-pentanediamide (THOPDA), and *N,N,N′,N′*-tetra(2-ethylhexyl)-3-oxa-pentanediamide (TEHOPDA), have shown strong extraction properties toward tri/tetravalent actinides and medium extraction affinities toward Tc(VII), Mo(VI), U(VI), Np(V), Fe(III), Cr(III), Ba(II), Ni(II), Ru(II), and Sr(II) (*186*). Although the increase in the substituted alkyl length lowered the extraction of the actinides, TEHOPDA was chosen as the best extractant among the three investigated diglycolamides to perform a cascade extraction experiment, because the stripping of the actinides was easier from the loaded solvent. Besides, it was reported in the literature that branching of the alkyl chain attached to the acyl N atoms of the diglycolamides suppresses the extraction of strontium from acidic solutions (*187*). The solvent therefore consisted of TEHOPDA dissolved at 0.25 M in a mixture of kerosene and *n*-octanol (70/30 vol%). 99.99% of U (initially 225 g/L in the feed) and 99.999% of Am, Pu, and Np (traces) were extracted from a spiked surrogate spent-fuel dissolution solution in four steps.

At the Indian Bhabha Atomic Research Center, engineering-scale inactive countercurrent tests (similar to those previously described for the TRUEX process) have also been performed on TEHOPDA, hereafter referred to as TEHDGA (*N,N,N′,N′*-tetra(2-ethylhexyl)diglycolamide) (*104, 188*). The objective was to validate the extraction of La(III) and Ce(III), used to mimic An(III) and Ln(III) coseparation from a surrogate feed ([HNO$_3$] = 4 M) simulating a PUREX raffinate, obtained from reprocessing a long-cooled pressurized heavy-water reactor spent fuel. The solvent consisted of TEHDGA dissolved at 0.2 M in a 30% *iso*decyl alcohol/*n*-dodecane mixture. *Iso*decyl alcohol was preferred to *N,N*-dihexyl-octanamide or TBP, as phase modifier, because of its lower affinity for nitric acid and hence its better

influence on third-phase formation with synthetic high level waste. The concentration of TEHDGA was optimized and set at 0.2 M to avoid the coextraction of other fission products, such as Mo and Sr. La(III) and Ce(III) were quantitatively stripped in dilute nitric acid (0.01 M). As in the TRUEX test, no third-phase formation was encountered, either in the five extraction stages or in the five stripping ones, and the final streams showed negligible amounts of entrained phases. The overall mass balances were satisfactory.

3.3.1.2   Second Step: An(III)/Ln(III) Separation

All partitioning processes described in today's literature that claim to separate the minor An(III) from the fission products by selective extraction of the An(III) actually perform the An(III)/Ln(III) partition from a feed arising from a front-end partitioning step, which has already separated the An(III) + Ln(III) fraction from a PUREX raffinate. There are, however, other processes that perform the An(III)/Ln(III) partition by using a selective hydrophilic complexant, introduced either in the feed to selectively complex the An(III) and prevent their extraction, or in the stripping solution to selectively back-extract the An(III) from the loaded solvent. The development and achievements of these two families of processes ("selective extraction of An(III)" and "selective complexation of An(III)") will be described hereafter.

3.3.1.2.1   *Selective Extraction of An(III)*

3.3.1.2.1.1   Nitrogen Donor Extractants   Synergistic mixtures: "N donor ligand + lipophilic acid." Since the 1980s, synergistic mixtures composed of a tridentate polyazine and a carboxylic acid have been studied (*189*). The tridentate polyazine usually provides the selectivity toward the An(III), while the carboxylic acid helps the extraction into the organic phase of the complexes formed between the An(III) and the tridentate polyazine ligand. Potentialities of 2,2′:6′,2″-terpyridine (terpy), 2,4,6-tri-2-pyridyl-1,3,5-triazine (TPTZ) (*142, 189–193*), 2-amino-4,6-di-(pyridine-2-yl)-1,3,5-triazine (ADPTZ) (*46*), 6-(5,6-dialkyl-1,2,4-triazin-3-yl)-2,2′-bipyridines (*71*), 2,6-bis-(4,6-di-pivaloylamino-1,3,5-triazin-2-yl)-pyridines (*43*), 2,6-bis-(benzimidazolyl)-4-pyridines (*198*), 2,6-dioxadiazolypyridines (*199*), or 2,6-bis-(benzoxazolyl)-4-pyridine derivatives (*194*) (Figure 3.15) have been assessed with α-bromocapric acid, and differences in extraction behavior have been explained by the basicity of the nitrogen-donor ligand.

Thermodynamic data determined by UV-visible spectroscopy and microcalorimetric titrations have highlighted a stability increase in the case of the Am(III)-ADPTZ complex compared with those of trivalent lanthanides (*46*). This difference is assumed to arise from a greater degree of covalence in the americium-nitrogen bond, in that complex formation is more exothermic for the Am(III)-ADPTZ complex. Quantum chemistry calculations (DFT) support this experimental result, showing a slightly greater covalence in the actinide-ligand bond that originates from a charge transfer from the ligand σ orbitals to the 5f and 6d orbitals of the actinide ion. ^{1}H NMR competition experiments showed that the tridentate terpy ligand has a higher affinity for U(III) in anhydrous pyridine than for Ce(III) or Nd(III) in the presence of iodide ions (*195*). The X-ray crystal structures of the solvates revealed
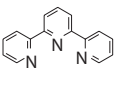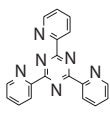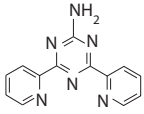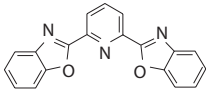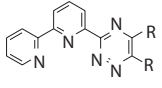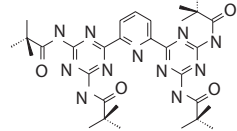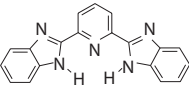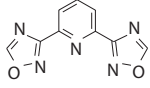
Terpyridine (terpy)	TriPyridyl-TriaZine (TPTZ)	2-amino-4,6-di-(pyridine-2-yl)-1,3,5-triazine (ADPTZ)	2,6-bis-(benzoxazolyl)-4-pyridine
6-(1,2,4-triazin-3-yl)-2,2′-bipyridine	2,6-bis(4,6-di-pivaloylamino-1,3,5-triazin-2-yl)-pyridine	2,6-bis-(benzimidazolyl)-4-pyridine	2,6-dioxadiazolypyridine

FIGURE 3.15 N-donor ligands used in synergistic mixtures with cation exchangers.

that the U-N(central pyridine) distances were shorter than the U-N(distal pyridines) distances, whereas the reverse order was found in lanthanide compounds. These differences could reflect the presence of a π back-bonding interaction between the uranium atom and the terpy ligand.

First results dealing with trivalent actinide/lanthanide group separation in laboratory-scale mixer-settlers, using a synergistic mixture, were reported in 1986 (*196*). The system combined TPTZ, directly dissolved at 0.003 M in the acidic feed ([HNO$_3$] = 0.125 M, spiked with ^{241}Am, ^{152}Eu, and ^{141}Ce), and dinonylnaphthalene sulfonic acid (HDNNS, dissolved at 0.05 M in carbon tetrachloride, used as the organic diluent to minimize phase-disengagement difficulties). Sixteen stages were employed for the extraction-scrubbing section and three stages for Am(III) stripping. Group separation of tracers was satisfactory: 99.9% of Am(III) was recovered, with only 2% of the initial Ln(III) content. However, for macroconcentrations, 5% of the Ln(III) were still present in the Am(III)-loaded organic phase (containing 99.5% of the initial Am(III)). This incomplete separation was attributed to temperature fluctuations in the mixer-settlers. Attempts to substitute hexachlorinated cobalt dicarbollide for HDNNS in the synergistic mixture with TPTZ failed because of the too strong extraction power of the hydrophobic anion, which attenuated the selectivity of TPTZ toward An(III) (*197*).

More recently, a countercurrent spiked test was run at the CEA Marcoule with a synergistic mixture composed of the tridentate nitrogen ligand 2-(3,5,5-trimethylhexanoyl-amino)-4,6-di(pyridin-2-yl)-1,3,5-triazine (TMHADPTZ, Figure 3.16) and octanoic acid. The surrogate An(III) + Ln(III) feed, containing 0.58 mM of Am(III), 1.6 μM of Cm(III), and 18 mM of various Ln(III), was buffered with a glycolic acid/sodium glycolate mixture to allow high $D_{An(III)}$ values and tune the pH variations (because $D_{An(III)}$ values vary with the third power of the pH). Although the observed Am(III)/Eu(III) separation factor was only 10 in batch tests with this synergistic mixture, a process flowsheet was elaborated for the separation of An(III) from Ln(III). This process flowsheet was tested in laboratory-scale mixer-settlers in 2000 (*3, 147*). The main results of this spiked test are indicated in Figure 3.17.
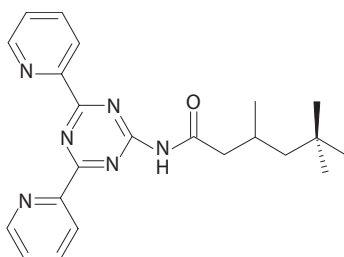
FIGURE 3.16   2-(3,5,5-Trimethylhexanoyl-amino)-4,6-di(pyridin-2-yl)-1,3,5-triazine(TMH ADPTZ).
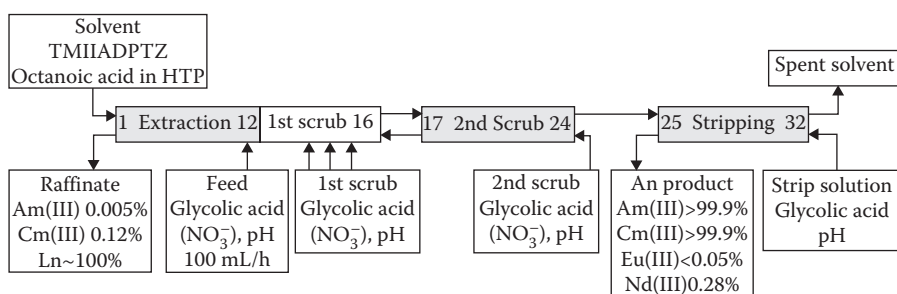
FIGURE 3.17   Synergistic system process flowsheet tested at the CEA Marcoule on a surrogate An(III) + Ln(III) product. (Courtesy of Madic, C., Lecomte, M., Baron, P., Boullis, B., *Compte-Rendu de Physique*, 3, 797–811, 2002.)

Although promising, this system has not been further developed because of its sensitivity to pH variations and the need to buffer the feed (either via a front-end step where the feed acidity is reduced through denitration, or via the introduction of large amounts of carboxylic acid in the scrubbing solution).

Bis-Triazinyl-Pyridines. Among the various tridentate polyazine compounds investigated for the past two decades, the only family of ligands that appear to extract trivalent actinides selectively over trivalent lanthanides from acidic media ([HNO$_3$] > 1 M) are the 2,6-bis-(5,6-dialkyl-1,2,4-triazin-3-yl)-pyridines (known as BTPs, Figure 3.18), discovered by German researchers (*200*) from the INE, during the NEWPART European collaborative project of the 4th EURATOM Framework Program (*145*). These soft N-donor ligands, which show unexpectedly high separation factors between An(III) and Ln(III) (SF$_{An/Ln}$ > 100), extract trivalent metallic cations through a solvation mechanism leading to the formation of M:L$_3$ complexes in which three tridentate BTP ligands bind to the trivalent metallic cation, which ends up almost completely dehydrated in its inner coordination-shell (*70, 156*).

The BTP ligands immediately drew the curiosity of the European scientific community in its quest for potential candidates for the development of minor-actinide

2,6-Bis-(5,6-dialkyl-1,2,4-triazin-3-yl)-pyridines (BTP)	
Bis-annulated-triazine-pyridine (BATP): CyMe$_4$-BTP	Bis-annulated-triazine-pyridine (BATP): ϕCyMe$_4$-BTP
6,6'-bis(5,6-dialkyl-[1,2,4]-triazin-3-yl)-[2,2']-bipyridines (BTBP)	Bis-annulated-triazine-bis-pyridine (BATBP): CyMe$_4$-BTBP
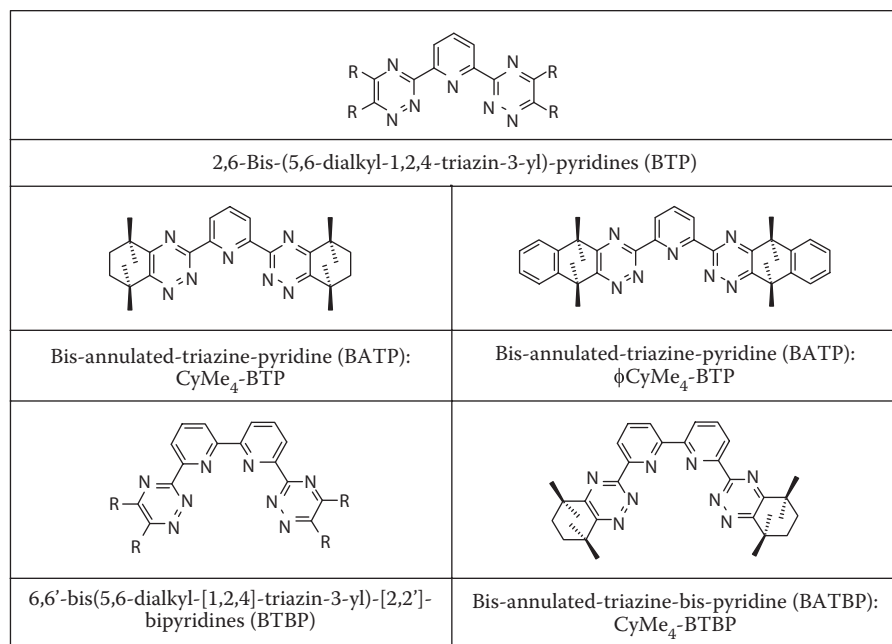
FIGURE 3.18   Soft N-donor polyazine extractants developed for An(III)/Ln(III) separation.

partitioning processes. A first BTP system, consisting of 2,6-bis(5,6-di-*n*-propyl-1,2,4-triazin-3-yl)-pyridine (*n*Pr-BTP) dissolved at 0.04 M in a mixture of HTP and *n*-octanol (70/30 vol%), was optimized from the standpoint of An(III) loading capacity and extraction/back-extraction kinetics (*201, 202*). It was applied to the partitioning of An(III) from Ln(III) both in miniature HFMs at the FZK-INE (Karlsruhe, Germany) (*203*) and in laboratory-scale mixer-settlers at the CEA Marcoule (*204*). In the 10.5-hour countercurrent alpha test performed at the CEA Marcoule in 1998, five stages of extraction, three stages of Ln(III) scrubbing, and four stages of An(III) stripping were implemented (6 mL mixing chamber and 17 mL settling chamber). Four complementary stages of An(III)-product scrubbing by introducing fresh *n*Pr-BTP solvent in the first stages of the An(III) stripping section, were implemented to maintain extractable palladium in the organic phase and therefore purify the An(III) product, as shown in Figure 3.19. The feed was a surrogate DIAMEX product (An(III) + Ln(III) fraction) containing all Ln(III) and Am(III) in nominal amounts ([Am(III)] = 126 mg/L) in [HNO$_3$] = 1 M (^{152}Eu(III) and ^{244}Cm(III) being at trace levels). Am(III) and Cm(III) were quantitatively extracted from the feed (> 99.85%). However, only 98.3% of Am(III) and 93.9% of Cm(III) were recovered in the product solution. DFs of Am(III) and Cm(III) versus Ln(III) were high but not satisfying. The mass ratio of the REEs in the actinides(III) output was about 7%, even if the concentration of Y(III) in the synthetic feed was mistakenly six times higher than that of an actual DIAMEX product solution. Less than 1% of Ru(III) but 70% of Fe(III) were coextracted with the An(III) in the solvent. Less than 1% of Pd(II) followed the An(III) product, although 20−25% mass-balance deviations were noted
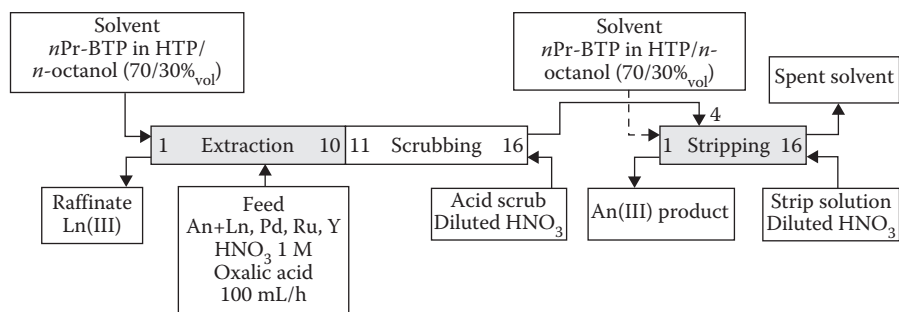
FIGURE 3.19 *n*Pr-BTP process flowsheet tested at the CEA Marcoule on a surrogate An(III) + Ln(III) product. (Courtesy of Hill, C., Hérès, X., Calor, J.N., Guillaneux, D., Mauborgne, B., Rat, B., Rivalier, P., Baron, P. 1999. Trivalent actinides/lanthanides separation using bis-triazinyl-pyridines. *Global 1999: Nuclear Technology – Bridging the Millennia*, August–September, Jackson Hole, WY.)

for both iron and palladium. Corrosion of the steel mixer blades accounted for the unexpected amounts of iron found in the different streams.

Despite the failure of this alpha test to meet the target specification of less than 5 wt% of Ln(III) in the An(III) product, countercurrent hot tests were scheduled within the NEWPART collaborative project on genuine highly active DIAMEX product solutions, first at the ITU and then at the CEA Marcoule. The results of the ITU hot test, carried out in centrifugal contactors (*205*) were rather encouraging, although the overall performance in terms of An(III) recovery yields was lower than 99.9%, in particular for Cm(III), 2.5% of which remained in the solvent, with another 2.5% left in the raffinate. The number of stripping stages was therefore increased in the flowsheet implemented in mixer-settlers in the hot cells of the ATALANTE facility at the CEA Marcoule. The observed DFs were very satisfactory ($1400 < DF_{An(III)/Ln(III)} < 450,000$), actually higher than expected by calculations, but the extraction and back-extraction yields of trivalent actinide elements were much lower than predicted by flowsheet modeling (2.5% of Am(III) and Cm(III) were left in the raffinate and 1.4% of Cm(III) in the spent solvent). Partial degradation of the *n*Pr-BTP ligand accounted for the unexpectedly bad results observed during the hot test. A 20% loss of *n*Pr-BTP was estimated by calculation (*147*).

Complementary laboratory experimental investigations of *n*Pr-BTP hydrolytic stability revealed that D_{Am} values decreased by 80% after two days of contact of the *n*Pr-BTP solvent with a 1 M nitric acid solution, but by 50% after only two hours, due to the artificial addition of nitrous acid (potentially formed by the alpha radiolysis of nitric acid during a hot test) at 0.02 M to the 1 M nitric acid solution (*206, 207*).

Thanks to gas chromatography and atmospheric-pressure chemical-ionization mass-spectrometry analyses, a mechanism of *n*Pr-BTP degradation has been proposed. The first step is assumed to be the attack at one CH_2 group on the α position of the triazine rings to form a nitro compound observed by ^{15}N NMR. In the second step, the compound is degraded into an alcohol (which is the main degradation product observed in the absence of acidic aqueous phase) or into a ketone (which is the main degradation product observed after the hydrolysis of *n*Pr-BTP by molar nitric

acid). A second CH$_2$ group can also be attacked, resulting in the formation of doubly functionalized compounds (dialcohols and diketones). The alcohol compounds can also lose one propyl chain. Side and minor reactions result in breaking triazinyl rings leading to cyano compounds (*208*).

It was further demonstrated that BTP ligands bearing branched alkyl groups on the α position of their triazine rings were more stable to hydrolysis than BTP ligands bearing linear alkyl groups. This is the reason why 2,6-bis-(5,6-di-*iso*-propyl-1,2,4-triazin-3-yl)-pyridine (*i*Pr-BTP) was chosen to develop a new process flowsheet for An(III)/Ln(III) partitioning (*209*). However, due to the low solubility of *i*Pr-BTP and its An(III) complexes in HTP/*n*-octanol mixtures and because of the peculiar kinetic behavior of *i*Pr-BTP compared with *n*Pr-BTP when extracting traces or macro amounts of An(III), *i*Pr-BTP had to be dissolved in pure *n*-octanol. Moreover, DMDOHEMA (or another surface-active reagent) had to be added as a phase-transfer catalyst to accelerate An(III) extraction. The optimized formulation of the *i*Pr-BTP system was as follows: [*i*Pr-BTP] = 0.01 M and [DMDOHEMA] = 0.5 M in *n*-octanol. In addition, glycolic acid (0.3 M, neutralized to pH 4 by NaOH) had to be used as the stripping agent to facilitate An(III) back-extraction.

An inactive countercurrent test was first carried out in the G1 facility at the CEA Marcoule in a battery of eight centrifugal contactors using a synthetic nitric acid solution containing Nd(III) and Eu(III) at 2 g/L and 100 mg/L, respectively, to assess the hydrodynamic behavior of the system, which appeared to be satisfactory (*206*).

The flowsheet described in Figure 3.20 was then implemented twice in small-scale centrifugal contactors in June 2001 in the ATALANTE hot cells (*3*):

1. First, as a "once-through" process, which lasted 8 hours and gave far better yields for the An(III) recovery than the hot test performed in 1999 with *n*Pr-BTP. More than 99.9% of Am(III) and more than 99.8% of Cm(III) were recovered from the genuine feed. An(III) losses in the raffinate solution and in the spent solvent, reached respectively 180 and 13 μg/L for Am(III) and 23 and 1 μg/L for Cm(III). A mean DF of 150 was estimated for An(III) versus Ln(III), but higher values were calculated for lighter Ln(III), which were also the major components initially present in the feed. Hence, the
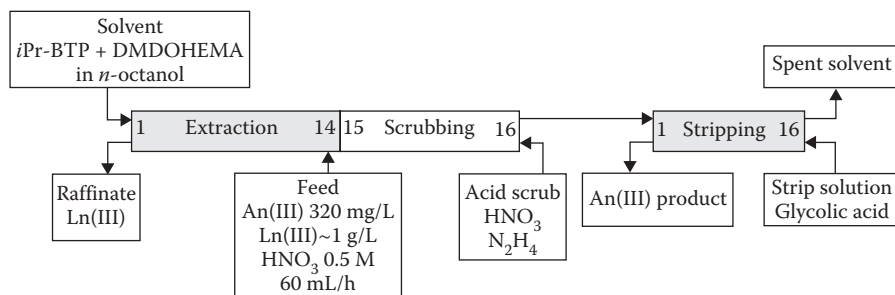
FIGURE 3.20 *i*Pr-BTP process flowsheet tested at the CEA Marcoule on a genuine DIAMEX An(III) + Ln(III) product. (Courtesy of Madic, C., Lecomte, M., Baron, P., Boullis, B. 2002. *Compte-Rendu de Physique*, 3, 797–811, 2002.)

amounts of Ln(III) in the An(III) product solution were lower than 2.5 wt%.

2. Second, as a "solvent recycle" process, which ran for 54 hours without solvent clean-up to treat 3.85 L of a DIAMEX An(III) + Ln(III) product. This second hot test, which generated 6.5 L of Am(III) + Cm(III) product, revealed partial degradation of *i*Pr-BTP, probably because of alpha/gamma radiolysis reflected by a 40% decrease in the solvent-extraction performance observed after two cycles (*207*).

Attempts to improve the chemical stability of BTP ligands by fully substituting the carbon atoms on the α position of the triazine rings led the organic chemists of the University of Reading to design and synthesize Bis-Annulated-Triazine-Pyridines (BATP, Figure 3.18), such as 2,6-bis(5,5,8,8-tetramethyl-5,6,7,8-tetrahydrobenzo[1,2,4] triazin-3-yl) pyridine (CyMe$_4$-BTP) or 2,6-bis(9,9,10,10-tetramethyl-9,10-dihydro-1,2,4-triaza-anthracen-3-yl) pyridine (BzCyMe$_4$-BTP), in which the labile α-benzylic hydrogens have been replaced by methyl groups (*210*). The hydrolytic stability of CyMe$_4$-BTP is as good as that of *i*Pr-BTP. It was demonstrated that the nature of the organic diluent (aliphatic, aromatic, nitro-aromatic) also influences the stability of the BTP ligands, especially those presenting radical-scavenging properties (*211, 212*).

The distribution ratio of Am(III) is much higher for CyMe$_4$-BTP than for *i*Pr-BTP when mixed with DMDOHEMA in *n*-octanol, and the observed An(III)/Ln(III) selectivity is outstanding for an N-soft-donor ligand: $SF_{Am/Eu} > 1500$ at equilibrium (*207*). Nevertheless, stripping becomes problematic, and further investigations and optimizations are still required before this system can be applied to countercurrent test implementation.

Bis-Triazinyl-BiPyridines. A new class of tetradentate N-donor polyazine ligands was designed at the University of Reading during the European collaborative project EUROPART of the EURATOM 6th Framework Program: the Bis-Triazinyl-BiPyridines (BTBPs) (*207*), consisting of two 5,6-dialkyl-[1,2,4]-triazinyl groups linked by a central dipyridyl moiety (Figure 3.18). The motivation for turning tridentate BTPs into tetradentate BTBPs was multiple:

- Increase the solubility of the nitrogen-donor ligands in aliphatic diluents
- Improve the An(III)/Ln(III) selectivity by increasing the denticity of the ligand
- Improve the hydrolytic/radiolytic stability of the BTPs

The extraction properties of the BTBPs toward trivalent lanthanides and actinides have been intensively investigated as a function of the nature of the organic diluent or phase-transfer catalyst and as a function of the ionic strength and acidity of the aqueous phase (*47, 210–215*).

The stoichiometry of the extracted M(III) complexes differs from that of the above-mentioned BTP ligands in that M:L$_2$ complexes (instead of M:L$_3$ complexes) have been identified by various techniques (e.g., X-ray crystallography, nuclear magnetic resonance, electro-spray ionization mass-spectrometry, and slope analysis in liquid-liquid extraction).

As in the case of the tetra-*n*-alkyl substituted BTP ligands, the tetra-*n*-alkyl substituted BTBP compounds suffer from a weak chemical stability when they are dissolved in HTP/*n*-octanol mixtures, because of the oxidation of their α-benzylic hydrogens. However, 6,6′-bis(5,5,8,8-tetramethyl-5,6,7,8-tetrahydro-benzo[1,2,4]tri-azin-3-yl)[2,2′]bipyridine (CyMe$_4$-BTBP, Figure 3.18), in which the labile α-benzylic hydrogens have been replaced by methyl groups, exhibits a good hydrolytic stability (comparable to that of CyMe$_4$-BTP) and a better apparent radiolytic stability compared with BTP compounds, probably due to its lower complex stoichiometry. In fact, the mass-action law differs and is more favorable in the case of the BTBPs: the $D_{M(III)}$ values, measured when investigating the effect of irradiation doses on BTBP ligands, follow a two-fold order of the extractant concentration in the organic phase (because M:L$_2$ complexes are formed), whereas in the case of the BTPs, the $D_{M(III)}$ values follow a three-fold order of the extractant concentration (because M:L$_3$ complexes are formed) (*207*).

CyMe$_4$-BTBP was envisaged for the development of an An(III)/Ln(III) partitioning process. The system formulation was optimized: [CyMe$_4$-BTBP] = 0.01 M and [DMDOHEMA] = 0.25 M in *n*-octanol, for the organic solvent, and [Glycolic acid] = 0.5 M, neutralized to pH 4 by NaOH, for the stripping solution (*216*). A flow-sheet was elaborated based on the extraction isotherms determined through a series of test-tube experiments. Nevertheless, kinetic problems were identified when implementing this system in centrifugal contactors at the FZJ and at the ITU (*217*). Due to the small hold-up volume compared to the flow rate in centrifugal contactors, the time for extraction was too short to reach the D_M values determined at equilibrium in batch tests. Kinetics experiments performed to investigate the D_M dependence of the flow rate showed that even with the lowest applicable flow rates, only 8% of the equilibrium D_{Am} value was reached for Am(III) extraction in the single-stage centrifuge spiked test and around 16% in the single-stage centrifuge hot test (the difference being due to the size of the centrifuges). Nevertheless, a countercurrent hot test was attempted at the ITU (*218*). The An(III) + Ln(III) product issued from the TODGA hot test carried out at the ITU in 2006 on a PUREX raffinate (see Section 3.3.1.1.6.1) was used as the feed, after increasing its acidity to 2 M. The concentration of CyMe$_4$-BTBP was increased to 15 mM in the mixture DMDOHEMA (0.25 M)/*n*-octanol to compensate for the low apparent $D_{M(III)}$ values measured in single-stage centrifuge experiments. The extraction section comprised nine stages followed by a three-stage scrub and a four-stage strip. All flow-rates were set to 10 mL/h due to the slow extraction/back-extraction kinetics of the CyMe$_4$-BTBP system (Figure 3.21). The "once-through" countercurrent test was successful, as more than 99.9% of Am(III) and Cm(III) ended up in the product with less than 0.1% of the most dominant lanthanides, thus demonstrating the ability of CyMe$_4$-BTBP system to separate An(III) from Ln(III). A validation of the process when recycling the solvent is now awaited.

3.3.1.2.1.2 Sulfur-donor Extractants The CYANEX 301 Process. Various dialkyl-(mono/di)-thio(phosphoric/phosphinic) acids, such as di(2-ethylhexyl)-di-thiophosphoric acid (HDEHDTP), bis(2,4,4-trimethylpentyl)-thiophosphinic acid (CYANEX 272), bis(2,4,4-trimethylpentyl)-monothiophosphinic acid (CYANEX

302), or the better known bis(2,4,4-trimethylpentyl)-dithiophosphinic acid (CYANEX 301), have been studied at the Institute of Nuclear Energy Technology (INET, Tsinghua, China) to separate An(III) from REEs. Like HDEHP from the TALSPEAK process, the oxygen-donor extractant CYANEX 272 presents the highest extraction efficiency for Ln(III), among the CYANEX compounds. On the contrary, its monothio analog CYANEX 302 is selective toward An(III), but much less than its dithio analog CYANEX 301, thus, demonstrating the importance of soft-donor atoms in the structure of the extractant for An(III)/Ln(III) separation (*219*). Nevertheless, commercial CYANEX 301 compound from the Canadian CYTEC company only contains approximately 80% bis(2,4,4-trimethylpentyl)-dithiophosphinic acid (HBTMPDTP, Figure 3.22) and requires prior purification by crystallization of its ammonium salt in benzene to become highly selective toward An(III): $SF_{Am/Eu} = D_{Am}/D_{Eu} = \sim 5900$ at pH > 3 (*91*). When mixed with a nitrogen soft ligand, such as 2,2′-bipyridine or 1,10-phenanthroline in toluene, HBTMPDTP presents Am/Eu separation factors that exceed 40,000 from nitrate solutions at pH > 3 (*69, 220*).

An empirical distribution ratio model was first elaborated to describe the extraction of Am(III) and Ln(III) in kerosene by purified HBTMPDTP, based on mass balances and mass-action laws of HBTMPDTP dimerization in kerosene, dissociation
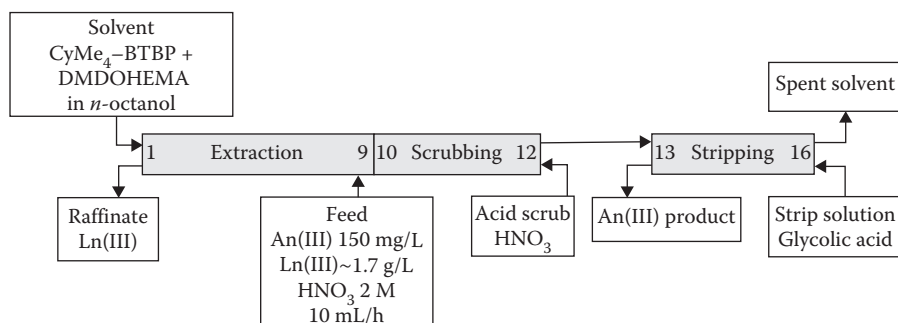
FIGURE 3.21 CyMe₄-BTBP process flowsheet tested at the ITU on a genuine TODGA An(III) + Ln(III) product. (Courtesy of Magnusson, D., Christiansen, B., Glatz, J.P., Malmbeck, R., Modolo, G., Serrano Purroy, D., Sorel, C. 2008. *ATALANTE 2008: Nuclear Fuel Cycles for a Sustainable Future*, May 2008, Montpellier, France.)
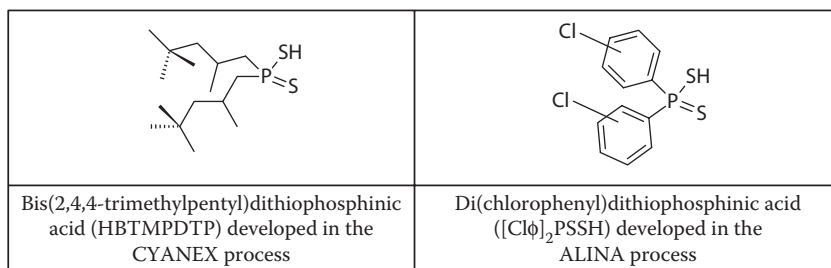
FIGURE 3.22 Soft S-donor dithiophosphinic acidics developed for An(III)/Ln(III) separation.

and distribution of HBTMPDTP in the aqueous phase, and trivalent metallic cation extraction (*221, 222*):

$$M^{3+} + 2(HBTMPDTP)_2 \xrightarrow{K_{ex}} M(BTMPDTP)_3 HBTMPDTP + 3H^+$$
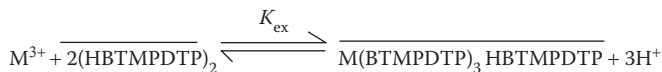
However, the formation of such 1:4 (metal:ligand) complexes, in which three molecules of HBTMPDTP lose their protons and one remains protonated, was later invalidated by SANS, visible absorption spectroscopy, and extended X-ray absorption fine structure experiments, which all support 1:3 (metal:ligand) complexes in the organic phase (*223*).

A method for computing countercurrent process parameters was developed to design practicable An(III)/Ln(III) separation flowsheets involving purified HBTMPDTP and was verified through multistage extraction-cascade experiments (four to six stages), using surrogate as well as genuine highly active An(III) + Ln(III) product solutions from the TRPO process, after pretreatment to adjust their pH to 3.5 (*224–226*). Spiked countercurrent extraction experiments showed that >99.99% Am(III) could be separated from the Ln(III) and >99% of Ln(III) from Am(III) within six stages.

A continuous flowsheet was further tested countercurrently by implementing a solution of purified CYANEX 301, dissolved at 0.5 M in kerosene and saponified to 0.8%, in a 10-stage miniature centrifugal-contactor battery (four stages for extraction, three stages for scrubbing with 0.5 M NaNO$_3$ at pH = 3.6, and three stages for Am(III) stripping by 0.5 M HNO$_3$). The feed, an An(III) + Ln(III) fraction from a previous TRPO process, was evaporated to dryness to remove nitric acid (approximately 4.7 M HNO$_3$), the residue was dissolved in 0.5 M NaNO$_3$ and contacted three times with the CYANEX 301 solvent to remove Fe(III), Mo(VI), and Pd(II). Its pH was then adjusted to 3.5 with NaOH (*227*). The results of the hot test were not satisfactory, as the separation of REEs from Am(III) did not meet the transmutation requirements, although better results should be obtained by optimizing process parameters, such as the number of stages and the pH of the scrubbing solution.

By combining purified CYANEX 301 (HBTMPDTP, 0.5 M) with TBP (0.25 M) in kerosene, the pH$_{1/2}$ value of Am(III) extraction was decreased from 3.16 to 2.45 (*228*). A multistage extraction cascade experiment, consisting of seven stages of extraction, three stages of scrubbing (with 0.1 M HNO$_3$), and two stages of Am(III) stripping (with 0.5 M HNO$_3$), showed that >99.99% of trace amounts of [241]Am(III) were extracted with <0.04% Nd(III) from the initial surrogate feed composed of palladium and neodymium nitrates ([Pd + Nd] = 0.5 M) at pH 3.

The ALINA Process. During the European collaborative project NEWPART under the Fourth EURATOM Framework Program (*145*), several bis(halogeno-phenyl)-dithiophosphinic acids, aryl derivatives of HBTMPDTP-bearing electron-attractor substituents (presenting negative mesomeric effects), were synthesized and tested at the FZJ with the intention of achieving An(III)/Ln(III) separation at pH values lower than 2 (*229, 230*). Batch experiments showed that it was possible to carry out this difficult separation with relatively high selectivity, even in strongly acidic media (up to
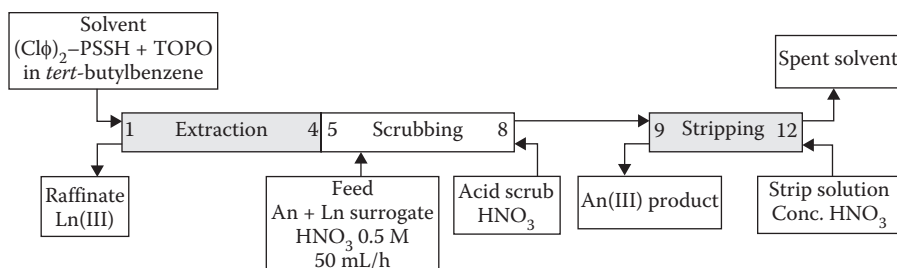
FIGURE 3.23 ALINA process flowsheet tested at the FZJ on a surrogate DIAMEX product. (Courtesy of Modolo, G., Odoj, R., Baron, P., *Global 1999: Nuclear Technology – Bridging the Millennia*, August–September 1999, Jackson Hole, WY.)

1 M HNO$_3$), using aromatic dithiophosphinic acids mixed with either TBP or TOPO. The higher hydrolytic and radiolytic resistance of aromatic dithiophosphinic acids compared with HBTMPDTP was also demonstrated. The formulation of a selective organic solvent was optimized in order to selectively extract trivalent actinides from DIAMEX An(III) + Ln(III) product solutions. It consisted of di(chlorophenyl) dithiophosphinic acid ([Clϕ]$_2$PSSH, Figure 3.22) and tetra-*n*-octylphosphine oxide (TOPO), respectively dissolved at 0.5 and 0.25 M in *tert*-butyl-benzene. Based on this solvent, the Actinide(III)-Lanthanide(III) INter-group separation in Acidic medium (ALINA) process was tested countercurrently, at the FZJ, using 12 miniature centrifugal extractors designed at Tsinghua University and a surrogate An(III) + Ln(III) feed simulating a DIAMEX product (*231*). The flowsheet consisted of four stages of extraction, four stages of scrubbing, and four stages of stripping (Figure 3.23). More than 96% of Am(III) was extracted from the feed and back-extracted with 3 M nitric acid; ~3% of the Ln(III) followed the An(III) stream, probably because the 1 M acid scrubbing was not efficient enough. Although in good agreement with the calculated predictions, the results of this spiked test showed that the process should be extended by two extraction steps and two scrubbing steps to achieve complete separation of An(III) and Ln(III).

The ALINA process has also been implemented in HFMs at the INE. The mass-transfer kinetics appeared fast, and an Am(III) extraction efficiency exceeding 99.9% was observed (*156, 203*).

3.3.1.2.2 *Selective Complexation of An(III)*

3.3.1.2.2.1 The ZEALEX Process Researchers from KRI have shown that the zirconium salt of dibutyl phosphoric acid (ZS-HDBP) was soluble in Isopar-L in the presence of 30% TBP. This super PUREX solvent, known as ZEALEX, extracts actinides (Np-Am) together with lanthanides and other fission products, such as Ba, Cs, Fe, Mo, and Sr from nitric acid solutions. The extraction yields depend on both the molar ratio between Zr and HDBP in the 30% TBP/Isopar-L mixture and the concentration of HNO$_3$ (*232*). Trivalent transplutonium and lanthanide elements can be stripped together from the loaded ZEALEX solvent by a complexing solution, mixing ammonium carbonate, (NH$_4$)$_2$CO$_3$, and ethylenediamine-*N,N,N′,N′*-tetraacetic acid (EDTA). An optimized version of the process should allow the separation of

An(III) from Ln(III) in a two-cycle flowsheet. In the first cycle, Ln(III) and An(III) are coextracted by 0.2 M ZS-HDBP dissolved in 30% TBP/Isopar-L and, in the second cycle, the An(III) are selectively stripped by a diethylenetriamine-*N,N,N′,N″,N″*-pentaacetic acid (DTPA) solution, while the Ln(III) are consecutively stripped by a mixture of nitric acid and hydrogen peroxide. DFs greater than 100 are expected by calculations, and less than 5% Ln(III) contamination is assumed (*233, 234*).

3.3.1.2.2.2 Di(2-ethylhexyl)-phosphoric Acid (HDEHP): The TALSPEAK Process   A comprehensive review has recently been published on the development and operational characteristics of the TALSPEAK (Trivalent Actinide-Lanthanide Separation by Phosphorus reagent Extraction from Aqueous Komplexes) process, developed in the late 1960s at the Oak Ridge National Laboratory (USA) to partition Ln(III) and An(III) between an acidic organophosphorus extractant and an aqueous phase buffered with a carboxylic acid and containing a polyaminopolycarboxylate complexant. Several combinations of different extractants and aqueous complexant/ buffer couples have been investigated, as well as the influence of various parameters, such as the nature of the organic diluent, the pH, and the temperature (*235, 236*). The most commonly tested TALSPEAK system involves:

- HDEHP as the cation-exchanger dissolved in di-*iso*-propylbenzene
- DTPA as the hydrophilic selective complexant of the An(III)
- Lactic acid as the aqueous buffer

It generally proceeds through the extraction of the Ln(III) at a pH ranging from 2 to 3, leaving the An(III) in the aqueous raffinate as polyaminopolycarboxylate complexes. Therefore, it requires a buffered feed, which could be the stripping solution of a front-end process (such as the TRUEX process).

A variant solvent formulation was developed in China (INET), involving (2-ethylhexyl)-phosphonic acid 2-ethylhexyl ester (HEHEHP) as the extractant (saponified to 40% with concentrated ammonia), dissolved at 1.5 M in kerosene, to recover, in 43 stages, 99% of Am(III) and remove 90% of Ln(III) from a 0.2 M nitrate feed (pH 1) (*237*).

In the "reverse" TALSPEAK process, the An(III) + Ln(III) fraction is first coextracted from a feed, the acidity of which has to be reduced to ~0.1 M by denitration or nitric acid extraction. An(III) are then selectively stripped using DTPA in citric acid (1 M) at pH 3 (hence the name "reverse" TALSPEAK process), and the Ln(III) are finally stripped by 6 M HNO_3. Attempts to apply this TALSPEAK variant to the treatment of actual UREX + raffinates are reported in the literature, but they involve several steps. The problematic Zr and Mo elements are first removed by direct extraction with HDEHP (0.8 M in di-*iso*-propylbenzene) from the high-acidity raffinate stream arising from the UREX + co-decontamination process (*238*). The remaining fission products and actinides can then be concentrated by acid evaporation and denitration processes. This concentrate is further diluted to a lower acidity (e.g., $[HNO_3] = 0.03$ M) to allow the coextraction of An(III) and Ln(III) by the TALSPEAK solvent.

3.3.1.2.2.3 Di-iso-decylphosphoric Acid: The DIDPA Process An(III) and Ln(III) can be partitioned using the DIDPA solvent (DIDPA and TBP, respectively dissolved at 0.5 and 0.1 M in *n*-dodecane) in a two-step process approach. First coextracted and costripped in a 4 M nitric acid solution in a first DIDPA cycle (see Section 3.3.1.1.4), the An(III) + Ln(III) fraction is partitioned in a second cycle after denitration of the An(III) + Ln(III) product by formic acid to reduce the nitric acid concentration to at least 0.5 M. In this second DIDPA cycle, An(III) and Ln(III) are first coextracted by the DIDPA solvent, and the An(III) are selectively stripped by DTPA (0.05–0.1 M) in a solution buffered at pH 3 with lactic acid (1 M). The trivalent lanthanides are further stripped with a 4 M nitric acid solution (*134*).

3.3.2 ONE-CYCLE PROCESSES: SEPARATION OF AN(III) FROM PUREX RAFFINATES

3.3.2.1 The SETFICS Process

The SETFICS process (Solvent Extraction for Trivalent *f*-elements Intragroup Separation in CMPO-Complexant System) was initially proposed by research teams of the former Japan Nuclear Cycle Development Institute (JNC, today JAEA) to separate An(III) from PUREX raffinates. It uses a TRUEX solvent (composed of CMPO and TBP, respectively dissolved at 0.2 and 1.2 M in *n*-dodecane) to coextract trivalent actinides and lanthanides, and a sodium nitrate concentrated solution (4 M $NaNO_3$) containing DTPA (0.05 M) to selectively strip the TPEs at pH 2 and keep the Ln(III) extracted by the TRUEX solvent (*239*). However, the DFs for heavy Ln(III) are rather poor. An optimized version of the SETFICS process has recently been proposed as an alternative process to extraction chromatography for the recovery of Am(III) and Cm(III) in the New Extraction System for TRU Recovery (NEXT) process. NEXT basically consists of a front-end crystallization of uranium, a simplified PUREX process using TBP for the recovery of U, Np, and Pu, and a back-end Am(III) + Cm(III) recovery step (*240, 241*).

Minimization of the secondary wastes produced by the SETFICS process was assessed during inactive countercurrent test campaigns. Although it improved the loading capacity of the TRUEX solvent in *n*-dodecane, the increase of TBP content from 1.2 to 1.4 M enhanced the extraction of nitric acid. This affected the pH in the stripping bank (which is only slightly buffered by DTPA), which lowered the complexation yields of An(III) by DTPA, and consequently decreased the separation of light lanthanides (*242*). Furthermore, the use of HAN as a "salt-free" substitute for sodium nitrate in both the acid scrubbing and An(III) stripping sections, as described in Figure 3.24, led to poorer decontamination of Nd and Sm than in previous tests. From the mass-balance data and the DFs observed for Nd, Sm, and Eu, it was concluded that the experimental flowsheet was not yet ideal for An(III) recovery and required further optimization (*243*).

A SETFICS countercurrent hot test was recently conducted with high loading of "salt-free" flowsheet (in order to reduce the solvent volume and the amount of waste stream by 50%) in the JAEA Chemical Process Facility (CPF) as part of the feasibility demonstration of the NEXT process. The solvent consisted of CMPO and TBP,
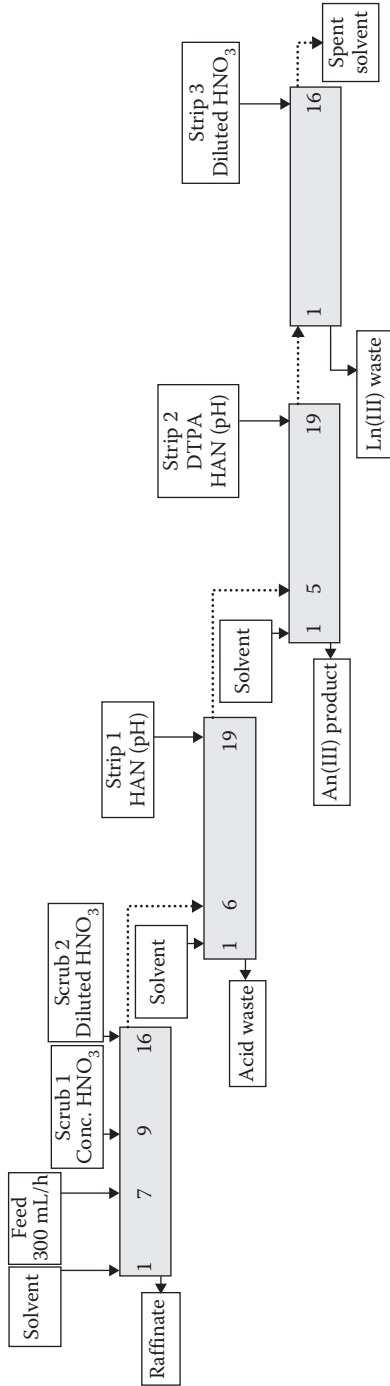
FIGURE 3.24 SETFICS process flowsheet tested by JNC on an inactive surrogate PUREX raffinate. (Courtesy of Hirano, H., Koma, K., Koyama, T., *7th Information Exchange Meeting on Actinide and Fission Product Partitioning and Transmutation*, October 2002, Jeju, Republic of Korea.)

respectively dissolved at 0.2 and 1.4 M in *n*-dodecane, and the feed was a genuine highly active solution issued from the first two steps of the NEXT process. Two batteries of 16 miniature centrifugal extractors were used consecutively to implement a 64-stage flowsheet Figure 3.25). In the first step, the trivalent actinides and lanthanides were coextracted using seven stages. The loaded solvent was scrubbed by nitric acid and HAN solutions using 25 stages. In the second step, the An(III) were selectively stripped by a salt-free DTPA (0.05 M)/HAN (2 M) solution using 16 stages, followed by the back-extraction of the remaining Ln(III) in dilute nitric acid. Americium and curium followed the An(III) product solution, and their total losses were kept below 1%. The DFs for the major fission products were >3100, >10, 1.8, and 1.9, respectively for Cs, Pr, Nd, and Sm. $DF_{An/Nd}$ was lower than in previous tests (*241*). HEDTA, which exhibits higher dissociation constants than DTPA, was proposed for the selective stripping of the An(III). Batch distribution data of Ln(III) in the presence of HEDTA showed that the required nitrate concentration was half that needed with DTPA to obtain the same D_{Nd} value. Nevertheless, Ln(III) intragroup separation appeared to be worse with HEDTA than with DTPA, foreseeing a less efficient An(III)/Ln(III) separation in countercurrent test applications. Furthermore, the An(III) stripping appeared to be very sensitive to pH variations (slope of −3 for the variation of log $D_{M(III)}$ versus pH).
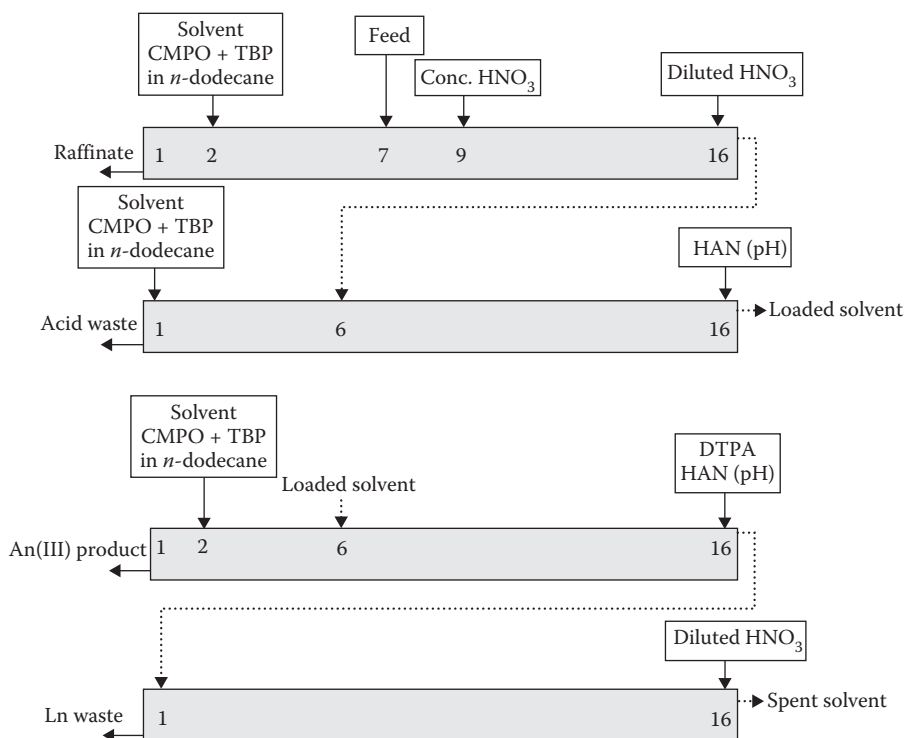
FIGURE 3.25 SETFICS process flowsheet tested at JAEA (CPF) on a highly active feed. (Courtesy of Nakahara, M., Sano, Y., Koma, Y., Kamiya, M., Shibata, A., Koizumi, T., Koyama, T. 2007. *Journal of Nuclear Science and Technology*, 44, 373–381, 2007.)

The use of fluorinated organic diluents, such as Fluoropole-732, has recently been suggested to suppress third-phase formation risks in the SETFICS solvent, even without TBP (*244*). A solvent consisting of CMPO, dissolved at 0.22 M in Fluoropole-732, was tested in active countercurrent tests performed at the Mining Chemical Combine in Russia in the scope of a collaboration between the research teams of JAEA and the KRI of Saint Petersburg. A spiked test was first run with 10 L of a surrogate feed to bring the equipment into reliable operating mode, and then a hot test was carried out to treat 12 L of HAW arising from reprocessing a fast-breeder-reactor spent nuclear fuel. Trivalent REEs and TPEs were quantitatively extracted: >99.97% Ce(III) and Am(III), and >98.7% La, Pr, and Nd. Upon HNO_3 washing, the TPEs were stripped by a solution of $NaNO_3$ (3 M) and DTPA (0.05 M) at pH = 2.5, which also stripped 41% of Sm, 48% of Eu, and 58% of Y; thus, no effective purification of the TPEs from the heavy REEs was observed, similarly to the classical SETFICS process. Contamination of the TPE stream by La, Nd, Pr, Ce, U, and Fe was 0.5%, 4.4%, 0.3%, 0.04%, 1.2%, and 3.6%, respectively. Increasing the concentration degree of the target elements in the strip product led to a decreased separation.

3.3.2.2   The DIAMEX-SANEX/HDEHP Process

The DIAMEX-SANEX/HDEHP process is probably the only single-step process that enables a complete selective An(III)/Ln(III) partitioning from non-pretreated PUREX raffinates (*245*). It combines two organic molecules possessing opposite but complementary extracting mechanisms:

- *N,N′*-Dimethyl-*N,N′*-dioctylhexylethoxymalonamide, used in the DIAMEX process, which extracts trivalent metallic cations from highly acidic feeds by solvation, thus avoiding any adjustment of the acidity of PUREX raffinates.
- Di(2-ethylhexyl) phosphoric acid, used in the TALSPEAK process, which extracts trivalent metallic cations at low acidity by proton exchange.

As in the SETFICS and TALSPEAK processes, the DIAMEX-SANEX/HDEHP process involves selectively back-extracting the trivalent actinides by a hydrophilic polyamino-carboxylate complexing agent, HEDTA, in a citric acid buffered solution (pH 3). However, the combination of HDEHP and DMDOHEMA at high acidity promotes the coextraction of some *d*-block transition metals, such as Pd(II), Fe(III), Zr(IV), and Mo(VI), which must be dealt with by specific stripping steps (as described on Figure 3.26) that increase the total volume of the output streams:

- The An(III) and some fission products (Ln(III), Pd(II), Fe(III), Zr(IV), Ru, and Mo(VI)) are first coextracted from the PUREX raffinate by the mixture of extractants (DMDOHEMA and HDEHP, respectively dissolved at 0.5 and 0.3 M in HTP).
- The interfering *d*-block transition metals, Mo and Pd, are stripped prior to the TPEs by a citrate solution at pH 3.
- The An(III) are selectively stripped by HEDTA in a citric acid buffered solution (pH 3), while the Ln(III) are maintained extracted in the organic phase by HDEHP.
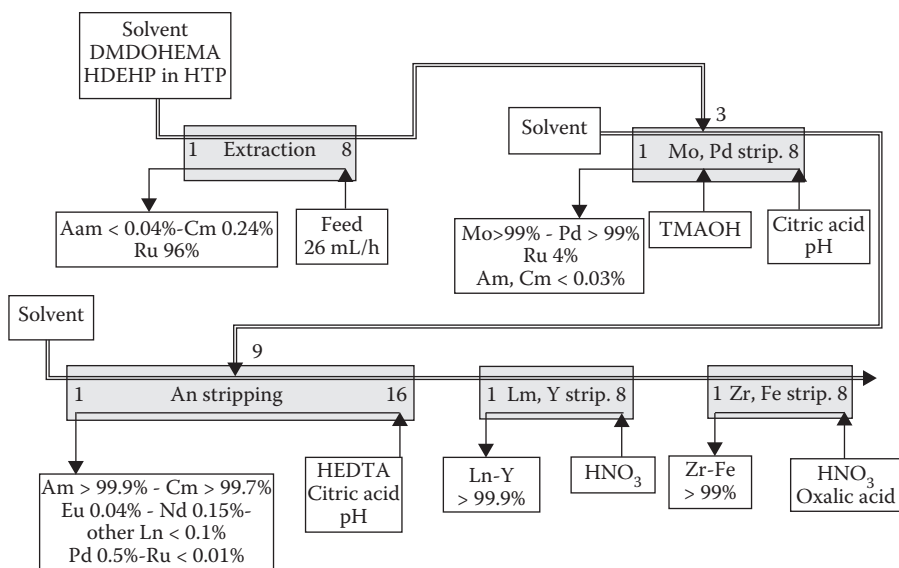
FIGURE 3.26 DIAMEX-SANEX/HDEHP process flowsheet tested at the CEA Marcoule on a genuine PUREX raffinate. (Courtesy of Madic, C., Lecomte, M., Baron, P., Boullis, B., *Compte-Rendu de Physique*, 3, 797–811, 2002.)

- The Ln(III) are back-extracted in 1 M nitric acid
- Zr and Fe are finally stripped by an acidic oxalic solution

The concept feasibility of this process was first validated by the successful implementation of an inactive countercurrent test using 48 stages of laboratory-scale mixer-settlers (6 mL mixing chamber and 17 mL settling chamber) in the G1 facility at the CEA Marcoule. This inactive test was followed by a countercurrent hot test in 2000, performed on a genuine highly active PUREX raffinate in the hot cells of the ATALANTE facility (*3, 147, 246*). The flowsheet was implemented in two sequences of approximately 6 hours each, as only 32 miniature centrifugal contactors were available in the hot cells:

1. Extraction (eight stages), Mo and Pd stripping (eight stages), and An(III) stripping (16 stages)
2. Ln(III) and Y(III) stripping (eight stages), and Zr and Fe stripping (eight stages)

The main results of this hot test can be summarized as follows:

- Satisfactory hydrodynamic behavior
- High recovery yields for An(III): >99.9% for Am(III) and >99.7% for Cm(III) (0.2% of Cm(III) remained in the raffinates, but this should be improved by two additional stages in the extraction section)
- Satisfactory An(III)/Ln(III) DFs: $DF_{An/Ln} > 800$ (less than 2 wt% of Ln(III) in the An(III) product solution)

- Satisfactory An(III)/fission products DFs: only 0.5% of Pd and less than 0.01% of Ru followed the An(III) fraction

It should be noted, however, that a simplified version of the DIAMEX-SANEX/HDEHP process was also successfully implemented on a genuine highly active DIAMEX product (An(III) + Ln(III) fraction) in 2005, as the second step of an An(III)/Ln(III) partitioning scheme, in the scope of the technical feasibility validation of minor-actinide separation proposed by the CEA to address the issues of the 1991 French radioactive waste management act (*154*).

The chemical stability of the DIAMEX-SANEX/HDEHP solvent with regard to acidic hydrolysis and gamma radiolysis has been investigated both in batch experiments and during a continuous 1800-hour test in which the solvent was recycled approximately 100 times and was subjected to a cumulative dose of ~800 kGy (at a dose rate of 1.3 kGy/h) and to ~250 hours of 3 M nitric acid hydrolysis at 40°C in the MARCEL facility of the CEA Marcoule (*247, 248*). A continuous regeneration of the spent solvent by alkali washing prevented the accumulation of degradation products (especially the monoamide and acid amide derived from DMDOHEMA), combined with an in-line adjustment of the extractant concentration allowed the process performances to remain constant during the 1800-hour run.

Current optimizations of the DIAMEX-SANEX/HDEHP process rely on the simplification of its flowsheet by minimizing the required number of stages and the volumes of the generated effluents through the use of more efficient hydrophilic complexing agents. Another optimization contemplated consists in avoiding the presence of the phosphorus acidic extractant at the extraction step (which induces the concomitant extraction of molybdenum, zirconium, and iron) (*249*). This option is made possible by introducing in the process flowsheet (right after the stripping of the lanthanides) an in-line separation of the two extractants (by specifically stripping the phosphorus acidic extractant into an appropriate buffered citric acid solution). The DMDOHEMA is thus recycled in a first "loop" of the process flowsheet (where An(III) and Ln(III) are coextracted at high acidity), and the acidic extractant in the second one (where the An(III) are selectively stripped by the carboxylate complexant). These modifications involve a search for a new organophosphorus acid which would offer the advantages of HDEHP, but which could be easily separated from DMDOHEMA. di-*n*-Hexylphosphoric acid (HDHP) was chosen as a substitute for HDEHP because it fulfills all the required criteria.

The coordination of trivalent 4*f* and 5*f* elements with DMDOHEMA and HDHP has been investigated in *n*-dodecane and HTP under different extraction conditions (high and low acidity) with the help of various techniques (liquid-liquid extraction, extended X-ray absorption fine structure spectroscopy, small-angle neutron/X-ray scattering, vapor pressure osmometry, and electrospray ionization mass spectrometry). The extraction of Eu(III) and Am(III) by HDHP-DMDOHEMA mixtures exhibits a change of extraction mechanism and a reversal of selectivity taking place at 1 M HNO_3 in the aqueous phase: below 1 M HNO_3, HDHP dominates the metal extraction, whereas DMDOHEMA is the predominant extractant at higher aqueous acidities. Results indicate modest antagonism between the two extractants in the extraction of Eu(III) and synergism in the extraction of Am(III). These data are interpreted as resulting from the formation of mixed DMDOHEMA/HDHP/M(III)

complexes containing two phosphoric and five malonamide moieties (*250, 251*). This stoichiometry has been further confirmed by electrospray ionization mass spectrometry studies on the DMDOHEMA/HDEHP couple of extractants (*52*).

3.4 CONCLUSION

The separation of trivalent minor actinides (Am, Cm, Cf) from trivalent lanthanides has been a challenging and key issue of the Partitioning and Transmutation strategy during the past decades, because no technology can transmute the actinides to a degree meaningful for waste management without prior chemical separation from the lanthanides because of their neutron-poisoning effect. The lanthanides present the same oxidation state (i.e., III) as the 5*f* TPEs in acidic solutions, the matrix usually employed to dissolve spent nuclear fuels. This physical feature similarity makes the chemical separation of An(III) from Ln(III) all the more tedious and difficult. Various hydrometallurgical processes based on solvent extraction have been developed around the world over almost a half century for An(III)/Ln(III) separation from acidic aqueous feeds. This review summarized the latest developments of An(III)/Ln(III) separation processes, the concept feasibility of which has been assessed through the implementation of countercurrent tests either at laboratory or at pilot scales. They all require prior implementation of the PUREX (or similar) process, which eliminates the two major actinides, uranium and plutonium (and potentially also the minor actinide neptunium). They are summarized in Figure 3.27 and can be broken down as follows:

- Two-cycle processes, which achieve the An(III)/Ln(III) separation only after a first cycle of An(III) + Ln(III) coextraction and separation from the rest of the fission products
- One-cycle processes, which allow the separation of An(III) from Ln(III) directly from PUREX raffinates

However, none of these hydrometallurgical processes allows the An(III) to be selectively extracted from PUREX raffinates. The two-cycle processes need a preliminary step in which "hard-donor" extractants bearing oxygen atoms easily coextract the trivalent (and sometimes higher oxidation states) 5*f* elements together with the trivalent 4*f* elements from acidic feeds. The compounds involved in these first-step processes can be mono- or bidentate ligands that extract either through a solvation mechanism, as in the case of the phosphine oxides (e.g., TRPO, TRUEX, or UNEX processes) and in the case of the diamides (e.g., DIAMEX or TODGA processes), or through a proton exchange mechanism, as in the case of the phosphoric acids (e.g., DIDPA process), which require a prior adjustment of the feed acidity below 1 M HNO_3. The acidity of the An(III) + Ln(III) fraction produced by these front-end processes is usually lower than that of the PUREX raffinate, allowing second-step processes to employ "soft-donor" extractants bearing either nitrogen or sulfur atoms inducing selectivity toward the An(III). The trivalent TPEs can thus be either selectively extracted, as in the case of N-donor polytriazines (e.g., BTP or BTBP) and S-donor dithiophosphinic acids (e.g., CYANEX or ALINA processes), or selectively stripped by an N-donor hydrophilic complexing agent such as DTPA (e.g., TALSPEAK or DIDPA processes).
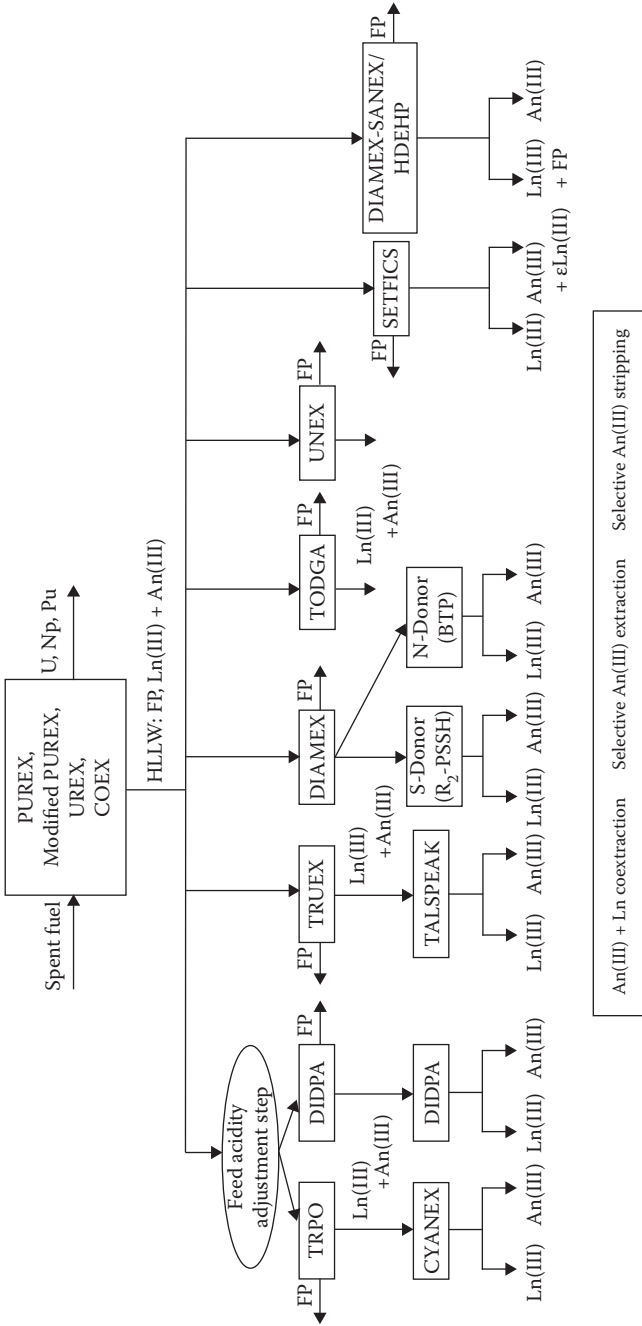
FIGURE 3.27 Overview of the aqueous processes developed around the world.

Historically, pairs of processes have been developed throughout the world to achieve An(III)/Ln(III) partitioning: TRUEX + TALSPEAK in the United States, TRPO + CYANEX in China, DIDPA + DIDPA in Japan, and DIAMEX + BTP or DIAMEX + ALINA in Europe, but cross combinations of processes are possible. The one-cycle processes (e.g., SETFICS and DIAMEX-SANEX/HDEHP) appear more attractive and more compact than the two-cycle processes, as they do not use two different solvent loops to carry out the separation of An(III) from Ln(III), but they sometimes generate much larger aqueous streams than the feed input.

Obviously, to date, there has been no implementation (at least reported in the recent literature) of any of these An(III)/Ln(III) partitioning processes at nuclear industrial scale. Studies are still in progress (i) to demonstrate the long-term sturdiness of these flowsheets and the chemical stability of the extractants employed, (ii) to master the impact of the extractant degradation products on the flowsheet efficiencies, (iii) to regenerate the spent solvents, (iv) to manage the secondary technological wastes generated, and (v) to convert the separated minor actinides into suitable precursors for new fuel fabrication. Nevertheless, the recent advances observed in the field of An(III)/Ln(III) separation by solvent extraction make the closure of the fuel cycle increasingly realistic and the sustainability of nuclear energy increasingly credible. Besides, research in test tubes on new structures of complexing/extracting ligands is still currently reported in the literature (i) to improve the efficiency of already known An(III)/Ln(III) separation systems, (ii) to strengthen ligand chemical stability, and (iii) to investigate new concepts for An(III)/Ln(III) separation from genuine high-active raffinates (Figure 3.28). These laboratory-scale studies might
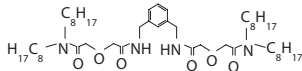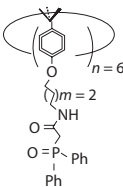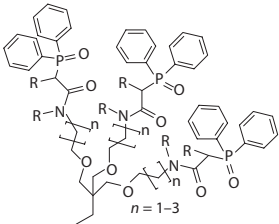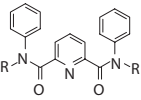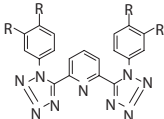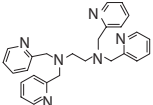
For the coextraction of An(III) and Ln(III)		
Bis-Diglycolamides [252]	CMPO-functionalized calixarenes [253,254]	CMP(O)-functionalized C-pivot tripodes 257–259]
For the separation of An(III) from Ln(III)		
N,N' -Dialkyl, *N,N'* -diaryl-dipicolinamides [261–263]	2,6-bis(1-Aryl-1-H-tetrazol-5-yl)pyridines (ATP, [265])	Hydrophobic derivatives of *N,N', N,N'* -tetrakis (2-methylpyridyl ethylenediamine (TPEN [266])

FIGURE 3.28 Examples of new extractant structures investigated at the laboratory scale (test tubes) for An(III)/Ln(III) separation.

be the premises of tomorrow's industrial separation processes. They involve, for instance, the following molecules:

- bis-Diglycolamides (*252*), CMP(O)-functionalized calixarenes (*253, 254*), CMP(O)-functionalized cyclotriveratrylenes (*255, 256*), CMP(O)-functionalized trityl or C-pivot tripodes (*257–259*), or phosphorylated calixarenes (*260*) for the coextraction of An(III) and Ln(III)
- *N,N′*-Dialkyl, *N,N′*-diaryl-dipicolinamides (*261–263*), dithiocarbamates (*264*), 2,6-bis(1-aryl-1-H-tetrazol-5-yl)pyridines (ATP, (*265*)), and hydrophobic derivatives of *N,N,N′,N′*-tetrakis(2-methylpyridyl)ethylenediamine (TPEN, (*266*)) for the separation of An(III) from Ln(III).

ACKNOWLEDGMENT

REFERENCES

1. Benedict, M., Pigford, T.H., Levi, H.W. 1981. *Nuclear Chemical Engineering*, 2nd ed., Mc Graw-Hill, New York, pp. 501–514.
2. Phillips, C. 1999. The thermal oxide reprocessing plant at Sellafield: Four years of active operation of the solvent extraction plant. *ISEC'99 Conference on Solvent Extraction for the 21st Century*, July, Barcelona, Spain.
3. Madic, C., Lecomte, M., Baron, P., Boullis, B. 2002. Separation of long-lived radionuclides from high active nuclear waste. *Compte-Rendu de Physique* 3: 797–811.
4. Elsden, A. 2003. Commercial reprocessing experience at BNFL. *Global 2003, Atoms for Prosperity: Updating Eisenhower's Global Vision for Nuclear Energy*, November, New Orleans, LA.
5. OECD/NEA. 1999. Actinide and fission product partitioning and transmutation. *Status and Assessment Report*, OECD, Paris.
6. Tani, S., Ozawa, M., Wakabayashi, T. 1993. Overview of partitioning and transmutation study in PNC. *Technical Meeting on Safety and Environmental Aspects of P&T of Actinides and FP, IAEA*, November–December, Vienna, Austria.
7. Takano, H., Ikegami, T. 2002. Activities on R&D partitioning and transmutation in Japan. *7th Information Exchange Meeting on Actinide and Fission Product Partitioning and Transmutation*, October, Jeju, Republic of Korea.
8. Rouyer, H. 1992. Separation and transmutation of actinides: The SPIN programme. General introduction. *Revue Genérale Nucléaire* 5: 407–413.
9. Madic, C., Bourges, J., Dozol, J.F. 1994. Brief overview of the long-lived radionuclide separation processes developed in France in connection with the SPIN program. *International Conference on Accelerator-Driven Transmutation Technologies and Applications*, July, Las Vegas, NV.
10. Camarcat, N., Bernard, P., Sicard, B. 1998. The 1991 long-lived radioactive waste management law. *NUCEF'98 Symposium Working Group*, November, Hitachinaka, Ibaraki, Japan.
11. Boullis, B. 1998. Partitioning studies in France: The SPIN program. *NUCEF'98 Symposium Working Group*, November, Hitachinaka, Ibaraki, Japan.
12. Boullis, B., Salvatores, M., Mouney, H. 1999. Separation and transmutation of long lived radionuclides: Recent advances of the French SPIN program. *Global 1999: Nuclear Technology – Bridging the Millennia*, August–September, Jackson Hole, WY.

13. Warin, D. 2002. Status of the French research programme for actinides and fission products Partitioning and Transmutation. *7th Information Exchange Meeting on Actinide and Fission Product Partitioning and Transmutation*, October, Jeju, Republic of Korea.

14. Baron, P., Lecomte, M., Boullis, B., Simon, N., Warin, D. 2003. Separation of the long lived radionuclides: Current status and future R&D program in France. *Global 2003, Atoms for Prosperity: Updating Eisenhower's Global Vision for Nuclear Energy*, November, New Orleans, LA.

15. Warin, D. 2007. Status of the French research program on P&T. *Journal of Nuclear Science and Technology* 44(3): 410–414.

16. Madic, C., Hudson, M.J. 1998. High-level liquid waste partitioning by means of completely incinerable extractants, EUR 18083 EN, European Commission, Luxembourg.

17. Madic, C., Hudson, M.J., Liljenzin, J.O., Glatz, J.P., Nannicini, R., Facchini, A., Kolarik, Z., Odoj, R. 2000. New partitioning techniques for minor actinides (NEWPART: F141-CT-96-0010), EUR 19149 EN, European Commission, Luxembourg.

18. Madic, C., Testard, F., Hudson, M.J., Liljenzin, J.O., Christiansen, B., Ferrando, M., Facchini, A., Geist, A., Modolo, G., Gonzales-Espartero, A., De Mendoza, J. 2004. New solvent extraction processes for minor actinides (PARTNEW: FIKW-CT-2000-00087), CEA-R-6066, France.

19. Dozol, J.F., Schwing-Weill, M.J., Arnaud-Neu, F., Böhmer, V., Ungaro, R., van Veggel, F.C.J.M., Wipff, G., Costero, A., Desreux, J.F., De Mendoza, J. 2000. Extraction and selective separation of long lived nuclides by functionalized macrocycles (FI4W-CT96-0022), EUR 19605 EN, European Commission, Luxembourg.

20. Dozol, J.F., Liger, K., Arnaud-Neu, F., Böhmer, V., Casensky, B., Casnati, A., Desreux, J.F., Grüner, B., Grüttner, C., De Mendoza, J., Pina, G., Selucky, P., Verboom, W., Wipff, G. 2004. Selective extraction of minor actinides from high activity liquid waste by organised matrices (CALIXPART FIKW-CT2000-00088).

21. Bhatnagar, V.P., Casalta, S., Hugon, M. 2002. Partitioning and transmutation research in the EURATOM fifth and sixth framework programmes. *7th Information Exchange Meeting on Actinide and Fission Product Partitioning and Transmutation*, October, Jeju, Republic of Korea.

22. Bhatnagar, V.P., Van Goethem, G. 2005. Overview of EU activities in partitioning and transmutation research in the EURATOM 6th and 7th framework programmes. *9th Information Exchange Meeting on Actinide and Fission Product Partitioning and Transmutation*, September, Nîmes, France.

23. Madic, C., Hudson, M.J., Baron, P., Ouvrier, N., Hill, C., Arnaud, F., Espartero, A.G., Desreux, J.F., Modolo, G., Malmbeck, R., Bourg, S., De Angelis, G., Uhlir, J. 2006. EUROPART: European research programme for partitioning of minor actinides within high active wastes issuing from the reprocessing of spent nuclear fuels. *9th Information Exchange Meeting on Actinide and Fission Product Partitioning and Transmutation*, September, Nîmes, France.

24. Herczeg, J.W. 2002. The Advanced Fuel Cycle Initiative: The future path for advanced spent fuel treatment and transmutation research in the United States. *7th Information Exchange Meeting on Actinide and Fission Product Partitioning and Transmutation*, October, Jeju, Republic of Korea.

25. Laidler, J.J. 2002. Development of separations technologies in the U.S. Partitioning and Transmutation programme. *7th Information Exchange Meeting on Actinide and Fission Product Partitioning and Transmutation*, October, Jeju, Republic of Korea.

26. Laidler, J.J., Bresee, J.C. 2004. The U.S. Advanced Fuel Cycle Initiative: Development of separations technologies. *ATALANTE 2004: Advances for Future Nuclear Cycles*, June, Nîmes, France.

27. Collins, E.D., Felker, L.K., Benker, D.E., Campbell, D.O. 2008. Closed nuclear fuel cycle technologies to meet near-term and transition period requirements. *ATALANTE 2008: Nuclear Fuel Cycles for a Sustainable Future*, May, Montpellier, France.

28. Nash, K. 1993. A review of the basic chemistry and recent developments in trivalent f-elements separations. *Solvent Extraction and Ion Exchange* 11(4): 729–768.
29. Nash, K. 1999. Aqueous complexes in separation of f-elements: Options and strategies for future development. *Separation Science and Technology* 34(6&7): 911–929.
30. Beitz, J. 1994. Similarities and differences in trivalent lanthanide- and actinide-ion solution absorption spectra and luminescence studies. In *Handbook on the Physics and Chemistry of Rare Earths* (Vol. 18, *Lanthanides/Actinides Chemistry*), eds. K.A. Gschneider, J.L. Eyring, G.R. Choppin, G.H. Lander, pp. 159–193. Elsevier Science B.V., Amsterdam.
31. Morss, L.R. 1994. Comparative thermochemical and oxidation-reduction properties of lanthanides and actinides. In *Handbook on the Physics and Chemistry of Rare Earths*, eds. K.A. Gschneider, J.L. Eyring, G.R. Choppin, G.H. Lander, pp. 239–257. Elsevier Science B.V., Amsterdam.
32. Rydberg, J., Musikas, C., Choppin, G.R. 1992. *Principles and Practices of Solvent Extraction*. Marcel Dekker, New York.
33. Rydberg, J., Cox, M., Musikas, C., Choppin, G.R. 2004. *Solvent Extraction Principles & Practice,* 2nd ed. Lavoisier, Paris.
34. Weaver, B. 1974. Solvent extraction in the separation of rare earths and trivalent actinides. In *Ion Exchange and Solvent Extraction*, Vol. 6, eds. J.A. Marinsky, Y. Marcus. Marcel Dekker, New York.
35. Nash, K. 1994. Separation chemistry for lanthanides and trivalent actinides. In *Handbook on the Physics and Chemistry of Rare Earths* (Vol. 18, *Lanthanides/Actinides Chemistry*), eds. K.A. Gschneider, J.L. Eyring, G.R. Choppin, G.H. Lander, pp. 198–238. Elsevier Science B.V., Amsterdam.
36. Choppin, G., Nash, K. 1995. Actinide separation science. *Radiochimica Acta* 70/71: 225–236.
37. Nash, K., Choppin, G. 1997. Separation chemistry for actinide elements: Recent developments and historical perspective. *Separation Science and Technology* 32(1–4): 255–274.
38. Mathur, J.N., Murali, M.S., Nash, K.L. 2001. Actinide partitioning – A review. *Solvent Extraction and Ion Exchange* 19(3): 357–390.
39. Nash, L.K., Madic, C., Mathur, J.N., Lacquement, J. 2006. Actinide separation science and technology. In *The Chemistry of the Actinide and the Transactinide Elements*, Vol. 4, 3rd ed., eds. L.R. Morss, N.M. Edelstein, J. Fuger, J.J. Katz, pp. 2622–2798. Springer, Dordrecht.
40. Wietzke, R., Mazzanti, M., Latour, J.M., Pécaut, J., Cordier, P.Y., Madic, C. 1998. Lanthanide(III) complexes of tripodal N-donor ligands: Structural models for the species involved in solvent extraction of actinides(III). *Inorganic Chemistry* 37(26): 6690–6697.
41. Lefrançois, L., Hébrant, M., Tondre, C., Delpuech, J.J., Berthon, C., Madic, C. 1999. Z,E Isomerism and hindered rotations in malonamides: An NMR study of N,N'-dimethyl-N,N'-dibutyl-2-tetradecylpropane-1,3-diamide. *Journal of Chemical Society, Perkin Transactions* 2: 1149–1158.
42. Karmazin, L., Mazzanti, M., Gateau, C., Hill, C., Pécaut, J. 2002. The important effect of ligand architecture on the selectivity of metal ion recognition in An(III)/Ln(III) separation with N-donor extractants. *Chemical Communications* 23: 2892–2893.
43. Drew, M.G.B., Hill, C., Hudson, M., Iveson, P.B., Madic, C., Youngs, T.G.A. 2004. Solvent extraction and lanthanide complexation studies with new terdentate ligands containing 1,3,5-triazine moieties. *Journal of the Chemical Society, Dalton Transactions* 2: 244–251.

44. Guillaumont, D. 2004. Quantum chemistry study of actinide(III) and lanthanide(III) complexes with tridentate nitrogen ligands. *Journal of Physical Chemistry* 108(33): 6893–6900.

45. Drew, M.G.B., Foreman, M.R.St.J., Hill, C., Hudson, M., Madic, C. 2005. 6,6'-*Bis*-(5,6-diethyl-[1,2,4]triazin-3-yl)-2,2'-bipyridyl the first example of a new class of quadridentate heterocyclic extraction reagents for the separation of americium(III) and europium(III). *Inorganic Chemistry Communications* 8: 239–241.

46. Miguirditchian, M., Guillaneux, D., Guillaumont, D., Moisy, P., Madic, C., Jensen, M., Nash, K.L. 2005. Thermodynamic study of the complexation of trivalent actinide and lanthanide cations by ADPTZ, a tridentate N-donor ligand. *Inorganic Chemistry* 44(5): 1404–1412.

47. Foreman, M.R.St.J., Hudson, M.J., Geist, A., Madic, C., Weigl, M. 2005. An investigation into the extraction of americium(III), lanthanides and *d*-block metals by 6,6'-bis-(5,6-dipentyl-[1,2,4]triazin-3-yl)-[2,2']bipyridinyl (C_5-BTBP). *Solvent Extraction and Ion Exchange* 23(5): 645–662.

48. Guillaumont, D., Guilbaud, P., Sorel, C., Gutierrez, F., Chalmet, S., Defranceschi, M. 2006. Modeling selectivity in liquid/liquid extraction. *Nuclear Science and Engineering* 153(3): 207–222.

49. Trumm, S., Panak, P.J., Foreman, M.R.St.J., Fanghänel, T., Geist, A. 2008. TRLFS-Studies on the complexation of Cm(III) and Eu(III) with BTBP-ligands in organic solution. *ATALANTE 2008: Nuclear Fuel Cycles for a Sustainable Future*, May, Montpellier, France.

50. Meridiano, Y., Berthon, L., Lagrave, S., Crozes, X., Sorel, C., Testard, F., Zemb, T. 2008. Correlation between aggregation and extracting properties in solvent extraction systems: Extraction of actinides (III) and lanthanides (III) by a malonamide in non acidic media. *ATALANTE 2008: Nuclear Fuel Cycles for a Sustainable Future*, May, Montpellier, France.

51. Vu, T.H., Charbonnel, M.C., Boubals, N., Couston, L., Arnaud, F. 2008. Thermodynamic and structural description of europium complexation in 1-octanol – H_2O solutions. *ATALANTE 2008: Nuclear Fuel Cycles for a Sustainable Future*, May, Montpellier, France.

52. Berthon, L., Zorz, N., Lagrave, S., Gannaz, B., Hill, C. 2008. Use of electrospray ionization mass spectrometry (ESI-MS) for the characterization of complexes 'ligand-metallic cations' in solution. *ATALANTE 2008: Nuclear Fuel Cycles for a Sustainable Future*, May, Montpellier, France.

53. Leclerc, E., Guillaumont, D., Guilbaud, P., Berthon, L. 2008. Mass spectrometry and theoretical investigation of di-alkylphosphoric acid-lanthanide complexes. *Radiochimica Acta* 96(2): 85–92.

54. Petit, L., Adamo, C., Maldivi, P. 2006. Toward a clear-cut vision on the origin of 2,6-di(1,2,4-triazin-3-yl)pyridine selectivity for trivalent actinides: Insights from theory. *Inorganic Chemistry* 45(21): 8517–8522.

55. Petit, L., Daul, C., Adamo, C., Maldivi, P. 2007. DFT modelling of the relative affinity of nitrogen ligands for trivalent f elements: An energetic point of view. *New Journal of Chemistry* 31: 1738–1745.

56. Gaunt, A.J., Reilly, S.D., Enriquez, A.E., Scott, B.L., Ibers, J.A., Sekar, P., Ingram, K.I.M., Kaltsoyannis, N., Neu, M.P. 2008. Experimental and theoretical comparison of actinide and lanthanide bonding in $M[N(EPR_2)_2]_3$ complexes (M = U, Pu, La, Ce; E = S, Se, Te; R = Ph, iPr, H). *Inorganic Chemistry* 47: 29–41.

57. Guillaumont, D., Guilbaud, P., Sorel, C., Gutierrez, F., Chalmet, S., Defranceschi, M. 2006. Modeling selectivity in liquid/liquid extraction. *Nuclear Science and Engineering* 153: 207–222.

58. Ahlström, P.E., Blomgren, J., Ekberg, C., Englund, S., Fermvik, A., Liljenzin, J.O., Retegan, T., Skarnemark, G., Eriksson, M., Seltborg, P., Wallenius, J., Westlén, D. 2007. Partitioning and transmutation. Current developments. In *A Report from the Swedish Reference Group for P&T-Research*, ed. Ahlström P.E. Svensk Kärnbränslehantering AB, Stockholm.

59. Burkin, A.R. 2001. *Chemical Hydrometallurgy: Theory and Principles*. Imperial College Press, London.

60. Adachi, T., Ohnuki, M., Yoshida, N., Sonobe, T., Kawamura, W., Takeishi, H., Gunji, K., Kimura, T., Suzuki, T., Nakahara, Y., Muromura, T., Kobayashi, Y., Okashita, H., Yamamoto, T. 1990. Dissolution study of spent PWR fuel: Dissolution behavior and chemical properties of insoluble residues. *Journal of Nuclear Materials* 174(1): 60–71.

61. Ritcey, G.M. 2006. Solvent extraction in hydrometallurgy: Present and future. *Tsinghua Science and Technology* 11(2): 137–152.

62. Ritcey, G.M. 2006. *Solvent Extraction. Principles and Applications to Process Metallurgy*, Vol. 1. G.M. Ritcey & Associates, Ottawa, Canada.

63. Marcus, Y. 1997. *Ion properties*. Marcel Dekker, New York.

64. Pearson, R.G. 1963. Hard and soft acids and bases. *Journal of the American Chemical Society* 85: 3533–3539.

65. Musikas, C., Cuillerdier, C., Livet, J., Forchioni, A., Chachaty, C. 1983. Azide interaction with 4*f* and 5*f* ions in aqueous solutions. 1. Trivalent ions. *Inorganic Chemistry* 22 (18):2513–2518.

66. Choppin, G.R. 1985. Separation of actinides in aqueous solution by oxidation state. In *Actinide/Lanthanide Separations*, eds. G.R. Choppin, J.D. Navratil, W.W. Schulz. Singapore: World Scientific.

67. Rizkalla, E.N., Sullivan, J.C., Choppin, G.R. 1989. Calorimetric studies of americium(III) complexation by amino carboxylates. *Inorganic Chemistry* 28: 909–911.

68. Choppin, G.R., Rizkalla, E.N. 1994. Lanthanides and actinides hydration and hydrolysis. In *Handbook on the Physics and Chemistry of Rare Earths* (Vol. 18, *Lanthanides/ Actinides: Chemistry*), eds. K.A. Gschneider, J.L. Eyring, G.R. Choppin, G.H. Lander, pp. 559–590. Elsevier Science B.V., Amsterdam.

69. Ionova, G., Ionov, S., Rabbe, C., Hill, C., Madic, C., Guillaumont, R., Modolo, G., Krupa, J.C. 2000. The problem of Am(III)/Eu(III) separation in the frame of hardness of cations and softness of cations and softness of extractants: Theoretical aspects. *ATALANTE 2000: Scientific Research on the Back-end of the Fuel Cycle for the 21st Century*, October, Avignon, France.

70. Berthet, J.C., Miquel, Y., Iveson, P.B., Nierlich, M., Thuéry, P., Madic, C., Ephritikhine, M. 2002. The affinity and selectivity of terdentate nitrogen ligands toward trivalent lanthanide and uranium ions viewed from the crystal structures of the 1:3 complexes. *Journal of the Chemical Society, Dalton Transactions* 3265–3272.

71. Hudson, M.J., Drew, M.G.B., Foreman, M.R.St.J., Hill, C., Huet, N., Madic, C., Youngs, T.G.A. 2003. The coordination chemistry of 1,2,4-triazinyl bipyridines with lanthanides(III) elements – implications for the partitioning of americium(III). *Journal of the Chemical Society, Dalton Transactions* 9: 1675–1685.

72. Colette, S., Amekraz, B., Madic, C., Berthon, L., Cote, G., Moulin, C. 2004. Eu interaction with a polyazaaromatic extractant studied by TRLIF: A thermodynamical approach. *Inorganic Chemistry* 43: 6745–6751.

73. Berthet, J.C., Nierlich, M., Miquel, Y., Madic, C., Ephritikhine, M. 2005. Selective complexation of uranium(III) over lanthanide(III) triflates by 2,2′:6′,2″-terpyridine. X-ray crystal structures of [M(OTf)$_3$(terpy)$_2$] and [M(OTf)$_2$(terpy)$_2$(py)][OTf](M = Nd, Ce, U) and of polynuclear μ-oxo uranium(IV) complexes resulting from hydrolysis. *Journal of the Chemical Society, Dalton Transactions* 2: 369–379.

74. Deneke, M.A., Rossberg, A., Panak, P.J., Weigl, M., Schimmelpfennig, B., Geist, A. 2005. Characterization and comparison of Cm(III) and Eu(III) complexed with *i*-C$_3$H$_7$-2,6-di(1,2,4-triazin-3-yl)pyridine using EXAFS, TRFLS, and quantum-chemical methods. *Inorganic Chemistry* 44: 8418–8425.

75. Miguirditchian, M., Guillaneux, D., François, N., Airvault, S., Ducros, S., Thauvin, D., Madic, C., Illemassene, M., Lagarde, G., Krupa, J.C. 2006. Complexation of lanthanide(III) and actinide(III) cations with tridentate nitrogen-donor ligands: A luminescence and spectrophotometric study. *Nuclear Science and Engineering* 153(3): 223–232.

76. Madic, C., Cordier, P.Y. 1997. Process for the selective separation of actinides (III) and lanthanides (III). Patent US5826161 A.

77. Mathur, J.N., Nash, K.L. 1998. Thermodynamics of extraction of Am(III) and Eu(III) from nitrate and thiocyanate media with octyl(phenyl)-*N,N*-di*iso*butylcarbamoylmethylphosphine oxide. *Solvent Extraction and Ion Exchange* 16(6): 1341–1356.

78. Musikas, C. 1986. Complexes des ions actinides en solutions aqueuses. *Journal of the Less-Common Metals* 122: 107–123.

79. Zhu, Y.J. 1985. Extraction of trivalent actinides with phosphine oxides. In *Handbook on the Physics and Chemistry of the Actinides*, eds. A.J. Freeman, C. Keller, pp. 469–513. Elsevier Science B.V., Amsterdam.

80. Chmutova, M.K., Ivanova, L.A., Litvina, M.N., Pribylov, G.A., Drozhko, D.E., Tananaev, I.G., Artyushin, O.A., Kalyanova, R.M., Pavlova, N.A., Mastryukova, T.A., Kuntsevich, A.D., Myasoedov, B.F. 2002. Extraction of actinides from HNO$_3$ solutions with solutions of dialkyl methylphosphonates. *Radiochemistry* 44(3): 261–265.

81. Burger, L.L. 1958. Uranium and plutonium extraction by organophosphorus compounds. *Journal of Physical Chemistry* 62(5): 590–598.

82. Peppard, D.P., Ferraro, J.R., Mason, G.W. 1957. Possible hydrogen bonding in certain interactions of organic phosphorus compounds. *Journal of Inorganic Nuclear Chemistry* 4(5–6): 371–372.

83. Peppard, D.P., Mason, G.W., Driscole, W.J., Sironen, R.J. 1958. Acidic esters of orthophosphoric acid as selective extractants for metallic cations. Tracer studies. *Journal of Inorganic Nuclear Chemistry* 7(3): 276–285.

84. McAlister, D.R., Horwitz, E.P. 2007. Characterization of extraction of chromatographic materials containing bis(2-ethyl-1-hexyl)phosphoric acid, 2-ethyl-1-hexyl (2-ethyl-1-hexyl) phosphonic acid, and bis(2,4,4-trimethyl-1-pentyl)phosphinic acid. *Solvent Extraction and Ion Exchange* 25(6): 757–769.

85. Bressee, J.C. 2007. The Global Nuclear Energy Partnership and the spent fuel takeback provision. *Global 2007: Advanced Nuclear Fuel Cycles and Systems*, September, Boise, ID.

86. Rochwerger, D., Thiévenaz, B., Ichimura, E., Takizawa, A., Takaki, N. 1999. Study of a closed nuclear system for fuel and waste. *Global 1999: Nuclear Technology – Bridging the Millennia*, August–September, Jackson Hole, WY.

87. Glatz, J.P., Haas, D., Magill, J., Wider, H. 2003. Partitioning and transmutation options in spent fuel management. *Global 2003, Atoms for Prosperity: Updating Eisenhower's Global Vision for Nuclear Energy*, November, New Orleans, LA.

88. Srinivasan, T.G., Vasudeva Rao, P.R., Sood, D.D. 1998. Diluent and extractant effects on the enthalpy of extraction of uranium(VI) and americium(III) nitrates by trialkyl phosphates. *Solvent Extraction and Ion Exchange* 16(6): 1369–1387.

89. Brahmmananda Rao, C.V.S., Srinavasan, T.G., Vasudeva Rao, P.R. 2007. Studies on the extraction of actinides by diamylamyl phosphonate. *Solvent Extraction and Ion Exchange* 25(6): 771–789.

90. Zhu, Y., Han, B., Wu, Q. 1999. Study on the integration of the PUREX process and the TRPO process in nuclear fuel cycle back end. *Global 1999: Nuclear Technology – Bridging the Millennia*, August–September, Jackson Hole, WY.

91. Zhu, Y., Song, C., Jiao, R. 1995. Partitioning studies in China and the separation of americium and fission product rare earths with dialkylphosphinic acid and its thio-sub-stituted derivatives. *Global 1995 International Conference on Evaluation of Emerging Nuclear Fuel Cycle Systems*, September, Versailles, France.

92. Chen, J., Wang, S., Jing, S. 2007. A pilot test of partitioning for the simulated highly saline high level waste. *Global 2007: Advanced Nuclear Fuel Cycles and Systems*, September, Boise, ID.

93. Song, C., Wang, J., Jiao, R. 1999. Hot test of total partitioning process for the treat-ment of high saline HLLW. *Global 1999: Nuclear Technology – Bridging the Millennia*, August–September, Jackson Hole, WY.

94. Xu, J., Liu, X., Liang, J., Chen, J. 2003. Research on PUREX-TRPO integrated process. *Global 2003, Atoms for Prosperity: Updating Eisenhower's Global Vision for Nuclear Energy*, November, New Orleans, LA.

95. Sätmark, B., Apostolidis, C., Courson, O., Malmbeck, R., Carlos, R., Pagliosa, G., Römer, K., Glatz, J.P. 2000. Advanced aqueous reprocessing in P&T strategies: Process demonstration on genuine fuels and targets. *ATALANTE 2000: Scientific Research on the Back-end of the Fuel Cycle for the 21st Century*, October, Avignon, France.

96. Christiansen, B., Apostolidis, C., Carlos, R., Courson, O., Glatz, J.P., Malmbeck, R., Pagliosa, G., Römer, K., Serrano-Purroy, D. 2004. Advanced aqueous reprocessing in P&T strategies: Process demonstration on genuine fuels and targets. *Radiochimica Acta* 92(8): 475–480.

97. Horwitz, E.P., Kalina, D.G., Kaplan, L., Mason, G.W., Diamond, H. 1982. Selected alkyl(phenyl)-*N,N*-dialkylcarbamoylmethylphosphine oxides as extractants for Am(III) from nitric acid media. *Separation Science and Technology* 17(10): 1261–1279.

98. Horwitz, E.P., Schulz, W.W. 1990. The TRUEX process: A vital tool for disposal of US defense nuclear wastes. *Conference on New Separation Chemistry for Radioactive Waste and Other Specific Applications*, May, Rome, Italy.

99. Spencer, B., Egan, B.Z., Beahm, E.C., Chase, C.W., Dillow, T.A. 1999. Dissolution of ORNL HLW sludge and partitioning of the actinides using the TRUEX process. *Separation Science and Technology* 34(6&7): 1021–1042.

100. Vandegrift, G.F., Regalbuto, M.C. 1995. Validation of the Generic TRUEX Model using data from TRUEX demonstrations with actual high-level waste. *5th International Conference on Radioactive Waste Management and Environmental Remediation*, September, Berlin, Germany.

101. Vandegrift, G.F., Regalbuto, M.C., Aase, S., Bakel, A., Battisti, A.T., Bowers, D., Byrnes, J.P., Clark, M.A., Cummings, D.G., Emery, J.W., Falkenberg, J.R., Gelis, A.V., Pereira, C., Hafenrichter, L., Tsai, Y., Quigley, K.J., Vander Pol, M.H. 2004. Designing and demonstration of the UREX+ process using spent nuclear fuel. *ATALANTE 2004: Advances for Future Nuclear Cycles*, June, Nîmes, France.

102. Laidler, J.J. 2006. Advanced spent fuel processing technologies for the United States GNEP programme. *9th Information Exchange Meeting on Actinide and Fission Product Partitioning and Transmutation*, September, Nîmes, France.

103. Facchini, A., Amato, L., Nannicini, R. 1996. A two-cycle process for enhanced actinide separation from radioactive liquid wastes. *Separation Science and Technology* 31(16): 2245–2256.

104. Manohar, S., Sharma, J.N., Shah, B.V., Wattal, P.K. 2007. Process development for bulk separation of trivalent actinides and lanthanides from radioactive high-level liquid waste. *Nuclear Science and Engineering* 156: 96–102.

105. Fujii, T., Yamana, H., Moriyama, H. 2002. Decontamination study of some noticeable fission products in the actinides recovery by TRUEX process. *7th Information Exchange Meeting on Actinide and Fission Product Partitioning and Transmutation*, October, Jeju, Republic of Korea.

106. Fujii, T., Yamana, H., Watanabe, M., Moriyama, H. 2002. Extraction study for TRUEX process using short-lived radionuclides produced by neutron irradiation of uranium. *Solvent Extraction and Ion Exchange* 20(2): 151–175.

107. Fujii, T., Aoki, K., Yamana, H. 2007; Extraction behavior of antimony in a TRUEX system. *Journal of Nuclear Science and Technology* 44(10): 1301–1305.

108. Fujii, T., Aoki, K., Yamana, H. 2006. Effect of nitric acid distribution on extraction behaviour of trivalent *f*-elements in a TRUEX system. *Solvent Extraction and Ion Exchange* 24(3): 347–357.

109. Belair, S., Labet, A., Mariet, C., Dannus, P. 2005. Modeling of the extraction of nitric acid and neodymium nitrate from aqueous solutions over a wide range of activities by CMPO. *Solvent Extraction and Ion Exchange* 23(5): 481–499.

110. Litvina, M.N., Chmutova, M.K., Myasoedov, B.F., Kabachnik, M.I. 1996. Extraction and separation factors of lanthanides and americium in aqueous nitric acid – Diaryl(dialkyl)-(dialkylcarbamoylmethyl)phosphine oxide systems. *Radiochemistry* 38(6): 494–499.

111. Babain, V.A., Smirnov, I.V., Shadrin, A.Y., Torgov, V.G., Shulman, R.S., Us, T.V., Podoinitsyn, S.V. 2002. Recovery of actinides and noble metals from HLW by neutral organophosphorus extractants. *Journal of Nuclear Science and Technology* S3: 306–308.

112. Kulyako, Y.M., Maliko, D.A., Chmutova, M.K., Litvina, M.N., Myasoedov, B.F. 1998. New method for actinide and rare-earth element recovery by diphenyl[dibutylcarbamoyl-methyl]phosphine oxide from nitric acid solutions. *Journal of Alloys and Compounds* 271–273: 760–764.

113. Kulyako, Y., Maliko, D., Trofimov, T., Chmutova, M., Myasoedov, B. 2002. Extraction of actinides and lanthanides with diphenyl[dibutylcarbamoylmehtyl]phosphine oxide in the absence of a solvent. *Journal of Nuclear Science and Technology* Sup 3: 302–305.

114. Malofeeva, G.I., Chmutova, M.K., Rozhkova, L.S., Petrukhin, O.M., Spivakov, B.Y., Myasoedov, B.F. 1998. Recovery of Eu(III) and Am(III) by solid-phase extraction with diphenyl(dialkylcarbamoylmethyl)-phosphine oxides. *Radiochemistry* 40(3): 241–246.

115. Myasoedov, B.F., Chmutova, M.K., Litvina, M.N., Kulyako, Y.M. 1998. The extraction of actinides by diphenyl(dibutylcarbamoylmethyl)phosphine oxide in the absence of a solvent. *Russian Chemical Bulletin* 47(9): 1690–1696.

116. Todd, T.A., Brewer, K.N., Law, J.D., Wood, D.J., Herbst, R.S., Romanovskiy, V.N., Esimantovskiy, V.N., Smirnov, I.V., Babain, V.A. 1999. Development of a universal solvent for the decontamination of acidic liquid radioactive waste. *Czechoslovak Journal of Physics* 49(S1): 931–936.

117. Todd, T.A., Brewer, K.N., Law, J.D., Herbst, R.S., Wood, D.J., Romanovskiy, V.N., Esimantovskiy, V.N., Smirnov, I.V., Babain, V.A., Zaïtsev, B. 1999. Development of a universal cobalt dicarbollide solvent for the removal of actinides, cesium and strontium from acidic wastes. *ISEC'99 Conference on Solvent Extraction for the 21st Century*, July, Barcelona, Spain.

118. Law, J.D., Herbst, R.S., Todd, T.A., Wood, D.J., Romanovskiy, V.N., Esimantovskiy, V.N., Smirnov, I.V., Babain, V.A., Zaïtsev, B.N. 1999. Demonstration of a universal solvent extraction process for the separation of actinides, cesium and strontium from actual acidic tank waste at the Idaho National Engineering and Development Laboratory. *Global 1999: Nuclear Technology – Bridging the Millennia*, August–September, Jackson Hole, WY.

119. Romanovskiy, V.N., Smirnov, I.V., Babain, V.A., Todd, T.A., Herbst, R.S, Law, J.D., Brewer, K.N. 2001. The universal solvent extraction (UNEX) process. I. Development of the UNEX process solvent for the separation of cesium, strontium, and the actinides from acidic radioactive waste. *Solvent Extraction and Ion Exchange* 19(1): 1–21.

120. Herbst, R.S., Law, J.D., Todd, T.A., Romanovskiy, V.N., Smirnov, I.V., Babain, V.A., Esimantovskiy, V.N., Zaïtsev, B. 2003. Development of the universal extraction (UNEX) process for the simultaneous recovery of Cs, Sr, and actinides from acidic radioactive wastes. *Separation Science and Technology* 38(12–13): 2685–2708.

121. Law, J.D., Herbst, R.S., Peterman, D.R., Todd, T.A., Romanovskiy, V.N., Babain, V.A., Smirnov, I.V., Esimantovskiy, V.N. 2005. Development of a regenerable strip reagent for treatment of acidic, radioactive waste with the Universal solvent extraction process. *Solvent Extraction and Ion Exchange* 23(1): 59–83.

122. Alekseenko, S., Babain, V., Bondin, V., Viznyl, A., Esimantovskiy, V., Krivitskiy, Y., Kuznetsov, G., Rodionov, S., Romanovskiy, V., Smirnov, I., Todd, T., Shklyar, L. 2005. Testing of UNEX-process on centrifugal contactor mockup of mining and chemical combine. *Global 2005: Nuclear Energy System for Future Generation and Global Sustainability*, October, Tsukuba, Japan.

123. Romanovskiy, V.N., Smirnov, I.V., Babain, V.A., Esimantovskiy, V.M., Todd, T.A., Herbst, R.S., Law, J.D. 2005. UNEX-process. State of the art and outlook. *Global 2005: Nuclear Energy System for Future Generation and Global Sustainability*, October, Tsukuba, Japan.

124. Romanovskiy, V.N., Babain, V.A., Smirnov, I.V., Todd, T.A., Herbst, R.S., Law, J.D. 2003. Regenerable stripping reagents for HLW reprocessing. *Global 2003, Atoms for Prosperity: Updating Eisenhower's Global Vision for Nuclear Energy*, November 2003, New Orleans, LA.

125. Peterman, D.R., Herbst, R.S., Law, J.D., Tillotson, R.D., Garn, T.G., Todd, T.A., Romanovskiy, V.N., Babain, V.A., Alyapyshev, M.Y., Smirnov, I.V. 2005. Diamide derivatives of dipicolinic acid as actinide and lanthanide extractants in a variation of the UNEX process. *Global 2005: Nuclear Energy System for Future Generation and Global Sustainability*, October, Tsukuba, Japan.

126. Rzhekhina, E.K., Karkosov, V.G., Alyapyshev, M.Yu., Babain, V.A., Smirnov, I.V., Todd, P.A., Law, J.D., Herbst, R.S. 2007. Reprocessing of spent solvent of the UNEX process. *Radiochemistry* 49(5): 493–498.

127. Rozen, A.M., Volk, V.I., Vakhrushin, A.Y., Zakharkin, B.S., Kartasheva, N.A., Krupnov, B.V., Nikolotova, Z.I. 1999. Extractants for exhaustive recovery of TPEs from radiochemical production waste. *Radiochemistry* 41(3): 215–221.

128. Sasaki, Y., Umetani, S. 2006. Comparison of four bidentate phosphoric and diamide compounds for the extractability of actinides. *Journal of Nuclear Science and Technology* 43(7): 794–797.

129. Smirnov, I.V. 2007. Anomalous effects in extraction of lanthanides and actinides with bidentate neutral organophosphorous extractants. Role of proton hydrate solvates. *Radiochemistry* 47(1): 44–54.

130. Myasoedov, B. 1999. Potentiality of bidendate neutral compounds. *Summer School on Separation of Long-lived Radionuclides*, September–October, Méjannes-le-Clap, France.

131. Morgalyuk, V.P., Molochnikova, N.P., Myasoedova, G.V., Tananaev, I.G. 2006. Extraction and sorption preconcentration of U(VI), Am(III), and Pu(IV) from nitric acid solutions with alkylenediphosphine dioxides. *Radiochemistry* 48(6): 580–583.

132. Kubota, M., Morita, Y., Yamaguchi, I., Yamagishi, I., Fujiwara, T., Watanabe, M., Mizoguchi, K., Tatsugae, R. 1998. Development of the four group partitioning process at JAERI. *NUCEF'98 Symposium Working Group*, November, Hitachinaka, Ibaraki, Japan.

133. Morita, Y., Glatz, J.P., Kubota, M., Koch, L., Pagliosa, G., Roemer, K., Nicholl, A. 1996. Actinide partitioning from HLLW in a continuous DIDPA extraction process by means of centrifugal extractors. *Solvent Extraction and Ion Exchange* 14(3): 385–400.

134. Morita, Y., Yamaguchi, I., Fujiwara, T., Koizumi, H., Kubota, M. 1998. The first test of 4-group partitioning process with real high-level liquid waste at NUCEF. *NUCEF'98 Symposium Working Group*, November, Hitachinaka, Ibaraki, Japan.

135. Morita, Y., Yamaguchi, I., Fujiwara, T., Koizumi, H., Kubota, M. 1999. The first test of 4-group partitioning process with real high-level liquid waste. *Global 1999: Nuclear Technology – Bridging the Millennia*, August-September, Jackson Hole, WY.

136. Morita, Y., Yamaguchi, I., Fujiwara, T., Koizumi, H., Tachimori, S. 2000. A demonstration of the 4-group partitioning process with real high-level liquid waste. *ATALANTE 2000: Scientific Research on the Back-end of the Fuel Cycle for the 21st Century*, October, Avignon, France.

137. Musikas, C. 1988. Potentiality of nonorganophosphorus extractant in chemical separations of actinides. *Separation Science and Technology* 23(12&13): 1211–1226.

138. Berthon, L., Martinet, L., Testard, F., Madic, C., Zemb, T. 2007. Solvent penetration and sterical stabilization of reverse aggregates based on the DIAMEX process extracting molecules: Consequences for the third phase formation. *Solvent Extraction and Ion Exchange* 25(5): 545–576.

139. Dozol, H., Berthon, C. 2007. Characterization of the supramolecular structure of malonamides by application of pulsed field gradients in NMR spectroscopy. *The Royal Society of Chemistry*. *Physical Chemistry Chemical Physics* 9: 5162–5170.

140. Bauduin, P., Testard, F., Berthon, L., Zemb, T. 2007. Relation between the hydrophile/hydrophobe ratio of malonamide extractants and the stability of the organic phase: Investigation at high extractant concentrations. *The Royal Society of Chemistry*. *Physical Chemistry Chemical Physics* 9(28): 3776–3785.

141. Testard, F., Bauduin, P., Martinet, L., Abécassis, B., Berthon, L., Madic, C., Zemb, T. 2008. Self-assembling properties of malonamide extractants used in separation processes. *Radiochimica Acta* 96(4–5): 265–272.

142. Charbonnel, M.C., Daldon, M., Berthon, C., Madic, C., Moulin, C. 1999. Extraction of lanthanides(III) and actinides(III) by *N,N'*-substituted malonamides: Thermodynamic and kinetic data. *ISEC'99 Conference on Solvent Extraction for the 21st Century*, July, Barcelona, Spain.

143. Madic, C., Blanc, P., Condamines, N., Baron, P., Berthon, L., Nicol, C., Pozo, C., Lecomte, M., Philippe, M., Masson, M., Hequet, C., Hudson, M.J. 1994. Actinide partitioning from high level liquid waste using the DIAMEX process. *RECOD'94*, April, London, UK.

144. Charbonnel, M.C., Nicol, C., Berthon, L., Baron, P. 1997. State of progress of DIAMEX process. *Global 1997: International Conference on Future Nuclear Systems*, October, Yokohama, Japan.

145. Courson, O., Lebrun, M., Malmbeck, R., Pagliosa, G., Römer, K., Sätmark, B., Glatz, J.P. 2000. Partitioning of minor actinides from HLLW using the DIAMEX process. Part 1 – Demonstration of extraction performances and hydraulic behaviour of the solvent in a continuous process. *Radiochimica Acta* 88: 857–863.

146. Courson, O., Malmbeck, R., Pagliosa, G., Römer, K., Sätmark, B., Glatz, J.P., Baron, P., Madic, C. 1998. Separation of minor actinides from genuine HLLW using the DIAMEX process. *5th Information Exchange Meeting on Actinide and Fission Product Partitioning and Transmutation*, November, Mol, Belgium.

147. Baron, P., Hérès, X., Lecomte, M., Masson, M. 2001. Separation of the minor actinides: The DIAMEX-SANEX concept. *Global 2001: Back-end of the Fuel Cycle: From Research to Solutions*, September, Paris, France.

148. Berthon, L., Morel, J.M., Zorz, N., Nicol, C., Virelizier, H., Madic, C. 2001. Diamex process for actinide partitioning: Hydrolytic and radiolytic degradations of malonamide extractants. *Separation Science and Technology* 36(5–6): 709–727.

149. Camès, B., Caniffi, B., Rudloff, D. 2008. Radiolytic and hydrolytic stability of extractant molecules. *ATALANTE 2008: Nuclear Fuel Cycles for a Sustainable Future*, May, Montpellier, France.

150. Nicol, C., Camès, B., Margot, L., Ramain, L. 2000. DIAMEX solvent regeneration studies. 2000. *ATALANTE 2000: Scientific Research on the Back-end of the Fuel Cycle for the 21st Century*, October, Avignon, France.

151. Camès, B., Saucerotte, B., Faucon, M., Rudloff, D., Gastaldi, M., Bisel, I. 2004. Long term evolution of recycled DIAMEX solvent properties under hydrolysis and radiolysis with or without solvent clean-up. *ATALANTE 2004: Advances for Future Nuclear Cycles*, June, Nîmes, France.

152. Bisel, I., Nicol, C., Charbonnel, M.C., Blanc, P., Baron, P., Belnet, F. 1998. Inactive DIAMEX test with the optimized extraction agent DMDOHEMA. *5th Information Exchange Meeting on Actinide and Fission Product Partitioning and Transmutation*, November, Mol, Belgium.

153. Duhamet, J., Lanoë, J.Y., Rivalier, P., Borda, G. 2008. Inactive experiments for advanced separation processes prior to high activity trials in ATALANTE. *ATALANTE 2008: Nuclear Fuel Cycles for a Sustainable Future*, May, Montpellier, France.

154. Baron, P., Masson, M., Rostaing, C., Boullis, B. 2007. Advanced separation processes for sustainable nuclear systems. *Global 2007: Advanced Nuclear Fuel Cycles and Systems*, September, Boise, ID.

155. Serrano-Purroy, D., Baron, P., Christiansen, B., Malmbeck, R., Sorel, C., Glatz, J.P. 2005. Recovery of minor actinides from HLLW using DIAMEX process. *Radiochimica Acta* 93(6): 351–355.

156. Gompper, K., Geist, A., Modolo, G., Deneke, M.A., Panak, P.J., Weigl, M., Fanghänel, T. 2005. R&D on partitioning at the German research centers Karlsruhe and Juelich. *Global 2005: Nuclear Energy System for Future Generation and Global Sustainability*, October, Tsukuba, Japan.

157. Modolo, G., Vijgen, H., Serrano-Purroy, D., Christiansen, B., Malmbeck, R., Sorel, C., Baron, P. 2007. DIAMEX countercurrent extraction process for recovery of trivalent actinides from simulated high active concentrate. *Separation Science and Technology* 42: 439–452.

158. Serrano-Purroy, D., Christiansen, B., Malmbeck, R., Glatz, J.P., Baron, P., Madic, C., Modolo, G. 2004. First DIAMEX partitioning using genuine High Active Concentrate. *ATALANTE 2004: Advances for Future Nuclear Cycles*, June, Nîmes, France.

159. Serrano-Purroy, D., Baron, P., Christiansen, B., Glatz, J.P., Madic, C., Malmbeck, R., Modolo, G. 2005. First demonstration of a centrifugal solvent extraction process for minor actinides from a concentrated spent fuel solution. *Separation Science and Technology* 45: 157–162.

160. Geist, A., Weigl, M., Gompper, K. 2004. Hydrometallurgical minor actinide separation in Hollow Fibre Modules. *ATALANTE 2004: Advances for Future Nuclear Cycles*, June, Nîmes, France.

161. Geist, A., Magnussen, D., Serrano-Purroy, D., Christiansen, B., Malmbeck, R., Gompper, K. 2006. Toward a hot DIAMEX test in Hollow Fibre Module micro-plant. *9th Information Exchange Meeting on Actinide and Fission Product Partitioning and Transmutation*, September, Nîmes, France.

162. Geist, A. 2008. Equilibrium model for the extraction of Am(III), Eu(III), and HNO_3 into DMDOHEMA in TPH. 2008. *ATALANTE 2008: Nuclear Fuel Cycles for a Sustainable Future*, May, Montpellier, France.

163. Tachimori, S., Sasaki, Y., Morita, Y., Suzuki, S. 2002. Recent progress of partitioning process in JAERI: Development of amide-based ARTIST process. *7th Information Exchange Meeting on Actinide and Fission Product Partitioning and Transmutation*, October, Jeju, Republic of Korea.

164. Tian, G., Zhang, P., Wang, J., Rao, L. 2005. Extraction of actinide(III, IV, V, VI) ions and TcO$_4^-$ by *N,N,N',N'*-tetra*iso*butyl-3-oxa-glutaramide. http://repositories.cdlib.org/lbnl/LBNL-57031

165. Mowafy, E.A., Aly, H.F. 2007. Synthesis of some *N,N,N',N'*-tetraalkyl-3-oxa-pentane-1,5-diamide and their application in solvent extraction. *Solvent Extraction and Ion Exchange* 25(2): 205–224.

166. Sasaki, Y., Sugo, Y., Tachimori, S. 2000. Actinide separation with a novel tridentate ligand, diglycolic amide for application to partitioning process. *ATALANTE 2000: Scientific Research on the Back-end of the Fuel Cycle for the 21st Century*, October, Avignon, France.

167. Sasaki, Y., Suzuki, S., Tachimori, S. 2001. Effect of acid on the extraction of Am(III) by TODGA. *Actinides-2001*, November, Hayama, Japan.

168. Sasaki, Y., Suzuki, S., Tachimori, S., Kimura, T. 2003. An innovative chemical separation process (ARTIST) for treatment of spent nuclear fuel. *Global 2003, Atoms for Prosperity: Updating Eisenhower's Global Vision for Nuclear Energy*, November, New Orleans, LA.

169. Sasaki, Y., Zhu, Z.X., Sugo, Y., Kimura, T. 2007. Extraction of various metal ions from nitric acid to n-dodecane by diglycolamide (DGA) compounds. *Journal of Nuclear Science and Technology* 44(3): 405–409.

170. Morita, Y., Sasaki, Y., Tachimori, S. 2001. Development of TODGA extraction process for high level liquid waste. Preliminary evaluation of actinide separation by calculation. *Global 2001: Back-end of the Fuel Cycle: From Research to Solutions*, September, Paris, France.

171. Narita, H., Yaita, T., Tachimori, S. 2004. Extraction of lanthanides with *N,N'*-dimethyl-*N,N'*-diphenyl-malonamide and 3,6-dioxaoctanediamide. *Solvent Extraction and Ion Exchange* 22(2): 135–145.

172. Sasaki, Y., Rapold, P., Arisaka, M., Hirata, M., Kimura, T., Hill, C., Cote, G. 2007. An additional insight into the correlation between the distribution ratios and the aqueous acidity of the TODGA system. *Solvent Extraction and Ion Exchange* 25(2): 187–204.

173. Tachimori, S., Sasaki, S., Suzuki, S. 2002. Modification of TODGA-*n*-dodecane solvent with a monoamide for high loading of lanthanides(III) and actinides(III). *Solvent Extraction and Ion Exchange* 20(6): 687–699.

174. Sasaki, Y., Zhu, Z.X., Sugo, Y., Kimura, T. 2005. Novel compounds, diglycolamides (DGA), for extraction of various metal ions from nitric acid to *n*-dodecane. *Global 2005: Nuclear Energy System for Future Generation and Global Sustainability*, October, Tsukuba, Japan.

175. Yaita, T., Herlinger, A.W., Thiyagarajan, P., Jensen, M.P. 2004. Influence of extractant aggregation on the extraction of trivalent *f*-element cations by tetraalkyldiglycolamide. *Solvent Extraction and Ion Exchange* 22(4): 553–571.

176. Jensen, M.P., Yaita, T., Chiarizia, R. 2007. Reverse-micelle formation in the partitioning of trivalent f-element cations by biphasic systems containing a tetraalkyldiglycolamide. *Langmuir* 23: 4765–4774.

177. Modolo, G., Vijgen, H., Schreinemachers, C., Baron, P., Dinh, B. 2003. TODGA process development for partitioning of actinides(III) from PUREX raffinate. *Global 2003, Atoms for Prosperity: Updating Eisenhower's Global Vision for Nuclear Energy*, November, New Orleans, LA.

178. Modolo, G., Asp, H., Schreinemachers, C., Vijgen, H. 2007. Development of a TODGA based process for partitioning of actinides from PUREX raffinate Part I: Batch extraction optimization studies and stability tests. *Solvent Extraction and Ion Exchange* 25(7): 703–721.

179. Modolo, G., Asp, H., Vijgen, H., Malmbeck, R., Magnusson, D., Sorel, C. 2007. Demonstration of a TODGA/TBP process for the recovery of trivalent actinides and lanthanides from a PUREX raffinate. *Global 2007: Advanced Nuclear Fuel Cycles and Systems*, September, Boise, ID.

180. Modolo, G., Asp, H., Vijgen, H., Malmbeck, R., Magnusson, D., Sorel, C. 2008. Demonstration of a TODGA-based continuous counter-current extraction process for the partitioning of actinides from a simulated PUREX raffinate, Part II: Centrifugal contactor runs. *Solvent Extraction and Ion Exchange* 26(1): 62–76.

181. Magnusson, D., Christiansen, B., Glatz, J.P., Malmbeck, R., Modolo, G., Serrano Purroy, D., Sorel, C. 2007. Partitioning of minor actinides from PUREX raffinate by the TODGA process. *Global 2007: Advanced Nuclear Fuel Cycles and Systems*, September, Boise, ID.

182. Magnusson, D., Christiansen, B., Glatz, J.P., Malmbeck, R., Modolo, G., Serrano Purroy, D., Sorel, C. 2008. Demonstration of minor actinide separation from a genuine PUREX raffinate by TODGA/TBP and SANEX reprocessing. *ATALANTE 2008: Nuclear Fuel Cycles for a Sustainable Future*, May, Montpellier, France.

183. Asp, H., Modolo, G., Schreinemachers, C., Vijgen, H. 2006. Development of a TODGA process for co-separation of trivalent actinides and lanthanides from a high-active raffinate. *9th Information Exchange Meeting on Actinide and Fission Product Partitioning and Transmutation*, September, Nîmes, France.

184. Sugo, Y., Sasaki, Y., Kimura, T., Sekine, T., Kudo, H. 2005. Radiolysis of TODGA and its effect on extraction of actinide ions. *Global 2005: Nuclear Energy System for Future Generation and Global Sustainability*, October, Tsukuba, Japan.

185. Sugo, Y., Sasaki, Y., Kimura, T., Sekine, T. 2007. Attempts to improve radiolytic stability of amidic extractants. *Global 2007: Advanced Nuclear Fuel Cycles and Systems*, September, Boise, ID.

186. Chen, J., Wang, S. 2005. A new conceptual reprocessing process based on the diamide derivative extraction. *Global 2005: Nuclear Energy System for Future Generation and Global Sustainability*, October, Tsukuba, Japan.

187. Tachimori, S., Suzuki, S., Sasaki, Y., Apichaibukol, A. 2003. Solvent extraction of alkaline earth metal ions by diglycolic amides from nitric acid solutions. *Solvent Extraction and Ion Exchange* 21(5): 707–715.

188. Sharma, J.N., Suri, A.K., Manohar, S., Chitnis, R.R., Shah, G.J., Wattal, P.K. 2004. Solvent extraction studies of synthetic high level waste using novel extractant tetra (2-ethylhexyl) dilycolamide (TEHDGA). *SESTEC-2004: Emerging Trends in Separation Science and Technology*, July, Mumbai, India.

189. Ekberg, C., Fermvik, A., Retegan, T., Skarnemark, G., Froeman, M.R.S., Hudson, M.J., Englund, S., Nilsson. M. 2008. An overview and historical look back at the solvent extraction using nitrogen donor ligands to extract ans separate An(III) from Ln(III). *Radiochimica Acta* 96(4–5): 225–233.

190. Cordier, P.Y., Rabbe, C., François, N., Madic, C., Kolarik, Z. 1998. Comparative study of some nitrogen bearing ligands for the An(III)/Ln(III) separation by liquid-liquid extraction. *NUCEF'98 Symposium Working Group*, November, Hitachinaka, Ibaraki, Japan.

191. Cordier, P.Y., François, N., Boubals, N., Madic, C., Hudson, M.J., Liljenzin, J.O. 1999. Synergistic systems for the selective extraction of trivalent actinides from mixtures of trivalent actinides and lanthanides. *ISEC'99 Conference on Solvent Extraction for the 21st Century*, July, Barcelona, Spain.

192. Nomura, K., Ozawa, M., Tanaka, Y., Baron, P., Madic, C. 1998. Study on Am/Eu extraction and separation with acid extractant and TPTZ. *NUCEF'98 Symposium Working Group*, November, Hitachinaka, Ibaraki, Japan.

193. Boubals, N., Drew, M.G.B., Hill, C., Hudson, M.J., Iveson, P.B., Madic, C., Russel, M.L., Youngs, T.G.A. 2002. Americium(III) and europium(III) solvent extraction studies of amide-substituted triazine ligands and complexes formed with ytterbium(III). *Journal of the Chemical Society, Dalton Transactions* 55–62.

194. Andersson, S., Ekberg, C., Foreman, M.R.S., Hudson, M.J., Liljenzin, J.O., Nilsson, M., Skarnemark, G., Saphiu, K. 2003. Extraction behavior of the synergistic system 2,6-bis-(benzoxazolyl)-4-dodecyloxylpyridine and 2-bromodecanoic acid using Am and Eu as radioactive tracers. *Solvent Extraction and Ion Exchange* 21(5): 621–636.

195. Berthet, J.C., Rivière, C., Miquel, Y., Nierlich, M., Madic, C., Ephritikhine, M. 2002. Selective complexation of uranium(III) over cerium(III) and neodymium(III) by 2,2':6',2"-terpyridine – X-ray crystallographic evidence for uranium-to-ligand π backbonding. *European Journal of Inorganic Chemistry* 6: 1434–1446.

196. Vitart, X., Musikas, C., Pasquiou, J.Y., Hoel, P. 1986. Séparation actinides-lanthanides à contre-courant en batterie de mélangeurs décanteurs. *Journal of the Less-Common Metals* 122: 275–286.

197. Rais, J., Tachimori, S. 1994. Extraction separation of tetravalent americium and lanthanides in the presence of some soft and hard donors and dicarbollide. *Separation Science and Technology* 29(10): 1347–1365.

198. Kolarik, Z., Müllich, U. 1997. Extraction of Am(III) and Eu(III) by 2-substituted benzimidazoles. *Solvent Extraction and Ion Exchange* 15(3): 361–379.

199. Weigl, M., Müllich, U., Geist, A., Gompper, K., Zevaco, T., Stephan, H. 2003. Alkyl-substituted 2,6-dioxazolylpyridines as selective extractants for trivalent actinides. *Journal of Radioanalytical and Nuclear Chemistry* 256(3): 403–412.

200. Kolarik, Z., Müllich, U., Gassner, F. 1999. Selective extraction of Am(III) over Eu(III) by 2,6-ditriazolyl- and 2,6-ditriazinylpyridines. *Solvent Extraction and Ion Exchange* 17(1): 23–32.

201. Weigl, M., Geist, A., Müllich, U., Gompper, K. 2002. Kinetics of novel extraction systems in the partitioning of nuclear waste. *7th Information Exchange Meeting on Actinide and Fission Product Partitioning and Transmutation*, October, Jeju, Republic of Korea.

202. Weigl, M., Geist, A., Müllich, U., Gompper, K. 2006. Kinetics of americium(III) extraction and back-extraction with BTP. *Solvent Extraction and Ion Exchange* 24(6): 845–860.

203. Geist, A., Weigl, M., Gompper, K. 2002. Effective actinide(III)-lanthanide(III) separation in miniature hollow fibre modules. *7th Information Exchange Meeting on Actinide and Fission Product Partitioning and Transmutation*, October, Jeju, Republic of Korea.

204. Hill, C., Hérès, X., Calor, J.N., Guillaneux, D., Mauborgne, B., Rat, B., Rivalier, P., Baron, P. 1999. Trivalent actinides/lanthanides separation using bis-triazinyl-pyridines. *Global 1999: Nuclear Technology – Bridging the Millennia*, August–September, Jackson Hole, WY.

205. Glatz, J.P., Courson, O., Malmbeck, R., Pagliosa, G., Roemer, K., Saetmark, B., Baron, P., Madic, C. 1999. Demonstration of partitioning schemes proposed in the frame of P&T studies using genuine fuel. *Global 1999: Nuclear Technology – Bridging the Millennia*, August–September, Jackson Hole, WY.

206. Hill, C., Guillaneux, D., Berthon, L., Madic, C. 2002. SANEX-BTP process development studies. *Journal of Nuclear Science and Technology* 3: 309–312.

207. Hill, C., Berthon, L., Madic, C. 2005. Study of the stability of BTP extractants under radiolysis. *Global 2005: Nuclear Energy System for Future Generation and Global Sustainability*, October, Tsukuba, Japan.

208. Hill, C., Berthon, L., Bros, P., Dancausse, J.P., Guillaneux, D. 2002. SANEX-BTP process development studies. *7th Information Exchange Meeting on Actinide and Fission Product Partitioning and Transmutation*, October, Jeju, Republic of Korea.

209. Hill, C., Berthon, L., Guillaneux, D., Dancausse, J.P., Madic, C. 2004. SANEX-BTP process development: From bench to hot test demonstration. *ATALANTE 2004: Advances for Future Nuclear Cycles*, June, Nîmes, France.

210. Hudson, M.J., Boucher, C., Braekers, D., Desreux, J.F., Drew, M.G.B., Foreman, M.R.St.J., Harwood, L.M., Hill, C., Madic, C., Marken, F., Youngs, T.G.A. 2006. New bis(triazinyl) pyridines for selective extraction of americium(III). *New Journal of Chemistry* 30: 1171–1183.

211. Nilsson, M., Andersson, S., Ekberg, C., Foreman, M.R.S., Hudson, M.J., Skarnemark, G. 2006. Inhibiting radiolysis of BTP molecules by addition of nitrobenzene. *Radiochimica Acta* 94(2): 103–106.

212. Retegan, T., Ekberg, C., Dubois, I., Fermvik, A., Skarnemark, G., Wass, T.J. 2007. Extraction of actinides with different 6,6'-bis(5,6-dialkyl-[1,2,4]-triazin-3-yl)-[2,2']-bipyridines. *Solvent Extraction and Ion Exchange* 25(4): 417–431.

213. Foreman, M.R.St.J., Hudson, M.J., Drew, M.G.B., Hill, C., Madic, C. 2006. Complexes formed between the quadridentate, heterocyclic molecules 6,6'-bis-(5,6-dialkyl-1,2,4-triazin-3-yl)-2,2'-bipyridine (BTBP) and lanthanides(III): Implications for the partitioning of actinides(III) and lanthanides(III). *Journal of the Chemical Society, Dalton Transactions* 13: 1645–1653.

214. Nilsson, M., Andersson, S., Drouet, F., Ekberg, C., Foreman, M., Hudson, M., Liljenzin, J.O., Magnusson, D., Skarnemark, G. 2006. Extraction properties of 6,6'-bis-(5,6-di-pentyl-[1,2,4]-triazin-3-yl)-[2,2']-bipyridinyl (C5-BTBP). *Solvent Extraction and Ion Exchange* 24(3): 299–318.

215. Nilsson, M., Ekberg, C., Foreman, M., Hudson, M., Liljenzin, J.O., Modolo, G., Skarnemark, G. 2006. Separation of actinides(III) from lanthanides(III) in simulated nuclear waste streams using 6,6'-bis-(5,6-dipentyl-[1,2,4]-triazin-3-yl)-[2,2']-bi-pyridinyl (C5-BTBP) in cyclohexanone. *Solvent Extraction and Ion Exchange* 24(6): 823–843.

216. Geist, A., Hill, C., Modolo, G., Foreman, M.R.St.J., Weigl, M., Gompper, K., Hudson, M.J. 2006. 6,6'-Bis(5,5,8,8-tetramethyl-5,6,7,8-tetrahydro-benzo[1,2,4]triazin-3-yl) [2,2']bipyridine, an effective extracting agent for the separation of americium(III) and curium(III) from the lanthanides. *Solvent Extraction and Ion Exchange* 24(4): 463–483.

217. Magnusson, D., Christiansen, B., Glatz, J.P., Malmbeck, R., Serrano-Purroy, D., Sorel, C. 2008. Towards an optimized flow-sheet for a SANEX demonstration process using centrifugal contactors. *ATALANTE 2008: Nuclear Fuel Cycles for a Sustainable Future*, May, Montpellier, France.

218. Magnusson, D., Christiansen, B., Glatz, J.P., Malmbeck, R., Modolo, G., Serrano-Purroy, D., Sorel, C. 2008. Demonstration of minor actinide separation from a genuine PUREX raffinate by TODGA/TBP and SANEX reprocessing. *ATALANTE 2008: Nuclear Fuel Cycles for a Sustainable Future*, May, Montpellier, France.

219. Musikas, C. 1984. Actinide-lanthanide group separation using sulfur and nitrogen donor extractant. In *Actinide/Lanthanide Separations*, eds. G.R. Choppin, J.D. Navratil, W.W. Schulz, pp. 19–30. World Scientific, Singapore.

220. Bhattacharyya, A., Mohapatra, P.K., Manchanda, V.K. 2006. Separation of americium(III) and europium(III) from nitrate medium using a binary mixture of Cyanex-301 with N-donor ligands. *Solvent Extraction and Ion Exchange* 24(1): 1–17.

221. Zhu, Y., Jiao, R. 1995. The extraction of americium and light lanthanides by HDEHDTP and CYANEX 302. *Radiochimica Acta* 69: 191–193.

222. Zhu, Y., Chen, J., Choppin, R.G. 1996. Extraction of americium and fission product lanthanides with CYANEX 272 and CYANEX 301. *Solvent Extraction and Ion Exchange* 14(4): 543–553.

223. Jensen, M.P., Bond, A.H., Rickert, P.G., Nash, K.L. 2002. Solution phase coordination chemistry of trivalent lanthanide and actinide cations with bis(2,4,4-trimeth-ylpentyl)dithiophosphinic acid. *Journal of Nuclear Science and Technology* (S3): 255–258.

224. Zhu, Y., Chen, J., Jiao, R. 1997. Hot test and process parameter calculation of purified CYANEX 301 extraction for separating Am and fission products. *Global 1997: International Conference on Future Nuclear Systems*, October, Yokohama, Japan.

225. Zhu, Y., Xu, J., Chen, J., Chen, Y. 1998. Extraction of americium and lanthanides by dialkyldithiophosphinic acid and *f-f* absorption spectra of the extraction complexes. *Journal of Alloys and Compounds* 271–273: 742–745.

226. Chen, J., Zhu, Y., Jiao, R. 1998. Separation of Am(III) from fission product lanthanides by bis(2,4,4-trimethylpentyl)-dithiophosphinic acid (HBTMPDTP) extraction: Process parameter calculation. *Nuclear Technology* 22: 64–71.

227. Chen, J., Tian, G., Jiao, R., Zhu, Y. 2002. Hot test for separating americium from fission product lanthanides by purified Cyanex 301 extraction in centrifugal contactors. *Journal of Nuclear Science and Technology* S3: 325–327.

228. Wang, X., Zhu, Y., Jiao, R. 2002. Separation of Am from lanthanides by a synergistic mixture of purified CYANEX 301 and TBP. *Journal of Radioanalytical and Nuclear Chemistry* 251(3): 487–492.

229. Modolo, G., Odoj, R. 1998. The separation of trivalent actinides from lanthanides by dithiophosphinic acids from HNO_3 acid medium. *Journal of Alloys and Compounds* 271–273: 248–251.

230. Modolo, G. 1998. Actinides(III)-lanthanides(III) group separation from nitric acid using new aromatic diorganyldithiophosphinic acids. *NUCEF'98 Symposium Working Group*, November, Hitachinaka, Ibaraki, Japan.

231. Modolo, G., Odoj, R., Baron, P. 1999. The ALINA-process for An(III)/Ln(III) group separation from strong acidic medium. *Global 1999: Nuclear Technology – Bridging the Millennia*, August–September, Jackson Hole, WY.

232. Fedorov, Y.S., Zilberman, B.Y., Shmidt, O.V. 2008. Liquid HLW processing using zirconium salt of dibutylphosphoric acid. *ATALANTE 2008: Nuclear Fuel Cycles for a Sustainable Future*, May, Montpellier, France.

233. Zilberman, B.Y., Fedorov, Y.S., Mishin, E.N., Shmidt, O.V., Goletskiy, N.D. 2003. Superpurex as an optimized TBP-compatible process for long-lived radionuclide partitioning. *Global 2003, Atoms for Prosperity: Updating Eisenhower's Global Vision for Nuclear Energy*, November, New Orleans, LA.

234. Zilberman, B.Y., Fedorov, Y.S., Shmidt, O.V., Goletskiy, N.D., Shiskin, D.N., Esymantovskiy, V.M., Rodionov, S.A., Egorova, O.N., Palenik, Y.V. 2007. Usage of dibutyl phosphoric acid and its zirconium salt for extraction of transplutonium elements and rare earths with their partitioning. *Global 2007: Advanced Nuclear Fuel Cycles and Systems*, September, Boise, ID.

235. Nilsson, M., Nash, K.L. 2007. Review article: A review of the development and operational characteristics of the TALSPEAK process. *Solvent Extraction and Ion Exchange* 25(6): 665–701.

236. Nilsson, M., Nash, K.L. 2008. TALSPEAK chemistry in advanced nuclear fuel cycles. *ATALANTE 2008: Nuclear Fuel Cycles for a Sustainable Future*, May, Montpellier, France.

237. He, P.J., Jiao, R.Z., Zhu, Y.J. 1996. HEHEHP fractional extraction process with three outlets for separation of Am from rare earths. *Nuclear Science and Techniques* 7(3): 161–165.

238. Collins, E.D., Benker, D.E., Bailey, P.D., Felker, L.K., Taylor, R.D., Delcul, G.D., Spencer, B.B., Bond, W.D., Campbell, D.O. 2005. Hot test evaluation of the reverse TALSPEAK process. *Global 2005: Nuclear Energy System for Future Generation and Global Sustainability*, October, Tsukuba, Japan.

239. Ozawa, M., Wakabayashi, T. 1999. Status on nuclear waste separation and transmutation technologies in JNC. *Global 1999: Nuclear Technology – Bridging the Millennia*, August–September, Jackson Hole, WY.

240. Nakahara, M., Sano, Y., Koma, Y., Kamiya, M., Shibata, A., Koizumi, T., Koyama, T. 2005. Actinides recovery by solvent extraction in NEXT process. *Global 2005: Nuclear Energy System for Future Generation and Global Sustainability*, October, Tsukuba, Japan.

241. Nakahara, M., Sano, Y., Koma, Y., Kamiya, M., Shibata, A., Koizumi, T., Koyama, T. 2007. Separation of actinide elements by solvent extraction using centrifugal contactors in the NEXT process. *Journal of Nuclear Science and Technology* 44(3): 373–381.

242. Funasaka, H., Sano, Y., Nomura, K., Koma, Y., Koyama, T., 2000. Current status of research and development on partitioning of long-lived-radionuclides in JNC. *ATALANTE 2000: Scientific Research on the Back-end of the Fuel Cycle for the 21st Century*, October, Avignon, France.

243. Hirano, H., Koma, K., Koyama, T. 2002. Waste minimization in actinides(III)/lanthanides(III) separation process from high-level liquid waste. *7th Information Exchange Meeting on Actinide and Fission Product Partitioning and Transmutation*, October, Jeju, Republic of Korea.

244. Shadrin, A., Kamachev, V., Kvasnitsky, I., Romanovsky, V., Bondin, V., Krivitsky, Y., Alekseenko, S. 2007. Extraction reprocessing of HLW by modified SETFICS-process. *Global 2007: Advanced Nuclear Fuel Cycles and Systems*, September, Boise, ID.

245. Hérès, X., Nicol, C., Bisel, I., Baron, P., Ramain, L. 1999. PALADIN: A one step process for actinides(III)/fission products separation. *Global 1999: Nuclear Technology – Bridging the Millennia*, August–September, Jackson Hole, WY.

246. Baron, P., Rostaing, C., Lecomte, M., Boullis, B., Warin, D. 2004. Process development for minor actinide separation. *ATALANTE 2004: Advances for Future Nuclear Cycles*, June, Nîmes, France.

247. Bisel, I., Camès, B., Faucon, M., Rudloff, D., Saucerote, B. 2007. DIAMEX-SANEX solvent behaviour under continuous degradation and regeneration operations. *Global 2007: Advanced Nuclear Fuel Cycles and Systems*, September, Boise, ID.

248. Bisel, I., Camès, B., Faucon, M., Rudloff, D., Saucerote, B. 2008. DIAMEX-SANEX solvent behavior under continuous degradation and regeneration operation. *ATALANTE 2008: Nuclear Fuel Cycles for a Sustainable Future*, May, Montpellier, France.

249. Hérès, X., Baron, P., Hill, C., Ameil, E., Martinez, I., Rivalier, P. 2008. The separation of extractants implemented in the DIAMEX-SANEX process. *ATALANTE 2008: Nuclear Fuel Cycles for a Sustainable Future*, May, Montpellier, France.

250. Gannaz, B., Antonio, M.A., Chiarizia, R., Hill, C., Cote, G. 2006. Structural study of trivalent lanthanide and actinide complexes formed upon solvent extraction. *Journal of the Chemical Society, Dalton Transactions* 38: 4553–4562.

251. Gannaz, B., Chiarizia, R., Antonio, M.A., Hill, C., Cote, G. 2007. Extraction of lanthanides(III) and Am(III) by mixtures of malonamide and dialkylphosphoric acid. *Solvent Extraction and Ion Exchange* 25(3): 313–337.

252. Modolo, G., Vijgen, H., Espartero, A.G., Prados, P., de Mendoza, J. 2008. Partitioning of minor actinides from high active raffinates using bis-diglycolamides (BisDGA) as new efficient extractants. *ATALANTE 2008: Nuclear Fuel Cycles for a Sustainable Future*, May, Montpellier, France.

253. Sansone, F., Fontanella, M., Casnati, A., Ungaro, R., Böhmer, V., Saadioui, M., Liger, K., Dozol, J.F. 2006. CMPO-substituted calix[6]- and calix[8]arene extractants for the separation of An^{3+}/Ln^{3+} from radioactive waste. *Tetrahedron* 62(29): 6749–6753.

254. Lamouroux, C., Rateau, S., Moulin, C. 2006. Use of electrospray ionization mass spectrometry for the study of Ln(III) complexation and extraction speciation with calixarene-CMPO in the fuel partitioning concept. *Rapid Communications in Mass Spectrometry* 20(13): 2041–2052.

255. Dam, H.H., Reinhoudt, D.N., Verboom, W. 2007. Influence of the platform in multicoordinate ligands for actinide partitioning. *New Journal of Chemistry* 31: 1620–1632.

256. Dam, H.H., Reinhoudt, D.N., Verboom, W. 2007. Multicoordinate ligands for actinide/lanthanide separations. *Chemical Society Review* 36: 367–377.
257. Dam, H.H., Beijleveld, H., Reinhoudt, D.N., Verboom, W. 2008. In the pursuit for better actinide ligands: An efficient strategy for their discovery. *Journal of the American Chemical Society* 130(16): 5542–5551.
258. Reinoso-Garcia, M.M., Jańczewski, D., Reinhoudt, D.N., Verboom, W., Malinowska, E., Pietrzak, M., Hill, C., Báča, J., Grüner, B., Selucky, P., Grüttner, C. 2006. CMP(O) tripodants: Synthesis, potentiometric studies and extractions. *New Journal of Chemistry* 30: 1480–1492.
259. Jańczewski, D., Reinhoudt, D.N., Verboom, W., Malinowska, E., Pietrzak, M., Hill, C., Allignol, C. 2007. Tripodal (N-alkylated CMP(O) and malonamide ligands: Synthesis, extraction of metal ions, and potentiometric studies. *New Journal of Chemistry* 31: 109–120.
260. Smirnov, I.V., Karavan, M.D., Efremova, T.I., Babain, V.A., Miroshnichenko, S.I., Cherenok, S.A., Kal'chenko, V.I. 2007. Extraction of Am, Eu, Tc and Pd from nitric acid solutions with phosphorylated calixarenes. *Radiochemistry* 49(5): 482–492.
261. Arisaka, M., Watanabe, M., Kimura, T. 2007. Separation of actinides(III) from lanthanides(III) by extraction chromatography using new N,N'-dialkyl-N,N'-diphenylpyridine-2,6-dicarboxamides. *Global 2007: Advanced Nuclear Fuel Cycles and Systems*, September, Boise, ID.
262. Babain, V.A., Alyapyshev, M.Y., Smirnov, I.V., Shadrin, A.Y. 2006. Extraction of Am and Eu with N,N'-substituted pyridine-2,6-dicarboxamides in fluorinated diluents. *Radiochemistry* 48(4): 331–334.
263. Babain, V.A., Alyapyshev, M.Y., Kiseleva, R.N. 2007. Metal extraction by N,N'-dialkyl,N,N'-diaryl-dipicolinamides from nitric acid solutions. *Radiochimica Acta* 95: 217–223.
264. Miyashita, S., Satoh, I., Yanaga, M., Okuno, K., Suganuma, H. 2007. Extraction based on *in situ* formation of dithiocarbamate for separation of Am(III) from Ln(III). *Global 2007: Advanced Nuclear Fuel Cycles and Systems*, September, Boise, ID.
265. Smirnov, I.V., Babain, V.A., Chirkov, A.V. 2007. New hydrolytically stable solvent for Am/Eu separation in acidic media. *Global 2007: Advanced Nuclear Fuel Cycles and Systems*, September, Boise, ID.
266. Matsumura, T., Takeshita, K. 2006. Extraction behavior of Am(III) from Eu(III) with hydrophobic derivatives of N,N,N',N'-tetrakis(2-methylpyridyl)ethylenediamine (TPEN). *Journal of Nuclear Science and Technology* 43(7): 824–827.

4 Extraction of Radioactive Elements by Calixarenes

Jean François Dozol
CEA, DEN, Cadarache

Rainer Ludwig
International Atomic Energy Agency A-1400

CONTENTS

4.1 NUCLEAR WASTE

Today, there are over 440 fission nuclear reactors in 31 countries, producing approximately 16% of the electrical energy used worldwide. When ^{235}U or odd isotopes of plutonium (^{239}Pu, ^{241}Pu) undergo nuclear fission, under action of neutrons, they split into two fission fragments consisting of lighter atoms than the original. The sum of their masses is slightly lower than that of the heavy atom. This mass difference consists of ejected neutrons and the release of binding energy, which can be used in nuclear reactors to produce electricity.

The fission products include every element from zinc through to the lanthanides. The majority of the mass yield of the fission products occurs in two peaks. These two peaks (expressed by atomic number) range from strontium to ruthenium and from tellurium to neodymium, respectively. By subsequent β decay reactions, these radioactive isotopes lead to stable isotopes. ^{239}Pu formed in situ undergoes fission similar to ^{235}U, leading to the formation of fission products. About one-fourth to one-third of the total fuel load of a reactor is removed from the core every 12–18 months and replaced with fresh fuel. Then, after several years of storage in pools, the spent-fuel rods are either sent to a definitive disposal (US policy) or reprocessed (France, UK, Japan, Russia…). In the future, the United States expects to reprocess spent fuels. Table 4.1 displays repartition of elements (kg/tU) produced by uranium fission for two burn-up values and two initial ^{235}U enrichment values (E), respectively.[1]

Fission reactors were also utilized for the production of plutonium. The first site was Hanford, and was established in 1943 to produce plutonium for nuclear weapons. To separate the valuable plutonium from other by-products, the spent uranium fuel was dissolved in nitric acid and chemically separated. Once the plutonium was removed, the rest was dumped in sludge tanks and was chemically converted to an alkaline solution for storage. In its alkaline form, the waste consists of two components, soluble salt and insoluble sludge. Both components contain highly radioactive residues from nuclear materials production. Radionuclides found in the sludge component include higher valent fission products (such as ^{90}Sr, lanthanides) and long-lived actinides (such as uranium and plutonium). Radionuclides found in the soluble salt component include isotopes of cesium and technetium, as well as traces of strontium and actinides. In the same way, nuclear materials production operations

TABLE 4.1

Repartition (kg/tU) According to Chemical Family of Fission Products

	UO$_2$ 33 GWd/tU ($E = 3.5\%$)	UO$_2$ 60 GWd/tU ($E = 4.5\%$)
Rare gas (Kr, Xe)	5.6	10.3
Alkali (Cs, Rb)	3	5.2
Alkaline earth (Sr, Ba)	2.4	4.5
Y and lanthanides	10.2	18.3
Zirconium	3.6	6.3
Chalcogenides (Se, Te)	0.5	1
Molybdenum	3.3	6
Halogens (I, Br)	0.2	0.4
Technetium	0.8	1.4
Platinoids (Ru, Rh, Pd)	3.9	7.7
Diverse (Ag, Cd, Sn, Sb)	0.1	0.3

Source: J.-G. Devezeaux de Lavergne and B. Boullis, *Clefs CEA*, 53, 36–53, 2005. With permission.

at the Savannah River Site (SRS) resulted in the generation of large quantities of the same type of waste.

4.1.1 REPROCESSING

Reprocessing is based on liquid-liquid extraction for the recovery of uranium and plutonium from used nuclear fuel (PUREX process). The spent fuel is first dissolved in nitric acid. After the dissolution step and the removal of fine insoluble solids, an organic solvent composed of 30% TriButyl Phosphate (TBP) in TetraPropylene Hydrogenated (TPH) or Isopar L is used to recover both uranium and plutonium; the great majority of fission products remain in the aqueous nitric acid phase. Once separated from the fission products, back-extraction combined with a reduction of Pu(IV) to Pu(III) allows plutonium to be separated from uranium; these two compounds can be recycled.[2]

After a few years, the radiotoxicity of spent fuel is dominated by ^{90}Sr and ^{137}Cs with half-lives of 29 and 30 years, respectively. After 300 years, their radioactivity is negligible. For the long term, the main radiotoxicity sources are some long-lived fission products (^{99}Tc, ^{129}I, ^{135}Cs…) and especially actinides. Currently, in Europe and Japan, high-activity solutions arising from the PUREX process are, after calcinations, incorporated in glass matrixes. In the future, these solid wastes are destined for disposal in geological formations. The major radionuclides in a typical aged spent fuel and their contributions are summarized in Table 4.2.[3]

Table 4.2 indicates that over 95% of the radiation in spent fuels presented for separation arises principally from ^{137}Cs and ^{90}Sr, the remaining part being mainly due to americium isotopes that are α emitters. Similarly, the bulk of some 1.5-W/kg heat load from radioactivity is due to these nuclides. Presently, two ways are followed, either the disposal of spent fuel (current policy in the United States) or the spent

TABLE 4.2

Radionuclides in Spent Fuel Aged for 10 Years in Descending Order of Activity

Radionuclide	Half Life (y)	Activity, Bq/kg	Content, mole/kg	Specific Dose Rate, eV/(kg/s)	Heat Load, W/kg	Radiolysis Rate, moles/ (kg hour)
^{137}Cs	30.07	3×10^{12}	6.8×10^{-3}	3.5×10^{18}	5.6×10^{-1}	2.1×10^{-4}
^{90}Sr	28.84	2×10^{12}	4.4×10^{-3}	5.6×10^{18}	8.9×10^{-1}	3.3×10^{-4}
^{99}Tc	211×10^{3}	8×10^{8}	1.3×10^{-2}	2.4×10^{14}	3.8×10^{-5}	1.4×10^{-8}
^{240}Pu	6.65×10^{3}	1×10^{8}	4.9×10^{-5}	1.0×10^{14}	1.6×10^{-5}	6.0×10^{-9}
^{135}Cs	2.3×10^{6}	1×10^{7}	1.7×10^{-3}	2.7×10^{12}	4.3×10^{-7}	1.6×10^{-10}
All low LET		5×10^{12}	2.6×10^{-2}	9.1×10^{18}	1.45	5.4×10^{-4}
^{241}Am	432	7×10^{10}	2.3×10^{-3}	4.0×10^{17}	6.3×10^{-2}	2.4×10^{-5}
^{243}Am	7.4×10^{3}	1×10^{9}	5.6×10^{-4}	5.4×10^{15}	8.7×10^{-4}	3.3×10^{-7}
^{239}Pu	24×10^{3}	8×10^{7}	1.5×10^{-4}	4.2×10^{14}	6.7×10^{-5}	2.5×10^{-8}
^{237}Np	2.14×10^{6}	1.5×10^{7}	2.4×10^{-3}	2.4×10^{14}	3.7×10^{-5}	1.4×10^{-8}
All high LET		7.1×10^{10}	5.4×10^{-3}	4.01×10^{17}	6.41×10^{-2}	2.4×10^{-5}
Grand total		5.1×10^{12}	3.1×10^{-2}	9.5×10^{18}	1.52	5.7×10^{-4}

Source: J.-G. Devezeaux de Lavergne and B. Boullis, *Clefs CEA*, 53, 36–53, 2005. With permission.

Note: Low Energy Transfer (LET) emitters (β and γ); High Energy Transfer (LET) emitters (α and recoil). All quantities are per kilogram of spent fuel.

fuel reprocessing in order to recover and recycle uranium and plutonium contained inside, wih vitrification of the high-activity waste (HAW) produced during reprocessing operations. To minimize the vitrified HAW volume to be disposed of in a deep geological repository and the radiotoxicity of the waste, several countries are studying advanced separation processes, as described below.

4.1.2 SEPARATION OF MINOR ACTINIDES (NEPTUNIUM, AMERICIUM, AND CURIUM)

A possible alternative management of HAW is to remove the long-lived nuclides, mainly actinides, and to destroy them by transmutation into short- or medium-lived fission products. About one-third of the mass of fission products belongs to the family of the lanthanide elements and must be separated from actinides because of the high neutron-capture cross sections of some of their isotopes (^{149}Sm, ^{155}Gd, ^{157}Gd…). These elements, like americium and curium, exist in the radioactive liquid waste at the +3 oxidation state, and thus the selective separation of lanthanides from actinides is complex, as reinforced by the fact that the molar ratio of lanthanides over actinides is close to 30 for spent fuels having a burn-up of 33 GWd t^{-1}. Upon modification of its valence, neptunium can be recovered during the PUREX process. Trivalent actinides (americium and curium) and lanthanide nitrates are coextracted in the DIAMEX process developed in France and Europe, and an additional extraction step

is necessary to accomplish the separation of actinides from lanthanides. Studies are in progress to "burn" neptunium and americium by transmutation in nuclear reactors. Promising results were obtained especially for burning americium. Management of curium is more complex.

4.1.3 Separation of Cesium and Strontium

Separation of these two radionuclides will reduce the short-term heat load in a geological repository and, when combined with the separation of Am and Cm, could strongly increase the capacity of the geological repository. It is forecasted that the separated cesium/strontium stream will be directed to a decay-storage for approximately 300 years, at which time the activity of the ^{137}Cs and ^{90}Sr will be below the limits for low-level waste. However, the long-lived ^{135}Cs, in spite of its relatively low residual radioactivity, will still need to be disposed of in a repository.

4.1.4 Recovery of other Fission Products

Lanthanides are coextracted with actinides and then separated from actinides, which are forecasted to be sent to a repository. The lanthanide elements comprise a unique series of metals in the periodic table. These metals are distinctive in terms of size, valence orbitals, electrophilicity, and magnetic and electronic properties, such that some members of the series are currently the best metals for certain applications. Increased use of the lanthanides in the future is likely, because their unusual combination of physical properties can be exploited to accomplish new types of chemical transformations. These elements coextracted with actinides and then separated from the latter, could in the future be recovered and used (among the lanthanides, only ^{151}Sm is a long-lived isotope (half-life 90 years)).[4]

Further progress has much to do with High-level liquid waste (HLLW) containing up to 1 kg rhodium and 2 kg palladium per 1 ton spent nuclear fuel depleted up to 80 GW/day. Rhodium obtained from fission consists of stable ^{103}Rh and trace amounts of short-lived radionuclides. As for palladium, it is a mixture of 83% stable isotopes and 17% of radioactive ^{107}Pd with a half life of 6.5×10^6 years. Its intrinsic radioactivity (soft β-emitter with E_{max} of 35 keV) is very weak, and it can be tolerated for many industrial applications. Recovered rhodium must be stored for 25–30 years for the short-lived radionuclides to be decayed; palladium can be used immediately. The platinoids can be recovered as an additional source of noble metals, extremely rare elements in the Earth's crust (especially Rh), irreplaceable for catalysis, alloying, hydrogen isotopes separation, thermonuclear engineering, etc. Moreover, removal of these elements from HLLW is desirable before immobilization, to eliminate complex problems during vitrification and also to improve the quality of final waste form.[5,6]

4.1.5 Medium Activity Waste

Nuclear industry operations, especially reprocessing, produce radioactive waste containing mainly large amounts of sodium nitrate and nitric acid and radionuclides at

much lower concentration. A way to reduce the volume of liquid waste to be send to a repository in geological formation is to concentrate it by evaporation: the concentrated part has to undergo a subsequent treatment while the pure distillate part can be released into the environment after radiological control. The treatment involves removing from this concentrate, long-lived nuclides (actinides, ^{90}Sr, ^{137}Cs), which can be disposed of in a repository in geological formations after vitrification and sending the bulk of the waste (inactive salts and the short-lived low-level and intermediate-level activity nuclides) to a subsurface repository, such as the Soulaisne repository in France.[7]

Large amounts of sodium waste arise from fast neutron reactors (Phenix and Superphenix in France, Dounreay in the UK, Monju in Japan), which are cooled by large amounts of liquid sodium, which is contaminated by ^{137}Cs during its functioning. We shall see that it is possible to remove radioactive cesium after conversion of liquid sodium to sodium hydroxide.

From the 1940s, several classes of inorganic ion exchangers have been used for cesium removal, such as zeolites, hexacyanoferrates, zirconium phosphates, ammonium phosphomolybdates, and crystalline silicotitanates. Generally, these compounds have only been able to efficiently remove cesium under restrictive conditions. The performances of most of these compounds strongly decreased as the acidity or salinity of liquid waste increased, either because of decreasing K_d values or instability of the inorganic ion exchangers. The most efficient compounds for removal of cesium are hexacyanoferrates, ammonium phosphomolybdates, or phosphotungstates. Unfortunately, cesium sorption with these compounds is hardly reversible. After saturation of these exchangers, two possibilities exist, either their reuse, which requires implementation of large volumes of high-salinity eluent and which produces new liquid waste, or their solidification with the cesium into ceramics. In the both cases, the concentration factors (CF) obtained are low.

Tetraphenylborate (TPB) was used at Savannah River to recover cesium from alkaline solutions, but attempts to treat HLW tanks with TPB resulted in the production of benzene (a TPB decomposition product) at levels that did not permit the safe operation of the process.[8] Crown ethers and dicarbollides were proposed as extractants to remove cesium from acidic HAW, but these compounds are not selective enough to allow cesium to be removed from solutions containing large amounts of nitric acid or sodium nitrate.[9] Dicarbollides were used in Russia at industrial scale to recover cesium from HAW, but the removal of cesium was only possible after partial denitration of the liquid waste.[10]

Complex mixtures (one-third of the elements of Mendeleev's table are present in solutions arising from the PUREX process) and harsh conditions (high acidity and strong irradiation generated by radioactive elements) of the chemical processing of nuclear fuels require the utilization of highly selective and radiation-resistant extractants, properties fulfilled by calixarenes. In the remainder of this chapter, the object will be to present results showing progress in the use of calixarenes to solve the various separation problems outlined above. Because of the multitude of compounds presented, the reader is referred to Section 4.7 of this chapter for structures and abbreviations.

4.2 CALIXARENES

Calixarenes are cyclic molecules made up of several phenol units linked via methylene groups. The most common calixarenes, calix[4]arenes, calix[6]arenes, or calix[8] arenes contain 4, 6, or 8 phenolic units, respectively. The use of the word "calix" was suggested by the shape of the tetramer, which can adopt a beaker-like conformation. Gutsche proposed the name calixarenes for cyclic oligomers resulting from condensation of formaldehyde with *p*-alkyl phenols.[11] Calixarenes are characterized by a narrow (or lower rim, the phenolic hydroxy groups), a wide (or upper rim, the aromatic positions para to the phenolic hydroxy groups), and a central annulus. These calixarenes or "parent calixarenes" are available in large quantities by simple one-pot procedures and can be easily modified in various ways by reactions that can be carried out either on the narrow rim or on the wide rim; they represent an ideal scaffold on which it is possible to assemble various functional groups, from three arrays of reactive centres (phenolic groups, the para position after dealkylation, and the methylene bridges) leading to a multitude of functionalized calixarenes (Figure 4.1).[11–14] See Section 4.7 for a tabulation of structures and abbreviations for individual compounds.

Calix[4]arenes are characterized by a three-dimensional basket shape, the internal volume being around 10 nm³. Calixarenes exist in different chemical conformations because rotation around the methylene bridge is possible. In calix[4]arene, four conformations are possible: cone, partial cone, 1,2-alternate, and 1,3-alternate. These four conformations are in dynamic equilibrium. Conformations can be locked, for instance, by placing a bulkier substituent than the ethyl group on the lower (or narrow) rim, this chain prevents the benzene units from rotating inside the calixarene cavity.

More recently, thiacalix[*n*]arenes were synthesized, in which methylene bridges of calix[*n*]arene are replaced by sulfur atoms.[15] This replacement leads to

- An enlargement of the cavity of calixarenes
- A potential oxidability to sulfoxide and sulfone for providing new sulfur-bridged calixarenes
- A possible coordination to specific metal ions controlled by the oxidation state of sulfur

The idea of implementing calixarenes to allow radionuclides to be selectively extracted from radioactive waste was launched by CEA Cadarache, in direct cooperation with the Vicens group in Strasbourg, and also in the framework of projects granted by the Commission of European Community (EC).

The first project, gathering eight teams from six EC countries where more than 140 new extractants were prepared and studied, not counting all the precursors and intermediates. Tests carried out with these compounds on simulated and real waste showed the excellent chemical and radiolytic performance of calixarene derivatives.

In the second project, gathering nine teams from six EC countries, more than 150 new extractants were prepared and studied, and the target was reached for the decategorization of waste. Dialkoxy calix[4]arene-crown-6 for cesium, octaamide calix[8] arenes, and CMPO-like calixarenes for actinides display much higher complexing and extracting abilities than other classical extractants, crown ethers, or dicarbollides proposed and sometimes used for this purpose.

(a)

Wide rim ⟶

Narrow rim ⟶

(b)   X = H: C[4] - X = *t*Bu : *t*BuC[4]

Cone

Partial cone

1,2-Alternate

1,3-Alternate
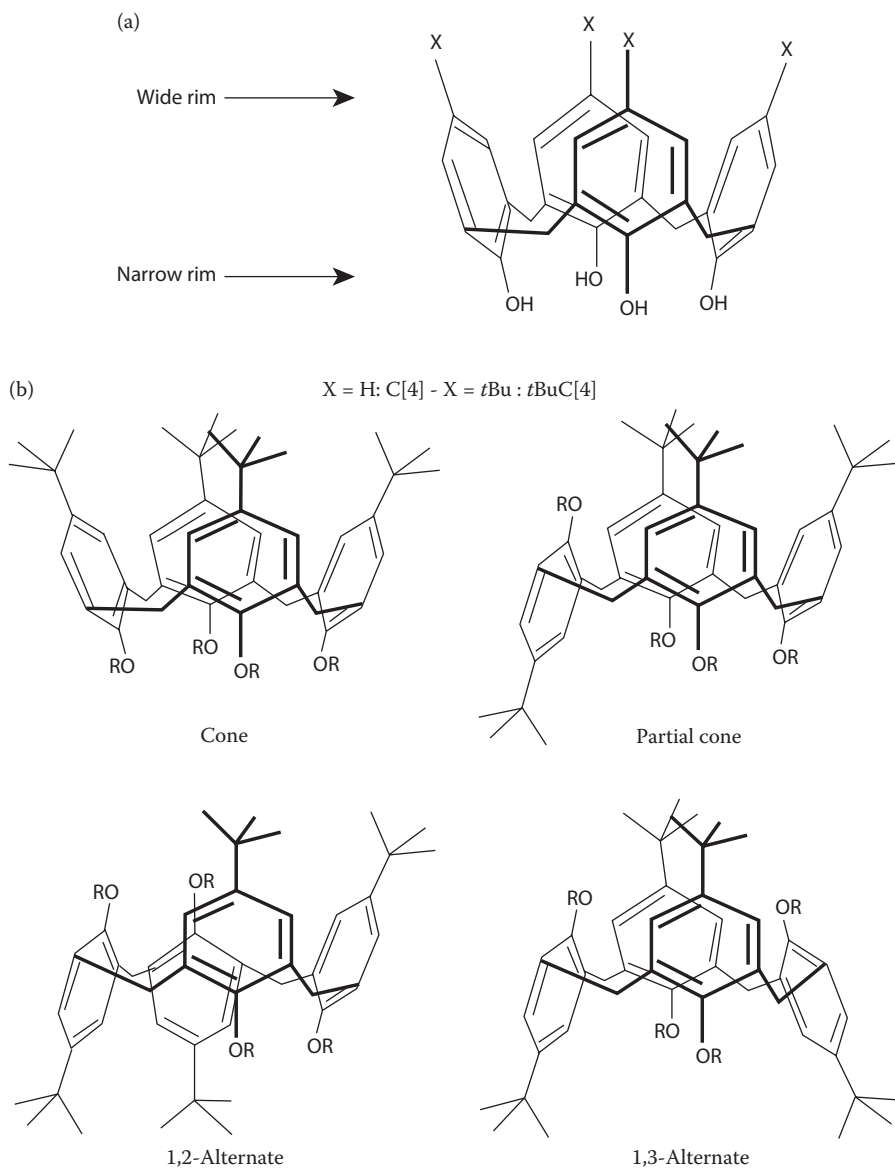
FIGURE 4.1   Calix[4]arenes (a) and their conformations (b).

In the third project, gathering twelve teams from seven EC countries, more than 160 new extractants were prepared and studied. The most promising compounds for the selective extraction of actinides are as follows

- Picolinamide derivatives show interesting Am/Eu selectivity, but an efficiency that is highly pH-dependent.

- Wide-rim tetra(CMPO) calix[4]arenes present good extraction abilities and also rather good selectivities at high acidity. But, the stability toward hydrolysis is not very good. N-methylated compounds exhibit low extraction efficiency, but higher stability toward hydrolysis when they are in contact with strong nitric acid (3 M).
- Tetra(CMPO) cavitands present nearly the same extraction properties as wide-rim tetra CMPO calix[4]arenes, but a slightly lower selectivity.
- Narrow-rim hexa(CMPO) calix[6]arenes are very promising, having very high distribution ratios, especially at high acidities, and also remarkable selectivities.

The main results obtained were published in various journals. The wholeness of the synthesis, of the complexing and extracting results, of the modelling, and of the X-ray and NMR investigations appear in the three Commission of EC final reports.[16–18]

4.3   EXTRACTION OF CESIUM

Three classes of extractants for cesium exist: dicarbollides, crown ethers, and calixarenes. Dicarbollides allow coextraction of cesium and strontium (by adding polyethylene glycol for the latter) from relatively high acidic liquid wastes arising from reprocessing of spent fuels. However, this lipophilic anion behaves as a cation exchanger; thus, its efficiency decreases as the acidity of the liquid wastes increases and does not enable cesium or strontium to be extracted from 3 M HNO_3 solutions arising from PUREX process. Stripping is also a problem requiring strong acid or displacing cations (e.g., guanidinium). Moreover, the selectivity for cesium over sodium is not sufficient for the extraction of cesium from solutions containing large amounts of sodium, especially with the use of polyethylene glycol for strontium extraction.

Most of the studies carried out on cesium extraction conclude that the most efficient crown ethers for extraction of this cation are benzo-21-crown-7 derivatives. Like dicarbollides, these compounds need a synergistic agent or polar diluent modifier to allow cesium to be extracted from very acidic solutions. The resulting selectivity for cesium over sodium is low. Only dialkoxy-calix[4]arene-crown-6 and calix[4]arene bis(crown-6) compounds allow objectives to be fulfilled: extraction of cesium at low-level concentration from acidic media.[19]

4.3.1   Parent Calixarenes

In 1982, *p-tert*-butyl-calix[*n*]arenes were studied by Izatt et al. for their capacity to transport cesium from an alkaline medium ([MOH] = 1 M) through bulk liquid membranes made of a mixture of diluents able to dissolve these compounds: methylene chloride, carbon tetrachloride, and dichloromethane. Experiments were carried out using *p-tert*-calix[8]arene to measure the rate of cesium transport under conditions of varying source pH. The values of the transport rate, small below a pH of 12, rise rapidly beyond this value, hence confirming that a proton is removed from the ligand in the complexation process. Under such conditions, tetramer, hexamer, and octamer (*n* = 4, 6, and 8, respectively) display a high selectivity for cesium over the other

alkaline cations. Transport rate increases as the size of the calixarene decreases, the highest permeability being obtained with the *p-tert*-butylcalix[4]arene (tBu[C4]).[20,21]

Up to 2003, the performance of calix[4]arenes (with and without *tert*-butyl groups in the *para* positions, respectively *t*Bu[C4] and [C4]) and calix[4]arene-crown-6 derivatives had not been compared under the same conditions (nature of the diluent, composition of the aqueous phase, etc.).[22]

Following the recommendation of Reinhoudt,[23] in almost the majority of cases, nitrophenyl alkyl ethers were used as diluents for the extraction tests by the Cadarache group, because they are able to dissolve calixarenes at relatively high concentration. Moreover, the basicity as well the dielectric constant of these diluents improves cation extraction by better solvation of the associated nitrate anions (Table 4.3).

Tests carried out in an acidic medium (4 M $NaNO_3$, 1 M HNO_3) or a neutral medium (4 M $NaNO_3$) show that the calix[4]arene-crown-6 ligands (dioctyloxy-calix[4]arene-2,4-crown-6 MC8, dioctyloxy-calix[4]arene-2,4-benzo crown-6 MC11, and dioctyloxy-calix[4]arene-2,4-dibenzo crown 6-MC14) in NPHE are more effective for cesium and rubidium extraction than C[4] or *t*BuC[4]. In an alkaline medium (4 M NaOH), C[4] and *t*BuC[4] become efficient for cesium removal, and in contrast to the three calix[4]arene-crown-6 ligands, the presence of potassium in the aqueous solution slightly improves their distribution ratios. The extraction efficiency of cesium from 4 M NaOH and 3.9 M NaOH/0.1 M KOH media, respectively, follows the sequences:

$$MC8 < C[4] < tBuC[4] < MC11 < MC14$$

$$MC14 < MC8 < MC11 < C[4] < tBuC[4]$$

The significant selectivity for cesium over rubidium ($S_{Cs/Rb} = 39$), compared with that obtained for the calix[4]arene-crown-6 derivatives (8 for MC8 and less than 5 for MC14), has to be pointed out. Replacement of 0.1 M of sodium hydroxide by potassium hydroxide strongly decreases the cesium distribution ratios for calix[4]arenes-crown-6 ($D_{Cs} < 1$). On the contrary, they are slightly increased for *t*BuC[4], leading to a cesium-over-rubidium selectivity exceeding 150. This selectivity value

TABLE 4.3
Physicochemical Characteristics of Nitro Phenyl Alkyl Ethers

Abbreviation	Alkyl Group	Mol. Weight (g mol^{-1})	Density (g cm^{-3})	Dielectric Constant (debye)	Viscosity (centipoise)	Surface Tension (dyne cm^{-1})
NPHE	Hexyl	223.3	1.066	25.7	8.9	34.3
NPOE	Octyl	251.3	1.036	31.8	13.4	34.3

Source: Workshop on Basic Research Needs for Advanced Nuclear Energy Systems – Report of the Basic Energy Sciences Workshop on Basic Research Needs for Advanced Nuclear Energy Systems, 2006.

is quite exceptional for two cations whose physical and chemical properties are so close.[22]

*t*BuC[4], even at a concentration of 10^{-3} M, allows cesium at trace level in solution to be quantitatively extracted from solutions containing sodium hydroxide (15 M) and also partially extracted (33%) from potassium hydroxide solutions. Under these conditions, selectivity for cesium over potassium and selectivity for cesium over sodium can be estimated to 7,500 and higher than 100,000, respectively.

^{1}H NMR measurements carried out on the organic phase (chloroform) after stirring with 6 M NaOH confirmed the high affinity and selectivity of these ligands for cesium. Upon complexation with C[4] and *t*BuC[4], the peak attributed to OH groups disappears, confirming the previous hypothesis of Izatt of the removal of a proton from the ligand.[20,21]

Parent resorcin[4]arenes also show Cs selectivity in extraction from alkaline media (pH 12), for example, into benzene.[24] With long alkyl chains appended to the bridging carbon atom, separation by flotation is possible.

As a general trend, cation-π interactions with the ligands under study are observed to increase in the Li^+-Cs^+ series, in other words, they follow the increasing order of size and "softness." This may be primarily a result of the largest cations being able to interact with more than one aromatic ring. Apart from the cesium complex structure cited above, several other crystal structures, recently reported, illustrate this trend. The Na^+ and Cs^+ complexes of monoanionic C[4] show exo-coordination of the former, with only O-bonding and formation of a dimeric species and endo-coordination of the latter, with both O- and π-bonding and formation of polymeric assemblies.[25]

Three complexes of K^+ with monoanionic C[4] and *t*BuC[4] in the cone conformation have been described with either O- and π-bonding or O-bonding alone,[26] whereas strong π-bonding of K^+ has been evidenced in the tetrametallic complex of four-fold deprotonated *t*BuC[4].[27] The comparison of K^+, Rb^+, and Cs^+ complexes of monoanionic C[4] and *t*BuC[4] is particularly interesting, as Cs^+ is always complexed in an endo fashion, whereas Rb^+ and K^+ can be either exo- or endo-coordinated.[28]

Such a difference in complexing behavior is likely the origin of the Cs^+/Rb^+, K^+ selectivity observed. It has been noted that, in simple aryloxide systems, the behavior of Rb^+ is more similar to that of Cs^+ than to that of K^+.[29] However, it may be tentatively advanced that the high Cs^+/Rb^+ selectivity observed is related to differing endo/exo preferences resulting from slightly different size, "softness," or solvation.

The cation-π interactions were evidenced by Prodi, who studied the photophysical properties of calix[4]arene-crown and their complexes with alkali metal ions. The presence of these cation ions usually caused weak effects on the absorption spectra, but sometimes caused marked changes in the intensity and wavelength maxima of the fluorescence bands of the calixarenes. The fluorescence quantum yields of complexes with alkali metal follows a precise trend for both MC46 and MC7, decreasing from potassium to cesium. These changes were explained by cation-π interactions between the metal ion and the two aromatic rings pointing toward it.[30]

From a practical point of view, these calixarenes could be used to remove cesium from very alkaline liquid waste containing significant amounts of potassium, the selectivity for cesium over potassium being the most important for a synthetic ligand.

4.3.2 Calixarene Mono Crown

4.3.2.1 Complexation Extraction Results

Ungaro, having observed that the 1,3-dimethoxy-*p-tert*-butylcalix[4]arene-crown-6 MC1 had a slight binding preference for cesium, first synthesized 1,3-dimethoxycalix[4] arene-crown-6 MC2 having six oxygen atoms in the polyether ring linking two phenolic groups. This compound, mainly in the cone conformation, undergoes a rearrangement into the 1,3-alternate conformation when it is put in the presence of cesium. These observations led Ungaro to prepare ligands having this conformation, di-*n*-propoxy MC6, di-*iso*-propoxy MC7, and di-*n*-octyloxy MC8 calix[4]arenes-crown-6 ethers, because substituents bulkier than ethyl block the interconversion between conformational isomers in dialkoxycalix[4]arene.

The first studies performed at Strasbourg University by the picrate extraction method developed by Pedersen reveals a high preference of calix-crowns fixed in the 1,3-alternate conformation for cesium. In contrast to its conformational isomer, di-isopropoxy-calix[4]arene-crown-6 in the cone conformation does not extract cesium (Table 4.4).

There is full agreement between the extraction and the complexation data, in that among the conformationally mobile 1,3-dimethoxy compounds, the crown-5 exhibits selectivity for potassium,[31] the crown-7 is completely unselective and quite inefficient, whereas MC2 and MC1 show selectivity for cesium. Interestingly, all ligands in the 1,3-alternate conformation display significant enhancement in the binding of

TABLE 4.4
Extraction Percentages (%*E*) of Alkali Picrates from Water into Dichloromethane

Ligand	Li+	Na+	K+	Rb+	Cs+
MC3	2	1.6	10	8.9	2.8
MC4	0.4	0.67	1.0	2.3	6.3
MC1	1.4	1.6	2.2	3.1	19.0
MC5	0.5	0.21	0.4	0.4	0.5
MC6	2.5	2.6	13.8	41.7	63.5
MC7	3.0	2.4	15.8	43.8	64.5
MC8	2.1	2.2	13.4	40	63.9
MC12	1.6	2.3	11.0	31.9	41.1
MC14	1.2	2.0	13.3	42.6	54.4
MC15	0.2	0.7	3.4	2.8	2.7
MC7 cone conformation	≤0.2	≤0.2	≤0.2	≤0.2	≤0.2

Source: From J.-F. Dozol, EUR-OP Reference: CG-NA-17615-EN-C (EUR-17615), European Commission, Nuclear Science and Technology, Luxembourg, 1997. With permission. From A. Casnati, et al., *J. Am. Chem. Soc.*, 117, 2767–2777, 1995. With permission.

Note: $C_L = C_{pic} = 2.5 \times 10^{-4}$ M; volume aqueous/organic phase = 1, T = 20°C.

TABLE 4.5
Complexation Data (Log β) of Some Calix[4]arene-crown-6 and Alkali Cations

Ligand	Li$^+$	Na$^+$	K$^+$	Rb$^+$	Cs$^+$
MC7	≤1	≤1	4.5	5.93	6.1
MC6	≤1	≤1	4.3	5.96	6.4
MC4	≤1	≤1	2.13	3.18	4.2
MC1	≤1	≤1	2.54	3.5	4.6

Source: J.-F. Dozol, EUR-OP Reference: CG-NA-17615-EN-C (EUR-17615), European Commission, Nuclear Science and Technology, Luxembourg, 1997. With permission. From A. Casnati, et al., *J. Am. Chem. Soc.*, **117**, 2767–2777, 1995. With permission.
Note: Complexation in MeOH at 25°C, $I = 0.01$ M (Et$_4$NCl or Et$_4$NClO$_4$).

cesium and no affinity for small cations such as lithium and sodium. Therefore, their cesium over sodium selectivity is excellent (Table 4.5).

Measurements performed by Hill in the Cadarache group on simulated radioactive waste confirmed the expectations from basic studies. Preorganized ligands (fixed in the 1,3-alternate conformation) display much higher efficiency and selectivity than the conformationally mobile methoxy substituent (Table 4.6). In comparison to most efficient crown ethers for extraction of cesium (*tert*-butylbenzo-21-crown-7 and decylbenzo-21-crown-7), calixarenes are, by far, more efficient and more selective. Extraction of cesium by crown ethers and calixarenes from solutions simulating radioactive waste (4 M NaNO$_3$, 1 M HNO$_3$, or 3 M HNO$_3$) proves the exceptional efficiency and selectivity of calixarenes-crown-6 in the 1,3-alternate conformation.[32]

Although the interpretation of the thermodynamic results obtained at Strasbourg University is rather complex due to the concomitant operation of several effects, some interesting features emerge from the data (Tables 4.7 and 4.8). The high efficiency of the calix[4]crown-6 in the complexation of cesium is controlled by the enthalpy term, which is one of the highest values found for a synthetic ligand toward cesium in methanol. This value is not counterbalanced by the entropy term, which is less negative than with other cyclic ligands such as the crown ether 18-crown-6 (18C6).[33]

The slightly less negative value found for the entropy term can be explained by the preorganization of the ligand in the 1,3-alternate conformation, where only a small part of the crown ether moiety is rather flexible. This flexibility is lost with the large cesium cation, which fits very well into the cavity created by the polyether ring and the aromatic nuclei.[34]

4.3.2.2 Modeling of Complexation and Extraction

The major aim of these studies, performed by the group of Wipff at the University of Strasbourg, was to understand and predict the binding of alkali ions by calix[4]arene-crown-6 as a function of the conformation of the ligands, the solvent, and the

TABLE 4.6

Extraction of Cesium and Sodium Cs/Na Selectivity and Competitive Extraction of Cesium in the Presence of an Excess of Sodium

Compound	D_{Na}^a	D_{Cs}^a	D_{Cs}/D_{Na}^a	D_{Cs}^b
21-Crown-7 ethers				
n-Decylbenzo-21C7	1.2×10^{-3}	0.3	250	0.12
tert-Butylbenzo-21C7	1.2×10^{-3}	0.3	250	0.12
Di(alkoxy)calix[4]arenes crown-*n*				
MC4	3×10^{-3}	4×10^{-2}	13	0.034
MC2	4×10^{-3}	4.2	>4,200	5.2
MC6	2×10^{-3}	19.5	>19,500	12
MC7	$<10^{-3}$	28.5	>28,500	18
MC8	$<10^{-3}$	33	>33,000	25
MC12	$<10^{-3}$	34	>34,000	45
MC14	$<10^{-3}$	31	>31,000	56
MC15	$<10^{-3}$	0.017	17	0.036
MC5	4×10^{-3}	7×10^{-3}	1.7	0.003
Calix[4]arenes bis(crown-*n*)				
BC1	2×10^{-3}	0.4	400	0,03
BC2	1.3×10^{-2}	19.5	1,500	10
BC3	$<10^{-3}$	0.3	>300	0.2
BC4	$<10^{-3}$	2×10^{-2}	>20	$<10^{-3}$
BC5	1.7×10^{-3}	32.5	19,000	20
BC8	$<10^{-3}$	23	>23,000	32
BC10	$<10^{-3}$	29.5	>29,000	32
BC11	$<10^{-3}$	7×10^{-2}	>70	0.39
Thiacalix[4]arenes bis(crown-*n*)				
Thiacalix[4]arene-bis (crown-5)	2.5×10^{-2}	$<10^{-3}$	25	
Thiacalix [4]arene-bis (crown-6)	1.5	$<10^{-3}$	1,500	

Note: Organic phase: 10^{-2} extractant agent in 1,2-nitrophenylhexylether.

ᵃ Aqueous feed solution: 5×10^{-4} M MNO_3, 1 M HNO_3.

ᵇ Aqueous feed solution: 1 M HNO_3, 4 M $NaNO_3$, 10^{-6} M $CsNO_3$.

environmental effects. Two aspects of ion-binding selectivity were considered, the complexation in a pure homogeneous solution and the extraction from an aqueous to an organic phase.[35,36]

The ligands initially considered are the conformationally mobile dimethoxy-calix[4] arene-crown-6 and its counterpart bearing a *tert*-butyl moiety wide-rim. Each has be considered in three conformations: cone, partial cone, and 1,3 alternate in the free state and then complexed by Na, K, Rb, and Cs. The conclusions are summarized below.

TABLE 4.7

Thermodynamic Parameters of the Complexation of Alkali Cations in Methanol at 25°C

Ligands	Calix[4]arene-diisopropoxy-crown-6			18-crown-6
Cations	K	Rb	Cs	Cs
log K (kJ mol^{-1})	4.5	5.93	6.1	4.8
$-\Delta G_c$ (kJ mol^{-1})	25.6	33.8	35	27.4
$-\Delta H_c$ (kJ mol^{-1})	18.1	40	50.2	47.2
$T \Delta S_c$ (kJ mol^{-1})	7.5	−6	−15	−19.8
ΔS_c (J K^{-1})	25.3	−21	−52	

Source: A. Casnati, A. Pochini, R. Ungaro, F. Ugozzoli, F. Arnaud, S. Fanni, M.-J. Schwing, R. J. M. Egberink, F. de Jong and D. N. Reinhoudt., *J. Am. Chem. Soc.,* **117**, 2767–2777, 1995. With permission.

TABLE 4.8

Dimethoxy-*p-tert*-butylcalix[4]arene-crown-6 in Water

		Na$^+$→K$^+$	K$^+$→Rb$^+$	Rb$^+$→Cs$^+$	Na$^+$→Cs$^+$
	ΔG_3	17.6	5.1	7.7	30.4
Cone	ΔG_4	21.1	6.6	8.9	36.6
	$\Delta G_3 - \Delta G_4$	−3.5	−1.5	−1.2	−6.2
Partial cone	ΔG_4	18.5	6.7	7.0	32.3
	$\Delta G_3 - \Delta G_4$	−0.9	−1.6	−0.7	−1.8
1,3 alternate	ΔG_4	15.0	3.2	5.9	24.1
	$\Delta G_3 - \Delta G_4$	2.6	1.9	1.8	6.3

Note: Differences in free energies and in free energies of binding (kcal mol^{-1}) using M$^+$ Aqvist parameters.

4.3.2.2.1 Gas Phase

For the three conformers, the binding sequence is Na > K > Rb > Cs. This is supported by energy component analysis on the trajectories, as well as by Free energy perturbation (FEP) calculations. Intrinsically, Cs$^+$ has the weakest interactions with both hosts. The largest contribution of the cation/host interaction energy comes from the ether ring rather than from the aromatic moieties. Each complex displays a clear conformational preference. Sodium is most stable in the cone conformation, whereas cesium is most stable in the 1,3-alternate conformation.

4.3.2.2.2 Water Solution

The binding selectivity ΔG_c depends on the conformation of the host and differs from the selectivity calculated in the gas phase. The selectivity $\Delta G_3 - \Delta G_4$ results from the difference in the free energies for the complexed ions ΔG_4 and for the free

ions in water ΔG_3. The thermodynamic cycle method was considered to be as in the scheme, where, assuming that the system is reversible, the relative binding selectivity is computed by the difference: $\Delta\Delta G = \Delta G_1 - \Delta G_2 = \Delta G_3 - \Delta G_4$ [37]

$$Calix + M_1^+ \xrightarrow{\Delta G_1} Calix / M_1^+$$

$$\Delta G_3 \downarrow \qquad\qquad \downarrow \Delta G_4$$

$$Calix + M_2^+ \xrightarrow{\Delta G_2} Calix / M_2^+$$
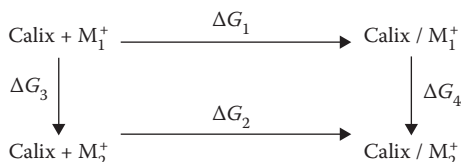
However, the ΔG_3-ΔG_4 difference, which measures the binding selectivity, is clearly conformation dependent. The cone and the 1,3-alternate conformations prefer sodium and cesium, respectively, whereas partial-cone conformation displays practically no preference. These results are consistent with the lifetime of inclusion complexes of MC2 simulated in water. In the cone conformation, cesium decomplexes, while sodium remains deeply encapsulated inside the phenolic oxygens. In the 1,3-alternate conformation, reverse results are observed, as sodium decomplexes in bulk water, while cesium remains encapsulated inside the polyether bridge. The simulation demonstrated for the first time that the binding selectivity depends on the conformation of the host and on differential solvation effects. Although simulations used the methoxy derivative, the replacement of methoxy by more bulky alkoxy groups should not alter the above conclusions: the alkyl chains remote from the cation-binding area, expected to increase the lipophicity of the ligand, have weak effects on its binding ability.

4.3.2.2.3 *Chloroform Solution*

The Na^+, K^+, Rb^+, and Cs^+ complexes were simulated in the cone, partial-cone, and 1,3-alternate conformations, first without counterion. It was found that the smallest Na^+ lies in a very deep position, surrounded by phenoxy-oxygens, not involving crown ether oxygens. As M^+ gets bigger, it moves "up" to the crown. Picrate as the counterion remains an intimate pair with the complexed M^+. The structure of the Na^+ complex is different, compared with the host-M^+ complex, because the picrate counterion pulls Na^+ more "exo" to the crown region. On the contrary, for Cs^+, the structures with and without picrate are very close, which demonstrates the good fit between Cs^+ and the 1,3-alternate host.

4.3.2.2.4 *Extraction of Alkali Cations from Pure Water to Pure Chloroform*

Combining the simulations in water and those in pure chloroform, the extraction selectivity was modeled by the following thermodynamic cycle. The assumption is made that the concentrations of the free ions in the organic phase and of the free or complexed ligand in water is negligible.[35,38] The extraction is defined as:

$$\Delta G_{extr} = \Delta G_1 - \Delta G_2 = \Delta G_{aq} - \Delta G_{org} \qquad (4.1)$$

It was calculated that the 1,3-alternate form of calix[4]arene-crown-6 will selectively extract, with or without picrate counterion, Cs^+ over Na^+. However, it was shown that the counterion reduces somewhat the preference for Cs^+.

The Cadarache group[39] focused its modeling contribution on di(isopropoxy)-calix[4]arene-crown-6. It was deduced from these simulations that the 1,3-alternate conformation is much more preorganized than the cone conformation to bind a large cation in water and in vacuo. It can be explained by the fact that the isopropoxy groups, which are near to the crown basis, can prevent the complexation of small cations by shielding the complexation site constituted by the four phenoxy oxygen atoms.

4.3.2.2.5   *Simulation In Vacuo with and without Counterion Nitrate*

All the simulations of the Cadarache group were performed with the 1,3-alternate conformation. For K^+, Rb^+, and Cs^+, without the anion, the cation is almost at equidistance from the six oxygen atoms of the crown. The presence of the nitrate lightly draws the cation to the upper part of the crown, farther from the mean plane defined by the six oxygen atoms of the crown, but there is no major structural modification in the complexes. On the contrary, the Na^+ cation, which is deep inside the calixarene cavity, goes immediately to the upper part of the crown with the counterion, for any initial location of the nitrate. These structural observations are in good agreement with those previously made by the team of the University of Strasbourg with the MC2 and the picrate counterion.

The energetic features were modified by the presence of the counterion. The energy of interaction between the cation and the nitrate is much higher (about 50 kcal/mol) than the energy of interaction between the cation and the calix-crown, this last value being considerably lowered (from 9 to 14 kcal/mole) with respect to its value without the anion. The presence of the anion weakened the interactions between the cation and the calix-crown and favored the affinity of the ligand for sodium, lowering the calculated selectivity cesium over sodium. The preponderance of the interactions between the sodium and its counterion, from both a structural and energetic point of view, underlines the lack of affinity of the calix-crown for such a small cation.

4.3.3   Bis(crown)calix[4]arenes

4.3.3.1   Extraction Results

Simultaneously with the synthesis of di(alkoxy) calix[4]arene-monocrown-6, Asfari et al. synthesized a new class of calixarenes, calix[4]arenes-bis(crown). As the di-alkoxy-calix[4]arene-monocrown-6, blocked in 1,3-alternate conformation by linking opposite phenolic oxygens by two polyethylene glycol chains, calix[4]arenes-bis(crown-6) containing six oxygen atoms are the most efficient for binding cesium. Calix[4]arenes-bis(crown-*n*) bearing five (BC1) or seven oxygen atoms (BC3) are not effective for cesium extraction and display a poor selectivity for cesium over sodium, comparable with selectivity found for 21-crown-7 ethers (Table 4.6).[34,40,41]

4.3.3.2   Stoichiometry of the Bis (Crown) Complex
             Cesium/Calixarene

Calix[4]arenes-bis-crown constrained to a 1,3-alternate conformation present two binding sites on each crown, which are linked by a π-basic benzene tunnel. In the 1:1 complexes, the cation switches from one binding site to the other through this

tunnel. This symmetrical ditopic arrangement is well adapted for the formation of 1:1 as well as 1:2 calix:metal complexes. The possibility of di-coordination of Cs was characterized by X-ray diffraction and by NMR. When the ratio calix/Cs is equal to 1/1.25, a coalescence attributed to a rapid metal-ligand exchange between *mononuclear* and *binuclear* species is observed by nuclear magnetic resonance (NMR). For a calix/Cs ratio equal to 1/2.5, only a triplet in the meso-CH_2-groups is detected, attributed to a symmetrical binuclear species. Molecular modeling based on the structure obtained from X-ray diffraction concludes that, in the water phase, by far the most likely species is the mononuclear complex, due to a higher stability than the binuclear one and to possible solvation of the second binding site. The modeling conclusions obtained in water medium are consistent with those obtained by liquid-liquid extraction.[41]

Electrospray Ionization/Mass Spectrometry (ES/MS), a soft-ionization desorption technique using polar solvents such as water, methanol, or acetonitrile, was used for direct measurement of cations in solution. The first measurements carried out with mono or bis(crown-6) calix[4]arenes from an equimolar cation-extractant solution confirm that the calixarenes mono(crown-6) extract only one cesium cation. On the contrary, in the same conditions, bis(crown-6) calix[4]arenes can extract two cesium cations for a ratio Cs/BC6 equal to 2.5. The binuclear complex (composed of two cesium cations) is the major species. Cesium/sodium selectivity measurements implementing various mono or bis(crown-6) calix[4]arenes were in agreement with liquid/liquid results.[42]

Thuéry reported the crystal structure of the complexes of sodium and of potassium with calix[4]arenes-bis(crown-6). One sodium ion and one water molecule are included in each crown cavity of the calixarene. The sodium ion is only bonded to three oxygen atoms of the crown, two from the nitrate ions and one from the water molecule. On the contrary, potassium is bound to the six oxygen atoms of the crown and to two oxygen atoms of the nitrate ions. The similarity between the potassium and the cesium suggests a lack of specificity of calixarene toward one or other of these two cations. However, the ligand/potassium complementarity is less satisfying than in the case of cesium (the distances between potassium ion and the oxygen atoms of the crown are not optimal), and the interactions between the cation and the electrons of the benzene rings are less important with potassium.[43]

A molecular dynamics (MD) study in vacuo and in water phase was undertaken on benzo and cyclohexano 21-crown-7 ether derivatives, the best fitted crown ether for complexation of cesium. In the gas phase, the crown ethers are highly flexible whatever the number and the position of benzo or cyclohexano groups. Notable differences in the hydrophobicity and complex stability appear in simulation in an explicit aqueous phase. Benzo derivatives are well preorganized in water for complexation, but the cation is not sufficiently shielded from the water phase. The conclusions are the same for the cyclohexano derivative. On the contrary, di- and tricyclohexano derivatives possessing a larger and more flexible crown, display a lack of preorganization to host alkali cations. Calixarene-crown-6 compounds are much better preorganized, the crown fits perfectly to cesium, and the rigid calixarene cavity hinders the binding of sodium cations.[44]

4.3.4 CALIXARENES BEARING AROMATIC GROUPS IN THE CROWN ETHER LOOP

4.3.4.1 Complexation and Extraction Results

MD simulations performed on calix[4]arene-monocrown-6 and on calix[4]arene-bis-crown-6 and their alkali complexes, suggested that incorporation of aromatic groups in the crown ether loop was a possible way to enhance cation binding and cesium over sodium selectivity.[45]

Results obtained with di-octyloxy-calix[4]arene-dibenzocrown-6 (MC14), di-isopropoxy-di(*tert*-butyl-benzo)crown-6 (MC15), and di-isopropoxy-calix[4]arene-octylbenzocrown-6 (MC13) synthesized by Casnati, confirmed the results of MD simulations. The comparison of the results obtained with MC13 with MC12 shows that the substitution of the crown part with one *tert*-octylbenzo group leads to a small decrease in extraction with all the cations of the series (Table 4.9). The substitution of the crown by two benzo groups does not significantly change the extraction level of the smallest cations. Cesium is less extracted by calix[4]arene-di-*n*-dioctyloxy-dibenzo-crown-6 than its counterpart without benzo groups. The further substitution of the two benzo units by *tert*-butyl groups prevents any extraction or complexation because of steric hindrance of the bulky *tert*-butyl groups. Benzo groups do seem to improve Cs/Na selectivity. In order to examine the origin of the stabilization of alkali complexes of MC14, thermodynamic parameters of complexation have been determined (Table 4.10). The trends are the same as those previously determined for the MC7 (Table 4.7) studied in methanol, that is, an enthalpic stabilization, an increase in enthalpy change from potassium to cesium, concomitant with a decrease in entropy change. This can be explained by a size complementarity between the crown and cesium, resulting in loss of freedom, and by desolvation of the cations. The exceptional selectivity for cesium over sodium higher than 30,000, displayed by calixarenes diluted in NPHE, is corroborated by the competitive extraction of cesium solutions containing large amounts of sodium (1 M HNO_3, 4 M $NaNO_3$).

TABLE 4.9

Dialkoxy Calix[4]arene Substituted Benzocrown-6: Extraction Percentages (%*E*) of Alkali Picrates from Water into Dichloromethane

Ligand	Li$^+$	Na$^+$	K$^+$	Rb$^+$	Cs$^+$
MC7	3.4	2.4	15.8	43.8	64.5
MC8	2.1	2.2	13.4	40.0	63.9
MC14	1.2	2.0	13.3	42.6	54.4
MC15	0.2	0.7	3.4	2.8	2.7
MC12	1.6	2.3	11.0	31.9	41.1

Source: A. Casnati, F. Sansone, J.-F. Dozol, H. Rouquette, F. Arnaud-Neu, D. Byrne, S. Fuangswasdi, M.-J. Schwing-Weill and R. Ungaro., *J. Incl. Phenom. Macrocyclic Chem.*, **41,** 193–200, 2001. With permission.

Note: $C_L = C_{pic} = 2.5 \times 10^{-4}$ M; volume aqueous/organic phase = 1, $T = 20°C$.

TABLE 4.10

Thermodynamic Functions of the Complexation of Alkali Cations by Dioctyloxycalix[4]arene-dibenzocrown-6 MC14 in Acetonitrile at 25°C

Thermodynamic Functions	K^+	Rb^+	Cs^+
Log β	5.47	5.7	5.7
$-\Delta G$ (kJ mol^{-1})	31.2	32.5	32.5
$-\Delta H$ (kJ mol^{-1})	17.4	29	42
$T \Delta S$ (kJ mol^{-1})	13.8	4	−10
ΔS (J K^{-1} kJ mol^{-1})	46	13	−34
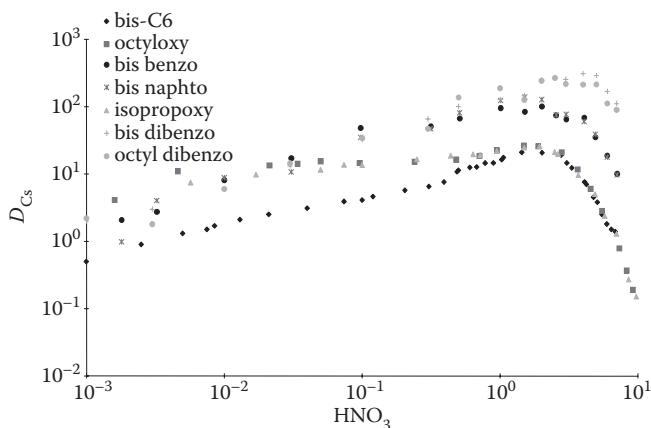
FIGURE 4.2 Distribution ratios of cesium at trace level as a function of HNO$_3$ concentration. Organic phase: calixarene 10^{-2} M in NPHE.

Very high distribution ratios are obtained with ligands including one and two benzo units in the polyethylene chain, $D_{Cs} = 45$ and $D_{Cs} = 56$, respectively. This enhancement of distribution ratios is explained by a lesser extraction of sodium, linked to a better complementarity of these ligands with cesium (Table 4.6).[46]

One goal of the project was the removal of cesium from highly acidic solutions of fission products arising from the PUREX process (3 M HNO$_3$). Cesium distribution ratios, much higher than those of two dibenzo 21-crown-7 ethers, strongly increase with the increasing concentration of nitric acid, to a value ranging between 2 and 3 M. The presence of benzene units on the crown bridge reduces the nitric acid extraction, strongly enhances that of cesium, and shifts the maximum of cesium extraction toward higher acidity ($D_{Cs} = 200$ for 3–4 M HNO$_3$ in NPHE). The EC goal is reached with these compounds, especially those including benzo and naphtho units in the crown (Figure 4.2).[47]

For the calix[4]arene-bis(crown-6), the trends are the same on adding a benzo (BC5) or a naphtho group (BC10) in improving the extraction efficiency and the selectivity for cesium over sodium. However, the distribution ratios, although higher

when benzo groups are added to the crown, are lower than those obtained with their mono-crown-6 counterparts.[40,48]

Results obtained by ES/MS confirm that the stability of calixarene/cation complexes depends upon the medium. The calixarene in solution presents a strong affinity for cesium, whereas in the gas phase, it displays a stronger affinity for sodium. Moreover, the stability of calixarene/Na^{+} complexation in a solvent phase is increased by the presence of water in the dilution system (up to 40% in acetonitrile), whereas other alkali complexes are destabilized by the presence of water. Finally, affinity for sodium, which is weak in the solution for calixarenes bearing benzo moieties, considerably increases in the gas phase. These results confirm the interpretation of the MD simulations in an aqueous phase, which lead the authors to conclude that cesium-over-sodium selectivity is governed by the hydration of the sodium cation in the complex, and by the higher hydrophobicity of the complexation site leading to an enhancement of selectivity for cesium over sodium.[49]

Replacement of sp[3] carbons by sp[2] carbons in the crown chain leads to a flattening of these chains. This change causes a higher binding of cesium and a lower binding of sodium, which was confirmed when unsymmetrical 1,3-alternate calix[4]arene-bis(crown-6) containing one crown-6 loop and a 1,2-arylene modified crown-6 was shown by NMR to complex cesium picrate in the 1,2-arylene crown-6 chain and the sodium in the crown-6 chain.[50] Studies of the complexing properties of BC9 (in which the three central ethylene links have been replaced by three fused 1,2-phenylenes) with sodium or cesium picrates shows an improvement of cesium complexation in comparison to the previously studied bis-crown-6 calixarenes and, on the contrary, no detectable sodium binding.[51]

Kim et al. confirmed the results previously described by Reinhoudt et al., which showed that monocrown-5 and biscrown-5 calix[4]arenes are efficient extractants for potassium.[52–54]

Kim et al. also studied diisopropoxy-calix[4]arene-crown-6 (MC7), diisopropoxy-calix[4]arenes-crown-7 (MC16), and several dibenzo derivatives including 6, 7, or 8 oxygen atoms in the crown, all these calixarenes displaying the 1,3-alternate conformation, dipropoxy-calix[4]arene (dibenzocrown-6) (MC17), dipropoxy-calix[4]arene (dibenzocrown-7) (MC18), dioctyloxy-calix[4]arenes (dibenzocrown-7) (MC19), dipropoxy-calix[4]arene (dibenzocrown-8) (MC20), dipropoxy-calix[4]arene (dibenzocrown-7) (MC21), and dioctyloxy-calix[4]arene (dibenzocrown-7) (MC22), the two latter including two butyl groups attached to the crown. NMR studies concluded that the upper four oxygen atoms in the crown ether play a very important role in metal complexation. On the contrary, the lower two oxygen atoms (phenolic hydroxy groups) play a minor role. Performance of these eight compounds was compared by transporting metal ions through a bulk liquid membrane (Table 4.11). The most efficient carriers are dipropoxy-calix[4]arene (dibenzocrown-6) (MC5) and, to a lesser extent, dipropoxy-calix[4]arenes crown-6 (MC6). Increasing the size of the crown results in a decrease by about 10-fold of the transport rate of cesium. It has to be pointed out that there is no more selectivity between the alkali cations for the dibenzo crown-8 derivative; all the cations are poorly extracted. The authors explain the better affinity of (MC17) in comparison to (MC7) by the flattening of the crown, induced by introduction of two benzo groups in this crown. The two butyl groups attached to

TABLE 4.11

Single-Ion Transport Values of Alkali Metal Ions through a Bulk Liquid Membrane

	Flux/10^{-8} mol s^{-1} m^{-2}				
Ligands	Li$^+$	Na$^+$	K$^+$	Rb$^+$	Cs$^+$
MC6	0.00	1.42	1.90	20.75	78.23
MC16	0.00	1.22	1.45	4.55	8.35
MC17	0.00	0.00	2.84	44.95	130.59
MC18	0.00	1.92	1.28	4.35	11.87
MC19	0.00	1.07	2.12	2.21	5.42
MC21	0.00	1.51	0.77	1.03	2.90
MC22	0.00	0.87	0.64	1.00	1.90
MC20	0.00	0.87	2.17	1.69	1.03

Note: Transport conditions: source phase, MNO$_3$ = 0.1 M; membrane-phase carrier 10^{-3} M in CH$_2$Cl$_2$; receiving phase, deionized water.

the crown ether (MC21) and (MC22), slightly tilted inside the cavity of the crown, hindering the introduction of cations in the crown (confirmation by examination of Corey–Pauling–Koltun space-filling models).[55,56] These transport measurements were confirmed by transport of alkali metals through polymeric membranes.[57]

4.3.4.2 MD Computation

Four calixarenes were studied by MD: MC7, BC2, BC5, and BC3. The aim of these simulations was to correlate the extracting behavior and the cesium over sodium selectivity to molecular properties, considering that a good extractant is first of all a good complexant and lipophilic enough to stay in the organic phase. For these simulations in water, considering that ion pairs are separated, the counterion was not taken into account. MD computations show that, for BC5, the distances between the cation and the six oxygen atoms of the complexing crown are almost the same $d(Cs^+ - Oc) = 3.31$ Å. They are a little larger and more heterogeneous for BC2. On the contrary, the complementarity between cesium and the oxygen donors of the crown is not satisfactory for BC3. By visualizing the MD trajectory, the evolution of the complexes and their interactions with water molecules can be observed. From the beginning of the simulation, one water molecule, located out of the ligand, is coordinated to the cesium for the calix[4]arenes crown-6; on the contrary, BC3 is coordinated to several water molecules that, after 75 ps of MD, provoke the decomplexation of cesium. The situation is very different for sodium complexes. In BC2/sodium complexes, a water molecule enters the complexing crown during the first picosecond of MD and stays in this stable position, completing the coordination sites of the cation. This introduction of water in the crown is not observed during the first 100 ps with BC5 and the BC3, due to the best shielding effect of surrounding water by the crown. The complexing crown of BC3 completely folded over sodium, preventing the solvation; on the other hand,

the other crown loop, free of cation, is well solvated with water. MC7 has the same behavior as BC2 with a best structural complementarity, similar to that of BC5.[58]

MD simulations were performed on the alkali cations to evaluate the host-guest complementarity in particular. A criterion of this complementarity is the ability of the extractant to provide a coordination environment similar to that of the hydration shell of the cation. Part of this environment (number of donor atoms and their statistical distance to the cation) can be evaluated by the summation of the radial distribution functions (rdfs) of the oxygen atom donor sites rdfOc, collected during MD simulations and their comparison with the rdf of the water oxygen atoms rdfOw, around the "free" cation under similar simulation conditions. The MD simulations were performed with several calix[4]arene-biscrowns: calix[4]arene-bis(crown-5) BC1, calix[4]arene-bis(crown-6) BC2, calix[4]arene-bis(crown-7) BC3, calix[4]arene-bis(dibenzo-crown-6) BC8, calix[4]arene-bis(tribenzo-crown-6) BC9, calix[4]arene-bis(naphtho-crown-6) BC10. From the simulations in vacuum in the absence of counterion, BC10, BC8, and BC9 display an excellent complementarity for Cs$^+$. BC2 is slightly too large, and BC1, too small, is better fitted for rubidium or potassium. Simulations in the vacuum with sodium nitrate give rise to a different location of the sodium cation, whatever the calixarene. This cation is shifted to the upper part of the crown, interacting with the nitrate anion and four oxygen atoms of the crown. This location leaves enough room for a water molecule in the crown. Previously, it was shown that the sodium binding was favored by one water molecule. The decrease of affinity toward sodium when benzo or naphtho moieties are present in the crown must be related to this hydrophobic unfavorable environment more than to a worse calixarene/sodium complementarity.

In water, the introduction of a counteranion (NO$_3^-$) induces a stronger electrostatic interaction, which tends to draw the cations out of the mean plane of the crown ether loop. Simulations with cesium nitrate and the various calix[4]arene-biscrowns show that the best fit is obtained with BC8 and BC9.[59]

A MD simulation on the extraction of Cs$^+$ by MC4 compared two diluents, CHCl$_3$ and the ionic liquid (IL) BMI + Tf$_2$N$^-$. With CHCl$_3$, the complex formation is limited to the interface, while the IL allows reaction in the vicinity of the interface, involving mixed solvation. In CHCl$_3$, the ligand and its Cs$^+$ complex are amphiphilic and prefer the interface, whereas in the IL, the complex is less surface active than the free ligand. The latter explains the better extraction of Cs$^+$ into the bulk organic phase by hydrophobic ILs. However, in the IL/water biphasic system, equilibrium is reached more slowly due to the lower diffusion coefficients and distribution of water into the IL phase.[60]

4.3.5 Dihydrocalix[4]arene

Sachleben et al. observed that for bis(alkoxy)calix[4]arene monocrown ethers, reducing the size of the alkoxy substituent from octyl to allyl increased the cesium extraction by 10%–30% and the cesium-to-potassium selectivity by 20%–40%, with little impact on cesium over sodium selectivity. A standard modeling approach was used to analyze the complementarity of the calix-crown cavity toward potassium and cesium. MM3 optimizations were performed by modifying the K$^+$ and Cs$^+$ complexes, replacing the 1,3-dioxybenzene-substituent with *tert*-butoxy, methoxy, or hydrogen groups.

A measure of complementarity, ΔU_{comp}, was obtained as the difference between the steric energy of the ligand in its bound form and the steric energy of the ligand in its binding conformation. In addition to the ligand strain ΔU_{comp}, summing each $[M^+]$-calixarene interaction energy provides a measure of the strength of the π-cation interactions E_π. Using the sum of ΔU_{comp} and E_π as gauge, authors observed that complementarity for both cations is best when the substituents are hydrogen and decrease in the order hydrogen > methoxy > *tert*-butoxy. Hydrogen substitution permits the cavity to open, thereby allowing the two arene donor groups to approach their preferred orientation with respect to the cation. Remarkably, the structure predicted for Cs/3c by molecular modeling is very similar to that found in the crystal structure.

Changing the calixarene from dioctyloxycalix[4]arenes MC8, MC11, and MC14 to the dihydro analogs MC30, MC31, and MC33, respectively, the extraction strength for cesium expressed in terms of distribution ratios D_{Cs}, decreases by roughly an order of magnitude. However, a much larger decrease is observed for the extraction of other alkali cations, corresponding to an increase of the selectivity (Table 4.12). These studies prove that enhanced selectivity for cesium over other alkali cations can be obtained by appropriate modifications of some portions of calix[4]arene crown-6.[61,62]

4.3.6 ENLARGED CALIX[4]ARENE CROWN-6

4.3.6.1 Calix[4]arene Propylene-crown-6

From the observation that ring-enlarged crown ethers, $(3m + n)$-crown-m, usually show decreased cation-binding ability in comparison to the corresponding symmetric

---

TABLE 4.12

Distribution Ratios for Alkali Metal Nitrates from Water to 1,2-Dichloroethane and the Corresponding Selectivities

Ligands	D_{Cs}	D_{Rb}	D_K	D_{Na}	D_{Li}
		$S_{Cs/Rb}$	$S_{Cs/K}$	$S_{Cs/Na}$	$S_{Cs/Li}$
MC30	0.403	<0.0070	<9.6 × 10⁻⁵	2.17 × 10⁻⁵	1.90 × 10⁻⁵
		>58	>4200	>23,000	>32,000
MC31	0.383	<0.0070	<9.6 × 10⁻⁵	<2.5 × 10⁻⁶	<5.8 × 10⁻⁷
		>54	>4000	>150,000	>660,000
MC33	0.116	<0.0070	<9.6 × 10⁻⁵	<2.5 × 10⁻⁶	<5.8 × 10⁻⁷
		>17	>1200	>47,000	>200,000
MC8	3.65	0.180	0.0152	22.0 × 10⁻⁵	2.98 × 10⁻⁵
		20	240	17,000	120,000
MC11	4.04	0.214	0.0141	3.9 × 10⁻⁵	0.99 × 10⁻⁵
		19	290	100,000	>450,000
MC14	1.61	0.178	0.0125	<2.5 × 10⁻⁶	0.97 × 10⁻⁵
		9.0	130	>640,000	170,000

Note: $C_L = C_{pic} = 2.5 \times 10^{-4}$ M; volume aqueous/organic phase = 1, T = 25°C.

crown ethers, but sometimes enhance selectivity, Casnati et al. proposed to improve the selectivity for cesium over potassium of these compounds by enlarging the crown of calix[4]arene crown-6 by the introduction of a propylene unit in place of the central ethylene unit. The authors modeled the structure of the complexes of "enlarged calix[4]arene crown-6" with potassium and cesium in the gas phase. The main conclusions of the modeling are the following. The calix[4]arene basket undergoes a significant conformational reorganization upon complexation, the opposite phenolic units are forced to rotate toward the exterior of the macrocycle to favor the binding of the metal ion, and the rotations increase as the size of the cation increases. The analysis of the interatomic M^+-O distances shows that the K^+ ion is tetra-coordinated (the K^+-O bond distances range from 2.64 to 2.89 Å) in contrast with cesium, which is hexa-coordinated (the Cs^+-O bond distances range from 3.00 to 3.43 Å). It is, however, surprising that a small shortening of the Cs^+-O distance is observed in spite of an enlargement of the size of the crown. Therefore, these data, which show a relevant difference in the coordination numbers of the two cations, suggesting an improved selectivity for cesium over potassium, prompted the authors to synthesize two calix[4]arene-propylene-crown-6 compounds. The binding properties of the two new ligands, MC23 and MC24, with propylene units were determined by Cram's method and compared to those of their counterparts with ethylene units. A strong decrease in cation-binding properties of propylene calix[4]arene crown-6 is observed. This effect is more significant for larger cations and with the dibenzo-crown-6 derivative. This discrepancy is ascribed to the fact that effects due to solvation and interaction with the counterion are not taken into account in the modeling.[63]

4.3.6.2 Thiacalix[4]arene

Another way to act on the selectivity of calix[4]arene-crown is to modify the size of the cavity of calixarene by replacing methylene by sulfur bridges. Crystal structures and extraction data obtained with the thiacalix[4]arene-bis(crown-5) and the thiacalix[4]arene-bis(crown-6) lead to the conclusion that these compounds are less interesting than calix[4]arene-crown-6 for the extraction of alkali cations (Table 4.6). In agreement with crystal structures, MD simulations showed that the thiacalix[4] arene cavity size was approximately 0.05 nm larger than that of calix[4]arene. MD simulations show that the cations are located close to the thiacalix[4]arene cavity with the possibility of migration through the latter and that the crown does not correctly fulfill its role of ligand.[64] Complexation studies confirm these extraction results: the replacement of the bridging CH_2 groups of calix[4]arene-bis(crown-*n*) by sulfur atoms of thiacalix[4]arene-bis(crown-*n*) leads to a strong decrease in complexation levels of alkali metal ions, but does not affect the selectivity within the series of crown ethers. No clear-cut conclusions about the possible interactions between these cations and the sulfur atoms can be drawn.[65]

In conclusion, calix[4]arene-bis(crown-6) and dialkoxy calix[4]arene crown-6, and especially their dibenzo derivatives, which display an important hydrophobicity, seem best suited for the extraction of cesium from very acidic media or media containing large amounts of sodium. In 2006, Mohapatra confirmed the high efficiency and selectivity of BC5 and BC10 for the extraction of cesium from simulated acidic high-activity level waste. The Cs distribution ratio follows the trend of diluent

dielectric constant. The selectivity factor over the other studied fission products and over U(VI) exceeds 200 (except I2). The Cs distribution ratio remains nearly constant up to equimolar amounts of Cs and extractant in aqueous and organic phases, respectively.[66] Their selectivity for cesium over potassium being relatively low, dihydrocalix[4]arenes would appear to be good candidates for the extraction of cesium containing large amounts of potassium.

4.3.7 PROTON-IONIZABLE CALIX[4]ARENE

Incorporating a proton-ionizable group into a macrocyclic ligand has a very important effect upon the efficiency with which a metal ion can be extracted into an organic medium. Transfer of hydrophilic anions, such as nitrate, from the aqueous phase into an organic phase to provide an electroneutral extraction complex with a macrocycle-complexed metal ion is energetically unfavorable, and markedly diminishes the extraction efficiency. With a proton-ionizable group in the ligand, ionization provides the requisite anion for formation of an electroneutral extraction complex without transfer of an aqueous-phase anion.

For the first time, Talanov synthesized two 1,3-alternate calix[4]arene-bis(crown-6) compounds with a proton-ionizable group (carboxylic BC17 or the more acidic N-(trifluoromethylsulfonyl)-carboxamide) BC18 located in front of one crown ether cavity (in para position to the phenolic hydroxy groups). Competitive extraction of alkali cations from aqueous nitrate solution (0.1 mM in each cation, pH 6) into 0.10 mM solutions of the ligand in chloroform showed no extraction for calix[4]arene crown-6 without an ionizable group. On the contrary, BC17 extracted only cesium (17.7%), and BC18 extracted both rubidium (17.0%) and cesium (56.5%).[67]

Moyer hypothesized that the incorporation of amine functionality into the calix-crown could improve the efficiency of release of cesium from the calix-crown upon protonation. Neutral calix-crowns extract Cs^+ by coextraction of an aqueous-matrix anion, such as nitrate. If the organic phase is then contacted with an acidic aqueous phase, the amine functionalities will become protonated, possibly destabilizing cesium complexation by charge-charge repulsion. Three classes of amine-derivatized calix-crowns were prepared to evaluate the relationship between the proximity of the amine groups to the cesium-binding cavity and the destabilizing effect on cesium binding. The first had the amine attached to the phenyl group of the benzocrown unit MC34 and BC19, the second was particular to mono crown calixarenes, in which the alkoxy group is a short alkyl chain with an amine terminus (MC35), and the last had the amine attached to one of the phenyl rings of the calixarene "upper rim" (BC20).

The calix[4]arene mono crowns MC34 and MC35 and calix[4]arene bis crowns BC19 and BC20 were compared to BC6 and MC8. The organic phase in each case consisted of a calix-crown at 2.5 mM in nitrobenzene, and extractions were carried out from alkaline and acidic nitrate aqueous solutions. A 100-fold decrease in cesium extraction strength is observed upon acidification of the aqueous phase. Under alkaline conditions, except for the bisamino-propoxy calix[4]crown, MC35, the presence of the amino group does not change D_{Cs} significantly. Extraction under acidic conditions decreases significantly relative to the nonaminated control compounds for all amino-substituted compounds, and most significantly for amino methyl calix-crown

BC20. Stripping under acidic conditions gives approximately the same value of D_{Cs} as extraction under nitric acid conditions, confirming that back-extraction is enhanced. A combination of high extraction ability under basic conditions and high stripping efficiency under acidic conditions make compound BC20 an attractive extractant candidate. For BC7, at low concentrations of cesium, the stoichiometry of the calix:cesium complex is 1:1. A further loading of BC7 can be achieved to give a calix:cesium ratio of 1:2, in agreement with the number of crown rings available to complex cesium. In contrast, the stoichiometry between BC20 and cesium remained unchanged, suggesting that one of the two crown cavities of this molecule is unsuitable for binding cesium, evidence that the nonfunctionalized crown ring contains the cesium. The implication is thus that positioning the methylamino group on one of the phenyl groups on the calixarene "belt" destabilizes cesium binding, although the amino group itself is ordinarily capable of acting as an electron-pair donor.[68–71]

The goal of further work was to evaluate the role of the amino group of amino methyl calix[4]arene-[bis-4-(2-ethylhexyl)benzo-crown-6] (BC20) in the extraction of cesium from acidic and basic mixtures of sodium nitrate and other concentrated salts. The extraction of cesium from nitrate media was measured as a function of extractant concentration, nitrate concentration, cesium concentration, and pH over the range 1–13. Rather than the nitrobenzene diluent used in previous studies, an alcohol-modified alkane was employed. The initial studies showed a moderate decrease in the extraction of cesium in acidic media, which indicated the binding of cesium by the calixarene-crown was weakened by the protonation of the amine group. The results also indicated that a 1:1:1 Cs-ligand-nitrate complex is formed in the organic phase. The formation constants of the complexes formed in the organic phase computed from empirical data showed that the attachment of the amine group to the calixarene-crown molecule reduced the binding stability for the cesium ion upon contact with an acidic solution. The small magnitude of the charge-charge repulsion effect likely implies that the cesium binding in BC20 occurs in the cavity opposite that of the pendent amino group, such that the positive charges are not in close proximity.[72]

A series of calix[4]arene-bis(crown-6) ligands BC21, BC22, and BC23 and three series of calix[4]arene-monocrown-6 ligands (MC36-MC41), (MC42-MC43), and (MC44-MC45) have been synthesized.[70] The lipophilic calix[4]arene-bis(crown-6) extractant series BC21, BC22, and BC23 has the same general structure as nonionizable BC6 with the exception that the lipophilic groups are 2-ethylhexyl instead of *tert*-octyl and the presence over the face of one crown ring of a proton-ionizable group. In addition to a carboxylic acid group, the ionizable groups include two N-(*X*) sulfonyl carboxamide groups in which the acidity of the function is "tuned" by varying the electron withdrawing ability of *X*. The change from $X = CH_3$ to CF_3 is expected to increase the ligand acidity by about three pKa units. Since calix[4] arene-biscrown-6 extractants have two crown units, there is a possibility that in addition to the complexation of cesium ion by one crown unit, the second crown unit could complex cesium, thereby escaping the switching mechanism. Additionally, the possibility of sodium or potassium ion binding by the second crown unit could reduce the cesium extraction selectivity. To eliminate these unwanted effects, the lipophilic calix[4]arene-monocrown-6 series (MC36-MC41) was prepared. To allow the effect of varying the proton-ionizable group's acidity to be assessed, ligands with

six different acidic functions located over the crown cavity were synthesized. These include a carboxylic acid group, four N-(X) sulfonyl carboxamide groups in which the acidity can be "tuned" by variation of X, and a very weakly acidic fluorinated alcohol group. For comparison of the proton-ionizable ligands with an analogous nonionizable extractant (MC36-MC41) with $R = H$ was also prepared.

For evaluation of the influence of proton-ionizable group positioning relative to the crown cavity, extractant series (MC42, MC43) and (MC44, MC45) were realized. In (MC42, MC43), the proton-ionizable group is located directly over the crown cavity. In (MC44, MC45), the proton-ionizable group points away from the crown cavity. For extractant series (MC42, MC43) and (MC44, MC45), the proton-ionizable groups are of the N-(X) sulfonyl carboxamide variety with $X = CH_3$ and CF_3 to provide for a substantial acidity variation. For this comparison, the 2-ethylhexyl groups were not needed, as the *n*-octyl chains confer sufficient solubility.

The proton-ionizable families (BC21–BC23) and (MC36–MC41) are not only strong extractants for cesium under alkaline conditions, but they also possess a striking switching-off effect under acidic conditions; D_{Cs} swings as much as six orders of magnitude between alkaline and acidic conditions. Under alkaline conditions, the value of D_{Cs} increases to an expected plateau (except for $R = CHCF_3OH$, whose presumed plateau occurs at unreachable alkalinity), where the ionizable protons are presumed to be quantitatively exchanged for sodium ions. At the plateau, the effective extraction reaction is thus expected to be an exchange of sodium for more strongly favored cesium, a pH-independent process. A constant plateau value of approximately 200 is reached for all N-sulfonylcarboxamide compounds. It may be seen that the pH effect is governed by the nature of the ionizable group. Among the N-sulfonylcarboxamides tested, the strength of extraction at a given pH value below the range of plateau values follows the order: X = trifluoromethyl > *p*-nitrophenyl > methyl ~ phenyl. Results for the mono crowns in chloroform were similar to the results of bis-crowns in toluene, though the magnitude of change in D_{Cs} values with pH swing was not as large. Bis-crowns exhibited less change in D_{Cs}, as the curves tend to level off at a higher value of D_{Cs} in the low-pH region, undoubtedly owing to the fact that the second crown ring is capable of extracting cesium nitrate unencumbered by the presence of the ionizable group. The authors make the important conclusion that the pH-switching effect is enhanced by a blocking effect of the ionizable group upon cesium binding. That is, the neutral ionizable group must make cesium binding unfavorable by steric or hydrogen-bonding interactions.[71]

4.3.8 PHOTOSENSITIVE CALIXARENES

Often, decomplexation of cations from extractants is difficult when strong binding ligands are used. As shown in this review, the binding ability and selectivity of most macrocyclic compounds are mainly governed by the size and shape of the cavity.[34]

Many systems are described in which changing the cavity shape by allosteric effects allows the cation binding ability and the selectivity of the receptor to be modified and controlled. For instance a photo-responsive *cis/trans* isomerizable azobenzene unit has been introduced in macrocyclic structures in order to change the receptors cavity shape, leading to a photo-control of ion extraction.

Several calix[4]arenes, including a photo-isomerizable azobenzene unit in the ether bridge, were synthesized. Two are in the cone conformation with six and eight oxygen atoms in the ether part of the bridge, respectively, and two others with four and six oxygen atoms, respectively, in which the presence of two glycolic chains requires the calixarenes to be in the 1,3-alternate conformation. X-ray structures show that the geometry of calix[4]arenes including azo groups in the crown can be tuned by modifying either the bridge length or the conformation of calixarene. However, none of these compounds can be considered as preorganized for cation complexation, because the oxygen-atom lone pairs are not all directed toward the cavity center.[73] Calix[4] arene-bis-crowns, including a photo-isomerizable azobenzene unit and six and eight oxygen atoms respectively in each ether bridge, were synthesized. The authors have shown that the *cis/trans* composition of the various compounds is dependent on the length of the glycolic chain capping the calixarene unit.[73]

Among these calixarenes, 1,3-calix[4]azobenzene crown-6 was more extensively studied. This compound is a mixture of *cis* and *trans* forms; the latter is the major form, being the more thermodynamically stable. The presence of alkali cations influences the photostationary state of the photosensitive ligand if the cations are complexed by one of the two isomers. By observing the reversibility of the photoisomerization, it is possible to determine the stability of complexes formed with the two isomers. The percentage of the *cis* isomer increases in the following order: $Na^+ < K^+ < Rb^+ < Cs^+$. The cations Na^+ and K^+ only slightly increase the percentage of the *cis* isomer under photostationary state, which suggests that these cations are moderately complexed by the *cis* form. On the contrary, the presence of Rb^+ or Cs^+ sharply increases the *cis* percent. The observed distribution ratios of Na^+, Rb^+, and Cs^+ show that rubidium and cesium are better extracted by *cis* isomer.[74,75]

4.3.9 Ion-Selective Electrodes (ISE)

Calix[4]arene-crown-6 derivatives MC7, MC8, and MC10 in the 1,3-alternate conformation, incorporated in poly(vinylchloride) membranes of CHEMFETs, exhibit high Cs^+ selectivity and Nernstian behavior. The selectivity Cs^+ over Na^+, given by $\log K^{pot}_{Cs,Na} = 3.3$, is slightly better than that observed for bis(18-crown-6) derivatives, $\log K^{pot}_{Cs,Na} = 3.0$. The CHEMFETs display a sub-Nernstian response in the presence of K^+ and NH_4^+ behavior, which can be explained, respectively, by the small difference between the stability constants of the Cs^+ and K^+ complexes and by the high ratio of NH_4^+ in favor of the membrane phase.[76]

MC2 and the three different conformers of the 1,3-diiso-propoxycalix[4]arene-crown-6 (cone, partial cone, 1,3-alternate (MC7)) were used in ion-selective electrodes (ISE) with two solvents (dibutyl sebamate and *o*-nitrophenyl octyl ether (NPOE)). As expected, the lowest detection limit was obtained for membranes containing the 1,3-diisopropoxy derivative in the 1,3-alternate conformation. To correlate the analytical results with the structural properties of the ligand and with the nature of the polymeric membrane, a multifactor ANalysis Of VAriance between groups (ANOVA) was carried out on selectivities toward monovalent and divalent ions. As for the alkali metal ions, a highly significant negative correlation ($p < 0.01$) between the $\log K^{pot}_{Cs,M}$ values and the ionic radius was found; for the smaller ions H^+,

Li⁺, and Na⁺, the four ionophores showed higher differences in selectivity than for the larger ions K⁺ and Rb⁺ as well as for alkaline earth metal ions. Better results than those previously reported with other ligands in terms of detection limits (5×10^{-7}) and $\log K_{Cs,M}^{pot}$ (4.46) were found for the 1,3-diisopropoxycalix[4]arene-crown-6 in the 1,3-alternate conformation.[77]

Four calix[4]arene dibenzocrown ether compounds MC17, MC18, MC20, and MC21 have been evaluated as cesium-selective ligands in solvent polymeric membrane electrodes. For an ISE based on MC17, potentiometric selectivities of ISEs based on MC17, MC18, MC20, and MC21 for cesium over other alkali metal cations, ammonium, and alkaline earth metal cations have been determined. For MC17-ISE, a remarkably high selectivity for cesium over sodium is observed, the selectivity coefficient $\log K_{Cs,M}^{pot}$ being ca. 5. As the size of the crown ether ring is enlarged from crown-6 (MC17) to crown-8 (MC21), the selectivity cesium over other alkali metal cations, such as sodium and potassium, is reduced successively.[57]

4.3.10 MEMBRANES BASED ON CALIXARENE CROWN-6

4.3.10.1 Transport of Cesium by Means of Supported Liquid Membranes (SLM)

Supported liquid membranes (SLM) consist of two aqueous phases separated by an organic phase. The aqueous phase, called the feed phase, contains the cations to be extracted by means of the membrane organic phase. These cations are then carried to the other aqueous phase, called the stripping phase. The organic phase, constituted by an extractant dissolved in diluent, impregnates a microporous support placed between the aqueous phases. The mass of organic phase is very low (1.5 mg cm⁻²) for a CELGARD 2500 membrane (25 μm thickness, 45% porosity). As in the University of Twente, experiments in Cadarache were carried out with the device developed by Stolwijk and implementing nitrophenyl hexyl ether (NPHE) or NPOE. These diluents were used because they lead to a stable membrane due to their very low solubility in water. Moreover, the basicity as well as the polarity of these diluents improves cation extraction by a better solvation of nitrate anions. The driving force of the process is due to the difference of the nitrate concentration in the feed phase 4 M (NaNO₃, 1 M HNO₃, or 3 M HNO₃) and in the receiving phase (deionized water).

Reusch and Cussler have shown that common ion pumping can be used to transport a salt against its concentration gradient.[78] When a secondary salt with the same anion and a low extraction constant is present in large excess, the anion gradient acts as a "pump" for the primary salt. Calixarenes displaying high affinity for cesium and showing no affinity for sodium are ideal for the transport of cesium from solutions containing sodium nitrate in large amounts (Table 4.13).

Stolwijk has reported a mathematical model that describes the initial flux as a function of the diffusion constant of the complex (D_M), the product (K_{ex}) of the association constant of the complex in the membrane and the partition ratio of the salt, the concentration of salt (a) in the aqueous phase and of the carrier (L_0) in the membrane phase, and the thickness of the membrane (d):

TABLE 4.13

Percentage of Transported Cations across the Membrane after 24 Hours

Ligands	%Cs$^+$	%Na$^+$
MC6	97.9	0.23
MC8	99.5	0.20
MC10	98.1	0.25

Note: Carrier concentration: 0.05 M, source phase: 10^{-3} M CsNO$_3$, 4 M NaNO$_3$, 1 M HNO$_3$.

$$J = \frac{D_M}{2d}\left[-K_{ex}a^2 + K_{ex}a^2\sqrt{1 + \frac{4L_0}{K_{ex}a^2}}\right] \tag{4.2}$$

To verify that carriers were not leaching from the membrane, cesium fluxes were measured for 24 h with diisopropoxy calix[4]arene crown-6 and di-NPOE calix[4]arene crown-6 (for this calixarene, the alkoxy group is replaced by a NPOE moiety) as carriers, after which both the source phase and the receiving phase were replaced. The cesium flux remained constant even after three replacements; thus it, was concluded that the carriers are not leaching from the membrane (Table 4.13).[79]

According to the Danesi model, the flux of cations through the membrane is equal to:

$$J = P_{Cs} \cdot C = \frac{D_{Cs} \cdot C}{\dfrac{D_{Cs}d_a}{D_a} + \dfrac{d_o}{D_o}} \tag{4.3}$$

where D_{Cs} is the distribution ratio of the permeating cation, d_a is the thickness of the aqueous diffusion boundary layer, d_o is the thickness of the membrane, and D_a and D_o are, respectively, the diffusion coefficient of cation in the aqueous and organic phases, and C is the concentration of transported cation. From this relation, the permeability P_{Cs} can be deduced:

$$P_{Cs} = \frac{D_{Cs}}{\dfrac{D_{Cs}d_a}{D_a} + \dfrac{d_o}{D_o}} \tag{4.4}$$

Moreover, the permeability can be deduced from transport experiments by plotting $-\log C/C_0$ versus time:

$$-\log\frac{C}{C_0} = \frac{S}{V}P_{Cs}t \tag{4.5}$$

Here, C_0 and C denote the initial concentration of cation and that of cation at time t, S is the membrane surface, and V is the volume of the feed solution.

Under certain conditions where d_a/D_a is negligible in front of d_o/D_o, P_{Cs} is proportional to D_{Cs}:

$$P_{Cs} = \frac{D_{Cs} D_o}{d_o} \tag{4.6}$$

The flux of cations is governed by the following two relations. At high cesium concentrations ($C > E/D$) (where E denotes the concentration of carrier in the membrane),

$$J = \frac{E D_o}{d_o} \tag{4.7}$$

while at lower cesium concentrations:

$$J = P \cdot C = \frac{D_{Cs} C D_o}{d_o} \tag{4.8}$$

Using the Danesi model of mass transfer, the Cadarache group was able to evaluate the permeabilities P_{Cs} (cm h^{-1}) of cesium cation through SLMs implementing different calixarenes crown-n (10^{-2} M) from acidic solutions containing large amounts of sodium nitrate to deionized water. As expected, the highest transport rates were obtained with dibenzo derivatives mono and bis (crown-6), which both display the highest hydrophobicity and cesium over sodium selectivity (Table 4.14).[10,33,80]

Repeated transport experiments, where both the aqueous feed and stripping solutions are renewed every day while the membrane remains the same as in the first run, were carried out. The decrease of the permeability P_{Cs} is explained by the partitioning of the carrier between the membrane and the aqueous solutions. Hill described the permeability decrease by the following relation:[80]

$$\log P_{Cs}^i = \log P_{Cs}^1 - (i-1)\log\left(1 + \frac{R}{K_p}\right) \tag{4.9}$$

Here, P_{Cs}^i and P_{Cs}^1 are the cesium permeability in the ith transport experiment and in the first run, respectively, and $R = (V_{feed} + V_{strip})/V_{SLM}$, V_{feed}, V_{strip}, and V_{SLM} are the volumes of feed and stripping aqueous phases and the volume of organic phase in the membrane, respectively. K_p is the apparent partition constant of the carrier between the SLM and both aqueous and stripping solutions. Values of this apparent partition constant can be deduced via linear regression of $\log P_{Cs}$ versus (i–1). They are equal to 128,100, 29,100, 106,700, and 295,000, respectively, for decyl-benzo-21-crown-7, calix[4]arene-bis(crown-6), calix[4]arene-bis(benzo-crown-6), and calix[4]arene-bis(naphtho-crown-6). Calix[4]arene-bis(crown-6) rapidly leaked off the membrane

TABLE 4.14

Permeability of Cesium through Supported Liquid Membranes

Compounds	P_{Cs}
21-Crown-7 ethers	
n-Decylbenzo-21C 7	0.09
tert-Butylbenzo-21C 7	0.09
di-Alkoxy calix[4]arenes crown-*n*	
MC4	0.034
MC2	0.4
MC6	1.6
MC7	1.3
MC8	1.9
MC12	2.1
MC14	4.3
MC5	0.05
Calix[4]arenes bis (crown-*n*)	
BC1	0.09
BC2	1.3
BC3	0.04
BC4	0.003
BC5	2.8
BC8	4.3
BC10	2.7
BC11	0.1

Note: Organic solution: Carrier 10^{-2} M in nitrophenyl hexyl ether. Aqueous feed solution: 4 M NaNO, 1 M HNO_3. Aqueous receiving solution: deionized water.

because of its low apparent partition constant, leading to membrane instability in less than 20 runs. Better stability and efficiency were observed with the more lipophilic benzo and naphtho derivatives, which present higher preorganization and hydrophobicity. Comparable behavior was achieved with the lipophilic dioctyloxy calix[4]arene-crown-6.

Small-angle neutron-scattering (SANS) experiments were performed on micellar solutions of cesium dodecylsulfate (1% w/w) in the presence of MC8 at different concentrations (0%, 3%, and 5%). An increase of calixarene concentration results in growth in size of micelles and in a strong decrease of micellar ionization factor $\alpha = Z/N$. These results confirm that dioctyl calix[4]arene(crown-6) is adsorbed at the micellar interface and entraps the cesium counterions, implying an efficient screening of the surfactant's negative charge and explaining the efficient ion transport across liquid membranes.[81]

4.3.10.2 Solid Membrane

In spite of satisfactory results in terms of durability, the main drawback to the practical application of SLMs is the observed decrease of permeability due to the progressive leaching of extractant during the successive runs. A way to overcome this drawback is to use a dense membrane containing the ligand chemically grafted on an insoluble matrix. Then, ions will be transported through the membrane by a facilitated diffusion process owing to the large solubility increase into the matrix related to the extractive strength of immobilized macrocycles. A new unsymmetrical calix[4]arene bis(crown-6) derivative was prepared for the purpose of attaching it to a silica network by a sol-gel process. Comparison of performances of SLM and solid membranes shows a sharp decrease of the selectivity for cesium over sodium attributable to the deformation of the complexing crown ring due to the constraint induced by the linking to silica network of the other crown of calix[4]arene bis(crown-6). Moreover, the diffusion and decomplexation steps are hindered by the parasitic transfer of nitrate anions, which induces a strong decrease of the transport driving force.[82,83]

4.3.11 EXTRACTION CHROMATOGRAPHY

Comparison of solvent extraction and extraction chromatography by BC5 and BC6 showed surprising differences: a high uptake of Cs by impregnated resin occurs over a broad range of 0.01–1 M HNO_3, while a sharp maximum in solvent extraction occurs at 3 M HNO_3. The equilibrium is rapidly reached and the calixarene is not washed out from the column. The loading capacity of 0.7 mg Cs/mL resin may improve upon optimization. Interference by K^+ is noticeable at higher levels.[84]

4.3.12 FLUORESCENT CALIXARENES

Although fluorescent calixarenes would be an appropriate section herein, especially as regards nuclear applications, the reader is referred to the recent and exhaustive review "Calixarene-derived Fluorescent Probes."[85]

4.3.13 TESTS OF CALIXARENES CROWN-6 ON ACTUAL RADIOACTIVE WASTE

Distribution ratios and transport were carried out on real HAW arising from dissolution of a mixed oxide of uranium and plutonium (MOX) fuel (burnup 34,650 MW d/tU), where uranium and plutonium have been previously extracted by TBP.[86] The experiments were performed in the CARMEN hot cell of CEA Fontenay aux Roses with two dialkoxy-calix[4]arene-crown-6 derivatives (diisopropoxy and dinitrophenyl-octyloxy). High cesium distribution ratios were obtained (higher than 50) by contacting the HAW solution with diisopropoxy calix[4]arene-crown-6 (0.1 M in NPHE). Moreover, the high selectivity observed with the simulated waste was confirmed for most of the elements and radionuclides (actinides or fission products: Eu, Sb, Ce, Mo, Zr, and Nd). The residual concentration or activity of elements, other than cesium, was less than 1% in the stripping solution, except for iron (2%) and ruthenium (8%); the extraction of these two cations, probably under a complexed

form, can be due to an interaction with NPHE. With MC7 and MC10, respectively, 77.5% and 86.3% of the cesium were transported from HAW to demineralized water in 9 hours. Only molybdenum and zirconium were detected in the stripping phase at very low level with the diisopropoxy calix[4]arene-crown-6 used as a carrier at a concentration 0.1 M in NPOE.

4.3.14   COEXTRACTION OF CESIUM AND TECHNETIUM

Extraction of tetrahedral pertechnetate anion from aqueous solutions using several crown ethers is well known. The coextraction of cesium (or strontium) and technetium from nuclear waste by calix[4]arene-crown-6 has been reported from alkaline media. Although technetium in its common pertechnetate form does not complex directly with crown ethers, pertechnetate extraction may be facilitated by crown ethers as the coanion of sodium (for alkaline nitrate waste). Pertechnetate at trace levels in the waste may be more than a 1000-fold more extractable than the smaller nitrate anion in ion-pair extraction processes.[87]

Recovery of technetium, present as pertechnetate in aqueous acidic solution, is of utmost importance because of its long half-life of 2.13×10^5 years and its relative mobility in the environment. The close relation between TcO_4^- and the isoelectronic perrhenate ReO_4^- makes the latter a widely used model for artificially produced technetium, which only possesses radioactive isotopes.

Calixarene crown-6 compounds, which are neutral extractants like crown ethers, are able to coextract technetium with cesium. Tests carried out with several calixarene-crown ethers (MC7, MC8, MC14, BC2, BC5, BC8, and BC10) show that the extraction of technetium, present in the aqueous phase at a concentration 10^{-5} M, is enhanced as the cesium concentration in the aqueous phase increases from 10^{-5} to 10^{-2} M. As expected, an increase of nitrate concentration prevents pertechnetate extraction in competition with nitrate anion. The extraction of technetium is only appreciable when the nitric acid does not exceed 1 M. Distribution ratios D_{Cs} (close to 8) are comparable for the various calixarenes. However, a decrease of extraction is observed for naphtho derivatives.[88,89]

Crystal structures of calix[4]arene-bis(crown-6) BC2 show that the perrhenate ion, present in excess in solution, has completely replaced the nitrate ion. The ReO_4^- ion presents the same variety of coordination modes as NO_3^- with a greater tendency to be noncoordinating. The origin of the dissociation is likely to be found in the low charge density, the high coordination number provided by the ligand, and in steric effects (the geometry of the ligand does not permit a close approach of the anion). The constancy of the binding strength and the lesser extraction of pertechnetate (or perrhenate) can be explained by the fact that those anions, which can be more distant from the calixarene than nitrate ions, are likely to be less sensitive to the presence of aromatic units on the crown, except for the bulky and very lipophilic naphtho units.[90]

4.3.15   BEHAVIOR OF CALIXARENES UNDER IRRADIATION

The use of calix[4]arene crown-6 compounds for the extraction of cesium from HAW necessitates the study of their behavior under irradiation. Calixarenes diluted

in nitrophenyl alkyl ethers were irradiated in the presence of HNO_3 (3 M) with a ^{60}Co source for 1500 hours, providing a dose of 3 MGy, equivalent to 10 years operation in a reprocessing plant. The behavior of calix[4]arene bis(crown-6) having undergone irradiation in the presence or in the absence of 3 M HNO_3 was examined by ES/MS. During irradiation of this calixarene diluted in NPOE, very few degradation products are formed, and the few are attributed to crown fragmentation products. On the contrary, the calixarene irradiated in the presence of nitric acid undergoes nitration, which leads to the formation of mono and dinitro products. These nitro groups are likely located at the para position of the phenoxy group.[91]

4.3.15.1 Identification of Nitro Derivatives

Nitro derivatives of bis-crown calix[4]arenes were prepared by reacting the latter with conc. HNO_3 at 0°C for 2.5 hours in a 1:2 mixture of 100% CH_3CO_2H/CH_2Cl_2. After evaporation of the solvents, the residue was separated by chromatography. All the products were identified by NMR, FAB mass spectrometry, and microanalysis. Whereas the structures of the mono nitro derivative (BC12), trinitro derivative (BC15), and tetranitro derivative (BC16) are easily assigned because the positions of the nitro groups are obvious, the authors were unable to choose between the two possible isomeric structures of the dinitro derivative, BC13 or BC14.[92]

The structure of the tetranitro derivative was confirmed by X-ray diffraction; in the solid state, this compound does not possess any symmetry element. The conformation of the calixarene structure is less symmetrical than for calix[4]arene(bis crown-6). The nitro groups appear to strongly modify the usual conformation of this calixarene, and a decrease in the preorganization toward cesium complexation can be expected.

Complexation measurements of the four nitro calixarenes with cesium picrates were carried out by means of NMR. Only the mononitro ligand displayed 100% complexation, while very low complexation ability was observed for the dinitro derivative (8%) and trinitro derivative (2%), and no complexation was observed for the tetranitro derivative. The decrease of complexation ability with the increasing number of nitro groups may arise from either a steric effect similar to that of *tert*-butyl groups preventing the cesium entering the crown ether or a deactivation of the oxygen donor atoms, as already observed in the case of benzocrown ethers substituted with electron-withdrawing nitro groups. The small difference in the shifts of the singlets for p-NO_2-ArH between the free mononitro derivative and the complex of this compound with cesium picrate seems to indicate that the cesium is not located close to these protons, but rather in the opposite crown cavity.[92]

Nitration of di-*iso*-propoxy calix[4]arene-crown-6 MC7 under different conditions (HNO_3/H_2SO_4, HNO_3/CH_3COOH, HNO_3/CF_3COOH) and different temperatures allowed the four nitro derivatives to be synthesized. NMR studies have suggested that nitration occurs mainly in the para position relative to the isopropoxy group, rather than in the para position relative to phenoxy. Distribution ratios were determined for several nitro derivatives of BC2 and MC7 (Table 4.15). The steric hindrance of the nitro moieties, which makes access of the cation to the complexation site difficult, is particularly evidenced by very low cesium distribution ratios for tetranitro calix[4]arene bis(crown-6) and dinitro di-*iso*-propoxy calix[4]arene crown-6. These

TABLE 4.15

Extraction of Cesium and Sodium—Cs/Na Selectivity—Competitive Extraction of Cesium in the Presence of an Excess of Sodium by Nitro Derivatives of Calix[4]arene-diisopropoxy-crown-6 and Calix[4]arene-bis-crown-6

Ligands	^{22}Na[a]	^{137}Cs[a]	^{137}Cs[b]
MC7	$<10^{-3}$	28.5	18.5
MC25	$<10^{-3}$	1.05	0.65
MC26	$<10^{-3}$	0.04	0.03
BC2	$<10^{-3}$	19.5	10
BC12	$<10^{-3}$	8.5	6
BC16	$<10^{-3}$	$6\ 10^{-3}$	$<10^{-3}$

Note: Organic phase: 10^{-2} extractant agent in 1,2-nitrophenylhexylether.

[a] Aqueous feed solution: 5×10^{-4} M MNO$_3$, 1 M HNO$_3$.

[b] Aqueous feed solution: 1 M HNO$_3$, 4 M NaNO$_3$, 10^{-6} M CsNO$_3$.

low values confirm that the nitration occurs mainly in the para position relative to the di-*iso*-propoxy position. In the para position to the phenoxy group, the decrease of distribution ratios should be less marked.[93]

Preparation of the different nitro derivatives of dialkoxy calix[4]arene crown-6, isolation, and identification of pure isomers of these derivatives should be very useful in subsequent identification of isomers arising from irradiation of calixarenes. For instance, the two isomers of the mononitro derivative (NO$_2$ para to alkoxy chain or para to phenoxy) were characterized. From the three possible isomers of the dinitro derivative, two were isolated and obtained in pure form, thus enabling interpretation of their NMR spectra. The structure of the trinitro derivative was clarified; as expected, two nitro moieties are in the para position relative to the two alkoxy chains; the third one is para to phenoxy.[94]

The radiolytic degradation of MC8 in aliphatic or aromatic solvent in contact with 3 M nitric acid, was studied by high-performance liquid chromatography directly coupled to electro-spray ionization mass spectrometry (LC/ESI-MS). More than 50 distinct degradation products were observed, and about 30 of these were identified. These compounds can be assigned to three categories, namely, products of reactions involving radical cleavage, or the addition of oxidation reactions or of aromatic substitution reactions. The major product, corresponding to substitution by a NO$_2$ group, was quantified by external standard calibration using a purified synthetic sample. Despite the observation of all these degradation compounds, MC8 appears to be remarkably stable under these drastic conditions. Combining hydrolysis (3 M HNO$_3$) and an extreme exposure to radiolysis (10^6 Gy), the total loss of MC8 reaches 33.5%, representing all the degradation compounds; of this total, nearly 20% is contributed by the various nitro compounds.[95]

4.3.15.2   MD Computation

MD simulations both in the gas phase, taking into account the influence of the nitrate counterion, and in explicit the water phase were performed on the Cs^+ and Na^+ complexes of the mononitrate derivative. From the simulations in the gas phase, it is concluded that the preferred crown loop for binding would depend on the proximity of the nitrate counterion. In a nondissociating medium, the cation should be located in the crown opposite to the nitro group; however, the binuclear complex is stable and should be observed in the presence of an excess of cesium. The presence of the nitro group is not expected to significantly modify the selectivity of the extractant, although liquid/liquid results show a weaker affinity for cesium (Table 4.15). The steric hindrance must be the origin of this decrease of affinity due to a more difficult access to the complexation site, as shown by results on the tetranitro derivative, which has no extraction properties for alkali cations.[91] This hindrance must be both to nitrate ion-pairing and to Cs binding alone, as the tests showing weakened extractants were done in a dissociating diluent (NPHE), as shown in Table 4.15.

4.3.16   Choice of a Phase Modifier for Calixarene Crown-6 Diluted in Aliphatic Hydrocarbon Diluents

The appearance of a third phase, incompatible with the process of liquid-liquid extraction, requires the use of a phase modifier to eliminate or to restrict this phenomenon by increasing the solubility of extractant in the organic phase. This modifier can also enhance the extraction ability of the extractant. Often, this phase modifier is implemented without explanations; on the contrary, the group of Oak Ridge undertook a thorough study, which will be described in the following paragraphs.

The strength of cesium extraction afforded by a lipophilic calix[4]arene-crown-6 ether extractant can be enhanced by the addition of alcohol-solvating components or "modifiers" to the solvent. The group of Oak Ridge discovered that alcohol modifiers of the type shown in Table 4.16 were especially effective with regard to enhancing cesium extraction strength by BC6 in aliphatic hydrocarbon diluents.[96] Cesium extraction strength was enhanced when the -R group contained electronegative elements such as fluorine. Modifier 1-(1,1,2,2-tetrafluoroethoxy)-3-(4-*tert*-octylphenoxy)-2-propanol (**1**) was found to possess insufficient long-term stability to alkaline conditions; the stability issue could be resolved with $-CH_2OCH_2CF_2CF_2H$ (**2**).

To investigate the effect of alcohol hydrogen-bond donor (HBD) strength in a systematic way, a series of modifiers possessing a common 4-*tert*-octylphenoxy ethanol core element were prepared, in which the properties of the substituent attached to the alcohol carbon atom were varied. These modifiers were evaluated with respect to both the cesium extraction strength they afforded when used in combination with BC6 and the HBD strength of the solvent as assessed using the solvatochromic parameter E_T^N.

The E_T^N values obtained at 25°C for solvents comprised of BC6 (0.005 M), modifiers **1–5**, and 4-*tert*-octylphenol (0.25 M) in 1,2-dichloromethane (1,2-DCE) show a good correlation with D_{Cs} values (Table 4.16). Both the D_{Cs} and E_T^N values for **1–5** increase as the expected acidity of the alcohol increases, based on increasing the

TABLE 4.16

Cesium Distribution Ratios and Corresponding E_T^N Values for Solutions of BOBCalixC6 at 0.005 M in 1,2-DCE, as a Function of Modifier at 0.25 M

Modifier[a]	D_{Cs}	E_T^N
None	1.20 ± 0.06	0.336 ± 0.006
$R = -CH_2OCH(CH_3)_2$	1.16 ± 0.06	0.387 ± 0.006
$R = -CH_2OCH_2CH_3$	1.23 ± 0.06	0.411 ± 0.004
$R = -CH_2OCH_2CF_3$	1.72 ± 0.09	0.476 ± 0.005
$R = -CH_2OCH_2CF_2CF_2H$	2.11 ± 0.10	0.490 ± 0.012
$R = -CH_2OCF_2CF_2H$	2.72 ± 0.14	0.520 ± 0.005
$R = -CF_3$	5.28 ± 0.26	0.609 ± 0.008
4-*tert*-Octylphenol	13.3 ± 0.7	0.649 ± 0.023

Note: Aqueous phase: 1 M NaNO$_3$, 1.0 mM CsNO$_3$, and ^{137}CsNO$_3$ at trace level. O/A = 1, T = 25°C.

[a] The R groups are appended to the cone unit.

number and proximity of the fluorine atoms to the hydroxyl group. Bringing the 1,1,2,2-tetrafluoroethyl moiety closer to the alcohol group results in further increases in both D_{Cs} and E_T^N, and simply attaching a trifluoromethyl group directly to the alcohol carbon atom results in a dramatic increase in both D_{Cs} and E_T^N. The strongest extraction is afforded by the strongest acid, 4-*tert*-octylphenol, which also gives the highest E_T^N value.

Some of the modifiers in this study (**1–5**) were also evaluated in the isoparaffinic diluent Isopar L for cesium extraction performance from a Savannah River waste simulant. The effect the modifiers have on the cesium distribution ratio in aliphatic diluents is more pronounced than it is in polar diluents, such as 1,2-DCE, previously used. The cesium distribution results are shown in Table 4.17 alongside those obtained from 1 M NaNO$_3$ in 1,2-DCE.

The observed trend in D_{Cs} obtained from the alkaline waste simulant by solvents using Isopar L diluent is the same as that observed from 1 M sodium nitrate using 1,2-DCE diluent. However, the differences between the stronger fluorinated modifiers and the weaker nonfluorinated modifiers are much more pronounced. This could be due to the fact that the stronger modifiers may be sufficiently acidic to be partly deprotonated when contacted with the alkaline simulant. The alkoxide form of the alcohol would serve as the counteranion to the extracted cesium, eliminating the need for an anion from the aqueous phase (e.g., nitrate) to be coextracted, and, in turn, making it energetically easier to transfer the cesium cation to the solvent phase, hence increasing the cesium distribution ratio.

The cesium distribution ratio afforded by alcohol modifiers, such as **1**, dissolved in hydrocarbon diluents, such as Isopar L or dodecane, increased dramatically as the concentration of the modifier increased from below 0.10 M to 1 M, then leveled off.

TABLE 4.17

Cesium Distribution Ratios for (a) Extraction of Cs from 1 M NaNO₃ Using Solutions of BC6 (0.005 M) and Modifier (0.25 M) in 1,2-DCE, and (b) Extraction of Cs from an Alkaline Waste Simulant Using Solutions of BC6 (0.010 M) and Modifier (0.20 M) in Isopar L

Modifier[a]	D_{Cs} in DCE (±5%)	D_{Cs} in Isopar L (±5%)
None	1.20 ± 0.06	Not measured
(**5**) $R = -CH_2OCH(CH_3)_2$	1.16 ± 0.06	$7.08 \ 10^{-2}$
(**4**) $R = -CH_2OCH_2CH_3$	1.23 ± 0.06	$9.10 \ 10^{-2}$
(**3**) $R = -CH_2OCH_2CF_3$	1.72 ± 0.09	2.82
(**2**) $R = -CH_2OCH_2CF_2CF_2H$	2.11 ± 0.10	6.35
(**1**) $R = -CH_2OCF_2CF_2H$	2.72 ± 0.14	11.18
$R = -CF_3$	5.28 ± 0.26	Not measured
4-Tert-octylphenol	13.3 ± 0.7	Not measured

Note: Aqueous phase: 1 M NaNO₃, 1.0 mM CsNO₃, and ¹³⁷CsNO₃ at trace level. O/A = 1, T = 25°C.

[a] The R groups are appended to the 1-position of 2-(*p-tert*-octylphenoxy) ethanol.

TABLE 4.18

Cesium Distribution Ratios and Corresponding E_T^N Values for 1,2-DCE Solutions of BC6 at 0.005 M as a Function of Modifier (1) Concentration

Modifier[a]	D_{Cs}	E_T^N
None	1.20 ± 0.06	0.336 ± 0.006
0.030	1.33 ± 0.07	0.412 ± 0.004
0.100	1.77 ± 0.09	0.471 ± 0.009
0.250	2.72 ± 0.14	0.520 ± 0.005
0.500	4.03 ± 0.20	0.557 ± 0.021
1.00	6.64 ± 0.33	0.590 ± 0.005

Note: Aqueous phase: 1 M NaNO₃, 1.0 mM CsNO₃, and ¹³⁷CsNO₃ at trace level. O/A = 1, T = 25°C.

This general phenomenon was observed when extracting cesium from neutral sodium nitrate as well as from alkaline solutions. In 1,2-DCE, however, the increase in D_{Cs} is less pronounced (possibly due to 1,2-DCE's higher polarity, which affords moderate D_{Cs} at low modifier concentrations). Nevertheless, both D_{Cs} and E_T^N increase as a function of the concentration of the alcohol modifier **1**, as shown in Table 4.18.

As the concentration of the modifier is increased, the net polarity of the solvent and accordingly both the cesium distribution ratio and the magnitude of the hypsochromic shift of the dye increases. The relationship between D_{Cs} and E_T^N as a function of modifier **1** concentration is nonlinear.

In conclusion, cesium extraction strength for the set of alcohol modifiers examined in this study correlates well with the solvatochromic parameter E_T^N, strengthening the hypothesis that extraction effectiveness is strongly linked to the HBD ability of the modifier. The presence of electron-withdrawing substituents attached to the alcohol carbon atom increase the HBD strength of the alcohol, and the electron-withdrawing power of the substituent increases as the number of electronegative fluorine atoms proximal to the hydroxyl group increases. The relationship between the modifier HBD strength and cesium extraction efficiency suggests that solvation of the BC6-Cs anion complex may be occurring via hydrogen-bonding interactions. In a recent paper, Sieffert confirmed this hypothesis by a MD study.[97]

Much stronger extraction may be obtained through the dual-host concept, in which the binding of the cation and anion by separate receptors compensates their unfavorable partitioning. In addition to stronger extraction, mixing two receptors offers great flexibility in the choice of receptors and in the separate control of cation and anion selectivity.

The addition of sulfonamide H-bond donors to the calix[4]arene-bis (benzo crown-6) enhances cesium extraction into 1,2-dichloroethane.[98,99] Enhancement with the simple monosulfonamide MSA was weak, while the two potentially bidentate disulfonamides, DSA1 and DSA2, yielded significantly stronger extraction. The two extractants acting together yield a stronger extraction than the sum of the two extractants acting independently (synergistic effect); thus, there must exist a new reaction involving the two extractants (cation receptor B and anion receptor R):

$$Cs_{(aq)}^+ + X_{(aq)}^- + B_{(org)} + R_{(org)} \rightleftharpoons CsB_{(org)}^+ + RX_{(org)}^- \tag{4.10}$$
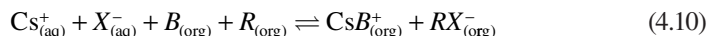
The 1:1 binding of cesium having been previously established, it was expected that the low organic-phase concentrations would disfavor ion pairing. The following equation quantifies the enhanced extraction in terms of the added Gibbs energy term for anion binding.

$$\Delta G_{ex}^0 = \Delta G_p^0(M^+) + \Delta G_{bind}^0(M^+) + \Delta G_p^0(X^-) + \Delta G_{bind}^0(X^-) \tag{4.11}$$

Here ΔG_p^0 and ΔG_{bind}^0 denote, respectively, the Gibbs energy for the partitioning step and the Gibbs energy for the binding step of cation M^+ and anion X^-.

The synergistic enhancement upon adding an anion receptor to a given cation receptor may be predicted from the anion-binding constant obtained under suitably analogous conditions. Based on 1:1 binding of the extracted ions according to Equation 4.10, an equation has been derived for conversion of the corresponding homogeneous anion-binding constants D_{cpx} to synergistic factors (SF) under the assumption that the

anion host effects negligible extraction by itself. Other key assumptions included low loading of the two hosts and negligible ion pairing. The relationship is:

$$\frac{D_{Cs\,syn2}}{D_{Cs\,B2}} = \frac{\left[Cs_{(init)\,R=0}\right]}{\left[Cs\right]_{(init)}} \frac{\left[NO_3^-\right]_{(aq)}}{\left[NO_3^-\right]_{(aq)R=0}} \frac{\left[B\right]}{\left[B\right]_{R=0}} \frac{\left[\Phi D_{Cs\,syn}+1\right]}{\left[\Phi D_{Cs\,synR=0}+1\right]}(1+D_{cpx}[R]_{(org)}) \quad (4.12)$$

The SF is given as SF = D_{Cs} syn/D_{Cs} B, the ratio of D_{Cs} obtained under synergistic conditions versus D_{Cs} obtained for the calix-crown alone. The variable Φ is the organic-to-aqueous phase volume ratio. The absence of an anion receptor is indicated by subscript $R = 0$, and the subscripts init, aq, and org refer to initial, aqueous, and organic.

A comparison of predicted and experimental SF for the experiment with calix-crown and sulfonamides shows partial agreement; an adequate agreement was obtained for values of SF up to 33. The sulfonamide receptors did nothing to perturb the Hofmeister bias except to attenuate it. They acted rather like HBD solvating agents than anion receptors, which tends to agree with structural results that show that the disulfonamides are not preorganized. To reverse the Hofmeister bias, the thermochemical analysis requires that the anion binding more than compensates for the unfavorable anion partitioning, and to escape completely from any Hofmeister bias, highly complementary and net strong interactions with selected anions must take place.

Pedersen and Frensdorff studied the binding and extraction of the cation by crown ethers, which require coextraction of an anion. Without the presence of an anion host, solvation directs selectivity, giving rise to Hofmeister bias selectivity favoring low anion charge density. Anions initially in aqueous solution must be dehydrated (at least partially) and are then resolvated in the solvent phase. Empirically, the HBD ability of the solvent medium is the single most important determinant of the solvation of small, inorganic anions.[100]

The stoichiometry of complexes involved in the extraction of CsNO$_3$ by BC6 was fairly straightforward for the metal, anion, and calixarene; such was not the case for the alcohol-based modifiers.[99,101] Three different alcohols, **1**, octylphenoxy ethanol, and *n*-octanol were investigated in these studies. Modifier concentrations below 0.03 M were not run because of the insolubility of BC6. The addition of moderate concentrations of the modifiers increases extraction, and the order of modifier strength goes in the same order as expected HBD acidity: **1** > octylphenoxy ethanol > *n*-ethanol. By a mass-action analysis of extraction data, it was deduced that the formation of 1:1:1:*n* metal:anion:calixarene:modifier complex species occurs, together with aggregates of the modifier and the latter with the calixarene. Results of equilibrium modeling, consistent with aggregation of the alcohol molecules with each other and with the calixarene-cesium nitrate complexes are supported by electrospray mass spectrometry and by X-ray crystallography showing, respectively, that the alcohol:anion adducts contain several alcohol molecules and that hexameric aggregates are present in the solid state for a derivative of one of the alcohol modifiers used for solvent extraction. In conclusion, the authors can model all the data for each modifier, including all

concentrations, assuming the formation of 1:1:1:*n* metal:anion:calixar-ene:modifier, along with the aggregation of the modifier, and the aggregation of the latter with the calixarene.

4.3.17 PROCESS FOR EXTRACTION OF CESIUM

4.3.17.1 Process for Extraction of Cesium from Acidic High-Activity Level Waste

In the previous studies, calixarenes were not directly usable in a liquid-liquid extraction process, because used in a diluent (nitro phenyl hexyl ether), the hydrodynamic properties were incompatible with such a process. The system has been modified in order to satisfy the following criteria: density, viscosity, kinetics, and absence of a third phase.[102]

Two systems based on crown-calixarenes, able to be used in liquid-liquid extraction process were chosen. Both systems use a modifier in the organic phase to avoid the occurrence of a third phase in the TPH (diluent used at the reprocessing plant of la Hague for the PUREX process) and ensure a sufficient cesium extraction.

System 1 is based on MC8 (0.065 M) but needs the addition of TBP (1.5 M) in the organic phase and the introduction of oxalic acid in the liquid waste to prevent the extraction of zirconium by TBP. It has been pointed out that the addition of oxalic acid is necessary for the PALADIN process, previously implemented for the extraction of minor actinides. The addition of TBP which extracts several cations, leads to a lesser selectivity of the solvent.

System 2 is based on 1,3-(2,4-di-ethyl-heptyloxy)-2,4-calix[4]arene-crown-6 (MC9) (0.1 M), more difficult to synthesize, but the monoamide (methyloctyl-1,2-dimethylbutanamide) (1 M) used as a phase modifier does not alter the selectivity of the organic phase.

4.3.17.2 Flowsheets, Experiments Realized with Simulated and Actual Waste

After acquisition of experimental data, flowsheet calculations were carried out. A theoretical recovery of cesium was fixed at 99.99%. Hydraulic tests and chemical transfer tests were first carried out with centrifugal contactors, then with pulsed columns, first on simulated effluents and then on actual effluents.

In the tests carried out in centrifugal extractors, the extraction and recovery of cesium higher than 99.99% were obtained on simulated effluents, with a very good coherence between calculated flowsheets and experimental results.[102] Tests confirmed the feasibility of the implementation of the "cesium process" in pulsed columns, the latter representing the most adapted contactors for the industrial implementation to overcome the drawback due to the presence of solid matter in waste to be treated.

For cesium extraction, "Couette" columns have been used. The operations in such a contactor can be easily extrapolated to a pulsed column, and the quantity of implemented solvent is less important. The hydrodynamic behavior is satisfactory for the two calixarene systems studied in spite of a more "emulsion-prone" behavior with system 2. The selectivity obtained compared to other elements is excellent.

```
┌─────────────────────────┐
│ Calix octyl 0.062 M/    │
│     TBP 1.5 M/TPH        │
├─────────────────────────┤
│        40 mL/h           │
└─────────────────────────┘
```

Extraction   Scrub   Stripping

Cs/HNO₃

F.P. without Cs/ HNO₃

H.A Feed
HNO₃4 M
Oxalic acid 0.2 M
F.P.
66 mL/h

Scrub feed
HNO₃ 4 M
4 mL/h

Strip feed
HNO₃ 0.05 M
40 mL/h
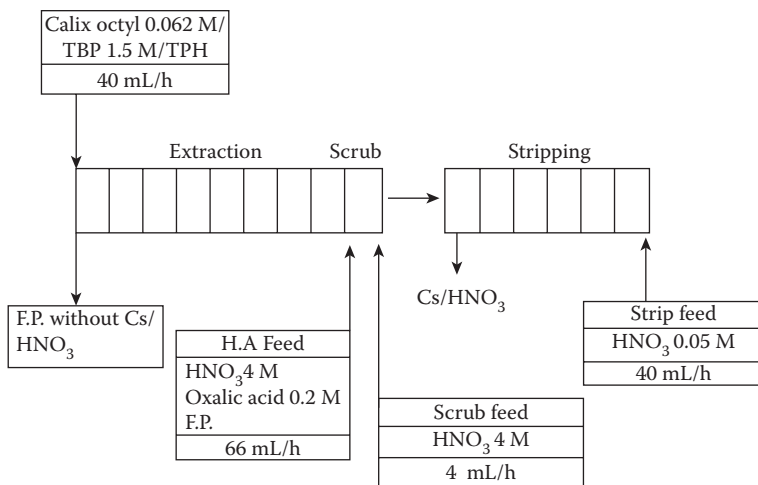
FIGURE 4.3 Flowsheet of cesium process for extraction of cesium from acidic high-activity level waste with MC8 (0.062 M) diluted in the mixture TBP (1.5 M)/TPH.

A complete flowsheet relative to each system was tested on a real effluent (DIAMEX raffinate with oxalic acid due to the lower selectivity of system 1 in the ATALANTE facility (CEA-Valrhô) with centrifugal contactors. An example of a flowsheet is given in the case of system 2 (relating to MC8 with TBP modifier) (Figure 4.3). The two selected systems (MC8/TBP, MC9/monoamide) display comparable performances in terms of efficiency. The extraction percentage obtained for cesium is 99.9%, the discharged solvent contains less than 0.01% cesium. A hydrodynamic behavior more favorable in some cases for system 1 (MC8/TBP) and a higher selectivity for system 2 (MC9/monoamide) are observed. The scientific feasibility of a cesium-selective extraction by calixarenes was thus demonstrated on an actual effluent.[103]

When the hot tests on genuine waste were undertaken, MC14 were synthesized in insufficient quantity to prepare for these tests or to be used. The dibenzo-calixarenes, such as MC14, have several advantages, as they are the best fitted to host cesium, and, in addition, they allow a lower extraction of the nitric acid in competition with cesium. Moreover, they are more lipophilic and could be more soluble in diluents such as TPH. In spite of the fact that alkyl substitution on the benzo group provokes nitration of the benzo groups, their solubility in these diluents can be increased by using long-chain alkyl benzo. Following the studies carried out in Oak Ridge (see above), it would be interesting to associate these calixarenes with modifiers such as alcohols or phenols, compounds that do not lead to a decrease of the selectivity of calix-crown-6 compounds. Unfortunately, as the project was postponed, these tests have never been realized.

Zhang proposed the chromatographic partitioning of cesium from HNO₃ (4 M) to implement the calixarene MC9 with TBP immobilized on a macroporous silica-based polymeric composite.[104] The authors do not explain the choice of the calixarene MC9, more difficult to synthesize than classical dipropoxy or octyloxy calix[4]

arenes, which were chosen by Simon for their higher solubility in aliphatic diluent. Satisfactory results in terms of adsorption of rubidium and cesium and elution by water were obtained.

4.3.17.3   Process for Extraction of Cesium from Alkaline High-Activity Level Waste

For the removal of cesium from high-level radioactive waste (HLW) stored in the underground tanks at the U.S. Department of Energy's (DOE) SRS, the Oak Ridge group initially proposed a solvent based on the calix[4]arene-bis-(*tert*-octylbenzo-crown-6) (BC6) and the phase modifier 1-(1,1,2,2-tetrafluoroethoxy)-3-(4-*tert*-octylphenoxy)-2-propanol (Cs-3) in the isoparaffinic diluent Isopar L.[105,106] The function of the phase modifier is to improve the overall solvation of BC6 and its ion-pair complexes, thereby increasing BOBCalixC6 solubility, increasing cesium extraction strength, and helping prevent third-phase formation. The insufficient alkaline stability of (Cs-3) phase modifier possessing the -CF$_2$CF$_2$H moiety, which reacts with itself following long-term exposure to warm alkali metals, led Bonnesen to prepare a series of phase modifiers possessing the -OCH$_2$CF$_2$CF$_2$H moiety. Of the four modifiers examined (containing the alkyl groups *tert*-octyl, *tert*-butyl, *tert*-amyl, or *sec*-butyl), the modifiers possessing the *sec*-butyl group (Cs-7SBT and the more purified analog Cs-7SB), were found to possess the best overall balance of properties with respect to cesium distribution and phase-coalescence behavior, resistance to solid hydrate formation, and cleanup following degradation (ability to wash out the phenol degradation product). The solvent composed of calix[4]arene-bis(*tert*-octylbenzo-crown-6) (BC6) (0.01 M), 1-(2,2,3,3-tetrafluoropropoxy)-3-(4-*sec*-butylphenoxy)-2-propanol (Cs-7SBT) at 0.50 M, and tri-*n*-octylamine (TOA) at 0.001 M, in Isopar L was retained as the prototype (though not the final) solvent of the Caustic Side Solvent-Extraction (CSSX) process.

The CSSX process flowsheet for the decontamination of high-level waste was demonstrated in a 33-stage, 2-cm contactor apparatus at the Savannah River National Laboratory (formerly the Savannah River Technology Center).[107] Simulated SRS average waste, simulated Tank 37H/44F composite waste, and actual Tank 37H/44F composite high-level waste were processed in three tests lasting 6, 12, and 48 hours, respectively.

The results of testing demonstrate that the process is capable of reducing the ^{137}Cs activity in high-level waste to below the Saltstone process requirement of 45 nCi/g. For Tank 37H/44F composite waste, the Saltstone requirement implies a decontamination factor (DF) of 13,000. During the actual-waste processing test, 106 L of Tank 37H/44F composite waste were processed, and the composite decontaminated raffinate met the Saltstone requirement. Instantaneous DFs as high as 2 million were achieved during stable hydraulic conditions. The DF values achieved the test objective for waste decontamination and demonstrated that minor chemical components present in actual tank waste do not adversely affect process performance.[107]

The results indicate that the process is robust and can tolerate and recover from disruptions in operation. In addition, hydraulic stage efficiencies in the extraction and strip sections were greater than the 80% design requirement. Test results showed that the loaded solvent could be stripped of cesium and recycled to the process with

an average solvent DF of 154,000 over the course of the entire 48-hour test. As expected, it was further demonstrated that heating of the strip section to greater than 30°C increases stripping performance markedly. A steady-state CF of 14.4 was achieved for Tank 37H/44F high-level waste. Uncertainties in the process flow measurements prevented achievement of the target CF of 15. Adjustment of the process flow in the latter hours of the high-level waste test allowed the CF to approach 15 to within 5% without exceeding the maximum throughput of the contactors.

Several specific studies for the development of CSSX process were carried out by the Oak Ridge team to correct some minor defects observed during tests or to improve the reliability of the process.[108]

The solvent was loaded with ^{137}Cs and subsamples were stored on a shaker table while in contact with the extract, scrub, or strip aqueous phases. Evidence of solvent degradation was evaluated for exposure times of 83 days; this resulted in estimated solvent doses of 1.24 Mrad, equivalent to the dose expected to be received during 16.5 years of operation at the SRS plant.

Distribution of cesium in the batch tests remained constant within experimental error; in addition, no third-phase formation was observed. The solvent concentrations of calix[4]arene-bis-(*tert*-octylbenzo-crown-6) and 1-(2,2,3,3-tetrafluoropropoxy)-3-(4-*sec*-butylphenoxy)-2-propanol remained constant within experimental error. Solvent degradation with irradiation was evidenced by a decrease TOA concentration decrease and an degradation product (4-*sec*-butylphenol) increase in the solvent phase. No decline in extraction or scrubbing performance of the irradiated solvents was observed. The stripping performance of the solvent was seriously impaired with irradiation; however, a mild caustic wash and replenishment of the TOA concentration restored the ability to strip the irradiated solvent.

Although solvent samples have been observed for approximately one year without any solids formation, work was completed to define a new solvent composition that was thermodynamically stable with respect to solids formation and to expand the operating temperature with respect to third-phase formation.[109] Chemical and physical data as a function of solvent component concentrations were collected. The data included BC6 solubility; cesium distribution ratio under extraction, scrub, and strip conditions; flowsheet robustness; temperature range of third-phase formation; dispersion numbers for the solvent against waste simulant, scrub and strip acids, and sodium hydroxide wash solutions; solvent density; viscosity; and surface and interfacial tension. These data were mapped against a set of predefined performance criteria. The composition of 0.007 M BC6, 0.75 M 1-(2,2,3,3-tetrafluoropropoxy)-3-(4-*sec*-butylphenoxy)-2-propanol, and 0.003 M TOA in the diluent Isopar L provided the best match between the measured properties and the performance criteria.

Experiments suggested a potential cesium-stripping problem in the CSSX process due to the presence of nitrite in the waste stimulant. The true reason for the cesium-stripping problem was, in fact, the presence of surfactant (sodium mono- and dimethyl naphthalene sulfonate) that can partition into the organic phase on extraction and then retain cesium upon stripping. To overcome this drawback, the authors proposed a caustic wash with a moderate concentration of sodium hydroxide sufficient to remove enough of these lipophilic anions to rejuvenate the solvent, therefore,

preventing any build-up. In addition, the authors studied the risk of forming nitrated organics that can build up in the solvent during operation of the CSSX process when the solvent is exposed to acidic nitrate solutions. They concluded that this risk was negligible.[110,111]

The developed cesium and potassium extraction model, based on extraction data obtained from simple aqueous media, was tested to ensure the validity of the prediction for the cesium extraction from actual waste.[112] The predicted values agreed with the measured values for the simulants; predicted values also agreed, with some exceptions, with measured values for the tank wastes. Discrepancies were attributed, in part, to the uncertainty in the cation/anion balance in the actual-waste composition, but likely more so to the uncertainty of the potassium concentration in the waste, given the demonstrated large competing effect of this metal on cesium extraction. It was demonstrated that the upper limit for the potassium concentration in the feed should not exceed 0.05 M, in order to maintain suitable cesium distribution ratios.

In October 2001, the USDOE announced its decision to implement the CSSX process, developed at Oak Ridge National Laboratory, for removing the radioactive fission product ^{137}Cs from high-level waste. Approximately 34 million gallons of waste left over from nuclear weapons production are stored in tanks at the SRS. Over 31 million gallons of that waste is solid or dissolved salts in which ^{137}Cs is the primary radioactive contaminant, comprising more than 98% of the total radioactivity in the salt. To remove cesium, the Modular Caustic-side Solvent-Extraction Unit (MCU) has been built at the SRS. Operations of this pilot-scale unit began in May 2008, and the separated ^{137}Cs stream, concentrated approximately 14-fold, is being vitrified. A larger facility, the Salt Waste Processing Facility, with 3–6 times the throughput of the MCU is in construction.

In the CSSX process, the solvent is contacted with the cesium-rich aqueous waste solution in an extraction stage to remove the cesium. Following separation of the aqueous and organic phases, the aqueous waste solution exits the MCU as a cesium-depleted effluent stream to be made into a grout. The solvent goes to a scrub stage where it is contacted with 0.05 M nitric acid solution to remove sodium, potassium, and other soluble salts, including any trace levels of aluminum, iron, or calcium. Neutralization of any hydroxide carryover from the waste also occurs in the scrub stage. The metals' removal and hydroxide neutralization are essential for a robust stripping-stage operation. The scrubbed cesium-laden solvent proceeds to a stripping stage, where it is contacted with 0.001 M nitric acid solution to remove the cesium. The nitric acid solution leaves the MCU as a cesium-rich effluent to be incorporated into glass. The solvent from the stripping stage moves to a wash stage, where it is contacted with 0.01 M sodium hydroxide solution to remove residual impurities and any solvent-degradation products before recycling to the extraction stage (Figure 4.4). The MCU will inevitably have variations in process parameters, which will impact the process performance by changing the final cesium concentration. This study evaluated the impact of parameter changes on process performance using a Spreadsheet Algorithm for Stagewise Solvent-Extraction (SASSE) model to help define acceptable ranges for the MCU process parameters. The SASSE model (developed at Argonne National Laboratory) outputs indicate that broad changes in
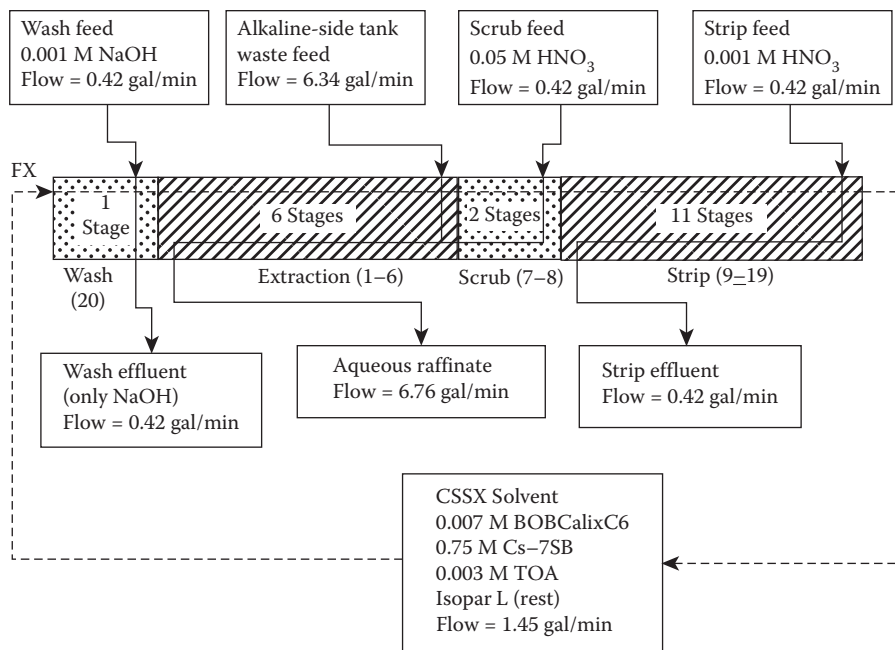
FIGURE 4.4 CSSX flowsheet for extraction of cesium from alkaline high-activity level waste.

the MCU process parameters for the extraction, scrub, and strip stages will not result in the final ^{137}Cs concentration exceeding the process target.[113]

4.3.18 Process for Coextraction of Cesium and Strontium

Extraction of strontium from acidic medium or from acidic medium containing large amounts of sodium nitrate by dicyclohexano-18-crown-6 derivatives and, particularly, its lipophilic analog with a *t*-butyl group appended to each cyclohexane rings DtBuC18C6, was extensively studied by Horwitz (SREX process).[114–116]

Laboratory experimentation having indicated that the SREX process was effective for partitioning ^{90}Sr from acidic radioactive waste solutions located at INL, these laboratory results were used to develop a flowsheet for countercurrent testing of the SREX process with dissolved pilot plant calcine.[117] Testing was performed using 24 stages of 2-cm diameter centrifugal contactors. Dissolved calcine spiked with [85]Sr was used as feed solution for the testing. The flowsheet tested consisted of an extraction section employing DtBuC18C6 (0.15 M) and TBP (1.5 M) in Isopar L, a 1.0 M $NaNO_3$ scrub section to remove extracted potassium from the SREX solvent, a 0.01 M HNO_3 strip section for the removal of strontium from the SREX solvent, a Na_2CO_3 (0.01 M) wash section to remove degradation products from the solvent, and a rinse section HNO_3 (0.1 M). The described flowsheet successfully extracted [85]Sr from the dissolved pilot plant calcine with a removal efficiency of 99.6%. Distribution ratios for [85]Sr ranged from 3.6 to 4.5 in the extraction section. With these distribution ratios,

a removal efficiency of approximately >99.99% was expected. It was determined that the lower-than-expected removal efficiency can be attributed to a stage efficiency of only 60% in the extraction section.

For the first time, to simultaneously extract cesium and strontium, Gerow proposed the coextraction of cesium and strontium by mixing two crown ethers, *bis*-(4,4'(5')-[1-hydroxy-2-ethylhexyl]-benzo)-18C6 (DHEHB18C6) and *bis*-(4,4'(5')-[1-hydroxyheptyl]-cyclohexano)-18C6 (DHHC18C6), specific extractants of cesium and strontium, respectively.[118–120] These crown ethers were dissolved in a mixture of nonylnaphthalene-sulfonic acid and TBP in kerosene. The crown compounds were found not to be sufficiently strong complexing agents to extract these metals from a nitric aqueous phase. However, the use of large organic soluble anions, which also functioned as liquid ion exchangers, made it possible to extract cesium from 3 M HNO_3. The use of 0.02 M DHHC18C6 diluted in the mixture 0.076 M (5 vol %) didodecylnaphthalene sulfonic acid (DNS)-27 vol % TBP-68 vol % kerosene gave the most favorable results for cesium extraction. A relatively low distribution ratio of 2.0 was obtained for the cesium extraction from 3 M HNO_3. Strontium is not extracted significantly at this acid concentration, while in the low acidity region, strontium is extracted by a liquid ion-exchange mechanism, and the addition of a crown ether does not significantly improve the distribution ratios.

Dozol proposed the removal of these nuclides from acidic waste containing large amounts of sodium by implementing an SLM containing both tBuB21C7 and DC18C6. The removal of cesium was incomplete due particularly to an insufficient selectivity cesium over sodium of tBuB21C7.[121–124]

Riddle mixed DtBuC18C6 with the calixarene-crown-6 used at Oak Ridge. The combination of DtBuC18C6, BC6, and Cs-7SB modifier in Isopar L proved to be an effective mixed solvent for the extraction of cesium and strontium from acidic nitrate media.[125] The synergistic properties for the extraction of strontium with this new mixed solvent show that not only can it be used for simultaneous extractions, but also for strontium removal alone. The combination of DtBuC18C6, BC6, and Cs-7SB modifier in Isopar L shows synergistic extraction of strontium while maintaining high cesium extraction. This synergy is due to the Cs-7SB modifier, whereas there is a slight antagonistic effect between the crown ether and calixarene-crown. The distribution ratios of both cations are temperature dependent:

$$D_{Sr} = 8.8, D_{Cs} = 7.7 \text{ at } 20°C, D_{Sr} = 25.0 \text{ and } D_{Cs} = 32.7 \text{ at } 25°C$$

This process, allowing coextraction of strontium and cesium, has been named the Fission Product Extraction process (FPEX).

Delmau proposed the combined extraction of cesium and strontium from caustic wastes by adding a crown ether and a carboxylic acid to the CSSX solvent.[126] The classical DtBuC18C6 and one carboxylic acid were combined with the components of the CSSX solvent optimized for the extraction of cesium, allowing for the simultaneous extraction of cesium and strontium from alkaline nitrate media simulating alkaline high-level wastes present at the SRS. The promising results of these batch tests showed that the system could reasonably be tested on actual waste.

4.4 EXTRACTION OF FISSION PRODUCTS OTHER THAN CESIUM

4.4.1 EXTRACTION OF STRONTIUM AND BARIUM

Previously, we saw that the extractants used for the extraction of strontium were DC18C6 derivatives or dicarbollide derivatives. Strontium can be effectively extracted with a synergistic mixture of dicarbollide and polyethylene glycols or crown ethers. A drawback of this process is the use of high-polarity diluents, such as nitrobenzene or chlorinated compounds, in order to solubilize the mixture of the extractants.[127]

Within the framework of the project granted by the EC, extractants of strontium based on calixarenes were synthesized in the hope of finding more efficient compounds in terms of effectiveness and selectivity than those previously quoted. In particular, these compounds, because of their poor selectivity for strontium over sodium, do not allow strontium to be extracted from liquid waste containing large amounts of sodium.[16,17]

4.4.1.1 *p-t*-Butyl calix[*n*]arene (di-*N*-alkyl)amide and Calix[*n*]arene (di-*N*-alkyl)amide

Several classes of synthesized calixarenes bearing several moieties (ether, ester, and amide derivatives), were tested for the extraction of strontium picrates (from aqueous solutions into dichloromethane).[128] Only a few of them show appreciable extraction levels. The *p-t*-butyl calix[6]arene hexa(di-*N*-ethyl)amide (CA4) shows a very high extraction level of alkaline earth cations with respect to alkali metal cations. Moreover, dealkylation of the calix[6]arene hexa(di-*N*-ethyl)amide (CA5) decreases the extraction of both sodium and strontium. As this decrease is much more important for sodium than for strontium, the Sr/Na selectivity, which increases from 3.12 to 9.4, is better than that achieved for DC18 derivative under the same conditions (8.7). These results were confirmed by extraction of strontium (5×10^{-4} M) from 1 M HNO_3 solutions, where it was found that *p-t*-butyl calix[4]arene tetra(di-N-ethyl) amide (CA2) (10^{-2} M in NPOE) extracts only sodium ($D_{Na} = 12.3$, $D_{Sr} < 0.001$).

Increasing the size of calixarenes favors the extraction of strontium and leads to a decrease of sodium extraction. For *p-t*-butyl calix[5]arene penta(di-*N*-pentyl)amide (CA3) (10^{-2} M in NPOE), $D_{Na} = 0.79$, $D_{Sr} = 1.5$. For *p-t*-butyl calix[6]arene hexa (di-*N*-ethyl)amide (CA4) (5×10^{-3} M in NPOE), $D_{Na} = 0.05$, $D_{Sr} = 3.8$. Under the same conditions (HNO_3 1 M), this compound displays higher selectivity than DC18C6.

Extraction data for alkali and alkaline earth cations showed that the replacement of two distal tertiary amides of the *p-tert*-butyl calix[4]arene tetra(di-*N*-ethyl)amide (CA2) by secondary or primary amides (CA1) leads to a sharp decrease of the extraction of these cations.

Quantum mechanis (QM) calculations showed that the interaction energy between strontium and amide carbonyl groups increased in the expected sequence: primary < secondary < tertiary amides, but could not explain the difference of complexation between (CA1) and (CA2), in particular in chloroform.[129] Another hypothesis based on the loss of internal H-bonds with the NH_2 protons was also rejected. MD simulations of $Sr(Pic)_2$ complexes of (CA1) and (CA2) for 1 ns at the water/chloroform

interface showed that (CA1) is much more surface active and attracted by water than (CA2). Complexes of the latter are lipophilic enough to be extracted to the organic phase, while those of (CA1) remain trapped at the interface. This behavior casts doubts on the interpretation of extraction experiments that use only traces of extractants and ions. It is important to perform extraction at different ligand concentrations, when the solubility of the latter allows it. Another consequence is that the extraction should be facilitated by surface-active species (for instance, lipophilic anions such as dicarbollides, picrates, fatty acids, or neutral surfactants).[17]

The X-ray structure of the L·Sr(Picrate)$_2$ (L = *p-tert*-butyl-calix[4]arene-tetra(diethylamide)) is reported, as well as MD simulations on the L · M^{2+} complexes in vacuo, in water, and in acetonitrile solutions for alkaline earth cations with a comparison of "converging" and "diverging" conformers.[130] In the simulated and solid-state structures of the L · M^{2+} complex, the ligand wraps around the complexed cations M^{2+} (more than it does with alkaline cations), which are completely encapsulated within the polar pseudo-cavity of L, without coordination to its counterion in the crystal or to solvent molecules in solution. In contrast to alkali cation complexes, which display conformational flexibility in solution, computations show that the alkaline earth cation complexes are of the converging type in water and in acetonitrile. Subtle structural changes from Mg^{2+} to Ba^{2+} are observed in the gas phase and in solution. Based on FBP calculations, a binding sequence of alkaline earth cations was determined; Mg^{2+} displays the weakest affinity for L, while Ca^{2+} and Sr^{2+} are the most stable complexes, which is in agreement with the experiment.

In mixtures with the hydrophobic dicarbollide anion, the extraction of Ca, Sr, and Ba by calixarenes with oxygen donor atoms improves, allowing the separation from alkali ions.[131] The competition by alkali ions is lower than in crown ether extraction systems. Separation factors S with CA2 in nitrobenzene are log S = 7 (Ca), 5.5 (Sr), and 5.4 (Ba).

4.4.1.2   *p*-Alkoxy calix[6]arene hexa(di-N-ethyl)amide

With the exception of magnesium, which is poorly extracted by all ligands, the *p*-alkoxy calix[6]arene hexa(di-*N*-ethyl)amide (CA8, CA10, CA12, and CA15) and calix[8]arene octa(di-*N*-ethyl)amide (CA9, CA11, CA13, CA14, and CA16) display a marked preference in the extraction of alkaline earth metals over sodium. The selectivity for strontium over sodium increases according to the sequence:

$$CA5 < CA6 < CA12 < CA7 < CA13 < CA9$$
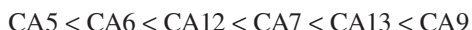
It has been pointed out that the octamers CA9 ($S_{Sr/Na}$ = 51.3) and CA13 ($S_{Sr/Na}$ = 42) are much more selective than the crown ether DC18C6 ($S_{Sr/Na}$ = 16.4) (Table 4.19).[132] These results were confirmed for extraction of strontium from acidic medium. For all the calixarenes tested except CA8, the distribution ratios are higher than those obtained with DC18C6.[133] The selectivity $S_{Sr/Na}$ is very high thanks to a negligible sodium extraction.

Within the hexamers studied, (CA12) is the most efficient for strontium extraction, while (CA8) and (CA15) bearing bulkier groups on the upper rim display lower distribution ratios. In general, octamers show higher distribution ratios and selectivity

TABLE 4.19

Distribution Ratios for Sodium and Alkaline Earth Picrates from Water into Dichloromethane

Ligands	Na$^+$	Mg^{2+}	Ca^{2+}	Sr^{2+}	Ba^{2+}
CA4	0.37	0.10	5.33	5.17	5.90
CA6	0.17	0.04	1.33	3.06	10.90
CA5	0.05	0.03	0.35	0.82	1.38
CA7	0.05	0.03	0.37	1.61	4.10
CA8	0.15	0.04	0.81	1.54	1.79
CA9	0.09	0.03	1.09	4.62	13.29
CA12	0.03	0.04	0.25	0.98	1.27
CA13	0.04	< 0.01	0.29	1.81	5.17
CA14	0.37	0.14	1.69	3.26	5.71
CA15	0.21	0.16	1.62	2.58	3.02
CA16	0.17	< 0.01	1.70	4.03	16.24

Note: $C_L = C_{pic} = 2.5 \times 10^{-4}$ M; volume aqueous/organic phase = 1, T = 20°C.

than their hexamer counterparts. The order of efficiency and selectivity is the following (Table 4.20):

$$CA13 < CA7 < CA9 < CA16 < CA14$$

To increase competition with large amounts of sodium, the concentration of NaNO$_3$ was raised to 4 M, while that of nitric acid was kept at 1 M; the radionuclides were present in solution at trace levels. In these conditions, all tested calixarenes still extract strontium. The order of efficiency (CA7 < CA12 < CA13 < CA16 < CA9) confirms the higher efficiency of octamers compared with hexamers and *p*-alkoxy compared with *p*-H or *p*-*tert*-butyl derivatives. A plot of the distribution ratio of strontium versus the nitric acid concentration in the aqueous phase gives evidence for the much better extracting ability of CA16 in comparison to that of crown ether; distribution ratios of CA16 (at a concentration 10^{-2} M in NPHE) reach 30 in the range of nitric acid concentration 2–4 M, while the distribution ratios of DC18C6 at a concentration 10-fold higher (10^{-1} M in NPHE) do not exceed 1 (Figure 4.5).

The X-ray crystal structures show an important difference between the hexamers and octamers. Hexamer CA4 forms a 1:1 complex with strontium, while the octamers form 2:1 complexes. In the hexamer, strontium is completely encapsulated in the polar region of the ligand and is coordinated only through oxygen donor atoms of the calixarene, while in the octamers CA6 and CA13 there is room also for one chloride and two acetic moieties to coordinate strontium. The structure of the strontium complex of CA13 shows that the *p*-alkoxy groups, which could participate in complexation, are inoperative. None of the oxygen atoms of the methoxy groups are coordinated to the strontium cations; however, the alkoxy groups play a role. Their electron-donating effect enhances the donor properties of the phenolic oxygen atoms

TABLE 4.20

Distribution Ratios for Sodium and Strontium and Selectivity Sr/Na in NPHE

	5 10^{-4} M M(NO$_3$)$_n$/1 M H(NO$_3$)			4 M NaNO$_3$/1 M H(NO$_3$)
Ligands	^{22}Na	^{85}Sr	D_{Sr}/D_{Na}	^{85}Sr
CA6	–	–	–	0.4
CA7	0.006	8.3	>8,300	1.3
CA8	<0.001	0.13	>130	0.5
CA9	<0.001	20	>20,000	5
CA12	<0.001	2.9	>2,900	1.8
CA13	<0.001	6.5	>6,500	2.2
CA14	<0.001	30	>30,000	0.34
CA15	<0.001	0.80	>800	1.09
CA16	<0.001	24	>24,000	3.8
DC18C6	0.006	0.28	>47	–

Note: ($C_L = 10^{-2}$ M).
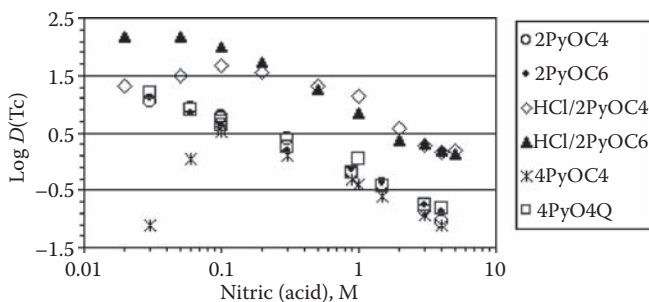
FIGURE 4.5 Strontium distribution ratios of DC18C6 (1) (10^{-1} M in NPHE) and CA16 (2) (10^{-2} M in NPHE) as a function of the nitric acid concentration.

bearing the amide groups, which explains the remarkable efficiency of the octamers. Formation of dinuclear species with octamers was confirmed by ESI mass spectrometry and by competitive spectrophotometry with 1-(2-pyridylazo)-2-naphthol (PAN).

With the aim of studying the origin of strontium over sodium selectivity observed for calixarenes bearing amide groups, Parma University determined the crystal structures of strontium complexes with CA4, CA6, and CA8.[134] The hexameric CA4 consists of one Sr^{2+} cation coordinated by the ligand. On the contrary, octameric CA6 and CA8 crystallized as dinuclear strontium complexes (Sr:L = 2:1), although equimolar amounts of strontium salt and ligand were used. This indicates a strong tendency of the first strontium ion to preorganize the chelating groups to host the second cation. In spite of unfavorable Coulomb interactions between two cations, this

2:1 (metal to ligand) stoichiometry was evidenced by NMR and mass spectrometry for calix[8]arenes.

The higher Sr^{2+}/Na^+ selectivity shown by calix[8]arene derivatives compared to those of tetramers and hexamers is mainly linked to the low binding ability of the larger calixarene ligands toward the sodium cation. Each polar niche for cation coordination in the calix[8]arenes is too large and cannot result in all the oxygen atoms being at 2.45–2.53 Å from the metal cation, as required for coordination of Na^+ to calix[4]arene tetraamide, whereas those of the calix[4/6]arenes can achieve the fine-tuning of the Na-O distances needed for strong bonding of the sodium cation.[134]

4.4.1.3   The Behavior of Ionizable, Crowned Calixarenes

Tu et al. synthesized *p-tert*-calix[4]arene-1,2-crown-*n* (*n* = 4, 5, and 6), where a crown-*n* polyether unit links alternate aromatic rings of the calix[4]arene; oxyacetic acid MCI6, MCI11, and MCI16 or *N-(X)*sulfonyl oxyacetamide groups (*X* = methyl (MCI7, MCI12, and MCI17), phenyl (MCI8, MCI13, and MC18), 4-nitrophenyl (MCI9, MCI14, and MCI19), and trifluoromethyl (MCI10, MCI15, and MCI20)) are attached to the remaining lower-rim positions, with variation of proton-ionizable groups, "tunable" ligand acidity was obtained. Extraction tests of alkaline earth metal cations from aqueous solutions (10.0 mM in each) by ligands (1.0 mM) in chloroform were carried out. MCI6, MCI11, and MCI16 in the cone conformation exhibits high selectivity for Ba^{2+} in competitive extraction of alkaline earth metal cations, the Ba^{2+}/Sr^{2+} selectivity exceeds 100. The extraction selectivity order ($Ba^{2+} > Sr^2 > Ca^{2+} > Mg^{2+}$) is the same whatever the size of the crown. For the three dicarboxilic acid ligands, only MCI6 exhibits appreciable extraction selectivity. For the calix-crown *N-(X)*sulfonyl oxyacetamide, all show extraction selectivity. However, the selectivity is considerably greater with MCI7 than with MCI12, and MCI17. Thus, expansion of the polyether ring size to better accommodate within the cavity does not lead to improved extraction selectivity.[135–139]

Zhou et al. studied the extraction of alkaline earth metal cations with *p-tert*-calix[4]arene-1,2-crown-5 under different conformations. The pH for half loading, $pH_{0.5}$, is a qualitative measure of ligand acidity. The $pH_{0.5}$ values for a given conformation decrease as the electron-withdrawing ability of *X* increases. Moreover, the ligand acidity increases uniformly as the conformation is varied in the order: 1,3-alternate < partial-cone < cone. This order is related to the proximity of the ionized groups to the complexed cations.[140]

When these crowned, ionizable calixarenes contain no *t*-Bu groups in the 4-position (MCI1, MCI2, MCI3, MCI4, and MCI5), the increased molecular flexibility causes the extraction to shift to higher pH (cone conformer), the selectivity for Ba^{2+} to disappear (partial cone conformer) or to be less pronounced (1,3-alternate conformer).[141]

4.4.1.4   Parent Calixarenes

In a test at "Mayak" nuclear fuel reprocessing plant in Russia, alkaline high-active waste was subjected to extraction by a mixture of parent *t*-butyl calix[6]arene, 2-{[bis(2-hydroxyethyl)amino]methyl}-4-alkylphenol, and a solubilizer in dodecane.

More than 99% of the Sr and Cs together with 90% of gross alpha-activity could be extracted in the presence of 8 M Na^+ and subsequently re-extracted into acidic media.[142]

4.4.2 EXTRACTION OF TECHNETIUM WITHOUT CESIUM COEXTRACTION

The extraction of Tc(VII) into 1,2-dichloroethane by two neutral *p-t*-butyl calix[4] arenes with four $-CH_2C(O)OC_2H_5$ or $-CH_2C(O)CH_3$ substituents at the phenolic oxygen atoms was investigated. Their difference is discussed in terms of the carbonyl group basicity, allowing stronger interaction of the keto group with Lewis acids. The distribution ratio increases significantly at higher NaOH concentration due to ion-pairing with extracted Na^+ (the ester slowly hydrolyzes under such condition). The presence of 1 M $NaNO_3$ reduces the distribution ratios. The extracted complex has a stoichiometry of 1:1 as seen from slope analysis. Thiacalix[4]arene in the cone conformation bearing ester groups is a more effective extractant from acidic solutions.[143,144]

Tc(VII) can be extracted by pyridinium-appended calixarenes as an ion pair.[145] Maximum extractability is observed at a range where the nitrogen becomes protonated, for example, from 0.1 to 0.2 M HNO_3. An exception is 2PyOC4, where D_{Tc} increases steadily from 4 M to 0.03 M HNO_3. The distribution ratios decrease with the acidity of the aqueous phase: competition by nitrate extraction was identified as the cause. A high percentage of Tc (90%) is extracted by 2PyOC6 in $CHCl_3$ at $NO_3^-/TcO_4^- = 500$ (15% at a ratio NO_3^-/TcO_4^- of 60,000). In agreement with the Hofmeister order, extraction from HCl is better by approximately one order of magnitude. Protonation of TcO_4^- was concluded not to be relevant under the investigated conditions (Figure 4.6). The extraction power of 2PyOC*n* (*n* = 4, 6, 8) is nearly identical, except in the weakly acidic range. This confirms conclusions on partially substituted calixarene pyridinium derivatives: not all py groups participate in binding. The position of the nitrogen atom in the py group is more important for the rigid calix[4] arene; for example, 2PyOC4 is more effective than 4PyOC4, especially in weakly acidic media, but 2PyOC6 and 3PyOC6 behave nearly identically. Comparison with amine-type commercial extractants Aliquat 336 and protonated tridodecylamine showed a macrocyclic enhancement effect for the calixarenes. Quaternization of the
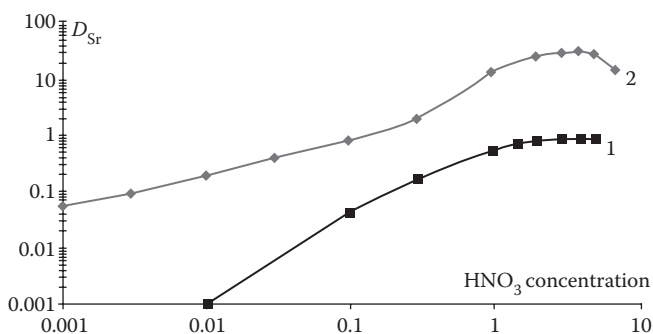
FIGURE 4.6 Technetium distribution ratios as a function of the nitric acid concentration.

pyridinum nitrogen atoms allows good extraction from diluted acid. For example, $\log D_{Tc} = 1$ for 2 mM 4PyOC4Q in CHCl$_3$, and stripping can be achieved with strongly acidic solutions.

4.5 EXTRACTION OF ACTINIDES

Three European projects have been devoted to the extraction of the long-lived elements and in particular of actinides.[16–18] Initially, the goal of the project was to decategorize the effluents by eliminating cesium, strontium, and actinides with a mixture of extractants. Then, a much more ambitious project was launched consisting in separating selectively the actinides from other elements including lanthanides, contained in high-activity liquid waste arising from the PUREX process, in only one step, stimulating the search for extractants based on the calixarenes bearing one or several ligands. For more information on the separation of actinides from lanthanides, it is recommended to refer to Chapter 3 of this book, dedicated to this subject.

Organophosphorus extractants have an exceptional ability to extract hard cations, particularly actinides and lanthanides, but monodentate organophosphorus ligands, even the most powerful ones such as alkylphosphine oxides (the most used is trioctyl phosphine oxide (TOPO)), only extract actinides(IV) and (VI) and to a lesser extent (V) from low acidity media. Due to their relatively low charge densities, actinides(III) and lanthanides usually show a weak complexing ability with most chelating agents in nitric acid solution. Some bidentate neutral ligands have been developed as useful extractants for actinides, for example, dihexyl-*N,N*-diethylcarbamoylmethylphosphonate (DHDECMP). Horwitz et al. synthesized and studied several carbamoylmethylphosphine oxide derivatives.[146–151] In carbamoylmethylphosphine oxides (CMPOs), the C = O and P = O groups act as the ligating functions, and compounds bearing numerous residues at the nitrogen (R$_1$, R$_2$) and phosphorus (R$_3$, R$_4$) atoms in various combinations have been tested. Among them, diphenyl-*N,N*-diisobutyl carbamoyl methyl phosphine oxide (DΦCMPO) and finally octyl(phenyl)-*N,N*-diisobutylcarbamoylmethylphosphine oxide (OΦCMPO) were chosen to remove actinides, whatever their oxidation states, from acidic medium activity waste (TRUEX Process).

These compounds, tested in NPHE at Cadarache, were used as reference compounds for the extraction of actinides by functionalized calixarenes (see below). The distribution ratios for neptunium mainly at the oxidation state (V), plutonium at the oxidation state (IV), and americium (III) are shown in Table 4.21 for OΦCMPO. They were also used as references for the americium over europium selectivity (Table 4.22).

TABLE 4.21

Distribution Ratios for Np, Pu, and Am From Aqueous Solutions 4 M NaNO$_3$, 1 M HNO$_3$ into a NPHE Solution of OΦD(iB) CMPO (10^{-2} M)

OΦCMPO	^{237}Np	^{239}Pu	^{241}Am
	0.85	22	1.2

TABLE 4.22
Distribution Ratios for Ce, Eu, Am, and Cm From HNO_3 Aqueous Solutions at Different Concentrations into a NPHE Solution of TOPO, DHDECMP, OΦD(iB) CMPO, and DΦD(iB) CMPO (0.25 M)

Ligands		0.01	0.1	1	1.5	2	3	4
TOPO (0.25 M)	Eu	–	–	2.95	0.11	–	0.28	< 0.01
	Am	–	–	1.6	0.07	–	0.17	0.01
DHDECMP (0.25 M)	Ce	0	0.02	1.8	3.9	6.1	8.3	9.7
	Eu	0.01	0.01	0.8	1.75	2.75	4.7	4.9
	Am	0	0.02	1.45	3.3	3.7	7.2	7.7
	Cm	0.01	0.02	0.97	1.95	3.05	5.0	5.45
OΦCMPO (0.25 M)	Ce	1.55	21.5	14	12.5	13	12.5	11.5
	Eu	1.15	15.7	105	105	125	90	75
	Am	2.5	32	200	160	195	150	105
	Cm	1.7	26	90	95	50	50	70
DiΦCMPO (0.25 M)	Eu	–	–	12	19.5	–	19	20
	Am	–	–	26	40	–	36	27

The header row above has a spanning header "HNO₃ Concentration":

| | | HNO₃ Concentration | | | | | | |

In the Strasbourg laboratory, which cannot handle radioactive substances, trivalent and tetravalent transuranic elements were simulated by lanthanides (generally europium) and thorium, respectively.

4.5.1 Selective Extraction of Actinides by Calixarenes Bearing Phosphine Oxide Moieties

4.5.1.1 Extraction by Phosphine Oxide (Grafted on the Narrow-Rim of) Calix[*n*]arenes

Extraction of thorium nitrate and europium nitrate (10^{-4} M) from 1 M HNO_3 into dichloromethane was carried out for 19 calixarenes totally or partially substituted on the lower rim by phosphine oxide moieties (CPo1-CPo17-CPo19-CPo20) and for one calixarene substituted by phosphinate (CPo18) (see Section 4.7).[128,152–154]

As expected, tetravalent thorium is better extracted than trivalent europium. All calixarenes are stronger extractants than TOPO or OΦCMPO. The dealkylated series is better than the alkylated one. For the dealkylated series and alkylated series, the sequence of increasing efficiency toward two cations is tetramer < octamer < hexamer.

The replacement of the phenyl groups on the phosphine oxide moieties by *n*-butyl groups leads to a complete loss of extraction. Increasing the length of the chain linking the calixarene to the phosphine oxide moieties leads to a decrease of extracting ability of both tetramer and hexamer (Table 4.23). The selectively substituted

TABLE 4.23

Percentage of Extraction (*E*%) of Europium and Thorium Nitrates from 1 M HNO$_3$ into Dichloromethane Containing the Ligand at Various Concentrations

Ligands	[Th(IV)]						[Eu(III)]
	10^{-4} M	$5\ 10^{-4}$ M	10^{-3} M	$5\ 10^{-3}$ M	10^{-2} M	$2.5\ 10^{-2}$ M	$2.5\ 10^{-2}$ M
TOPO	0	0	0	1.4	10.2	64.2	0[a]
OΦCMPO	0	0	0	1.6	12.2	70.4	0[b]
CPo1	0	5.6	26.8	96.1	100	100	0
CPo2			0				
CPo3	2.6	46.9	79.8	100	100	100	24.6
CPo4	0	23.6	62.5	98.8	100	100	20.8
CPo5			0				
CPo6			55				29.6
CPo7	9.4	79.4	94.8	100	100	100	94.3
CPo8	0	0	0	30.6	60.1	88.4	0
CPo9			0				
CPo10	5.1	62.6	87.9	100	100	100	92.0
CPo11	0	1.9	4.6	28.4	50.0	76.5	
CPo12					20	45	
CPo13					0		
CPo14	0	0	1.1	10.3	24.0	54.5	
CPo15					0	6	
CPo16	0	1.1	3.6	38.8	68.2	91.4	
CPo17	0	0	0	17.0	46.9	85.9	
CPo18					60		
CPo19					15		
CPo20					0		

[a] %$E = 18$ ($C_L = 0.25$ M).
[b] %$E = 69.5$ ($C_L = 0.25$ M).

calixarenes are less efficient than the fully substituted ones. The more efficient compounds are CPo16 > CPo17 > CPo14 > CPo19.

Extraction of neptunium, plutonium, and americium from simulated radioactive liquid waste was carried out in particular with *tert*-butyl and dealkylated tetramers, hexamers, and octamers of calixarene [ethoxy(diphenylphosphine oxide)]. Among these six calixarenes, the highest distribution ratios were obtained with the dealkylated calix[8]arene. Using a different sample of the dealkylated hexamer, the Strasbourg group concluded that this compound is the most efficient. This discrepancy can be explained by the presence of impurities, detected by NMR, which were probably responsible for the poor performances of the dealkylated hexamer tested at Cadarache.

The analysis of the extraction by CPo21 data reveals a 1:1 metal ion-to-ligand ratio for europium and thorium. The selectivity factors indicate a good selectivity toward these two cations with respect to Mn^{2+}, Pb^{2+}, Cd^{2+}, Fe^{2+}, Ni^{2+}, and Co^{2+}, among which only cadmium is a weakly radioactive fission product.[155] A synergistic extraction of almost three orders of magnitude was evidenced for the extraction of La^{3+}, Nd^{3+}, Eu^{3+}, Ho^{3+}, Lu^{3+} with 4-benzoyl-3-methyl-1-phenyl-5-pyrazolone and CPo21; however, it does not improve the separation factors between lanthanides.[156]

4.5.2 SELECTIVE EXTRACTION OF ACTINIDES BY COMPOUNDS BEARING CMPO MOIETIES

4.5.2.1 Extraction by Wide-Rim CMPO Calix[4]arenes and Oligomers

Horwitz et al. showed that the trivalent americium is coordinated to three CMPO molecules and three nitrate anions in an overall neutral complex, another molecule of nitric acid being hydrogen bound to each of the carbamoyl oxygen atoms.[157,158] Several molecules of CMPO are included in complexes formed with other cations such as plutonium.

From this observation, it is interesting to construct molecules in which several CMPO ligands are combined in a suitable mutual arrangement. These new ligands, as expected, show in general not only improved extraction properties on the basis of the chelate effect (favorable entropic factors), but also higher extraction selectivity due to differences in the stoichiometry of the complexes and in the steric requirements. Calixarenes offer an ideal platform for the arrangement of various ligating functions either at the wide or the narrow rim, which allows an independent control of factors such as solubility in organic diluents or insolubility in aqueous phases by the introduction of appropriate hydrophobic residues. Several calixarenes bearing CMPO moieties on the wide rim and their linear counterparts were synthesized by Böhmer et al.[16,17,159]

4.5.2.1.1 Extraction by CMPO Linear Oligomers

With the aim of getting a better understanding of the structural requirements for effective complexation, two series of linear oligomers (propoxy and pentoxy groups) were prepared up to the pentamer.[17] For the pentoxy series ($O_5 1$ $n = 0$, $O_5 2$ $n = 1$, $O_5 3$ $n = 2$, $O_5 4$ $n = 3$, $O_5 5$ $n = 4$), complexation constants with europium have been determined out in methanol in comparison to CPw3 (Table 4.24) (see Section 4.7).

All compounds form 1:1 and 1:2 species as the calixarenes. Monomer $O_5 1$ forms more stable complexes than OΦCMPO. A slight increase in the stability of the 1:1 complexes is observed when a supplementary unit is added to the ligand (from $O_5 2$ to $O_5 5$). For 1:2 complexes, a large stabilization is noticed on going from $O_5 1$ to $O_5 2$ and $O_5 3$, but not for $O_5 4$ or $O_5 5$. These results are consistent with the assumption that only one arm of each ligand may be involved in the complexation.

All the products were soluble in NPHE only at a very low concentration ($\leq 10^{-3}$ M). At this concentration, $O_5 1$ is not very effective for actinide removal, whereas $O_5 2$ shows a relatively high efficiency toward plutonium (Table 4.25). Adding a new CMPO

TABLE 4.24

Stability Constants ($\log \beta_{xy}$) of Europium Complexes with Wide-Rim CMPO Calix[4]arenes and Linear Counterparts in Methanol ($I = 0.05$ M NaNO$_3$)

Complexes M:calix	CMPO	O$_5$1	O$_5$2	O$_5$3	O$_5$4	O$_5$5	CPw1	CPw2	CPw3	CPw14	CPw15	CPw16
1:1	3.6	4.5	5.0	5.5	5.6	6.2	4.4	6.2	6.2	5.6	5.7	6.3
1:2	5.5	7.7	9.0	10.3	9.9	10.1	8.4	11.0	11.1	10.5	10.9	12.0

TABLE 4.25

Distribution Ratios for Eu, Np, Pu, and Am from Aqueous Solutions 4 M NaNO$_3$, 1 M HNO$_3$ into a NPHE Solution of Linear Oligomers or Calixarenes Bearing the CMPO Moieties on the Wide Rim (10^{-3} M)

	C_{Ligand}	^{152}Eu	^{237}Np	^{239}Pu	^{241}Am
OΦCMPO	10^{-2} M		0.85	22	1.2
O$_5$1	10^{-3} M	<0.001	0.5	0.3	<0.001
O$_5$2	10^{-3} M	1.2	0.9	23	1.8
O$_5$3	10^{-3} M	13	2	20	17
CPw3	10^{-3} M	>100	2	>100	>100
CPw4	10^{-3} M	>100	2	20	45
CPw5	10^{-3} M	>100	2	90	>100
CPw6	10^{-3} M	–	4	>100	>100
CPw7	10^{-3} M	>100	2	80	>100
CPw8	10^{-4} M		1.1	27	27
CPw9	10^{-4} M		1.5^a	24^a	21^a
CPw10	10^{-3} M	>100	12	>100	61
CPw11	10^{-3} M	>100	2	>100	>100
CPw12	10^{-3} M	>100	3	>100	>100
CPw13	10^{-3} M	>100	3	>100	>100

^{a} Precipitation of a part of actinides.

group (O$_5$3) does not improve the extracting ability toward plutonium, but enhances strongly that of americium, which needs three CMPO molecules to be extracted.

4.5.2.1.2   Extraction by Wide-Rim CMPO Calixarenes

Complexation studies of some lanthanides and thorium in methanol have been undertaken in order to better understand the solution behavior of OΦCMPO and CPw3.[160] The stability of the complexes increases along the lanthanides series as a consequence of the increase in the charge density of the cations due to the lanthanide contraction (Table 4.25).

The complexes with the two rigid derivatives CPw3 and CPw2 have similar stabilities (log β_{11} = 6.2), whereas the stability of the flexible tetramethoxy derivative CPw1 is much lower (log β_{11} = 4.4). The stability increases with the number of propoxy groups (from CPw14 to CPw16), that is, when the molecule becomes increasingly rigid.

Extraction of thorium and europium by these same compounds shows an increase from O$_5$1 to O$_5$5 (Table 4.26). Thorium is equally extracted by the linear tetramer and pentamer, whereas europium is even better extracted by linear tetramer than by the linear pentamer. Most of the CMPO calixarenes extract europium better than TOPO and OΦCMPO. All these extractants are stronger extractants of thorium than europium, because similar efficiencies require ligand concentrations of 10^{-3} M for

TABLE 4.26

Percentage of Extraction (%) of Europium and Thorium Nitrates from 1 M HNO$_3$ into Dichloromethane at 20°C

Ligands	Eu^{3+}		Th^{4+}	
	$C_L = 10^{-3}$ M	$C_L = 10^{-2}$ M	$C_L = 10^{-4}$ M	$C_L = 10^{-3}$ M
OΦCMPO	69.5		12.2	
TOPO	18		10.2	
O$_s$1	–	6	–	4
O$_s$2	–	18.3	–	22
O$_s$3	15	94	–	4.3
O$_s$4	43.4	100	15.2	–
O$_s$5	17	–	21.7	–
CPw1	35		60	
CPw2	64		61.8	
CPw3	58		61	
CPw4	24		26	
CPw5	68		53	
CPw6	68		63	
CPw7	72		54	
CPw8	69.5		51.5	
CPw9	59		50	
CPw10	–		46	
CPw11	20		32	
CPw12	40		39	
CPw13	49		43	
CPw14	45		69	
CPw15	48		66	
CPw16	60		66	

europium and only 10^{-4} M for thorium. An increase of the alkyl chain length from C_{10} to C_{18} does not cause any regular change in the extraction efficiency. The cyclic pentamer extracts thorium slightly less than its tetramer counterpart. The mixed derivatives (CPw14–CPw16), which correspond to the progressive replacement of four CH_3 groups at the narrow rim of CPw1 by bulkier C_3H_7 groups, show slightly but still significantly higher extraction values for thorium than their counterparts bearing four identical groups.

For all the calix[4]arenes, whatever the length of the linear alkyl branched to the narrow rim, the solubility in NPHE remained very low ($\sim 10^{-3}$ M) and even lower than 10^{-3} M for the longest alkyl chains (C_{16} CPw8, C_{18} CPw9) (Table 4.25).[159] It was surprising that compared to the high lipophilicity introduced by such radicals, interactions with NPHE arose more with phenyl-phenyl interactions than with alkyl chains Van der Waals interactions. All the calixarenes prepared in Mainz exhibit high extracting power toward actinides whatever their valencies. When the solubility

of the compounds is equal to 10^{-3} M, the distribution ratios for americium and plutonium exceed 100. In comparison, OΦCMPO used at a concentration ten-fold higher (10^{-2} M) displayed lower distribution ratios ($D_{Pu} = 22$, $D_{Am} = 1.2$). Calixarenes bearing $C_{12}H_{25}$ alkoxy chains CPw6 and the three calixarenes bearing mixed alkoxy groups were the most powerful extractants of actinides, particularly of plutonium and americium. Calix[5]arene CPw10, with five functionalized groups and a larger cavity, is as efficient as the calix[4]arene for the extraction of plutonium. A decrease of D_{Am} and, in contrast, a sharp increase of D_{Np} is observed. It can be explained by a lesser fitting of the calixarene cavity for trivalent americium and by a better adjustment of the cavity to linear NpO_2^+.

Böhmer et al. synthesized the counterpart of CPw3 CPw19, where phenyl groups linked to phosphorus were replaced by hexyl residues, which was compared with OΦCMPO for the extraction of nine lanthanides (La, Pm, Sm, Eu, Gd, Tb, Ho, Er, and Yb) and two minor actinides (Am and Cm) from an aqueous phase containing 4 M $NaNO_3$ and 10^{-2} M HNO_3. While distribution ratios are comparable for all cations with OΦCMPO, a marked decrease of the distribution ratios along the lanthanide series is observed, from 140 for lanthanum to 0.19 for ytterbium, corresponding to a separation factor of about 700. The observed selectivity nearly disappears for CPw19. These results are in agreement with those obtained for two CMPO molecules, where a relatively low selectivity is observed ($D_{La}/D_{Lu} \sim 10$) for DΦCMPO derivative, whereas no discrimination is obtained with DBCMPO derivative. The experiment was repeated using 3 M nitric acid; the separation factor D_{Am}/D_{Eu} is slightly higher (10.2) than in the presence of sodium nitrate (7.5) (Figure 4.7).[161–163]

It is interesting to compare the extraction of different lanthanides from acidic medium (1.5 M HNO_3) by OΦCMPO at a concentration 0.25 M, 250 times higher than that of CPw3 or that of tetramer O_54, the acyclic analogue of CPw3. For the lightest
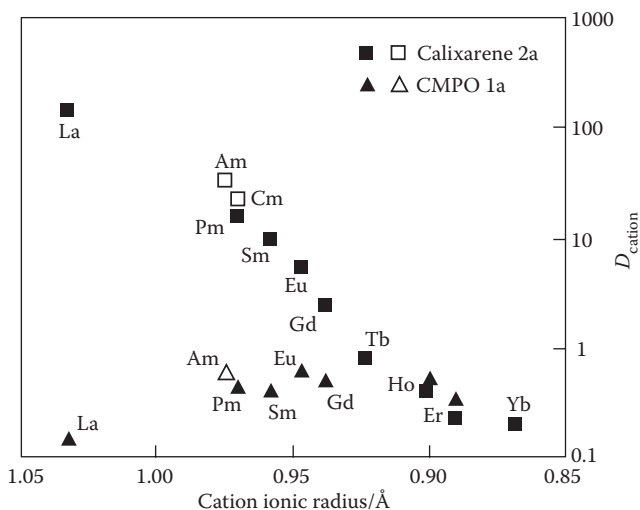
FIGURE 4.7 Extraction of lanthanides, americium, and curium by (1a) OΦCMPO (0.2 M) and (1b) CPw3 (10^{-3} M) in chloroform. Aqueous phase: 4 M $NaNO_3$ and 10^{-2} M HNO_3.

TABLE 4.27

Distribution Ratios for Lanthanides and Actinides from Aqueous Solutions 1.5 M HNO$_3$ into a NPHE Solution of OΦCMPO (0.25 M), O$_5$4, and CPw3 (10^{-3} M)

	OΦCMPO	O$_5$4	CPw3
La	62	3.4	280
Ce	12.4	5.4	23
Nd	115	5.9	220
Sm	130	7.8	77
Eu	105	7.2	36
Am	160	6.6	> 300
Cm	95	8.3	120
Pu	85	10	5.1

lanthanides, distribution ratios for OΦCMPO (0.25 M) and CPw3 (1 M) are comparable. As the atomic number increases, a very strong decrease of lanthanide extraction is observed for CPw3. On the contrary, for OΦCMPO and O$_5$4, this decrease is much less pronounced; for the latter, distribution ratios for the first lanthanides are much lower and almost unvarying along the lanthanide series (Table 4.27). With classical extractants like di(2-ethylhexyl) phosphoric acid (HDEHP), distribution ratios increase as the atomic number of lanthanides increases. This is explained by the higher charge density due to the ionic radius contraction of the lanthanides. For CPw3, and more generally for calixarenes bearing CMPO groups, the reverse trend is observed due to a good adjustment between the size of the lightest lanthanide cations and that of the cavity formed by the four CMPO moieties. This unexpected discrimination led us to use these calixarenes, initially synthesized for the extraction of actinides whatever their valencies, for a possible way to separate the latter from lanthanides. Tests carried out at several acidities showed the same trend. That is, only the lightest lanthanides were significantly extracted by CMPO calixarenes.[17] One has to point out the peculiar behavior of cerium, which displays low distribution ratios in comparison to lanthanum or neodymium. This difference of behavior can be explained by a partial or total oxidation of this cation to the IV oxidation state. The ionic radius of cerium(IV) being lower than that of cerium(III), the tetravalent ion is less fitted to the cavity formed by the CMPO groups than the trivalent cerium.

Böhmer et al. synthesized phosphinate (CPw20), phosphonate (CPw21), and phosphoric acid (CPw22) derivatives. The most basic phosphine oxide functions in CPw19 lead to a maximum of extraction for a nitric concentration of 1 M. With the phosphonate derivative CPw20, which is the strongest extractant, a maximum is reached for a higher acidity (3 M). This compound is relatively efficient at low acidity (10^{-2} M) and for acidity higher than 1.5 M. Calixarene CPw22 bearing phosphoric acid moieties displays low distribution whatever the acidity. Comparison of CPw19 and CPw3 confirms the importance of phenyl groups, essential for obtaining a selectivity along the lanthanide series and for a better americium over europium selectivity.

TABLE 4.28

Distribution Ratios for Eu and Am from Aqueous Solutions of HNO₃ at Different Concentrations into a NPHE Solution of CPw19–CPw22 Calixarenes

Ligands		10^{-2}	10^{-1}	1	1.5	2	3	4
		HNO₃ concentration (M)						
CPw19	Eu	0.11	0.19	0.40	0.31	0.24	0.19	0.18
	Am	0.16	0.37	0.67	0.51	0.37	0.28	0.29
CPw20	Eu	0.02	0.06	1.8	3.7	–	6.1	3.9
	Am	0.07	0.45	12	14.5	–	41	21
CPw21	Eu	< 0.01	< 0.01	0.02	0.02	0.02	0.05	0.07
	Am	$-^{a}$						
CPw22	Eu	0.85	0.15	0.22	0.72	0.64	0.69	0.60
	Am	1.0	0.16	0.32	1.2	1.1	1.2	1

[a] Not measured.
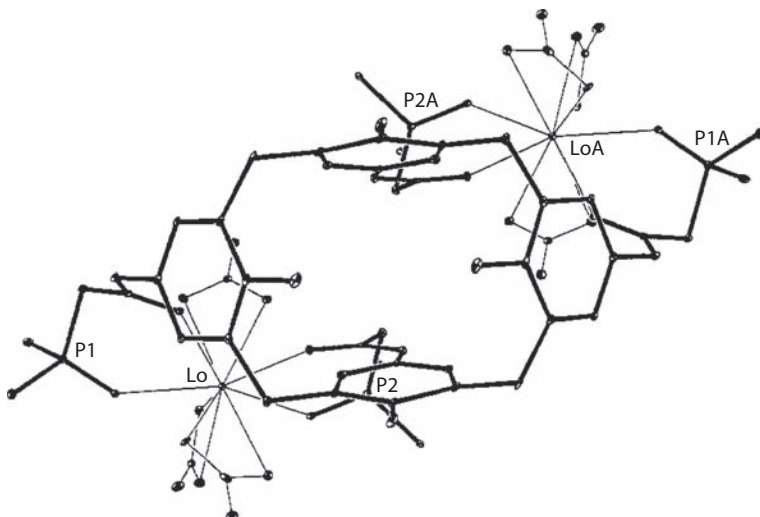
Phenyl groups and the alkyl chains (C3) are not represented

FIGURE 4.8 X-ray structure of lanthanide calixarene complex ((La(NO₃)₃)₂ (CPw2).

It has been pointed out that CPw20, possessing only a phenyl group and an ethoxy group linked to the phosphorus atom, displays relatively high extraction ability and separation factor $S_{Am/Eu}$ (Table 4.28).[17]

All the complexes metal:wide-rim CMPO calix[4]arene studied by crystallographic analysis have the 2:1 M:calix stoichiometry. Cations are complexed by two bidentate CMPO, which keep them apart from the cavity of the calix[4]arene. Thus, these complexes are not real inclusion complexes (Figure 4.8).

There was evidence for two subgroups among the lanthanides, for which the coordination number of the metal is 10 (from La to Eu) and 9 (From Eu to Lu). Europium, which presents the two coordination numbers, 9 in the complexes of 2:1 stoichiometry and 9 and 10 in a complex of 5:2 stoichiometry, ensures the transition between the two subgroups. Lutetium, the smallest of lanthanide cations, presents also two coordination numbers, 8 and 9. This change of coordination number is the consequence of the decrease of the ionic radius along the series of lanthanides. The conformation of the calix[4]arene is identical for the various complexes. Moreover, the conformation of a complex of CMPO calixarene is close to that of a complex of $O_5 2$, with a small deformation close to the skeleton. The dimer seems to be the smallest entity representative of the behavior of a CMPO calixarene. No structural explanation for the selectivity of the CMPO calixarene can be found. Moreover, CPw19 forms with europium nitrate a complex in any point similar to that obtained with CPw2. The complexes formed with the calixarene CMPO are not inclusion complexes. The selectivity of these compounds does not find an obvious structural explanation. However, the conjunction of two effects, the chelating effect and the macrocyclic effect, could be the cause of it. The fact that the two CMPOs are linked implies that only two partners instead of three intervene in the reaction of the formation of a 1:2 M:CMPO complex (the chelating effect). The macrocyclic effect is related to the position of the CMPO and their oxygen atoms in a confined space. Lanthanides are thus better extracted by calixarene CPw3 than by its linear tetramer analogue $O_5 4$ and, in contrast to $O_5 4$ discrimination between lanthanides, is clearly marked for CPw3. The resultant of these two effects can be described as "preorganization."[164]

Complexation studies were carried out by electrospray ionization mass spectrometry (ESI-MS) with three lanthanides (La, Eu, and Yr) at a concentration of 10^{-4} M, while the ratio of concentration of CPw2 versus calixarene ($r = [calix]_{org}/[Ln]_{aq}$) was varied between 0.1 and 10.[165] The behavior of the three lanthanides is the same: the 1:1 Ln:calix-CMPO complex is always predominant in the range of concentration studied; the 2:1 Ln:calix-CMPO appears in the case of metal excess with a maximum for $r = 0.5$, while the percent of 1:2 Ln:calix-CMPO increases as the concentration of ligand increases, but does not exceed 10% for $r = 10$. These studies show that two factors play a key role in the selectivity of CMPO derivatives, firstly the presence of phenyl groups on the phosphorus atom, which confers the selectivity to CMPO ligands, secondly the calixarene structure, which amplifies this selectivity due to its preorganization. Indeed the noncyclic derivative ($O_5 2$), in spite of the presence of phenyl units, does not display noticeable selectivity.

As the extraction of actinides, which are hard cations, requires very powerful extractants, so in some cases back-extraction can be incomplete and can be enhanced by adding soluble complexing agents like methylene diphosphonic acid (MDPA) to the stripping solution. Horwitz et al. proposed to implement thermodynamically unstable complexing agents that are diphosphonic acids and diphosphonic acid derivatives like 1-hydroxyethylidenediphosphonic acid (HEDPA) capable of complexing with metal ions, especially metal ions in the II, III, IV, V, and VI oxidation states, to form stable, water-soluble metal ion complexes.[166] Subsequently, the complexing agents can be decomposed, under mild conditions, into inorganic compounds that degrade the

TABLE 4.29

Distribution Ratios for Several Fission Products [M] = 10^{-4} from Aqueous Solutions (3 M HNO_3) into NPHE by CMPO (0.25 M) and CPw3 (10^{-3} M)

Ligands	Zr	Nb	Mo	Ru	Rh	Pd
OΦCMPO	15	21	14	0.07	0.001	2.4
CPw3	0.05	0.09	0.09	0.01	0.004	1.9

Note: Contact time between aqueous phase and organic phase was 3 days.

complex and release the metal ion. These compounds were used to facilitate the stripping of actinides and avoid their hydrolysis in pure water.[167]

Calixarenes display strong transport abilities in spite of their low concentration (10^{-3} M in NPHE) in SLMs. High permeabilities were obtained for americium and plutonium and to a lesser extent for neptunium. Implemented at a concentration 10-fold higher, OΦCMPO displays comparable values only for plutonium. With the most efficient calixarene (CPw13), 92% of the plutonium in the feed was transported after 2 h and 99.75% after 6 h.

Solutions arising from the PUREX process contain many fission products and, in particular, some fission products and corrosion products that can be extracted by OΦCMPO or DMDBTDMA used in the DIAMEX process (cf Chapter 3 on the Ln/An separation). In particular, with the latter, zirconium(IV) nitrate is better extracted than either the lanthanides or actinides, but its extraction may be reduced to acceptable levels by complexing it with oxalic acid or ketomalonic acid. Extraction of molybdenum may be suppressed by complexation with hydrogen peroxide. Iron, which is almost always present from corrosion of process equipment, also has a high affinity for DMDBTDMA, but Fe(III) is extracted slowly, and it may be possible to use this property to separate it from the actinides and lanthanides. In contrast to OΦCMPO, which displays high distribution ratios for cations such as Zr, Nb, Mo, and Pd, CPw3 shows a significant affinity only for palladium (Table 4.29). It has to be pointed out that this coextraction of palladium can be interesting from the perspective of the recovery of palladium. Similarly, under the same conditions (contact time of six days), corrosion products are 10-fold less extracted by CPw3 ($D_{Fe} = 0.4$, $D_{Co} = 0.01$) than by OΦCMPO ($D_{Fe} = 3.3$, $D_{Co} = 0.11$).[168]

Cavitands, prepared by the Twente group, differ from the wide-rim CMPO calixarene not only by the basic scaffold, but also by the distance to the rim and in the amido function (tertiary amide versus secondary amide). In comparison to CMPO calixarenes, compounds Cv1 and Cv2 did not lead to improvements in terms of extracting ability or selectivity.[17,169]

4.5.2.1.3 Extraction by Wide-rim N-methylated CMPO Calixarenes

Two calix[4]arene tetraethers (pentoxy CPw17 and tetradecyloxy CPw18) bearing four -N(Me)-CO-CH_2-P(O)Ph_2 residues on their wide-rim were synthesized for the first time.[170] Their ability to extract lanthanides and actinides from an acidic aqueous

TABLE 4.30

Distribution Ratios for the Extraction of Several Lanthanides and Americium from Aqueous Solutions (3–4 M HNO$_3$) into NPHE by CPw3 and CPw17 Calixarenes

Ligands	La	Ce	Nd	Sm	Eu	Am
CPw17/3 M HNO$_3$	2.1	1.8	0.72	0.21	0.14	0.87
CPw17/4 M HNO$_3$	6.3	5.6	2.4	0.74	0.41	2.95
CPw3/3 M HNO$_3$	145	–	135	60	45	156

phase to organic phases (CH$_2$Cl$_2$, and NPHE) was studied. The most striking is the 100-fold decrease of europium distribution ratios displayed by CPw17, which differs from CPw3 only by the replacement of H by CH$_3$ unit on the nitrogen atom of amide. However, CPw17, in comparison to the corresponding -NH- analogs, is a less efficient extractant; the selectivity for the light over the heavy lanthanides is less pronounced, but CPw17 displays a higher Am/Eu selectivity than CPw3 (Table 4.30). Moreover, CPw17 is more resistant to nitric acid and to irradiation. While for CPw17 the europium distribution ratios remain practically unchanged after 22 days of contact of this compound with 3 M nitric acid, they decrease strongly for CPw3 after 10 days. Complexation measurements of La and Eu in methanol showed that CPw17 formed a 1:1 M:L complex in contrast to CPw3, for which a 2:1 complex was detected. However, the small differences in the stability constants do not explain the better extracting ability of CPw3 (see Section 4.7).

The crystallographic structure of CPw17 obtained at the University of Liège shows that the four methyl groups do not prevent this ligand from adopting the most preferred conformation of the calix[4]arenes. An open geometry, in which two phenyl rings in the macrocyclic unit are pointing outward while the two other rings are parallel and oriented vertically, is indeed adopted by CPw17. The relatively low extracting ability of this macrocycle is thus not due to steric effects.

Desreux et al. studied the stoichiometry and the dynamic behavior of Gd^{3+} complexes by the dispersion of the nuclear magnetic relaxation dispersion (NMRD).[170] Formation of the complex is accompanied by the removal of solvent molecules from the first coordination sphere of the paramagnetic sphere, which induces changes in the solution relaxation time T_1. The relaxation rate $1/T_1$ decreases as the relaxation of the solvent nuclei becomes slower, because it takes place in the bulk of the solution rather than close to unpaired electronic spins. Ligands CPw3 and CPw17 form aggregates at a large ligand/Gd(III) concentration ratio. The formation of oligomers is evidenced in NMRD titration curves by an increase of the relaxation rates between 1 and 20 MHz brought about by a lengthening of the rotational correlation times. Although calixarene CPw17 is barely different from CPw3, it forms larger aggregates with Gd(III) (Figure 4.9).

The rotational correlation times of the largest aggregates of Gd(CPw3) and Gd(CPw17) are 649 and 1360 ps, respectively, and their radii are 1.2 and 1.6 nm. The opposite was expected, because the methylation of the amide functions precludes
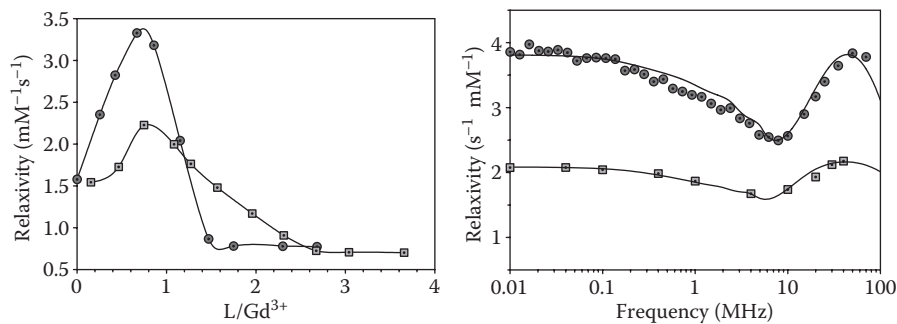
FIGURE 4.9 Relaxation titration curves (left) and NMRD dispersion curves (right) of ligands CPw3 (▣) and CPw17 (⊙) in anhydrous acetonitrile.

the formation of hydrogen bonds. Calixarene CPw17 is also a much poorer extractant than its nonmethylated counterpart, and this difference could be related to their aggregation state. The assumption of the formation of oligomeric structures of CPw3 due to its relative flexibility is confirmed by a crystallographic analysis of the dimeric structure $Eu_5(CPw3)_2(NO_3)_{15}$ $2H_2O$ in which one of the cations is coordinated to two CMPO arms belonging to different calixarene units.[164]

Oligomeric assemblies were also found by light diffusion scattering, although their small size is just at the limit of the possibilities of this technique. It is noteworthy that oligomerization is the first step in the formation of a third phase, a major problem in solvent-extraction processes. Aggregation phenomena, which are also supported by dynamic light-scattering measurements, probably play a role in the extraction, but certainly other factors have to be taken into account.[18]

4.5.2.1.4 Extraction by Rigidified Wide-rim CMPO Calixarenes

Conformationally rigidified tetra-CMPO derivatives have been prepared from calix[4] arene bis(crown ether) in which adjacent oxygen atoms are bridged at the narrow rim by two short diethylene glycol links, and in which the wide rim bears different residues: diphenylphosphine oxide (CPr1), dihexylphosphine oxide (CPr2), phosphinate (CPr3), and phosphonate (CPr4).[171] The rigidified bis(crown ether) ligand CPr1 is a more effective extractant than its pentylether counterpart. CPr1 requires only one-tenth of the concentration ($C_L = 10^{-4}$ M) to obtain the same distribution ratios as CPw3, while OΦCMPO needs a 2000-fold higher concentration to obtain the same distribution ratios. CPr3, more efficient than CPr4, which displays distribution ratio values comparable to those of the not-rigidified CPw3-bearing CMPO groups, is an especially interesting compound, as the highest extraction is achieved for americium (Figure 4.10). Tests performed at different cation concentrations show the influence of nitric acid. At a concentration of 10^{-5} M for each lanthanide, the distribution ratios are relatively independent of nitric acid concentration, contrary to what is observed at a concentration ten-fold lower, where the distribution ratios sharply decrease as the nitric acid concentration increases. The enhancement of distribution ratios can be explained by a better preorganization of the ligating functions owing to the rigidity, which on the other hand, did not appreciably change the selectivity for americium
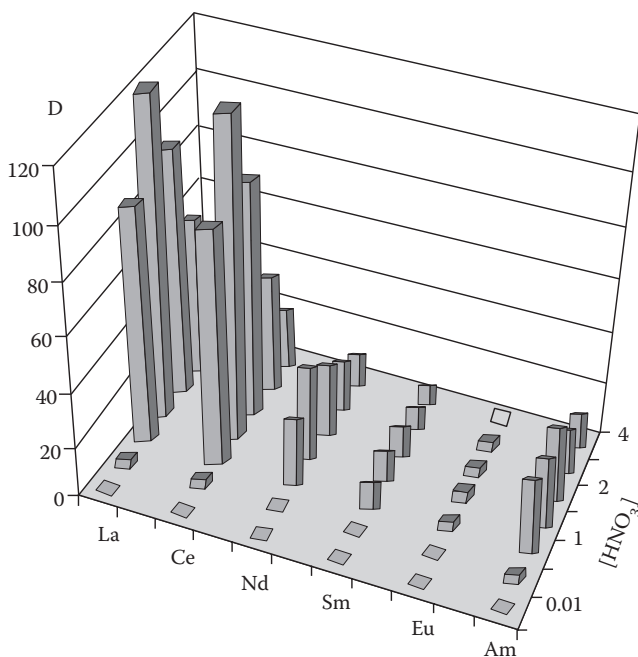
FIGURE 4.10 Distribution ratios of lanthanides (10^{-6} M) for CPr1 as a function of HNO_3 concentration (0.01 M, 0.1 M, 1 M, 1.5 M, 2 M, 3 M, and 4 M).

and light lanthanides over heavy ones observed for pentylether CMPO calixarenes. NMR relaxivity titration curves and nuclear magnetic relaxation dispersion (NMRD) profiles showed that large oligomers were formed (see Section 4.7).

4.5.2.1.5 Extraction by Sulfur Derivatives of Wide-rim CMPO Calixarenes

To try to improve the discrimination between trivalent actinides (Am and Cm), Böhmer synthesized the counterpart of CPw3 by replacing amidic oxygen atom and the oxygen atom of the phosphine oxide by sulfur atoms. As expected, hard lanthanide and actinide cations were much less extracted by the sulfur counterpart; to improve the extraction, TOPO was added to the organic phase, increasing the extracting ability of the mixture, but without improving the selectivity for actinides over lanthanides.[168]

4.5.2.1.6 Extraction by CMPO or Diphosphine Wide-rim Calixarenes

Atamas et al. synthesized calixarenes in which the phosphorus atoms of four CMPO or diphosphine residues are linked to the wide rim of these calixarenes via a CH_2 spacer.[172] When compared with CPw2, the calixarenes CPw30 and CPo22 extract Yb more efficiently, in contrast with La and Eu, which are less effectively extracted; the selectivity along the lanthanide series is less marked. Complexation measurements were carried out in methanol in the presence of $NaNO_3$ ($5 \cdot 10^{-2}$ M); the La and

Eu complexes are significantly less stable than those measured with CPw2. Contrary to the latter, which additionally forms strong 2:1 M:calix complexes, the CPw29 and CPo22 form only 1:1 complexes, which hints at the involvement of the four ligating arms in their complexes. Comparison of CPw29 and CPo22 versus CPw2 (extraction from acidic solutions by calixarenes diluted in NTFB) shows that the latter is by far the most efficient and the most selective calixarene; the selectivity factors $S_{Am/Eu}$ for CPw2 and CPw29 are 22 and 2, respectively.

4.5.2.2 Extraction by Narrow-rim CMPO Calixarenes

Functional groups attached to the wide rim of calix[4]arene fixed in the cone conformation are divergently oriented. This situation may change, if such groups are attached to the narrow rim, thus, primarily having a more convergent orientation. As the extraction ability (and even the selectivity) of calixarene-based ionophores is significantly dependent on the *p*-substituents, *t*-butyl substituted compounds (CPn1-CPn4), *t*-octyl derivatives (CPn5-CPn6), and the unsubstituted derivatives (CPn7-CPn9) were synthesized by the Mainz group[173] (see Section 4.7).

The binding of some lanthanide cations with OΦCMPO, CPw2, CPw3, CPw17, and CPn3 has been investigated using two experimental methods: UV absorption spectrophotometry (in the presence of nitrate or chloride anions) and ESI-MS. In the case of OΦCMPO, UV spectrophotometric measurements in methanol show the formation of ML, ML_2, and ML_3 species with $LaCl_3$. The same stoichiometries are also observed in this solvent by ESI-MS, which provides additional information. For $La(NO_3)_3$, mainly singly charged species are observed (coordination of two NO_3^-), while for $LaCl_3$, mainly doubly charged complexes are detected (coordination of one Cl^-). With the calix[4]arene-bearing CMPO moieties, the same stoichiometries have been established by ESI-MS and UV spectrophotometry for the complexation of $La(NO_3)_3$: ML and M_2L with CPw2 and CPw3, and ML with CPw17 and CPn3. The most stable 1:1 complexes are those formed with the wide-rim derivatives in chloride medium. Their stability decreases remarkably in the series in contrast to the stability of the complexes with OΦCMPO, which increases with the electronic density of the cations (Table 4.31).[174]

All the compounds synthesized are highly efficient for Th^{4+} extraction even more than their wide-rim counterparts. The lanthanides are extracted to a much lesser extent. The highest extraction is obtained for La^{3+} with the derivatives CPn3 and CPn6 having a spacer of four CH_2 groups. For all cations, the extraction depends upon the length of the alkyl chain linking the functional groups to the phenolic oxygen of the calixarene. Butyl chains seem the optimum in terms of efficiency. For each ligand, the extraction level is close for La^{3+} and Eu^{3+} and then decreases for Yb^{3+}. The extraction level, comparable for *t*-butyl and octyl, is higher than for their *p*-H counterparts (Table 4.32).

The grafting of CMPO moieties on the narrow rim affords a strong decrease of extracting ability toward lanthanides, trivalent actinides, and tetravalent plutonium from acidic solutions. The distribution ratios for the different calixarenes in NPHE are low, except for CPn3 for which the number of carbon atoms in the spacer is four, but even for this compound, the distribution ratios are lower than those obtained with their wide-rim counterparts (Figure 4.11).

TABLE 4.31

Stability Constants ($\log \beta \pm \sigma_{N-1}$) of Lanthanide Complexes with OΦCMPO and CPw2, CPw3, CPw17, and CPn3 in MeOH ($I = 0.05$ M) Determined by UV Spectrophotometry

Ligands	Complexes	Cl⁻			NO₃⁻		
		La³⁺	Eu³⁺	Yb³⁺	La³⁺	Eu³⁺	Yb³⁺
OΦCMPO	ML	4.63 ± 0.05	4.99 ± 0.05	5.6 ± 0.3	—ᵃ	—ᵃ	—ᵃ
	ML₂	8.5 ± 0.2	9.35 ± 0.05	10.5 ± 0.4	—ᵃ	—ᵃ	—ᵃ
	ML₃	12.4 ± 0.2	13.5 ± 0.1	14.5 ± 0.5	—ᵃ	—ᵃ	—ᵃ
CPw1	ML	n.d.	7.00 ± 0.02	n.d.	n.d.	4.0 ± 0.1	n.d.
	M₂L	n.d.	11.5 ± 0.4	n.d.	n.d.	8.09 ± 0.02	n.d.
CPw2	ML	8.5 ± 0.1	7.2 ± 0.1	6.8 ± 0.5	6.0 ± 0.2	5.6 ± 0.3	3.5 ± 0.5
	M₂L	13.9 ± 0.3	11.9 ± 0.3	12.01 ± 0.03	10.6 ± 0.4	11.0 ± 0.3	8.6 ± 0.4
CPw3	ML	n.d.	n.d.	n.d.	6.9 ± 0.4	6.0 ± 0.3	5.7 ± 0.2
	M₂L	n.d.	n.d.	n.d.	12.2 ± 0.3	11.1 ± 0.4	10.3 ± 0.1
CPw17	ML	7.1 ± 0.1	7.6 ± 0.2	ᵃ	5.4 ± 0.2	5.3 ± 0.2	—ᵃ
CPn2	ML	5.77 ± 0.08	5.0 ± 0.5	5.0 ± 0.5	—ᵃ	—ᵃ	—ᵃ
CPn2	ML	6.4 ± 0.2	5.1 ± 0.1	5.1 ± 0.1	—ᵃ	—ᵃ	—ᵃ

ᵃ Below detection limits.

TABLE 4.32
Percentage Extraction, %E, and, in Brackets, Distribution Ratios, D, for Lanthanides and Thorium Nitrates by Narrow-Rim Calixarenes CMPO from 1 M HNO$_3$ into Dichloromethane: T = 20°C, C$_M$ = 10^{-4} M

Ligands	R		La^{3+} C$_L$ = 10^{-3} M	Eu^{3+} C$_L$ = 10^{-3} M	Yb^{3+} C$_L$ = 10^{-3} M	Th^{4+} C$_L$ = 10^{-4} M
CPn1	t-Butyl	2	19	16	2.6	76
CPn2		3	13	12.5	<2	83
CPn3		4	70	68	37	96
CPn4		5	30	19	6	86
CPn5	Octyl	3	11	10	<2	80.6
CPn6		4	71	70	22	95
CPn7	H	2	9	5	<2	70
CPn8		3	9	7.3	<2	75.3
CPn9		4	52.5	54	15.1	90.2
CPn10	t-Butyl	3/5	33.3	34	17	87
CPn11		4/5	47	54	28	91
CPn12		3/4	69	72	23	77
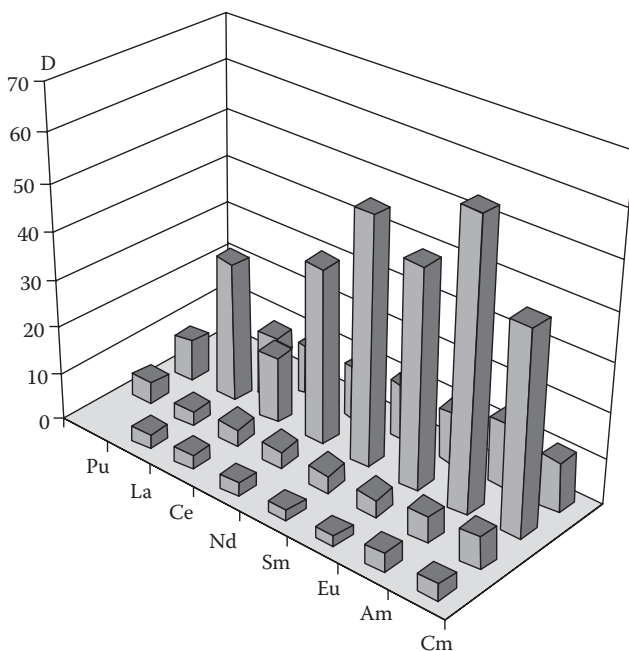
FIGURE 4.11   Distribution ratios of lanthanides (10^{-5} M), Am, and Cm (trace level) from 3 M HNO$_3$ solutions into NPHE with CPn1, CPn2, CPn3, and CPn4.
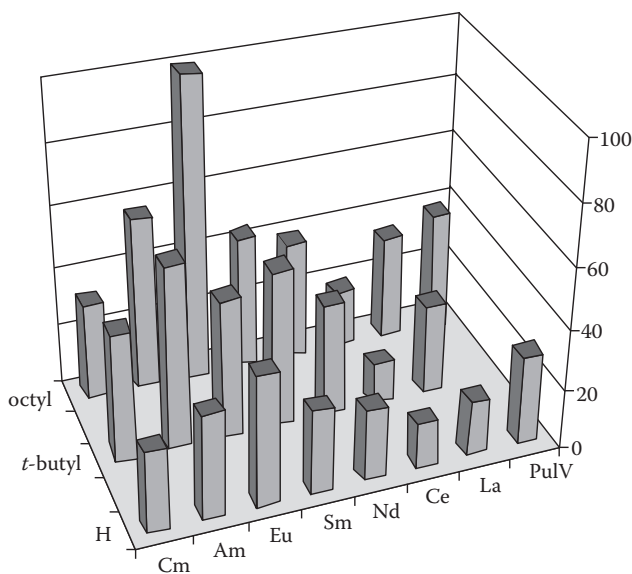
FIGURE 4.12 Distribution ratios of lanthanides (10^{-5} M), Pu, Am, and Cm (trace level) from 3 M HNO_3 solutions into NPHE with CPn3, CPn6, and CPn9.

CPn1, CPn2, and CPn4 display a low intralanthanide selectivity or a low affinity for actinides in comparison to lanthanides. However, the distribution ratios of lanthanides decrease with increasing atomic number for ligand CPn1, as observed for macrocyclic compounds. On the contrary, compounds possessing a longer spacer, CPn2 and CPn4, behave like classical extractants, that is, their extracting ability increases with the increasing charge density of lanthanide cations. More peculiar is the behavior of CPn3, for which an extraction maximum is observed for neodymium, samarium, and europium; then the distribution ratios sharply decrease for the heaviest lanthanides (Figure 4.12). The comparison of the three calixarenes with the same spacer (butyl chain) shows that the substitution of the aromatic H by butyl or octyl appreciably increases the distribution ratios and the selectivity. The selectivity of europium over other lanthanides is pronounced for the octyl derivative CPn6. One has to point out that high americium distribution ratios are obtained for the *t*-butyl derivative CPn3 (Figure 4.13).

In order to see if it was possible to tune the efficiency and possibly the selectivity of this series of compounds, mixed derivatives bearing two different chain lengths have been studied: CPn10 ($n = 3, 5$), CPn11 ($n = 4, 5$), and CPn12 ($n = 3, 4$). Extraction data obtained with CPn12 are similar or slightly lower than with the homo derivative ($n = 4$), but much higher than with the derivative ($n = 3$). CPn10 and CPn11 display extraction percentages intermediate between those of the corresponding symmetrical derivatives (Table 4.32) (see Section 4.7).

Complexation in methanol in the presence of chloride anions has been followed for two "symmetrical" ligands, CPn8 ($n = 3$) and CPn9 ($n = 4$), and for the mixed CPn10 and CPn12. Only 1:1 complexes form with the four ligands. With the "symmetrical" ones, the stability sequence is $La^{3+} > Eu^{3+} \sim Yb^{3+}$. With the mixed ligand CPn12, the
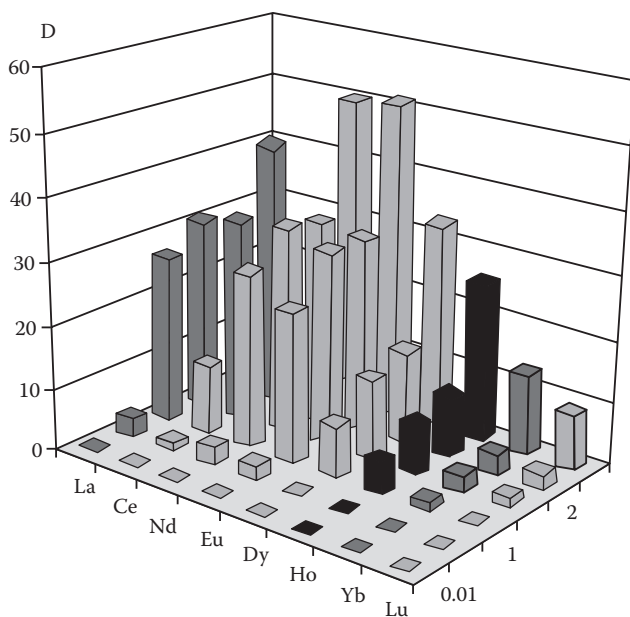
FIGURE 4.13 Distribution ratios of lanthanides (10^{-5} M) for CPn3 as a function of HNO_3 concentration (0.01 M, 0.1 M, 1 M, 1.5 M, 2 M, and 3 M).

stability decreases along the series, whereas CPn10 is almost nonselective. NMR spectroscopy was applied at the University of Liège for unraveling the solution structures and the dynamic properties of calixarene lanthanide complexes. Both the induced paramagnetic dipolar shifts and the solvent relaxation times (NMRD) were used in these studies, the former to establish solution structures and the latter to study aggregation states. It was confirmed that complexed calixarenes substituted on the narrow rim remain monomeric in solution, while their analogues substituted on the wide rim form polymers with metal ions. This can be explained by the fact that the latter maintain the CMPO ligands and the complexed cations outside the cavity of the calix[4]arene.[175]

This difference of behavior of calixarenes bearing CMPO residues either on the wide rim or on the narrow rim was confirmed by extraction of europium (from nitric acid solutions by CPw2 and CPn2 diluted in chloroform) by implementing ESI-MS for the two calixarenes. Complexes with 1:1 and 1:2 Eu:calix-CMPO stoichiometry were evidenced. The major species for CPw2 is the 1:2 complex, while for CPn2 the predominant complex is the 1:1 complex.[165]

It was shown that narrow-rim CMPO derivatives form stronger 1:1 lanthanide complexes than their wide-rim counterparts. However, lanthanide extraction results display a stronger extracting ability. This discrepancy can be explained by the fact that, contrary to the wide-rim CMPO calixarenes that form polymeric species, a part of less lipophilic monomeric narrow-rim CMPO calixarene piles up at the interface instead of being extracted, as predicted by Wipff for the extraction of strontium by mixed amide calixarenes (see Section 4.4.1.1). This assumption is all the more

probable, as the ligand concentration is weak (10^{-3} M). The higher distribution ratios observed for wide-rim CMPO calixarenes seem to have for origin the faculty to form polymers. This seems particularly obvious in the case of rigid calixarenes such as CPr1.

The presence of both CMPO and amide residues on the narrow rim of the calixarene does not lead to an enhancement of Am/Eu selectivity (about 2) (CPn13, CPn14, CPn15) like that observed for their counterparts with amide groups grafted on the wide rim (CPw25, CPw26, and CPw27).

4.5.2.3   Adamantyl Calix[*n*]arene-CMPO

Starting from *p*-adamantylcalix[4]-[6]arenes functionalized with carboxylic acid or ester groups at the adamantane nuclei, eight *p*-adamantylcalix[4]arene derivatives bearing four CMPO-like functions $[(CH_2)_nNHC(O)CH_2P(O)Ph_2]$ at the wide (CAd1, CAd2, CAd3, n = 0, 1, 2) or narrow (CAd5, CAd6, CAd7, CAd8, CAd9, and CAd10, n = 2–4) rims were synthesized for the first time as well as the hexamer bearing six CMPO groups at the wide-rim of CAd4.[176] They were studied as extractants for a series of *f*-block elements, including radioactive [152]Eu(III), [241]Am(III), [233]U(VI), and [239]Pu(IV). For comparative purposes, N-(1-adamantyl)CAd11, N-(1-adamantylmethyl)CAd12, and DΦCMPO were used as reference compounds (see Section 4.7). Adamantylated calixarenes have been chosen as molecular platforms for several reasons:

- These compounds can be easily obtained on a multigram scale from *p*-H-calix[4,6]arenes and 3-*R*-1-hydroxyadamantanes (*R* = H, alkyl, aryl, or other functional groups).
- The main drawback of calixarene CMPO is their low solubility in most diluents; the presence of the bulky and lipophilic adamantane nuclei should improve it.
- The adamantyl unit provides several positions for the introduction of additional substituents, which opens the road for the further development of this type of ligand (possible fine-tuning of selectivity, creation of new binding sites at the wide rim, etc.).

To enhance the effectiveness of extraction, *m*-nitro-trifluoromethylbenzene (NTFB) was used as a more polar solvent. The Am and Eu extraction in NTFB and dichloromethane as receiving phases were compared. Under these conditions, the extraction ability is about ten times higher in NTBF than in dichloromethane. Studies of the extraction of americium(III) and europium(III) from 3 M HNO_3 solutions to organic phases (dichloromethane, NTFB) show (Table 4.33):

- A relatively good solubility in dichloromethane, as the concentration of CAd1 and CAd2 in this diluent reached 2×10^{-2} M.
- As for wide-rim CMPO calixarenes, the extraction ability for all the adamantyl-calixarene ligands is much better than for their monomeric analogues (CAd11, CAd12) and DiΦCMPO.

TABLE 4.33

Distribution Ratios for Am and Eu from Aqueous Solutions (3 M HNO$_3$) into Dichloromethane for Adamantyl-Calixarenes at Various Ligand Concentrations

Ligands	D	[C$_L$] mM								
		0.25	0.5	1.0	2.0	3.0	4.0	5.0	10	20
CAd1	D_{Am}							0.27	1.0	2.1
	D_{Eu}							0.19	0.62	1.7
CAd2	D_{Am}	0.29	0.60	1.9	6.6	17	17	32	240	920
	D_{Eu}	0.19	0.44	1.2	4.1	9.0	14	26	125	570
CAd3	D_{Am}	0.11	0.39	0.66	1.08	5.2	10.5			
	D_{Eu}	0.08	0.25	0.47	1.03	2.6	6.1			
CAd4	D_{Am}		0.15	0.33	0.86		3.3			
	D_{Eu}		0.12	0.24	0.61		2.3			
CAd5	D_{Am}	0.58	1.4	2.4	8.8	22				
	D_{Eu}	0.49	1.1	2.8	7.0	16				
CAd6	D_{Am}	0.06	0.11	0.27	0.71	1.2				
	D_{Eu}	0.04	0.08	0.25	0.48	0.8				
CAd7	D_{Am}	0.11	0.22	0.44	1.1	1.6				
	D_{Eu}	0.08	0.14	0.38	0.64	1.0				
CAd8	D_{Am}	0.32	0.70	1.2	4.9	14				
	D_{Eu}	0.19	0.45	1.8	3.0	9.2				

- The extraction percentage increases strongly with increasing length of the spacer for all types of ligands, and best extraction results were found for CAd2 and CAd7; the separation factor $S_{Am/Eu}$ did not exceed 2, which is close to the narrow rim CMPO calixarenes.
- Variation of the spacer length between CMPO groups attached to the 1,3- and 2,4-positions of the calixarene platform did not lead to appreciable improvements, in terms of extraction or selectivity.

As on the wide-rim CMPO compounds, the plots of log D_{Am} versus log C_L for several compounds suggests that the extracted complexes are a 1:2 cation/ligand species. For all the ligands tested, americium is extracted slightly more efficiently than europium, though the ratio $S_{Am/Eu}$ does not exceed 2. Apparently, this is connected with the weaker preorganization of adamantyl-calixarenes as well as CMPO-calixarenes on the narrow rim in comparison with CMPO-calixarenes on the wide rim. Preorganization of the ligating functions on a suitable platform (e.g., a calixarene) still remains the determining factor in increasing the extraction of americium and europium in comparison with simple ligands.

All calixarenes bearing CMPO residues on the wide rim display a higher affinity for thorium. The hexamer CAd4 is the most effective for thorium, while lanthanides are better extracted by CAd2. Without spacers (CAd1), the ligating CMPO functions

seem "shielded" by the adamantane groups, while the C_2 spacers (CAd4) are too long, leading to a loss of preorganization of the CMPO groups. There is no important difference for the lanthanide extraction by tetrameric (CAd1-CAd3) or hexameric ligands (CAd4). Enlargement of the calixarene size mainly leads to a better extraction of tetravalent thorium. No notable selectivity was found; the separation factors D_{Am}/D_{Eu} are in the range of 0.8–1.9 for all the adamantyl-calixarene compounds. Plots of log D versus log C_L are linear with slopes ranging between 1.5 and 1.9. The extraction seems to occur with the formation of at least ML and ML_2 complexes with close stabilities.

The wide-rim CMPO calix[4]arenes are the most efficient compounds for the extraction of trivalent actinides and lanthanides. They are also the compounds that display the highest selectivity along the lanthanide series, provided that phosphorus atoms are linked to phenyl groups. They also display a higher selectivity than the calixarene-bearing diphosphine oxide, where the phosphorus atom is linked to phenyl units CPo21.[176–178]

4.5.2.4   Extraction by CMPO-Calixarenes Possessing More than Four CMPO Units

4.5.2.4.1   Extraction by Octa-CMPO-Calixarenes

Mainz University workers attached eight CMPO groups to a calix[4]arene skeleton fixed in the 1,3-alternate (CPwn1) and the 1,2-alternate (CPwn2) conformations, respectively. Four of these groups are directly bound to the wide rim and four via a C_3-spacer to the narrow rim. Surprisingly, (CPwn2) shows an interesting selectivity within the lanthanide series. The distribution ratios for La^{3+}, Eu^{3+}, and Yb^{3+} nitrates from 1 M HNO_3 into dichloromethane are 1.56, 0.75, and 0.25, respectively (see Section 4.7).[18]

4.5.2.4.2   Extraction by CMPO-Calix[6,8]arenes

The Parma group synthesized a series of calix[6,8]arenes bearing CMPO units. In all of them, the CMPO units are linked to the lower rim of the calixarene mostly via C_3 spacers. CP_61, CP_62, and CP_63 are hexamers, CP_81 and CP_82 are octamers, while CP_61 and CP_82 bear *tert*-butyl and benzyloxy units, respectively, at the upper rim. This affects both the conformational properties of the macrocycle and the electron-donating character of the phenolic oxygen atoms at the lower rim. CP_62 has a longer spacer (C_4) between the calix and the CMPO unit. CP_61, having bulky groups both at the upper (*tert*-butyl) and at the lower rim (CMPO) on a medium-sized calixarene skeleton (hexamer) is conformationally restricted in solution and is present as a mixture of conformers[179] (see Section 4.7).

Since in the case of *p*-H calixarenes, a precipitate occurred at the water/organic interphase, extraction tests were carried at a concentration of 10^{-4} M for these compounds. The presence of *tert*-butyl or benzyloxy at the wide rim helps to solubilize the complexes. The distribution ratios are compared to wide-rim CPw3 and narrow-rim CPn3 (Table 4.34).[179] For all CMPO-calix[6,8]arenes, distribution ratios of the two cations studied (Eu and Am) increase with increasing HNO_3 concentration, in agreement with what is observed with tetramers bearing CMPO residues

TABLE 4.34

Distribution Ratios and Selectivity $S_{Am/Eu}$ for Am and Eu From Aqueous Solutions into a NPHE Solution of CMPO-calix[6,8]Arenes (10^{-3} M)

Ligands	[L] (M)		[HNO$_3$] (M)						
			0.001	0.01	0.1	1	2	3	4
CP$_6$1	10^{-3}	D_{Eu}	0.29	0.56	5.1	26.4	27.7	35.5	26.6
		D_{Am}	0.44	0.82	11.1	>100	>100	>100	>100
		$S_{Am/Eu}$	1.5	1.5	2.2	>3	>3	>3	>3
CP$_6$2	10^{-3}	D_{Eu}	1.6	0.6	1.2	5.9	—[a]	—[a]	—[a]
		D_{Am}	2.8	0.9	2.1	20.6	—[a]	—[a]	—[a]
		$S_{Am/Eu}$	1.7	1.5	1.7	3.5	—[a]	–	–
CP$_6$3	10^{-3}	D_{Eu}	0.47	0.25	0.56	3.0	nd	nd	10.6
		D_{Am}	0.85	0.34	0.95	4.5	nd	nd	20.7
		$S_{Am/Eu}$	1.8	1.4	1.7	1.5	–	–	1.9
CP$_8$1	10^{-3}	D_{Eu}	—[b]	7.8	9.2	21.9	nd	nd	nd
		D_{Am}	—[b]	14.6	18.3	32.8	nd	nd	nd
		$S_{Am/Eu}$	–	1.9	2.0	1.5	–	–	–
CP$_8$2	10^{-3}	D_{Eu}	3.8	5.6	4.2	10.7	12.5	14.7	32
		D_{Am}	3.8	7.1	12.6	12.6	18.0	> 100	—[b]
		$S_{Am/Eu}$	1	1.3	3.0	1.2	1.4	> 6	

Note: nd: not determined; nr: not reported.

[a] Important precipitation at the interphase.

[b] Content of the aqueous layer too low to allow a precise determination of D.

on the narrow rim, while tetramers bearing CMPO residues on the wide rim usually display a maximum at a nitric acid concentration of 2 M. The efficiency and selectivity obtained with hexamers seem close to the wide-rim CMPO tetramers. Functionalized calix[8]arene had a poor solubility and a third phase appeared during extraction experiments. Among functionalized calix[6]arene, CP$_6$1 (narrow-rim hexa CMPO calixarene) seems to be the most promising, with very high distribution ratios, especially at high acidities, and also an interesting Am over Eu selectivity.

In collaboration with the Mainz group, Parma University workers synthesized CMPO-calix[6]arenes CP$_6$4 and CP$_6$5, bearing three CMPO binding sites onto the narrow and wide rim, respectively. CP$_6$5 and to a lesser extent CP$_6$4 display relatively low distribution ratios and a selectivity $S_{Am/Eu}$ lesser than 2.5.[18]

4.5.2.4.3 Dendritic Octa-CMPO-Calix[4]arenes

First studies on dendrimeric polyamines from the second (D_2) to the fifth generation (D_5) leading to molecules carrying 8, 16, 32, and 64 CMPO-functions were carried out; D_2 and D_4 are shown as an example (see Section 4.7). These compounds, though soluble in chloroform or NPHE, are probably too soluble in the aqueous phases (eventually due to protonation under acidic conditions) for a liquid-liquid extraction

procedure. Consequently, Dozol made profit of their relative solubility in water to use these compounds as complexing agents and to separate the complexes formed in water by filtration.

For complexation experiments, a known mass of dendrimer was dissolved in the aqueous phase containing actinides (dissolution was accelerated by ultrasonication), and the solution was filtered. The filtrate was recovered and contacted with a new known mass of dendrimer and filtered again. These operations were repeated three or four times.

Distribution ratios (K_d) were determined from the following relation:

$$K_d = \frac{([C]_{in} - [C]_{fin})}{[C]_{in}} \frac{V}{m_{ext}}$$

where:
C_{in} = Initial concentration (or activity) of nuclides
C_{fin} = Initial concentration (or activity) of nuclides
V = Volume of aqueous phase
m_{ext} = Mass of dendrimer

As expected, the distribution ratios K_d are constant, even though the concentration of dendrimer changes. K_d is also independent of the size of the filters. It is likely that the polymer is adsorbed on the organic filters. This hypothesis is confirmed by using different "generation" dendrimers and hence of compounds of different size. Distribution ratios were shown to be independent of the dendrimer size and also of the cation concentration (Table 4.35).

The selectivity factor is not sufficient to allow actinides to be separated from lanthanides. However, this process, easy to implement, can be used to remove actinides at low concentration from acidic waste containing even large amounts of sodium.[180]

TABLE 4.35

Distribution Ratios $K_{d\,Am}$ and $K_{d\,Eu}$ and Selectivity $S_{Am/Eu}$ for Dendrimer of Different Generations—Filtration 0.2 μm

| Dendrimer | Conc (M) | | Aqueous Phase: HNO$_3$ 3 M + Dendrimer | | |
			1st Filtration	2nd Filtration	3rd Filtration
D_2	10^{-4}	$K_{d\,Eu}$	1,170	1,200	970
D_3	10^{-5}	$K_{d\,Eu}$	1,090	1,380	
		$K_{d\,Am}$	2,820	4,240	
		$S_{Am/Eu}$	2.59	3.07	
D_4	10^{-5}	$K_{d\,Eu}$	1,510	9,20	2,600
		$K_{d\,Am}$	3,370	2,120	4,860
		$S_{Am/Eu}$	2.23	2.31	1.87
D_5	5 10^{-6}	$K_{d\,Eu}$	1,070	2,280	1,790
		$K_{d\,Am}$	1,070	2,280	1,790
		$S_{Am/Eu}$	3.08	2.09	2.83

4.5.2.4.4   Dendritic Calixarenes

Following the idea that a high local concentration of CMPO functions would be benefi-
cial, dendritic polyamines of the poly(propylene imine) (PPI) and of the polyamidoamine
(PAMAM) type were attached to calix[4]arenes leading to four compounds in the cone
conformation with eight CMPO functions attached to the narrow rim with C_3 spacer
(CD1) or C_4 spacer (CD2) or to the wide-rim (CD3 and CD4) these dendritic calixarenes
were prepared by Maniz group.[181] The extraction ability is low in comparison to wide- or
narrow-rim tetra-CMPOs for all the compounds whether the CMPO residues are located
on the wide or the narrow rims. Solubility problems were encountered with some com-
pounds, which could probably be solved by the introduction of more lipophilic residues.
However, the extraction results show that simple accumulation of CMPO groups is not
sufficient to improve the extracting ability and the selectivity of extractants. Contrary to
what is observed for tetramers bearing CMPO residues on the wide rim, NMR relax-
ation studies show that probably CD3 forms exclusively a monomeric 2:1 metal/ligand
complex in which the two cations are totally encapsulated by the CMPO and amino
coordinating groups and are essentially unsolvated (see Section 4.7).

4.5.2.4.5   Magnetic Particles Bearing CMPO Calix[4]arenes

Nuñez et al. proposed the use of magnetic fluidized-bed separation technology and
the development of magnetically assisted chemical separation (MACS) systems for
nuclear-waste remediation.[182,183] These combine the selectivity of a solvent exchange
ligand system with improved separation, resulting in a system that can be used at
low concentrations. The magnetic particles can then be stripped, to enable re-use,
or vitrified. Adsorption of CMPO to magnetic acrylamide particles enhances the
extraction of americium and plutonium through a synergistic relationship between
the extractant and magnetic particle.

   A magnetic particle-based process that applies calix[4]arene-bearing CMPO on
the wide rim and covalently attached by spacer (C_3, C_5, and C_{10}) on the narrow rim
with particle surface was developed.[184,185] Efficient extraction of americium, euro-
pium, and cerium from simulated acidic nuclear waste has been achieved due to
the use of highly porous magnetic silica particles, which allow a higher density of
CMPO-calix[4]arenes to be implemented. The C_3–C_5 spacer leads to more effective
extraction of europium and americium than the highly flexible C_{10} spacer; however,
a higher selectivity $S_{Am/Eu}$ is observed for the longer spacers (from 1.28 for the C_3
spacer to 2.3–2.4 for the longer C_5 and C_{10} spacers). The possibility of recycling the
magnetic particles was demonstrated by back-extraction of europium from the par-
ticle surface. The complexation capacity of the particles did not change within four
complexation back-extraction cycles.

4.5.3   Calixarene Picolinamide

Picolinamides are possible binding groups able to achieve the actinide/lanthanide
separation. The Parma group has undertaken a study aimed at introducing picolin-
amide groups on both rims of calix[n]arenes. The picolinamide-binding group was
introduced at the narrow rim of calix[4]arenes (CPi2, CPi3, and CPi3), of calix[6]
arenes (CPi6, CPi7, and CPi8), or of calix[8]arenes (CP9 and CP10) also using

different spacers such as propyl or butyl chains. In order to study the effect of softer binding groups on the extraction properties of these derivatives, the thiopicolinamide CPi5 was prepared from CPi4. Compounds with picolinamide linked to the wide rim directly (CPi11) or through a methyl spacer (CPi12) were also synthesized. Monomer N-butylpicolinamide (CPi1) was used as a model compound[186] (see Section 4.7).

To increase the distribution ratios, a solution of lithium nitrate 1 M was used. This salt, which has a common anion with europium and americium to be extracted but a cation which is usually negligibly extracted by other calixarenes, should increase the distribution ratios according to the relation $D_M = K_{ex}[L]^m[NO_3^-]^n$. It seems that these calixarenes, as several nitrogen ligands do, present a certain affinity for this lithium cation. The lipophilic dicarbollide anion (BrCosan), which is known to facilitate cation extraction, was implemented and led to a strong increase of the extraction of cations from 10^{-3} M HNO_3 solutions. Under these conditions, only thiopicolinamide was not able to significantly extract trivalent actinides.[187]

Dynamics studies were carried out on the effect of CCD$^-$ (chlorinated cobalt-dicarbollide) anions on the Eu^{3+} lanthanide cation extraction by a calix[4]arene-CMPO ligand L, focusing on the water-"oil" interface, where oil is modeled by chloroform.[188] The free L ligand and its EuL^{3+} complex are found to adsorb and to concentrate at the interface, but they are too hydrophilic to be extracted. The addition of CCD$^-$ anions under dilute conditions (either covalently linked to L or as separated CCD$^-$ H_3O^+ ions) also leads to the same conclusions. However, at high concentrations, CCD$^-$ anions saturate the interface and promote the extraction of EuL^{3+} to the oil phase. Moreover, for the uncomplexed $Eu(CCD)_3$ salt, accumulation of CCD$^-$ anions at the interface creates a negative charge, which attracts the hydrated Eu^{3+} ions, therefore facilitating their complexation by interfacial ligands. MD studies on the extraction of M^{3+} ions (M = f-element) by CMPO-type CPw5, mixed with partly chlorinated cosan, and by an analogue ligand with $C_{10}H_{20}$-cosan arms gave insight into the synergistic extraction mechanism and the importance of interfacial phenomena,[189] for example:

1. The calixarene-M^{3+} complex is formed at the interface and remains there due to its surface activity; neutralization by cosan anions removes the amphiphilic character and allows diffusion into the bulk organic phase
2. The cosan anion itself is surface-active (though not amphiphilic), saturating the interface at higher concentration, thus promoting the removal of the complex from the interface
3. The interfacial cosan anion creates a negative surface charge, attracting Ln^{3+} to the interface, thus promoting the kinetics of the complexation

CPi6 displays a slightly higher americium-over-europium selectivity than the monomer CPi1. Most of the ligands, in the presence of dicarbollide, display distribution ratios higher than 100, and the americium-over-europium selectivity exceeds 10 for four ligands (CPi3, CPi4, CPi7, and CPi11). The size of the calixarene ring does not play an important role in the extracting ability of americium, octamers being slightly more efficient to extract americium than hexamers and tetramers. Increasing acidity leads to a protonation of the basic pyridine nitrogen atoms, which prevents the extraction of trivalent cations (Table 4.36).[190]

TABLE 4.36

Distribution Ratios[a] and Selectivity for the Extraction of Am and Eu from Aqueous Solutions 10^{-3} M HNO_3 into a NPHE/3 $\times$ 10^{-3} M [Bromocosan] Solution of Picolinamide Calixarenes

Ligand	CPi1	CPi2	CPi3	CPi4	CPi5	CPi7	CPi8	CPi9	CPi10	CPi11	CPi12
[L] (M)	0.1	0.01	0.01	0.01	0.001	0.005	0.005	0.005	0.002[b]	0.01	0.01
D_{Eu}	6.0	19.6	1.43	16.4	0.23	29.2	16.7	98	150	0.81	26.4
D_{Am}	16.5	173	16.3	210	0.20	>300	60.5	>300	>300	11.5	158
$S_{Am/Eu}$	2.7	8.8	11.4	12.8	0.9	>10	3.6	>3	>2	13.8	6.0

[a] Due to uncertainties associated with measurements at low activity in the aqueous phase (<50 KBq L^{-1}), D_M values greater than 300 should be considered with care.

[b] Significant precipitation occurred for CPi9.

Under the same conditions, in contrast to what is observed for calix[4]arene-bearing CMPO moieties, with CPi12, distribution ratios of lanthanides increase from the lightest lanthanide, lanthanum, to europium. Americium can be easily separated from the lightest lanthanides (separation factor $D_{Am/La} > 20$, $D_{Am/Ce} = 15$, $D_{Am/Nd} = 10$, $D_{Am/Sm} = 7.5$, $D_{Am/Eu} = 6$), which are the most abundant lanthanides in fission-product solution. Cavitands bearing picolinamide (Cv5) or thiopicolin-amide (Cv6) residues seems much less selective than their calixarene counterparts, giving $S_{Am/Eu} < 2$.[18]

4.5.4 Extraction by CMPO Calixarenes with Mixed Functionalities

4.5.4.1 Extraction by Wide-Rim Calixarenes Bearing One to Three CMPO Residues

Böhmer et al. synthesized calix[4]arenes fixed in the cone conformation and sub-stituted at their wide rim by one to three CMPO residues and hydrogen atoms in the remaining positions: CPw23 (with one CMPO unit), CPw24 (with two CMPO units in opposite positions), and CPw25 (with three CMPO units).[191] These calix-arenes were tested with their counterpart bearing four CMPO groups (CPw3) and the linear trimer for the extraction of La, Eu, and Th from 1 M HNO_3 in dichlo-romethane and for Sm, Eu, Gd, Er, Pm, and Am from solutions containing 10^{-2} M HNO_3, 4 M $NaNO_3$. CPw3 is much more efficient than the four other calixarenes even the calixarene bearing three CMPO residues CPw25. It definitively reveals that all four CMPO groups are required to obtain excellent extraction ability. In spite of the fact that the fixed cone conformation of the calixarene orients the CMPO ligands in one direction, inducing a better preorganization, CPw25 is less effective than the linear trimer. This phenomenon can be explained by an easier formation of a 2:1 M:calix complex in the case of the trimer (Table 4.37) (see Section 4.7).

4.5.4.2 Extraction by Wide-Rim Calixarenes Bearing Malonamide or Carboxylate Residues

Böhmer et al. also synthesized calixarenes bearing one or more CMPO moi-eties and another functionality (malonamide or carboxylate). These calixarenes display lower extracting ability than CPw3, and contrary to expectations, these functions do not lead to a new order of selectivity. Calix[4]arenes bearing one or two adjacent malonic acid groups (NH-C(O)-CH$_2$-COOH) adjacent to CMPO functions at the wide rim were unstable and decomposed during the complex-ation studies.

4.5.4.3 Extraction by Wide-Rim Calixarenes Bearing Amide Residues

Quite unexpectedly, the tris-CMPO monoacetamide CPw26, the bis-CMPO diamides CPw27 and CPw28 and, to a lesser extent, the monoamine CPw25 show much better Am/Eu selectivity than the corresponding tetrakis-CMPO derivatives. The mono- and tris-CMPO derivatives CPw23 and CPw24 were synthesized in order to gain a deeper insight into the structural requirements for an efficient

TABLE 4.37

Distribution Ratios[a] and Selectivity of Am and Eu from HNO_3 Solutions by Several Calixarenes into a NPHE Solution of CPw23–CPw29 (10^{-3} M)

		HNO₃ Concentration				
		0.01 M	**1 M**	**2 M**	**3 M**	**4 M**
CPw23	D_{Eu}	$4\ 10^{-3}$	$12\ 10^{-4}$		$13\ 10^{-3}$	
	D_{Am}	$5\ 10^{-3}$	$15\ 10^{-4}$		$13\ 10^{-4}$	
	$S_{Am/Eu}$	1.2	1.5			
CPw24	D_{Eu}	0.1	0.24	0.56	0.65	0.77
	D_{Am}	0.15	1.25	2.15	3.2	2.1
	$S_{Am/Eu}$	1.5	5.2	3.9	5	2.8
CPw25	D_{Eu}	$<10^{-3}$	0.05	0.19	1.2	0.46
	D_{Am}	0.0016	0.27	0.72	4.65	1.05
	$S_{Am/Eu}$	2.2	5.4	3.8	3.8	2.3
CPw26	D_{Eu}	0.018		2.15	7.7	
	D_{Am}	0.06		19	90	
	$S_{Am/Eu}$	3.4		8.6	12	
CPw27	D_{Eu}	0.47	1	0.45	1.2	
	D_{Am}	0.65	8.1	2.4	7.1	
	$S_{Am/Eu}$	1.4	8.1	5.4	5.9	
CPw28	D_{Eu}	$<5\ 10^{-3}$	0.66	0.56	0.55	
	D_{Am}	$4\ 10^{-2}$	6.3	1.45	5.2	
	$S_{Am/Eu}$	> 8	9.5	2.6	9.4	0.36
CPw29	D_{Eu}	0.03	0.14	0.24	0.29	0.7
	D_{Am}	<0.01	0.5	0.8	0.8	1.9
	$S_{Am/Eu}$	–	3.3	3.3	2.7	0.7
CPw29 BrCosan (3×10^{-3} M)	D_{Eu}	7.6	3.3	0.7	0.7	1.0
	D_{Am}	<0.01	8.8	1.0	1.2	1.5
	$S_{Am/Eu}$	5.4	2.7	1.6	1.7	0.36

calixarene-based CMPO-extractant. As expected, reducing the number of CMPO units results in a decrease of europium extraction; especially when only one CMPO unit is grafted to the calixarene CPw23. This decrease of extracting ability is accompanied by an unexpected increase of americium selectivity over europium $D_{Am/Eu}$, which is higher than 8 for calixarenes when one or two CMPO units are replaced by amide moieties (CPw26, CPw27, and CPw28) (Table 4.38). It is commonly accepted that the use of donor atoms softer than oxygen, especially N and S, can afford a higher selectivity for similarly sized actinides over lanthanides. However, these softer donor atoms often give rise to less stable complexes. In order to find a good compromise between efficiency and selectivity, the possibility to introduce both soft and hard donor atoms on the calixarene scaffold was explored. Therefore, calix[4]arenes were synthesized having both hard groups (CMPO) and

TABLE 4.38

Selectivity Americium over Lanthanides from Aqueous Solutions 3M HNO$_3$ into a NPHE Solution of CPw23–CPw28 (10^{-3} M)

CPw24	D_{La}	D_{Ce}	D_{Nd}	D_{Sm}	D_{Eu}	D_{Am}
	4.3	4.0	1.85	0.88	0.60	2.30
	$D_{Am/La}$	$D_{Am/Ce}$	$D_{Am/Nd}$	$D_{Am/Sm}$	$D_{Am/Eu}$	$D_{Am/Am}$
	0.53	0.57	1.23	2.59	3.84	1
CPw25	D_{La}	D_{Ce}	D_{Nd}	D_{Sm}	D_{Eu}	D_{Am}
	0.67	0.64	0.32	0.18	0.12	0.43
	$D_{Am/La}$	$D_{Am/Ce}$	$D_{Am/Nd}$	$D_{Am/Sm}$	$D_{Am/Eu}$	$D_{Am/Am}$
	0.65	0.68	1.35	2.35	3.7	1
CPw26	D_{La}	D_{Ce}	D_{Nd}	D_{Sm}	D_{Eu}	D_{Am}
	97	79	28	7.5	3.7	36
	$D_{Am/La}$	$D_{Am/Ce}$	$D_{Am/Nd}$	$D_{Am/Sm}$	$D_{Am/Eu}$	$D_{Am/Am}$
	0.37	0.45	1.27	4.77	9.8	1
CPw27 (10^{-3} M)	D_{La}	D_{Ce}	D_{Nd}	D_{Sm}	D_{Eu}	D_{Am}
	10.5	9.05	3.45	1.14	0.69	4.15
	$D_{Am/La}$	$D_{Am/Ce}$	$D_{Am/Nd}$	$D_{Am/Sm}$	$D_{Am/Eu}$	$D_{Am/Am}$
	0.39	0.46	1.19	3.60	5.98	1
CPw28 (10^{-3} M)	D_{La}	D_{Ce}	D_{Nd}	D_{Sm}	D_{Eu}	D_{Am}
	16.5	14.1	5.3	1.6	0.83	6.55
	$D_{Am/La}$	$D_{Am/Ce}$	$D_{Am/Nd}$	$D_{Am/Sm}$	$D_{Am/Eu}$	$D_{Am/Am}$
	0.40	0.47	1.24	4.14	7.94	1

softer picolinamide-binding groups. CPw29, which bears three CMPO and one picolinamide groups at the wide rim of pentoxy-calix[4]arene, displays lower D_{Eu} and D_{Am} than its analogue bearing four CMPO moieties CPw3, without improving the selectivity $S_{Am/Eu}$. It seems that the arm bearing the picolinamide residue hinders the extraction of cations without enhancing the discrimination between actinides and lanthanides[18] (see Section 4.7).

Parma University workers also synthesized CPn16 bearing three CMPO and one picolinamide residue at the narrow rim of *p-tert*-butylcalix[4]arene. They also synthesized CPn17 and CPn18, bearing two CMPO and two thiopicolinamide residues linked to the phenolic oxygen atom by spacers of different length. As for their wide-rim counterpart, the picolinamide groups do not modify the selectivity of these compounds (Table 4.39).

In order to find compounds able to perform an efficient lanthanide/actinide separation, the Twente group prepared two cavitands (Cv1 and Cv2) functionalized with CMPO groups and two cavitands (Cv3 and Cv4) with carbamoylmethylphosphonate (CMP) groups[192,193] (see Section 4.7). Distribution ratios displayed by CMPO cavitands are much lower than those found for the calixarene counterpart. This important decrease of extracting ability of cavitand is probably due to the presence of a carbon atom between the benzene unit and the nitrogen atom, causing N-protonation below pH 2. Furthermore, the Am/Eu selectivity is less than that of CMPO-calix[4]

TABLE 4.39

Distribution Ratios[a] and Selectivity for the Extraction of Am and Eu from Aqueous Solutions [HNO$_3$] into a NPHE Solution of Picolinamide CMPO Calixarenes (10^{-3} M)

		HNO$_3$ Concentration						
Ligands		10^{-3} M	10^{-2} M	10^{-1} M	1 M	2 M	3 M	4 M
CPw29	D_{Eu}	0.03	0.03	<0.01	0.14	0.24	0.29	0.36
	D_{Am}	0.03	<0.01	0.2	0.5	0.8	0.8	0.7
	$S_{Am/Eu}$	1.1	–	–	3.3	3.3	2.7	1.9
CPw29 BrCosan	D_{Eu}	42.3	7.6	11.1	3.3	0.7	0.7	0.7
3 × 10^{-3} M								
	D_{Am}	0.03	<0.01	7.2	8.8	1.0	1.2	1.0
	$S_{Am/Eu}$	1.3	5.4	0.6	2.7	1.6	1.7	1.5
CPn16	D_{Eu}	0.49	0.18	0.35	2.5	2.3	2.9	3.7
	D_{Am}	0.77	0.3	0.97	6.9	4.9	5.3	5.9
	$S_{Am/Eu}$	1.6	1.7	2.8	2.8	2.1	1.9	1.6
CPn17	D_{Eu}		<0.01	0.85	0.44	0.58	0.39	
	D_{Am}		<0.01	1.52	1.02	1.4	0.8	
	$S_{Am/Eu}$		–	1.8	2.3	2.4	2.1	
CPn18	D_{Eu}						0.1	
	D_{Am}						0.2	
	$S_{Am/Eu}$						2.2	
CPn18 BrCosan	D_{Eu}						7.8	
3 × 10^{-3} M								
	D_{Am}						12.5	
	$S_{Am/Eu}$						1.6	

arene, but higher than that observed for OΦCMPO, particularly for Cv2. It has to be pointed out that, in contrast to CMPO calixarenes, selectivity between lanthanides is not marked.

Important works were devoted to the synthesis of calixarenes bearing different groups (malonamide, glycolamide, pyrazolone, thiopyrazolone, terpyridine, TTFA). Unfortunately, none of these compounds displayed a sufficient extracting ability.

4.5.4.4 Dicarbollide (Cosan) and Calixarenes

In certain cases, cosan derivatives were used to improve the distribution ratios. In particular, it was interesting to know if linking a calixarene and cosan could lead to a synergistic effect in comparison to a mixture of these compounds. For the first time, very sophisticated synthesis led to mixed compounds with cosan linked to the wide rim or narrow rim of calixarenes or cavitands, Cos1 and Cos2, precursors of new extractants.[18]

Mixtures between cosan and neutral thiacalixarene CAc9 (cone conformer) are also characterized by a strong synergistic effect in the extraction of Eu^{3+}, D_{Eu} increasing from below detection limits to $\log D = 1.9$ (0.3 M HNO_3, 0.05 M of each synergist in chlorobenzene).[194] The effect of the anion on selectivity over alkali ions and on D_{Eu} is most pronounced at ratios CAc9:cosan 1:1 and 0.6:0.4, respectively. Various complexes are extracted, depending on the phase compositions, with CAc9 Eu(cosan)$_3$ existing at high metal loading. The rates of forward and backward phase transfer can be accelerated by pre-equilibrating the mixture in the absence of metal ions.

The combination of cosan and CMPO groups on the calix[4]arene skeleton turned out to produce a strong intramolecular allosteric effect.[195] For example, the extractability of Am(III) and Ln(III) increases in the order Cos3, CPn1 < Cos6 mixed with Cos7 < Cos5 (1,3-alternate) < Cos4 (cone). With 1 mM Cos4 in 1,2-dichloroethane, $\log D > 2$ from 1 M HNO_3. The synergistic enhancement factor for Cos6 + Cos7, 1 mM each, equals 10,000 at pH 1. The efficiency of Cos5 is also surprising, taking into account the charge separation, but the flexible spacers may contribute to it. The diluent promotes extraction in the order of nitrobenzene < dichloroethane < octan-2-one:TPH (1:1 mixture).

The ligands Cos8–Cos13 show strongly enhanced extraction abilities for trivalent actinides and lanthanides in comparison to the previously reported simple covalent combination of one Cosan$^-$ with one CMPO group or to various synergistic mixtures of calixarenes substituted exclusively with two Cosan$^-$ or two CMPO moieties. These compounds are the first examples of molecules bearing combinations of hydrophobic anionic groups, Cosan$^-$ and chelating functions for trivalent lanthanides and actinides CMPO in a geometrically predefined manner. The combination of the two groups on a calix[4]arene platform affords extractants with strongly increased extraction efficiency for europium and americium from acidic aqueous phases. However, as expected from the behavior of Cosan, distribution ratios decrease strongly as the HNO_3 concentration increases.[196] Distribution ratios of more than 100 for a 10^{-5} M extractant concentration are obtained with Cos10. They are unprecedented and substantially higher than those reported previously for the covalent combination of one Cosan$^{(-)}$ with one CMPO group.[187]

Comparison of derivatives in the *cone* and *1,3-alternate* conformations shows that the four groups must be attached to the same side of the molecule. Modification of the spacer length for the CMPO groups (with constant spacer of the Cosan groups) shows that the distances from the platform must be similar to allow a cooperative action. A similar cooperative effect is observed when the same concentration of CMPO/Cosan groups is offered by a 1:1 mixture of the tetra-substituted calix[4]arenes Cos3 and CPn4. Complexation studies with Cos10 for La^{3+}, Eu^{3+}, and Yb^{3+} in methanol carried out by UV spectrophotometry and microcalorimetry revealed the formation of ML and ML_2 complexes.[196] This formation of ML_2 complexes is quite unusual for narrow-rim CMPO calixarenes. The $\log \beta$ values of the complexes of La^{3+}, Eu^{3+}, and Yb^{3+} with Cos10 range from 9.6 to 11.7 and from 7.2 to 7.5 with Cos7 corresponding to a low selectivity between lanthanides. Similarly, the discrimination between europium and americium is not marked.

4.5.5 Extraction of Uranium (Uranophiles)

U(VI) was found to be well complexed and extracted by proton-ionizable calix[n] arenes (n = 5, 6) bearing carbonyl groups. This is ascribed to their oxygen donor atoms achieving a planar arrangement, thus matching the free UO_2^{2+} coordination sites. For example, 2 mM CAc1 in o-dichlorobenzene extracts U(VI) quantitatively at pH 8 with $pH_{0.5}$ = 3.5 (2.6 mmol L in $CHCl_3$, 2.6 mmol UO_2^{2+}) and a stoichiometry at maximum loading of the fully deprotonated form being $[CAc1^{6-} \cdot (UO_2^{2+})_3]$.[197] The interference of Ni(II) and Zn(II) if present in 10-fold excess can be eliminated by use of the hydroxamate CAc2; $pH_{0.5}$ = 3.8. This ligand can also effectively compete with carbonate in five-fold excess in complexing U(VI) at pH 10.[198]

However, the excess of ionizable groups constitutes a drawback of these ligands, because they are able to interact with interfering ions, thus reducing the selectivity. With CAc3 as alternative, only monovalent ions such as K^+ are coextracted as $[CAc3^{3-} \cdot UO_2^{2+} \cdot K^+]$ with $pH_{0.5}$ = 4.2.[199] The U(VI) distribution ratio as a function of pH is very similar between CAc3 and CAc4.[200] The extraction constant for $[CAc4^{2-} \cdot UO_2^{2+}]$ is 7.1×10^{-5} (M) at I = 0.04 ($NaNO_3$). Calix[6]arene via p-sulfonamide tethered to polymer is an efficient adsorbant for U(VI) due to the acidity of the phenolic -OH groups.[201]

4.5.6 The Coextraction of Light Alkali and f-element Ions

In the course of Ln(III) extraction experiments, a new extraction mechanism was discovered: the uptake of two different metal cations by calix[4]arene CAc5 in the cone conformation. This positive allostericity renders the calix[4]arene more selective in mutual Ln(III) extraction than the analogous calix[6]arene CAc1 at a similar level of extraction power.[202,203] A similar effect was observed for Am^{3+} in the extraction by CAc5 ($+Na^+$) and by CAc8 ($+K^+$).[204]

The same effect is observed with CAc7 and partially -COOH derivatized calix[4] arenes in the extraction of Ln(III) (and other ions). It was explained by structural changes to the molecule, being rigidified by Na^+ bound to ethereal oxygen atoms, preorganizing the COOH groups for chelating Ln^{3+}.[205–207] It can be applied to membrane transport, where the transport rate is enhanced by a factor of 100.[208,209]

4.5.7 Am(III) Separation by Calix[6]arenes Bearing Mixed Functional Groups

Intended as charge-matching extractants for Ln(III), CAc11 and CAc12 turned out to preferentially extract Am(III) from acidic media.[210,211] The effect was also observed with the half-open cavity CAc10, though at lower D-values ascribed to partial ion hydration. It was not observed with CAc1 or CAc6, bearing an excess of strongly electrostatically interacting groups, nor with calix[4]arenes bearing monodentate groups on short spacers. It is interpreted in terms of cation-π interactions of relativistically expanded d, f-orbitals when An(III) is located in proximity to the calixarene π-system. However, crystal-structural evidence could not yet be provided (Table 4.40).

TABLE 4.40

Values of Log(K_{ex}/dm³ mol⁻¹) for the Extraction from Water to Chloroform According to: $M^{3+} + H_6L \rightleftharpoons MH_3L + 3H^+$ (I) or $M^{3+} + 2H_3L \rightleftharpoons ML \cdot H_3L + 3H^+$ (II) pH 2.6–3.2, 1 kBq/mL ²⁴¹Am or 0.1 mM of each Ln^{3+}

Ligands	Am[a]	Nd[b]	Nd[a]	Eu[b]	Er[b]	Eqn.
CAc6	4.14	4.14	−4.53	−4.60	−4.63	(I)
CAc10	nd	−5.48	nd	5.47	−6.10	(II)
CAc11	−2.92	−4.12	−4.11	−4.29	−4.87	(II)
CAc12	−2.52	−4.31	−4.55	−4.56	−5.24	(II)

[a] Single element extraction.

[b] Competitive extraction of six lanthanides.

The structural feature was later applied to alpha-halogenated calixarenes, allowing extraction from more acidic media.[212]

4.6 CONCLUSIONS
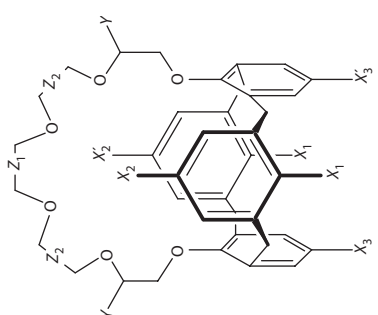
In the early 1990s, there existed several classes of extractants for actinides (CMPO), for cesium and more generally alkali cations, and for strontium and alkaline earth cations (crown ethers and cosan). The combination of these extractants and the grafting of these functions on calixarene platforms have led to new classes of extremely efficient and selective extractants, in particular calixarene-crown, which are presently applied in the United States to treat the huge amounts of waste at the SRS. Calixarenes/ CMPO, crown ethers/cosan, CMPO/cosan, and more recently calixarenes/CMPO/ cosan are promising compounds. It is desirable that these studies, conducted at the international level, continue in particular to obtain a better understanding of the complex mechanisms of extraction of these compounds.[127,187]

This review has shown that calixarenes, with functional groups at the upper or lower rim, provide more or less rigid preorganized cavities, which can be tuned to incorporate a metal cation, with a good degree of selectivity. This selectivity can be enhanced in some cases by mixing ligating functions on the same molecular platform. Aggregation phenomena also play a role in the extraction of cations by calixarenes; in particular the higher distribution ratios observed for wide-rim CMPO in comparison to narrow-rim CMPO calixarenes seem to have for origin the faculty for wide-rim CMPO to form self-assembled polymers.
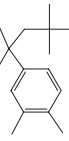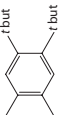
The main drawback of CMPO calixarenes is their low solubility in most of the diluents. Their concentration in the organic phase is not sufficient to allow lanthanides and actinides to be coextracted from HAW. Adamantyl groups improve the solubility of CMPO calixarenes. It would be interesting to continue to study these compounds and possibly to seek other ways to achieve a sufficient solubility (e.g., 0.1 M) of these calixarenes.

4.7 COMPOUNDS

Mono Crown Calix[4]arenes
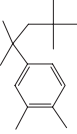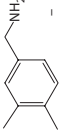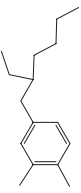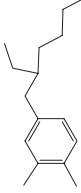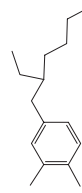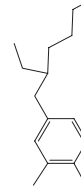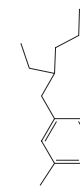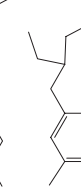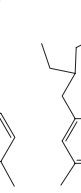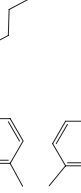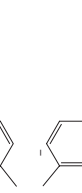
	X_1	X_2	X_3	Y	Z_1	Z_2
MC1	$-O-CH_3$	t-Butyl	t-Butyl	H-	$-CH_2-CH_2-$	$-CH_2-CH_2-$
MC2	$-[O-(CH_2)_2]_2-OH$	H-	H-	H-	$-CH_2-CH_2-$	$-CH_2-CH_2-$
MC3*	$-O-CH_3$	H-	H-	H-	0	$-CH_2-CH_2-$
MC4	$-O-CH_{3v}$	H-	H-	H-	$-CH_2-CH_2-$	$-CH_2-CH_2-$
MC5	$-O-CH_3$	H-	H-	H-	$CH_2-CH_2-O-CH_2-CH_2$	$-CH_2-CH_2-$
MC6	$-O-CH_2-CH_2-CH_3$	H-	H-	H-	$-CH_2-CH_2-$	$-CH_2-CH_2-$
MC7	$-O-CH-(CH_3)_2$	H-	H-	H-	$-CH_2-CH_2-$	$-CH_2-CH_2-$
MC8	$-O-C_8H_{17}$	H-	H-	H-	$-CH_2-CH_2-$	$-CH_2-CH_2-$
MC9	$-O-(CH_2)_2-O-CH_2(C_2H_5)-CH_2(C_2H_5)-C_3H_7$	H-	H-	H-	$-CH_2-CH_2-$	$-CH_2-CH_2-$
MC10	$-C_8H_{16}O(C_6H_4)NO_2$	H-	H-	H-	$-CH_2-CH_2-$	$-CH_2-CH_2-$

MC11	[dimethylbenzene]	-CH$_2$-CH$_2$-	H-	H-	H-	-O-C$_8$H$_{17}$
MC12	[di-tert-alkylbenzene]	-CH$_2$-CH$_2$-	H-	H-	H-	-O-CH-(CH$_3$)$_2$
MC13	[di-tert-alkylbenzene]	-CH$_2$-CH$_2$-	H-	H-	H-	-O-C$_8$H$_{17}$
MC14	-CH$_2$-CH$_2$-	[methylbenzene]	H-	H-	H-	-O-C$_8$H$_{17}$
MC15	-CH$_2$-CH$_2$-	[di-tbut methylbenzene]	H-	H-	H-	-O-CH-(CH$_3$)$_2$
MC16	CH$_2$-CH$_2$-O-CH$_2$-CH$_2$	-CH$_2$-CH$_2$-	H-	H-	H-	-O-CH-(CH$_3$)$_2$
MC17	-CH$_2$-CH$_2$-	[benzene]	H-	H-	H-	-O-CH$_2$-CH$_2$-CH$_3$
MC18	CH$_2$-CH$_2$-O-CH$_2$-CH$_2$	[benzene]	H-	H-	H-	-O-CH$_2$-CH$_2$-CH$_3$
MC19	CH$_2$-CH$_2$-O-CH$_2$-CH$_2$	[benzene]	H-	H-	H-	-O-C$_8$H$_{17}$
MC20	CH$_2$-CH$_2$-O-CH$_2$-CH$_2$-O-CH$_2$-CH$_2$	[benzene]	H-	H-	H-	-O-CH$_2$-CH$_2$-CH$_3$
MC21	CH$_2$-CH$_2$-O-CH$_2$-CH$_2$	[benzene]	-C$_4$H$_9$	H-	H-	-O-CH$_2$-CH$_2$-CH$_3$

(Continued)

Mono Crown Calix[4]arenes (*Continued*)

	X_1	X_2	X_3	Y	Z_1	Z_2
MC22	$-O-C_8H_{17}$	H-	H-	$-C_4H_9$	$CH_2-CH_2-O-CH_2-CH_2$	[o-tolyl structure]
MC23	$-O-CH-(CH_3)_2$	H-	H-	H-	$-CH_2-CH_2-CH_2-$	$-CH_2-CH_2-$
MC24	$-O-CH-(CH_3)_2$	H-	H-	H-	$-CH_2-CH_2-CH_2-$	[xylene structure]
MC25	$-O-CH-(CH_3)_2$	$X_2 = NO_2 X_2' = H$	$X_3 = H_2 X_3' = H$	H-	$-CH_2-CH_2-$	$-CH_2-CH_2-$
MC26	$-O-CH-(CH_3)_2$	$X_2 = NO_2 X_2' = NO_2$	$X_3 = HX_3' = H$	H-	$-CH_2-CH_2-$	$-CH_2-CH_2-$
MC27	$-O-CH-(CH_3)_2$	$X_2 = NO_2 X_2' = H$	$X_3 = NO_2 X_3' = H$	H-	$-CH_2-CH_2-$	$-CH_2-CH_2-$
MC28	$-O-CH-(CH_3)_2$	$X_2 = NO_2 X_2' = NO_2$	$X_3 = NO_2 X_3' = H$	H-	$-CH_2-CH_2-$	$-CH_2-CH_2-$
MC29	$-O-CH-(CH_3)_2$	$X_2 = NO_2 X_2' = NO_2$	$X_3 = NO_2 X_3' = NO_2$	H-	$-CH_2-CH_2-$	$-CH_2-CH_2-$
MC30	H-	H-	H-	H-	$-CH_2-CH_2-$	$-CH_2-CH_2-$
MC31	H-	H-	H-	H-	[xylene structure]	$-CH_2-CH_2-$
MC32	H-	H-	H-	H-	[di-tert-butyl xylene structure]	$-CH_2-CH_2-$
MC33	H-	H-	H-	H-	$-CH_2-CH_2-$	[xylene structure]
MC34	$-O-C_8H_{17}$	H-	H-	H-	[benzylamine-substituted structure, NH_2] –	$-CH_2-CH_2-$

MC35	-O-C$_3$H$_7$NH$_2$	H-	H-		H-	-CH$_2$-CH$_2$
MC36	-O-C$_8$H$_{17}$	X_2 = COOHX'_2 = H	H-	H-		H-	-CH$_2$-CH$_2$
MC37	-O-C$_8$H$_{17}$	X_2 = C(O) NHSO$_2$CH$_3$$X'_2$ = H	H-	H-		H-	-CH$_2$-CH$_2$-
MC38	-O-C$_8$H$_{17}$	X_2 = C(O) NHSO$_2$CF$_3$$X'_2$ = H	H-	H-		H-	-CH$_2$-CH$_2$-
MC39	-O-C$_8$H$_{17}$	X_2 = C(O) NHSO$_2$C$_6$H$_5$$X'_2$ = H	H-	H-		H-	-CH$_2$-CH$_2$-
MC40	-O-C$_8$H$_{17}$	X_2 = C(O) NHSO$_2$C$_6$H$_4$-4-NO$_2$$X'_2$ = H	H-	H-		H-	-CH$_2$-CH$_2$-
MC41	O-C$_8$H$_{17}$	X_2 = CH(CF$_3$)OHX'_2 = H	H-	H-		H-	-CH$_2$-CH$_2$-
MC42	-O-C$_8$H$_{17}$	X_2 = C(O) NHSO$_2$CH$_3$$X'_2$ = H	H-	H-		H-	-CH$_2$-CH$_2$-
MC43	-O-C$_8$H$_{17}$	X_2 = C(O) NHSO$_2$CF$_3$$X'_2$ = H	H-	H-		H-	-CH$_2$-CH$_2$-

(Continued)

Mono Crown Calix[4]arenes (*Continued*)

	X_1	X_2	X_3	Y	Z_1	Z_2
MC44	-O-C$_8$H$_{17}$	H	H-	H-	R = C(O)NHSO$_2$CH$_3$	-CH$_2$-CH$_2$-
MC45	O-C$_8$H$_{17}$	H	H-	H-	R = C(O)NHSO$_2$CF$_3$	-CH$_2$-CH$_2$-
MC46*	-O-CH-(CH$_3$)$_2$	H-	H-	H-	0	-CH$_2$-CH$_2$-
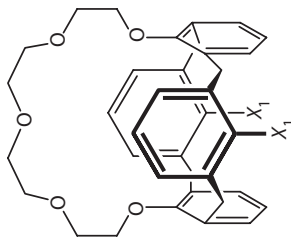
* MC3: X_1 = -O-CH$_3$; MC46: X_1 = -O-CH-(CH$_3$)$_2$.

Bis(crown)Calix[4]arenes
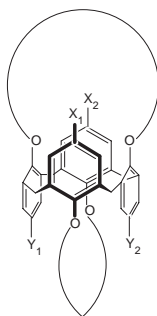
	X_1	X_2	Y_1	Y_2	Crowns
BC1	-H	-H	-H	-H	
BC2	-H	-H	-H	-H	
BC3	-H	-H	-H	-H	
BC4	-H	-H	-H	-H	
BC5	-H	-H	-H	-H	
BC6	-H	-H	-H	-H	
BC7	-H	-H	-H	-H	
BC8	-H	-H	-H	-H	
BC9	-H	-H	-H	-H	
BC10	-H	-H	-H	-H	

Bis(crown)Calix[4]arenes (*Continued*)

	X_1	X_2	Y_1	Y_2	Crowns
BC11	-H	-H	-H	-H	
BC12	-NO$_2$	-H	-H	-H	
BC13	-NO$_2$	-NO$_2$	-H	-H	
BC14	-NO$_2$	-H	-NO$_2$	-H	
BC15	-NO$_2$	-NO$_2$	-NO$_2$	-H	
BC16	-NO$_2$	-NO$_2$	-NO$_2$	-NO$_2$	
BC17	-COOH	-H	-H	-H	
BC18	-C(O)NHSO$_2$CF$_3$	-H	-H	-H	
BC19	-H	-H	-H	-H	
BC20	-CH$_2$NH$_2$	-H	-H	-H	
BC21	-COOH	-H	-H	-H	
BC22	C(O)NHSO$_2$CH$_3$	-H	-H	-H	
BC23	C(O)NHSO$_2$CF$_3$	-H	-H	-H	

Ionizable 1,2 Crown Calix[4]arenes
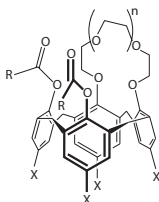
	n	*X*	*R*
MCI1	1	H	OH
MCI2	1	H	NHSO$_2$CH$_3$
MCI3	1	H	NHSO$_2$C$_6$H$_5$
MCI4	1	H	NHSO$_2$C$_6$H$_4$-4-NO$_2$
MCI5	1	H	NHSO$_2$CF$_3$
MCI6	1	*t*-Butyl	OH
MCI7	1	*t*-Butyl	NHSO$_2$CH$_3$
MCI8	1	*t*-Butyl	NHSO$_2$C$_6$H$_5$
MCI9	1	*t*-Butyl	NHSO$_2$C$_6$H$_4$-4-NO$_2$
MCI10	1	*t*-Butyl	NHSO$_2$CF$_3$
MCI11	2	*t*-Butyl	OH
MCI12	2	*t*-Butyl	NHSO$_2$CH$_3$
MCI13	2	*t*-Butyl	NHSO$_2$C$_6$H$_5$
MCI14	2	*t*-Butyl	NHSO$_2$C$_6$H$_4$-4-NO$_2$
MCI15	2	*t*-Butyl	NHSO$_2$CF$_3$
MCI16	3	*t*-Butyl	OH
MCI17	3	*t*-Butyl	NHSO$_2$CH$_3$
MCI18	3	*t*-Butyl	NHSO$_2$C$_6$H$_5$
MCI19	3	*t*-Butyl	NHSO$_2$C$_6$H$_4$-4-NO$_2$
MCI20	3	*t*-Butyl	NHSO$_2$CF$_3$

Amide Calixarenes

CA1   CA2-CA16
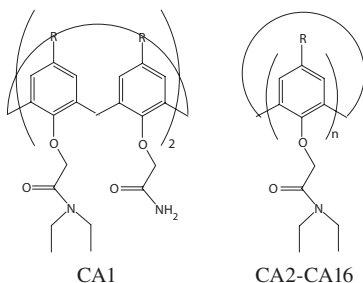
		n	*R*	*R′*
p-tert-butyl calix[4]arene tetra(di-*N*-ethyl)amide	CA2	4	*t*-Butyl	C$_2$H$_5$NH$_2$
p-tert-butyl calix[5]arene penta(di-*N*-pentyl)amide	CA3	5	*t*-Butyl	C$_5$H$_{11}$NH$_2$

Amide Calixarenes (*Continued*)

		n	*R*	*R′*
p-tert-butyl calix[6]arene hexa(di-*N*-ethyl)amide	CA4	6	*t*-Butyl	$C_2H_5NH_2$
Calix[6]arene hexa(di-*N*-ethyl)amide	CA5	6	-H	$C_2H_5NH_2$
p-*tert*-butyl calix[8]arene octa(di-*N*-ethyl)amide	CA6	8	*t*-Butyl	$C_2H_5NH_2$
Calix[8]arene octa(di-*N*-ethyl)amide	CA7	8	-H	$C_2H_5NH_2$
Hexa(benzyloxy)calix[6]arene hexa(di-*N*-ethyl)amide	CA8	6	$-OCH_2C_6H_5$	$C_2H_5NH_2$
Octa(benzyloxy)calix[8]arene hexa(di-*N*-ethyl)amide	CA9	8	$-OCH_2C_6H_5$	$C_2H_5NH_2$
Hexa(hydroxy)calix[6]arene hexa(di-*N*-ethyl)amide	CA10	6	-OH	$C_2H_5NH_2$
Octa(hydroxy)calix[8]arene hexa(di-*N*-ethyl)amide	CA11	8	-OH	$C_2H_5NH_2$
Hexa(methoxy)calix[6]arene hexa(di-*N*-ethyl)amide	CA12	6	$-OCH_3$	$C_2H_5NH_2$
Octa(methoxy)calix[8]arene hexa(di-*N*-ethyl)amide	CA13	8	$-OCH_3$	$C_2H_5NH_2$
Octa(pentyloxy)calix[8]arene hexa(di-*N*-ethyl)amide	CA14	8	$-O(CH_2)_4CH_3$	$C_2H_5NH_2$
Hexa(octyloxy)calix[6]arene hexa(di-*N*-ethyl)amide	CA15	6	$-O(CH_2)_7CH_3$	$C_2H_5NH_2$
Octa(octyloxy)calix[8]arene hexa(di-*N*-ethyl)amide	CA16	8	$-O(CH_2)_7CH_3$	$C_2H_5NH_2$

Pyridinium Calixarenes
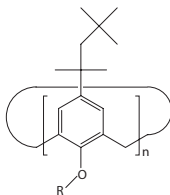
Ligands	*n*	*R*
2PyOC4	4	
2PyOC6	6	
4PyOC4	4	
4PyOC4Q	4	

Phosphine Oxide Calixarenes
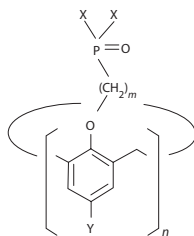
Ligands	*m*	*n*	*X*	*Y*
CPo1	2	4	C_6H_5	$t\text{-}C_4H_9$
CPo2	2	4	$n\text{-}C_4H_9$	$t\text{-}C_4H_9$
CPo3	2	4	C_6H_5	H
CPo4	2	6	C_6H_5	$t\text{-}C_4H_9$
CPo5	2	6	$n\text{-}C_4H_9$	$t\text{-}C_4H_9$
CPo6	2	6	C_6H_5	$C_{12}H_{25}$
CPo7	2	6	C_6H_5	H
CPo8	2	8	C_6H_5	$t\text{-}C_4H_9$
CPo9	2	8	$n\text{-}C_4H_9$	$t\text{-}C_4H_9$
CPo10	2	8	C_6H_5	H
CPo11	4	4	C_6H_5	$t\text{-}C_4H_9$
CPo12	4	6	C_6H_5	$t\text{-}C_4H_9$
CPo21	1	6	C_6H_5	$t\text{-}C_4H_9$
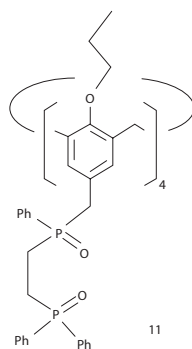
Cpo22
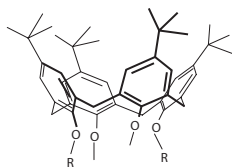
Ligands	R
CPo13	$(CH_2)_4PO(Ph)_2$
CPo14	$(CH_2)_4PO(Ph)_2$
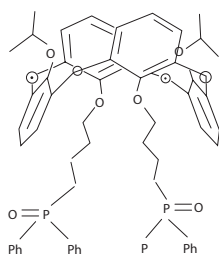
Cpo15
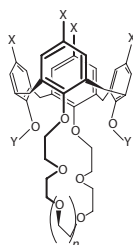
Ligands	N	X	Y
CPo16	0	$(CH_2)_2PO(Ph)_2$	$t\text{-}C_4H_9$
CPo17	1	$(CH_2)_2PO(Ph)_2$	H
CPo18	0	$(CH_2)_2OPO(Ph)_2$	$t\text{-}C_4H_9$
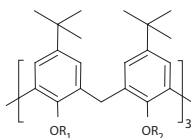
Ligands	R_1	R_2
CPo19	$(CH_2)_4PO(Ph)_2$	CH_3
CPo20	$(CH_2)_2PO(Ph)_2$	CH_3

Wide-rim CMPO Calixarenes
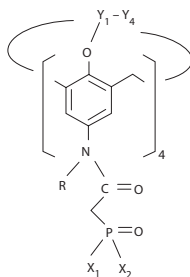
Ligands	n	R	X_1	X_2	Y_1	Y_2	Y_3	Y_4
CPw1	4	H	C_6H_5	C_6H_5	CH_3			
CPw2	4	H	C_6H_5	C_6H_5	C_3H_5			
CPw3	4	H	C_6H_5	C_6H_5	C_5H_{11}			
CPw4	4	H	C_6H_5	C_6H_5	$CH_2CH(C_2H_5)$ (C_4H_9)			
CPw5	4	H	C_6H_5	C_6H_5	$C_{10}H_{21}$			
CPw6	4	H	C_6H_5	C_6H_5	$C_{12}H_{25}$			
CPw7	4	H	C_6H_5	C_6H_5	$C_{14}H_{29}$			
CPw8	4	H	C_6H_5	C_6H_5	$C_{16}H_{33}$			
CPw9	4	H	C_6H_5	C_6H_5	$C_{18}H_{37}$			
CPw10	5	H	C_6H_5	C_6H_5	$C_{14}H_{29}$			
CPw11	4	H	C_6H_5	C_6H_5	CH_3	$CH_2CH(C_2H_5)$ (C_4H_9)	CH_3	$CH_2CH(C_2H_5)$ (C_4H_9)
CPw12	4	H	C_6H_5	C_6H_5	CH_3	$C_{10}H_{21}$	CH_3	$C_{10}H_{21}$
CPw13	4	H	C_6H_5	C_6H_5	CH_3	$C_{18}H_{37}$	CH_3	$C_{18}H_{37}$
CPw14	4	H	C_6H_5	C_6H_5	CH_3	CH_3	CH_3	C_5H_{11}
CPw15	4	H	C_6H_5	C_6H_5	CH_3	CH_3	C_5H_{11}	C_5H_{11}
CPw16	4	H	C_6H_5	C_6H_5	CH_3	C_5H_{11}	C_5H_{11}	C_5H_{11}
CPw17	4	CH_3	C_6H_5	C_6H_5	C_5H_{11}			
CPw18	4	CH_3	C_6H_5	C_6H_5	$C_{14}H_{29}$			
CPw19	4	H	C_6H_{13}	C_6H_{13}	C_5H_{11}			
CPw20	4	H	C_6H_5	$O\ C_2H_5$	C_5H_{11}			
CPw21	4	H	$O\ C_2H_5$	$O\ C_2H_5$	C_3H_7			
CPw22	4	H	C_6H_5	OH	C_5H_{11}			
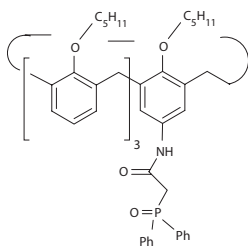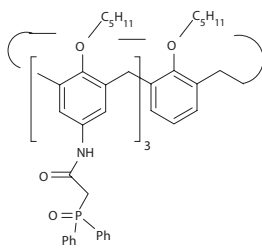
CPw23 CPw24 CPw25
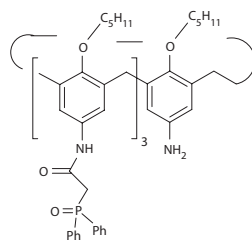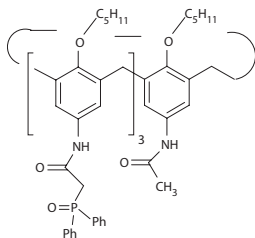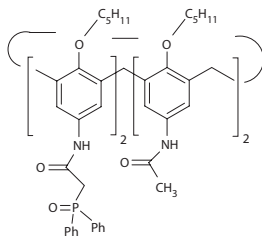
CPw26 CPw27 CPw28
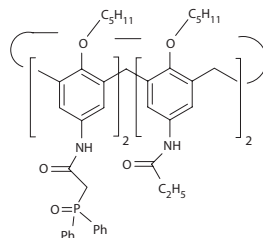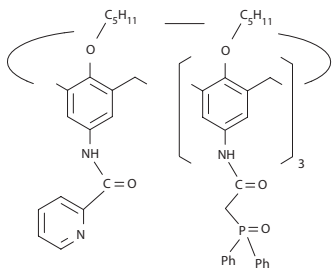
CPw29 CPw30
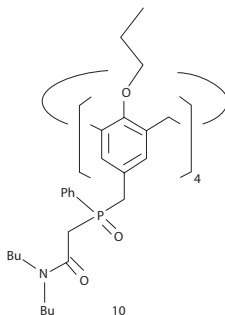
Calixarenes
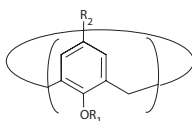
Ligands	R_1	R_2
CPh21	$n\text{-}C_3H_7$	$O(CH_2)_2PO(Ph)_2$
CPh22	$n\text{-}C_3H_7$	$(CH_2)PO(Ph)_2$
CPh23	$n\text{-}C_3H_7$	$(CH_2)PO(OEt)_2$
CPh24	$C_2H_4OC_2H_5$	$PO(Ph)_2$
CPh25	$C_2H_4OC_2H_5$	$PO(OEt)_2$

Rigidified CMPO Calixarenes
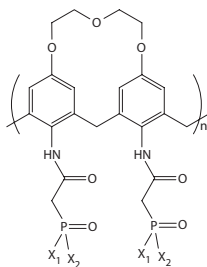
Ligands	X_1	X_2
CPr1	C_6H_5	C_6H_5
CPr2	C_6H_{13}	C_6H_{13}
CPr3	C_6H_5	OC_2H_5
CPr4	OC_2H_5	OC_2H_5

Narrow-rim CMPO Calixarenes
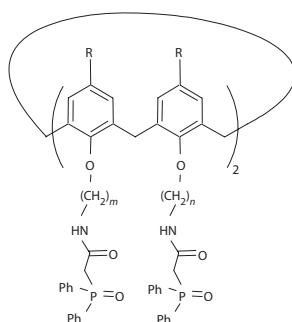
Ligands	m	n	R
CPn1	2	2	t-Butyl
CPn2	3	3	t-Butyl
CPn3	4	4	t-Butyl
CPn4	5	5	t-Butyl
CPn5	3	3	C_8H_{17}
CPn6	4	4	C_8H_{17}
CPn7	2	2	H
CPn8	3	3	H
CPn9	4	4	H
CPn10	3	5	t-Butyl
CPn11	4	5	t-Butyl
CPn12	3	4	t-Butyl
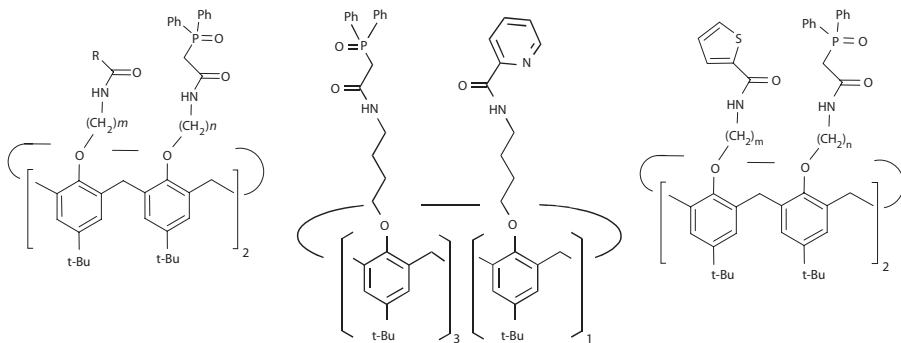
Ligands	m	n	R
CPn13	3	4	C_4H_9
CPn14	4	3	CH_3
CPn15	4	4	CH_3

CPn16

Ligands	m	n
CPn17	4	4
CPn18	4	3

Adamantyl CMPO Calixarenes
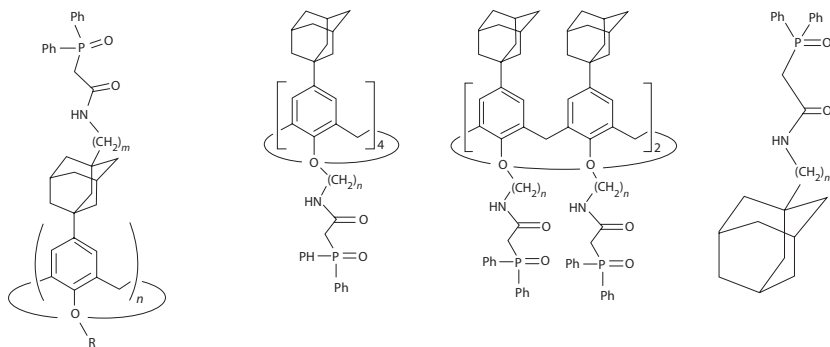
Ligands	n	m	R
CAd1	4	0	n-Bu
CAd2	4	1	n-Bu
CAd3	4	2	n-Pr
CAd4	6	2	Me

Ligands	n
CAd5	2
CAd6	3
CAd7	4

Ligands	n
CAd8	2
CAd9	3
CAd10	4

Ligands	n
CAd11	0
CAd12	1

Calixarenes Functionalized on the Wide Rim and Narrow Rim
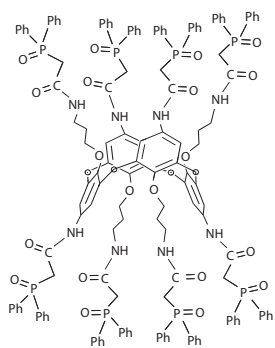
CPwn1
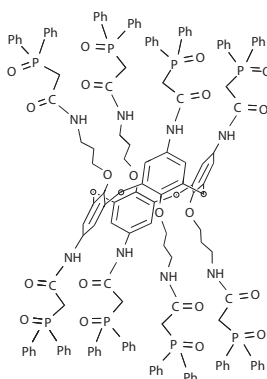
CPwn2

Dendrimers
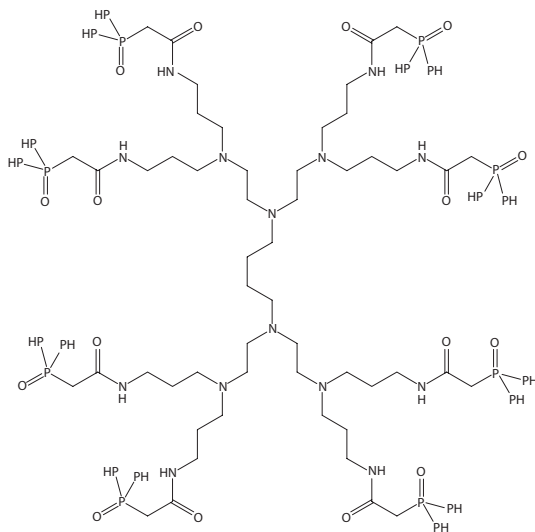
D2
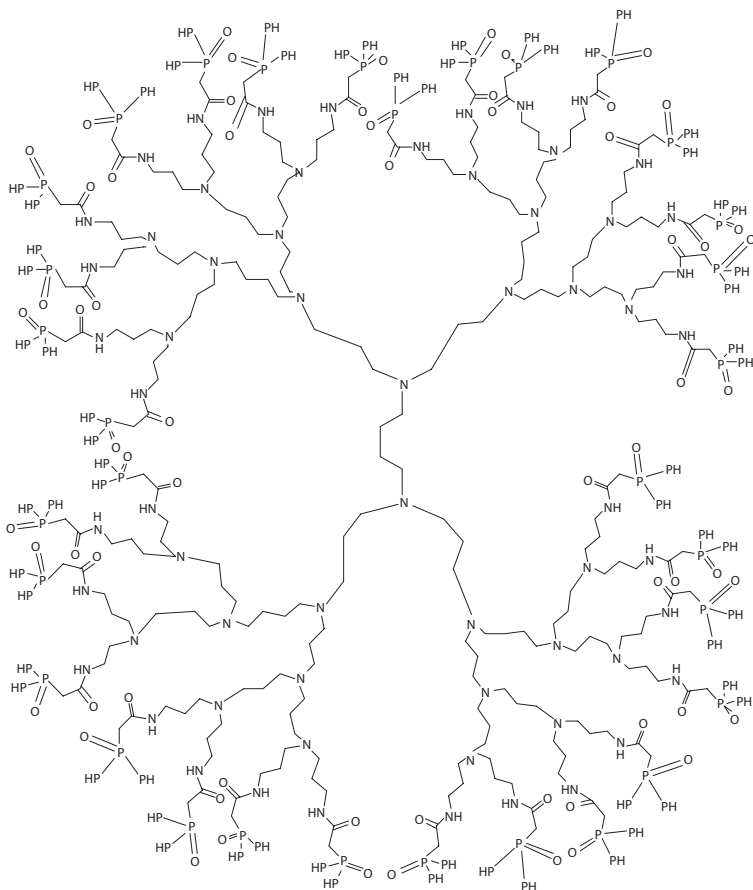
D4

Dendrimer Calixarenes
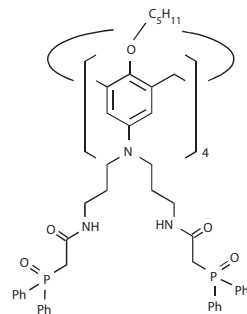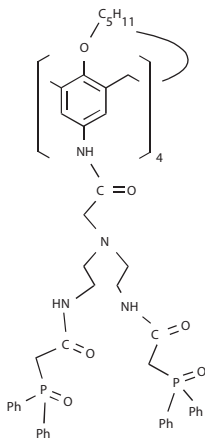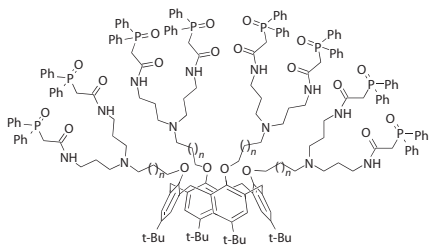
Ligands	*n*
CD1	1
CD2	2

CD3   CD4

CMPO Calix[6,8]arenes
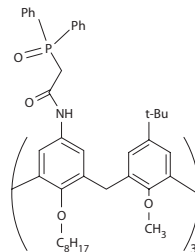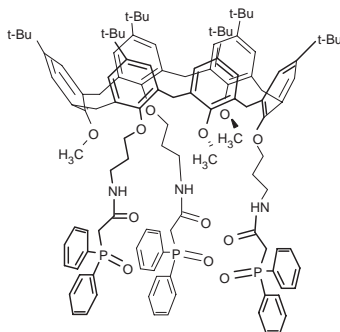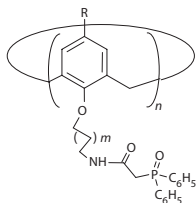
Ligands	*m*	*n*	*R*
CP$_6$1	1	6	*t*-Butyl
CP$_6$2	1	6	H
CP$_6$3	2	6	H
CP$_8$1	1	8	H
CP$_8$2	1	8	OCH$_2$C$_6$H$_5$

CP$_6$4   CP$_6$5

Picolinamide Calixarenes
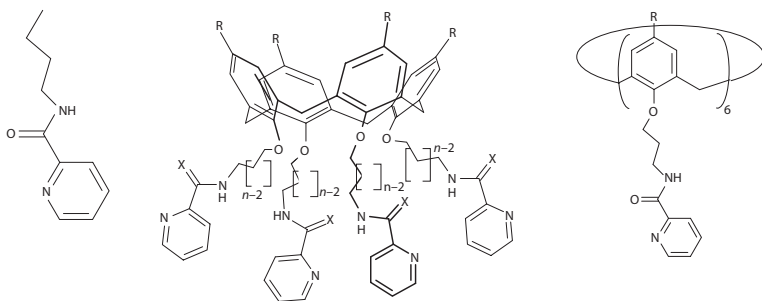
Ligands		n	R	X	Ligands	m	n	R
CPi1	CPi2	3	t-Bu	O	CPi6	3	6	t-Bu
	CPi3	3	H	O	CPi7	3	6	H
	CPi4	4	t-Bu	O	CPi8	4	6	H
	CPi5	3	t-Bu	S	CPi9	3	8	H
					CPi10	3	8	OBn
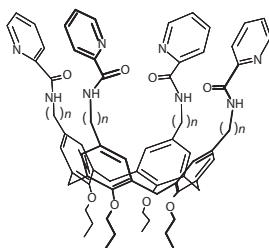
Ligands	n
CPi11	0
CPi12	1

Cosan Calixarenes

Cos1

Cos2

Cos3: R = R =

Cos5: R =

Cos4: R =
R =

Cos6: R =
R =

Cos7: R =
R =

Z =

Cos 8: *m* = 2
Cos 9 – Cos 13: *m* = 3, 4, 5, 6, 7

Cos 8: *m* = 2
Cos 9 – Cos 13: *m* = 3, 4, 5, 6, 7
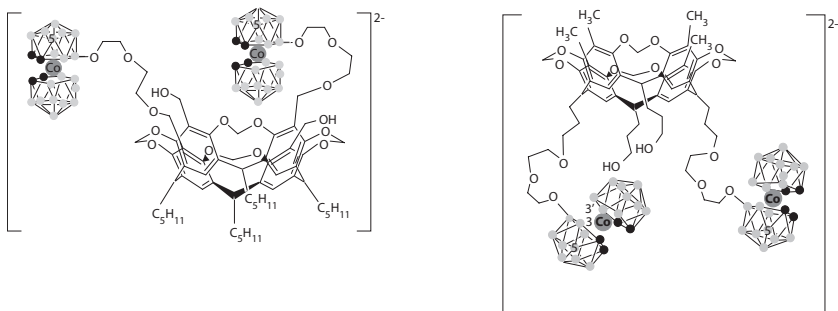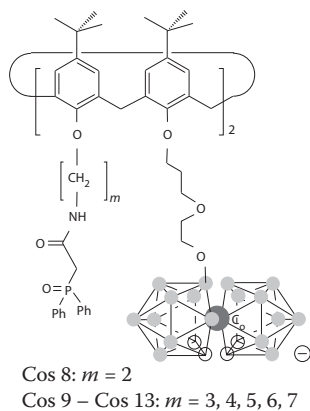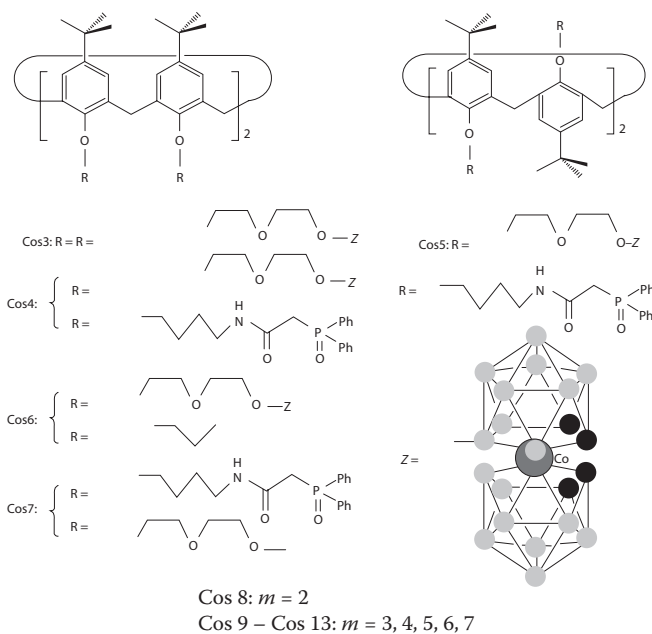
Various Calixarenes for Actinide Extraction
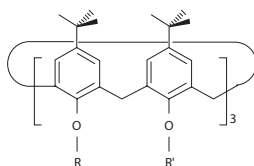
CAc1: R = R′ = CH₂COOH
CAc2: R = R′ = CH₂C(O)N(H)OH
CAc3: R = CH₂COOH, R′ = CH₃
CAc4: R = CH₂C(O)N(H)OH, R′ = CH₃

CAc1: $n = 6$
CAc5: $n = 4$ } R = t-butyl
CAc6: $n = 6$
CAc7: $n = 4$ } R = t-octyl

CAc8

CAc9

O — $CH_2COOC_2H_5$

CAc10: R = $-CH_3$
CAc11: R = $CH_2C(O)N(C_2H_5)_2$
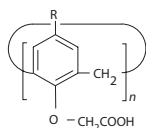
CAc12
R' = t-OCtyl
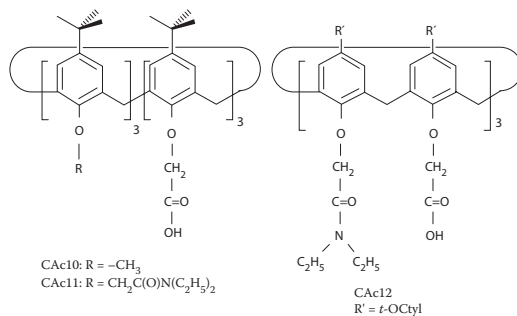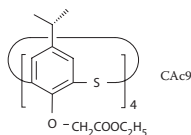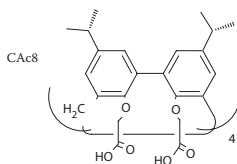
Oligomers
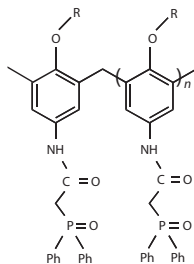
Ligands	n	R
O_51	0	C_5H_{11}
O_52	1	C_5H_{11}
O_53	2	C_5H_{11}
O_54	3	C_5H_{11}
O_55	4	C_5H_{11}

Crown Ethers
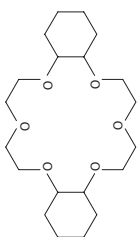
DHEHB18C6
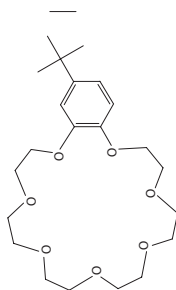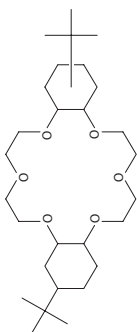
DHHC18C6

D*tw*ButC18C6

*t*ButB21C7

DC18C6
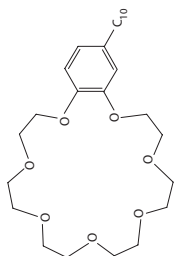
*t*ButB21C7
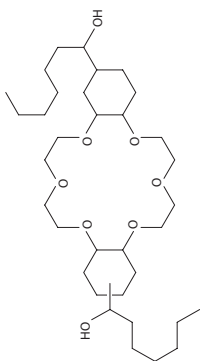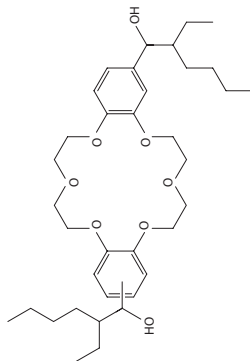
Cosan
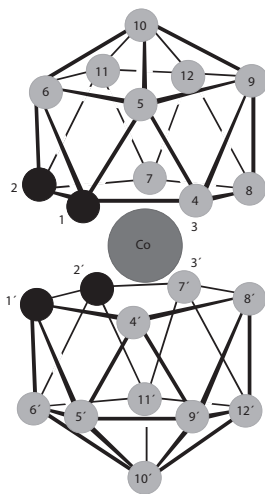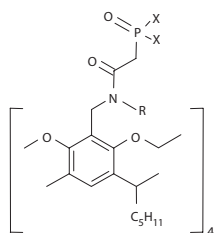
Cavitands

Ligands	X	R
Cv1	C_6H_5	H
Cv2	C_6H_5	C_3H_7
Cv3	OC_2H_5	H
Cv4	OC_2H_5	C_3H_7
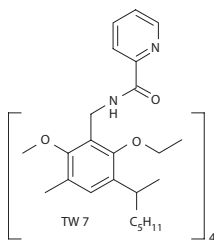
Cv5
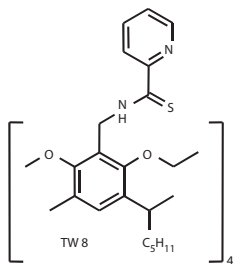
Cv6
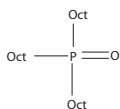
TOPO
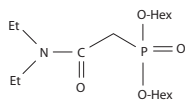
DHDECMP
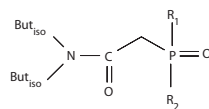
Ligands	R_1	R_2
OΦCMPO	Oct	Φ
DΦCMPO	Φ	Φ
DBCMPO	But	But
DOCMPO	Oct	Oct
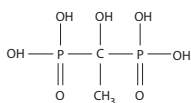
Methylene diphosphonic acid (MDPA)
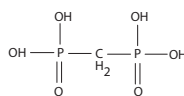
1-Hydroxy ethylidene-1,1-diphosphonic acid (HEDPA)
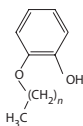
$n = 5$ NPHE, $n = 7$ NPOE
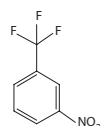
Trifluoromethylbenzene (NTFB)

Alcohols
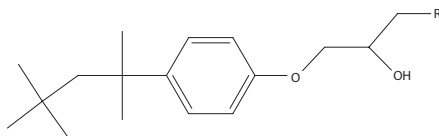
1	$R = -OCF_2CF_2H$
2	$R = -OCH_2CF_2CF_2H$
3	$R = -OCH_2CF_3$
4	$R = -OCH_2CH_3$
5	$R = -OCH_2(CH_3)_2$

Sulfonamides
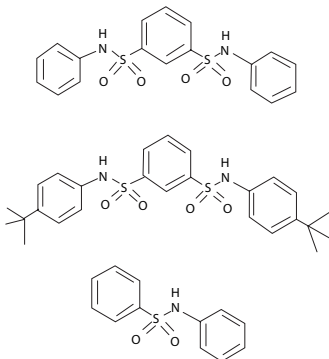
di-(N-(phenyl)sulfonylcarboxamide)-1,3-benzene (DSA1)
di(tert-butyl) N-(phenyl)sulfonylcarboxamide)-1,3-benzene (DSA2)
(N-(phenyl)sulfonylcarboxamide)benzene (MSA)

REFERENCES

1. J.-G. Devezeaux de Lavergne and B. Boullis, *Clefs CEA*, 2005, **53**, 36–53.
2. A. Poczynajło, *J. Radioanal. Nucl. Chem.*, 1998, **125**, 445–485.
3. Workshop on Basic Research Needs for Advanced Nuclear Energy Systems – Report of the Basic Energy Sciences Workshop on Basic Research Needs for Advanced Nuclear Energy Systems, 2006.
4. F. Cotton and G. Wilkinson, *Advanced Inorganic Chemistry*, 6th edn., John Wiley & Sons, New York, 1999.
5. K. A. Venkatesan, B. R. Selvan, M. P. Antony, T. G. Srinivasan and R. P. R. Vasudea, *Hydrometallurgy*, 2007, **86**, 221–229.
6. K. Kolarik and E. V. Renard, *Platinum Metals Rev.*, 2005, **49**, 79–90.
7. L. Cecille, M. Casarci, J.-F. Dozol, W. Faubel and A. Turner, 3rd EU Conference on Radioactive Waste Management and Disposal, Elsevier Appl. Sci., Luxembourg, 17–21 September, 1991.

8. M. J. Barnes, B. B. Anderson, T. L. White and K. B. Martin, *Tetraphenylborate decomposition testing using Savannah River Site high level waste*, USDOE Report WSRC-TR-2001-00251, 2001.

9. C. Hill, J.-F. Dozol, V. Lamare, H. Rouquette, S. Eymard, B. Tournois, J. Vicens, Z. Asfari, C. Bressot, R. Ungaro and A. Casnati, *J. Incl. Phenom. Mol. Recognit. Chem.*, 1994, **19**, 399–408.

10. J.-F. Dozol, N. Simon, V. Lamare, H. Rouquette, S. Eymard, B. Tournois, D. De Marc and R. M. Macias, *Sep. Sci. Technol.*, 1999, **34**, 877–909.

11. C. D. Gutsche, *Calixarenes*, The Royal Society of Chemistry, Cambridge, UK, 1989.

12. J. Vicens and V. E. Böhmer, eds., *Calixarenes. A Versatile Class of Macrocyclic Compounds*, Kluwer Academic, Dortrecht, 1991.

13. V. Böhmer, *Angew. Chemie*, 1995, **107**, 785–818.

14. C. D. Gutsche, *Calixarenes Revisited*, The Royal Society of Chemistry, Cambridge, UK, 1998.

15. N. Iki and S. Miyano, *J. Incl. Phenom. Macrocyclic Chem.*, 2001, **41**, 99–105.

16. J.-F. Dozol, V. Böhmer, M. A. McKervey, F. Lopez-Calahorra, D. N. Reinhoudt, M. J. Schwing, R. Ungaro and G. Wipff, *New macrocyclic extractants for radioactive waste treatment: Ionizable crown ethers and functionalized calixarenes*, EUR-OP Reference: CG-NA-17615-EN-C (EUR-17615), European Commission, Nuclear Science and Technology, Luxembourg, 1997.

17. J.-F. Dozol, M. J. Schwing-Weill, F. Arnaud-Neu, V. Böhmer, R. Ungaro, F. C. J. M. Van Veggel, G. Wipff, A. Costero, J. F. Desreux and J. De Mendoza, *Extraction and selective separation of long-lived nuclides by functionalised macrocycles*, EUR 19605, 2000.

18. K. Liger, J.-F. Dozol, F. Arnaud-Neu, V. Böhmer, B. Casensky, A. Casnati, J.-F. Desreux, B. Gruner, C. Grüttner, J. De Mendoza, G. Pina, P. Selucky, W. Verboom and G. Wipff, *Selective extraction of minor actinides from high activity liquid waste by organised matrices*, Final Report FIKW-CT-2000-00088, CEC, 2004.

19. J.-F. Dozol, M. Dozol and R. M. Macias, *J. Incl. Phenom. Macrocyclic Chem.*, 2000, **38**, 1–22.

20. R. M. Izatt, J. D. Lamb, R. T. Hawkins, P. R. Brown, S. R. Izatt and J. J. Christensen, *J. Am. Chem. Soc.*, 1983, **105**, 1782–1785.

21. S. R. Izatt, R. T. Hawkins, J. J. Christensen and R. M. Izatt, *J. Am. Chem. Soc.*, 1985, **107**, 63–66.

22. J.-F. Dozol, Z. Asfari, F. Arnaud-Neu, J. Vicens and P. Thuéry, *Radiochim. Acta*, 2004, **92**, 175–182.

23. D. Reinhoudt, Personal communication.

24. Y. Koide, T. Oka, A. Imamura, H. Shosenji and K. Yamada, *Bull. Chem. Soc. Jpn.*, 1993, **66**, 2137–2142.

25. P. Thuery, Z. Asfari, J. Vicens, V. Lamare and J.-F. Dozol, *Polyhedron*, 2002, **21**, 2497–2503.

26. T. A. Hanna, L. Liu, L. N. Zakharov, A. L. Rheingold, W. H. Watson and C. D. Gutsche, *Tetrahedron*, 2002, **58**, 9751–9757.

27. E. D. Gueneau, K. M. Fromm and H. Goesmann, *Chem. Eur. J.*, 2003, **9**, 509–514.

28. T. A. Hanna, L. Liu, A. M. Angeles-Boza, X. Kou, C. D. Gutsche, K. Ejsmont, W. H. Watson, L. N. Zakharov, C. D. Incarvito and A. L. Rheingold, *J. Am. Chem. Soc.*, 2003, **125**, 6228 –6238.

29. A. Bilyk, A. K. Hall, J. M. Harrowfield, M. W. Hosseini, B. W. Skelton and A. H. White, *Inorg. Chem.*, 2001, **40**, 672–686.

30. L. Prodi, F. Bolletta, M. Montalti, A. Casnati, F. Sansone and R. Ungaro, *New J. Chem.*, 2000, **24**, 155–158.

31. A. Casnati, A. Pochini, R. Ungaro, C. Bocchi, F. Ugozzoli, R. J. M. Egberink, H. Struijk, R. Lugtenberg, F. de Jong and D. N. Reinhoudt, *Chem. Eur. J.*, 1996, **2**, 436–445.

32. C. Hill, Ph.D. Thesis, Universite Louis Pasteur de Strasbourg, 1994.
33. A. Casnati, A. Pochini, R. Ungaro, F. Ugozzoli, F. Arnaud, S. Fanni, M.-J. Schwing, R. J. M. Egberink, F. de Jong and D. N. Reinhoudt, *J. Am. Chem. Soc.*, 1995, **117**, 2767–2777.
34. R. Ungaro, A. Casnati, F. Ugozzoli, A. Pochini, J.-F. Dozol, C. Hill and H. Rouquette, *Angew. Chemie Int. Ed.*, 1994, **33**, 1506–1509.
35. G. Wipff and M. Lauterbach, *Supramol. Chem.*, 1995, **6**, 187–207.
36. M. Lauterbach and G. Wipff, in *Physical Studies in Supramolecular Chemistry*, eds. L. Echegoyen and A. Kaifer, Kluwer, Dordrecht, Editon edn., 1996, pp. 65–102.
37. P. A. Kollman, *Chem. Rev.*, 1993, **93**, 2395–2417.
38. A. Varnek and G. Wipff, *J. Comput. Chem.*, 1996, **17**, 1520–1531.
39. V. Lamare, C. Bressot, J.-F. Dozol, J. Vicens, Z. Asfari, R. Ungaro and A. Casnati, *Sep. Sci. Technol.*, 1997, **32**, 175–191.
40. Z. Asfari, C. Bressot, J. Vicens, C. Hill, J.-F. Dozol, H. Rouquette, S. Eymard, V. Lamare and B. Tournois, *Analyt. Chem.*, 1995, **67**, 3133–3139.
41. F. Arnaud-Neu, Z. Asfari, B. Soley and J. Vicens, *New J. Chem.*, 1996, **20**, 453–463.
42. F. Allain, H. Virelizier, C. Moulin, C. K. Jankowski, J.-F. Dozol and J. C. Tabet, *Spectroscopy*, 2000, **14**, 127–139.
43. P. Thuery, M. Nierlich, V. Lamare, J.-F. Dozol, Z. Asfari and J. Vicens, *Supramol. Chem.*, 1997, **8**, 319–332.
44. V. Lamare, D. Haubertin, J. Golebiowski and J.-F. Dozol, *J. Chem. Soc. Perkin Trans.*, 2001, **2**, 121–127.
45. V. Lamare, J.-F. Dozol, F. Ugozzoli, A. Casnati and R. Ungaro, *Eur. J. Org. Chem.*, 1998, 1559–1568.
46. A. Casnati, F. Sansone, J.-F. Dozol, H. Rouquette, F. Arnaud-Neu, D. Byrne, S. Fuangswasdi, M.-J. Schwing-Weill and R. Ungaro, *J. Incl. Phenom. Macrocyclic Chem.*, 2001, **41**, 193–200.
47. A. Casnati, F. Sansone, J.-F. Dozol, H. Rouquette, F. Arnaud-Neu, D. Byrne, S. Fuangswasdi, M.-J. Schwing-Weill and R. Ungaro, *J. Incl. Phenom. Macrocyclic Chem.*, 2001, **41**, 193–200.
48. P. Thuery, M. Nierlich, C. Bressot, V. Lamare, J.-F. Dozol, Z. Asfari and J. Vicens, *J. Incl. Phenom. Mol. Recogn. Chem.*, 1996, **23**, 305–312.
49. C. K. Jankowski, F. Allain, C. Lamouroux, H. Virelizier, C. Moulin, J.-C. Tabet, V. Lamare and J.-F. Dozol, *Spectrosc. Lett.*, 2003, **36**, 327–340.
50. Z. Asfari, P. Thuery, M. Nierlich and J. Vicens, *Tetrahedron Lett.*, 1999, **40**, 499–502.
52. J. S. Kim, W. K. Lee, D. Y. Ra, Y. I. Lee, W. K. Choi, K. W. Lee and W. Z. Oh, *Microchem. J.*, 1998, **59**, 464–471.
53. W. F. Nijenhuis, E. G. Buitenhuis, F. deJong, E. J. R. Sudhölter and D. N. Reinhoudt, *J. Am. Chem. Soc.*, 1991, **113**, 7963–7968.
54. E. G. Reichwein-Buitenhuis, H. C. Visser, F. D. Jong and D. N. Reinhoudt, *J. Am. Chem. Soc.*, 1995, **117**, 3913–3921.
55. J. S. Kim, J. H. Pang, I. Y. Yu, W. K. Lee, I. H. Suh, J. K. Kim, M. H. Cho, E. T. Kim and D. Y. Ra, *J. Chem. Soc., Perkin Trans.* 1999, **2**, 837–846.
56. J. S. Kim, I. H. K. Suh, J. Kuk and M. H. Cho, *J. Chem. Soc., Perkin Trans.* 1998, **1**, 2307–2312.
57. J. S. Kim, A. Ohki, R. Ueki, T. Ishizuka, T. Shimotashiro and S. Maeda, *Talanta*, 1999, **48**, 705–710.
58. V. Lamare, C. Bressot, J.-F. Dozol, J. Vicens, Z. Asfari, R. Ungaro and A. Casnati, *Sep. Sci. Technol.*, 1997, **32**, 175–191.
59. V. Lamare, J.-F. Dozol, S. Fuangswasdi, F. Arnaud-Neu, P. Thuery, M. Nierlich, Z. Asfari and J. Vicens, *J. Chem. Soc., Perkin Trans.* 1999, **2**, 271–284.
60. N. Sieffert and G. Wipff, *J. Phys. Chem. B*, 2006, **110**, 19497–19506.

61. R. A. Sachleben, A. Urvoas, J. C. Bryan, T. J. Haverlock, B. P. Hay and B. A. Moyer, *J. Chem. Soc., Chem. Commun.*, 1999, 1751–1752.
62. R. A. Sachleben, J. C. Bryan, N. L. Engle, T. J. Haverlock, B. P. Hay, A. Urvoas and B. A. Moyer, *Eur. J. Org. Chem.*, 2003, **2003**, 4862–4869.
63. A. Casnati, N. Della Ca, F. Sansone, F. Ugozzoli and R. Ungaro, *Tetrahedron*, 2004, **60**, 7860–7876.
64. V. Lamare, J.-F. Dozol, P. Thuery, M. Nierlich, Z. Asfari and J. Vicens, *J. Chem. Soc., Perkin Trans.* 2001, **2**, 1920–1926.
65. S. Bouhroum, F. Arnaud-Neu, Z. Asfari and J. Vicens, *Russ. Chem. Bull., Int. Ed.*, 2004, **53**, 1544–1548.
66. P. K. Mohapatra, S. A. Ansari, A. Sarkar, A. Bhattacharyya and V. K. Manchanda, *Analyt. Chim. Acta*, 2006, **571**, 308–314.
67. V. S. Talantov, G. G. Talantova and R. A. Bartsch, *Tetrahedron*, 2000, **41**, 8221–8224.
68. M. G. Gorbunova, P. V. Bonnesen, N. L. Engle, E. Bazelaire, L. H. Delmau and B. A. Moyer, *Tetrahedron Lett.*, 2003, **44**, 5397–5401.
69. E. Bazelaire, M. G. Gorbunova, P. V. Bonnesen, B. A. Moyer and L. H. Delmau, *Solvent Extr. Ion Exch.*, 2004, **22**, 637–661.
70. E. Bazelaire, M. G. Gorbunova, P. V. Bonnesen, B. A. Moyer and L. H. Delmau, *Solvent Extr. Ion Exch.*, 2004, **22**, 637–661.
71. B. A. Moyer, E. Bazelaire, P. V. Bonnesen, R. Custelcean, L. H. Delmau, M. E. Ditto, N. L. Engle, M. G. Gorbunova, T. J. Haverlock, T. G. Levitskaia, R. Bartsch, M. A. Surowiec and H. Zhou, *Next generation extractants for cesium separation from high-level waste*, FY 2005 Annual Report, Environnmental Management Science Program, Project #73803, 2005.
72. B. W. Harmon, D. D. Ensor, L. H. Delmau and B. A. Moyer, *Solvent Extr. Ion Exch.*, 2007, **25**, 373–388.
73. P. Thuery, M. Lance, M. Nierlich, N. Reynier, V. Lamare, J.-F. Dozol, M. Saadioui, Z. Asfari and J. Vicens, *Anales de Quimica Int. Ed.*, 1997, **93**, 324–331.
74. M. Saadioui, Z. Asfari, J. Vicens, N. Reynier and J.-F. Dozol, *Chem. Rev.*, 1997, **28**, 223–244.
75. N. Reynier, J.-F. Dozol, M. Saadioui, Z. Asfari and J. Vicens, *Tetrahedron Lett.*, 1998, **39**, 6461–6464.
76. R. J. W. Lugtenberg, Z. Brzozka, A. Casnati, R. Ungaro, J. F. J. Enbersen and D. N. Reinhoudt, *Analyt. Chim. Acta*, 1995, **310**, 263–267.
77. C. Bocchi, M. Careri, A. Casnati and G. Mori, *Analyt. Chem.*, 1995, **67**, 4234–4238.
78. C. F. Reusch and E. L. Cussler, *AIChE J.*, 1973, **19**, 736–741.
79. T. B. Stolwijk, J. R. Sudholter and D. N. Reinhoudt, *J. Am. Chem. Soc.*, 1987, **109**, 7042–7047.
80. Z. Asfari, C. Bressot, J. Vicens, C. Hill, J.-F. Dozol, H. Rouquette, S. Eymard, V. Lamare and B. Tournois, Cesium Removal from Nuclear Waste Water by Supported Liquid Membranes Containing Calix-bis-brown Compounds, in *ACS Symposium Series 642* (Anaheim CA, April 2–6, 1995), eds. R. A. Bartsch and J. D. Way, American Chemical Society, Washington, DC, Editon edn., 1996, pp. 376–390.
81. G. Capuzzi, F. Pini, L. Dei, P. Lo Nostro, E. Fratini, R. Gilles and P. Baglioni, *Physica B*, 2000, **276–278**, 384–385.
82. Z. Asfari, X. Nicolle, J. Vicens, J.-F. Dozol, A. Duhart, J. M. Harrowfield, B. W. Skelton and A. H. White, *J. Incl. Phenom. Macrocyclic Chem.*, 1999, **33**, 251–262.
83. A. Duhart, J.-F. Dozol, H. Rouquette and A. Deratani, *J. Mebrane Sci.*, 2001, **185**, 145–155.
84. M. L. Dietz, D. D. Ensor, B. Harmon and S. Seekamp, *Sep. Purif. Technol.*, 2006, **41**, 2183–2204.

85. J. S. Kim and D. T. Quang, *Chem. Rev.*, 2007, **107**, 3780–3799.

86. J.-F. Dozol, V. Lamare, N. Simon, R. Ungaro and A. Casnati, in *ACS Symposium Series 757 (Calixarenes for Separations)*, eds. G. Lumetta, R. D. Rogers and A. S. Gopalan, American Chemical Society, Washington, DC, Editon edn., 2000, pp. 12–25.

87. B. A. Moyer, P. V. Bonnesen, L. H. Delmau, T. J. Heverlock, R. A. Sachleben, R. A. Leonard, C. Conner and G. L. Lumetta, ISEC'99, Barcelona, 1999.

88. M. Grunder, J.-F. Dozol, Z. Asfari and J. Vicens, *J. Radioanal. Nucl. Chem.*, 1999, **241**, 59–67.

89. J.-F. Dozol, N. Simon, V. Lamare, A. G. Carrera, D. De Marc, S. Eymard, H. Rouquette and B. Tournois, International Symposium and XI Reunion National Conference on Solvent Extraction, Moscow, 21–27 June, 1998.

90. P. Thuery, M. Nierlich, Z. Asfari, J. Vicens and J.-F. Dozol, *Polyhedron*, 2000, **19**, 1749–1756.

91. V. Lamare, J.-F. Dozol, F. Allain, H. Virelizier, C. Moulin, C. Jankowski and J.-C. Tabet, in *ACS Symposium Series 757 (Calixarenes for Separations)*, eds. G. Lumetta, R. D. Rogers and A. S. Gopalan, American Chemical Society, Washington, DC, Editon edn., 2000, pp. 56–70.

92. H. Dozol, Z. Asfari, J. Vicens, P. Thuery, M. Nierlich and J.-F. Dozol, *Tetrahedron Lett.*, 2001, **42**, 8285–8287.

93. C. K. Jankowski, J.-F. Dozol, F. Allain, J.-C. Tabet, R. Ungaro, A. Casnati, J. Vicens, Z. Asfari and J. Boivin, *Pol. J. Chem.*, 2002, **76**, 701–711.

94. C. K. Jankowski, M. R. Van Calsteren, N. Aychet, J.-F. Dozol, C. Moulin and C. Lamouroux, *Can. J. Chem.*, 2005, **83**, 1098–1113.

95. C. Lamouroux, N. Aychet, A. Lelièvre, C. K. Jankowski and C. Moulin, *Rapid Commun. Mass Spectrom.*, 2004, **18**, 1493–1503.

96. C. R. Duchemin, N. L. Engle, P. V. Bonnesen, T. J. Haverlock, L. H. Delmau and B. A. Moyer, *Solvent Extr. Ion Exch.*, 2001, **19**, 1037–1058.

97. N. Sieffert and G. Wipff, *Phys. Chem. Chem. Phys.*, 2007, **9**, 3763–3775.

98. K. Kavallieratos and B. A. Moyer, *Chem. Commun.*, 2001, 1620–1621.

99. B. A. Moyer, P. V. Bonnesen, R. Custelcean, L. H. Delmau and B. P. Haym, *Kemija u Industriji (Zagrep)*, 2005, **54**, 65–87.

100. Y. Marcus, *J. Sol. Chem.*, 1991, **20**, 929–944.

101. L. H. Delmau, T. J. Lefranc, P. V. Bonnesen, J. C. Bryan, D. J. Presley and B. A. Moyer, *Solvent Extr. Ion Exch.*, 2005, **23**, 23–57.

102. N. Simon, B. Tournois, S. Eymard, G. Volle, P. Rivalier, J. Leybros, J.-Y. Lanoe, N. Reynier-Tronche, G. Ferlay and J.-F. Dozol, Atalante 2004, International Conference on Advances for future nuclear fuel cycles, Nîmes, France, June, 2004.

103. *Les déchets radioactifs à haute activité et à vie longue. Recherche et résultat.* Loi du 30 décembre 1991. Dossier Final/Décembre, 2005.

104. A. Zhang, Y. Wei, H. Hoshi, Y. Koma and M. Kamiya, *Solvent Extr. Ion Exch.*, 2007, **25**, 389–405.

105. L. H. Delmau, P. V. Bonnesen, G. J. Van Berkel and B. A. Moyer, *Improved performance of the alkaline-side CSEX process for cerium extraction from alkaline high-level waste obtained by characterization of the effect of surfactant impurities,* ORNL/TM-1999/209, ORNL, USA, 1999.

106. P. V. Bonnesen, L. H. Delmau, B. A. Moyer and G. J. Lumetta, *Solvent Extr. Ion Exch.*, 2003, **21**, 141–170.

107. M. A. Norato, M. H. Beasley, S. G. Campbell, A. D. Coleman, M. W. Geeting, J. W. Guthrie, C. W. Kennell, R. A. Pierce, R. C. Ryberg, D. D. Walker, J. D. Law and T. A. Todd, *Demonstration of the caustic-side solvent extraction process for the removal of 137Cs from Savannah River Site high level waste*, WSRC-MS-2001-00201 Report, 2001.

108. R. D. Spence, L. N. Klatt, L. H. Delmau, F. V. Sloop, P. V. Bonnesen and B. A. Moyer, ORNL/TM-2001/49 Report, ORNL, 2001.

109. L. N. Klatt, J. F. Birdwell, P. V. Bonnesen, L. H. Delmau, L. J. Foote, D. D. Lee, R. A. Leonard, T. G. Levitskaia, M. P. Maskarinec and B. A. Moyer, ORNL/TM-2001/258 Report, ORNL, 2001.

110. L. H. Delmau, T. J. Haverlock and B. A. Moyer, ORNL/TM-2002/104 Report, ORNL, 2002.

111. P. V. Bonnesen, F. V. Sloop and N. L. Engle, ORNL/TM-2002/115 Report, ORNL, 2002.

112. L. H. Delmau, T. J. Haverlock, J. Sloop, F.V. and B. A. Moyer, ORNL/TM-2003/011 Report, ORNL, 2003.

113. K. Adu-Wusu, D. D. Walker, T. B. Edwards and S. D. Fink, AIChe 2006 Spring National Meeting Session 14: Nuclear Engineering Div., Advances in the Separations and Immobilization of Nuclear Waste, Orlando, FL, 2006.

114. E. P. Horwitz, M. L. Dietz and D. D. Fisher, *Solvent Extr. Ion Exch.*, 1990, **8**, 199–208.

115. E. P. Horwitz, M. L. Dietz and D. D. Fisher, *Solvent Extr. Ion Exch.*, 1990, **8**, 557–572.

116. E. P. Horwitz, M. L. Dietz and D. D. Fisher, *Solvent Extr. Ion Exch.*, 1991, **9**, 1–25.

117. J. D. Law, D. J. Wood and T. A. Todd, INEEL/EXT-99-00001 Report, 1999.

118. I. H. Gerow and M. W. Davis, *Sep. Sci. Technol.*, 1979, **14**, 395–414.

119. I. H. Gerow, J. E. Smith and M. W. Davis, *Sep. Sci. Technol.*, 1981, **15**, 519–548.

120. R. G. Shuler, C. B. Bowers, J. E. Bowers, J. E. Smith, V. Van Brunt and M. W. Davis, *Solvent Extr. Ion Exch.*, 1985, **3**, 567–604.

121. J.-F. Dozol, J. Casas and A. M. Sastre, *J. Membrane Sci.*, 1993, **114**, 237–246.

122. J.-F. Dozol, J. Casas and A. M. Sastre, *Sep. Sci. Technol.*, 1993, **28**, 2007–2022.

123. J.-F. Dozol, J. Casas and A. M. Sastre, *Sep. Sci. Technol.*, 1994, **29**, 1999–2018.

124. J.-F. Dozol, J. Casas and A. M. Sastre, *Sep. Sci. Technol.*, 1995, **30**, 435–448.

125. C. L. Riddle, J. D. Baker, J. D. Law, C. A. McGrath, D. H. Meikrantz, B. J. Mincher, D. R. Peterman and T. A. Todd, *Solvent Extr. Ion Exch.*, 2005, **23**, 449–461.

126. L. H. Delmau, P. V. Bonnesen, N. L. Engle, T. J. Haverlock, F. V. Sloop Jr. and B. A. Moyer, *Solvent Extr. Ion Exch.*, 2006, **24**, 197–225.

127. B. Grüner, J. Plesek, J. Baca, J.-F. Dozol, V. Lamare, I. Cisarova, M. Belohradsky and J. Caslavsky, *New J. Chem.*, 2002, **26**, 867–875.

128. F. Arnaud-Neu, M.-J. Schwing-Weill and J.-F. Dozol, Calixarenes for nuclear waste treatment in *Calixarenes 2001*, eds. Z. Asfari, V. Böhmer, J. Harrowfield and J. Vicens, Kluwer, Dordrecht, Editon edn., 2001, p. 642.

129. F. Arnaud-Neu, S. Barboso, F. Berny, A. Casnati, N. Muzet, A. Pinalli, R. Ungaro, M. Schwing-Weill and G. Wipff, *J. Chem. Soc., Perkin Trans.* 1999, **2**, 1727–1738.

130. N. Muzet, G. Wipff, A. Casnati, L. Domiano, R. Ungaro and F. Ugozzoli, *J. Chem. Soc., Perkin Trans.* 1996, **2**, 1065–1075.

131. P. Vanura and I. Stibor, *Collect. Czech. Chem. Commun.*, 1998, **63**, 2009–2014.

132. S. Fanni, F. Arnaud-Neu, M. A. McKervey, M. J. Schwing-Weill and K. Ziat, *Tetrahedron Lett.*, 1996, **37**, 7975–7978.

133. A. Casnati, S. Barboso, H. Rouquette, M.-J. Schwing-Weill, F. Arnaud-Neu, J.-F. Dozol and R. Ungaro, *J. Am. Chem. Soc.*, 2001, **123**, 12182–12190.

134. A. Casnati, L. Baldini, N. Pelizzi, K. Rissanen, F. Ugozzoli and R. Ungaro, *J. Chem. Soc., Dalton Trans.*, 2000, 3411–3415.

135. C. Tu, K. Surowiec and R. A. Bartsch, *Tetrahedron Lett.*, 2006, **47**, 3443–3446.

136. C. Tu, D. Liu, K. Surowiec, D. W. Purkiss and R. A. Bartsch, *Org. Biomol. Chem.*, 2006, **4**, 2938–2944.

137. H. Zhou, K. Surowiec, D. W. Purkiss and R. A. Bartsch, *Org. Biomol. Chem.*, 2006, **4**, 1104–1114.

138. C. Tu, K. Surowiec and R. A. Bartsch, *Tetrahedron*, 2007, **63**, 4184–4189.

139. C. Tu, K. Surowiec, J. Gega, D. W. Purkiss and R. A. Bartsch, *Tetrahedron*, 2008, **64**, 1187–1196.

140. H. Zhou, K. Surowiec, D. W. Purkiss and R. A. Bartsch, *Org. Biomol. Chem.*, 2005, **3**, 1676–1684.

141. H. Zhou, D. Liu, J. Gega, K. Surowiec, D. W. Purkiss and R. A. Bartsch, *Org. Biomol. Chem.*, 2007, **5**, 324–332.

142. I. V. Smirnov, A. Y. Shadrin, V. A. Babain, M. V. Logunov, M. K. Chmutova and V. I. Kal'tchenko, *ACS Symp. Ser.*, 2000, **757 (*Calixarenes for Separations*)**, 107.

143. I. S. Antipin, G. A. Pribylova, S. E. Solovyeva, I. G. Tananaev, A. I. Konovalov and B. F. Myasoedov, in *Recent Advances in Actinide Science (Proc. Actinide Conf., Actinides 2005)*, eds. I. May and R. Alvarez, Royal Society of Chemistry, Cambridge, Editon edn., 2006, vol. 305, pp. 557–559.

144. I. S. Antipin, S. E. Solovieva, I. I. Stoikov, I. S. Vershinina, G. A. Pribylova, I. G. Tananaev and B. F. Myasoedov, *Russ. Chem. Bull. (Translation of Izvestiya Akademii Nauk, Seriya Khimicheskaya)*, 2004, **53**, 127–132.

145. R. Ludwig and T. K. D. Nguyen, *J. Nucl. Radiochem. Sci.*, 2005, **6**, 227–231.

146. D. G. Kalina, E. P. Horwitz, L. Kaplan and A. C. Muscatello, *Sep. Sci. Technol.*, 1981, **16**, 1127.

147. E. P. Horwitz, D. G. Kalina, L. Kaplan, G. W. Mason and H. Diamond, *Sep. Sci. Technol.*, 1982, **17**, 1261–1279.

148. E. P. Horwitz and D. G. Kalina, *Solvent Extr. Ion Exch.*, 1984, **2**, 179–200.

149. E. P. Horwitz, D. G. Kalina, H. Diamond, G. F. Vandegrift and W. W. Schulz, *Solvent Extr. Ion Exch.*, 1985, **3**, 75–109.

150. E. P. Horwitz, K. A. Martin, H. Diamond and L. Kaplan, *Solvent Extr. Ion Exch.*, 1986, **4**, 449–494.

151. Z. Kolarik and E. P. Horwitz, *Solvent Extr. Ion Exch.*, 1988, **6**, 61–91.

152. J. F. Malone, D. J. Marrs, M. A. McKervey, P. O'Hagan, N. Thompson, A. Walker, F. Arnaud-Neu, O. Mauprivez, M.-J. Shwing-Weill, J.-F. Dozol, H. Rouquette and N. Simon, *J. Chem. Soc., Chem. Commun.*, 1995, 2151–2153.

153. F. Arnaud-Neu, J. K. Browne, D. Byrne, D. J. Marss, M. A. McKervey, P. O. O'Hagan, M. J. Schwing-Weill and A. Walker, *Chem. Eur. J.*, 1999, **5**, 175–186.

154. M.-J. Schwing-Weill and F. Arnaud-Neu, *Gazz. Chim. Ital.*, 1997, **127**, 687–692.

155. M. R. Yaftian, M. R. Razipour and D. Matt, *J. Radioanal. Nucl. Chem.*, 2006, **270**, 357–361.

156. M. Atanassova, V. Lachkova, N. Vassilev, S. Varbanov and I. Dukov, *J. Incl. Phenom. Macrocyclic Chem.*, 2007, **58**, 173–179.

157. K. A. Martin, E. P. Horwitz and J. R. Ferraro, *Solvent Extr. Ion Exch.*, 1986, **4**, 1149.

158. S. D. Baker, B. J. Mincher, D. H. Meikrantz and J. R. Berreth, *Solvent Extr. Ion Exch.*, 1988, **6**, 1049.

159. F. Arnaud-Neu, V. Böhmer, J.-F. Dozol, C. Grüttner, R. A. Jacobi, D. Kraft, O. Mauprivez, H. Rouquette, M.-J. Schwing-Weill, N. Simon and W. Vogt, *J. Chem. Soc., Perkin Trans.* 1996, **2**, 1175–1182.

160. S. E. Matthews, M. Saadioui, V. Böhmer, S. Barboso, F. Arnaud-Neu, M.-J. Schwing-Weill, A. G. Carrera and J.-F. Dozol, *J. Prakt. Chem.*, 1999, **341**, 264–273.

161. L. H. Delmau, N. Simon, M.-J. Schwing-Weill, F. Arnaud-Neu, J.-F. Dozol, S. Eymard, B. Tournois, V. Böhmer, C. Grüttner, C. Musigmann and A. Tunayar, *J. Chem. Soc., Chem. Commun.*, 1998, 1627–1628.

162. L. H. Delmau, Ph.D. Thesis, Strasbourg University, 1997. Extraction of Trivalent Lanthanides and Actinides by Functionalized Calixarenes. Study of the Structure of the Complexes in Solution by Nuclear Magnetic Resonance.

163. L. H. Delmau, N. Simon, M.-J. Schwing-Weill, F. Arnaud-Neu, J.-F. Dozol, S. Eymard, B. Tournois, C. Grüttner, C. Musigmann, A. Tunayar and V. Böhmer, *Sep. Sci. Technol.*, 1999, **34**, 863–876.

164. S. Cherfa, Ph.D. Thesis, University Paris XI Orsay, 1998.

165. C. Lamouroux, S. Rateau and C. Moulin, *Rapid Commun. Mass Spectrometry*, 2006, **20**, 2041–2052.

166. K. L. Nash and E. P. Horwitz, *Inorg. Chim. Acta*, 1990, **169**, 245.

167. K. L. Nash and P. G. Rickert, *Sep. Sci. Technol.*, 1993, **28**, 25–41.

168. A. G. Carrera, Ph.D. Thesis, Barcelona University, 2000. Extraction of the Lanthanides and Actinides by Means of Calixarenes Bearing CMPO Groups.

169. M. M. Reinoso-Garcia, W. Verboom, D. Reinhoudt, F. Brisach, F. Arnaud-Neu and K. Liger, *Solvent Extr. Ion Exch.*, 2005, **23**, 425–437.

170. C. Schmidt, M. Saadioui, V. Böhmer, V. Host, M.-R. Spirlet, J.-F. Desreux, F. Brisach, F. Arnaud-Neu and J.-F. Dozol, *Org. Biomol. Chem.*, 2003, **1**, 4089–4096.

171. A. Arduini, V. Böhmer, L. Delmau, J.-F. Desreux, J.-F. Dozol, M. A. G. Carrera, B. Lambert, C. Musigmann, A. Pochini, A. Shivanyuk and F. Ugozzoli, *Chem. Eur. J.*, 2000, **6**, 2135–2144.

172. L. Atamas, O. Klimchuk, V. Rudzevich, V. Pirozhenko, V. Kalchenko, I. Smirnov, V. Babain, T. Efremova, A. Varnek, G. Wipff, F. Arnaud-Neu, M. Roch, M. Saadioui and V. Böhmer, *J. Supramol. Chem.*, 2002, **2**, 421–427.

173. S. Barboso, A. G. Carrera, S. E. Matthews, F. Arnaud-Neu, V. Böhmer, J.-F. Dozol, H. Rouquette and M.-J. Schwing-Weill, *J. Chem. Soc., Perkin Trans.* 1999, **2**, 719–723.

174. H. Herschbach, F. Brisach, J. Haddaoui, M. Saadioui, E. Leize, A. V. Dorsselaer, F. Arnaud-Neu and V. Böhmer, *Talanta*, 2007, **74**, 39–46.

175. B. Lambert, V. Jacques, A. Shivanyuk, S. E. Matthews, A. Tunayar, M. Baaden, G. Wipff, V. Böhmer and J. F. Desreux, *Inorg. Chem.*, 2000, **39**, 2033–2041.

176. V. A. Babain, M. Y. Alyapyshev, M. D. Karavan, V. Böhmer, L. Wang, E. A. Shokova, A. E. Motornaya, I. M. Vatsouro and V. V. Kovalev, *Radiochim. Acta*, 2005, **93**, 749–756.

177. A. Motornaya, I. Vatsouro, E. Shokova, V. Hubscher-Bruder, M. Alyapyshev, V. Babain, M. Karavan, F. Arnaud-Neu, V. Böhmer and V. Kovalev, *Tetrahedron*, 2007, **63**, 4748–4755.

178. A. E. Motornaya, I. M. Vatsouro, E. A. Shokova, V. Hubscher-Bruder, M. Y. Alyapyshev, V. Babain, M. D. Karavan, F. Arnaud-Neu, V. Böhmer and V. V. Kovalev, *J. Supramol. Chem.*, 2003, **2**, 421–427.

179. F. Sansone, M. Fontanella, A. Casnati, R. Ungaro, V. Böhmer, M. Saadioui, K. Liger and J.-F. Dozol, *Tetrahedron*, 2006, **62**, 6749–6753.

180. J.-F. Dozol, C. Schmidt, P. Wang and V. Böhmer, United States Patent 20060205920, 2006.

181. P. Wang, M. Saadioui, C. Schmidt, V. Böhmer, V. Host, J. F. Desreux and J.-F. Dozol, *Tetrahedron*, 2004, **60**, 2509–2515.

182. L. Nuñez, B. A. Buchholz and G. F. Vandegrift, *Sep. Sci. Technol.*, 1995, **30**, 1455–1471.

183. L. Nuñez, B. A. Buchholz and M. Kaminski, *Sep. Sci. Technol.*, 1996, **31**, 1393–1407.

184. S. E. Matthews, P. Parzuchowski, A. G. Carrera, C. Grüttner, J.-F. Dozol and V. Böhmer, *J. Chem. Soc., Chem. Commun.*, 2001, 417–418.

185. C. Grüttner, S. Rudershausen, S. E. Matthews, P. Wang, V. Böhmer and J.-F. Dozol, *Eur. Cells Mater.*, 2002, **3**, 48–51.

186. M. Formica, V. Fusi, M. Micheloni, R. Pontellini and P. Romani, *Coord. Chem. Rev.*, 1999, **184**, 347–363.

187. B. Grüner, J. Plesek, J. Baca, I. Cisarova, J.-F. Dozol, H. Rouquette, C. Vinas, P. Selucky and J. Rais, *New J. Chem.*, 2002, **26**, 1519–1527.

188. G. Chevrot, R. Schurhammer and G. Wipff, *J. Phys. Chem. B*, 2006, **110**, 9488–9498.
189. B. Coupez and G. Wipff, *Comptes Rendus Chim.*, 2004, **7**, 1153–1164.
190. A. Casnati, N. Della Ca', M. Fontanella, F. Sansone, F. Ugozzoli, R. Ungaro, K. Liger and J.-F. Dozol, *Eur. J. Org. Chem.*, 2005, 2338–2348.
191. F. Arnaud-Neu, S. Barboso, B. V. F. Brisach, L. Delmau, J.-F. Dozol, O. Mogck, E. F. Paulus, M. Saadioui and A. Shivanyuk, *Austr. J. Chem.*, 2003, **56**, 1113–1119.
192. H. Boerrigter, W. Verboom, F. deJong and D. N. Reinhoudt, *Radiochim. Acta*, 1998, **81**, 39–45.
193. H. Boerrigter, W. Verboom and D. N. Reinhoudt, *Liebigs Annalen/Recueil*, 1997, 2247–2254.
194. M. Kyrs, K. Svoboda, P. Lhotak and J. Alexova, *J. Radioanal. Nucl. Chem.*, 2003, **258**, 497–509.
195. L. Mikulasek, B. Gruener, C. Danila, V. Böhmer, J. Caslavsky and P. Selucky, *Chem. Commun.*, 2006, 4001–4003.
196. L. Mikulasek, B. Grüner, C. Dordea, V. Rudzevich, V. Böhmer, J. Haddaoui, V. Hubscher-Bruder, F. Arnaud-Neu, J. Caslavsky and P. Selucky, *Eur. J. Org. Chem.*, 2007, **2007**, 4772–4783.
197. S. Shinkai, Y. Shiramama, H. Satoh, O. Manabe, T. Arimura, K. Fujimoto and T. Matsuda, *J. Chem. Soc., Perkin Trans.* 1989, **2**, 1167–1171.
198. T. Nagasaki, S. Shinkai and T. Matsuda, *J. Chem. Soc., Perkin Trans.* 1990, **1**, 2617–2618.
199. K. Araki, N. Hashimoto, H. Otsuka, T. Nagasaki and S. Shinkai, *Chem. Lett.*, 1993, **22**, 829–832.
200. B. Boulet, C. Bouvier-Capely and C. Cossonnet, *Solvent Extr. Ion Exch.*, 2006, **24**, 319–330.
201. S. Shinkai, H. Kawaguchi and O. Manabe, *J. Polym. Sci., Part C, Polym. Lett.*, 1988, **26**, 391–396.
202. R. Ludwig, K. Inoue and T. Yamato, *Solvent Extr. Ion Exch.*, 1993, **11**, 311–330.
203. K. Ohto, K. Inoue, M. Goto, F. Nakashio, T. Nagasaki and S. Shinkai, ISEC'93, York (UK), 1993.
204. R. Ludwig, S. Tachimori and T. Yamato, *Nukleonika*, 1998, **43**, 161–174.
205. K. Ohto, M. Yano, K. Inoue, T. Nagasaki, M. Goto, F. Nakashio and S. Shinkai, *Polyhedron*, 1997, **16**, 1655–1661.
206. J. Soedarsono, A. Hagege, M. Burgard, Z. Asfari and J. Vicens, *Ber. Bunsen-Ges. Phys. Chem.*, 1996, **100**, 477–481.
207. K. Ohto, H. Ishibashi, S. Kuwata and K. Inoue, Solvent Extraction for the 21st Century, Proceedings of ISEC '99, Barcelona, 11–16. July, 1999.
208. T. Kakoi, T. Ohshima, T. Nishiori, F. Kubota, M. Goto, S. Shinkai and F. Nakashio, *J. Membr. Sci.*, 1998, **143**, 125–135.
209. T. Oshima, T. Kakoi, F. Kubota, K. Ohto, M. Goto and F. Nakashio, *Sep. Sci. Technol.*, 1998, **33**, 1905–1917.
210. R. Ludwig, K. Kunogi, T. K. D. Nguyen and S. Tachimori, *J. Chem. Soc., Chem. Commun.*, 1997, 1985–1986.
211. T. K. D. Nguyen, K. Kunogi and R. Ludwig, *Bull. Chem. Soc. Jpn.*, 1999, **72**, 1005–1011.
212. R. Ludwig, T. K. D. Nguyen and E. Herrmann, Advances in Nuclear and Radiochemistry: Proc. NRC-6, Aachen 29 August to 3 September, 2004.

5 Quantitative Structure-Property Relationships in Solvent Extraction and Complexation of Metals

Alexandre Varnek
Université Louis Pasteur

Vitaly Solov'ev
Institute of Physical Chemistry and Electrochemistry
of Russian Academy of Sciences

CONTENTS

> The most fundamental and lasting objective of synthesis is not production of new compounds but production of properties

> **George S. Hammond**
> *Norris Award Lecture, 1968*

5.1   INTRODUCTION

The development of new reagents for selective binding and separation of metal ions in solutions represents a real challenge because of the complexities of intra- and intermolecular interactions associated with metal ion (M)-ligand (L) binding in the liquid phase.[1] In solution, the stability of complexes depends on the number and type of the coordination centers of L, its topology and flexibility/rigidity and solvent effects. In some cases, complexation is accompanied by proton dissociation or association, as well as by the formation of contact- or solvent-separated ion pairs with a counterion. Compared with complexation in homogeneous solutions, extraction processes are more complex because they involve various chemical and physical interactions of molecular species (extractant, coextractant, and counterions) situated in two immiscible liquid phases.[2] Even in the simplest case, an extraction process involves the formation of a metal-ligand complex in one of the phases or at the liquid-liquid interface, followed by its diffusion into the organic phase. The formation of more complex species like inverse micelles, vesicles, etc., also affects extraction equilibria.

At least three theoretical approaches can be used for computer-aided designs of new metal binders: quantum mechanics, force-field molecular modeling, and chemoinformatics. These approaches are complementary; a decision to apply a particular one depends on the target problem. Quantum mechanics and force-field molecular modeling are suitable tools to study coordination patterns of metal/ligand complexes, conformational transformations of ligands upon complexation, and explicit solvation effects. However, they are mostly useful for interpreting known phenomena, not to predict directly the thermodynamic or kinetic parameters of metal complexation or extraction. Quantum mechanics calculations are still time consuming to treat explicitly solvent effects and complex aggregates formed in liquid phase(s).

Due to simplified representations of intra- and intermolecular interactions, force-field molecular mechanics and dynamics simulations[3] can be performed on large systems of up to 4,000–5,000 solvent molecules, several ligand molecules, metal cations, and counterions.[4] However, the force-field approaches suffer from numerous methodological problems related to the construction of empirical atom-atom potentials and the assessment of entropy terms. Therefore, quantum mechanics and force-field molecular modeling give microscopic insight into metal complexation or extraction phenomena, but still fail to assess quantitatively the metal-binding affinity of ligands with reasonable accuracy. Unlike these approaches, chemoinformatic methods provide a direct link between molecular structure and any property, and, therefore, they could become a realistic solution for computer-aided designs of new complexants or extractants.

Chemoinformatics is a relatively new field dealing with the combination of chemical information resources to transform data into information and information into knowledge.[5] Its three main applications are: (i) management (storage, organization, and search) of chemical data; (ii) development of predictive qualitative or quantitative models linking molecular structure and related properties; and (iii) computer-aided designs of new compounds possessing the desired properties. The first one is related to the development of chemical databases, and substructural and similarity search techniques, whereas the others concern establishing and utilizing qualitative Structure-activity relationships (SAR) and Quantitative structure-activity (or property) relationships (QSAR/QSPR). All these applications are closely related: SAR and QSPR models can be derived only from analyses of available experimental data. Thus, chemoinformatics applies an inductive learning approach (development of models from the data), which contrasts with quantum mechanics applying mostly deductive inference (application of fundamental theory to particular systems). Unlike molecular models used in quantum mechanics (ensembles of nuclei and electrons) or in force-field molecular modeling (ensembles of atoms and bonds), chemoinformatics describes a molecule by means of some characteristics (molecular descriptors) related to its structure and somehow related to modeled properties. Selected descriptors define a *chemical space* in which each molecule is represented as a vector.

Chemoinformatic approaches open new opportunities for computer-aided developments of new, efficient metal binders. Generally, the strategy of an in-silico design involves three main steps: (i) acquisition, storage, and organization of experimental data; (ii) development and validation of SAR or QSAR/QSPR; and (iii) applying those models to screen large datasets of real or virtual chemical structures. To develop robust models, one should select a pertinent set of descriptors, choose an appropriate machine-learning method(s), and choose a reasonable procedure of validation of these models.[5] Traditionally, QSAR is used in the modeling of biological, pharmaco-kinetic, and pharmaco-dynamical properties, whereas QSPR corresponds to models for any other chemical or physical properties.

A QSAR/QSPR model can be defined as a mathematical relationship, $Y = f(X)$, between any physical, chemical, or biological property (Y) of a molecule and its chemical structure.[6] The main problems here are to define a functional dependence (f), to select a set of pertinent molecular descriptors (X), and to establish a protocol

for obtaining and validating the model. A predictive QSPR model linking stability constant values with the structure of ligand L, on the one hand, has to involve descriptors accounting for the structural diversity and topology of L as well as different binding mechanisms, and, on the other hand, it should be based on a reasonable mathematical approach that accounts for possible nonadditive effects.

The first empirical correlations (1950s–1980s) between complexation or extraction constants and some physicochemical parameters of ligands and metals were developed for a small series of ligands belonging to one chemical class; see previous reviews[1,7–12] and references therein. One of these correlations—linear free energy relationships (LFER)—uses as descriptors experimental stability constants obtained in similar complexation reactions with a reference species (a proton, another metal, or another ligand). These correlations are always limited by the availability of related experimental data. Another popular type of correlation—"parametric equations"—concerns equations of the additive-multiplicative type (Drago, Edwards, Pearson, Misono, and Hancock), Hammet-like relationships, or more complicated (Brown–Sylva–Ellis) relationships. These were obtained using the experimental data for some model reactions and, therefore, are also limited by available experimental data. The predictive performance of these correlations is rather uncertain, because they were observed for limited sets of molecules and, as a rule, were not properly validated (see Section 2.3). However, they give a certain idea about the trends of complex stabilities as a function of some molecular characteristics and, therefore, could be considered as predecessors of QSPR technologies.

Following the evolution of structure-property methods in the drug design area at the beginning of the 1990s, various types of descriptors (topological, electronic, physicochemical, and fragment, issued from molecular mechanics calculations, etc.), were used in metal complexation and extraction. The linear regression approach was used in most cases; only one work involving the artificial neural network (ANN) method has been published (see Section 4.2). Unlike simple correlations, some of these studies involved validation of the models on independent test set(s). The datasets used for the training were large enough (up to 100 ligands) and more structurally diverse than those used in the "era of correlations." The application of those models for predictions was still very restricted because of the limited number of chemical classes used for the training and an insufficiently robust validation procedure.

In recent years, QSPR modeling of metal complexation and extraction has attained a higher level because of the application of various types of descriptors and machine-learning approaches, proper validation procedures, new modeling strategies (divide and conquer[13] models' applicability domain (AD),[13] and others). Predictive models were successfully developed on large (several hundred), structurally diverse sets of ligands. Successful computer-aided designs of new metal binders have been performed.[14,15]

Formally, complexation stability constants in water ($\log K$) and extraction constants ($\log K_{ex}$) can be related via partitioning coefficients of the free ligand and its complex between the aqueous and organic phases.[16] However, the latter are rarely available, and therefore the relationships between $\log K$ and $\log K_{ex}$ are not widely used. Nevertheless, in many cases, the binding ability of ligands to metal in complexation and extraction processes follows the same trend. In this respect, information

about metal binding in a homogeneous solution is useful to interpret the processes taking place in systems involving two immiscible liquids. On the other hand, the quantitative assessment of thermodynamic parameters of complexation and extraction is more difficult, and, therefore, QSPR modeling should be performed individually for each of them.

The goal of this work is to provide an overview of QSPR studies in metal complexation and extraction and to discuss under which conditions QSPR modeling may become a valuable tool for computer-aided design of new metal binders. Early empirical correlations will be analyzed here only for comparison with "regular" QSPRs.

This paper is organized according to the following. In the first two sections, we briefly describe the methods of obtaining and validating of predictive structure-property models and give some information about existing databases on metal complexation and extraction. The main section is devoted to the analysis of empirical correlations and QSPR models developed for metal complexation and extraction. Finally, two examples of computer-aided (*in silico*) designs of new extractants are reported.

5.2   GENERAL INFORMATION ABOUT QSPR MODELING

To build a QSPR model, one should carefully select available experimental data, and choose the initial pool descriptors (from which the program selects the most appropriate ones) as well as a mathematical approach linking those descriptors with a given property. Then, a suitable strategy of model validation should be applied in order to obtain a quantitative assessment of the quality of predictions. Finally, some rules should be established in order to prevent the application of the models to compounds too different from those used for obtaining the models.

5.2.1   Descriptors

Nowadays, more than 4000 types of descriptors are known.[17] There exist different ways to classify them. With respect to the type of molecular representation used for their calculations—chemical formula, molecular graph, or spatial positions of atoms—one speaks about 1D, 2D, and 3D descriptors, respectively. Descriptors can be global (describing the molecule as a whole) and local (only selected parts are considered). One could distinguish information-based descriptors, which tend to code the information stored in molecular structures, and knowledge-based (or semiempirical) descriptors issued from the consideration of the mechanism of action. Most of those descriptors can be obtained with the DRAGON, CODESSA PRO, and ISIDA programs.

DRAGON[18] is a well-known commercial software for the calculation of more than 3,000 descriptors. Formally, they are divided into 22 "blocks": constitutional descriptors, topological descriptors, walk and path counts, connectivity indices, information indices, 2D autocorrelations, edge adjacency indices, Randic molecular profiles, GETAWAY descriptors, topological charge indices, eigenvalue-based indices, charge descriptors, and some others. CODESSA PRO,[19] a commercial program

for QSAR/QSPR analysis, calculates constitutional, topological, geometrical, electrostatic, molecular surface, quantum-chemical, Molecular Orbitals related, and thermodynamic descriptors.

The ISIDA package[20] for computer-aided designs of new compounds generates several types of fragment descriptors. The latter represent selected substructures (fragments) of molecular graphs and their occurrences in molecules; they constitute one of the most important types of molecular descriptors. Their main advantage is related to the simplicity of their calculation, storage, and interpretation (see review articles[21–24]). Substructural fragments are information-based descriptors. Due to their versatility, they could be efficiently used to create a chemical space that separates active and nonactive compounds. ISIDA[20] generates two classes of substructural molecular fragment (SMF) descriptors: "sequences" and "augmented atoms." The sequences may contain connected atoms and bonds, atoms only, or bonds only. For each type of sequence, the minimal ($n_{min} \geq 2$) and maximal ($n_{max} \leq 15$) number of constituent atoms is defined. An "augmented atom" represents a particular atom with its environment including either neighboring atoms and bonds, or atoms only, or bonds only. Linear QSPR models involving fragment descriptors can be easily interpreted, taking into account the values and signs of fragment contributions. For example, stability constants ($\log K$) of potassium complexes with phosphoryl-containing podands in mixed THF-CHCl$_3$ solvent are calculated using 14 fragment descriptors,[25] some of which bring high positive (O-C-C-O, C-P=O) or negative (C-C-C, P-C-C-P) contributions into $\log K$, whereas others (C-C$_{ar}$- C$_{ar}$- C$_{ar}$ and some others) are less important (Figure 5.1).
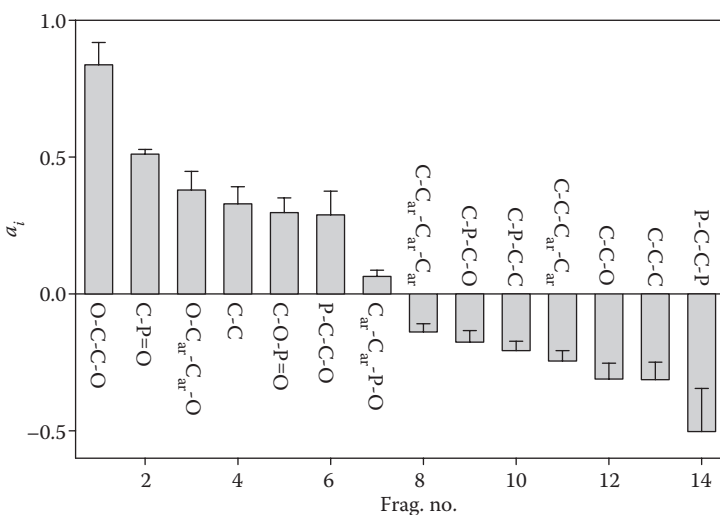
FIGURE 5.1   QSPR modeling of the stability constant $\log K$ of potassium complexes K$^+$ with phosphoryl-containing podands in THF-CHCl$_3$ (4:1 v/v) at 298 K:[25] fragment contributions (a_i) in the linear model $\log K = a_o + \Sigma a_i N_i$, where N_i is an occurrence of the ith fragment.

5.2.2 MACHINE-LEARNING METHODS

Generally, tens of different machine-learning techniques are used in QSAR/QSPR studies. In this chapter, we describe only those that have been recently applied in studies of solvent extraction and complexation of metals.

5.2.2.1 Multiple Linear Regression (MLR)

The multiple linear regression (MLR) method was historically the first and, until now, the most popular method used for building QSPR models. In MLR, a property is represented as a weighted linear combination of descriptor values: $Y = A^T X$, where Y is a column vector of property to be predicted, X is a matrix of descriptor values, and A is a column vector of adjustable coefficients calculated as $A = (X^T X)^{-1} X^T Y$. The latter equation can be applied only if the matrix $X^T X$ can be inverted, which requires linear independence of the descriptors ("multicollinearity problem"). If this is not the case, special techniques (e.g., singular value decomposition (SVD)[26]) should be applied.

5.2.2.2 Artificial Neural Networks

An artificial neural network is a mathematical model that mimics biological neural networks. In this model, simple nodes ("neurons") are connected together to form a network of nodes ("neural network"). The neurons may receive signals from their neighbors and form the signals toward some other neighbors. Thus, an artificial neural network represents an adaptive system that fits its parameters looking for rather complex mathematical relationships between "input" neurons (descriptors) and "output" neurons (modeled activity). In most cases, a three-layer architecture (input layer–hidden layer–output layer) is used for QSAR/QSPR studies. In particular, in the metal complexation and extraction area, Radial Basis Function Neural Network (RBFNN)[27] and Associative Neural Network (ASNN)[28,29] approaches have been used. The RBFNN approach approximates modelled properties by a linear combination of Gaussians. The ASNN approach[28,29] represents a combination of an ensemble of feed-forward neural networks and k-nearest neighbors (kNN) calculations in the space of ensemble residuals.

5.2.2.3 Support Vector Regression (SVR)

Support Vector Machine (SVM) is a classification and regression method developed by Vapnik.[30] In support vector regression (SVR), the input variables are first mapped into a higher dimensional feature space by the use of a kernel function, and then a linear model is constructed in this feature space. The kernel functions often used in SVM include linear, polynomial, radial basis function (RBF), and sigmoid function. The generalization performance of SVM depends on the selection of several internal parameters of the algorithm (C and ε), the type of kernel, and the parameters of the kernel.[31]

5.2.2.4 *k*-Nearest Neighbors

In the kNN method, the property Y of the target compound is calculated as an average (or weighted average) of that for its kNN in the space of descriptors selected for the model. Different metrics (Euclidian distances, Tanimoto similarity coefficients, etc.), can be used to identify the neighbors. Their number k is optimized using a cross-validation procedure for the training set.

5.2.3 SELECTION AND VALIDATION OF MODELS

The most frequently used procedure of QSPR modeling involves a split of the initial dataset into two subsets: training and test sets. The models are built on the training set followed by "prediction" calculations for the test set. Some recommendations for selecting the compounds for the test set are given in numerous publications (see Refs. 32 and 33 and references therein). According to most of them, the following rules should be respected: (i) experimental methods for property determination in the training and test sets should be similar; (ii) the property values of the compounds in the test set should not exceed the property value in the training set by more than 10% and (iii) the distribution; of property values for the training and test sets should be similar to respect uniform sampling of the data. In fact, the validation of the model on only one test set does not guarantee its robustness because of possible bias of the training and test sets. In order to avoid any uncertainties related to the selection of a particular test set, a more severe n-fold cross-validation (n-fold CV) technique is recommended. In this procedure, the entire dataset is divided in n nonoverlapping pairs of training and test sets. Each training set covers $(n–1)/n$ of the dataset, while the related test set covers the remaining $1/n$. Thus, predictions could be made for all molecules of the initial dataset, as each of them belongs to one of the test sets.

Several statistical parameters are used to assess the quality of fitting of models at the training stage: squared correlation coefficient (R^2), standard deviation (s, only for the linear models), root-mean square error (RMSE), and Fischer criterion. The robustness of models can be estimated using a leave-one-out (LOO) cross-validation technique, in which the models are built on the subset of (N–1) compounds, where N is a size of the training set, followed by predictions for one remaining compound. Then, this procedure is repeated N times to "predict" all compounds in the training set, which allows one to calculate the squared LOO correlation coefficient (Q^2) and related s or RMSE (LOO) values. It should be noted that the LOO technique does not represent a real test of prediction ability of the models, because the descriptor selection is usually done before for the whole training set containing all N compounds. The real assessment of the quality of predictions can be done only by applying the model on the external test set(s). In this case, a coefficient of determination ($R^2_{abs} = 1–\Sigma(Y_{exp}–Y_{pred})^2/\Sigma(Y_{exp}–<Y>_{exp})^2$) and related RMSE ($RMSE_{abs} = (\Sigma(Y_{exp}–Y_{pred})^2/N)^{1/2}$) are calculated using predicted (Y_{pred}) and experimental (Y_{exp}) property values. They characterize the ability of the model to reproduce quantitatively the experimental data. Typically, RMSE values increase in the order RMSE (fitting) < RMSE (LOO) < RMSE (n-fold CV), as demonstrated in Figure 5.2. The reason is obvious: to calculate the RMSE (fitting), the program applies a QSPR model on the compounds used for the development of that model, whereas in other procedures the program at the model-building stage only partially (in LOO) or never (in n-fold CV) uses the information about compounds to be predicted.

Generally, a QSPR program generates many models, one or several of which are to be selected according to the above-mentioned statistical parameters obtained for the training stage. Instead of selecting only one model, some programs apply an Ensemble Modeling approach, which allows one to combine the information issuing from several individual models. For example, at the training stage, the ISIDA program
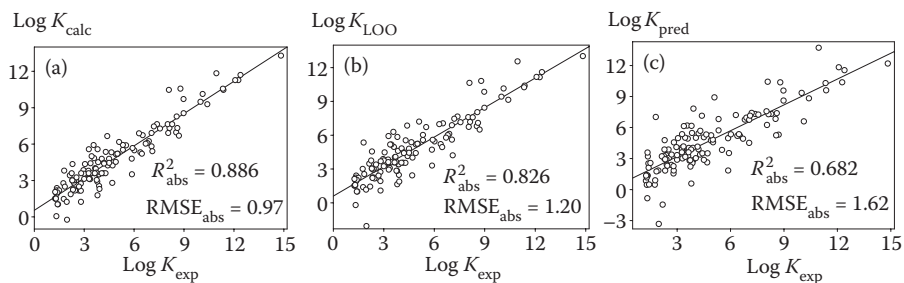
FIGURE 5.2 Modeling of stability constant (log K) of the (Sr^{2+})L complexes of organic ligands (L) in water using the MLR approach. The three plots show the linear correlation "calculated versus experimental log K" obtained for the entire set of 130 ligands at the fitting stage (a), in leave-one-out cross-validation procedure (b), and in external five-fold cross-validation (c).

selects M "best" models for which $Q^2 \geq Q^2_{lim}$, where Q^2_{lim} is a user-defined threshold. Thus, for each compound from the test set, the program applies a Consensus Model representing an arithmetic mean of predictions made with these M models; those leading to outlying values can be excluded according to Grubbs's statistics.[34,35] According to observations in Refs. 36–38, a consensus model smoothes the inaccuracies of individual models, thus, improving the quality of property predictions.

When applying a model, the program should check its AD, which measures the similarity between a test-set compound and the compounds from the training set. If the given test compound is identified as being outside AD, the predictions are not reliable. Several methods to establish AD have been reviewed by Tetko et al.[39]

5.3   DATABASES ON METAL COMPLEXATION AND EXTRACTION

5.3.1   COMPLEXATION DATABASES

The main source of experimental data on complexation of metals in aqueous and nonaqueous solutions is the IUPAC Stability Constants Database (SC-DB) found at http://www.acadsoft.co.uk/. The SC-Database is a compilation of literature data; it contains all significant stability constants and associated thermodynamic data published from 1887 to the present day, including all stability constants included in the book volumes published by the Chemical Society of London (now the Royal Society of Chemistry) and by IUPAC. The SC-Database is maintained by L.D. Pettit in cooperation with K.J. Powell and kept up-to-date through regular upgrades. The Version 4.66 has about 109,750 records for 9,426 ligands from about 22,900 references. The database uses EdChemS sketcher of 2D structures[20,40] with an implemented (sub) structural search option. There is a possibility to estimate a variation of stability constants as a function of temperature (T) and ionic strength (I) using van't Hoff and the Davies equations, respectively. The latter is extremely important for preparation of the data for structure-property modeling, because, ideally, stability constants should be measured under the same experimental conditions (T and I).

The NIST Critically Selected Stability Constants of Metal Complexes (NIST Standard Reference Database 46, http://www.nist.gov/srd/nist46.htm) provides

coverage of thermodynamic parameters for complexation in aqueous solutions with protons and various metal ions. Version 8.0 contains more than 50,000 equilibrium constants involving more than 6,200 ligands, as well as some data on the heats and entropies of reactions and entropies. Although presentation of 2D molecular structures of ligands are given, the structural (substructural) search option is not available.

The Joint Expert Speciation System (JESS), (http://jess.murdoch.edu.au/jess/jess_home.htm) contains 180,000 equilibrium constants for 72,000 reactions as well as 26,000 enthalpy values collected from 11,500 literature sources.

The THECOMAC database contains the stability constant, enthalpy, and entropy values for the complexations of the alkaline and alkaline earth metal cations with cyclic polyethers in water and organic solvents, and includes more than 3,500 records. Each record contains 22 textual and digital fields and 2D chemical structures of ligands. The database includes thermodynamic values for 330 cyclic polyethers containing oxygen coordination centers only.[41]

5.3.2 EXTRACTION DATABASES

The number of publications on solvent extraction is smaller than that for complexation reactions, but still it is rather large. Thus, a bibliographic search performed with SciFinder Scholar using "SOLVENT," "EXTRACTION," and "METAL" as keywords, resulted in about 13,000 references, some of them concerning several individual extraction systems. This information could probably be enriched by numerous publications in the Russian, Japanese, and Chinese scientific literature, which is not covered by "western" bibliographic databases (see Refs. 42–47). Much information is still buried in reports at various nuclear-energy research institutions. According to our estimates, about 25,000 papers on extraction chemistry (including Russian, Japanese, and Chinese bibliographic sources, industrial reports, etc.), reviewing 60,000–70,000 extraction systems have been published since 1970. Given also that there are many publications in which extraction information is reported but was not the main focus of the work, it is clear that a huge volume of data is very diversely spread and requires extreme diligence for its proper collation.

The first database project, SEPSYS,[48,49] was initiated in 1983 by W.J. McDowell. This is a bibliographic database containing about 4,500 records; its development has been stopped. Nevertheless, it was significant in providing an early means to precisely identify the literature dealing with the separation of a target species from a matrix of competing species, a capability that "standard" bibliographic databases cannot provide.

An INTERNET compatible database for solvent extraction of metal ions (SEDATA), developed by H. Watarai et al., contains about 9,600 equilibrium constants, including distribution constants, extraction constants, and adduct formation constants, for more than 1,400 ligands and 82 metal ions.[50] Raw data points of extraction curves are also incorporated to be reconstructed as a figure. However, SEDATA contains no fields for 2D chemical structures of extractants and allows one to perform a search using only eight fields (classification, metal, valence, reagent, solvent, title of the paper, author, and year).

Solvent eXtraction Database (SXD) software has been developed by A. Varnek et al.[51] Each record of SXD corresponds to one extraction equilibrium and contains 90 fields to store bibliographic information, system descriptions, chemical structures of extractants, and thermodynamic and kinetic data in textual, numerical, and graphical forms. A search can be performed by any field including 2D structure. SXD tools allow the user to compare plots from different records and to select a subset of data according to user-defined constraints (identical metal, content of aqueous or organic phases, etc.). This database, containing about 3,500 records, is available on the INTERNET (http://infochim.u-strasbg.fr/sxd).

As the thermodynamic parameters of complexation or extraction depend on many different factors (ligand, metal, solvent, counterion, pH, ionic strength, temperature, etc.), the descriptors used should describe all of them. However, in most of the cases, the models are developed on subsets of data measured for one particular metal in similar conditions. This allows one to simplify the modeling task and to link the property with only one factor—chemical structure of ligands. For many different metal ions suitable sized subsets of stability constants of their complexes with organic ligands in the given solvent, could be selected from a database or collected from the literature. As stability constants depend on ionic strength (I) and temperature (T), their original values should be recalculated for selected "standard" values of I and T. For the given equilibrium, a database may contain several experimental estimations of stability constants, and the choice of data for the modeling represents a real challenge (see critical surveys and evaluations of stability constants by the IUPAC Commission on Equilibrium Data[52–57]). For solvent extraction, very few datasets of reasonable size, that is, containing more than 20 data points measured exactly at the same conditions, are available. In this respect, the complexation databases provide more data for the modeling than the extraction databases.

5.4 QUANTITATIVE RELATIONSHIPS BETWEEN STRUCTURE AND METAL-BINDING AFFINITY

In this section, two types of structure–metal binding ability relationships will be described. The first one concerns empirical linear correlations between equilibrium constants of complexation or extraction and some descriptors. In most cases, these correlations are obtained for relatively small datasets (less than 20 molecules) without any validation. We do not intend to analyze them in detail; only their general characteristics will be reported. The second type of relationships were obtained in "regular" QSPR studies involving the selection of pertinent descriptors from their large initial pools, and the stage of the models, validation on external test set(s).

5.4.1 EMPIRICAL CORRELATIONS IN METAL COMPLEXATION AND EXTRACTION

5.4.1.1 Complexation

Empirical approaches to predict the stability constants of metal complexes in solution (mostly in water) are discussed in the book by Kumok[11] and in reviews by Hancock and Martell,[9] Dimmock et al.,[7] Hancock,[8] and Hay.[10] Generally, two types

of correlations are used: LFER and parametric equations. LFERs represent linear correlations between the $\log K_i$ of one group of reactions with the $\log K_j$ for a second group of reactions. They could be applied to assess the $\log K$ only for the ligands (metals) involved in correlations (*missed values*), whereas the parametric equations could be formally applied for any ligand (metal).

Several types of LFER have been observed for metal-ligand complexes.

1. For the series of ligands L^i, correlations between stabilities of the complexes of metal M^1 and that for reference cation (proton or metal M^2)

$$\log K(ML^i) = a \cdot pK_a(L^i) + b \tag{5.1}$$

$$\log K(M^1L^i) = a \cdot \log K(M^2L^i) + b \tag{5.2}$$

2. For the series of metals M^i, correlation between stabilities of the complexes of ligand L^1 and that for reference ligand L^2

$$\log K(M^iL^1) = a \cdot \log K(M^iL^2) + b \tag{5.3}$$

3. Correlations between stability constants $\log K(ML)$ of the complexes of multidentate ligands and a sum of $\log K(ML^i)$ of monodentate "ligands" obtained by splitting L into constituent fragments L^i. Thus, Hancock[8] suggested an additive scheme, linking the stability constants of metal complexes of aminocarboxylates with the stabilities of related NH_3 and CH_3COO^- complexes. Harris[58] extended this approach for more structurally diverse ligands containing amine, pyridyl, carboxylate, imidazolo, and thioether groups, forming five- or six-membered chelate rings.

Several types of parametric equations are known. Thus, stabilities $\log K(M^iL)$ of the complexes of a series of metals M^i with one ligand L correlate with the physical properties of the metal ion. A variety of functional dependencies have been observed with metal properties that include the charge, ionic radius, electronegativity, and ionization potential.[10] More complex equations (like Brown–Sylva–Ellis equations[59]) represent $\log K(ML)$ values as a function of metal and ligand parameters. Some equations (e.g., Misono[60] or Edwards[61] equations) are based on the Hard-Soft Acid-Base approach. Thus, the Edwards[61] equation,

$$\log(K(M^1L) / K(M^2L)) = \alpha E_n + \beta H \tag{5.4}$$

accounts for the softness (α and E_n) and hardness (β and H) parameters for the metal and ligand, respectively. Hancock et al.[9] have suggested a more extended equation,

$$\log K(ML) = E_A E_B + C_A C_B - D_A D_B \tag{5.5}$$

which takes into account not only the electrostatic (E) and covalent (C) contributions of acid A and base B in metal-ligand bonding, but also their steric hindrance (D).

An interesting way to take into account all coordinating centers has been suggested by Schneider et al.,[62] who used the electron-donor parameters (ED_i) for the donor atoms of macrocyclic ligands to correlate with the free energy of complexation (ΔG) of crown ethers and cryptands with alkali cations and with ammonium cation in methanol, water, or chloroform. The ED parameters for the functional groups have been calculated from the experimental free energies of 1:1 H-bond complexes.[63] Several reasonable linear correlations $\Delta G = a + b\Sigma ED_i$ (where i counts all electron-donor groups of the molecule) have been obtained only for subsets of ligands with a particular size of the macrocycle, but not for the whole set.

It should be noted that the above-mentioned LFER and parametric equations have been derived for a relatively small series of ligands and metals. Therefore, their application for prediction is limited to the class of metals or ligands used for fitting the empirical parameters of those equations. Nevertheless, they have contributed to the fundamental understanding of complexation phenomena, especially for the classes of ligands and metals studied.

The growing size of the complexation databases opens an opportunity to use empirical equations for predicting of the stability of metal complexes of a wide spectrum of ligands. Recently, a series of linear correlations has been developed for stability constants $\log K$ for the 1:1 complexes of 13 lanthanide cations M^{3+} with organic ligands in water. The set of experimental data retrieved from IUPAC SC-DB contained the stability constants for the 2,854 complexes of lanthanides with 450 ligands, including 50 macrocyclic (crown ethers and cryptands) ligands (Figure 5.7). Equation 5.2 has been applied to establish all possible linear correlations between the stability constants of two different lanthanide ions. It has been found that standard deviations (s) of those correlations vary as a function of the difference of ionic radii of the two metals (Figure 5.3). This allows one to assess $\log K$ with well-defined accuracy. Thus, from Figure 5.3 it follows that the
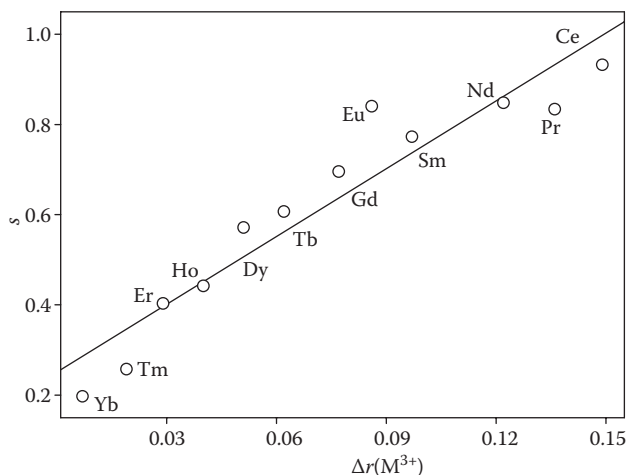
FIGURE 5.3   The 1:1 complexation of lanthanide ions (M^{3+}) with organic ligands in water: standard deviation (s) of Equation 5.2 as a function of the difference between ionic radii r (for CN=6) of the M^{3+}/Lu^{3+} pairs of lanthanides.

assessment of $\log K$ for the Lu complexes is the most accurate ($s = 0.2$) if one uses the correlation for Yb. However, if the data for a given ligand for the Yb-series are not available, one should use the correlations with other metals, starting with those corresponding to smaller values of s. Nevertheless, this approach is limited by the ligands involved in the correlations; the number of missed values is rather large. Thus, for the case of lanthanides, the number of all metal/ligand combinations ($13 \times 450 = 5,850$) is large compared to the number of experimental $\log K$ values (2,854) in the dataset.

5.4.1.2 Extraction

Most empirical correlations for the solvent extraction of metals have been reviewed by Rozen and Krupnov.[12] Due to the problem of availability of consistent datasets, most of them were developed for a small series of 3–20 data points for monodentate ligands. Some of these equations are similar to those obtained for the metal complexation. For instance, Rozen et al.[64] have observed correlations between $\log K_{ex}$ and pK_a (Equation 5.1) for the series of extractants for uranyl ion-bearing P=O, C=O, As=O, and N=O electron donor groups. Correlations between K_{ex} and group electronegativities or Taft parameters of substituents of the P=O group have been found for the extraction of actinides by some neutral phosphoryl-containing ligands.[12] However, the validity of this approach is limited because of the nonadditive effects of the substituents, as has been shown for the extraction of uranyl by a series of substituted ketones Alk_2CO, $AlkC(O)NAlk'_2$, and $(NAlk'_2)_2CO$. Therefore, Rozen[65] and Varnek[66] suggested the use of descriptors' characteristics derived for the whole molecule, such as atomic charges,[12,67] energies of 1s-orbitals of oxygen atoms,[12] electrostatic potential distributions,[66,67] chemical softness, and donor-acceptor interaction energies.[68] Rozen et al.[12] also suggested the correlation of $\log K_{ex}$ with interaction energies of the extractant with the model compound (H^+, Li^+) calculated by quantum-mechanics methods.

The influence of steric effects on the thermodynamic parameters of extraction has been discussed in numerous publications (see the review in Ref. 12 and references therein). For a small series of selected extractants, a decrease of $\log K_{ex}$ as a function of the length of alkyl substituents has been discovered.[69,70] However, in other cases, this dependence passes through a maximum or is not regular at all.[71] The point is that the increase in the volume and branching of the substituents leads to some changes of molecular properties: decrease of solubility in the aqueous phase, increase of steric hindrance upon the complexation, decrease of the extractant's aggregation, etc.[12] Some of these factors strengthen extraction, but others weaken it.

5.4.2 QSPR Modeling of Different Classes of Complexants and Extractants

Publications on QSPR modeling of metal complexation and extraction reviewed here are listed in Table 5.1. Some details of these studies are given below.

TABLE 5.1
QSPR Modeling of Metal/Ligand Complexation and Metal Ion Extraction

No.	Modeled Property	Metal Ion(s)	n_{tot}[a]	Ligands — Ligand Type(s)	Figure	Solvent(s) or Diluent	Machine-Learning Method[b]	Descriptors	n_{tr}/n_{test}[c]	Ref.
						Complexation				
1	Log K ΔH	Ca^{2+}	56	Organic acids, phosphates and phosphonates; aminocarboxylates, crown ethers, cryptands, phenols, podands, heterocyclic and aromatic compounds		H_2O	MLR	Molecular fragments, molecular and atomic properties, topological indices	48/7	72
2	Log K	Na^+, Ca^{2+}, Zn^{2+}	106	Crown ethers, cryptands, antibiotics, and spherands		17 pure, 3 mixed	MLR	Calculated by MM energy components, surface tension of solvent, solvation parameters	254/60[d]	73
3	Log K	Na^+	22	Spherands		$CDCl_3$ satur. with D_2O	MLR	See No. 3	e	73
4	Log K	Na^+ K^+ Cs^+	14 15 16	Crown ethers		MeOH	ANN	Number of aromatic rings and oxygen atoms, size of macrocycle	10/4 10/5 11/5	74

(Continued)

TABLE 5.1
(Continued)

No.	Modeled Property	Metal Ion(s)	n_{tot}[a]	Ligands Ligand Type(s)	Figure	Solvent(s) or Diluent	Machine-Learning Method[b]	Descriptors	n_{tr}/n_{test}[c]	Ref.
5	Log K	K^+	76	Phosphoryl-containing podands	5.6 (c)	THF:CHCl$_3$ (4:1 vol)	MLR, CM-MLR	SMF	71/5	25, 75
6	Log K	Na^+	61	Crown ethers	5.6 (a)	MeOH	MLR	SMF	56/5	75
7	Log K	Mg^{2+}, Ca^{2+}, Mn^{2+}, Fe^{2+}, Co^{2+}, Ni^{2+}, Cu^{2+}, Zn^{2+}, Cd^{2+}	17	Amino acids, adenosine, and its phosphate derivatives		H_2O	MLR	Topological	55/55[f]	76
8	Log K	Na^+, K^+, Cs^+	69, 123, 31	Crown ethers	5.6 (a)	MeOH	CM-MLR	SMF	60/9, 113/10[g,h], 28/3	25, 77
9	Log K	Gd^{3+}	28	Aminocarboxylates, aza-crown ethers	5.4	H_2O	MLR, ANN	Topological, quantum-chemical	20/8	78
10	Log K	Mg^{2+}, Ca^{2+}, Mn^{2+}, Fe^{2+}, Co^{2+}, Ni^{2+}, Cu^{2+}, Zn^{2+}, Cd^{2+}	25	Amino acids, adenosine and its phosphate derivatives, heterocyclic (aromatic) rings		H_2O	MLR	Topological	75/75[f]	79

#	Property	Metal ion	N	Compounds	Value	Medium	Methods	Descriptors	Validation	
11	Log K	Sr^{2+}	130	Organic acids, phosphates and phosphonates; amino acids, aminocarboxylates, (aza)crown ethers, phenols, heterocyclic and aromatic compounds	5.6 (b)	H_2O	CM-MLR	SMF	115/15[i]	38
12	Log K	14 lanthanides Ln^{3+}	63	Aminocarboxylates, aza-crown ethers	5.5	H_2O	MLR	*Metals*: atomic and physical properties, *ligands*: CODESSA descriptors	e	80
13	Log K	Ag^+ Eu^{3+}	161 241	Organic acids, amino acids, aminocarboxylates, (tio) crown ethers, (tio) cryptands, podands, phenols, heterocyclic and aromatic compounds, adenosine derivatives	5.7	H_2O	ASNN, SVM, *k*NN, MMLP, RBFNN, MLR, and CM-MLR	SMF, atom-type E-state indices, atom type E-state counts	Five-fold CV[j]	36
14	Log β_2	Ag^+ Eu^{3+}	112 81	See above no. 13 in this table	5.7	H_2O	See No. 14	See No. 14	Five-fold CV[j]	36
15	Log K	Ce^{3+} Eu^{3+} Tb^{3+} Lu^{3+}	198 239 186 189	See above no. 13 in this table	5.7	H_2O	CM-MLR, DC-MLR, ASNN, and SVM	SMF	Five-fold CV[j]	13

(Continued)

TABLE 5.1
(Continued)

No.	Modeled Property	Metal Ion(s)	n_{tot}[a]	Ligands Ligand Type(s)	Figure	Solvent(s) or Diluent	Machine-Learning Method[b]	Descriptors	n_{tr}/n_{test}[c]	Ref.
					Extraction					
16	$Log\ D$	UO_2^{2+}	22	Amides		Toluene	MLR	Sum of atomic charges, calculated by MM association energy	15/3	81
17	$Log\ K_{ex}$	UO_2^{2+}	12	Aryl diphosphonates		$CHCl_3$	MLR	SMF	e	75
18	$Log\ D$	UO_2^{2+}	22	Amides		Toluene	MLR	SMF	19/3	51
19	$Log\ D$	UO_2^{2+}	32	Phosphoryl-containing podands	5.6 (c)	$1,2\text{-}DCE^k$	MLR	SMF	29/3	51
20	$Log\ D$	Hg^{2+} Pt^{2+} In^{3+}	25 25 25	Phosphoryl-containing podands	5.6 (c)	$1,2\text{-}DCE^k$	MLR	SMF	22/3 22/3 22/3	25, 51
21	D_{Am}/D_{Eu}	Am^{3+} Eu^{3+}	47	Nitrogen-containing heterocycles	5.11	$1,1,2,2\text{-}TCE^l$	MLR	DRAGON descriptors	36/11	82
22	$Log\ D$	UO_2^{2+}	32	Phosphoryl-containing podands	5.6 (c)	$1,2\text{-}DCE^k$	CM-MLR, MLR	SMF, CODESSA descrs	$29/3^m$; *in silico:* 8^n	15
23	D_{Am}/D_{Eu}	Am^{3+} Eu^{3+}	46	Nitrogen-containing heterocycles	5.11	$1,1,2,2\text{-}TCE^l$	CM-MLR, MLR, RBFNN, and ASNN	SMF, CODESSA descriptors	36/10 Blind test: 1°	83

24	Log D	UO_2^{2+}	19	Amides	Toluene	CM-MLR, MLR, RBFNN, ASNN, and SVM	SMF, CODESSA descriptors	19/0; *in silico:* 21[n]	14
25	Log K_{ex}	Lanthanides Ln^{3+}	3	Alkyl phosphates	Toluene	LR	Ligand's strain energy	e	84, 85
26	Log K_{ex}	Lanthanides Ln^{3+}	6	Alkyl phosphates, calixarenes	Toluene	LR	Ligand's strain energy	e	86

[a] n_{tot} is the total number of ligands in the whole dataset.

[b] Machine-learning method: Multiple Linear Regression (MLR), combination the most robust models (consensus model (CM)) with Multiple Linear Regression (CM-MLR), Divide and Conquer (DC) approach in combination with Multiple Linear Regression (DC-MLR), Artificial Neural Networks (ANN), Associative Neural Networks (ASNN), Support Vector Machines (SVM), k-Nearest Neighbors (kNN), Maximal Margin Linear Programming (MMLP), Radial Basis Function Neural Network (RBFNN).

[c] n_{tr}/n_{test} is the number of compounds in the training/test set.

[d] Metal/ligand/solvent combinations.

[e] Models were not validated.

[f] Metal/ligand combinations.

[g] Four different combinations of training/test sets were used.

[h] Additional test set of 13 ethylene glycols and glymes was used.

[i] Three different combinations of training/test sets were used.

[j] Five-fold external cross-validation.

[k] 1,2-DCE is 1,2-dichloroethane.

[l] 1,1,2,2-TCE is 1,1,2,2-tetrachloroethane.

[m] Two different combinations of training/test sets were used.

[n] The number of newly designed ligands, then synthesized and tested experimentally.

[o] Additional validation has been performed on one new compound.

5.4.2.1 Complexation

Raevsky et al.[72] used molecular fragments as well as topological and physico-chemical ($\log P$, molecular refraction) descriptors to build QSPR models for stability constants and ΔH of complexation of 56 ligands with Ca^{2+} in water. The main idea was to split the initial dataset into clusters and to build the models on those clusters. Each test compound should first be attributed to "its" cluster, followed by applying the models developed for that cluster. Two different clustering techniques were used to obtain two to four clusters from the training set of 49 compounds. Validation calculations performed for $\log K$ on the remaining seven compounds led to relatively poor correlations between the predicted and experimental data. Thus, using the reported data,[72] we obtained a determination coefficient $R^2_{abs} = 0.4$.

The article by Shi et al.[73] was devoted to the modeling of stability constants of the 1:1 complexes in five different systems: (a) 314 metal ion-macrocycle-solvent (including three mixed solvents) combinations; (b) 88 ammonium ion-crown ether-solvent (including one mixed solvent) combinations; (c) 24 reactions of H^+ with crown ether in water, (d) 26 reactions of Na^+ with spherands in $CDCl_3$; (e) 78 reactions of ammonium with spherands in $CDCl_3$ combinations; and (f) 73 reactions of organic ligands with combinations of neutral guests in different solvents (including one mixed solvent). The main idea of this work was to build models on the descriptors associated with the mechanism of complexation. Thus, the free energy of complexation was considered as a sum of two terms corresponding, respectively, to the host-guest interactions in the gas phase and solvation of the formed complex. Molecular structures of free ligands and their complexes were modeled using the AMBER or MMP2 force fields. Molecular dynamics simulations were used to obtain the lowest energy conformers, followed by an energy minimization procedure to calculate their energies. Solvation processes were considered in the framework of continuum solvation models involving the energy of formation of the cavity in the solvent and solute-solvent interactions. Thus, the force-field energy components (bond stretch, angle bending, torsional van der Waals, electrostatic, and hydrogen-bonding energy) for the lowest energy conformers, internal strain energy, and its components were calculated as the difference of energies of complexed and free ligands, and Mulliken–Jaffe electronegativities were used as descriptors of the gas-phase free-energy term, whereas the surface tension of the solvents, charges, and ionic radii of metal cations, dipole moments of the solvent and ligand molecules, as well as the effective radii of ligands (found in force-field calculations) were used to describe the solvation term. The linear regression models were built on a training set containing 80% of the complexation reactions from the initial dataset, followed by their validation on the test set containing the remaining 20% of reactions. A forward stepwise variables selection procedure was used to select the most pertinent variables leading to the models containing from 6 to 12 descriptors. Generally, these models displayed reasonable prediction ability, although for some systems the number of outliers moved up to 25% of the test-set reactions.

The neural network approach has been successfully used by Gakh et al.[74] to model the stability constants of Na^+, K^+, and Cs^+ complexes with some unsubstituted

regular crown ethers and their benzo and dibenzo derivates in methanol. A three-layer architecture, input layer–hidden layer–output layer, was used. The number of aromatic rings, the size of the macrocycle, and the number of oxygen atoms were used as input vectors in the training sets containing 14–16 ligands. The average error was about 0.3 $\log K$ units for the validation sets containing four to five molecules. Models developed from this have been used to predict the binding properties of some hypothetical crown ethers. Thus, the calculated values of $\log K$ as a function of the number of (-CH$_2$CH$_2$O-) and (-CH$_2$CH$_2$O-+-C$_6$H$_4$O-) units have been plotted. The observed trend corresponds well with available experimental data and molecular mechanics calculations.

Toropov et al.[76,79] developed QSPR models for the complexes of nine alkaline-earth and transition metals with some amino acids, phosphate derivatives of adenosine, and heterocyclic compounds based on topological indices. Although the numbers of examples in the datasets were big enough, 110[76] and 150,[79] they involved only a few different ligands (17 and 25 molecules, respectively). The validation calculations were performed on the test sets containing the same ligands as in the training sets, which could explain the well observed performance of the predictions.[76,79]

Multiple regression analysis and neural networks were applied by Qi et al.[78] to build models for stability constants of Gd^{3+} with cyclic and acyclic aminocarboxylates and aza-crowns (Figure 5.4). The best MLR model obtained on the whole set of 28 ligands involved three quantum-chemical and two topological descriptors. Then, those five descriptors were used to train a backpropagation neural network on the training set of 20 ligands. Validation calculations performed on the test set of eight ligands confirmed the reasonable prediction performance of the model.

Svetlitski et al.[80] have developed QSPR models for the stability constants of the 1:1 complexes between 63 organic ligands (Figure 5.5) and 14 lanthanides. The ligand dataset included mostly aminocarboxylates and aza-crowns. Calculations were performed using the CODESSA PRO program, which generates up to 900 theoretical descriptors and applies a variable selection procedure to build linear regressions. Two

R = Me, Ar, CH$_2$C(O)NHMe, CH$_2$C(O)NHCH$_2$CH$_2$OMe, CH$_2$C(O)NMeCH$_2$CH$_2$OMe

R = CH$_2$CO, CH$_2$COOH Y = Alk, AlkOAlkOAlk

R = H, CH$_2$COOH, CH$_2$P(O)(OH)$_2$, CH$_2$C(OH)Me X = N and O (no R) in different combinations; n = 1–4
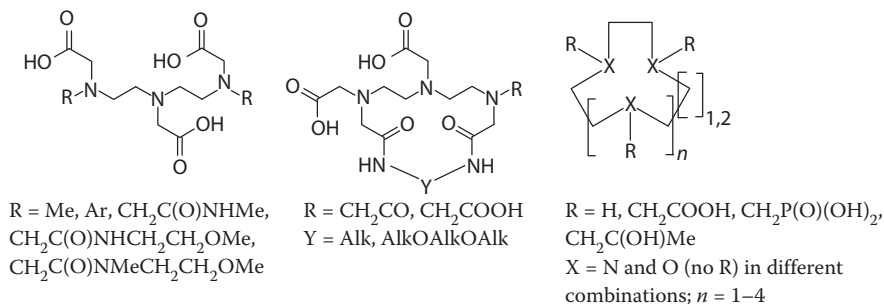
FIGURE 5.4 Gd^{3+} binders. (From Qi, Y.-H.; Zhang, Q.-Y.; Xu, L. *J. Chem. Inf. Comput. Sci.* 42 (6), 1471–1475, 2002. With permission.)

$R_1–R_4 = H, CH_2COOH, CH_2CH_2COOH, CH(COOH)_2, OH, CH_2P(O)(OH)_2$
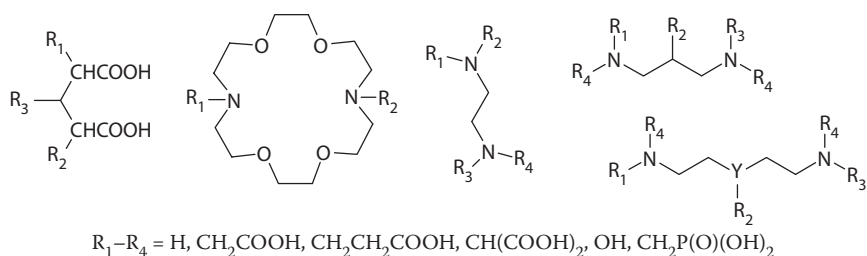
FIGURE 5.5   Lanthanide binders. (From Svetlitski, R.; Lomaka, A.; Karelson, M., *Sep. Sci. Technol.* 41 (1), 197–216, 2006. With permission.)

types of models were developed: "one metal and various ligands" (**I**) and "one ligand and various metals" (**II**). All 14 models **I** involved four theoretical descriptors of different types: topological indices (e.g., average information content); geometrical parameters (shadow plane YZ); constitutional descriptors (number of double bonds, relative number of N atoms); electronic properties (energies of LUMO and HOMO); hydrogen-bonding descriptors (H-donor FCPSA); partial surface area descriptors (square root of charged surface area for atom C, etc.); and binding interactions (maximal Coulombic interactions for bonds C–C and C–H, etc.). Each model was built on a particular combination of those descriptors, which always varies from one model to another one. Each of the 63 models **II** (one per ligand) was built on two or three descriptors selected by the program from the initial pool of 23 physical properties of lanthanides (ionization potentials, atomic radius, density, melting point, etc.). All these models are different with respect to the types of descriptors involved. A reasonable quality of linear correlations has been achieved: 47 of the 63 models **II** for ligands $R^2 > 0.90$, and only six had $R^2 < 0.80$, whereas for all 14 models **I** for metals resulted in $R^2 > 0.84$. However, these models were not validated on the independent test sets. The authors[80] tried to assess "missed" log K values for some unknown complexes involving the 63 ligands studied, using both models **I** and **II**. However, the relatively small correlation coefficient $R^2 = 0.588$ observed for the linear correlation log K (models **I**) versus log K (models **II**) revealed a weak convergence of these approaches.

Multilinear regression analysis using SMF descriptors has been applied to model stability constants of the 1:1 complexes of alkali and alkaline-earth cations. Thus, QSPR models have been obtained for the sets of 69 (Na^+), 123 (K^+), and 31 (Cs^+) complexes of crown ethers; 13 (K^+) complexes of ethylene glycols and glymes (Figure 5.6a) in methanol;[25,75,77] complexes of Sr^{2+} with a diverse set of 130 organic ligands (Figure 5.6b) in water;[38] and complexes of K^+ with 76 phosphoryl-containing podands (Figure 5.6c) in the mixed solvent THF:CHCl$_3$ (4:1 v/v).[25,75] The RMSE of predictions varied from 0.3 (for alkali cations) to 0.9 log K units (for Sr^{2+}). The models for strontium complexation have been used for screening of a combinatorial library of virtual ligands generated with ISIDA. Some hypothetical efficient Sr^{2+} binders were suggested.[38]

The efficiency of several popular machine-learning methods ANN, SVM, *k*NN, Maximal Margin Linear Programming, RBFNN, and MLR, to build predictive

(a)

R = H, Alk,
(OAlk)$_n$, AlkOH,
CH$_2$NHAlk, Ar,
CH$_2$OAr, ArOH
X = H, Alk,
=O (no R)
n = 0–5, 7, 8

R, X = H, Alk
n = 0–3
m = 1–3

R = H, Alk,
Ph, (OAlk)$_n$
X = H, Me
n = 1–3

R = H, Alk
n = 1, 2

n = 0–2

n = 0, 1
m = 1, 2

n = 4–7

n = 3, 4

R = Me, Et; n = 2–4

n = 0, 1; R = H, CH$_2$CH$_2$OH

(b)

R—P—OH
O
OH

R = Alk, OAlk, OAr,
AlkOH, AlkNR$_2$

OH   OH
O   O
R

R = Alk, Alk(OR)$_n$Alk,
AlkNH$_2$, AlkOAlk,
Alk(COOH)$_n$Alk,
Alk(NR)$_n$Alk(COOH)$_m$

O   O
OH—P—R—P—OH
OH   OH

R = Alk, AlkOH,
OAr, Alk(NR)$_n$Alk

O   O
OH—P—O—P—OH
R   OH

R = Alk, OAlk, OAr

R$_2$—N
R$_1$
R$_3$

R$_1$, R$_2$, R$_3$ = H, Alk,
Ar(OH)$_n$,
AlkP(O)(OH)$_2$,
Alk(COOH)$_n$, AlkNR$_2$

R$_1$ R$_1$
N—X—N
R$_2$ R$_2$

X = Alk, (OAlk)$_n$, Ar,
Alk(N(CH$_2$COOH)$_2$)
R$_1$, R$_2$ = H, AlkOH,
Alk(COOH)$_n$,
AlkP(O)(OH)$_2$

R$_2$ R$_1$
N   N
N   N
R$_3$ R$_4$

R$_1$ – R$_4$ = H, CH$_2$P(O)(OH)$_2$,
CH$_2$COOH, AlkOH, Alk, AlkOMe

R$_1$
O   N
N   N
R$_1$ R$_2$

O   O
R—X   X—R
O

n

X = O (no R), N
R = CH$_2$COOH,
AlkOH, AlkOAlk,
CH$_2$P(O)(OH)$_2$
n = 0–2

R
O   X
R—N   N—R
X   O
R'

X = O (no R), N
R = H, CH(COOH)$_2$,
AlkOMe, AlkOH,
CH$_2$P(O)(OH)(OR)

(c)

O   O
R—P—X—P—R
R   R

O
Ph—P—X—O
Ph

O
Y—P—R
R

O
R—P—X
R

O
Y   X—P—R
R

O
O=P
O   X—P—Ph
Ph
3

R = OMe, OEt, Bu, OBu, Ph; X, Y = (CH$_2$)k, (OCH$_2$CH$_2$)$_n$, (CH$_2$)$_k$ C$_6$H$_4$(OCH$_2$CH$_2$)$_n$

FIGURE 5.6 (a) Typical ligands used for log K modeling for the complexation of alkali cations in methanol,[25,75,77] (b) Sr^{2+} cations in water,[38] (c) and K$^+$ cations in the mixed solvent THF:CHCl$_3$ (4:1 v/v).[25,75]

QSPR models for stability constants (log K) for the 1:1 (M:L) and log β_2 for the 1:2 complexes of metal cations Ag$^+$ and Eu^{3+} were compared by Tetko et al.[36] The calculations were performed on diverse sets of organic molecules, including 161 (Ag$^+$) and 241 (Eu^{3+}) ligands for log K and 112 (Ag$^+$) and 81 (Eu^{3+}) ligands for log β_2 (Figure 5.7) in water at 298 K and ionic strength 0.1 M. The methods were tested on three types of descriptors: molecular descriptors including

$$R_2-N(R_1)-R_3$$

$R_1 - R_3 =$ H, CH$_2$COOH, C$_n$H$_{2n-1}$(COOH)$_2$, AlkP(O)(OH)$_2$, C$_n$H$_{2n}$S(O)$_2$OH, AlkOH, ArOH, AlkN(R)(CH$_2$COOH)

$$R_1-N(R_2)-N(R_1)-X-R_2$$

X = C$_n$H$_{2n}$', c-C$_n$H$_{2n-2}$, C$_n$H$_{2n}$OH, Ar, (C$_n$H$_{2n}$O)$_m$', C$_n$H$_{2n}$(NCH$_2$COOH)$_m$' AlkP(O)(OH)Alk R$_1$, R$_2$ = H, CH$_2$COOH, C$_n$H$_{2n}$(COOH)$_2$, ArS(O)$_2$OH, C$_n$H$_{2n}$OCmH$_{2m}$', C$_n$H$_{2n}$(OH), AlkP(O)(OH)$_2$, C$_n$H$_{2n}$NXCmH$_{2m}$', CH$_2$C(O)NHR', Ar, ArOH

$$\left[R-C(=O)-OH \right]_m$$

R = Alk, c-Alk, Ar, AlkNH$_2$, Alk(OH)$_{n'}$, AlkSH, ArOAlk, Ar(OH)$_{n'}$, Alken
m = 1–6

$$\left[R-OH \right]_n$$

R = Ar, n = 1–3

$$HO-C(=O)-R-C(=O)-OH$$

R = Alk, Ar, C$_n$H$_{2n}$OC$_m$H$_{2m}$', C$_n$H$_{2n-1}$OH, C$_n$H$_{2n}$NXC$_m$H$_{2m}$'

$$HO-P(=O)(OH)-R-P(=O)(OH)-OH$$

R = Alk, C$_n$H$_{2n}$NXC$_n$H$_{2n}$

$$R-P(=O)(OH)-R-OH$$

R = Alk, OAlk, OAlk(OH)$_{n'}$, Ar, OAr

$$\left[R-S(=O)_2-OH \right]_n$$

R = Alk, Ar, ArOH, Ar(OH)$_p$(COOH)$_m$(NH2)$_k$
n = 1–3

n = 0, 1

k, m = 1, 2

R = Ar, n = 1–3

R, R$_1$–R$_4$ = H, CH$_2$COOH, CHMeCOOH, CH$_2$P(O)(OH)$_2$, CH$_2$P(O)(OH)Et; AlkOH
X = O (no Ri), N; n = 0–3

FIGURE 5.7 Metal binders studied.[13,36]

E-state indices, counts of atoms determined for E-state atom types, and fragment (SMF) descriptors. Individual structure-complexation property models obtained with nonlinear methods demonstrated a significantly better performance than the models built using MLR. However, the consensus models calculated by averaging several MLR models display a prediction performance as good as the most efficient nonlinear techniques. The use of SMF descriptors and E-state counts provided similar results, whereas E-state indices led to less significant models. For the best models, the *RMSE* of the $\log K$ predictions is 1.3–1.6 for Ag^+ and 1.5–1.8 for Eu^{3+}.

The accuracy of $\log K$ predictions for the complexation of lanthanide cations M^{3+} in water at 298 K and ionic strength 0.1 M as a function of the metal and machine-learning method has been assessed.[13] The 5-fold validation calculations were performed on diverse sets of organic ligands containing from 157 (Tm^{3+}) to 308 (Gd^{3+}) compounds. It has been shown that for a given metal, a difference between $RMSE_{abs}$ values obtained with different methods doesn't exceed 0.2–0.5 log K units (Figure 5.8). The overall accuracy of predictions is 2–2.5 log K units obtained for the range of variations of $\log K$ from 0.2 to 26. It should be noted that the $RMSE_{abs}$ for consensus models obtained at the fitting stage is rather small ($RMSE_{abs} \cong 1$ log K unit). This value corresponds to the correlation between log K and selected descriptors and estimates the quality of the fitting procedure rather than the real predictive performance of the model ($RMSE_{abs} \cong 2$–2.5).

An attempt to build QSPR models for large structurally diverse sets of crown ethers and to extract the information hidden in the experimental data about the macrocyclic effect (ME) was made by Varnek and Solov'ev et al.[25,77] using an ensemble modeling approach and SMF descriptors. The calculations were performed on
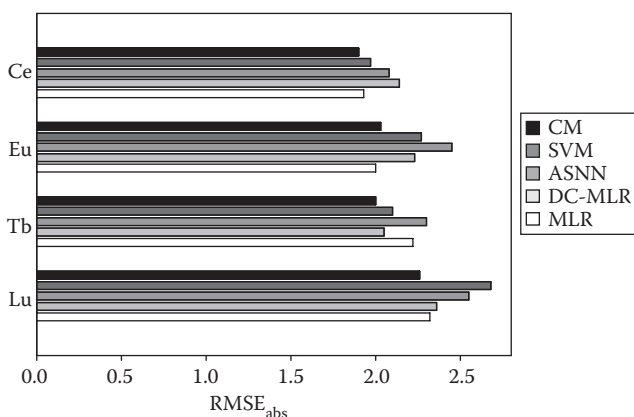
FIGURE 5.8   QSPR modeling of log K of Ce^{3+} (large size), Eu^{3+}, Tb^{3+} (middle size), and Lu^{3+} (small size) cations with organic ligands in water using linear (MLR, DC-MLR) and nonlinear (ASNN and SVM) machine-learning techniques.[13] Root-mean square error (RMSE) of predictions was obtained with the Five-fold cross-validation procedure. A consensus model was calculated for each compound as an arithmetic average of predictions obtained with all of the above-mentioned methods.
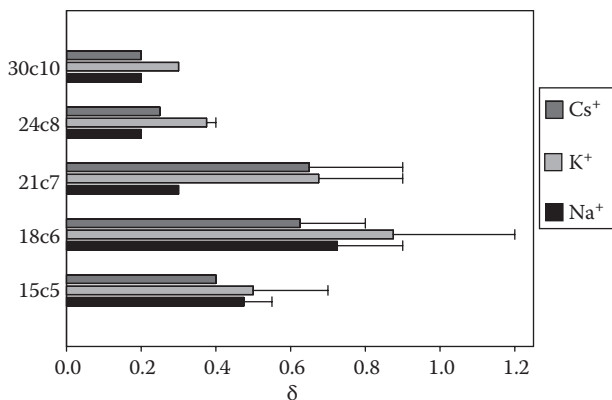
FIGURE 5.9 The macrocyclic effect contribution of stabilities of complexes (δ = ME/log K) for different macrocyclic scaffolds for the Na$^+$ (■), K$^+$ (■), and Cs$^+$ (■) crown ether complexes, respectively.[77,25] Error bars show variation of δ for a given type of ligand.

experimental stability constants for Na$^+$, K$^+$, and Cs$^+$ complexes in methanol, from which 10%–15% of the compounds were assigned to the test sets. The studied ligands included "regular" crown ethers with different cavity sizes (-CH$_2$-CH$_2$-O-)$_n$ (n = 4–12); their benzo, dibenzo, cyclohexyl, dicyclohexyl, and neutral lariat derivatives; and several "nonregular" crown ethers (Figure 5.6a). The main goal of this work was to estimate a ME[87] representing a difference between the stability constants of the complexes of a crown ether and its acyclic analog. In such a way, the ME has been estimated in the literature only for a few crown ethers; no conclusions concerning the ME for most substituted crown ethers were drawn because of a lack of experimental data for the corresponding acyclic ligands. The consensus model with reasonable statistical parameters ($Q^2 > 0.8$, R^2 (test) > 0.9, s (test) < 0.2) was obtained for the multilinear regression log $K = a_o + \Sigma a_i N_i + ME_j$, where a_i are fragment contributions, N_i is the number fragments of i type, and ME_j is a descriptor accounting for the ME for a macrocyclic scaffold of j type. Thus, structure-property modeling led to a quantitative assessment of the ME for a diverse set of crown ethers (Figure 5.9), without any information on the stability constants for the corresponding acyclic analogs. Moreover, the latter could be directly predicted with reasonable accuracy (Figure 5.10) from the above equation, putting ME = 0. So, QSPR models developed for one class of metal binders were successfully used to predict the properties of another class.

5.4.2.2 Extraction

There are very few publications devoted to regular QSPR studies in solvent extractions.

Rabbe et al.[81] have built QSPR models on a dataset of 19 alkyl- and phenyl-substituted monoamides R$_1$C(O)NR$_2$R$_3$ (R$_1$=H, Alk, R$_2$, R$_3$=Alk, Ar). A linear correlation between uranyl distribution ratio (log D) values and two descriptors, one of which
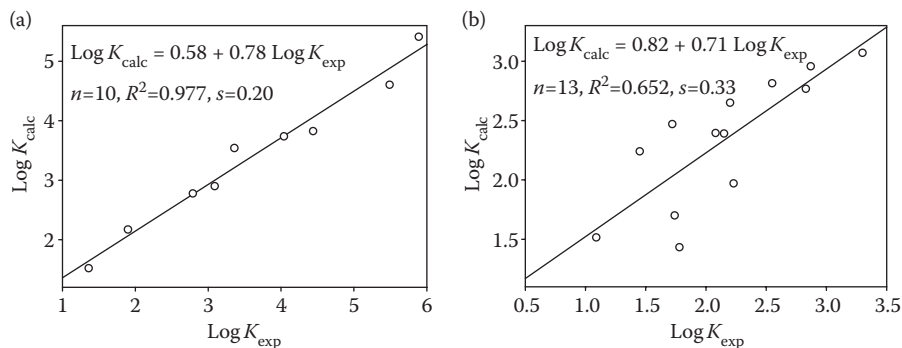
FIGURE 5.10 Assessment of stability constant (log K) values of the complexes of crown ethers and their acyclic analogs with K^+ in methanol.[25, 77] Linear correlations between predicted and experimental log K values for the test set (a) of crown ethers and for the set of acyclic ligands (b) in Figure 5.6a. As QSPR models were built on the training set containing exclusively crown ethers, it is not surprising that predictions for the test set (a) are more reliable.

was derived from quantum mechanics calculations (the sum of point charges at C, N, O, and C_α atoms) and another one (association energy) from molecular mechanics calculations, has been established. Validation of the model developed was performed on three test compounds whose binding affinities varied in a very narrow range, log $D = 0.62–0.71$.

For three dialkyl-hydrogen phosphate ligands, Comba et al.[84] have derived a relationship linking the differences between the complexation strain energies of the lanthanide cation M and La^{3+} with their extraction constants K_{ex}: $\Delta U_M - \Delta U_{La} = \alpha \log(K_{ex,M}/K_{ex,La})$. For a given M, its complexation strain energy was calculated with the MOMEC force field[88] as a difference of strain energy of the 1:1 ligand/M complex and that of free ligand plus an unbound M complex with nine water molecules. Later on, this approach was validated by Yoshizuka et al.,[86] who found the same relationship as in Ref. 84 for small dataset, including four dialkyl-hydrogen phosphate ligands and two calixarene acetic acid derivatives. It should be noted that Hay et al., for the complexation of 18-crown-6 and its nine derivatives with K^+ in methanol (log K)[89] as well as for a synergistic adduct formation constant for Sr^{2+} and Ba^{2+} extraction by dialkylphosphoric acids and different stereoisomers of dicyclohexyl-18-crown-6 (log K_s),[90,91] found a linear correlation between macrocyclic ligand strain energies and log K and log K_s, respectively.

A number of publications by Varnek and Solov'ev, et al.[14,15,25,51,75,83] were devoted to QSPR modeling based on the SMF descriptors implemented in TRAIL and then in ISIDA programs. First, these descriptors were used to model extraction constants for the uranyl cation extracted by 12 diphosphoryl-containing ligands ($R_2P(O)CH_2P(O)R_2$, R = Ph, 3-XC_6H_4, 4-XC_6H_4, X = Me, Cl, Br) from water to chloroform.[75] As the total number of molecules was not large enough, the authors were unable to select molecules for the validation set. The modeling

R, R$_1$ = H, Alk
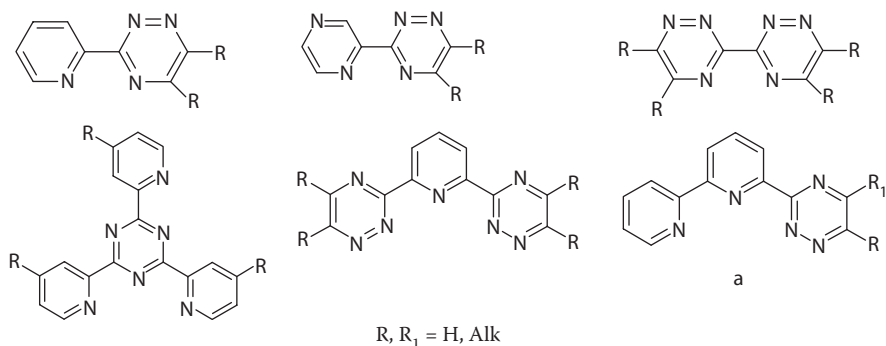
FIGURE 5.11   Polyazaheterocyclic ligands for Am and Eu separation.[82,83]

of distribution ratios (log D) of Hg, Pt, or In extracted by phosphoryl-containing podands (Figure 5.6c) has been reported.[51] The models were built on the training sets of 22 compounds following their validation on the test sets of three compounds.

QSPR modeling of the separation factor (SF) (the ratio D_{Am}/D_{Eu} of the distribution ratios for Am^{3+} and Eu^{3+}) for a set of 47 polyazaheterocyclic ligands (Figure 5.11) was the subject of two publications. First, Drew et al.[82] obtained linear models based on topological descriptors weighted by some atomic properties (Sanderson electronegativity, polarizibility, etc.). The models were built on a subsets including only bidentate or tridentate ligands as well as on a training set containing both types of and of ligands. Later on, Varnek et al.[83] used substructural fragment descriptors and both linear (MLR) and nonlinear (neural networks, support vector machine) methods implemented in the ISIDA program to build models on two different training sets. All models developed[82,83] showed good performance in the predictive calculations on a selected test set of 10 compounds. However, a real challenge for those models has become a prediction of the SF for a new polyazaheterocyclic ligand (structure a, R$_1$ = t-Bu, R = H in Figure 5.11) synthesized at the University of Reading in the framework of the EUROPART project and tested experimentally at CEA Marcoule when the modeling work had been finished. The calculations show that only models based on ISIDA fragment descriptors lead to reasonable estimations of log SF = 1.07–1.46 compared to the experiment (log SF = 1.0), whereas the models from Ref. 82 lead to a broad range of predicted log SF = 0.75–5.13 for this compound.

5.4.3   SOFTWARE FOR THE PREDICTION OF STABILITY CONSTANTS

Information about three programs able to predict the stability constants of metal complexes has been reported in the literature.

The LOGKEST program by Hancock[8] assesses the stability constants of the 1:1 complexes of 75 metal ions in aqueous solutions with several types of organic ligands. LOGKEST makes calculations in three stages: (i) for monodentate ligands, Equation

5.5 is used to predict $\log K$; (ii) for n-dentate polyamines forming with metal five-membered chelate rings, $\log K$ is proportional to the stability constant ($\log \beta_n$) of 1:n (M:L) complex with NH_3:$\log K$(polyamine) = $1.152 \log \beta_n + (n-1)\log 55.5$; and (iii) for more complex systems, some empirical corrections related to chelate ring size, bulk alkyl substituents, groups bearing neutral oxygen donors, and macrocyclic rings are made.

The "Stability Constant Estimator" by Hay et al.[10] for 1:1 complexes in water applies empirical correlations 1–3, equations by Hancock[8] and by Brown–Sylva–Ellis[59] as well as correlations with some physical properties of metals. This program includes 88 ligands and 74 metal ions. The correlations were trained on 1,431 stability constants.

The COmplexation of METals (COMET) program[13] applies MLR, ASNN, and SVM models developed by the ISIDA package.[20] Formally, these models could be applied for any query ligand. However, a given model is not applied if the query ligand is too different from the compounds used for the development of the models and, therefore, is considered to be outside of the model's AD. The program outputs results of predictions obtained with both the individual and consensus models. The current version of COMET performs calculations for stability of the 1:1 complexes of alkaline-earth and lanthanides cations in water at 298 K and ionic strength 0.1 M. The models were trained on 3,340 complexation reactions involving more than 600 ligands. The models for the 1:1 and 1:2 M:L complexes for other metals in water and in some nonaqueous solvents are in preparation. Potentially, QSPR models linking thermodynamics and kinetic characteristics for solvent extraction could also be included in COMET.

5.5   *IN SILICO* DESIGN OF NEW EXTRACTANTS

Theoretical ("*in silico*") design of compounds possessing the desired properties is an ultimate objective of modeling. In chemoinformatics, it involves several stages, shown in Figure 5.12. The sets of carefully selected experimental data (1) are used
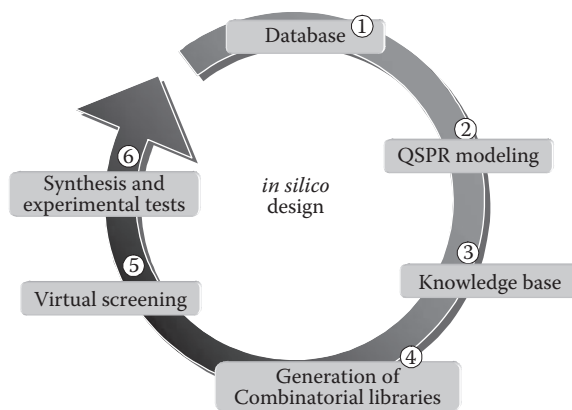
FIGURE 5.12   Workflow for *in silico* design of new metal binders.

for obtaining and validating QSPR models (2), which are then stored in the knowledge base (3). These models can be applied to virtual screenings (5) of databases containing either real or virtual structures. Selected hits can be synthesized and experimentally tested (6), in turn providing the database with new information. As a rule, a database of virtual structures represents a combinatorial library (4) generated by uniting different combinations of selected molecular fragments.[14,15] For example, in ISIDA, combinatorial libraries are generated from the Markush structures,[15,38,92,93] representing a user-defined molecular scaffold with n substituents R_i. If the list for each R_i contains n_i candidates, the total number of generated structures is $N = \prod_{i=1}^{n} n_i$. Potential substituents R_i could be rationally chosen using information about descriptors involved in QSPR models, thus enriching the virtual library with potentially active compounds, on the one hand, and decreasing its size, on the other hand.[14,15]

In this section, we demonstrate the performance of this approach to generate "*in silico*" novel extractants belonging to two families: monoamides[14] and phosphoryl-containing podands.[15] Most of the calculations were performed with the ISIDA program.[20] In order to validate the theoretical predictions, a synthesis of suggested molecules and corresponding extraction experiments was performed after the calculations had been completed.

5.5.1 MONOAMIDES

Alkyl-substituted monoamides are known as extractants for the uranyl cation and they could potentially be considered as alternatives to organophosphorus compounds in nuclear fuel reprocessing. In toluene, the uranyl cation forms complexes with two monoamide molecules. These relatively simple molecules were selected for computer-aided design,[14] taking into account a lot of synthetic and experimental work that must be done to prove the modeling predictions.

Structure-property models were trained on a set of 19 alkyl-substituted monoamides for which the distribution ratio of uranyl nitrate extracted from water to toluene (D) was reported by Siddall[94] and by Rabbe et al.[81] In the modeling with the ISIDA program, fragment descriptors (atom/bond sequences or augmented atoms) were used together with several different machine-learning techniques: MLR, kNN, RBFNN, ASNN, and SVM. Some models involving physicochemical descriptors were obtained with the CODESSA PRO program. The virtual combinatorial library containing about 10,500 alkyl-substituted monoamides was generated with ISIDA by systematically attaching different alkyl substituents to the C and N atoms of the monoamide scaffold.

A screening of the virtual combinatorial library was performed in several steps. As potential extractants must be insoluble in the water phase, the ISIDA-Log S module incorporating QSPR models for aqueous solubilities (log S)[95] has been used for filtering the library. Thus, the compounds for which log $S \le -3$ were considered insoluble in water; other compounds were excluded. A subset containing 9,306 potentially insoluble molecules has been screened using the "structure-log D" models. The main goal of screening was the selection of potentially efficient extractants. However, in
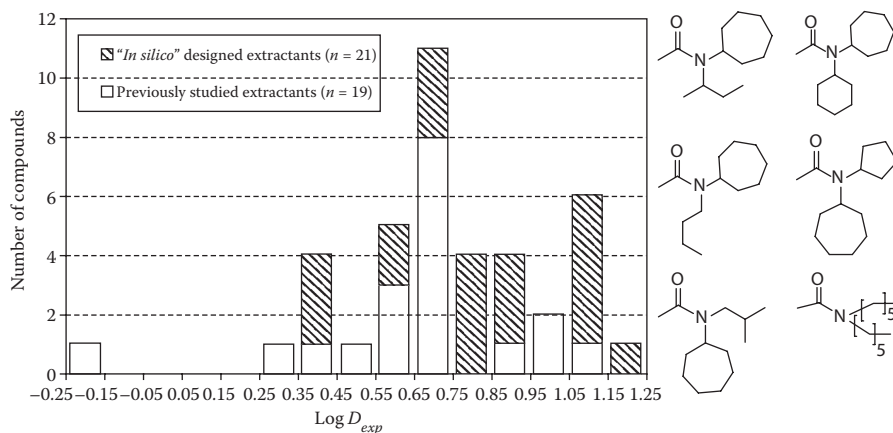
FIGURE 5.13 Experimental distribution ratio of UO_2^{2+} for the initial set of 19 amides (blank bars) and for 21 newly designed amides (filled bars). Structures on the right correspond to the most efficient new extractant ($\log D > 1$). (From Varnek, A.; Fouches, D.; Kireeva, N.; Klimchuk, O.; Marcon, G.; Tsivadze, A.; Solov'ev, V. *Radiochimica Acta* 2008, 96(8), 505–511. With permission.)

order to assess the performance of a theoretical approach to reproduce the whole range of $\log D$ variations, both strong and weak uranyl binders were selected as hits. The screening and hits selection was performed using the ISIDA consensus model involving more than 200 individual linear models. More time-consuming calculations involving the ASNN, RBFNN, SVM, and CODESSA PRO models were applied only for those selected hits. The compounds with problematic synthetic feasibilities were excluded from the hits list. The remaining compounds were recommended to experimentalists.

A distribution of experimental values of $\log D$ for the datasets of initial and novel compounds is given in Figure 5.13. One can see that the population of efficient extractants is much higher among novel compounds than that for previously studied molecules. Thus, the number of molecules with $\log D > 0.9$ is four for the initial set and nine for the new set of monoamides. One of the novel molecules displays a slightly larger affinity for uranyl than previously known extractants. Figure 5.14 demonstrates a prediction performance of structure-property models for 21 novel extractants: a reasonable linear correlation $\log D_{pred}$ versus $\log D_{exp}$ has been observed ($R_{rel}^2 = 0.675$, $R_{abs}^2 = 0.573$, $RMSE_{abs} = 0.16$).

5.5.2 PHOSPHORYL-CONTAINING PODANDS

Phosphoryl-containing podands are acyclic molecules with polyether spacer(s) linking two (in monopodands), three (in dipodands and tripodands), or four (in tripodands) terminal phosphine oxide groups (Figure 5.6c). Variations of the lengths of the spacers, of the molecular topology, and of the substituents at the phosphorus
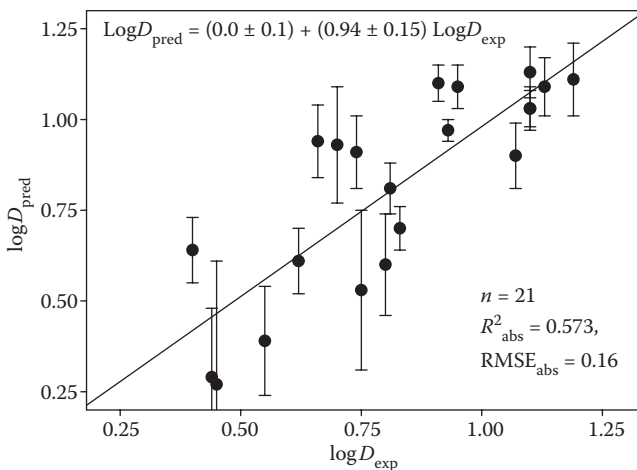
FIGURE 5.14 Experimental versus predicted log D values for 21 designed monoamides.[14]

atoms may lead to desirable complexation or extraction properties of podands for selected metal cations. In particular, these molecules extract the uranyl cation by forming 1:1 complexes[96] whose structures have not been studied so far. Analysis of the data from the SXD[51] shows that the set of distribution ratios (log D) for uranyl extraction in 1,2-dichloroethane for 32 podands[96] is one of the largest available in the literature datasets, where extraction properties of the compounds were studied strictly under the same conditions.

Two different approaches were used[15] for a QSPR modeling of log D: one based on classical structural and physicochemical descriptors (implemented in the CODESSA PRO program) and another based on fragmental descriptors (implemented in the ISIDA program). Three statistically significant models obtained with ISIDA involved as descriptors either sequences of atoms and bonds, or atoms with their close environment (augmented atoms). The best models from CODESSA PRO included its own molecular descriptors as well as fragmental descriptors obtained with ISIDA. At the second step, a virtual combinatorial library of 2,024 podands was generated for the Markush structure $R_1R_2R_3P{=}O$ for which a set of "optimal" substituents R_1, R_2, and R_3 was prepared using fragment contributions a_i calculated by ISIDA for the three best models obtained at the training stage. The activity of each compound in the combinatorial library was evaluated by an ISIDA consensus model. Eight hits were selected among many potential candidates in order to span the range of log D variation for experimentally studied molecules. Their extraction ability was also assessed using the best models of CODESSA PRO. Then, these eight podands were prepared and experimentally studied as uranyl extractants using the same protocol as for the compounds from the parent set.[96] Comparison of experimental log D values with those predicted by ISIDA and CODESSA PRO (Figure 5.15) shows that both QSPR approaches reasonably estimate log D for seven of the eight compounds from the "blind" test set.
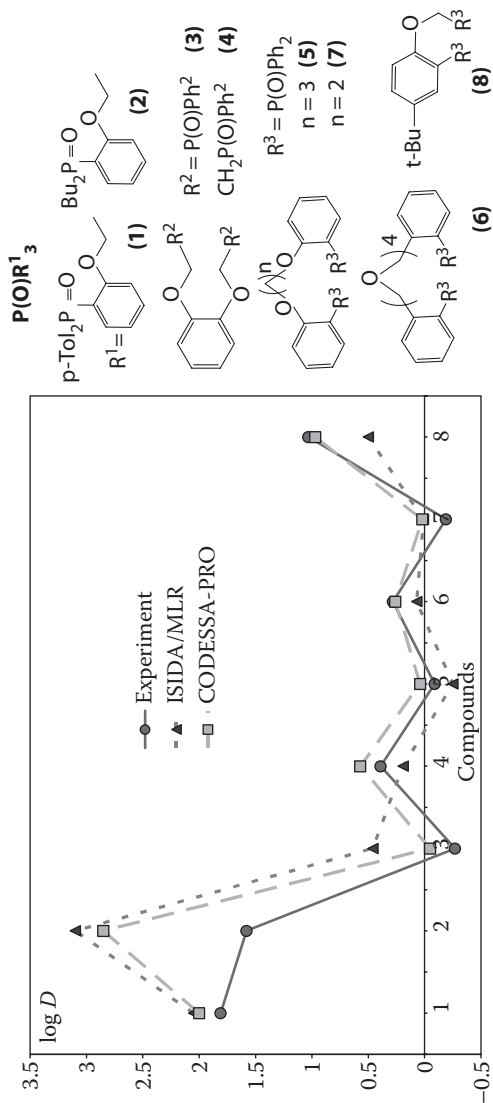
FIGURE 5.15 Experimental and predicted log D values for eight designed phosphoryl-containing podands.[13]

5.6   DISCUSSION

5.6.1   PREDICT OR INTERPRET?

QSPR modeling has two main objectives: to interpret studied phenomena and to predict modeled property values (*Y*) for new compounds. These two goals are hardly attainable simultaneously. In fact, a model could be easily interpreted if it involves relatively few descriptors and the mathematical dependence between *Y* and the descriptors is reasonably simple. A multilinear regression is a good example: descriptors with positive (negative) contributions describe the molecular character-istics that tend to increase (decrease) *Y*. In this context, nonlinear neural network or support vector machine models could hardly be used for interpretation purposes because of the mathematical complexity of these approaches.[97] On the other hand, the predictive performance of nonlinear models is, as a rule, higher than that of individual linear models. If one uses ensemble modeling techniques involving many individual linear and nonlinear models, the predictive performance of the approach usually improves significantly without any hope of obtaining a reasonable interpre-tation of the models. Thus, in improving the predictive ability of the models, one often deteriorates their interpretability. An interplay between them is always a ques-tion of trade-off.

5.6.2   WHAT DESCRIPTORS DO WE NEED?

The quality of QSPR models always depends on the molecular descriptors involved. The descriptors should be able to discriminate between active and inactive com-pounds and, desirably, to characterize related chemical, physical, or biological pro-cesses. In this respect, the success of fragment descriptors to produce predictive models on large and diverse datasets is quite understandable: they possess a good discriminative power (one can always find the fragments present only in active com-pounds) and they implicitly contain information about related chemical properties. Mixing fragments and physicochemical descriptors improves the performance of the models.[15] Application of large and informationally rich descriptor pools together with pertinent machine-learning methods may allow one to develop models describ-ing not only restricted series of compounds, but also entire complexation or extrac-tion systems as a "metal-ligand-medium," where the latter concerns solvent(s), counterion(s), ionic strength, etc.

The parameters derived from force-field molecular mechanics calculations (ligand strain energies, cation-ligand interaction energies) represent another type of attrac-tive descriptors.[81,84,89] Their main advantage is a direct link with the 3D structure of the complexes and accounting for steric effects and the specificities of metal-ligand interactions. On the other hand, strain energies vary from one conformer to another. Therefore, for conformationally flexible ligands and their complexes, one should identify a reference state (e.g., global energy minimum) for which strain energies are calculated; otherwise, the descriptor calculations are ambiguous. This represents a clear obstacle for virtual screening because the generation of those descriptors for each query compound is a time-consuming task.

5.6.3   Complementarity of QSPR and 3D Modeling Approaches

Combining chemoinformatics and 3D molecular modeling approaches might be very useful for the development of new metal binders. Thus, the above-mentioned existence of linear correlations between the strain energy ΔU of ligands and thermodynamic parameters of complexation and extraction shows that ΔU represents a useful criterion for the selection of new ionophores. This approach has been used in the HostDesigner program[98–101] dedicated to *de novo* designs of new metal binders. In HostDesigner, the library of tridimensional constituent fragments is used to generate a large number of 3D molecular structures followed by selection of the most promising candidates according to some geometry and energy (ΔU) criteria. Using this strategy, new efficient ligands for lanthanides extraction[102,103] and Cs^+/alkali cation extraction separations[104] have been designed.

5.6.4   New Strategies in QSPR

Despite the availability of several commercial and academic user-friendly programs for structure-property modeling, QSPR studies are still far from routine procedures. Depending on the particular dataset used for the training, various strategies (multitask learning, divide and conquer, etc.), should be applied. As soon as the model is developed, its AD should be identified. Special attention should be paid to the models' validations. We believe that a "classical" training/test-sets setup is not sufficient because of the ambiguities of the test-set selection. A more rigorous external n-fold CV procedure is required to obtain a realistic assessment of the prediction performances of models.

5.7   CONCLUSION

In this work, we have demonstrated that modern QSPR modeling methods are becoming an important tool for computer-aided designs of new metal binders. Further developments depend not only on new data-mining techniques and descriptors applied, but also on the quality of the experimental data used for the training and validation of the models. Thus, both theoretical and experimental chemists should make an effort to build a basis for predictive structure-property modeling that will accelerate the development of target molecules and materials.

REFERENCES

1. Beck, M.; Nagypal, I. *Chemistry of Complex Equilibria*. Akademiai Kiado: Budapest, 1989.

2. *Science and Practice of Liquid-Liquid Extraction*. J.D. Thornton, Ed., Oxford Science Publications, Clarendor Press: Oxford, 1992; Vols. 1 and 2.

3. Leach, A. *Molecular Modelling. Principles and Applications.* Prentice Hall: Upper Saddle River, NJ, 2001.

4. Varnek, A.; Wipff, G. Molecular modelling in solvent extraction: Ionophores in pure solutions and at the liquid/liquid interface. *Solvent Extr. Ion. Exch.* 1999, 17 (6), 1493–1505.

5. Leach, A.; Gillet, V. *An Introduction to Chemoinformatics*. Kluwer Academic: Dordrecht, 2003.

6. Gasteiger, J. Chemoinformatics: A new field with a long tradition. *Anal. Bioanal. Chem.* 2006, 384, 57–64.

7. Dimmock, P.W.; Warwick, P.; Robbins, R.A. Approaches to predicting stability constants. *Analyst* 1995, 120 (8), 2159–2170.

8. Hancock, R.D. Approaches to predicting stability constants. A critical review. *Analyst* 1997, 122, 51R–58R.

9. Hancock, R.D.; Martell, A.E. Ligand design for selective complexation of metal ions in aqueous solution. *Chem. Rev.* 1989, 89 (8), 1875–1914.

10. Hay, B.P.; Castleton, K.J.; Rustad, J.R. *Stability Constant Estimator User's Guide*; PNNL-11434. Pacific Northwest National Laboratory: Springfield, 2001; pp. 1–47.

11. Kumok, V.N. *Regularities in Stability of Coordination Compounds in Solutions*. University of Tomsk: Tomsk, 1977.

12. Rozen, A.M.; Krupnov, B.V. Dependence of the extraction ability of organic compounds on their structure. *Russ. Chem. Rev.* 1996, 65 (11), 973–1000.

13. Varnek, A.; Fourches, D.; Kireeva, N.; Klimchuk, O.; Marcou, G.; Tsivadze, A.; Solov'ev, V. Computer-aided design of new metal binders. *Radiochimica Acta* 2008, 96 (8), 505–511.

14. Varnek, A.; Fourches, D.; Solov'ev, V.; Klimchuk, O.; Ouadi, A.; Billard, I. Successful 'in silico' design of new efficient uranyl binders. *Solvent Extr. Ion Exch.* 2007, 25 (4), 433–462.

15. Varnek, A.; Fourches, D.; Solov'ev, V.P.; Baulin, V.E.; Turanov, A.N.; Karandashev, V.K.; Fara, D.; Katritzky, A.R. "In silico" design of new uranyl extractants based on phosphoryl-containing podands: QSPR studies, generation and screening of virtual combinatorial library, and experimental tests. *J. Chem. Inf. Comp. Sci.* 2004, 44 (4), 1365–1382.

16. Petrukhin, O.M. Coordination chemistry and analytical methods of metal separation. *Russ. J. Coord. Chem.* 2002, 28 (10), 681–696.

17. Todeschini, R.; Consonni, V. *Handbook of Molecular Descriptors*. Wiley-VCH: Weinheim, 2000.

18. DRAGON Program. Version 5.4. www.talete.mi.it/download.htm, 2006.

19. CODESSA PRO Program. http://www.codessa-pro.com/manual/manual.htm, 2008.

20. ISIDA (In Silico Design and Data Analysis) Program. http://infochim.u-strasbg.fr/recherche/isida/index.php, 2008.

21. Japertas, P.; Didziapetris, R.; Petrauskas, A. Fragmental methods in the design of new compounds. Applications of the advanced algorithm builder. *QSAR* 2002, 21 (1), 23–37.

22. Zefirov, N.S.; Palyulin, V.A. Fragmental approach in QSPR. *J. Chem. Inf. Comp. Sci.* 2002, 42 (5), 1112–1122.

23. Varnek, A.; Fourches, D.; Solov'ev, V.P. Encoding and exchange of chemical information using substructural molecular fragments. *Abstracts of Papers, 229th ACS National Meeting*, San Diego, CA, March 13–17, 2005, COMP-048.

24. Baskin, I.; Varnek, A. Building a chemical space based on fragment descriptors. *Comb. Chem. High Throughput Screening* 2008, 11 (8), 661–668.

25. Solov'ev, V.P.; Varnek, A.A. Structure-property modeling of metal binders using molecular fragments. *Russ. Chem. Bull.* 2004, 53 (7), 1434–1445.

26. Golub, G.H.; Reinsch, C. Singular value decomposition and least squares solutions. *Numer. Math.* 1970, 14, 403–420.

27. Frank, E.; Hall, M.; Trigg, L.; Holmes, G.; Witten, I.H. Data mining in bioinformatics using Weka. *Bioinformatics* 2004, 20 (15), 2479–2481.

28. Tetko, I.V. Associative neural network. *Neural Process. Lett.* 2002, 16 (2), 187–199.

29. Tetko, I.V. Neural network studies. 4. Introduction to associative neural networks. *J. Chem. Inf. Comp. Sci.* 2002, 42 (3), 717–728.

30. Vapnik, V.N. *Statistical Learning Theory.* John Wiley & Sons: New York, 1998.

31. Ivanciuc, O. Applications of support vector machines in chemistry. In *Reviews in Computational Chemistry*, Lipkowitz, K.B.; Cundari, T.R. Eds. Wiley-VCH: Weinheim, 2007; Vol. 23, pp. 291–400.

32. Oprea, T.I.; Waller, C.L.; Marshall, G.R. Three-dimensional quantitative structure-activity relationship of human immunodeficiency virus (I) protease inhibitors. 2. Predictive power using limited exploration of alternate binding modes. *J. Med. Chem.* 1994, 37 (14), 2206–2215.

33. Tropsha, A.; Gramatica, P.; Gombar, V.K. The importance of being earnest: Validation is the absolute essential for successful application and interpretation of QSPR models. *QSAR Comb. Sci.* 2003, 22 (1), 69–77.

34. Grubbs, F.E. Procedures for detecting outlying observations in samples. *Technometrics* 1969, 11 (1), 1–21.

35. Muller, P.H.; Neumann, P.; Storm, R. *Tafeln der mathematischen Statistik.* VEB Fachbuchverlag: Leipzip, 1979.

36. Tetko, I.V.; Solov'ev, V.P.; Antonov, A.V.; Yao, X.J.; Fan, B.T.; Hoonakker, F.; Fourches, D.; Lachiche, N.; Varnek, A. Benchmarking of linear and non-linear approaches for quantitative structure-property relationship studies of metal complexation with organic ligands. *J. Chem. Inf. Model.* 2006, 46 (2), 808–819.

37. Katritzky, A.R.; Kuanar, M.; Slavov, S.; Dobchev, D.A.; Fara, D.C.; Karelson, M.; Acree, W.E. Jr.; Solov'ev, V.P.; Varnek, A. Correlation of blood–brain penetration using structural descriptors. *Bioorg. Med. Chem.* 2006, 14 (14), 4888–4917.

38. Solov'ev, V.P.; Kireeva, N.V.; Tsivadze, A.Y.; Varnek, A.A. Structure-property modelling of complex formation of strontium with organic ligands in water. *J. Struct. Chem.* 2006, 47 (2), 298–311.

39. Tetko, I.V.; Bruneau, P.; Mewes, H.-W.; Rohrer, D.C.; Poda, G.I. Can we estimate the accuracy of ADME-Tox predictions? *Drug Discov. Today* 2006, 11 (15/16), 700–707.

40. Katritzky, A.R.; Fara, D.C.; Yang, H.; Karelson, M.; Suzuki, T.; Solov'ev, V.P.; Varnek, A. Quantitative structure-property relationship modeling of beta-cyclodextrin complexation free energies. *J. Chem. Inf. Comp. Sci.* 2004, 44 (2), 529–541.

41. Solov'ev, V.P.; Vnuk, E.A.; Strakhova, N.N.; Raevsky, O.A. *Thermodynamics of Complexation of the Macrocyclic Polyethers with Salts of Alkali and Alkaline-Earth Metals (Russ.).* VINITI: Moscow, 1991.

42. Martinov, B.V. *Extraction by Organic Acids and their Salts (Russ.).* ENERGOATOMIZDAT: Moscow, 1989.

43. Mejov, E.A. *Handbook on Extraction by Amines and Quaternary Ammonium Bases (Russ.).* ENERGOATOMIZDAT: Moscow, 1987.

44. Mejov, E.A. *Handbook on Extraction by Amines and Quaternary Ammonium Bases (Russ.).* ENERGOATOMIZDAT: Moscow, 1999.

45. Nikolotova, Z.I. *Handbook on Extraction of Lanthanides and Actinides by Neutral Extractants (Russ.).* ENERGOATOMIZDAT: Moscow, 1987.

46. Nikolotova, Z.I. *Extraction of Lanthanides and Actinides by Neutral Extractants (Russ.).* ENERGOATOMIZDAT: Moscow, 1999.

47. *Handbook on Solvent Extraction (Russ.).* A.M. Rozen, Ed., ATOMIZDAT: Moscow, 1976; Vol. 1–3.

48. McDowell, W.J.; Michelson, D.C.; Moyer, B.A.; Coleman, C.F. In *A Data Base for Solvent Extraction Chemistry*, Proceedings of the International Solvent Extraction Conference (ISEC '83), Am. Inst. Chem. Eng., Denver, CO, August 1983; pp. 257–258.

49. McDowell, W.J.; Michelson, D.C.; Moyer, B.A.; Coleman, C.F. A source of solvent extraction information. *Solvent Extr. Ion Exch.* 1983, 1(1), 1–4.

50. Watarai, H.; Fujiwara, M.; Tsukahara, S.; Suzuki, N.; Akiba, K.; Saitoh, K.; Hasegawa, Y.; Kato, M. Construction of an INTERNET compatible database for solvent extraction of metal ions. *Solvent Extr. Res. Dev. Jpn.* 2000, 7, 197–205.

51. Varnek, A.A.; Wipff, G.; Solov'ev, V.P. Towards an information system on solvent extraction. *Solvent Extr. Ion. Exch.* 2001, 19 (5), 791–837.

52. Anderegg, G.; Arnaud-Neu, F.; Delgado, R.; Felcman, J.; Popov, K. Critical evaluation of stability constants of metal complexes of complexones for biomedical and environmental applications. *Pure Appl. Chem.* 2005, 77 (8), 1445–1495.

53. Arnaud-Neu, F.; Delgado, R.; Chaves, S. Critical evaluation of stability constants and thermodynamic functions of metal complexes of crown ethers (IUPAC Technical Report). *Pure Appl. Chem.* 2003, 75 (1), 71–102.

54. Portanova, R.; Lajunen, L.H.J.; Tolazzi, M.; Piispanen, J. Critical evaluation of stability constants for alpha-hydroxycarboxylic acid complexes with protons and metal ions and the accompanying enthalpy changes. Part II. Aliphatic 2-hydroxycarboxylic acids. *Pure Appl. Chem.* 2003, 75 (4), 495–540.

55. Popov, K.; Ronkkomaki, H.; Lajunen, L.H.J. Critical evaluation of stability constants of phosphonic acids. *Pure Appl. Chem.* 2001, 73 (10), 1641–1677.

56. Lajunen, L.H.J.; Portanova, R.; Piispanen, J.; Tolazzi, M. Critical evaluation of stability constants for alpha-hydroxycarboxylic acid complexes with protons and metal ions and the accompanying enthalpy changes. Part I. Aromatic ortho-hydroxy carboxylic acid. *Pure Appl. Chem.* 1997, 69 (2), 329–381.

57. Sjoberg, S. Critical evaluation of stability constants of metal-imidazole and metal-histamine systems. *Pure Appl. Chem.* 1997, 69 (7), 1549–1570.

58. Harris, W.R. Structure–reactivity relation for the complexation of Ni, Cd, Zn, and Fe. *J. Coord. Chem.* 1983, 13, 17–27.

59. Brown, P.L.; Sylva, R.N.; Ellis, J. An equation for predicting the formation constants of hydroxo-metal complexes. *J. Chem. Soc., Dalton Trans.* 1985, (4), 723–730.

60. Misono, M.; Saito, Y. Evaluation of softness from the stability constants of metal-ion complexes. *Bull. Chem. Soc. Jpn.* 1970, 43 (12), 3680–3684.

61. Edwards, J.O. Correlation of relative rates and equilibria with a double basicity scale. *J. Am. Chem. Soc.* 1954, 76 (6), 1540–1547.

62. Schneider, H.J.; Rudiger, V.; Raevsky, O.A. The incremental description of host-guest complexes: Free energy increments derived from hydrogen bonds applied to crown ethers and cryptands. *Org. Chem.* 1993, 58 (14), 3648–3653.

63. Raevsky, O.A.; Grigor'ev, V.Y.; Solov'ev, V.P. Modeling of structure – activity relationships. II. The estimation of electron-donor and -acceptor functions of active centres in molecules of physiologically active compounds. *Khim. Farm. Zh. (Russ.)* 1989, 23 (11), 1294–1300.

64. Rozen, A.M.; Nikolotova, Z.I.; Kartasheva, N.A.; Skotnikov, A.S. Effect of the structure of organic compounds on their extractability. *Radiokhim. (Russ.)* 1983, 25 (5), 603–608.

65. Rozen, A.M.; Khimenko, N.M.; Krupnov, B.V. Electronic structures of carboxylic acid amides. *Zh. Fiz. Khimii (Russ.)* 1989, 63 (5), 1239–1248.

66. Varnek, A.A.; Kuznetsov, A.N.; Petrukhin, O.M. Electrostatic potential distribution and extraction ability of some organophosphorus compounds. *Zh. Structurnoi Khim. (Russ.)* 1989, 30, 44–48.

67. Varnek, A.A.; Glebov, A.S.; Kuznetsov, A.N. Charge density distribution, electrostatic potential and complex formation ability of some neutral agents. *Portugal Phys.* 1988, (1), 59–61.

68. Varnek, A.A.; Kuznetsov, A.N.; Petrukhin, O.M. Calculation of the indexes of extractability of some neutral organo-phosphorus compounds within the framework of electron density functional method. *Koord. Khim. (Russ.)* 1991, 17, 1038–1043.

69. Rozen, A.M.; Nikolotova, Z.I. Relation of the extraction capacity of organic compounds to their structure and to the electronegativity of the substituting groups. *Zh. Neorg. Khimii (Russ.)* 1964, 9 (7), 1725–1742.

70. Rozen, A.M.; Khol'kin, A.I. Analogy between characteristics of extraction by binary and neutral extractants. *Dokl. Akad. Nauk SSSR (Russ.)* 1988, 301 (3), 661–664.

71. Yuan, C. *Some Problems in Chemical Structures and Properties of Organic Extractants*, Int. Solvent Extraction Conf. ISEC'80, Liege, Belgium, 6–12 September, Liege, Belgium, 1980; pp. 1–10.

72. Raevskii, O.A.; Sapegin, A.M.; Chistyakov, V.V.; Solov'ev, V.P.; Zefirov, N.S. Development of a model for the relation between structure and complex forming ability. *Koord. Khim. (Russ.)* 1990, 16 (9), 1175–1184.

73. Shi, Z.G.; McCullough, E.A. A computer-simulation – statistical procedure for predicting complexation equilibrium-constants. *J. Inclusion Phenom. Mol. Recognit.* 1994, 18 (1), 9–26.

74. Gakh, A.A.; Sumpter, B.G.; Noid, D.W.; Sachleben, R.A.; Moyer, B.A. Prediction of complexation properties of crown ethers using computational neural networks. *J. Inclusion Phenom. Mol. Recognit. Chem.* 1997, 27 (3), 201–213.

75. Solov'ev, V.P.; Varnek, A.A.; Wipff, G. Modeling of ion complexation and extraction using substructural molecular fragments. *J. Chem. Inf. Comput. Sci.* 2000, 40 (3), 847–858.

76. Toropov, A.A.; Toropova, A.P. QSPR modeling of complex stability by optimization of correlation weights of the hydrogen bond index and the local graph invariants. *Russ. J. Coord. Chem.* 2002, 28 (12), 877–880.

77. Varnek, A.A.; Wipff, G.; Solov'ev, V.P.; Solotnov, A.F. Assessment of the macrocyclic effect for the complexation of crown-ethers with alkali cations using the substructural molecular fragments method. *J. Chem. Inf. Comput. Sci.* 2002, 42 (4), 812–829.

78. Qi, Y.-H.; Zhang, Q.-Y.; Xu, L. Correlation analysis of the structures and stability constants of gadolinium(III) complexes. *J. Chem. Inf. Comput. Sci.* 2002, 42 (6), 1471–1475.

79. Toropov, A.A.; Toropova, A.P.; Nesterova, A.I.; Nabiev, O.M. QSPR modeling of complex stability by correlation weighing of the topological and chemical invariants of molecular graphs. *Russ. J. Coord. Chem.* 2004, 30 (9), 611–617.

80. Svetlitski, R.; Lomaka, A.; Karelson, M. QSPR modelling of lanthanide-organic complex stability constants. *Separat. Sci. Technol.* 2006, 41 (1), 197–216.

81. Rabbe, C.; Sella, C.; Madic, C.; Godard, A. Molecular modeling study of uranyl nitrate extraction with monoamides. II. Molecular mechanics and lipophilicity calculations. Structure-activity relationships. *Solvent Extr. Ion Exch.* 1999, 17 (1), 87–112.

82. Drew, M.G.B.; Hudson, M.J.; Youngs, T.G.A. QSAR studies of multidentate nitrogen ligands used in lanthanide and actinide extraction processes. *J. Alloy Comp.* 2004, 374 (1–2), 408–415.

83. Varnek, A.; Fourches, D.; Sieffert, N.; Solov'ev, V.P.; Hill, C.; Lecomte, M. QSPR modelling of the AmIII/EuIII separation factor: How far can we predict? *Solvent Extr. Ion. Exch.* 2007, 25, 1–26.

84. Comba, P.; Gloe, K.; Inoue, K.; Krueger, T.; Stephan, H.; Yoshizuka, K. Molecular mechanics calculations and the metal ion selective extraction of lanthanoids. *Inorg. Chem.* 1998, 37 (13), 3310–3315.

85. Yoshizuka, K.; Inoue, K.; Comba, P. Quantitative structure-property relationship of extraction equilibria of lanthanoid series using molecular mechanics calculations. *Kagaku Kogaku Ronbunshu* 2000, 26 (4), 517–522.

86. Yoshizuka, K. Advance of computational technology for simulating solvent extraction. *Analyt. Sci.* 2004, 20 (5), 761–765.

87. Cabbines, D.K.; Margerum, D.W. Macrocyclic effect on the stability of copper(II) tetramine complexes. *J. Am. Chem. Soc.* 1969, 91, 6540–6541.

88. Comba, P.; Hambley, T.W.; Okon, N.; Lauer, G. *MOMEC – A Molecular Modeling Package for Inorganic Compounds*. CVS: Heidelberg, 1997.

89. Hay, B.P.; Rustad, J.R.; Hostetler, C.J. Quantitative structure-stability relationship for potassium ion complexation by crown ethers. A molecular mechanics and ab initio study. *J. Am. Chem. Soc.* 1993, 115 (24), 11158–11164.

90. Dietz, M.L.; Bond, A.H.; Chiarizia, R.; Huber, V.J.; Herlinger, A.W.; Hay, B.P. Ligand reorganization energies as a basis for the design of synergistic metal ion extraction systems. *Chem. Commun.* 1999, (13), 1177–1178.

91. Bond, A.H.; Chiarizia, R.; Huber, V.J.; Dietz, M.L.; Herlinger, A.W.; Hay, B.P. Synergistic solvent extraction of alkaline earth cations by mixtures of di-n-octylphosphoric acid and stereoisomers of dicyclohexano-18-crown-6. *Anal. Chem.* 1999, 71 (14), 2757–2765.

92. Solov'ev, V.P.; Varnek, A. Anti-HIV activity of HEPT, TIBO, and cyclic urea derivatives: Structure-property studies, focused combinatorial library generation, and hits selection using substructural molecular fragments method. *J. Chem. Inf. Comp. Sci.* 2003, 43 (5), 1703–1719.

93. Varnek, A.; Solov'ev, V.P. "In silico" design of potential anti-HIV actives using fragment descriptors. *Combinat. Chem. High Throughput Screening* 2005, 8 (5), 403–416.

94. Siddall III, T.H. Effects of structure of N,N-disubstituted amides on their extraction of actinide and zirconium nitrates and of nitric acid. *J. Phys. Chem.* 1960, 64, 1863–1866.

95. Varnek, A.; Fourches, D.; Hoonakker, F.; Solov'ev, V.P. Substructural fragments: A universal language to encode reactions, molecular and supramolecular structures. *J. Comp.-Aided Mol. Design* 2005, 19 (9–10), 693–703.

96. Turanov, A.N.; Karandashev, V.K.; Baulin, V.E. Extraction of uran and thorium with neitral phosphoryl containing podands from nitric acid solutions. *Radiokhim. (Russ.)* 1998, 40 (1), 36–43.

97. Baskin, I.I.; Ait, A.O.; Halberstam, N.M.; Palyulin, V.A.; Zefirov, N.S. An approach to the interpretation of backpropagation neural network models in QSAR studies. *SAR and QSAR Environ. Res.* 2002, 13 (1), 35–41.

98. Hay, B.P.; Firman, T.K. HostDesigner: A program for the de novo structure-based design of molecular receptors with binding sites that complement metal ion guests. *Inorg. Chem.* 2002, 41 (21), 5502–5512.

99. Hay, B.P.; Zhang, D.; Rustad, J.R. Structural criteria for the rational design of selective ligands. 2. Effect of alkyl substitution on metal ion complex stability with ligands bearing ethylene-bridged ether donors. *Inorg. Chem.* 1996, 35 (9), 2650–2658.

100. Hay, B.P.; Oliferenko, A.A.; Uddin, J.; Zhang, C.; Firman, T.K. Search for improved host architectures: Application of de novo structure-based design and high-throughput screening methods to identify optimal building blocks for multidentate ethers. *J. Am. Chem. Soc.* 2005, 127 (48), 17043–17053.

101. Hay, B.P.; Firman, T.K.; Lumetta, G.J.; Rapko, B.M.; Garza, P.A.; Sinkov, S.I.; Hutchison, J.E.; Parks, B.W.; Gilbertson, R.D.; Weakley, T.J.R. Toward the computer-aided design of metal ion sequestering agents. *J. Alloy Comp.* 2004, 374, 416–419.

102. Lumetta, G.J.; Rapko, B.M.; Garza, P.A.; Hay, B.P.; Gilbertson, R.D.; Weakley, T.J.R.; Hutchison, J.E. Deliberate design of ligand architecture yields dramatic enhancement of metal ion affinity. *J. Am. Chem. Soc.* 2002, 124 (20), 5644–5645.

103. Lumetta, G.J.; Rapko, B.M.; Hay, B.P.; Garza, P.A.; Hutchison, J.E.; Gilbertson, R.D. A novel bicyclic diamide with high binding affinity for trivalent f-block elements. *Solvent Extr. Ion Exch.* 2003, 21 (1), 29–39.

104. Sachleben, R.A.; Bryan, J.C.; Engle, N.L.; Haverlock, T.J.; Hay, B.P.; Urvoas, A.; Moyer, B.A. Rational design of cesium-selective ionophores: Dihydrocalix[4]arene crown-6 ethers. *Eur. J. Org. Chem.* 2003, (24), 4862–4869.

6 Simultaneous Removal of Radionuclides by Extractant Mixtures

Vasily A. Babain
VG Khlopin Radium Institute

CONTENTS

6.1 INTRODUCTION

The disposition of the radioactive waste resulting from spent nuclear-fuel reprocessing is one of the major problems of nuclear technology. Many of these wastes are high-level (HLW) and present a potential environmental hazard. Because of the expense associated with long-term storage, it is desirable to minimize the volume of radioactive waste and store it as material with maximal chemical stability to avoid the dissipation of radionuclides in the environment.

Different radionuclides have different chemistry, so it seems reasonable to include each nuclide in a specific matrix that is most stable for the desired nuclide. It is possible to find stable matrices for incorporation of numerous nuclides with similar chemical properties. The target elements for such incorporation are the long-lived radionuclides (transuranic elements), ^{90}Sr, ^{137}Cs, and Tc. Many extraction processes have been proposed for radionuclide removal from radioactive wastes. Typically, the goal of the processes is to extract one radionuclide or multiple radionuclides

with similar chemical properties.[1–3] In contrast to the PUREX process, where only uranium and plutonium are the center of attention, extraction of long-lived radionuclides has currently become the priority task. The revived interest in fractionating high-level waste is connected mainly with an increase of fuel burn-up and will be especially important for mixed oxide (MOX) fuel and fuels for fast reactors.

After a few years of storage, the main radioactive heat emitters in HLW are ^{90}Sr and ^{137}Cs. In addition, extremely long-lived actinides—neptunium, plutonium, americium, and curium—should be collected for transmutation in the future. Therefore, different flowsheets can be proposed for waste processing. It is possible to extract each radionuclide in the special extraction (sorption) cycle, for example, uranium and plutonium in the PUREX process, and after that, minor actinides (MAs) by the TRUEX process,[4] strontium by the SREX process,[5,6] and cesium by sorption[7] or extraction.[8]

The flowsheet of the UREX process, developed in the United States, includes the following extraction cycles: (1) separation of uranium and technetium, (2) separation of plutonium, (3) separation of cesium and strontium, (4) separation of MAs and Rare Earth Elements (REE), and (5) group separation of MA from REE metals.[9,10] Flowsheet development in Europe[11] includes a modified PUREX process and, after that, the DIAMEX process for separation of MAs and lanthanides, the SANEX process for separation of MAs from lanthanides, and a special cycle for Am/Cm separation. Cesium and strontium will be in the raffinate of the DIAMEX process, and this raffinate will be vitrified, or cesium can be preliminarily extracted.[12]

All these stages can be realized, but the total cost of such multicyclic processing will be very high. It needs special equipment and buildings for realization of each cycle. It should be mentioned also that each cycle has some additional secondary liquid wastes that need to be vitrified, leading to additional cost. Therefore, the idea to combine the removal of some radionuclides in one extraction cycle seems to be very promising. Thus, an alternative to such multicycle schemes may be simultaneous extraction of several radionuclides. For example, the process for simultaneous extraction and separation of lanthanides and MAs using octyl(phenyl)-*N,N*-diisobutylcarbamoylmethylphosphine oxide (CMPO) (SETFICS process) was tested and shows positive results.[13–16] All of these nuclides can be extracted and group separation can be done in the stripping stages. In this process, two separate processes, classical TRUEX and An/Ln separation, are united. Such a combination results in a more complex flowsheet, but no additional tanks for the intermediate product, An-Ln concentrate, are needed.

There are special extractants to extract each class of radionuclides: crown ethers for cesium and strontium; and phosphine oxides, carbamoylmethylphosphine oxides, and diamides for actinides, etc. It is unrealistic to have a single extractant that can extract all target nuclides with nearly the same effectiveness. So, a promising technical decision is to mix extractants for different radionuclides and extract them simultaneously.

The goal of this work is to discuss the advantages and drawbacks of combined extraction of different nuclides by extractant mixtures. It is not a review of synergistic extraction as such, but rather only a technological view on the use of extractant mixtures in radiochemistry.

Mixtures of extractants have been used for extraction many times. The use of the PUREX extractant tri-*n*-butyl phosphate (TBP) in paraffinic hydrocarbons as

a modified diluent for many other extractants, such as carbamoylmethylphosphine oxides, crown ethers, and phosphine oxides, is very popular. The extraction ability in such systems depends mainly on the concentration of the stronger extractant, because target metals (Sr for crowns, lanthanides and Am for phosphine oxides, etc.) are practically not extracted by TBP. In other extraction systems, two or more extractants have been used to extract not one, but multiple, metals simultaneously. In the following sections, there is an attempt to classify extraction systems by the extractants employed. The most popular is the mixing in one solvent of neutral and acidic compounds. It is known that crown ethers extract rare earths and actinides much better in a mixture with different compounds, from carboxylic acids to chlorinated cobalt dicarbollide (CCD).

6.2 EXTRACTION OF NUCLIDES BY MIXTURE OF ACIDS AND NEUTRAL COMPOUNDS

6.2.1 CCD AND ADDITIVES

CCD and its brominated analog (Br-COSAN) are very widely studied as potential components of extraction mixtures for radionuclide separation. These compounds were proposed for extraction more than 30 years ago,[17] and already in the first publications, polyethylene glycols (PEGs) were used for simultaneous extraction of cesium and strontium. An excellent review of extraction by carborane compounds was recently published;[18] so, in this paper, mainly works published after 2003 and not included in the previous review will be discussed.

It is well known that pure CCD in polar diluents (nitroaromatic) effectively and very selectively extracts cesium. The addition of PEGs or crown ethers[19] sharply increases the extraction ability toward alkaline-earth metals. However, at the same time, the addition of PEG or crown ethers suppresses the extraction of cesium. Extraction of strontium increases with increasing PEG concentration up to a CCD:PEG mole ratio of about 1:1 and also decreases with higher PEG concentration. The behaviors of such systems have been discussed in many works and reviewed.[18] Therefore, component concentrations in the solvent were chosen to obtain acceptable distribution ratios. Ideally, distribution ratios for both metals, cesium and strontium, should be the same. In practice, it is not easy to achieve, because the feed solution content is not the same in all cases, and distribution ratios for Sr and Cs depend on acidity and salt concentrations in a different manner. Thus, it is enough to achieve distribution ratios of more than 1, better between 3 and 10. Such ratios are optimal to attain full extraction of metals in an acceptable number of extraction stages and subsequently to attain the full stripping of metals. Extremely high distribution ratios in an extraction stage create a problem with stripping in many cases.

The search for, and study of, new additives to CCD are going on intensively. In the last few years, some new works were published where extraction systems based on CCD were studied. Not only works involving classical synergistic additives, such as PEG and crown ethers[20–22] and bidentate organophosphorus compounds,[23–25] were studied, but also calixarenes[26–28] and phosphorylated PEGs.[29] A theoretical investigation on the interaction of CCD with calixarenes in extraction has been carried out.[30]

As was shown first by Rais and Tachimori,[31] a synergistic effect was also observed for mixtures of CDD with heterocyclic compounds. This direction was also actively investigated in the last years. Mixtures of CCD with N-tridentate heterocyclic compounds,[32] diamides of dipicolinic acid (DPA),[33–35] and calixarenes with heterocyclic reaction centers[36–38] were studied for extraction. For the most part, extraction of MAs and separation of MAs from lanthanides were the center of attention in these works. But, it should be mentioned that all solvents with CCD also extract cesium.

A new class of synergistic additives, diamides of DPA, showed very strong extraction properties in mixtures with CCD[33–35] for the extraction of MAs. By themselves, though pure tetraalkyldiamides of DPA are rather weak extractants. These compounds have moderate extraction ability for uranium[39] and very low extraction ability for MAs.[33,40] However, the mixture of tetraalkyldiamides of DPA and CCD shows a very strong extraction ability for americium and cesium. Symmetrical dialkyldiaryldiamides in polar diluents show good extraction of americium in chloroform[41] and particularly in fluorinated diluents.[42,43] A great difference between the extraction of americium by tetralkyl and dialkyldiaryldiamides becomes negligible for mixtures of diamides with CCD. In both cases, extraction increases considerably, but for tetraalkyldiamides, such an increase is higher. In contrast to organophosphorous compounds, extraction of cesium by a mixture of CCD and diamide decreased to a lesser extent. Use of DPA as a component of the UNEX process instead of carbamoylmethylphosphine oxide has some technological advantages. First of all, the solubility of tetralkyl derivatives of DPA (e.g., tetrabutyl) is higher than for carbamoylmethylphosphine oxide. Therefore, maximal saturation of the organic phase will also be higher, and it is possible to process solutions with high concentration of REEs (and MAs). It is most important for the potential processing of high burn-up fuel waste with a high concentration of fission products. One positive feature of DPA is its better extraction of americium compared with europium. This difference is not as high as for bis(triazinyl)pyridines (separation factor for Am/Eu is about 5–6), but such separation is in an acidic medium (0.5–1.0 M nitric acid), and, this separation factor in principle is enough to separate MAs from REEs in a multistage extraction cascade. Mixtures of CCD and DPA do not extract strontium and other divalent ions. However, a modified UNEX solvent (CCD + DPA + PEG) is able to extract all long-lived radionuclides from acidic solution, including solutions with a high concentration of REEs. In this case, the problem exists of achieving reasonable distribution ratios for all major metals. As it was shown, the most effective coextractant for Sr is PEG-400. But Slovafol-909 is more accepted for this solvent, because for a mixture of CCD, Slovafol-909, and DPA, distribution ratios for Cs, Sr, and An are more balanced.[43] This solvent was tested under dynamic conditions with a "warm" solution.[44] Modified "diamidic" UNEX solvent—0.08 M CCD, 0.05 M tetrabutyldiamide of dipicolinic acid (TBDPA), 0.8 vol % Slovafol-909 in *meta*-nitrobenzotrifluoride (F-3)—was used for the extraction of radionuclides from a simulated warm solution. Concentrations of metals in the feed solution are shown in Table 6.1.

A standard flowsheet consisting of eight extraction stages, two stages of scrubbing, and eight stages of stripping was used. A 0.4 M solution of oxalic acid was used as the scrub solution, and 2 M methylaminecarbonate (MAC) with 10 g/L nitrilotriacetic

TABLE 6.1

The Composition of the Feed Solution

Element	Concentration (mg/L)	Element	Concentration (mg/L)
Al	100	Fe	480
Ba	120	Mo	970
Ca	100	Na	500
Ce	2100	Nd	2100
Co	210	Ni	100
Cr	140	Sr	230
Cs	350	Zr	820
Mn	150	HNO$_3$	2.9 M

Source: Data from Babain, V.A., Smirnov, I.V., Logunov. M.V., Alyapysev, M. Yu., et al., *Voprosi radiatsionnoy bezopasnosti*, 4 (44), 3–12, 2006. With permission.

Note: Radioactive isotope content in feed solution: 1.6×10^7 Bq/L for ^{241}Am, 2.6×10^7 Bq/L for ^{137}Cs, 1.3×10^7 Bq/L for ^{154}Eu, and 4.5×10^7 Bq/L for ^{90}Sr and ^{90}Y.

acid (NTA) was used as the strip solution. Dynamic testing with mixer-settlers was continued for 48 hours, and the solvent was recycled nine times. Extraction of Am was 99.3%; Cs, 99.3%; Sr, 99.5%; and Eu, 95%. Good hydrodynamic properties of the solvent was shown, and no radionuclides in the recycled solvent were found.[44]

Calixarenes, a relatively new class of multidentate extractants, have been very widely investigated in the last 10 years. Some of these extractants, those containing CMPO groups, show extremely high extraction ability[45] for americium and europium. But a great hope for sharply increasing the selectivity of extraction and possible Am/Eu separation because of the rigid geometry of such compounds has not been realized; selectivity is very close to the selectivity for monodentate analogs. Another way to increase the extraction ability of calixarenes involves the use of the mixture of calixarenes with CCD[26,27] or Br-COSAN.[28] Influence on extraction depends on the calixarene structure to a great extent. As a rule, if the calixarene as such has extraction ability for a metal, the addition of CCD or Br-COSAN may be expected to greatly increase the extraction ability. But sometimes such a mixture may extract metals that are not extracted separately by the individual mixture components.[26] The extraction chemistry of such systems is very interesting. It is evident that some supramolecular complexes exist in many cases; therefore, in some cases, extraction equilibrium is achieved slowly, requiring several hours.[26,27] Such an effect is not observed for CCD-PEG mixtures, where equilibrium is reached in only minutes.Extremely high extraction ability together with usually low extraction capacity for metals makes extraction systems employing calixarenes most promising for concentration of radionuclides from solution with a low concentration of metals. An interesting extraction system was proposed involving the mixture of CCD, substituted PEG (Slovafol-909), and the zirconium salt of dibutylphosphoric acid (Zr-DBP).[46]

Solution of Zr-DBP in TBP-Isopar L was proposed earlier for the processing of radioactive wastes.[47] The authors state that the advantages of this solvent were

TABLE 6.2

Influence of HNO$_3$ Concentration on the Distribution Ratios for Individual Elements in Extraction with a Mixture of 0.05 M CCD, 0.06 M Zr-DBP (Zr:HDBP = 1:9), and Slovafol-909 (PEG) in F-3

[HNO$_3$] (M)	Ce	Eu	Y	Am	Cm	Cs	Sr	Mo	Fe
0.5	3600	4300	>1000	127	132	43	>1000		
1	264	384	640	52	66	20.5	600	3.4	12
1.5	54	113	210	25	41	12.9	460	2.2	0.93
2.5	8.1	29	160	5.1	7	4.9	310	1.5	0.54
3.0		7.0		1.0				1.7	0.41
5	0.54	2.7	42	0.25	0.4	1.25	24	1.9	1.4
8	0.11	0.64	16	0.07	0.08	0.64	0.64	3.7	20
10	0.02	0.12	2	0.013	0.015	0.16	0.16	5.5	>50

Source: Data from Shishkin, D.N., Galkin, B. Ya., Fedorov, Yu, S., Zilberman, B. Ya., Shmidt, O.V., *Radiochemistry*, 45 (6), 577–580, 2003. With permission.

Note: The initial aqueous phase contains 0.0007–0.02 M element (Ce in experiments with trace amounts of TPE).

its compatibility with the PUREX extractant and the low price of the extractant. The addition of CCD increases the extraction ability for lanthanides and americium. The addition of PEG also increases the strontium extraction. Data on the extraction of different metals by the proposed solvent are presented in Table 6.2.[46] It was supposed that the system can be used for HLW partitioning,[46] as it recovers all the elements from strongly acidic solutions and consists of relatively cheap and available components; however, the problem of back-extraction of some elements (e.g., Fe, Zr, and Y) requires additional studies. No data about the extraction capacity of this system were presented.

6.2.2 EXTRACTION BY CROWN ETHERS WITH DIFFERENT ACIDS

The idea to combine the crown ethers with acids to improve the extraction ability was studied in 1979.[48] In this work, it was shown that both strontium and cesium can be extracted from an aqueous HNO$_3$ phase containing the metal nitrates into an organic phase containing kerosene or CCl$_4$ as a diluent and complexing agents dissolved in the diluent. The most promising results obtained, thus, far have required the use of a mixture of three metal complexing agents: tributyl phosphate, di(2-ethylhexyl) phosphoric acid, and 4,4′(5′)-di-*tert*-butylbenzo-24-crown-8. The highest distribution ratios obtained (organic/aqueous) were 1.45 ± 0.05 for Cs$^+$ and 200 for Sr^{2+}. The development of this idea, involving the use of 0.02 M bis-(4,4′(5′)-[α-hydroxyheptyl]benzo)-18-crown-6 in 0.076 M (5 vol %) didodecylnaphthalene sulfonic acid (DNS)/27 vol % TBP/68 vol % kerosene, gave the most favorable results for cesium extraction.[49] This system shows good hydrodynamic properties, but only cesium is extracted from 3 M nitric acid. Strontium is extracted only at low concentration of nitric acid. For both proposed extraction systems, stripping of metals is possible only in a narrow range of pH.

We can see here one of the most complicated problems of extractant mixing: we cannot predict the character of the change of extraction ability. For different ions, it can change in a different manner. Also, when extraction is from an acidic aqueous phase, stripping becomes a problem for such systems. It is possible to strip metals from a solution containing only the crown ether by water. But, for a mixture of crowns with organophilic acids, water stripping is not possible; alternatives include only stripping with highly concentrated acid, or low-concentrated acid in a narrow pH range, or complexant solutions. Thus, we apparently combine not only positive, but also negative features of both extractants. Sometimes, though, it is not important. For example, it was shown[50,51] that both cesium and strontium can be extracted effectively from alkaline solutions by a mixture of carboxylic acids and 4,4′(5′)-di(*tert*-butyl)cyclohexano-18-crown-6. This process was tested with alkaline nitrate media simulating alkaline HLWs present at the U.S. Department of Energy Savannah River Site. For this process, it is possible to use relatively weak carboxylic acids, because they are dissociated in the alkaline media and increase extraction. On the other hand, stripping can then be done by acid stripping agents, and low concentrations of mineral acid are needed to achieve good stripping. It was also shown that using stronger acid (e.g., trichloroacetic instead of carboxylic) moves the extraction to a lower pH range.[52] Data about CCD-crown mixtures also confirm that extraction moves to a more acidic range with an increase in acid strength.

The situation with different metals is almost opposite. It was shown that the influence of dibenzo-24-crown-8, dicyclohexyl-18-crown-6 (DCH18C6), or trioctylphosphine oxide on the extraction of europium by dinonylnaphthalenesulfonic acid (HDNNS) in benzene from nitrate and perchlorate solutions is negative. That is, an antisynergistic or antagonistic effect is observed.[53]

6.2.3 Extraction by Organophosphorus Acids with Neutral Extractants

A mixture of well-known extractants, di-(2-ethylhexyl)phosphoric acid (HDEHP) and CMPO, in *n*-paraffin was used for the study of combined extraction of different actinides (americium, plutonium, and uranium) and lanthanides (cerium and europium) and their separation from fission products (cesium, strontium, ruthenium, and zirconium).[54] Combined extraction of MAs and lanthanides was studied together with group separation of MAs from lanthanides by selective stripping with a solution of diethylenetriaminepentaacetic acid (DTPA), formic acid, and hydrazine hydrate. This solution strips only MAs, leaving lanthanides in the organic phase. Subsequently, the lanthanides are stripped using a mixture of DTPA and sodium carbonate.

Extraction of americium and lanthanides by a mixture of dihexylphosphoric acid (HDHP) and *N,N′*-dimethyl-*N,N′*-dioctylhexylethoxymalonamide (DMDOHEMA) was studied.[55] The authors compared extraction of metals by these extractants separately and by their mixture. An interesting influence on lanthanide extraction is shown in Figure 6.1. A synergistic effect is observed for lanthanides from La to Dy, but for metals from Ho to Lu, the addition of malonamides results in decreasing extraction. No data about metal stripping were presented, but it is evident that in this case too, it is not possible to strip metals by water, as for malonamides.
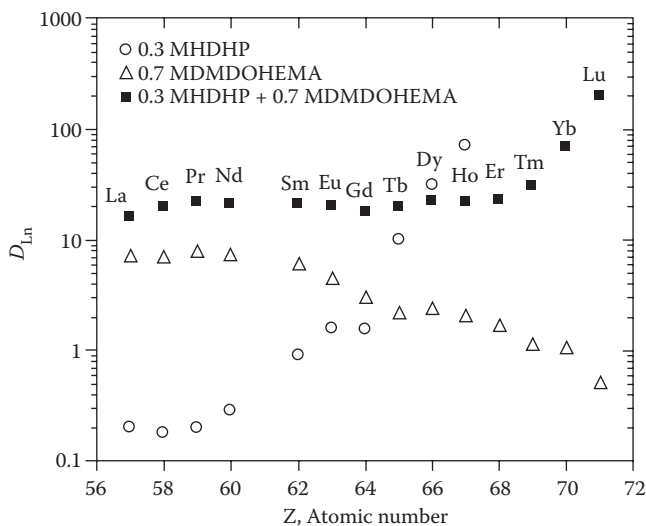
FIGURE 6.1 Distribution ratio of lanthanide ions extracted by 0.3 M HDHP (empty circles), 0.7 M DMDOHEMA (empty triangles), and the 0.3 M HDHP/0.7 M DMDOHEMA mixture (full squares) in *n*-dodecane from a solution of 1 M HNO_3 and 2 M $LiNO_3$ at 238°C. (From Gannaz, B., Chiarizia, R., Antonio, M.R., Hill, C., Cote, G., *Solvent Extr. Ion Exch.* 25 (3), 313–337, 2007. With permission.)

The solvent comprised of 0.5 M DMDOHEMA and 0.3 M HDEHP in total petroleum hydrocarbon (TPH) diluent was used for separation of Am and Cm from lanthanides and fission products. A proposed technological flowsheet (PALADIN process) was tested in 2000.[56] The flowsheet of this process is given in Figure 6.2.

In connection with the PALADIN process, the authors studied the extraction and separation of target elements—MAs and fission products and Mo, Pd, Zr, and Fe (corrosion product). Addition of HDEHP was explained by the necessity to keep the lanthanides in the organic phase in the Am stripping process by a solution of 0.5 M N-(2-hydroxyethyl) ethylenetrinitrilotriacetic acid (HEDTA) and 0.5 M citric acid at pH 3. A high decontamination factor (> 800) for Am and Cm separation from lanthanides was achieved. However, large volumes of stripping solution for lanthanides (1 M nitric acid) and stripping solution for zirconium and iron (1 M nitric acid and 0.8 M oxalic acid) were used.

Development of a related flowsheet was discussed.[57] In the first step (extraction), the DIAMEX solvent was used as the organic phase (Figure 6.3). Therefore, only actinides and lanthanides were extracted. HDHP was added to the organic phase, saturated by metals before stripping. It was possible to separate actinides from lanthanides (as in PALADIN or TALSPEAK process) by a strip solution containing polyaminocarboxylic acid in buffer solution. HDHP was removed to the water phase by neutralization, whereupon the obtained DIAMEX solvent was used again for extraction, and HDHP was regenerated by acidification of the water phase. The advantage of this flowsheet is depression of Mo and Zr extraction, but a new secondary waste solution with a high concentration of organic salt is obtained. Also, solvents disobeying the CHON (carbon, hydrogen, oxygen, nitrogen) criterion were used in these two flowsheets.
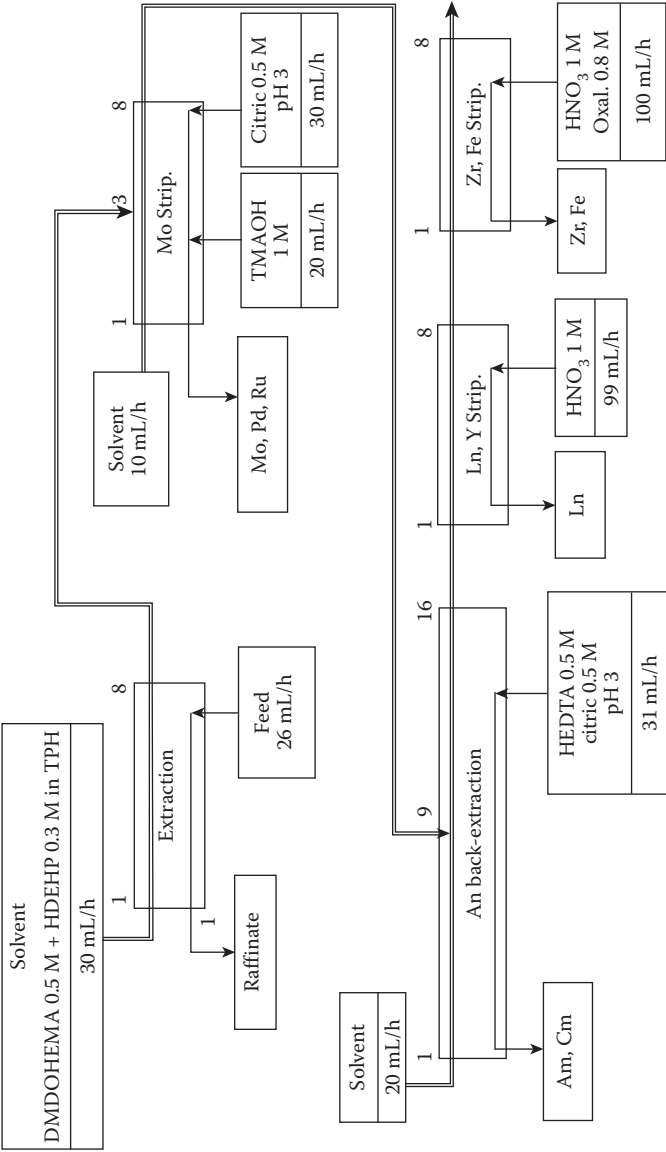
FIGURE 6.2 PALADIN process test flowsheet. (From Madic, C., Lecomte, M., Baron, P., Boullis, B., *C.R. Physique* 3 (7–8), 797–811, 2002. With permission.)
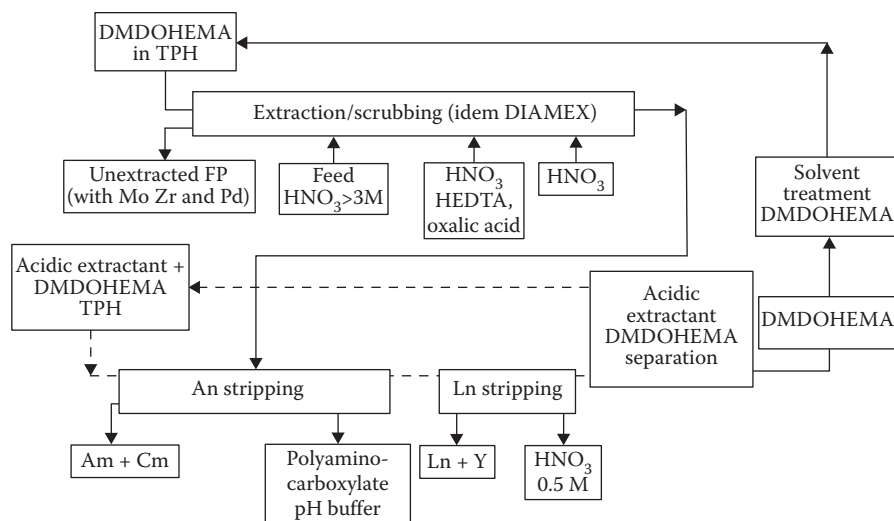
FIGURE 6.3 DIAMEX-SANEX flowsheet with organophosphorus acid regeneration in extraction cycle. (From Heres, X., Ameil, E., Martinez, I., Baron, P., Hill, C., Extractant separation in Diamex Sanex Process. Presentation on Global'07 conference. With permission.)

6.3 EXTRACTION OF RADIONUCLIDES BY MIXTURES OF DIFFERENT NEUTRAL EXTRACTANTS

6.3.1 MIXTURE OF DIFFERENT CROWN ETHERS

Crown ethers were proposed for extraction of cesium using the CSEX process[58] and of strontium by the SREX process[5] from acidic solutions. Two diluents were used, either 1-octanol or a hydrocarbon mixture with TBP modifier. In both cases, very effective extraction of the target components was achieved. Therefore, an "advanced integrated system" combining the CSEX and SREX processes for the extraction of cesium and strontium was proposed.[59] The two crown ethers, bis[4,4′(5′)-(2-hydroxyalkyl)benzo]-18-crown-6 and bis[4,4′(5′)-(*tert*-butyl)cyclohexano]-18-crown-6), are diluted in the mixture phase containing 1.2 M TBP and 5 vol % lauryl nitrile in the isoparaffinic diluent Isopar L. The process enables 99.99% of cesium and strontium to be recovered from acidic liquid wastes (3.78 M) containing mainly aluminium (0.486 M), calcium (0.778 M), zirconium (0.225 M), and to a lesser extent sodium (0.015 M). In this case, no interference of extraction ability and no antisynergistic or antagonistic effect are observed. The main reason for lack of such effects may be the similarity of extraction mechanisms for extraction of Cs and Sr by different crowns and quite likely the lack of significant mutual extractant interaction.

Similar work was done in Russia. Traditionally, heavy, mostly fluorinated, diluents were used for extraction. The fluorinated alcohols, mainly 1,1,7-trihydrododecafluoroheptan-1-ol ($HCF_2CF_2CF_2CF_2CF_2CF_2CH_2OH$, THDFH), offer the best compromise between viscosity, density, solubility in aqueous solutions, and dissolving ability; therefore, preference was given to this compound as diluent for alkyl

crown ethers showing very good influence on extraction ability for different crown ethers,[60,61] dibenzocrown ethers,[62] phosphorylated crown ethers, and their mixtures with alkyl crown ethers.[63] For example, dibenzo-18-crown-6 in dodecafluoroheptanol effectively extracts cesium and rubidium,[62] whereas the extraction ability of its solution in a diluent such as chloroform is low. In all cases, solvents containing crown ethers in fluorinated alcohol diluent processed a stronger extraction ability than obtained with other diluents (e.g., chloroform, octanol, etc.).

In the late 1980s in the USSR, the specialists of "Mayak" PA and the All-Union Research Institute of Chemical Technology (VNIICT) developed the extraction technology on the basis of DCH18C6 adapted to recovery of strontium-90 and tested it on real solutions. In the course of pilot-industrial tests, ~110 m^3 HLW were reprocessed, and ~1.5×10^6 Ci of ^{90}Sr were recovered into concentrate.[61] Therefore, extraction of both cesium and strontium by a mixture of two crowns seems very attractive. After selection and comparison of many crown ethers, dibenzo-21-crown-7 (DB21C7) was selected as the cesium extractant.[64] Mixture of these two crown ethers shows the best results when a mixture of THDFH and synthanol (mixture of PEG ethers of normal C$_{12}$-C$_{14}$ aliphatic alcohols) was used as the diluent. Data for extraction of Cs and Sr for varying crown ether concentrations are shown in Table 6.3.

Barium and lead are also well extracted. A solution of the potassium salt of ethylenediaminetetraacetic acid (EDTA) with pH=8–9 was proposed to strip the lead and regenerate the solvent for further use. The high radiation stability of this solvent was also shown. Distribution ratios for extraction of Sr by DCH18C6 in THDFH and Cs by DB21C7 in THDFH after irradiation are shown in Table 6.4.

Two dynamic experiments with the extractant mixture of 0.06 M DB21C7 with 0.08 M DCH18C6 in the mixed diluent THDFH/synthanol (87:13 v:v) were performed. The technological flowsheet (see Figure 6.4) includes eight stages of extraction, two

TABLE 6.3

Extraction of Cesium and Strontium from 3 M Nitric Acid

DCH18C6 and DB21C7 (mol/L)	D_{Sr}	D_{Cs}
0.04	1.65	1.16
0.05	2.3	2.3
0.06	2.99	3.47
0.07	3.66	4.64
0.08	4.33	5.79
0.09	5.0	6.95
0.1	5.67	8.11

Source: Data from Glagolenko, J.V., Logunov, M.V., Mamakin, I.V., et al. Extraction of radionuclides by crown ether-containing extractants. Pat WO2006036083 (Publ. 6.4.2006). With permission.

Note: Initial aqueous phase: [Sr] = 1 g/L, [Cs] = 1 g/L, [HNO3] = 1 M. Organic phase: [DCH18C6] = [DB21C7]; THDFH + synthanol (87:13 v:v) as diluent.

TABLE 6.4

Radiation Influence on Extraction

Crown-Ether	Extracted Metal	Distribution Ratio				
		Before Irradiation	After Dose 100 KGy	% of Initial	After Dose 285 KGy	% of Initial
DCH18C6	Sr	3.6	3.4	94.4%	3.0	83.
DB21C7	Cs	2.83	2.83	100%	2.65	93.8

Source: Glagolenko, J.V., Logunov, M.V., Mamakin, I.V. et al. Extraction of radionuclides by crown ether-containing extractants. Pat WO2006036083 (Publ. 6.4.2006).

Note: Organic phase: solution of corresponding crown-ether in THDFH.
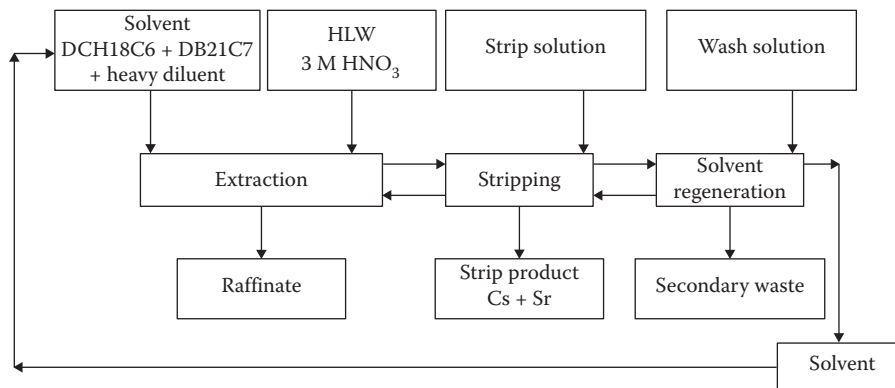
FIGURE 6.4 Test flowsheet for cesium and strontium extraction by crown mixture.

stages of scrubbing with deionized water, eight stages of stripping with deionized water, and regeneration of solvent using the potassium salt of EDTA at pH = 8–9.

Simulated solutions of Russian waste and INL (Idaho National Laboratory, USA) waste were used as feed solutions. Extraction of cesium was 98.4%, and of strontium, 98.1%. A problem with low solubility of the crown ethers (<180 mg/L for all type of solutions) was shown in the tests. The authors pointed out the main positive features of the proposed flowsheet: a salt-free strip product with very low nitric acid concentration (<0.1 M), possibility to extract both cesium and strontium, and low losses of extractants. A last step in the modification of this solvent was the addition of polyalkylphosphonitrilic acid to the mixture of crown ethers.[65] Positive results were obtained for extraction of not only Cs and Sr, but also MAs from simulated HLW.

6.3.2 MIXTURE OF CROWNS AND CALIXARENES

Calix-crowns extract cesium from acidic and alkaline solutions with extremely high Cs/Na selectivity.[66–71] Because their selectivity is higher, it seems promising to use the calix-crown instead of DB21C7 for extraction of cesium in mixtures with the

corresponding crown ether for extraction of strontium. Indeed, such mixture shows very promising properties for simultaneous extraction of cesium and strontium.[72,73] The new FPEX process solvent used in this study was a mixture of 0.15 M DtBuCH18C6, 0.007 M BOBCalixC6, and 0.75 M Cs-7SB modifier in Isopar L. Formulas of these compounds are presented in Figure 6.5.

The influence of the two active components with one another was studied. It was shown that increasing the DtBuCH18C6 concentration in the mixture results in increasing Sr distribution ratios, but slightly decreasing cesium distribution ratios (see Figure 6.6).
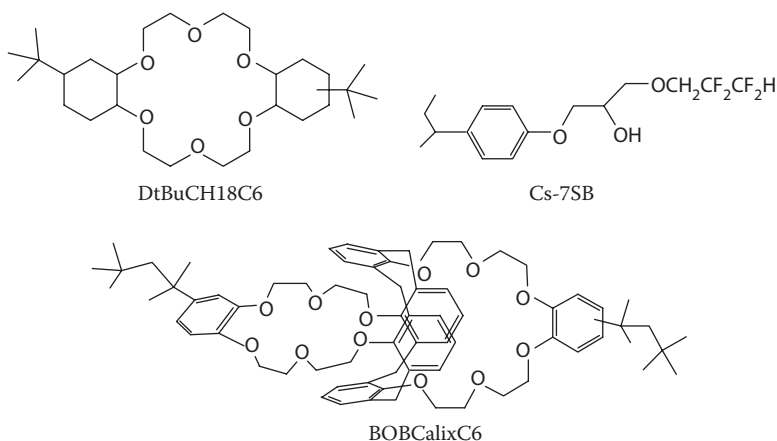
FIGURE 6.5 The structures of the FPEX solvent, consisting of 4,4′,(5′)-di(*tert*-butylcyclohexano)-18-crown-6(DtBuCH18C6),calix[4]arene-bis(*tert*-octylbenzo-crown-6) (BOBCalixC6), and 1-(2,2,3,3-tetrafluoropropoxy)-3-(4-*sec*-butylphenoxy)-2-propanol modifier (Cs-7SB).
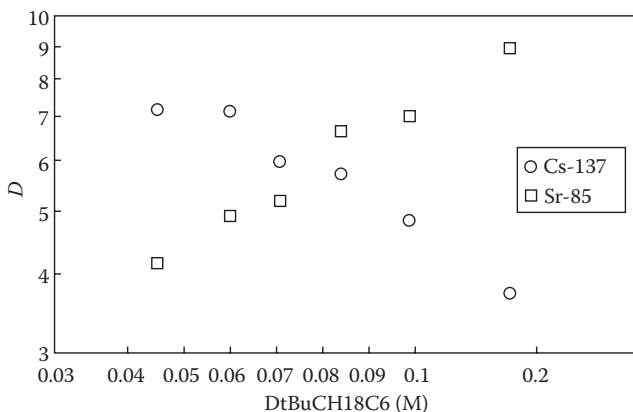
FIGURE 6.6 D_{Cs} and D_{Sr} in 1 M HNO$_3$ versus DtBuCH18C6 concentration in the CSSX solvent (0.007 M BOBCalixC6, 0.75 M Cs-7SB modifier, and 0.003 M TOA in Isopar L). (From Riddle, C.L., Baker, J.D., Law, J.D., McGrath, C.A., Meikrantz, D.H., Mincher, B.J., Peterman, D.R., Todd, T.A., *Solvent Extr. Ion Exch.* 23 (3), 449–461, 2005. With permission.)

Very good results for the combined extraction of Cs and Sr from acidic solution were achieved. Increasing the modifier content also increases the distribution ratios. However, there are no data about the extraction of other metals by this solvent. Neutral crown ethers and calix-crowns extract cesium and strontium by a similar mechanism, namely ion-pair extraction. Therefore, a combination of extractants of this type are close to additive in terms of the resulting extraction, typically with slight if any mutual weakening. The weakening can be explained, at least in part, by the additional extraction of nitric acid, because of the increase in the greater total concentration of extractants in the organic phase.

6.3.3 Mixture of Crowns and Neutral Organophosphorus Compounds

Phosphine oxides and carbamoylmethylphosphine oxides are very effective extractants for MAs and have been investigated widely. A combination of crown ethers with carbamoylmethylphosphine oxide was proposed to obtain combined extraction of MAs and strontium from acidic solutions.[74,75] Simultaneous extraction of actinides, technetium, and strontium was achieved using a mixture of 0.2 M DtBuCH18C6, 0.2 M CMPO, and 1.2 M diamylamylphosphonate (DAAP) in Isopar L. It was shown that all targeted metals—strontium, uranium, americium, and technetium—are extracted by this solvent from 1 to 2 M nitric acid. Dynamic testing was performed with a flowsheet consisting of six stages of extraction, five stages of scrubbing by two scrub solutions, three stages of stripping, five stages of scrubbing after stripping, and finally one stage of carbonate washing to remove residual uranium and technetium (Figure 6.7). There are two strip products in this flowsheet; one contains Sr with actinides, except uranium, and the second contains uranium and technetium. Cesium is not extracted by this solvent and should remain in the raffinate. A new stripping agent, tetrahydrofurantetracarboxylic, acid, was used for this process. There was no explanation reported for the many scrubbing stages. Unfortunately, two salt reagents were used, aluminum nitrate for scrubbing of the saturated solvent and sodium carbonate for solvent regeneration.

More detailed investigation of this extraction system was reported.[75] Tetrahydrofuran-2,3,4,5-tetracarboxylic acid (THFTCA) properties, such as the distribution of THFTCA into the organic phase as a function of its concentration and acidity, were studied, and the separation of UO_2^{2+} ion from Np(IV), Eu(III), Am(III), and Pu(IV) was optimized. This system seems promising to extract main radionuclides except cesium.

The mixture of DCH18C6 ether with different alkyl phosphine oxides (POR, mixture of isomers $C_5H_{11}(C_7H_{15}-C_9H_{19})_2P(O)$) was proposed.[76] Lanthanides (cerium and promethium) and strontium are extracted from 1 M nitric acid with an organic phase consisting of 0.1 M DCH18C6 ether and 0.8 M POR in tetrachloroethane. Distribution ratios are 6.7 for strontium, 14 for cerium, and 21 for promethium. Strontium was stripped by water and REEs by 4 M nitric acid, so separation can be done on stripping. However, at nitric acid content in the aqueous phase above 2 M, only strontium is extracted in the organic phase. In this case, the solvent is working as a crown solution, and POR is used as an additional diluent for Sr extraction.
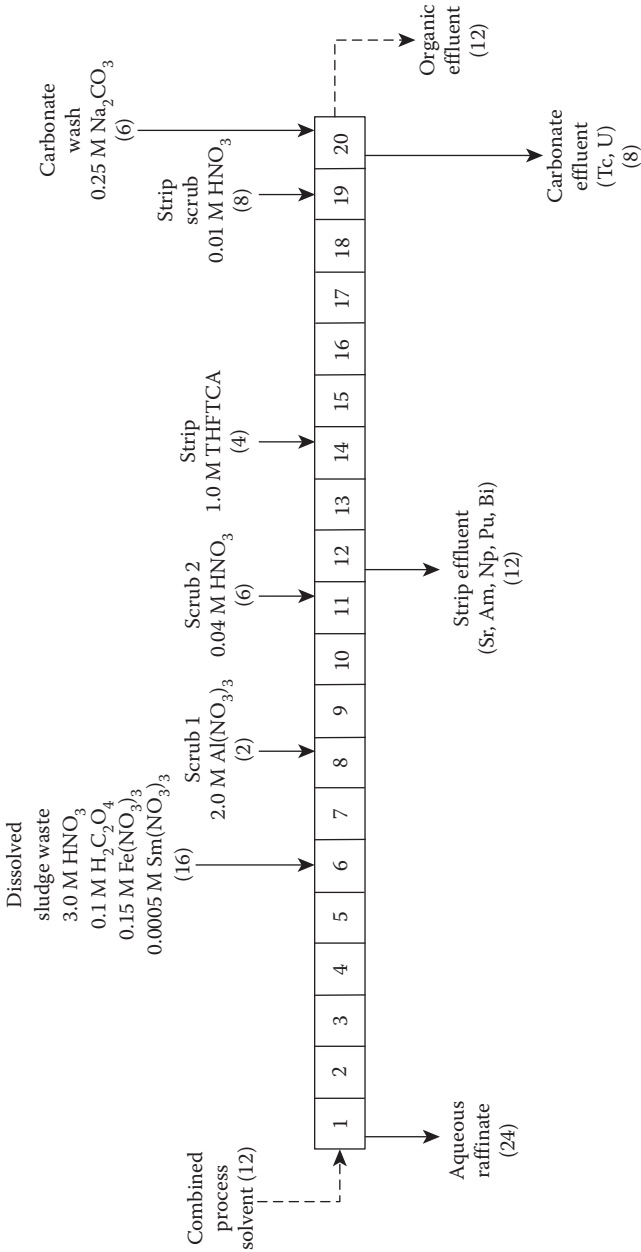
FIGURE 6.7 The flowsheet of a combined crown ether-carbamoylmethylphosphine oxide process. (From Horwitz, E.P., Dietz, M.L., Diamond, H., Rogers, R.A., Leonard, R.A., *Chemical Pretreatment of Nuclear Waste for Disposal*, Plenum Press, New York, 1994. With permission.)

6.4 CONCLUSION

The data presented show that in many cases the combination of two or three extractants gives very positive results regarding the possibility to simultaneously extract different radionuclides. At the same time, the combination of two extractants is the combination of not only their advantages but also their drawbacks.

For example, metals may be stripped from neutral-extractant combinations by diluted nitric acid or simply by water. Stripping is only possible by high concentrations of nitric acid or by complexant solutions after the addition of acidic coextractants (e.g., HDEHP) to such systems. Extraction ability of extractant mixtures can change in different ways. Synergistic or antisynergistic (antagonistic) effects can be observed for metal extraction. Coextractants play different roles in extraction mixture. Not only can they change the extraction ability, but they can also act as phase modifiers. Sometimes coextractants can increase the solubility of a given extractant in the solvent and therefore the extraction capacity. The key question of influence of one extractant on the other lies in the extraction mechanism. When the extraction mechanism is basically the same (mixture of crowns, crown-calixarene mixture), results can approach superposition of extractant strengths (additive extraction). Mutual influence is not very strong in such cases. More or less high synergistic effect can usually be observed with mixtures of extractants with different extraction mechanisms (e.g., mixture of an acid with a neutral extractant).

There are many different technological tasks for HLW processing, an important one being to extract all the MAs. Cesium and strontium should be in the raffinate and converted to glass. Actinides should also be vitrified to a stable form for storage and transmutation in the future. A disadvantage of such a version is the high volume of the Cs-Sr vitrified fraction, which includes all stable nonextracted metals. Alternatively, preliminary extraction of cesium and strontium would make the next process (MAs extraction) easier. In this version, cesium and strontium can be vitrified commonly or separately, but the activity of the resulting solid will be higher than in the first process. The raffinate after Cs and Sr extraction can be processed to extract actinides or directly converted to a solid form (of course, with lower concentration of actinides and higher volume). There are many examples of common extraction of cesium and strontium. Interest in such technologies is connected with the fact that these radionuclides have the most gamma radioactivity and heat generation over the first few hundred years of storage. Therefore, their removal makes the next processing easier. A known process of cesium and strontium extraction using CCD and PEG in *meta*-nitrobenzotrifluoride has been working on an industrial scale for some years at the "Mayak" facility (Ozersk, Russia). By the end of 2001, 1200 m^3 of HLW was treated on the UE-35 installation of the Mayak Production Association, and 50×10^6 Ci of Cs and Sr have been recovered.[77] The combination of both approaches is embodied in the UNEX process,[34,35,78] where not only MAs, but also cesium and strontium are extracted in one cycle. All tested versions of the UNEX process were with simultaneous extraction and simultaneous stripping of radionuclides. But there are possibilities to separate different nuclides in a modified UNEX process with selective stripping. Such a modified flowsheet would be more

complicated, but it is much more compact in comparison with use of several extraction cycles for separation of different nuclides separately.

Optimization of the solvent content for extraction of all desired nuclides with very similar distribution ratios is also a serious task in the search for optimal mixed solvents. Dependencies of distribution ratios with change of extractant concentrations are not predictable as a rule. Thus, only experimental work can give an answer about final solvent content.

Currently, the situation seems promising for the study of new solvents for common radionuclide extraction. However, to date, only empirical investigation has been performed. The problem of gaining a quantitative description of coextractant influence on one another has practically not been investigated. But the attractive target, to create a simple and cost-effective flowsheet for HLW processing, is the serious reason to continue the efforts in this direction.

REFERENCES

1. Horwitz, E.P., Schulz, W.W. Solvent extraction in the treatment of acidic high-level liquid waste: Where do we stand? In Bond, A.H., Dietz, M.L., Rogers, R.D. Eds., *Metal Ion Separation and Preconcentration: Progress and Opportunities*, ACS Symposium Series 716. ACS, Washington, DC, (1999), pp. 20–50.
2. Mathur, J.M., Murali, M.S., Nash, K.L. Actinides partitioning—A review. *Solvent Extr. Ion Exch.* (2001), 19 (3), 357–390.
3. Paiva, A.P., Malik, P. Recent advances on the chemistry of solvent extraction applied to the reprocessing of spent nuclear fuels and radioactive wastes. *J. Radioanal. Nucl. Chem.* (2004), 261 (2), 485–496.
4. Horwitz, E.P., Kalina, D.G., Diamond, H., Vandegrift, G.F., Schulz, W.W. The TRUEX process – a process for the extraction of the transuranic elements from nitric acid wastes utilizing modified Purex solvent. *Solvent Extr. Ion Exch.* (1985), 3 (1&2), 75–109.
5. Horwitz, E.P., Dietz, M.L., Fisher, D.E. SREX. A new process for the extraction and recovery of strontium from acidic nuclear waste streams. *Solvent Extr. Ion Exch.* (1991), 9 (1), 1–25.
6. Wood, D.J., Law, J.D., Tullock, P.A. Extraction of lead and strontium from hazardous waste streams by solvent extraction with 4,4',(5')-di-(t-butyldicyclohexo)-18-crown-6. *Solvent Extr. Ion Exch.* (1997), 15 (1), 65–78.
7. Todd, T.A., Mann, N.R., Tranter, T.J., Šebesta, F., John, J., Motl, A. Cesium sorption from concentrated acidic tank wastes using ammonium molybdophosphate-polyacrylonitrile composite sorbents. *J. Radioanal. Nucl. Chem*. (2002), 254 (1), 47–52.
8. Dozol, J.F., Dozol, M., Macias, R.M. Extraction of strontium and cesium by dicarbollides, crown ethers and functionalized calixarenes. *J. Incl. Phenom. Macrocyclic Chem.* (2000), 38 (1–4), 1–22.
9. Regalbuto, M.C., Copple, J.M., Leonard, R., Pereira, C., Vandegrift, G.F. Solvent extraction process development for partitioning and transmutation of spent fuel. In *Actinide and Fission Product Partitioning and Transmutation*. Eighth Information Exchange Meeting, NEA, Paris, France, November 9–11, 2004, pp. 373–385.
10. Pereira, C., Vandegrift, G., Regalbuto, M., Aase, S., Bakel, A., Bowers, D., Byrnes, J., Clark, M., Emory, J., Falkenberg, J.R., Gelis, A., Hafenrichter, L., Leonard, R., Quigley, K., Tsai, Y., Pol, M.V., Laidler, J. Lab-scale demonstration of the UREX+2 process using spent fuel. In *Waste Management* Conference, WM Symposia, Tempe, AZ, February 27 to March 3, 2005.

11. Madic, C., Boullis, B., Baron, P., Testard, F., Hudson, M.J., Liljenzin, J.-O., Christiansen, B., Ferrando, M., Facchini, A., Geist, A., Modolo, G., Espartero, A.G., De Mendoza, J. Futuristic back-end of the nuclear fuel cycle with the partitioning of Mas. *J. Alloys Compd.* (2007), 444–445, 23–27.

12. Hill, C., Dozol, J.-F., Lamare, V., Rouquette, H., Eymard, S., Tournois, B., Vicens, J., Asfari, Z., Bressot, C., Ungaro, R., Casnati, A. Nuclear waste treatment by means of supported liquid membranes containing calixcrown compounds. *J. Incl. Phenom. Macrocyclic Chem.* (1994), 19 (1–4), 399–408.

13. Koma, Y., Watanabe, M., Nemoto, S., Tanaka, Y. A counter current experiment for the separation of trivalent actinides and lanthanides by the SETFICS process. *Solvent Extr. Ion Exch.* (1998), 16 (6), 1357–1367.

14. Ozawa, M., Koma, Y., Nomura, K., Tanaka, Y. Separation of actinides and fission products in high-level liquid wastes by the improved TRUEX process. *J. Alloys Compd.* (1998), 271–273, 538–543.

15. Shadrin, A., Babain, V., Kamachev, V., Koyama, T., Kamiya, N. Fluoropole-732 as a diluent for SETFICS-process. *Proc. Int. Conf. Global '03*, Atomic Nuclear Society, La Grange Park, IL, November 16–22, 2003, pp. 728–731.

16. Shadrin, A., Kamachev, V., Kvasnitsky, I., Romanovsky, V., Bondin, V., Krivitsky, Y., Alekseenko, S. Extraction reprocessing of HLW by modified SETFICS-process. *Proc. of Global '05*, Atomic Energy Society of Japan, Tokyo, Japan, October 9–13, 2005, Paper No. 129.

17. Rais, J., Selucky, P., Kyrs, M. Extraction of caesium into nitrobenzene in the presence of univalent polyhedral borate anions. *J. Inorg. Nucl. Chem.* (1976), 38 (7), 1376–1378.

18. Rais, J., Grüner, B. Extraction with metal Bis(dicarbollide) anions. In Marcus, Y., SenGupta, A.K. Eds., *Ion Exchange and Solvent Extraction*, Vol. 17. Marcel Dekker, New York, 2004, pp. 243–334.

19. Vaňura, P. The extraction behavior of some dicarbollylcobaltate crown extraction systems. *J. Radioanal. Nucl. Chem.* (1998), 228 (1–2), 43–46.

20. Valentová, Z., Vaňura, P., Makrlík, E. Extraction of microamounts of strontium into nitrobenzene by using hydrogen dicarbollylcobaltate in the presence of dicyclohexyl-18-crown-6. *J. Radioanal. Nucl. Chem.* (2006), 267 (2), 471–475.

21. Vaňura, P., Makrlík, E. Extraction of microamounts of yttrium from water into nitrobenzene using hydrogen dicarbollylcobaltate in the presence of 15-crown-5. *J. Radioanal. Nucl. Chem.* (2006), 267 (1), 251–254.

22. Luther, T.A., Herbst, R.S., Peterman, D.R., Tillotson, R.D., Garn, T.G., Babain, V.A., Smirnov, I.V., Stoyanov, E.S., Antonov, N.G. Some aspects of fundamental chemistry of the Universal Extraction (UNEX) process for the simultaneous separation of major radionuclides (cesium, strontium, actinides, and lanthanides) from radioactive wastes. *J. Radioanal. Nucl. Chem.* (2006), 267 (3), 603–613.

23. Smirnov, I.V., Babain, V.A., Shadrin, A.Yu., Efremova, T.I., Bondarenko, N.A., Herbst, R.S., Peterman, D.R., Todd, T.A. Extraction of americium and europium by diphosphine dioxides and their mixtures with chlorinated cobalt dicarbollide. *Solvent Extr. Ion Exch.* (2005), 23 (1), 1–21.

24. Smirnov I.V. Anomalous effects in extraction of lanthanides and actinides with bidentate neutral organophosphorus extractants. Role of proton hydrate solvates. *Radiochemistry* (2007), 49 (1), 44–54.

25. Stoyanov, E.S., Smirnov, I.V. Proton solvates, $H^+ \cdot nH_2O \cdot mL$, formed by diphosphine dioxides with chlorinated cobalt(III) dicarbollide acid. *J. Mol. Struct.* (2005), 740 (1–3), 9–16.

26. Kyrš, M., Svoboda, K., Lhoták, P., Alexová, J. Solvent extraction of europium from nitric acid solutions into chlorobenzene in the presence of calixarenes and dicarbollides. *J. Radioanal. Nucl. Chem.* (2002), 254 (3), 455–464.

27. Kyrš, M., Svoboda, K., Lhoták, P., Alexová, J. Synergistic solvent extraction of Eu, Sr and Cs into chlorobenzene solutions of the three conformers of tetrathiocalixarene and dicarbollide. *J. Radioanal. Nucl. Chem*. (2003), 258 (3), 497–509.

28. Reinoso-García, M.M., Verboom, W., Reinhoudt, D.N., Brisach, F., Arnaud-Neu, F., Liger, K. Solvent extraction of actinides and lanthanides by CMP(O)- and N-acyl(thio) urea-tetrafunctionalized cavitands: Strong synergistic effect of cobalt bis(dicarbollide) ions. *Solvent Extr. Ion Exch*. (2005), 23 (3), 425–437.

29. Stoyanov, E.S., Vorob'yova, T.P., Smirnov, I.V. Cationic complexes of Eu(III) and Sr(II) with diphosphine dioxides in organic extracts. *J. Struct. Chem*. (2005), 46 (5), 829–838.

30. Coupez, B., Wipff, G. The synergistic effect of cobalt-dicarbollide anions on the extraction of M^{3+} lanthanide cations by calix[4]arenes: A molecular dynamics study at the water–'oil' interface. *C.R. Chimie* (2004) 7(12), 1153–1164.

31. Rais, J., Tachimori, S. Extraction separation of tervalent americium and lanthanides in the presence of some soft and hard donors and dicarbollide. *Sep. Sci. Technol.* (1994), 29 (10), 1347–1365.

32. Krejzler, J., Narbutt, J., Foreman, M.R.St.J., Hudson, M.J., Casensky, B., Madic, C. Solvent extraction of Am(III) and Eu(III) from nitrate solution using synergistic mixtures of N-tridentate heterocycles and chlorinated cobalt dicarbollide. *Czech. J. Phys.* (2006), 56 (Suppl. D), D459–D467.

33. Alyapyshev, M.Yu., Babain, V.A., Smirnov, I.V. Extractive properties of synergistic mixtures of dipicolinic acid diamides and chlorinated cobalt dicarbollide. *Radiochemistry* (2004), 46 (3), 270–271.

34. Romanovskiy, V.N., Babain, V.A., Alyapyshev, M.Yu., Smirnov, I.V., Herbst, R.S., Law, J.D., Todd, T.A. Radionuclide extraction by 2,6-pyridinedicarboxylamide derivatives and chlorinated cobalt dicarbollide. *Sep. Sci. Technol.* (2006), 41 (10), 2111–2127.

35. Peterman, D.R., Herbst, R.S., Law, J.D., Tillotson, R.D., Garn, T.G., Todd, T.A., Romanovsky, V.N., Babain, V., Alyapyshev, M. Yu, S., Smirnov, I.V. Diamide derivatives of dipicolinic acid as actinide and lanthamide extractants in a variation of the UNEX process. *Proc. Int. Conf. Global'07,* Boise, ID, September 9–13 (2007), pp. 1106–1110, *Amer. Nucl. Soc*., La Grange Park, USA.

36. Galletta, M., Macerata, E., Mariani, M., Giola, M., Casnati, A., D'Arpa, O., Ungaro, R. A study on synergistic effects and protonation of a selected calixarene based picolinamide ligand used in the An/Ln separation. *Czech. J. Phys.* (2006), 56 (Suppl. D), D453–D458.

37. Casnati, A., Della Ca', N., Fontanella, M., Sansone, F., Ugozzoli, F., Ungaro, R., Liger, K., Dozol, J.-F. Calixarene based picolinamide extractants for the selective An/Ln separation from radioactive waste. *Eur. J. Org. Chem.* (2005), 2005 (11), 2338–2348.

38. Mariani, M., Macerata, E., Galletta, M., Buttafava, A., Casnati, A., Ungaro, R., Faucitano, A., Giola, M. Partitioning of MAs: Effects of gamma irradiation on the extracting capabilities of a selected calixarene-based picolinamide ligand. *Rad. Phys. Chem.* (2007), 76, 1285–1289.

39. Mowafy, E.A., Shalash, A.M., El-Naggar, I.M. Extraction of certain radionuclides by bipicolinamides as new extractants from nitric acid medium. *Ind. J. Chem. A* (2003), 42 (12), 3012–3016.

40. Nigond, L., Condamines, P.Y., Cordier, J., Livet, C., Madic, C., Cuillerdier, C., Musikas, C., Hudson, M.J. Recent advances in the treatment of nuclear wastes by the use of diamide and picolinamide extractants. *Sep. Sci. Technol.* (1995), 30 (7–9), 2075–2099.

41. Shimada, A., Yaita, T., Narita, H., Tachimori, S,, Kimura, T., Okuno, K., Nakano, Y. Extraction of Am(III) and lanthanide(III) ions from HNO_3 solutions using N,N'-dimethyl-N,N'-diphenylpyridine-2,6- dicarboxyamide. *Solvent Extr. Res. Dev. Jpn.* (2004), 11, 1–10.

42. Babain, V.A., Alyapyshev, M.Yu., Smirnov, I.V., Shadrin, A.Yu. Extraction of Am and Eu with N,N′-substituted pyridine-2,6-dicarboxamides in fluorinated diluents. *Radiochemistry* (2006), 48 (4), 369–373.

43. Babain, V.A., Alyapyshev, M.Yu., Kiseleva, R.N. Metal extraction by N,N'-dialkyl-N,N'-diaryl-dipicolinamides from nitric acid solutions. *Radiochim. Acta* (2007), 95 (4), 217–223.

44. Logunov, M.V., Skobtsov, A.S., Mesentsev, V.A., Mashkin, A.N., Babain, V.A., Smirnov, I.V., Alyapysev, M.Yu., UNEX process for processing of HLW with high concentration of rare-earth metals. II. *Voprosi radiatsionnoy bezopasnosti* (2006), 4 (44), 3–12. (In Russian.)

45. Delmau, L.H., Simon, N., Schwing-Weill, M.-J., Arnaud-Neu, F., Dozol, J.-F., Eymard, S., Tournois, B., Grüttner, C., Musigmann, C., Tunayar, A., Böhmer, V. Extraction of trivalent lanthanides and actinides by 'CMPO-like' calixarenes. *Sep. Sci. Technol*. (1999), 34 (6), 863–876.

46. Shishkin, D.N., Galkin, B.Ya., Fedorov, Yu.S., Zilberman, B.Ya., Shmidt, O.V. Partitioning of high-level waste with an extractant based on chlorinated cobalt dicarbollide and dibutylphosphoric acid zirconium salt. *Radiochemistry* (2003), 45 (6), 577–580.

47. Shmidt, O.V., Zilberman, B.Ya., Fedorov, Yu.S., Suglobov, D.N., Puzikov, V.A., Mashirov, L.G., Palenik, Yu.V., Glekov, R.G. Extraction properties of dibutylphosphoric acid zirconium salt in recovery of transplutonium and rare-earth elements from nitric acid solution. *Radiokhimiya* (2002), 44 (5), 428–433.

48. Gerow, I.H., Davis, Jr., M.W. The use of 24-crown-8's in the solvent extraction of $CsNO_3$ and $Sr(NO_3)_2$. *Sep. Sci. Technol.* (1979), 14 (5), 395–414.

49. Gerow, I.H., Smith, Jr., J.E., Davis, Jr., M.W. Extraction of Cs and Sr from HNO_3 solution using macrocyclic polyethers. *Sep. Sci. Technol.* (1981), 16 (5), 519–548.

50. Moyer, B.A., McDowell, W.J., Ontko, R.J., Bryan, S.A., Case, G.N. Complexation of strontium in the synergistic extraction system dicyclohexano-18-crown-6, versatic acid, carbon tetrachloride. *Solvent Extr. Ion Exch.* (1986), 4 (1), 83–93.

51. Delmau, L.H., Bonnesen, P.V., Engle, N.L., Haverlock, T.J., Sloop, Jr., F.V., Moyer, B.A. Combined extraction of cesium and strontium from alkaline nitrate solutions. *Solvent Extr. Ion Exch.* (2006), 24 (2), 197–217.

52. Samy, T.M., Imura, H., Suzuki, N. Solvent extraction of lanthanoid(III) with 18-crown-6 from aqueous trichloroacetate solutions to 1,2-dichloroethane. *J. Radioanal. Nucl. Chem.* (1988), 126 (2), 153–163.

53. Ramadan, A., Mahmoud, M., Khalifa, S.M., Souka, N. Extraction of Eu(III) by dinonyl-naphthalenesulfonic acid and synergistic effects of crown ethers and trioctylphosphine oxide. *J. Radioanal. Nucl. Chem.* (1993), 176 (6), 457–470.

54. Dhami, P.S., Chitnis, R.R., Gopalakrishnan, V., Wattal, P.K., Ramanujam, A., Bauri, A.K. Studies on the partitioning of actinides from high level waste using a mixture of HDEHP and CMPO as extractant. *Sep. Sci. Technol.* (2001), 36 (2), 325–335.

55. Gannaz, B., Chiarizia, R., Antonio, M.R., Hill, C., Cote, G. Extraction of lanthanides(III) and Am(III) by mixtures of malonamide and dialkylphosphoric acid. *Solvent Extr. Ion Exch.* (2007), 25 (3), 313–337.

56. Madic, C., Lecomte, M., Baron, P., Boullis, B. Separation of long-lived radionuclides from high active nuclear waste. *C.R. Physique* (2002), 3 (7–8), 797–811.

57. Heres, X., Ameil, E., Martinez, I., Baron, P., Hill, C. Extractant separation in Diamex-Sanex process. *Proc. Int. Conf. Global' 2007,* Boise, ID, September 9-13, (2007), p. 699. *Amer. Nucl. Soc.,* La Grange Park, USA.

58. Dietz, M.L., Horwitz, E.P., Bartsch, R.A., Barrans, R.E., Rausch, Jr., D. Composition and process for separating cesium ions from an acidic aqueous solution also containing other ions. US Patent No. 5888398. Issued March 30, 1999.

59. Horwitz, E.P., Dietz, M.L., Leonard, R.A. Proc. of the Efficient separations and processing crosscutting program. Technical Exchange Meeting, January 28–30, (1997), Gaithersburg, MD, Report PNNL-SA-28461, Pacific Northwest National Laboratory, Richland, WA.

60. Mamakin, I.V., Nardova, A.K., Filippov, E.A. Method for extraction recovery of strontium. RU Patent 1706661 (Publ. 23.01.1992, Bull. Inv. N 3).

61. Filippov, E.A., Dzekun, E.G., Nardova, A.K. Mamakin, I.V., Gelis, V.M., Mityutin, V.V. Application of crown-ethers and ferrocyanide-based inorganic materials for cesium and strontium recovery from high-level radioactive wastes. In *Proc. Symp. Waste Management*, Tucson, AZ, Vol. 2, 1992, pp. 1021–1024.

62. Smirnov, I.V., Babain, V.A. Method of extractive extraction of cesium and rubidium. Patent RU 1.695.547 (Publ. 04.27.1997. Bull. Inv. 12/1997).

63. Smirnov, I.V., Babain, V.A., Bardov, A.I. Method for extraction recovery of cesium. Patent RU 1768216 (Publ. 15.10.1992, Bull. Inv. N 38).

64. Glagolenko, J.V., Logunov, M.V., Mamakin, I.V., Polosin, V.M., Rovni, S.I., Starchenko, V.A., Shishclov, J.P., Yakovlev, N.G. Extraction of radionuclides by crown ether-containing extractants. Pat WO2006036083 (Publ. 6.4.2006).

65. Filippov, E.A., Ruzin, L.I., Mamakin, I.V. Development of complex flowsheet of HLW partitioning by solvents on the base of crown ethers and polyorganophosphazenes in heavy diluent. In Khol'kin, A.I. Ed., *Khimiya i tekhnologiya ekstraktsii* (*Extraction Chemistry and Technology*), Vol. 2. Moscow, 2001, pp. 50–63. (In Russian.)

66. Dozol, J.F., Simon, N., Lamare, V., Roquette, H., Eymard, S., Tournois, B., DeMarc, D., Macias, R.M. Solution for Cs removal from high-salinity acidic or alkaline liquid waste: The crown calix[4]arenes. *Sep. Sci. Technol.* (1999), 34 (6&7), 877–909.

67. Leonard, R.A., Conner, C., Liberatore, M.W., Sedlet, J., Aase, S.B., Vandergrift, G.F., Delmau, L.H., Bonnesen, P.V., Moyer, B.A. Development of a solvent extraction process for cesium removal from SRS tank waste. *Sep. Sci. Technol.* (2001), 36 (5&6), 743–766.

68. Casnati, A., Pochini, A., Ungaro, R., Ugozzoli, F., Arnaud, F., Fanni, S., Schwing, M.J., Egberink, R.J.M., DeJong, F., Rienhoudt, D.N. Synthesis, complexation and membrane transport studies of 1,3-alternate calix[4]arene crown-6 conformers: A new class of cesium selective ionophores. *J. Am. Chem. Soc.* (1995), 117, 2767–2777.

69. Sachleben, R.A., Bonnesen, P.V., Descazeaud, T., Haverlock, T.J., Urvoas, A., Moyer, B.A. Surveying the extraction of cesium nitrate by 1,3-alternate calix[4]- arene crown-6 ethers in 1,2-dichloroethane. *Solvent Extr. Ion Exch.* (1999), 17 (6), 1445–59.

70. Bonnesen, P.V., Haverlock, T.J., Engle, N.L., Sachleben, R.A., Moyer, B.A. Development of process chemistry for the removal of cesium from acidic nuclear waste by calix[4]arene-crown-6 ethers. In Lumetta, G.J., Rogers, R.D., Gopalan, A.S. Eds., *Calixarenes for Separations*, ACS Symposium Series 757. ACS, Washington, DC, 2000, pp. 27–44.

71. Bonnesen, P.V., Delmau, L.H., Moyer, B.A., Leonard, R.A. A robust alkaline-side CSEX solvent suitable for removing cesium from Savannah river high level waste. *Solvent Extr. Ion Exch.* (2000), 18 (6), 1079–1108.

72. Riddle, C.L., Baker, J.D., Law, J.D., McGrath, C.A., Meikrantz, D.H., Mincher, B.J., Peterman, D.R., Todd, T.A. Fission product extraction (FPEX): Development of a novel solvent for the simultaneous separation of strontium and cesium from acidic solutions. *Solvent Extr. Ion Exch.* (2005), 23 (3), 449–461.

73. Meikrantz, D.H., Todd, T.A., Riddle, C.L., Law, J.D., Peterman, D.R., Mincher, B.J., McGrath, C.A., Baker, J.D. Cesium and strontium extraction using a mixed extractant solvent including crown ether and calixarene extractants. Pat WO2006016892 (Publ. 16-02-16-2006).

74. Horwitz, E.P., Dietz, M.L., Diamond, H., Rogers, R.D., Leonard, R.A. Combined TRUEX-SREX extraction/recovery process. In Horwitz, E.P., Schulz, W.W. Eds., *Chemical Pretreatment of Nuclear Waste for Disposal*. Plenum Press, New York, 1994, pp. 81–100.

75. Nash, K.L., Horwitz, E.P., Diamond, H., Rickert, P.G., Muntean, J.V., Mendoza, M.D., Di Giuseppe, G. Selective separation of uranyl ion from TRUs in a combined solvent extraction process using tetrahydrofuran-2,3,4,5-tetracarboxylic acid. *Solvent Extr. Ion Exch.* (1996), 14 (1), 13–33.

76. Prokopchuk, Ju.Z., Logunov, M.V., Trukhanov, S.Ja. Method of strontium and rare-earth elements extraction. Pat RU 2027671.

77. Zilberman, B.Ya. Romanovskii, V.N. Extraction studies at the Khlopin Radium Institute. *Radiochemistry* (2003), 45 (3), 211–218.

78. Romanovskiy, V.N., Smirnov, I.V., Babain, V.A., Todd, T.A., Herbst, R.S., Law, J.D., Brewer, K.N. The universal solvent extraction (UNEX) process. I. Development of the UNEX process solvent for the separation of cesium, strontium, and the actinides from acidic radioactive waste. *Solvent Extr. Ion Exch.* (2001), 19 (1), 1–21.

7 Third-phase Formation in Liquid/Liquid Extraction: A Colloidal Approach

Fabienne Testard
Commissariat á l'Energie Atomique, CEA Saclay

Th. Zemb and P. Bauduin
Institut de Chimie Séparative de Marcoule

Laurence Berthon
Commissariat á l'Energie Atomique, CEA Marcoule

CONTENTS

381

7.1   INTRODUCTION

Hydrometallurgy using liquid/liquid extraction is one of the processes chosen to extract actinides from high-level radioactive liquid wastes. The "Plutonium-URanium EXtraction" (PUREX) process, for example, has been used worldwide since 1950 to separate U(VI) and Pu(IV) from the spent nuclear fuel dissolution liquor (*1*). Due to the high radiotoxicity of minor actinides, specific extraction systems are still under investigation (*2*) to separate additional radionuclides from spent nuclear fuel (*3*). In all liquid/liquid processes, the high loading of the organic solvent with metal salts or acids can sometimes cause a third phase to form. That is, the organic phase splits into two phases of different compositions and densities. In a centrifuge test, third-phase formation generally involves a very viscous phase for which the contactors are not designed to handle. In pulsed columns or Couette-type separators, a viscous emulsion with a lifetime incompatible with processing would occur if a "third phase" arose during operation. This phenomenon is a major drawback in terms of industrial process implementation, as it may cause damage in the continuous countercurrent extraction process. An even more substantial issue is nuclear criticality that may occur when fissile matter becomes locally highly concentrated in the third phase.

It is clear that the problem of third-phase formation has been brought about by the protocol preference to use alkane diluents, because of their excellent hydraulics, low water solubility, high stability, low toxicity, resistance to radiolytic degradation, and low density. Given that extractants and often extraction complexes are highly polar, it is easy to understand the phase incompatibility. Ultimately, the dichotomy between the extraction chemistry we design to occur and the poorly solvating diluent environment in which it must occur frames how we approach the design of extractants and the formulation of solvents. Indeed, this dichotomy lies as the heart of science and technology of solvent extraction itself.

Thus, third-phase formation must be avoided in industrial applications of solvent extraction, and so the precise mechanisms responsible for its occurrence must be understood. Considerable work has thus been devoted to third-phase formation in liquid/liquid extraction. Numerous qualitative studies have been carried out to identify the experimental factors influencing and leading to third-phase formation (*4*). The aim of research in this field is to progress from localization on a phase map to predictive modeling. It has been found empirically, for example, that phase separation could be prevented by tuning the lipophilicity of the extractant molecule or by modifying the nature of the diluent (by increasing polarity, decreasing molecular size, or increasing the branching of alkyl chains) (*5*). Although parameter studies allow the formulation to be modified, there is still a

need for a predictive model of third-phase formation. As highlighted by Chiarizia et al. (*6, 7*), a comprehensive description is still lacking for both the mechanisms of formation and the energetics of the phenomenon at molecular and supramolecular scale.

Considering an extractant solution as a molecular solution does not explain third-phase formation. In line with the pioneering work of Osseo-Asare (*8*), the third phase can be understood by considering the organic phase as a complex fluid involving reverse micelles or a microemulsion (*9*). Reverse micelles consist of a water core containing ionic species, such as salt stabilized by an extractant layer dispersed in an organic medium. A microemulsion is a thermodynamically stable isotropic solution, consisting of water, oil, surfactant, and often a cosurfactant (*10–13*). In the history of microemulsion nomenclature, the third-phase transition corresponds to a transition between a "Winsor II" and a "Winsor III" system. Winsor II is a reverse (i.e., water-in-oil) microemulsion in equilibrium with an aqueous phase, and a Winsor III system is a microemulsion (middle phase) in equilibrium with both the aqueous and oil phases (*14*). The third phase is thus the middle phase of the Winsor III system. Osseo-Asare reviewed the experimental evidence published before 1997 of the existence of reverse micelles in tri-*n*-butyl phosphate (TBP) organic phases. At that time, little was known about the size and shape of these reverse micelles. An idea of the size can either be obtained directly by light scattering in a dilute system or can be inferred from aggregation numbers obtained by various techniques. It was, however, observed that under certain conditions the third-phase formation is related to an extensive aggregation of the metal or acid-extractant complexes in the organic phase for TBP (*8*) and other phosphorous-based extractants (*8, 15–17*). Since 1998, progress in understanding third-phase formation has been driven by direct determination of molecular aggregation obtained via small-angle X-rays and neutron scattering (*18*). Erlinger et al. (*19*) established for the first time the microstructure of the reverse micelles in malonamide organic phases and found evidence that short-range attractive interactions between reverse micelles are at the origin of the phase separation. This approach was then used to explain third-phase formation in several other organic extractant phases, such as TBP (*6, 7, 20–29*), *N,N,N′,N′*-tetraoctyl-3-oxapentanediamide (TODGA) (*30, 31*), diphosphonic acid (*32*), octyl(phenyl)-*N,N′*-diisobutylcarbamoylmethylphosphine oxide (CMPO) (*33*), malonamide (*34–37*), etc.

For all the systems studied, it is now acknowledged that the self-assembling properties of both the extractant and the metal or acid–extractant complexes produce polar cores that are unstable due to short-range attractive interactions. The speciation of supramolecular structure is thus highly important for further progress toward a complete description of liquid/liquid extraction processes (*38*).

In this review, we summarize recent progress in understanding the aggregation states of organic extractant phases in relation to third-phase formation. The organic extractant phase is described from a colloidal standpoint to interpret the phase-separation boundary. The aim is to provide the basis for developing a theoretical approach to predict third-phase formation. Finally, the structure of the third phase is described.

The new features are detailed in this review most using diamide as a model system and illustrated with published data on other extractant systems. Figure 7.1 summarizes the structure of the different extractants cited in this chapter. The mixture of extractants as synergistic systems and extractants, such as the N-polydentate ligands BTP (*39, 40*), BTBP (*41, 42*), or bis-malonamide (*43*), will not be treated here. These extractants have low solubility in alkane and are generally used in chlorinated solvent or octanol or diamide/alkane solution to enhance their solubility.
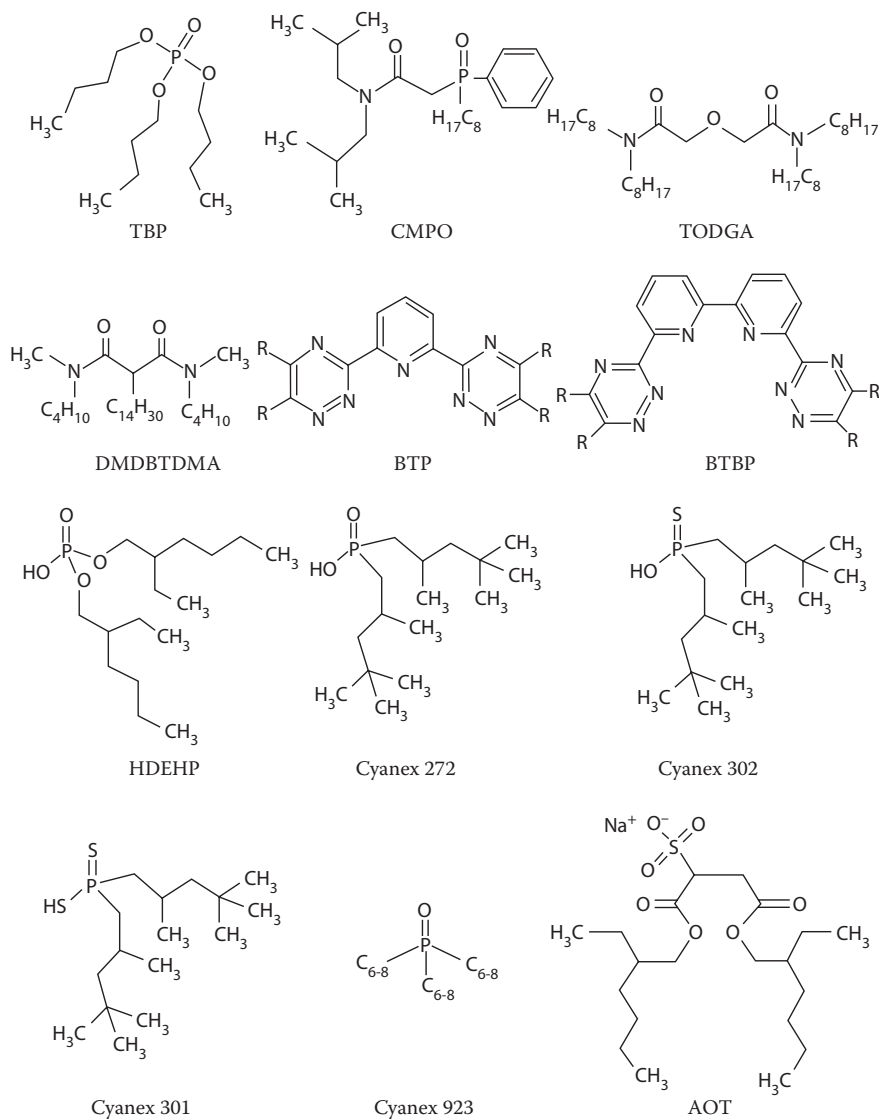
FIGURE 7.1   Formula of the different extractants cited in this review.

7.2   EXTRACTANT SOLUTIONS ARE COMPLEX FLUIDS

7.2.1   AMPHIPHILIC PROPERTIES OF EXTRACTANT

Since the pioneering work by Osseo-Asare (8), it is now well established that extractant solutions are complex fluids rather than molecular solutions. As this author reviewed, self-association of extractants has been observed using a variety of techniques such as infrared spectroscopy, nuclear magnetic resonance, light scattering, calorimetry, and vapor pressure osmometry (VPO) (8). Extractants are amphiphilic due to the conjunction between the polar part of the chelating group and the apolar part of the alkyl chains used to increase their solubility in an organic diluent. Remarkable interfacial activity is observed at the diluent/ aqueous solution macroscopic interface, indicated classically by a decrease in the interfacial tension "γ" as the extractant concentration increases, as shown for a malonamide at the dodecane/water interface (Figure 7.2) (37). The smooth break observed in the γ-log[extractant] curves at the oil/water interface corresponds to the formation of aggregates in the organic phase and can be associated with a critical micellar concentration (cmc) as observed with classical surfactants. The cmc is ideally the threshold concentration of surfactants at which micellization occurs, but for low-surfactant properties, aggregation begins at lower concentration. Therefore, conversely to what is generally admitted, the cmc is not always equal to the concentration of monomers in the solution, which can be determined using the closed association model (44). The chemical potential of the pseudo-phases (micelles and monomers) is imposed by the monomer concentration (45).
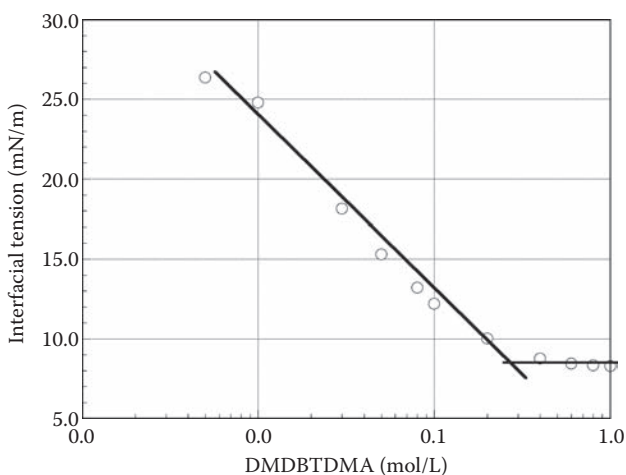
FIGURE 7.2   Interfacial tension at the *n*-dodecane/water interface versus DMDBTDMA concentrations at 25°C for DMDBTDMA/dodecane equilibrated with an aqueous solution containing $Nd(NO_3)_3$ (0.2 M), $LiNO_3$ (1 M), and HNO_3 (0.01 M). A straight line is drawn to estimate the CMC, although in an extractant system (with low surfactant properties), the aggregation is gradual and begins at a concentration lower than the cmc. (From L. Martinet, Organisation Supramoléculaire des Phases Organiques de Malonamides du Procédé d'Extraction DIAMEX. PhD thesis. Rapport CEA-R-6105, 2005.)

The decrease in interfacial tension is related to the amount of extractant adsorbed at the interface through the Gibb's adsorption equation (*46*). The molecular areas of the extractant at the interface can thus be directly obtained from this equation. As an example, an area of 104 ± 8 Å^2 is obtained for the *N,N′*-dimethyl dibutyltetradecylmalonamide (DMDBTDMA) at the dodecane/water interface (*4, 34*). For classical surfactants, it should be noted that a nearly constant area per molecule with the addition of salt strongly suggests that anions and cations are adsorbed and extracted as pairs (*47*). Thus, the variation of the area per molecule with added salt can provide information on the mechanism of extraction.

The cmc values obtained are listed in Table 7.1 for different extractants (malonamides, di(2-ethylhexyl)phosphoric acid (HDEHP), and TBP) (*37, 48–50*) in dodecane contacted with an aqueous phase of various ionic strengths. A high cmc (>0.1 M) indicates a weak surfactant, while a low cmc (<0.1 M) is associated with a "good" surfactant. The cmc range is relatively large and is very dependent on the nature and concentration of the salt in the aqueous phase, even with opposite trends. The interfacial tension measures the amphiphilic properties of the extractant and of extractant complexes with water and electrolyte. Most extractant systems investigated to date, by necessity belong to the class of "poor" surfactants, except the ionic ones such as carbon acids and primary amines, and like most surfactants in nonpolar media (*10*), they self-aggregate in a progressive stepwise process (*10*).

TABLE 7.1

Critical Micellar Concentration (cmc) and Area per Molecule (σ) at the Dodecane/Aqueous Phase Interface for Different Extractants and Salinities

Extractant/Diluant	Aqueous Phase	cmc/$\pm$0.05 M	σ/$\pm$7A^2
TBP/C$_{12}$H$_{26}$[a]	H$_2$O	0.28	84
	HNO$_3$ 2 M	0.36	95
	HNO$_3$ 4 M	0.45	102
	HNO$_3$ 10 M	0.57	103
HDEHP/C$_{12}$H$_{26}$[b]	HNO$_3$ 10^{-3} M	0.008	181
	HNO$_3$ 0.1 M	0.002	184
	HNO$_3$ 1 M	0.0002	182
DMDBTDMA/C$_{12}$H$_{26}$[c]	HNO$_3$ 1 M	0.27	–
	HNO$_3$ 3 M	0.1	–
	HNO$_3$ 5 M	0.01	–

[a] With drop-weight method. *Source:* S. Nave, C. Mandin, L. Martinet, L. Berthon, F. Testard, C. Madic, and T. Zemb, *Phys. Chem. Chem. Phys.*, 6(4):799–808, 2004. With permission.

[b] With interfacial-tension measurements. *Source:* G. F. Vandegrift and E. P. Horwitz, *J. Inorg. Nucl. Chem.*, 42, 119–125, 1979.

[c] With pendant-drop method. *Source:* L. Martinet. Organisation Supramoléculaire des Phases Organiques de Malonamides du Procédé d'Extraction DIAMEX. PhD thesis, Thèse de doctorat de l'Université Paris XI Orsay. Rapport CEA-R-6105, 2005.

In highly agitated systems where the diffusion is made insignificant, and in which the homogeneous steps are fast, the macroscopic interface between the aqueous and organic phase can be the limiting kinetic step of the extraction of the metal salt (*51, 52*). It is, thus, important to understand the behavior of the extractants at the interface to have a kinetic as well as a thermodynamic view of liquid/liquid extraction. Wipff et al. used molecular dynamics simulations to gain microscopic insights into the preferred conformation and distribution of different extractants at the interface. They found that the interface could stabilize a high-energy conformer of the malonamide favorable to complexation, resulting in a catalysis phenomenon (*53*). In their simulations, the malonamides do not form a regular monolayer, which is otherwise more favorable for liquid/liquid extraction, as a thick monolayer could decrease the interface crossing of the species. They also came to similar conclusions with other extractants: significant adsorption and orientation preferences are demonstrated for TBP in agreement with its amphiphilic nature (*54*). Baaden et al. (*55–57*) provided microscopic images of TBP at the water/oil interface, oil being modeled by chloroform, with the effect of TBP concentration and acidity of the aqueous phase. Dithiophosphonic acids were studied at the interface (*58*). In all these simulations, the aggregation of extractant in the bulk is frequently observed with increasing extractant concentrations.

Surface-tension measurements evidence the amphiphilic nature of extractants, but do not give any information on the physical size and shape of the aggregates. Number-averaged aggregation numbers can be determined by VPO (*15, 37, 49, 59–61*). VPO measurement is based on vapor-pressure reduction in solutions described by Raoult's law. It allows the determination of the osmolality of organic extractant phases, that is, the concentration of solute particles present in solution, whether they are extractant monomers or micelles. The osmolality is equal to the molarity when only monomers are present in solution. Conversely, if all the extractants participate in micelle aggregates, osmolality=molarity/n, where the molarity is the extractant initial concentration and n is the aggregation number averaged over all types and sizes present in a given phase. Therefore, a plot of osmolality/molarity versus molarity allows the determination of n, as shown in Figure 7.3 for a malonamide organic phase. Some number-averaged aggregation numbers obtained by VPO for different experimental conditions are listed in Table 7.2. Average aggregation numbers are typically at least one order of magnitude smaller than the classical values obtained with surfactants. Under process conditions, however, namely with a high solute load in the organic phase or when approaching the third phase, the aggregation number can increase by several orders of magnitude.

Nuclear Magnetic Resonance (NMR) is widely used to obtain structural and dynamic information in reverse-micelle systems (*62, 63*) and has therefore been used to elucidate the self-association properties of extractants. When the extractant generates a characteristic signal whose position and structure should change during aggregate formation, the aggregation of the extractants can be studied with NMR. Jensen et al. (*28*) obtained the equilibrium constant for oligomer formation for the extraction of trivalent lanthanide and actinide cations by purified Cyanex 272, Cyanex 301, and Cyanex 302 using the chemical shift of the P-SH or P-OH proton. Gaonkar et al. (*64*) studied the formation of reverse-micellar aggregates in the extraction system
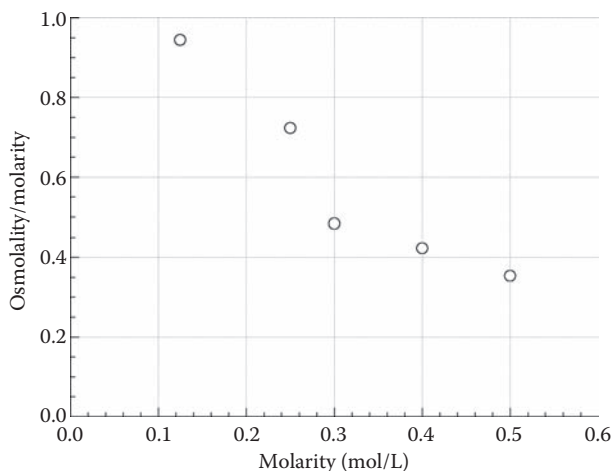
FIGURE 7.3   Osmolality/molarity versus molarity plots for the DMDBTDMA, *n*-dodecane system contacted with water at 60°C. (From L. Martinet, Organisation Supramoléculaire des Phases Organiques de Malonamides du Procédé d'Extraction DIAMEX. PhD thesis. Rapport CEA-R-6105, 2005. With permission.)

TABLE 7.2

Number-Averaged Aggregation Numbers *<n>* for Different
Extractant- and Aqueous Phase Conditions Obtained by VPO

Examples from literature	*<n>*
TODGA 0.1 M in heptane contacted with HNO_3	2–7[a]
DMDBTDMA in dodecane (HNO_3, $Nd(NO_3)_3$, $LiNO_3$)	4–5[b]
$H_2DEH(MDP)$ 0.1 M in toluene contacted with H_2O	2[c]
$H_2DEH(MDP)$ 0.1 M in toluene contacted with $H_2O/Th(IV)$	>14[d]
TBP 0.24 M in hexane contacted with H_2O	2[e]

Source:

[a] T. Yaita*,* A. W. Herlinger, P. Thiyagarajan, and M. P. Jensen, *Solvent Extr. Ion Exch.*, 22(4): 553–571, 2004.

[b] L. Martinet, PhD thesis. Rapport CEA-R-6105, 2005.

[c] R. Chiarizia, R. E. Barrans, J. R. Ferraro, A. W. Herlinger, and D. R. McAlister, *Sep. Sci. Technol.*, 36(5–6): 687–708, 2001.

[d] A. W. Herlinger, *Polyhedron*, 16(11): 1843–1854: 1997.

[e] C. H. Huang and R. G. Bautista, *Sep. Sci. Technol.*, 19(8–9): 515–529, 1984.

(HDEHP), benzene/$CaCl_2$ (0.05 M) using ^{1}H-NMR. Using NMR, Modolo et al. (*65*) followed the aggregation of bis(chlorophenyl)dithiophosphinic acid $(ClPh)_2PSSH$ and its effect on extraction. Several examples are described in Osseo-Asare's review for the TBP-diluent system (*8*). Nigond et al. (*66*) have shown the self-association of DMDBTDMA in benzene and in TPH (aliphatic hydrocarbon) by ^{1}H-NMR using a mass-action model. The type of diluent, the diamide concentration, and the acidity

influence aggregation. Later, Lefrançois et al. (*67*) characterized the DMDBTDMA-dodecane system by ^{1}H-NMR by increasing the solubilized nitric acid. They suspected a change in the shape of DMDBTDMA aggregates, from a reverse micelle-like closed structure to an open "bicontinuous" phase related to the third-phase transition. It is known that microemulsion microstructure can range from simple droplets to several classes of connected structures of high conductivity (*68*). Finally, Dozol et al. (*69*) have used ^{1}H-NMR to measure the self-diffusion coefficients of various malonamides in dodecane. They evidenced transitions in aggregation organization with increasing extractant concentrations in the diluent.

7.2.2 Phase Diagram

Third-phase formation occurs with high loading of metal salts or acids in the organic phase. There are several ways to represent the third-phase data. To determine the extension domain of a given phase, it is common to use ternary or binary phase diagrams. As there are "*N*" components, even a phase prism is not sufficient. Projections of phase diagrams on a plane, called pseudo-phase diagrams, are used in the literature. A pseudo-phase diagram can be drawn by plotting the extractant concentration in the organic phase on one axis and the ionic strength in the aqueous phase in equilibrium (metal salt or inorganic acid concentration of the aqueous phase in contact) on the other axis (Figures 7.4 and 7.5 (a)). This type of representation is common in the colloidal field.

The tendency of a given system to form a third phase can also be illustrated by indicating the maximum solute concentration in the organic phase, or limiting organic concentration (LOC) (Figure 7.5 (b)) (*70*). However, this representation sometimes does not coincide with the formation of a third phase, as in the case of DMDBTDMA in dodecane contacted with water. A maximum of solubilization can be measured, but no third-phase formation is observed. But, generally with the extraction of salt, the LOC corresponds to the limit of third-phase formation. This is the most common representation of third-phase formation in industry or in the literature for liquid/liquid extraction.
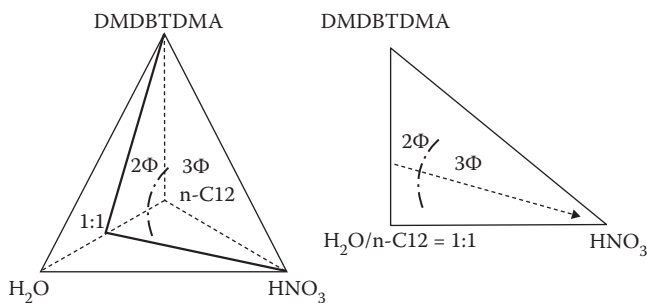
FIGURE 7.4 Quaternary phase diagram of the water, HNO$_3$/DMDBTDMA, dodecane system, and pseudobinary phase diagram DMDBTDMA/HNO$_3$ obtained from a cut in the quaternary phase diagram. The binary phase diagram is one possible representation to identify the extension domain of the third-phase formation. "2Φ" and "3Φ" indicate regions of respective two and three phases. (From L. Martinet, Organisation Supramoléculaire des Phases Organiques de Malonamides du Procédé d'Extraction DIAMEX. PhD thesis. Rapport CEA-R-6105, 2005. With permission.)
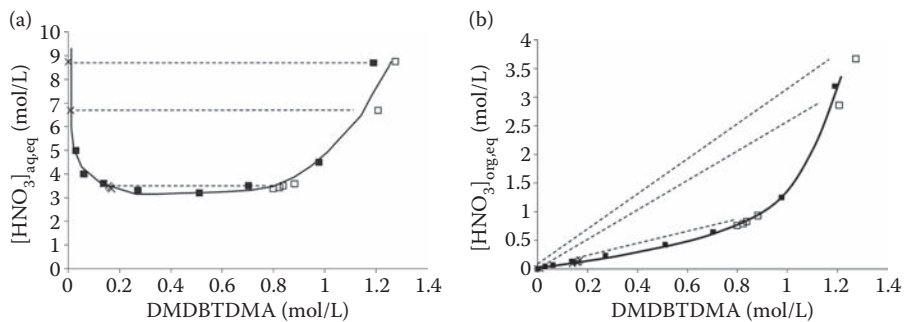
FIGURE 7.5 Two different representations of a binary phase diagram for the DMDBTDMA, dodecane system contacted with nitric acid aqueous phase at 25°C. (a) Acid concentration in the aqueous phase in equilibrium versus extractant concentration in the organic phase. (b) Acid concentration in the organic phase at equilibrium versus extractant concentration in the organic phase (LOC representation). The full line is a guide for the eyes. The tie-lines are represented on the phase diagrams and are determined through chemical analysis of the third phase and the diluted phase after the splitting of the extractant solution (titrations of both phases are represented by the empty symbols). The full symbols correspond to the experimental determination of third-phase formation and LOC, respectively. (From F. Testard, P. Bauduin, L. Martinet, B. Abécassis, L. Berthon, and C. Madic, *Radiochim. Acta*, 96: 1–8, 2008. With permission.)

Experimentally, the third-phase limit is determined by a stepwise increase of solute in the aqueous phase until phase instability occurs, then the concentration of the solute just before the third-phase formation is taken as the two- to three-phase sample (third phase or LOC).

Another method for obtaining the extension domain of the organic extractant phase before third-phase formation is to prepare a solution under the conditions of formation of a third phase, and allow it to equilibrate. Chemical analysis of the third phase and the dilute organic phase in equilibrium with the aqueous phase identifies tie-lines in the phase diagrams (Figure 7.5) (a tie-line joins the composition of the two phases (dilute and concentrated) in equilibrium after the splitting of the organic phase into two phases).

From the experimental results shown in Figure 7.5, we can conclude (*70*) that the third-phase formation corresponds to equilibrium between an organic solution with a high concentration of extractant (generally above 1 mol/L) and a dilute organic solution, namely nearly pure solvent. The third phase thus has the same chemical composition and the same structure—as demonstrated by the typical signatures observed in small-angle scattering spectra—as an organic phase with a high extractant concentration loaded with a solute at concentrations below the LOC.

7.2.3 Extractant Aggregates can be Described as Sticky Hard Spheres

Despite several studies on the self-assembling properties of extractants, few details on the structure of the aggregates were available before 1997. Small-angle neutron or X-ray scattering (SANS or SAXS, respectively) are powerful tools for characterizing

the state of aggregation of extractants with or without extracted metal ions in complex form. Generally, the aggregation properties are studied in the region of the biphasic domain of the phase diagram where the organic phase is in equilibrium with the aqueous phase, approaching the third-phase transition.

The first class of extractants studied by SANS was the alkylphosphoric acid family used in liquid-membrane extraction to transport metal ions from water (*71–77*). Neuman et al. used the NaDEHP-alkane system as a model of an acidic organo-phosphorus extraction system. These extractants behave as surfactants and form reverse microemulsions in alkanes. It was found that, depending on the nature of the metal ions M^{n+} and, in some cases, on the amount of extracted water, the extractant or the metal salts of HDEHP (NaDEHP or $M^{n+}(DEHP^-)_n$ with $M^{n+} = Ca^{2+}$, Co^{2+}, Ni^{2+}, Cu^{2+}, Mn^{2+}, Al^{3+}, and Cr^{3+}) either form rod-shaped reverse micelles (sometimes giant quasi-one-dimensional reverse micelles) or exist as small reverse aggregates of low aggregation numbers with a spherical structure. Using both SANS and NMR, Neuman et al. (*78–80*) proposed the concept of an "open" water channel in contact with the nonpolar solvent rather than the "closed" water channel in the polar core of the reverse micelles to describe the giant aggregates formed by the nickel salt of HDEHP. This is reminiscent of sphere-to-cylinder transitions known with stiff surfactants (*81*). A major problem in terms of industrial process applications with these extractant systems is the large increase in viscosity with metal salt loading in the organic phase. The higher viscosity is a direct consequence of the elongation of the aggregates when cations are extracted. This macroscopic change illustrates how the aggregation properties of the extractant and their metal salt complexes cannot be ignored in the understanding of liquid/liquid extraction.

The bifunctional extractant octyl(phenyl)-*N,N′*-diisobutylcarbamoylmethylphosphine oxide and related compounds (*16, 17*) were also studied by SANS to elucidate the size and shape of the macromolecular aggregates formed during metal salt extraction.

In all these cited studies, the extractant solutions were described only from the point of view of the shape of the aggregates without taking into account interactions between aggregates. This can lead to large errors in determining the aggregation numbers (*82*). The concentration used for an industrial process is quite high (generally above 0.5 M), and interactions between aggregates can no longer be ignored.

In 1998, Erlinger et al. (*19, 83*) were the first to elucidate the structure of malonamides in dodecane by considering the interactions between aggregates. They showed that a DMDBTDMA (>0.2 M) dodecane solution contacted with a water or a nitric acid solution contains reverse micelles interacting through an attractive potential. The aggregation number is between 4 and 10 and the radius of the polar core between 0.5 and 1.2 nm. Indeed, the reverse micelles are structurally divided in terms of a polar core composed of extracted ion pairs, coextracted water, and polar heads of malonamide, which are surrounded by a shell composed of the extractant hydrocarbon chain, as shown schematically in Figure 7.6 for DMDBTDMA. The polar cores of the micelles interact attractively through oil via Van der Waals attraction (characterized by the Hamaker constant "*A*"), while protruding chains of the reverse micelles sterically stabilize the aggregates. The sum of these two contributions (attractive and repulsive) gives a resulting interaction as a function of the separation distance *r* between the two aggregates. The Baxter sticky hard-sphere
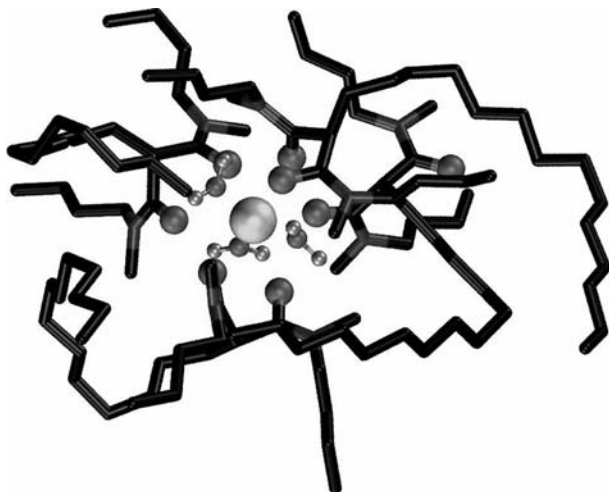
FIGURE 7.6 Schematic view of DMDBTDMA reverse micelle. The polar core is composed of extracted ion pairs, coextracted water, and polar heads of malonamide, surrounded by the hydrophobic chains of the extractant. (From F. Testard, P. Bauduin, L. Martinet, B. Abécassis, L. Berthon, and C. Madic, *Radiochim. Acta*, 96: 1–8, 2008. With permission.)
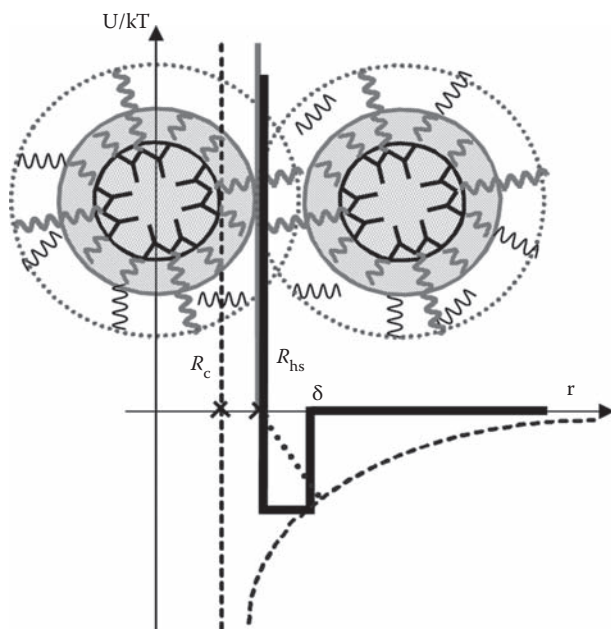
FIGURE 7.7 Schematic Baxter (—), Van der Waals attraction (---), and steric stabilization (….) potential curves describing the interaction between two DMDBTDMA aggregates. R_c is the radius of the polar core, R_{hs} is the hard-sphere radius, and (δ-R_{hs}) represents the distance of the effective attractive interaction. (From L. Martinet, Organisation Supramoléculaire des Phases Organiques de Malonamides du Procédé d'Extraction DIAMEX. PhD thesis. Rapport CEA-R-6105, 2005. With permission.)

approximation (*84*) can be used in a first step to calculate the short-range interactions, as shown in Figure 7.7. The model developed by Baxter is general to any colloidal dispersion when the sum of interparticle interactions can be considered as a short-range step. Therefore, reverse micelles separated by a distance r interact via a square-well attraction effective potential $U(r)$ defined in Equation 7.1.

$$\frac{U(r)}{kT} = \begin{vmatrix} \infty & \text{for } 0 \leq r \leq R_{hs} \\ \lim_{\delta \to R_{hs}} \ln\left[12\tau(\delta - R_{hs})/R_{hs}\right] & \text{for } R_{hs} \leq r \leq \delta \\ 0 & \text{for } r \geq \delta \end{vmatrix} \tag{7.1}$$

$U(r)$ is approximated by a repulsive hard core together with a rectangular attractive well of width $(\delta - R_{hs})$ approaching zero and infinite depth, where R_{hs} is the hard-sphere radius and δ is the attractive distance limit. The attractive step is a combination of Van der Waals attraction between the polar cores and steric repulsion. The difference $(\delta - R_{hs})$ represents the extent of the effective attractive interaction, in which R_{hs} is the "hard sphere" radius of the particles. In the model used for the extractant system, the hard sphere of the aggregates is considered to contain the extracted water, the extracted ion pair, and the extractant headgroup with the first carbon atoms of the extractant alkyl chains. Generally, the Baxter potential is taken for $(\delta - R_{hs})$ of the order of 10% of the hard-sphere radius, R_{hs}. The reciprocal of the parameter τ is the "stickiness parameter" expressed in $k_B T$ units; τ^{-1} represents the strength of adhesion, namely, the higher the value of τ^{-1} becomes, the deeper will be the attractive potential well and the stronger the attractive interactions. This sticky hard-sphere description reproduces the experimental SAXS and SANS spectra of malonamides in dodecane equilibrated with an aqueous phase of different compositions, as shown
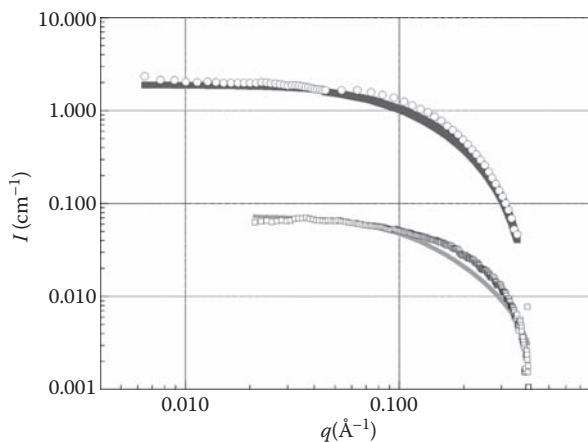
FIGURE 7.8 X-ray (square) and neutron (circle) scattering data for DMDBTDMA in *n*-dodecane contacted with water. Lines correspond to the simultaneous fit to the experimental X-ray and neutron data with the Baxter sticky hard-sphere approach. [DMDBTDMA] = 0.5 M, [Monomers] = 0.28 M, aggregation number = 4.4, and $U/k_B T = -1.7$.

for a given example in Figure 7.8. The composition of the system and the monomeric extractant concentration being determined, only two parameters (the aggregation number and the stickiness parameter) are needed for this methodology. The intermicellar interaction can also be traduced using the Hamaker constant "*A*." Depending on the experimental conditions, a value in the range of $2-4\ k_B T$ is obtained, in agreement with the values obtained for a polarizable fluid dispersed in oil (*85*).

This sticky hard-sphere description was then used to analyze extractant solutions of TBP (*7, 23–25, 27, 86*), TODGA (*30, 31*), and malonamide (*19, 34–37, 83*). In the medium concentration range, the same observations were obtained for all these extractant solutions. The aggregation numbers are, in general, small and range from 4 to 10; the polar core radius is of the order of 1 nm and contains the polar part of the extractant with a few water molecules and acid or metal salt. The range of attractive interactions is comparable whatever the type of extractant used and remains below $2.5\ k_B T$. The organic extractant phase can thus be described by a polar core interacting through oil via Van der Waals attraction. With this simple description, the aggregates formed by extractants and the interactions between aggregates are characterized, providing an explanation for the third-phase formation under certain experimental conditions as described below.

7.2.4   ORIGIN OF PHASE SPLITTING EXPLAINED BY THE STICKY HARD-SPHERE DESCRIPTION

Third-phase formation occurs with high loading of metal salts or acids in the organic phase. The general phenomenon of third-phase formation is illustrated in the case of DMDBTDMA in Figure 7.9 (b), where increasing the nitric acid concentration in the aqueous phase in equilibrium with dodecane containing 0.8 M DMDBTDMA induces phase separation. SANS experiments at a given extractant concentration and
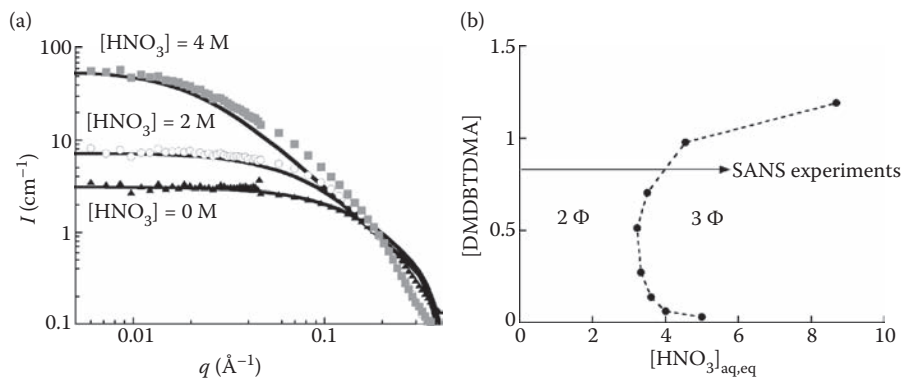
FIGURE 7.9   (a): SANS spectra of the DMDBTDMA (0.8 M), dodecane solution contacted with nitric acid aqueous phases. When the third-phase boundary is approached, characteristic low-*q* increase in SANS is measured. The scattered intensity of D-dodecane is constant and equal to $9 \times 10^{-3}\ cm^{-1}$. (b): Third-phase boundary experimentally determined as an [extractant] versus $[HNO_3]_{aq,eq}$ map for DMDBTDMA/dodecane solution. (From F. Testard, P. Bauduin, L. Martinet, B. Abécassis, L. Berthon, and C. Madic, *Radiochim. Acta*, 96: 1–8, 2008. With permission.)

along a dilution line of solute in the organic phase proved that the change in the attractive interactions between aggregates is the key parameter for understanding the third-phase formation (*83*). To illustrate this point, SANS spectra of the organic phase of DMDBTDMA (0.8 M) in dodecane equilibrated with aqueous phases of different nitric acid concentrations are shown in Figure 7.9 (a). The increase in the intensity at low *q* corresponds to an increase in the attractive interactions between swollen reverse micelles. The theoretical scattered intensity obtained with the Baxter approximation suggests that by increasing the initial aqueous nitric acid concentration $[HNO_3]_{ini,aq}$ from 0 to 4 M, the attractive potential goes from $-1.8\ k_BT$ to $-2.5\ k_BT$ for a typical range in the attractive potentials of 1–2 nm. By increasing $[HNO_3]_{ini,aq}$ and before the third-phase formation occurs, the small reverse micelles are thus subjected to two contrasting mechanisms. The thermal energy k_BT keeps the micelles dispersed in the solvent, while the energy of intermicellar attraction makes the micelles stick together. The organic phase becomes unstable when the energy of attraction becomes larger than about twice the thermal energy, leading to phase separation between a dilute and a concentrated phase. The Van der Waals attractions between the cores of reverse micelles have thus been shown to be the key to understanding the onset of the "third phase," analogous to a "liquid-gas" phase separation known in the field of microemulsions.

By increasing the ionic strength, that is, the acid or metallic salt concentration, in the aqueous phase, the concentration of the extracted acid or salt in the organic phase increases and induces an increase in the attractions between reverse micelles (see below). Numerically, all the terms can be evaluated (*7, 37, 83*). It can then clearly be concluded that this effect is the origin of the third-phase formation.

With a similar approach for SANS data of extractant micellar systems, Chiarizia et al. reexamined the third-phase formation in a TBP, *n*-dodecane system loaded with HNO_3-U(VI) (*7, 22, 23*), HNO_3-Th(IV) (*6, 20, 25*), HNO_3-Zr(IV) (*6*), HNO_3-Pu(IV) (*87*), and different inorganic acids (*26, 27, 88*). Nave et al. (*49*) also studied the TBP-dodecane system by varying the nitric acid concentration in the aqueous phase. The mechanism of third-phase formation in the TBP-alkane solution is also driven by attractive interactions between reverse micelles and can be described by the sticky hard-sphere approach. The liquid-liquid transition driven by short-range Van der Waals interactions between polar cores is therefore general.

As described by Tachimori et al. (*5*), depending on the temperature and aqueous acidity, third-phase formation is also observed when TODGA in *n*-dodecane is contacted with a nitric acid solution. The mechanism is similar to the one described above as shown by Nave et al. (*31*) and in agreement with the data of Yaita et al. (*61*) for TODGA, *n*-octane, and *n*-heptane solution equilibrated with an aqueous phase containing nitric acid. Recently, Jensen et al. (*30*) have shown that the formation of tetrameric reverse micelles in the organic phase is driven by the extraction of neodymium salts or high nitric acid content. They explained the unusual behavior observed with trivalent lanthanide and actinide cations in TODGA, *n*-alkane extractions systems by the preformed tetrameric reverse micelles in solution. This is also supported by the fact that TODGA tetrameric species with metal salt are not formed in solvents that impede the formation of tetrameric reverse micelles in the absence of salt. Finally, the other malonamide/*n*-alkane systems loaded with metal salt or

other inorganic acids can also be described by the sticky hard-sphere approach (*34, 36, 37, 89*).

Molecules that self-assemble into reverse micelles with low surfactant properties are generally "efficient" extractants (such as HDEHP, TBP, malonamides, etc.). Their adsorptions at the interface permit the complexation of the aqueous solute and their low surfactant properties permits the avoidance of the formation of very stable emulsion. Hence, ions are extracted, but typically there is less than one water molecule per ion extracted. Exact determination of coextracted water is still important, however, for interpreting the conductivity values and for evaluating the polar core volumes. Typical values are found for the Hamaker constant, because polar cores are supersaturated salt solution.

This self-organization in reverse micelles interacting through a sticky potential is actually general in extractant solutions for extractant concentrations typically between 0.2 and 1 M, namely for the concentration ranges usually used in industrial processes.

7.2.5 Predicting the Phase Diagram

7.2.5.1 Sticky Hard-Sphere Description

Two steps are necessary to avoid third-phase formation in liquid/liquid extraction: identifying the mechanism of attraction and then determining the quantities involved. In the Baxter approximation, when the size of species, concentration, and potentials are known, the position of a liquid-liquid phase separation, namely the third phase, corresponds to the divergence of the osmotic compressibility. The reason for the success of the Baxter model is that the divergence of compressibility location is analytic (*90*) and gives the limit of the two-phase region (liquid-gas transition, corresponding in our case to a transition between a concentrated and a dilute solution) characterized by a critical point located at $\Phi_c = 12\%$ and $\tau = 0.097$ (Φ_c is the volume fraction of the aggregated extractant molecules and τ is a dimensionless measure of the temperature). When the Baxter model is used, the parameter τ could be a function of temperature, salt concentration, or pH of the solution, as long as its variation could affect a phase separation. In the particular case of DMDBTDMA/dodecane contacted with aqueous solution containing nitric acid (*83*), the stickiness parameter τ^{-1} varies linearly with the extracted nitric acid concentration. The limit of the phase separation can be related to the extracted nitric acid concentration, and, thus, the third-phase limit can be reproduced. The results obtained are given in Figure 7.10 for the DMDBTDMA/dodecane system equilibrated with nitric acid aqueous phase (*83*). The position of the third-phase limit can thus be predicted without any parameter from liquid-state theory, once the magnitude of the attractive interaction has been determined via scattering experiments. As shown in Figure 7.10, this prediction of phase boundary can be used for DMDBTDMA concentrations below 0.6 M corresponding to a volume fraction of aggregates below 33%. At higher aggregate concentrations, the prediction is below the phase separation observed experimentally. This is probably because chains of neighboring aggregates are in close contact at high volume fractions, or to the fact that supramolecular organization is more complex than spherical aggregates at high volume fractions. The potential obtained from the sticky hard-sphere approximation is, thus, too simple to obtain the full phase diagram. However, within a limited concentration range, it has been
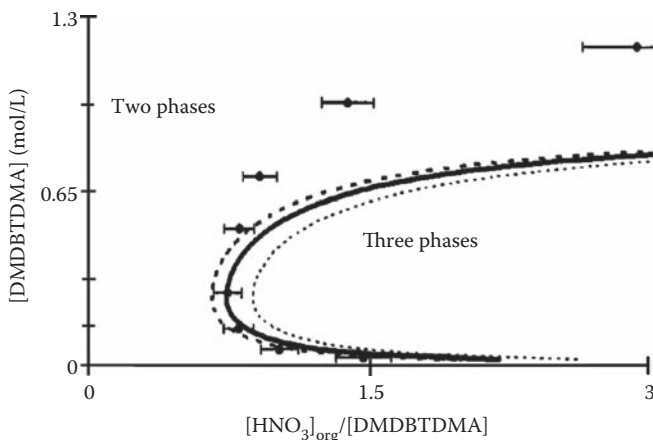
FIGURE 7.10 Pseudo-binary phase diagram of the water, HNO$_3$/DMDBTDMA, dodecane system to identify the third-phase limit. Experimental points (circles) and theory (lines) obtained from Baxter sticky hard-sphere approach. The theoretical line is obtained with the experimental determination of the linear variation of the stickiness parameter τ^{-1} versus [HNO$_3$]/[DMDBTDMA]. The different lines illustrate the impact of the error in this τ^{-1} experimental linear law. (From C. Erlinger, L. Belloni, T. Zemb, and C. Madic, *Langmuir*, 15: 2290–2300, 1999. With permission).

demonstrated that it is possible to reproduce the re-entrant, nonmonotonic path of the phase limit on the binary pseudo-phase diagram ([DMDBTDMA], [HNO$_3$]).

This approach proves that a phase diagram can be modeled when the solution microstructure is known (i.e., aggregation number and micellar aggregate number per unit volume) together with an experimental determination of the potential between aggregates. If the variation of the potential versus various parameters (metal salt in the organic phase) can be obtained experimentally, the limits of the phase separation can be reliably correlated with theory.

Despite this important step toward a model of the phase diagram in liquid/liquid extraction, no other models using this approach are described in the literature for other conditions or other extractant systems. It is likely that a model of third-phase formation in liquid/liquid extraction could be obtained by considering the aggregates in solution. However, a Baxter approximation would not work if the polar cores of the micelles are nonspherical on average or connected. Thus, the determination of the phase diagram could be obtained if the large diversity of structure of aggregates and a complex potential are considered instead of simply spherical reverse micelle with sticky hard-sphere potential. To our knowledge, such an approach was not presented in the literature until now.

7.2.5.2 Flory–Huggins Description

There are some similarities between third-phase formation in liquid/liquid extraction and the critical phenomenon of "cloud points" in aqueous solutions of nonionic polyethoxylated surfactants (*12, 91*). When a nonionic micellar solution is heated to a certain temperature, it becomes turbid, and by further increasing the temperature,

the solution separates into a dilute and a concentrated surfactant phase. Cloud-point phenomena have been modeled (*92*) with the Flory–Huggins theory of polymer solutions. The same approach has been used by Lefrançois et al. (*93*) to interpret and parameterize the third-phase formation in the extraction of HNO_3 by a malonamide in dodecane. Reverse micelles, instead of polymers in the Flory–Huggins theory, are assumed to arrange on a lattice. The interaction parameter χ_{12} can be estimated from the Hildebrand solubility parameters and is equal to $\chi_{12} = (V_1/RT) (\delta_1 - \delta_2)^2$, where V_1 is the molar volume of solvent, and δ_i is the solubility parameter of the solvent (1) or the solute (2). The interaction parameter χ_{12} between aggregates and diluent has been shown to be correlated with the nitric acid content in the organic phase. χ_{12} is another way of expressing the penetrating power (*94*) of the diluent in the apolar chain of the extractants. Lefrançois et al. (*93*) obtained good agreement between the theoretical phase-separation curves and the experimental data. By entering the relevant molecular parameters (molar volume and solubility) in the model, the authors derived the third-phase formation for different diluents: the more penetrating the diluent, the higher the ionic strength required to obtain a third phase. As for the model based on the Baxter approach, this parameter model can be used if the supramolecular structure with the interaction potential of the solution is known. To our knowledge, the use of phase-separation theory of polymers for reverse aggregates has not been extended to other systems, particularly when metal salt or modifiers are added to the system.

7.2.6 Effect on Conductivity

Conductivity measurement is an effective way of following the transitions of the supramolecular structures in the organic extractant phase. The conductivity of apolar solvent is typically between 10^{-10} and 10^{-16} µS m^{-1}, rising to $1-10$ µS m^{-1} when reverse micelles are present in the solvent. Moreover, the conductivity increases with the clustering or connection of the reverse micelles. The structure of the organic phase can thus be followed by conductivity measurements (*68, 95, 96*). An increase or a decrease in the normalized conductivity along dilution lines in a phase diagram indicates a change in the structure of the solution or a change in the interaction between aggregates. Experimentally, for a given extractant concentration, an increase in the conductivity is observed when approaching a third phase with increasing amounts of extracted salt in the organic phase at a given extractant concentration (*83*). Using the Baxter approximation to describe the structure of the solution allows the observed behavior of conductivity to be rationalized. The simplest approach is to consider that the conductivity is proportional to the number of first neighbors, λ, of a given reverse micelle. This number can be obtained analytically for sticky hard spheres using the analytical description of the Baxter model (*90*). The comparison between the calculated and observed conductivity is shown in Figure 7.11(a) for the DMDBTDMA, *n*-dodecane system contacted with nitric acid phase. As a rough approximation, it can be concluded that the conductivity of extractant aggregate solutions is due to ions exchanging between polar cores of micelles.

Another example with TBP is shown in Figure 7.11(b), where it is shown that the conductivity of TBP-dodecane solution equilibrated with nitric acid aqueous phase decreases as the temperature rises. The cmc is known to increase with temperature

(a)

(b)
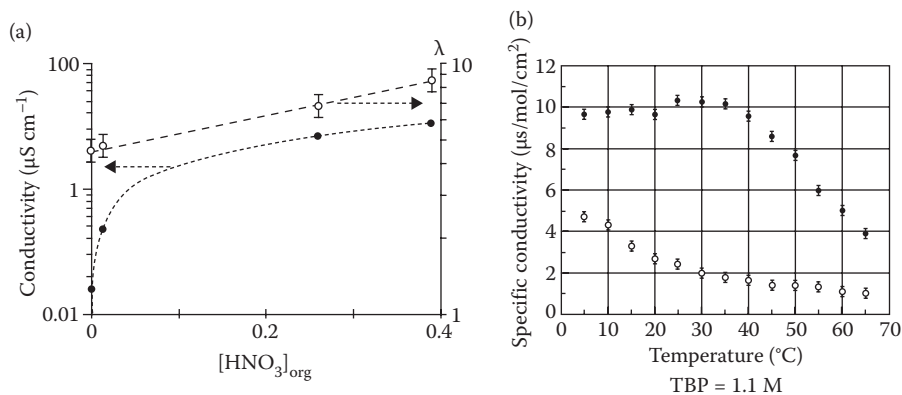
FIGURE 7.11 (a): Conductivity measurements (•) and number of closest neighbors λ (○) versus $[HNO_3]_{org}$ for a 0.5 M DMDBTDMA/dodecane solution. λ is obtained with the Baxter sticky hard-sphere approach. (From C. Erlinger, L. Belloni, T. Zemb, and C. Madic, *Langmuir*, 15: 2290–2300, 1999. With permission) (b): Variation of the specific conductivity versus temperature of (1.1 M) TBP/*n*-dodecane organic phases equilibrated with $[HNO_3]_{aq,ini}$ = 2 M (○) and $[HNO_3]_{aq,ini}$ = 12 M (•). (From S. Nave, C. Mandin, L. Martinet, L. Berthon, F. Testard, C. Madic, and T. Zemb, *Phys. Chem. Chem. Phys.*, 6(4): 799–808, 2004. With permission.)

in that the monomer-micelle equilibrium between pseudophases shifts toward monomers when the temperature increases. This can be interpreted by a transformation of reverse-micellar solution into a regular molecular solution by modest heating. This was confirmed by the decreasing intensity of the SAXS signal produced by the solution when the temperature increases (*49*).

Rao et al. (*4*) showed that with TBP solutions a higher ionic strength is needed to obtain third-phase formation at higher temperatures; that is, the LOC increases with the temperature. This means that for a given ionic strength, third-phase formation is prevented by a temperature increase. This is in direct relation with the variation of the aggregate structure and interactions between aggregates with increasing temperature. The third-phase formation is a direct consequence of the attractive interaction between aggregates; thus, any parameters that decrease the strength of the attractive interactions or suppress the aggregates will prevent third-phase formation.

Conductivity has been widely used to estimate the degree of ionization of the extracted species (*8, 97, 98*). In relation with the supramolecular organization, conductivity is also a simple and powerful technique for following the variation in the structure of the extractant solutions and thus the formation of a third phase. Measuring the conductivity of the solvent phase, used as "sensor" in chemical engineering, therefore also provides efficient and reliable "warning" of the approach of a third-phase transition.

7.3 STABILITY DOMAINS

7.3.1 INFLUENCE OF CHAIN LENGTH

The molecular structures of the diluent and the extractant play a central role in third-phase formation. The literature describes several examples of the LOC variation due

to changing the nature of the diluent or the chain length of the extractant. Rao et al. (*99, 100*) showed the importance of the diluent and extractant chain length on third-phase formation in TBP solutions. In their review of third-phase formation with neutral organophosphorus extractant, Rao and Kolarik (*4*) showed that decreasing the carbon chain length resulted in an increase in the LOC for the extraction of metal salts. They also emphasized that in contrast to the LOC values, the distribution ratios of metals forming a third phase are negligibly dependent on the molecular size and structure of the aliphatic diluent. Generally, the third-phase formation is obtained with aliphatic diluents, whereas no third phase is observed when aromatic diluents are used. Recently, Chiarizia et al. (*88*) showed in a systematic study that in the case of TBP phase, the critical concentration of $HClO_4$ decreases appreciably when the length of the alkyl chain increases in the diluent molecule. Tachimori et al. (*5*) determined the LOC value in TODGA (0.1 M), *n*-alkane/HNO_3 (1 M), Nd(III) extraction systems, showing that LOC decreased from 0.015 M for undecane to 0.014 M for dodecane and 0.010 M for tetradecane. Kedari et al. (*101*) described the effect of the diluent on the liquid/liquid extraction of Ir(IV) and HCl using Cyanex 923 (C923). The following order of LOC values were obtained for different diluents in decreasing order: toluene ≈ xylene > cyclohexane > *n*-octane > *n*-nonane > kerosene > *n*-dodecane; no third phase was detected when toluene and xylene were used as diluents.

Among these examples, a general trend is always observed: third-phase formation is favored by larger alkane diluent molecules, the LOC is lower with a linear alkane chain diluent than with branched alkanes, and, generally, the third phase is prevented when aromatic diluents are used. In the language of surface wetting, short-chain solvents better wet the protruding chains.

On the other hand, studies of the extractant chain length are less common and reveal the opposite trend. Rao et al. (*4*) reviewed the effect of changing the chain length in monofunctional organophosphorus extractants. They proposed that increasing the carbon chain length of the alkyl group of trialkyl phosphate leads to increased compatibility with the diluent; thus, increasing the LOC. Vidyalakshmi et al. (*100*) studied the influence of the molecular structure of amide extractants on third-phase formation in the extraction of uranyl nitrate and nitric acid. In general, the LOC values were found to increase when the total number of carbon atoms of the amide increased from 14 to 22. Pathak et al. (*102*) studied organophosphorus extractants with sterically hindered alkyl groups. Under similar experimental conditions, the branched-chain extractants do not form a third phase, whereas linear alkyl-chain extractants lead to instability. Sazaki et al. (*103*) have shown that the LOC increased with the length of the alkyl chain attached to the N atom of diglycolamide extractants. In former studies, Sazaki (*104*) and Gasparini (*105*) reported that no third-phase formation is observed for a C/O ratio above 17 for monoamine and 13 for diglycolamide.

Here again, a general trend is observed in all these studies: the organic extractant phase is stabilized by a long-chain extractant; this is related to the steric stabilization component of the intermicellar potential.

These competing effects of third-phase formation with changing the chain length of both diluent and extractant can be understood together using the description of reverse micelles interacting through a sticky hard-sphere potential as shown by

Berthon et al. (*34*), who systematically studied third-phase formation during the extraction of nitric acid by a malonamide-alkane system of changing the alkyl chain length both of the malonamide extractant (central chain) and of the diluents. They found that malonamide reverse micelles exhibit similarities with classical reverse micelles of Aerosol-OT (AOT) (bis (ethylhexyl) sodium sulfoccinate) (*106*). Third-phase formation is favored by increasing the chain length (C6–C18) of the diluent (Figure 7.12), as well as by decreasing the central chain length (from C18 to C14) of the malonamide extractant. This behavior is consistent with the general trends observed in the published data on other extractant systems as described above. This provides quantitative examples of increased steric repulsion obtained by solvent penetration as well as by increasing the length of chains protruding from the reverse aggregate.

Conversely, it was shown that the composition of the polar core depends only on the polar heads of the malonamide and on the initial salt concentration in the aqueous phase in equilibrium. The extraction efficiencies of HNO_3 and H_2O are independent of the diluent and extractant chain lengths (*34*). Diluent-extractant interactions and variations in the amphiphilic balance of the extractant thus do not influence the extraction equilibrium of HNO_3 and H_2O. Here again, this conclusion is consistent with published results for other extractant systems.

The sticky hard-sphere approach accounts for these general features and suggests that extractant solutions share several properties with classical reverse-micelle solutions of AOT. Third-phase formation is a consequence of the interactions between aggregates, resulting from universal Van der Waals attractions and steric stabilization. Above a certain attraction limit, a liquid-liquid phase transition is obtained between two organic phases containing high and low concentration of the reverse micelles (and thus of the extractant). In the concentrated solution, polar cores may connect or coalesce. One universal feature of liquid-liquid separation is the existence of a critical point when the two liquids in coexistence have the same composition. Using longer extractant chains or shorter (or branched) diluent chains increases the steric
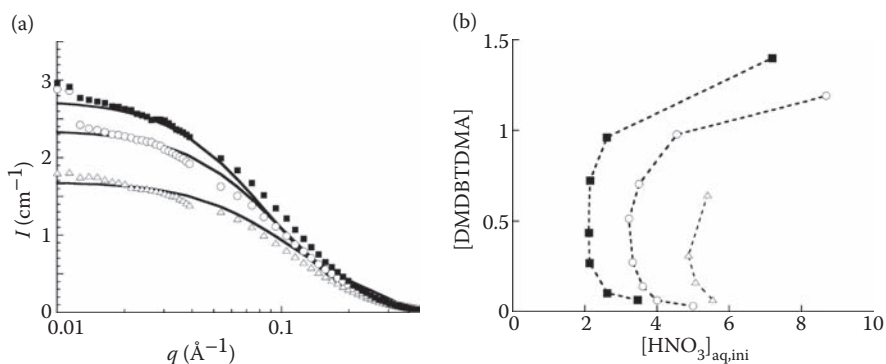
FIGURE 7.12   (a): SANS spectra of the organic phase DMDBTDMA 0.8 M in different oil contacted with a nitric acid aqueous phase. (b): Third-phase boundary experimentally determined as a [extractant] versus $[HNO_3]_{aq,eq}$ map for DMDBTDMA in different oil. Hexadecane (■), dodecane (○), hexane (Δ). (From L. Martinet, Organisation Supramoléculaire des Phases Organiques de Malonamides du Procédé d'Extraction DIAMEX. PhD thesis. Rapport CEA-R-6105, 2005. With permission.)

stabilization and thus, prevents third-phase formation. As in reverse microemulsions, two effects are important: (1) the chain protruding from any aggregate stabilizes polar solutes in oils, and (2) short or branched oils ("penetrating chain" (*94*)) penetrate and swell the outer layer of the reverse micelle with a consequent stabilization effect. Diamide solutions thus behave as AOT reverse microemulsions, and the phase stability is governed by the same rules. Leung et al. (*107*) used a simple model of spherical reverse micelles interacting through an attractive potential to obtain general data on phase transition in the case of AOT microemulsions. The two important classes of phase instability encountered with water-in-oil microemulsions can be predicted based on the competition between the interfacial free energy and the free energy of interaction:

(a) Emulsification failure, where the "internal" phase is expelled by the oil phase: The microemulsion is in equilibrium with water in excess. The maximum droplet radius is limited by the high cost in energy to create more interface.

(b) Liquid/liquid phase separation driven by attractive interactions between micelles: The final state after phase separation is a micellar-rich and micellar-poor water-in-oil solution. From a thermodynamic point of view, such demixing can be considered as liquid/gas phase demixing.

The most complicated case, which is not predicted by Leung et al. (*107*), is the domain where both instabilities coexist, the so-called Winsor III microemulsion in equilibrium with both water and oil in excess.

Leung et al. (*107*) explained the effect of temperature, salt, oil nature, ionic strength, and the addition of alcohol on the phase transition in AOT reverse micelles. Depending on the nature of the instability, the parameters have an opposite effect on the maximum of water solubilization. In the case of an extractant solution, we are dealing with the second class of instability, the liquid/gas transition resulting from an increase in the attractive interaction between reverse micelles. We can thus conclude that in the extractant case, the maximum solute solubilization (equivalent to a LOC in the language of liquid-liquid extraction studies) increases if a parameter variation can decrease the attraction between the droplets. This can be obtained by increasing the repulsion part of the potential or by increasing the rigidity of the interfacial film. Experimentally, phase separation will be prevented by decreasing the chain length of the solvent (importance of the "penetration" power of the solvent), or by increasing the chain length of the surfactant, or by adding a cosurfactant with a long alkyl chain to increase the rigidity of the interfacial film, as illustrated schematically in Figure 7.13.

As noted at the beginning of this section for TBP (*4*) or TODGA (*5*), the LOC of HNO_3 or metal salts is increased by decreasing the diluent chain length, that is by increasing the repulsive part of the intermicellar potential. On the other hand, as described in the case of malonamide (*34*) or amide extractant (*100*), the LOC values were found to increase by increasing the total number of carbon atoms in the chain length of the extractant. Here again, phase separation is prevented by increasing the repulsive contribution to the interaction potential. Finally, the third phase can be
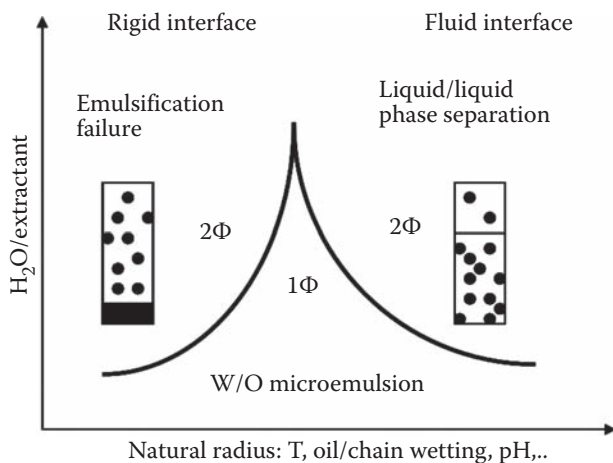
FIGURE 7.13 Maximum of water solubilization versus the parameters influencing the rigidity of the interface and the attraction between water droplets. In the emulsification-failure case, the inside water is expelled by the oil phase. The liquid/liquid phase separation is driven by attractive interaction between micelles; in the final state a micellar-poor phase is in equilibrium with a micellar-rich phase. (Readapted from R. Leung and D. O. Shah, *J. Colloid Interface Sci.*, 120(2): 330–344, 1987.)

prevented by adding a modifier. Dhamodaran et al. (*4, 108*) observed that an increase in the carbon chain length of the alcohol from C4 to C9 led to a monotonous increase in LOC in the Th(IV)-TBP system. Regarding the rule of Leung et al. (*107*), this can be explained by an increase in the rigidity of the interfacial film by increasing the chain length of the modifier. Another possible explanation is increased steric stabilization induced by the short chain alcohol seen as a cosurfactant increasing the effective volume V of the apolar chains of an aggregate.

The phase stability of organic extractant phases and classical reverse microemulsions are thus governed by the same rule. This general conclusion would not have been valid for extractant systems in the case of an emulsification failure mechanism, namely rejection of the "internal" phase, but this was not observed in liquid/liquid extraction systems when salt is extracted.

7.3.2 Influence of the Nature of the Polar Core

The presence of reverse micelles in extractant systems was found to be related to third-phase formation through an increase in the attraction potential between micelles above approximately two times the thermal energy. The effect of different cations or anions of the extracted metallic salt or acid on the third-phase formation can be explained by this approach.

7.3.2.1 Salt Extraction and Influence of Polarizability

In contact with water, HNO_3 and metal salts such as uranyl nitrate, thorium nitrate, or zirconium nitrate, extractants dissolved in the diluent form small reverse micelles. Upon extraction of metal salts, the swollen micelles interact through attractive forces

between their polar cores. The most direct way to evidence this is to estimate the structure factor at zero angles in a scattering experiment. The osmotic compressibility increase is a direct translation of the attractive interparticle potential (*109*). Intermicellar interactions lead to third-phase formation under certain conditions as described above. In the presence of reverse micelles, the molecular speciation of species remains complex and relatively unknown. Generally, the authors are interested in the structure of the organic phases as a function of their compositions rather than as a function of the complex stoichiometry. The sticky hard-sphere potential approach can be used if the global composition of the polar core of the micelle is considered with a spherical shape for the reverse micelle. The limit of the model is obtained if the shape of the reverse micelle is strongly modified by the extracted salt, as for example a transition from sphere to rod.

Chiarizia et al. (*7, 22, 23*) systematically studied the TBP, *n*-dodecane/HNO_3, $UO_2(NO_3)_2$ solvent-extraction system using SANS. They observed an increase in the diameter of the aggregates by increasing the amount of $UO_2(NO_3)_2$ or HNO_3. This reflects the swelling of the reverse micelles when solutes are solubilized in the polar core of the reverse micelles. At the same time, an increase in the short-range attraction forces between polar cores of the micelles due to dipole-dipole interactions is also observed. As shown in Figure 7.14 (a) (redrawn from Ref. (*7*)), the attraction potential becomes more attractive as the amount of solute increases in the reverse micelles, and reaches about $-1.8\ k_B T$ (which corresponds to an effective Hamaker constant of about $4.3\ k_B T$) at the limit of third-phase formation.

Similar results have been obtained for the diamide/dodecane (*37, 70*) system contacted with an HNO_3, or $UO_2(NO_3)_2$, or $Nd(NO_3)_3$ aqueous phase (Figure 7.14 (b)). For all the systems, assuming the spherical reverse micelles are interacting through
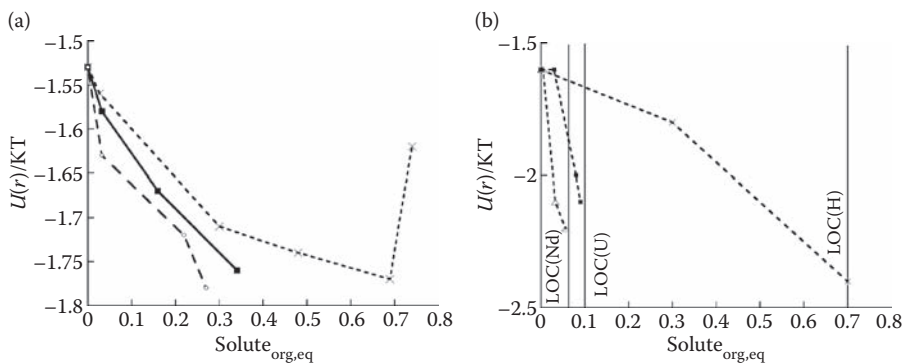
FIGURE 7.14 Interaction potential $U/k_B T$ versus solute concentration in the organic phase at equilibrium. (a) The data are obtained from Baxter modeling of SANS data for the TBP (0.73 M), *n*-dodecane system equilibrated with uranyl nitrate (■), or nitric acid (×), or a mixture of both salts (○) (Redrawn from R. Chiarizia, K. L. Nash, M. P. Jensen, P. Thiyagarajan, and K. C. Littrell, *Langmuir*, 19: 9592–9599, 2003). (b) The data are obtained from Baxter modeling of SANS data for the DMDBTDMA, dodecane system equilibrated with (×) nitric acid or (■) uranyl nitrate, $LiNO_3$ (1 M), HNO_3 (0.01 M), or (Δ) neodymium nitrate, $LiNO_3$ (0.1 M), HNO_3 (0.01 M). (From F. Testard, P. Bauduin, L. Martinet, B. Abécassis, L. Berthon, and Madic C, *Radiochim. Acta*, 96: 1–8, 2008. With permission.)

an effective attractive potential, the attraction increases with the amount of extracted salt in the polar core of the reverse micelles and again the critical energy of attraction for the third-phase appearance is around 2.3 k_BT, regardless of the extracted solute. The major difference between the extracted salts is how rapidly the energy of attraction $|-U(r)|$ increases with the quantity of metal nitrate. The increase is greater with $UO_2(NO_3)_2$ than with HNO_3, indicating that less uranyl is necessary to obtain the third phase. This must be correlated with the higher LOC obtained with HNO_3 than with uranyl nitrate. That is, the addition of a given amount of metal nitrate is more efficient for increasing the attraction between micelles if the metal nitrate is more polarizable. As the polarizability is much higher for uranyl than for protons, we propose here that the more polarizable the core of the micelles is, the higher is the attractive interactions between reverse micelles, and the lower the LOC. This is consistent with the Hofmeister series classification (47).

There is only one systematic example in the literature of the influence of the polarizability of metal cations on the attraction between extractant reverse micelles. Chiarizia et al. (6) investigated third-phase formation in the extraction of U(VI), Th(IV), and Zr(IV) nitrates from HNO_3 solutions by n-alkane solution of TBP. They have shown that the attractive interactions (and thus, the occurrence of a third phase) for different extracted cations follow their polarizability. A much lower concentration of Zr(IV) than Th(IV) is required to obtain a phase separation, indicating that Zr^{4+} is more effective at producing phase splitting than the larger Th^{4+} cation. In addition, the effect of metal nitrate on third-phase formation is always much more important than with nitric acid alone. To illustrate the relation between cation polarizability and phase-splitting efficiency, the authors quantified the slope of a plot of $-U(r)$ versus total nitrate concentration. This allows comparisons of extraction data that are always dependent on the amount of nitric acid in the aqueous solution. As shown in Figure 7.15 (reproduced from Ref. (6)), they evidenced a linear correlation between the derivative of $U(r)$ and the cation hydration enthalpy (110).
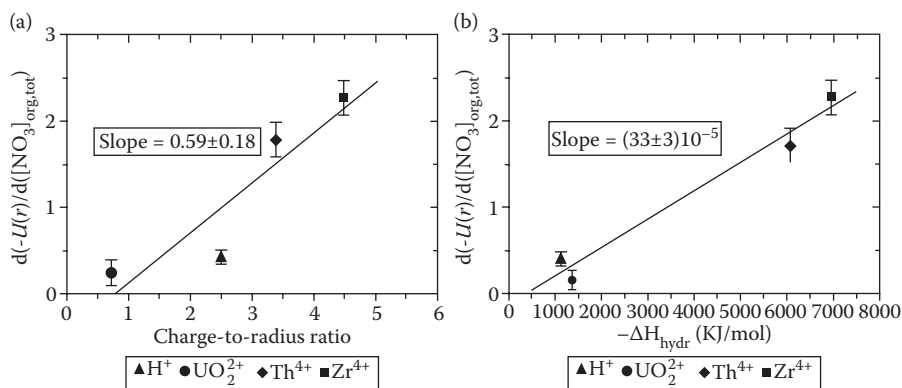
FIGURE 7.15 Plot of $d(-U(r))/d([NO_3]_{org,tot})$ versus (a) the charge-to-size ratio or (b) the enthalpy of hydration for the extraction of the nitrates of various cations. (From R. Chiarizia, M. P. Jensen, P. G. Rickest, Z. Kolarik, M. Borowski, and P. Thiyagerrajan, *Langmuir*, 20: 10798–10808, 2004. With permission.)

Three main effects are universal and do not depend on the system studied. The favorable effect of a cation on third-phase formation is measured by the slope of the energy of attraction between the reverse micelles plotted versus the cation concentration in the organic phase or the total nitrate concentration for different salt. Whatever the nature of the extracted cations, third-phase formation is observed when the energy of attraction is near $2k_BT$. Finally, the tendency toward phase splitting correlates well with the hydration enthalpy of the cations.

7.3.2.2 Extraction of Inorganic Acids and Polarizability

Inorganic acids are not equal in promoting third-phase formation, as the phenomenon is strongly dependent on the nature of the anions. Condamines et al. (*111*) have shown that inorganic acids such as $HClO_4$, H_2SO_4, H_3PO_4, and HCl are less extracted than HNO_3 by dialkylamide diluted in alkane. This is surprising in comparison with the classical Hofmeister series (*112, 113*), HNO_3 should not be the best extracted in the series given according to Hofmeister. They explained this by the hydrophobicity of the amide, which prevents the coextraction of water. Inversions in the Hofmeister series are also observed in protein separations and are related to the polarizability of the "active" site (*114*). Nigond et al. (*66*) have observed that $HClO_4$ is more effective than HNO_3 in promoting a third phase in the amide-TPH system. For TBP systems, Chiarizia et al. concluded that HCl is more effective than HNO_3 in forming a third phase (*26, 27*). In similar systems, it has been shown that $HClO_4$ is also more effective than either HNO_3 or HCl in promoting TBP phase splitting (*115, 116*). Thus, contrary to the case of cations, the tendency toward phase splitting seems not to be correlated with the hydration enthalpy of the anions (*88*). Chiarizia et al. (*26, 88*) recently investigated the liquid/liquid extraction of several mineral acids (HNO_3, $HClO_4$, H_2SO_4, HCl, and H_3PO_4) by TBP under identical conditions, to compare the efficiency of the acids in promoting third-phase formation with their specific properties. They evidenced the important role of coextracted water on the efficiency of anions in promoting third-phase formation. In an earlier study, Nave et al. (*49*) described the relation between third-phase formation and polar-core polarizability for the extraction of two acids, perchloric acid and nitric acid. In the case of nitric or perchloric acid extraction by TBP in *n*-dodecane, the third phase is obtained at lower concentration with the most polarizable anion (perchloric acid). Phase splitting is observed near an acidity of 2 M for $HClO_4$ and 15 M for HNO_3 for TBP (1.1 M) in dodecane (Figure 7.16 (b)). SAXS attributes this difference to the higher effective attraction interaction between polar cores when perchloric acid is extracted. Figure 7.16 (a) compares the SAXS patterns for TBP (1.1 M) solution contacted with H_2O, 2 M HNO_3, and 0.5 M $HClO_4$, respectively. The aggregates formed in the three cases have the same shape, as all the three plots merge into the same curve at high q values, while the large increase in intensity in the low q range indicates high osmotic compressibility and hence strong attractive interparticle interactions for the $HClO_4$ solution. Reverse micelles containing ClO_4^- ions thus have a more polarizable polar core, inducing predominant dispersion forces (van der Waals interactions) between polar cores, as suggested by Ninham et al. (*117*) (polarizability of ClO_4^- and NO_3^- are, respectively, 7.47 and 4.13 $Å^3$ (*110*)).
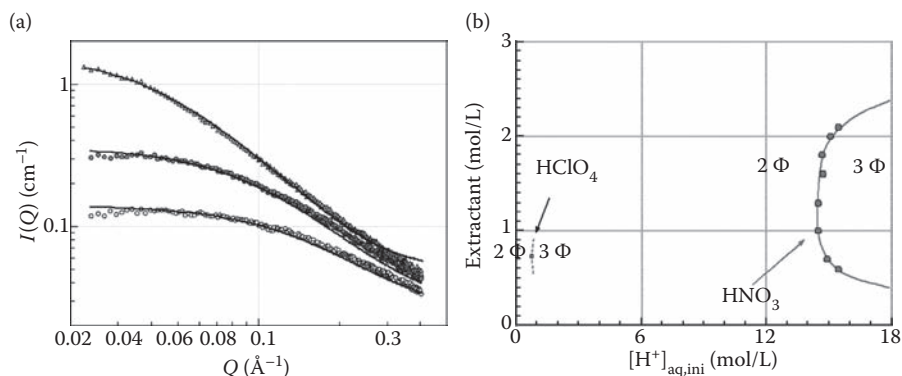
FIGURE 7.16   (a) Small-angle X-ray scattering data for TBP (1.1 M) in n-dodecane contacted with H_2O (○), 2 M HNO_3 (●), and 0.5 M $HClO_4$ (▲). Lines represent the fit of the data. The wave vector "q" is noted "Q." (b) Pseudo-phase diagram [extractant] versus $[H^+]_{aq,ini}$ for different acid in the aqueous phase ($HClO_4$ or HNO_3). (From S. Nave, C. Mandin, L. Martinet, L. Berthon, F. Testard, C. Madic, and T. Zemb, *Phys. Chem. Chem. Phys.*, 6(4): 799–808, 2004. With permission.)

Regarding the other acids from Chiarizia's studies (*88*), the effectiveness of inorganic acids in promoting third-phase formation is not simply related to the physicochemical parameters (e.g., polarizability) of the relevant anions. The acids can be ranked by decreasing LOC values as follows: $HClO_4 > H_2SO_4 > HCl > H_3PO_4 > HNO_3$. Regarding the ability of the anions to coextract water, the extraction of $HClO_4$ is accompanied by a large amount of water, contrary to the extraction with H_3PO_4 or HNO_3. The LOC order correlates with the amount of extracted water in the organic phase at the concentration point at which phase splitting occurs, as shown in Figure 7.17 (redrawn from the data of Ref. (*88*)). Table 7.4 indicates the LOC values, the amount of coextracted water, and the polarizability of the different anions. Third-phase formation during extraction of inorganic acids by TPB in dodecane seems to be primarily due to the ability of the various acids to carry hydration water into the organic phase. With regard to the above argument of increasing attractive interactions when approaching third-phase formation, the water incorporated in the reverse micelles makes the micellar core more polar and hence more unstable in terms of phase stability.

Far from third-phase formation, Kanellakopulos et al. (*118*) showed in an earlier study that the extraction behavior of given electrolytes with the same cation is primarily influenced by the solvation properties of the associated anions. They found that the electrolyte phase distribution can be explained by single ion solvation, by comparing the equilibrium constants for the extraction of acids by undiluted TBP with the free energies of transfer for the anions (Table 7.3).

The distribution of acids between water (*w*) and TBP phase (*s*) is given by:

$$(H^+)_w + (X^-)_w \overset{K}{\rightleftharpoons} (HX)_s \tag{7.2}$$
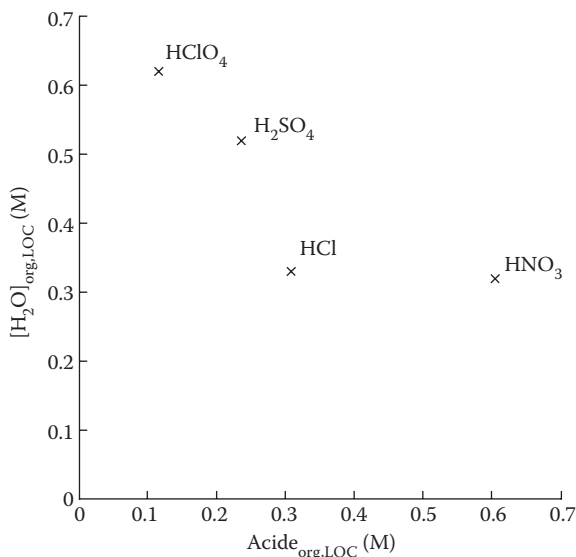
FIGURE 7.17 Water organic-phase concentration versus acid organic concentration at the LOC conditions for TBP/*n*-octane system equilibrated with different acidic aqueous phases. (Redrawn from R. Chiarizia and A. Briand, *Solvent Extr. Ion Exch.*, 25: 351–371, 2007.)

TABLE 7.3

Phase Distribution Constants K for the Extraction of Acids by TBP (Undiluted) at Dilute Concentration and Free Energies of Transfer for the Anions

Electrolyte	Log K	$\Delta_{ws}G°$ (kJ/mol) for Anions
HClO$_4$	1.86 ± 0.07	$+24.9 \pm 0.7$
HNO$_3$	0.74 ± 0.06	38.2 ± 1.2
HCl	-1.12 ± 0.07	48 ± 0.9

Source: B. Kanellakopulos, V. Neck, and J. I. Kim, *Radiochim. Acta*, 48(3–4): 159–163, 1989.

---

and their equilibrium constants by:

$$K(A) = \frac{[HX]_s}{[H^+]_w \cdot [X^-]_w} \tag{7.3}$$

The different solvation properties of the anions are directly influencing the extraction behavior of their acids (Equations 7.4 and 7.5).

$$(H^+)_w + (X^-)_w \overset{K}{\rightleftharpoons} (HX)_s \overset{{}_sKa}{\rightleftharpoons} (H^+)_s + (X^-)_s \tag{7.4}$$
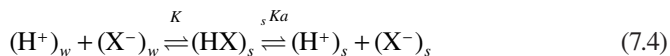
TABLE 7.4

Values of LOC, [TBP]/[Acid], and [H₂O]/[Acid] in Third Phase for the Extraction of Different Inorganic Salt by TBP (0.73 M) in *n*-Dodecane at 23±0.5°C

Electrolyte	LOC	[TBP]/[Acid] in Third Phase	[H₂O]/[Acid] in Third Phase	ΔG°$_{hyd}$ (kJ/mol) of the Anions	Polarizabilities of the Anions (A³)
$HClO_4$	0.116	2.5	4.1	−214	7.47
H_2SO_4	0.236	1.2	1.6	−335	5.47
HCl	0.308	0.88	2.2	−347	3.42
H_3PO_4	0.604	0.62	0.4	−473	5.79
HNO_3	0.804	–	–	−306	4.13

Note: ΔG°$_{hyd}$: absolute free energy change for transfer of ion from gas phase to infinite diluted solution, polarizabilities obtained from molar refractivity.

Source: Data are from R. Chiarizia and A. Briand, *Solvent Extr. Ion Exch.*, 25: 351–371, 2007. With permission.

$$K(A) = \frac{[HX]_s}{[H^+]_w.[X^-]_w} = \frac{[H^+]_s.[X^-]_s\,Ka}{[H^+]_w.[X^-]_w} \qquad (7.5)$$

where $_sKa$ is the association constant in the TBP phase.

The order found for the equilibrium constant ($HClO_4 > HNO_3 > HCl$) shows that the lower the free energy of transfer is, the higher is the equilibrium constant.

From these results on third-phase formation and measurement of extraction constants, it turns out that two important features must be taken into account for the formulation of a liquid/liquid extraction system: how easily the salt is transferred from water to the organic extractant phase, and the stability of the organic extractant phase obtained by increasing the amount of extracted salt. These points can be in contradiction. For example, $HClO_4$ is better extracted than HNO_3, but the resulting organic phase is less stable with $HClO_4$ than with HNO_3. In applications, and for extraction plant design, a compromise between the efficiency of extraction (i.e., high extraction constant values) and the stability of the extractant phase must be found to optimize the liquid/liquid extraction processes.

7.4   STABILITY OF MICELLES AND SHAPE TRANSITIONS

In the preceding sections, we focused on a description of the organic extractant phases when the microstructure can be assumed to comprise spherical reverse micelles interacting through an attractive potential. While spherical reverse micelles have been evidenced for TBP, diamide, and TODGA organic solutions, the polymorphism of the aggregates can be more complex when other extractants are used or when the extractant concentrations exceed 1 M. A trivial and direct observation of shape transition is when the conductivity of the organic phase increases by more than one order of magnitude. NaDEHP in heptane, a model of an acidic organophosphorus extraction system (*48, 59*), forms giant rod-like reverse micelles whenever metal

salt is extracted. Large aggregates have also been evidenced by VPO measurement (*35, 37*). Large aggregation numbers are incompatible with a spherical shape due to surface and volume constraints (*68*). Some authors reported that third-phase formation is preceded by a large increase in the size of the aggregates or by polymerization of the metal-extractant complexes in some organic phases, as for example reported by Thiyagrajan et al. (*16, 17, 74*) with octyl(phenyl)-*N,N'*-diisobutylcarbamoyl-methylphosphine oxide (CMPO) extractant.

Assuming that different polymorphisms can be found in the extractant systems, a better understanding also comes from other phase-separation mechanisms studied in classical amphiphilic systems such as soaps and lipids. The first, largely described here, is the phase separation resulting from increased attractive interactions. The second occurs when a sphere-to-rod transition is observed for the shape of the aggregates. The attraction between cylinders is higher than between spheres when attraction is dominated by van der Walls (VdW) forces between polar cores (*119*). For micellar solutions (reverse or not), the liquid-liquid phase transition cannot be unambiguously attributed to either shape or attractive interactions only, as it appears that these two effects coexist in nonionic surfactants solutions (*91, 120–123*).

Another mechanism assuming the formation of connected, flexible, rod-like micelles is sometimes put forward to explain phase demixing (*124*). In this case, the phase separation results from an increase in the attraction due to the formation of junctions between the elongated aggregates. Nevertheless, this mechanism has not yet been evidenced experimentally in extractant systems.

Bauduin et al. (*125*) have shown that the shape of the aggregates is directly at the origin of the macroscopic observation by Dozol et al. (*69*): third-phase formation when a solution of *N,N'*-dimethyl-*N,N'*-dibutyl-pentyl malonamide (DMDBPMA > 1 M) in dodecane is contacted with water, whereas no third-phase formation is observed when a solution of DMDBTDMA in dodecane is contacted with water over the entire concentration range. The only difference between these two malonamide is the length of the central alkyl chain (five carbons for DMDBPMA and 14 carbons for DMDBTDMA, respectively). Using small-angle scattering, the authors showed that at concentrations near 1 M, a transition from reverse micelles to reverse cylindrical micelles is observed for DMDBPMA and not for DMDBTDMA (Figure 7.18). This shape transition coincides with the third-phase formation, and the phase separation is thus due to an elongation of the aggregates in this case. If the concentration is increased above 1.2 M, DMDBTDMA undergoes a transition from reverse micelles to lamella, being sterically stabilized by the longer alkyl chains compared with DMDBPMA. The stability of the organic phase can thus be determined a priori from the aggregation behavior of the extractant-solvent system. This study confirms that the aggregation state at supramolecular scale plays a major role in extraction systems, especially in predicting phase instability.

7.4.1 Packing Parameter

The shape of the aggregates can be related to the dimensionless packing parameter (*P*) defined by Israelachvili (*119, 126*) as the ratio $V/\sigma{\cdot}l$, where V is the apolar volume
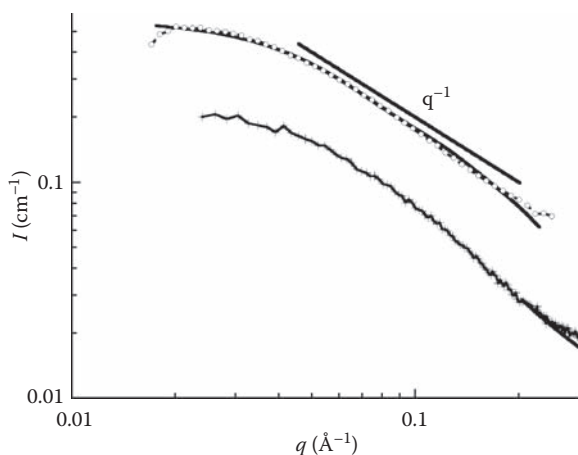
FIGURE 7.18 Sphere-to-rod transition in DMDBPMA, n-dodecane solution. 0.54 M (+) of DMDBPMA is fitted with sticky hard-sphere ($N_{agg} = 4$ and $U/k_BT = -1.92$) and 1.25 M (o) of DMDBPMA is fitted by monodisperse cylinders of finite length, $L = 87$ Å, and radius, $R = 5$ Å. The presence of cylinders is also confirmed by the q^{-1} dependence in the spectra.

of the amphiphile, σ the optimum area per polar head group at the interface between hydrophobic and hydrophilic parts, and l the average chain length. The optimum area σ is the area that minimizes the free energy of the surfactant monolayer at the oil-water interface; the effective volume V must include cosurfactant and penetrating oil; and l is 80% of the extended chain length. The spontaneous packing parameter P_0 for any water-surfactant-oil system can thus be estimated, P_0 being dependent on a molecular system. Efficient extractants generally form reverse micelles and thus, have a spontaneous packing parameter value around 3 (*10*). Israelachvili and Ninham (*119*) also showed that any aggregate shape corresponds to an effective packing parameter (related to the solution constraints). The effective packing parameter must refer to the effective geometry adopted by the surfactant in the interfacial film (taking into account all the constraints of concentration, temperature, ionic strength, etc.), and not only to the molecular volumes of the surfactant alone. The value of the effective parameter is directly related to the possible shape of the aggregates in solution. For example, a packing parameter of less than 1 corresponds to direct aggregates (oil in water); a value near 1 corresponds to aggregates with zero curvature such as lamellar phase or vesicles. If P is greater than 1, the system becomes increasingly lipophilic, and transitions are observed from lamellar phase to reverse cylindrical micelles and then to reverse spherical micelles (*119*). The difference between the effective packing parameter (related to the constraint of the solution) and the spontaneous one gives the free energy of curvature, namely the energy required to bend the film to adopt the constraints of the sample. This difference controls the formation of aggregates with any shape.

The packing parameter of the neighboring surfactant molecules reflects the molecular dimension and is related to the macroscopic curvatures (Gaussian and mean curvature) of the surface imposed by the topology of the coverage relation (*127*).

Using the packing parameter, the sample composition can be modified to impose a packing variation toward better solution stability. As an example, if the DMDBPMA-dodecane solution forms a third phase because of the rod-like shape of the aggregates, the addition of a molecule that increases the packing parameter of the extractant will induce a transition toward the sphere and will thus, prevent the third-phase formation. The role of the added modifier can be explained simply using this concept.

7.4.2 Influence of Added Modifier

7.4.2.1 Modifier and Supramolecular Structure

In the liquid/liquid extraction field, the third phase is often prevented by adding a modifier to the solution. Modifiers are generally polar molecules containing a hydrocarbon chain and a polar component such as long-chain alcohols (octanol, isodecanol, and p-nonyl phenol), TBP, or amides. As the metal solvate is more compatible with a polar diluent, increasing the polarity of the solvent by adding a modifier results in a higher LOC. Kertes et al. (*115*) suggested that the effect of a polar modifier is to increase the solubility of the complexes due to a secondary solvation of the complex. The protruding alkyl chain of the modifiers around the complex tends to increase its solubility. This is the main explanation given for the effectiveness of the modifier in preventing the third phase, but a clear understanding of the effect of the modifier is still required. Several experimental results are described in the literature. The main studies concern the use of alcohol with different chain lengths, as described in the review by Rao et al. (*4*) for TBP systems.

Smith et al. (*128*) developed a modified amide phase system to extend the operational stability range of the alkylmalonamide-dodecane system. They obtained a more extensive domain of stability over the temperature and acidity concentration range.

Tachimori et al. (*5*) and Sazaki et al. (*104*) studied the effect of adding a monoamide modifier to a TODGA (0.1 or 0.2 M)-dodecane/Nd(III) extraction system. N,N-dihexyloctanamide (DHOA) was used as a representative monoamide modifier. It was shown that adding this modifier suppressed the third phase and that the amount of extracted Nd(III) reached the stoichiometric value. DHOA alone has a very weak extractability for Nd(III), and the explanation given is increased solvent polarity within an outer-sphere organization.

Kedari et al. (*101*) studied the influence of adding a modifier on a solvent extraction with an Ir(IV)-Cyanex 923 system. Cyanex 923 is a commercial neutral organophosphorus extractant widely used for extraction of metal ions or inorganic acids. They observed that decanol is not efficient as a modifier probably because of an interaction with Cyanex 923. TBP can only be used at 4 M HCl; otherwise the efficiency is poor. This highlights the fact that the interaction of the modifier with the extractant can modify the efficiency of the extraction.

Delmau et al. (*129*) studied the self-association of fluorinated alcohols used as diluent modifiers for the selective extraction of cesium from caustic media by calixarene-crown ethers. They found that the salt distribution ratio is enhanced by the modifiers and explained this by a solubilization effect of the modifier due to its amphiphilic properties.

The adjunction of a modifier thus changes the physicochemical properties of the extractant and directly influences the maximum solute concentration in the organic phase (LOC). The role of the modifier is generally attributed to a specific experimental system and is generally not linked to a particular supramolecular organization. Abecassis et al. (*89*) studied the impact of octan-1-ol used as a modifier on the self-assembling properties of the DMDBTDMA in dodecane. Octanol (an H-bonded liquid) is known to form oligomers through intermolecular hydrogen bonds constituting regions of high electronic density (*130, 131*) compared to the aliphatic parts. Octanol is not a molecular solution, and its addition to a diamide/alkane solution organized into reverse micelles must have some consequences on the supramolecular organization. When small amounts of octanol are added, the organization into reverse micelles is maintained and a cosurfactant effect is observed. A "cosurfactant" is a molecule that cannot form micelles by itself in a given solvent, but once a micelle is formed by a surfactant or an extractant molecule, a cosurfactant molecule participates in the micellar structure. The scattering spectra are typical of reverse micelles, but the external specific surface area of the polar aggregates is modified by the presence of the cosurfactant. The dynamic properties of the extractant film can be modified with possible consequences on extraction capacities, but, to date, no systematic studies have been done to relate the molecular exchange, extraction kinetics, and structural properties of the aggregates.

When octanol is added in large amount and used as a cosolvent, a structural transition occurs in the molecular organization of the solution. A new structure appears organized in a hydrogen-bond network that contains the diamide. When present, this hydrogen-bonded network has a specific SAXS signature (*132–134*). Indeed, upon the addition of octanol, the scattering spectrum is modified from a classical reverse-micelle spectrum to a spectrum containing a broad peak, characteristic of a mean distance in the sample between regions of high electronic density, as shown in Figure 7.19.
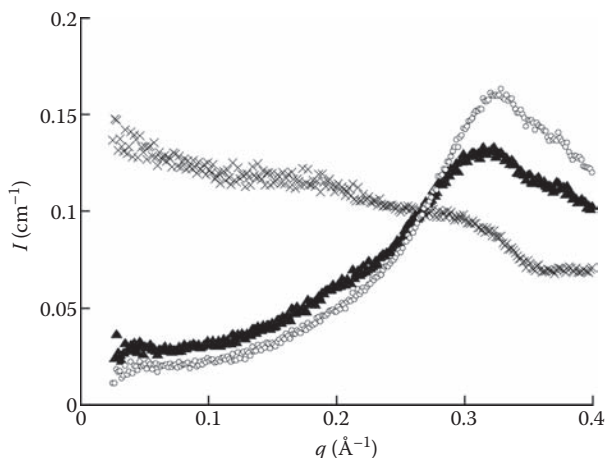
FIGURE 7.19   Small-angle X-ray scattering spectra of solutions of [DMDOHEMA] = 0.7 M in various solvents: (×): extractant reverse micelles in dodecane; or extractant dispersed in structured solvent: (▲) for $\phi_{dodecane}/\phi_{octanol} = 24/76$ and (**O**) octanol. (From F. Testard, P. Bauduin, L. Martinet, B. Abécassis, L. Berthon, and C. Madic, *Radiochim. Acta*, 96: 1–8, 2008. With permission.)

This transition from reverse micelles to a tridimensional H-bond network has a direct consequence on third-phase formation. Moreover, the structure of the solution does not depend on the nitric acid concentration. Third-phase formation is thus prevented. Significant variations in extraction properties can be expected concurrently with this micelle-to-cosolvent microstructural transition. Without octanol, polar microdomains are clearly separated from the apolar solvent by an interface, whereas in the second system, the transition between polar and apolar areas is spatially more extended and probably creates an "open" structure as in a network. Nevertheless, a systematic study with structural determination in relation with the extraction ability is not yet available in the literature. Regarding the efficiency of the extractant solution containing modifiers, the key issue is also the competition for complexation between the complexing agent and the cosurfactant head-group.

7.4.2.2   Using the Packing Parameter to Explain the Role of Modifiers

The packing parameter concept can be used to understand the role of the modifier on the structure, as shown by Bauduin et al. (*135*) DMDBBPMA-alkane solutions form a third phase when equilibrated with water. The third phase can be suppressed by the addition of alcohols of various chain lengths. As shown in Figure 7.20, the minimum amount of *n*-alcohol sufficient to make the third phase disappear (C_{min}) was determined for DMDBTDMA-dodecane or heptane solutions. For both systems, the following general trend in the alcohol efficiency is observed: $C_5H_{11}OH < C_7H_{15}OH$
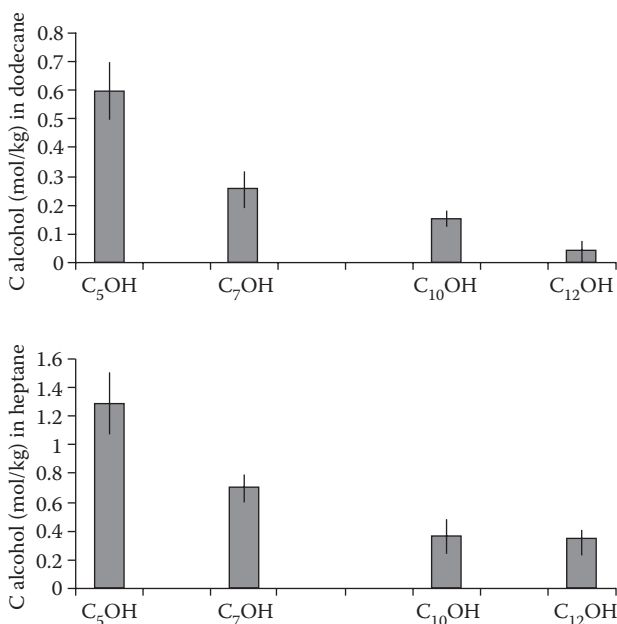
FIGURE 7.20   Amount of alcohol required to disrupt the third-phase formation observed when DMDBPMA XM (>1 M)/in dodecane or heptane is contacted with a water solution ($C_nOH = C_nH_{2n+1}OH$). (From P. Bauduin, F. Testard, L. Berthon, and Th. Zemb. *J. Phys. Chem. B*, 112: 12354–12360, 2008. With permission.)

$< C_{10}H_{21}OH < C_{12}H_{25}OH$, $C_{12}H_{25}OH$ being the most efficient alcohol in disrupting ordered phases, that is being efficient at lower concentrations. The extractant packing parameter is more influenced by dodecanol than by pentanol. The addition of a small amount of dodecanol is sufficient to increase the extractant packing parameter and thus to impose a change in the structure of the solution toward spherical aggregates.

DMDBPMA molecules form rod-like micelles, so the effective packing parameter is about 2; for spherical reverse micelles, P is approximately 3. In comparison to DMDBPMA and spherical micelle-forming extractants, modifiers have $P > 3$ due to the very low σ values. Hence, they do not form reverse rod-like or spherical micelles in oil, but rather form "poorly defined" or "softer" aggregates such as dimers, trimers, etc. The addition of alcohol to the extractant leads to comicellization and the overall P of the extractant-modifier couple increases. Adding modifiers to extractant solutions thus disrupts the rod-like or spherical aggregates. By disrupting rod-like DMDBPMA micelles, which cause phase splitting, the addition of a modifier prevents phase instability. P increases with the alkyl chain length of n-alcohols: the longer the n-alcohol, the more efficient it is in disrupting aggregates and hence in preventing third-phase formation, as observed experimentally. The addition of a small amount of dodecanol is then sufficient to prevent third-phase formation in DMDBPMA systems.

The trend for the different alcohols according to their ability to suppress the third phase in the DMDBTDMA-alkane system is consistent with the results reported by Dhamodaran and Srinivasan and summarized in the review of Rao et al. (*4*). Dhamodaran et al. showed that increasing the carbon chain length of the alcohol from C4 to C9 leads to a monotonous increase in LOC in the Th(IV)-TBP system. Srinivasan et al. showed a similar effect of alcohol between butanol and heptanol on the LOC of a Pu(IV)-TBP system.

7.5   MICROSTRUCTURE OF THE CONCENTRATED PHASES OF EXTRACTANT

The origin of third-phase formation is unambiguously related to the supramolecular organization of the extractant, as shown by the numerous papers on this subject in the last 10 years, but few structural investigations have focused on the third phase. From the phase diagram, it is clear that the third phase has the same chemical composition and the same structure as an organic phase with a high extractant concentration loaded with a solute at concentrations below the LOC. Thus, the structure of the third phase can be understood using the concentrated region of the phase diagram determined and studied with two different approaches from coordination chemistry and supramolecular organization.

7.5.1   LAMELLAR STRUCTURE IN CONCENTRATE REGIME

Few studies in the literature concern the structure of concentrated phases of extractant in diluent. Recently, Bauduin et al. (*125*) have investigated the structure of DMDBPMA-dodecane and DMDBTDMA-dodecane solutions in the concentrate regime. Figure 7.21 clearly shows the difference in the microstructure of the
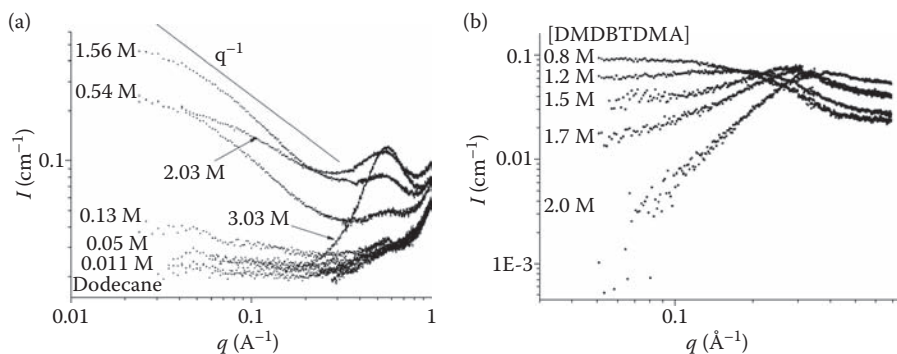
FIGURE 7.21 SAXS spectra of malonamide/dodecane solution from dilute to concentrate regime. (a) DMDBPMA and (b) DMDBTDMA. (From P. Bauduin, F. Testard, L. Berthon, and T. Zemb, *Phys. Chem. Chem. Phys.*, 9: 3776–3785, 2007. With permission.)

solutions. The scattering data need to be plotted on a logarithmic scale, because scattered intensities differ by orders of magnitude. Spherical reverse micelles formed in DMDBPMA-dodecane solutions at low concentrations become rod-like micelles at about 1 M, and at high concentrations the spectra show a strong and broad "correlation peak." The maximum of the peak, q_{peak}, can be used to determine the corresponding typical correlation length $D*$ through the expression $D*=2p/q_{peak}$ where $D*$ corresponds to the average distance between polar heterogeneities in the solution, that is, regions of higher electronic density constituted by the polar components of aggregated extractant molecules in an aliphatic hydrocarbon medium of lower electronic density. For higher concentration, the q_{peak} values are around 0.55 Å^{-1} ($D* = 11.4$ Å in real space) and remain nearly constant with the concentration.

For DMDBTDMA-dodecane, spherical reverse micelles are formed below 1 M, and the intensity at low q values is observed to decrease due to an increase in the repulsive potential between reverse micelles when the concentration increases. Furthermore, as for DMDBPMA, a correlation peak appears with increasing concentration, but here in the q range from 0.16 to 0.31 Å^{-1}. The position of the peak is shifted to higher q values as the DMDBTDMA concentration increases. The $D*$ values range from around 40.2 Å at 1.2 M DMDBTDMA to 16.7 Å for nearly pure DMDBTDMA (2 M). Comparing the experimental results with the known dilution laws of the different corresponding topologies establishes that DMDBTDMA is organized into lamella, being sterically stabilized by the long alkyl chains, while DMDBPMA is organized into unstabilized disordered lamella (shown in Figure 7.22) (*125*).

Therefore, in concentrated media, malonamide extractant does not organize into spherical micelles, and the structure becomes increasingly organized as the solution viscosity increases.

This order can also be found at lower concentration when metal-extractant complexes are involved instead of a single extractant. The corresponding physical chemistry is not known, and a specific theory has to be developed for ion adsorption, by analogy with weak polyelectrolytes, the closest analog to the network of hydrogen bonds decorated with complexing molecules.
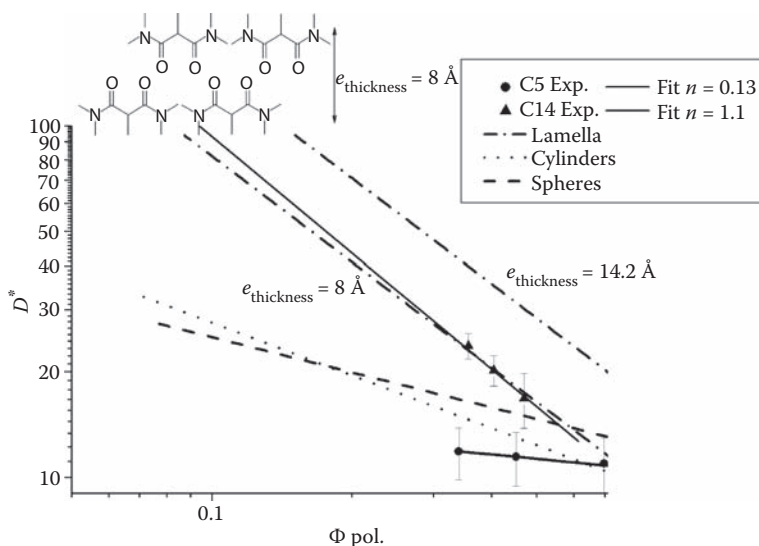
FIGURE 7.22   Variation of D^* (obtained from the maximum of the broad peak in SAXS data) for DMDBTDMA-dodecane or DMDBPMA-dodecane solutions. The theoretical dilution law for lamella, cylinders, and sphere are drawn to obtain the structure of the different solutions. Sphere for DMDBPMA (C5) and triangle for DMDBTDMA (C14). (From P. Bauduin, F. Testard, L. Berthon, and T. Zemb, *Phys. Chem. Chem. Phys.*, 9: 3776–3785, 2007. With permission.)

Figure 7.23 summarizes the four possible different organizations found in some extractant/diluent solutions. The presence in a given system of any of the four microstructures described here could have profound consequences on its dynamic and kinetic properties.

7.5.2   Liquid Crystalline State and Solid in the Third Phase

Very little structural information is available on the species formed in the third phase. Until recently, the third phase was principally investigated from a coordination chemistry point of view without any relation with the supramolecular organization of the species. Borkowski et al. (*20, 21*) studied the third phase of U(VI) or Th(IV), HNO_3/TBP, alkane systems. They demonstrated the presence of a significant amount of HNO_3 weakly bonded to the P = O group of TBP in the third phase. The amount of bound HNO_3 found when using UO_2^{2+} was greater than when Th^{4+} was used. Kumar et al. (*136*) investigated the speciation studies for U(IV), Pu(IV), and Th(IV) in the third phase from experimental results found in the literature. Earlier publications such as Kolarik et al. (*137*) concluded that for a Pu(IV)-TBP system, the solvate composition remained the same in the third phase and in the regular organic solution. Boukis et al. (*138*) and Jensen et al. (*28*) later reported that $UO_2(NO_3)_2 \cdot 2TBP \cdot HNO_3$ is found in the third phase, while $UO_2(NO_3)_2 \cdot 2TBP$ is found in the normal extractant phase. The analysis of several other publications allowed Kumar et al. (136) to conclude that during third-phase formation, extended solvates are formed for U(VI), Pu(IV), and Th(IV).
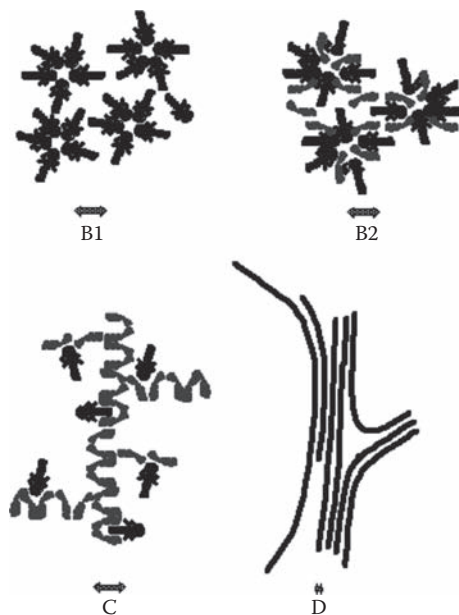
FIGURE 7.23 Four organized microstructures recognized for extractant solutions (black: extractant molecule, gray: cosurfactant or cosolvent). (B1) W/O micelles or reverse aggregates of surfactant molecules. (B2) W/O micelles with another solute acting like a cosurfactant. (C) Random dynamical networks in organized solvent, acting like adsorption sites for solubilized complexing molecules. (D) Microphase separation containing "tactoids," that is, coexistence of locally condensed structures such as a hexagonal phase. (From F. Testard, L. Berthon, and Th. Zemb, *C.R. Chimie,* 10: 1034–1041, 2007. With permission.)

Kedari et al. (101) observed similar IR spectra for the third phase obtained in the Ir(IV)-Cyanex 923 extraction system for different initial concentration of HCl in the aqueous phase. Bal et al. (*139*) recently investigated the structure of the precipitates in the third phases obtained after extraction of molybdenum(VI) and vanadium(V)-Aliquat 336 organic solutions. Chiarizia et al. (*7, 23*) characterized the third phase of the U(VI)-HNO₃/TBP-dodecane extraction system, and reported the formation of extended solvates in the third phase. SANS data reveals that the heavy organic phase can be understood as a continuous phase of $UO_2(NO_3)_2 \cdot 2TBP \cdot HNO_3$ composition with dispersed "pockets" containing an average of two molecules of dodecane.

From macroscopic observations, it appears that in the DMDBTDMA-dodecane system the nature of the third phase (liquid, gel, or solid) (*140*) depends to a large extent on the extracted species. In some cases, microphase separations can be obtained, that is, the coexistence of a more crystalline phase with domains of diluted phase that do not separate upon centrifugation. In classical colloidal literature (*141*), this situation is described as a dispersion of tactoids in the form of small amounts of liquid crystals, giving macroscopically a gel.

In the DMDBTDMA-alkane system (*37, 140*), the third phase is a gel when neodymium nitrate or thorium nitrate are extracted at high concentration, but

contains a precipitate when uranyl nitrate is extracted (with an induction period related to the concentration of the species). In the case of the gel, the SANS patterns reveal the microphase separation. For the solid in the third phase obtained with uranyl nitrate from DMDBTDMA-dodecane, the SANS patterns clearly show a correlation peak corresponding to 17 Å in real space. The diffraction correlogram for the third phase was compared with the structure of a DMDBTDMA-$UO_2(NO_3)_2$ crystal obtained from the third phase after filtration, washing, and recrystallization. It can be concluded from the similarity of the two spectra that the third phase is ordered over large distances (>500 Å) and that the third phase is organized into a crystal with a lattice parameter of 33 Å with interleaved layers of hydrophobic extractant chains and of uranyl nitrate. A supramolecular organization is still present in the third phase in relation with the speciation of the extracted salt and extractant.

7.6   CONCLUSIONS

The colloidal approach provides a better understanding of third-phase formation than earlier models relying solely on coordination chemistry or regular solution theory, for example. The presence of reverse micelles with a polarizable core is the key to understanding phase separation. In some cases, the structure of the aggregates can change from spherical to cylindrical or lamellar structures leading to third-phase formation under different conditions. The third-phase formation is thus a consequence of the self-assembling properties of both the extractants and the solute-extractant complexes. Despite the very low aggregation numbers (between 4 and 10) of the reverse micelles, the colloidal concepts can be used to describe the liquid/liquid extraction. This approach places the extractant at the center of the extraction studies.

Regarding the liquid/liquid extraction from the metal standpoint is rather different. This is the classical approach of coordination chemistry (most of the publications in this area). Today, it is still difficult to establish a direct link between the two descriptions of the organic extractant phases. To better understand liquid/liquid extraction, the aggregation number and coordination number must be measured separately for each system and set of initial conditions. This is the only way to determine the role of the aggregates in the extraction efficiency. This important point was emphasized by Yaita et al. (*61*). In this way, Gannaz et al. has used an approach combining studies on both supramolecular and molecular speciation of extractant systems of the DIAMEX-SANEX process (*36*).

In the aggregates, not all the extractant molecules are coordinated with the ion. According to coordination chemistry, this is equivalent to considering that some extractants are present as outer-sphere ligands in the complex. This can account for some discrepancies between the slope analysis and the stoichiometry of the complexes found by other methods. Extractants that are not directly bound to the metal can be considered to be involved in a process of solubilization of the complexes formed at the water/oil interface.

Although the role of the self-assembling properties of the extractant in the stability of the organic phase has now been demonstrated, this is not yet the case for the

extraction efficiency. A recent approach considering the extractant as a potential surface where ions can adsorb may allow discriminating between the chelating role of the extractant and the role of the aggregate in the extraction efficiency (*142*).

ACKNOWLEDGMENTS

REFERENCES

1. W. W. Schulz and J. D. Navratil. *Science and Technology of Tributyl Phosphate*. CRC Press, Boca Raton, FL, 1984.
2. C. Madic, B. Boullis, P. Baron, F. Testard, M. J. Hudson, J.-O. Liljenzin, B. Christiansen, M. Ferrando, A. Facchini, A. Geist, G. Modolo, A. G. Espartero, and J. de Mendoza. Futuristic back-end of the nuclear fuel cycle with the partitioning of minor actinides. *J. Alloys Compd.*, 444–445:23–27, 2007.
3. A. P. Paiva and P. Malik. Recent advances on the chemistry of solvent extraction applied to the reprocessing of spent nuclear fuels and radioactive wastes. *J. Radioanal. Nucl. Chem.*, 261:485–496, 2004.
4. P. R. V. Rao and Z. Kolarik. A review of third phase formation in extraction of actinides by neutral organophosphorus extractants. *Solvent Extr. Ion Exch.*, 14(6):955–993, 1996.
5. S. Tachimori, Y. Sasaki, and S. Suzuki. Modification of TODGA-n-dodecane solvent with a monoamide for high loading of lanthanides(III) and actinides(III). *Solvent Extr. Ion Exch.*, 20(6):687–699, 2002.
6. R. Chiarizia, M. P. Jensen, P. G. Rickert, Z. Kolarik, M. Borkowski, and P. Thiyagarajan. Extraction of zirconium nitrate by TBP in n-octane: Influence of cation type on third phase formation according to the "sticky spheres" model. *Langmuir*, 20(25): 10798–10808, 2004.
7. R. Chiarizia, K. L. Nash, M. P. Jensen, P. Thiyagarajan, and K. C. Littrell. Application of the Baxter model for hard spheres with surface adhesion to sans data for the U(VI)-HNO$_3$, TBP-n-dodecane system. *Langmuir*, 19(23):9592–9599, 2003.
8. K. Osseo-Asare. Aggregation, reversed micelles, and microemulsions in liquid-liquid extraction: The tri-n-butyl phosphate-diluent-water-electrolyte system. *Adv. Colloid Interface Sci.*, 37:123–173, 1991.
9. Y. Chevalier and T. Zemb. The structure of micelles and microemulsions. *Rep. Prog. Phys.*, 53(3):279–371, 1990.
10. H. F. Eicke. Surfactants in nonpolar solvents. Aggregation and micellization. *Topics Curr. Chem.*, 87:85–145, 1980.
11. T. P. Hoar and J. P. Schulman. Transparent water-in-oil dispersions: the oleopathic hydro-micelle. *Nature*, 152:102–103, 1943.
12. M. Kahlweit and R. Strey. Phase-behavior of ternary-systems of the type H$_2$O-oil-nonionic amphiphile (microemulsions). *Angewandte Chemie. International edition in English*, 24(8):654–668, 1985.

13. H. Watarai. Microemulsions in separation sciences. *J. Chromatogr. A*, 780(1–2):93–102, 1997.

14. P. A. Winsor. *Solvent Properties of Amphiphilic Compounds*. Butterworth Scientific, London, 1954.

15. R. Chiarizia, V. Urban, P. Thiyagarajan, and A. W. Herlinger. Aggregation of p,p′-di(2-ethylhexyl) methanediphosphonic acid and its Fe(III) complexes. *Solvent Extr. Ion Exch.*, 16(5):1257–1278, 1998.

16. H. Diamond, P. Thiyagarajan, and E. P. Horwitz. Small-angle neutron-scattering studies of praseodymium-CMPO polymerization. *Solvent Extr. Ion Exch.*, 8(3):503–513, 1990.

17. P. Thiyagaran, H. Diamond, and E. P. Horwitz. Small-angle neutron-scattering studies of the aggregation of $Pr(NO_3)_3$-CMPO and $PrCl_3$-CMPO complexes in organic-solvents. *J. Appl. Crystallogr.*, 21:848–852, 1988.

18. P. Lindner and Th. Zemb. *Neutron X-rays & Light: Scattering Methods Applied to Soft Condensed Matter*. North Holland, Amsterdam, Rev Sub edition, 2002.

19. C. Erlinger, D. Gazeau, T. Zemb, C. Madic, L. Lefrancois, M. Hebrant, and C. Tondre. Effect of nitric acid extraction on phase behavior, microstructure and interactions between primary aggregates in the system dimethyldibutyltetradecylmalonamide (DMDBTDMA) n-dodecane water: A phase analysis and small angle x-ray scattering (SAXS) characterisation study. *Solvent Extr. Ion Exch.*, 16(3):707–738, 1998.

20. M. Borkowski, R. Chiarizia, M. P. Jensen, J. R. Ferraro, P. Thiyagarajan, and K. C. Littrell. Sans study of third phase formation in the $Th(IV)$-HNO_3/TBP-n-octane system. *Sep. Sci. Technol.*, 38(12–13):3333–3351, 2003.

21. M. Borkowski, J. R. Ferraro, R. Chiarizia, and D. R. McAlister. Ft-ir study of third phase formation in the U(VI) or $Th(IV)$/HNO_3, TBP/alkane systems. *Solvent Extr. Ion Exch.*, 20:313–330, 2002.

22. R. Chiarizia, M. P. Jensen, M. Borkowski, J. R. Ferraro, P. Thiyagarajan, and K. C. Littrell. Sans study of third phase formation in the $U(VI)$-HNO_3/TBP-n-dodecane system. *Sep. Sci. Technol.*, 38(12–13):3313–3331, 2003.

23. R. Chiarizia, M. P. Jensen, M. Borkowski, J. R. Ferraro, P. Thiyagarajan, and K. C. Littrell. Third phase formation revisited: The U(VI), HNO_3-TBP, n-dodecane system. *Solvent Extr. Ion Exch.*, 21(1):1–27, 2003.

24. R. Chiarizia, M. P. Jensen, M. Borkowski, and K. L. Nash. A new interpretation of third-phase formation in the solvent extraction of actinides by TBP. *Separations for the Nuclear Fuel Cycle in the 21st Century*, 933:135–150, 2006.

25. R. Chiarizia, M. P. Jensen, M. Borkowski, P. Thiyagarajan, and K. C. Littrell. Interpretation of third phase formation in the $Th(IV)$-HNO_3, TBP-n-octane system with Baxter's "sticky spheres" model. *Solvent Extr. Ion Exch.*, 22(3):325–351, 2004.

26. R. Chiarizia, P. G. Rickert, D. Stepinski, P. Thiyagarajan, and K. C. Littrell. Sans study of third phase formation in the HCl-TBP-n-octane system. *Solvent Extr. Ion Exch.*, 24(2):125–148, 2006.

27. R. Chiarizia, D. C. Stepinski, and P. Thiyagarajan. Sans study of third phase formation in the extraction of HCl by TBP isomers in n-octane. *Sep. Sci. Technol.*, 41(10):2075–2095, 2006.

28. M. P. Jensen and A. H. Bond. Influence of aggregation on the extraction of trivalent lanthanide and actinide cations by purified Cyanex 272, Cyanex 301, and Cyanex 302. *Radiochim. Acta*, 90(4):205–209, 2002.

29. M. P. Jensen, R. Chiarizia, J. R. Ferraro, M. Borkowski, K. L. Nash, P. Thiyagarajan, and K. C. Littrell. New insights in third phase formation in the $U(VI)$-HNO_3-TBP-alkane system. In *Proceeding of the International Solvent Extraction Conference 2002* (ISEC 2002), 2002.

30. M. P. Jensen, T. Yaita, and R. Chiarizia. Reverse-micelle formation in the partitioning of trivalent f-element cations by biphasic systems containing a tetraalkyldiglycolamide. *Langmuir*, 23(9):4765–4774, 2007.

31. S. Nave, G. Modolo, C. Madic, and F. Testard. Aggregation properties of n,n,n′,n′-tetraoctyl-3-oxapentanediamide (TODGA) in n-dodecane. *Solvent Extr. Ion Exch.*, 22:1–25, 2004.

32. R. Chiarizia, R. E. Barrans, J. R. Ferraro, A. W. Herlinger, and D. R. McAlister. Aggregation of dialkyl-substituted diphosphonic acids and its effect on metal ion extraction. *Sep. Sci. Technol.*, 36(5–6):687–708, 2001.

33. Z. Kolarik and E. P. Horwitz. Extraction of metal nitrates with octyl(phenyl)-n,n-diisobutyl-carbamoylmethyl phosphine oxides in alkane diluents at high solvent loading. *Solvent Extr. Ion Exch.*, 6(1):61–91, 1988.

34. L. Berthon, L. Martinet, F. Testard, C. Madic, and Th. Zemb. Solvent penetration and sterical stabilization of reverse aggregates based on the diamex process extracting molecules: Consequences for third phase formation. *Solvent Extr. Ion Exch.*, 25:545–576, 2007.

35. L. Bosland. Etude thermodynamique et cinétique de l'extraction des nitrates de lanthanides par un malonamide (N,N' diméthyl –N,N' dioctyl hexyléthoxy malonamide ou DMDOHEMA). PhD thesis, Thèse de l'école centrale Paris. Report CEA-R-6099, 2006.

36. B. Gannaz. Spéciation moléculaire et supramoléculaire de systèmes d'extraction liquide-liquide à base de malonamide et/ou d'acides dialkylphosphoriques pour la séparation An(III)/Ln(III). PhD thesis, Université Paris XI Orsay, 2006.

37. L. Martinet. Organisation Supramoléculaire des Phases Organiques de Malonamides du Procédé d'Extraction DIAMEX. PhD thesis, Thèse de doctorat de l'Université Paris XI Orsay. Rapport CEA-R-6105, 2005.

38. G. Cote. The supramolecular speciation: A key for improved understanding and modelling of chemical reactivity in complex systems. *Radiochim. Acta*, 91(11):639–643, 2003.

39. M. R. S. J. Foreman, M. J. Hudson, A. Geist, C. Madic, and M. Weigl. An investigation into the extraction of americium(III), lanthanides and d-block metals by 6,6′-bis-(5,6-dipentyl-1,2,4)triazin-3-yl)-2,2')bipyridinyl(c-5-btbp). *Solvent Extr. Ion Exch.*, 23(5):645–662, 2005.

40. M. J. Hudson, M. G. B. Drew, M. R. S. Foreman, C. Hill, N. Huet, C. Madic, and T. G. A. Youngs. The coordination chemistry of 1,2,4-triazinyl bipyridines with lanthanide(III) elements – implications for the partitioning of americium(III). *Dalton Trans.*, (9):1675–1685, 2003.

41. M. Nilsson, S. Andersson, F. Drouet, C. Ekberg, M. Foreman, M. Hudson, J. O. Liljenzin, D. Magnusson, and G. Skarnemark. Extraction properties of 6,6′-bis-(5,6-dipentyl-1,2,4)triazin-3-yl)-2,2′)bipyridinyl (C5-BTBP). *Solvent Extr. Ion Exch.*, 24(3):299–318, 2006.

42. M. Nilsson, C. Ekberg, M. Foreman, M. Hudson, J. O. Liljenzin, G. Modolo, and G. Skarnemark. Separation of actinides(III) from lanthanides(III) in simulated nuclear waste streams using 6,6′-bis-(5,6-dipentyl-1,2,4)triazin-3-yl)-2,2′)bipyridinyl (c5-btbp) in cyclohexanone. *Solvent Extr. Ion Exch.*, 24(6):823–843, 2006.

43. C. Madic, F. Testard, M. J. Hudson, J. O. Liljenzin, B. Christianson, M. Ferrando, A. Facchini, A. Geist, G. Modolo, A. Gonzalez Espartero, and J. de Mendoza. Nuclear science and technology partitioning: New solvent extraction processes for minor actinides (partnew) contract no fikw-ct2000-00087. Technical report, 2003.

44. D. F. Evans and H. Wennerström. *The Colloidal Domain: Where Physics, Chemistry, Biology, and Technology Meet*. Wiley-VCH, New York, 1999.

45. S. J. Chen, D. F. Evans, B. W. Ninham, D. J. Mitchell, F. D. Blum, and S. Pickup. Curvature as a determinant of microstructure and microemulsions. *J. Phys. Chem.*, 90(5):842–847, 1986.

46. J.W. Gibbs. *The Collected Works of J.W. Gibbs*. Longmans, Green, London, Vol. I, 1928.

47. A. Aroti, E. Leontidis, M. Dubois, and T. Zemb. Effects of monovalent anions of the Hofmeister series on DPPC lipid bilayers part I: Swelling and in-plane equations of state. *Biophys. J.*, 93(5):1580–1590, 2007.

48. A. G. Gaonkar and R. D. Neuman. Interfacial activity, extractant selectivity and reversed micellization in hydrometallurgical liquid/liquid extraction systems. *J. Colloid Interface Sci.*, 119:251–261, 1987.

49. S. Nave, C. Mandin, L. Martinet, L. Berthon, F. Testard, C. Madic, and T. Zemb. Supramolecular organisation of tri-n-butyl phosphate in organic diluent on approaching third phase transition. *Phys. Chem. Chem. Phys.*, 6(4):799–808, 2004.

50. G. F. Vandegrift and E. P. Horwitz. Interfacial activity of liquid-liquid extraction reagents. *J. Inorgan. Nuclear Chem.*, 42:119–125, 1979.

51. W. Nitsch and M. Weigl. Action of amphiphile layers on the kinetics of interfacial reactions at liquid/liquid interfaces. *Langmuir*, 14:6709–6715, 1998.

52. M. Weigl, A. Geist, A. Mullich, and K. Gompper. Kinetics of americium (III) extraction and back extraction with BTP. *Solvent Extr. Ion Exch.*, 24:845–860, 2006.

53. R. Diss and G. Wipff. Lanthanide cation extraction by malonamide ligands: From liquid-liquid interfaces to microemulsions. A molecular dynamics study. *Phys. Chem. Chem. Phys.*, 7(2):264–272, 2005.

54. P. Beudaert, V. Lamare, J. F. Dozol, L. Troxler, and G. Wipff. Theoretical studies on tri-n-butyl phosphate: Md simulations in vacuo, in water, in chloroform, and at a water/chloroform interface. *Solvent Extr. Ion Exch.*, 16(2):597–618, 1998.

55. M. Baaden, F. Berny, and G. Wipff. The chloroform TBP aqueous nitric acid interfacial system: A molecular dynamics investigation. *J. Mol. Liq.*, 90(1–3):1–9, 2001.

56. M. Baaden, M. Burgard, and G. Wipff. TBP at the water-oil interface: The effect of TBP concentration and water acidity investigated by molecular dynamics simulations. *J. Phys. Chem. B*, 105(45):11131–11141, 2001.

57. M. Baaden, R. Schurhammer, and G. Wipff. Molecular dynamics study of the uranyl extraction by tri-n-butylphosphate (TBP): Demixing of water/oil/TBP solutions with a comparison of supercritical CO_2 and chloroform. *J. Phys. Chem. B*, 106(2):434–441, 2002.

58. B. Coupez, C. Boehme, and G. Wipff. Importance of interfacial phenomena and synergistic effects in lanthanide cation extraction by dithiophosphinic ligands: A molecular dynamics study. *J. Phys. Chem. B*, 107(35):9484–9490, 2003.

59. A. W. Herlinger, J. R. Ferraro, R. Chiarizia, and E. P. Horwitz. An investigation of p,p′-di(2-ethylhexyl) methanediphosphonic acid and some of its metal complexes. *Polyhedron*, 16(11):1843–1854, 1997.

60. C. H. Huang and R. G. Bautista. The aggregation and interactions of tributyl-phosphate and tricaprylmethylammonium nitrate in hexane by osmometry. *Sep. Sci. Technol.*, 19(8–9):515–529, 1984.

61. T. Yaita, A. W. Herlinger, P. Thiyagarajan, and M. P. Jensen. Influence of extractant aggregation on the extraction of trivalent f-element cations by a tetraalkyldiglycolamide. *Solvent Extr. Ion Exch.*, 22(4):553–571, 2004.

62. L. Coppola, U. Olsson, R. Muzzalupo, G. A. Ranieri, and M. Terenzi. Microstructures in an oil-in-water microemulsion: A NMR self-diffusion study. *Mol. Cryst. Liq. Cryst. Sci. Tech. Mol. Cryst. Liq. Cryst.*, 299:451–456, 1997.

63. B. Lindman and U. Olsson. Structure of microemulsions studied by NMR. *Berichte Der Bunsen-Gesellschaft-Phys. Chem. Chem. Phys.*, 100(3):344–363, 1996.

64. A. G. Gaonkar, T. M. Garver, and R. D. Neuman. H^1-NMR spectroscopic investigation of reversed micellization in metal organophosphorous surfactant system. *Colloids and Surfaces*, 30(3–4):265–273, 1988.

65. G. Modolo and S. Nabet. Thermodynamic study on the synergistic mixture of bis(chlorophenyl) dithiophosphinic acid and tris(2-ethylhexyl) phosphate for separation of actinides(iii) from lanthanides(iii). *Solvent Extr. Ion Exch.*, 23(3):359–373, 2005.

66. L. Nigond, C. Musikas, and C. Cuillerdier. Extraction by n,n,n′,n′-tetraalkyl-2-alkyl-propane-1,3-diamides. 1. H_2O, HNO_3 and $HClO_4$. *Solvent Extr. Ion Exch.*, 12(2):261–296, 1994.

67. L. Lefrancois, J. J. Delpuech, M. Hebrant, J. Chrisment, and C. Tondre. Aggregation and protonation phenomena in third phase formation: An NMR study of the quaternary malonamide/dodecane/nitric acid/water system. *J. Phys. Chem. B*, 105(13):2551–2564, 2001.

68. Th. Zemb. The doc model of microemulsions: Microstructure, scattering, conductivity and phase limits imposed by sterical constraints. *Colloid Surface A*, 129:435, 1997.

69. H. Dozol and C. Berthon. Characterisation of the supramolecular structure of malonamides by application of pulsed field gradients in NMR spectroscopy. *Phys. Chem. Chem. Phys.*, 9:5162–5170, 2007.

70. F. Testard, P. Bauduin, L. Martinet, B. Abécassis, L. Berthon, and Madic C. Self-assembling properties of malonamide extractants used in separation processes. *Radiochim. Acta*, 96:1–8, 2008.

71. R. D. Neuman and S. J. Park. Characterization of association microstructures in hydrometallurgical nickel extraction by di(2-ethylhexyl) phosphoric-acid. *J. Colloid Interface Sci.*, 152(1):41–53, 1992.

72. R. D. Neuman, N. F. Zhou, J. G. Wu, M. A. Jones, A. G. Gaonkar, S. J. Park, and M. L. Agrawal. General-model for aggregation of metal-extractant complexes in acidic organophosphorus solvent-extraction systems. *Sep. Sci. Technol.*, 25(13–15):1655–1674, 1990.

73. D. C. Steytler, D. L. Sargeant, G. E. Welsh, B. H. Robinson, and R. K. Heenan. Ammonium bis(ethylhexyl) phosphate: A new surfactant for microemulsions. *Langmuir*, 12(22):5312–5318, 1996.

74. P. Thiyagarajan, H. Diamond, P. R. Danesi, and E. P. Horwitz. Small-angle neutron-scattering studies of cobalt(ii) organo-phosphorus polymers in deuteriobenzene. *Inorg. Chem.*, 26(25):4209–4212, 1987.

75. Z. J. Yu, T. H. Ibrahim, and R. D. Neuman. Aggregation behavior of cobalt(II), and nickel(II) and copper(II) bis(2-ethylhexyl) phosphate complexes in n-heptane. *Solvent Extr. Ion Exch.*, 16(6):1437–1463, 1998.

76. Z. J. Yu and R. D. Neuman. Giant rodlike reversed micelles formed by sodium bis(2-ethylhexyl) phosphate in n-heptane. *Langmuir*, 10(8):2553–2558, 1994.

77. Z. J. Yu and R.D. Neuman. Giant rodlike reversed micelles. *J. Am. Chem. Soc.*, 116:4075, 1994.

78. T. H. Ibrahim and R. D. Neuman. Nanostructure of open water-channel reversed micelles. i. H^1-NMR spectroscopy and molecular modeling. *Langmuir*, 20(8):3114–3122, 2004.

79. T. H. Ibrahim and R. D. Neuman. Molecular modeling study of the aggregation behavior of nickel(II), cobalt(II), lead(II) and zinc(II) bis(2-ethylhexyl) phosphate complexes. *J. Colloid Interface Sci.*, 294(2):321–327, 2006.

80. R. D. Neuman and T. H. Ibrahim. Novel structural model of reversed micelles: The open water-channel model. *Langmuir*, 15(1):10–12, 1999.

81. I. S. Barnes, P. J. Derian, S. T. Hyde, B. W. Ninham, and T. N. Zemb. A disordered lamellar structure in the isotropic-phase of a ternary double-chain surfactant system. *J. Physique*, 51(22):2605–2628, 1990.

82. T. Zemb and P. Charpin. Micellar structure from comparison of x-ray and neutron small-angle scattering. *J. Physique*, 46(2):249–256, 1985.

83. C. Erlinger, L. Belloni, T. Zemb, and C. Madic. Attractive interactions between reverse aggregates and phase separation in concentrated malonamide extractant solutions. *Langmuir*, 15(7):2290–2300, 1999.

84. R. J. Baxter. Percus-yevick equation for hard spheres with surface adhesion. *J. Chem. Phys.*, 49(6):2770–2774, 1968.

85. V. A. Parsegian. *Van der Waals Forces: A Handbook for Biologists, Chemists, Engineers and Physicists*. Cambridge University Press, New York, 2006.

86. R. Chiarizia, M. Jensen, M. Borkowski, and K. L. Nash. New interpretation of third phase formation in the solvent extraction of actinides by TBP. *Abstracts of Papers of The American Chemical Society*, 227:U1251–U1252, 2004.

87. J. Plaue, A. Gelis, K. Czerwinski, P. Thiyagarajan, and R. Chiarizia. Small-angle neutron scattering study of plutonium third phase formation in 30% TBP/HNO$_3$/alkane diluent systems. *Solvent Extr. Ion Exch.*, 24(3):283–298, 2006.

88. R. Chiarizia and A. Briand. Third phase formation in the extraction of inorganic acids by TBP in n-octane. *Solvent Extr. Ion Exch.*, 25(3):351–371, 2007.

89. B. Abecassis, F. Testard, T. Zemb, L. Berthon, and C. Madic. Effect of n-octanol on the structure at the supramolecular scale of concentrated dimethyldioctylhexylethoxyma-lonamide extractant solutions. *Langmuir*, 19(17):6638–6644, 2003.

90. S. V. G. Menon, V. K. Kelkar, and C. Manohar. Application of Baxter model to the theory of cloud points of nonionic surfactant solutions. *Phys. Rev. A*, 43(2):1130–1133, 1991.

91. M. Corti and V. Degiorgio. Micellar properties and critical fluctuations in aqueous-solutions of non-ionic amphiphiles. *J. Phys. Chem.*, 85(10):1442–1445, 1981.

92. R. Kjellander. Phase-separation of non-ionic surfactant solutions – a treatment of the micellar interaction and form. *J. Chem. Soc.-Faraday Trans. II*, 78:2025–2042, 1982.

93. L. Lefrancois, F. Belnet, D. Noel, and C. Tondre. An attempt to theoretically predict third-phase formation in the dimethyldibutyltetradecylmalonamide (DMDBTDMA)/dodecane/water nitric acid extraction system. *Sep. Sci. Technol.*, 34(5):755–770, 1999.

94. D. F. Evans, D. J. Mitchell, and B. W. Ninham. Oil, water, and surfactant – properties and conjectured structure of simple microemulsions. *J. Phys. Chem.*, 90(13):2817–2825, 1986.

95. A. Bumajdad and J. Eastoe. Conductivity of mixed surfactant water-in-oil microemulsions. *Phys. Chem. Chem. Phys.*, 6(7):1597–1602, 2004.

96. A. Bumajdad and J. Eastoe. Conductivity of water-in-oil microemulsions stabilized by mixed surfactants. *J. Colloid Interface Sci.*, 274(1):268–276, 2004.

97. P. Biddle, A. Coe, H. A. C. Mckay, J. H. Miles, and M. J. Waterman. Some properties of mineral acid solutions in tri-n-butyl phosphate as functions of water concentration. *J. Inorgan. Nuclear Chem.*, 29(10):2615–2627, 1967.

98. E. Hesford and H. A. C. Mckay. The extraction of mineral acids by tri-normal-butyl phosphate (TBP). *J. Inorgan. Nuclear Chem.*, 13(1–2):156–164, 1960.

99. P. R. V. Rao, R. Dhamodaran, T. G. Srinivasan, and C. K. Mathews. The effect of diluent on 3rd phase-formation in thorium nitrate-TBP system – some novel empirical correlations. *Solvent Extr. Ion Exch.*, 11(4):645–662, 1993.

100. V. Vidyalakshmi, M. S. Subramanian, T. G. Srinivasan, and P. R. V. Rao. Effect of extractant structure on third phase formation in the extraction of uranium and nitric acid by N,N-dialkyl amides. *Solvent Extr. Ion Exch.*, 19(1):37–49, 2001.

101. C. S. Kedari, T. Coll, and A. Fortuny. Third phase formation in the solvent extraction system ir(IV) – Cyanex 923. *Solvent Extr. Ion Exch.*, 23(4):545–559, 2005.

102. P. N. Pathak, D. R. Prabhu, and V. K. Manchanda. Distribution behaviour of U(VI), Th(IV) and Pa(V) from nitric acid medium using linear and branched chain extractants. *Solvent Extr. Ion Exch.*, 18(5):821–840, 2000.

103. Y. Sasaki, Z. X. Zhu, Y. Sugo, H. Suzuki, and T. Kimura. Extraction capacity of diglyco-lamide derivatives for Ca(II), Nd(III) and Zr(IV) from nitric acid to n-dodecane containing a solvent modifier. *Anal. Sci.*, 21(10):1171–1175, 2005.

104. Y. Sasaki, Y. Sugo, S. Suzuki, and T. Kimura. A method for the determination of extraction capacity and its application to N,N,N′,N′-tetraalkyl derivatives of diglycol-amide-monoamide/n-dodecane media. *Anal. Chim. Acta*, 543(1-2):31–37, 2005.

105. G. M. Gasparini and G. Grossi. Long-chain disubstituted aliphatic amides as extracting agents in industrial applications of solvent-extraction. *Solvent Extr. Ion Exch.*, 4(6): 1233–1271, 1986.

106. S. Nave, J. Eastoe, R. K. Heenan, D. Steytler, and I. Grillo. What is so special about Aerosol-OT? 2. Microemulsion systems. *Langmuir*, 16(23):8741–8748, 2000.

107. R. Leung and D. O. Shah. Solubilization and phase-equilibria of water-in-oil micro-emulsions. 2. Effects of alcohols, oils, and salinity on single-chain surfactant systems. *J. Colloid Interface Sci.*, 120(2):330–344, 1987.

108. R. Dhamodaran, T. G. Srinivasan, and P. R. Vasudevan, Rao. Effect of alcohols on third phase formation in extraction of Th(IV) by tributyl phosphate. In *Proceeding of Nuclear and radiochemistry Symposium*. S. G. KulKarni, S. B. Manohar, D. D. Sood (eds). Babha Atomic Research Centre, Bombay, 1995. pp. 126–127.

109. J.-P. Hansen and I. R. McDonald. *Theory of Simple Liquids*. 2nd edn. Academic Press, New York, 1986.

110. Y. Marcus. *Ion Properties*. 3rd edn. CRC Press, Boca Raton, FL, 2004.

111. N. Condamines and C. Musikas. The extraction by N,N-dialkylamides. 1. HNO_3 and other inorganic acids. *Solvent Extr. Ion Exch.*, 6(6):1007–1034, 1988.

112. K. D. Collins and M. W. Washabaugh. The Hofmeister effect and the behavior of water at interfaces. *Q. Rev. Biophys.*, 18(4):323–422, 1985.

113. W. Kunz, J. Hendle, and B. W. Ninham. Zur Lehre von der Wirkung der Salze (about the science of the effect of salts). Franz Hofmeister's historical papers. *Curr. Opin. Colloid Interface Sci.*, 9:19–37, 2004.

114. K. D. Collins. Ions from the Hofmeister series and osmolytes: Effects on proteins in solution and in the crystallization process. *Methods*, 34(3):300–311, 2004.

115. A. S. Kertes. The chemistry of the formation and elimination of a third phase in organo-phosphorous and amine extraction systems. In *Solvent Extraction Chemistry of Metals*. H. A. C. McKay, T. V. Healy, I. L. Jenkins, and A. Naylor, Macmillan, London, 1965. pp. 377–399.

116. Y. Marcus and A. S. Kertes. *Ion Exchange and Solvent Extraction of Metal Complexes*. Wiley-Interscience, New York, 1969.

117. B. W. Ninham and V. Yaminsky. Ion binding and ion specificity: The Hofmeister effect and Onsager and Lifshitz theories. *Langmuir*, 13(7):2097–2108, 1997.

118. B. Kanellakopulos, V. Neck, and J. I. Kim. Preferential solvation of single ions and the TBP-extraction behavior of acids, uo2(tco4)2 and uo2(no3)2. *Radiochim. Acta*, 48(3–4):159–163, 1989.

119. J. N. Israelachvili, D. J. Mitchell, and B. W. Ninham. Theory of self-assembly of hydrocarbon amphiphiles into micelles and bilayers. *J. Chem. Soc.-Faraday Trans. II*, 72:1525–1568, 1976.

120. A. Bernheim-Groswasser, E. Wachtel, and Y. Talmon. Micellar growth, network forma-tion, and criticality in aqueous solutions of the nonionic surfactant C12E5. *Langmuir*, 16(9):4131–4140, 2000.

121. D. Blankschtein, G. M. Thurston, and G. B. Benedek. Theory of phase-separation in micellar solutions. *Phys. Rev. Lett.*, 54(9):955–958, 1985.

122. A. Blom, G. G. Warr, and E. J. Wanless. Morphology transitions in nonionic surfactant adsorbed layers near their cloud points. *Langmuir*, 21(25):11850–11855, 2005.

123. O. Glatter, G. Fritz, H. Lindner, J. Brunner-Popela, R. Mittelbach, R. Strey, and S. U. Egelhaaf. Nonionic micelles near the critical point: Micellar growth and attractive interaction. *Langmuir*, 16(23):8692–8701, 2000.

124. S. Safran and L. Turkevich. Phase diagrams for microemulsions. *Phys. Rev. Lett.*, 50:1930–1933, 1983.

125. P. Bauduin, F. Testard, L. Berthon, and T. Zemb. Relation between the hydrophile/ hydrophobe ratio of malonamide extractants and the stability of the organic phase: Investigation at high extractant concentrations. *Phys. Chem. Chem. Phys.*, 9(28):3776– 3785, 2007.

126. J. N. Israelachvili. *Intermolecular and Surface Forces with Applications to Colloidal and Biological Systems*. Academic Press, London, 1991.

127. S. Hyde, S. Andersson, K. Larsson, Z. Blum, T. Landh, S. Lidin, and B. W. Ninham. *The Language of Shape, the Role of Curvature in Condensed Matter: Physics, Chemistry and Biology*. Elsevier Science B.V., Amsterdam, 1997.

128. B. F. Smith, K. V. Wilson, R. R. Gibson, M. M. Jones, and G. D. Jarvinen. Amides as phase modifiers for N,N′-tetraalkylmalonamide extraction of actinides and lanthanides from nitric acid solutions. *Sep. Sci. Technol.*, 32(1–4):149–173, 1997.

129. L. H. Delmau, P. V. Bonnesen, A. W. Herlinger, and R. Chiarizia. Aggregation behaviour of solvent modifiers for the extraction of cesium from caustic media. *Solvent Extr. Ion Exch.*, 23(2):145–169, 2005.

130. S. E. Debolt and P. A. Kollman. Investigation of structure, dynamics, and solvation in 1-octanol and its water-saturated solution – molecular-dynamics and free-energy perturbation studies. *J. Am. Chem. Soc.*, 117(19):5316–5340, 1995.

131. P. Sassi, A. Morresi, M. Paolantoni, and R. S. Cataliotti. Structural and dynamical investigations of 1-octanol: A spectroscopic study. *J. Mol. Liq.*, 96–97:363–377, 2002.

132. M. Tomsic, M. Bester-Rogac, A. Jamnik, W. Kunz, D. Touraud, A. Bergmann, and O. Glatter. Nonionic surfactant Brij 35 in water and in various simple alcohols: Structural investigations by small-angle x-ray scattering and dynamic light scattering. *J. Phys. Chem. B*, 108(22):7021–7032, 2004.

133. M. Tomsic, M. Bester-Rogac, A. Jamnik, W. Kunz, D. Touraud, A. Bergmann, and O. Glatter. Ternary systems of nonionic surfactant Brij 35, water and various simple alcohols: Structural investigations by small-angle x-ray scattering and dynamic light scattering. *J. Colloid Interface Sci.*, 294(1):194–211, 2006.

134. M. Tomsic, A. Jamnik, G. Fritz-Popovski, O. Glatter, and L. Vlcek. Structural properties of pure simple alcohols from ethanol, propanol, butanol, pentanol, to hexanol: Comparing Monte Carlo simulations with experimental SAXS data. *J. Phys. Chem. B*, 111(7):1738–1751, 2007.

135. P. Bauduin, F. Testard, L. Berthon, and Th. Zemb. Solubilization in alkanes by alcohols as reverse hydrotropes or «lipotropes». *J. Phys. Chem. B*, 112:12354–12360, 2008.

136. S. Kumar and S. B. Koganti. An extended Setschenow model for Pu(IV) third phase formation in 20 tri-n-butyl phosphate based nuclear solvent extraction system. *Solvent Extr. Ion Exch.*, 21(3):423–433, 2003.

137. Z. Kolarik. The formation of a third phase in the extraction of Pu(IV), U(VI) and Th(IV) nitrates with tributyl phosphate in alkane diluents. In *Proceeding of the International Solvent Extraction Conference* (ISEC-77), 1977.

138. N. Boukis and B. Kanellakopoulos. Extraction phase distribution of uranyl nitrate with tri-n-butyl phosphate: Part II – The formation of a third phase in the system $UO_2(NO_3)_2$-TBP-HNO_3. Technical report, Kernforschungszentrum Karlsruhe (KfK-3352), 1983.

139. Y. Bal, K. E. Bal, G. Cote, and A. Lallam. Characterization of the solid third phases that precipitate from the organic solutions of aliquat (r) 336 after extraction of molybdenum(VI) and vanadium(V). *Hydrometallurgy*, 75(1–4):123–134, 2004.

140. F. Testard, L. Martinet, L. Berthon, S. Nave, B. Abecassis, C. Madic, and Th. Zemb. The four types of supramolecular organisation of extractant molecules used in separation processes. In *2nd ATALANTE 2004 Conference: Advances for Future Nuclear Fuel Cycles*, 2004.

141. H. R. Kruyt. *Colloid Science*. Elsevier, New York, 1952.

142. F. Testard, L. Berthon, and Th. Zemb. Liquid-liquid extraction: An adsorption isotherm at divided interface? *C. R. Chimie*, 10:1034–1041, 2007.

8 Radiolysis of Solvents Used in Nuclear Fuel Reprocessing

Laurence Berthon and Marie-Christine Charbonnel
Commissariat à l' Energie Atomique

CONTENTS

8.1 INTRODUCTION

The international context for nuclear energy has led the scientific community to draw up common strategies to plan for new generation reactors. Recycling (individual or by families) of nuclear materials is a primary objective and requires efficient processes to be established (*1, 2*). To meet such needs, liquid-liquid extraction remains a favored route.

However, applying extraction by solvent to the nuclear field is not an easy task for the solvent that undergoes multiple attacks—chemical, thermal, but especially radiolytic. This multiplicity is reinforced by the biphasic nature of the chemical system and the presence of numerous solutes, be it in aqueous or organic phase. Radiolysis of such a system thus leads to the formation of a multitude of radicals and ionized species (including the reactive species H$^\bullet$, OH$^\bullet$, solvated electrons, H$_2$, or H$_2$O$_2$), which recombine in molecular products shared between the two phases.

The experience gained from the PUREX process, in operation for a half century, is rich in lessons learned about the potential consequences this can cause:

- Degradation of the solvent formulation (loss of efficiency due both to the partial disappearance of the extractant at the heart of the process and to the formation of degradation products that may be competitive);
- Alteration of the physicochemical properties (density, viscosity, interfacial tension, etc.);
- Modification of the extraction kinetics (presence of precipitates, of interface-active substances, etc.);
- Modification of the redox properties of the metallic ions to be extracted by reaction with the many radical species present.

During the reprocessing of fuel using the PUREX process, the degradation of tri-*n*-butyl phosphate (TBP) by hydrolysis nevertheless represents an important part, as

the surrounding medium is particularly reactive (presence of high concentrations of nitric acid).

To develop a new liquid-liquid extraction process in the nuclear field, it is therefore imperative to consider the stability of the molecules proposed as a major criterion and to integrate systematic degradation studies in order to check the robustness of the solvent submitted to radiolysis, particularly in terms of efficiency and of selectivity.

The published studies of degradation have not, however, been approached with the same methodologies. The main axes have been the following:

- Experimental studies of irradiation carried out on the extractant, either pure or in solution, under representative conditions (presence of diluent, of aqueous phase, of acid and/or metallic solutes, of complexants, etc.). Most of these approaches consist in measuring the impact of the dose delivered on:
  - The composition of the organic phase (qualitative and/or quantitative analyses);
  - The efficiency and the selectivity of the extractant by the measurement of the distribution ratios of different metallic cations;
  - The physicochemical properties of the system.

The objective of such an approach is to correlate the evolution of the solvent's composition with the modification of its properties.

- The proposition of a solvent-regenerating treatment (sometimes called solvent cleanup) to eliminate unwanted degradation products as they occur (basic scrubbing, distillation, etc.).
- Carrying out integration studies using experimental loops that enable the solvent to be submitted sequentially and cyclically to all the treatments (extraction-irradiation-scrubbing-regenerating treatment).

Selection of the radiolysis conditions is of primary importance. If studies carried out with a pure extractant enable the intrinsic stability of the molecules to be verified, radiolysis in solution and especially in a basic medium are indispensable to guarantee the approaches' good representativity, as much from the point of view of species' formation as from that of their distribution (potential elimination of the shortest degradation products, the most polar to the aqueous phase). The characteristics of the irradiation source (nature, dose rate, integrated dose) and also the temperature are essential parameters. Thus, the nature of the irradiation depends on the composition of the fuel, and the dose rate is dependent on the burn-up and cooling time of the fuel, while the exposure time of a solvent depends on the implementation conditions of the proposed process (flowsheet and nature of the contactors).

This review groups the information published on degradation of the main families of extractants studied in the frame of long-lived minor-actinide and fission-product recovery (*1–4*) (see Chapter 1): alkyl-phosphorus compounds (phosphates, phosphonic acids, bifunctional compounds like CMPO), amide compounds (dialkyl-amides, malonamides, and diglycolamides), N-donor compounds, and macrocycles like crown ethers and calixarenes (Table 8.1). The multicomponent systems based on the chlorinated cobalt dicarbollide process have not been considered.

TABLE 8.1
Acronyms and Formulae of Different Extractants

Phosphates

TBP: Tri-*n*-butyl
 phosphate
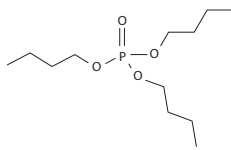
T*i*AP: Tri-*iso*-amyl
 phosphate
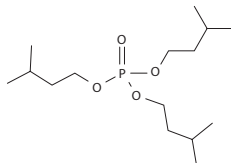
T*n*AP: Tri-*n*-amyl
 phosphate
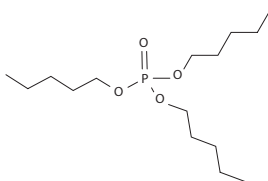
Dialkylphosphoric acids

HDEHP: Di(2-ethylhexyl)
 phosphoric acid
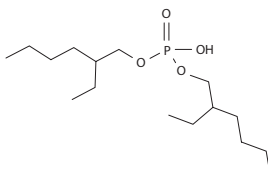
HBDMBP: Bis(1,3-
 dimethylbutyl) phosphoric
 acid
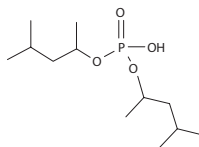
HD*i*DP: Di-*iso*-decyl
 phosphoric acid
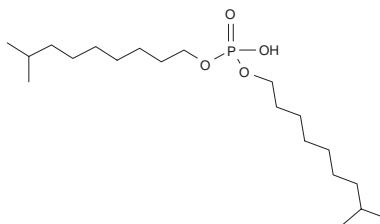
HDHOEP:
 Di(hexyloxyethyl)
 phosphoric acid
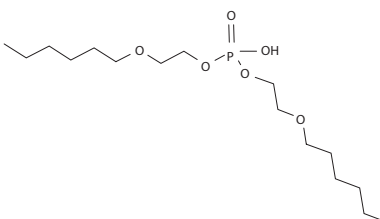
TABLE 8.1 (Continued)

Dialkyldithiophosphinic Acids

Ph$_2$PS$_2$H: Di(phenyl)
dithiophosphinic acid
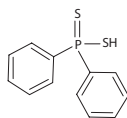
(ClPh)$_2$PS$_2$H:
Bis(chlorophenyl)
dithiophosphinic acid
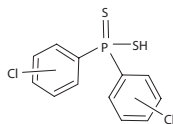
CMPO

OΦD(iB)CMPO:
Octyl(phenyl)-*N,N*-di-
iso-butylcarbamoyl
methylphosphine oxide
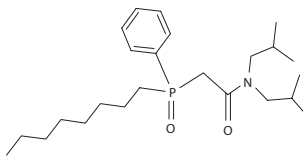
DOD(iB)CMPO:
Dioctyl-*N,N*-di-*iso*-
butylcarbamoylmethyl
phosphine oxide
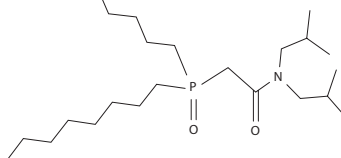
DΦD(iB)CMPO:
Diphenyl-*N,N*-di-
iso-butylcarbamoyl
methylphosphine oxide
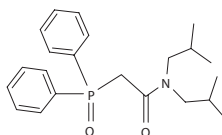
Monoamides

DBEHA: *N,N*-di-*n*-butyl-
2-ethylhexanamide
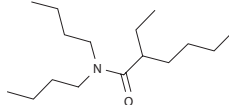
D*i*BEHA: *N,N*-di-*iso*-
butyl-2-ethylhexanamide
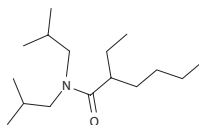
DBOA: *N,N*-di-*n*-
butyloctanamide
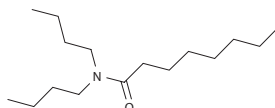
D*i*BOA: *N,N*-di-
iso-butyloctanamide
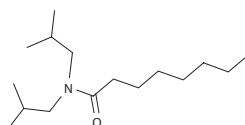
(*continued*)

TABLE 8.1   (Continued)

DEHBA: *N,N*-di(2-
ethylhexyl)-*n*-butanamide
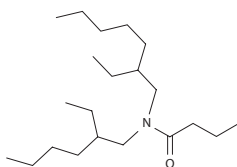
DEH*i*BA: *N,N*-di(2-
ethylhexyl)-*iso*-
butanamide
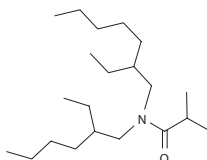
DEHDMBA: *N,N*-di(2-
ethylhexyl)-3,3-dimethyl
butanamide
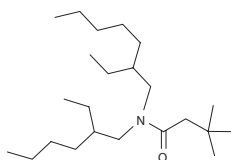
DEHHA: *N,N*-di(2-
ethylhexyl)hexanamide
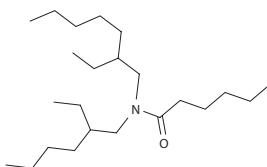
MBEHA: *N*-methyl-*N*-
butyl-2-ethylhexanamide
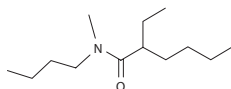
Malonamides

DMDBHDEMA:
N,N′-dimethyl-*N,N′*-
dibutylhexyldiethoxy
malonamide
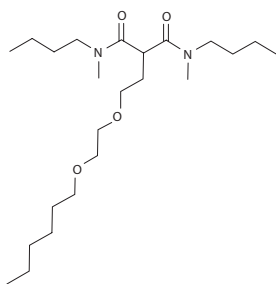
DMDOHEMA: *N,N′*-
dimethyl-*N,N′*-
dioctylhexylethoxy
malonamide
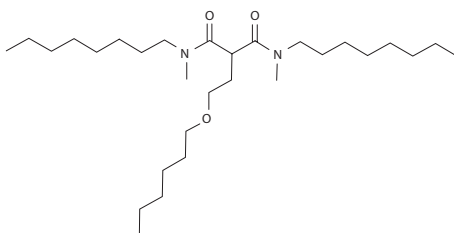
TABLE 8.1 (Continued)

DMDBDDEMA:
N,N'-dimethyl-*N,N'*-
dibutyldodecylethoxy
malonamide
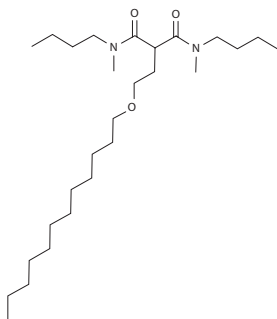
DMDBTDMA: *N,N'*-
dimethyl-*N,N'*-
dibutyltetradecyl
malonamide
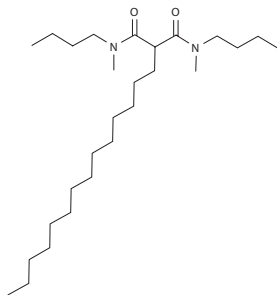
Diglycolamides

TODGA *N,N,N',*
N'-tetraoctyl-3-
oxapentane-1,5-diamide
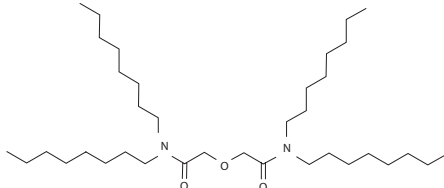
T(OPh)DGA *N,N, N',*
N'-tetrakis(*p*-octyl-
phenyl)-3-oxapentane-
1,5-diamide
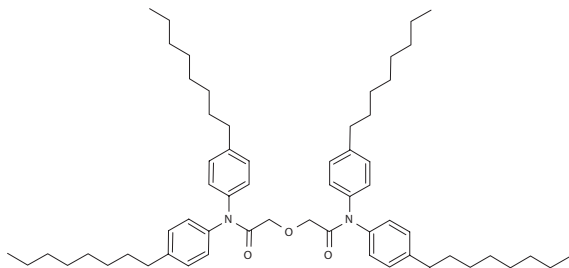
TOFDA *N,N, N',N'*-
tetraoctyl-furan-2,5-
diamide
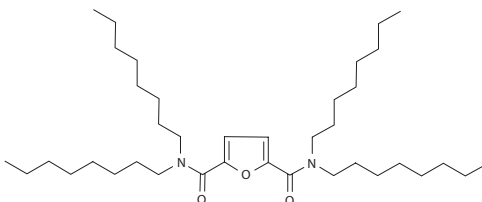
(continued)

TABLE 8.1   (Continued)

Nitrogen Polyaromatic Molecules
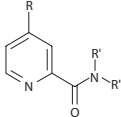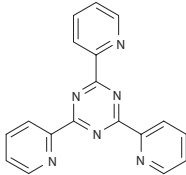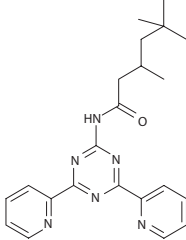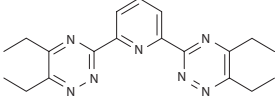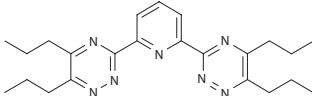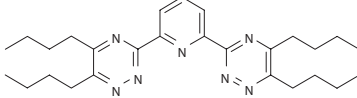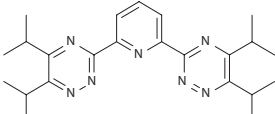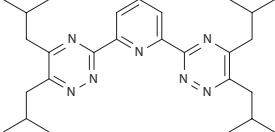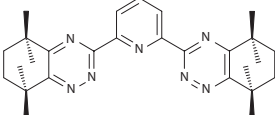
Picolinamides

TPTZ: 2,4,6-tri-(2-pyridyl)-1,3,5-triazine

TMHADPTZ: 2-(3,5,5-trimethylhexanoylamino)-4,6-di(pyridine-2-yl)-1,3,5-triazine

Et-BTP: 2,6-bis(5,6-diethyl[1,2,4]triazine-3-yl)-pyridine

***n*Pr-BTP:** 2,6-bis(5,6-di-*n*-propyl[1,2,4]triazine-3-yl)-pyridine

***n*Bu-BTP:** 2,6-bis(5,6-di-*n*-butyl[1,2,4]triazine-3-yl)-pyridine

***i*Pr-BTP:** 2,6-bis(5,6-di-*iso*-propyl[1,2,4]triazine-3-yl)-pyridine

***i*Bu-BTP:** 2,6-bis(5,6-di-*iso*-butyl[1,2,4]triazine-3-yl)-pyridine

CyMe$_4$-BTP: 2,6-bis(5,5,8,8-tetramethyl-5,6,7,8-tetrahydrobenzo[1,2,4]triazine-3-yl) pyridine

TABLE 8.1 (Continued)

BzCyMe₄-BTP: 2,6-bis(9,9,10,10-tetramethyl-9,10-dihydro-[1,2,4]-triazaanthrane-3-yl) pyridine
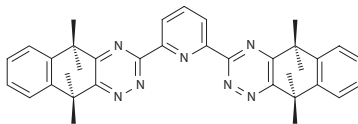
C5-BTBP: 6,6′-bis(5,6-dipentyl-1,2,4-triazin-3-yl)-2,2′-bipyridine
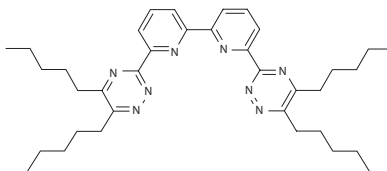
CyMe₄-BTBP: 6,6′-bis(5,5,8,8-tetramethyl-5,6,7,8-tetrahydro-benzo[1,2,4]triazin-3-yl)-[2,2′]-bipyridine
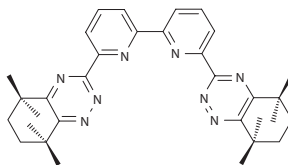
Crown Ethers

DCH18C6: Dicyclohexano-18-crown-6
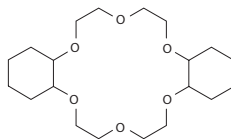
D*t*BuCH18C6: Di-*t*-butylcyclohexano-18-crown-6
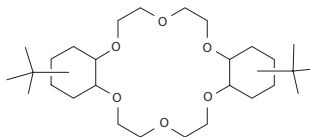
Calixarenes

octMC6: Di(*n*-octyloxy) calix[4]arene-crown-6
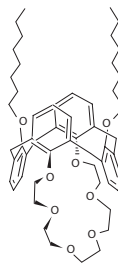
***i*PrMC6:** Di(*iso*-propyloxy)calix[4]arene-crown-6
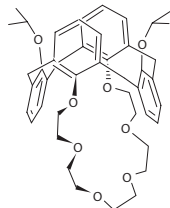
(*continued*)

TABLE 8.1   (Continued)

BC6: 1,3-*alt*-calix[4]
  arene-bis(crown-6)
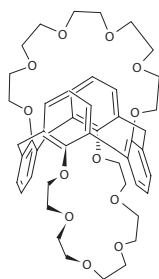
BOBCalixC6: Calix[4]
  arene-bis(*tert*-octylbenzo-
  crown-6)
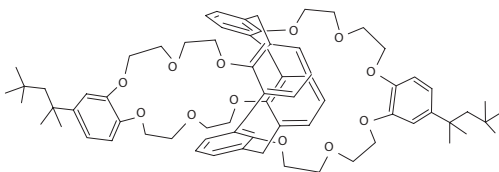
The part of this chapter concerning the TBP molecule remains the largest, as this ligand has been considered the reference extractant system for more than one reason: not only is the information published abundant (enabling a comprehensive view of the parameters acting on radiolysis, and the analysis of many influences), and has been summarized in several review articles, but also the degraded solutions have recently been analyzed by high-performance techniques that enable the identification of compounds, which though minor are nevertheless influential, and finally different scientific teams have proposed degradation mechanisms on the molecular scale. It should also be emphasized that the PUREX process's position at the head of reprocessing exposes the TBP solvent to considerable radiolysis.

After a brief presentation of the major analytical tools selected to degrade and analyze solvents, the results of degradation studies will be reported. The main points will be the presentation of the chemical damage to extractant (qualitative studies of the solvent, including identification of degradation products and presentation of a simplified degradation scheme), the macroscopic factors governing the degradation, and the impact of radiolysis on extracting capabilities. The following section provides a review of more fundamental studies related to the radiolytic degradation mechanism of organic solvent. Finally, the last part has been devoted to the establishment of the relation between the solvent's formulation (structure of the extractant, composition of the organic phase) and its radiolytic stability.

8.2   EXPERIMENTAL CONDITIONS

8.2.1   Irradiation Tools

The radiolytic degradation of solvents was usually performed by irradiation of synthetic solutions rather than industrial samples. In more than 90% of studies, samples were exposed to γ-irradiation with a ^{60}Co source, and sometimes with a ^{137}Cs

source (*4–7*). Some studies were carried out on chemical extraction systems with α-irradiations either with an external beam from a cyclotron (*8*) or by direct introduction of α-emitters (^{239}Pu (*9*), ^{238}Pu (*9–11*), ^{241}Am (*12, 13*), ^{244}Cm (*14, 15*)) in the solutions. Few experiments were performed with β-irradiation using a ^{90}Sr source (*16*). Other authors investigated radiolysis with electron accelerators (*9, 17–19*). However, studies with a comparison of two different radiation modes were rare (*8, 11, 16*).

It must be remembered that irradiation experiments can be performed with monophasic systems (in the absence of an aqueous phase) or in extraction conditions in the presence of an aqueous phase, in static or dynamic conditions (organic and aqueous phases continuously stirred with a dedicated stirrer unit (*20*), magnetic stirrer, or sparging with air).

However, the conditions are often far from those of industrial situations. In order to better simulate solvent degradation during the PUREX process, a test loop was created in the 1990s in a CEA laboratory (Fontenay-aux-Roses, France), with the EDIT loop (Extraction Désextraction Irradiation Traitement) (*21, 22*). The laboratory simulation of industrial conditions consisted of a succession of representative physical and chemical treatments after the irradiation of the solvent (i.e., alkali and acid treatments, distillation). Indeed, these treatments can modify the final solvent composition because of the elimination of some compounds or the occurrence of secondary reactions. A few years later, the MARCEL (Module Avancé de Radiolyse dans les Cycles d'Extraction Lavage) test loop was built at Marcoule to follow the regeneration efficiencies of degraded solvents involved in actinide separation processes (*4, 5*).

8.2.2 ANALYTICAL TECHNIQUES

Examination of such degraded solvents is difficult from the analytical point of view. In multicomponent extractant-diluent/aqueous phase systems, free radicals are produced by radiolysis of major compounds: water, acid, extractant, and diluent. These radicals, after dimerization or coupling with other compounds, are responsible for the formation of several families of compounds. For instance, in the PUREX process, the exposure of the solvent to radiolysis gives rise to a mixture of over 200 secondary products, most of them in trace quantities.

Research groups have used numerous analytical methods to analyze irradiated solvents. The earliest techniques, based on global analysis, allowed the identification of specific chemical functions among the degradation products, including acid-base or conductometric titration and infrared and visible absorption spectrometry (*11, 23–30*). Then, various chromatographic techniques became indispensable to separate individual species: thin-layer chromatography (*11, 31–34*); gas chromatography equipped with a flame ionization detector (GC-FID), with an electron-capture detector (*35*), with a mass spectrometer detector (GC-MS), or coupled to an infrared spectrophotometer (GC-IRTF) (*7, 8, 21, 22, 26, 34, 36–51*); ion chromatography (*52–54*); high-speed analytical isotachophoresis (*55*); or capillary electrophoresis (*56*). In the 1990s, NMR was applied to raw solutions, without any complicated pretreatment or separation steps, to identify specific solutes (*29, 57–61*). Nowadays, electrospray ionization mass spectrometry, which allows analysis of organic solutes at low levels in the solvent (*62–69*) or after liquid chromatographic separation (*70–72*), has become a useful tool.

Sometimes, the gas production rate was measured and the nature of the compounds analyzed by gas chromatography using a thermal conductivity detector or by mass spectrometry (*10, 12, 17, 73–76*).

8.2.3 RADIOLYSIS QUANTIFICATION

Authors have used different units to express total dose or dose rate. Total doses have been expressed as W h L^{-1}, eV g^{-1}, eV mL^{-1}, rad, Gy… The dose rates correspond to a dose divided by time units. On the basis of the SI units of measurement, the following equalities can be calculated (*77*):

$$1 \text{ Gy} = 100 \text{ rad} = 1 \text{ J kg}^{-1} = (1/3600) \text{ W h kg}^{-1} = 6.241 \times 10^{15} \text{ eV g}^{-1}$$

In this review, the dose has been expressed in Gy as often as possible to facilitate comparison.

The radiolytic degradation of a molecule or the formation of new species can be quantified by a radiation-chemical yield related to the energy absorbed, and the term *G*-value represents the number of molecule changes for each 100 eV of energy absorbed. Thus, $G(X)$ refers to the number of molecules of a product *X* formed on irradiation per 100 eV of energy absorbed and $G(-Y)$ refers to the loss of a material *Y* destroyed on irradiation (*78*).

8.3 RADIOLYTIC DEGRADATION OF EXTRACTANT SYSTEMS

8.3.1 ORGANOPHOSPHORUS COMPOUNDS

8.3.1.1 Trialkyl Phosphates

8.3.1.1.1 *Tri-n-butyl Phosphate Systems*

TBP is the extractant used throughout the world in spent nuclear-fuel reprocessing plants. Since the 1950s, the stability of the TBP molecule has been the subject of many investigations, and some comprehensive reviews have already been published. The first, published by Davis in 1984 (*77*), identified the degradation products and the specific role of diluents. In the review written in 1995 by Tahraoui (*79*), interest had been aroused in the degradation mechanisms. Schemes of TBP and diluent radiation-chemical transformations occurring on the decomposition of the solvent were discussed. In the period 1995–2003, with the development of the mass-spectrometry technique (GC-MS, gas chromatography and tandem mass spectrometry; ESI-MS, electrospray ionization and tandem mass spectrometry), the structure of minor degradation products (isomeric dimers of TBP, their oxidation products, and their lower homologues) could be established (*21, 22, 47, 62, 80, 81*). The behavior of high-molecular-weight compound rich fractions has also been investigated (*50, 82, 83*).

8.3.1.1.1.1 *Degradation Products from the Radiolysis of TBP/diluent/nitric Acid*

8.3.1.1.1.1.1 *Qualitative Analysis.* Degradation products from the radiolysis of TBP include di-*n*-butyl phosphoric acid (HDBP), mono-*n*-butyl phosphoric acid

(H_2MBP), phosphoric acid (H_3PO_4), and oligomer-type compounds. Gaseous products, such as hydrogen, saturated hydrocarbons, and olefins (CH_4, C_2H_2, C_2H_4, C_2H_6, C_3H_6, C_3H_8, C_4H_8, C_4H_{10}, pentenes, pentanes) are also formed (*73, 77, 84*).

The large volume of data published on the radiolysis of TBP was difficult to compare because of differing experimental conditions, for example, the irradiation procedures. The most reliable data were provided by experiments in which aqueous-organic emulsions were irradiated under conditions representative of processes, like the EDIT loop (*21, 22*). Figure 8.1 presents an overall degradation scheme obtained from recent studies (*21, 22, 34, 43, 50*) using chromatographic techniques for preliminary separation and mass spectrometry for characterization. The products resulted from hydrolysis, nitration, and oxidation of both TBP and diluents, dimerization of both TBP and diluents, radical combinations involving alkyl and TBP radicals, etc. The constituents can be separated into three distinct groups, as discussed below.

Degradation products from the diluent (Figure 8.1, Compounds A and B). Compounds A include alkane dimers and fragments of dodecane. Compounds B result from nitration and oxidation of the diluent. These nitration and oxidation reactions arise from the actions of HNO_3, O_2, H_2O, and their radiolysis products on organic components.

Degradation products from TBP (Figure 8.1, Compounds I, II, III, IV, and V).

– Compounds I are formed by homolytic breaking of the C-C bond on the butyl chain.
– Compounds II correspond to isomers resulting from nitration and oxidation of TBP.
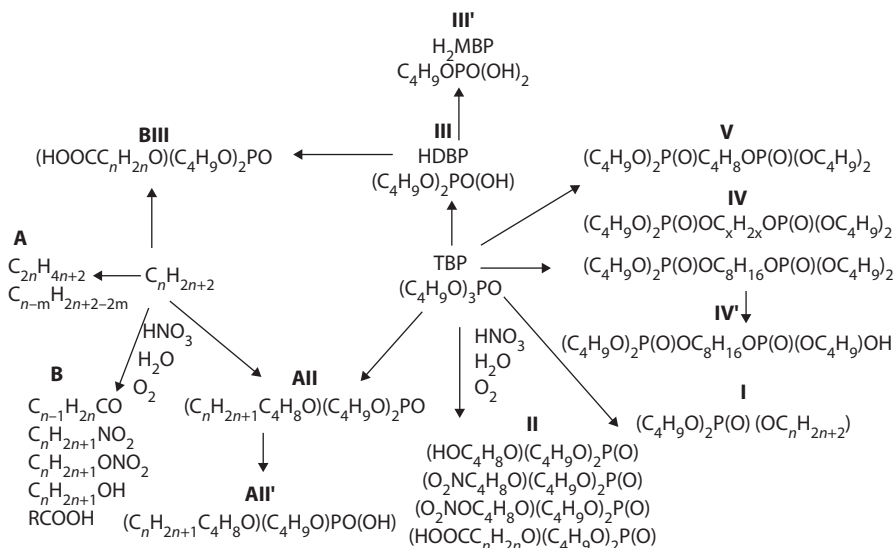
FIGURE 8.1 Scheme of formation of radiolysis products accumulated in the organic phase of the extraction system TBP-*n*-paraffin-HNO_3 aqueous solution. (Drawn from data in Refs. (*21, 22, 34, 43, 50*).)

- Compound III (HDBP) results from hydrolysis of TBP (breaking of the C-O bond) and, in turn, undergoes further hydrolysis to form III′ (H_2MBP).
- Compounds IV correspond to isomers of diphosphates, where the two phosphate groups are connected by a C_nH_{2n} chain, with $n \leq 8$. The central alkyl chain comes from the combination of two radicals and can therefore be linear or branched on different positions (see Section 8.4.1.1). These compounds can undergo hydrolysis to form IV′ compounds.
- Compounds V correspond to isomers of phosphate-phosphonates and probably result from radical recombination between $(C_4H_9O)_2P(O)O(C_4H_8)^{\bullet}$ and $(C_4H_9O)_2(O)P^{\bullet}$. The isomers differ from one another by the position of the new P-C bond along the C_4H_8 radical.

Mixed degradation products (Figure 8.1 Compounds AII and BIII)

- Compounds AII result from radical recombination involving alkyl and TBP radicals, which then undergo further hydrolysis to form AII′.
- Compounds BIII are long-chain carboxylic acids, which can arise from HDBP secondary reactions.

Numerous gaseous products are also released, such as H_2, CH_4, CO, CO_2, C_1-C_4 hydrocarbons, and several nitrogen-containing compounds (HNO_3, N_2, NO, N_2O, and NO_2) (*17, 73, 75, 77, 84*).

8.3.1.1.1.1.2   Quantitative Aspects.   The quantity of data on the yield of degradation is so large and so scattered (due to various irradiation procedures, chemical compositions, and uncertainties of analytical techniques) that a comparison remains difficult. The next paragraph illustrates the importance of experimental variables on the qualitative and quantitative radiolytic degradation. The most reliable and recent data, obtained from experiments carried out under conditions simulating the industrial process, are presented in Tables 8.2 and 8.3 (*22, 34*). In solution, HDBP was always the predominant component, with G(HDBP) close to 1.5 ± 0.2 molecules/100 eV (*34*), a value similar to the mean yield given by Shultz (1–1.5 for water-saturated TBP) (*77*). The more detailed identification performed by Lesage focused on minor phosphate components of the TBP-irradiated solutions.

   In the gas phase, the highest yield measured is always for H_2. But, as shown in Table 8.4, the G values of gaseous compounds containing nitrogen rise when the radiolysis is performed in the presence of HNO_3. No recent studies have been published.

8.3.1.1.1.2   Factors Governing the Degradation.   Much data on radiation-chemical degradation of solvent have been published, but there are some discrepancies in the results from various researchers because of the difference in procedure and experimental conditions: diluent, acidity, irradiation dose, dose rate, etc. In a 1984 review, Davis reported the influence of experimental conditions on the yield of TBP degradation products (*77*).

   In the following section, the main trends on the influence of experimental conditions, such as atmosphere, irradiation (nature, dose, and dose rate), and composition of the organic and aqueous phases, have been summarized. Generally, radiolysis of

TABLE 8.2

Accumulation of Radiolysis Products in the Organic Phase during Irradiation of TBP Solutions

	Concentration (mol L^{-1})		
	TBP	**TBP-H$_2$O ($V_{org} = 2V_{aq}$)**	**TBP-HNO$_3$ 3 M ($V_{org} = 2V_{aq}$)**
HDBP	0.17	0.12	0.19
H$_2$MBP	0.006	0.0050	0.010
Modified phosphates[a]	0.050	0.050	0.10
Diphosphates	0.030	0.04	0.005
Phosphate phosphonates	0.012	0.006	0.0008
TBP destruction[b]	0.31	0.24	0.31

Source: Adamov, V.M., Andreev, V.I., Belyaev, B.N., Markov, G.S., Polyakov, M.S., Ritori, A.E., Yu Shil'nikov, A.Y. *Kerntechnik* 55(3): 133–137, 1990. With permission.

Note: Conditions: gamma irradiation of a two-phase system (2 V_{org}–V_{aq}) with a ^{60}Co source at 1.14 MGy (dose rate 1.7 to 2.0 Gy s^{-1})–22 ± 2°C.

[a] Modified phosphates include isomers of oxybutyl dibutyl phosphates, nitrobutyl dibutyl phosphates, butyl nitrate, dibutyl phosphates, and octyl dibutyl phosphates.

[b] The value of TBP destruction was determined as the sum of the molar concentrations of HDBP, H$_2$MBP, modified phosphates, and twice the molar concentrations of phosphorus-containing dimeric products.

the TBP-diluent systems was examined for 20–30% TBP in contact with various aqueous nitric solutions.

8.3.1.1.1.2.1   External Parameters

8.3.1.1.1.2.1.1   Nature of the Irradiation Source. The degradation of TBP-diluent in contact with an aqueous phase did not reveal any qualitative influence of the nature of the radiation (γ, β, α, accelerator radiation). Moreover, the yield value of the decomposition products of TBP (*8, 9, 11, 26, 84*), nitro and carbonyl products (RNO$_2$, RNO$_3$, RCOOH, and RCOR′) (*16*), alkanes (C5–C8), and butanol (*8*) were almost identical, whatever the nature of radiations. Nevertheless, after radiolysis of TBP in *n*-dodecane without aqueous solution, the yield of H$_2$MBP was substantially lower under α-irradiation than under γ-irradiation (G_α (H$_2$MBP) = 0.158 and G_γ(H$_2$MBP) = 0.443) (*8*).

The same effect was observed on the yield of hydrogen (the main gas product of radiolysis) by Kulikov (*11*) in biphasic samples (30% TBP in paraffin-3 mol L^{-1} HNO$_3$), with a higher yield under γ-radiolysis (G_γ(H$_2$) ≈ 2.7 and G_α(H$_2$) ≈ 2.0).

8.3.1.1.1.2.1.2   Irradiation Dose and Dose Rate. In most cases, an increase of the dose led to an increase of the degradation products. For a radiation dose lower than 0.1 MGy, the yield of the TBP decomposition products was independent of the irradiation dose and G(HDBP) > G(H$_2$MBP) (*85*). Above 0.2 MGy, the value of G for the majority of identified phosphorus products decreased with increasing absorbed dose

TABLE 8.3

Concentration of the Phosphorus Degradation Products Observed after Radiolysis of TBP

Structures	Name	Concentration μL L^{-1} (ppm)
	TBP Derivatives	
A-OC$_2$H$_4$CH(OH)CH$_3$	3-Hydroxy TBP	66,000
A-OCH$_2$C(O)C$_2$H$_5$	2-Oxo TBP	600
A-OC$_4$H$_8$NO$_2$	x-Nitro TBP (x = 1, 2, 3, 4)	200
A-OC$_4$H$_8$ONO$_2$	x-Nitroxy TBP (x = 2, 3, 4)	13,000
A-OC$_2$H$_4$CH(OCOC$_y$H$_{2y+1}$)CH$_3$	O-Esters	60
A-OC$_3$H$_6$CH$_2$OCOC$_y$H$_{2y+1}$ (y = 0–3)		
A-OC$_3$H$_6$COOC$_y$H$_{2y+1}$ (y = 1–4)	C-esters	10
A-OC$_4$H$_8$OC$_y$H$_{2y+1}$ (y = 2–4)	x-Alkoxy TBP	10
A-OC$_y$H$_{2y+1}$ (y = 1–17)	TBP homologs	8,000
A-OC$_3$H$_6$COOH	3-Carboxy propyl DBP	Traces
		Total $\approx$ 88,000 ppm or 8.8%
	TBP Dimer Derivatives	
A-OC$_8$H$_{16}$O-A	TBP-TBP (dimers)	300
A-OC$_y$H$_{2y}$O-A (y = 1–7)	TBP dimers lower homologs	170
A-OC$_y$H$_{2y}$-A (y = 2–4)	Phosphate-phosphonates	30
A-O(C$_8$H$_{15}$ONO$_2$)O-A	Nitroxy TBP-TBP	2
A-OC$_8$H$_{16}$O-B-OC$_4$H$_8$ONO$_2$		
A-O(C$_8$H$_{15}$OH)O-A	Hydroxy TBP-TBP	20
A-OC$_8$H$_{16}$O-B-OC$_4$H$_8$OH		
A-OC$_4$H$_8$-O-C$_4$H$_8$O-A	TBP-O-TBP	3
		Total $\approx$ 500 ppm or 0.05%

Source: Lesage, D., Virelizier, H., Jankowski, C.K., Tabet, J.C. *Spectroscopy* 13: 275–290, 1997.

Note: A- = (C$_4$H$_9$O)$_2$PO-; -B- = (C$_4$H$_9$O)PO-. Conditions: Gamma irradiation with ^{60}Co source at 0.6 MGy in the EDIT test loop that simulated the nuclear fuel reprocessing, room temperature.

(*34, 73*). Moreover, for doses higher than 1 MGy, the HDBP concentration increase rate slowed down and was correlated with a build-up in the concentration of H$_2$MBP (*85, 86*). This behavior came from the equality between the rates of formation and decomposition of HDBP. The concentration of high-molecular-weight organophosphates (Figure 8.1 Compounds I, II, IV, and V in the degradation scheme) increased much more sharply with an increasing absorbed dose than that of HDBP (*51*).

The dose rate seems to have no significant influence on G(HDBP) and G(H$_2$MBP) (*25*), or on the yield of RNO and RNO$_2$ compounds (*27*).

8.3.1.1.1.2.1.3   Effect of the Temperature.   The effect of temperature up to 50°C on the radiolytic degradation of TBP-hydrocarbon systems is insignificant. On the other hand, in the presence of CCl$_4$, an increase in temperature to 50°C results in

TABLE 8.4

***G* Values for Gaseous Products during Irradiation of 19.5% TBP/Odorless Kerosene -H_2O-0.6 M HNO_3**

Gas	*G* Values (for dose up to 0.5–1 MGy)
H_2	1.18
CH_4	0.094
CO	0.031
N_2	0.267
CO_2	0.073
N_2O	0.39
NO	0.58
Hydrocarbons	0.33

Source: From Rigg T., Wild, W., Radiation Effect in Solvent Extraction Processes. *Progress in Nuclear Energy* Series III, Pergamon Press: London, Vol. 2, 7–6, 320–331. 1958.

considerable degradation of the extractant and the diluent, particularly in the presence of uranyl nitrate (*28*).

8.3.1.1.1.2.2   Chemical System Parameters

8.3.1.1.1.2.2.1   Nature of the Diluents.   Diluents can inhibit or sensitize TBP radiolysis. The effect of various diluents (aliphatic hydrocarbons, aromatic and halocarbons) on TBP degradation products was examined over a wide range of nitric acid concentrations (*26*).

The highest yield of degradation products (HDBP, H_2MBP, phosphoric acid, carbonyl compounds) occurred in the TBP-CCl_4-HNO_3 system (*87*). As a result, it has been suggested that the considerable amounts of hydrochloric acid produced could accelerate the process of degradation. On the other hand, the use of carbon tetrachloride as diluent resulted in a very low yield of nitro compounds. An important sensitization effect was also reported by Nash with tetrachloroethylene $G(–TBP) = 3.8 \pm 0.6$ and 9.2 ± 3 for pure molecule and TCE solution (*41*).

In contrast, in the TBP-aromatic diluent system, G(HDBP), $G(H_2$MBP), and G(gaseous products) decreased (*88*), due to the aromatic diluents' protective effect (*23, 26, 39, 73, 88–90*).

The use of aliphatic hydrocarbons as diluents led to an intermediate yield of degradation products, and Canva et al. (*90*) concluded that some saturated hydrocarbons (hexane, cyclohexane, and dodecane) sensitize or increase the decomposition of TBP. Though Egorov et al. (*91*) observed an increase in the radiolytic and chemical stability of TBP with the carbon chain length of the diluent (*n*-octane < *n*-dodecane < mixture *n*-C14/*n*-C15), Adamov (*92*) did not notice any change in the composition of the radiolysis TBP-alkane solution when *n*-undecane was replaced by higher hydrocarbons (up to C17). Otherwise, a length of 12–14 carbons was considered as optimal to avoid difficulties in removing the high-molecular-weight products in the regeneration stage. Though the chemical and radioactive stability of branched aliphatic hydrocarbons

and olefins seemed to be lower than for linear hydrocarbons (*93*), the radiation resistance of TBP solutions in *iso-* and *n*-paraffins was almost the same (*94*).

The radiation resistance of TBP-aliphatic compound solutions could be improved by the introduction of aromatic derivatives; the addition of only 10% of aromatic diluents or 0.1 mol L^{-1} mono-*iso*-propyldiphenyl reduced the global concentration of the degradation products by half (*91, 94*).

In conclusion, despite their protective effect as regards degradation, the use of aromatic diluents has been avoided because of their low flash point. The classical diluents selected for PUREX process operations were hydrocarbons, either pure compounds (i.e., *n*-dodecane), or mixtures of different products (i.e., hydrogenated polypropylene tetramer, odorless kerosene, etc.) (*93*). Halocarbon diluents had two major drawbacks linked to their radiolytic behavior: sensitization of TBP degradation and the production of extremely corrosive chloride ions (*89, 93, 95*).

8.3.1.1.1.2.2.2　Concentration of TBP.　The rate of TBP decomposition and the yields of major acids G(HDBP) and G(H$_2$MBP) increased with the concentration of TBP (*8, 85, 88*). On the other hand, the yield of gaseous radiolysis products coming from the diluent decomposition decreased with an increasing fraction of TBP (*88, 96*).

8.3.1.1.1.2.2.3　Nitric Acid Concentration.　Like TBP and diluent, nitric acid extracted in solvent was decomposed by irradiation with a high yield value: G(−HNO$_3$) = 5.2 and 6.2 for TBP solution in contact with [HNO$_3$] = 3 mol L^{-1} and [HNO$_3$] = 5 mol L^{-1}, respectively. Species like nitrogen dioxide (NO$_2$) formed by irradiation of HNO$_3$ were highly reactive to TBP fragments (*97*). Thus, in the presence of nitric acid, the radiation-induced decomposition of TBP solutions was significantly increased (*97*). For a given dose, the yield of acidic TBP degradation products (HDBP and H$_2$MBP) increased slightly with the concentration of nitric acid in dodecane (*26, 27, 43, 85, 98*), but the influence was considerable in the system containing CCl$_4$ (*26, 99*). Otherwise, for the TBP-alkane system, the global yields of oxidation products (hydroxy, nitro, and carbonyl compounds) increased markedly with increasing concentrations of nitric acid (from 0.5 to 3 mol L^{-1}) (*27, 43*).

But the organic phases containing dissolved water and nitric acid (<2 mol L^{-1}) released less gas during irradiation compared with the related dry solvents, owing to a reduction in the yields of hydrogen and methane (*84*).

In the presence of nitric acid, the radiolysis of TBP led to new degradation products, named "modified phosphates" in Ref. (*43*), corresponding to type II compounds (see Figure 8.1). In these phosphate isomers, the butyl radical was functionalized by OH, NO$_2$, and ONO$_2$ groups, giving compounds like (OHC$_4$H$_8$O)(C$_4$H$_9$O)$_2$PO, (O$_2$NC$_4$H$_8$O)(C$_4$H$_9$O)$_2$PO, (O$_2$NOC$_4$H$_8$O)(C$_4$H$_9$O)$_2$PO, and (HOOCC$_n$H$_{2n}$O)(C$_4$H$_9$O)$_2$PO.

Thus, adding HNO$_3$ to the system mainly produced a redirection of the radiation-chemical processes. As a result, nitration products appeared, and the radiation-chemical yield of oxidation products (Figure 8.1 compounds II) increased, primarily due to a reduction of the radiation-chemical yield of condensation products (Figure 8.1 compounds AII, I, IV, and V) (*43*).

8.3.1.1.1.2.2.4   Presence of Metallic Salts.   The presence of major cations such as uranium(VI) (*27*) and plutonium(IV) significantly increased the yields of formation of HDBP and H_2MBP. This effect was stronger than the effect of the nitric acid concentration (*9*). For example, the presence of nitric acid in the organic phase increased G(HDBP) from 0.7 to 1.1 molecules/100eV when $[HNO_3]_{org}$ reached 0.7 mol L^{-1}. In the same conditions, a change of uranium(VI) nitrate concentration in the organic phase from 3×10^{-2} to 0.3 mol L^{-1} increased G(HDBP) from 1.9 to 3.1 molecules/100 eV, and the total yield of gas generation from 2.8 to 3.6. The same effect was observed with plutonium. Moreover, the presence of uranium(VI) changed the composition of the gases generated during radiolysis. The main compound was H_2 (92%) in the absence of uranium, but the ratio decreased in the presence of uranium: from 71% to 25% for organic uranium(VI) concentrations varying from 3×10^{-2} to 0.3 mol L^{-1}. Meanwhile, the concentration of short alkanes (CH_4 and C_2H_6) increased from 29% to 75% (*9*).

Otherwise, the effect of uranyl or zirconium nitrates and molybdic acid on nitro and carbonyl compounds was negligible (*27*), while the presence of palladium reduced the yield of nitro derivative but caused an increase of the yield of carbonyl compounds (*27*).

8.3.1.1.1.2.2.5   Effect of the Atmosphere.   The composition of radiolysis products depends substantially on the degree of saturation of the irradiated system with oxygen. In a nitrogen atmosphere, the major radiolysis products of the system TBP-diluent-HNO_3 were alkyl-nitro and -nitrate compounds. However, in the presence of oxygen, the yields of these compounds were sharply reduced, and an accumulation of carbonyl compounds was measured (*11, 25*).

For irradiation doses lower than 0.05 MGy, when oxygen or air was bubbled through the two-phase system, the formation rate of acidic radiolysis products remained constant and greater than the rate of formation in an oxygen-deficient system. For irradiation doses higher than 0.05 MGy, the rate of formation of HDBP fell and that of H_2MBP increased, and at γ-ray doses of over 1–1.5 MGy, equilibrium concentrations of HDBP were formed in solution (*85, 100*).

8.3.1.1.1.3   Effects of Degradation.   The accumulation of degradation products in the solvent can lead to different types of damage that disrupt the PUREX process:

– A decrease in the decontamination performance of uranium and plutonium for fission products (mainly ruthenium, zirconium, cerium, and niobium) (*19, 27, 84, 88, 101–106*).
– An increase of product loss, namely, uranium and plutonium, in aqueous raffinates (*84, 101*).
– The formation of emulsions, suspensions, and cruds at the liquid-liquid interfaces, which disturb the continuous extraction process (*84, 101, 102, 107–111*).
– The evolution of physicochemical properties of the phases, mainly the organic (the viscosity (*51*), the interfacial tension, etc.).

The presence of fission products in suspensions or precipitates also increased the γ-activity undergone by the solvent (*103*).

A particular scientific interest has been aroused in the complexing properties of degradation products, because of the major relation to a decrease in extraction efficiency. The following section is a summarized account of the results.

8.3.1.1.1.3.1 Complexing Ability of Degradation Products

8.3.1.1.1.3.1.1 Major Compounds HDBP and H₂MBP. HDBP, the main degradation product of TBP, is partially soluble in aqueous phases; the distribution ratio is highly dependent on the composition of the two phases (*89, 112, 113*). This molecule can form strong complexes with Pu(IV), Th(IV), Zr(IV), U(VI), Np(VI), and other cations, causing modification of An(IV) and An(VI) distributions (*89, 114, 115*) and various problems in the PUREX process (*27, 89, 116–119*). The behavior of HDBP solution complexes is not easily understood because various compositions could be present in solution or as solid compounds.

The stoichiometry of the complexes between HDBP and U(VI) changes with the acidity, that is, at high nitric acidity, the presence of $[UO_2(NO_3)_2(HDBP)TBP]$ and $[UO_2(NO_3)_2(HDBP)_2]$, and at low nitric acidity, the forms $[UO_2(NO_3)(DBP)(HDBP)_x]$, $[UO_2(DBP)_2(HDBP)_x]$ (where $x = 1$ or 2) dominate. The presence of such complexes can explain the difficulties in U(VI) recovery (*114, 115, 120*). Otherwise, various authors have indicated the presence of insoluble compounds for enriched uranium solutions (*121–124*). Recently, Powell identified the solid forms with various spectroscopic methods: at lower acid concentrations, the well-characterized polymer $UO_2(DBP)_2$ precipitates as a yellow powder, whereas a sticky solid or gels are formed at high acidity. The global formula is $UO_2(NO_3)(H(DBP)_2)(HDBP)_2$ (*106*).

The complexes formed with Pu(IV) lead to the formation of precipitates. In TBP kerosene solution, when the ratio HDBP/Pu $\gg 2$, the formula is $[Pu(NO_3)_2(DBP)_2]_n$ (with an average degree of polymerization of 11) (*125*). Furthermore, in γ-irradiated TBP-dodecane solution, a precipitate corresponding to the formula $Pu_2(NO_3)_2MBP(DBP)_4(H_2MBP)_2$ has been observed; its solubility is dependent on the MBP concentration (*126, 127*).

The complexes formed with Zr(IV) can lead to the formation of stable emulsions, called cruds (*27, 89, 107, 108, 128, 129*), present at the aqueous-organic interface and stabilized by microsolid particles. Chemical analysis of interphase precipitate showed that its main components were Zr and HBDP. The precipitation depends on the acidity, the concentration of HDBP, and the concentration of Zr (*130*). In the solid form, the formula proposed is $Zr(NO_3)_2(DBP)_2$ (*101*). In solution, several Zr-HDBP complexes have been detected (*59, 64, 109, 110, 123, 131, 132*).

Complexes between HDBP and lanthanides have also been observed, but their low solubility leads to third phases observed at low acidity (containing several species with different chemical forms) (*133*). During electron irradiation of the TBP/dodecane/3 mol L⁻¹ HNO₃ system, Guedon et al. (*129*) observed the precipitation of $Fe(DBP)_3$ for high concentrations of HDBP (>3 g L⁻¹). The formation of complexes between nitrato-nitrosyl ruthenium and HDBP-H₂MBP mixtures has also been suggested (*103*).

H₂MBP has comparable complexing ability for metallic cations (*100, 134*), but because of its lower formation yield and its higher aqueous solubility, the damage is effectively more limited than for HDBP. Studies are therefore less numerous.

8.3.1.1.1.3.1.2   Minor Radiolytic Compounds.   Even at low concentrations, some degradation products may produce different physicochemical effects, which can influence process performance.

8.3.1.1.1.3.1.2.1   Compounds from Diluent Degradation.   The diluent used during the extraction process is also prone to degradation under the influence of radiation. Unlike the TBP decomposition products, these compounds are not removed by aqueous alkaline treatments, but slowly accumulate and reduce the solvent's performance (*19, 79*).

Among the functionalized compounds, nitroalkanes seem to be the source of most side-complexing:

- Nitroparaffins in the enol form lead to a synergistic extraction of Zr in the presence of TBP (*23*).
- In the presence of nitric acid, nitroparaffins turn into hydroxamic acids, RCONHOH (*16, 135*). Experiments performed with the addition of hydroxamic acids in the range 10^{-4}–10^{-3} mol L^{-1} in HNO_3/TBP/odorless kerosene proved a strong correlation between the zirconium retention in solvent mixtures and the presence of hydroxamic acids (*136*). Ruthenium retention, which increases with the hydroxamic acid concentration and aging time of loaded organic phase (*104*), has been explained by a slow reaction between hydroxamic acid in the organic phase and RuNO. The new species can be extracted easily by TBP, thus causing Ru retention. Nevertheless, the presence and the amount of hydroxamic acid is controversial (concentrations between 10^{-8} and $4\ 10^{-4}$ mol L^{-1} have been measured) (*104, 137, 138*).
- Carboxylic acids formed by the hydrolysis of nitro compounds have been identified as complexing uranium(VI) (*79, 139*).
- Stieglitz (*140*) concluded that the carbonyl function is most probably responsible for the Hf and Zr complexation by degraded solvent.

8.3.1.1.1.3.1.2.2   Minor Degradation Products from TBP   The main compounds responsible for the retention of metallic ions in organic phase are long-alkyl-chain acid organophosphates (Figure 8.1 AII′) and oligomeric butyl phosphates (Figure 8.1 IV and V) (*83, 141*).

- Compounds AII′, like HDBP, possess high affinity for tetravalent Zr and Pu, due to the acid phosphate groups.
- The high solubility of compounds IV and V in organic phase explains the accumulation of such species in the solvent without efficient aqueous treatments. Nevertheless, formation is very slow and the concentration stays at a low level. In order to enhance knowledge of such compounds, preconcentration by distillation (in the residue fraction), followed by steric exclusion chromatography has been performed (*143*). Plutonium retention measured on the various fractions showed high values for dimeric butyl phosphates and the functionalized TBP families (*82*). In 2001, Tripathi confirmed that the fraction enriched in high-molecular-weight products exhibits very high plutonium retention (*50*).

Otherwise, TBP derivatives with high boiling points and containing $C = O$ groups are zirconium complexing compounds (*31*).

8.3.1.1.1.3.2 Physicochemical Properties of Degradation Products   The degradation compounds formed can also modify the physical properties of the chemical system and thereby disturb hydrodynamic behavior.

8.3.1.1.1.3.2.1 Density and viscosity of the organic phase   Density and viscosity of the solvent (TBP-diluent-aqueous phase) change insignificantly after irradiation, whatever the diluent (dodecane, mesitylene, or CCl_4) (*26, 51, 142*). For example, for 30% TBP-*n*-dodecane-0.56 mol L^{-1} HNO_3, the density varies from 0.837 to 0.847 after irradiation at 0.5 MGy, and the viscosity from 1.96 to 2.38 mN s m^{-2} (*51*).

Some experiments were also conducted with the addition of identified degradation products to fresh solvent (*51*). The effect on density and viscosity remains slight, except for

- Some compounds like HDBP + *n*-dodecanol, for which a synergetic effect was observed in the viscosity (8.1% increase, whereas individual effects of 1.3% and ~2.5% were measured for HDBP and *n*-dodecanol, respectively);
- For methyl, alcohol, or nitro derivatives of TBP, where the addition of 0.1% to fresh solvent resulted in substantial increases in the viscosity of the solvent (~10%).

8.3.1.1.1.3.2.2 Interfacial properties.   The effect of the aqueous phase on interfacial tensions of irradiated TBP-diluent/nitric acid systems was measured (*142*). For neutral and acidic aqueous phase, the interfacial tension was similar for fresh and irradiated systems, but in contact with 0.6 mol L^{-1} NaOH solution, which is representative of alkaline treatment, a decrease of interfacial tension was observed.

Various synthetic solutions were prepared to identify the products responsible for this behavior. Measurements indicated that the main degradation products, such as HDBP, alcohols, nitro compounds, hydroxamic acid, and carboxylic acids with short alkyl chains have no influence on the interfacial tension (*142, 144*). However, the negative effect of the chain length of carboxylic acids is significant (*142, 144*) (cf. Figure 8.2). Lauric acid ($C_{11}H_{23}COOH$) forms sodium salts (soaps) in contact with 0.5 mol L^{-1} of Na_2CO_3 solution, and in extreme cases, above 3×10^{-3} mol L^{-1} of sodium laurate in an organic phase of 30% TBP in normal paraffin hydrocarbons (NPH), the phases cannot be separated even after one day (*145*).

8.3.1.1.1.3.2.3 Flash point and fire point.   An increase in irradiation leads to a lowering of the flash point and fire point of PUREX solvent (*146*). For example, after an absorbed dose of 300 W h L^{-1}, the flash point of 30% TBP-dodecane was about 16°C lower than that of fresh solvent.

8.3.1.1.1.3.2.4 Removal of degradation products from spent solvents.   Several methods of regeneration have been used to maintain the PUREX process solvent quality (*143*): chemical scrubbing treatment, specific management of solvent streams, and regeneration of solvent by distillation.
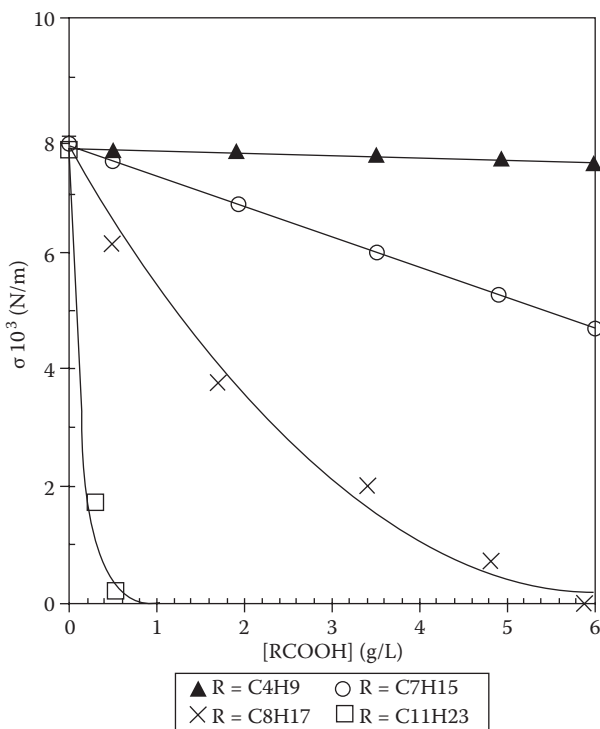
FIGURE 8.2 Interfacial tension of 30% TBP-*n*-dodecane in respect to 0.6 M NaOH as a function of RCOOH concentration of organic acid. (Drawn from Nowak, Z., Nowak, M., *Nukleonika*, 26(1): 19–26, 1981.)

– Chemical methods are used to solubilize degradation products in aqueous phases. Alkaline solutions remove acidic products (HDBP, H₂MBP, and long-chain carboxylic acids) from the solvent (*36, 89, 128, 147, 148*). A regular solvent scrubbing appears to be beneficial for long-term use of PUREX solvent, because it appears to limit the increase of high-molecular-weight phosphates (*83*).

– A good solvent management in a PUREX plant includes diluent scrubbing of high-level radioactive aqueous streams and optimum solvent and diluent routing between extraction cycles (*143*). Diluent scrubbing allowed the removal of the TBP solubilized in the aqueous phase, avoiding the progressive formation of poorly soluble salts of di-*n*-butylphosphate (*149*).

– Distillation under reduced pressure allowed separation of the TBP-diluent mixture components into three fractions: diluent, 60% TBP, and distillation residue. The first two fractions can be reused in the process, but the residue contains high-molecular-weight degradation products, which are not eliminated by alkaline scrubbing. Distillation removes the degradation products that are responsible for poor hydrodynamic behavior and for the retention of radioactive products such as plutonium, zirconium, and ruthenium (*143*).

Some authors have studied the effects of treatment with solid sorbents. Activated alumina was found to be very effective for secondary cleanup after alkaline scrubbing to remove compounds responsible for the decrease of interfacial tension and the complexing of plutonium. The drying of the solvent improves the capacity of activated alumina (*102, 150, 151*).

8.3.1.1.2   *Other Trialkylphosphates*

The degradation of several trialkylphosphates has been investigated, because lengthening the alkyl chain can enhance the actinide loading capacity in normal long-chain diluents. The main degradation products were the related dialkyl phosphoric acid $HO(RO)_2P = O$ and monoalkyl phosphoric acid $(HO)_2(RO)P = O$ (*18, 84, 152*). The yield of formation of the main compound $HO(RO)_2P = O$ varied from 2.83 for $R = CH_3$ to 1.47 for $R = C_5H_{11}$ (*18*).

The radiolytic degradations of tri-*iso*-amyl phosphate (T*i*AP) (*152*) and tri-*n*-amyl phosphate (T*n*AP) (*153*) have been investigated. The variations in physical properties (density, viscosity, and phase disengagement time) were similar to data obtained for degraded TBP systems (*153*). Both TAP systems exhibited marginal plutonium retention at high dose level, and precipitates were produced by prolonged γ-irradiation. In the case of T*i*AP, the authors suggest a rapid evolution of the soluble compounds $Pu(NO_3)_4(TiAP)(HDiAP)$ and $Pu(NO_3)_4(HDiAP)_2$ to $Pu(NO_3)_2(DiAP)_2$, an insoluble species that was predominant at high doses or for aging solutions. This compound's solubility in *n*-dodecane is, surprisingly, lower than the corresponding DBP-compound. Recently, Venkatesan also considered the presence of the more lipophilic higher molecular-weight organophosphates as the reason for plutonium retention with T*n*AP (*153*). In conditions representative of the first extraction cycle (0.2 kGy), the original quality of the solvent can be restored by classical scrubbing with sodium carbonate.

8.3.1.2   **Dialkyl Phosphoric Acids**

8.3.1.2.1   *Di(2-ethylhexyl) Phosphoric Acid Systems*

Di(2-ethylhexyl) phosphoric acid (HDEHP) is an extractant molecule used for An(III)/Ln(III) separation. Used in TALSPEAK-type processes in a mixture with TBP, or in the DIAMEX-SANEX process in a mixture with a malonamide (*154–157*), it has also been proposed, in a mixture with TBP, to remove strontium from PUREX acid waste solution in the Hanford B plant (*158*). Therefore, numerous studies have focussed on the radiolytic degradation of HDEHP and its effects on the extraction of Sr(II), lanthanides(III), and actinides(III) (*10, 158–163*).

8.3.1.2.1.1   Degradation Products from the Radiolysis of HDEHP Systems.   The main radiolytic degradation products are in the organic phase, mono(2-ethylhexyl) phosphoric acid (H_2MEHP), 2-ethylhexanol, and polymeric species, but also a certain amount of ortho phosphoric acid (H_3PO_4) was detected in the aqueous phase. The nature of the short compounds identified in the gas fraction was classical: H_2, unsaturated and saturated hydrocarbons (from 1 to 4 carbons), O_2, and N_2 (*10, 74, 158–160, 164*).

8.3.1.2.1.2   Factors Governing Degradation

8.3.1.2.1.2.1   Influence of the Aqueous Phase   The presence of an aqueous phase during irradiation increases the radiolytic destruction of HDEHP (*158, 160*) and leads to an increase of the polymeric species, particularly under acidic conditions.

Changing the composition of the aqueous phase (1 mol L^{-1} lactic acid + 0.05 mol L^{-1} DTPA or HNO_3 3 mol L^{-1}) has a negligible effect on the global yields of HDEHP decomposition products in solution. However, substantial changes have been observed in the gaseous composition in the presence of lactic acid (the yields of H_2 doubled and CO_2 appeared, whereas O_2 completely disappeared), and the amount of oxidation products increased, contrary to nitration derivatives, which decreased (*12*).

8.3.1.2.1.2.2   Influence of the Diluent   The presence of NPH as diluent did not modify the yield of radiolysis products (*12, 160*). As noted for TBP, the decomposition of the extractant in CCl_4 is higher than in benzene and paraffins (*10, 74*).

8.3.1.2.1.2.3   Influence of the type of Irradiation   For pure HDEHP, the yields G(-HDEHP) and G(H_2MEHP) are similar for α- (^{238}Pu emitters) and γ-irradiation (^{60}Co source). Some difference has been observed for hydrogen formation: G(H_2)$_\gamma$ = 2.5 and G(H_2)$_\alpha$ = 1.9 molecules per 100 eV (*10*).

Differences are more significant for solutions diluted in *n*-paraffins. The yields of decomposition products on α-radiolysis (with ^{238}Pu or ^{241}Am) are 15–20% greater than for γ-radiolysis (*10, 12*).

8.3.1.2.1.3   Effects of Degradation   The effects of radiolytic degradation are highly dependent on the experimental conditions:

- For solutions irradiated in the absence of an aqueous phase, the extraction of Am(III) and lanthanides(III) both increased, but the separation factor $SF_{Nd/Am}$ decreased (*160*).
- The γ-irradiation of HDEHP-*n*-paraffin solutions stirred with 0.1 mol L^{-1} nitric acid solutions led to an initial slight increase of D_{Am} and D_{Nd}, followed by a subsequent decrease for an absorbed dose of over 200 Wh L^{-1} (~0.7 MGy) (*160*).
- The γ-irradiation of HDEHP-*n*-paraffins in contact with TALSPEAK-type aqueous phase at pH 3 (DTPA + lactic acid) increased D_{Am} and D_{Ln}, and slightly decreased the separation factors $SF_{Ln/Am}$ (*12, 161*). The effect was stronger when lactic acid was replaced by $NaNO_3$, as presented in Figure 8.3 (*161*).

In order to understand these changes better, a comprehensive study related to the effect of each individual major degradation product was undertaken (*161*) and the main results summarized:

- In the absence of an aqueous phase, the increased $D_{M(III)}$ were attributed to the synergic effect brought about by H_2MEHP: D_{Am} measured in a mixture
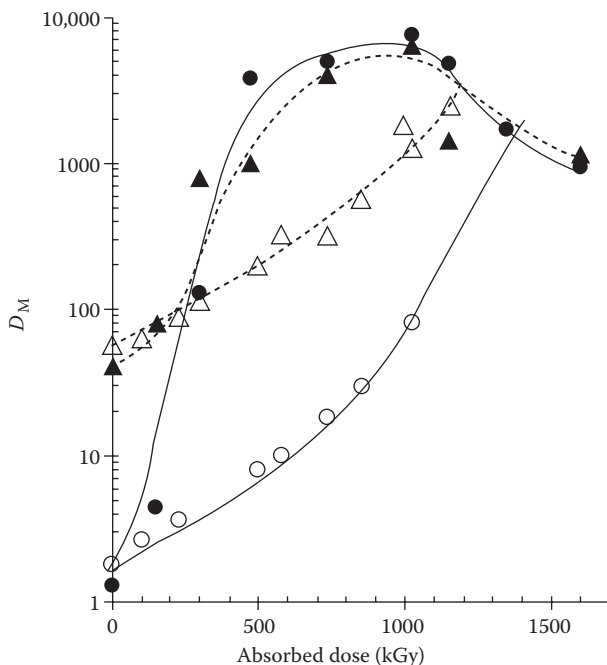
FIGURE 8.3 Radiation effects on $D_{Nd(III)}$ and $D_{Am(III)}$ by γ-irradiation (at a dose rate 1–5 kGy h^{-1}) of HDEHP solution in the presence of aqueous phase. (Organic phase: 0.5 M HDEHP in NPH. Aqueous phase at pH 3: 0.05 M DTPA-1 M NaNO$_3$, Nd ($\triangle$), Am ($\bullet$). 0.05 M DTPA, 1 M lactic acid, Nd ($\blacktriangle$), Am ($\circ$)). (Drawn from Nilsson, M., Nash, K.L., *Solvent Extr. Ion Exch.* 25: 665–701, 2007 Tachimori, S., Nakamura, H., *J. Radioanal. Chem.* 52(2):343–354, 1979.)

of HDEHP-H$_2$MEHP (2–3 in mol) was 1000 times higher than data obtained with HDEHP alone (*160, 162, 165*).

- In the presence of nitric acid, the degradation was more important due to the hydrolysis of H$_2$ MEHP in the aqueous phase, and the resulting H$_3$PO$_4$ degradation product led to competitive aqueous complexing of Am(III) and Ln(III) (*160*).
- With a Talspeak-type aqueous phase at pH 3, the value of D$_{Am}$ and D$_{Nd}$ first increased with the H$_2$MEHP/HDEHP ratio and then decreased (*161*). This overall behavior has been explained by the radiolytic decomposition of DTPA and the formation of H$_2$MEHP. The replacement of nitrate by lactate in the aqueous phase gave a protective effect, by slowing down the degradation of DTPA and therefore delaying the negative effects.

Concerning strontium extraction, the principal radiolytic effect was a two- to threefold decrease (*158*). Schultz explained this effect by the polymerization of HDEHP with H$_2$MEHP via hydrogen bonding, making HDEHP molecules either unavailable or less available for binding with strontium. According to Tachimori (*163*), the

decrease of D_{Sr} was explained by the decomposition of HDEHP and the formation of H_2MEHP.

8.3.1.2.1.4   Removal of Degradation Products from Spent Solvents. H_2MEHP could be removed from irradiated HDEHP solutions by alkaline scrubbing (dilute NaOH or Na_2CO_3 solutions) (*158*). However, in the presence of large amounts of H_2MEHP in the organic phase, emulsions have been observed during the alkaline cleanup treatment (*164*).

In the context of the DIAMEX-SANEX process development, the stability of the solvent (a mixture of malonamide and HDEHP extractants in alkane) was studied in the MARCEL loop (γ-irradiation followed by alkali treatments). No accumulation of HDEHP degradation products was observed, and most of the physical and chemical properties of the solvent were maintained (*5*).

8.3.1.2.2   Other Dialkyl Phosphoric Acids

Several dialkyl phosphoric acids have been studied under different experimental conditions (*32, 71, 166*). The main trends are the following:

- The presence of a nitric acid aqueous phase increased the extractant's degradation (*32, 166*).
- The shortening of the alkyl chain of dialkyl phosphoric acid was beneficial, as degradation products present a higher solubility in the aqueous phase. In the case of HBDMBP (bis(1,3-dimethylbutyl)phosphoric acid), no extractant degradation products remained present in the organic phase (*71*). On the other hand, increasing the alkyl chain seemed to improve the stability of the dialkylphosphoric acid: under similar conditions, the yields of monoester were 2.1 for HDEHP and 1.1 molecules/100 eV for HD*i*DP (di-*iso*-decyl phosphoric acid). Moreover, the formation of H_3PO_4, which had been found in the radiolysis of HDEHP, was not observed after γ-irradiation of HD*i*DP (*32*).
- The introduction of an ethoxy group to the alkyl chain weakened the molecule, as shown by Tachimori's study with HDHoEP (di(hexyloxyethyl)phosphoric acid). Under the same conditions, the yields of monoester were 6.6 for HDHOEP and 2.1 for HDEHP. Furthermore, the presence of an oxygen atom in the alkyl chain led to the formation of a supplementary degradation product (a diacidic compound, probably formed by the scission of the ether bond), compared to HDEHP or HD*i*DP (*32*).

8.3.1.3   Trialkyl Phosphine Oxides (TRPO)

Chinese scientists used trialkyl phosphine oxides (TRPO) to remove long-lived radioactive nuclides from high-level liquid waste (*67, 167*). TRPO is the trademark of a Chinese commercial product, consisting of a mixture of several TRPO (with alkyl chains from hexyl to octyl). The TRPO process has been tested in China and at ITU in Karlsruhe (*2, 168–174*).

8.3.1.3.1   Degradation Products from the Radiolysis of TRPO Systems

The degradation products obtained by γ-irradiation of 30% TRPO in kerosene were dialkylphosphinic acids $R_2P(O)OH$ and alkylphosphonic acids $RP(O)(OH)_2$.

Compounds with higher molecular weights were also identified at high irradiation doses (above 3 MGy). Zhang et al. proposed the following structure for these polymeric species: $RR'PO(CH_2)_mC(OH)[(CH_2)_nCH_3]COOH$ or $RR'POCH[(CH_2)_mCH_3]C(OH)[(CH_2)_nCH_3]COOH$ (*67, 167*).

8.3.1.3.2 Effect of Degradation

An increase of the irradiation dose (over 2 MGy) led to an increase in plutonium retention. The nitric acid concentration had a limited effect.

The addition of 0.01 mol L^{-1} dialkylphosphinic acids and alkylphosphonic acids in a nonirradiated 30% TRPO-kerosene system had no effect on the extraction of Pu(IV) with TRPO. Thus, these acids were not complexing materials for plutonium. The polymeric species were responsible for plutonium retention and emulsification in contact with NaOH or deionized water. The effective elimination of these compounds was obtained by vacuum distillation of the irradiated TRPO-kerosene (*67, 167*).

8.3.1.4 Sulfur Donors

8.3.1.4.1 Influence of the Structure of the Extractant

Sulfur-containing organophosphorus compounds are prone to oxidation and degradation, especially in the presence of acids and strong oxidants. Their hydrolytic and thermal stability increase in the order dialkyl dithiophosphoric acids (($RO)_2PSSH$) < dialkyl dithiophosphinic acids (R_2PSSH), due to the absence of the weak ether bridge.

Dialkyl dithiophosphinic acids have been investigated as extractants for An/Ln separation (*29, 49, 60, 61, 175, 176*). In this context, the radiolytic degradation of Cyanex 301 (whose main constituent is di(2,4,4,-trimethylpentyl)dithiophosphinic acid) has been studied (*29, 60*). The main degradation products are oxygenated compounds R_2PSOH and R_2POOH. The high influence of Cyanex 301's purity on its stability explains the wide differences found among published results. After radiolysis of 0.5 mol L^{-1} Cyanex 301 in alkane under 0.1 MGy, a loss of 94% and ~50% of the initial concentration was measured for commercial and purified extractant, respectively (*29, 60*). Otherwise, the efficiency of Cyanex 301 for An(III) extraction was maintained up to 0.1 MGy, but the separation factor $SF_{Am/Eu}$ decreased from 1000 to about 10 after irradiation at 0.7 MGy (*60*).

The radiolytic resistance of the two aromatic dithiophosphinic acids, Ph_2PS_2H and $(ClPh)_2PS_2H$, considered for actinide(III)/lanthanide(III) separation, was higher. After radiolysis under 1 MGy of $(ClPh)_2PS_2H$ 0.5 mol L^{-1} in toluene, ^{31}P-NMR analysis indicated a degradation of 30–40% (*49, 61*). Thus, the substitution of aromatic groups for alkyl groups and the incorporation of chlorine into phenyl rings on the Cyanex 301 structure increased its radiolytic stability. Furthermore, the dichloro derivative $(Cl_2Ph)_2PS_2H$ seemed to be more resistant to oxidation by nitric acid than $(ClPh)_2PS_2H$ (*49*).

8.3.1.4.2 Influence of the Chemical Composition

The dilution of $(ClPh)_2PS_2H$ in toluene lowered its radiolytic stability. At an integrated dose of 1 MGy, the degradation was lower than 5% for the pure molecule (not in solution), whereas 30–40% of the ligand had disappeared for a 0.5 mol L^{-1} solution in toluene (*49*). The presence of a 0.5 mol L^{-1} aqueous nitric solution had a

slight influence on the stability of $(ClPh)_2PS_2H$ 0.5 mol L^{-1} in toluene (increasing the degradation of ~5–10%).

8.3.1.4.3 Effect of Degradation

The effect of radiolysis on the extraction of Am(III) and Eu(III) by Ph_2PS_2H and $(ClPh)_2PS_2H$ in a mixture with TBP in toluene was negligible up to a total dose of 0.1 MGy. At higher levels, such as 0.7 MGy, D_{Am} decreased slightly, whereas D_{Eu} clearly increased, resulting in a significant drop in Am/Eu separation factors (*61*).

The same behavior was observed with the system $(ClPh)_2PS_2H$-TOPO-toluene. The decrease of D_{Am} has mainly been explained by the reduction in the extractant's concentration (*49*).

8.3.2 Mixed Compounds: The Case of the CMPO Extractants

8.3.2.1 Octyl(phenyl)-*N,N*-di-*iso*-butylcarbamoylmethyl Phosphine Oxide

The OΦD(iB)CMPO [octyl(phenyl)-*N,N*-di-*iso*-butylcarbamoylmethyl phosphine oxide] molecule is a neutral bifunctional organophosphorus extractant selected to recover actinides in the TRUEX process. This extractant is mainly used in mixtures with TBP (added to increase solubility and the loading capacity) in diluents like aliphatic hydrocarbons or chlorinated diluents (CCl_4 or $Cl_2C = CCl_2$) (*2, 177–180*).

8.3.2.1.1 Degradation Products

Numerous studies have applied gas chromatography to determine the concentration of CMPO and of a variety of organophosphorus compounds. The CMPO degradation products identified are summarized in Figure 8.4.

More recent studies completed the analysis of degraded solutions with the capillary GC-MS technique (*46*) and proposed the identification of four CMPO degradation products, compounds (1) to (4) in Figure 8.4. In previous studies (*20, 42*),
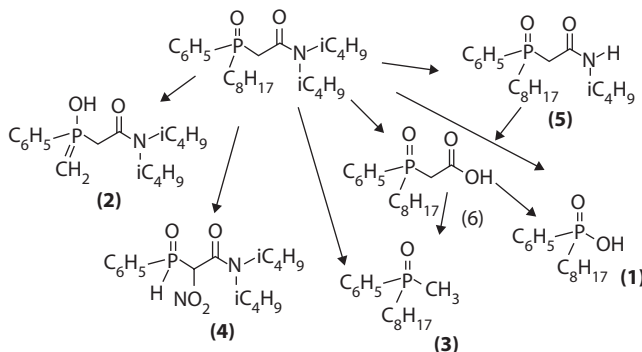
FIGURE 8.4 Pathway for the hydrolytic and radiolytic degradation of CMPO. (Drawn from data in Nash, K.L., Gatrone, R.C., Clark, G.A., Rickert, P.G., Horwitz, E.P., *Sep. Sci. Technol.* 23: 1355–1372, 1988; Mathur, J.N., Murali, M.S., Ruikar, B., Nagar, M.S., Sipahimalani, A.T., Bauri, A.K., Banerji, A., *Sep. Sci. Technol.* 33(14): 2179–2196.)

compounds (2) and (4) were not observed, but on the other hand, two other compounds OΦPOCH$_2$COOH (5) and OΦPOCH$_2$CONH(C$_4$H$_9$) (6) were identified. This discrepancy could be explained by the difference in experimental conditions (stirring or not during irradiation, aqueous acidity, etc.).

In CCl$_4$ and tetrachloro ethylene, the products identified were phosphinic acid (1), phosphinylacetic acid (5), and methyl(octyl)(phenyl) phosphine oxide (3) (*40, 41*). But gas chromatography alone was not able to identify 50% of the unknown compounds.

As was the case for monofunctionalized ligands, the weaker bonds were C-N, P-CH$_2$, and CH$_2$-CO, while the P = O, C = O, and hydrocarbon chains were the least likely to suffer radiolytic damage.

Nash did not observe any influence of acidity on the production rate for the major CMPO radiolysis products in the range of aqueous acidity from 1 to 5 mol L^{-1} (*41, 42*). A similar resistance was found for CMPO and TBP molecules in the absence of diluent, G(-CMPO) = 3.74 ± 0.4, and G(-TBP = 3.8 ± 0.6 molecules/100 eV (*41*).

8.3.2.1.2   *Influence of the Diluent*

Intensive studies on hydrolysis and gamma radiolysis of OΦD(iB)CMPO were carried out in decalin (*40*), *n*-dodecane (*20, 41, 46*), TCE (tetrachloroethylene) (*42*), and CCl$_4$ (*40*). The stability of CMPO in dodecane was greater than in chlorinated diluents, as shown by G-values established in the presence of an acidic aqueous phase for the disappearance of CMPO; in the presence of TBP in the organic phase (to simulate solvent in TRUEX process conditions), G(-CMPO) = 1.2 ± 0.3 in dodecane, and 4.5 ± 0.3 molecules/100 eV in tetrachloroethylene (*42*). This protective effect of dodecane on CMPO was quite unusual.

8.3.2.1.3   *Effect of Degradation*

Most of the studies focused on the influence of CMPO radiolysis on two important steps of the TRUEX process for americium recovery: extraction and stripping. The effect of radiolysis on CMPO-diluent solutions was extremely different under these two process conditions (see Table 8.5), with a major increase in D_{Am} values at pH 2, but a moderate decrease for 2–3 mol L^{-1} HNO$_3$.

In the presence of TBP molecules, the effect of radiolysis on D_{Am} at high and low acidities was reduced, which allowed authors to declare a protective effect of TBP (*40, 42*).

The presence of acidic degradation products of both TBP and CMPO (HDBP, compounds (1) and (5)—strong extracting agents) was responsible for the dramatic elevation of D_{Am} at low acidities. Specific studies have indicated that HDBP could increase americium extraction even for such small amounts as 5×10^{-2} mol L^{-1} (*41*), and that D_{Am} depends on phosphinic acid (1) concentration to the power of three (*40*). The increase of D_{Am} measured at low acidity under dynamic conditions compared to static radiolysis has been attributed to the formation of larger amounts of acidic degradation products, such as (1) and (2) (*46*).

When contacted with 2 mol L^{-1} HNO$_3$, the radiolyzed solutions showed little decline of D_{Am}, though an important loss of CMPO molecules had been measured (*41*). Neutral compounds like phosphine oxide (3) could replace some CMPO molecules around the metal ion.

TABLE 8.5

Effect of Radiolysis on Am Extraction by Irradiated CMPO Solutions

Conditions of Radiolysis		D_{Am}	
Dose		$[HNO_3]_{aq}$ in Extraction Tests	
(MGy)	Presence of TBP 0.74 M	2 M	0.01 M
0	None	8.5	6.3×10^{-3}
0.117	None	3.6	4.2
0.24	None	0.43	1.6×10^3
0.24	Addition of TBP after irradiation	0.49	1.4×10^2
0.24	Addition of TBP before irradiation	2.1	8.1×10^1

Irradiation with ^{60}Co source (2.5 kGy h^{-1})—vigorous stirring with a magnetic bar at 50°C of equal volume of organic phase (CMPO 0.25 M in CCl$_4$) and 5 M HNO$_3$

Extraction with the same volume of pre-equilibrated irradiated organic phase and HNO$_3$ skiped with ^{241}Am—25°C (40)

Conditions of Radiolysis		D_{Am}	
Dose		$[HNO_3]_{aq}$ in Extraction Tests	
(MGy)		3 M	0.01 M
0		25.5	0.016
0.152		22.3	1.5
0.305		21.5	7.1
1.062		13.9	247.3

Irradiation with a ^{60}Co source without stirring of CMPO 0.2 M + TBP 1.2 M in *n*-dodecane pre-equilibrated with 3 M HNO$_3$

Extraction with the same volume of organic phase (prewashed for HNO$_3$ 0.01 M measurements) and aqueous phase (46)

Some measurements were carried out on Ru, Zr, and Fe. The extraction of ruthenium was not affected by irradiation, whereas D_{Zr} and D_{Fe} increased dramatically, under all acidic conditions. The important effect of HDBP has been studied: a tolerable limit of 0.015 mol L^{-1} was proposed to avoid a sharp increase in the extraction of Fe and Zr (46).

The effect of α-radiolysis on the OΦD(iB)CMPO-TBP-*n*-dodecane system has been studied, and the change in D_{Am} at pH 2 was similar for both γ- and α-radiolyses (13).

8.3.2.1.4 Removal of Degradation Products

Carbonate cleanup was successful in restoring extraction efficiency to radiolyzed solutions when the diluent was CCl$_4$ (40) or tetrachloroethylene (41). With paraffinic hydrocarbons as diluents, a secondary clean-up operation was needed (181). Several efficient sorbents have been proposed, for example, macroporous anion-exchange resins, acid-washed activated charcoal, acid-washed alumina (20), or basic alumina (46).

8.3.2.2 Influence of the CMPO Structure

Several carbamoylmethyl phosphine oxides were compared: dioctyl, octyl(phenyl), and diphenyl-*N,N*-di-*iso*-butylCMPO [DOD(iB)CMPO, OΦD(iB)CMPO, and DΦD(iB) CMPO]. For γ-radiolysis of CMPO diluted in CCl_4 in contact with 5 mol L^{-1} nitric acid, the *G*-values of CMPO disappearance were 4.9, 7.4, and 6.4 molecules/100 eV for DOD(iB)CMPO, OΦD(iB)CMPO, and DΦD(iB)CMPO, respectively. The stability depended somewhat on the substituent on the P = O group, indicating that degradation was probably initiated on the amidic site of the molecule (*40*). Unlike dithiophosphinic acids (*49*) or diamide extractants (*182, 183*), the substitution of phenyl groups for alkyl groups seemed to reduce the stability of the molecule (*40*).

8.3.1 Amide Extractants

8.3.3.1 *N,N*-dialkyl Amides

N,N-dialkyl aliphatic amides R-CO-NR´R˝ have been studied as an alternative to TBP for the reprocessing of nuclear fuel or actinide separation (*184–190*). These extractants offer advantages over TBP, especially their complete incinerability and the innocuous nature of their degradation products. Amide solutions were often pre-equilibrated with aqueous nitric solutions before irradiation, in order to be as representative of process conditions as possible. The main degradation products were carboxylic acids and secondary amines, which had little influence on the separation of U(VI) and Pu(IV) from fission products. If the length of the alkyl chain R´ was short enough, the main degradation products could easily be removed by scrubbing steps.

8.3.3.1.1 Degradation Products

In most studies, the presence of amines and carboxylic acids has been proposed from the emergence of large vibration bands on infrared spectra at 3470–3480 cm^{-1} and 1720–1725 cm^{-1}, respectively (*191–193*). The vibration bands of amines were not always detected, for example with short alkyl chain R´ or R˝ like DBEHA (*N,N*-dibutyl-2-ethyl hexanamide) or *N*-methyl-*N*-butyl-2-ethylhexanamide (MBEHA) (*194*); this absence was explained by the formation of volatile amines. Musikas noted that very small amounts of secondary amine were also observed with longer radicals (DEHHA: *N,N*-di(2-ethylhexyl)hexanamide) and supposed that the secondary amine could degrade in acidic conditions faster than it had appeared (*189*). A qualitative study of degradation products was performed by GC-MS analysis after electronic bombardment of 1 mol L^{-1} DEHHA dodecane-HNO$_3$. Numerous short compounds were identified: 3-heptanol, 3-heptanone, 2-ethylhexanal, 2-ethylhexanol, and carboxylic acids RCOOH (with $R = C_4H_9, C_5H_{11}, CH(C_2H_5)-C_5H_{11}$). Volatile compounds were measured by GC after specific trapping in a sorption tube. The compounds detected were alkanes and olefins (C3 to C8), RCHO (C3 to C7), ketones, and alcohols. In the gas phase, the classical compounds H_2 (87%), N_2, CO, N_2O, CO_2, and CH_4 were identified (*195*).

Other amide compounds were also identified from radiolysis of DEHDMBA (*N,N*-di(2-ethylhexyl)-3,3-dimethyl butanamide) and mixtures of DEHBA [*N,N*-di(2-ethylhexyl)-*n*-butanamide]–DEHiBA [*N,N*-di(2-ethylhexyl)-i*so*-butanamide] in TPH by CPG-FTIR: light primary and secondary amides and functionalized tertiary amides with high molecular masses (*196*). Carboxylic acids represented a large

proportion of the degradation products: in the case of DEHBA or DEH*i*BA, one-third of degraded amide. However the main part (80%) was eliminated in the aqueous phase (propionic acid, *n*-butyric, and *iso*-butyric acids).

Authors have often used FTIR spectroscopy to estimate the quantity of residual amide after irradiation, and sometimes the quantity of carboxylic acids (ν = 1720–30 cm^{-1}). Musikas selected specific titration in nonaqueous medium to determine the concentration of amide, amine, and carboxylic acids (*189*).

The amounts of degraded amide extractant were slightly higher than those observed with TBP in the same conditions (*187,188, 189, 191, 192, 197, 198*).

8.3.3.1.2   Factors Governing Degradation

Unlike the extractant TBP (*26, 27, 98*), the radiolysis yields strongly depended on the nitric acid concentration (*188, 189*); after irradiation of DEHHA in TPH in the presence of nitric acid aqueous phase, the G(-amide) = 3.6 and 0.9 for 4 and 0.5 mol L^{-1} HNO$_3$, respectively.

On the other hand, the radiolysis of amides was increased in the presence of *n*-dodecane (*183, 199*), as mentioned for TBP (*90*).

8.3.3.1.3   Influence of the Monoamide Structure

The nature of the alkyl group had some influence on the stability of the amide extractants (a factor of 2 has been observed for high doses), and interest had meanwhile been aroused in the establishment of tendencies (*191, 192, 194, 200*). But the effect was strongly dependent on the diluent.

In *n*-dodecane, the order of stability (shown in Figure 8.5) was DBOA (*N,N*-dibutyloctanamide) > D*i*BEHA (*N,N*-di(*iso*-butyl)-2-ethylhexanamide) > D*i*BOA (*N,N*-di-*iso*-butyloctanamide) > MBEHA ≈ DBEHA (*191, 194, 200*). The most stable amides were therefore *N,N*-di-*n* alkyl *n*-alkylamides (15% degraded after 0.6–0.8 MGy), whereas the proportion reached 20–25% for branched amides (on N and CO) (*189, 191, 194, 200*) and 35–40% for some branched amides (on N or CO) (*191, 194, 196, 200*).

The tendency observed in benzene with 11 molecules (*192*) was slightly different:

– The branching of the alkyl group R bound to the C = O group reduced the stability in the order α-branching > *n*-chain ≈ β-branching;
– The branching of the alkyl groups at the N-atom stabilized the extractant;
– As the length of the alkyl groups R increased, the stability decreased;
– The presence of different alkyl groups on N-atom decreased the stability (i.e., RCONR′(CH$_3$) were less stable than symmetrical amides RCONR′$_2$).

In this case, the highest stability was observed for the branched amide (*i*Pr)$_2$NCOCH(C$_2$H$_5$)C$_4$H$_9$

8.3.3.1.4   Effect of Degradation on Extraction Behavior

8.3.3.1.4.1   U(VI), Pu(IV), and Th(IV) Extraction.   The influence of the dose was similar for numerous *N,N*-di-*n*-alkyl-*n*-alkylamides in alkane: a gradual decrease of $D_{U(VI)}$ (up to a factor of 1.5 to 2) from 0.1 to 1 MGy (*187, 191, 197, 200*), and then a
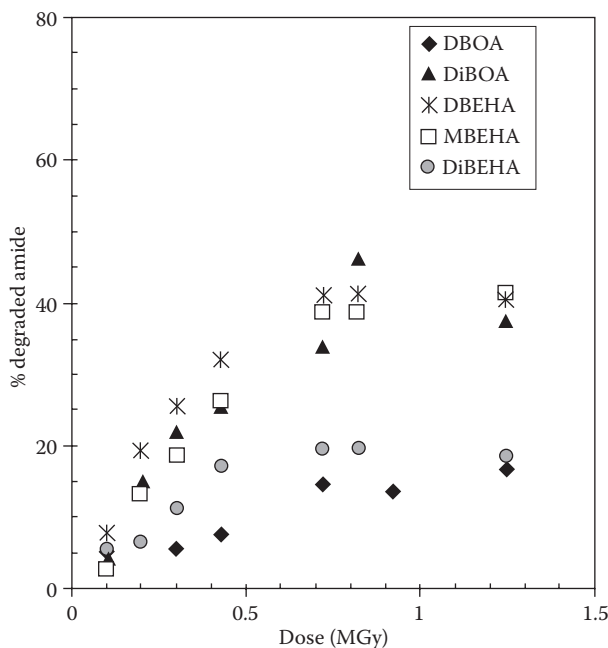
FIGURE 8.5 Effect of the structure on the radiolytic stability of *N,N*-dialkyl aliphatic amides in *n*-dodecane: % degraded extractant. Experimental conditions: irradiation with a 2000 Curie ^{60}Co gamma-irradiator (4.2 kGy h^{-1} dose rate) of 0.5 M monoamide in *n*-dodecane solution pre-equilibrated with 3.5 M HNO$_3$. DBOA: *N,N*-dibutyloctanamide, DiBOA: *N,N*-di-iso-butyloctanamide, DBEHA: *N,N*-dibutyl-2-ethylhexanamide, MBEHA: *N*-methyl,*N*-butyl-2-ethylhexanamide, DiBEHA: *N,N*-di-iso-butyl-2-ethylhexanamide. (Drawn from data in Ruikar, P. B., Nagar, M.S., Subramanian, M.S., Gupta, K.K., Varadanajan, N., Singh, R.K., *J. Radioanal. Nucl. Chem.*, 1: 171–178, 1995; Ruikar, P.B., Nagar, M.S., Subramanian, M.S., *J. Radioanal. Nucl. Chem., Lett.,* 176(2): 103–111, 1993; Ruikar, P.B., Nagar, M.S., Subramanian, M.S., *J. Radioanal. Nucl. Chem.,* 159(1): 167–173, 1992.)

distribution ratio remaining stable (see Figure 8.6a). This behavior has been attributed to the decrease of the extractant concentration (*197*) (14–30% at 1 MGy). HNO$_3$ concentration seemed to have no influence (*187*).

For an irradiation dose of 0.35 MGy, the extent of the decrease in D_U was the same (30–35%) in the case of 0.5 mol L^{-1} DEH*i*BA and 5% TBP; but with higher concentrations of TBP (0.5 or 1 mol L^{-1} in dodecane (*191*) and benzene (*194*)), it must be remembered that $D_{U(VI)}$ systematically increased after gamma irradiation.

In benzene, Mowafi observed some differences between symmetrical amides RCONR$'_2$ and unsymmetrical amide RCON(CH$_3$)R′. The influence of the dose on $D_{U(VI)}$ was stronger for *N*-methyl-*N*-alkyl amides (reduction of factor 4 compared to factor 1.7–1.8 for RCONR$'_2$) (*192*), related to the extractant's lower stability.

However, the effect on Pu(IV) extraction was totally different: after a first step, where the decrease with the dose was very low (factor of 2), the extraction increased rapidly and then decreased (Figure 8.6b) (*194, 200*). The last two steps have been explained by authors as:
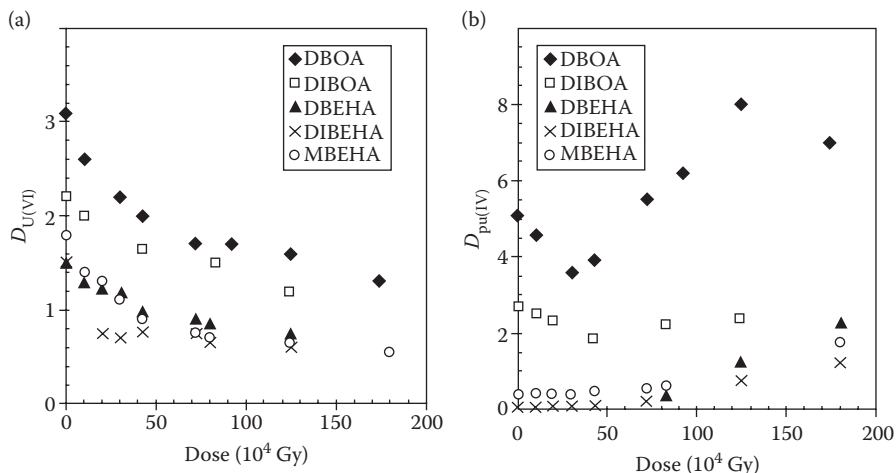
FIGURE 8.6 Effect of the dose on the extraction of U(VI) (a) and Pu(IV) (b) by γ-irradiated amides. Experimental conditions: irradiation with a 2000 Curie ^{60}Co gamma-irradiator (4.2 kGy h^{-1} dose rate) of 0.5 M monoamide in *n*-dodecane solution pre-equilibrated with 3.5 M HNO$_3$-extraction: equal volume of organic and aqueous phase (3.5 M HNO$_3$ with tracers) at 25 ± 0.1°C. DBOA: *N,N*-di-butyloctanamide, D*i*BOA: *N,N*-di-*iso*-butyloctanamide, DBEHA: *N,N*-dibutyl 2-ethylhexanamide, MBEHA: *N*-methyl,*N*-butyl-2-ethylhexanamide, D*i*BEHA: *N,N*-di-*iso*-butyl-2-ethylhexanamide. (Figure drawn from data in Ruikar, P.B., Nagar, M.S., Subramanian, M.S., *J. Radioanal. Nucl. Chem., Lett.,* 176(2): 103–111, 1993; Ruikar, P.B., Nagar, M.S., Subramanian, M.S., *J. Radioanal. Nucl. Chem.,* 159(1): 167–173, 1992.)

- A synergistic extraction of Pu(IV) by carboxylic acids;
- Hydrolytic disturbances of the organic phase, such as the formation of third phase and emulsification.

Nevertheless, extraction tests by the addition of the primary acidic compound (hexanoic acid coming from the degradation of *N,N*-diethyl-2-hexyl hexanamide) were performed by Musikas (*189*): the distribution ratios of U(VI) and Pu(IV) at 0.5 and 4 mol L^{-1} HNO$_3$ remained constant, even for amounts related to a degradation of 0.2 MGy.

The extraction of Th(IV) was not affected by the gamma radiolysis over the entire range from 0 to 1 MGy for both symmetrical and N-methyl amides (*192*).

With cyclic amides, *N*-alkyl-caprolactams, the tendency was similar, namely no obvious change in the extraction of Th(IV) and U(VI) was observed in the range 10^2–10^4 Gy. But if the gamma-ray irradiation dose was higher than 10^4 Gy, $D_{U(VI)}$ decreased with the increased dose, as observed for TBP. This effect was stronger when one radical on nitrogen was branched (2-ethylhexyl instead of *n*-octyl) (*201*).

8.3.3.1.4.2 Extraction of Other Fission Products. The extraction of lanthanides by monoamides is weak, but some authors have performed tests after irradiation, showing that, for a similar dose (1 MGy), D_{Eu} could decrease slightly (from 10^{-2} to 0.2×10^{-2}) (*191*) or remained stable (*194*) for 0.5 mol L^{-1} amide in *n*-dodecane, but could increase (from 0.5–0.6 to 4–6) (*192*) for 0.5 mol L^{-1} amide in benzene. The irradiation seemed to have no influence on Am(III) extraction (*191*).

Distribution ratios of ruthenium evolved irregularly with the dose absorbed. With some amides, after a high increase (factors of 20–30 up to 1 MGy), the extraction decreased, as shown for Pu(IV), but more drastically (factors of 10 to 300 from 1 to 2 MGy) (*188, 191*). Other authors indicated an absence of ruthenium extraction ($D_{Ru} < 10^{-2}$) over the entire range studied (0 to 1.8 MGy) (*194*). On the other hand, the decontamination factors for U and Pu with respect to ruthenium(III) employing irradiated amides were comparable to the corresponding values with TBP (*191*).

But with *N*-alkyl-caprolactams, the influence of the dose on the extraction of ruthenium was strong, especially above 10 kGy, where a sharp increase in the extraction was observed (*201*).

The extraction of Zr increased with the absorbed γ-dose (factor of 20 up to 0.7–0.8 MGy for linear amides in *n*-dodecane (*191*) and factors of 4–6 up to 0.3–0.6 MGy for shorter amides in benzene) (*192*). Beyond this threshold, the extraction decreased slightly. This effect is more noticeable with *N*-methyl amides (*192*). As for Pu(IV), the first step has been explained by authors by a synergistic extraction due to the presence of carboxylic acids as degradation products (*191*). Nevertheless, the degradation had a stronger effect on the decontamination factors of U and Pu with respect to Zr(IV) than with TBP (*191*). Typically, decontamination factors were $DF_{M/Zr} = 7$ and 12 for, respectively, U(VI) and Pu(IV) with TBP and 5 with the monoamide DHOA at an irradiation dose of 300 MGy (*193*).

With cyclic amides (*N*-alkyl-caprolactams), Zr distribution ratios increased with γ-irradiation in the range 0.1–10 kGy and decreased slightly beyond this. The increase in the first step has been explained by the formation of large molecular compounds like $C_8H_{17}NHC_5H_{10}COOH$, which have a better extracting capability (*201*). For higher doses, this compound was supposed to be radiolyzed into smaller compounds that would be soluble in the aqueous phase.

8.3.3.1.5   Removal of Degradation Products

The main degradation products of *N,N*-dialkyl-monoamides were easily removed with dilute acid/water or during the extraction-scrub-strip sequence, unlike those of TBP, which need specific alkali treatments (*187, 193*).

8.3.3.2   Malonamides

In the context of minor actinide partitioning from high-level radioactive liquid wastes, malonamides have been proposed either as the single extractant in the DIAMEX process (*202–210*) or in a mixture with dialkylphosphoric acid in the DIAMEX-SANEX process (*156, 211, 212*). The semideveloped formula of the selected malonamides is $R(CH_3)NCO(CHR´)CONR(CH_3)$ (R and R´ are alkyl or oxyalkyl groups). Degradation behavior was one of the main criteria selected when optimizing the malonamide molecule's formula. To minimize the formation of surfactant compounds, like long-alkyl-chain carboxylic acids, the number of carbon atoms was shared between the radicals R and R´. The introduction of an oxygen in the central chain R´ was interesting because an additional cleavage became possible (*202, 213*). These studies led to the selection of the reference molecule, DMDOHEMA (*N,N´*-dimethyl-*N,N´*-dioctyl hexyloxyethyl malonamide ($C_8H_{17}(CH_3)NCO)_2CH(C_2H_4OC_6H_{13})$).

8.3.3.2.1 Degradation Products from the Radiolysis of Malonamide Systems

Malonamide degradation under hydrolysis and radiolysis has been studied in detail using GC-FTIR and GC-MS techniques. Figure 8.7 shows a degradation scheme for the molecule DMDOHEMA (*214*). The main degradation products identified in the organic solution after radiolysis in the presence of nitric acid aqueous phase were: bifunctional compounds (amide-acid, amide lactone), monomides, diamides, *N*-nitrosoamines, carboxylic acids, and amines (*3, 4, 48, 214*).

The first step was the hydrolysis of the amide group, resulting in the formation of a carboxylic acid (1) and a secondary amine (10). By the loss of CO_2, the carboxylic acid (1) yielded the monoamide (3). Another reaction was the hydrolysis of the ether function of the central oxy-alkyl group, leading to alcohols. From these two successive breaks, an acid-alcohol was formed, and an intramolecular reaction between the alcohol function and the acid function led to a lactone (2). In the same way, new attacks of the amide group of compounds (3) and (2) resulted in the formation of the carboxylic acid (9). Other reactions occurred and led to diamides (5, 6, 7), formamide (4), *N*-nitrosamine (8), and alcohols. The presence of dialkylphosphoric acid in solution did not change the nature of the malonamide DMDOHEMA degradation products (*71*).

8.3.3.2.2 Quantitative Data

Table 8.6 gives the concentrations of the main degradation products after gamma radiolysis of three malonamides in TPH: DMDOHEMA, DMDBTDMA (*N,N´-*dimethyl-*N,N´-*dibutyltetradecyl malonamide) and DMDBDDEMA (*N,N´-*dimethyl-*N,N´-*dibutyldodecyloxyethyl malonamide). The extractant concentration decrease was quite high, and the main degradation products were acid compounds. Under similar conditions, malonamides were less stable than TBP, with an average factor of 6 to 9 (*48*).

8.3.3.2.3 Factors Governing Degradation

Quantitative studies of radiolytic and hydrolytic degradations of the "malonamide-alkane-nitric acid" system by potentiometric or gas chromatographic titrations gave the following results (*48*):

- Studies allowed the estimation of *G*-value: 3.7 molecules/100 eV for 0.65 mol L^{-1} DMDOHEMA in TPH in the presence of 3 mol L^{-1} aqueous nitric acid.
- An increase of the temperature led to a decomposition of the amide-acid (1) into monoamide (3).
- An increase of the acidity in the aqueous phase slightly reduced the stability of amide compounds, not only the initial malonamide, but also the monoamide (3) and diamides (5) and (6). At the same time, the concentration of the amide-acid (1) increased.
- The quantity of monoamide (3) produced was low, owing to competitive reactions between its formation and its degradation by radiolysis.
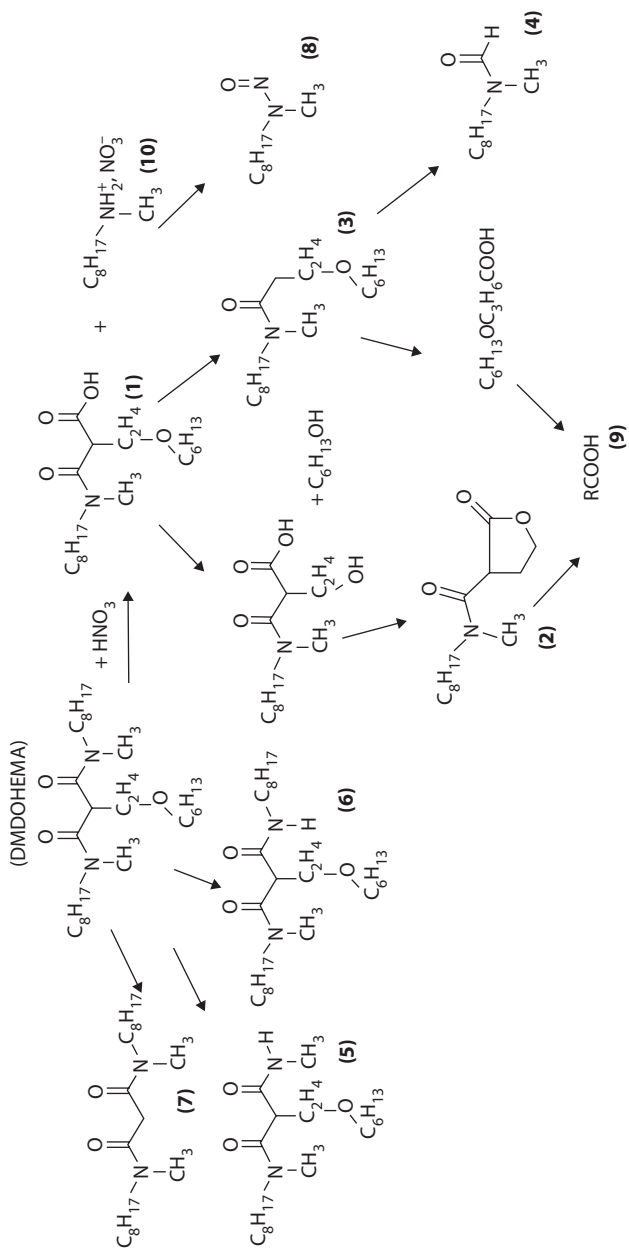
FIGURE 8.7 Simplified scheme for the hydrolytic and radiolytic degradation of DMDOHEMA. (Redrawn from Berthon, L., Camès, B., *CEA Report*: CEA-R-5892, 206–211, 2000.)

TABLE 8.6

Concentrations (in mol L⁻¹) of the Main Solutes in Organic Solutions after Radiolysis Under 0.75 MGy

	[Diamide]	[Amide-Acid]	[Monoamide]	[Carboxylic Acids]	[Amine]
DMDBTDMA	0.68	0.15	0.02	0.29	0
DMDBDDEMA	0.64	0.23	0.01	0.28	0
DMDOHEMA	0.57	0.08	0	0.33	0.13

Source: From Berthon, L., Morel, J.M., Zorz, N., Nicol, C., Virelizier, H., Madic, C. *Sep. Sci. Technol.* 36 (5–6): 709–728, 2001.

Note: Irradiation with a ^{60}Co source (4 kGy h⁻¹ dose rate) at room temperature. Equal volume of organic phase (1 M malonamide in TPH) and aqueous phase (4 M HNO_3).

In the presence of dodecane, as for other extractants like TBP or monoamides, radiolysis was increased (*182, 199*).

The degradation by gamma radiolysis of the mixed solvents DMDOHEMA-organophosphoric acid has been studied in the presence of acidic aqueous phase. Some *G*-values related to the disappearance of DMDOHEMA have been estimated:

- G(-DMDOHEMA) = 5.5 molecules/100 eV for 0.65 mol L⁻¹ DMDOHEMA, 0.45 mol L⁻¹ HBDMBP in TPH in the presence of pH 3 or 0.5 mol L⁻¹ HNO_3 aqueous phase (*71*);
- G(-DMDOHEMA) = 4.9 molecules/100 eV for 0.5 mol L⁻¹ DMDOHEMA, 0.3 mol L⁻¹ HDEHP in TPH in the presence of 3 mol L⁻¹ HNO_3 (*5*).

The effect of the presence of dialkyl phosphoric acid was moderate, with an increase of the malonamide degradation probably by hydrolysis, as has been observed in specific hydrolysis experiments (*71*).

8.3.3.2.4 Influence of the Structure

Cuillerdier compared the radiolytic stability of several malonamides [(C₄H₉(CH₃)NCO)₂CHR″] in *t*-butylbenzene in contact with nitric acid as a function of the central alkyl chain R″ (3.3 kGy h⁻¹, 40°C) (*215*). The order of stability, established on the total concentration of amide functions measured by potentiometry in nonaqueous medium, was: H < C₂H₅ < C₂H₄OC₆H₁₃ ≈ C₂H₄OC₂H₄OC₆H₁₃. The authors then proposed the following tendencies:

- The stability decreased with the aqueous solubility of the malonamide;
- The presence of a long oxyalkyl radical R″ appeared to protect the molecule from degradation;
- The presence of a second oxygen in R″ had no significant effect.

More recently, a comprehensive study of the radiolytic behavior of three malonamides (DMDBTDMA, DMDBDDEMA, and DMDOHEMA) in alkane was carried

out (*48*). Though the extractants present the same generic behavior, some differences linked to the structure were observed:

– The presence of an oxygen in the central chain led to an additional cleavage (formation of the hexanol and bifunctional compounds presented in Figure 8.7, and identified for high irradiation), but a comparable concentration of carboxylic functions in organic phase and similar stability of the molecule, even in contact with 4 mol L^{-1} HNO$_3$, G(-DMDBTDMA) = 5.2 and G(-DMDBDDEMA) = 5.5 molecules/100 eV.

– A lengthening of the alkyl chain on the nitrogen atom (from C$_4$H$_9$ to C$_8$H$_{17}$) led to an increasing lipophilicity of the related amine formed by degradation (compound (4) in Figure 8.7 for DMDOHEMA). Thus, the presence of the amine (R´CH$_3$NH) was observed only after degradation of DMDOHEMA, because of the higher lipophilicity of CH$_3$(C$_8$H$_{17}$)NH compared to the water-soluble CH$_3$(C$_4$H$_9$)NH.

8.3.3.2.5   Effect of Degradation

8.3.3.2.5.1   Extracting Properties.   Extraction efficiency of malonamides was checked after gamma radiolysis:

– On the metallic ions (Eu(III), Am(III), Pu(IV), and U(VI)) with DMDBHEEMA in *t*-butylbenzene (*215, 216*);

– On Am(III) and Eu(III) with DMDBTDMA, DMDOHEMA, and DMDBDDEMA in TPH (*48*).

The influence of the dose was quite low (see Figure 8.8), and the efficiency of the solvent for the extraction of actinides (III, IV, and VI) and back-extraction of trivalent cations was maintained up to 0.6–0.7 MGy. No precipitation was observed after contact of radiolyzed solutions with metallic ions.

In order to specify the individual role played by each degradation product, measurements were carried out with synthetic organic solutions of "malonamide + degradation product." The presence of degradation products led systematically to a decrease of D_{Nd} and D_{Am}, in the following order: amine > carboxylic acid > monoamide ≈ hexanol, as presented for Am(III) in Figure 8.9.

The impact of DMDOHEMA-TPH radiolysis under continuous degradation was studied in the laboratory-scale MARCEL γ-irradiation facility. A retention of Mo in the DMDOHEMA-TPH solvent was observed (about 30–40% of Mo was missing from the aqueous phase), which has been linked to the MDOHEMA accumulation (*217*).

8.3.3.2.5.2   Hydraulic Behavior.   The influence of the main DMDOHEMA degradation products on the hydraulic performances of the process flowsheet was investigated by the determination of the emulsion settling time after mixing the irradiated solvent with nitric acid solution (0.1 mol L^{-1}). This settling time increased with the irradiation dose. Experiments performed with synthetic solutions of monoamide and
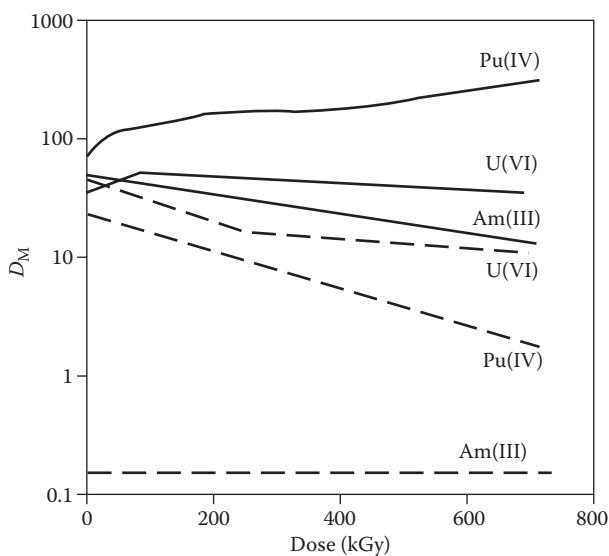
FIGURE 8.8   Effect of radiation dose on the distribution ratios of various actinides from 0.5 M (- - -) or 5 M HNO_3 (–) by 1 M DMDBHDEMA in *tert*-butylbenzene. (Redrawn from Thiollet, G., Musikas, C., *Solvent Extr. Ion Exch.* 7(5): 813–827, 1989. With permission.)
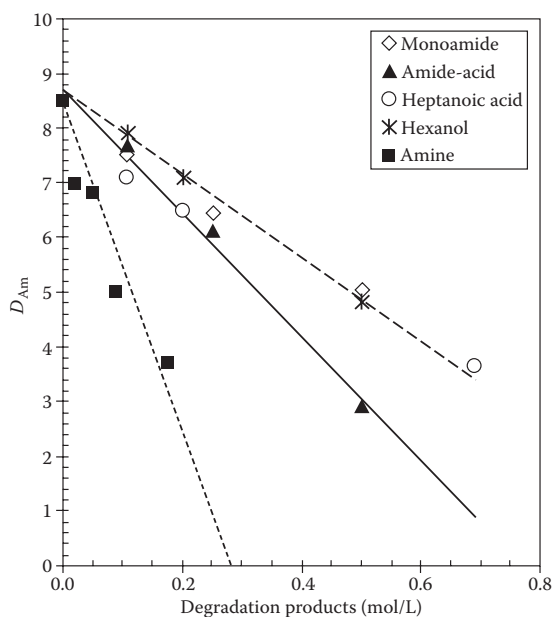
FIGURE 8.9   Distribution ratios of Am(III) as a function of the degradation product concentration in a synthetic DMDOHEMA solution. Equal volumes of organic and aqueous phases (degradation product added in 0.65 M DMDOHEMA in TPH-3 M HNO_3-25°C). (Drawn from Berthon, L., Morel, J.M., Zorz, N., Nicol, C., Virelizier, H., Madic, C. *Sep. Sci. Technol.*, 36(5–6): 709–728, 2001.)

amide-acid in malonamide solution indicated that these main degradation products were not responsible for the increase in the phase-disengagement time (*4*).

After long-term degradation in the MARCEL γ-irradiation facility, no influence was observed on the physical properties of the DMDOHEMA-TPH solvent (density, refraction index, interfacial tension), but a slight increase of solvent viscosity was observed (*217*).

8.3.3.2.6   Removal of Degradation Products from Spent Solvents

8.3.3.2.6.1   In the DIAMEX Process   To remove the basic species (e.g., amine) and acidic degradation products (e.g., carboxylic acids and amide-acid) of DMDOHEMA, various scrubbings, acidic and alkaline treatments, respectively, have been tested. The amine was quantitatively eliminated by acidic scrubbing (nitric acid 0.1 mol L^{-1}), which corresponds to the stripping step in the DIAMEX process (*218*). An alkaline solvent cleanup step has been specifically defined. Regeneration efficiency has been studied in the MARCEL test loop under continuous operation: extraction/ scrubbing/solvent degradation (radiolysis and hydrolysis) and stripping (*4*). The efficiency of the alkaline treatment has been shown in the fact that some hydrolysis and radiolysis degradation products that remained (mono and diamide compounds) did not modify the classical solvent properties (hydrodynamic behavior, surface tension, density, viscosity, and extractant properties) (*6*).

8.3.3.2.6.2   In the DIAMEX-SANEX Process   The presence of HDEHP decreased the alkaline treatment's efficiency for removing amide-acid (*5*). Nevertheless, solvent endurance was tested in the MARCEL test loop for a total of 1800 hours, equivalent to about 100 solvent recycling cycles. After alkaline treatment, some degradation products remained in the solvent (monoamide, MDOHEMA, but also the acid-amide). These remaining degradation products had no influence on the process performance (settling properties and extractant properties: the Mo, Zr, Fe, Pd, and Nd distribution ratios and the americium/europium separation factors) (*5*).

8.3.3.3   Diglycolamides

N,N,N′,N′-tetraoctyl-3-oxapentane-1,5-diamide (TODGA) was studied as an extractant for minor actinides such as Am(III) and Cm(III) from a PUREX raffinate or for actinides(III) and (IV) from spent nuclear fuel, in the context of the ARTIST process (*219–228*). Therefore, some stability studies were undertaken recently.

8.3.3.3.1   Nature of the Degradation Products

Degradation of TODGA under hydrolysis and radiolysis was studied using FTIR, GC-MS, and NMR spectroscopies. TODGA was more sensitive to radiation than mono- and malonamide, as attested by the *G*-value for neat extractants: *G*(-TODGA) = 8.5 ± 0.9, *G*(-DMDODDEMA) = 7.5 ± 0.8, and *G*(-DOHA) = 5.6 ± 0.6 molecules/100 eV (*199*).

The cleavage of both the $C = O_{amide}$ and the $C\text{-}O_{ether}$ bonds was observed by the weakening of the related IR absorption, at 1,653 and 1,124 cm^{-1}, respectively. The main degradation products identified in organic phases after radiolysis

in the presence of nitric acid aqueous phase were dioctylamine (DOA), *N,N*-dioctyl-3-oxapentan-1,5-amide acid, *N,N*-dioctylacetamide (DOAA), *N,N*-dioctylglycolamide (DOGA), and *N,N*-dioctylformamide (DOFA) (*199, 229*). The schematic diagram in Figure 8.10 summarizes TODGA's radiolytic degradation paths (*199*).

DOA was formed by the hydrolytic cleavage of the amide-bond, as observed for other amide extractants (*48, 189*). DOAA and DOGA were formed mutually by the cleavage of the ether-bond. The formation of DOFA was caused by the cleavage of the bond adjacent to the ether-bond.

No data has yet been published on the quantitative ratio of each degradation product. However, radiolysis should lead to lower amounts of acidic compounds than malonamides, because of the absence of any alkyl (or oxyalkyl) chain between the two amide groups.

8.3.3.3.2   Factors Governing Degradation

8.3.3.3.2.1   Influence of the Aqueous Phase.

Different TODGA-dodecane solutions were irradiated without HNO_3, or stirred with 0.1 or 3.0 mol L^{-1} HNO_3 during irradiation (*199*). The residual TODGA concentrations in the organic phase were comparable, which indicates that HNO_3 has an insignificant effect on the overall stability of the molecule. Nevertheless, the influence of nitric acid was important to the ratio of the degradation products (*199*). Gas chromatography analyses indicated that in the presence of HNO_3, reaction (a) was favored (see Figure 8.10), resulting in the formation of amide acid, as observed with malonamides (Figure 8.7). In the absence of nitric acid, reaction (b) was preponderant; reaction (c) was a secondary reaction in all cases.
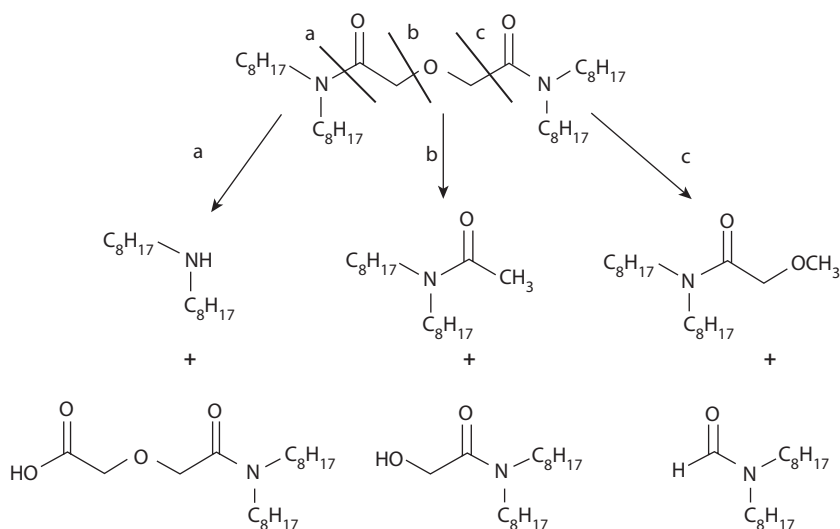
FIGURE 8.10   Schematic diagram of the radiolytic degradation of TODGA. (Drawn from Sugo, Y., Sasaki, Y., Tachimori, S., *Radiochim. Acta*, 90: 161–165, 2002.)

8.3.3.3.2.2 Influence of the Diluent. The degradation of TODGA increased in the presence of *n*-dodecane (*182, 183, 199*), as observed with other amide extractants (*182, 199*) or TBP (*90*). The same effect was observed with 1-octanol, though as mentioned by Sugo (*182, 183*), the reaction mechanisms with alkane and alcohol are different. The sensitization effect of dodecane was explained by a charge-transfer reaction from radical cations of *n*-dodecane to TODGA molecules in the primary process (*182*) (see detailed discussion in Section 4.2). This sensitization effect was reduced by the introduction of additives, like aromatic diluents (benzene, benzylalcohol, nitrobenzene), or solutes, like monoamides, as presented in Figure 8.11.

8.3.3.3.2.3 Influence of the Irradiation Dose. The TODGA concentration decreased exponentially with the dose. After γ-radiolysis of 0.1 mol L^{-1} TODGA in dodecane pre-equilibrated with 3.0 mol L^{-1} nitric acid, G(-TODGA) = 0.38 μmol J^{-1} (or 3.7 molecules for 100 eV of absorbed energy) (*229*).

8.3.3.3.3 Effect of Degradation

The extraction of Am(III), Pu(IV), and U(VI) from 3.0 mol L^{-1} HNO$_3$ using 0.1 mol L^{-1} TODGA in *n*-dodecane was studied (*229*). Extraction efficiency at high acidity was maintained, even after irradiation with 0.42 MGy, where the concentration of TODGA
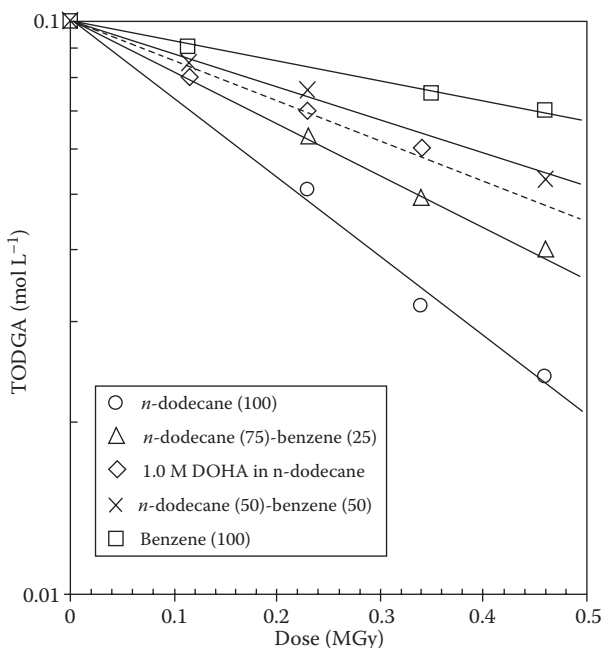
FIGURE 8.11 Effect of the addition of benzene and monoamide DOHA on the radiolysis of TODGA. Conditions: gamma-irradiation from ^{60}Co source (125 C kg^{-1} h^{-1}) in air, at room temperature of 0.1 M TODGA in solution. The numeral in parenthesis indicates a volume percentage in diluent. (Redrawn from Sugo, Y., Sasaki, Y., Tachimori, S., *Radiochim. Acta*, 90: 161–165, 2002. With permission.)

was reduced (lower than 0.03 mol L^{-1}). Other experiments performed with 0.2 mol L^{-1} TODGA (with and without 0.5 mol L^{-1} TBP) in TPH, in contact with 3.0 mol L^{-1} nitric acid showed only a slight decrease in D_{Am} above 0.6 MGy and no significant influence on D_{Eu} (227). On the other hand, at low acidity, the values of D_{Am} increased after irradiation of the solvent (as presented in Figure 8.12), which could lead to potential difficulties in the splitting step with dilute nitric acid. Specific investigations into the behavior of *N,N*-dioctyl-3-oxapentan-1,5-amide acid (Figure 8.10a) allowed it to be established that this compound played a noticeable role at low acidity, as do classical acidic extractants, and had a synergistic effect on the extraction at high acidity. D_{Am} increases from 24 to 80 in the presence of 0.02 mol L^{-1} of the amide acid (229).

8.3.3.3.4 Influence of the Extractant Structure

The protective effect of aromatic diluents has encouraged authors to test the radiolytic stability of TODGA derivatives possessing an aromatic moiety. Two molecules were synthesized: *N,N,N′N′*-tetra(*p*-octylphenyl)diglycolamide (T(OPh)DGA) and *N,N,N′,N′*-tetra-octylfuran-2,5-diamide (TOFDA) (183). The order of radiolytic stability was T(OPh)DGA > TOFDA > TODGA, which indicates that the presence
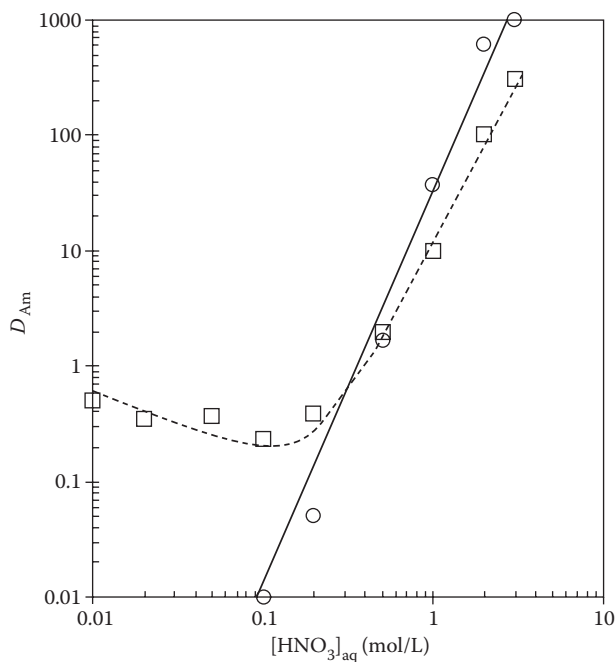
FIGURE 8.12 Influence of irradiation on extraction of Am(III) from HNO$_3$ by 0.1 M TODGA in *n*-dodecane before (o) and after 422 kGy (□). Gamma irradiation of 0.1 M TODGA in *n*-dodecane pre-equilibrated with HNO$_3$ with ^{60}Co source—4.8 kGy h^{-1} dose rate—in air at room temperature. Extraction: equal volume of organic and aqueous phase (HNO$_3$ spiked with tracer –1.0 × 10^{16} Bq). Temperature: 25 ± 0.1°C. (Redrawn from Sugo, Y., Sasaki, Y., Kimura, T., Sekine, T., Kudo, H. *Proceeding of the International Conference Global 2005*, Tsukuba, Japan, 9–13 October, Paper No. 368, 2005.)

of aromatic cycles in diglycolamides improves their stability. The smaller effect observed for TOFDA has been explained by a lower degree of aromaticity of the furan cycle compared to benzene.

8.3.4 NITROGEN DONORS

Several systems involving nitrogen polydentate extractants were investigated in order to separate An(III) from Ln(III). The main N-donors investigated are picolinamides, 2,4,6-tri(2-pyridyl)-1,3,5-triazines (TPTZ) (*203, 211, 230–233*), 2-(3,5,5-trimethylhexanoylamino)-4,6-di(pyridine-2-yl)-1,3,5-triazine (TMHADPTZ) (*203, 211*), bis-triazinyl-1,2,4-pyridines (BTP) (*3, 4, 174, 203, 211, 234–236*), and 6,6′-bis(5,6-dialkyl-1,2,4-triazin-3-yl)-2,2'-bipyridines (BTBP) (*4, 237–239*). Among these, the only degradation studies reported in the literature concern BTP and BTBP extractants. The aim of the research was to improve the radiolytic and hydrolytic stability of these otherwise efficient molecules, their main drawback. In fact, the strong sensitivity of the ligand *n*Pr-BTP (2,6-bis(5,6-*n*-propyl-1,2,4-triazin-3yl)-pyridine) selected in 1999 to perform a countercurrent test on a genuine highly active effluent explained the low efficiency in the process (*202, 235, 236*) and justified the interest of radiolysis investigations.

8.3.4.1 Degradation Products

The majority of degradation studies have focused on process data (the influence on extracting properties such as D_{Am} and $SF_{Am/Eu}$). Nevertheless, a few publications reported some identification of hydrolysis or radiolysis degradation products for *n*Pr-BTP and *i*Pr-BTP by gas phase chromatography (GC-MS), and electro-spray ionization (ESI) or atmospheric-pressure chemical ionization (APCI)-mass spectrometry (*4, 236, 240*). In nitric media, the main chemical attack was the addition of a nitrous moiety to one of the $(CH \text{ or } CH_2)_{propyl}$ groups located on the α-position of the triazinyl rings, to form a nitro compound, which evolved into the related alcohol and ketone derivatives. A second similar attack on another propyl group could occur, leading to dialcohols and diketones. Other reactions, such as the loss of one alkyl chain or the disruption of the triazinyl rings, led to cyanocompounds (*4, 66*). Surprisingly, after radiolysis of *i*Pr-BTP under 0.1 MGy, the main compounds detected by APCI-MS were heavier than the initial BTP, resulting from the addition of one or two $C_8H_{17}O$-groups arising from the diluent octanol (*4, 240*).

No quantitative data have yet been published on the residual ligand concentration and the amount of degradation products.

8.3.4.2 Effect of Degradation

An increase of the irradiation dose led to an important decrease of

- Americium extraction (a factor of 10^6 after only 20 kGy with Et-BTP in hexanol (*241*) and a decrease greater than 99% after an absorbed dose of 100 kGy with *i*Pr-BTP in a mixture with DMDOHEMA in octanol (*240*));
- Am/Eu selectivity (*237, 240*) ($SF_{Am/Eu}$ dropped from 150 to almost 30 after an irradiation of only 17 kGy with the system C5-BTBP-cyclohexanone, see Figure 8.13).
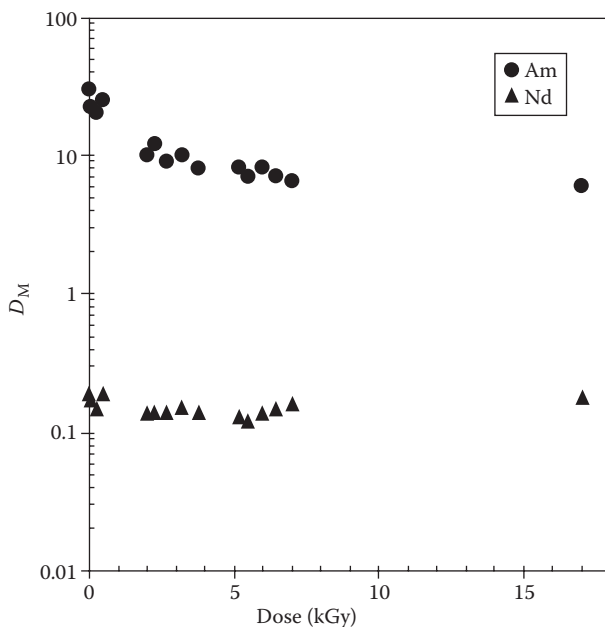
FIGURE 8.13 Influence of the dose on the extraction of Am(III) and Eu(III) by 0.005 M C5-BTBP in cyclohexanone. Irradiation of 0.005 M C5BTBP in cyclohexanone with a ^{60}Co source (dose rate to water 40 Gy h^{-1}). Extraction: equal volumes of irradiated organic and aqueous phase (0.01M HNO$_3$-0.99 M NaNO$_3$ spiked with ^{241}Am and ^{152}Eu) at room temperature (20°C). (Redrawn from Nilsson, M., Anderson, S., Drouet, F., Ekberg, C., Foreman, M., Hudson, M., Liljenzin, J.O., Magnusson, D., Skarnemark, G. *Solvent Extr. Ion Exch.* 24: 299–318, 2006. With permission.)

However, variable effects on D_{Am} were observed with BTBPs, depending on the ligand and the diluent (cyclohexanone or hexanol), namely an increase to almost a factor of 2 or a decrease to a factor of 3–4 have been reported after 20 kGy for CyMe$_4$-BTBP and C5-BTBP, respectively (*237, 242*). The radiolytic stability of BTPs and BTBPs seemed favored by an increase in their initial concentration (*240*).

8.3.4.2.1 Influence of the Extractant Structure

To avoid chemical attack on the α-benzylic hydrogens and thus improve the stability of such polyazines, ligands with annulated rings were studied (see CyMe$_4$-BTP or BzCyMe$_4$-BTP in Table 8.1). Based on extraction tests, the following stability scale has been proposed: *n*-alkyl-BTP < *i*Pr-BTP ≤ CyMe$_4$-BTP < BzCyMe$_4$-BTP (*240, 243*). Molecules bearing branched alkyl groups, such as *i*Pr-BTP and CyMe$_4$-BTP, appeared to be less hydrolyzed than related linear alkyl compounds (i.e., *n*PrBTP or *n*BuBTP) (*66, 244*), but the improved radiolytic stability of CyMe$_4$-BTP was still too unsatisfactory to be used in a process (*240*). The incorporation of an annulated aromatic π-system added significant extra resistance to radiolysis (*243*).

In the BTBP family, the same tendency has been observed: the annulated CyMe$_4$-BTBP was more resistant to nitric hydrolysis than the alkylated compound C5-BTBP

(*245*). Recently, unexpected results were obtained with CyMe₄-BTBP in cyclohexanone or hexanol: a slight increase of D_{Am} after radiolysis (*242*). The hydrolytic stability of tetra-*n*-alkyl substituted-BTP and BTBP was comparable, but the radiolytic stability of CyMe₄-BTBP seemed better than that of CyMe₄-BTP (*240*).

8.3.4.2.2 Influence of the Diluent

The nature of the organic diluent was proved to influence the stability of BTP molecules. Nitrobenzene and the chlorinated diluent $C_2H_2Cl_4$ improved the hydrolytic stability of *n*-PrBTP (*236*). For radiolysis, the same protective effect was observed in the presence of nitrobenzene.

- For Et-BTP in 1-hexanol irradiated with 20 kGy, D_{Am} was a factor of 10^4 greater with only 10% of nitrobenzene as compared with hexanol alone, as shown in the data plotted in Figure 8.14 (*241*).
- For CyMe₄-BTP in *n*-octanol irradiated with 100 kGy, the degraded portion decreased to 15% in the presence of nitrobenzene, instead of 80% (*243*).

However, no significant effect was observed with other aromatic diluents such as *tert*-butyl benzene, 2,4-dinitrophenol, 2-nitrobiphenyl, or 2,2-dinitrobiphenyl (*241*).
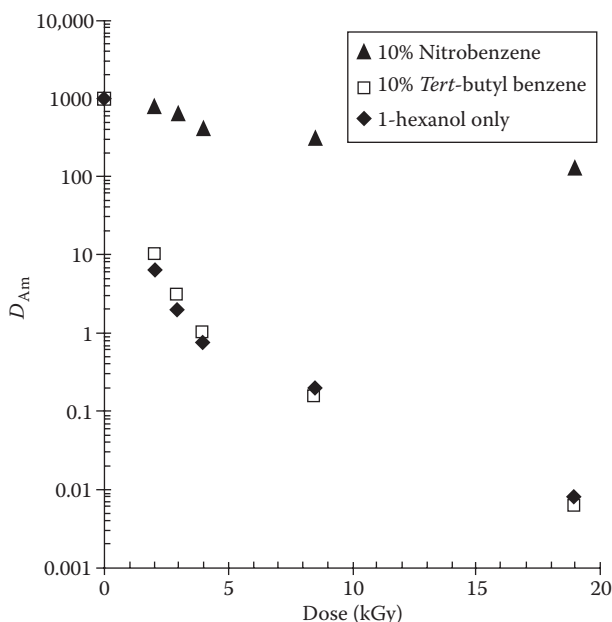
FIGURE 8.14 Influence of the diluent composition on the distribution ratios of Am(III) after irradiation of Et-BTP. Irradiation with a gamma ^{60}Co source (dose rate to water 40 Gy h⁻¹). Extraction with equal volumes of organic phase (Et-BTP 1.8×10^{-3} M) and aqueous phase (trace amount of ^{241}Am in 0.99 M NaClO₄ and 0.01 M HClO₄). (Drawn from Nilsson, M., Anderson, S., Ekberg, C., Foreman, M.R.S., Hudson, M.J., Skarnemark, G. *Radiochim. Acta* 64: 103–106, 2006.)

In a recent study, Retegan compared the radiolytic stability of C5-BTBP and CyMe$_4$-BTBP in hexanol or in cyclohexanone (*242*). No protective effect of a cyclic diluent was observed on europium extraction, whereas surprising results were obtained with americium. The behavior needs to be more precisely defined.

8.3.5 MACROCYCLIC EXTRACTANTS

8.3.5.1 Crown Ethers

The crown ethers were investigated mainly for the removal of Sr or Cs from nuclear-waste streams (*246–250*), and some studies reported their interest as selective extractants of plutonium (*251*). Different crown ether derivatives with the addition of alkyl chains have been examined, in order to increase the lipophilicity of the molecule and prevent major extractant losses due to high solubility in aqueous phases. These extractants were described as radiolytically resistant, and their stability increased in the order benzocrown > dicyclohexanocrown > crown (*44*).

8.3.5.1.1 Degradation Products

The radiolytic degradation of a representative dicyclohexano-18-crown-6 (DCH18C6) was investigated in different media (aqueous solution, chloroform, toluene, cyclohexane, 1-octanol…) (*7, 252–254*). Several radiolytic degradation products were separated and identified (see Figure 8.15) (*253*). Degradation products had a lower molecular weight than DCH18C6 and lost their macrocyclic structure by the opening of the crown ring. Further, as a general rule, the degradation gave rise to products with configuration retention, that is *cis* configuration (*253*).

Volatile products (hydrogen and ethylene) were also produced after radiolysis of pure crown ethers. Their formation yields were measured: $G(H_2)$ ranged from
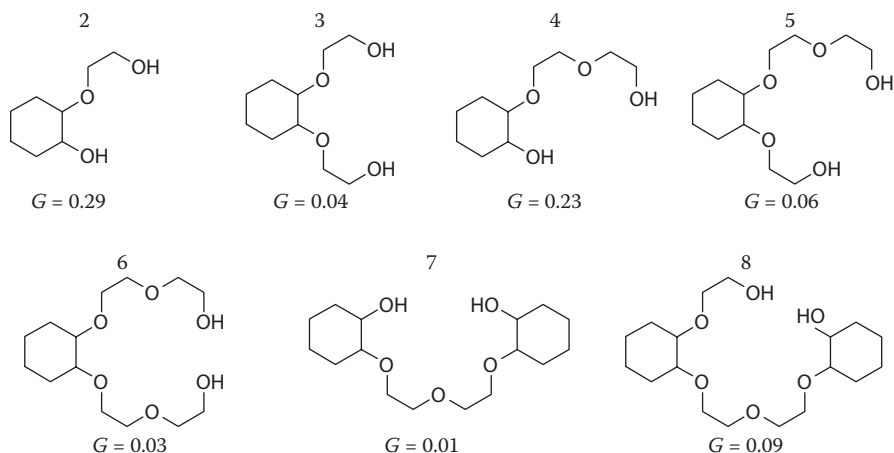
FIGURE 8.15   Structures of the DCH18C6 radiolytic products after γ-irradiation and their radiochemical yield, *G* determined at an irradiation dose of 3.2 MGy. (From Draye, M., Favre-Reguillon, A., Foos, J., Guy, A., Lemaire, M. *Radiochim. Acta* 78: 105–109, 1997. With permission.)

1 to 2 and G(ethylene) ranged from 0.02 to 0.15 molecule/100 eV, depending on the irradiation conditions (*76*).

After irradiation with 3.3 MGy of a DCH18C6 solution in 1 mol L^{-1} nitric acid containing 20 g L^{-1} of uranyl nitrate, compounds 2 and 4 (presented in Figure 8.15 with their radiolytic yields) were shown to be the main products of radiolysis; nevertheless, 50% of DCH18C6 remained unchanged. In these conditions, the disappearance yield G(-DCH18C6) was estimated to be 0.72 molecule/100 eV (*7*).

An increase in the acidity from 1 to 2 mol L^{-1} had a very slight influence on the macrocycle degradation. But the presence of a high concentration of uranium (250 g L^{-1}) in the DCH18C6 solution decreased the radiolysis of DCH18C6 and changed the distribution of degradation products: the least fragmented product (compound 8) was the main compound ($G \sim 0.16$ molecule/100 eV) (*252*).

8.3.5.1.2   Influence of the Diluent

The radiolytic degradation of DCH18C6 was strongly influenced by the nature of the diluents. An experimental approach with gas chromatography concluded on the following order of stability: chloroform > cyclohexane >1-octanol > toluene (*254*). The degradation inhibition in toluene was explained, as for previous extractants, by a lower ionization potential of toluene than that of crown ether. DCH18C6 suffered extensive decomposition in chloroform solution. Moreover, crown ethers exhibited high affinity toward inorganic chloroform radiolysis products (such as HCl, C_2Cl_6…) resulting in the formation of complexes (*44, 255*).

8.3.5.1.3   Influence on Extraction Behavior

The variation of strontium distribution ratios D_{Sr} from nitric acid solution was investigated as a function of the irradiation dose. In toluene DCH18C6 solution, D_{Sr} was minimally affected by radiolysis, but decreased with the absorbed dose in the other nonaromatic solvents (*254*). Nevertheless, the distribution ratios measured after radiolysis were higher than expected, given the remaining extractant concentration, indicating some contribution from the degradation products (e.g., after an irradiation of 0.84 MGy, 70% of the crown ether was destroyed in chloroform, while the distribution ratio exhibited a decrease of only 30%) (*254*).

Extraction of U(VI) and Pu(IV) from 1 to 8 mol L^{-1} HNO$_3$ solutions by radiolytically degraded DCH18C6 in toluene was studied (*256*). A decrease in the distribution ratios for both U and Pu was observed for irradiation in the range 0.010–0.071 MGy, with a higher effect for Pu(IV). For 0.2 mol L^{-1} DCH18C6-toluene solution in contact with 3 mol L^{-1} nitric acid, D_U decreased from 0.21 to 0.12 and D_{Pu} from 64.3 to 6.42 after a dose of 0.07 MGy. This behavior was explained by both diluent and extractant degradation.

Some degradation products (compounds 2, 3, and 4, see Figure 8.15) were synthesized to evaluate their influence on extraction (*252, 253*). The simultaneous addition of these three compounds at a concentration of 2×10^{-3} mol L^{-1} did not modify the extraction of Pu, U, and Sr (DCH18C6 0.134 mol L^{-1} in chloroform -HNO$_3$ 4.9 mol L^{-1}), but higher amounts (7.35×10^{-3} mol L^{-1} for each compound) led to a slight decrease of D_{Pu}, whereas no effect was observed on D_U and D_{Sr}.

The radiolytic behavior of a solution of D*t*BuCH18C6 (di-*t*-butylcyclohexano-18-crown-6) in 1-octanol was assessed by measuring the distribution ratio of strontium

under the extraction and stripping conditions of the SREX process ($[HNO_3] = 3$ mol L^{-1} and 0.01 mol L^{-1}, respectively) (*248*). At high acidity, the extraction was constant up to absorbed doses of ~0.24 MGy, then significantly declined until ~0.4 MGy, to reach one-third of the reference value. In stripping conditions, degradation led to an increase of D_{Sr} even for low irradiation doses. D_{Sr} increased by nearly a factor of 3 after an absorbed dose of ~0.24 MGy. This behavior was attributed to the degradation of both the extractant and the diluent.

8.3.5.2 Calixarenes

Calixarenes are potential platforms on which specific binding arms can be grafted. The extractive properties of these molecules for metallic ions depend on the cavity size, the conformation, and the nature of the ligating groups. Different calix[4]arene-crown-6 derivatives in the 1,3-alternate conformation have been studied for Cs recovery from both basic and acidic solutions (*257–262*). Calixarene-based picolinamide ligands have been proposed as candidates for separating actinides from lanthanides (*263, 264*).

The stability of calixarene molecules under hydrolysis and radiolysis was quite high, but the nature of the substituents and the chemical environment caused some differences.

8.3.5.2.1 Degradation Products

Representative calix[4]arene-crown-6 derivatives (monocrowns such as *i*Pr-MC-6 or octMC-6 (di(*n*-octyloxy)calix[4]arene-crown-6) and biscrown as BC-6 (1,3-alt-calix[4]arene-bis-crown-6), see Table 8.1), have been irradiated under various conditions and the solution examined by techniques based on mass spectrometry: ESI/MS, GC/MS (or GC/MS/MS), and LC/ESI-MS (*68, 69, 72*). In the absence of nitric acid, very few degradation products were formed, even after an irradiation dose of 3 MGy. The molecular weight of BC-6 degradation products indicated partial crown ring degradation (*68, 69*). In the presence of nitric acid, radiolysis led to the formation of a large number of derivatives resulting from cleavage or additional reactions and from aromatic nitration and oxidation, as presented in Figure 8.16 for octMC-6 ligand.

The binding of NO_2 groups on the calixarene took place on the aromatic rings in the para position (never on the crown moiety) (*68, 69, 72*), and mononitro-calixarene was always the most abundant compound, with the presence, to a lesser extent, of dinitro-compound. Despite the large number of compounds, the crown ether structure was conserved, which is an indirect indication of such ligands' good stability.

8.3.5.2.2 Quantitative Data

A quantitative investigation performed using the HPLC/DAD (Diode Array Detector) technique showed that the amount of degraded octMC-6 was quite high. In contact with 3 mol L^{-1} nitric acid, the proportion of degradation after an irradiation of 1 MGy was estimated to be 33% in *o*-nitrophenyl octyl ether (NPOE) and 88% in dodecane. The quantity of octMC6-NO_2 reached 50% of degradation products (*72*).
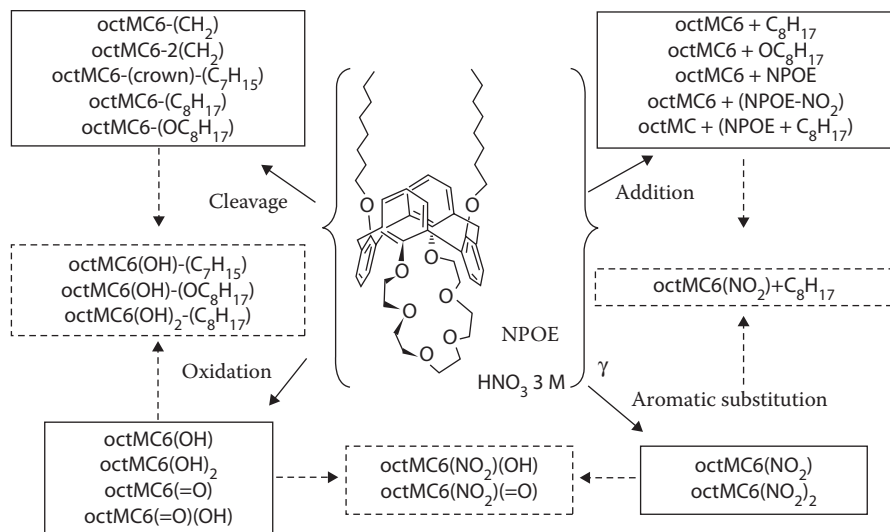
FIGURE 8.16 Major radiolytic degradation compounds of (octMC6) in NPOE/HNO₃. (Redrawn from Lamouroux, C., Aychet, N., Lelievre, A., Jankowski, C.K., Moulin, C., *Rapid Commun. Mass Spectrom.*, 18: 1493–1503, 2004.)

The related radiolytic yields were low: in contact with 3 mol L⁻¹ nitric acid, G(-octMC6) ≈ 0.034 and 0.082 for 5×10^{-2} mol L⁻¹ solution in NPOE and 10^{-2} mol L⁻¹ in dodecane, respectively (*72*). But the low concentration of ligand partly explained the values.

Moreover, in the solid form, the monocrown MC-6 was slightly less stable than the biscrown BC-6 analog (after a 3 MGy dose, 60 and 50% of the molecules were degraded, respectively), but the opposite effect was noted for a solution 10^{-2} mol L⁻¹ in NPOE (the amounts of unchanged extractant were 52% and 68%, respectively) (*69*).

The stability under irradiation of the calix[4]arene-bis(*tert*-octylbenzo-crown-6) (BOBCalixC6)-based solvent system (mixture composed of calix[4]arene, an aromatic fluoro-propanol as modifier, and trioctylamine in aliphatic diluent) was tested under chemical and radiolytic conditions representative of the alkaline-side process (*265*). After γ-irradiation doses as high as 0.16 MGy, no significant loss of BOBCalixC6 was measured (less than 10%).

8.3.5.2.3 Influence of the Diluent

The nature of the diluent has an important role on the degradation rate of calixarene (see Table 8.7). In dodecane, the loss of calixarene was very high, compared with measurements in the aromatic NPOE diluent. As already mentioned with other ligands (like TBP), aromatic diluents had a protective effect, explained by a lower ionization potential. However, serious radiolytic damage (e.g., a considerable rise in viscosity) has been observed with NPOE alone (*68*). Therefore, authors, such as Lamouroux, have suggested the use of a mixture NPOE-dodecane (*72*).

TABLE 8.7

Influence of the Experimental Conditions on the Degradation Rate of the Calixarene OctMC6-H (Irradiation 1 MGy)

[Ligand] (Mol L^{-1})	Diluent	Presence of Aqueous Phase	Degradation Rate (%)
5×10^{-2}	NPOE	–	6.5 ± 2
5×10^{-2}	NPOE	Contact with 3 M HNO$_3$	33.5 ± 2
10^{-2}	*n*-Dodecane	–	80 ± 2
10^{-2}	*n*-Dodecane	Contact with 3 M HNO$_3$	88 ± 2

Source: From Lamouroux, C., Aychet, N., Lelievre, A., Jankowski, C.K., Moulin, C. *Rapid Commun. Mass Spectrom.*, 18: 1493–1503, 2004.

Note: Irradiation with a ^{60}Co source (6.3 kGy h^{-1} dose rate) in the presence of air at 22°C. Organic phase (5 mL) is irradiated alone or in the presence of an equal volume of aqueous phase.

8.3.5.2.4 Influence on Extraction Behavior

Since the main degradation product of BC6 was assumed to be the mononitro derivative (BC6-NO$_2$), nitro compounds have been synthesized and the distribution ratios measured. Extraction results with 1 mol L^{-1} nitric acid showed that the presence of nitro groups reduced the extraction of cesium: D_{Cs} were 19.5, 8.5, and 6×10^{-3} for solutions 10^{-2} mol L^{-1} of BC6, BC6-NO$_2$, and BC6-4NO$_2$, respectively (*68*), whereas the extraction of Na$^+$ was slightly affected. Theoretical approaches by molecular dynamics simulations indicated that the nitro group was not ideally located to efficiently participate in the complexing of Cs$^+$ or Na$^+$, and therefore the loss of efficiency with nitro compounds arose from steric hindrance around the complexing site.

Recent studies have been published on representative process systems.

- Variation of cesium distribution ratios (D_{Cs}) was investigated as a function of the irradiation dose for BOBCalixC6 under process conditions (*265*). The extraction, scrubbing, and stripping performances were not significantly affected by gamma irradiation doses as elevated as 0.08 MGy, which was consistent with the high stability of the calixarene.
- The effect of radiolysis on complexed solutions proposed for the FPEX process was investigated. The calixarene BOBCalixC6 was present with substituted-18-crown-6, aromatic fluoro-propanol as modifier, and trioctylamine in aliphatic diluents (*35*). The effect of gamma irradiation was negligible up to 0.02 MGy. An important change of coloration and the appearance of a third phase was observed, but due to the nitration of the modifier. Instead of the BC-6 and oct-MC6 calixarenes, which presented a decrease of Cs extraction after radiolysis, the presence of alkylated phenyl moieties provided protection for the Cs site.

– The radiolytic behavior of a substituted picolinamide calix[6]arene, studied for the separation of actinides from lanthanides, was recently investigated by Mariani (*263*). For doses ranging from 0.014 to 0.055 MGy, the distribution ratios of both Am(III) and Ln(III) strongly increased, whereas after absorbed doses higher than 0.10 MGy, they decreased to values lower than those measured for nonirradiated samples. The selectivity for Am/Eu remained constant. Comparable experiments under a nitrogen atmosphere indicated the role of oxygen in the radiolysis, because the distribution ratios decreased by factors of 10 and 1.5–5 for Am-Eu and other lanthanides, respectively. The increase for lower doses was then explained by the formation of oxidized radiolytic products. No evidence of new products was obtained with the ESI-MS technique.

8.4   DEGRADATION MECHANISM

For the successful application of solvent extraction to the treatment of highly radio-active materials, it was essential to grasp the nature of radiation-chemical phenomena occurring in the extractant environment. Numerous studies have focused on the degradation mechanism of TBP, and some on HDEHP or TODGA through specific investigations of radical transient species. Some experiments have also been performed on lower molecular amides, using pulse radiolysis or electron spin resonance (ESR), in aqueous phase (*266–268*), in THF (*269*), in methyl cyanide (*270*), or in Freon (*271*). Attention has been paid to the radiolysis mechanisms of liquid alkanes often selected as diluents in the reprocessing process (*272–278*).

The following paragraph deals with the experimental approach to the degradation mechanism of different molecules and with the role of the diluent. Theoretical studies related to stability remain rare, and calculations were often performed on pure ligands in the gas phase, thereby omitting the important role of surrounding solutes.

The radiolytic mechanism of an organic molecule's degradation could occur through different routes: a direct process with an energy transfer from the radiation to the ligand (resulting in primary radicals of excited and ionized species), homolytic radical cleavages that generate two free radicals, or indirect radiolysis (energy transfer from radicals of various solutes to the ligand). It should be noted that C-H bonds are usually broken more easily than C–C or C–O bonds, and lead to reactive and mobile H• radicals.

8.4.1   RADIOLYTIC DEGRADATION OF PURE EXTRACTANTS

Studies focusing on the degradation of pure molecules allowed the ligands' points of fragility to be checked.

8.4.1.1   Tri-*n*-butyl Phosphate (TBP)

The experiments performed to study the TBP degradation mechanism (*18, 279–287*) consisted mainly of the identification of final products, but also included the examination of the radical intermediates by ESR (*288, 289*) or by pulse radiolysis and

flash photolysis (285, 286, 290–292). Various reaction steps have been postulated and results give rise to the following issues.

Some scientists emphasized that the degradation of TBP was due to dissociative electron capture via the following reaction (279, 283, 285, 286):

$$e^-_{solv} + (C_4H_9O)_3P = O \rightarrow C_4H_9^{\bullet} + (C_4H_9O)_2P = OO^- \tag{8.1}$$
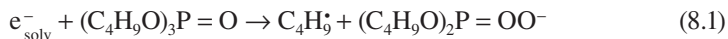
However, other experiments based on the analysis of acid products (*280, 293*) indicated that the decomposition of TBP was mainly due to the cleavage of excited TBP molecules (TBP*) as follows:

$$TBP^* \rightarrow C_4H_9^{\bullet} + (C_4H_9O)_2P = OO^{\bullet} \tag{8.2}$$
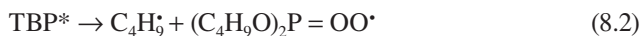
According to Zhang, the excited site of TBP was located on the $P = O$ bond (*287*), and several active species were formed by γ-radiolysis, such as excited singlets, excited triplets, and positive ions (*293*).

With pulse radiolysis and flash photolysis, Jin *et al.* have recently focused on the examination of TBP excited species (*291*). The authors concluded that the decomposition of TBP occurred through two processes: dissociative electron capture (Equation 8.1) and decomposition of TBP excited molecules (Equation 8.2).

The identification of radicals coming from the scission of specific bonds was carried out by several teams.

8.4.1.1.1 C–O and P–O Bond Scission

The PO_4^{3-} anion in TBP is very stable under radiation. The rupture of the P–O bond is much less probable than the cleavage of the C–O bond, which was confirmed by the low quantity of butanol analyzed (*96*).

According to Kerr and Webster (*279*), the radiolysis of TBP leads to alkyl radicals R$^{\bullet}$ and OP(OR)$_2$OR$^{\bullet}$. Investigations of the radical intermediates, by ESR examination or by use of electron scavengers, provided clear evidence regarding the formation of R$^{\bullet}$ radicals by dissociative electron capture (Equation 8.1) (*294*).

According to Symons and Haase, the O atom of the ester group is the effective electron-gain center rather than the other two electron-capture centers (P and oxygen atoms of the $P = O$ group) (*294, 295*). The phosphoranyl radical formed in Equation 8.3 has a high probability of undergoing fragmentation by β-scission with the ejection of an alkyl radical, as in Equation 8.4.

$$(C_4H_9O)_3P^{\bullet} = O + e^- \rightarrow (C_4H_9O)_3P^{\bullet} = O^- \tag{8.3}$$

$$(C_4H_9O)_3P^{\bullet} = O^- \rightarrow C_4H_9^{\bullet} + (C_4H_9O)_2P = OO^- \tag{8.4}$$
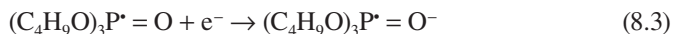
8.4.1.1.2 C–C Bond Scission

The partial charges of the alkyl chain's carbon atoms are quite different (*294*); the C in the α-position to oxygen possesses the largest density of positive charge. As a result, the scission of C_α–C_β bonds was easier than other C–C bonds.

8.4.1.1.3 C–H Bond Scission

The TBP's butyl chain can form four different radicals by C-H bond scissions: three secondary alkyl radicals (TBP-C$_\alpha^\bullet$, TBP-C$_\beta^\bullet$, TBP-C$_\gamma^\bullet$) and one primary radical TBP-C$_\delta^\bullet$, as presented in Figure 8.17. Different studies show that the unpaired electron is mainly located on the C in the γ-position of the butyl group (*281, 282, 295, 296*).

8.4.1.2 Phosphates or Phosphonates

The ESR spectra of free radicals arising from the action of hydroxyl radicals on several phosphorous compounds (trialkyl phosphate and dialkyl phosphonate) have been studied. In all cases, the radicals observed are due to the removal of a hydrogen atom from the carbon atom adjacent to the oxygen in the ester group (C$_\alpha$-atoms) (*289*).

In addition, recent calculations of the partial charges on carbon atoms of the alkyl chains of several trialkylphosphates have indicated that in all cases, the C$_\alpha$-atoms possessed the highest density of positive charge (*294*).

8.4.1.3 Di(2-ethylhexyl) Phosphoric Acid

The mechanism of HDEHP radiolysis has been investigated by ESR spectroscopy after γ-irradiation (*74, 159*). The formation of the radical C$_4$H$_9$-C$^\bullet$(CH$_3$)C$_2$H$_5$ formed by the removal of a hydrogen atom from the alkyl chain of HDEHP has been proposed (*159*). A large *G*-value (about 6 molecuels/100 eV) for the formation of this latter radical indicated that the ester bond of HDEHP is likely to crack at the C-O position by radiolytic excitation. However, the split alkyl radicals are liable to recombine with phosphate groups and reform HDEHP (*159*). The following reactions (Equations 8.5 and 8.6), were proposed to explain the formation of 1-methyl-1-ethylpentyl radical.

$$(8.5)$$
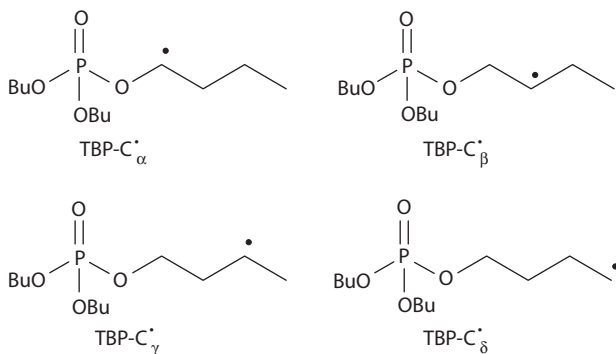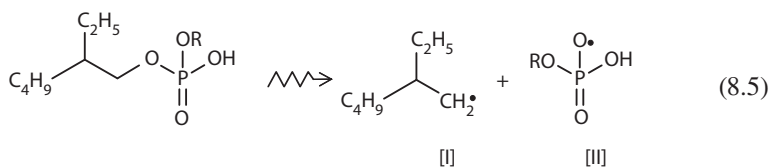
FIGURE 8.17 Primary radicals formed under radiolysis from tributyl phosphate (TBP).

$$(8.6)$$
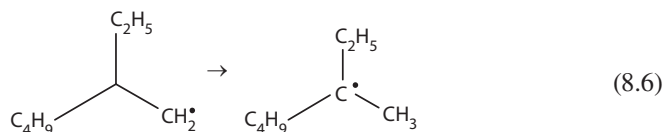
The 1-methyl-1-ethylpentyl radical [I] and its neighboring molecule may then transfer hydrogen or methyl radical to yield 3-methylheptane or n-heptane (*159*). Radical [II] was proposed but without any identification. By recombination, it would take part in the formation of H_2MEHP.

8.4.1.4   Amides

The behavior of two substituted organic acetamides (*N,N*-diethyl- and *N,N*-dipropyl-) were studied by ESR techniques. The spectra were characteristic of free radicals involving H-atom loss from the N-alkyl groups (*297*).

8.4.2   INFLUENCE OF THE DILUENT ON DEGRADATION

Different studies indicate that diluents can inhibit or sensitize an extractant's radiolysis. For example, in the cases of alkyl phosphates, amide extractants, or crown ethers, aromatic additives act as protectors (*39, 84, 88, 90, 199, 254, 298*), while saturated hydrocarbons often sensitize the decomposition of the extractant (*90, 182, 183, 199, 299*). Figure 8.18 illustrates this sensitization effect of n-dodecane on various oxygen-donor ligands (diglycolamide, malonamide, and monoamides) (*199*).

Recently, the primary processes were investigated using pulse radiolysis with two extractant-alkane systems (*182, 292*). Transient optical absorption spectra proved that in the presence of ligands like TODGA, the excited species of n-dodecane (singlet excited state and radical cation) disappeared immediately. Results showed that an energy transfer occurred from the excited alkane to the extractant molecule (TBP, TOPO, or amide), which constituted an additional decomposition route, as described in the following set of reactions:

$$[\text{diluent}] \rightarrow [\text{diluent}]^{\bullet+} + e^- \qquad (8.7)$$

$$[\text{diluent}]^{\bullet+} + [\text{extractant}] \rightarrow [\text{extractant}]^{\bullet+} + [\text{diluent}] \qquad (8.8)$$

$$[\text{extractant}]^{\bullet+} \rightarrow \text{degradation products} \qquad (8.9)$$
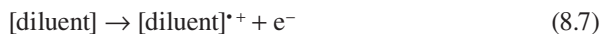
The charge-transfer reaction from the excited diluent to the ligand was brought about by the difference in their ionization potentials (*79, 182, 183*). Thus, if the potential of the diluent is higher than the potential of the extractant, the reaction (Equation 8.8) could occur and results in a greater degradation of the extractant because of the subsequent reaction (Equation 8.9). Conversely, if the diluent has a low ionization potential (like aromatic compounds, see Table 8.8), the charge-transfer reaction (Equation 8.8) would be inhibited and the diluent acts as an "ionization
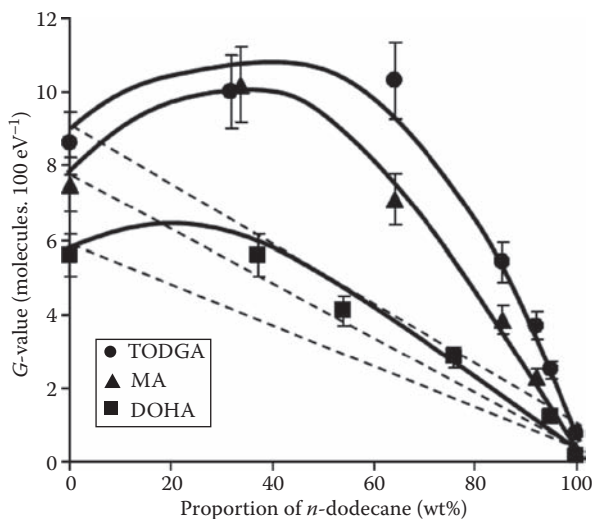
FIGURE 8.18 Sensitization effect of *n*-dodecane on the radiolysis of the glycolamide TODGA, a malonamide (*N,N'*-dioctyl-*N,N'*-dimethyl-2(3'-oxapentadecyl)-propane-1,3-diamide) and a monoamide DOHA. Conditions: gamma-irradiation from ^{60}Co source (125 C kg^{-1} h^{-1}) in air, at room temperature. The solid lines indicate the experimental *G*-value with an error of about 10%. The dotted lines indicate the theoretical *G*-value based on the direct effect on the radiolyis. (Redrawn from Sugo, Y., Sasaki, Y., Tachimori, S., *Radiochim. Acta*, 90, 161–165, 2002. With permission.)

sink," thus, protecting the extractant molecule against further degradation (in the case of studies with TBP, TODGA, crown ethers, etc.).

The high ionization potential of CCl_4 (Table 8.8) was consistent with the sensitization observed with TBP. CCl_4, partially water-soluble, was also described as an effective e$^-$ scavenger, and the ionic degradation mechanism seemed to predominate in the TBP-CCl_4 system (*87*).

The ionization potential of some extractants (TODGA and DOHA) calculated by quantum chemistry (*182*) was lower than that of *n*-dodecane, which was consistent with the sensitization effect of these diluents observed by experimental approaches (*182, 183*).

8.4.3 INFLUENCE OF AN AQUEOUS NITRIC ACID PHASE ON THE RADIOLYTIC DEGRADATION OF TBP

The yield of radiolysis products depends strongly on the presence of an aqueous phase in the system, and on its composition. The presence of water and nitric acid in the solvent produces additional free radicals by radiolysis (*14, 302, 303*), leading to functionalized compounds of extractants and diluents (*304*). In the case of alkanes, specific compounds like nitroparaffins, alcohols, hydroxamic acids, and nitronic acids have been identified (*21, 43, 51*). Taharaoui and Morris have summarized the results published in this field (*79*).

TABLE 8.8
Ionization Potential (IP) Values of Some Diluents

Diluent	IP (eV)	References
Propane	11.5	300
iso-Butane	11.4	300
Cyclobutane	11.0	300
Hexane	10.43	90
n-Heptane	9.83	301
Dodecane	10 ± 0.2	79, 90
n-Dodecane	9.40	301
Cyclohexane	10.3	90
Cyclohexane	9.82	301
Cyclohexane	9.24	90
Benzene	9.24	90, 300
Toluene	8.82	90
Toluene	8.78	300
Methanol	10.96	300
Dimethyl ether	10.04	300
Tetrachloromethane	11.47	301
Tetrachloromethane	11.5	79

Radiolysis of HNO_3 generates different radicals (*305*), but at high acidity, HNO_3 can also act as a hydroxyl radical scavenger (*306*). Moreover, postirradiation effects have been observed (variation of the concentration of radicals, for example) (*305*).

In spite of the complexity of the solutions, some authors have managed to identify the main degradation routes in the presence of HNO_3: the radiolysis of TBP proceeded by the preferential loss of a radical H$^{\bullet}$ from C-H bonds (*21, 50*), followed by O-C, C-C, or O-P bond cleavages (*21*). The four primary radicals (presented in Figure 8.17) interact with species present in the medium, and the classical further reactions are dimerization, coupling with dodecane, and reaction with O_2 to give the related hydroxy-TBPs, which can undergo further oxidation or form nitrates (*21*). The low amount of TBP-dimers (0.3%) and lower homologues has been explained by the involvement of TBP fission prior to dimer formation (*22*).

8.4.4 EFFECT OF INHIBITORS ON TBP DEGRADATION

To limit the radiolytic degradation of extractants, the influences of free-radical inhibitors have been measured. The addition of dimethoxybenzaldehydes (DMBA), particularly 3,5- and 3,4-DMBA, to the PUREX solvent could improve its stability and decrease its contamination (*307*). DMBA has a double effect, including a protective effect for the excited molecules of TBP (because of its low ionization potential), and the aldehyde radiolysis products could react with the HDBP present and therefore inhibit its complexing properties.

Another family of inhibitors, hydrogen-donating agents such as *iso*-propyl and 1,4-di-*iso*-propyl benzenes, was investigated by Lamouroux in order to reduce the formation of TBP-TBP dimers, which exhibit a very high plutonium retention of TBP (*47*). The presence of at least one mobile hydrogen on the *iso*-propyl group could produce a benzylic tertiary radical stabilized by resonance. The addition of such compounds reduced the concentration of the TBP-TBP dimers by about 50%.

8.5   RELATION BETWEEN THE FORMULATION OF THE SOLVENT AND THE RADIOLYTIC STABILITY OF THE EXTRACTANT

From the studies published, it appears that it may be possible to improve the radiolytic stability of an extractant system. Of course, it is difficult to obtain a universal proposal, and the various experimental conditions selected to perform the radiation experiments (nature of the diluents, acidity, and the presence of other solutes either in the aqueous or organic phase) have made the comparison of extractants' stability difficult. Nevertheless, systematic tendencies have been summarized in the following section, related to the modification of the extractant alone or related to the composition of the solvent (organic phase).

8.5.1   MODIFICATIONS TO THE EXTRACTANT FORMULAE

8.5.1.1   Presence of Oxygen Atoms

Many extractants contain one or several oxygen atom(s), with specific donor properties ($P = O$ or $C = O$ groups) or as ether bridges. Generally, the presence of such heteroatoms in a molecule introduces an additional fragility point and leads to a lower overall radiolytic stability. In molecules with ether bridge(s) (–C–O–C–), the easy cleavage of the C–O bond can have drastic consequences on the molecule, for example in crown ethers, for which the cleavage of C–O bonds led to an opening of the ring (*7, 253*). In the diamide family, the introduction of such a bridge between the two amide functions weakens the molecule: the stability of malonamides is higher than of diglycolamides (*183, 199*). The replacement of an alkyl group by an alkoxy chain anywhere in the molecule often inserted a weakness in the molecule. For example, the alkoxy derivative di(hexyloxyethyl)phosphoric acid (HDHOEP) was more degraded by γ-radiolysis than the alkyl derivative HDEHP, and an additional degradation product was observed (*32*). Related oxygenated bifunctionalized molecules were less stable than mono derivatives; for example, the radiolytic stability of monoamides was higher than that of malonamides (*182, 199, 216*). On the other hand, the presence of an alkoxy radical grafted onto the central carbon of malonamides, instead of alkyl chains, led to an additional cleavage without decreasing the overall stability of the molecule (*48, 202, 213*). The presence of two ether functions in this chain had no significant influence on the stability of malonamides (*215*).

With oxygen donors like organophosphorus extractants (presence of $P = O$ group) or amide-based molecules (presence of $(N)C = O$ group), the main cleavage occurs in the α-position of the chemical function. The introduction of an O atom into this sensitive α-position was responsible for a lower stability, because the cleavage of an

O–P bond was easier than that of a C–P. In the alkylphosphorus family, the radiolytic stability decreased in the order phosphine oxides TOPO $[(C_8H_{17})_3PO]$ > dibutylbutyl phosphonate $[(C_4H_9O)_2(C_4H_9)PO]$ > tributyl phosphate $[(C_4H_9O)_3PO]$ (*308*), which is consistent with the number of carbon-oxygen-phosphorus linkages. In the same way, the hydrolytic and thermal stability decreased in the order dialkyl dithiophosphinic acids $[(RO)R´PSSH]$ > dialkyl dithiophosphoric acids $[(RO)_2PSSH]$, due to the elimination of one ether bridge (*29*).

In conclusion, the controlled introduction of an oxygen atom into a molecule could be an advantage. In the case of extractants with long alkyl chain(s), the presence of an oxygen atom could lead to the formation of shorter degradation products, easier to remove by classical aqueous scrubbing because of their higher aqueous solubilities and/or their lower interfacial activity (the main drawback of long-chain carboxylic acids in contact with alkaline aqueous solution) (*142, 144*). This strategy has been applied to the optimization of malonamide formulae for the DIAMEX process (*202, 213*).

8.5.1.2 Nature of the Substituents

To enhance the solubility of extractants in organic diluents, alkyl chains are often grafted onto strategic parts of the molecules; sometimes the replacement by an aryl part has also been proposed.

8.5.1.2.1 Alkyl Substituents

Lengthening the alkyl chains in extractants seemed to slightly increase their resistance to degradation:

- The stability of trialkyl phosphates $(RO)_3PO$ increased from the methyl derivative to the pentyl ester (18, 84, 152);
- The same tendency has been observed for dialkylphosphoric acids $(RO)_2(HO)PO$; for example, the stability of HD*i*DP ($R = iso$-decyl) was greater than that of HDEHP ($R = $ ethylhexyl) (*32*);
- In the malonamide family, the stability increased with the length of the central alkyl chain in the order $H < C_2H_5 < C_2H_4OC_6H_{13} \approx C_2H_4OC_2H_4OC_6H_{13}$ (*215*).

It should be noted that several authors have indicated the increase of the yield of hydrogen with the molecular weight of the extractant (*18, 84*), which is consistent with a higher probability of C–H cleavages.

Considering the nature of degradation products, increasing the chain length can lead to more lipophilic compounds with higher molecular weights, which are more difficult to eliminate by classical aqueous scrubbing. For example, an increase in the alkyl chain length on the nitrogen atom (from C_4H_9 to C_8H_{17}) on malonamides led to an increasing lipophilicity of the amine formed by degradation and to its increased solubility in the organic phase (*48*).

The introduction of a branched, instead of linear, alkyl chain has been studied with monoamides, but the results depended on the nature of the diluent, and no systematic tendency could be deduced (*191, 192, 194, 200*). For the trialkylphosphate

family, the behavior of *n*-amyl and *iso*-amyl derivatives was similar (*152, 153*). In the polynitrogen family of BTPs, the presence of branched alkyl groups on the triazine cycles was favorable. The following scale of stability has been proposed: *n*-alkyl-BTP < *i*Pr-BTP ≤ CyMe$_4$-BTP (*240, 243*), an order consistent with the hydrolysis protection given by the sensitive carbon (on the α-position of the triazinyl rings).

8.5.1.2.2 Aryl Subtituents

The stabilizing effect of aromatic diluents has already been discussed (Section 8.4.2 on the mechanism), but the presence of an aromatic moiety inside the extractant also improves its radiolytic stability.

- In the family of phosphonates (RO)$_2$R′PO, the aryl derivatives were more stable than the related alkyl compounds, and the benefit was higher than the effect observed from alkylphosphate to alkylphosphonate (*96*). The same tendency has been observed with dithiophosphinic acids (RO)R′PSSH; namely, aromatic ligands were more resistant to hydrolysis and radiolysis than aliphatic compounds (*49, 61*). It was noted that the introduction of chlorine into the phenyl rings reinforced the radiolytic stability of the extractant (*49, 61*).
- In the family of crown ethers, the following order of stability was observed: benzocrown > dicyclocrown > simple crown (*44*).
- With polynitrogen polyaromatic ligands, the addition of an aromatic ring significantly increased the molecule's resistance to radiolysis, as shown by results with BzCyMe$_4$-BTP (*243*), but the introduction of a saturated cyclohexyl group (CyMe$_4$-BTP) already had a favorable effect in comparison with tetraalkyl-substituted BTPs (*240*).

The combined effect of the nature and the position of the aromatic moiety in the TODGA skeleton was studied with two newly designed molecules: T(OPh)DGA, where two octylphenyl groups have been introduced on each N atom, and TOFDA, where the central framework of TODGA was replaced by a furan ring. Both molecules were more resistant to radiation than TODGA. The stability increased in the order TODGA < TOFDA < T(OPh)DGA, suggesting a lower aromaticity of the furan cycle than phenyl (*183*).

The positive effect of an aromatic substituent was not systematic. With CMPO extractants, the introduction of phenyl groups on P = O (one or two, instead of linear octyl chains) led to less stable molecules (*40*). This atypical behavior was explained by the higher sensitivity of the amide group to hydrolysis, leading to a preferential attack around the amide function in the first step of the degradation pathway. The presence of an aromatic part on the P = O group has a negligible influence.

8.5.1.2.3 Presence of a Sulfur Atom in the Extractant Molecule

The sulfur-containing extractants have a poor hydrolytic stability; for example, dialkyl monothiophosphinic acid and dithiophosphinic acid were completely oxidized after a few days in contact with 5 mol L^{-1} HNO$_3$ (*309*). The radiolytic stability was also dramatic in that dialkyl dithiophosphinic acid (i.e., Cyanex 301) was

completely destroyed after a 0.1 MGy irradiation dose (*29*). The introduction of an aromatic group, which enhanced the stability, was necessary to carry out a test under process conditions (*49*).

8.5.2 COMPOSITION OF THE ORGANIC PHASE

8.5.2.1 Choice of the Diluent

The selection of a suitable diluent is important to limit radiolytic degradation. Diluents currently used in nuclear applications are hydrocarbons, despite their well-known sensitization effect on radiolysis, as mentioned for alkylphosphates or amide extractants (*90, 182, 183, 199*), and as discussed in Section 8.4.2. To avoid this negative effect or to enhance the solubility of ligands and metallic complexes, other diluents have been selected and their influence on degradation investigated.

- The extractant's stability can be improved if the selected diluent has a lower ionization potential than the extractant, like aromatic compounds (*183*). This protective effect has been observed for numerous extractants: alkyl phosphates, alkyl phosphonates, amides, and calixarenes (*25, 39, 68, 84, 90, 199, 298*), but not with aryl phosphonates in toluene (*96*). The protective effect of aromatic diluents was not systematic with the BTPs-octanol systems, where the addition of (or replacement by) nitrobenzene enhanced the stability of BTPs (*241, 244*), whereas the addition of *tert*-butyl benzene did not modify the resistance of BTP under radiation. The difference has been explained by the ability of nitrobenzene to remove solvated electrons and hydroxyl alkyl radicals (*241*).

  Even so, aromatic diluents could cause important damage, as in the case of NPOE, a diluent proposed to solubilize calixarenes. In particular, a considerable increase in the viscosity of the organic phase was observed after radiolysis (*68*).
- Some new extractants were not soluble in alkanes; thus, a long-chain alcohol like *n*-octanol had to be selected. The degradation of the diglycolamide TODGA was similar for *n*-octanol and dodecane solutions (*182, 183*). With polyaromatic nitrogen donors like the *i*Pr-BTP molecule, a similar hydrolysis effect was measured in pure *n*-octanol and alkane-octanol (70–30% in volume) (*244*).

8.5.2.2 Presence of Additional Ligands

The presence of additional solutes in the organic phase often enhances the radiolytic stability of extractants; this behavior has been described for the following examples:

- In the TRUEX process, the presence of TBP decreases the radiolytic degradation of CMPO (*41*);
- The presence of monoamide inhibited the radiolysis of TODGA in dodecane (*183, 199*);

- In the DIAMEX-SANEX process, the presence of malonamide protected HDEHP (*5, 10, 32*); but it should be noted that the presence of dialkyl phosphoric acid in the organic phase had a slightly negative effect on the malonamide's stability (*5, 48, 71*);
- The same protective effect was observed in the TALSPEAK process, where the lactic acid added to the aqueous phase reduced the degradation of DTPA (*161*).

8.6   COMPARISON OF EXTRACTANTS' STABILITY

Though the chemical families retained in the context of nuclear fuel reprocessing are very different, depending on the metallic ion to be recovered and the composition of the initial feed, an attempt to establish a scale of extractants' sensitivity toward radiolysis is presented in the following paragraph:

- The least stable extractants are *S* donor molecules (*29, 49, 60*) and the alkyl-BTP or BTBP molecules (*66, 240, 241, 244*);
- The most stable are the macrocyclic extractants, with radiolytic degradation yields lower than 1 molecule/100 eV (*7*), and especially the calix-arenes G(-calixarene) <0.1 (*72*);
- O-donor extractants have an intermediate stability.

Among the O-donor extractants, the molecules containing amide functions were slightly less stable than the reference TBP (*48, 187, 188, 189, 191, 192, 197, 198*) and dialkylphosphoric acids (G(-TBP) ≈ 1 to 1.5 (77), G(-HDEHP) ≈ 1.5 to 2 (*10*), and G(-malonamide$_{DMDOHEMA}$) ≈ 4 molecules 100 eV (*48*)).

The following order of stability can be proposed: amide (diglycolamides < malonamides < monoamides (*183, 199, 216*)) ≈ CMPO ≤ HDEHP ≈ TBP (*10, 42, 77*) < trialkylphosphonate < trialkyl phosphine oxide (*308*).

However, the yield value has to be carefully considered. In fact, though calixarenes present the lowest degradation G values, a loss of 50% of the molecule was observed under an irradiation dose of 1 MGy (*72*), which is comparable to the degradation rate of malonamides (loss of 40% under irradiation dose of 0.75 MGy) (*48*). This difference can be explained by the definition of the yield, which took into account the number of molecules, and therefore favored processes in which the concentration of the extractant was low (e.g., calixarene 10^{-2} mol L^{-1}).

Nevertheless, the radiolytic (and hydrolytic) stability of an extractant must be considered not only from the quantitative, but also from the qualitative aspect. The objective is not perfect resistance to the aggressive medium, but sufficient for an industrial implementation of the process. The nature of the stable compounds, their distribution in the process steps, and their impact are also important when proposing an efficient solvent cleanup. For such studies, dedicated representative loops in which the main treatments, "extraction-irradiation-stripping-solvent treatment," could be run on the solvent are of key importance.

8.7   CONCLUSIONS

In each step of nuclear fuel reprocessing, the solvent is exposed to various radio-active sources and consequently prone to more degradation than solvents in other industrial fields. The resulting damage can be either chemical or physical. Numerous experimental studies have been carried out; most of them were applied research and therefore restricted to studying the impact of degradation on process performance in order to develop an adequate cleanup treatment.

Nevertheless, with the "oldest" extraction system in the nuclear field, the TBP-alkane solvent has been studied since the 1950s, and authors have succeeded in pro-posing a detailed qualitative and quantitative description of the radiolysis. Many authors have focused on the primary process of the mechanism for pure TBP (*18, 279–281, 283–287*). The formation rate of TBP degradation products has been esti-mated under several experimental conditions and a degradation scheme proposed with rate constants (*9, 311–313*). An empirical equation allowing the calculation of the yield of TBP decomposition and degradation product formation in the presence of HNO_3, $Pu(NO_3)_4$, and $UO_2(NO_3)_2$ has been proposed (*9, 11*).

With more recent extractants, scientists have begun to use, as with TBP some years ago, a global approach: determination of ligand destruction rate, identification of main degradation products, and especially the effect on extraction performance. Detailed investigations need a major effort, and teams have often considered this aspect as side studies. The studies published are often presented almost as an after-thought in a parametric extraction study and therefore do not seem to be an important aspect in the development strategy for new processes. As a result, the comprehensive understanding of such multicomponent and biphasic systems' degradation mecha-nisms under radiation remains a scientific challenge. To advance in the elucidation of the radiation process, only a few fundamental and original investigations have been performed, such as those mentioned in the following examples.

- Pulsed radiolysis has been used to study the primary process of TBP, TOPO (*292*), and TODGA (*182*) degradation. This approach allowed an experimental proof of the charge-transfer reaction from the alkane cation to the extractant, already previously proposed by various authors (*90*), to be obtained. Recent studies with a series of aliphatic alcohols have dem-onstrated the interest of pulse radiolysis to measure the rate constants for radical production and recombination (*314*).
- Experimental approaches using mass-spectrometric fragmentations of pure extractant are of interest to identify the fragility points in the TBP molecule and explain the TBP fragmentation pathways (*81*).
- Molecular dynamics simulations have been performed on the complexing of cesium and sodium by a nitro derivative of a calixarene (BC6) to esti-mate the influence of a nitro group on cesium selectivity (*68*).
- An interesting kinetic approach to radiolysis in liquid-liquid systems by mathematic modelling has been proposed (*315, 316*). The authors confirmed that in most cases the formation of destructive radicals can be considered

as slow, and the radiolysis of solutes in emulsion will proceed in a kinetic regime, but a change to a diffusional regime could occur under specific conditions (such as low substrate solubility, high doses, and thick phase layers). Recommendations were given to ensure the best experimental conditions.

- Other research has focused on a phenomenon that is important but outside the subject of this review: the influence of radiolysis on the redox behavior of actinide ions in nitric acid aqueous solution or in extraction systems (*116–119, 317–320*).

- Only a few papers have described the influence of the nature of the radiation (α or γ exposure) on the degradation of extractants and the formation of degradation products in the TBP-alkane and HDEHP-alkane systems (*8–12*), or with CMPO (*13*). If certain authors indicate lower HDEHP degradation during gamma radiolysis (G_γ(-HDEHP) = 1.5 compared to G_α(-HDEHP) = 2.2 molecules/100 eV) (*10*), other studies give comparable degradation rates. Local irradiation (privileged positioning of the α-particles (^{238}Pu or ^{241}Am) close to the extractant) does not seem to produce greater damage than irradiation by a ^{60}Co source.

- Even so, the basic data to aid an understanding of the elementary mechanisms remain very incomplete. To fill the gap in comprehensive studies related to radiolysis of such multicomponent systems, investigations in the following directions could be undertaken.

- Scientists should focus on the initial steps of the processes (identification of the transient radical species with dedicated techniques like ESR or pulsed radiolysis), the kinetic aspect, and sensitive external parameters, like the nature of the radiation (α, β, γ, e$^-$), to control the accumulation of radiation-induced damage. Dedicated tools need to be built.

- Side phenomena, like the effect of radiolysis on the redox behavior of metallic solutes and the speciation of complexes with degradation products, should also be examined in more detail.

- The study of simple systems (considered as model systems) is required, but representative systems must also be investigated. A progressive approach should enable the integration of knowledge acquired from the model systems.

- In each step, theoretical chemistry can enhance understanding and help to reach a comprehensive modeling of the effect of radiation.

From such studies, it can be expected that progress will be made toward the prevention of extractant degradation and the design of more stable extractants.

REFERENCES

1. Nash, K.L., Madic, C., Mathur, J.N., Laquement, J. 2006. Actinide separation science and technology, in *The Chemistry of the Actinide and Transactinide Elements*; Morss, L.R., Edelstein, N.M., and Fuger, J. Eds.; Springer: Dordrecht, Vol. 4, 2622–2798.
2. Mathur, J.N., Murali, M.S., Nash, K.L. 2001. Actinide partitioning – A review. *Solvent Extr. Ion Exch.* 19(3): 357–390.

3. Madic, C., Hudson, M.J., Liljenzin, J.O., Glatz, J.P., Nannicini, R., Facchini, A., Kolarik, Z., Odoj, R. 2000. New partitioning techniques for minor actinides. *European Report*, EUR 19149.

4. Madic, C., Testard, F., Hudson, M.J., Liljenzin, J.O., Christiansen, B., Ferrando, M., Facchini, A., Geist, A., Modolo, G,, Gonzales-Espartero, A., De Mendoza, J. 2004 European project on Partitioning: PARTNEW – New solvent extraction processes for minor actinides – Final Report. Report *CEA*-R-6066.

5. Bisel, I., Camès, B., Faucon, M., Rudloff, D., Saucerotte, B. 2007. DIAMEX-SANEX solvent behavior under continuous degradation and regeneration operation. *Proceeding of the International Conference on Advanced Nuclear Fuel Cycles and Systems, Global 2007*, Boise, ID, 9–13 September, 1857–1860.

6. Cames, B., Saucerotte, B., Faucon, M., Rudloff, D., Gastaldi, M., Bisel, I. 2004. Long term evolution of recycled DIAMEX solvent properties under hydrolysis and radiolysis with or without solvent clean-up. *Proceeding of Atalante 2004, Advances for Future Nuclear Fuel Cycles*, Nimes, France, June 21–25, 1–13.

7. Draye, M., Chomel, R., Doutreluingne, P., Guy, A., Foos, J., Lemaire, M. 1993. Radiolytic products study of dicyclohexano-18-crown-6, a selective extractant for nuclear fuel reprocessing. *J. Radioanal. Nucl. Chem. Lett.* 175(1): 55–62.

8. Ladrielle, T., Wanet, P., Lemaire, D., Apers, D.J. 1983. Alpha and gamma induced radiolysis of tributyl phosphate. *Radiochem. Radioanal. Lett.* 59(5–6): 355–364.

9. Kulikov, I.A., Kermanova, N.V., Vladimirova, M.V. 1983. Radiolysis of TBP in presence of plutonium and uranium. *Soviet Radiochem.* 25: 310–316. (Translated from *Radiokhimiya* 25(3): 330–336.)

10. Vladimirova, M.V., Kulikov, I.A., Milovanova, A.S. 1979. Radiation-chemical behavior of the system D2EHPA in paraffin-3.0 M HNO_3 with α- and γ-radiolysis. *Soviet Radiochem.* 21(6): 789–791. (Translated from *Radiokhimiya* (21)6: 925–926.)

11. Kulikov, I.A., Kermanova, N.V., Sosnovskii, O.A., Shesterikov, N.N., Vladimirova, M.V. 1981. Effect of α- and γ-radiations on the decomposition of tributylphosphate and the distribution ratios of Pu^{4+} and Zr^{4+}. *Soviet Radiochem.* 23: 664–669. (Translated from *Radiokhimiya* 23(6): 825–831.)

12. Kulikov, I.A., Milovanova, A.S., Shesterikov, N.N., Vladimirova, M.V. 1990. Effect of α- and γ-irradiations on Am^{3+} and Ce^{3+} distribution coefficients in an extraction system based on DEHP. *Soviet Radiochem.* 32(3): 232–236. (Translated from *Radiokhimiya* 32(3): 101–105.)

13. Buchholz, B.A., Nunez, L., Vandergrift, G.F. 1996. Effect of α-radiolysis on TRUEX-NPH solvent. *Sep. Sci. Technol.* 31(16): 2231–2243.

14. Andreichuk, N.N., Rotmanov, K.V., Frolov, A.A., Vasil'ev, V.Y. 1988. Steady-state concentrations of nitrogen oxides formed in the α-radiolysis of nitric acid solution. *High Energy Chem.* 22(6): 414–417. (Translated from *Khimiya Vysokikh Energii* 22(6): 498–501).

15. Bibler, N.E. 1972. Gamma and alpha radiolysis of aqueous solutions of diethylene triaminepentaacetic acid, *J. Inorg. Nucl. Chem*. 34: 1417–1425.

16. Huggard, A.J., Warner, B.F. 1963. Investigations to determine the extent of degradation of TBP/odorless kerosene solvent in the new separation plant, Windscale. *Nucl. Sci. Eng*. 17: 638–650.

17. Burr, J.G. 1958. The radiolysis of tributyl phosphate. *Radiat. Res.* 8: 214–221.

18. Wilkinson, R.W., Williams, T.F. 1961. The radiolysis of tri-n-alkyl phosphates. *J. Chem. Soc.* 4098–4107.

19. Egorov, G.F., Afanas'ev, O.P. 1983. Radiation chemistry of hydrocarbon diluents in solvent-extraction processes. A*tomic Energy* 54(5): 349–534. (Translated from *Atomnaya Énergiya* 347–350.)

20. Chiariza, R., Horwitz, E.P. 1990. Secondary cleanup of TRUEX process solvent. *Solvent Extr. Ion Exch*. 8(6): 907–941.

21. Lesage, D., Virelizier, H., Jankowski, C.K., Tabet, J.C. 1997. Identification of minor products obtained during radiolysis of tributylphosphate (TBP). *Spectroscopy* 13: 275–290.

22. Lesage, D., Virelizier, H., Jankowski, C.K., Tabet, J.C. 1998. Identification of isomeric tributylphosphate dimers formed by radiolysis using tandem mass spectrometry and stable isotopic labelling. *Eur. Mass Spectrom*. 4: 47–54.

23. Blake, C.A., Davis, W., Schmitt, J.M. 1963. Properties of degraded TBP-Amsco solutions and alternative extractant-diluent systems. *Nucl. Sci. Eng.* 17: 626–637.

24. Hughes, E. 1966. Applications of absorption spectrophotometry (infrared and visible) to the determination of impurities in tributyl phosphate and degraded tributyl phosphate/ kerosene mixtures. *PG Report 737*.

25. Barelko, E.V., Solyanina, I.P. 1975. Radiolysis of solutions of TBP in contact with nitric acid. II. Processes of oxidation and nitration. *Atomic Energy* 38(1): 25–29. (Translated from *Atomnaya Énergiya* 38(1): 23–26.)

26. Nowak, Z. 1977. Radiolytic degradation of extractant-diluent systems used in the PUREX process. *Nukleonika* 22: 155–171.

27. Nowak, Z., Nowak, M., Seydel, A. 1979. The radiolysis of TBP-dodecane-HNO$_3$ systems. *Radiochem. Radioanal. Lett*. 38(5–6): 343–354.

28. Nowak, Z., Seydel, A. 1981. The effect of temperature on the radiolysis of extraction systems containing TBP. *Nukleonika* 26(1): 27–33.

29. Chen, J., Jiao, R., Zhu, Y. 1996. A study on radiolytic stability of commercial and purified Cyanex 301. *Solvent Extr. Ion Exch*. 14(4): 555–565.

30. Ruikar, P.B., Nagar, M.S., Subramanian, M.S. 1991. Quantitative analysis of some extractants by infrared spectrometry. *J. Radioanal. Nucl. Chem.* 155(6): 371–376.

31. Rochon, A.M., Nowak, Z., Zagorski, Z.P. 1976. On compounds complexing zirconium in irradiated (TBP-dodecane) 0.5 M HNO$_3$ systems. *Radiochem. Radioanal. Lett*. 27(1): 1–8.

32. Tachimori, S., Nakamura, H., Sato, A. 1979. A study of radiation effects on the extraction of americium(III) with acidic organophosphates. *J. Radioanal. Chem.* 50(1–2): 143–151.

33. Tripathi, S.C., Ramanujam, A., Nadkarni, M.N., Bandyopadhyay, C. 1986. Thin-layer chromatographic separation and determination of dibutylphosphoric acid in a mixture of monobutylphophoric acid and tributyl phosphate. *Analyst* 111: 239–240.

34. Adamov, V.M., Andreev, V.I., Belyaev, B.N., Markov, G.S., Polyakov, M.S., Ritori, A.E., Yu Shil'nikov, A.Y. 1990. Identification of decomposition products of extraction systems based on tri-*n*-butyl phosphate in aliphatic hydrocarbons. *Kerntechnik* 55(3): 133–137.

35. Mincher, B.J., Mezyk, S.P., Bauer, W.F., Elias, G., Riddle, C., Peterman, D.R. 2007. FPEX gamma-radiolysis in the presence of nitric acid. *Solvent Extr. Ion Exch.* 25: 596–601

36. Nowak, Z., Nowak, M. 1975. Regeneration of extraction systems used in the PUREX process. *Soviet Radiochem.* 17(3): 361–367. (Translated from *Radiokhimiya* 17(3): 362–370.)

37. Lee, Y.C., Ting, G. 1979. Determination of dibutyl and monobutyl phosphate kerosene mixtures by solvent extraction and gas chromatography. *Anal. Chim. Acta* 106: 373–378.

38. Kuo, C.H., Shih, J.S., Yeh, Y.C. 1982. Determination of dibutyl and monobutyl phosphates in mixtures of kerosene and tributyl phosphate. *Analyst* 107: 1190–1194.

39. Bellido, A.V., Rubenich, M.N. 1984. Influence of the diluent on the radiolytic degradation of TBP in TBP, 30% (v/v)-diluent-HNO$_3$ systems. *Radiochim. Acta* 36: 61–64.

40. Chiariza, R., Horwitz, E.P. 1986. Hydrolytic and radiolytic degradation of octyl(phenyl) butyl carbamoylmethyl phosphine oxide and related compounds. *Solvent Extr. Ion Exch.* 4(4): 677–723.

41. Nash, K.L., Gatrone, R.C., Clark, G.A., Rickert, P.G., Horwitz, E.P. 1988. Hydrolytic and radiolytic degradation of ОФD(iB)CMPO: Continuing studies. *Sep. Sci. Technol.* 23: 1355–1372.

42. Nash, K.L., Rickert, P.G., Horwitz, E.P. 1989. Degradation of the TRUEX process solvent. *Solvent Extr. Ion Exch.* 7(4): 655–675.

43. Adamov, V.M., Andreev, V.I., Belyaev, B.N., Markov, G.S., Polyakov, M.S., Ritori, A.E., Yu Shil'nikov, A.Y. 1992. Identification and formation mechanism of decomposition products of tri-*n*-butyl phosphate extraction systems in aliphatic hydrocarbons. *Soviet Radiochem.* 34(1): 150–157. (Translated from *Radiokhimiya* 34(1): 189–197.)

44. Matel, L. 1990. Radiation-chemical changes of benzo-15-crown-5 in chloroform. *J. Radioanal. Nucl. Chem. Lett.* 146(2): 85–93.

45. Ali, M.A., Al-Ani, A.M. 1991. Gas chromatographic determination of tributyl phosphate, dibutyl phosphate and butyl phosphate in kerosene solutions. *Analyst* 116, 1067–1069.

46. Mathur, J.N., Murali, M.S., Ruikar, B., Nagar, M.S., Sipahimalani, A.T., Bauri, A.K., Banerji, A. 1998. Degradation, cleanup, and reusability of octylphenyl-N,N′-diisobutylcarbamoyl methyl phosphine oxide (CMPO) during partitioning of minor actinides from high level waste (HLW) solution. *Sep. Sci. Technol.* 33(14): 2179–2196.

47. Lamouroux, C., Virelizier, H., Moulin, C., Jankowski, C.K. 2001. Application of gas chromatography-tandem mass spectrometry to the analysis of inhibition of dimerisation of tributylphosphate under radiolysis. Identification of isomeric tributylphosphate-alkylbenzene inhibitor coupling products. *J. Chromatogr. A* 917: 261–275.

48. Berthon, L., Morel, J.M., Zorz, N., Nicol, C., Virelizier, H., Madic, C. 2001. Diamex process for minor actinide partitioning: hydrolytic and radiolytic degradations of malonamide extractants. *Sep. Sci. Technol.* 36(5–6): 709–728.

49. Modolo, G., Seekamp, S. 2002. Hydrolysis and radiation stability of the alina solvent for actinides(III)/lanthanide(III) separation during the partitioning of minor actinides. *Solvent Extr. Ion Exch.* 20(2): 195–210.

50. Tripathi, S.C., Ramanujam, A., Gupta, K.K., Bindu, P. 2001. Studies on the identification of harmful radiolytic products of 30% TBP-n-dodecane-HNO_3 by gas-liquid chromatography. II. Formation and characterization of high molecular weight organophosphates. *Sep. Sci. Technol.* 36(13): 2863–2883.

51. Tripathi, S.C., Ramanujam, A. 2003. Effect of radiation-induced physicochemical transformations on density and viscosity of 30% TNP – *n*-dodecane-HNO_3 system. *Sep. Sci. Technol.* 38(10): 2307–2336.

52. Lash, R.P., Hill, C.J. 1979. Ion chromatographic determination of dibutylphosphoric acid in nuclear fuel reprocessing streams. *J. Liquid Chromatogr.* 2(3): 417–427.

53. Shoji, Y., Minami, T., Ichihashi, T., Hyodo, H., Ohta, M. 1987. Determination of degradation products of TBP by ion chromatography. *NAIG Annual Review* 71–75.

54. Dodi, A., Verda, G. 2001. Improved determination of tributyl phosphate degradation products (mono- and dibutyl phosphates) by ion chromatography. *J. Chromatogr. A* 920: 275–281.

55. Bocek, P., Dolnik, V., Deml, M., Janak, J. 1980. Separation and determination of the degradation products of tributyl phosphate by high-speed analytical isotachophoresis. *J. Chromatogr.* 195: 303–305.

56. Rivasseau, C., Blanc, P. 2001. Determination of C_4-C_{14} carboxylic acids by capillary zone electrophoresis – Application to the identification of diamide degradation products and partitioning studies. *J. Chromatogr. A* 920: 345–358.

57. Uetake, N. 1987. Determination of degradation products in tributyl phosphate using ^{31}P Fourier transform NMR spectroscopy. *Analyst* 112: 445–448.

58. Vaufrey, F., Berthon, C., Chachaty, C., Madic, C. 1994. NMR and nuclear fuel reprocessing *J. Chim. Phys*. 91: 806–812.

59. Berthon, C., Vaufrey, F., Livet, J., Madic, C. 1996. Liquid-liquid extraction and NMR, in *Proceedings of International Solvent Extraction Conference, ISEC'1996*; Shallcross, D.C., Paimin, R., Prvcic, L.M. Eds.; the University of Melbourne: Australia. Vol II, 1349–1354.

60. Modolo, G., Odoj, R. 1998. Influence of the purity and irradiation stability of cyanex 301 on the separation of trivalent actinides from lanthanides by solvent extraction. *J. Radioanal. Nucl. Chem*. 228(1–2): 83–88.

61. Modolo, G., Odoj, R. 1999. Synergistic selective extraction of actinides(III) over lanthanides from nitric acid using new aromatic diorganyldithiophosphinic acids and neutral organophosphorus compounds. *Solvent Extr. Ion Exch.* 17(1): 33–53.

62. Lamouroux, C. 2000. Contribution et complémentarité des techniques de spectrométrie de masse à l'étude des molécules issues de la dégradation radiolytique du tributyl phosphate. PhD thesis: Thèse de doctorat de l'université Paris VI.

63. Lamouroux, C., Virelizier, H., Moulin, C., Tabet, J.C., Jankowski, C.K. 2000. Direct determination of dibutyl and monobutyl phosphate in a tributyl phosphate/nitric aqueous-phase system by electrospray mass spectrometry. *Anal. Chem.* 72: 1186–1191.

64. Lamouroux, C., Moulin, C., Tabet, J.C., Jankowki, C.K. 2000. Characterization of zirconium complexes of interest in spent nuclear fuel reprocessing by electrospray ionization mass spectrometry. *Rapid Commun. Mass Spectrom*. 14: 1869–1877.

65. Berthon, L., Piveteau, B. 2000. Contribution of electrospray mass spectrometry to the study of the organic species and metal-ligand complexes in solution. *Proceeding of Atalante 2000, Scientific Research on the Back-end of the Fuel Cycle for the 21st Century*, 24–26 October, Avignon, France, 3–21.

66. Hill, C., Berthon, L., Bros, P., Dancausse, J.P., Guillaneux, D. 2002. SANEX-BTP process development studies. *Proceeding of the 7th International Exchange Meeting on Actinide and Fission Product Partitioning*, Jeju, Korea, 14–16 October, 453–461.

67. Zhang, P., Song, C.L., Liang, J.F., Xin, R.X. 2003. Identification of radiolytic degradation products of γ-irradiated 30% trialkylphosphine oxide-kerosene solution. *Solvent Extr. Ion Exch.* 21(1): 91–108.

68. Lamare, V., Dozol, J-F., Allain, F., Virelizier, H., Moulin, C., Jankowski, C-K., Tabet, J-C. 2000. Behavior of calix[4]arene-bis-crown-6 under irradiation: Electrospray-mass spectrometry investigations and molecular dynamics simulation on Cs^+ and Na^+ complexes of a degradation compound, in *ACS Symposium Series 757, Calixarenes Molecules for Separations*; Lumetta G., Rogers R.D., Gopalan A.S. Eds.; American Chemical Society: Washington, DC, 56–70.

69. Jankowski, C.K., Allain, F., Dozol, J-F., Virelizier, H., Tabet, J-C., Moulin, C., Lamouroux, C. 2003, Preliminary study of the stability of calyx[4]arene crown compounds under radiolysis. *Rapid Commun. Mass Spectrom*. 17: 1247–1255.

70. Beom, Y.H., Hee, L.H., Sil, M.H. 2003. Determination of radiolysis products in zirconium salt of di-(2-ethylhexyl) phosphoric acid by high performance liquid chromatography/mass spectrometry. *J. Liquid Chromatogr. Rel. Technol.* 26(15): 2593–2604.

71. Berthon, L., Journet, S., Lalia, V., Morel, J.M., Zorz, N., Berthon, C., Amekraz, B. 2004. Use of chromatographic techniques to study a degraded solvent for minor actinides partitioning: qualitative and quantitative analysis. *Proceeding of Atalante 2004, Advances for Future Nuclear Fuel Cycles*, Nimes, France, June 21–25, 2–8.

72. Lamouroux, C., Aychet, N., Lelievre, A., Jankowski, C.K., Moulin, C. 2004. High-performance liquid chromatography with electrospray ionization mass spectrometry and diode array detection in the identification and quantification of the degradation products of calix[4]arene crown-6 under radiolysis. *Rapid Commun. Mass Spectrom*. 18: 1493–1503.

73. Burger, L.L., Mc Clanahan, E.D. 1958. Tributyl phosphate and its diluent systems. *Ind. Eng. Chem.* 50(2): 153–156.

74. Kuzin, V.D., Semushin, A.M., Romanovskii, V.N. 1969. Stability of di(2-ethylhexyl) hydrogen phosphate against radiation. *High Energy Chem.* 3: 248–249. (Translated from *Khimiya Vysokikh Energii* 3: 274–275.)

75. Holland, J.P., Merklin, J.F., Razvi, J. 1978. The radiolysis of dodecane-tributyl phosphate solutions. *Nucl. Instr. Methods* 153: 589–593.

76. Zatonsky, S.V., Povolotskaya, O.S. 1987. On the radiation resistance of crown ethers. *J. Radioanal. Nucl. Chem. Lett.* 117(6): 364–367.

77. Davis, W. Jr. 1984. Radiolytic behavior, in *Science and Technology of Tributyl Phosphate*, *Vol I, Synthesis, Properties, and Analysis*; Schulz, W.W., Navratil, J.D., Talbot, A.E. Eds.; CRC Press: Boca Raton, FL, 221–265.

78. Spinks, J.W.T., Wodds, R.J. 1990. *An Introduction to Radiation Chemistry*, 3rd edn. John Wiley & Sons: NewYork/Chichester /Brisbane/Totonto/Singapore.

79. Tahraoui, A., Morris, J.H. 1995. Decomposition of solvent extraction media during nuclear reprocessing: literature review. *Sep. Sci. Technol.* 30(13): 2603–2630.

80. Lesage, D. 1995. Contribution à l'étude des produits de dégradation du solvant de retraitement des combustibles nucléaires par utilisation de la spetrométrie de masse, ses différents couplages ainsi que par l'emploi d'isotopes stables. PhD thesis: Thèse de l'université Paris VI.

81. Lesage, D., Virelizier, H., Tabet, J.C., Jankowski, C.K. 2001. Study of mass spectrometric fragmentations of tributyl phosphate via collision-induced dissociation. *Rapid Commun. Mass Spectrom.* 15: 1947–1956.

82. Pozo, C. 1993. Application of steric exclusion chromatography for the separation of degradation products of the solvent used for the reprocessing of the nuclear fuels. *Rapport CEA*-R-5647.

83. Tripathi, S.C., Sumathi, S., Ramanujam, A. 1999. Effects of solvent recycling on radiolytic degradation of 30% tributyl phosphate-n dodecane-HNO$_3$ system. *Sep. Sci. Technol*. 34(14): 2887–2903.

84. Rigg, T., Wild, W. 1958. Radiation effect in solvent extraction processes, in *Progress in Nuclear Energy*, Series III. Process Chemistry, Pergamon Press: London, Vol. 2, 7–6, 320–331.

85. Kulikov, I.A., Kermanova, N.V., Vladimirova, M.V. 1985. Gamma-radiolysis of TBP and DBPA in the presence of HNO$_3$. *Soviet Radiochem.* 27: 58–63. (Translated from *Radiokhimiya* 27(1): 65–70.)

86. Barelko, E.V., Solyanina, I.P., Babakina, G.S. 1976. Influence of radiation on the extraction of radiozirconium and radioiodine by solutions of n-tributyl phosphate (TBP). *Soviet Radiochem.* 18(4): 573–577. (Translated from *Radiokhimiya* 1976, 18(4): 667–671.)

87. Hromadova, M., Čech, R., Rajec, P. 1992. A study of changes in the yields of radiolytic products in two-phase systems with tributyl phosphate. *J. Radioanal. Nucl. Chem.* 163(1): 99–105.

88. Barelko, E.V., Solyanina, I.P., Tsvetkova, Z.I. 1966. Radiation-chemical stability of TBP in solutions of hydrocarbons. A*tomic Energy* 21(4): 946–950. (Translated from *Atomnaya Énergiya* 21(4): 281–285.)

89. Burger, L.L. 1958. The decomposition reactions of tributyl phsophate and its diluents and their effect on uranium recovery processes. *Progress in Nuclear Energy* Series III; Pergamon Press: London, Process Chemistry, Vol. 2, 7–5, 307–319.

90. Canva, J., Pagès, M. 1965. Effet de protection et de sensibilisation dans la décomposition radiolytique du phosphate de tributyle. *Radiochim. Acta* 4: 88–91.

91. Egorov, G.F., Ilozhev, A.P., Nikiforov, A.S., Smelov, V.S., Shevchenko, V.B., Schmidt, V.S. 1979. Choice of organic diluents for the extractive regeneration of the spent fuel of

nuclear power plants. *Soviet Atomic Energy* 47: 591–596. (Translated from *Atomnaya Énergiya* 47(2): 75–79.)

92. Adamov, V.M., Andreev, V.I., Belyaev, B.N., Lyubtsev, R.I., Markov, G.S., Polyakov, M.S., Ritori, A.E., Yu Shil'nikov, A. 1987. Radiolysis of an extraction system based on solutions of tri-n-butylphosphate in hydrocarbon diluents. *Soviet Radiochem.* 29(6): 775–781. (Translated from *Radiokhimiya* 29(6): 822–829.)

93. Vandegrift, G.F. 1984. Diluent for TBP extraction systems, in *Science and Technology of Tributyl Phosphate, Vol I, Synthesis, Properties, and Analysis*; Schulz, W.W., Navratil, J.D., Talbot, A.E. Eds.; CRC Press: Boca Raton, FL, 69–136.

94. Renard, E.V., Pyatibratov, Y.P., Neumoev, N.V., Vhizhov, A.A., Kulikov, I.A., Gol'dfarb, Y.Y., Sirotkina, I.G., Semenova, T.I. 1988. Isoparaffinic diluents for tri-*n*-butyl phosphate. Chemical, radiation-chemical stability, effect on tetravalent plutonium and thorium extraction. *Soviet Radiochem.* 30(6): 734–745. (Translated from *Zhurnal Strukturnoi khimii* 30(6): 774–787.)

95. Egorov, G.F., Afanas'ev, O.P., Zilberman, B.Y., Makarychev-Mikhailov, M.N. 2002. Radiation-chemical behavior of TBP in hydrocarbon and chlorohydrocarbon diluents under conditions of reprocessing of spent fuel from nuclear power plants. *Radiochemistry* 44(2): 151–156. (Translated from *Radiokhimiya* 44(2): 140–145.)

96. Wagner, R.M., Kinderman, E.M., Towle, L.H. 1959. Radiation stability of organophosphorus compounds. *Ind. Eng. Chem.* 51(1): 45–46.

97. Krishnamurthy, M.V., Sampathkumar, R. 1992. Radiation-induced decomposition of the tributyl phosphate-nitric acid system: role of nitric acid. *J. Radioanal. Nucl. Chem. Lett.* 166(5): 421–429.

98. Nowak, Z., Nowak, M. 1973. Radiolytic and thermal degradation of dodecane – 30% TBP-HNO$_3$ systems. *Radiochem. Radioanal. Lett.* 14(3): 161–168.

99. Kurtekov, M.M., Pushlenkov, M.F., Zil'berman, B.Y., Gryaznova, A.S., Efremova, T.I. 1967. Behavior of the extractant TBP + CCl$_4$ under irradiation. *Soviet Radiochem.* 9(1): 32–36. (Translated from *Radiokhimiya* 9(1): 32–37.)

100. Barelko, E.V., Solyanina, I.P. 1973. Radiolysis of solutions of TBP in contact with nitric acid. Formation of radiolysis products of the extraction reagent. *Atomic Energy* 35(4): 898–902. (Translated from *Atomnaya Énergiya* 35(4): 239–243.)

101. Hardy, C.J., Scargill, D. 1961. Studies on mono- and di-n-butylphosphoric acids. III. The extraction of zirconium from nitrate solution by di-n-butylphosphoric acid. *J. Inorg. Nucl. Chem.* 17: 337–349.

102. Neace, J.C. 1983. Diluent degradation products in the PUREX solvent. *Sep. Sci. Technol.* 18(14&15): 1581–1594.

103. Faugeras, P., Talmont, X. 1968. Radiolysis and hydrolysis of TBP and their effects. *Proceedings of the 5th International Conference on Solvent Extraction Chemistry*, Jerusalem, Israel, 16–18 September, 411–423.

104. Huang, H.X., Zhu, G.H., Hou, S.B. 1989. Retention of ruthenium-nitrosyl complexes in 30% TBP-kerosene-laurohydroxamic acid. *Radiochim. Acta* 46: 159–162.

105. Nakamura, T., Fukasawa, T., Sasahira, A. 1991. Formation mechanism of interfacial crud in solvent cleanup process for fuel reprocessing. *J. Nucl. Sci. Technol.* 28(3): 255–257.

106. Powell, B.A., Navratil, J.D., Thompson, M.C. 2003. Compounds of hexavalent uranium and dibutylphosphate in nitric acid systems. *Solvent Extr. Ion Exch.* 21(3): 347–368.

107. Zimmer, E., Printz, G., Merz, E. 1984. Investigations of crud formation in the PUREX process. *Fuel Reprocess. Waste Manag. Proc. Am. Nuc. Soc. Int. Top. Meet.* 1: 459–466.

108. Zimmer, E., Borchardt, J. 1986. Crud formation in the PUREX and THOREX processes. *Nucl. Technol.* 75: 332–337.

109. Miyake, C., Hirose, M., Yoshimura, T., Ikeda, M., Imoto, S., Sano, M. 1990. 'The third phase' of extraction process in juel reprocessing, (I) Formation conditions, compositions and structures of precipitates in Zr-degradation products of TBP systems. *J. Nucl. Sci. Technol.* 27(2): 157–166.

110. Miyake, C., Hirose, M., Yoshimura, T., Ikeda, M., Imoto, S., Sano, M. 1990. 'The third phase' of extraction process in juel reprocessing, (II) EXAFS study of zirconium monobutylphosphate and zirconium dibutylphosphate. *J. Nucl. Sci. Technol.* 27(3): 256–261.

111. Smith, D.N., Edwards, H.G.M., Hugues, M.A., Courtney, B. 1997. Odorless kerosene degradation and the formation of interfacial deposits during the alkaline solvent wash in the PUREX process. *Sep. Sci. Technol.* 32(17): 2821–2849.

112. Solovkin, A.S., Lobanov, A.V., Rubisov, B.N. 1989. Mathematical model of distribution of dialkylphosphoric acids in water-nitric acid-organic solvent-trialkyl phosphate two-phase systems. *Soviet Radiochem.* 31(1): 113–119. (Translated from *Radiokhimiya* 31(1): 117–124.)

113. Zilberman, B.Y., Goletskii, N.D., Shmidt, O.V., Puzikov, E.A., Blazheva, I.V., Egorov, G.E., Afanas'ev, O.P. 2007. Distribution of HDBP in two-phases systems consisting of aqueous nitric acid, organic diluent (with or without TBP), and HDBP or its zirconium salt. *Radiochemistry* 49(4): 391–396. (Translated from *Radiokhimimiya* 49(4): 344–347.)

114. Fedorov, Y.S., Zilberman, B.Y., Kulikov, S.M., Blazheva, I.V., Mishin, E.N., Wallwork, A.L., Denniss, I.S., May, I., Hill, N.J. 1999. Uranium(VI) extraction by TBP in the presence of HDBP. *Solvent Extr. Ion Exch.* 17: 243–257.

115. May, I., Taylor, R.J., Wallwork, A.J., Hasting, J.J., Fedorov, Y.S., Zilberman, B.Y., Mishin, E.N., Arkhipov, S.A., Blazheva, I.V., Poverkova, L.Y., Livens, F.R., Charnock, J.M. 2000. The influence of dibutylphosphate on actinide extraction by 30% tributyl-phosphate. *Radiochim. Acta* 88: 283–293.

116. Vladimirova, M.V., Fedoseev, D.A., Kulikov, I.A., Milovanova, A.S., Boikova, I.A., Sosnovskii, O.A., Kermanova, N.V., Bulkin, B.I. 1982. Radiation-chemical behavior of actinoids in extraction systems. I. Pu(IV), Np(IV), Th(IV) in a 30% tri-n-butyl phosphate- n-dodecane solution during γ-radiolysis. *Soviet Radiochem.* 24(1): 33–38. (Translated from *Radiokhimiya* (24)1: 38–42.)

117. Vladimirova, M.V., Fedoseev, D.A., Kulikov, I.A., Boikova, I.A., Milovanova, A.S., Kermanova, N.V. 1984. Radiation-chemical behavior of Pu(IV) in extraction systems. *Soviet Radiochem.* 26(1): 84–89. (Translated from *Radiokhimiya* (26)1: 89–94.)

118. Vladimirova, M.V., Fedoseev, D.A., Boikova, I.A., Milovanova, A.S. 1984. Radiation-chemical behavior of actinoids in extraction systems. II. Pu(IV) + U(VI) in solution of 30% TBP + n-dodecane in γ-radiolysis. *Soviet Radiochem.* 26(1): 29–36. (Translated from *Radiokhimiya* (26)1: 32–40.)

119. Vladimirova, M.V., Fedoseev, D.A., Milanova, A.S., Boikova, I.A. 1987. Actinoid radiation chemistry in solvent extraction systems. 5. Pu(IV) + Zr(IV) in 30% TBP + *n*-dodecane on γ-radiolysis. *Soviet Radiochem.* 29(1): 84–88. (Translated from *Radiokhimiya* 29(1): 87–92.)

120. Hahn, H.T., Vander Wall, E.M. 1964. Complex formation in the dilute uranyl nitrate-nitric acid-dibutyl phosphoric acid-tributyl phosphate-amsco system. *J. Inorg. Nucl. Chem.* 26: 191–192.

121. Mikhailov, V.A., Grigor'eva, E.F. 1964. Salts of dialkyl hydrogen phosphates. *J. Inorg. Chem.* 9: 477–481.

122. Krutikov, P.G., Solovkin, A.S. 1970. (Di-n-butyl phosphato)-compounds of uranyl. *Russ. J. Inorg. Chem.* 15(6): 825–827.

123. Teterin, E.G., Shesterikov, N.N., Krutikov, P.G., Solovkin, A.S. 1971. Infrared spectroscopic study of the zirconium complex of di-n-butyl phosphoric acid (DBP). *Russ. J. Inorg. Chem.* 16: 77–80.

124. Burns, J.H. 1983. Solvent-extraction complexes of the uranyl ion. 2. Crystal and molecular structures of *catena*-Bis(μ-di-*n*-butyl phosphato-*O,O'*) dioxouranium(VI) and Bis(μ-di-*n*-butyl phosphato-*O,O'*)bis[(nitrato)(tri-*n*-butylphophine oxide) dioxouranium(VI)]. *Inorg. Chem.* 22: 1174–1178.

125. Sokina, L.P., Solovkin, A.S., Teterin, E.G., Bogdanov, F.A., Shesterikov, N.N. 1978. Dibutyl phosphates of tetravalent plutonium, zirconium, and thorium, formed in solutions of tri-*n*-butyl phosphate (TBP). *Soviet Radiochem.* 20(1): 19–24. (Translated from *Radiokhimiya* 20(1): 28–34.)

126. Vladimirova, M.V., Fedoseev, D.A., Teterin, E.G., Boikova, I.A., Kuzinets, I.E., Milanova, A.S., Shesterikov, M.N., Ragimov, T.K. 1985. Radiation chemical behavior of actinides in extraction systems. III. Pu(IV) precipitates from gamma-irradiated 30% TBP + *n*-dodecane. *Soviet Radiochem.* 27(6): 748–755. (Translated from *Radiokhimiya* (27)6: 804–812.)

127. Fedosev, D.A., Artemova, L.A., Romanovskaya, I.A., Dunaeva, M.Y., Vladimirova, M.V. 1996. Radiation-chemical behavior of plutonium in the 30% tributyl phosphate + *n*-dodecane system under conditions of repeated γ-irradiation and regeneration of extractant. *Radiochemistry* 38(1): 78–80. (Translated from *Radiokhimiya* 38(1): 84–87.)

128. Sugai, H. 1992. Crud in solvent washing process for nuclear fuel reprocessing. *J. Nucl. Sci. Technol.* 29: 445–453.

129. Guedon, V., Thieblemont, J.C., Revel, Y. 1994. Etude de la précipitation des produits de fission ou de corrosion sous l'effet de la dégradation radiolytique du solvent de retraitement. *J. Nucl. Sci. Technol.* 31(1): 48–61.

130. Uetake, N. 1989. Precipitation formation of zirconium-dibutyl phosphate complex in PUREX process. *J. Nucl. Sci. Technol.* 23(3): 329–338.

131. Mesisenhelder, J.H., Siczek, A.A. 1980. An infrared study of zirconium retention in 30% tributyl phsophate. *Radiochim. Acta* 27: 223–227.

132. Edwards, H.G.M., Hugues, M.A., Smith, D.N., Courtney, B. 1995. Preparation and vibrational spectroscopy of di-*n*-butyl phosphate complexes of zirconium nitrate. *J. Mol. Struct.* 351: 65–76.

133. Zhang, P., Kimura, T. 2006. Complexation of Eu(III) with dibutyl phosphate and tributyl phosphate. *Solvent Extr. Ion Exch.* 24: 149–163.

134. Maya, L. 1981. Zircoium behavior in the system HNO_3-30% tributyl phosphate-dodecane in the presence of monobutyl phosphoric acid. *J. Inorg Nucl. Chem.* 43: 379–384.

135. Lane, E.S. 1963. Performance and degradation of diluents for TBP and the cleanup of degraded solvents. *Nucl. Sci. Eng.* 17: 620–625.

136. Healy, T.V., Pilbeam, A. 1974. Metal retention by hydroxamic acids in irradiated TBP solutions. *Proceedings of the International Solvent Extraction Conference ISEC'74*, 8–14 September, Lyon, France, Vol. 1, 459–467.

137. Zaitsev, V.D., Karasev, A.L., Egorov, G.F. 1987. Formation of hydroxamic acids in the radiolysis of tri-n-butyl phosphate containing nitric acid. *Soviet Atomic Energy* 63(1): 524–527. (Translated from *Atomnaya Énergiya* 63(1): 26–29.)

138. Di Furia, F., Modena, G., Scrimin, P., Gasparini, G.M., Grossi, G. 1982–1983. The role of hydroxamic acids in the retention of fission products in TBP diluents. A quantitative study in a model system. *Sep. Sci. Technol.* 17(12): 1451–1468.

139. Ishihara, T., Ohwada, K. 1966. Chemical degradation of kersosene diluent with nitric acid. *J. Nucl. Sci. Technol.* 3(1): 20–26.

140. Stieglitz, L. 1971. Investigation on the nature of degradation products in the system 20 vol.-% tributyl phosphate-dodecane-nitric acid. I. Enrichment of complexing products and infra-red study. *Proceedings of the International Solvent Extraction Conference*, 19–23 April, Society of Chemical Industry: London, Vol. I, 155–159.

141. Stieglitz, L., Becker, R. 1982. Chemical and radiolytic solvent degradation in the PUREX process, in *Nukleare Entsorgung Nuclear Fuel Cycle*; Baumgärtner, F., Ebert, K., Gelfort, E., Lieser, K.H. Eds.; Verlag-Chemie: Weinheim, Deerfield Beach, FL, Basel, 333–350.

142. Nowak, Z., Nowak, M. 1981. Examination of the interfacial tension of the radiation degraded TBP-diluent systems. *Nukleonika*, 26(1): 19–26.

143. Ginisty, C., Guillaume, B. 1990. Solvent distillation studies for a PUREX reprocessing. *Sep. Sci. Technol.* 25(13–15): 1941–1952.

144. Huss, V. 1991. Etude de la dégradation d'un solvant industriel : le mélange TBP/isopar. PhD thesis: Thèse de l'université d'Aix Marseille III.

145. Tallent, O.K., Mailen, J.C., Dodson, K.E. 1985. PUREX diluent chemical degradation. *Nucl. Technol.* 71: 417–425.

146. Ikeda, H. 2004. Safety design of PUREX liquids system – The flash and fire points. *J. Nucl. Sci. Technol.* 41(4): 534–536.

147. Sugai, H., Munakata, K. 1992. Destruction of emulsions stabilized by precipitates of zirconium and tributyl phosphate degradation products. *Nucl. Technol.* 99: 235–241.

148. Araujo, B.F., Matsuda, H.T., Kuada, T.A., Araujo, J.A. 1992. Continuous removal of radiolytic products from TBP extraction systems. *J. Radioanal. Nucl. Chem. Lett.* 166(1): 75–84.

149. Germain, M., Pluot, P. 1980. Diluent washing of aqueous phase using centrifugal contactors. *Proceedings of the International Solvent Extraction Conference ISEC'80*, 6–12 September, Liege, Belgium, 80–218.

150. Mailen, J.C. 1988. Secondary Purex solvent cleanup: Laboratory development. *Nucl. Technol.* 83: 182–189.

151. Reif, D.J. 1988. Canyon solvent cleaning with activated alumina. *Nucl. Technol.* 83: 190–196.

152. Vladimirova, M.V., Fedoseev, D.A., Boikova, I.A., Milanova, A.S. 1987. Actinoid radiation chemistry in solvent-extraction systems. 6. Pu(IV) in 33% TIAP + n-dodecane on γ-radiolysis. *Soviet Radiochem.* 29(1): 89–94. (Translated from *Radiokhimiya* (29) 1: 92–99.)

153. Venkatesan, K.A., Robertselvan, B., Antony, M.P., Srinivasan, T.G., Vasudeva Rao, P.R. 2006. Physical and plutonium retention properties of hydrolytic and radiolytically degraded tri-*n*-amyl phosphate. *Solvent Extr. Ion Exch.* 24: 747–763.

154. Weaver, B., Kappelmann, F.A. 1964. TALSPEAK: A new method of separating americium and curium from the lanthanides by extraction from an aqueous solution of aminopolyacetic acid complex with a monoacidic organophosphate or phosphonate. *Report ORNL-3559*, Oak Ridge National Laboratory, Oak Ridge, TN.

155. Weaver, B., Kappelmann, F.A. 1968. Preferential extraction of lanthanides over trivalent actinides by monoacidic organophosphates from carboxylic acids and from mixtures of carboxylic and aminopolyacetic acids. *J. Inorg. Nucl. Chem.* 30: 263–272.

156. Hérès, X., Nicol, C., Bisel, I., Baron P., Ramain, L. 1999. Paladin: A one step process for actinide(III)/fission product separation. *Proceedings of the International Conference on Future Nuclear Systems, Global'99*: *Nuclear Technology – Bridging the Millennia*, Jackson Hole, WY, 29 August to 3 September, American Nuclear Society: La Grange Park, IL, 585–591.

157. Nilsson, M., Nash, K.L. 2007. Review article: A review of the development on operational characteristics of the TALSPEAK process. *Solvent Extr. Ion Exch.* 25: 665–701.

158. Schulz, W.W. 1972. Radiolysis of Hanford B Plant HDEHP extractant. *Nucl. Technol.* 13: 159–167.

159. Tachimori, S., Ito, Y. 1979. Radiation damage of organic extractant in partitioning of high-level liquid waste, (I) Radiolysis of di(2-ethylhexyl)phosphoric acid by irradiation with cobalt-60 gamma rays. *J. Nucl. Sci. Technol.* 16(1): 49–56.

160. Tachimori, S. 1979. Radiation effects on the extraction of americium (III) with di(2-ethylhexyl) phosphoric acid. *J. Radioanal. Chem.* 50(1–2): 133–142.

161. Tachimori, S., Nakamura, H. 1979. Radiation effects on the separation of lanthanides and transplutonides by the Talspeak-type extraction. *J. Radioanal. Chem.* 52(2): 343–354.

162. Tachimori, S., Kroos, B., Nakamura, H. 1978. Effect of radiolysis products of di-(2ethylhexyl)phosphoric acid upon the extraction of lanthanides. *J. Radioanal. Chem.* 43: 53–63.

163. Tachimori, S. 1978. Effects of radiolysis of di(2-ethylhexyl)phosphoric acid upon the extraction of strontium(II). *J. Radioanal. Chem.* 44: 25–35.

164. Mannone, F., Dwoschak, H. 1984. Chemical separation of actinides from high activity liquid wastes – Final report. *JRC Ispra Report*, S.A./1.07.03.84.02.

165. Tachimori, S. 1979. Synergistic extraction of americium with MEHPA-DEHPA mixed solvent from nitric acid solution. *J. Radioanal. Chem.* 49(1): 31–35.

166. Morita, Y., Kubotas, M., Shin, Y.J. 1990. Radiolysis of diisodecyl phosphoric acid and its effect on the extraction of neptunium. *Solvent Extr. Ion Exch.* 8(4&5): 529–555.

167. Zhang, P., Song, C.L., Liang, J.F., Xin, R.X. 2001. Extraction and retention of plutonium with γ-irradiated 30% trialkyl phosphine oxide-kerosene solution. *Solvent Extr. Ion Exch.* 19(1): 79–89.

168. Glatz, J.P., Song, C., Koch, L., Bokelund, H., He, X. 1995. Hot tests of the TRPO process for the removal of TRU elements from HLLW. *International Conference on Evaluation of Emerging Nuclear Fuel Cycle Systems: Global'95,* Versailles, France, 10–14 September.

169. Zhu, Y., Jiao, R. 1994. Chinese experience in the removal of actinides from highly active waste by trialkyl phosphine oxide extraction. *Nucl. Technol.* 108: 361–369.

170. He, X.H., Yan Y.S., Zhang, Q., Lui, B.R. 1998. Recent advances of annular centrifugal extractor for hot test of nuclear waste partitioning process. *Nucl. Sci. Technol.* 9: 157–162.

171. Jianchen, W., Chongli, S. 2001. Hot test of trialkyl phosphine oxide (TRPO) for removing actinides from highly saline high-level liquid waste (HLLW). *Solvent Extr. Ion Exch.* 19(2): 231–242.

172. Xuegang, L., Junfu, L., Jingming, X. 2004. Simplified Chinese TRPO Process to extract and recover transuranium elements from high-level liquid waste. *Solvent Extr. Ion Exch.* 22(2): 163–173.

173. Sätmark, B., Apostolidis, C., Courson, O., Malmbeck, R., Carlos, R., Pagliosa, G., Römer, K., Glatz, J.P. 2000. Advanced aqueous reprocessing in P&T strategies: process demonstrations on genuine fuels and targets. *Proceeding of the Conference Atalante 2000, Scientific Research on the Back-end of the Fuel Cycle for the 21st Century*, Avignon, France, 24–26 October, Paper No. O2-02.

174. Christiansen, B., Apostolidis, C., Carlos, R., Courson, O., Glatz, J.P., Malmbeck, R., Pagliosa, G., Römer, K., Serrano-Purroy, D. 2004. Advanced aqueous reprocessing in P&T strategies: process demonstrations on genuine fuels and targets. *Radiochim. Acta* 92: 475–480.

175. Zhu, Y., Chen, J., Jiao, R. 1996. Extraction of Am(III) and Eu(III) from nitrate solution with purified Cyanex 301. *Solvent Extr. Ion Exch.* 14(1): 61–68.

176. Tian, G., Zhu, Y., Xu, J. 2001. Extraction of Am(III) and Ln(III) by dialkyldithiophosphinic acid with different alkyl groups. *Solvent Extr. Ion Exch.*, 19(6): 993–1005.

177. Horwitz, E.P., Kalina, D.G. 1984. The extraction of Am(III) from nitric acid by octyl(phenyl)-N,N-diisobutylcarbamoylmethyl phosphine oxide-tri-n-butyl phosphate mixtures. *Solvent Extr. Ion Exch.* 2(2): 179–200.

178. Horwitz, E.P., Kalina, D.G., Diamond, H., Vandegrift, G.F. 1985. The TRUEX process – a process for the extraction of the transuranic elements from nitric acid wastes utilizing modified PUREX solvent. *Solvent Extr. Ion Exch.* 3(1&2): 75–109.

179. Vandegrift, G.F., Leonard, R.A., Steindler, M.A., Hortwitz, E.P., Basile, L.J., Diamond, H., Kalina, D.G., Kaplan, L. 1984. Transuranic decontamination of nitric acid solutions by the TRUEX solvent extraction process-preliminary development studies. Report *ANL-84-45*, Argonne National Laboratory, Argonne, IL.

180. Schultz, W.W., Horwitz, E.P. 1988. The Truex process and the management of liquid TRU waste. *Sep. Sci. Technol.* 23(12&13): 1191–1210.

181. Tse, P.K., Reichley-Yinger, L., Vandegrift, G.F. 1990. Truex process solvent clean-up with solid sorbents. *Sep. Sci. Technol.* 25(13–15): 1763–1775.

182. Sugo, Y., Izumi, Y., Yoshida, Y., Nishijima, S., Sasaki, Y., Kimura, T., Sekine, T., Kudo, H. 2007. Influence of diluent on radiolysis of amides in organic solution. *Rad. Phys. Chem.* 76: 794–800.

183. Sugo, Y., Sasaki, Y., Kimura, T., Sekine, T. 2007. Attempts to improve radiolytic stability of amidic extractants. *Proceeding of the International Conference on Advanced Nuclear Fuel Cycles and Systems, Global 2007,* Boise, ID, 9–13 September, 1870–1873.

184. Siddall, III, T.H. 1960. Effects of structure of N,N-disubstituted amides on their extraction of actinide and zirconium nitrates and of nitric acid. *J. Phys. Chem.* 64, 1863–1866.

185. Siddall, III, T.H. 1961. Application of amides as extractants. US AEC Report *DP 541*, E.I. Du Pont de Nemours and Co., Aiken, SC.

186. Gasparini, G.M., Grossi, G. 1980. Application of N,N-dialkyl amides in the separation of some actinides. *Sep. Sci. Technol.* 15(4): 825–844.

187. Gasparini, G.M., Grossi, G. 1986. Long chain disubstituted aliphatic amides as extracting agents in industrial applications of solvent extraction. *Solvent Extr. Ion Exch.* 4(6): 1233–1271.

188. Musikas, C. 1987. Solvent extraction for the chemical separations of the 5f elements. *Inorg. Chim. Acta* 140: 197–206.

189. Musikas, C. 1988. Potentiality of nonorganophosphorus extractants in chemical separations of actinides. *Sep. Sci. Technol.* 23(12&13): 1211–1226.

190. Condamines, N., Musikas, C. 1992. The extraction by *N,N*-dialkylamides. II. Extraction of actinide cations. *Solvent Extr. Ion Exch.* 10(1): 69–100.

191. Ruikar, P. B., Nagar, M.S., Subramanian, M.S., Gupta, K.K., Varadanajan, N., Singh, R.K. 1995. Extraction behavior of uranium (VI), plutonium(IV) and some fission products with gamma pre-irradiated *n*-dodecane solutions of *N,N'*-dihexyl substituted amides. *J. Radioanal. Nucl. Chem.* 1: 171–178.

192. Mowafi, E.A. 2004. The effect of previous gamma-irradiation on the extraction of U(VI), Th(IV), Zr(IV) Eu(III) and Am(III) by various amides. *J. Radioanal. Nucl. Chem.* 260(1): 179–187.

193. Manchanda, V.K., Pathak, P.N. 2004, Amides and diamides as promising extractants in the back end of the nuclear fuel cycle: an overview. *Sep. Purif. Technol.* 35: 85–103.

194. Ruikar, P.B., Nagar, M.S., Subramanian, M.S. 1993. Extraction of uranium, plutonium and some fission products with γ-irradiated unsymmetrical and branched chain dialkylamides. *J. Radioanal. Nucl. Chem., Lett.* 176(2): 103–111.

195. Revais, C. 1990, Etude du comportement d'un alkylamide: le *N,N*-di(2ethyl hexyl) hexanamide en vue de son utilisation comme extractant pour le retraitement des combustibles nucléaires, Thesis of the University J. Fourier, Grenoble.

196. Charbonnel, M.C. 1991. Private communication.

197. Pathak, P.N., Prabhu, D.R., Ruikar, P.B., Manchanda, V.K. 2002. Evaluation of di(2-ethylhexyl)isobutyramide (D2EHIBA) as a process extractant for the recovery of [233]U form irradiated Th. *Solvent Extr. Ion Exch.* 20(3): 293–311.

198. Suzuki, S., Yaita, T., Sugo, Y., Kimura, T. 2007. Study on selective separation of uranium(VI) by new *N,N*-dialkyl carboxamides. *Proceeding of the International Conference on Advanced Nuclear Fuel Cycles and Systems, Global 2007,* Boise, ID, 9–13 September, 1137–1141.

199. Sugo, Y., Sasaki, Y., Tachimori, S. 2002. Studies on hydrolysis and radiolysis of *N,N,N',N'*-tetraoctyl-3-oxapentane-1,5-diamide. *Radiochim. Acta* 90: 161–165.

200. Ruikar, P.B., Nagar, M.S., Subramanian, M.S. 1992. Extraction behavior of uranium, plutonium and some fission products with gamma-irradiated N,N'-dialkylamides. *J. Radioanal. Nucl. Chem.* 159(1): 167–173.

201. Bao, B., Shen, C., Bao, Y., Wang, G., Qian J., Cao, Z. 1994. Extraction of U(VI), Th(IV) and some fission products from nitric acid by N,N-disubstituted amides and effect of γ-ray irradiation on the extraction. *J. Radioanal. Nucl. Chem.* 178(1): 99–107.

202. Baron, P., Berthon, L., Charbonnel, M.C., Nicol, C. 1997. State of progress of Diamex process. *Proceedings of the International Conference on Future Nuclear Systems, Global' 97, Challenge Towards Second Nuclear Era with Advanced Fuel Cycles*, 5–10 October, Yokohama, Japan.

203. Madic, C., Lecomte, M., Baron, P., Boullis, B. 2002. Separation of long-lived radionuclides from high active nuclear waste. *C.R. Phys.* 3: 797–811.

204. Facchini, A., Amato, L., Modolo, G., Nannicini, R., Madic, C., Baron, P. 2000. Transient- and steady-state concentration profiles in a Diamex-like countercurrent process for Am(III) + Ln(III) separation. *Sep. Sci. Technol.* 35(7): 1055–1068.

205. Malmbeck, R., Courson, O., Pagliosa, G., Römer, K., Sätmark, B., Glatz, J.P., Baron, P. 2000. Partitioning of minor actinides from HLLW using the DIAMEX process. Part 2 – 'Hot' continuous counter-current experiment. *Radiochim. Acta* 88: 865–871.

206. Courson, O., Lebrun, M., Malmbeck, R., Pagliosa, G., Römer, K., Sätmark, B., Glatz, J.P. 2000. Partitioning of minor actinides from HLLW using the DIAMEX process. Part 1- demonstration of extraction performances and hydraulic behaviour of the solvent in a continuous process. *Radiochim. Acta* 88: 857–863.

207. Serrano-Purroy, D., Baron, P., Christiansen, B., Glatz, J.P., Madic, C., Malmbeck, R., Modolo, G. 2005. First demonstration of a centrifugal solvent extraction process for minor actinides from a concentrated spent fuel solution. *Sep. Purif. Technol.* 45: 157–162.

208. Serrano-Purroy, D., Christiansen, B., Glatz, J.P., Malmbeck, R., Modolo, G. 2005. Towards a DIAMEX process using high active concentrate. Production of a genuine solution. *Radiochim. Acta* 93: 357–361.

209. Sorel, C. 2006. Technical feasibility of the Diamex process. In *Proceeding of Actinide and Fission Product Partitioning and Transmutation*, *Ninth Information Exchange Meeting*, Nimes, France, 25–29 September, 719–717.

210. Modolo, G., Vijgen, H., Serrano-Purroy, D., Christiansen, B., Malmbeck, R., Sorel, C., Baron, P. 2007. Diamex counter-current extraction process for recovery of trivalent actinides from simulated high active concentrate. *Solvent Extr. Ion Exch.* 42: 439–452.

211. Baron, P., Hérès, X., Lecomte, M., Masson, M. 2001. Separation of the minor actinides: the DIAMEX-SANEX concept. *Proceedings of the International Conference on Back-end of the Fuel Cycle: From Research to Solutions (Global 2001)*, Paris, France, 9–13 September, 2001.

212. Gannaz, B., Chiarizia, R., Antonio, M.R., Hill, C., Cote, G. 2007. Extraction of Lanthanides(III) and Am(III) by mixtures of malonamide and dialkylphosphoric acid. *Solvent Extr. Ion Exch.* 25: 313–337.

213. Charbonnel, M.C., Berthon, L. 1998. Optimisation de la molecule extractante pour le procédé DIAMEX, in *Rapport Scientifique 1997*. CEA, Direction du Cycle du Combustible. Eds. Report: CEA-R-5801: 114–119.

214. Berthon, L., Camès, B. 2000. Procédé DIAMEX : Dégradation hydrolytique et radiolytique de l'extractant diamide DMDOHEMA, in *Rapport Scientifique 1999.* CEA, Direction du Cycle du Combustible. Eds. *Report:* CEA-R-5892: 206–211.

215. Cuillerdier, C., Musikas, C., Hoel, P., Nigond, L., Vitart, X. 1991. Malonamides as new extractants for nuclear waste solutions. *Sep. Sci. Technol.* 26(9): 1229–1244.

216. Thiollet, G., Musikas, C. 1989. Synthesis and uses of the amides extractants. *Solvent Extr. Ion Exch.* 7(5): 813–827.

217. Cames, B., Saucerotte, B., Faucon, M., Rudloff, D., Faucon, M., Bisel, I. 2006. DIAMEX solvent behaviour under continuous degradation and regeneration operation. *Proceeding of Actinide and Fission Product Partitioning and Transmutation*, *Ninth information Exchange Meeting*, Nimes, France, 25–29 September, 701.

218. Nicol, C., Cames, B., Margot, L., Ramain, L. 2000. DIAMEX solvent regeneration studies. *Proceeding of Atalante 2000, Scientific Research on the Back-end of the Fuel Cycle for the 21st Century,* 24–26 October, Avignon, France, 3–22.

219. Sasaki, Y., Sugo, Y., Suzuki, S., Tachimori, S. 2001. The novel extractants, diglycolamides, for the extraction of lanthanides and actinides in HNO_3-n-dodecane system. *Solvent Extr. Ion Exch.* 19(1): 91–103.

220. Sasaki, Y., Suzuki, S., Tachimori, S., Kimura, T. 2003. An innovative chemical separation process (ARTIST) for treatment of spent nuclear fuel. *Proceeding of the International Conference Global 2003*, New Orleans, LA, 16–20 November, 1266–1269.

221. Sasaki, Y., Kitatsyji, Y., Sugo, Y., Asakura, T., Kimura, T. 2007. Chemical separation of actinides from high level radioactive liquid waste using diglycolamide (DGA) compounds. *Proceeding of the International Conference on Advanced Nuclear Fuel Cycles and Systems, Global 2007*, Boise, ID, 9–13 September, 1117–1120.

222. Ansari, S.A., Pathak, P.N., Manchanda, V.K., Husain, M., Prasad, A.K., Parmar, V.S. 2005. *N,N,N',N*'-tetraoctyl diglycolamide (TODGA): a promising extractant for actinide-partitioning from high-level waste (HLW). *Solvent Extr. Ion Exch*. 23: 463–479.

223. Modolo, G., Vijgen, H., Schreinemachers, C., Baron, P., Dinh, B. 2003. TODGA process development for partitioning of actinides (III) from PUREX raffinate. *Proceeding of the International Conference Global 2003,* New Orleans, LA, 16–20 November, 1926–1930.

224. Asp, H., Modolo, G., Schreubemachers, C., Vijgen, H. 2006. Development of a TODGA process for co-separation of trivalent actinides and lanthanides form a high-active raffinate. *Proceeding of Actinide and Fission Product Partitioning and Transmutation*, *Ninth information Exchange Meeting*, Nimes, France, 25–29 September, 197–208.

225. Modolo, G., Asp, H., Vijgen H., Malmbeck, R., Magnusson, D., Sorel, C. 2007. Demonstration of a TODGA-based continuous counter-current extraction process for the partitioning of actinides from a PUREX raffinate. Part I: batch extraction optimization studies and stability tests. *Solvent Extr. Ion Exch.* 25: 703–721.

226. Modolo, G., Asp, H., Vijgen, H., Malmbeck, R., Magnusson, D., Sorel, C. 2007. Demonstration of a TODGA/BTP process for recovery of trivalent actinides and lanthanides from a PUREX raffinate. *Proceeding of the International Conference on Advanced Nuclear Fuel Cycles and Systems, Global 2007*, Boise, ID, 9–13 September, 1111–1116.

227. Modolo, G., Asp, H., Schreinemachers, C., Vijgen H. 2007. Development of a TODGA based process for partitioning of actinides from a PUREX raffinate. Part I: batch extraction optimization studies on stability tests. *Solvent Extr. Ion Exch.* 25: 703–721.

228. Modolo, G., Asp, H., Schreinemachers, C., Vijgen, H. 2008. Development of a TODGA based process for partitioning of actinides from a PUREX raffinate. Part II: centrifugal contactor runs. *Solvent Extr. Ion Exch.* 26: 62–76.

229. Sugo, Y., Sasaki, Y., Kimura, T., Sekine, T., Kudo, H. 2005. Radiolysis of TODGA and its effect on extraction of actinides ions. *Proceeding of the International Conference Global 2005,* Tsukuba, Japan, 9–13 October, Paper No. 368.

230. Cordier, P.Y., Hill, C., Baron, P., Madic, C., Hudson, M.J., Liljenzin, J.O. 1998. Am(III)/Eu(III) separation at low pH using synergistic mixtures composed of carboxylic acids and neutral nitrogen polydendate ligands. *J. Alloys Comp*. 271–273: 738–741.

231. Cordier, P.Y., François, N., Boubals, N., Madic, C., Hudson, M.J., Liljenzin J.O. 1999. Synergistic systems for the selective extraction of trivalent actinides from mixtures of trivalent actinides and lanthanides. In *Solvent Extraction for the 21st Century, Proceedings of International Solvent Extraction Conference, ISEC'1999*;. Cox, M., Hidalgo, M.,. Valiente, M. Eds.; Society of Chemical Industry (SCI): London, Vol. 1, 317–322.

232. Enarsoson, A., Spjuth, L., Liljenzin, J.O., Källvenius, G., Hudson, M.J., Iveson, P.B., Russell, M.L., Madic, C., Cordier, P.Y. 1999. Separation of trivalent americium and europium with some substituted oligopyridines and triazines in synergy with 2-bromo-decanoic acid. In *Solvent Extraction for the 21st Century, Proceedings of International Solvent Extraction Conference, ISEC'1999*; Cox, M., Hidalgo, M., Valiente. M. Eds.; Society of Chemical Industry (SCI): London, Vol. 1, 323–328.

233. Hagström, I., Spjuth, L., Enarsson, A., Liljenzin, J.O., Skalberg, M.A., Hudson, M.J., Iveson, P.B., Madic, C., Cordier, P.Y., Hill, C., François, N. 1999. Synergistic solvent extraction of trivalent americium and europium by 2-bromodecanoic acid and neutral nitrogen-containing reagents. *Solvent Extr. Ion Exch.* 17(2): 221–242.

234. Kolarik, Z., Müllich, U., Gassner, F. 1999. Selective extraction of Am(III) over Eu(III) by 2,6-ditriazolyl- a,d 2,6-ditriazinylpyridines. *Solvent Extr. Ion Exch.* 17(1): 23–32.

235. Hill, C., Heres, X., Calor, J.N., Guillaneux, D., Mauborgne, B., Rat, B., Rivalier, P., Baron, P. 1999. Trivalent actinides/lanthanides separation using bis-triazinyl-pyridines. *Proceedings of the International Conference on Future Nuclear Systems, Global'99*: *Nuclear Technology – Bridging the Millennia*, Jackson Hole, WY, 29 August to 3 September, American Nuclear Society, Inc.: La Grange Park, IL.

236. Hill, C., Guillaneux, D., Berthon, L. 2002. Sanex-Btp process development studies, in *Proceeding of the International Solvent Extraction Conference ISEC 2002*; K.C. Sole, P.M. Cole, J.S. Preston, D.J. Robinson Eds.; South African Institute of Mining and Metallurgy: Johannesburg, 1205–1209.

237. Nilsson, M., Anderson, S., Drouet, F., Ekberg, C., Foreman, M., Hudson, M., Liljenzin, J.O., Magnusson, D., Skarnemark, G. 2006. Extraction properties of 6,6-bis-(5,6-dipentyl-[1,2,4] triazin-3-yl)-[2,2']bipyridinyl (C5-BTBP). *Solvent Extr. Ion Exch.* 24: 299–318.

238. Nilsson, M., Ekberg, C., Foreman, M., Hudson, M., Liljenzin, J.O., Modolo, G., Skarnemark, G. 2006. Separation of actinides(III) from lanthanides(III) in simulated nuclear waste streams using 6,6'-bis-(5,6-dipentyl-[1,2,4] triazin-3yl)-[2,2']bipyridinyl (C5-BTBP) in cyclohexanone. *Solvent Extr. Ion Exch.* 24: 823–843.

239. Geist, A., Hill, C., Modolo, G., Foreman, M.R.J., Weigl, M., Gompper, K., Hudson, M.J. 2006. 6,6'-Bis(5,5,8,8-tetramethyl-5,6,7,8-tetrahydro-benzo[1,2,4]triazin-3-yl) [2,2'] bipyridine, an effective extracting agent for the separation of americium(III) and curium(III) from the lanthanides. *Solvent Extr. Ion Exch.* 24: 463–483.

240. Hill, C., Berthon, L., Madic, C. 2005. Study of the stability of BTP extractants under radiolysis. *Proceeding of the International Conference Global 2005*, Tsukuba, Japan, 9–13 October, Paper No. 283.

241. Nilsson, M., Anderson, S., Ekberg, C., Foreman, M.R.S., Hudson, M.J., Skarnemark, G. 2006. Inhibiting radiolysis of BTP molecules by addition of nitrobenzene. *Radiochim. Acta* 64: 103–106.

242. Retegan, T., Ekberg, C., England, S., Fermvik, A., Foreman, M.R.S., Skarnemark, G. 2007. The behaviour of organic solvents containing C5-BTBP and CyMe4-BTBP at low irradiation doses. *Radiochim. Acta* 95: 637–642.

243. Hudson, M.J., Boucher, C.E., Braekers, D., Desreux, J.F., Drew, M.G.B., Foreman, M.R.St J., Harwood, L.M., Hill, C., Madic, C., Marken, F., Youngs, T.G.A. 2006. New bis(triazinyl) pyridines for selective extraction of americium(III). *New J. Chem.* 30: 1171–1183.

244. Hill, C., Guillaneux, D., Berthon, L., Madic, C. 2002. Sanex-Btp process development studies. *J. Nucl. Sci. Technol.* Suppl 3: 309–312.

245. Foreman, R.S., Hudson, M.J., Drew, M.G.B., Hill, C. Madic, C. 2006. Complexes formed between the quadridentate heterocyclic molecules 6,6'-bis-(5,6-dialkyl-s1,2,4-triazin-3-yl)-2,2'-bipyridine (BTBP) and lanthanides(III): Implications for the partitioning of actinides(III) and lanthanides(III). *Dalton Trans.* 9: 1645–1653.

246. Blasius, E., Klein, W., Schön, U. 1985. Separation of strontium from nuclear waste solutions by solvent extraction with crown ethers. *J. Radioanal. Nucl. Chem.* 89(2): 389–398.

247. Horwitz, E.P., Dietz, M.L., Fisher, D.E. 1990. Extraction of strontium from nitric acid solutions using dicyclohexano-18crown-5 and its derivatives. *Solvent Extr. Ion Exch.* 8(4&5): 557–572.

248. Horwitz, E.P., Dietz, M.L., Fisher, D.E. 1991. SREX: a new process the extraction and recovery of strontium from acidic nuclear waste streams. *Solvent Extr. Ion Exch.* 9(1): 1–25.

249. Dietz, M.L., Horwitz, E.P., Jensen, M.P., Rhoads, S. 1996. Substituted effects in the extraction of cesium from acidic nitrate media with macrocyclic polyethers. *Solvent Extr. Ion Exch.* 14(3): 357–384.

250. Sacheben, R.A., Deng, Y., Moyer, B.A. 1997. Ion-pair extraction of alkali metal nitrate salts by lipohilic, benzo-substituted 24-crown-8 ethers. *Sep. Sci. Technol.* 32(1–4): 275–284.

251. Lemaire, M., Guy, A., Chomel, R., Foos, J. 1991. Dicyclohaxano-18-crown-6 ether: a new selective extractant for nuclear fuel reprocessing. *J. Chem. Soc. Chem. Commun.* 1152–1154.

252. Draye, M., Favre-Reguillon, A., Chomel, R., Faure, R., Guy, A., Foos, J., Lemaire, M. 1996. Radiochemical stability of the dicyclohexano-18-crown-6 ether (DCH18C6): synthesis and tests in radioactive medium of the DCH18C6 radiolytic products. *Bull. Soc. Chim. Fr.* 133, 183–197.

253. Draye, M., Favre-Reguillon, A., Foos, J., Guy, A., Lemaire, M. 1997. Radiochemical stability of dicyclohecano-18-crown-6 ether (DCH18C6) and its use in a recovery process of strontium from acidic nuclear waste stream. *Radiochim. Acta* 78: 105–109.

254. Tagaki, N., Izumi, Y., Ema, K., Yamamoto, T., Nishizawa, T. 1999. Radiolytic degradation of a crown ether for extractability of strontium. *Solvent Extr. Ion Exch.* 17(6): 1461–1471.

255. Matel, L., Bilbao, T. 1989. Extraction of strontium using an irradiated extraction agent of crown structure. *J. Radioanal. Nucl. Chem.* 137(3): 183–190.

256. Shukla, J.P., Kumar, A., Singh, R.K. 1994. Influence of gamma-irradiation on extraction and cation-transport of uranium(VI) and plutonium(IV) by dicyclohexano-18-crown-6. *J. Nucl. Sci. Technol.* 31(10): 1066–1072.

257. Haverlock, T.J., Bonnesen, P.V., Sacheben, R.A., Moyer, B.A. 1997. Applicability of a calixarene-crown compound for the removal of cesium from alkaline tank waste. *Radiochim. Acta* 76: 103–108.

258. Bonnesen, P.V., Delmau, L.H., Moyer, B.A. 2000. A robust alkaline-side CSEX solvent suitable for removing cesium from Savannah River high level waste. *Solvent Extr. Ion Exch.* 18(6): 1079–1107.

259. Leonard, R.A., Conner, C., Liberatore, M.W., Sedlet, J., Aase, S.B., Vandegrift, G.F., Delmau, L.H., Bonnesen, P.V., Moyer, B.A. 2001. Development of a solvent extraction process for cesium removal from SRS tank waste. *Sep. Sci. Technol.* 36(5&6): 743–766.

260. Dozol, J.F., Simon, N., Lamare, V., Rouquette, H., Eymard, S., Tournois, B., De Marc, D. 1999. A solution for cesium removal from high-salinity acidic or alkaline liquid waste: the crown calix[7]arenes. *Sep. Sci. Technol.* 34(6&7): 877–909.

261. Grunder, M., Dozol, J.F., Asfari, Z., Vicens, J. 1999. Simultaneous removal of technetium and cesium by functionalized calixarenes from acidic liquid waste. *J. Radioanal. Nucl. Chem.* 241(1): 59–67.

262. Riddle, C.L., Baker, J.D., Law, J.D., Mc Grath, C.A., Meikrantz, D.H., Mincher, B.J., Peterman, D.R., Todd, T.A. 2005. Fission product extraction (FPEX): Development of a novel solvent for the simultaneous separation of strontium and cesium from acidic solutions. *Solvent Extr. Ion Exch*. 23: 449–461.

263. Mariani, M., Macerata, E., Galletta, M., Buttafava, A., Casnati, A., Ungaro, R., Faucitano, A., Giola, M. 2007. Partitioning of minor actinides: Effect of gamma irradiation on the extracting capabilities of selected calixarene-based picolinamide ligand. *Rad. Phys. Chem.* 76: 1285–1289.

264. Casnati, A., Della Ca', N., Fontanella, M., Sansone, F., Ugozzoli, F., Ungaro, R., Liger, K., Dozol, J.F. 2005. Calixarene based picolinamide extractant for the selective An/Ln separation from radioactive waste. *Eur. J. Org. Chem.* 11: 2338–2348.

265. White, T.L., Peterson, R.A., Wilmarth, W.R., Norato, M.A., Crump, S.L., Delmau, L.H. 2003. Stability study of Cs extraction solvent. *Sep. Sci. Technol*. 38: 2667–2683.

266. Tran-Thi, T.H., Koulkès-Pujo, A.M., Sutton, J., Anitoff, O. 1984, Pulse radiolysis of amides and their aqueous organic mixtures. Effect of the environment on the reactivity of the presolvated electrons. *Radiat. Phys. Chem.* 23(1–2): 77–87.

267. Dusaucy, A.C., De Doncker, J., Couillard, C., De Laet, M., Tilquin, B. 1987. Radical production evidenced by dimer analysis in γ-irradiated amides in aqueous solutions and in the solid state. *J. Chem. Soc. Faraday Trans. I* 83: 125–133.

268. Simic, M., Hayon, E. 1973. Interaction of solvated electrons with the amide and amide groups. Acid-base properties of $RC(OH)NH_2$ radicals. *J. Phys. Chem*. 77(8): 996–1001.

269. Tran-Thi, T.H., Koulkès-Pujo, A.M. 1983. Electron and organic radical anion solvation. Pulse radiolysis of tetrahydrofuran and its solutions of N-methylacetamide or pyrrolidone. *J. Phys. Chem.* 87: 1166–1169.

270. Tran-Thi, T.H., Koulkès-Pujo, A.M., Gilles, L., Genies, M., Sutton, J. 1980. Transient species formed by pulse radiolysis of solutions of N-methylacetamide (NMA) in methyl cyanide. Comparison of the reaction mechanisms of electrolysis and radiation chemistry. *Radiat. Phys. Chem.* 15: 209–215.

271. Belevskii, V.N., Tyurin, D.A., Chuvylkin, N.D. 1998. Reactivity of radical cations in the radiolysis of amides. An ESR study and quantum chemical calculation. *High Energy Chem.* 32(5): 305–315. (Translated from *Khimiya Vysokikh Energii* 32(5): 342–352.)

272. Auslooss, P., Rebbert, R.E., Schwarz, F.P., Lias, S.G. 1983. Pulse- and gamma ray-radiolysis of cyclohexane: ion recombination mechanisms. *Radiat. Phys. Chem*. 21(1–2): 27–43.

273. Katsumura, Y., Yoshida, Y., Tagawa, S., Tabata, Y. 1983. Study on the excited state of liquid alkanes and energy transfer process by means of picosecond pulse radiolysis. *Radiat. Phys. Chem*. 21(1–2): 103–111.

274. Tagawa, S., Hayashi, N., Yoshida, Y., Washio, M., Tabata, Y. 1989. Pulse radiolysis studies on liquid alkanes and related polymers. *Radiat. Phys. Chem.* 34(4): 503–511.

275. Saeki, A., Kobawa, T., Yoshida, Y., Tagawa, S. 2001. Study on geminate ion recombination in liquid dodecane using pico- and subpicosecond pulse radiolysis. *Radiat. Phys. Chem.* 60: 319–322.

276. Soebianto, Y.S., Katsumura, Y. Ishigure, K., Kubo, J., Koizumi, T. 1992. Protection in radiolysis of n-hexadecane – 2. Radiolysis of n-hexadecane in the presence of additives. *Radiat. Phys. Chem.* 40(6): 451–459.

277. Soebianto, Y.S., Katsumura, Y., Ishigure, K., Kubo, J., Hamakawa, H., Kudoh, H., Seguchi, T. 1996. Radiation induced oxidation of liquid alkanes as a polymer model. *Radiat. Phys. Chem.* 48(4): 449–456.

278. Yoshida, Y., Ueda, T., Kobayashi, H., Tagawa, S. 1993. Studies of geminate ion recombination and formation of excited states in liquid *n*-dodecane by means of a new picosecond pulse radiolysis system. *Nucl. Instr. Meth. Phys. Res. A* 327: 41–43.

279. Kerr, C.M.L., Webster, K., Williams, F. 1972. Electron spin resonance evidence for dissociative electron capture in γ-irradiated phosphate esters. *J. Phys. Chem.* 76(20): 2848–2850.

280. Wu, J.L., Fu, Y.X., Wang, W.Q. 1984. Energy transfer kinetics in irradiated tributyl phosphate to diphenyl sulfoxide and methyl isobutyl ketone. *Radiat. Phys. Chem.* 23(5): 601–606.

281. Kuruc, J., Zubarev, V.E., Macášek, F. 1988. ESR spectra of radicals at a low-temperature X-radiolysis of phosphates. *J. Radioanal. Nucl. Chem. Lett.* 127(1): 37–49.

282. Kuruc, J., Zubarev, V.E., Bugaenko, L.T., Macášek, F. 1988. X- and gamma-radiolysis of phosphate esters. Electron spin resonance study by the spin trap technique. *J. Radioanal. Nucl. Chem. Lett.* 127(3): 177–192.

283. Zaitsev, V.D., Khaihin, G.I. 1989. Formation of solvated electrons during radiolysis of liquid tri-n-butyl phosphate. *High Energy Chem.* 23(2): 79–82. (Translated from *Khimiya Vysokikh Énergii* 23(2): 99–102.)

284. Zaitsev, V.D., Protasova, E.L., Khaikin, G.I. 1993. Kinetics of primary electron-ion pair recombination in liquid trialkyl phsophate radiolysis. *High Energy Chem.* 27(1): 28–34. (Translated from *Khimiya Vysokikh Énergii* 27(1): 30–36.)

285. Zaitsev, V.D., Protasova, E.L., Khaikin, G.I. 1994. Radiation-chemical behavior and spectral characteristics of solvated electrons in liquid trialkyl phosphates. *High Energy Chem.* 28(1): 21–24. (Translated from *Khimiya Vysokikh Énergii* (28)1: 30–33.)

286. Zaitsev, V.D., Khaikin, G.I. 1994. Precursors of dibutylphosphoric acid upon radiolysis of tributyl phosphate. *High Energy Chem.* 28(4): 269–272. (Translated from *Khimiya Vysokikh Énergii* (28)4: 308–311.)

287. Zhang, N., Wu, J.L. 1991. Scavenger effects in the radiolysis of cyclohexane: 4-methyl-4-phenyl-2-pentanone system and cyclohexane:tributyl phosphate system. *Radiat. Phys. Chem.* 38: 383–388.

288. Begum, A., Subramanian, S., Symons, M.C.R. 1970. Unstable intermediates. Part LXXI. Electron spin resonance spectra of γ-irradiated trimethyl phosphate. *J. Chem. Soc. A* 1334–1336.

289. Lucken, E.A.C. 1966. The electron spin resonance spectra of the free radicals arising from the action of Fenton's reagent on the methyl and ethyl esters of phosphoric and phosphonic acid. *J. Chem. Soc. A* 1354–1356.

290. Jin, H., Pan, X., Wu, J., Li, F., Lui, A., Gu, H. 1996. Microsecond pulse radiolysis of benzophenone tributyl phosphate system. *Radiat. Phys. Chem.* 47(6): 815–816.

291. Jin, H., Wu, J., Zhang, X., Fang, X., Yao, S., Zuo, Z., Lin, N. 1999. The examination of TBP excited state by pulse radiolysis. *Radiat. Phys. Chem.* 544: 245–251.

292. Du, Y., Wu, J., Li, F., Liu, A. 1999. A pulse radiolysis study on energy transfer mechanism in trioctylphosphineoxide-cyclohexane and tributylphosphate-cyclohexane systems by using benzophenone as a probe. *Radiat. Phys. Chem.* 54: 455–461.

293. Zhang, N., Wu, J.L. 1992. Using 4-methyl-4-phenyl-2-pentanone as a singlet probe of benzene, cyclohexane, tributyl phosphate and its multiple scavenger effects. *Radiat. Phys. Chem.* 39: 287–291.

294. Sheng, H.Y., Wang, Z.Z., Chen, Y.H., He, Y.H., Wang, Q.Z., Chen, J.T., Liu, R.Z. 1989. A study of the radiation chemistry of phosphorus compounds. *Radiat. Phys. Chem.* 33(6): 585–597.

295. Haase, K.D., Schulte-Frohlinde, D., Kourim, P., Vacek, K. 1973. Low-temperature radiolysis of organic phosphates studied by electron spin resonance. *Int. J. Radiat. Phys. Chem.* 5: 351–360.

296. Vashman, A.A., Savel'ev, Y.I. 1970. The formation of radicals in the low-temperature radiolysis of tributl phosphate and certain organophosphorus extraction reagents. *Soviet Radiochem.* 12(1): 9–13. (Translated from *Radiokhimiya* (12)1: 12–17.)

297. Holton, D.M., Edwards, P.P. 1984. Electrons, alkali metal-electron species, and radical anions in substituted organic amides. *J. Phys. Chem.* 88: 3855–3859.

298. Canva, J., Pagès, M. 1964. Effets des rayonnements ionisants sur le phosphate de tributyle (TBP). *Bull. Soc. Chim. France* 5: 909–911.

299. Giefer, D.L., Merklin, J.F. 1975. The radiolysis of decalin-TBP solutions. *Nucl. Instr. Meth.* 128: 609–610.

300. Dewar, M.J.S., Zoebisch, E.G., Healy, E.F., Stewart, J.J.P. 1985. AM1: A new general purpose quantum mechanical molecular model. *J. Am. Chem. Soc.* 107: 3902–3909.

301. Brede, O., Mehnert, R., Naumann, W. 1987. Kinetics of excitation and charge transfer reactions in non-polar media. *Chem. Phys.* 115: 279–296.

302. Katsumura, Y., Jiang, P.Y., Nagaishi, R., Oishi, T., Ishigure, K. 1991. Pulse radiolysis study of aqueous nitric acid solutions. Formation mechanism, yield, and reactivity of NO_3 radical. *J. Phys. Chem.* 95: 4435–4439.

303. Neta, P., Huie, R.E., Ross, A.B. 1988. Rate constant for reactions of inorganic radicals in aqueous solution. *J. Phys. Chem. Ref. Data* 17(3): 1027–1284.

304. Titov, A.I. 1963. The free radical mechanism of nitration. *Tetrahedron* 19: 557–580.

305. Nowak, Z., Nowak, M., Michalik, J., Owczarczyk, A. 1972. ESR study of irradiated TBP-dodecaneHNO$_3$ systems. *Radiochem. Radioanal. Lett.* 12(2–3): 78–88.

306. Clay, P.G., Witort, M. 1974. Radiolysis of tri-n-butyl phosphate in aqueous solution. *Radiochem. Radioanal. Lett.* 19(2): 101–107.

307. Banko, K., Nowak, M. 1986. The effect of some aromatic aldehydes on stabilization of extractives properties of PUREX-solvent. *Nukleonika* 31(10–12): 325–343.

308. Zhu, Y.J. 1985. Extraction of trivalent actinides with phosphone oxides, in *Handbook on the Physics and Chemistry of the Actinides*; Freeman, A.J., Keller, C. Eds.; Elsevier Science Publishers B.V.: Amsterdam, 469–511.

309. Menoyo, B., Elizalde, M.P., Almela, A. 2002. Determination of the degradation compounds formed by the oxidation of thiophosphinic acids and phosphine sulfides with nitric acid. *Anal. Sci.* 18: 799–804.

310. Rai, D., Strickert, R.G., Ryan, J.L. 1980. Alpha radiation induced production of HNO_3 during dissolution of Pu compounds. *Inorg. Nucl. Chem. Lett.* 16: 551–555.

311. Vladimirova, M.V., Kulikov, I.A., Bulkin, V.I., Sonovskii, O.A. 1989. TBP radiolysis kinetics in single-phase and two-phase systems. *Soviet Radiochem.* 31(1): 33–35. (Translated from *Radiokhimiya* 31(1): 36–39.)

312. Tashiro, Y., Kodama, R., Sugai, H., Suzuki, K., Matsuoka, S. 2000. Nonphosphate degradation products of tributylphosphate and their reactivities in purex media under extreme conditions. *Nucl. Technol.* 129: 93–100.

313. Egorov, G.F., Tkhorzhnitskii, G.P., Zilberman, B.Y., Shmidt, O.V., Goletskii, N.D. 2005. Radiation chemical behavior of tributyl phosphate, dibutylphosphoric acid, and its zirconium salt in organic solution and two-phase systems. *Radiochemistry* 47(4): 392–397 (Translated from *Radiokhimiya* 47(4): 359–363.)

314. Janata, E. 2003. Some examples of pulse radiolysis. *Rad. Phys. Chem.* 67, 287–290.

315. Macasek, F., Cech, R. 1984. Macrokinetics of radiolysis in systems with liquid-liquid partition of substrates. I – A general approach to mathematical models of simulated solvent extraction systems. *Rad. Phys. Chem*. 23(4): 473–479.

316. Macasek, F., Cech, R. 1984. Macrokinetics of radiolysis in systems with liquid-liquid partition of substrates. II. Radiation yields in 2-liquid systems. *Rad. Phys. Chem*. 23(4): 481–484.

317. Vladimirova, M.V., Fedoseev, D.A., Romanovskaya, I.A., Artemova, L.A., Gubina, M.Y. 1989. Radiation-chemical behavior of Np(VI) in irradiated solutions of tri-n-butyl phosphate. *Soviet Radiochem*. 31(1): 29–33. (Translated from *Radiokhimiya* 31(1): 32–36.)

318. Vladimirova, M.V., Fedoseev, D.A., Romanovskaya, I.A., Gubina, M.Y., Artemova, L.A. 1991. Radiation-chemical behavior of actinides in extraction systems. VII. Oxidation of U(IV) in solutions of TBP in *n*-dodecane. *Soviet Radiochem*. 33(6): 680–684. (Translated from *Radiokhimiya* 33(6): 118–125.)

319. Vladimirova, M.V. 1992. Mathematical modelling of radiation-chemical processes in HNO_3 solutions of Pu. 3. Refined quantitative characteristics of the model for 3 and 6M HNO_3. *Soviet Radiochem*. 34(6): 711–720. (Translated from *Radiokhimiya* 34(6): 89–102.)

320. Nagaishi, R. 2001. A model for radiolysis of nitric acid and its application to the radiation chemistry of uranium ion in nitric acid medium. *Rad. Phys. Chem*. 60(4–5): 369–375.

9 Automation of Extraction Chromatographic and Ion Exchange Separations for Radiochemical Analysis and Monitoring

Jay W. Grate and Matthew J. O'Hara
Pacific Northwest National Laboratory

Oleg B. Egorov
IsoRay Medical Inc.

CONTENTS

9.1 INTRODUCTION

Radiochemical analysis, complete with the separation of radionuclides of interest from the sample matrix and from other interfering radionuclides, is often an essential step in the determination of the radiochemical composition of a nuclear sample or process stream. Although some radionuclides can be determined nondestructively by gamma spectroscopy, where the gamma rays penetrate significant distances in condensed media and the gamma ray energies are diagnostic for specific radionuclides, other radionuclides that may be of interest emit only α or β particles. For these, samples must be taken for destructive analysis and radiochemical separations are required. However, even for gamma-emitting radionuclides, purification or concentration to a smaller volume in the range of a detector may be desirable and advantageous to facilitate detection and to provide better selectivity by reducing spectral complexity and interferences.

For process-monitoring purposes, the radiochemical separation and detection methods must be rapid so that the results will be timely. These results could be obtained by laboratory analysis or by radiochemical process analyzers operating on-line or at-site. In either case, there is a need for automated radiochemical analysis methods to provide speed, throughput, safety, and consistent analytical protocols. Classical methods of separation used during the development of nuclear technologies, namely manual precipitations, solvent extractions, and gravity-feed ion exchange, are slow and labor intensive. Fortunately, the convergence of digital instrumentation for pre-programed fluid manipulation and the development of new separation materials for column-based isolation of radionuclides has enabled the development of automated radiochemical analysis methodology.

Classic separation methods such as liquid-liquid extraction and ion exchange are well known.[1–3] Ion exchange is readily employed in column formats. Liquid-liquid extraction can also be implemented in column formats using solvent-impregnated resins as extraction chromatographic materials. The organic liquid extractant is immobilized in the pores of a polymer material. Under suitable conditions, the analyte of interest partitions into the immobilized organic phase while other matrix species and interferences are washed away in the mobile aqueous phase. After the wash step, retained analytes are rapidly released in one or more steps by changing the aqueous eluent, such that the analytes now partition back into the mobile phase. The development of solvent-impregnated resins, their physical chemistry, technological applications for metal and radionuclide recovery, and analytical uses were described in detail in volume 13 of this series by Cortina and Warshawsky.[4]

Column-based separation approaches are well suited for the isolation of radionuclides from complex sample matrixes in a rapid automated format. The development of automated radioanalytical methods is, in fact, closely coupled to the availability of extraction chromatographic materials. In this review, we will focus on the

application of radiochemical separations in automated fluidic formats for the analysis of radionuclide-containing samples.

9.2   SEPARATION APPROACHES

9.2.1   REQUIREMENTS FOR SEPARATIONS IN RADIOCHEMISTRY

Separations are essential in the determination of α- or β-emitting radionuclides from aqueous solutions. Short ranges and rapid energy dispersion in the liquid characterize these particles. β particles are emitted with broad energy spectra, and the β spectra of different radionuclides are not well resolved. Although α particles are emitted with characteristic energies, they are not detected with good energy resolution in liquids. Detection by scintillation does not provide adequate energy resolution for selective detection of individual α emitters. Thus, for radiometric analysis of aqueous samples, separations are required to remove interferences and isolate the α- or β-emitting radionuclide of interest prior to counting, and separations may be desirable for the radiometric determination of gamma-emitters from complex matrixes.

If α emitters are separated and collected by fraction collection, the preparation of very thin counting sources in a consistent matrix is required to obtain high-energy resolution. These are placed in close proximity to a diode detector, typically in vacuum. Nevertheless, α energy peak overlap can still occur for various combinations of radionuclides if they are not chemically separated, for example, ^{241}Am/^{238}Pu and ^{237}Np/^{234}U.

When using mass spectrometric detection, an intrinsically multivariate technique that is selective for particular mass-to-charge ratios, there are still significant reasons to perform separations first. In inductively coupled plasma mass spectrometer (ICP-MS), for example, it is desirable to separate the species of interest so that the sample is always introduced into the system in a consistent matrix.[5–7] Mass spectrometry is intrinsically subject to isobaric interferences as well as interferences created by the formation of molecular ions.[8–15] In addition, interferences can occur due to tailing of peaks when one isotope is present at a much higher concentration than an isotope with an adjacent mass number. Some examples of potential interferences in mass spectrometry include ^{238}U/^{238}Pu, ^{241}Pu/^{241}Am, ^{99}Tc/^{99}Ru, and ^{238}UH/^{239}Pu. A large excess of ^{238}U could interfere in the measurement of ^{237}Np. The use of ICP-MS for radiochemical analysis has been reviewed recently, and interference issues were discussed in detail.[14,15]

Both radiometric and mass spectrometric detection approaches have been used in automated radiochemical analysis, depending on the radionuclides of interest and the capabilities of the laboratory involved. The tradeoffs between radiation counting and atom counting have been described.[14,16,17] Short-lived fission products may be advantageously detected with radiation detection, whereas long-lived (low specific activity) radionuclides can be determined with better sensitivity using ICP-MS.

In the analysis of total uranium, colorimetric detection methods are also possible, depending on the detection limits required. This is a case of measuring a radioactive element, as opposed to a specific radioisotope of an element. In this case, separation methods are used to preconcentrate the uranium to increase the analysis sensitivity and decrease the detection limits.[18–21]

9.2.2 Solid-Phase Separation Materials for Radiochemical Analysis

The most important solid-phase separation materials for column-based separations in modern radioanalytical chemistry are extraction chromatographic materials, and these have been particularly important in automated radioanalytical chemistry. Solid-phase extraction materials based on the covalent attachment of ligands to solid supports also exist, and they have found application in large-scale separation processes for waste or effluent treatment.[22–25] They have been commercialized as "Analig" or "SuperLig" materials by IBC Advanced Technologies (American Fork, UT). However, they are less well characterized or used for small-column analytical separations.

Extraction chromatographic materials for analytical separations have been commercialized by Eichrom Technologies, Inc. (Darien, IL). These typically use extractants and solvents known in the field of liquid/liquid extraction for radiochemical separations. Some of the extractants and solvents used are shown in Scheme 9.1.

DtBuCH18C6 (in Sr Resin)

Aliquat 336 (in TEVA-Resin)

CMPO (in TRU-Resin)

DP[PP] (in UTEVA-Resin)

HDEHP (in Ln Resin)

H2DEH[MDH]
(DIPEX extractant in Actinide Resin)

DGA (in DGA=Resin)
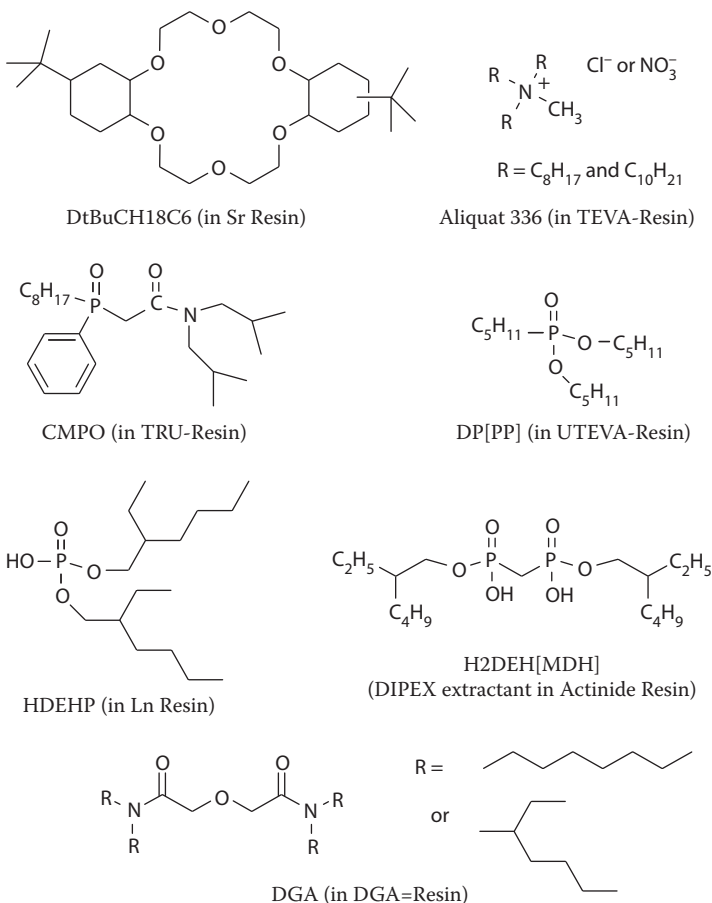
SCHEME 9.1

The selectivity of the solvent-impregnated resins generally follows from the known selectivity of the liquid/liquid extraction system, although exceptions have been noted. Horwitz, Dietz, and coworkers at Argonne National Laboratory pioneered the development of these extraction chromatographic materials and their analytical uses.[26–29] The weight distribution ratios, D_w, and column capacity factors, k', for radionuclides and potential interferences are well characterized in the literature. The weight distribution ratio, D_w, is the ion quantity per weight of resin divided by the ion quantity per volume of solution at equilibrium, typically in milliliters per gram. For radioactive isotopes, this is determined in a batch contact experiment where the activity of the solution is known before, A_o, and after equilibrating with the resin material, A_s, according to $D_w = ((A_o - A_s)/W)/(A_s/V)$, where W is the weight of the resin and V is the volume of the solution. The capacity factor, $k' = D(V_s/V_m)$, which indicates the number of free column volumes to peak maximum, is given by the volume distribution ratio, D, times the phase volume ratio, where V_s is the volume of the stationary phase and V_m is the volume of the mobile phase.[30,31] The volume distribution ratio, D, as normally determined in liquid-liquid extraction, can be obtained by dividing the milliliter of organic extractant or solution per gram of resin into D_w. The validity of the relationships between D, D_w, and k' have been verified experimentally.[4]

Extraction chromatography can be differentiated from other forms of chromatography as follows. Classical chromatography utilizes differences in distribution ratios to achieve separation as species migrate at different rates down a column. Ion chromatography binds all appropriately charged ions, which are then gradually eluted by increasing the eluting power of the mobile phase. Extraction chromatography selectively binds particular species or groups of species according to the complexants or extractants used in the immobilized organic phase. After the wash step, the selected species are abruptly released by changes in the mobile phase or by carrying out reaction chemistry (e.g., redox reactions) on the sorbed species. Thus, this separation format relies on the selective uptake and release properties of the separation material, rather than on the high chromatographic efficiency of a long separation column.

Extraction chromatographic methods generally provide columns with high capacities, tolerate high levels of potential interferences and a variety of sample matrixes, allow flexibility in sample loading conditions, and work at low pressures. These are the features that are well suited for radiochemical separations in general and automated radiochemical separations in particular.

9.3   AUTOMATION APPROACHES

9.3.1   Fluidic Methods

Fluidic approaches move samples, reagents, and eluents from place to place entirely through a system of pumps, valves, and tubing. Fluidic methodology from the field of flow injection (FI) analysis has been adapted to the needs of automated radiochemistry. In its original form, FI used a multichannel peristaltic pump and an injection valve in a continuous forward flow paradigm to mix the sample with reagents and
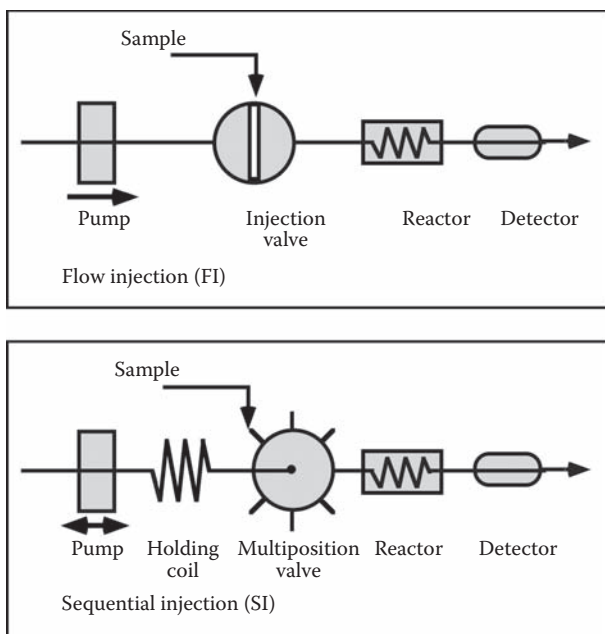
FIGURE 9.1 Schematic diagrams of flow injection and sequential injection fluidic automation approaches.

deliver the products to a flow-through detector.[32–34] This approach has been used to automate serial assays for many application areas, including environmental measurements, biochemistry, and clinical analysis. A schematic diagram of a typical FI approach is shown in Figure 9.1.

Further developments in the field lead to sequential injection (SI) methods that use programmed flow, including flow reversals, with a digital syringe pump as the preferred fluid drive.[34–43] Samples, reagents, or eluents are selected by the multiposition valve and pulled into a holding coil. By changing the position of the valve and reversing the pump flow direction, the solution that was pulled into the holding coil can be pushed out to the downstream reactor, separation column, and/or detector. A typical SI system is shown schematically in Figure 9.1. To automate separations, a column can be included in the FI or SI system upstream from the detector, that is, in the position of the reactor shown in Figure 9.1, or as shown in Figures 9.2 and 9.3. SI systems are fully automated with a computer, providing precise control of volumes, flow rates, and timing.

In the SI methodology, solutions can be pulled into the holding coil and pushed downstream one at a time, or multiple solutions can be pulled into the holding coil in sequence and "stacked" there prior to pushing them downstream. The volumes of the solutions pulled into the holding coil are determined by the pump flow rate and timing; therefore, changes in these volumes can easily be made in programming without physical changes to the system. Solution volumes can be in the milliliter to microliter range. The pump does not contact the sample or the reagents, and can be
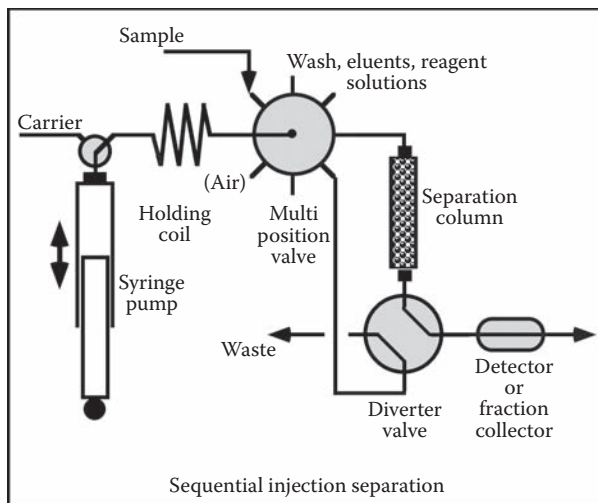
FIGURE 9.2   Schematic diagram of a sequential injection separation fluidic system.
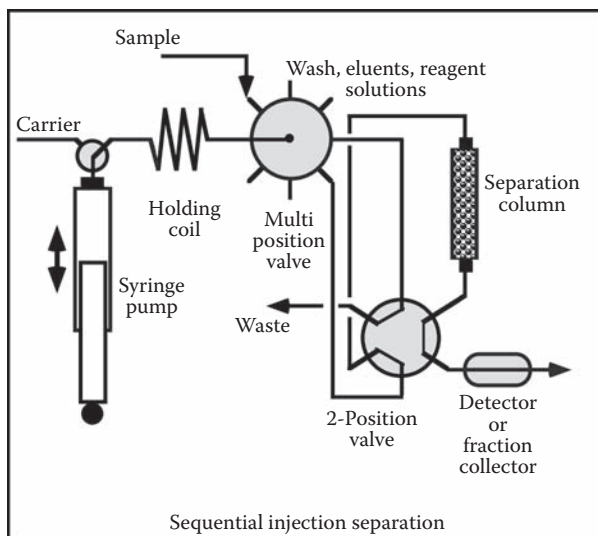
FIGURE 9.3   Schematic diagram of a SI separation system using a 6-port 2-position valve to isolate the separation column. The 6-port valve is shown in the column elution position.

located remotely from the remainder of the system. Thus, SI systems are quite versatile and meet the requirements for delivering samples and reagents to low-pressure separation columns.

An example of a SI separation system is shown in Figure 9.2.[44] The column is followed by a diverter valve so that the column effluent can be sent to waste during sample load and wash steps. This approach prevents matrix components and high-activity interferences from fouling the detector. During the elution of the radionuclide

of interest, the column effluent is sent to the on-line detector. Using a 4-port 2-position valve for the diverter valve, as shown, provides a path by which a wash solution can be sent through the detector without going through the column first.

An alternative SI separation system configuration is shown in Figure 9.3, using a 6-port 2-position valve to isolate the separation column.[45] This configuration enables the same two functions as the 4-port 2-position valve just described, namely, diversion of column wash solutions to waste and bypassing the column to wash the detector flow cell. It also enables reversal of flow through the column, so that a sample can be loaded from one end of the column and then eluted back off of that end without going through the whole column packing.

The fluidic system can be configured to deliver samples to a fraction collector, to a flow-through radioactivity detector, or to an ICP-MS. Adaptations of SI fluidics for separations, as well as methods including flow reversal through the column, column switching, and renewable separation columns have been described in detail previously.[46] For handling larger solution volumes than those typically handled for simple serial analyses, while keeping dispersion between solutions low, a "separation-optimized" SI approach was developed using an air segment between the carrier fluid and solutions pulled into a large-bore holding coil.[44,47,48] (Figure 9.2 shows one port of the multiposition valve set aside for pulling in air segments.) This prevents dispersion between solutions in the holding coil. After pushing the solution forward, and expelling the air segment to waste, a sharp contact boundary between the carrier and the solution is created at the valve. Radiochemical separations automated with FI and SI methods will be discussed below.

Within the mass spectrometry community, some groups have chosen to adapt commercial instrumentation to perform extraction chromatography as a front end to ICP-MS. For example, the Perkin–Elmer Model FIAS-400 is a FI system designed for atomic spectrometries that has been used to automate extraction chromatographic separations for actinide analyses.[49–54] The PrepLab liquid handling system for ICP-MS has similarly been adapted for extraction chromatographic separations.[55–59] High performance ion chromatographic (HPIC) systems from Dionex have been outfitted with columns containing extraction chromatographic resins, although some columns for this system have been much longer than those normally used for extraction chromatography.[60,61]

With regard to terminology, we will use FI to mean flow injection as described above with an injection valve for sample introduction. Similarly, we will use SI as described above to mean sequential injection in which solutions are pulled into a holding coil via a multiposition valve, and pushed out through this valve to the separation system. The combination of a SI fluid-handling system with a separation column can be called "SI chromatography." Some papers apply FI and SI terms more loosely to flow-based systems that may or may not follow these formal fluid-handling approaches as just defined.

9.3.2 Robotic Methods

Modern robotic instrumentation represents an increasingly important approach in biological science and analytical chemistry. A variety of routine analytical operations

can be performed from sample preparation to separations. Robotic systems typically use either a robotic arm or an x–y–z Cartesian system to move tools, apparatus, and liquids from place to place. The latter systems may include a fluidic subsystem to deliver liquids to a dispensing tip. The tip is moved by the x–y–z system to specific locations on the deck containing, for example, multiwell plates or solid-phase extraction columns.

A Zymark robotic arm system has been described for processing samples of diluted spent nuclear fuel samples for analysis.[62] This system implemented an extraction chromatographic separation using immobilized tri-n-octylphosphine oxide (TOPO), a well-known extractant in radiochemistry. This column chemistry was used to separate U and Pu from the highly radioactive fission product matrix. The U and Pu fractions were collected for subsequent analysis using α spectroscopy and isotope-dilution mass spectroscopy. Ziegler et al. investigated TOPO-based extraction chromatographic material in detail, focusing on U/Pu separation.[63] Ascorbic acid in formic acid was developed as a rapid reductant for stripping Pu from the column. Direct filament loading for thermal ionization mass spectrometry (TIMS) was discussed, as well as a Pu, Np, and U separation method. The separation methodology was developed for implementation with a Zymark XP robot in a glove box.

The use of UTEVA-Resin, an extraction chromatographic resin to be described in more detail below, has also been described for robotic separations of actinides in a glove box.[64–66] These authors designed their process to allow columns to run dry between steps to simulate what could happen in an unattended open-column process. In addition, corrosive solvents were avoided. They reported >90% recoveries and fractions that were suitable for thermal ion mass spectrometry (TIMS) source preparation without further purification or treatment.

Buegelsdijk et al. described a fully automated system for preparation of dissolved Pu metal samples using the Zymate II (Zymark Corporation) laboratory robot.[67] The sample preparation steps included bar-code label reading, weighing the sample, and transfer to the dissolution vessel.

Laboratory robotics represents an attractive approach for the automation of sample preparation and separation steps in radiochemical analysis, and for many years, such methods have been routinely used by laboratories serving the analytical needs of the International Atomic Energy Association.[64,68–72] However, there are currently a limited number of published studies containing technical details on the radiochemical separations and how they were automated. Accordingly, the remainder of this chapter will focus on fluidic approaches.

9.4   AUTOMATED FLUIDIC RADIOCHEMICAL SEPARATIONS

9.4.1   Development of Automated Fluidic Separation Approaches

Although best known for simple serial assays in homogeneous solution, such as colorimetric reactions, FI methods have also been developed that perform separations or utilize solid phases.[33,34,42,73–76] The use of solid-phase separation columns in FI or SI systems for radiochemical analysis gathered momentum in the 1990s.

In 1992, Cordera et al. described a FI system with an on-line ion-exchange column to preconcentrate uranium and thorium prior to reaction with Arsenazo III for spectrophotometric determination.[21] In 1995, Grudpan et al. incorporated an ion-exchange preconcentration column as part of the injection valve of a FI system for colorimetric determination of uranium using 4-(2-pyridylazo)resorcinol.[18] In 1998, Grudpan's group described a similar FI system for uranium analysis using UTEVA-Resin packing in a preconcentrating minicolumn.[19,20]

In 1994, Dadfarnia and McLeod described the analysis of uranium in surface waters and sea water using a simple FI system with an alumina column for preconcentration.[77] Species eluted from this column were delivered to an ICP-MS as the detector. Also in 1994, Hollenbach et al. described the automation of extraction chromatographic methods based on TRU-Resin and TEVA-Resin to separate and preconcentrate U, Th, and Tc from soil samples, using ICP-MS for detection.[49,125] In 1996, Aldstadt et al. described the use of FI and extraction chromatography using TRU-Resin to determine U in environmental samples by ICP-MS.[78]

In 1995, Nevissi and Strebin described a simple fluidic system to deliver sample and reagents to a TRU-Resin column for the separation of Pu and Am.[79] A filter was included on-line to capture a precipitate containing the actinides; dissolution of the precipitate transferred the sample onto the column downstream. Radionuclides were detected with α-spectrometry off-line.

In 1996, Grate et al. described a SI method to automate a Sr-Resin extraction chromatographic separation of ^{90}Sr from tank-waste samples, with on-line detection using a flow-through scintillation detector.[80] This report was followed by several additional papers within a few years, which described on-line extraction chromatographic separations for ^{99}Tc or actinides in FI and SI systems using TEVA-Resin or TRU-Resin.[44,47,48,81–83] The use of FI and SI methods to automate radiochemistry was summarized in the journal *Analytical Chemistry* in 1998,[84] and was later described in additional detail in a book chapter[46] and in ACS Symposium Series papers.[85,86] This group described the use of a SI extraction chromatographic separation involving TRU-Resin as a front end for ICP-MS in 2001.[87]

By the late 1990s and into the 2000s, a number of additional groups became involved in automated fluidic separations for radiochemical analysis, especially as a front end for ICP-MS. Published journal articles on fluidic separations for radiometric or mass spectrometric detection are summarized in Tables 9.1 through 9.5. The majority of such studies have used extraction chromatographic separations, and these will be the main focus of the remainder of this chapter. Section 9.4 describes methods that combine separation and detection. Section 9.5 describes a fully automated system that combines sample preparation, separation, and detection.

Although the automated extraction chromatographic separations are designed from existing separation chemistry and manual procedures, several issues are typically investigated when they are automated. These investigations ensure that the separations are performing satisfactorily, help to define parameters for the automated procedure, and provide confidence that the automated method will perform properly over and over again while unattended. Separation issues examined include solution compositions for the load, wash, and elute steps; column crossover effects, removal of interferences during the wash step, and analyte recoveries. Sample issues are

TABLE 9.1

Fission Product Separations in Flow Systems: Tc

Year	Separation Chemistry	Purpose/Approach	Detection	References
1994	Aliquat 336 TEVA-Resin	^{99}Tc determination in soil samples using extraction chromatography in FI system to separate and concentrate	ICP-MS	49
1998	Aliquat 336 TEVA-Resin	^{99}Tc determination in SI system using stopped-flow detection for nuclear waste	On-line liquid scintillation	44
1999	Aliquat 336 TEVA-Resin	^{99}Tc separated on-line using renewable separation column to release resin with ^{99}Tc rather than elute from the column	Off-line liquid scintillation on resin	83
1999, 2001	Aliquat 336	^{99}Tc sensing in water using impregnated polymer containing both extractant and scintillating fluors	Radiometric column sensor	95,97
2000, 2003	Aliquat 336	^{99}Tc sensing in water using impregnated polymer containing both extractant and scintillating fluors	Radiometric column sensor	96,98
2000, 2001	Aliquat 336 TEVA-Resin	^{99}Tc sensing in water using column containing mixture of TEVA-Resin particles and scintillating plastic beads	Radiometric column sensor	96,97

addressed to ensure that the speciation (typically the valence state) of the analytes and interferences are rigorously controlled prior to separation, and experiments are done to determine the effects of complex sample matrixes. Column-size and flow-rate effects may be assessed, and column reuse is often evaluated. The overall speed, sample throughput, and reproducibility are investigated.

9.4.2   FISSION PRODUCTS

9.4.2.1   Technetium

^{99}Tc is a long-lived fission product with a half-life of 2.13×10^5 years. A high fission yield of ~6% results in the production of significant quantities from the fission of enriched uranium. As a result, ^{99}Tc is present in spent nuclear fuel, nuclear waste, and in process streams associated with spent-fuel reprocessing. Due to the long half-life, large quantities, and because it is very mobile in the environment as the water-soluble pertechnetate anion, ^{99}TcO$_4^-$, it is very important to contain ^{99}Tc in nuclear operations and monitor its concentration. ^{99}Tc monitoring is advantageous in technetium removal processes in the processing of nuclear waste into stable waste forms

TABLE 9.2
Fission Product Separations in Flow Systems: Sr and Y

Year	Separation Chemistry	Purpose/Approach	Detection	References
1996	Crown ether Sr-Resin	^{90}Sr determination in aged nuclear waste by SI method	On-line liquid scintillation	80
1999	Crown ether Sr-Resin	^{90}Sr determination by rapid automated SI formats, nuclear waste	On-line or off-line radiometric detection	47
1999	Crown ether Sr-Resin	^{90}Sr separated on-line using renewable separation column approach	On-line liquid scintillation	83
2002	Crown ether wetting film	^{90}Sr separation using automated wetting film instead of column, spiked environmental samples	Off-line counting	146
2004	Crown ether Sr-Resin	Sr (stable and radioactive) separated by multisyringe FI	Off-line, ICP-AES or counting	121
2000, 2001	Crown ether	^{90}Sr sensing in water using column containing polymer impregnated with both extractant and scintillating fluors	Radiometric column sensor	96,124
2001	Crown ether Sr-Resin	^{90}Sr sensing in water using column containing mixture of Sr-Resin particles and solid scintillator particles	Radiometric column sensor	124
2000	MnO$_2$ cotton filter	^{90}Sr/^{90}Y separation by capture of ^{90}Y on MnO$_2$-impregnated column	Off-line counting	45
2003	MnO$_2$ cotton filter	^{90}Sr determination in combination with ^{226}Ra determination, using MnO$_2$-impregnated column separation	Off-line counting	126
1999	HDEHP	^{90}Sr/^{90}Y sensing in water using column containing extractant and scintillating fluors	Radiometric column sensor	95
2005	HDEHP C18 support	Y (stable and radioactive) separated by multisyringe FI	Off-line, ICP-AES, or counting	123

and the reprocessing of spent nuclear fuels. ^{99}Tc is a pure β emitter with a specific activity of 629 Bq/μg; thus, radiometric determination relies on detecting its β particle emission ($\beta_{max} = 294$ keV). Its low specific activity also makes it an excellent candidate for determination by ICP-MS.

Analytical methods normally require separation of ^{99}Tc from inactive matrix constituents and various interfering radionuclides. These separations can be carried out

TABLE 9.3

Actinide Separations in Flow Systems using CMPO Chemistry on TRU-Resin

Year	Purpose/Approach	Detection	References
1994	^{230}Th and ^{234}U determinations in soil samples using extraction chromatography in FI system to separate and concentrate	ICP-MS	49
1995	Am and Pu separation with an on-line column in a simple flow system	Off-line α spectroscopy	79
1996	^{238}U determination in groundwater using extraction chromatography in FI system to separate and concentrate	ICP-MS	78
1998	Actinide separation method development in automated FI format	On-line liquid scintillation	81
1998	Pu separation method development investigating on-column redox reactions in automated FI format	On-line liquid scintillation	82
1999	Pu, Am, and Cm determination in aged nuclear waste using SI system to automate separations of groups and individual actinides	Off-line α spectroscopy	48
1999	^{241}Am determination in dissolved vitrified nuclear waste using renewable separation column to pack fresh resin for each sample	Off-line α spectroscopy	83
1999	^{238}U and ^{232}Th determination in biological materials using FI system with column separation for matrix removal and preconcentration	ICP-MS	131
2001	^{238}U, ^{232}Th, ^{239}Pu, ^{240}Pu, ^{237}Np, ^{241}Am, and ^{243}Am determination in biological materials using FI system with column separation	SF-ICP-MS	132
2001	SI separations of actinides to address isobaric, molecular ion, and spectral interferences. Am, Pu, and Np isotopes determined in dissolved vitrified nuclear waste	ICP-MS	87
2001	FI separation of U and Th to remove matrix interferences using two 6-port 2-position valves	ICP-MS	134
2004	Actinide determinations in urine matrix using column separation automated in ion chromatographic instrument	ICP-MS	60
2005	^{241}Am determination in urine with on-line separation and preconcentration using FI system	ICP-MS	52
2005	Pu determination in urine with on-line separation and preconcentration using FI system	ICP-MS	51

(Continued)

TABLE 9.3   (Continued)

Year	Purpose/Approach	Detection	References
2005	U and Th determinations in urine with on-line separation and preconcentration using FI system	SF-ICP-MS	53
2007	Actinide separations conditions investigated using column separation automated in ion chromatographic instrument	ICP-MS	61
2000, 2002, 2005, 2005	Actinide sensing in aqueous solutions using TRU-Resin type materials impregnated with both extractant and scintillating fluors	Radiometric column sensors	96,135–137

TABLE 9.4

Actinide Separations in Flow Systems using DP[PP] Chemistry on UTEVA-Resin

Year	Purpose/Approach	Detection	References
2001	Actinide isotope analysis method development using FI technique for column separation and preconcentration	ICP-MS	138
2001	U determination in seawater using FI technique for column separation and preconcentration with 10-port 2-position valve	ICP-MS	139
2002	U determination in urine using FI technique for column separation and preconcentration	ICP-MS	141
2004	U and Th determination in urine and blood using FI technique for column separation and preconcentration	ICP-MS	140
2004	Briefly compares UTEVA-Resin unfavorably with TRU-Resin for actinide separations for ICP-MS	ICP-MS	60
2005	Pu determination method development with on-line column separation using PrepLab system	ICP-MS	59
2006	Pu determination in soil with on-line column separation using PrepLab system	ICP-MS	58
2006	^{234}U and ^{230}Th determination in marine sediments with on-line column separation using FI	ICP-MS	142

by a variety of methods, including ion exchange, solvent extraction, precipitation, and extraction chromatography, and often, multistep combinations of such methods are employed.[88–94] Traditionally, these ^{99}Tc separation and analysis steps were carried out manually, exposing the analyst to hazardous chemicals and open sources of radioactivity during tedious, time-consuming and costly procedures.

The prevailing extraction-chromatographic approach for ^{99}Tc separation is the use of Aliquat 336, a liquid quaternary ammonium salt (see Scheme 9.1), as an anion

TABLE 9.5

Plutonium Isotope Separations in Flow Systems using Aliquat 336 Liquid Anion Exchange Chemistry on TEVA-Resin

Year	Purpose/Approach	Detection	References
2000	Pu determinations in sediments using on-line tandem Sr-Resin and TEVA-Resin columns in PrepLab system	SF-ICP-MS	56
2002	Pu determinations in seawater using on-line tandem Sr-Resin and TEVA-Resin columns in PrepLab system	SF-ICP-MS	57
2004	Pu and Np determinations in environmental samples using on-line column separation in PrepLab system	SF-ICP-MS	55
2007	Pu determinations in samples with high U levels, with on-line separation and preconcentration using FI system	ICP-MS	50
2008	Pu determinations in urine with on-line separation and preconcentration using FI system	SF-ICP-MS	143

exchanger in TEVA-Resin. ^{99}Tc in the anionic pertechnetate form, ^{99}TcO$_4^-$, is retained on the resin under neutral to weakly acidic conditions, and eluted using strong acids. The extraction equilibrium is shown in Equation 9.1, where A$^+$ indicates the quaternary ammonium group and the bar above a species indicates that it is immobilized on the resin.

$$\text{TcO}_4^- + \overline{(\text{A}^+\text{NO}_3^-)} \rightleftharpoons \overline{(\text{A}^+\text{TcO}_4^-)} + \text{NO}_3^- \tag{9.1}$$
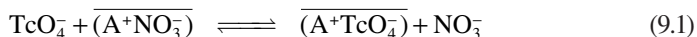
In 0.1 M HNO$_3$ solution, pertechnetate ion is retained with capacity factor k' ~10^4.[30] The capacity factor decreases markedly with increasing nitric acid concentration (k' ~2 in 8 M HNO$_3$)[30] and, after washing the column with dilute nitric acid, the retained Tc(VII) can be eluted using 6–12 M HNO$_3$. This separation is selective, with most metal ions being removed during the column wash. However, tetravalent actinides can be retained along with ^{99}Tc. Tetravalent Pu retention is significant even in dilute nitric acid (capacity factor ~50 in 0.1 M HNO$_3$). However, by incorporating a suitable complexing reagent in the wash solution, actinide retention on TEVA-Resin can be lowered.

Hollenbach et al. captured ^{99}Tc from standards or soil sample digestates on a TEVA-Resin column for on-line purification and preconcentration prior to ICP-MS determination.[49] A wash solution of 0.5 M HNO$_3$ was used to remove interferences prior to elution with 8 M HNO$_3$ solution. A Re isotope, which behaves similarly to pertechnetate on TEVA-Resin, was used as an internal standard. Recoveries from the column varied from 97 to 99.5%, and columns could be reused over a hundred times. The use of the on-line column separation reduced detection limits by 10-fold and alleviated matrix and isobaric interferences compared to direct sample injection. This pioneering study adapted FIAS-200 and FIAS-400 FI systems to perform sample injection and extraction-chromatographic separations upstream from the ICP-MS.

Egorov et al. developed a SI system incorporating a TEVA-Resin column to perform automated ^{99}Tc separations with on-line detection using a flow-through liquid scintillation counter.[44] The SI system was designed like the system in Figure 9.2, including the "purge" line for delivering fluids from the multiposition valve to the diverter valve, thus bypassing the column. In addition, the "separation optimized" SI method (mentioned above), using air segments to prevent mixing between the carrier and the solutions pulled into a large-bore holding coil, was introduced in this study. Column conditioning, sample load, and column wash procedures were carried out with 0.1 M HNO_3. For the first half of the column wash, the solution also contained 0.2 M HF to complex and remove tetravalent actinides. A solution of 6 M HNO_3 was selected for elution as a tradeoff between higher acid concentrations that result in faster elution and sharper elution peaks, and lower acid concentrations that lead to less quenching, and hence higher detection efficiencies, in the liquid scintillation determination.

Detector traces for the removal of high-activity fission products in the wash step and elution of ^{99}Tc are shown in Figure 9.4. ^{99}Tc is present at much lower activities than the more abundant fission products that pass unretained through the column and detector flow cell. Nevertheless, during elution of the column with the 6 M HNO_3, the ^{99}Tc is readily seen in the vertically expanded inset. The SI separation procedure provided a decontamination factor of 10^4 for removal of ^{137}Cs or ^{90}Sr from the ^{99}Tc.

In this radiometric detection approach, the detection limit could be lowered by using a stopped-flow procedure that captured 89% of the eluted ^{99}Tc within a 2.5-mL flow-through counting cell. Continuous-flow and stopped-flow detector traces are
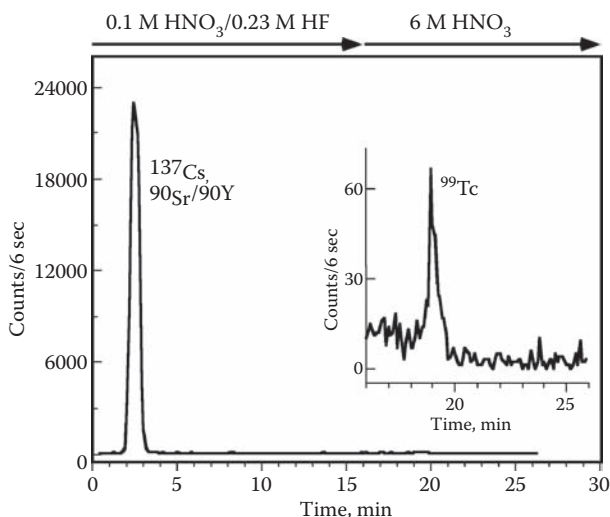
FIGURE 9.4 Extraction chromatographic separation of ^{99}Tc(VII) from other fission products in the sample using a sequential injection separation system with a TEVA-Resin column. The signal for the ^{99}Tc is shown in the vertically expanded trace in the inset. (Reproduced from Egorov, O. B., O'Hara, M. J., Ruzicka, J., and Grate, J. W., *Anal. Chem.*, 70, 977–984, 1998. With permission.)

compared in Figure 9.5. Because this analysis does not use an internal standard like the ICP-MS determination described above, consistency of ^{99}Tc recovery, peak position, and peak shape are very important for accurate analyses. It was shown that ^{99}Tc determinations were reproducible for at least 15 runs, and carryover from sample to sample was negligible: no ^{99}Tc activity was detectable in blank runs following high-activity standards.

Because the system was set up with a diverter valve as shown in Figure 9.2, samples could be processed onto the column and washed, with solutions going to waste, while the previous sample was stopped in the detector for counting. On completion of the counting interval, the detector flow cell could be washed, and then the sample already processed and separated on the column could be eluted to the detector. Using a count time of 15 minutes, the analysis time was 40 minutes for the first sample and 20 minutes for each subsequent sample or blank.

The method was demonstrated in the analysis of samples of processed Hanford tank waste, with good agreement between automated SI method results and results obtained using a conventional multistep manual procedure.

In subsequent work, it was shown that a renewable separation-column approach could be used to capture and purify ^{99}Tc on a TEVA-Resin column set up between a pair of 2-position valves, as shown in Figure 9.6.[83] After loading the sample and washing away interferences, the separation material was released from the column and delivered downstream to a collection vial. Scintillation cocktail was added to the vial off-line and the ^{99}Tc was determined radiometrically. In this approach, there is no need to elute the ^{99}Tc with strong acid, and a fresh suspension of separation material is delivered to the column body for each sample.
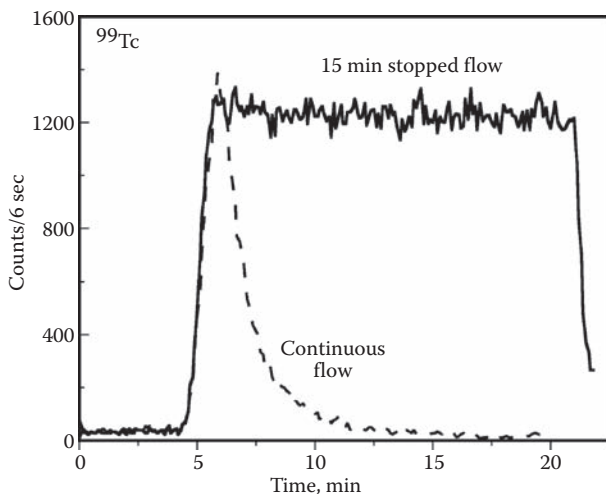
FIGURE 9.5   Continuous- and stopped-flow detector traces for the automated SI separation of ^{99}Tc(VII) on a TEVA-Resin column. (Adapted from Egorov, O. B., O'Hara, M. J., Ruzicka, J., and Grate, J. W., *Anal. Chem.*, 70, 977–984, 1998. Copyright 1998 Am. Chem. Soc. With permission.)
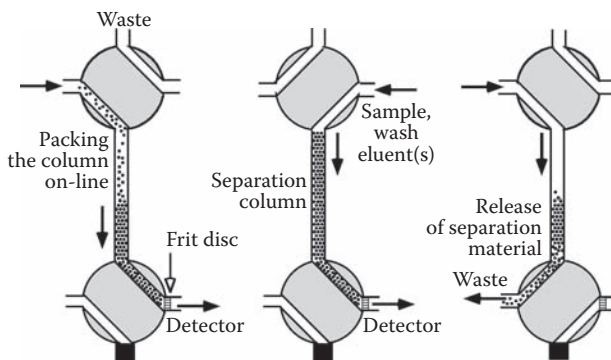
FIGURE 9.6 Renewable separation-column approach for automatically packing a column on-line, localizing the column packing between a pair of 2-position valves.

Radionuclide sensors have been developed that combine radiochemical separation and scintillation detection in a single, column-based device. Aliquat 336 was impregnated on resins in the development of radionuclide sensors for ^{99}Tc.[95–98] Both the extractant and some organic fluor molecules were coimpregnated on macroporous polymer beads. This created a dual-functionality material that provides selective radionuclide uptake due the extractant, while the combination of polymer and fluors gave the material scintillating properties. Scintillation light reported when radionuclides were being collected in the column material. Such dual-functionality materials and radionuclide sensors for water monitoring were recently reviewed.[99] Sensors were also prepared by creating an intimate mixture of TEVA-Resin particles and scintillating plastic beads.[96,97] Selective radiochemical sensors may have applications in nuclear process monitoring.

9.4.2.2 Strontium

^{90}Sr is a high-abundance fission product that decays with a half-life of 29 years to ^{90}Y. ^{90}Y has a half-life of 64 hours, decaying to stable ^{90}Zr. Both of these radioisotopes are β emitters, and together they are primary heat-generating isotopes in nuclear waste. ^{90}Sr is of considerable concern due to the large quantities produced, its long half-life, and its extreme radiotoxicity due to its tendency to substitute for calcium in bone tissue.

Analytical determination of ^{90}Sr requires that it is separated from a variety of interfering radionuclides prior to quantification by counting methods. Because the relative half-lives of ^{90}Sr and ^{90}Y lead to secular equilibrium, a variety of approaches are possible. By isolating Sr, ^{90}Sr can be quantified by β counting. Alternatively, after isolating the Sr, the ingrowth of ^{90}Y can be followed. If free of other interferences, the total activity of the ^{90}Sr and ^{90}Y can be determined when they are in secular equilibrium. Finally, the activity of ^{90}Y can be determined after separating it from a sample of ^{90}Sr and ^{90}Y in secular equilibrium. A variety of classical and chromatographic methods can be used to achieve the required chemical separations, including precipitation, liquid-liquid extraction, ion exchange, and thin-layer chromatography.[100–115] Typically, multistep combinations of separation methods are used, which is time consuming and costly.

The prevailing extraction-chromatographic method for ^{90}Sr separation entails the use of Sr-Resin.[116–119] This material is prepared by impregnating a porous polymer with a 1-octanol solution of the crown ether 4,4′(5′)-bis(*t*-butylcyclohexano)-18-crown-6 (DtBuCH18C6). This material will extract and retain Sr from 2–8 M HNO$_3$ solutions, while most of the matrix constituents are not retained and are removed with a column wash. The separated Sr is released by elution with water or weak nitric acid. The extraction equilibrium is shown in Equation 9.2, where the bar above a species indicates that it is immobilized on the resin.[4]

$$Sr^{2+} + 2NO_3^- + \overline{DtBuCH18C6} \rightleftharpoons \overline{Sr(DtBuCH18C6)(NO_3)_2} \qquad (9.2)$$
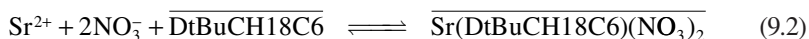
Horwitz et al. have discussed a number of applications for Sr-Resin, including the analysis of ^{90}Sr in high-level nuclear wastes.[117–119] In conventional practice, isolation of ^{90}Sr with Sr-Resin is a manual open-column procedure with quantification of the eluted ^{90}Sr carried out as a separate counting step.

Grate et al. described a rapid automated method for the determination of ^{90}Sr using a SI separation system that combined a Sr-Resin separation column with on-line liquid scintillation counting. The original system used a peristaltic pump; however, it was similar in function to the SI separation system shown in Figure 9.3.[80] Carrier, wash, and sample zones were stacked in the holding coil, with the carrier also serving as the eluent. Figure 9.7 shows the separation of ^{90}Sr from ^{90}Y in a standard sample.[80] The column is loaded and washed using 8 M HNO$_3$, where ^{90}Y is unretained. ^{90}Sr is subsequently eluted with water. Because of dispersion between the water and the acid, the ^{90}Sr is actually eluted in weak nitric acid solution. The eluent plot in the lower portion of Figure 9.7 (dashed trace referring to the right y-axis) shows the column crossover from 8 M nitric acid to water, with ^{90}Sr elution beginning in low acid concentrations.

Subsequent work used a SI system with a syringe pump as the fluid drive, and radiometric detection was carried out either on-line or off-line.[47] Each solution was loaded and dispensed to the column in separate operations using air segments in the holding coil, according to the separation-optimized solution-handling approach. This approach created sharper boundaries between the water and acid zones, leading to a much more rapid column crossover from acid to water, as shown in Figure 9.8. This plot compares the acid concentrations in the eluent from a Sr-Resin column using a stacked-zone SI method and a separation-optimized SI method.[47] Normally, abrupt changes in solution composition are favorable for rapid and sharp analyte elution. In this case, however, it was found that ^{90}Sr recovery was poor using water as the eluent and a very rapid column crossover in an automated system.[47] Excellent recoveries were achieved by eluting with 0.05 M HNO$_3$.

Using separation-optimized SI with 0.05 M HNO$_3$ as the eluent and 1-octanol saturated solutions, ^{90}Sr recoveries were 96%, and carryover from one sample into a subsequent blank run was typically 1–2%.[47] Blank runs or column clean-up procedures can be used to reduce or eliminate carryover between samples. Recoveries were not sensitive to elution flow rates, and columns could be used repeatedly. There were no significant performance differences between Sr-Resin materials with 20–50
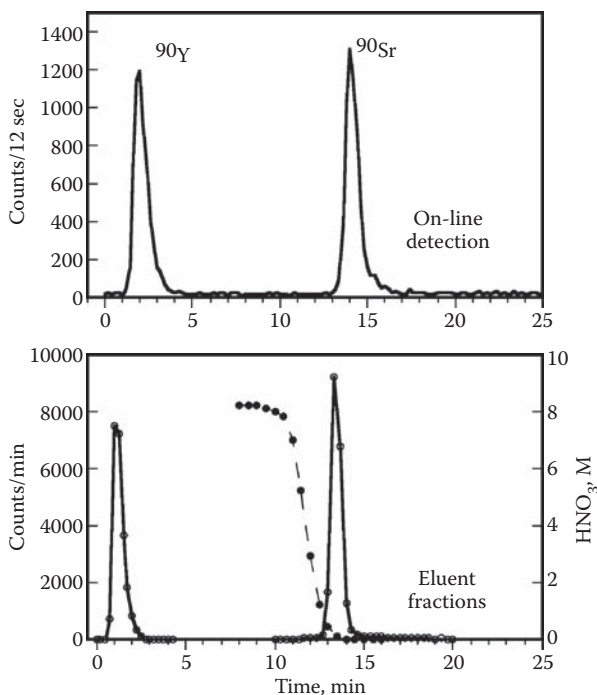
FIGURE 9.7 Detector traces for the automated SI separation of ^{90}Sr on a Sr-Resin column in the top plot, with analytical results for eluents obtained by fraction collection in the lower plot. (Adapted from Grate, J. W., Strebin, R. S., Janata, J., Egorov, O., and Ruzicka, J., *Anal. Chem.*, 68, 333–340, 1996. Copyright 1996 Am. Chem. Soc. With permission.)

or 50–100 micron diameter particle sizes. The use of the octanol-saturated solutions, however, was important in repeated column usage, as the Sr-Resin can lose the impregnated solvent with use, and it was observed that recoveries and carryover both suffered if solutions that were not octanol-saturated were used. (It is noteworthy, however, that Dietz has developed an extraction-chromatographic material for ^{90}Sr using the DtBuCH18C6 crown ether impregnated on the resin without 1-octanol or any other remaining cosolvent.[120])

Sr-Resin can retain a number of potential interferences in the radiometric determination of ^{90}Sr.[47] Tetravalent Pu and Np are strongly retained under strong-acid load conditions and coelute with Sr. (This retention of tetravalent actinides under strong-acid conditions is likely due to the charge-charge interactions between the anionic hexanitrato complex and the cationic complex of the crown ether with H_3O^+.) In typical nuclear waste, however, ^{90}Sr activity is orders of magnitude higher than the actinide activities, and interference is not a problem. Nevertheless, the incorporation of 0.1 M HF in the 8 M HNO_3 column wash solution effectively removes Pu(IV) with a decontamination factor of 1000. Ba is also retained on Sr-Resin. Nevertheless, with a sufficient volume of 8 M HNO_3 for the column wash, most of the Ba can be removed. Figure 9.9 shows the removal of Pu(IV) and Ba from a Sr-Resin column using column wash solutions. (The retention of Pu(IV) by Sr-Resin has been used to
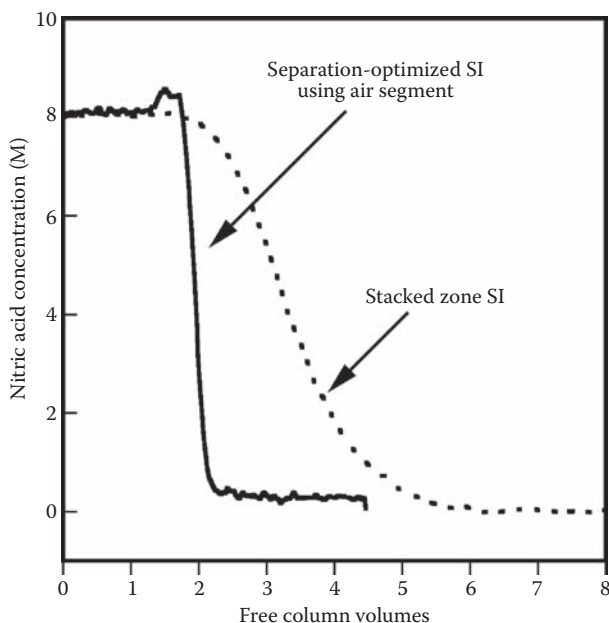
FIGURE 9.8 Comparison of the acid concentrations of the Sr-Resin column eluents, determined spectrophotometrically, for conversion from 8 M HNO$_3$ to water using stacked zone SI methodology (dashed line) and "separation-optimized" SI methodology that separates carrier and solution using an air segment. (Adapted from Grate, J. W., Fadeff, S. K., and Egorov, O., *Analyst,* 124, 203–210, 1999. Copyright 1999 Royal Society of Chemistry. With permission.)
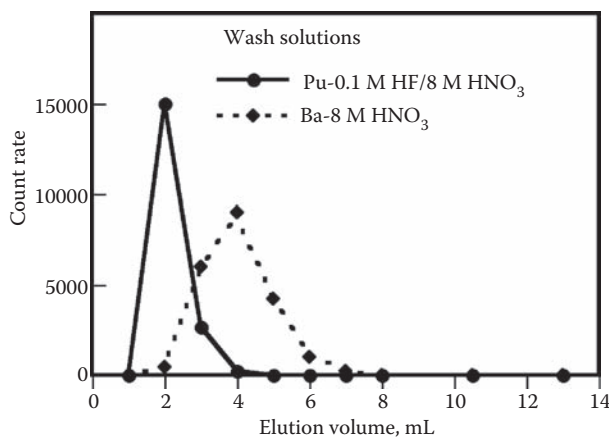
FIGURE 9.9 Removal of Pu and Ba from a Sr-Resin column in the column wash solutions. Data are from eluent fraction collection. (Adapted from Grate, J. W., Fadeff, S. K., and Egorov, O., *Analyst,* 124, 203–210, 1999. Copyright 1999 Royal Society of Chemistry. With permission.)

advantage in tandem column separations that capture and wash Pu on Sr-Resin and elute it to TEVA-Resin for focusing and further purification in the determination of Pu isotopes in seawater and sediments.[56,57])

In the analysis of sets of aged nuclear-waste samples, Grate et al. demonstrated two approaches.[47] In one approach, eight Sr-Resin columns were set up in parallel with column switching provided by a multiposition valve. Each of the eight samples was analyzed in series, switching to a new column for each sample. The analysis of one sample using on-line detection required 22 minutes, and the set of eight could be completed in 3 hours. Using on-line detection right after separation, there is no need to correct for ^{90}Y ingrowth. In the second approach, samples were separated, and eluents were collected using a fraction collector. Without on-line detection, a set of eight samples could be processed in 1 hour and then set aside for off-line quantification. This approach may suit the work-flow in some process laboratories, but it does require recording the time from separation to counting for ^{90}Y ingrowth corrections.

Sr-Resin separations can also be set up in a renewable separation-column approach[83] as described above for ^{99}Tc determinations, and illustrated in Figure 9.6. In this case, the sample was separated and eluted from the column. The advantage of the renewable column approach was that fresh column material could be provided for each separation. The carryover on Sr-Resin columns, described above, is largely due to the resin material. It was shown that automatically replacing the resin material largely eliminated carryover from one sample to the next.

Fajardo et al. have described a "multisyringe FI" approach for automating Sr-Resin column separations.[121] These authors used off-line counting and ICP-AES to determine radioactive and stable Sr. The multisyringe approach,[39,122] as set up for Sr-Resin separations, is shown in Figure 9.10. This system uses flow reversals and a holding coil associated with each syringe, so in this respect it can be regarded as a modified SI system. Instead of a multiposition valve, a series of 3-port solenoid valves were used to select solutions to pull into the system, and direct them for pushing out to the column. These authors analyzed for Sr in water, soil, and milk samples. The primary potential interference of concern in these studies was Pb, which is strongly retained on Sr-Resin. Pb is retained even in 0.05 M HNO_3 when Sr is eluted; it does not appear in the Sr fractions as an interference; however, it could consume binding sites on the resin in subsequent reuse of the column. A 0.5 M H_2SO_4 cleaning step was inserted into the procedure between analyses to remove Pb.

Another multisyringe FI separation system design has been used in the analysis of stable and radioactive Y, using an extraction-chromatographic material containing HDEHP adsorbed on a C_{18} support.[123] Separated samples were analyzed off-line by ICP-AES and proportional counting. This system used four syringe pumps in parallel.

HDEHP has also been used in the development of extractive scintillating materials for ^{90}Sr and ^{90}Y sensing.[95] The polymeric bead material contains both an impregnated extractant and organic fluor molecules. Both ^{90}Sr and ^{90}Y are retained from 0.001 M HCl solution using HDEHP. The sensor-column scintillation signal results from the sum of the radioactive species. Elution with 2 M HCl removes ^{90}Sr, leaving ^{90}Y on the sensor column for determination. This provides two measurements to determine two unknowns. The ^{90}Y can be removed from the sensor with 4 M HCl.

Multisyringe separation system
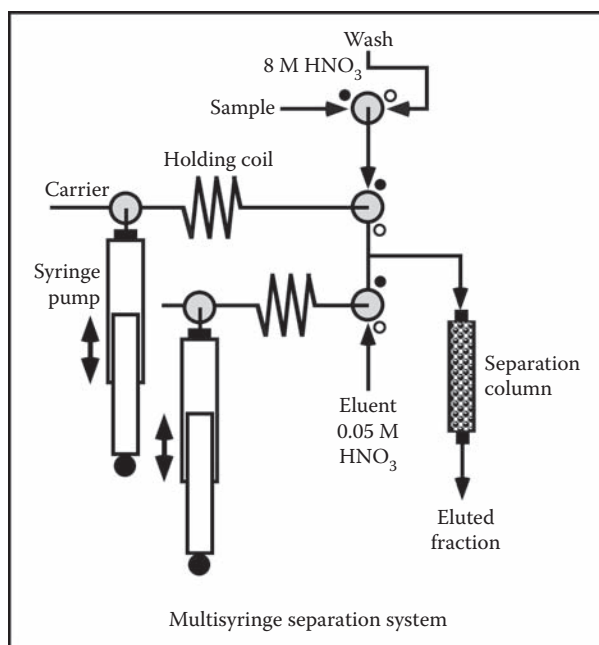
FIGURE 9.10 Schematic diagram of a multisyringe separation system using solenoid valves rather than a multiposition valve. Normally open and normally closed ports on the solenoid valves are marked with open and closed circles, while the common port is unmarked. System is shown with wash and eluent solutions for Sr determination using a Sr-Resin separation column.

The crown ether chemistry used for ^{90}Sr separations (e.g., as Sr-Resin) has been used for the development of ^{90}Sr sensors in two ways. In one approach, polymer particles were impregnated with both the extractant and with organic fluor molecules to create a dual-functionality extractive scintillating resin.[96,124] In the second approach, Sr-Resin particles were intimately mixed with solid scintillating particles to make a composite bed column with ^{90}Sr sensing properties.[124] In either case, retention of ^{90}Sr results in a scintillation signal.

Another material used in separations for the determination of ^{90}Sr or ^{90}Y has been manganese dioxide.[45] This material has been deposited on cotton filters packed in a column body to create a solid-phase extraction column, which was then used to retain ^{90}Y from 40 mL water samples. Under these conditions, ^{90}Sr was poorly retained. The ^{90}Y could then be removed along with manganese dioxide using a hydroxylamine solution. In contrast to separations using Sr-Resin, this approach avoids strong acids, capturing the ^{90}Y from neutral water solutions. This system had been previously described for determination of ^{226}Ra in environmental samples.[125] The SI separation system, shown in Figure 9.3, used a syringe pump, holding coil, and multiposition valve for introduction of the sample and reagents. A 6-port 2-position valve downstream was used to isolate the separation column, functioning to divert waste solutions, enabling flow reversal through the column for

loading in one direction and eluting in another direction, and providing a purge line route that bypasses the column. This separation approach has also been adapted for simultaneous determination of ^{90}Sr and ^{226}Ra with off-line radiometric determination.[126] The quantity of ^{90}Sr initially present is determined from the measured ^{90}Y activity assuming secular equilibrium conditions existed in the original sample.

9.4.3 ACTINIDES

Actinides have significant abundance in irradiated nuclear fuel, long radioactive half-lives, and high radiological and chemical toxicities, and they raise concerns with criticality and nuclear proliferation. Accordingly, actinide analyses are important in process solutions, nuclear wastes, and environmental samples.

Actinides can be separated from matrix elements, other radionuclides, and each other using extraction-chromatographic materials such as TEVA-Resin, TRU-Resin, and UTEVA-Resin. The capacity factors for various actinides on these resins, as a function of nitric or hydrochloric acid concentrations are shown in Figures 9.11 and 9.12.[30,31,127] Elution peaks or collected fractions from column separations can be
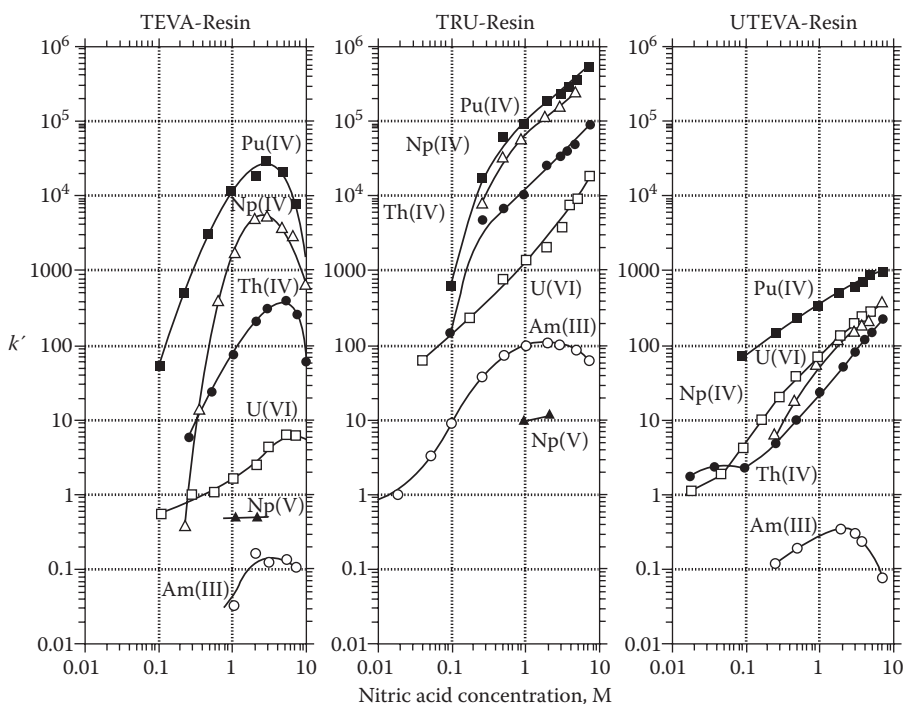
FIGURE 9.11 Capacity factor*s*, k′, against nitric acid concentration for three resins used in actinide separations. (Data for these plots were originally published in Refs*. 30, 31, 127, and data traces were adapted from www.eichrom.com where they are shown in color. With permission.) (From Horwitz, E. P., Dietz, M. L., Chiarizia, R., Diamond, H., Maxwell, S. L., and Nelson, M. R., *Anal. Chim. Acta*, 310, 63–78, 1995. With permission.)
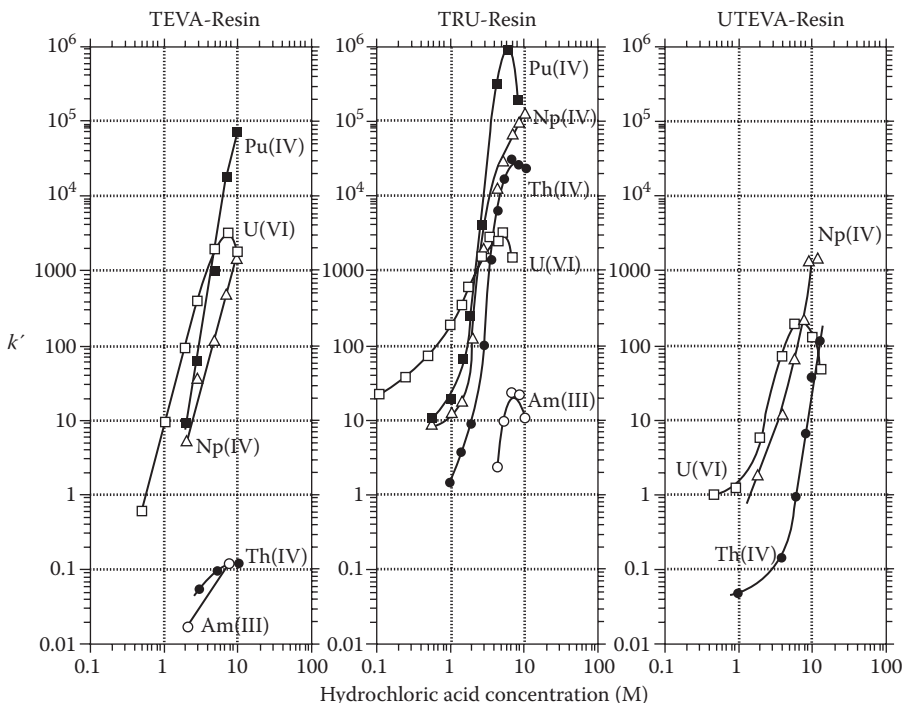
FIGURE 9.12   Capacity factors, k′, against hydrochloric acid concentration for three resins used in actinide separations. (Data for these plots were originally published in Refs. 30, 31, 127, and data traces were adapted from www.eichrom.com where they are shown in color. With permission.) (From Horwitz, E. P., Dietz, M. L., Chiarizia, R., Diamond, H., Maxwell, S. L., and Nelson, M. R., *Anal. Chim. Acta*, 310, 63–78, 1995. With permission.)

analyzed by methods such as α spectroscopy or ICP-MS. The latter method can be implemented as an on-line detector, and the majority of studies automating actinide separations using fluidic systems have been carried out as front-end processes for ICP-MS analyses.[14,15]

A large number of such studies have been reported, and these are summarized in Tables 9.3 through 9.5. In this section, we will highlight selected examples to illustrate the separation chemistries and automation approaches used.

9.4.3.1   TRU-Resin Separations

The largest number of automated extraction-chromatographic separations for actinides have used TRU-Resin, and many of these have coupled the column to ICP-MS as an on-line separation (see Table 9.3). TRU-Resin is impregnated with the neutral bifunctional organophosphorus complexant, octyl(phenyl)-*N,N*-diisobutylcarbamoylmethylphosphine oxide (CMPO) in tri-*n*-butyl phosphate (TBP).[26,127,128] The organic stationary phase in this resin binds trivalent, tetravalent, and hexavalent actinide nitrato complexes from nitric acid solutions (see Figure 9.11). The extraction equilibria for representative species are shown in Equations 9.3–9.5, where the bar above a species indicates that it is immobilized on the resin.[4]

$$Am^{3+} + 3NO_3^- + \overline{3\,CMPO} \rightleftharpoons \overline{(CMPO)_3 Am(NO_3)_3} \quad (9.3)$$

$$Pu^{4+} + 4NO_3^- + \overline{2\,CMPO} \rightleftharpoons \overline{(CMPO)_2 Pu(NO_3)_4} \quad (9.4)$$

$$UO_2^{2+} + 2NO_3^- + \overline{2\,CMPO} \rightleftharpoons \overline{(CMPO)_2 UO_2(NO_3)_2} \quad (9.5)$$
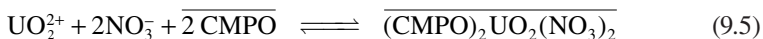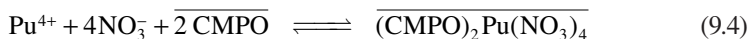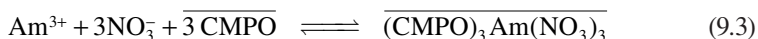
Actinide retention increases with increasing nitric acid concentration. Tetravalent actinides are more strongly retained than trivalent actinides. Chloro complexes of tetravalent and hexavalent actinides, but not trivalent actinides, are retained from hydrochloric acid solutions (see Figure 9.12). Actinides retained on TRU-Resin columns from nitric acid load solutions can be recovered, individually or in groups, using different acid solutions and/or complexants as eluents. In addition, on-column redox chemistry can be used to shift the valence state of Pu through multistep separation processes so that Pu can be isolated individually.

Hollenbach et al. coupled a TRU-Resin column to an ICP-MS using a FI system for solution handling.[49] The determination of ^{230}Th and ^{234}U entailed loading the sample on the column in nitric acid solution, washing with 4 M HNO_3, and eluting the actinides together in 0.1 M ammonium oxalate solution. This complexant solution produced sharper elution peaks than either dilute nitric acid or water. ^{229}Th and ^{233}U were used as internal standards, and columns could be reused over a hundred times. Potential interferences due to ThH were discussed.

Aldstadt et al. described the determination of U in groundwater using a FI system with a TRU-Resin column coupled on-line to an ICP-MS. The system used three 2-position valves and a flow-reversal scheme to load the sample in one direction and elute in the reverse direction. The system provided an enrichment factor on the order of 30-fold compared to direct groundwater analysis. Separate elution of Pu and Th in a group prior to eluting U was also discussed.

Egorov and Grate examined automated actinide separations on TRU-Resin, starting with FI systems, then progressing to SI systems, and finally coupling the SI system to an ICP-MS detector.[48,81,82,87] Figure 9.13 illustrates some of the types of actinide separations that can be obtained. Plot (a) illustrates purification of the actinides as a group. The unretained or slightly retained fission products are removed during the column wash with 2 M nitric acid.[48,84] The actinides are released from the column using the complexant ammonium hydrogen oxalate (bioxalate).

Sequential separation of actinides in valence state groups is shown in plot (b) of Figure 9.13. After loading the actinides under reducing conditions (i.e., Pu as Pu(III) and Np as Np(IV)) and washing away the fission products, the trivalent actinides, including Pu(III), are eluted with 4 M hydrochloric acid. The tetravalent actinides are released selectively with an oxalic acid solution. Remaining hexavalent actinides (U) are removed from the column using ammonium bioxalate solution.[48,84] Careful valence state adjustment of the sample is carried out with reagents prior to the separation process, so that the actinides are in known states prior to the separation, and will accordingly be retained and released as desired.
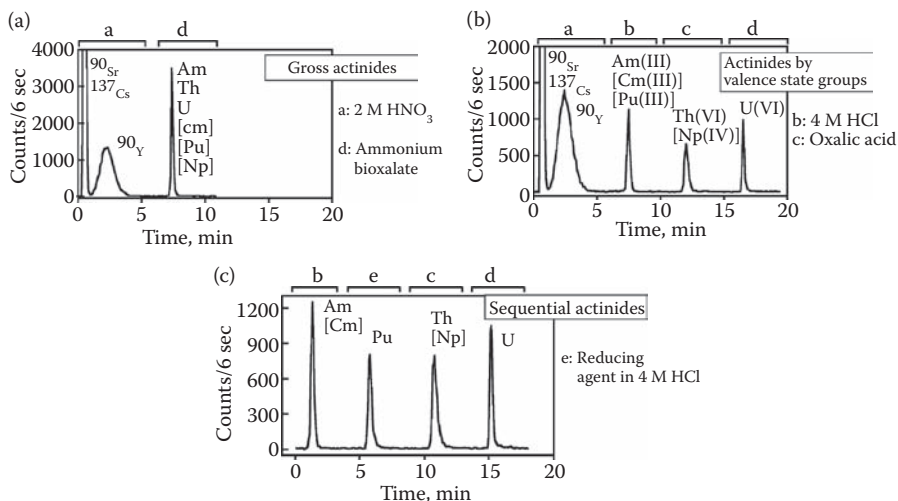
FIGURE 9.13 Group and individual actinide separations using TRU-Resin extraction-chromatographic material: (a) from fission products as a single group (gross actinides); (b) actinide separation from the fission product with release from the column as valence state groups; and (c) elution of the actinides using on-column redox chemistry to separate Pu from Am and the other trivale*n*t f-element species (the initial elution of fission products is omitted from (c)). (Adapted from Grate, J. W., Egorov, O. B., and Fiskum, S. K., *Analyst,* 124, 1143–1150, 1999. Copyright 1999 Royal Society of Chemistry. With permission.)

Individual separation of Pu is possible by toggling the valence state of plutonium, as indicated in plot (c) of Figure 9.13, showing only the actinide elution steps after washing away the fission products. This separation is essentially the same as that in the middle plot with the addition of Pu valence state adjustments. Although the Pu is loaded as Pu(III), it is oxidized on-line using sodium nitrite after the fission product elution and wash. The Pu is thus in the tetravalent state during the elution of the trivalent actinides. Then a reducing agent in hydrochloric acid solution is added to convert Pu(IV) back to Pu(III), which is then unretained and is individually released. The other trivalents have already been released in the prior step.

The conditions for Pu reduction and elution were examined in detail, and a variety of reducing agents were tested.[82] A flow system with an on-line scintillation detector was used to show the elution behavior in detail under well-controlled flow conditions. It was found that reduction and elution with hydroquinone was slow, resulting in broad tailing peaks and incomplete reduction. Some Pu remained in the Pu(IV) state and could be eluted with a complexant on completion of the reductant/HCl elution step. However, by choosing other reductants, rapid reduction and clean elution as a sharp peak could be obtained. These results are shown in Figure 9.14.

The role of nitrite in oxidizing the Pu(III) to Pu(IV) before the elution of the trivalents, and its effects on the subsequent reduction of Pu(IV) back to Pu(III) were also discussed in detail. Sodium nitrite is an efficient and fast oxidizing reagent to convert Pu(III) to Pu(IV) in acidic solutions without further oxidizing Pu to higher
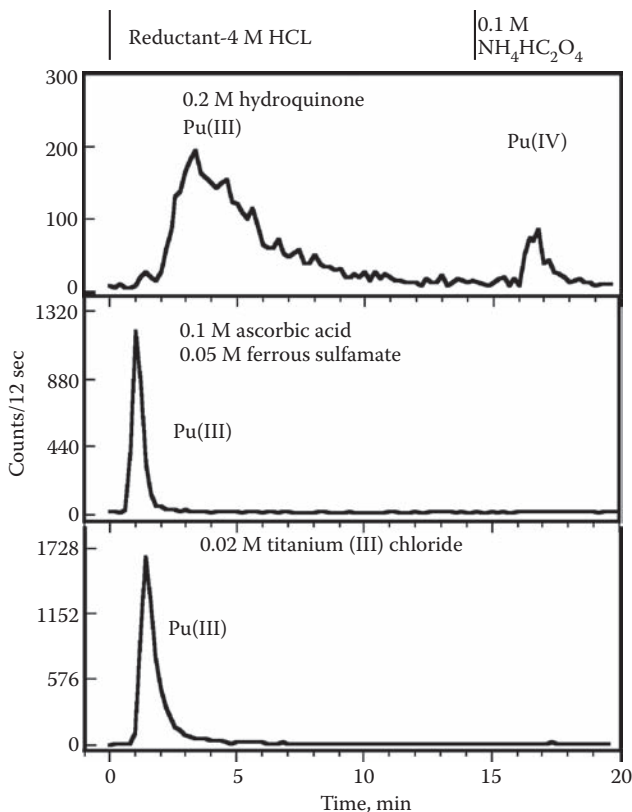
FIGURE 9.14 Comparison of reductants for on-column conversion of Pu(IV) to Pu(III) in order to release the Pu from the TRU-Resin selectively. (Adapted from Grate, J. W. and Egorov, O., *Anal. Chem.*, 70, 3920–3929, 1998. Copyright 1998 Am. Chem. Soc. With permission.)

valence states.[129,130] However, nitrite is unstable in acid. An injection sequence was developed to automatically prepare fresh acidic nitrite solution on-line from a stable aqueous solution of sodium nitrite 2 M nitric acid.

Using the renewable separation-column approach, TRU-Resin can be used to conduct Am-Pu separations without the need to elute the remaining actinides off the resin.[83] Instead, the resin could simply be replaced prior to the next sample. In addition, it was shown that TRU-Resin could be automatically loaded into a separation column as part of an "open-architecture" radiochemical separation workstation, where the instrument would load the desired separation material, and then select reagents appropriate to the separation desired, all under computer control according to the operator's needs for the sample at hand.[83]

Most recent studies describing fluidic automation of TRU-Resin separations have been directed to ICP-MS analysis. Evans et al. used a FI system with a TRU-Resin column to concentrate U and Th from a variety of aqueous and biological standard reference materials.[131] After the wash step with 2 M HNO_3, these analytes were

eluted with 0.1 M ammonium bioxalate. The ICP-MS system was equipped with an electrothermal vaporization sample-introduction system. In subsequent work, this group analyzed several actinide isotopes using a TRU-Resin column separation and sector-field ICP-MS (SF-ICP-MS).[132] Two elution approaches were described: either elution as a single group using ammonium bioxalate, or elution in two groups using titanium(III) chloride in 4 M HCl to release trivalent Am and Pu, and then ammonium bioxalate to release Th, Np, and U. The sequential separation prevented $^{238}U^1H$ from interfering with the determination of ^{239}Pu in biological and environmental samples. (This group has also described ICP-MS analysis approaches where a separation column containing polymer beads was dynamically loaded with picolinic acid to retain and separate actinides from the sample matrix and from each other.[133])

Hill et al. used ICP-MS and FI with TRU-Resin column separations for determination of U and Th in natural waters.[134] High analyte recoveries were found even in waters with high dissolved organic matter, which normally presents a problem if samples are concentrated using typical ion-exchange or chelating resins. Samples on the TRU-Resin column were washed with nitric acid as usual and eluted in ammonium bioxalate.

Egorov et al. demonstrated the use of SI fluid handling to couple TRU-Resin column separations to ICP-MS.[87] The SI system is shown in Figure 9.15. Reagents were selected and delivered via a holding coil and multiposition valve using SI methods, while the sample was introduced downstream using an injection valve as in FI methodology. The SI system for handling the clean, "cold" reagents was set up and maintained outside the "hot" zone. The separation approach shown in Figure 9.13b, which separates actinides by valence state groups, was used to alleviate potential interferences, including $^{241}Am/^{241}Pu$, $^{244}Cm/^{244}Pu$, and $^{238}Pu/^{238}U$ isobaric interferences; $^{239}Pu/^{238}U^1H$ and $^{233}U/^{232}Th^1H$ polyatomic interferences; and $^{237}Np/^{238}U$ spectral interference. Reductive sample pretreatment ensured that Pu would be in the Pu(III) state and Np in the Np(IV) state for this separation. It was noted that Np(V) is essentially unretained by TRU-Resin in nitric acid. Although separation-optimized SI procedures with an air segment were used for most operations, reagents for the elution of trivalent and then tetravalent actinides were stacked in the holding coil and pushed out in sequence in order to provide uninterrupted elution and detection of these species. Because of dispersion between the two reagent zones, there is effectively a gradient elution aspect to this method. These authors also demonstrated a reagent sequence to first elute Pu(IV) and Np(IV) together using 0.5 M HNO_3–0.05 M oxalic acid followed by the remaining actinides in one or more steps using additional reagents. This approach enables elution of Np and Pu together for analyses where these are the species of interest that must be separated from the remaining actinides.

Hang et al. used a HPIC instrument to create a FI separation system that was coupled to ICP-MS, as shown in Figure 9.16.[60] They packed a 30-cm column with TRU-Resin, which is a much longer TRU-Resin column than would normally be used for actinide separations. Water and diluted urine samples were loaded and washed in 3 M HNO_3. Gradient elution from 1.0 M HCl–0.032 M oxalic acid to 0.01 M HCl–0.032 M oxalic acid released Np, Am, and Pu. Subsequent elution with additional 0.01 M HCl–0.032 M oxalic acid released Th and U. This procedure separated actinides according to valence states, with the retention order V < III < IV < VI, and hence with release in the order Np(V), Am(III), Pu(IV), Th(IV), and
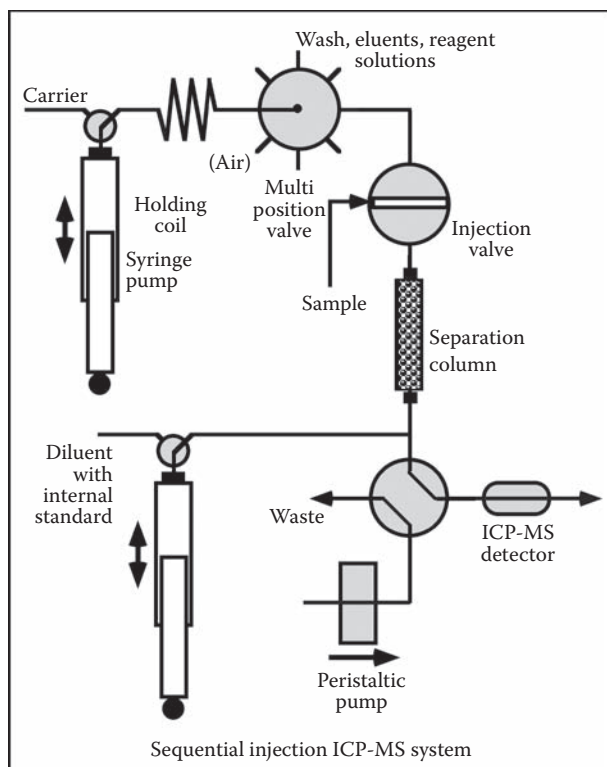
FIGURE 9.15 Design of a SI separation system for on-line separation of actinides for ICP-MS detection, where the SI system handles clean solutions and reagents outside the radioactivity containment glove box, while the injection valve and separation column downstream handle radioactive solutions.

U(VI). The long separation column—preconditioned, loaded, and washed with 3 M HNO$_3$—was credited with the apparent retention of Np(V) and Am(III) under this elution program. These authors also examined UTEVA-Resin for this actinide analysis application but concluded that TRU-Resin was to be preferred for retention of actinides from urine.

Subsequent work by Petersen et al. also used TRU-Resin columns with a HPIC instrument; however, the effects of column length were investigated and a 3-cm length was selected.[61] Other parameters such as resin size and flow rate were examined, and eluent compositions were studied to minimize the use of oxalic acid. Decreased oxalic acid concentrations reduced the frequency of instrument cleaning. In the final scheme, the Np and Am were eluted in hydrochloric acid, followed by Pu and Th together as tetravalent species in a gradient that added oxalic acid. Last to elute was U. Coelution of Pu and Th was considered satisfactory because isobaric interferences between these elements was not a problem.

The commercial FIAS FI accessory for atomic spectroscopies has also been used to couple TRU-Resin column separations to ICP-MS, as described by Epov et al.[51–53]
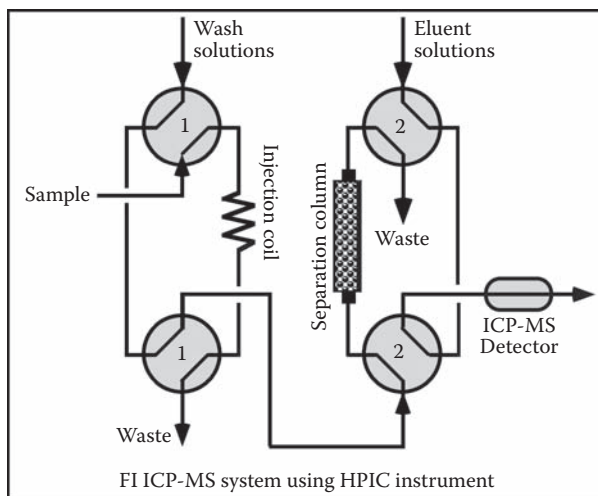
FIGURE 9.16 Design of an automated fluidic system based on the coupling of a high performance ion-chromatography system to an ICP-MS, where the ion-exchange column has been replaced with a TRU-Resin column.

The TRU-Resin column served to preconcentrate the actinide of interest from urine or digested urine samples. Methods were developed for the analysis of Pu in urine, Am in urine, as well as U and Th in urine. After column washing, the actinides were eluted in a single step, using ethylenediaminetetraacetic acid for Am or Pu, and ammonium bioxalate for the U/Th determinations. Column reusability was quite limited if urine samples were not digested first.

CMPO, the selective extractant chemistry in TRU-Resin, can be impregnated into polymers that also contain organic fluor molecules to develop sensor materials, as described previously for crown ether and liquid anion-exchange chemistry. Actinide sensing by this approach has been described.[96,135–137] Such sensor chemistries have potential for use in the development of on-line monitors.

9.4.3.2 UTEVA-Resin Separations

Several groups have described the use of UTEVA-Resin separations coupled to ICP-MS for actinide analyses (see Table 9.4). UTEVA-Resin contains the extractant dipentyl pentylphosphonate (DP[PP]), which is also known as diamylamyl phosphonate (DAAP).[31] This extractant retains actinides from nitric acid solutions as nitrato complexes, with increasing uptake as nitric acid concentrations increase (see Figure 9.11). Extraction equilibria for representative species are shown in Equations 9.6 and 9.7, where the bar above a species indicates that it is immobilized on the resin.[4]

$$Th^{4+} + 4NO_3^- + \overline{3\ DP[PP]} \rightleftharpoons \overline{(DP[PP])_3 Th(NO_3)_4} \qquad (9.6)$$

$$UO_2^{2+} + 2NO_3^- + \overline{2\ DP[PP]} \rightleftharpoons \overline{(DP[PP])_2 UO_2(NO_3)_2} \qquad (9.7)$$
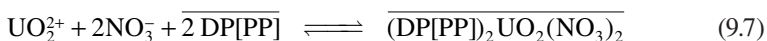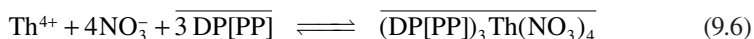
Loading the sample in nitric acid solution, the tetravalent actinides are strongly retained along with hexavalent uranium. However, trivalent actinides like Am(III) and Pu(III) are not retained from nitric acid solutions (unlike TRU-Resin). Pu retained as Pu(IV) can be removed from the column by reducing it to Pu(III). Tetravalent actinides and U(VI) are also retained in strong hydrochloric acid solution, with retention sharply dropping off as hydrochloric acid concentrations decrease (see Figure 9.12). Th(IV) is less retained in hydrochloric acid solutions than U(VI). Actinides retained on UTEVA-Resin from nitric acid solutions can be released with diluted nitric acid or low hydrochloric acid concentrations.

Betti et al. examined the elution of multiple actinides in detail.[138] Noting that Am(III), Pu(III), and Np(V) are unretained in nitric acid, these authors used a sample pretreatment approach that first reduced the sample with ferrous ion to obtain Np(IV), and then used nitrite to convert the reduced Pu(III) to Pu(IV). In column separations, the sample was loaded and washed in 3 M HNO_3, removing Am(III) in the wash. The nonretention of Am(III) was desirable to prevent isobaric interferences with other actinides. Then Pu(IV), Np(IV), and Th(IV) were eluted together in 2 M HCl−0.1 M oxalic acid, followed by elution of U with 0.025 M HCl. This separation is shown in Figure 9.17. By including 0.1 M oxalic acid in the 2 M HCl eluent, the tetravalent actinides were released with sharper, faster peaks, improving the separation from the subsequent U peak. Without oxalic acid in the 2 M HCl eluent, the tetravalents elute as broader overlapped peaks in the order Th-Np-Pu. With oxalic acid, the order changes to Np-Pu-Th and the peaks are more closely overlapped, thus providing the improved separation from U. The separation procedure was coupled to an ICP-MS using FI methods and used in the analysis of dissolved sediments and dissolved irradiated nuclear fuels.

Kang et al. used a UTEVA-Resin column as part of a 10-port valve FI system coupled to ICP-MS.[139] Samples were loaded in 3 M HNO_3 and eluted in 0.02 M HNO_3. This simple method was developed for the preconcentration and analysis of U in seawater. Similar procedures for the analysis of U in urine or U and Th in body fluids
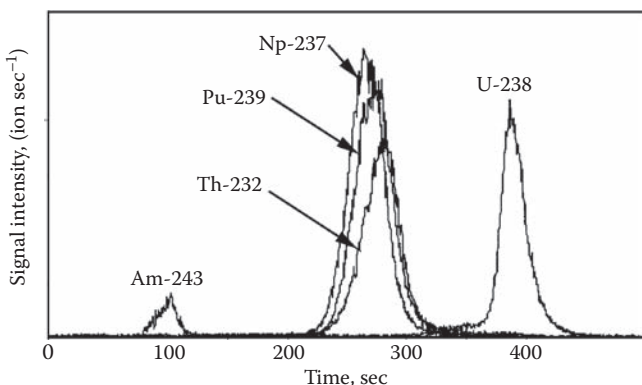
FIGURE 9.17   Separation of actinides on UTEVA-Resin with ICP-MS detection. (Adapted from Perna, L., Betti, M., Moreno, J. M. B., and Fuoco, R., *J. Anal. At. Spectrom.*, 16, 26–31, 2001. Copyright 2001 Royal Society of Chemistry. With permission.)

have been developed by Kuwabara, Tolmachyov, and Noguchi.[140,141] For U analysis, a FI system performed sample load in 4 M HNO_3 and U elution in 0.05 M HCl. In the U/Th analysis case, a FI system loaded the sample in 6.5 M HNO_3 and eluted U and Th together in 0.025 M oxalic acid, which was selected to reduce the formation of molecular interferences compared to using dilute hydrochloric acid as eluent. Godoy et al. also used a simple elution procedure for the analysis of U and Th isotopes in ocean sediments, loading the dissolved sample on the UTEVA column in 3 M HNO_3 and eluting U and Th together in 0.05 M ammonium oxalate.[142] A FI system was used, and the purpose of the analysis was to evaluate uranium series disequilibrium.

Ohtsuka et al. used UTEVA-Resin to set up a Pu analysis method, taking advantage of the ability to retain Pu in the Pu(IV) state, wash away other trivalents, and then selectively reduce and elute the Pu as Pu(III), thus separating it from still-retained U.[58,59] Samples were loaded and washed in 3 M HNO_3, and Pu(III) was released with 0.01 M ascorbic acid in 3 M HNO_3. Ascorbic acid provides rapid reduction and is destroyed in the ICP-MS torch. A decontamination factor of 6 to 7 orders of magnitude was estimated for the Pu-U separation. After Pu elution, U could be removed in dilute nitric acid. Chemical recovery of Pu was 70% in the analysis of several sediment reference samples. These authors used the PrepLab system set up as shown in Figure 9.18.

9.4.3.3   TEVA-Resin Separations

TEVA-Resin is an extraction-chromatographic material based on Aliquat 336, which is a liquid quaternary ammonium salt, as described previously in connection with ^{99}Tc separations.[30] It acts as a strongly basic anion-exchange material, retaining tetravalent actinides from 2–4 M HNO_3 solutions as anionic nitrato complexes (see Figure 9.11). Am(III), Np(V), and U(VI) are much less retained. The extraction

Peristaltic pump

Sample, wash, eluent solutions

Separation column

Waste

ICP-MS Detector

Peristaltic pump

Preplab system example
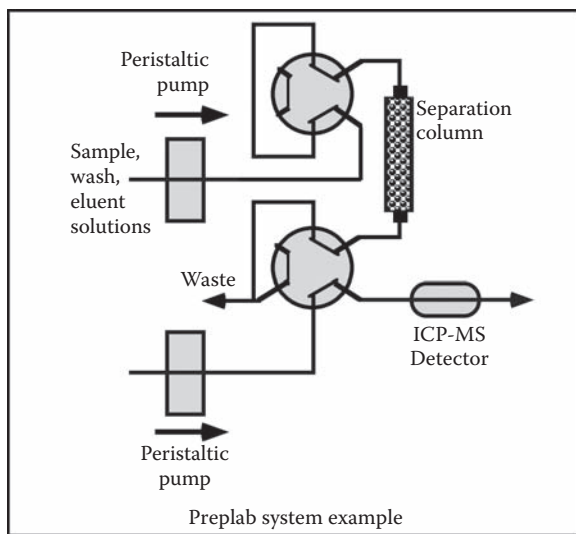
FIGURE 9.18   FI separation system for ICP-MS based on the PrepLab instrument.

equilibrium for a representative tetravalent species is shown in Equation 9.8, where A^+ indicates the quaternary ammonium group and the bar above a species indicates that it is immobilized on the resin. In strong nitric acid, the Pu(IV) species in solution would be the dianion, $Pu(NO_3)_6^{2-}$.

$$Pu^{4+} + 4NO_3^- + \overline{2\,(A^+NO_3^-)} \rightleftharpoons \overline{(A^+)_2\,Pu(NO_3)_6^{2-}} \tag{9.8}$$
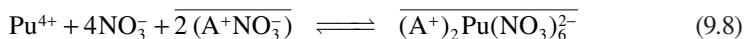
As the nitric acid concentration decreases, the retention of tetravalent actinides decreases. In strong hydrochloric acid, Pu(IV), Np(IV), and U(VI) are strongly retained, but Th(IV) and Am(III) are not (see Figure 9.12). By adjusting acid concentrations and valencies, a number of separations can be set up. For example, after loading the actinides and washing the column, which will remove unretained Am(III), U(VI) can be eluted with 2 M HNO_3, followed by Th(IV) with 3 M HCl.[30] The tetravalent actinides Pu(IV) and Np(IV) can be eluted with 0.5 M HCl. Pu(IV) on the column can be reduced and released as Pu(III) to separate it from Np(IV). As an on-line separation method for ICP-MS analyses, TEVA-Resin has been used primarily to isolate Pu, or Pu and Np. It has also been used in tandem column separations for Pu analysis. Separation of the U from Pu is important to reduce the interference of $^{238}U^1H$ with ^{239}Pu determination. TEVA-Resin column separations used in conjunction with ICP-MS for the separation and determination Pu isotopes are summarized in Table 9.5.

Kim et al. used tandem columns of Sr-Resin with TEVA-Resin, taking advantage of the affinity of Sr-Resin for Pu(IV).[56,57] Elution of the Pu(IV) from Sr-Resin provides broad peaks, which could be focused by capturing the Pu on TEVA-Resin. It was then eluted to an autosampler, which delivered it to the ICP-MS. A PrepLab system was used to automate the fluidic separations. For the analysis of soil digestates,[56] the sample was loaded and washed on Sr-Resin in 4 M HNO_3, followed by elution and capture on TEVA-Resin using 0.8 M HNO_3. A solution of 2 M HCl was used to elute Pu from the TEVA-Resin to the autosampler. Chemical recoveries of Pu exceeded 90% given proper valence state adjustment prior to the analysis, and the decontamination factor for removing U was on the order of four to five orders of magnitude. A similar tandem column approach was used for the analysis of Pu isotopes in seawater.[57]

Kim has also described a single-column TEVA separation for Pu analysis, again using the PrepLab system for fluid handling.[55] After using ascorbic acid to reduce Np(V) and Pu(VI) in soil digestates to Np(IV) and Pu(IV), samples were loaded and washed in 5 M HNO_3. Then 9 M HCl was used to strip Th, and 1 M HNO_3 was used to strip residual U. Pu and Np were eluted to the autosampler with 0.5 M HNO_3. Using a sector field ICP-MS for detection, this method was applied to the analysis of environmental levels of Np and Pu in sediment samples. Kim has recently reviewed ICP-MS methods for Pu isotope determinations.[15]

Epov et al. used TEVA-Resin in the isolation of Pu for the analysis of Pu in the presence of much higher U concentrations, using the FIAS-400 fluidic system.[50] These authors also selected ascorbic acid to adjust the valence state of Pu to Pu(IV). Samples were loaded and washed in 4 M HNO_3, removing the trivalent actinides. Elution with 1 M HNO_3 removed most U and some Th. Finally, 0.02 M HCl was

used to elute Pu together with Np and some Th. The low concentration of HCl was selected for Pu elution after examining concentrations from 2 to 0.5 M. The method was applied to digested sediment samples.

Lariviere developed a procedure for Pu analysis in urine, coupling a FI separation to ICP-MS.[143] Samples were loaded and washed on TEVA-Resin using 3 M HNO_3. With sufficient washing, U was removed; then, 5 M HCl was used to remove Th. Finally, 0.01 M ammonium oxalate was used to elute Pu. This final eluent was selected after examining figures of merit for four possible eluents, 0.01 M ammonium oxalate and 0.1 M HCl both being satisfactory and considered to be better than 0.01 M HNO_3 or 0.1 M ammonium oxalate.

9.5   AUTOMATED PROCESS MONITORING

Conventional radiochemical analysis of nuclear process or waste samples in the laboratory entails three primary activities: sample preparation, radiochemical separation, and detection. Each of these activities may entail multiple steps. The automated fluidic methods described above, typically also carried out in the laboratory, link separation and detection. Sample preparation has, in many cases, been carried out first by manual laboratory methods.

Process monitoring poses two additional challenges compared to these automated fluidic separation methods. First, methodology for automated sample preparation must be developed, and second, the entire sample preparation-separation-detection system must be developed to operate on-line or at-site under unattended computer control, including sample transport through all the steps. Sample preparation is particularly critical for nuclear-waste and nuclear-process streams due to the complexity of the sample matrix and the uncontrolled valence states of several of the potential analytes.

This task is challenging for the monitoring of α- and β-emitting radionuclides for reasons discussed above. However, even for gamma-emitting radionuclides, situations may exist where separations or concentration to a smaller volume in the range of a detector may be desirable.

Scientists at PNNL have developed an automated radiochemical sample preparation-separation-detection system for the determination of total ^{99}Tc in nuclear-waste process streams.[46,85,86,144,145] This analyzer was designed to support a technetium removal process planned as part of the development of a nuclear-waste processing plant. The process stream composition is both complex and variable, with a high pH, high salt matrix. Depending on the source of the feed, the total base content, the concentration of organics, and complexant concentrations will vary, as will the aluminum, nitrate, nitrite, dichromate, and radionuclide composition.

Sample preparation is required to cope with the sample matrix, the interferences, and the speciation of ^{99}Tc. The separation processes for isolating ^{99}Tc prior to radiometric detection require that the ^{99}Tc be in the pertechnetate ($^{99}TcO_4^-$) state. However, in waste samples with high organic content, much of the ^{99}Tc may be present in reduced valence states. Therefore, to determine the total ^{99}Tc content, all the ^{99}Tc must be oxidized to the pertechnetate state prior to ion-exchange or extraction-chromatographic separation.

Egorov et al. developed an automated radiochemical analysis system that incorporated an on-line microwave-assisted sample preparation system as a front end to a fluidic radiochemical separation system with on-line radiometric detection. This system is shown in simplified schematic form in Figure 9.19.[46,85,86,144,145] Designed for the determination of total ^{99}Tc in aged low-activity waste streams, the analyzer performed the steps required to acidify the caustic sample, vent evolved gases, oxidize the sample using peroxidisulfate, load and then separate pertechnetate from radioactive interferences on an anion-exchange column, and deliver the sample to a flow-through scintillation detector.

The scheme in Figure 9.19 shows a simplification of the separation unit, using a 2-position valve to reverse the flow through the column for load/wash and elute steps, and an additional 2-position valve as a detector diverter valve. The system also incorporated several zero-dead volume syringe pumps and several additional valves to route sample and reagents through the system.

The microwave unit of the sample-preparation system provides heating during sample acidification and oxidation procedures. Heating promotes the dissolution of $Al(OH)_3$ precipitates formed during the acidification step, as well as the removal of nitrites, as gaseous NO_x species, which could interfere with subsequent oxidation.
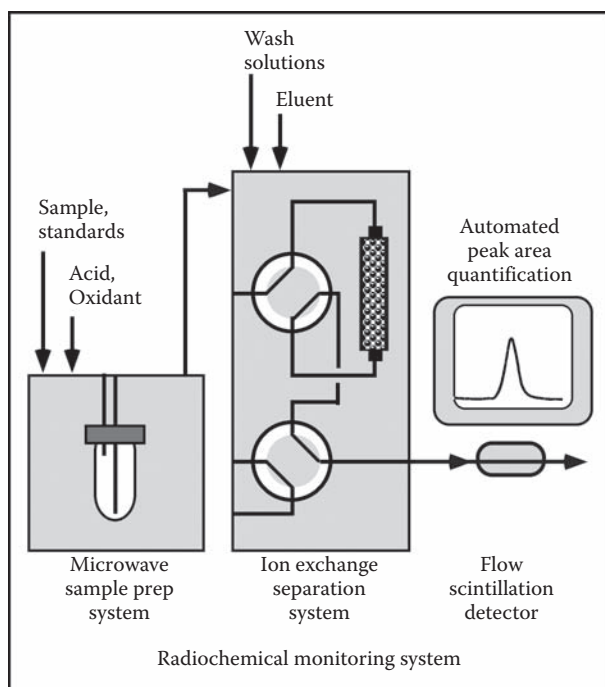
FIGURE 9.19 Simplified schematic diagram illustrating sample preparation, separation, and detection for an on-line analyzer for the continuous monitoring of the total ^{99}Tc content of nuclear-waste process streams. A number of zero-dead volume syringe pumps and valves are not shown.

The acid addition and heating protocol were designed to avoid excessive foaming and boiling within the microwave-digestion vessel.

An additional heating protocol is applied with the addition of sodium peroxidisulfate to promote complete oxidation of reduced ^{99}Tc species and destruction of at least a portion of the organic species. It was determined that reduced technetium species can be completely oxidized by the peroxidisulfate without having to oxidize all the organic carbon first. The overall sample-preparation procedure was designed to leave the ^{99}Tc as pertechnetate in an acidic solution composition that is compatible with the subsequent anion-exchange separation. The solution must be made sufficiently acidic to completely dissolve the aluminum hydroxides, but not so acidic that pertechnetate is not retained on the anion-exchange resin.

A macroporous strongly basic anion-exchange resin (Bio-Rad AG MP-1 M) was selected for the separation step. Although the elution kinetics of an extraction-chromatographic anion-exchange material such as TEVA-Resin (described above) are superior, the solid-phase anion-exchange resin was selected to obtain longer column life and reusability. Using column flow reversal, pertechnetate could be eluted rapidly from the solid-phase material. The separation selectivity provided reliable separation of pertechnetate from the major radioactive constituents, such as the fission products ^{90}Sr, ^{90}Y, and ^{137}Cs. A combination of column wash steps using dilute nitric acid, nitric-oxalic acid, sodium hydroxide, and moderately concentrated nitric acid was developed to ensure reliable separation of pertechnetate from anionic species of Sn, Sb, and Ru.

The separated pertechnetate was determined in a flow-through detector using lithium glass solid scintillator. A fully automated standard-addition technique was implemented as part of the analytical protocol to ensure accurate results with varying sample matrix compositions. After every fourth sample analysis, the sample was repeated after spiking it with a ^{99}Tc standard in nitric acid during the sample acidification step. The injected volume of the spike solution was calculated for each sample, based on the signal from the previous unspiked sample, to provide good measurement precision. Peak areas from the detector signals were determined automatically.

The total time for analysis—including sample preparation, separation, and detection—was 12.5 minutes for one sample, or 22 minutes for the sample and spiked sample. In tests on actual Hanford nuclear-waste samples, comparing results from the automated analyzer method to laboratory ICP-MS determinations, the analyzer method proved to be accurate in the determination of total ^{99}Tc.

9.6   DISCUSSION

The development of solvent-impregnated resins and extraction-chromatographic procedures has enabled the automation of radiochemical separations for analytical radionuclide determinations. These separations provide preconcentration from simple matrices like groundwater and separation from complex matrixes such as dissolved sediments, dissolved spent fuel, or nuclear-waste materials. Most of the published work has been carried out using fluidic systems to couple column-based separations to on-line detection, but robotic methods also appear to be very promising. Many approaches to fluidic automation have been used, from individual FI and SI systems to commercial FI sample-introduction systems for atomic spectroscopies.

Column-based separation formats are convenient and fast, but they are not the only options available. Miro et al. have shown, for example, that liquid-liquid extraction can be implemented in a fluidic system for ^{90}Sr separation by creating a wetting film of extractant inside a flow-system tubing wall.[146] A SI separation system (see Figures 9.3 and 9.4) was set up with a holding coil, multiposition valve, and 2-position diverter valve, replacing the separation column with an extraction coil. After coating the coil with extractant solution, the sample was loaded and the extractant was washed. Captured ^{90}Sr in the extractant film was recovered by using an organic solvent that stripped the extractant from the coil.

The DGA extractant,[147] shown in Scheme 9.1, has been coated on magnetic particles for magnetically assisted chemical separations (MACS).[148] By capturing the actinides from aqueous solutions into the extractant, and then separating the extractant though a magnetic solid-liquid separation, the actinides are separated from the aqueous solution. This approach has been demonstrated with a number of extractants for separating actinides, and applications to nuclear waste streams have been discussed.[148–150] Magnetic separation processes can be automated, and it was demonstrated that the extractant-loaded particles could be stripped and reused.

The Dipex extractant shown in Scheme 9.1, as actinide-Resin, has not been used in an automated separation scheme. With two phosphoryl groups, this extractant is very effective at retaining actinides, but it is difficult to recover them by elution. For laboratory analysis, schemes have been developed to strip the extractant from the resin after capturing the actinides.[151]

Some extractants have been used in the development of selective sensors for radionuclides. These have been noted in Tables 9.1 through 9.3 and briefly mentioned above. They were recently reviewed in detail.[99] In addition to column sensor formats, extractants have been coated onto passivated ion-implanted planar silicon (PIPS) diodes to create selective radionuclide sensors.[152,153] Though not a focus of this review, it is worth noting the such sensors, combining separation and detection in a single functional unit, have potential for use in process-monitoring applications.

Finally, the development of automated radiochemical separations has enabled the possibility of open-architecture radiochemical analyzer workstations. Instead of having a system set up to perform only one procedure with a particular separation material, workstations could be set up with the capability of performing a variety of radiochemical separations, which would be selected from software menus by the user. At the direction of the computer, the instrument would then load a separation material into a column, using the renewable separation column methodology,[83] or select from a number of different separation columns already configured on the system. The separation would proceed according to preprogramed instructions, selecting solutions and eluents from a variety of such reagents already available via selection valves. This approach was briefly demonstrated with renewable separation columns, using the same system to perform ^{90}Sr separations on Sr-Resin and actinide separations on TRU-Resin.[83]

Radiochemical analysis will continue to be important in many aspects of the use of nuclear fuels, including spent-fuel analysis; monitoring reprocessing for process performance or safeguards; analyzing environmental samples for contamination; and

performing bioassays for the health of workers in the nuclear industry or potentially contaminated citizens in a nuclear event. In the instance of capturing diverted nuclear materials, analysis will be required to support forensics and attribution. Whether in the laboratory or integrated into a processing plant, automation will be important to provide timely analytical results, reduce costs, improve worker safety, and develop high-throughput capabilities that will be needed in nuclear emergencies.

Process monitoring, with on-line instruments that operate autonomously for extended periods of time, presents significant challenges and opportunities. The requirements for monitors will vary with the application they support. Where the monitor is set up to support a particular separation process, the analytical objectives may be to determine a single species. The technetium monitor described above, designed to support a technetium removal process, is such an example. On the other hand, some processes may seek to determine multiple actinides in a process stream. These actinides could be a selected group of the transuranic (TRU) elements, or the multiple isotopes of a particular actinide like plutonium.

Process monitors in the nuclear field must deal with complex sample matrixes. Depending on the process, the feed may be strongly acidic or strongly basic, and most likely it will be high ionic strength. In most processes, the feed composition will be variable. The instrumentation, chemistry, and analytical approach must be sufficiently robust to provide effective sample processing and accurate analytical information, regardless of inconsistent feed composition.

Opportunities remain to develop new or improved separation chemistries, and the engineered solid-phase materials that utilize them, in order to support radioanalytical needs. Selectivity remains a key issue in order to support isolation of particular elements or groups of elements from complex sample matrixes. Selectivity to support determination of TRU actinides in the presence of large excesses of uranium is often required. The engineered form is also significant, as it must enable the separation chemistry to work while providing a robust material that can be used over and over again.

Process-monitoring instrumentation and methodology can be designed to cope with shortcomings of the separation chemistry or the engineered separation material. Methods such as matrix modification and renewable column techniques, which are described above, can be quite helpful in this regard. Nevertheless, improved materials and separations, where the material does not leach extractant, is highly selective for the analyte(s) of interest, works effectively in the face of complex and variable feed compositions, and where the eluent solutions are not too corrosive, can enable simpler, more robust, monitoring instrumentation.

ACKNOWLEDGMENTS

REFERENCES

1. Choppin, G. R., Separation processes for actinide elements, *Sep. Sci. Technol.*, 19, 911–925, 1984–1985.
2. Rydberg, J., Cox, M., Musikas, C., and Choppin, G. R., Eds., *Solvent Extraction Principles and Practice*, 2nd ed., Marcel Dekker: New York, 2004, 2622–2798.
3. Nash, K. L., Madic, C., Mathur, J. N., and Lacquement, J., Actinide separation science and technology, in *The Chemistry of the Actinide and Transactinide Elements*, 3rd ed., Vol. 4, Morss, L. R., Edelstein, N. M., Fuger, J., and Katz, J. L., Eds., Springer: Dordrecht, 2006.
4. Cortina, J. L. and Warshawsky, A., Developments in solid-liquid extraction by solvent-impregnated resins, *Ion Exch. Solvent Extr.*, 13, 195–293, 1997.
5. Denoyer, E. R., Expanding ICP-MS capabilities using flow injection, *Am. Lab.*, 24, 74–82, 1992.
6. Colodner, D., Salters, V., and Duckworth, D. C., Ion sources for analysis of inorganic solids and liquids by MS, *Anal. Chem.*, 66, 1079A-1089A, 1994.
7. Thompson, J. J. and Houk, R. S., Inductively coupled plasma mass spectrometric detection for multielement flow injection analysis and elemental speciation by reversed phase liquid chromatography, *Anal. Chem.*, 58, 2541–2548, 1986.
8. Tan, S. H. and Horlick, G., Background spectral features in inductively coupled plasma/ mass spectrometry, *Appl. Spectrosc.*, 40, 445–460, 1986.
9. Garcia Alonso, J. I., Babelot, J.-F., Glatz, J.-P., Cromboon, O., and Koch, L., Applications of glove-box ICP-MS for the analysis of nuclear materials, *Radiochim. Acta*, 62, 71–79, 1993.
10. Garcia Alonso, J. I., Sena, R., Arbore, P., Betti, M., and Koch, L., Determination of fission products and actinides in spent nuclear fuels by isotope dilution ion chromatography inductively coupled plasma mass spectrometry, *J. Anal. At. Spectrom.*, 10, 381–393, 1995.
11. Garcia Alonso, J. I., Determination of fission products and actinides by inductively coupled plasma mass spectrometry using isotope dilution analysis: A study of random and systematic errors, *Anal. Chim. Acta*, 312, 57–78, 1995.
12. Smith, M. R., Farmer, O. T., Reeves, J. H., and Koppenaal, D. W., Radionuclide detection by ion-chromatography and on-line ICP/MS and beta detection: Fission product rare earth element measurements, *J. Radianal. Nucl. Chem.*, 194, 7–13, 1995.
13. Crain, J. S. and Alvarado, J., Hydride interference on the determination of minor actinide isotopes by inductively coupled plasma mass spectrometry, *J. Anal. At. Spectrom.*, 9, 1223–1227, 1994.
14. Lariviere, D., Taylor, V. F., Evans, R. D., and Cornett, R. J., Radionuclide determination in environmental samples by inductively coupled plasma mass spectrometry, *Spectrochim. Acta, Part B*, 61, 877–904, 2006.
15. Kim, C. S., Kim, C. K., Martin, P., and Sansone, U., Determination of Pu isotope concentrations and isotope ratio by inductively coupled plasma mass spectrometry: A review of analytical methodology, *J. Anal. At. Spectrom.*, 22, 827–841, 2007.
16. Smith, M. R., Wyse, E. J., and Koppenaal, D. W., Radiounuclide detection by inductively coupled plasma mass spectrometry: A comparison of atomic and radiation detection methods, *J. Radioanal. Nucl. Chem.*, 160, 341–354, 1992.

17. Ross, R. R., Noyce, J. R., and Lardy, M. M., Inductively coupled plasma-mass spectrometry: An emerging method for analysis of long-lived radionuclides, *Radioact. Radiochem.*, 4, 24–37, 1993.

18. Grudpan, K., Laiwraungrath, S., and Sooksamiti, P., Flow injection spectrophotometric determination of uranium with in-valve ion-exchange column preconcentration and separation, *Analyst*, 120, 2107–2110, 1995.

19. Grudpan, K., Jakmunee, J., and Sooksamiti, P., Flow-injection in-valve solid-phase extraction spectrophotometric determination of uranium in geological samples, *Lab. Rob. Autom.*, 10, 25–31, 1998.

20. Grudpan, K., Jakmunee, J., and Sooksamiti, P., Spectrophotometric determination of uranium by flow injection analysis using U/TEVA. Spec chromatographic resin, *J. Radioanal. Nucl. Chem.*, 229, 179–181, 1998.

21. Pavon, J. L. P., Pinto, C. G., Garcia, E. R., and Cordero, B. M., Flow-injection determination of thorium and uranium after on-line ion-exchange preconcentration on dowex 50-x8, *Anal. Chim. Acta*, 264, 291–296, 1992.

22. Izatt, R. M., Bradshaw, J. S., and Bruening, R. L., Accomplishment of difficult chemical separations using solid phase extraction, *Pure Appl. Chem.*, 68, 1237–1241, 1996.

23. Izatt, R. M., Review of selective ion separations at BYU using liquid membrane and solid phase extraction procedures, *J. Incl. Phenom. Mol. Rec. Chem.*, 29, 197–220, 1997.

24. Izatt, R. M., Bradshaw, J. S., Bruening, R. L., and Bruening, M. L., Solid phase extraction of ions of analytical interest using molecular recognition technology, *Am. Lab*, 26, no. 18, 28c–28m, 1994.

25. Izatt, S. R., Bruening, R. L., Krakowiak, K. E., and Izatt, R. M., The selective separation of anions and cations in nuclear waste using commercially available molecular recognition technology (mrt) products, in *Proceedings of Waste Management 2003 Symposium WM'03*, http://www.Wmsym.Org/abstracts/2003/html/prof379.html, February 23–27, Tuscon, AZ, 2003, 1–11.

26. Dietz, M. L. and Horwitz, E. P., Novel chromatographic materials based on nuclear waste processing chemistry, *LC-GC*, 11, 424–436, 1993.

27. Horwitz, E. P., McAlister, D. R., and Dietz, M. L., Extraction chromatography versus solvent extraction: How similar are they? *Sep. Sci. Technol.*, 41, 2163–2182, 2006.

28. Horwitz, E. P., Extraction chromatography of actinides and selected fission products: Principles and achievement of selectivity, in *International Workshop on Application of Extraction Chromatography in Radionuclide Measurement (IRMM)*, Geel, Belgium, 1998, 27–37.

29. Dietz, M. L., Horwitz, E. P., and Bond, A. H., Extraction chromatography: Progress and opportunities, *ACS Symp. Ser.*, 716, 234–250, 1999.

30. Horwitz, E. P., Dietz, M. L., Chiarizia, R., Diamond, H., Maxwell, S. L., and Nelson, M. R., Separation and preconcentration of actinides by extraction chromatography using a supported liquid anion exchanger: Application to the characterization of high-level nuclear waste solutions, *Anal. Chim. Acta*, 310, 63–78, 1995.

31. Horwitz, E. P., Dietz, M. L., Chiarizia, R., Diamond, H., Essling, A. M., and Graczyk, D., Separation and preconcentration of uranium from acidic media by extraction chromatography, *Anal. Chim. Acta*, 266, 25–37, 1992.

32. Ruzicka, J. and Hansen, E. H. *Flow Injection Analysis*, 2nd ed., Vol. 62, Wiley-Interscience: New York, 1988, 498.

33. Fang, Z. *Flow Injection Separation and Preconcentration*, VCH: Weinheim, 1993.

34. Ruzicka, J., Discovering flow injection; journey from sample to live cell and from solution to suspension, *Analyst*, 119, 1925–1934, 1994.

35. Ruzicka, J. and Marshall, G. D., Sequential injection: A new concept for chemical sensors, process analysis and laboratory assays, *Anal. Chim. Acta*, 237 (2), 329–343, 1990.

36. Ivaska, A. and Ruzicka, J., From flow injection to sequential injection: Comparison of methodologies and selection of liquid drives, *Analyst*, 118, 885–889, 1993.

37. Christian, G. D., Sequential injection analysis for electrochemical measurements and process analysis, *Analyst*, 119, 2309–2314, 1994.

38. Taljaard, R. E. and van Staden, J. F., Application of sequential-injection analysis as process analyzers, *Lab. Rob. Autom.*, 10, 325–337, 1998.

39. Cerda, A., Estala, J. M., Forteza, R., Cladera, A., Becerra, E., Altimira, P., and Sitjar, P., Flow techniques in water analysis, *Talanta*, 50, 695–705, 1999.

40. Cerda, V., Cerda, A., Cladera, A., Oms, M. T., Mas, F., Gomez, E., Bauza, F., Miro, M., Forteza, R., and Estela, J. M., Monitoring of environmental parameters by sequential injection analysis, *Trends Anal. Chem.*, 20, 407–418, 2001.

41. Lenehan, C. E., Barnett, N. W., and Lewis, S. W., Sequential injection analysis, *Analyst*, 127, 997–1020, 2002.

42. Grudpan, K., Some recent developments on cost-effective flow-based analysis, *Talanta*, 64, 1084–1090, 2004.

43. Ruzicka, J., From beaker chemistry to programmable microfluidics, *Collect. Czech. Chem. Commun.*, 70, 1737–1755, 2005.

44. Egorov, O. B., O'Hara, M. J., Ruzicka, J., and Grate, J. W., Sequential injection system with stopped flow radiometric detection for automated analysis of 99Tc in nuclear waste, *Anal. Chem.*, 70, 977–984, 1998.

45. Mateos, J. J., Gomez, E., Garcias, F., Casas, M., and Cerda, V., Rapid Sr-90/Y-90 determination in water samples using a sequential injection method, *Appl. Radiat. Isot.*, 53, 139–144, 2000.

46. Grate, J. W. and Egorov, O. B., Automated radiochemical separation, analysis, and sensing, in *Handbook of Radioactivity Analysis*, 2nd ed., L'Annunziata, M. F., Ed., Elsevier, Academic Press: San Diego, 2003, 1129–1164.

47. Grate, J. W., Fadeff, S. K., and Egorov, O., Separation-optimized sequential injection method for rapid automated separation and determination of 90Sr in nuclear waste, *Analyst*, 124, 203–210, 1999.

48. Grate, J. W., Egorov, O. B., and Fiskum, S. K., Automated extraction chromatographic separations of actinides using separation-optimized sequential injection techniques, *Analyst*, 124, 1143–1150, 1999.

49. Hollenbach, M., Grohs, J., Mamich, S., Kroft, M., and Denoyer, E. R., Determination of technetium-99, thorium-230 and uranium-234 in soils by inductively coupled plasma mass spectrometry using flow injection preconcentration, *J. Anal. At. Spectrom.*, 9, 927–933, 1994.

50. Epov, V. N., Evans, R. D., Zheng, J., Donard, O. F. X., and Yamada, M., Rapid fingerprinting of Pu-239 and Pu-240 in environmental samples with high U levels using online ion chromatography coupled with high-sensitivity quadrupole ICP-MS detection, *J. Anal. At. Spectrom.*, 22, 1131–1137, 2007.

51. Epov, V. N., Benkhedda, K., Cornett, R. J., and Evans, R. D., Rapid determination of plutonium in urine using flow injection on-line preconcentration and inductively coupled plasma mass spectrometry, *J. Anal. At. Spectrom.*, 20, 424–430, 2005.

52. Epov, V. N., Benkhedda, K., Brownell, D., Cornett, R. J., and Evans, R. D., Comparative study of three sample preparation approaches for the fast determination of americium in urine by flow injection ICP-MS, *Can. J. Anal. Sci. Spectrosc.*, 50, 14–22, 2005.

53. Benkhedda, K., Epov, V. N., and Evans, R. D., Flow-injection technique for determination of uranium and thorium isotopes in urine by inductively coupled plasma mass spectrometry, *Anal. Bioanal. Chem.*, 381, 1596–1603, 2005.

54. Benkhedda, K., Lariviere, D., Scott, S., and Evans, D., Hyphenation of flow-injection preconcentration and ICP-MS for the rapid determination of 226ra in natural waters, *J. Anal. At. Spectrom.*, 20, 523–528, 2005.

55. Kim, C. S., Kim, C. K., and Lee, K. J., Simultaneous analysis of Np-237 and Pu isotopes in environmental samples by ICP-SF-MS coupled with automated sequential injection system, *J. Anal. At. Spectrom.*, 19, 743–750, 2004.

56. Kim, C. S., Kim, C. K., Lee, J. I., and Lee, K. J., Rapid determination of Pu isotopes and atom ratios in small amounts of environmental samples by an on-line sample pre-treatment system and isotope dilution high resolution inductively coupled plasma mass spectrometry, *J. Anal. At. Spectrom.*, 15, 247–255, 2000.

57. Kim, C. S. and Kim, C. K., Determination of Pu isotopes in seawater by an on-line sequential injection technique with sector field inductively coupled plasma mass spectrometry, *Anal. Chem.*, 74, 3824–3832, 2002.

58. Ohtsuka, Y., Takaku, Y., Nishimura, K., Kimura, J., Hisamatsu, S., and Inaba, J., Rapid method for the analysis of plutonium isotopes in a soil sample within 60 min, *Anal. Sci.*, 22, 309–311, 2006.

59. Ohtsuka, Y., Takaku, Y., Kimura, J., Hisamatsu, S., and Inaba, J., Development of rapid plutonium analysis for environmental samples by isotope dilution/inductively coupled plasma mass spectrometry with on-line column, *Anal. Sci.*, 21, 205–208, 2005.

60. Hang, W., Zhu, L. W., Zhong, W. W., and Mahan, C., Separation of actinides at ultra-trace level from urine matrix using extraction chromatography-inductively coupled plasma mass spectrometry, *J. Anal. At. Spectrom.*, 19, 966–972, 2004.

61. Peterson, D. S., Plionis, A. A., and Gonzales, E. R., Optimization of extraction chromatography separations of trace levels of actinides with ICP-MS detection, *J. Separat. Sci.*, 30, 1575–1582, 2007.

62. Zahradnik, P. and Swietly, H., The robotized chemical treatment of diluted spent fuel samples prior to isotope dilution analysis, *J. Radioanal. Nucl. Chem.*, 204, 145–157, 1996.

63. Ziegler, H. and Mayer, K., Development of an optimized method for faster and more reliable automated U/Pu/Np separations, *Radiochim. Acta*, 86, 123–128, 1999.

64. Richer, P., Brandalise, B., Apostolidis, C., Molinet, R., and Mayer, K., Development of a robotized separation method for U-Pu samples using UTEVA resin, in *Proc. Int. Workshop on the Application of Extraction Chromatography in Radionuclide Measurements*, IRMM, Geel, 9–10 November, 1998.

65. Morgenstern, A., Apostolidis, C., Carlos-Marquez, R., Mayer, K., and Molinet, R., Single-column extraction chromatographic separation of U, Pu, Np, and Am, *Radiochim. Acta*, 90, 81–85, 2002.

66. Apostolidis, C., Molinet, R., Richir, P., Ougier, M., and Mayer, K., Development and validation of a simple, rapid, and robust method for the chemical separation of uranium and plutonium, *Radiochim. Acta*, 83, 21–25, 1998.

67. Beugelsdijk, T. J. and Hollen, R. M., Robotics and automation in radiochemical analysis, in *Handbook of Radioactivity Analysis*, 1st ed., L'Annunziata, M. F., ed., Academic Press: San Diego, CA, 1998, 693–718.

68. Midorikawa, M., Sato, Y., Hara, S., Konno, K., and Iwanaga, M., The on-site laboratory for the rokkasho reprocessing plant in Japan, in *Addressing Verification Challenges*; IAEA-CN-148/103, International Atomic Energy Association, Vienna, 2007, 663–671.

69. Takahashi, M., Uchikoshi, S., Midorikawa, M., Ishikawa, M., and Adachi, T., Development of a digital-analog robotic system for input solution and mixed oxide samples, in *International Nuclear Safeguards 1994 Vision for the Future*; Volume 1 of 2, IAEA-SM-333/53, International Atomic Energy Association, Vienna, 1994, 761–767.

70. Brandalise, B., Ougier, M., Wellum, R., Wojnowski, D., and Koch, L., Robotized equipment for the on-site analysis of fissile material, in *International Nuclear Safeguards 1994 Vision for the Future*; Volume 1 of 2, IAEA-SM-333/37, International Atomic Energy Association, Vienna, 1994, 755–760.

71. Deron, S., Donohue, D., Bagliano, G., Kuhn, E., and Sirisena, K., The IAEA's analytical capabilities for safeguards, in *International Nuclear Safeguards 1994 Vision for the Future*; Volume 1 of 2, IAEA-SM-333/221, International Atomic Energy Association, Vienna, 1994, 717–738.

72. Surugaya, N., Taguchi, S., Kurosawa, A., and Watahiki, M., Improvement of analytical activities in the Tokai reprocessing plant, Japan, by measuring destructive and non-destructive assays, in *Addressing Verification Challenges*; Vol. IAEA-CN-148/104, International Atomic Energy Association, Vienna, 2007, 673–679.

73. Ruzicka, J. and Scampavia, L., From flow injection to bead injection, *Anal. Chem.*, 71, 257A–263A, 1999.

74. Miro, M. and Hansen, E. H., Solid reactors in sequential injection analysis: Recent trends in the environmental field, *Trends Anal. Chem.*, 25, 267–281, 2006.

75. Miro, M. and Frenzel, W., A critical examination of sorbent extraction preconcentration with spectrophotometric sensing in flowing systems, *Talanta*, 64, 290–301, 2004.

76. Miro, M. and Frenzel, W., Flow-through sorptive preconcentration with direct optosensing at solid surfaces for trace-ion analysis, *Trends Anal. Chem.*, 23, 11–20, 2004.

77. Dadfarnia, S. and McLeod, C. W., On-line trace enrichment and determination of uranium in waters by flow injection inductively coupled plasma mass spectrometry, *Appl. Spectrosc.*, 48, 1331–1336, 1994.

78. Aldstadt, J. H., Kuo, J. M., Smith, L. L., and Erickson, M. D., Determination of uranium by flow injection inductively coupled plasma mass spectrometry, *Anal. Chim. Acta*, 319, 135–143, 1996.

79. Nevissi, A. E. and Strebin, R. S., Automated radiochemical procedure for plutonium and americium measurement, *J. Radioanal. Nucl. Chem.*, 197, 211–218, 1995.

80. Grate, J. W., Strebin, R. S., Janata, J., Egorov, O., and Ruzicka, J., Automated analysis of radionuclides in nuclear waste: Rapid determination of Sr-90 by sequential injection analysis, *Anal. Chem.*, 68, 333–340, 1996.

81. Egorov, O., Grate, J. W., and Ruzicka, J., Automation of radiochemical analysis by flow injection techniques: Am-Pu separation using TRU-resin sorbent extraction column, *J. Radioanal. Nucl. Chem.*, 234, 231–235, 1998.

82. Grate, J. W. and Egorov, O., Investigation and optimization of on-column redox reactions in the sorbent extraction separation of americium and plutonium using flow injection analysis, *Anal. Chem.*, 70, 3920–3929, 1998.

83. Egorov, O., O'Hara, M. J., Grate, J. W., and Ruzicka, J., Sequential injection renewable separation column instrument for automated sorbent extraction separations of radionuclides, *Anal. Chem.*, 71, 345–352, 1999.

84. Grate, J. W. and Egorov, O. B., Automating analytical separations in radiochemistry, *Anal. Chem.*, 70, 779A–788A, 1998.

85. Egorov, O. B., O'Hara, M. J., Addleman, R. S., and Grate, J. W., Automation of radiochemical analysis: From groundwater monitoring to nuclear waste analysis, *ACS Symp. Ser.*, 868, 246–270, 2004.

86. Grate, J. W., Egorov, O. B., and O'Hara, M. J., Sensors and automated analyzers for radionuclides, *ACS Symp. Ser.*, 904, 322–341, 2004.

87. Egorov, O. B., O'Hara, M. J., Farmer, O. T., III, and Grate, J. W., Extraction chromatographic separations and analysis of actinides using sequential injection techniques with on-line inductively coupled plasma mass spectrometry (ICP MS) detection, *Analyst*, 126, 1594–1601, 2001.

88. Banavali, A. D., Raimondi, J. M., Moreno, E. M., and McCurdy, D. E., The determination of technetium-99 in low level radioactive was, *Radioact. Radiochem.*, 6, 26–35, 1995.

89. Dale, C. J., Warwick, P. E., and Croudace, I. W., An optimized method for technetium-99 determination in low level waste by extraction into tri-n-octylamine, *Radioact. Radiochem.*, 7, 23–27, 1996.

90. Holm, E., Rioseco, J., Ballestra, S., and Walton, A., Radiochemical measurements of technetium-99 sources and environmental levels, *J. Radioanal. Nucl. Chem.*, 123, 167–169, 1988.

91. Lavrukhina, A. K. and Pozdnyakov, A. A., *Analytical Chemistry of Technetium, Promethium, Astatine and Francium*; Ann Arbor-Humphery Science, Ann Arbor, MI, 1970, 1–92.

92. Nevissi, A. E., Silverston, M., R.S., S., and Kaye, J. H., Radiochemical determination of technetium-99, *J. Radioanal. Nucl. Chem. Articles*, 177, 91–99, 1994.

93. Silva, R. J., Evans, R., Rego, J. H., and Buddemeier, R. W., Methods and results of ^{99}Tc analysis of Nevada test site groundwaters, *J. Radioanal. Nucl. Chem.*, 124, 397–405, 1988.

94. Harvey, C. O., Separation of technetium by cation exchange and solvent extraction prior to measurement by beta counting. PNNL Technical Procedure pnl-alo-432, 1993, Pacific Northwest National Laboratory, Richland, WA.

95. Egorov, O. B., Fiskum, S. K., O'Hara, M. J., and Grate, J. W., Radionuclide sensors based on chemically selective scintillating microspheres: Renewable column sensor for analysis of 99Tc in water, *Anal. Chem.*, 71, 5420–5429, 1999.

96. DeVol, T. A., Roane, J. E., Williamson, J. M., Duffey, J. M., and Harvey, J. T., Development of scintillating extraction media for separation and measurement of charged-particle-emitting radionuclides in aqueous solutions, *Radioact. Radiochem.*, 11, 34–46, 2000.

97. DeVol, T. A., Egorov, O. B., Roane, J. E., Paulenova, A., and Grate, J. W., Extractive scintillating resin for 99Tc quantification in aqueous solutions, *J. Radioanal. Nucl. Chem.*, 249, 181–189, 2001.

98. Ayaz, B. and DeVol, T. A., Application of mno2 coated scintillating and extractive scintillating resins to screening for radioactivity in groundwater, *Nucl. Instrum. Methods Phys. Res., Sect. A*, 505, 458–461, 2003.

99. Grate, J. W., Egorov, O., O'Hara, M. J., and DeVol, T. A., Radionuclide sensors for environmental monitoring: From flow injection solid phase absorptiometry to equilibration-based preconcentrating minicolumn sensors with radiometric detection, *Chem. Rev.*, 108, 543–563, 2008.

100. Amano, H. and Yanase, N., Measurement of 90Sr in environmental samples by cation-exchange and liquid scintillation counting, *Talanta*, 37, 585–590, 1990.

101. Borcherding, J. and Nies, H., An improved method for the determination of 90Sr in large samples of seawater, *J. Radioanal. Nucl. Chem.*, 98, 127–131, 1986.

102. Cobb, J., Warwick, P., Carpenter, R. C., and Morrison, R. T., Determination of strontium-90 in water and urine samples using ion chromatography, *Analyst*, 119, 1759–1764, 1994.

103. Fourie, H. O. and Ghijsels, J. P., Radiostrontium in biological material: A precipitation and extraction procedure eliminating the use of fuming nitric acid, *Health Phys.*, 17 (5), 685–689, 1969.

104. Gattavecchia, E. and Tonelli, D., Determination of 90Sr by thin layer radiochromatography, *J. Radioanl. Nucl. Chem.*, 152, 391–399, 1991.

105. Kramer, G. H. and Davies, J. M., Isolation of strontium-90, yttrium-90, promethium-147, and cerium-144 from wet ashed urine by calcium oxalate coprecipitation and sequential solvent extraction, *Anal. Chem.*, 54, 1428–1431, 1982.

106. Kuno, Y., Sato, S., Ohno, E., and Masui, J., Rapid determination of strontium-90 in highly radioactive solutions of nuclear fuel reprocessing plant, *Anal. Sci.*, 9, 195–198, 1993.

107. Lamb, J. D., Nordmeyer, R. R., Drake, P. A., Elder, M. P., Miles, R. W., and Lah, R. P., Ion chromatographic separation for analysis of radiostrontium in nuclear reprocessing solutions of high ionic strength, *J. Radioanal. Nucl. Chem.*, 134, 317–331, 1989.

108. Noshkin, V. E. and Mott, N. S., Separation of strontium from large amounts of calcium, with application to radiostrontium analysis, *Talanta*, 14, 45–51, 1967.

109. Porter, C. R., Kahn, B., Carter, M. W., Vehnberg, G. L., and Pepper, E. W., Determination of radiostrontium in food and other environmental samples, *Environ. Sci. Technol.*, 1 (9), 745–750, 1967.

110. Wilken, R. D. and Diehl, R., Strontium-90 in environmental samples from northern Germany before and after the Chernobyl accident, *Radiochim. Acta*, 41, 157–162, 1987.

111. Wilken, R.-D. and Joshi, S. R., Rapid methods for determining 90Sr, 89Sr, and 90Y in environmental samples: A survey, *Radioact. Radiochem.*, 3, 15–27, 1991.

112. Smulek, W. and Lada, W. A., Separation of alkali and alkaline earth metals by polyethers using extraction chromatography. Effect of diluent, *J. Radioanal. Chem.*, 50, 169–178, 1979.

113. Wood, D. J., Elshani, S., Du, H. S., Natale, N. R., and Wai, C. M., Separation of 90Y from 90Sr by solvent extraction with ionizable crown ethers, *Anal. Chem.*, 65, 1350–1354, 1993.

114. Kremliakova, N. Y., Novikov, A. P., and Myasoedov, B. F., Extraction chromatographic separation of radionuclides of strontium, cesium, and barium with the use of tvex-dch18c6, *J. Radioanal. Nucl. Chem. Lett.*, 145, 23–28, 1990.

115. Alfaro, J., Apfel, T., Diercks, H., Knochel, A., Gupta, R. S., and Todter, K., Trace analysis of the radiounclides 90Sr and 89Sr in environmental samples iii: Development of a fast analytical method, *Angew. Chem. Int. Ed. Engl.*, 34, 186–189, 1995.

116. Dietz, M. L., Horwitz, E. P., Nelson, S. M., and Wahlgren, M., An improved method for determining 89Sr and 90Sr in urine, *Health Phys.*, 61, 871–877, 1991.

117. Horwitz, E. P., Dietz, M. L., and Fisher, D. E., Separation and preconcentration of strontium from biological, environmental, and nuclear waste samples by extraction chromatography using a crown ether, *Anal. Chem.*, 63, 522–525, 1991.

118. Horwitz, E. P., Chiarizia, R., and Dietz, M. L., A novel strontium-selective extraction chromatographic resin, *Solvent Extr. Ion Exch.*, 10, 313–336, 1992.

119. Horwitz, E. P., Dietz, M. L., and Chiarizia, R., The application of novel extraction chromatographic materials to the characterization of radioactive waste solutions, *J. Radioanal. Nucl. Chem., Articles*, 161, 575–583, 1992.

120. Dietz, M. L., Yaeger, J., Sajdak, L. R., and Jensen, M. P., Characterization of an improved extraction chromatographic material for the separation and preconcentration of strontium from acidic media, *Sep. Sci. Technol.*, 40, 349–366, 2005.

121. Fajardo, Y., Gomez, E., Mas, F., Garcias, F., Cerda, V., and Casas, M., Multisyringe flow injection analysis of stable and radioactive strontium in samples of environmental interest, *Appl. Radiat. Isot.*, 61, 273–277, 2004.

122. Miro, M., Cerda, V., and Estela, J. M., Multisyringe flow injection analysis: Characterization and applications, *Trends Anal. Chem.*, 21, 199–210, 2002.

123. Fajardo, Y., Gomez, E., Garcias, F., Cerda, V., and Casas, M., Multisyringe flow injection analysis of stable and radioactive yttrium in water and biological samples, *Anal. Chim. Acta*, 539, 189–194, 2005.

124. DeVol, T. A., Duffey, J. M., and Paulenova, A., Combined extraction chromatography and scintillation detection for off-line and on-line monitoring of strontium in aqueous solutions, *J. Radioanal. Nucl. Chem.*, 249, 295–301, 2001.

125. Caldes, A., Gomez, E., Garcias, F., Casas, M., and Cerda, V., A sequential injection method for radium determination in environmental samples, *Radioact. Radiochem.*, 10, 16–21, 1999.

126. Mateos, J. J., Gomez, E., Garcias, F., Casas, M., and Cerda, V., Implementation of a sequential injection pre-treatment method for simultaneous radium and strontium determination, *Int. J. Environ. Anal. Chem.*, 83, 515–521, 2003.

127. Horwitz, E. P., Chiarizia, R., Dietz, M. L., Diamond, H., and Nelson, D. M., Separation and preconcentration of actinides from acidic media by extraction chromatography, *Anal. Chim. Acta*, 281, 361–372, 1993.

128. Horwitz, E. P., Dietz, M. L., Diamond, H., LaRosa, J. J., and Fairman, W. D., Concentration and separation of actinides from urine using a supported bifunctional organophosphorus extractant, *Anal. Chim. Acta*, 238, 263–271, 1990.

129. Cleveland, J. M. *The Chemistry of Plutonium*, Gordon and Breach, New York, 1970.

130. Wick, O. J., Ed., *Plutonium Handbook. A Guide to Technology*, Vol. 1, Gordon and Breach, New York, 1967.

131. Truscott, J. B., Bromley, L., Jones, P., Evans, E. H., Turner, J., and Fairman, B., Determination of natural uranium and thorium in environmental samples by ETV-ICP-MS after matrix removal by on-line solid phase extraction, *J. Anal. At. Spectrom.*, 14, 627–631, 1999.

132. Truscott, J. B., Jones, P., Fairman, B. E., and Evans, E. H., Determination of actinide elements at femtogram per gram levels in environmental samples by on-line solid phase extraction and sector-field-inductively coupled plasma-mass spectrometry, *Anal. Chim. Acta*, 433, 245–253, 2001.

133. Truscott, J. B., Jones, P., Fairman, B. E., and Evans, E. H., Determination of actinides in environmental and biological samples using high-performance chelation ion chromatography coupled to sector-field inductively coupled plasma mass spectrometry, *J. Chromatogr., A*, 928, 91–98, 2001.

134. Unsworth, E. R., Cook, J. M., and Hill, S. J., Determination of uranium and thorium in natural waters with a high matrix concentration using solid-phase extraction inductively coupled plasma mass spectrometry, *Anal. Chim. Acta*, 442, 141–146, 2001.

135. Roane, J. E. and DeVol, T. A., Simultaneous separation and detection of actinides in acidic solutions using an extractive scintillating resin, *Anal. Chem.*, 74, 5629–5634, 2002.

136. Roane, J. E. and DeVol, T. A., Evaluation of an extractive scintillation medium for the detection of uranium in water, *J. Radioanal. Nucl. Chem*, 263, 51–57, 2005.

137. Fjeld, R. A., Roane, J. E., Leyba, J. D., Paulenova, A., and DeVol, T. A., Sequential and simultaneous radionuclide separation-measurement with flow-cell radiation detection, *ACS Symp. Ser.*, 868, 105–119, 2004.

138. Perna, L., Betti, M., Moreno, J. M. B., and Fuoco, R., Investigation on the use of UTEVA as a stationary phase for chromatographic separation of actinides on-line to inductively coupled plasma mass spectrometry, *J. Anal. At. Spectrom.*, 16, 26–31, 2001.

139. Kang, G. H., Lee, G. H., Jung, R.-S., Han, J. K., Kil, H.-S., and Shink, D. K., The study for determination of uranium by flow injection inductively coupled plasma mass spectrometry, *Anal. Sci.*, 17 Supplement, i1005–i1009, 2001.

140. Tolmachyov, S. Y., Kuwabara, J., and Noguchi, H., Flow injection extraction chromatography with ICP-MS for thorium and uranium determination in human body fluids, *J. Radioanal. Nucl. Chem.*, 261, 125–131, 2004.

141. Kuwabara, J., Tolmachyov, S., and Noguchi, H., The development of flow injection technique for rapid uranium determination in urine, *J. Nucl. Sci. Technol.,* Suppl. 3, 556–559, 2002.

142. Godoy, M. L. D. P., Godoy, J. M., Kowsmann, R., Santos, G. M., and Cruz, R. P., 234u and 230th determination by FIA-ICP-MS and application to uranium-series disequilibrium in marine samples, *J. Environ. Radioactivity*, 88, 109–117, 2006.

143. Lariviere, D., Cumming, T. A., Kiser, S., Li, C., and Cornett, R. J., Automated flow injection system using extraction chromatography for the determination of plutonium in urine by inductively couple plasma mass spectrometry, *J. Anal. At. Spectrom.*, 23, 354–360, 2008.

144. Egorov, O. B. and O'Hara, M. J., Development and testing of the automated 99Tc monitor. Final report, PNWD-3327, 2003, Battelle, Pacific Northwest Division, Richland, WA.

145. Egorov, O. B., O'Hara, M. J., and Grate, J. W., Microwave-assisted sample treatment in a fully automated flow-based instrument: Oxidation of reduced technetium species in the analysis of total technetium-99 in caustic aged nuclear waste samples, *Anal. Chem.*, 76, 3869–3877, 2004.

146. Miro, M., Gomez, E., Estela, J. M., Casas, M., and Cerda, V., Sequential injection Sr-90 determination in environmental samples using a wetting-film extraction method, *Anal. Chem.*, 74, 826–833, 2002.

147. Horwitz, E. P., McAlister, D. R., Bond, A. H., and Barrans, R. E., Novel extraction of chromatographic resins based on tetraalkyldiglycolamides: Characterization and potential applications, *Solvent Extr. Ion Exch.*, 23, 319–344, 2005.

148. Shaibu, B. S., Reddy, M. L. P., Murali, M. S., and Manchanda, V. K., N,N,N',N'-tetraoctyl-3-oxapentane-1,5-diamide impregnated magnetic particles for the uptake of lanthanides and actinides from nuclear waste streams, *Radiochim. Acta*, 95, 159–164, 2007.

149. Shaibu, B. S., Reddy, M. L. P., Prabhu, D. R., Kanekar, A. S., and Manchanda, V. K., N,N'-dimethyl-N,N'-dibutyl tetradecyl malonamide impregnated magnetic particles for the extraction and separation of radionuclides from nuclear waste streams, *Radiochim. Acta*, 94, 267–273, 2006.

150. Shaibu, B. S., Reddy, M. L. P., Bhattacharyya, A., and Manchanda, V. K., Evaluation of Cyanex 923-coated magnetic particles for the extraction and separation of lanthanides and actinides from nuclear waste streams, *J. Magn. Magn. Mater.*, 301, 312–318, 2006.

151. Burnett, W. C., Corbett, D. R., Schultz, M., Horwitz, E. P., Chiariza, R., Dietz, M., Thakkar, A., and Fern, M., Pre-concentration of actinide elements from soils and large volume water samples using extraction chromatography, *J. Radioanal. Nucl. Chem.*, 226, 121–127, 1997.

152. Egorov, O. B., Addleman, R. S., O'Hara, M. J., Marks, T., and Grate, J. W., Direct measurement of alpha emitters in liquids using passivated ion implanted planar silicon (PIPS) diode detectors, *Nucl. Instrum. Methods Phys. Res., Sect. A*, 537, 600–609, 2005.

153. Addleman, R. S., O'Hara, M. J., Grate, J. W., and Egorov, O. B., Chemically enhanced alpha-energy spectroscopy in liquids, *J. Radioanal. Nucl. Chem.*, 263, 291–294, 2005

10 Design Principles and Applications of Centrifugal Contactors for Solvent Extraction

Ralph A. Leonard
Argonne National Laboratory

CONTENTS

10.1   INTRODUCTION

Solvent extraction separates heavy metals (in particular, the actinides) from lighter metals and from each other and has been an important tool for nuclear chemistry over the last 60 years. As seen in the other chapters of this book, solvent-extraction chemistry remains of vital interest for nuclear fuel reprocessing and for the cleanup and segregation of nuclear waste.

Improvements in equipment design have made possible the multistage countercurrent operations needed for solvent-extraction flowsheets. Initially, packed columns were used because they had no moving parts. However, they were soon replaced by pulsed columns, which, because of their greater efficiency, did not need to be as high as the packed columns (Richards, 1957). Pulsed columns are still in use today. However, because of cost benefits from reducing the height of the solvent extraction facility, mixer-settler units have also been developed. At first, only gravity mixer-settlers (mixers with gravity settling zones) were used. Later, centrifugal mixer-settlers (mixers with centrifugal settling zones that are commonly called "centrifugal contactors") were developed at Savannah River Laboratory (SRL) (Davis and Jennings, 1961; Kishbaugh, 1963; Webster et al., 1969). The centrifugal contactor has the advantage of compact size coupled with high throughput and high extraction efficiency. Long (1978) gives the relative size of these four types of equipment for running solvent-extraction flowsheets. This reference shows that, for a given plant throughput, the centrifugal contactor is the same low height as the mixer-settler and is much more compact. Since 1966, the SRL contactor has been in use at the Savannah River Plant (Aiken, SC) for processing highly radioactive feeds. This application of the SRL contactors demonstrates the usefulness of centrifugal contactors when processing radioactive materials.

In the late 1960s, a modified centrifugal contactor was developed at Argonne National Laboratory (ANL) while work was being done on the original SRL contactor (Bernstein et al., 1973). The Argonne contactor is similar to the SRL contactor, except that it eliminates the paddle mixer under the centrifugal rotor and mixes the liquids in an annular region between the rotor and its housing. This change simplifies the contactor design, lowers its cost, and makes it easier to maintain the contactor remotely. At the same time, the Argonne "annular" centrifugal contactor retains the advantages of the SRL unit.

Centrifugal contactors are generally reliable, easy to use, and relatively inexpensive to build, operate, and maintain. The compact contactor stages give low liquid holdup, fast startup and shutdown, and greater criticality safety by geometry, while achieving high mass-transfer efficiency. The high efficiency allows the contactor to be made up of well-defined stages that are added only as needed. The low liquid holdup reduces the solvent exposure to radiation and the total solvent inventory. Low solvent inventory is especially important for solvents that are more expensive. It also permits the contactor to reach steady state quickly compared with other types of solvent-extraction equipment. This benefit is critical for engineering-scale tests, where one has to limit the amount of waste generated. Finally, a bank of contactors can be shut down and restarted a short time later while maintaining its stage-to-stage concentration profile in a steady state.

In this chapter, Section 10.2 gives an overview of the operation of the Argonne centrifugal contactor. Section 10.3 focuses on the design principles for this contactor. Section 10.4 discusses the worldwide applications of this contactor to solvent-extraction processes of interest to the nuclear and other industries. Comparisons with other types of contactors are made throughout the text, and a separate section is devoted to them in Section 10.4. However, because of their widespread use and the author's particular experience with them, the ANL contactor and its variations remain the primary focus.

10.2   OVERVIEW OF CONTACTOR DESIGN AND OPERATION

The contactor design for a single stage is shown schematically in Figure 10.1. Two immiscible liquids flow into the annular (Couette) mixing zone. Typically, the more-dense phase is aqueous, and the less-dense phase is organic. As shown in Figure 10.1, the two phases usually enter through inlet ports that are on opposite sides of the contactor wall. The mixing zone is the region between the spinning rotor and the stationary housing. The rapid Couette mixing in this region creates a turbulent liquid-liquid dispersion that promotes good mass transfer between the two phases. As the mixing occurs, the dispersion flows by gravity to the bottom of the mixing zone, reaching the bottom vanes, where it is guided to the inlet of the rotor located on the bottom face of the rotor. Once the dispersion passes through this opening, it is in the centrifugal separating zone of the rotor. Here, the dispersion band forms a vertical cylinder in the middle of the separating zone, shown as the darkest region of the separating zone in Figure 10.1. The dispersion breaks rapidly under the high centrifugal forces, typically 100–400 g. The separated more-dense phase moves out to the rotor wall and flows upward through the underflow to the upper weir. After the liquid flows over the upper weir, it is slung into the upper collector ring in the contactor housing, then into the more-dense-phase exit. The separated less-dense phase moves in toward the center of the rotor and flows up to the lower weir (LW). After the liquid flows over the LW, it is slung out into the lower collector ring and leaves the contactor via the less-dense-phase exit. The exit port in each of the collector rings is tangential to the ring so that the momentum of the liquid being slung from the rotor helps carry the liquid out of the stage. A slinger ring just above the lip of the upper collector
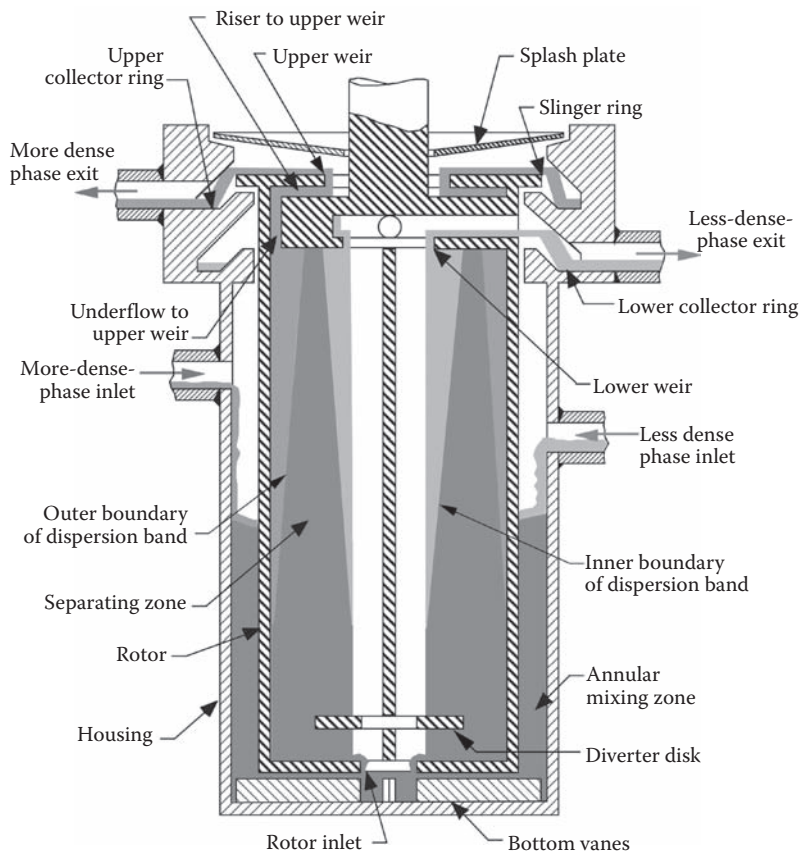
FIGURE 10.1 Schematic of annular centrifugal contactor.

ring prevents the more-dense phase from leaking down into the lower collector ring. Such leakage is undesirable, as it would increase other-phase carryover in the less-dense phase. The splash plate above the upper weir catches any liquid that is splashed upward and keeps it from reaching the motor or rotor bearings.

As shown in Figure 10.1, the inner and outer boundaries of the dispersion band are sloped. As the rotor speed increases, these surfaces become more vertical. The slope represents the balance between the gravity forces and the centrifugal forces acting on the dispersion. Typically, at normal rotor speeds, the centrifugal forces are much greater than the gravity forces. When this is the case, the inner and outer boundaries of the dispersion band are essentially vertical so that the dispersion band forms a hollow right cylinder.

The annular centrifugal contactor is designed so that each stage achieves the required mixing and subsequent separation. Besides the conditions specified above, at least five additional factors must be considered. First, to allow the dispersion to flow by gravity from the mixing zone into the rotor, stationary radial vanes under the rotor must dissipate the rotational velocity of the dispersion. Second, the rotor inlet (RI) must be small

enough with respect to the LW that the dispersed liquids are pumped up to the lower rotor weir. Third, the axial vanes inside the rotor must keep the liquids spinning at the same speed as the rotor. Fourth, a diverter disk, located inside the rotor a short distance above the RI, forces the entering dispersion outward into a region of higher centrifugal force and, thus, into a region that separates the two phases faster. Fifth, the radii for the lower and upper weirs must be chosen carefully so that the two vertical boundaries (inner and outer) of the dispersion band are located within the separating zone of the rotor, that is, between the LW and the underflow to the upper weir.

Photographs can better illustrate the operation and parts of the contactor. Figure 10.2 shows the mixing zone of a 2-cm contactor with a transparent acrylic housing. In view (a), the rotor is not turning and the mixing zone is drained of liquid. In view (b), which is from Leonard et al. (1997), the rotor is turning at 3600 rpm with both organic (30% tributyl phosphate (TBP) in normal dodecane (nDD)) and aqueous phase (0.01 M HNO$_3$) flowing into the mixing zone at 30 mL/min.

The separating zone is illustrated in Figures 10.3 through 10.5. The inside of a 2-cm rotor, looking up from the bottom, is shown in Figure 10.3. In this photograph, the rotor is held in place by a finger clamp, and the rotor top and rotor bottom have been removed. One can see the four vanes inside the separating zone, the dispersion disk with a center hole, and, at the far end of the separating zone, the underflow holes to the riser to the upper weir. The two holes near the outside of the dispersion disk are for two screws that hold the bottom of the rotor onto the rotor body. Because the screw holes can leak, the rotor bottom is normally welded onto the rotor body. This rotor is an experimental one that allows different designs for the rotor bottom to be tested.
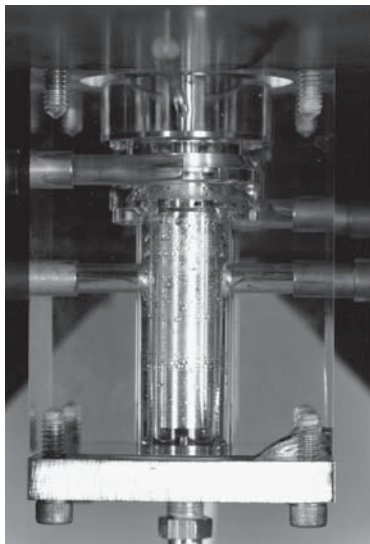
(a) Empty   (b) Operating
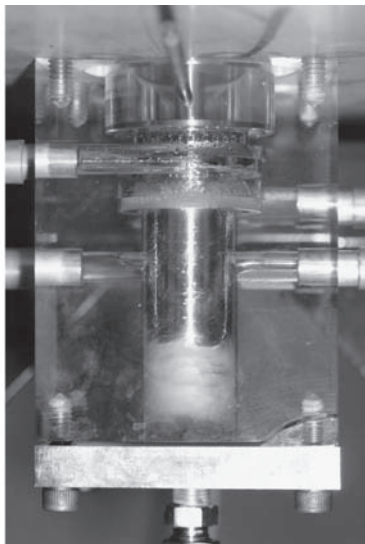
FIGURE 10.2   Mixing zone of a 2-cm annular centrifugal contactor. (Figure 10.2b: Reprinted from Leonard, R. A., D. B. Chamberlain, and C. Conner., *Sep. Sci. Technol. 32*(1–4), 193–210, 1997. With permission of Taylor & Francis Ltd., http://www.tandf.co.uk/journals.)
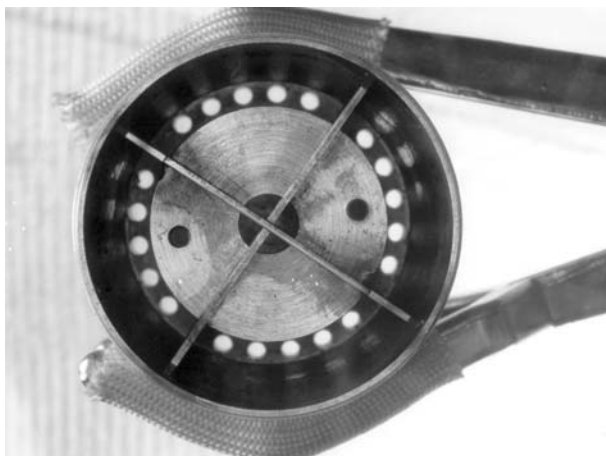
FIGURE 10.3 Inside view of a 2-cm contactor rotor with the bottom removed.

FIGURE 10.4 Inside bottom view of a 4-cm contactor rotor.

The inside of the separating zone of a 4-cm rotor is shown in Figure 10.4. In this photograph, the rotor is resting on a rubber stopper. The outside of the rotor bottom and the inside of the upper weir with the four weir vanes can be seen. As with the rotor bottom, the upper weir is held on by two screws in this experimental rotor. In production rotors, the upper weir is welded onto the rotor body.

The inside of a 25-cm rotor is shown in Figure 10.5. This photograph, which was taken during assembly of the rotor, shows the eight vanes in the separating zone. Some of the four rectangular exit ducts for the LW are visible, as are some of the openings for the exit ducts of the upper weir. The region between these two sets of openings is more complex than shown in Figure 10.1 because this rotor has an air-controlled upper weir.

The inside of the upper region of a 4-cm rotor can be seen in Figure 10.6. One can see the holes of the underflow as they open into the riser that leads to the upper weir. The upper weir, which has been removed from the rotor body, is face up so that the vanes in the riser area are hidden. These riser vanes can be clearly seen

FIGURE 10.5   Inside view of a 25-cm contactor rotor.

in Figure 10.4. The inside of the rotor bottom can also be seen because it was not attached to the rotor for this photograph. The large diameter of the rotor shaft gives the rotor the stiffness it needs to operate at 3600 rpm. One of the four exit ducts (a circular hole) for the flow over the LW is visible in the upper region on the outer surface of the rotor body. There are no exit ducts for the overflow of the upper weir, which is at the pressure of the air inside the rotor housing.

Different views of the contactor housing are shown in Figures 10.7 through 10.9. In the inside of the 12-cm contactor housing shown in Figure 10.7, one can see the eight vanes at the bottom of the housing, the openings to the lower and upper collector rings, the circular ledge above the upper collector ring where the splash plate will rest, and some of the bolt holes in the flange above the circular ledge that are used to attach the housing to the motor mount plate. In the top side view of the 25-cm contactor housing shown in Figure 10.8, one can see the tangential exit ports for both the upper and lower collector rings, as well as the opening into the lower collector ring. This photograph was taken during construction, before the lip to hold the splash plate and the flange had been welded to the housing of the motor mount plate. A side view of the same 25-cm contactor housing is shown in Figure 10.9, in which one can see the perpendicular inlet ports below the region of the collector rings, a bottom flange that allows different bottom designs to be tested, and three small holes into the lower side of the housing that allow experimental measurements of the mixing zone liquid level. These three small holes on the side and a bottom flange are not included
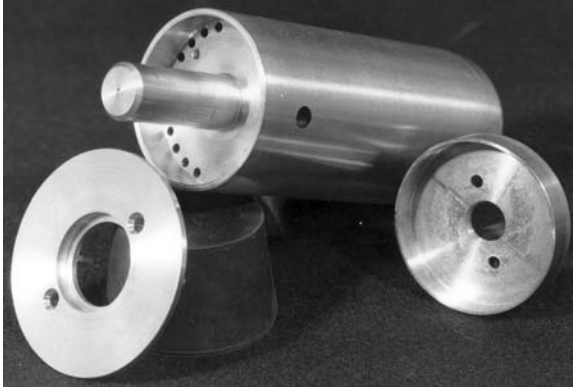
FIGURE 10.6   Inside top view of a 4-cm contactor rotor.
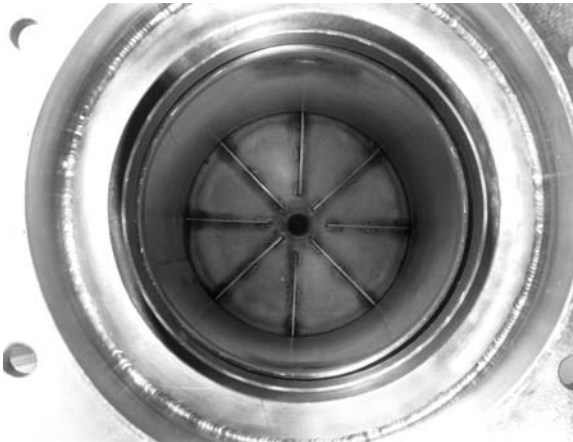
FIGURE 10.7   Top view of a 12-cm contactor housing.

FIGURE 10.8   Top side view of a 25-cm contactor housing.
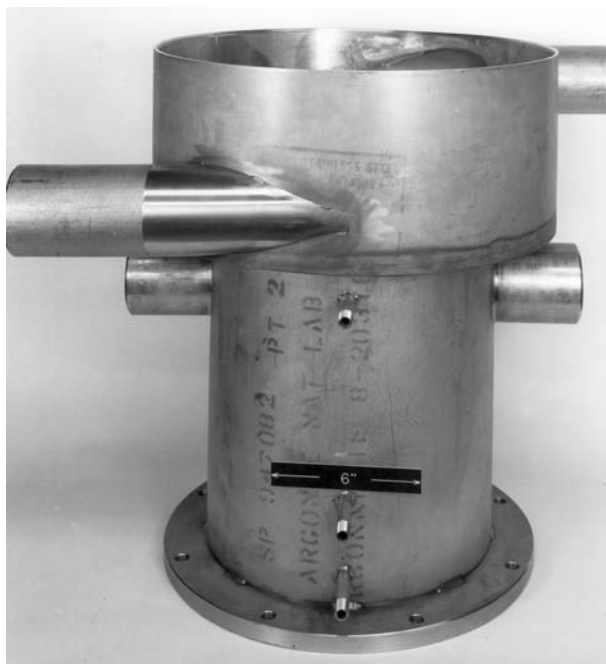
FIGURE 10.9   Side view of a 25-cm contactor housing.

in production contactors, which instead have the bottom of the contactor housing welded to the side of the housing.

A four-stage 4-cm contactor is shown in Figure 10.10. The organic-phase side of the contactor bank is operating at a flow rate of 615 mL/min. The aqueous phase on the other side of the contactor is flowing in a countercurrent direction at the same flow rate. Note how the flowing liquid in the interstage lines fills less than half of the cross section of the lines so that air can flow freely from stage to stage. The organic phase (30% TBP in nDD) is in full recycle so that the exiting liquid is immediately returned to the feed port by a pump that is not visible in the photo. The organic feed line to the contactor is full of liquid. Note that the contactor motors are not the face-mounted type. The motor mount plate bends up 90° in the back so that the motor can be mounted on the side. As will be discussed in the next section, this side-mount design is not the recommended way to attach a motor.

In a typical contactor, throughput is limited by the volume of the separating zone in the following way. The maximum throughput for the contactor rotor occurs when the total contactor throughput is increased so that the dispersion band has the same volume as the separating zone, and the weir diameters are such that the dispersion band is contained within this region. For a given total throughput, the position of the dispersion band depends on the organic-to-aqueous (O/A) flow ratio as well as the weir radii. As a rotor must be operated over a wide range of O/A flow ratios during process startup, and sometimes during shutdown as well, the nominal maximum throughput for the contactor is less than the

FIGURE 10.10   View of operating four-stage 4-cm contactor.

maximum throughput. A method for determining how much less is discussed in Section 10.3. A good engineering design practice is to keep the nominal throughput for a contactor to no more than 67% of the nominal maximum throughput. For most applications, phase separation is generally considered satisfactory if each effluent from a contactor stage contains <1% of the other phase entrained in it. This condition results in high stage efficiency. The maximum throughput for a given set of conditions (O/A flow ratio and set of weirs) is defined as when the other-phase carryover reaches 1%. As the total throughput decreases, the other-phase carryover drops below 1%.

While <1% other-phase carryover is good for stage-to-stage operation, in general, other-phase carryover should be much less at the exit ports. Typically, as the total throughput becomes significantly less than the maximum throughput, the other-phase carryover drops to low values, on the order of 0.04%, that is, 400 ppm, or less. Recent tests in a 4-cm contactor showed an average solvent entrainment in the aqueous effluent of 120 ppm, with a maximum value of 240 ppm (Arafat et al., 2001). If this concentration of entrainment is still too high, up to 90% of it can be removed by coalescers (Pereira et al., 2002). Note that other-phase carryover will never be zero, as some of each phase will be dissolved in the other phase. The dissolved material cannot be removed by a coalescer or a centrifuge.

10.3   DESIGN PRINCIPLES FOR CENTRIFUGAL CONTACTORS

This section discusses the design and operation of a single stage (Figure 10.2), fol-
lowed by a multistage contactor (Figure 10.10). Other design and operational consid-
erations are also reviewed.

10.3.1   Single Stage

This subsection describes the design of a contactor stage and how that design affects
contactor operation. It will be shown when to add or avoid a particular feature. The
discussion follows the flow of the two immiscible liquids through a contactor stage:
liquid entry, mixing, separation, and liquid exit. Finally, criteria for motor selection
are reviewed.

10.3.1.1   Liquid Entry

The two immiscible liquids enter the annular contactor from a point fairly high up
in the mixing zone. This point is chosen to be high so that the entering liquids are
above the liquid-liquid dispersion. However, the point cannot be so high that the
entering liquids splash up and enter the lower collector ring, bypassing the contactor
rotor. Typically, the entry points for the two phases are about 180° from each other
around the rotor housing, because the aqueous interstage lines are on one side of the
bank of contactor stages and the organic interstage lines are on the other side. This
configuration is easy to fabricate and highlights the countercurrent flow of the two
phases. However, the position of the entry ports around the wall of the contactor
housing should make no difference to contactor operation. In fact, when contactors
are used as centrifugal separators to separate oil from water, both phases must enter
via the same entry port.

Besides the height of the two inlet ports and their position around the side
of the contactor housing relative to each other, the orientation of each feed port
relative to the inside surface of the rotor housing must also be considered. In
early units, the inlet port was placed so that it was tangential to the inside wall of
the rotor housing. However, in tests that compared tangential with perpendicular
inlet ports, there was no difference in the operation. This result was attributed
to the liquid level of the dispersion in the annular mixing zone being below that
of the inlet ports. When the liquid level rises to the level of the inlet ports, the
two orientations can make a difference. In fact, being even slightly off the per-
pendicular toward the tangential position improves performance (Leonard et al.,
2001a). With the inlet port in the perpendicular position, the spinning liquid in
the annular mixing zone enters the port and creates a static head that backs up
the incoming liquid into the inlet line. This liquid backup can, in some cases,
limit contactor throughput. Thus, tangential inlet ports are recommended so that
the stage will operate satisfactorily even if the liquid level in the mixing zone
reaches the inlet ports. In this case, the spinning liquid assists in pulling the
liquid out of the tangential inlet port.

The above discussion assumes that the liquid comes from the adjacent contactor
stage. At certain stages, including both end stages, some of the entering liquid will

be external feeds. When the external feed is the only liquid of that phase entering a stage, the normal feed entry port can be used. If an interstage feed is used as well, either (1) the interstage line can have a side tube added where the external feed can be introduced, or (2) a third opening into the annular mixing zone can provide an entry port for an external feed. The first option has been the more popular. However, it requires a special interstage line and, therefore, is now being replaced by the second option. A third opening into the annular mixing zone could be the highest of the three ports shown in Figure 10.9. It could also be the vertical port shown at the extreme right in Figure 10.11. Contactors do not normally come with a third opening into the annular mixing zone on the side of the contactor housing. If a third side port is desired, it should be specified when the contactor is ordered. It is recommended that this port be oriented tangentially rather than perpendicularly to the housing wall. The tangential orientation should be such that the spinning rotor will drag any entering liquid into the annular mixing zone. The third port to the annular mixing zone, shown in Figure 10.11, allowed the liquid in the mixing zone to overflow before it backed up into the motor bearings. If a third entry port is included on every stage, it can introduce an external feed at any stage. This port can be useful in day-to-day contactor operations.

FIGURE 10.11   End of a bank of 2-cm contactors.

10.3.1.2   Mixing Zone

The gap for the annular mixing zone is balanced between being so narrow that the dispersion rises up and enters the lower collector ring, and so wide that mixing becomes poor and stage efficiency suffers. In a 2-cm contactor in which the annular gap was too wide, contactor operation exhibited a problem related to the absence of phase inversion (Leonard et al., 1980a). Once the mixing zone had the organic phase as the continuous phase, this condition remained even at low O/A flow ratios, such as 0.2 and 0.3, instead of the aqueous phase becoming the continuous phase. This condition gave the dispersion a high structural viscosity that inhibited its flow into the RI. Instead, the dispersion backed up into the annular mixing zone until it flowed out the less-dense-phase exit port. This problem was corrected by making the gap smaller (Leonard et al., 1997).

When contactors are developed for a new solvent-extraction process, typically a single-stage contactor is built first. Its annular gap is sometimes made too wide so that an insert can be added to reduce the gap. Various gap widths are then tested, and the one that gives the best operation is specified for the new contactor stages. This procedure allows one to maximize the performance of the mixing zone. Typically, an annular gap that is about 9% of the rotor diameter will balance these competing needs. As the annular gap is increased with other factors being held constant, the liquid height in the mixing zone decreases. As the annular gap is decreased, the shear rate increases. If shear rates are high enough, a stable or persistent emulsion could form. In general, liquid-liquid pairs chosen for solvent extraction are tested to check that the dispersions formed by the two immiscible liquids do not become stable emulsions.

The bottom of the mixing zone contains stationary vanes attached to the bottom of the contactor housing. These vanes stop the rotation of the dispersion that is created in the annular gap and allows the dispersion to flow under the rotor. The opening into the rotor is located at the center of the bottom surface of the rotor. If the bottom vanes were not there, the dispersion would back up in the annular mixing zone and flow out via the lower collector ring. If this happened, a breaking dispersion would flow out the less-dense-phase exit port.

The height of the bottom vanes is not very important. Typically, it is 0.3 cm plus 6% of the rotor diameter. The gap between the top of the bottom vanes and the bottom of the rotor should be small: typically, 0.15 cm plus 2% of the rotor diameter. Larger gaps will give increased liquid height in the annular mixing zone. Usually, there are eight vanes under the rotor. Use of four vanes would increase the average liquid height in the annular mixing zone; however, the variation of liquid height with time (pulsing) would also increase.

In addition to the number of vanes, the vane height, and the gap between the vanes and the rotor, the vanes can be straight or curved. In almost every case, practice at ANL has used straight vanes that extend to the inner wall of the contactor housing, as shown in Figure 10.7. One type of commercial annular centrifugal contactors, made by CINC Industries (Carson City, NV), has curved vanes that extend halfway into the annular mixing zone (Meikrantz et al., 1998b). Macaluso (2008), who designed these vanes, investigated the extension of eight curved vanes

into the annular region under the rotor, from vanes that stop at the outer edge of the rotor, to vanes that extend out to the inner wall of the rotor housing. A clear plastic sleeve was installed at the lower end of the contactor housing so that the flow patterns in the annular mixing zone could be viewed in 12.5- and 25-cm contactors. The curved vanes were oriented so that they direct the liquid to the inlet opening at the bottom of the rotor. With straight vanes, some turbulence was noted on the back side of each vane. This turbulence created foaming and aeration of a mixture of water and No. 2 diesel fuel, which prevented steady feeding to the rotor. As rotor speed was increased, the liquid level in the mixing zone formed a wave around the annulus. The curved vanes were tested to reduce the turbulence and the wave and to provide a steady feed to the RI. When the curved vanes extended to the wall, they overfed the rotor. The length of the vanes was cut in increments of 0.32 cm and tested until the vanes were at the outer diameter of the rotor. At the end of the testing, the optimal length for the curved bottom vanes was halfway into the annular mixing zone. At this length, the correct amount of liquid was taken from the mixing zone, and the turbulence and the wave were eliminated. More experimental work would be useful to determine the effect of (1) bottom-vane length on contactor operation with straight vanes, and (2) these two series of bottom-vane configurations on the stage efficiency. The lower turbulence of the curved vanes could reduce stage efficiency. However, less turbulence should give better oil-water separations.

When CINC licensed the contactor design from the U.S. Department of Energy, the main use of the contactor was to separate oil from water (Meikrantz, 1990). This is still an important application for CINC. When oil-water separations are the only objective, minimal mixing is desirable. To facilitate this, CINC provides a no-mix sleeve for the mixing zone. The sleeve keeps the two immiscible phases from contacting the spinning rotor and, thus from being mixed further. The two-phase liquid could also be fed to the bottom of the contactor just below the RI. However, feeding liquid into the annular region smoothes out flow fluctuations and provides a more constant flow rate to the separating zone of the contactor. This smoothing of flow fluctuations is also a benefit for multistage solvent extraction where both mixing and separation occur.

Several factors that affect liquid height have already been mentioned. When these factors are held constant, liquid height is roughly proportional to total throughput and rotor speed, and inversely proportional to rotor diameter. When only total throughput is varied, liquid height increases with throughput only to a point, and then it flattens out (Leonard et al., 2002b). More experimental and theoretical work would be useful. Some initial work in this area has been done by Wardle et al. (2008), who modeled the flow in the mixing zone of a 5-cm contactor by using computational fluid dynamics (CFD). The model calculations show the varying annular liquid height (ALH) and the air bubbles in the liquid that are observed experimentally. Wardle et al. found that 100 h of computer time was required for the CFD model to calculate 1 s of flow in the mixing zone. The photos in Figure 10.12 show the air entrained in the liquid phase and the variation of the liquid phase position with time. This 12-cm contactor was operated at 1800 rpm with only one phase, the solvent (30% TBP in nDD), flowing at 20 L/min. These

(a) Photo 1   (b) Photo 2
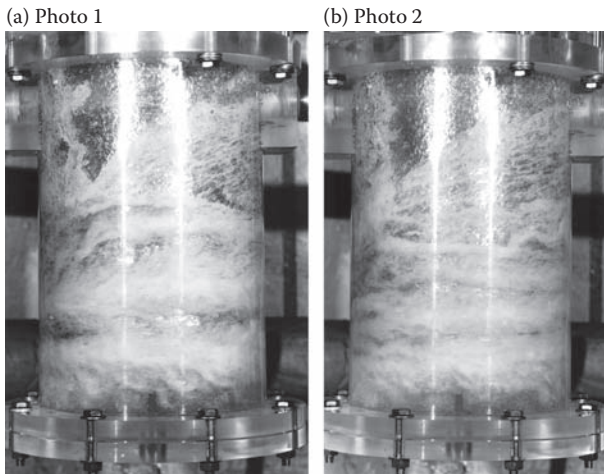
FIGURE 10.12 Variations in the mixing zone with time at constant operating conditions for a 12-cm annular centrifugal contactor.

two photos show the difficulty in measuring the ALH. To take these photographs, the normal stainless-steel contactor housing was replaced in the mixing zone with a transparent acrylic housing.

Typically, rotor speed will decrease as rotor diameter increases, so that the rotor is always operated 20–30% below its first critical speed. The net result is that for contactors ranging in size from 2 to 25 cm, the dispersion height in the annular mixing zone does not exceed the length (total height) of the mixing zone. The length of the mixing zone is fixed by the height of the vanes under the rotor, the gap between these vanes and the rotor, and most importantly, the length of the separating zone. The length of the separating zone will be discussed in Section 10.3.1.3.

The RI (the opening at the bottom of the rotor) should be small enough that any liquid entering will be pumped up to the LW as more liquid flows into the rotor. To determine the maximum radius for the RI that will meet this specification, $r_{RI,Max}$, use the following equation for pressure between two points (j and k) in a single liquid inside a rotor, that is, for unrestricted liquid movement between two points in the same liquid in a rotational field:

$$p_k - p_j = \left(\frac{\rho\omega^2}{2}\right)(r_k^2 - r_j^2) - \rho g(H_k - H_j) \qquad (10.1)$$

where p is the pressure in Pa, ρ is the liquid density in kg/m³, ω is the rotor speed in rad/s, g is the gravitational acceleration in m/s², r is the radius from the center of the rotor to the specified point in m, and H is the height of the specified point above a common reference plane in m. Equation 10.2 is obtained by applying Equation 10.1 to the liquid at the RI as point j with radius r_{RI} and the liquid surface over the LW as point k with radius r_{LW} and solving for $r_{RI,max}$:

$$r_{\text{RI,Max}} = \left(r_{\text{LW}}^2 - \frac{2gL}{\omega^2} \right)^{1/2} \tag{10.2}$$

where L is the height of the LW above the RI in m. Note that the pressure difference term is zero because the diverter disk has a hole in it. This condition allows the pressure over the liquid in the separating zone to be the same at every point. If the radius of the RI is less than or equal to $r_{\text{RI,max}}$, the rotor is considered to be fully pumping, as it can pump the liquid from the bottom of the rotor up to the LW. If the radius of the RI is greater than $r_{\text{RI,max}}$, the rotor is said to be partially pumping. The liquid can only be pumped part way up the rotor. The height that the liquid can be pumped, L_{p}, is given by Equation 10.2 if $r_{\text{RI,max}}$ is replaced with r_{RI}, L is replaced by L_{p}, and the equation solved for L_{p}. When a rotor is partially pumping, the liquid level in the annular mixing zone must rise by the height $L - L_{\text{p}}$ so that liquid can flow through the rotor. Equation 10.2 shows that $r_{\text{RI,max}}$ depends not only on the radius of the LW, but also on the gravitational acceleration, the length of the separating zone, and the rotor speed.

In Equation 10.2, the value for r_{LW} should be the radius of the LW less the maximum liquid rise over the weir. The liquid rise over the weir can be estimated by the correlation given by Davis and Jennings (1961). The value for the rotor speed should be the lowest speed at which the rotor will be operated. Note that, if L in Equation 10.2 is replaced by x, the distance below the LW of a point on the air–liquid interface inside the rotor, then $r_{\text{RI,max}}$ becomes the radius for this air-liquid interface at distance x below the LW.

The inlet radius for the contactor rotor should be chosen so that the rotor is always fully pumping. This condition ensures good contactor operation with no surprises, for example, dispersion backing up in the mixing zone and flowing out the less-dense-phase exit port. This recommended design rule for the RI radius was ignored in one case. In this case, the flow in the interstage lines of the 2-cm contactor was low and, as a result, controlled by surface tension and gravity head rather than the liquid momentum (Leonard et al., 2001a). This behavior is typical for a small unit like the 2-cm contactor. The result is that the liquid in the interstage lines moves as slugs rather than a continuous flow of liquid. This behavior was especially true for the aqueous phase, which did not wet the interstage lines, as they were made of a fluorocarbon-type polymer. The volume of the liquid slugs was about the volume of the liquid in the mixing zone. In single-stage operation, the extraction efficiency of the annular mixing zone was 98% or slightly better at an O/A of 1.0, while in multistage operation, the erratic liquid flow into the mixing zone and its large volume relative to that of the mixing zone lowered the effective stage efficiency to about 60% at O/A ratios away from 1.0, that is, near 0.2 and 3 (Leonard et al., 1999). By opening the RI, the volume of the liquid in the mixing zone was doubled so that the liquid slugs had less effect. In addition, a stainless-steel wire rope was inserted into the interstage line between contactor stages to reduce the volume of the liquid slugs. The metal fibers of the wire rope form a wick that sucked in the slug and elongated it. The slug volume entering the mixing zone was reduced by a factor of

30, from an average of 1.9 ± 0.4 mL to 0.06 mL at the entrance to the mixing zone. This reduced slug volume was probably more important in improving stage efficiency than increasing the RI radius (Leonard, 2001a). In subsequent units where a stainless-steel wire rope could not be used, the fluorocarbon-type polymer for the interstage lines was replaced by stainless steel, which was wetted by both the aqueous and organic phases. For either the stainless-steel wire ropes or the stainless-steel interstage lines, the stage efficiency for multistage operation was increased from 60% to 82–90%. For larger units with interstage flow rates above 100 mL/min, fluid momentum from the spinning rotor is retained by the liquid and helps it travel in the interstage lines in a steady stream, that is, without liquid slugs. This condition ensures that stage efficiencies for multistage operation will be higher, close to those for single-stage operation.

For the mixing-zone dimensions suggested above, stage efficiency should be $94\% \pm 7\%$ based on values for single-stage contactors ranging from 2 to 25 cm (Leonard et al., 1999). If the liquid flow between stages is smooth and the annular mixing zone has a reasonable volume of dispersion, the efficiency for multistage operation should be greater than 90%, typically greater than 95%. Based on the limited information available (4- and 25-cm contactors), however, this does seem to be the case (Leonard et al., 1999). As O/A flow ratios become very large (10) or very small (0.1) compared with 1.0, small flow fluctuations become important. At such O/A flow ratios in a small contactor, stage efficiency can drop to about 90% in single-stage operation. In a multistage 2-cm contactor, which is designed following the rules described above, the stage efficiency can drop below 90% but will remain above 80% over the required operating range (Leonard et al., 2001a). When the multistage 2-cm contactor is not well designed, the apparent stage efficiency can drop to 60% (Leonard et al., 2001a).

In tests of a caustic-side solvent-extraction (CSSX) flowsheet, multistage 25-cm contactors with curved vanes at the bottom of the mixing zone (CINC V-10 units) achieved an average stage efficiency of $86\% \pm 3\%$ for the extraction section and $65\% \pm 11\%$ for the strip section (Lentsch et al., 2008). When the curved vanes were replaced with straight vanes, the average stage efficiency for the extraction section was about the same, $88\% \pm 7\%$. However, for the strip section, which had a lower flow rate, the average stage efficiency increased significantly, to $82\% \pm 3\%$. In tests of the CSSX process in a 5-cm contactor (CINC V-2 unit), straight vanes seemed to yield higher stage efficiency than curved vanes (Birdwell et al., 2001).

A recent literature review by Vedantam and Joshi (2006) on the annular centrifugal contactor, focused on the annular mixing zone. In particular, their paper discusses work on Taylor-vortex flow in the annular zone, where the Taylor vortices have a structured flow. However, as shown by Figure 10.12 and Wardle et al. (2008), for the highly turbulent flow that results in the mixing required for high stage efficiencies in solvent extraction, the annular flow is highly turbulent with little structure. Also, a significant amount of air is entrained with the liquid phase. Thus, the review by Vedantam and Joshi (2006) is of limited use in designing annular centrifugal contactors for solvent extraction.

10.3.1.3 Separating Zone and Contactor Scale-up

The separating zone is the determining factor with regard to contactor throughput. As such, it is the key to scaling-up any contactor design. The importance of the separating zone has been verified at Argonne in contactor sizes ranging from 2 to 25 cm. Because the volume of the separating zone is so important, contactor size is characterized by the diameter of the rotor. The maximum throughput for a contactor rotor can be calculated from the dimensionless dispersion number, N_{Di} (also called the "Leonard number," N_{Le}), which is given by Leonard et al. (1981) as

$$N_{Di} = \frac{q}{V}\sqrt{\frac{\Delta Z}{r_{Avg}\omega^2}} \tag{10.3}$$

where q is the volumetric flow rate in m^3/s, V is the volume of the separating zone in m^3, ΔZ is the thickness of the dispersion band in meters, and r_{Avg} is the average radius for the dispersion band in meters. As stated above, ω is the rotor speed in rad/s. The dispersion band in the separating zone is assumed to be a hollow vertical cylinder, where ΔZ is the thickness of the cylinder wall. For a contactor rotor operating at maximum throughput, the outer wall of the dispersion band will be at the inner edge of the underflow and have the radius r_U. The inner wall of the dispersion band will be at the physical radius of the LW, which is designated r_{LW*}. When the dispersion completely fills the separating zone from r_{LW*} to r_U, the average radius for the dispersion band is given by Leonard et al. (1981) as

$$r_{avg} = \frac{2(r_U^3 - r_{LW*}^3)}{3(r_U^2 - r_{LW*}^2)} \tag{10.4}$$

and ΔZ becomes $r_U - r_{LW*}$. As can be seen in Leonard (1995), N_{Di} is typically about 8×10^{-4} for solvents that use linear or branched hydrocarbons, for example, normal dodecane or Isopar L, as the diluent. For solvents that use chloro- or fluorocarbons as the diluent, for example, CCl_4, N_{Di} is approximately 16×10^{-4}. The dispersion number can be measured for any pair of immiscible liquids (aqueous and organic phase) in a batch test using a 100-mL graduated cylinder with a ground-glass stopper (Leonard, 1995). The measurement involves creating a dispersion by hand shaking the cylinder and noting the time required for the dispersion to break.

For a given contactor diameter, the maximum contactor throughput can be estimated as follows. The volume of the separating zone (V) is a right cylinder with an outer radius of r_U, an inner radius of r_{LW*}, and a length of L. Note that L is a vertical dimension. The maximum ratio for L relative to the inside diameter of the rotor ($D_{R,i}$) is typically 2.2. If this ratio is increased above 2.2 for a given rotor diameter, L is increased, and the maximum throughput increases proportionally. However, the nominal maximum throughput, which will be described in the next paragraph, is increased by a much smaller amount. This effect has to do with the increased liquid rise over the weirs at the higher flow rates. In addition, the ratio of r_{LW*}/r_U should be a minimum of 0.46, as further decreases in r_{LW*} relative to r_U will not result in further increases in total throughput. The ratio of $D_U/D_{R,i}$, where D_U is the diameter of the

inner edge of the underflow, is typically about 0.91. The ratio of $D_{R,i}/D_{R,o}$, where $D_{R,o}$ is the outside diameter of the rotor, is typically about 0.97. Then, if the rotor diameter, the rotor speed, and the dispersion number for the two immiscible phases are known, Equations 10.3 and 10.4 can be used to estimate the maximum contactor throughput.

The nominal maximum contactor throughput is always less than the maximum contactor throughput because, at startup and shutdown, the contactor must be able to operate at all O/A flow ratios, not only the O/A value required for steady-state operation. To illustrate this point, we will look at the operating curves for a typical contactor over a wide range of flow ratios, typically, from 0.1 to 10. In this discussion, it is assumed that the aqueous (A) phase is the more-dense phase; the organic (O) phase is the less-dense phase; and the dispersion number, the rotor speed, and all rotor dimensions except the radius of the more-dense-phase (upper or aqueous-phase) weir are fixed. A typical operating curve is shown in Figure 10.13 for an O/A flow ratio of 1.0 with an aqueous density of 1000 g/L and an organic density of 855 g/L. If the more-dense-phase weir radius is too small, greater than 1% aqueous phase will be mixed with the organic-phase effluent (>1% A in O). If the more-dense-phase weir radius is too large, greater than 1% organic phase will be mixed with the aqueous-phase effluent (>1% O in A). The optimum throughput occurs at some intermediate radius for the rotor at this O/A flow ratio. In Figure 10.13, this intermediate radius is about 34.3 in arbitrary units for a flow rate of about 23.3 in arbitrary units. The curve is determined by operating the contactor at various radii for the more-dense-phase weir and increasing the flow rate while holding the O/A flow ratio constant. When either or both effluents have more than 1% of the other phase, the limit of the satisfactory operating region is reached.

Figure 10.14 shows the operating curve generated when this series of tests is repeated for O/A flow ratios of 0.1 and 10. Note that, for each O/A flow ratio, the maximum throughput is about 23.3 in arbitrary units. However, each O/A flow ratio requires a different more-dense-phase weir radius to achieve its maximum throughput. As seen in Figure 10.14, the region of fully stable contactor operation for all three O/A ratios has a nominal maximum throughput of 17.5 in arbitrary units, which is 75% of the maximum throughput. Since good engineering design practice is that the nominal throughput be no more than 67% of the nominal maximum throughput, the nominal throughput for this contactor with these phase densities is 11.8 in arbitrary units. Note that the optimum radius for the more-dense-phase weir is slightly lower, 34.0 in arbitrary units compared to 34.3 for an O/A flow ratio of 1.0, to achieve the nominal maximum throughput.

The nominal maximum throughput is dependent on phase density. For the contactor corresponding to the case shown in Figure 10.14, but with a less-dense organic phase, 810 g/L, the nominal maximum throughput increases to 20.8 in arbitrary units, that is, 89% of the maximum throughput (see Figure 10.15). Note that the more-dense-phase weir radius to yield the nominal maximum throughput increases to 35.3 in arbitrary units, which is at the edge of complete inoperability (>1% O in A) for the case shown in Figure 10.14. If the organic phase is denser, 900 g/L, then the nominal maximum throughput decreases to 13.0 in arbitrary units, that is, 56% of the maximum throughput (see Figure 10.16). Note that, for this case to achieve the nominal maximum throughput, the more-dense-phase weir radius must decrease to
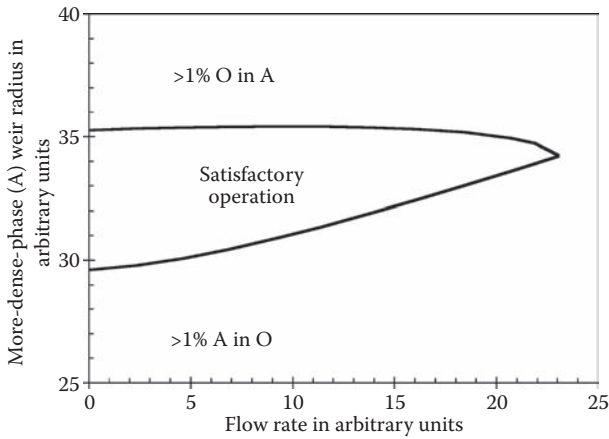
FIGURE 10.13 Typical shape of an operating curve for a centrifugal contactor with an aqueous-phase density of 1000 g/L, an organic-phase density of 855 g/L, and an O/A flow ratio of 1.0.
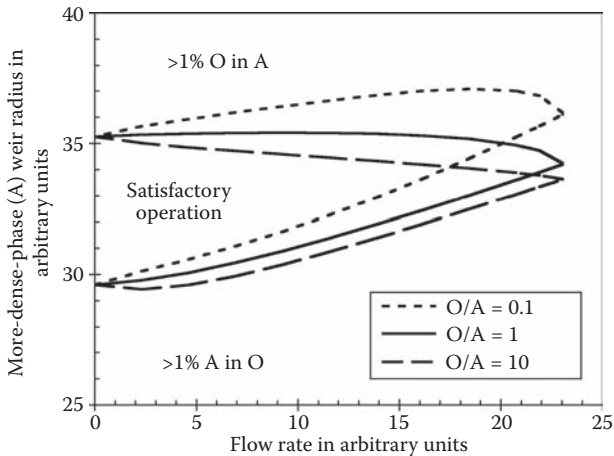
FIGURE 10.14 Operating curves for the same centrifugal contactor with an aqueous-phase density of 1000 g/L, an organic-phase density of 855 g/L, and O/A flow ratios of 0.1 to 10.

32.5 in arbitrary units. If the optimum radius for an organic-phase density of 855 g/L (34.0 in arbitrary units) was used for this case, the contactor would be inoperable (>1% O in A) except at low O/A flow ratios and high flow rates. As the density of the organic phase approaches that for the aqueous phase, the operating curves for the different O/A flow ratios move further apart and, accordingly, the nominal maximum throughput decreases relative to the maximum throughput.

    For the Argonne 2-cm contactor (Leonard et al., 1997), the rotor shaft diameter limited the minimum size for the upper weir. As a result, the minimum size for the
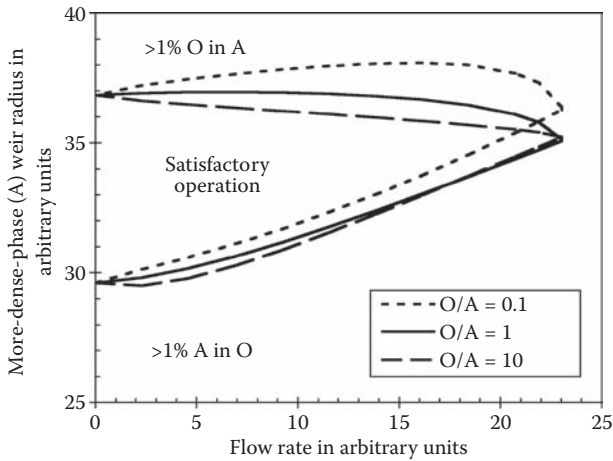
FIGURE 10.15 Operating curves for the same centrifugal contactor with an aqueous-phase density of 1000 g/L, an organic-phase density of 810 g/L, and O/A flow ratios of 0.1 to 10.
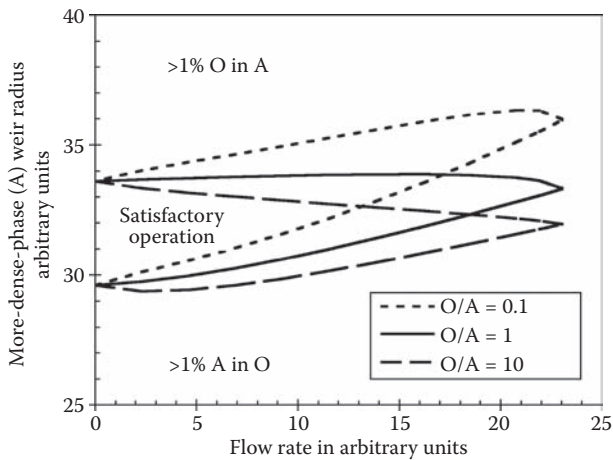
FIGURE 10.16 Operating curves for the same centrifugal contactor with an aqueous-phase density of 1000 g/L, an organic-phase density of 900 g/L, and O/A flow ratios of 0.1 to 10.

LW also had to be larger so that r_{LW*}/r_U was considerably greater than 0.46. This condition decreased the volume per unit length in the separating zone, thus, allowing $L/D_{R,i}$ to be considerably greater than the value of 2.2 mentioned earlier. The final volume of the separating zone was about the same as would be attained if r_{LW*}/r_U was 0.46 and $L/D_{R,i}$ was 2.2.

Inside the separating zone of the typical contactor rotor are four vertical vanes that divide the rotor into four quadrants (see Figure 10.4). The vanes are formed by

two sheets of metal that extend from one side of the rotor to the other. They also extend the full length of the separating zone (see Figure 10.5) and force the entering liquid to immediately attain the full rotational speed of the rotor and stay at that speed. Thus, the dispersion experiences the full centrifugal force of the contactor for the entire time it is in the rotor. A small weep hole at the bottom outer edge of each vane allows the liquid surface in the various quadrants to be at the same radius for a given height. Near the bottom of the separating zone, a horizontal disk, called a "diverter disk," is embedded in the vertical vanes. This disk extends into the middle of the separating zone, thus forcing all of the dispersion into a region of higher centrifugal force. The center of the disk is open so that entrained air can move up to the LW and escape over that weir. This design prevents pressurization of the lower region of the rotor, which would reduce liquid flow into the rotor. The vertical vanes next to the LW can extend into the center of the rotor or can stop at the edge of the weir. While both designs work, each design gives a slightly different weir coefficient (Leonard et al., 1980b). For a given rotor design, one needs to specify this design parameter and then use it consistently so that all the rotors perform the same.

The route for the less-dense phase leaving the rotor is fairly simple. When the separated less-dense phase flows inward and up over the LW, the liquid is thrown out into a channel (like a rain gutter) and moves to one of four sets of exit channels, one in each quadrant of the rotor. Each set of channels consists of a series of holes or a single rectangular channel that allows the less-dense phase to be flung by the rotor into the lower collector ring.

The route for the more-dense phase is more complex. The separated more-dense phase flows outward and up into the underflow. Each of the four sets of underflow channels is either a series of drilled holes (see Figure 10.3) or a slot. Each quadrant of the rotor has one set of underflow channels between the four sets of exit channels for the less-dense phase. At the exit of each underflow channel is a riser that carries the more-dense-phase liquid inward up to the upper weir. This riser is created when the top plate is placed on the rotor, shown in Figure 10.6. In the SRL and ANL contactors, the riser is narrow so that it will carry out fine particles that might be entrained in the more-dense phase. In the CINC contactor, the underflow channel is very short; thus, the riser to the upper weir is very wide, so that entrained particles have little possibility of being carried out in the more-dense phase. This design may not prove problemmatic. The particles could settle out and create a narrow riser channel to the upper weir, which then carries out any additional particles. When the more-dense phase reaches the upper weir, it flows up over the weir and is spun out. In some contactors, the rotor is open above the upper weir, and the liquid is thrown out into the upper collector ring, as shown in Figure 10.1. Other contactors have a cover over the upper weir. The liquid is thrown out into a channel (again, like a rain gutter) and moves to one of four sets of exit channels, one in each quadrant of the rotor. Each set of channels consists of a series of holes or a single rectangular channel (see upper rectangular openings in Figure 10.5), which allows the more-dense phase to be flung by the rotor into the upper collector ring.

Just as contactors typically have four vertical vanes in the separating zone, they also have four vertical vanes in the riser to the upper weir. Also, these vanes can stop at the edge of the upper weir or continue on to the center of the rotor. Typically, these

vanes go to the center of the rotor, as the radius of the upper weir may be changed for different solvent-extraction processes. This design is possible with the CINC rotors, as each upper weir is held in place by a cover plate above the upper weir. An o-ring seals the upper weir to the body of the rotor. After removal of the cover, the upper weir, and the o-ring, the upper weir can be replaced with another weir having a different inside diameter for the same process. Once the best diameter is found for the upper weir, its diameter does not have to be changed, and the weir can be welded in place. In the SRL contactors (Webster et al., 1969; Long, 1978), and in the first ANL contactors (Bernstein et al., 1973), an air-controlled weir was used for the upper weir. This design allowed the diameter of the upper weir to be effectively changed by changing the air pressure over the weir. Because of the mechanical complexity in maintaining the air pressure, however, the air-controlled weir is no longer used.

The underflow channel or channels in each quadrant should be either a single open channel or a series of holes next to the outer wall of the rotor. The underflow area should be as large as possible so that the effect on contactor performance is minimized. From ANL experience with contactors ranging from 2 to 25 cm in rotor diameter, the total underflow area for all four quadrants should be 5.8% of the outside diameter of the rotor squared.

As the diameter of the LW is fixed relative to the edge of the underflow as explained above, the diameter of the upper weir is chosen so that the dispersion band will be contained between the edge of the underflow and the edge of the LW. With no dispersion band, the radius of the interface in the separating zone (r_i) can be calculated by the following equation (Davis and Jennings, 1961):

$$(r_i^2 - r_{UW}^2)\rho_{MD} = (r_i^2 - r_{LW}^2)\rho_{LD} \qquad (10.5)$$

where ρ_{MD} is the density of the more-dense phase, ρ_{LD} is the density of the less-dense phase, r_{UW} is the radius of the liquid surface over the upper weir, and r_{LW} is the radius of the liquid surface over the LW. Note that the liquid rise over each weir can be calculated by using equations given by Davis and Jennings (1961) and Leonard et al. (1980b). In Equation 10.5, the densities of the two immiscible phases are very important. As a first approximation, the interface position should be chosen so that equal volumes for the dispersion band are between the interface radius and the inner edge of the underflow radius and between the interface radius and the edge of the LW radius. The radius of the more-dense-phase weir is then chosen to achieve the desired interface position in the rotor.

For a given process flowsheet and throughput, the two liquid densities at a given stage and the radius of the LW are fixed. Thus, once the interface position is also chosen, the radius of the upper weir can be calculated from Equation 10.5. If most of the flow is over the upper weir, the liquid rise over this weir will push its radius toward that of the LW, and the interface position for the dispersion band in the separating zone will move toward the edge of the LW. Conversely, if most of the flow is over the LW, the liquid rise over this weir will push its radius in, away from that of the upper weir, and the interface position for the dispersion band in the separating zone will move out toward the inner edge of the underflow. As deduced from Equation 10.5 and suggested by at in Figure 10.14, when the densities of the two phases are within

15% of each other, the value for the upper weir starts to be sensitive to the interface position. As deduced from Equation 10.5 and suggested by in Figure 10.16, when the densities of the two phases are 10% from each other, the interface position is sensitive to both the flow rate and the O/A flow ratios. For this reason, one should avoid flowsheets that have the densities of the two phases this close together. However, Figure 10.16 shows that centrifugal contactors can be used by reducing the nominal maximum throughput and making the more-dense-phase weir radius smaller. This is possible because the point where the lower curve of the operating envelope intersects the *y*-axis is independent of the differences in densities between the two immiscible phases.

10.3.1.4   Liquid Exit

The liquid exit for each phase in a multistage operation catches the liquid being slung from the rotor and moves it on to the next stage or to an effluent tank. For single-stage operation, the exiting liquid always goes to an effluent tank. Each liquid phase exiting from the upper portion of the contactor rotor is caught by its own collector ring so that the two phases are kept separate. The width of each collector ring is about 25% of the inside diameter of the contactor housing. Each liquid exits its collector ring through a tangential port that allows the liquid momentum imparted as the liquid leaves the rotor to move the liquid from the collector ring into the interstage line. When the liquid flow is small, typically less than 100 mL/min, the liquid loses its momentum in the collector ring and flows out the collector ring by gravity. In this situation, surface-tension forces also become important and give rise to the liquid slugging mentioned above.

The wall where the liquid exiting the rotor first strikes the contactor housing should be set at an angle so that the liquid is directed downward, as evident in Figure 10.1. In most ANL contactors, a splash plate appears above the upper weir. This plate catches any liquid that splashes upward and drips it back down onto the spinning rotor so that the liquid can be spun out again. The splash plate, shown in Figure 10.1, is trapped between the motor and the rotor and is removed with the motor/rotor assembly. The slinger ring on the rotor is also shown in Figure 10.1. The slinger ring is just above the lip of the upper collector ring. The gap between the slinger ring and the lip of the collector ring is kept small so that liquid cannot easily splash back and fall into the lower collector ring. If liquid puddles in the collector ring and starts to flow by gravity over the lip of the collector ring, the slinger ring will reverse most of this flow and result in significant momentum to the liquid it touches. This momentum will send the liquid back out into the upper collector ring and help to move it to the tangential exit port. There is no slinger ring for the lower collector ring. Such a ring would trap the rotor in the housing, thereby making removal of the motor/rotor assembly difficult. A lower slinger ring is not really needed because if a small amount of less-dense-phase liquid escapes to the mixing zone, it will be recycled back through the contactor rotor to the lower collector ring with no harm to the overall operation.

The cross-sectional area available for flow in the collector ring should match that for the exit port or interstage line. This condition allows a smooth transition, as the liquid leaves the collector ring with no hydraulic jumps that would cause the flow to

slow down. For this same reason, the interstage line should have a constant diameter. In the SRL and ANL designs, the interstage lines curve gently around to the next stage. In this way, liquid momentum is conserved and the liquid flows smoothly into the next stage. The interstage lines should be large enough that the flowing liquid fills no more than half of the cross-sectional area available for flow. The same rule should hold for the exit lines to an effluent tank. In both cases, the liquid flow is governed by liquid flow in an open channel with a free surface. By keeping the interstage lines open, the air pressure around the rotor will be the same in all stages. Lines for external feed into a contactor stage, since, typically, they are driven by a pump, can be much smaller. This condition prevents other-phase flow by gravity into these lines, at least during contactor operation.

So far, we have discussed the optimum contactor design. Some designs are less than optimal, either because of an operating error or the need to address some additional design constraint. The contactor still works, but the maximum achievable throughput will be less. One such case occurs when the direction of rotor rotation is reversed. Typically, this reversal is due to an installation or operating error. We have tested such operation at Argonne, and the contactor still worked, although the maximum throughput was reduced. In a hypothetical contactor design, a contactor housing could be machined out of a single steel block. In this design, the collector ring might not be a ring at all. Instead, it could a flat square trough that catches the liquid exiting from the rotor. There would have to be a circular opening in the center of the trough so that the contactor rotor could be inserted. For such a square collector, the interstage line might be a vertical hole drilled in the housing block in one corner of the trough. At the bottom of this vertical interstage passage, the line could make a sharp 90° turn into the next stage. While such a design has not been tested relative to a circular collector ring with a tangential exit port, its maximum throughput would most likely be less. However, because of its compactness, such a design might still be useful. In fact, it could eliminate the use of external interstage lines.

10.3.1.5 Motor

The motor above the contactor serves four functions by driving the rotor. First, it mixes the two immiscible liquids. Second, it creates the centrifugal force that rapidly separates the liquid-liquid dispersion. Third, it lifts the less-dense phase so that it can flow by gravity to the next stage or to an effluent tank. Finally, it lifts the more-dense phase so that it can also flow by gravity to the next stage or to an effluent tank. At the same time, all the bearings are kept out of the liquid so that they have a normal long life. All of the contactors built at SRL and ANL use the bearings in the motor as the bearings for the rotor. As long as a well-balanced motor/rotor assembly spins at less than 70–80% of its first critical speed, the contactor will not have excessive vibrations because of the spinning rotor. Leonard et al. (1993) developed a method for calculating the first critical speed of the motor/rotor assembly using an electronic spreadsheet. As noted in this reference, the first critical speed must be calculated and measured with the liquids in the contactor rotor.

The initial SRL and ANL contactors used motorized spindles to drive the contactor rotors. These spindles have a large-diameter shaft that gives good stiffness to the motor/rotor assembly. The shaft is also hollow so that it can supply air to the

air-controlled weir. However, these spindles are expensive and have a long delivery time. More recent contactors were designed with the diameter of the upper weir set so that an air-controlled weir was not required (Leonard, 1983). These contactors can use inexpensive off-the-shelf motors. For contactors larger than 4 cm, motors already designed to operate in a corrosive environment are commercially available. For high radiation environments, the motors must have electrical insulation and bearing lubricant that can stand up to radiation, which will increase the motor cost.

A key feature of all contactor designs used in high radiation environments is the ability to remove and replace the motor/rotor assembly easily by using remote maintenance tools. A typical design for a unit that is 4 cm or smaller has two nuts at the top of the motor/rotor assembly holding it in place (see Figure 10.17 and Leonard et al. (1997)). For larger units, additional nuts may be required. In all cases, the nuts are designed to be attached and removed remotely. An air-powered torque wrench is used to unscrew the nuts. A hook at the top of the motor/rotor assembly and tapered guide pins of unequal height allow the assembly to be removed and reinserted easily by using an overhead crane.

While some CINC units have a bearing at the bottom of the rotor, it is now being eliminated whenever possible. The bottom bearing is very expensive, hard to replace, and, if the contactor runs dry, cannot be lubricated and will thus, fail. In a production contactor, the bearing noise should be monitored so that bearing problems can be identified and corrected before the bearing fails.

In all CINC contactors and the latest ANL contactor (a 15-cm unit that has been designed but not yet built), the motor rotor and the contactor rotor are isolated from each other with respect to their vibrations. This separation is accomplished by means

FIGURE 10.17   Eight-stage 4-cm centrifugal contactor with face-mounted motors.

of a flexible coupling between the motor and the contactor rotor. In this design, the contactor rotor needs two sets of bearings on its shaft above the rotor body. The downside to this design is that it now has four sets of bearings that can fail instead of two. The upside is that the motor can be chosen to supply just the power needed. (For larger contactors where the motor bearings were also the rotor bearings, the motor was chosen for the large diameter of its motor shaft and thus had much more power than needed.) Because the flexible coupling isolates the vibrations of the motor and rotor, the critical speed for the contactor rotor can be calculated without having to consider the motor interactions. Also, as the motor is being operated at the conditions it was designed for, it is below its first critical speed. As before, the design of the motor/rotor assembly must be such that it can be removed easily as one piece.

10.3.2 MULTISTAGE DESIGN AND OPERATION

After a single contactor stage has been designed and the unit has been built and successfully tested with the desired process fluids at the required flow rates, a multistage unit can be designed and built. This section looks at the overall design and operation of the many stages usually required for a process flowsheet.

The earlier photos show several multistage centrifugal contactors. An operating four-stage 4-cm contactor is shown in Figure 10.10. In this contactor, the motors are side-mounted. The support frame is the L-shaped angle iron to which the motors are mounted. The end of a bank of 2-cm contactors is shown in Figure 10.11. Notice that these motors are face mounted.

Figure 10.17 shows an eight-stage 4-cm contactor. The motors are also face mounted, as discussed by Leonard (1988). There is only one leg between the two four-stage banks of contactors. In later units, one leg has been put at each end of each bank of contactors. This design makes it easier to handle individual banks of four contactor stages. A four-stage 10-cm contactor is shown in Figure 10.18. In this photograph, an overhead crane is lifting one of the motor/rotor assemblies out of the contactor housing.

10.3.2.1 Design

A solvent-extraction flowsheet is broken down into sections such as extraction, scrub, and strip. For each section, one or more component in a process fluid must be moved from one phase to the other phase with a specified degree of completeness. The first design problem is to determine the number of stages for each section to accomplish the required component transfer. With the well-defined stages of the centrifugal contactor, the following extraction factor (E) can be used to estimate the number of stages required:

$$E = RD \tag{10.6}$$

where D is the distribution ratio for a given component at a given stage (its concentration in the organic phase divided by its concentration in the aqueous phase at equilibrium), and R is the O/A flow ratio in that stage. When the extraction factor is greater than one, more of the component goes to the organic phase at that
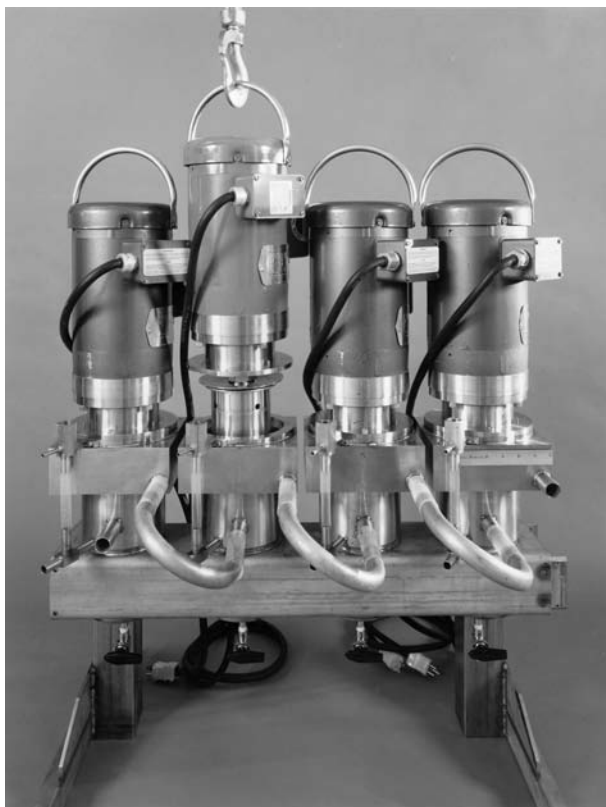
FIGURE 10.18   Four-stage 10-cm centrifugal contactor with one stage being removed.

stage. When the extraction factor is less than one, more of the component goes to the aqueous phase at that stage. The number of stages required in each section can be estimated from the design rules for solvent extraction given by Leonard (1999). As the extraction factor becomes greater than 2, the decontamination factor for the extraction section increases exponentially and approaches E^n. As the extraction factor becomes less than 0.5, the stripping factor for the strip section approaches E^{-n}. This correlation shows the power of countercurrent solvent extraction to achieve very high concentrations or very good stripping in a relatively small number of stages if the extraction factor can be made appropriately high or low, respectively. While the distribution ratio is normally fixed, the O/A flow ratio can be adjusted to obtain an appropriate extraction factor for good separations. Of course, contactor users cannot control the flow ratios as much as they might like because the organic phase flows at the same rate from stage to stage and from section to section.

The design rules given by Leonard (1999) are based on many assumptions, such as the D value being constant in a section. In general, processes are more complex. As a result, the final calculation should be done in a more rigorous fashion through a stage-to-stage calculation, where the D value for each component in each stage is specified. In addition, the following should be specified: amount of other-phase

carryover for each phase, the mass-transfer efficiency at each stage, the effect of the various component concentrations on the *D* value of each component (including solvent loading), and the effect of taking a continuous stage sample at one or more stages. Such a calculation can be done with the Spreadsheet Algorithm for Stagewise Solvent Extraction (SASSE) developed by Leonard and Regalbuto (1994). The SASSE worksheet for the process as given in their article provides a simple yet powerful tool for analyzing the flowsheet. It can also help to clarify any estimates made by using the design rules.

Multistage contactors must be designed to withstand variations in the various feed parameters. This robustness can be accomplished in several ways: (1) determine the number of stages based on the mass-transfer efficiency of 80% at each stage, even though, with well-designed centrifugal contactors, it should be greater than 95%, (2) calculate the number of stages required in a section based on 100% stage efficiency and then add 25% more stages, or (3) use the robustness factor (Bonnesen et al., 2000), which is defined as the SASSE-calculated decontamination factor for a section divided by the desired decontamination factor. In the example given by Bonnesen et al. (2000), the number of stages is increased while using the lowest expected stage efficiency (95%) and the highest expected other-phase carryover (1%). The correct number of stages is the one in which the robustness is greater than 3. This value is the minimum obtained when using SASSE to evaluate the flowsheet over the range of flow rates, temperatures, and *D*-value variations that are expected in a commercial plant facility. Depending on the process characteristics and the importance of always remaining at or above the desired decontamination factor, the design value for the robustness could be greater than or less than 3. It should always be greater than 1.

10.3.2.2 Operation

For both single-stage and multistage operation, the more-dense phase must be in all contactor stages before the flow of the less-dense phase is started. Otherwise, the less-dense phase flows the wrong way, that is, out the more-dense-phase exit. As the extraction-section feed has the component or components to be extracted, often at a very high decontamination factor, the actual extraction-section feed should not be used during process startup. If this is done, flushing the component or components being extracted from stage 1, the stage where the solvent is being fed, will take a long time. To prevent this condition, and indeed to ensure that the aqueous effluent from the extraction section (the aqueous raffinate) is always at or lower than its desired concentration, a dummy feed should be used for the aqueous feed to the extraction section during contactor startup. The dummy feed should have many of the characteristics of the actual feed, especially the feed density, but it should not have the component or components to be extracted. For example, the aqueous feed to the extraction section could be the aqueous raffinate from a previous campaign in which the components to be extracted have already been removed. After the contactor stages are filled with the more-dense phase, the less-dense phase feed should be started. When the less-dense phase has filled each contactor stage, then the dummy feed can be replaced by the actual feed. Note that the contactor rotors should be turned on before any liquid is fed to the contactor.

After the contactor stages have been filled with the more-dense (aqueous) phase and the less-dense (organic) phase is started, the organic phase will displace some of the aqueous phase, thus, temporarily speeding up the flow of the aqueous phase. This condition can be a problem if the contactor stages are operating near their hydraulic capacity. In this case, the flow of the aqueous phase should be slowed or stopped until the organic phase has filled the unit. When the organic phase starts flowing out the organic exit port, the aqueous phase flow returns to the process flow rate.

Once the actual extraction-section aqueous feed is started, the process should be close to steady state after three residence times of the fluid have passed through the contactor stages. This action will typically take 15 to 30 min. If the above startup procedure is used, the decontamination factor for the extraction section will always be greater than the desired value, even during startup. Once steady-state operation is reached, the process is easy to control. The operator needs to check that the required feed flow rates are maintained, that the feed in each feed tank is appropriate, and that the rotors are spinning at the proper speed. Also, the feed tanks need to be monitored to avoid them running dry, and the effluent tanks need to be monitored for overflow. In plant operation, these tasks are usually automated.

In a normal contactor, the flow of the liquid between stages cannot be seen because the interstage lines are made of metal. However, in some 2-cm contactors, the metallic interstage lines were replaced with Teflon-type tubing that is translucent. Flow in the interstage lines for the aqueous and organic phases in test CS25 (Leonard et al., 2001a) are shown in Figure 10.19. These four photographs show the wire ropes used to reduce slug flow in the interstage lines (discussed earlier). Figure 10.19a shows the aqueous liquid flowing from stage 5 to stage 4, where the interstage line is open as the liquid flows into stage 4. Figures 10.19b through d show the organic liquid flowing from stage 3 to stage 4 at various times. The organic liquid level and condition change with time in the interstage line going to stage 4, while the aqueous flow to this stage is stable and the aqueous interstage line remains open throughout
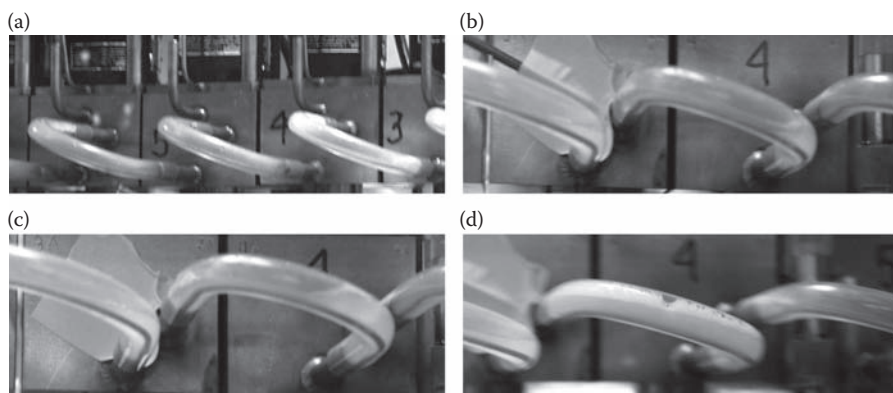
FIGURE 10.19 Varying liquid levels in the interstage lines of a 2-cm contactor. (a) Aqueous side—open interstage line at stage 4. (b) Organic side—almost open interstage line at stage 4. (c) Organic side: half-filled interstage line at stage 4. (d) Organic side: foam-filled interstage line at stage 4.

the test. In this contactor, the aqueous interstage lines enter the mixing zone slightly off the perpendicular and, as a result, work much better than the organic interstage lines that enter the mixing zone on the perpendicular. As long as the liquid does not back up into the stage from which it is exiting, overall contactor operation will not be affected. For the mixing zone liquid to interact with the entering liquid, the level of the liquid in the mixing zone needs to be up to the level of the liquid inlets. In spite of the interaction between the organic phase entering the mixing zone and the dispersion in the mixing zone, test CS25 was a success.

The contactor stages running a process flowsheet can be shut down either very quickly or normally. In normal shutdown, the actual aqueous feed to the extraction section is replaced by the dummy feed. Operation is continued until all the components to be extracted are flushed from the unit to the desired level. At this point, if desired, the organic flow can be stopped. Then, any aqueous cleaning solutions required are introduced at the appropriate feed ports. These flows are continued until they have achieved their cleaning goals. Finally, an aqueous feed of dilute acid or base or water is introduced as rinse to the appropriate feed ports to clear the contactor of all cleaning solutions. If desired, some diluent can be flowed through the units to pick up any solvent. All this time, the rotors are kept turning at their regular speed. After the rotors are turned off, any cleaning or rinsing solution must be pumped very slowly through the contactor so that the liquid is not forced up into the bearings closest to the contactor rotor at any stage. When the contactor rotor is connected directly to the motor, these are the lower motor bearings. When the contactor rotor vibrations are isolated from the motor by a flexible coupling, these are the lower rotor bearings.

In a quick shutdown, all the rotors and pumps are turned off at the same time. All the liquid is left in the stage where it was at shutdown. This procedure can be used to obtain a concentration profile of the various components from stage to stage at essentially steady-state operation. Thus, it is commonly used during tests of a new process flowsheet. It can also be used to handle an operating problem, for example, if a contactor motor fails. In this case, the motor/rotor assembly can be removed and a spare unit inserted. This operation can be done quickly, even in a fully remote facility, if the contactor is designed as discussed above. The process can then be restarted at essentially steady state. If a quick shutdown occurs because liquid has accumulated in one or more stages so that they are full of liquid even when not running, the unit must be restarted carefully. The first stage that is turned on should be stage 1, which is the stage where the organic feed is entering and the aqueous raffinate is exiting. When this stage is cleared of excess liquid, stage 2 is started. This process is repeated for each stage until all stages are running normally. Then, the process feeds are restarted. This restart procedure keeps excess liquid from being pumped into the motor or contactor rotor bearings.

In an unpublished large-scale test under computer control, an annular contactor was shut down by turning off the rotor motors and the feed pumps. During the shutdown, the computer did not turn off one of the feed pumps. This pump kept operating until the contactor was filled with liquid, which was detected by an operator. In this case, the above restart procedure (turning on one stage at a time starting with stage 1 was followed so that all the excess liquid could be removed from the

contactor stages without pumping some of the liquid into the contactor rotor bearings. The procedure worked well.

10.3.3 OTHER DESIGN CONSIDERATIONS

This section concerns other design and operational matters for both single- and multistage contactors.

10.3.3.1 Support Frame

A support frame is needed to hold the contactor stages in place and to keep the same distance from one stage to the next so that the interstage lines on each side are all the same. The support frame must be stiff enough that its first natural frequency is at least 30% higher than the contactor rotor speed. If the contactor rotor speed approaches the first natural frequency of the support frame, then the support frame will develop vibration problems. For larger contactors, a typical support frame will hold four to six contactors. At ANL, 4- and 10-cm contactors have been built in banks with four stages each. In these banks, the stages were in a straight line (Leonard, 1988). The 25-cm SRL contactors were built with six stages in a bank. In these banks, the stages were in two rows of three stages each (Webster et al., 1969). For smaller 2-cm contactors, the early units were built in banks of eight with a single motor driving all eight in-line stages (Leonard et al., 1980a). Later 2-cm contactors were built in banks of four, with the stages in a straight line; see Leonard et al. (1997) as well as Figures 10.11 and 10.17. In these units, each stage had its own motor. Four stages of contactors are easier to handle in a glovebox or a shielded-cell facility than banks of eight stages. In the ANL units, the interstage lines are attached with commercial off-the-shelf couplings that allow them to be removed easily. For the 25-cm SRL contactor, the interstage lines were welded in place. For a process that is still being developed and tested, detachable interstage lines are recommended. Once the process is fixed and if access to the equipment is difficult or impossible, as in a highly radioactive processing canyon, it is recommended that the interstage lines be welded in place. In a nonradioactive plant, normal tubing or pipe couplings would probably be used.

Box beams can be used in the support frame to make it as stiff as possible while minimizing the amount of steel required, as shown in Figure 10.11 and discussed by Leonard (1988). In early work, simple rules of thumb were used to estimate support-frame vibrations. Now, with computer-aided drawings, computer programs can make more-precise vibration calculations. Computer-aided drawing programs can also calculate the first natural frequency of the contactor rotor. This eliminates the need for the spreadsheet calculations given by Leonard et al. (1993). Basing the calculations on the as-drawn contactor rotor should be faster and more accurate than the older spreadsheet method. The first natural frequency for the support frame should be 20% to 30% above the motor speed, as is the case for the motor/rotor assembly or the contactor rotor with contactor rotor bearings.

10.3.3.2 Purge Air

As shown by Leonard (1988), purge air can be used to protect motor (or rotor) bearings from corrosive fumes in the contactor stage. This approach can work well as

long as the solvent-extraction liquids are not forced into the space above the contactor rotor body. The purge air is required when motors are not designed for corrosive service, and the bearings are not made of stainless steel. When the motor or the contactor rotor bearings are designed to stand up to the fumes of the solvent-extraction liquids, no purge air is required. Eliminating the purge air simplifies contactor design as well as operation and maintenance. Thus, designers should work to eliminate the need for purge air to protect the motor or rotor bearings. However, note that many radiation-resistant seals require such an air purge.

A multistage 4-cm contactor was built at ANL to be used with an aqueous phase that included 8 M HCl. As the motor shaft and bearings were carbon steel, an air purge was used at each stage to protect the motor shaft and bearings. The contactor housing and rotors were made of Hastelloy C276 because they cannot be protected by the purge air. The purge air provided good protection for the motors. The contactor housings had to be replaced after four years of operation, as the acid destroyed the weld joints that held the inlet and exit tubes to the contactor housing. Based on the rate at which 8 M HCl attacks Hastelloy C276, about four years of operation was expected. A newer alloy, Hastelloy C22, should perform even better when contactors are required for use with HCl solutions.

10.3.3.3   Bottom Drains

Many contactors include a drain at the bottom of the contactor housing (e.g., see Leonard et al., 1988). It is very useful for cleaning stages and for determining a stage-to-stage concentration profile when evaluating a process flowsheet. On the other hand, it provides a place for liquid to accumulate and can be very hard to use in a remote-handled facility. In addition, equipment is required to handle the liquid that is drained from the contactor stages. The 25-cm SRL contactors were built without bottom drains for these reasons. When needed, the 18-stage SRL contactor unit was cleaned by flushing with water and other liquids. Such unit flushing techniques obviously worked well, as it was possible to keep the SRL contactor in operation for almost 40 years without liquid drains. Thus, the need for bottom liquid drains on a production unit requires careful consideration. In many cases, such drains may not be desirable. All of the units built at ANL include a bottom drain.

10.3.4   TEMPERATURE CONTROL

In most processes using centrifugal contactors and other solvent-extraction equipment, temperature is set by the temperature of the room or the hot cell. However, the recent development of a process to remove Cs from nuclear waste required that the extraction section be cooled while the strip section was heated (Leonard et al., 2003). In the testing of this flowsheet, heating and cooling bars were attached to the sides of the contactor housing. A fluid, whose temperature was controlled, was passed through these bars to control process temperature. In some cases, the external feed line was cooled. In other cases, the room temperature was varied. In still other cases, motor heat was used to help warm up the stages. At the crucial first stage of the strip section, a heat lamp was found to help the separation. As temperature-sensitive flowsheets are identified, for example, where a third phase could form as the temperature

drops, temperature control will become a more important issue. Further work in this area would be beneficial.

10.3.5 LARGE CONTACTORS

Using the design rules stated above, 2- to 25-cm contactors have been built. A 25-cm contactor operating at a total flow rate of 100 L/min and an O/A flow ratio of 1.0 is shown in Figure 10.20. In general, as contactor size is increased, the rotor speed is decreased so that the maximum rotor speed is 20 to 30% below its first critical speed. The operating speed is dropped from 3600 rpm at rotor diameters of 4 cm and smaller, to 1800 rpm at rotor diameters of 9 cm and larger. At high rotor speeds and large contactor diameters, the power in the mixing zone becomes more than is needed to achieve good stage efficiency. This excess power can heat up the process liquids and waste electrical energy. Intense mixing can also emulsify the solvent-extraction dispersion; however, the author has not seen such an emulsion at ANL. Finally, high speeds with large rotor diameters could also require a bearing at the rotor bottom. As discussed above, such bottom bearings are not recommended. Either the rotor shaft should be made stiffer so that the rotor has a higher first natural frequency or the rotor speed should be lowered.

FIGURE 10.20   Operating single-stage 25-cm contactor.

In the future design of high-throughput contactors with rotor diameter greater than 25 cm, a smaller rotor diameter may be needed in the lower region of the separating zone. The transition to this lower region could be either tapered or abrupt. For a given liquid throughput, the liquid height in the annular mixing zone would be higher. This added height would provide a buffer region that would smooth out flow fluctuations. This design change would also lower the power required to drive the rotor and, accordingly, lower the day-to-day costs for a full-scale operating plant. The rotor diameter in this lower region should be large enough that the liquid in the annular region is turbulent. In this way, good mixing with high stage efficiency is maintained.

10.3.6 Emulsion Formation

The organic and aqueous phases chosen for solvent extraction typically do not form emulsions. The tendency to form emulsions can be evaluated by measuring the dispersion number (Leonard, 1995). For the solvents tested, the lowest dispersion numbers were observed at the highest O/A flow ratios. The 0.25 M Na_2CO_3 aqueous phase gave lower dispersion numbers than 0.1 M HNO_3. In addition, solvent degradation products can create an organic phase that will form emulsions. Because of the high centrifugal forces, the use of centrifugal contactors can sometimes eliminate the need for off-line processing of off-normal emulsified product batches (Meikrantz et al., 1998a). An emulsion was created during CSSX operation with the wrong equipment configuration at a high O/A flow ratio (5) and a very low HNO_3 concentration (0.001 M) for the aqueous phase (Fink et al., 2005). The emulsion remained stable for several weeks. Several methods were tried to break the emulsion. The best method was to pass the emulsion through the contactor at a very low flow rate so that the emulsion had a long residence time (20 min.) in the separating zone of the contactor rotor. In another test of the CSSX process, emulsion formation was found in the mixing zone but not in the separating zone of a 5-cm contactor (Birdwell et al., 2001). In a third test of the CSSX process, emulsion formation was related to the solvent composition (Birdwell et al., 2002). In this work, foam in the interstage line was also found to contain some emulsion. In a test of the TRUEX (transuranic extraction) flowsheet as a part of the overall uranium extraction (UREX) process, emulsion formation was observed while washing the solvent with 0.25 M Na_2CO_3 at an O/A of 4 (Law et al., 2006). When the emulsion was washed with 0.1 M HNO_3, the emulsion was destroyed.

10.3.7 Control of Mixing

In the first annular centrifugal contactor built at ANL, the outside wall of the rotor had vertical vanes, and the inside wall of the contactor housing had vertical baffles. This design gave very good mixing, but was found to be more than needed for typical solvent extraction. Contactors with the vanes and baffles removed usually achieved good mass-transfer efficiency. Where molten metal and molten salt are the two immiscible phases, so that the density difference is very large and the interfacial tension is very high, vanes and baffles are required in the annular mixing

zone (Chow and Leonard, 1993). The special two-diameter rotor, discussed above for large contactors, can also control the mixing when the annular mixing is still more than is needed. In some cases, reduced mixing might prevent emulsion formation. In all cases, the reduced operating costs are a benefit.

Mixing can also be controlled by designing the inside of the contactor housing with two diameters. In the upper region of the housing, the diameter would be large so that mixing is low. In the lower region, the diameter would be smaller so that the annular gap is small and the mixing is high. In addition, with the smaller annular gap at the bottom, the ALH would be higher than with the larger annular gap throughout the mixing zone for the same throughput. Such a configuration should be easier to build than the two-diameter rotor design and would allow a separating zone with a constant cross-sectional area. If an insert is used to create the smaller bottom annular gap, various mixing-zone configurations could easily be tested by making a number of inserts. In fact, this approach is reasonable to use with all contactors, at least while a process is being developed.

10.3.8 AQUEOUS AND ORGANIC PROPERTIES

When evaluating whether or not an aqueous and organic (solvent) pair is suitable for carrying out a solvent extraction, the most important characteristic is the distribution ratios of the components to be extracted and of those to be left in the fluid. Once the distribution ratios are found to be favorable, the immiscible liquid-liquid pair must be characterized to determine if the pair can be used in commercial solvent-extraction equipment. This characterization is best done by the batch dispersion-number test (Leonard, 1995). This test can be performed easily and quickly with no special equipment. If the results are favorable, the densities of the two phases need to be considered. If the difference is less than 10%, plant operation could be difficult. As a rule of thumb, the density difference should be 15% or greater. The liquid viscosity is important in that more power will be required to turn the rotor if the viscosity is higher. The liquids also need to be able to flow easily from stage to stage.

10.3.9 ZERO-POINT ANALYSIS

When rotors are made, they should have the desired hydraulic performance. Also, contactor fabricators may want to compare the hydraulic performance of a set of rotors with one or more previous sets of rotors. To do this, the zero-point test has been devised (Leonard et al., 2002b). In this test, a rotor is operated in a single-stage unit or as a single stage in a multistage unit with a single liquid phase, usually water. The water is pumped to the unit at a fixed flow rate, and the output flow from the more-dense-phase exit is measured. Then, the flow rate is increased, and the test repeated several times. At some point, the liquid will not only flow out of the more-dense-phase exit, but also the less-dense-phase exit. The average of the highest flow rate with no flow out of the less-dense-phase exit and the lowest flow rate with flow out of the less-dense-phase exit is called the "zero-point flow rate," or simply, "the zero point." Beyond the zero point, the flow rate increase is continued, and the liquid flow out of both exit ports is measured. Then, one plots the total flow rate on the *x*-axis of a

chart and the flow rate out the less-dense-phase exit on the *y*-axis. The curve formed by the data above the zero-point flow rate is extrapolated to the *x*-axis to obtain a second measure of the zero point. Use of this second measure is preferred, as it should avoid flow or volume surges in the rotor that could make the zero point appear to be lower than it really is. A typical zero-point result is shown in Leonard et al. (2002b).

The zero-point analysis characterizes the rotor hydraulics in two ways. First, the zero-point value gives the liquid flow rate over the more-dense-phase weir just as the liquid in the separating zone rises to the edge of the less-dense-phase weir. Second, the slope of the curve above the zero point measures the liquid rise over the more-dense-phase weir relative to the liquid rise over the less-dense-phase weir. Thus, if all rotors in a set have about the same zero point and the same slope above the zero point, then they can all be expected to operate about the same in two-phase flow.

It is possible to estimate when the zero point will occur. The rise of the liquid surface over the more-dense-phase weir is calculated as the flow rate increases. This calculation is possible with the equations given by Davis and Jennings (1961). The zero point occurs when the radius of the liquid surface over the more-dense-phase weir matches the physical radius of the less-dense-phase weir. This calculated zero point is an approximation and needs to be corrected by use of Equation 10.1 for the air (gas) pressure on the liquid surface of both weirs and the height of the more-dense-phase weir above the less-dense-phase weir. If the liquid flowing though the underflow has a significant pressure drop, that needs to be included as a correction to the zero-point calculation.

10.3.10 Siphon Formation

Estimation of the zero-point flow rate has identified a previously unexpected behavior in centrifugal contactors. In work with 12.5- and 25-cm contactors, the CINC V-5 and V-10, the measured zero-point flow rate was found to be significantly above the calculated value, even when the various approximation errors were considered (Campbell et al., 2008). In both contactors, the upper weir had a cover over the weir with exit channels through which the more-dense-phase liquid had to flow to leave the rotor. When a weir is closed in this way, the air pressure over the weir can be calculated by using Equation 10.1, where the density is that of air and the height term can be neglected. A reasonable hypothesis is that, before the zero point is reached, the flow over the upper weir is so great that the exit channels are completely filled with liquid, causing a liquid siphon to form in the filled exit channels of the rotor that are downstream from the more-dense-phase weir. The siphon pressure can also be estimated by using Equation 10.1, where the density is now that of the more-dense-phase liquid. The liquid siphon greatly increases the negative pressure over the more-dense-phase weir relative to atmospheric pressure, causing a large increase in the flow rate over the more-dense-phase weir and, so, the zero-point flow rate. To test this hypothesis, a hole or holes could be drilled in the cover plate over the upper weir. This hypothesis was not tested during this series of tests.

The expected zero point was found in one of the tests with these two CINC contactors. However, as the slope above the zero point was being measured, the flow out the LW suddenly dropped to zero. If the total flow to the contactor was lowered

slightly, flow out the lower exit resumed; if it was increased, that flow stopped. At the point when the flow out the lower exit stopped, the flow out the upper exit had probably become so large that the upper exit channels were filled with liquid, and a siphon formed. In a second test done at the same time for a different more-dense-phase weir configuration in the contactor, as the slope above the zero point was being measured, the flow out the LW dropped, but not to zero. As the total throughput was increased further, the flow out the LW started to increase from this lower value. This result suggests that only a weak siphon formed over the upper weir.

In recent tests on a 5-cm contactor, the CINC V-2 model, estimates of the upper weir diameter indicated an apparent weir diameter much larger than the actual one (Leonard et al., 2002). As this contactor has a covered upper weir, a siphon probably formed to cause the unexpected results. Note that a siphon could also be formed over the LW as it is always closed. To the author's knowledge, this phenomenon has never been observed. For normal contactor operation, even with a closed upper weir, a siphon will probably not form, as it occurs only at very high flow rates. When a siphon is formed, the general contactor operation represented by Equation 10.5 no longer applies, since it is assumed that the pressure over the liquid surface on both weirs is the same. The formation of a siphon is an area where more research is needed. Some work has been started in this area. Experimental and modeling work by Wardle (2008) showed that a siphon can form above the upper weir on a 5-cm contactor when it is covered. Holes drilled in this cover reduced the effect of the siphon.

10.3.11 THREE LIQUID PHASES

Under certain conditions, the two immiscible liquid phases used in a solvent-extraction flowsheet can become three liquid phases. This situation can occur when a high concentration of acid or a heavy metal has been extracted from the aqueous phase into the organic phase, exceeding the ability of the solvent to solubilize the organic-phase complexes formed. When the extractant is loaded with the heavy metal, the solvent phase can form two immiscible organic phases in which the diluent-rich solvent becomes a less-dense organic phase, while the extractant-rich solvent with the heavy metal becomes a more-dense organic phase. As long as the more-dense organic phase is less dense than the aqueous phase, the organic phase can be separated from the aqueous phase. In designing for this separation, one does not use the average density of the two organic phases. Instead, the separation should be between the more-dense organic phase and the aqueous phase. Quite often, the density of these two phases will be within 10% of each other. This condition makes separation difficult, as the region of satisfactory operation for different O/A flow ratios diverges, as shown in Figure 10.16. Consequently, solvent extraction should not be used when three liquid phases might form. Flowsheets are typically designed so that three liquid phases are never formed.

Leonard et al. (1983) operated an annular centrifugal contactor with three liquid phases forming in the mixing zone. With a weir designed to separate the more-dense organic phase from the aqueous phase, a good separation was achieved. However, problems occurred during startup and shutdown, where the contactor went through all the O/A flow ratios. Multistage operation made these problems worse. One test using

three liquid phases in a four-stage 2-cm contactor created a flow oscillator. This result reinforces the wisdom of designing solvent-extraction flowsheets so that three liquid phases do not form. The reader is referred to standard texts on solvent-extraction chemistry, for example, Peterson and Wymer (1963) and to Chapter 7 by Fabienne Testard in this volume, for more information on the formation of three liquid phases.

10.3.12 Cleaning

Sometimes, contactor cleaning is required because of a serious process upset or the need to run a different flowsheet. A contactor may be cleaned by flushing it with one or more cleaning and rinsing liquids. The choice of liquid or liquids is based on the organic and aqueous phases used in the flowsheet and the components to be removed. A second liquid may be needed to rinse out the first liquid and perhaps do some cleaning of its own. If needed, other liquids can be employed until cleaning and rinsing are complete. Usually, the last rinse liquid will be water.

If frequent cleaning is anticipated, the contactor design should eliminate all possible sources that would hold up liquid and prevent it from flowing to the contactor drain. Parts should be welded or otherwise assembled to eliminate crevices. Interstage lines should be sloped so that all liquid flows out and into the stage. The inside bottom of the rotor should be sloped slightly to the center so that all liquid leaves the rotor. The inside bottom of the contactor housing should be sloped slightly between the bottom vanes so that the liquid there flows to the drain in the middle. If the contactor housing has no bottom drain, a special tube should be made to remove the remaining liquid at the bottom. The tube would be inserted into the housing from the top after the motor/rotor assembly is removed. A housing around the tube would allow it to be self-guiding to the bottom of the contactor housing at the center. Once in place, a pump or vacuum would be applied to the other end of the tube to draw out all the liquid at the bottom of the contactor housing.

If cleaning is being done to gather valid stage samples, the system that collects these samples at the end of the test should also be easy to clean and be thoroughly cleaned before the test. The test itself should not undo the cleaning effort. Stage temperatures at the end of the test should be recorded. Then, the stage samples should be carefully collected, equilibrated at the stage temperature, and analyzed. Even when cleaning is not sufficient to collect valid stage samples, analysis of the stage samples can still provide clues to contactor operation. To validate the cleaning effort and the subsequent stage samples, the concentration of the effluent sample from a stage should be compared with that of the stage sample from the same stage. If they are within experimental error, then the cleaning efforts and stage sampling are considered valid. An example is given by Leonard et al. (2003) of a multistage solvent-extraction test where contactor cleaning was good, but where acid contamination from the cleaning solution itself caused minor problems.

10.3.13 Evaporative Losses

The typical solvent has at least one component that is slightly volatile, usually the diluent. As the solvent is constantly recycled through the contactor stages, some of

the volatile component will evaporate so that the solvent composition changes over time. In most cases, the loss of the volatile component can be determined as a function of time by measuring the solvent density. The use of an air purge acts to carry off the volatile component, thereby speeding up its loss. The contactor rotors also pump air through the bank of contactors. The lower (less-dense-phase) weir in the contactor rotor is especially effective in pumping out air because it has a covered exit port and gets air from the annular mixing zone via the RI and the open space in the center of the separating zone. The air is pumped out of the lower exit of the contactor rotor and the contactor housing along with the less-dense-phase effluent.

With a highly volatile diluent, such as carbon tetrachloride, the solvent loss can be quite high (Leonard, 1988). Even with a diluent that is considered nonvolatile, but which does have a small vapor pressure, the diluent loss from the solvent can be important (Leonard et al., 2003). In both cases, the solvent was returned to its original state by replacing the lost diluent. Measurements of diluent loss from solvent in a 33-stage 2-cm contactor ranged from 0.05 to 0.48 mL/min when the diluent was Isopar L (Leonard et al., 2002a). The lower loss rate is considered to be more typical for this particular system.

10.3.14 RADIATION

To minimize the impact of the radiation encountered when processing nuclear materials, motors and other equipment must be designed to have a reasonable service life for the radiation doses that will be encountered in the process plant. This protection is provided in two ways. First, any equipment that is affected by radiation must be made as radiation-resistant as possible. Second, the exposure of that equipment to radiation must be minimized.

The contactor parts that are affected by radiation consist of the electrical components (e.g., insulation, capacitors, resistors, and transistors) and mechanical components (e.g., parts made of plastic and the lubricant for the bearings in the motor/rotor assembly and the pumps). Typically, an electrical motor is chosen that will have only insulation as an electrical component. This electrical insulation must have the best possible radiation resistance. For the bearings in electrical motors as well as any other bearings that are part of the motor/rotor assembly, special lubricating oils that are radiation resistant must be used. The kind of oil will depend on the expected radiation to the equipment over its operating lifetime. Finding radiation-resistant greases, lubrication oils, and electrical insulation is a major design problem and should be addressed early in any contactor development work. Two references that the author has found helpful are by Stewart (1985) and Vandergriff (1990).

Most radiation-resistant equipment is protected by use of shielding, increasing the distance from the radiation source, and decreasing the exposure time to achieve an acceptable plant operating life. The choice of shielding will depend on the amount and type of radiation, as well as the weight and volume of the shielding that would be required. Increasing the distance from the radiation source works, as the effect of radiation falls off as the square of the distance from the source. Decreasing time works, as the radiation effects are proportional to the length of exposure. For this reason, the Savannah River Site (SRS) switched from mixer-settlers to SRL centrifugal

contactors. When this switch was made, the solvent exposure during each processing cycle was only one-twentieth as long as before. As a result, the solvent lasted about 20 times longer.

10.4 APPLICATIONS OF CENTRIFUGAL CONTACTORS

Centrifugal contactors have found many applications. In the simplest and most widely used case, they are used to separate oil from water. Many of the CINC contactors are used for this separation. When only liquid-liquid separation (demixing) is important, the annular mixing zone becomes a hindrance rather than an advantage. For that reason, CINC has designed a sleeve for the mixing zone so that the oil-water mixtures to be separated are not dispersed further. When applying centrifugal contactors to solvent-extraction flowsheets, both mixing and separating are required.

While solvent extraction is widely used in the petroleum, chemical, and pharmaceutical industries, acceptance of centrifugal contactors has been slow. Potential buyers have to be convinced that centrifugal contactor can not only replace the existing solvent-extraction equipment, but also perform better. For most existing processes, no money, time, or personnel are available for making process improvements that involve taking out existing equipment when that equipment is working satisfactorily.

Centrifugal contactors could find application in several non-nuclear areas, including the making of lube oils for the petroleum industry. A bank of centrifugal-contactor units with well-defined stages would seem to be more versatile than the Podbielniak centrifugal contactor (Baker Perkins Inc., now B&P Process Equipment, Saginaw, MI) that is typically used now. In the pharmaceutical industry, as new antibiotics are identified, annular centrifugal contactors could be introduced as a part of the overall product development. In existing processes, the equipment used is part of the drug specification and approval procedure, which is a long and costly task. For this reason, equipment changes to existing product lines are unlikely. As the benefits of centrifugal contactors to new processes are demonstrated, these units should become more common.

As the focus of this book is on nuclear fuel reprocessing and nuclear-waste cleanup, we will focus on applications in these areas. This section will look at the reprocessing of nuclear fuel and the cleanup and segregation of nuclear waste with SRL and ANL contactors. Finally, other centrifugal contactors used for nuclear processing in France, Japan, Russia, and China will be discussed.

10.4.1 REPROCESSING OF SPENT NUCLEAR FUEL

The centrifugal contactor was first used to reprocess spent nuclear fuel at the SRS in 1966 (Webster et al., 1969). For almost 40 years, this 18-stage 25-cm SRL contactor was used for the extraction and scrub sections (the A-bank) of the PUREX (plutonium-uranium extraction) process at the SRS. Contactor operation stopped when the facility in which they were housed was shut down in 2003. This 18-stage contactor replaced a 24-stage mixer-settler. Mixer-settlers continued to be used for the rest of the processing, as most of the radiation was removed in the A-bank. The ability to

use a multistage ANL centrifugal contactor to handle the A-bank of the PUREX process was demonstrated at Argonne with a 2-cm contactor (Leonard et al., 1980a). For these PUREX tests, only eight stages were available. They were first used to run the extraction and scrub sections of the PUREX flowsheet. Then, the eight stages were cleaned and used to run the strip section.

Recently, the UREX process has been demonstrated for recycling spent nuclear fuel (Regalbuto et al., 2004). In this process, the dissolved fuel is partitioned into various groups of constituents by means of several solvent-extraction flowsheets. This grouping allows the fissionable fuel elements to be recovered and reused while the fission products can be disposed of in the most economical way. Some separated fission products may go directly to low-level waste. Other separated groups (e.g., Cs-137, Sr-90) are stored until the elements decay. Then, they are disposed of at greatly reduced activity as low-level waste. The remaining fission products are disposed of as high-level waste (HLW). Finally, actinides would go back to the reactor where they are either used as fuel or transmuted into fission products that are easier to dispose of when that fuel is recycled. One of the UREX processes, UREX+, consists of five solvent-extraction flowsheets (Vandegrift et al. 2004). In this process the separated groups consist of (U), (Tc), (Cs and Sr), (Pu and Np), (Am and Cm), and the rare earth fission products. All of the UREX+ flowsheets were demonstrated twice, first with simulated dissolved spent nuclear fuel and then with actual spent nuclear fuel that had been dissolved in concentrated nitric acid. A second UREX process, UREX+2, consists of three solvent-extraction flowsheets and one ion-exchange process (Pereira et al., 2005). In this process, the separated groups are the same as those of UREX+. All of the UREX+2 steps were demonstrated with spent nuclear fuel that had been dissolved in nitric acid. The 24-stage 2-cm contactor used to carry out these process flowsheets is shown in a hot cell at Argonne in Figure 10.21.

10.4.2 CLEANUP AND SEGREGATION OF NUCLEAR WASTE

Besides reprocessing nuclear fuel, the contactor can also be used to clean up and segregate nuclear waste. Two plants are being built at the SRS to remove radioactive Cs from tank waste by running a solvent-extraction flowsheet designed to treat highly caustic waste (Caustic-Side Solvent Extraction or CSSX) in centrifugal contactors. One plant is small and allows for some hands-on maintenance. It was built quickly using an existing building and is being used to remove Cs from wastes that have

FIGURE 10.21   24-stage 2-cm centrifugal contactor in hot cell.

relatively low radioactivity. This plant, the Modular Caustic-Side Solvent Extraction Unit (MCU), has been running since May 2008 (Geeting, 2008). The other plant, which will be larger and take longer to build, will be able to remove Cs from tank wastes that are highly radioactive. Bonnesen et al. (2000) and Leonard et al. (2001b) describe some of the CSSX development work, formerly called the "Alkaline-Side CSEX process." The CSSX flowsheet was verified experimentally at Argonne using a simulated waste feed (Leonard et al., 2003). In the final test, a 33-stage 2-cm ANL contactor was run continuously for four days. The test was repeated at the SRS using actual tank waste in its 2-cm ANL contactor (Campbell et al., 2001; Walker et al., 2005). Based on the success of these tests, work was started on the two CSSX plants at the SRS: the MCU, which is running, and the larger plant the salt waste processing facility, which is being built.

Horwitz et al. (1985) proposed a process for cleanup and segregation of nuclear waste. In this process, called TRUEX, the aqueous waste from the extraction section of the PUREX process, the acidic aqueous raffinate, is processed to remove trace amounts of transuranic elements, mainly Am and Pu. The TRUEX process was first demonstrated at Argonne using a 10-stage batch countercurrent test (Vandegrift et al., 1984). Following the success of this test, a continuous countercurrent test of the TRUEX process was successfully run in a 14-stage 4-cm annular centrifugal contactor (Leonard et al., 1985). Although proven at the laboratory scale, this process has not been demonstrated in plant-scale contactors. However, based on the results in smaller contactors, plant-scale operation of the TRUEX process should work well and is widely accepted in many countries as standard technology.

10.4.3 OTHER CENTRIFUGAL CONTACTORS

While this chapter and this applications section has focused on ANL and CINC contactors, other centrifugal contactors have been used to process nuclear materials. Some of these contactors and the flowsheets tested using them are discussed here.

10.4.3.1 France

Since 1974, France has focused on using nuclear power as its primary source of electrical power. As of 2004, nuclear power accounted for 79% of the electricity generated in France. To support this industry, centrifugal contactors have been developed and used to process nuclear materials. An article in this area by workers at the French Atomic Energy Commission (Commissariat à l'Énergie Atomique or CEA) (Bergeonneau et al., 1979) describes a centrifugal contactor (referred to in this article as an ECP type) where the inner cylinder of the annular mixing zone is stationary and the outer cylinder rotates. In this unit, both the light and heavy phases enter at the top of the unit and flow down the stationary center core. This design seems to be the precursor to the Rousselet-Robatel (www.rousselet-robatel.com) multistage centrifugal contactor, which has two to ten contactor stages on a single vertical shaft (Hafez, 1983). This same reference also shows a monostage centrifugal contactor much like the SRL unit. Instead of a paddle mixer below the rotor, the Rousselet-Robatel contactor has a turbine mixer. The mixing zone below the rotor includes a shroud attached to the rotor. The shroud looks like a smaller rotor with a smaller

diameter and shorter length. If the feeds had been introduced on the outside of the shroud, the unit would have provided less intense annular mixing than that obtained when the outer wall of the main contactor rotor is used. In fact, the feed is introduced below the shroud, and a turbine mixer that extends down from the shroud provides the mixing. As this mixer can be replaced, various turbine-mixer designs can be used. This flexibility should allow for good control of the two-phase mixing required just before the dispersion enters the separating zone inside the contactor rotor. A paper by Rivalier et al. (2004) proposed that the shroud be used as an annular mixing zone with the shroud diameter being less than the rotor diameter. In this way, the two immiscible liquids are subjected to low mixing forces while maintaining good separation through the high gravitational forces in the separating zone of the rotor.

The monostage centrifugal contactor shown on the Rousselet-Robatel web site (www.rousselet-robatel.com) has the upper weir for the light phase and the LW for the heavy phase. Rousselet-Robatel can build contactor rotors either way depending on the need. The contactor rotor is trapped in the contactor housing, both of which are made of stainless steel. However, the contactor motor can be removed easily if it needs to be replaced. The size of the Rousselet-Robatel contactors ranges from 4 to 80 cm with nominal throughputs ranging from 50 to 80,000 L/h (0.83–1330 L/min). As the diameter of the contactor rotor increases, the rotor speed drops from 3600 rpm to 870 rpm. Rousselet-Robatel also makes a line of Teflon-type (PVDF) contactors with rotor diameters from 4 to 62 cm and nominal throughputs ranging from 50 to 60,000 L/h (0.83–1000 L/min). Four stages of a 36-cm contactor made of PVDF by Rousselet-Robatel are shown in Figure 10.22.

Recently, Rousselet-Robatel added a line of centrifugal contactors with annular mixing zones. The laboratory monostage centrifugal contactors have diameters of 1.2 and 2.5 cm. Their nominal throughputs are 2 and 10 L/h (0.033 and 0.167 L/min), respectively. Figure 10.23 shows the 1.2-cm contactor being assembled using remote manipulators. Rivalier and Lanoe (2000) have described a 1.2-cm centrifugal contactor that can be used as a single-stage unit or be mounted in a rack to provide compact multistage operation. As each stage has its own block, different interstage

FIGURE 10.22 Four-stage 36-cm centrifugal contactor made of PVDF by Rousselet-Robatel. (Photograph was supplied by Rousselet-Robatel and is reprinted with permission.)

FIGURE 10.23   1.2-cm Annular centrifugal contactor by Rousselet-Robatel being assembled using remote manipulators. (Photograph was supplied by Rousselet-Robatel and is reprinted with permission.)

blocks can be added to provide intermediate inlet and outlet ports. The individual blocks touch the adjacent blocks so that there is a seal between the blocks. This seal allows the interstage flows to go directly from one block to the next with no external interstage lines. The annular centrifugal contactor by Rousselet-Robatel is now also available with rotor diameters of 4 and 13 cm. A 19-cm annular centrifugal contactor is being developed.

The CEA has sponsored the ATALANTE conferences to provide an international forum for presentation and discussion of the advances for future fuel cycles and waste management that are needed for sustainable development of nuclear energy. Abstracts of the papers from the Avignon (2000) and Nimes (2004) conferences are available on the web at www-atalante2004.cea.fr. They demonstrate that centrifugal contactors are being used for flowsheets covering various nuclear processes.

10.4.3.2   Japan

As Japan has few natural resources, it has embraced the peaceful use of nuclear technology to provide a substantial portion of its electricity. Today, nuclear energy accounts for about 30% of its total electricity production with five operating reactors.

Recent contactor work has focused on developing an 8.4-cm annular centrifugal contactor operating at 3500 rpm to give a nominal throughput of 6.7 L/min (400 L/h) for a future reprocessing plant using PUREX (Washiya et al., 2000, 2005). The motor/rotor is connected through magnetic couplings. Initial tests were done with two-stage units. However, the contactors are available in blocks (two contactor stages side by side) of four and eight stages as well. In tests using a uranium-bearing feed, stage efficiency was 95–98% in the extraction section and 85–90% in the strip section. The ability to perform maintenance remotely is also being tested. Internal reflux of the aqueous phase at a stage is being considered to increase stage efficiency for the solvent wash step. The effect on contactor performance of a single dead stage was evaluated in a bank of 16 stages. Special lines have been added between stages so that a single dead stage will not shut down the whole process until the stage is fixed. Takeuchi et al. (2005) extended this work to evaluate the effect of process temperatures from 28 to 55°C in the 12-stage strip section. A stainless-steel block containing four contactor stages is shown in Figure 10.24. Note how there are no external
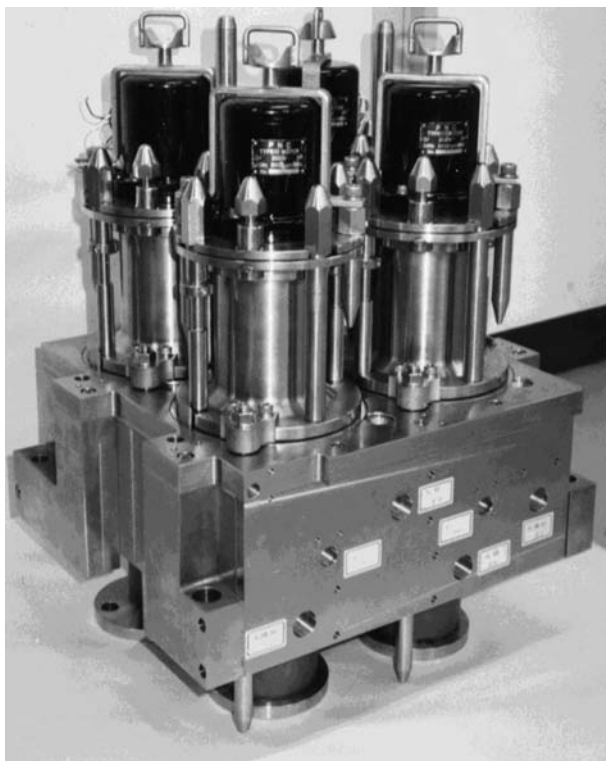
FIGURE 10.24 Four-stage 8.4-cm centrifugal contactor made by the Japan Atomic Energy Agency (JAEA). (Photograph is reprinted from Takeuchi, M., T. Washiya, H. Nakabayashi, et al. Engineering Test of Stripping Performance by Multi-Centrifugal Contactor System for Spent Nuclear Fuel Reprocessing. 13th International Conference on Nuclear Engineering, May 16–20, 2005, Beijing, China. With permission of ASME.)

interstage lines, as the interstage lines are drilled into the block itself. In these tests, the stage efficiency in the strip section was higher, 97–98%. Okamura et al. (2007) tested ball bearings and magnetic bearings to determine which bearing was the most reliable. Both bearings did well. Further testing is planned to determine the best bearing based on cost and lifetime.

10.4.3.3 Russia

The centrifugal contactors developed in Russia follow the design of the SRL contactor in that mixing of the two phases occurs under the rotor rather than in the annular region. Kuznetsov et al. (1996) report three contactor designs (defined here as ETs, ETsR, and ETsT), which have rotor diameters ranging from 3.3 to 40 cm, 2–16 cm, and 10–32 cm, respectively. The materials of construction can be stainless steel, titanium, zirconium, or a fluorocarbon-type polymer. The ETs contactors have sloped internal trays inside the separating zone of the rotor that shorten the settling distance for the coalescing dispersion and, therefore decrease the time to break. Kuznetsov et al. (1996) report that this design increases throughput by 2 to 2.5 times while giving stage efficiencies of 95%.

The ETsR and ETsT contactors have no sloped internal trays inside the rotor. The ETsR contactors, which are designed for remote servicing, have rotors that are a vertical right cylinder for the top 25–35% of the rotor length. Below the right cylinder, the outer walls of the rotor slope inward to form a cone that is truncated before it comes to a point. The paddle mixer is attached in the region where the conic section is truncated. It appears that the bottom of the conic section and the paddle mixer can be removed and exchanged for another paddle mixer design. The LW of the rotor appears to be a tube or tubes whose length from the wall of the rotor can be adjusted to control the position of the dispersion band in the separating zone. The ETsT contactors are designed for continuous removal of solids with the heavy phase. The concentration of the solids can be up to 5 g/L. The rotor body is tapered in from the top to the bottom so that the solids settling out in the separating zone will be carried upward to the more-dense-phase exit. The exiting channels for the more-dense phase appear to be small so that the solids can be entrained easily in the exiting liquid. The ETsT contactor sketch shows that contactor rotor bearings are below the motor bearings. Between the two sets of bearings is a disk that probably isolates the vibrations in the motor from the vibrations in the contactor rotor. A guide pin is used when the motor/rotor assembly is lowered into the contactor housing. Power requirements are given for each contactor model for all three designs. These Russian contactors appear to have been used in a wide range of solvent-extraction applications since they were developed in the early 1970s.

The 3.3-cm Russian contactors were used to test a cobalt-dicarbollide-based solvent-extraction process for separating Cs, Sr, and the actinides from dissolved HLW (Law et al., 2001, Herbst et al., 2002). These contactors were designed and fabricated in Moscow, Russia, by the Research and Development Institute of Construction Technology (NIKIMT). They are operated at 2700 rpm and have a nominal throughput of 417 mL/min (25 L/h). Figure 10.25 shows the 26-stage 3.3-cm contactor bank used in these tests. A recent summary of this work is given by Romanovskiy et al. (2005).

FIGURE 10.25 Twenty-six-stage 3.3-cm centrifugal contactor made of stainless steel by NIKIMT. (Photograph supplied by Jack Law and reprinted with the permission of Idaho National Laboratory (INL).)

10.4.3.4 China

The centrifugal contactors developed in China follow the design of the ANL contactor in that mixing of the two phases takes place in the annular region. In addition, a more-dense-phase weir with a fixed diameter is used in place of the air-controlled weir of older ANL contactors and the 25-cm SRL contactor (Xiangming et al., 1998). The Institute of Nuclear and new Energy Technology (INET) at Tsinghua University, Beijing, China, has fabricated annular centrifugal contactors of this design in sizes from 1.0 to 23 cm. They are made from various materials, including stainless steel, titanium, plastic, and glass-fiber reinforced plastic (GFRP). The 1.0-cm contactor, which has a stage volume of only 4 mL, has been very popular; over 200 stages have been made. It has been used in Germany (Karlsruhe Nuclear Research Center) and the UK (British Nuclear Fuel Ltd.) as well as in China. The motor bearings are separate from the contactor rotor bearings. There is a coupling between the motor and rotor. The motor/rotor assembly, which is held down only by a wing nut, can be removed easily as one piece. Duan et al. (2007) report that no screws or nuts are required to connect the motor/rotor assembly to the contactor housing. They further report that a computer located outside the hot cell controls rotor speed. The motor is covered with stainless steel to protect it from the corrosive acidic fumes. At the bottom of the mixing zone, stage liquid can be sampled automatically at the end of a flowsheet test. This feature is useful in hot cell operation. The 1.0-cm contactor is available as a one- or a four-stage block. For both the one- and four-stage blocks, additional stages can be added by pushing the blocks together. The interstage lines, which are in the block (there are no external interstage lines), are sealed between
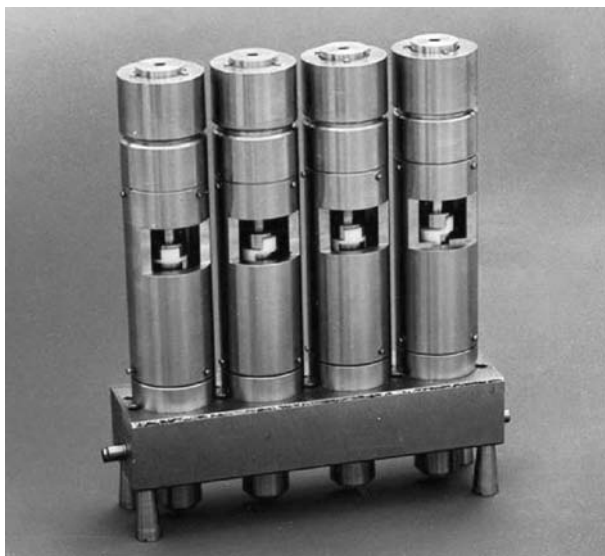
FIGURE 10.26 Photograph of a four-stage 1-cm annular centrifugal contactor. (Photograph is reprinted from Xiangming, H., *Chem. Eng. Comm. 195*(10), 1127–1239, 2008. With permission of Taylor & Francis Ltd., http://www.tandf.co.uk/journals.)

blocks using a Teflon o-ring for each interstage flow line. Fifty stages of the 1.0-cm contactor can be laid out in a space covering 24×65 cm in a hot cell (Xiangming, 2008). A four-stage block of these 1.0-cm contactors is shown in Figure 10.26.

A 7.0-cm annular centrifugal contactor has been developed in China for use at the semi-industrial scale. Duan et al. (2005) have shown how stage efficiency varies with the rotor speed, the total flow rate, and the number of stages. They also developed operating curves where the maximum total throughput is plotted against the O/A flow ratio for different diameters of the more-dense-phase weir. These operating curves can be replotted as the diameter of the more-dense-phase weir against the maximum total throughput for various O/A flow ratios to give the operating curves shown in Figures 10.13 through 10.16. The 7.0-cm contactor has a nominal throughput of 290 L/h (4.83 L/min) if made of steel and 200 L/h (3.3 L/min) if made of GFRP (Zhou et al., 2006a). The GFRP contactor is useful when the aqueous phase contains H_2SO_4 or HCl. A schematic of the GFRP contactor is shown in Figure 10.27. Note that the motor is not on top of the contactor. Instead, the motor is located at a distance from the contactor and transmits its power to the contactor rotor via a belt drive. By changing the size of the pulley on the motor and the contactor rotor, one can vary the speed of the contactor rotor.

The INET annular centrifugal contactors are being used to partition high-level liquid waste so that the back end of the nuclear fuel cycle can be simplified. In particular, the TRPO process has been developed at INET for this application (Song, 2000), where "TRPO" is the extractant in the process solvent. Also known as Cyanex 923, TRPO is a trialkyl phosphine oxide that is made commercially by Cytec Industries (formerly American Cyanamid). It has a high affinity for the actinides. Further
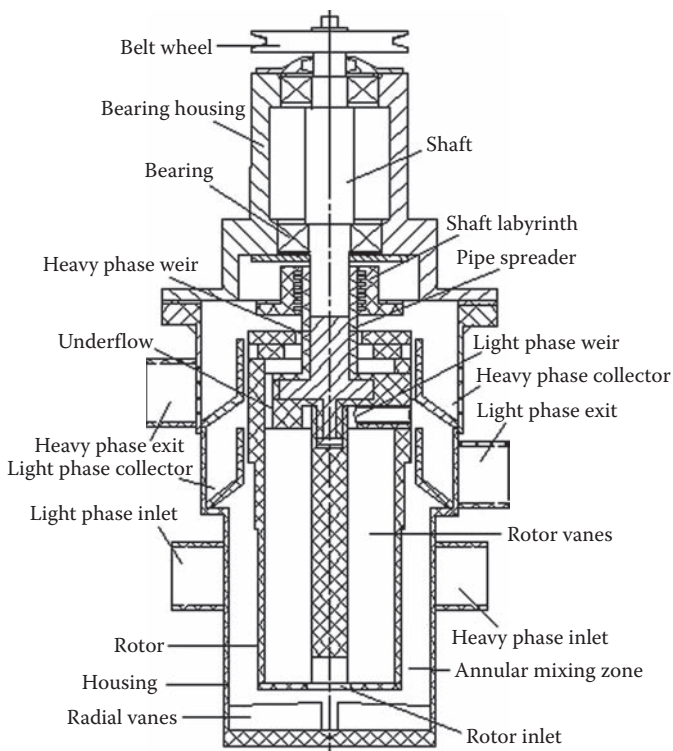
FIGURE 10.27 Schematic of a GFRP annular centrifugal contactor. (Photograph is reprinted from Zhou, J., W. Duan, and X. Zhou., *Sep. Sci. Technol. 41*(9), 1941–1952, 2006a. With permission of Taylor & Francis Ltd., http://www.tandf.co.uk/journals.)

details on the use of the 1.0- and 7.0-cm INET contactors used to develop the TRPO process are given by Duan et al. (2007).

The INET contactors have also been applied to non-nuclear processes, such as the removal of a specific rare metal (yttrium) from other rare metals (Zhou et al., 2007), hydrocortisone from fermentation liquor (Zhou et al., 2006b), phenol from wastewater (Xu et al., 2006), and caffeine from coffee beans (Duan et al., 2006). As described by Zhou et al. (2007), the contactor rotor is driven by a motor that is not above the contactor. Instead, a belt connects the motor to the top of the rotor shaft. This design is possible because these materials are not radioactive, and hands-on maintenance is thus possible.

ACKNOWLEDGMENTS

was also reviewed by Cliff Conner, Parsons Corporation, Aiken, SC, and Mark Geeting, Washington Savannah River Company, Aiken, SC. It was edited by Argonne employee Joseph E. Harmon.

REFERENCES

Arafat, H. A., M. C. Hash, A. S. Hebden, and R. A. Leonard. 2001. *Characterization and Recovery of Solvent Entrained During the Use of Centrifugal Contactors*. Argonne National Laboratory Report ANL-02/08, Argonne, IL.

Bernstein, G. J., D. E. Grosvenor, J. F. Lenc, and N. M. Levitz. 1973. A High-Capacity Annular Centrifugal Contactor. *Nucl. Technol. 20*, 200–202.

Birdwell, Jr., J. F., and K. K. Anderson. 2001. *Evaluation of 5-cm Centrifugal Contactor Hydraulic and Mass Transfer Performance for Caustic-side Solvent Extraction of Cesium.* Oak Ridge National Laboratory Report ORNL/TM-2001/137, Oak Ridge, TN.

Birdwell, Jr., J. F., K. K. Anderson, and D. E. Hobson. 2002. *Investigation of Emulsion Formation in Solvent Washing in the Caustic-side Solvent Extraction (CSSX) Process.* Oak Ridge National Laboratory Report ORNL/TM-2002/126, Oak Ridge, TN.

Bergeonneau, P., C. Jaonen, M. Germain, and A. Bathellier. 1979. Uranium, Neptunium, and Plutonium Kinetics of Extraction by Tributylphosphate and Trilaurylamine in a Centrifugal Contactor. Proceedings of International Solvent Extraction Conference (ISEC 77), September 9–16, 1977, Toronto, Canada, vol. 2, 612–619.

Bonnesen, P. V., L. H. Delmau, B. A. Moyer, and R. A. Leonard. 2000. A Robust Alkaline-Side CSEX Solvent Suitable for Removing Cesium from Savannah River High Level Waste. *Solvent Extr. Ion Exch. 18*(6), 1079–1107.

Campbell, S. G., M. W. Geeting, C. W. Kennell, et al. 2001. *Demonstration of Caustic-side Solvent Extraction with Savannah River Site High Level Waste*. Westinghouse Savannah River Company Report WSRC-TR-2001-00223, Aiken, SC.

Campbell, S. G., E. A. Brass, S. J. Brown, and M. W. Geeting. 2008. Catalog Solvent Extraction: Anticipate Process Adjustments. Proceedings of ISEC 2008 International Solvent Extraction Conference, September 15–19, Tucson, AZ, vol. 1, 739–744.

Chow, L. S. and R. A. Leonard. 1993. U.S. Patent 5,254,076, Centrifugal Pyrocontactor, October 19.

Davis, Jr., M. W. and A. S. Jennings. 1961. Equipment for processing by solvent extraction. In *Chemical Processing of Reactor Fuels*, ed., J. F. Flagg. Academic Press: New York, 271–303.

Duan, W., C. Song, Q. Wu, et al. 2005. Development and Performance of a New Annular Centrifugal Contactor for Semi-Industrial Scale. *Sep. Sci. Technol. 40*(9), 1871–1883.

Duan, W., X. Zhou, and J. Zhou. 2006. Extraction of Caffeine with Annular Centrifugal Contactors. *Solvent Extr. Ion Exch. 24*(2), 251–259.

Duan, W., J. Wang, J. Chen, et al. 2007. Development of Annular Centrifugal Contactors for TRPO Process Tests. *J. Radioanal. Nucl. Chem. 273*(1), 103–107.

Fink, S. D., M. L. Restivo, T. B. Peters, et al. 2005. *Entrainment of Solvent in Aqueous Stream from CINC V-5 Contactor.* Savannah River National Laboratory Report WSRC-TR-2005-00187, Aiken, SC.

Geeting, M. 2008. Washington Savannah River Company, Aiken, SC, personal communication, May 7.

Hafez, M. 1983. Centrifugal contactors. In *Handbook of Solvent Extraction*, eds., T. C. Lo, M. H. I. Baird, and C. Hanson. Wiley: New York, 459–474.

Herbst, R. S., J. D. Law, T. A. Todd, et al. 2002. Development and Testing of a Cobalt Dicarbollide Based Solvent Extraction Process for the Separation of Cesium and Strontium from Acidic Tank Waste. *Sep. Sci. Technol.*, *37*(8), 1807–1831.

Horwitz, E. P., D. G. Kalina, H. Diamond, et al. 1985. The TRUEX Process – A Process for the Extraction of the Transuranium Elements from Nitric Acid Wastes Utilizing Modified PUREX solvent. *Solvent Extr. Ion Exch. 3*, 75–109.

Kishbaugh, A. A. 1963. *Performance of a Multistage Centrifugal Contactor*. Savannah River Laboratory Report DP-841, Aiken, SC.

Kuznetsov, G. I., A. A. Pushkov, A. V. Kosogorov, and L. I. Shklyar. 1996. Centrifugal Extractors TSENTREK. *Russ. Chem. Industry 28*(2), 81–95.

Law, J. D., R. S. Herbst, T. A. Todd, et al. 2001. Flowsheet Testing of the Universal Solvent Extraction Process for the Simultaneous Separation of Cesium, Strontium, and the Actinides from Dissolved INEEL Calcine. Proceedings of WM-01, February 25–March 1, 2001, Tucson, AZ.

Law, J., D. Meikrantz, T. Garn, et al. 2006. The Testing of Commercially Available Engineering- and Plant-Scale Annular Centrifugal Contactors for the Processing of Spent Nuclear Fuel. 15th Pacific Basin Nuclear Conference, October 15–20, Sydney, Australia, Idaho National Laboratory Report INL/CON-06011498 PREPRINT, Idaho Falls, ID.

Lentsch, R. D., A. B. Stephens, K. E. Bartling, and S. A. Singer. 2008. Caustic-side Solvent Extraction Full-Scale Test. WM2008 Conference, February 24–28, Phoenix, AZ.

Leonard, R. A., G. J. Bernstein, A. A. Ziegler, and R. H. Pelto. 1980a. Annular Centrifugal Contactors for Solvent Extraction. *Sep. Sci. Technol. 15*, 925–943.

Leonard, R. A., R. H. Pelto, A. A. Ziegler, and G. J. Bernstein. 1980b. Flow over Circular Weirs in a Centrifugal Field. *Can. J. Chem. Eng. 58*, 531–534.

Leonard, R. A., G. J. Bernstein, R. H. Pelto, and A. A. Ziegler. 1981. Liquid-liquid Dispersion in Turbulent Couette Flow. *AIChE J. 27*, 495–503.

Leonard, R. A., A. A. Ziegler, R. A. Wigeland, et al. 1983. Operation with Three Liquid Phases in a Staged Liquid-liquid Contactor. *Sep. Sci. Technol. 18*, 1563–1579.

Leonard, R. A., G. F. Vandegrift, D. G. Kalina, et al. 1985. *The Extraction and Recovery of Plutonium and Americium from Nitric Acid Waste Solutions by the TRUEX Process—Continuing Development Studies*. Argonne National Laboratory Report ANL-85-45, Argonne, IL.

Leonard, R. A. 1988. Recent Advances in Centrifugal Contactor Design. *Sep. Sci. Technol. 23*, 1473–1487.

Leonard, R. A., M. O. Wasserman, and D. G. Wygmans. 1993. *A Vibration Model for Centrifugal Contactors*. Argonne National Laboratory Report ANL-92/40, Argonne, IL.

Leonard, R. A. and M. C. Regalbuto. 1994. A Spreadsheet Algorithm for Stagewise Solvent Extraction. *Solvent Extr. Ion Exch. 12*(5), 909–930.

Leonard, R. A. 1995. Solvent Characterization using the Dispersion Number. *Sep. Sci. Technol. 30*, 1103–1122.

Leonard, R. A., D. B. Chamberlain, and C. Conner. 1997. Centrifugal Contactors for Laboratory-scale Solvent Extraction tests. *Sep. Sci. Technol. 32*(1–4), 193–210.

Leonard, R. A. 1999. Design Rules for Solvent Extraction. *Solvent Extr. Ion Exch. 17*(3), 597–612.

Leonard, R. A., C. Conner, M. W. Liberatore, et al. 1999. *Evaluation of an Alkaline-Side Solvent Extraction Process for Cesium Removal from SRS Tank Waste Using Laboratory-Scale Centrifugal Contactors*. Argonne National Laboratory Report ANL-99/14, Argonne, IL.

Leonard, R. A., S. B. Aase, H. A. Arafat, et al. 2001a. *Development of an Improved 2-cm Centrifugal Contactor for Cesium Removal from High-Level Waste*. Argonne National Laboratory Report ANL-01/23, Argonne, IL.

Leonard, R. A., C. Conner, M. W. Liberatore, et al. 2001b. Development of a Solvent Extraction Process for Cesium Removal from SRS Tank Waste. *Sep. Sci. Technol. 36*(5&6), 743–766.

Leonard, R. A., S. B. Aase, H. A. Arafat, et al. 2002a. *Simulant Flowsheet Test with Modified Solvent for Cesium Removal Using Caustic-side Solvent Extraction*. Argonne National Laboratory Report ANL-02/22, Argonne, IL.

Leonard, R. A., M. C. Regalbuto, S. B. Aase, et al. 2002b. *Hydraulic Performance of a 5-cm Contactor for Caustic-side Solvent Extraction*. Argonne National Laboratory Report ANL-02/18, Argonne, IL.

Leonard, R. A., S. B. Aase, H. A. Arafat, et al. 2003. Experimental Verification of Caustic-side Solvent Extraction for Removal of Cesium from Tank Waste. *Solvent Extr. Ion Exch.* 21(4), 505–526.

Long, J. T. 1978. *Engineering for Nuclear Fuel Reprocessing*. American Nuclear Society: La Grange Park, IL.

Meikrantz, D. H. 1990. U.S. Patent 4,959,158, Method for Separating Disparate Components in a Fluid Stream, September 25.

Meikrantz, D., S. Meikrantz, and M. George. 1998a. Continuous Liquid-liquid Extraction Via an Improved Centrifugal Contactor. Online Chemical Engineering Information (special shared content with CINC) at www.cheresources.com/centcontactor.pdf.

Meikrantz, D. H., L. L. Macaluso, H. W. Sams, III, et al. 1998b. U.S. Patent 5,762,800, Centrifugal Separator, June 9.

Macaluso, L. L. 2008. Private communication. Advanced Machine Design, Carson City, NV.

Okamura, N., M. Takeuchi, and H. Ogino, et al. 2007. Development of Centrifugal Contactors with High Reliability. Global 2007, September 9–13, 2007, Boise, ID.

Pereira, C., H. A. Arafat, J. R. Falkenberg, et al. 2002. *Recovery of Entrained CSSX Solvent from Caustic Aqueous Raffinate Using Coalescers*. Argonne National Laboratory Report ANL-02/34, Argonne, IL.

Pereira, C., G. F. Vandegrift, M. C. Regalbuto, et al. 2005. Lab-Scale Demonstration of the UREX+2 Process using Spent Fuel. Proceedings of WM-05, February 27–March 3, Tucson, AZ.

Peterson, S. and R. G. Wymer 1963. *Chemistry in Nuclear Technology*. Addison-Wesley: Reading, MA.

Regalbuto, M. C., J. M. Copple, R. Leonard, et al. 2004. Solvent Extraction Process Development for Partitioning and Transmutation of Spent Fuel. 8th Information Exchange Meeting on Actinide and Fission Product Partitioning and Transmutation, November 9–11, 2004, Las Vegas, NV.

Richards, R. B. 1957. Aqueous reprocessing—an introduction. In *Symposium on the Reprocessing of Irradiated Fuels*, Book 1. U.S. Atomic Energy Commission Report No. TID-7534, Belgium, 3–21.

Rivalier, P. and J-Y. Lanoe. 2000. Development of a New Miniature Short-residence-time Annular Centrifugal Solvent Extraction Contactor for Tests of Process Flowsheets in Hot Cells. ATALANTE 2000, October 24–26, Avignon, France.

Rivalier, P., F. Gandi, and J. Duhamet. 2004. Development of a New Annular Centrifugal Solvent Extraction Contactor. ATALANTE 2004, June 21–24, Nimes, France.

Romanovskiy, V. N., I. V. Smirnov, V. A. Babain, et al. 2005. UNEX-Process, State of the Art and Outlook. Proceedings of GLOBAL 2005, Paper 353, October 9–13, Tsukuba, Japan.

Song, C. 2000. Study of Partitioning of Long Lived Nuclides from HLLW in Tsinghua University. Proceedings of the International Symposium on Energy Future in the Asia/ Pacific Region, Beijing, China, 89–99.

Stewart, D. C. 1985. *Data for Radioactive Waste Management and Nuclear Applications*. Wiley: New York.

Takeuchi, M., T. Washiya, H. Nakabayashi, et al. 2005. Engineering Test of Stripping Performance by Multi-Centrifugal Contactor System for Spent Nuclear Fuel Reprocessing. 13th International Conference on Nuclear Engineering, May 16–20, Beijing, China.

Vandegrift, G. F., R. A. Leonard, M. J. Steindler, et al. 1984. *Transuranic Deconta-mination of Nitric Acid Solutions by the TRUEX Solvent Extraction Process–Preliminary Development Studies*. Argonne National Laboratory Report ANL-84-45, Argonne, IL.

Vandegrift, G. F., M. C. Regalbuto, S. B. Aase, et al. 2004. Lab-Scale Demonstration of the UREX + Process. Proceedings of WM-04, February 29–March 4, Tucson, AZ.

Vandergriff, K. U. 1990. *Designing Equipment for Use in Gamma Radiation Environments.* Oak Ridge National Laboratory Report ORNL/TM-11175, Oak Ridge, TN.

Vedantam, S. and J. B. Joshi. 2006. Annular centrifugal contactors—A Review. *Trans IChemE, Part A, Chem. Eng. Res. Design 84*(A7), 522–542.

Walker, D. D., M. A. Norato, S. G. Campbell, et al. 2005. Cesium Removal from Savannah River Site Radioactive Waste using the Caustic-side Solvent Extraction (CSSX) Process. *Sep. Sci. Technol. 40*(1–3), 297–309.

Wardle, K. E. 2008. Computational and experimental analysis of the flow in an annular cen-trifugal contactor. PhD diss., Univ. of Wisconsin-Madison.

Wardle, K. E., T. R. Allen, and M. H. Anderson. 2008. Free Surface Flow in the Mixing Zone of an Annular Centrifugal Contactor. *AIChE J. 54*, 74–84.

Washiya, T., H. Ogino, and A. Aoshima. 2000. Development of a Centrifugal Contactor for Fast Reactor Spent Fuel Reprocessing. ATALANTE 2000, October 24–26, Avignon, France.

Washiya, T., M. Takeuchii, H. Ogino, and S. Aose. 2005. Development of Centrifugal Contactor System in JNC. Proceedings of GLOBAL 2005, October 9–13, Tsukuba, Japan.

Webster, D. S., A. S. Jennings, A. A. Kishbaugh, and H. K. Bethmann. 1969. Performance of centrifugal mixer-settler in the reprocessing of nuclear fuel. In *Recent Advances in Reprocessing of Irradiated Fuel, Nuclear Engineering–Part XX*, eds. W. A. Rodger and D. E. Ferguson. American Institute of Chemical Engineers, New York, Chem. Eng. Prog. Symp. Ser. No. 94, vol. 65, 70–77.

Xiangming, H., Y. Yushun, Z. Quanrong, and L. Binren. 1998. Recent Advances of Annular Centrifugal Extractor for Hot Test of Nuclear Waste Partitioning Process. *J. Nucl. Sci. Technol. 9*(3), 157–162.

Xiangming, H. 2008. Development of a Compact Miniature Annular Centrifugal Contactor for Hot Cell Placement. *Chem. Eng. Comm. 195*(10), 1127–1239.

Xu, J., W. Duan, X. Zhou, and J. Zhou. 2006. Extraction of Phenol in Wastewater with Annular Centrifugal Contactors. *J. Haz. Mat. B131*, 98–102.

Zhou, J., W. Duan, and X. Zhou. 2006a. Development and Performance of a Glass Fiber Reinforced Plastic Centrifugal Contactor. *Sep. Sci. Technol. 41*(9), 1941–1952.

Zhou, J., W. Duan, X. Zhou, and C. Zhang. 2006b. Extraction of Hydrocortisone from the Fermentation Liquor with Annular Centrifugal Contactors. *Sep. Sci. Technol. 41*(3), 573–581.

Zhou, J., W. Duan, X. Zhou, and C. Zhang. 2007. Application of Annular Centrifugal Contactors in the Extraction Flowsheet for Producing High Purity Yttrium. *Hydrometallurgy 85*, 154–162.

11 Neoteric Solvents as the Basis of Alternative Approaches to the Separation of Actinides and Fission Products

Mark L. Dietz
University of Wisconsin-Milwaukee

CONTENTS

11.1 INTRODUCTION

Despite the demonstrated effectiveness of solvent-extraction (SX) processes employing conventional organic diluents in nuclear-fuel reprocessing and

617

nuclear-waste treatment,[1,2] recently there has been growing interest in the possibilities afforded by less conventional alternatives. In large measure, this interest has been driven by the increasing appeal of processes exhibiting both high efficiency and selectivity *and* minimal environmental impact, a combination of characteristics not readily obtained with traditional extraction systems, which are frequently characterized by the use of toxic, volatile, or flammable diluents. Nash[3] and others[4] have noted that any of several "unconventional" systems, in particular aqueous biphases,[5] solid sorbents incorporating supported extractants,[6] supercritical fluids (SCFs) (particularly supercritical carbon dioxide, SC-CO_2),[7] or ionic liquids (ILs),[8] may ultimately provide a viable alternative to traditional, aqueous-based actinide (An) and fission-product (FP) separations. At present, however, the need for high salt concentrations to generate a biphase, while acceptable in analytical applications, argues against the utility of aqueous two-phase systems for many large-scale separations.[9] Similarly, despite attempts to improve the physical stability of solid-supported extractants,[10–12] their suitability for process-scale applications remains questionable. In contrast, both supercritical carbon dioxide and ILs, certain drawbacks notwithstanding, appear to offer promise as the basis for new separation schemes for Ans and FPs. In this chapter, we provide an overview of progress in the application of these two classes of so-called "neoteric"[13] solvents to the development of such schemes. The objective here is not to provide an exhaustive review of all potentially relevant IL and SCF literature, but rather to highlight those studies that have the most direct bearing on the issue of the utility of these novel solvents for large-scale An and FP separations, such as are encountered in nuclear fuel reprocessing and waste management.

11.2　SUPERCRITICAL FLUIDS (SCFs)

11.2.1　Background

The use of SCFs by far constitutes the more thoroughly explored "nontraditional" approach to An and FP separations, both in terms of the development of workable technology and an examination of the underlying chemistry. As is well known, the generation of a SCF is straightforward; one simply applies heat and pressure sufficient to exceed the critical point of the substance of interest (e.g., H_2O and CO_2). Upon reaching the supercritical state, the substance exhibits physical properties intermediate between those of its gaseous and liquid states. For example, while the viscosity of the fluid is gas-like, its density and solvating power most closely resemble those of the liquid phase. This unique combination of properties, together with the ease with which they can be "tuned" by changing the temperature or pressure applied, has led to considerable interest in the potential application of SCFs in chemical separations.[14,15] Although any of a variety of compounds (e.g., NH_3, NO_2, H_2S, CO, CO_2, and H_2O) can be employed as supercritical solvents, several practical considerations have made carbon dioxide the solvent of choice for a wide range of extractive separations. That is, unlike a number of other substances, CO_2 has a readily accessible critical temperature (31°C) and pressure (72.9 atm). In addition, it is readily available, inexpensive, nontoxic, nonflammable, and environmentally benign. Moreover, solubilized materials can be quickly and easily recovered

from it by depressurization, permitting facile recycling of the CO_2 and minimizing waste generation. Along with these many virtues, however, SC-CO_2 exhibits one significant limitation. That is, although its solvent properties can be varied over a wide range (to mimic such solvents as pentane, toluene, carbon tetrachloride, and benzene), unmodified SC-CO_2 is suitable only for the extraction of nonpolar (e.g., alkanes) and slightly polar species.[16] Metal salts, because of both the charge neutralization requirement and the weakness of solute–solvent interactions, are generally not soluble in SC-CO_2.[17] It has long been recognized, however, that solubilization of a metal ion can be effected by use of a complexing agent that is itself soluble in the SCF. Unfortunately, many common complexing agents have been found to be essentially insoluble in carbon dioxide.

11.2.2 Fluorinated Ligands as Supercritical Fluid-Soluble Complexants

In 1991, Laintz et al.[18] reported that fluorination of diethyl dithiocarbamate (DDC), a widely used chelating agent for the extraction of trace metal ions, significantly enhances its solubility and that of its metal complexes in SC-CO_2. For any of a number of metal-FDDC complexes, in fact, this solubility approaches 10^{-3} M under appropriate conditions (50°C and 100 atm), 2–3 orders of magnitude greater than that observed for the nonfluorinated analogs. In follow-up work,[19] these same investigators demonstrated the feasibility of applying FDDC for metal ion extraction into SC-CO_2, describing experimental approaches for the extraction of Cu^{2+} from both an aqueous solution and a silica surface:

$$Cu^{2+}_{aq} + 2LiFDDC_{SCF} \rightarrow CuFDDC_{2 \ SCF} + 2Li^+_{aq} \tag{11.1}$$

The following year, this "*in-situ* chelation SCF extraction" approach was extended to the extraction of lanthanides (Lns) and Ans from various solid samples for possible application to nuclear-waste management and analysis.[20] Because the LiFDDC complex employed previously for copper extraction is ineffective for the complexation of f-block elements,[21] a fluorinated ß-diketone, 2,2-dimethyl-6,6,7,7,8,8,8-heptafluoro-3,5-octanedione (FOD), was used instead. Despite the relatively high solubility (>0.05 M) of La(FOD)$_3$, and the analogous europium complex in SC-CO_2, and the known volatility of Ln-FOD complexes, extraction of La^{3+}, Eu^{3+}, and Lu^{3+} from cellulose-based filter papers was found to be poor (<12%) unless the sample matrix was prewetted and the polarity of the SC-CO_2 modified by the addition of methanol (5% v/v). Under these conditions, recoveries exceeding 90% were achieved in 10 minutes or less. The authors speculated that the addition of water leads to adduct formation with the Ln(FOD)$_3$ complexes, weakening their apparently strong interaction with the cellulose matrix. Much the same results were obtained for uranyl ion, with quantitative recovery achievable only from a wetted paper using methanol-modified CO_2. Interestingly, the working pH range for effective extraction was found to be wider in SC-CO_2 than in conventional solvents such as benzene.

In related work,[20] these same authors evaluated a fluorinated crown ether carboxylic acid, *sym*-difluorobenzo-16-crown-5 oxyacetic acid, for use in the SCF extraction of uranyl ion and lanthanides, again from a cellulose matrix. Although this compound

and its analogs had previously been shown to be effective extractants for these ions in conventional SX,[22] only a small fraction of either the trivalent lanthanides or uranyl ion were extracted into SC-CO_2, even after wetting of the matrix and the addition of methanol as a phase modifier. Thus, as was the case for lanthanide extraction by FOD, the behavior of the extractant in the SCF was found to be not entirely predictable based on observations made in conventional organic solvents.

Although these and related investigations (many of which have been the subject of prior reviews[23–25]) did demonstrate that SC-CO_2 could serve as a solvent into which An and FP ions are efficiently extracted under appropriate conditions, the results obtained also suggested that only if a chelating agent were fluorinated would it and its metal complexes be sufficiently soluble to provide the basis of a workable extraction process. Fluorinated analogs of many useful extractants are either unavailable or not readily synthesized, however. Moreover, fluorinated compounds are generally expensive, an undesirable attribute for any extractant for which large-scale application is envisioned.[26] Thus, while promising, these initial results failed to demonstrate that SCF extraction (SFE) could represent a viable approach to An and FP separations on other than an analytical scale.

A partial solution to this problem was proposed by Wai et al.[27] in a report concerning the extraction of FP strontium into SC-CO_2 by crown ethers. It is well known that strontium can be selectively extracted from acidic, nitrate-containing aqueous phases by 18-membered crown ethers with cavity diameters in the 2.6–2.8 Å range, such as dicyclohexano-18-crown-6 (DCH18C6), into various halogenated or oxygenated aliphatic solvents.[28,29] Unless the macrocycle employed is fluorinated, however, the analogous extraction process into SC-CO_2 is inefficient because of the limited solubility of the metal complexes formed in CO_2. Wai suggested that a less difficult approach to improving the extraction efficiency would be to pair a conventional extractant (e.g., DCH18C6) with fluorinated counterions, which would both facilitate formation of the requisite electrically neutral metal complex and render it more CO_2 soluble. In fact, while direct extraction of Sr^{2+} from water or nitric acid into SC-CO_2 with an excess of DCH18C6 is poor ($\leq 1\%$ extraction), the addition of pentadecafluoro-n-octanoic acid (PFOA) results in near-quantitative (ca. 98%) extraction under appropriate conditions (60°C; 100 atm pressure; 1:10:50 mole ratio of Sr^{2+}:DCH18C6:PFOA). As expected, the extraction efficiency falls off considerably as the aqueous acidity rises and the counterion becomes protonated. Unfortunately, extraction is not especially efficient under the conditions of high acidity typical of the extraction stages of a reprocessing scheme, but rather is most efficient under typical stripping conditions (i.e., at low acidity). Thus, while counterion fluorination can facilitate the extraction of strontium (and by analogy, that of other cations) by a neutral extractant into SC-CO_2, the variation in extraction efficiency with aqueous acidity follows a trend opposite to that desired.

11.2.3 Silicon-Functionalized Ligands as Supercritical Fluid-Soluble Complexants

Recent work by Dietz et al. has sought to identify approaches to increasing ligand "CO_2-philicity" not plagued by the expense and limited scope of fluorination.

Building on prior studies demonstrating that certain silicone polymers exhibit not insignificant solubility in SC-CO_2,[30,31] these investigators have examined the effect of discrete, well-defined, silicon-containing functional groups on the solubility of alkylenediphosphonic acid derivatives.[32–34] Although these compounds are well known as powerful and versatile An extractants,[35–37] they are not especially soluble in SC-CO_2.[38] In initial experiments, a series of oligo(dimethylsiloxane)-substituted tetraalkyl *gem*-diphosphonates (Figure 11.1) were prepared and their compatibility with carbon dioxide evaluated under subcritical conditions. (Data from such experiments, while obviously obtained at lower pressures than would be employed in SFE, are nonetheless indicative of the relative affinity of the various compounds for CO_2.) These measurements showed that the presence of siloxane substituents enhances the affinity of *gem*-diphosphonates for CO_2. Moreover, the enhancement was found to depend on the number of siloxane substituents (with increased substitution yielding greater enhancement) and their structure. Attempts to extend this approach to the functionalization of diphosphonic acids, however, were only partly successful. That is, once prepared, the compounds were found to exhibit signs of decomposition upon standing, clearly an undesirable property for any prospective extractant. Nonetheless, an important point was made: that the concept of improving the affinity of a ligand for CO_2 by incorporation of a simple (i.e., nonpolymeric) silicon-bearing substituent has merit.

In subsequent work, attention was directed to an alternative family of target molecules: di-[3-(trimethylsilyl)-1-propyl]-esterified alkylenediphosphonic acids (TMSP-esterified DPAs) (Figure 11.2). These compounds were chosen for consideration for several reasons. First, commercially available materials could be employed for the esterification, reducing the expense of the final product. Also, the chemistry required for the synthesis, in contrast to that needed for the preparation of methylsiloxane-substituted compounds, is straightforward. Finally, separation of the trimethylsilyl functionality from the remainder of the molecule by a propyl group was expected to provide improved chemical stability. In fact, TMSP-esterified DPAs were found to be sufficiently stable as to permit their use in conventional SX systems comprising aqueous phases containing up to 8 M HNO_3, as is
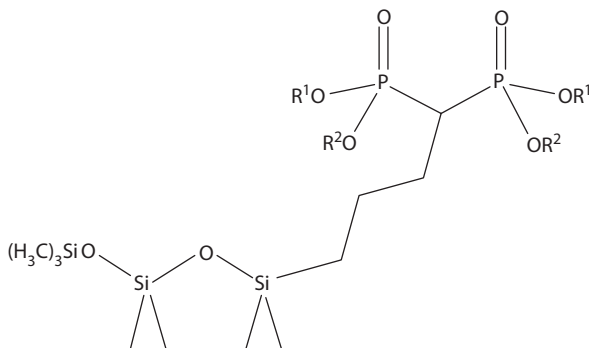
FIGURE 11.1 Representative oligo(dimethylsiloxane)-substituted tetraalkyl *gem*-diphosphonates (R^1 and R^2=methyl, ethyl, 2-ethylhexyl).
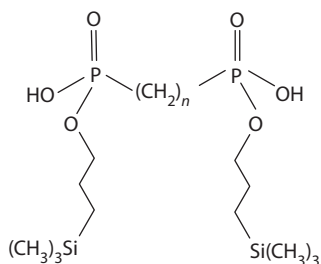
FIGURE 11.2 Representative di-[3-(trimethylsilyl)-1-propyl]-esterified alkylenediphospho-nic acids ($n=1-6$).
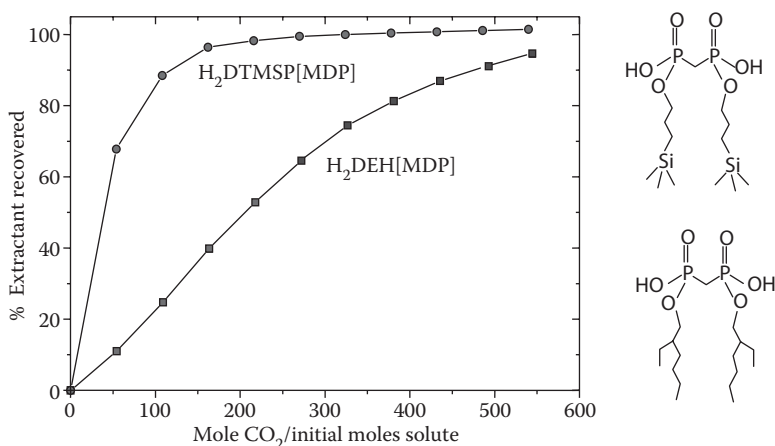
FIGURE 11.3 Percent recovery of 3-(trimethylsilyl)-1-propyl- and 2-ethylhexyl-substituted methylene diphosphonic acids from glass beads at 250 bar and 60°C.

the case for the analogous unsubstituted compounds. More importantly, as shown in Figure 11.3, which compares the results of dynamic transfer experiments for di-[3-trimethylsilyl)-1-propyl]-methylenediphosphonic acid (H_2DTMSP[MDP]) with its 2-ethylhexyl (nonsilicon bearing) analog, H_2DEH[MDP], the transfer (hence the solubility in SC-CO_2) was found to be significantly greater for the silyl ester under the experimental conditions, even after correction (by application of molecular connectivity indices) for differences in the branching pattern of the two compounds. Overall, the silicon-functionalized material is roughly a factor of 10 more soluble than would be anticipated based on branching alone. In fact, its mea-sured solubility, 0.054 M at 60°C and 200 atm pressure, is adequate for application in SC-CO_2. Clearly then, discrete, monodisperse, silicon-based functional groups can markedly improve the compatibility of alkylenediphosphonic acids with CO_2. Because this work is only in its early stages, however, it remains to be seen if silicon functionalization represents an inexpensive, "generic" alternative to fluorination for the enhancement of ligand/extractant solubility in SC-CO_2.

11.2.4 SUPERCRITICAL CO₂ SOLUBILITY OF "CONVENTIONAL" EXTRACTANTS—REVISITED

As already noted, examination of the behavior of a variety of conventional complexants suggests that only modest solubility in SC-CO_2 can be expected for typical nonfluorinated compounds. In 1993, however, Levy et al. reported that tri-*n*-butyl phosphate (TBP) can serve as a phase modifier in the SFE of polar organic analytes.[33] Because TBP (diluted in an appropriate diluent) is well known as an extractant for the removal of Ans (e.g., U and Pu) and certain FPs (e.g., lanthanides) from acidic aqueous media and because TBP had been shown to synergize the extraction of various metal ions (e.g., Th^{4+} and UO_2^{2+}) from solid and liquid matrices by fluorinated ß-diketones into SC-CO_2,[40,41] it was quickly recognized that it should be possible to extract these same metal ions into TBP-modified SC-CO_2.[42] That is, in this instance, SC-CO_2 would serve as a diluent, in analogy to a conventional organic solvent. To test this concept, the extraction of a series of lanthanides from various acidic, nitrate-containing aqueous phases was examined.[42] When initial experiments showed that none of the test elements could be extracted from 1 M HNO_3 even with 30% v/v TBP-modified SC-CO_2, an aqueous phase comprising a mixture of 6 M HNO_3 and 3 M $LiNO_3$ was adopted, as these conditions represent those for which maximum extraction is observed in conventional systems. Under these optimized conditions, near-quantitative extraction could be achieved for certain of the lanthanides (e.g., Sm^{3+}) if thenoyltrifluoroacetone (TTA), a second extractant that serves as a synergist, was added. The authors attributed the modest extraction efficiencies typically observed to the likelihood that the temperatures and pressures employed were inadequate to ensure that the system was in the supercritical state.

Later work by Lin et al. overcame this problem by bubbling SC-CO_2 through a vessel containing TBP upstream of the extraction vessel.[43] Using this approach, super-saturation of the fluid phase by the extractant was avoided and a supercritical phase containing ca. 11% (on a molar basis)[44] of TBP was consistently obtained (at 60°C and 120 atm pressure). This TBP-saturated CO_2 was then employed to extract uranyl and thorium ions from nitric acid solutions of various concentrations. The extraction of both ions increased with rising aqueous acidity, consistent with the extraction reactions observed in conventional systems (e.g., TBP-dodecane), such as that shown here for uranium:

$$UO_2^{2+}{}_{aq} + 2NO_3^-{}_{aq} + 2TBP_{org} \rightarrow UO_2(NO_3)_2(TBP)_{2org} \tag{11.2}$$
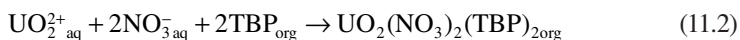
Moreover, under a particular set of conditions, the extraction efficiencies for the SC-CO_2 system were typically found to be very similar to the corresponding values in dodecane. The strong correlation between the SFE and conventional SX results for the two ions suggests that the solvation behavior of SC-CO_2 is similar to that of dodecane for the TBP system. Substitution of a stronger Lewis base, such as triphenyl- (TPPO), tributyl- (TBPO), or trioctylphosphine oxide (TOPO) for TBP, generally yielded higher extraction efficiencies for both uranium and thorium. For both TBPO and TOPO, in fact, extraction was nearly quantitative over the entire range of

acidities examined (0.1–6.0 M HNO$_3$). Synergistic systems comprising mixtures of either TBP or TPPO and TTA yielded similarly high values.

Subsequent work by some of these same investigators[45] revealed that the uranyl nitrato-TBP complex, UO$_2$(NO$_3$)$_2$·2TBP, is itself extraordinarily soluble in SC-CO$_2$ under certain conditions, thus providing a partial explanation for the relatively efficient extraction of uranium by TBP observed. In particular, UV-visible spectroscopic measurements carried out over a range of temperatures (40°C–60°C) and pressures (100–300 atm) demonstrated that concentrations comparable to those encountered in the waste streams for the PUREX process (0.13–0.47 M in the organic phase) are readily achievable. Not unexpectedly, the complex solubility was found to vary markedly with both temperature and pressure. Specifically, higher fluid densities were accompanied by greater complex solubility, with the relationship between the two parameters (except at very high pressures) being well-described by the Chrastil model:[46]

$$\log S = k \log D + C \qquad (11.3)$$

where S is the complex solubility (in g/L), D is the density of the SFC (in g/L), and k and C are constants related to the average number of solvent molecules associated with the metal complex and the enthalpy of solvation, respectively.

Since these reports, it has been shown that solubility in SC-CO$_2$ is not only a characteristic of TBP and a few trialkylphosphine oxides, but also of a variety of organophosphorus reagents, most notably *bis*(2,4,4-trimethylpentyl)phosphinic acid and its dithio- and monothio- analogs, available commercially as Cyanex 272, Cyanex 301, and Cyanex 302, respectively.[47] SFE studies of FP lanthanides from buffered (pH 3) aqueous phases employing these reagents have shown that all are effective for the extraction of the heavy lanthanide ions ($Z \geq 69$), with the sulfur-containing reagents exhibiting higher selectivity for these ions compared with Cyanex 272, whose oxygen donor atoms lend it (not unexpectedly) significant affinity for nearly all of the lanthanides.

Taken together, the results of these studies clearly demonstrate that efficient extraction of metal ions into SC-CO$_2$ (in particular, An and FP ions) need not require functionalization (in particular, fluorination) of the ligand employed. Rather, certain inexpensive, "off-the-shelf" extractants unexpectedly provide adequate metal complex solubilization and satisfactory extraction efficiency. This strongly suggests that large-scale SFC-based schemes for An and FP separations might indeed be practical.

11.2.5 SUPERCRITICAL FLUID-BASED APPROACHES TO NUCLEAR FUEL REPROCESSING

In fact, the first description of such a scheme, involving the application of SFE to spent nuclear fuel reprocessing, appeared shortly after publication of these results. Specifically, Smart et al.[48] outlined two possible approaches to SC-CO$_2$-based reprocessing. In the first, dubbed the "wet SF-PUREX process," SC-CO$_2$ merely serves as a replacement for the organic solvent (i.e., a normal paraffinic hydrocarbon) used in
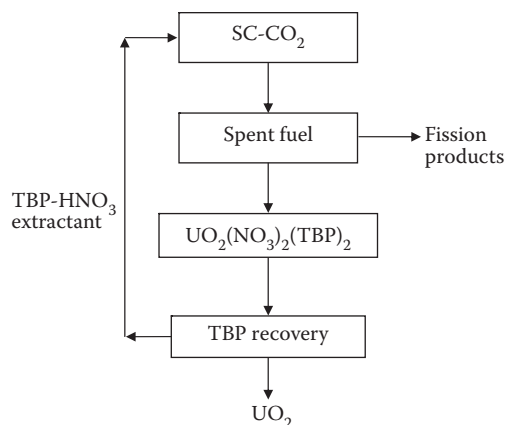
FIGURE 11.4 A "dry" process for the reprocessing of spent nuclear fuel using SC-CO$_2$.

the conventional PUREX process. Such an arrangement has several potential advantages over its conventional analog, among them faster mass transport, higher rates of extraction, and tunable metal ion extraction efficiency.[49] In addition, replacement by SC-CO$_2$ of the normal paraffinic hydrocarbons typically used eliminates the need for disposal of degraded organic solvent, thus, reducing secondary waste generation. Obviously, however, since nitric acid is required to dissolve the spent fuel, this process would still produce acidic, high-level aqueous waste. In the second approach, referred to as "dry SF-PUREX" (Figure 11.4), the need for an initial dissolution of the spent fuel in nitric acid would be eliminated by direct solubilization of uranium and plutonium from their respective oxides into SC-CO$_2$. That such an approach may be feasible was suggested by the results of a series of earlier studies by Wai and coworkers. These investigators had shown that UO$_2$(NO$_3$)$_2$(TBP)$_2$ has an unexpectedly high solubility in SC-CO$_2$ (ca. 0.42 M at 40°C and 200 atm).[45] In a subsequent report, they showed that UO$_3$ could be dissolved in SC-CO$_2$ by employing a synergistic combination of HTTA and TBP, forming UO$_2$(TTA)$_2$(TBP)$_2$:[50]

$$UO_{3\,S} + 2HL_{SCF} + TBP_{SCF} \rightarrow UO_2(L)_2TBP_{SCF} + H_2O \qquad (11.4)$$
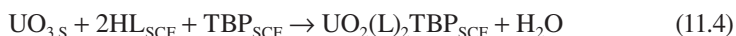
where HL is a fluorinated ß-diketone. Although this reaction was not found to be effective for the dissolution of UO$_2$, other related work showed that nitric acid itself forms a highly soluble 1:1 complex with TBP in SC-CO$_2$,[51] a complex readily prepared simply by mixing TBP with a concentrated nitric acid solution in the appropriate proportions.[49] Subsequent investigation demonstrated that this complex can oxidize UO$_2$ to the hexavalent state, leading to formation of highly soluble UO$_2$(NO$_3$)$_2$(TBP)$_2$.[52] Thus, a TBP-HNO$_3$ complex can effect the direct dissolution of UO$_2$ in supercritical carbon dioxide:

$$3UO_{2\,S} + 8TBP \cdot HNO_{3\,SCF} \rightarrow 3UO_2(NO_3)_2\,(TBP)_{2\,SCF}$$
$$+ 2TBP_{SCF} + 2NO + 4H_2O_{SCF} \qquad (11.5)$$
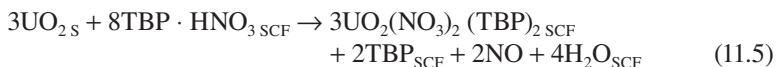
Alkali, alkaline earth, and a number of transition metals are not extracted by this complex into $SC-CO_2$.[49] Similarly, experiments examining the behavior of various FP oxides (e.g., ZrO_2, MoO_3, RuO_2, and CeO_2) under the same conditions have led to the conclusion that with the exception of Nd, decontamination factors of 400 or more (vs. uranium) can be readily obtained for all common FP elements.[53] The TBP-nitric acid adduct thus exhibits significant extraction selectivity for uranium.

One potential limitation of the "dry" process is that the rate of UO_2 dissolution is slow.[54] In an effort to remedy this, Wai et al. investigated the effect of ultrasonic irradiation on the kinetics of solubilization of UO_2 by the TBP-HNO_3 complex.[55] Prior work by this same author had established the utility of ultrasound in improving the rate of dissolution of UO_3 in $SC-CO_2$ containing a mixture of 4,4-trifluoro-1-(2-thienyl)-1,3-butanedione (HTTA) and TBP.[54] In the absence of ultrasound, only a small fraction ($< 10\%$) of the UO_3 initially present was found to dissolve, even when an hour of dynamic extraction ($T = 60°C$; $P = 150$ atm) was preceded by a static extraction step specifically designed to enhance the solubilization. The same sequence performed in the presence of ultrasound (i.e., by immersing the extraction vessel in an ultrasonic bath), however, yielded nearly 90% solubilization of the oxide, a result attributed by the authors to removal from the oxide surface of the $UO_2(TTA)_2(TBP)_2$ complex formed, thereby allowing further reaction of the oxide with TTA to take place more efficiently. The rate of dissolution of UO_2 powder by the TBP-HNO_3 complex is similarly increased upon irradiation.[55] That is, while ca. 5% (the exact percentage varying with the precise form of the TBP-HNO_3 complex employed) of the UO_2 originally present (as a coating on glass beads) was extracted in the absence of ultrasound, recoveries of 77–90% were observed under the same conditions (20 minutes of dynamic extraction) upon application of ultrasound, representing an order of magnitude increase in dissolution efficiency. The dissolution data were found to be modeled by an equation of the form:

$$E = 100(1 - e^{-\lambda t}) \tag{11.6}$$

where E is the recovery efficiency (in percent), λ is the recovery rate constant (in min^{-1}), and t is the extraction time (in minutes). From a rate-constant value, the corresponding "dissolution half-life" can be calculated, and from this, an estimate of the time required for complete dissolution made (by assuming that this will require five half-lives). From the results obtained, it appears that complete dissolution requires 30–60 minutes of contact time. Consideration of the possible steps involved in the dissolution process led the authors to conclude that the effect of ultrasound is likely the result of improved transport of the $UO_2(NO_3)_2(TBP)_2$ complex formed from the surface of the glass beads to the $SC-CO_2$ arising from the increase in interfacial contact area caused by sonication.

Since publication of this work, Japanese researchers have undertaken an effort to demonstrate the feasibility of direct dissolution of UO_2 from spent nuclear fuels by the TBP-HNO_3 complex in $SC-CO_2$.[49] Ultimately, the project is directed at the extraction of both uranium and plutonium from mixed oxide fuels and from irradiated nuclear fuel. Ideally, soluble uranyl and plutonium nitrate complexes will form and dissolve in the CO_2 phase, leaving the FPs as unwanted solids. As in the conventional

PUREX process, recovery of uranium and plutonium, in this case from the SC-CO_2 phase, would be accomplished simply by contact of the phase with water.

Although there is considerable evidence that these schemes will ultimately prove to be feasible, at this point, they remain largely conjectural. Of particular note in this context is the work of Samsonov et al.,[56] in which the solubility of a variety of An oxides (UO_2, UO_3, U_3O_8, PuO_2, NpO_2, and ThO_2), both alone and in mixtures, was determined in SC-CO_2 ($T=65°C$; $P=250$ atm) containing the TBP-HNO_3 complex. In all cases, uranium was found to be extracted quantitatively via the expected route: oxidation to the hexavalent state and formation of the highly soluble $UO_2(NO_3)_2(TBP)_2$ complex in the SC-CO_2 phase. In contrast, the extraction efficiencies of Pu, Np, and Th were found to be extremely poor ($<0.1\%$), both from individual oxides and mixtures with UO_2. Curiously, no attempt was made to identify conditions suitable for the extraction of both uranium and plutonium (if indeed such conditions exist), an obvious first step in any proposed SCF-based replacement for the PUREX process. It is worth noting, too, that although the schemes described generally represent an opportunity for waste-stream reduction, none constitutes an entirely "green" approach to spent-fuel reprocessing. Even the proposed "dry SF-PUREX process," for example, will result in the generation of a large volume of aqueous, nitric acid-containing strip solution for uranium recovery. Design of a more environmentally benign approach to spent-fuel reprocessing will require new methods for the recovery of uranium and the concomitant recycling of the TBP extractant. If, for example, $UO_2(NO_3)_2(TBP)_2$ could be converted to UO_2 in SC-CO_2 and the TBP regenerated, the dry process would be rendered both more economically viable and environmentally acceptable. Reports indicating that metal ß-diketonates can be reduced to the metallic state in SC-CO_2,[57,58] (e.g., low-temperature reduction of copper hexafluoroacetylacetonate by hydrogen in the presence of a palladium catalyst) strongly suggests that the required conversion and extractant recycle might indeed be feasible.

11.3 IONIC LIQUIDS (ILs)

11.3.1 BACKGROUND

ILs comprise a relatively new and in many respects, remarkable class of solvents. Although described as early as 1914,[59] it is only since 1992, with the first report of air- and water-stable ILs,[60] that the potential of these compounds in chemical separations has come to be widely appreciated. Since this time, studies by a number of authors have detailed both the physicochemical properties and the tremendous range of potential applications of these materials.[61–65] Given the enormous structural diversity exhibited by ILs, it is difficult to provide a simple, yet all-encompassing definition of the term. Briefly, however, ILs typically comprise any of a wide range of bulky, (usually) asymmetric organic cations paired with any of a number of inorganic (e.g., halides, PF_6^-) or organic ($CF_3SO_3^-$) anions.[66] Stated another way, ILs can be thought of as low-melting, (usually) organic analogs of classical molten salts. The wholly ionic nature of these solvents imparts them with a number of unique properties vis-à-vis conventional molecular solvents, most notably a near-absence of vapor pressure, an ability to solubilize a wide variety of solutes, and (often) an extraordinary degree of

thermal stability, and it is properties such as these that have drawn the attention of those considering their use as solvents for An and FP separations. The appeal of ILs in this application is readily apparent. Their miniscule vapor pressure eliminates the possibility of the fugitive emissions that plague processes based on volatile organic solvents (VOCs). Similarly, the ability to solubilize a variety of solutes provides for flexibility in process design and the possibility of high solvent loadings, while the high thermal stability suggests that ILs might readily withstand the rigorous conditions associated with reprocessing applications, thereby reducing the need for solvent cleanup and thus, secondary waste generation.

Interestingly, it is the partitioning behavior of an important FP, radiostrontium, which was the subject of one of the first extraction studies performed with ILs. In 1999, Dai et al.[67] examined its partitioning behavior between water and a variety of dialkylimidazolium-based ILs containing the crown ether dicyclohexano-18-crown-6 (DCH18C6), an extractant previously demonstrated to selectively complex strontium ion.[68] For most of the ILs studied, extraordinarily high values of the strontium distribution ratio (D_{Sr}, defined as $[Sr]_{org}/[Sr]_{aq}$) were observed, exceeding 10^4 in one instance, far larger than those observed for any conventional (i.e., molecular) organic solvent under the same conditions. Not only was strontium extraction found to be efficient, but also readily tunable. That is, by varying either the substituent on the imidazolium cation or the nature of the IL anion, significant changes in the magnitude of the D_{Sr} value observed could be effected. Thus, the tunable structure of the IL was found to translate into tunable performance as an extraction solvent. Shortly after this initial, highly encouraging report, Visser et al.[69] extended the work of Dai[67] to encompass three different crown ethers (18-crown-6, DCH18C6, and di-*tert*-butylcyclohexano-18-crown-6 (DtBuCH18C6)), three different 1-alkyl-3-methylimidazolium hexafluorophosphate ILs of systematically varying hydrophobicity ($[C_n mim^+][PF_6^-]$, with $n = 4$, 6, or 8), and a variety of aqueous phases containing either mineral acids or metal salts (e.g., $Al(NO_3)_3$). In many of the systems examined, the results obtained were precisely those anticipated based on the known extraction behavior of strontium with the same crown ethers dissolved in molecular organic solvents. For example, as expected, extraction was found to be more efficient for the di-*tert*-butylcyclohexano-substituted crown ether than for DCH18C6. Similarly, under a given set of conditions, D_{Sr} was found to fall as the chain length of the 1-alkyl-3-methylimidazolium salt (*n* in $C_n mim^+$) increased, much as it does for a homologous series of conventional solvents (e.g., alcohols). In other instances, however, the results were entirely unanticipated. For example, the extraction selectivity for strontium over cesium was poor, despite known differences in the tendency of 18C6 and its derivatives to form complexes with the two ions.[68] Along these same lines, for extraction from nitric acid solution by DtBuCH18C6 into $[C_4 mim^+][PF_6^-]$, the extraction efficiency for strontium was observed to decline to a minimum at ca. 1 M HNO_3, then increase again, a behavior not observed in any conventional solvent, for which increasing D_{Sr} values normally accompany rising acid concentrations. The following year, Bartsch and coworkers[70] observed yet another peculiarity in the behavior of ILs as diluents for metal ion extraction. That is, unlike extraction into conventional organic solvents (e.g., 1-octanol), for which a change in aqueous-phase anion is typically found to yield a significant change in the efficiency of extraction of a variety of cations by crown ethers, a change in

anion was found to have no appreciable impact on alkali metal ion partitioning into $[C_8mim^+][PF_6^-]$. It is the subsequent investigation of these peculiarities that has led to important insights into metal ion partitioning into ILs and to an indication of their viability as "drop-in" replacements for conventional solvents (i.e., VOCs) in SX processes for the recovery of Ans and FPs.

11.3.2 Fundamental Aspects of Metal Ion Partitioning into Ionic Liquids

In 2001, for example, Dietz and Dzielawa[71] carried out a systematic comparison of the extraction of strontium ion by DCH18C6 into several $[C_nmim^+][Tf_2N^-]$ ILs (where $Tf_2N^- = bis$[(trifluoromethyl)sulfonyl]imide) with that seen for an analogous series of n-alcohols. Unexpectedly, extraction into the ILs was found to differ in several important respects, among them the relationship of extraction efficiency to organic-phase water content, the effect of increasing aqueous-phase nitric acid concentration on the efficiency of strontium extraction, the influence of aqueous-phase anion (e.g., Cl^- vs. NO_3^-) on extraction efficiency, and the effect of extractant loading on the aqueous solubility of the organic phase. Of particular note among these was the difference in the shape of the nitric acid dependency of D_{Sr}, which declined with rising acidity for the ILs, while increasing for the alcohols over the same range. Taken together, these results clearly indicated that the process by which strontium is extracted into an IL cannot be the same as that observed in a conventional solvent, for which partitioning of a neutral strontium nitrato crown ether complex is observed:

$$Sr^{2+} + 2NO_3^- + DCH18C6_{org} \rightleftharpoons Sr(NO_3)_2 \cdot DCH18C6_{org} \qquad (11.7)$$
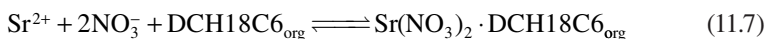
(Here the "org" subscript designates an organic phase species, while the absence of a subscript corresponds to a species present in the aqueous phase.) Rather, the data are consistent with an ion-exchange process by which a 1:1 strontium-crown ether complex is exchanged for the cationic constituent of the IL:

$$Sr(DCH18C6)^{2+} + 2[C_nmim^+] [Tf_2N^-] \rightleftharpoons$$
$$[Sr(DCH18C6)^{2+}] [Tf_2N^-]_2 + 2C_nmim^+ \qquad (11.8)$$
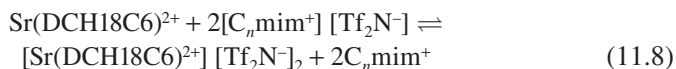
Subsequent work by the same authors,[72] who employed EXAFS and ion chromatography to determine the structure of the extracted species in a representative n-alcohol and IL, revealed that while a neutral complex bearing two axial nitrate anions is extracted into 1-octanol, a cationic 1:1 strontium-DCH18C6 complex in which the axial positions are occupied by water molecules is the predominant partitioning species in $[C_5mim^+][Tf_2N^-]$. Therefore, it is apparent that the difference in the mode of strontium ion partitioning in the two systems has as its origin the differing nature of the extracted species in the two solvents, with the ionic medium favoring the partitioning of a charged species.

Follow-up work by a number of other authors concerning the extraction of various Ans and FPs by crown ethers, calixarenes,[73,74] aza-crown ethers,[75] and organophosphorus

reagents[76] has, almost without exception, found that the use of a neutral extractant in combination with a dialkylimidazolium IL leads to cation exchange as the predominant mode of metal ion distribution. In addition, in those instances in which information has been obtained regarding the extracted species, its form in the IL has been found to differ from that seen in the conventional organic solvent. The extraction of uranyl ion from acidic nitrate media into a "TRUEX-like" diluent comprising CMPO in a TBP-modified IL (i.e., $[C_4mim^+][PF_6^-]$ or $[C_8mim^+][Tf_2N^-]$), for example, has been shown to involve partitioning of the cationic complex $UO_2(NO_3)(CMPO)^+$,[76] while a neutral $UO_2(NO_3)_2(CMPO)_2$ complex is extracted into conventional, dodecane-based TRUEX solvent.[76] It has been noted that the solvation of ionic species should be more favorable in an IL than in a conventional diluent.[67] Thus, it is not surprising that cationic complexes are often found to predominate in IL systems.

It can be argued that the apparent prevalence in the ILs of extracted complexes not observed in ordinary solvents opens up the possibility of novel, potentially more efficient and selective extraction processes. Although in principle this is true, in actual practice, the partitioning of charged complexes leads to several problems that complicate the design of workable extraction systems. First, the ion-exchange processes that are responsible for metal ion partitioning into an IL in these systems inevitably lead to contamination of the aqueous phase with one of the constituents of the IL, a problem both from the perspective of process economics and "greenness." In addition, the nature of the dependency of D_M upon nitric acid (i.e., nitrate) concentration in these systems is such as to favor extraction at low acidity, the conditions ordinarily employed for the stripping of extracted metal ions from a loaded process solvent. This can make necessary the use of complexing agents for the recovery of extracted metal ions (e.g., EDTA or citric acid, which have been used by Nakashima et al.[77] to remove extracted lanthanides from CMPO in $[C_4mim^+][PF_6^-]$) or even render stripping difficult or impractical. Finally, it has recently been reported that in certain systems, the extraction of both neutral and charged complexes can occur, their relative importance determined by process conditions.[78] The result in this case can be a rather complex dependency of D_M on aqueous-phase composition. In the extraction of uranyl ion into $[C_5mim^+][Tf_2N^-]$ by TBP, for example, rising nitric acid concentration is initially accompanied by falling D_U values until ca. 1 M HNO_3 is reached. At higher acidities, D_U increases with increasing aqueous acidity. The result is (interestingly) a U-shaped (i.e., parabolic) acid dependency for which uranium extraction is equally efficient at both high and low acidities and stripping is possible only over a narrow range of nitric acid concentrations.[79] Clearly, the design of a workable uranium extraction process employing such a system would not be straightforward. (It is interesting to note that such a complex dependency is not observed for TBP in the analogous PF_6^- IL.[80] The use of hexafluorophosphate-based ILs, however, is widely regarded as impractical, given the tendency of the anion to degrade to form hydrofluoric acid.[81])

11.3.3   Overcoming the Limitations of ILs as Extraction Solvents

It is apparent that the problems associated with the direct substitution of ILs for conventional organic diluents in extraction processes involving neutral extractants

are not insignificant. There exists, however, considerable incentive to overcome them. That is, aside from the general characteristics of ILs that make them seemingly well-suited to application as extraction solvents (noted above), ILs exhibit several additional properties that make them good candidates for use in An and FP separations. For example, initial investigations by several authors have shown that 1,3-dialkylimidazolium salts are comparatively radiation resistant, and thus experience little degradation even after exposure to high doses of α, β, and γ radiation.[82,83] Seddon and coworkers,[82] for example, have reported that less than 1% of the chloride and nitrate forms of these ILs decomposed after being subjected to a 400 kGy radiation dose. Such results indicate that the stability of these ILs is comparable to that of an aromatic molecule such as benzene, a not unexpected observation given the presence of an aromatic imidazolium ring in the IL. Most notable is that this stability far exceeds that of, for example, the TBP/kerosene mixtures that constitute the basis of the PUREX process. In addition, ILs are (in certain important respects) safer solvents for the processing of nuclear materials than are conventional solvents, including water. Their extraordinarily low vapor pressure (and resultant nonvolatility) has already been noted. Many ILs are also nonflammable and combustion resistant. Finally, the likelihood of a criticality accident in an IL is less than in an aqueous solution, a result of the lower hydrogen to nonhydrogen atom ratio of the IL and the accompanying lesser ability of the IL to moderate neutrons, thus lowering the probability of fission and raising the system's critical mass. It has been reported, for example, that plutonium has an infinite critical mass (meaning that no criticality accidents can occur as the solution volume is increased) at concentrations in $[C_2mim^+][BF_4^-]$ of ≤ 1000 g/L, two orders of magnitude higher than the corresponding value in water.[84]

Given all of this, it is not surprising that much effort has recently been directed at overcoming the limitations of ILs as solvents for An and FP separations employing neutral extractants. In particular, attempts have been made to reduce or eliminate loss of the IL cation or anion to the aqueous phase (i.e., to suppress ion-exchange processes) and to identify conditions under which the partitioning process associated with metal ion extraction into an IL is the same as that observed in systems employing conventional organic diluents. Progress (albeit modest) has, in fact, been made toward addressing both of these challenges.

It is evident from Equation 11.8 that the ion-exchange process by which the IL cation is lost to the aqueous phase should be increasingly disfavored as the hydrophobicity of the cation (as reflected in the value of n in C_nmim^+) increases. Work by the author[78,85] in which the extraction of strontium ion and the co-extraction of nitrate anion into a series of $[C_nmim^+][Tf_2N^-]$ ILs containing DCH18C6 was evaluated as a function of n showed that for the C_5-IL, the amount of coextracted nitrate is far less than the amount of strontium ion transferred, and is thus insufficient to produce a neutral strontium-crown ether-nitrato complex, an observation consistent with ion exchange as the dominant mode of partitioning. Increasing n, however, is accompanied by increasingly significant nitrate coextraction, as would be expected for a shift from ion exchange to neutral complex extraction. Also consistent with such a shift is a change in the slope of the nitric acid dependency of D_{Sr} with increasing n, from decreasing D_{Sr} with rising $[HNO_3]$ (for $n=5$) to increasing D_{Sr} with rising acidity

(for $n=10$).[78] In the latter case, in fact, the acid dependency strongly resembles that observed for *n*-alcohols, for which extraction of a neutral strontium-nitrate crown-ether complex is well-established.[71]

Fluorination of the alkyl side chains of the IL cation has also been suggested as a means of increasing its hydrophobicity, thereby favoring extraction of the neutral strontium-nitrato crown-ether complex (Equation 11.7). Accordingly, partially fluorinated analogs of C_{5-}, C_{8-}, and $[C_{10}mim^+][Tf_2N^-]$ have also been evaluated as solvents for the extraction of radiostrontium from acidic nitrate media.[86] Unexpectedly, these solvents are no more effective at suppressing ion exchange than is simply lengthening the alkyl chain. Moreover, D_{Sr} values are often significantly less than those observed in the nonfluorinated ILs under the same conditions. The diminution of ion exchange in these systems thus comes at the price of reduced extraction efficiency.[86] Nonetheless, taken together with the results of studies of increasing IL cation chain length, these results suggest that the problem of IL loss to the aqueous phase (i.e., ion exchange) can readily be overcome. More recent results, however, indicate that this may not always be the case.

In experiments designed to explore the generality of observations made for strontium ion,[71] the partitioning of a representative monovalent ion, Na^+, was studied under the same conditions.[87] The results obtained revealed the presence of a previously unidentified pathway for cation partitioning into an IL. More to the point, they showed that simply increasing the IL cation hydrophobicity is not always adequate to rule out the possibility of an ion-exchange process. The presence of this alternative path for extraction was indicated by the absence of an effect of IL cation hydrophobicity on the shape of the nitric acid dependency of D_{Na}. That is, for *both* $[C_5mim^+]$ $[Tf_2N^-]$ and its C_{10}-analog, D_{Na} was found to decline with increasing nitric acid concentration. In fact, at high acidity, the dependencies were virtually superimposable, indicating that precisely the same process is taking place in the two solvents. When infrared spectroscopy revealed the presence of a $DCH18C6-H_3O^+$ adduct in the IL phases, it became evident that this process comprises a second form of ion exchange in which sodium ion is exchanged for the crown-complexed acid:

$$Na^+ + DCH18C6-H_3O^+_{org} \rightleftharpoons H_3O^+ + Na-DCH18C6^+_{org} \qquad (11.9)$$
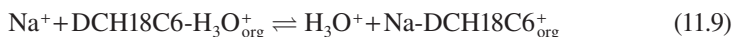
Such a reaction would obviously not be influenced by IL cation chain length, but rather by the propensity of the crown ether to form a hydronium ion adduct. Clearly, too, this process does not result in the *direct* loss of the IL cation to the aqueous phase. The preconditioning process (i.e., contact of the IL phase with nitric acid solution prior to attempts to extract sodium ion) leading to the formation of the crown ether-hydronium ion adduct, however, results in the dissolution of the IL phase:

$$H_3O^+ + DCH18C6_{org} + C_nmim^+Tf_2N^-_{org} \rightleftharpoons$$
$$DCH18C6-H_3O^+Tf_2N^-_{org} + C_nmim^+ \qquad (11.10)$$
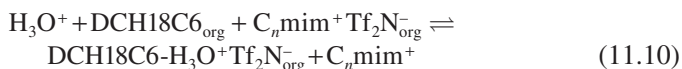
Thus, the "extractant-mediated" ion-exchange process (Equation 11.9) can result in substantial *indirect* solubilization losses of the IL cation. In fact, at sufficiently

high acid concentrations, increasing concentrations of the crown ether in the IL phase are accompanied by a corresponding increase in the dissolution of the IL in the aqueous phase. Were this behavior confined solely to DCH18C6 and related crown ethers, it would not be especially troubling. Recent work by the author in which the effect on IL solubilization of the presence of various neutral organophosphorus reagents (e.g., TBP, tributylphosphine oxide), however, indicates that extractant protonation and the increased IL cation solubility in the aqueous phase that accompanies it, may represent a general characteristic of IL-neutral extractant combinations.[88] Of course, the adverse impact of this process, like that of the direct exchange of a metal-extractant complex for the cationic constituent of the IL (Equation 11.8), can be reduced (although not completely eliminated, it appears) by the use of ILs incorporating relatively hydrophobic ($n \geq 10$ in $C_n mim^+$) cations. Attention to extractant basicity (with weakly basic extractants being less prone to protonation and exchange) and, in the case of DCH18C6, stereochemistry[89] (with *trans-* forms of the crown ether less subject to these same problems) has also been demonstrated to be of value in diminishing its effect.

Luo et al.[90] have described yet another approach to reducing the impact of ion exchange in metal ion extraction by neutral extractants in ILs, one which relies on modifying neither the structure of the IL nor the properties of the extractant. Instead, a "sacrificial" species that transfers in preference to the IL cation upon metal ion extraction (thereby reducing loss of the IL) is added to the IL phase. Ideally, the sacrificial species should exhibit no affinity for the extractant (in order not to interfere with extraction of the metal ion of interest) and be more hydrophilic than the IL cation (in order to favor its loss to the aqueous phase upon metal ion transfer). Tests with sodium tetraphenylborate indicate that its addition to a solution of a calix-crown ether in $[C_4 mim^+][Tf_2 N^-]$ reduces the loss of the IL induced by cesium extraction by nearly one-quarter with no adverse effect on the efficiency of cesium extraction.

11.3.4 ACIDIC EXTRACTANT-IL SYSTEMS

It is reasonable to conclude that the problems which plague IL-based An and FP extraction systems employing neutral extractants could be avoided simply by focusing instead on the use of acidic extractants. For these, a neutral (and thus extractable) species can be formed without the need for coextraction of a matrix anion (e.g., nitrate). That is, the extractant alone can both generate the requisite hydrophobic metal complex and satisfy the charge-neutralization requirement. It is interesting to note, however, that the few published reports describing the behavior of acidic extractant-IL combinations relevant to reprocessing applications indicate that they can be affected by problems similar to those seen for systems based on neutral extractants. In an examination of the extraction of lanthanides (e.g., Eu^{3+}) by the well-known extractant 2-thenoyltrifluoroacetone (HTTA) into $[C_4 mim^+][Tf_2 N^-]$, for example, Jensen et al.[91] found that *anion* exchange also represents a possible mechanism for metal ion transfer into an IL. In particular, the slopes of the extractant and acid dependencies of D_{Eu} at constant perchloric acid and HTTA concentration, respectively, are consistent with the partitioning of $Eu(tta)_4^-$, a conclusion supported by both UV-visible spectroscopy and EXAFS measurements. In addition, the absence

of measurable cation coextraction indicates that this anionic complex is exchanged for the anionic component of the IL (i.e., Tf_2N^-).

In contrast, in a subsequent study of the extraction of uranium by *bis*-(2-ethylhexyl)phosphoric acid (HDEHP) and of Ans (e.g., Am^{3+}) and lanthanides by Cyanex 272, Cocalia et al.[92] found through a combination of radiotracer partitioning measurements, UV-visible spectroscopy, and EXAFS investigations that both the general extraction behavior and metal ion coordination environment of the investigated ions are the same in either $[C_{10}mim^+][Tf_2N^-]$ or dodecane. In either solvent, for example, uranyl ion is extracted by a pair of H-bonded extractant dimers, while the extraction of Am requires three such monodeprotonated dimers. Thus, despite obvious differences in structure between dodecane and the IL, in this instance, the two diluents behave nearly identically in many respects as extraction solvents. It is important to note, however, that higher metal ion distribution ratios were observed in dodecane than in the IL. (In the case of Am extraction from dilute nitric acid, the difference was nearly a factor of 10.) Thus, the unique solvation environment of the IL does not necessarily lead to enhanced extraction efficiency. Equally important to note is the fact that this study employed a relatively hydrophobic IL, one for which prior work with strontium extraction by DCH18C6 (described above) would have suggested that similarities to the behavior of a conventional solvent are to be expected. Taken together with the results of Jensen[91], these results suggest that the mechanistic complications (i.e., ion exchange and the concomitant IL solubilization losses) arising from the use of ILs bearing relatively short alkyl side chains as diluents (e.g., C_nmim^+, with $n \le 8$) are not confined to systems employing neutral extractants.

11.3.5 TASK-SPECIFIC IONIC LIQUIDS (TSILS)

In contrast to conventional SX systems, in which the solvent (diluent) and extractant constitute distinct entities, ILs offer the possibility of incorporating an extracting moiety into either the cationic or anionic component of the solvent. Since the first description of such "task-specific" ILs (TSILs) by Davis et al.[93] in 2001, a number of examples of this unique class of solvents have been prepared and characterized,[94,95] among them several TSILs capable of the extraction of Ans.[96–98] Davis, for example, has described the synthesis of a phosphonamide IL in which a phosphine oxide group (such as that seen in CMPO) is appended to the imidazolium cation. Although the extraction of tri-, tetra-, and hexavalent Ans using the hexafluorophosphate form of the TSIL is very efficient, it has also been found to be both nonselective and pH independent,[96] clearly problematic from the perspective of the design of a workable extraction process. Subsequent work by Ouadi et al.[97] also employed an imidazolium substructure onto which was grafted an extracting moiety, in this case, a 2-hydroxybenzylamine functionality. Evaluation of the resultant TSIL as an extractant for americium, either neat or as a solution in $C_4mim^+Tf_2N^-$, showed that maximum extraction is achieved at a pH of ca. 10. At lower pH values, the TSIL is mainly in its LH_3^+ (acidic) form, while at higher pH, the solubility of the TSIL in the aqueous phase becomes significant. In both cases, the result is reduced extraction efficiency. Thus, the TSIL is not suitable for the extraction of Am (and by analogy other Ans)

from acidic media, as would be required in nuclear-fuel reprocessing applications. In addition, given that the metal ion partitioning data are consistent with an ion-exchange process in which an anionic Am complex is exchanged for the anionic constituent of the IL, it is evident that this system will be plagued by the same sort of solubilization losses encountered with more "conventional" ILs.

An additional potential limitation of TSILs has become apparent as the result of recent investigations of the uranium extraction behavior of a novel class of ILs comprising a quaternary ammonium cation bearing phosphoryl groups.[98] That is, in two of the three systems examined, a simple mixture of TBP in a conventional IL was found to yield significantly better results (in terms of uranium extraction efficiency) than those obtained using the analogous TSIL. Thus, the effort required to functionalize the IL cation (or anion) with an extracting moiety may often not be worthwhile. It seems reasonable to conclude from the few results available to date that TSILs, while seemingly offering much promise, remain unproven with respect to their applicability in the design of novel An and FP separation processes. Much work, in fact, remains to be done to establish the relationship between TSIL structure and extraction performance and to evaluate the practical utility of these unique solvents in large-scale separation applications.

11.4   CONCLUSIONS

It is apparent from the foregoing discussion that both ILs and supercritical carbon dioxide do indeed offer promise as alternative solvents in the reprocessing of spent nuclear fuel and the treatment of nuclear wastes. It is equally apparent, however, that considerable additional work lies ahead before this promise can be fully realized. Of particular importance in this context is the need for an improved understanding of the fundamental aspects of metal ion transfer into ILs, for a thorough evaluation of the desirability of extractant functionalization of ILs, and for the development of new methods for both the recovery of extracted ions (e.g., uranium) and the recycling of extractants in supercritical CO_2-based systems. Only after such issues have been addressed might these unique solvents reasonably be expected to provide the basis of improved approaches to An or FP separations.

REFERENCES

1. Horwitz, E. P.; Schulz, W. W. Solvent extraction in the treatment of acidic high-level liquid waste: Where do we stand? In *Metal Ion Separation and Preconcentration: Progress and Opportunities*, eds. A. H. Bond, M. L. Dietz, and R. D. Rogers, American Chemical Society, Washington, DC, 1999, pp. 20–50.
2. Dietz, M. L.; Horwitz, E. P. Combining solvent extraction processes for actinide and fission product separations. In *Science and Technology for Disposal of Radioactive Tank Waste*, eds. W. W. Schulz and N. J. Lombardo, Plenum Press, New York, 1998, pp. 231–243.
3. Nash, K. L.; Lumetta, G. J.; Clark, S. B.; Friese, J. Significance of the nuclear fuel cycle in the 21st century. In *Separations for the Nuclear Fuel Cycle in the 21st Century*, eds. G. J. Lumetta, K. L. Nash. S. B. Clark, and J. I. Friese, American Chemical Society, Washington, DC, 2006, pp. 3–20.

4. Wai, C. M.; Gopalan, A. S.; Jacobs, H. K. An introduction to separations and processes using supercritical carbon dioxide. In *Supercritical Carbon Dioxide: Separations and Processes*, eds. A. S. Gopalan, C. M. Wai, and H. K. Jacobs, American Chemical Society, Washington, DC, 2003, pp. 2–8.

5. Huddleston, J. G.; Griffin, S. T.; Zhang, J.; Willauer, H. D.; Rogers, R. D. Metal ion separations in aqueous biphasic systems and using aqueous biphasic extraction chromatography. In *Metal Ion Separation and Preconcentration: Progress and Opportunities*, eds. A. H. Bond, M. L. Dietz, and R. D. Rogers, American Chemical Society, Washington, DC, 1999, pp. 79–100.

6. Dietz, M. L., Recent progress in the development of extraction chromatographic methods for radionuclide separation and preconcentration. In *Radioanalytical Methods at the Frontier of Interdisciplinary Science*, eds. C. Laue and K. Nash, American Chemical Society, Washington, DC, 2004, pp. 161–176.

7. Wai, C. M.; Waller, B. *Ind. Eng. Chem. Res.* 39, 4837, 2000.

8. Dietz, M. L. *Sep. Sci. Technol.* 41, 2047, 2006.

9. Nash, K. L. Twenty-first century approaches to actinide partitioning. In *Separations for the Nuclear Fuel Cycle in the 21st Century*, eds. G. J. Lumetta, K. L. Nash. S. B. Clark, and J. I. Friese, American Chemical Society, Washington, DC, 2006, pp. 21–40.

10. Alexandratos, S. D.; Ripperger, K. P. *Ind. Eng. Chem. Res.* 37, 4756, 1998.

11. Dietz, M. L.; Horwitz, E. P.; Bond, A. H. Extraction chromatography: Progress and opportunities. In *Metal Ion Separation and Preconcentration: Progress and Opportunities*, eds. A.H. Bond, M.L. Dietz, and R.D. Rogers, American Chemical Society, Washington, DC, 1999, pp. 234–250.

12. Nii, S.; Masutani, M.; Takeuchi, H. Extraction of heavy metal ions using encapsulated extractant-impregnated resins. In *Solvent Extraction for the 21st Century (Proceedings of ISEC '99)*, Vol. 2, eds. M. Cox, M. Hidalgo, and M. Valiente, Society of Chemical Industry, London, 2001, pp. 1279–1283.

13. Seddon, K. R. *Kinetics and Catalysis* 37, 693, 1996.

14. Darr, J. A.; Poliakoff, M. *Chem. Rev.* 99, 495, 1999.

15. Phelps, C. L.; Smart, N. G.; Wai, C. M. *J. Chem. Ed.* 73, 1163, 1996.

16. Jessop, P. G.; Leitner, W. Supercritical fluids as media for chemical reactions. In *Chemical Synthesis Using Supercritical Fluids*, eds. P. G. Jessop and W. Leitner, Wiley-VCH, New York, 1999, pp. 9–13.

17. Gawenis, J. A.; Kauffman, J. F.; Jurisson, S. S. *Anal. Chem.* 73, 2022, 2001.

18. Laintz, K. E.; Wai, C. M., Yonker, C. R.; Smith, R. D. *J. Supercrit. Fluids*, 4, 194, 1991.

19. Laintz, K. E.; Wai, C. M.; Yonker, C. R.; Smith, R. D. *Anal. Chem.* 64, 2875, 1992.

20. Lin, Y.; Brauer, R. D.; Laintz, K. E.; Wai, C. M. *Anal. Chem.* 65, 2549, 1993.

21. Alfassi, Z. B.; Wai, C. M. *Preconcentration Techniques for Trace Elements*. CRC Press: Boca Raton, FL, 1992.

22. Tang, J.; Wai, C. M. *Anal. Chem.* 58, 3233, 1986.

23. Erkey, C. *J. Supercrit. Fluids* 17, 259, 2000.

24. Ashraf-Khorassag, M.; Combs, M. T.; Taylor, L. T. *J. Chromatogr. A* 774, 37, 1997.

25. Wai, C. M.; Wang, S. *J. Chromatorgr. A* 785, 369, 1997.

26. Smart, N. G.; Carleson, T.; Kast, T; Clifford, A. A.; Burford, M. A.; Wai, C. M. *Talanta* 44, 137, 1997.

27. Wai, C. M.; Kulyako, Y.; Yak, H. K.; Chen, X.; Lee, S. J. *Chem. Comm.* 2533, 1999.

28. Horwitz, E. P.; Dietz, M. L.; Fisher, D.E. *Solvent Extr. Ion Exch.* 9, 1, 1991.

29. Horwitz, E. P.; Dietz, M.L.; Fisher, D.E. *Solvent Extr. Ion Exch.* 8, 557, 1990.

30. DeSimone, J. M.; Maury, E. E.; Menceloglu, Y. Z.; McClain, J. B.; Romack, T. J.; Combes, J. R. *Science* 265, 356, 1994.

31. Hoefling, T. A.; Enick, R. M.; Beckman, E. J. *J. Phys. Chem.* 95, 7127, 1991.

32. McAlister, D. R.; Dietz, M. L.; Stepinski, D.; Zalupski, P. R.; Dzielawa, J. A.; Barrans, R. E., Jr.; Hess, J. N.; Herlinger, A. W. *Sep. Sci. Technol.* 39, 761, 2004.

33. Dietz, M. L.; McAlister, D. R.; Stepinski, D.; Zalupski, P. R.; Dzielawa, J. A.; Barrans, R. E., Jr.; Hess, J. N.; Rubas, A. V.; Chiarizia, R.; Lubbers, C.; Scurto, A. M.; Brennecke, J. F.; Herlinger, A. W. Recent progress in the development of supercritical carbon dioxide soluble metal ion extractants: Solubility enhancement through silicon functionalization. In *Nuclear Waste Management: Accomplishments of the Environmental Management Sciences Program*, ed. T. Zachry, American Chemical Society, Washington, DC, 2006, pp. 250–267.

34. Dzielawa, J. A.; Rubas, A. V.; Lubbers, C.; Stepinski, D. C.; Scurto, A. M.; Barrans, R. E., Jr.; Dietz, M. L.; Herlinger, A. W.; Brennecke, J. F. *Sep. Sci. Technol.*, 43, 2503, 2008. In press.

35. Chiarizia, R.; Horwitz, E. P.; Rickert, P. G.; Herlinger, A. W. *Solvent Extr. Ion Exch.* 14, 773, 1996.

36. Chiarizia, R.; Herlinger, A. W.; Horwitz, E. P. *Solvent Extr. Ion Exch.* 15, 417, 1997.

37. Chiarizia, R.; Herlinger, A. W.; Chang, Y. D.; Ferraro, J. R.; Rickert, P. G.; Horwitz, E. P. *Solvent Extr. Ion Exch.* 16, 505, 1998.

38. Herlinger, A. W.; McAlister, D. R.; Chiarizia, R.; Dietz, M. L. *Sep. Sci. Technol.* 38, 2741, 2003.

39. Levy, J. M.; Dolata, L.; Ravey, R. M.; Storozynsky, E.; Holowczak, K. A. *J. High Res. Chrom.* 16, 368, 1993.

40. Lin, Y.; Wai, C. M.; Jean, F. M.; Brauer, R. D. *Environ. Sci. Technol.* 28, 1190, 1994.

41. Lin, Y.; Wai, C. M. *Anal. Chem.* 66, 1971, 1994.

42. Laintz, K. E.; Tachikawa, E. *Anal. Chem.* 66, 2190, 1994.

43. Lin, Y.; Smart, N. G.; Wai, C. M. *Environ. Sci. Technol.* 29, 2706, 1995.

44. Page, S. H.; Sumpter, S. R.; Goats, S. R.; Lee, M. L. *J. Supercrit. Fluids* 6, 95, 1993.

45. Carrott, M. J.; Waller, B. E.; Smart, N. G.; Wai, C. M. *Chem. Commun.* 373, 1998.

46. Addleman, R. S.; Carrott, M. J.; Wai, C. M. *Anal. Chem.* 72, 4015, 2000.

47. Smart, N. G.; Carleson, T. E.; Elshani, S.; Wang, S.; Wai, C. M. *Ind. Eng. Chem. Res.* 36, 1819, 1997.

48. Smart, N. G.; Wai, C. M.; Phelps, C. *Chem. Brit.* 34, 34, 1998.

49. Wai, C. M. Reprocessing spent nuclear fuel with supercritical carbon dioxide. In *Separations for the Nuclear Fuel Cycle in the 21st Century*, ed. G. J. Lumetta, K. L. Nash, S. B. Clark, and J. I. Friese, American Chemical Society, Washington, DC, 2006, pp. 57–67.

50. Carrott, M. J.; Wai, C. M. *Anal. Chem.* 70, 2421, 1998.

51. Wai, C. M.; Lin, Y.; Ji, M.; Toews, K. L.; Smart, N. G. Extraction and separation of uranium and lanthanides with supercritical fluids. In *Metal Ion Separation and Preconcentration: Progress and Opportunities*, eds. A. H. Bond, M. L. Dietz, and R. D. Rogers, American Chemical Society, Washington, DC, 1999, pp. 390–400.

52. Samsonov, M. D.; Wai, C. M.; Lee, S.-C.; Kulyako, Y.; Smart, N. G. *Chem. Commun.* 1868, 2001.

53. Shimada, T.; Ogumo, S.; Sawada, K.; Enokida, Y.; Yamamoto, I. *Anal. Sci.* 22, 1387, 2006.

54. Trofimov, T. I.; Samsonov, M. D.; Lee, S. C.; Smart, N. G.; Wai, C. M. *J. Chem. Technol. Biotechnol.* 76, 1223, 2001.

55. Enokida, Y.; El-Fatah, S. A.; Wai, C. M. *Ind. Eng. Chem. Res.* 41, 2282, 2002.

56. Samsonov, M. D.; Trofimov, T. I.; Vinokurov, S. E.; Lee, S. C.; Myasoedov, B. F.; Wai, C. M. Dissolution of actinide oxides in supercritical carbon dioxide modified with various organic ligands. In *Proceedings of the International Solvent Extraction Conference 2002, ISEC 2002*, eds. K. C. Sole, P. M. Cole, J. S. Preston, and D. J. Robinson, SAIMM, Johannesburg, South Africa, 2002, pp. 1187–1192.

57. Blackburn, J. M.; Long, D. P.; Cabanes, A.; Watkins, J. J. *Science* 294, 141, 2001.

58. Wai, C. M.; Ohde, H.; Kramer, S. *United States Patent* 6,653,236; 2003.

59. Walden, P. *Bull. Acad. Sci. St. Petersburg* 405, 1914.

60. Wilkes, J. S.; Zaworotko, M. J. *J. Chem. Soc. Chem. Commun.* 965, 1992.

61. Adams, C. J.; Earle, M. J.; Seddon, K. R. *Chem. Commun.* 1043, 1999.

62. Karodia, N.; Guise, S.; Newlands, C.; Andersen, J. *Chem. Commun.* 2341, 1998.

63. Fuller, J.; Carlin, R. T.; Osteryoung, R. A. *J. Electrochem. Soc.* 144, 3881, 1997.

64. Earle, M. J.; Seddon, K. R. *Pure Appl. Chem.* 72, 1391, 2000.

65. Zhao, D.; Wu, M.; Kou, Y.; Min, E. *Catal. Today* 74, 157, 2002.

66. Olivier-Bourbigou, H.; Magna, L. *J. Mol. Catal. A* 182/3, 419, 2002.

67. Dai, S.; Ju, Y. H.; Barnes, C. E. *J. Chem. Soc. Dalton Trans.* 1201, 1999.

68. Izatt, R. M.; Pawlak, K.; Bradshaw, J. S.; Breuning, R. L. *Chem. Rev.* 91, 1721, 1991.

69. Visser, A. E.; Swatloski, R. P.; Reichert, W. M.; Griffin, S. T.; Rogers, R. D. *Ind. Eng. Chem. Res.* 39, 3596, 2000.

70. Chun, S.; Dzyuba, S. V.; Bartsch, R. A. *Anal. Chem.* 73, 3737, 2001.

71. Dietz, M. L.; Dzielawa, J. A. *Chem. Commun.* 2124, 2001.

72. Jensen, M. P.; Dzielawa, J. A.; Rickert, P.; Dietz, M. L. *J. Am. Chem. Soc.* 124, 10664, 2002.

73. Shimojo, K.; Goto, M. *Anal. Chem.* 76, 5039, 2004.

74. Sieffert, N.; Wipff, G. *J. Phys. Chem. A* 110, 1106, 2006.

75. Luo, H.; Dai, S.; Bonnesen, P. V. *Anal. Chem.* 76, 2773, 2004.

76. Visser, A. E.; Jensen, M. P.; Laszak, I.; Nash, K. L.; Choppin, G. R.; Rogers, R. D. *Inorg. Chem.* 42, 2197, 2003.

77. Nakashima, K.; Kubota, F.; Maruyama, T.; Goto, M. *Ind. Eng. Chem. Res.* 44, 4368, 2005.

78. Dietz, M. L.; Dzielawa, J. A.; Laszak, I.; Young, B. A.; Jensen, M. P. *Green Chem.* 5, 682, 2005.

79. Dietz, M. L; Stepinski, D. C. *Talanta* 75, 598, 2008.

80. Giridhar, P.; Venkatesan, K. A.; Srinivasan, T. G.; Rao, P. R. V. *J. Radioanl. Nucl. Chem.* 265, 31, 2005.

81. Swatloski, R. P.; Holbrey, J. D.; Rogers, R. D. *Green Chem.* 5, 361, 2003.

82. Baston, G. M. N.; Bradley, A. E.; Gorman, T.; Hamblett, I.; Hardacre, C.; Hatter, J. E.; Healy, M.J.F.; Hodgson, B.; Lewin, R.; Lovell, K.V.; Newton, G.W.A.; Nieuwenhuyzen, M.; Pitner, W. R.; Rooney, D. W.; Sanders, D.; Seddon, K. R.; Simms, H. E.; Thied, R. C. Ionic liquids for the nuclear industry: A radiochemical, structural, and electrochemical investigation. In *Industrial Applications for Green Chemistry*, eds. R. D. Rogers and K. R. Seddon, American Chemical Society, Washington, DC, 2002, pp. 162–177.

83. Allen, D.; Baston, G.; Bradly, A. E.; Gorman, T.; Haile, A.; Hamblett, I.; Hatter, J. E.; Healey, M. J. F.; Hodgson, B.; Lewin, R.; Lovell, K. V.; Newton, B.; Pitner, W. R.; Rooney, D. W.; Sanders, D.; Seddon, K. R.; Sims, H. E.; Thied, R. C. *Green Chem.* 4, 152, 2002.

84. Harmon, C. D.; Smith, W. H.; Costa, D. A. *Radiat. Phys. Chem.* 60, 157, 2001.

85. Dietz, M. L. Fundamental aspects of metal ion transfer into ionic liquids: Implications for the design of ionic liquid-based solvent extraction systems. In *Proceedings of the DAE-BRNS Biennial Symposium on Emerging Trends in Separation Science and Technology*, SESTEC, Delhi, India, 2008, pp. 5–11.

86. Heitzman, H.; Young, B. A.; Rausch, D. J.; Rickert, P.; Stepinski, D.; Dietz, M. L. *Talanta* 69, 527, 2006.

87. Dietz, M. L.; Stepinski, D. C. *Green Chem.* 7, 747, 2005.

88. Rickert, P. G.; Stepinski, D. C.; Rausch, D. J.; Bergeron, R. M.; Jakab, S.; Dietz, M. L. *Talanta* 72, 315, 2007.

89. Dietz, M. L.; Jakab, S.; Yamoto, K.; Bartsch, R. A. *Green Chem.* 10, 174, 2008.

90. Luo, H.; Dai, S.; Bonnesen, P. V.; Buchanan, A. C., III; Holbrey, J. D.; Bridges, N. J.; Rogers, R. D. *Anal. Chem.* 76, 3078, 2004.

91. Jensen, M. P.; Neuefeind, J.; Beitz, J. V.; Skanthakumar, S.; Soderholm, L. *J. Am. Chem. Soc.* 125, 15466, 2003.

92. Cocalia, V. A.; Jensen, M. P.; Holbrey, J. D.; Spear, S. K.; Stepinski, D. C. Rogers, R. D. *Dalton Trans.* 1966, 2005.

93. Visser, A. E.; Swatloski, R. P.; Reichert, W. M.; Mayton, R.; Sheff, S.; Wierzbicki, A.; Davis, J. H.; Rogers, R. D. *Chem. Commun.* 135, 2001.

94. Davis, J. H., Jr. Working salts: syntheses and uses of ionic liquids containing functionalized ions. In *Ionic Liquids: Industrial Applications for Green Chemistry*, eds. R. D. Rogers and K. R. Seddon, American Chemical Society, Washington, DC, 2002, pp. 247–258.

95. Davis, J. H., Jr. *Chem. Lett.* 33, 1072, 2004.

96. Gutowski, K. E.; Bridges, N. J.; Cocalia, V. A.; Spear, S. K.; Visser, A. E., Holbrey, J. D.; Davis, J. H., Jr., Rogers, R. D. Ionic liquid technologies for utilization in nuclear-based separations. In *Ionic Liquids IIIB: Fundamentals, Progress, Challenges, and Opportunities – Transformations and Processes*, eds. R. D. Rogers and K. R. Seddon, American Chemical Society, Washington, DC, 2005, pp. 33–48.

97. Ouadi, A.; Gadenne, B.; Heseman, P.; Moreau, J. J. E.; Billard, I.; Gaillard, C.; Mekki, S.; Moutiers, G. *Chem. Eur. J.* 12, 3074, 2006.

98. Ouadi, A.; Klimchuk, O.; Gaillard, C.; Billard, I. *Green Chem.* 9, 1160, 2007.

Index

Ion Exchange and Solvent Extraction
A Series of Advances

The growth in the world's nuclear industry, motivated by peaking world oil supplies, concerns about the greenhouse effect, and domestic needs for energy independence, has resulted in a heightened focus on the need for next-generation nuclear fuel-cycle technologies. **Ion Exchange and Solvent Extraction: A Series of Advances, Volume 19** provides a comprehensive look at the state of the science underlying solvent extraction in its role as the most powerful separation technique for the reprocessing of commercial spent nuclear fuel.

Capturing the current technology and scientific progress as it exists today and looking ahead to potential developments, the book examines:

- the overall state of solvent extraction in reprocessing
- new molecules for increased selectivity and performance
- methods for predicting extractant properties
- actinide-lanthanide group separation
- simultaneous extraction of radionuclides by mixing extractants
- the cause and nature of third-phase formation
- the effects of radiation on the solvent and its performance
- analytical techniques for measuring process concentrations
- new centrifugal contractors for more efficient processing
- new chemistry using novel media

The long-term vision of many professionals in the field entails a proliferation-free nuclear energy economy in which little or no waste is stored or released into the environment and all potential energy values in spent nuclear fuel are recycled. This text opens a window on that possibility, offering insight from world leaders on the cutting edge of nuclear research.